INTERIM REPORT

Accession No. 7912180099

Contract Program or Project Title:

Water Reactor Safety Research

Subject of this Document:

Papers presented at 7th WRSR Information Meeting, Nov. 5-9, 1979
Meeting agenda attached.

Type of Document:

Papers presented at 7 th Water Reactor Safety Research Information Meeting, November 5 -9, 1979 at the National Bureau of Standards

Author(s):

See agenda

Date of Document:

November 5 -9, 1979

Responsible NRC Individual and NRC Office or Division:

Stanley A. Szawlewicz, Division of Reactor Safety Research

This document was prepared primarily for preliminary or internal use. It has not received full review and approval. Since there may be substantive changes, this document should not be considered final.

POOR ORIGINAL

Prepared for
U.S. Nuclear Regulatory Commission
Washington, D.C. 20555

INTERIM REPORT

1600 ·001

7912180 099

FINAL AGENDA

SEVENTH WATER REACTOR SAFETY RESEARCH
INFORMATION MEETING

AT THE

NATIONAL BUREAU OF STANDARDS
ADMINISTRATION BUILDING 101
GAITHERSBURG, MARYLAND

NOVEMBER 5 - 9, 1979

Registration

Registration desks will be located in the hallway between the Red and Green Auditoriums.

Registration will begin before the meetings and extend into the morning coffee break.

A registration fee of $6.00 for each day of attendance will be charged each meeting participant to defray expenses.

Cafeteria tickets will be issued at the time of registration.

Entry to the cafeteria for the special prepaid luncheons will be through the use of cafeteria tickets only.

1600 002

AGENDA

SEVENTH WATER REACTOR SAFETY RESEARCH
INFORMATION MEETING

MONDAY, NOVEMBER 5, 1979

RED AUDITORIUM - ALL PARTICIPANTS

9:15 am -	Introductory Remarks	J. M. Hendrie S. Levine T. E. Murley G. L. Bennett, NRC
9:25 am -	Highlights of WRSR Achievements in FY-79	L. S. Tong, NRC

Three Mile Island Accident

9:40 am -	What NRC Is Doing In Response to TMI	H. R. Denton, NRC
10:05 am -	Coffee Break	
10:20 am -	Status in the Understanding of TMI	W. V. Johnston, NRC
10:45 am -	Radiological Aspects of TMI Accident	F. J. Miraglia, NRC

LOFT PROGRAM

MORNING SESSION - RED AUDITORIUM

Chairman: G. D. McPherson, NRC

11:10 am -	Overview of the LOFT Program	G. D. McPherson, NRC
11:20 am -	Analysis of LOFT Tests L2-2, L2-3 and L3-0	L. P. Leach, EG&G
12:00 pm -	Results of the PBF/LOFT Lead Rod Test Program	D. J. Varacalle, EG&G
12:20 pm -	Status of LOFT Two-Phase Flow Instrumentation Calibration	W. J. Quapp, EG&G
12:35 pm -	Planning for Small Breaks and Other Future Tests	G. D. McPherson, NRC
12:45 pm -	Discussion	
1:00 pm -	Lunch	

MONDAY, NOVEMBER 5, 1979

SEPARATE EFFECTS TESTS AND ANALYSES

AFTERNOON SESSION - RED AUDITORIUM

Semiscale Program

Chairman: H. Sullivan, NRC

2:00 pm - Highlights of Semiscale Tests and Analysis, Nov. 1978-Nov. 1979	R. G. Hanson, EG&G
2:20 pm - Results from Semiscale Three Mile Island Experiments	T. K. Larson, EG&G
2:40 pm - Preliminary Results from Semiscale Small Break Test	E. A. Harvego, EG&G

Instrumentation Programs of NRC

Chairman: Y. Y. Hsu, NRC

3:00 pm - Introduction - U.S. Instrumentation Activities	Y. Y. Hsu, NRC
3:15 pm - Coffee Break	
3:30 pm - Pulsed Neutron Generator for Two-Phase Flow Measurement	G. E. Rochau, SANDIA
3:50 pm - Pulsed Neutron Activation Calibration Technique	P. Kehler, ANL
4:10 pm - Instrumentation For Film Dynamics In Two-Phase Flow	J. E. Chen, Lehigh Univ.
4:30 pm - Advanced Instrumentation for Reflood Studies	B. Eads, ORNL
5:00 pm - Advanced Spool Piece Development and Signal Analysis	K. Turnage C. E. Davis, ORNL
5:30 pm - Adjourn	

MONDAY, NOVEMBER 5, 1979

SEPARATE EFFECTS TESTS AND ANALYSES

AFTERNOON SESSION - CONFERENCE ROOM "A"

Thermalhydraulic Model Development: I. Heat Transfer

Chairman: L. B. Thompson, NRC

2:00 pm -	Transient CHF Correlations	J. C. M. Leung, ANL
2:25 pm -	Progress in Low Quality and Subcooled Post-CHF Studies	D. C. Groeneveld, AECL
2:50 pm -	Non-Equilibrium Post-CHF Heat Transfer	J. E. Chen, Lehigh Univ.
3:15 pm -	Coffee Break	
3:30 pm -	Predictions of Core Rewet Behavior	R. A. Nelson, EG&G
3:55 pm -	Cladding Rewets Observed in LOFT Large Break LOCA Tests	E. L. Tolman, EG&G
4:20 pm -	Rewetting in the Semiscale MOD-1 and MOD-3 Cores	D. M. Snider, EG&G
5:00 pm -	Discussion	
5:30 pm -	Adjourn	

TUESDAY, NOVEMBER 6, 1979

SEPARATE EFFECTS TESTS AND ANALYSES

MORNING SESSION - RED AUDITORIUM

2D/3D Program

Chairman: W. S. Farmer, NRC

9:15 am -	Introduction	L. S. Tong, NRC
9:30 am -	Japanese Safety Research Programs - ROSA, CCTF, and SCTF	M. Nozawa, JAERI
10:15 am -	Coffee Break	

Reflood Tests and Analysis

Chairman: L. B. Thompson, NRC

10:30 am -	Results of NRC/W/EPRI FLECHT SEASET Program	L. E. Hochreiter, W
11:15 pm -	Gravity Reflood Oscillations in a PWR	P. Griffith Y. L. Cheung, MIT
11:45 pm -	Invited Paper - Experimental Capabilities of the HDR Plant with Emphasis on Blowdown Testing	K. Muller-Dietsche, KfK, FRG
12:15 pm -	Discussion	
1:00 pm -	Lunch	

TUESDAY, NOVEMBER 6, 1979

LOFT PROGRAM

MORNING SESSION - CONFERENCE ROOM "A"

Workshop on Instrumentation Programs

Chairman: N. Kondic, NRC

9:15 am -	Introduction	N. Kondic, NRC
9:30 am -	Status of Two-Phase Flow Standards Selection	J. R. Fincke, EG&G
9:50 am -	Video Optical Systems for the 2D/3D Multinational Refill-Reflood Program	W. L. Kirchner, LASL
10:15 am -	Coffee Break	
10:30 am -	Reactor Noise Applications to Two-Phase Flow Studies	R. W. Albrecht, U. of Washington
10:50 am -	Void Fraction Measurement Using Neutrons	S. Banerjee, McMaster U.
11:10 am -	Holographic and Laser Doppler Studies	R. S. Tankin, HWU
11:35 am -	Survey of INEL Advanced Instrumentation	J. V. Anderson, EG&G
12:25 pm -	Discussion	
1:00 pm -	Lunch	

TUESDAY, NOVEMBER 6, 1979

SEPARATE EFFECTS TESTS AND ANALYSES

AFTERNOON SESSION - RED AUDITORIUM

BWR Safety Research Program

Chairman: W. D. Beckner, NRC

2:00 pm -	Introduction - Boiling Water Reactor Safety Research Programs	W. D. Beckner, NRC
2:15 pm -	BWR BD/ECC Program - System Response With ECC Injection	G. L. Sozzi, GE
2:45 pm -	A Comparison of RELAP Calculations With TLTA Test 6406	G. E. Wilson, EG&G
3:15 pm -	Coffee Break	

TUESDAY, NOVEMBER 6, 1979

SEPARATE EFFECTS TESTS AND ANALYSES

AFTERNOON SESSION - RED AUDITORIUM

BWR Safety Research Program (Cont'd)

3:30 pm - BWR Core Spray Distribution	G. E. Dix, GE
4:00 pm - An Improved RELAP-4 Jet Pump Model	T. R. Charlton, EG&G
4:30 pm - Discussion	
5:00 pm - Adjourn	

TUESDAY NOVEMBER 6, 1979

SEPARATE EFFECTS TESTS AND ANALYSES

MORNING SESSION - CONFERENCE ROOM "B"

Thermalhydraulic Model Development:
Session II - Interfacial Mass Transfer

Chairman: Y. Y. Hsu, NRC

9:15 am - Nonequilibrium Phase Change Studies	N. Abuaf, BNL
9:45 am - Steam-Water Mixing Studies	S. G. Bankoff R. S. Tankin M. C. Yuen, NWU
10:15 am - Coffee Break	
10:30 am - Droplet Entrainment Studies of Dispersed Flow Through Tie Plate in LOCA by LDA Method	R. S. L. Lee J. Srinivasan S. K. Cho, SUNY
11:00 am - Droplet Cross Flow Phenomena in an LPWR Upper Plenum	W. L. Kirchner J. C. Dallman, LASL
11:30 am - Two-Fluid Model and Momentum Interaction Between Phases	M. Ishii T. C. Chowla, ANL
12:00 pm - Phase Distribution and Separation Phenomena	R. T. Lahey, RPI
12:30 pm - Discussion	
1:00 pm - Lunch	

TUESDAY, NOVEMBER 6, 1979

SEPARATE EFFECTS TESTS AND ANALYSES

AFTERNOON SESSION - CONFERENCE ROOM "B"

Thermalhydraulic Model Development: Session II (Cont'd)

2:00 pm -	Steam Generator Flow Instabilities and Natural Circulation	P. Griffith D-Y. Hsia R. Bjorge, MIT
2:45 pm -	Heat Transfer Modeling for Steam Generators	P. Saha, BNL
3:15 pm -	Coffee Break	
3:30 pm -	Steam Generator Modeling and Comparisons With FLECHT SEASET Data	G. E. Wilson, EG&G
4:00 pm -	Discussion	
4:30 pm -	Adjourn	

WEDNESDAY, NOVEMBER 7, 1979

SEPARATE EFFECTS TESTS AND ANALYSES

MORNING SESSION - CONFERENCE ROOM "A"

Workshop on ECC Bypass

Chairman: W. D. Beckner, NRC

9:15 am -	Summary of the Small Scale ECC Bypass Research Information Letter	W. D. Beckner, NRC
9:40 am -	Downcomer Flow Topology Results at 2/15 Scale	R. P. Collier, BCL
9:55 am -	Flashing Transients and ECC Interactions	C. J. Crowley, Creare
10:15 am -	Coffee Break	
10:30 am -	Summary of Air Water Flooding Experiments	H. J. Richter, Dartmouth C.
10:50 am -	Discussion	

Poster Session in Hallway - 11:00 am - 1:00 pm

RSR Data Bank at INEL
Reactor Safety Research Data Repository at ORNL

WEDNESDAY, NOVEMBER 7, 1979

LOFT PROGRAM

MORNING SESSION - CONFERENCE ROOM "B"

9:15 am - 1:00 pm with 10:15 am Coffee Break

Panel Discussion on LOFT Program Results

Chairman: G. D. McPherson, NRC

WEDNESDAY, NOVEMBER 7, 1979

AFTERNOON SESSION - CONFERENCE ROOM "A"

EPRI R&D Program

Chairman: W. B. Loewenstein, EPRI

2:00 pm - The EPRI Safety R&D Program	W. B. Loewenstein, EPRI
2:30 pm - Pump Two-Phase Performance Results	K. Nilsson, EPRI
3:15 pm - Coffee Break	
3:30 pm - Analysis of Optional Transients in LWRs Using RETRAN	J. Naser, EPRI
4:00 pm - Operating Effectiveness - Human Factors Research & Disturbance Analysis Safety System	J. Prestele, A. Long, EPRI
4:30 pm - BWR Pipe Cracking Research	R. Smith, EPRI
5:00 pm - Discussion	
5:30 pm - Adjourn	

1600 010

MONDAY, NOVEMBER 5, 1979

RED AUDITORIUM - ALL PARTICIPANTS

9:15 am - 11:10 am - Introductions, Research Highlights, and Presentations on the Three Mile Island Accident - See Page 1 of the agenda.

METALLURGY AND MATERIALS RESEARCH

MORNING SESSION - GREEN AUDITORIUM

11:15 am - Introductory Remarks — C. Z. Serpan, Jr., NRC

Symposium on Tearing Instability and Ductile Shelf Testing Technology

Chairman: P. Albrecht, NRC

11:25 am -	Application of Tearing Instability Analysis to Primary Systems	P. C. Paris, Wash Univ.
11:45 am -	Computer-Interactive Unloading Compliance Test Method Validation	J. P. Gudas, NSRDC
12:05 pm -	Key Curve Analysis of Ductile Shelf Fracture Toughness	J. A. Joyce, U.S. Naval Academy
12:25 pm -	Ductile Shelf Fracture Toughness of Irradiated Steels	F. J. Loss, NRL
12:45 pm -	Discussion	
1:00 pm -	Lunch	

MONDAY, NOVEMBER 5, 1979

METALLURGY AND MATERIALS RESEARCH

AFTERNOON SESSION - GREEN AUDITORIUM

Vessel and Piping Integrity

Chairman: P. Albrecht, NRC

2:00 pm -	Influence of Critical Parameters on Cyclic Crack Growth Rate	W. Cullen, NRL
2:20 pm -	Design Rules for Multiple Interacting Nozzles in Vessels	S. Moore, ORNL
2:40 pm -	Revaluation of Criteria for Postulating Cold Leg Breaks	R. J. Eiber, BCL
3:00 pm -	Coffee Break	

Chairman: M. Vagins, NRC

3:20 pm -	Two-Phase Jet Loads	D. Tomasko, Sandia
3:40 pm -	Development of Large-Displacement, Non-Linear, Elastic-Plastic Code for Pipe Whip Analysis	G. H. Powell, Univ. of Calif./Berkeley
4:00 pm -	Standard Crack Arrest Specimen and Analysis	G. R. Irwin, Univ. of Maryland
4:20 pm -	Crack Initiation and Arrest of Cracks from Deep Flaws Under Thermal Shock Loading	R. D. Cheverton, ORNL
4:40 pm -	Determination of K-Factors for Arbitrarily Shaped Flaws at Pressure Vessel Nozzle Corners	J. W. Bryson, ORNL
5:00 pm -	Adjourn	

TUESDAY, NOVEMBER 6, 1979

METALLURGY AND MATERIALS RESEARCH

MORNING SESSION - GREEN AUDITORIUM

Irradiation Effects and Neutron Dosimetry

Chairman: C. Z. Serpan, Jr., NRC

9:15 am -	Notch Ductility Degradation of Low Alloy Steels with Low-to-Intermediate Neutron Fluence Exposures	J. R. Hawthorne, NRL
9:45 am -	Progress Report of Pressure Vessel Surveillance Dosimetry Improvement	W. N. McElroy, HEDL
10:15 am -	Coffee Break	
10:30 am -	Validation of Predictions of Flux and Spectrum in a Pressure Vessel Wall Environment	F. B. K. Kam, ORNL
11:00 am -	Invited Paper - Embrittlement Saturation of Reactor Pressure Vessel Steels	D. Pachur, KFA Julich, FRG

Steam Generator Tube Integrity and Stress Corrosion

Chairman: J. Muscara, NRC

11:30 am -	Feasibility of Studies on a Retired Steam Generator	R. Clark, PNL
12:00 pm -	The EPR Method for the Detection of Sensitization in Stainless Steels	W. L. Clarke, GE
12:30 pm -	Stress Corrosion Cracking Predictability in Steam Generator Tubes	D. Van Rooyen, BNL
1:00 pm -	Lunch	

1600 013

TUESDAY, NOVEMBER 6, 1979

METALLURGY AND MATERIALS RESEARCH

AFTERNOON SESSION - GREEN AUDITORIUM

Non-Destructive Examination

Chairman: J. Muscara, NRC

2:00 pm -	Quantified Flaw Detection and Evaluation During In-Process Welding of Nuclear Components	D. W. Prine, GARD
2:30 pm -	Acoustic Emission/Material Property Relationships, Signature Analyses and Equipment Design for Continuous Monitoring of Reactors	P. Hutton, PNL
2:55 pm -	The Application of the Internal Friction Damping Nondestructive Evaluation Technique for Detecting Incipient Cracking of BWR Primary Piping Systems	L. L. Yeager A. A. Hochrein, Jr., Daedalean Associates
3:15 pm -	Coffee Break	
3:30 pm -	Improved Ultrasonic Flaw Detection and Characterization Using 3-D Imaging from Synthetic Aperture and Spotlight Mode	C. Vanden Broek, U. of Michigan
4:00 pm -	Improved Multi-Frequency Eddy Current Test and Analyses for In-Service Inspection of Steam Generator Tubes	C. V. Dodd, ORNL
4:20 pm -	Proposed Improved Test Standard for Steam Generator Tube Inspection	R. Clark, PNL
4:40 pm -	Ultrasonic Testing Flaw Detection Probability and Reliability of Piping Steels	F. L. Becker, PNL
5:10 pm -	Discussion	
5:30 pm -	Adjourn	

WEDNESDAY, NOVEMBER 7, 1979

ANALYSIS DEVELOPMENT PROGRAM

MORNING SESSION - RED AUDITORIUM

9:15 am -	Introduction	S. Fabic, NRC

Code Development Program

Session A-1: Improvements in Existing Codes

Chairman: W. C. Lyon, NRC

9:30 am -	RELAP-4/MOD 7 Development	S. R. Behling, EG&G
10:10 am -	Coffee Break	
10:30 am -	WRAP-BWR-EM System Development and Applications	M. R. Buckner, SRL
11:00 am -	WRAP-PWR-EM System Development and Applications	F. Beranek, SRL
11:30 am -	Application of RAMONA-III and IRT Codes to BWR and PWR Analysis	D. J. Diamond W. G. Shier, BNL
12:00 pm -	RELAP-4 Application to TMI-2 Accident	S. R. Behling, EG&G
12:30 pm -	RELAP-5 Development and Applications	V. H. Ransom, EG&C
1:00 pm -	Lunch	

WEDNESDAY, NOVEMBER 7, 1979

ANALYSIS DEVELOPMENT PROGRAM

AFTERNOON SESSION - RED AUDITORIUM

Code Development Program

Session A-2: Development and Application of Advanced Codes

Chairman: L. M. Shotkin, NRC

2:00 pm -	Variation of Doppler Reactivity Coefficient With Depletion	A. Radkowsky, GWU Tel Aviv Univ.
2:20 pm -	TRAC Code Development Status	R. J. Pryor, LASL
2:50 pm -	TRAC Hydrodynamics and Heat Transfer	D. R. Liles D. A. Mandell F. L. Addessio, LASL
3:20 pm -	Coffee Break	
3:35 pm -	TRAC Applications to the 2D/3D Facilities	P. B. Bleiweis, LASL
4:00 pm -	Analysis of TMI Accident Using TRAC	J. R. Ireland, LASL
4:30 pm -	Constitutive Modeling for Steam-Water Interactions	B. J. Daly, LASL
5:00 pm -	Numerical Simulation of Hydroelastic Motion with Application to the Full-Scale HDR Tests	W. C. Rivard, LASL
5:25 pm -	TRAC Code Sensitivity Studies	M. McKay, LASL
5:50 pm -	Adjourn	

THURSDAY, NOVEMBER 8, 1979

ANALYSIS DEVELOPMENT PROGRAM

MORNING SESSION - RED AUDITORIUM

Continuation of Session A-2: Development and Application of Advanced Codes

Chairman: S. Fabic, NRC

9:15 am -	COBRA -TF Development and Application to Semiscale S-07-6 Test	M. Thurgood, PNL
9:40 am -	COBRA-TF Reflood Model	J. M. Kelly, PNL
10:10 am -	Coffee Break	

Code Assessment and Sensitivity Studies

Chairman: N. Zuber, NRC

10:30 am -	Assessment of RELAP 4/MOD 6	T. R. Charlton, EG&G
11:00 am -	TRAC Code Developmental Assessment	K. A. Williams, LASL
11:30 am -	TRAC Code Independent Assessment at LASL: Part A	J. C. Vigil T. D. Knight, LASL

THURSDAY, NOVEMBER 8, 1979

ANALYSIS DEVELOPMENT PROGRAM

MORNING SESSION - RED AUDITORIUM

Code Assessment and Sensitivity Studies (Cont'd)

12:00 pm -	TRAC Code Independent Assessment: Part B	P. Saha U. S. Rohatgi, BNL
12:30 pm -	Statistical Analysis of the Blowdown Phase of a LOCA in a PWR as Calculated by RELAP 4/MOD 6	M. Berman R. K. Byers G. P. Steck, SANDIA
1:00 pm -	Lunch	

AFTERNOON SESSION - RED AUDITORIUM

Containment Analyses and Related Programs

Chairman: R. L. Cudlin, NRC

2:00 pm -	BEACON Development and Assessment	C. R. Broadus, EG&G
2:30 pm -	Objective and Results of the German Containment Standard Problem - Invited Paper	H. Karwat, TUM/FRG W. Winkler, GRS/FRG
3:10 pm -	Coffee Break	
3:25 pm -	Invited Paper - First Results of Large Scale Pressure Suppression System Experiments at the GKSS Facility	D. Seeliger E. Aust, GKSS
3:45 pm -	Invited Paper - Distribution of Hydrogen Released Within Compartmented Containment in Consequence of a LOCA: Analysis and Verification	H. L. Jahn, GRS G. Langer, Battelle/Frankfurt
4:15 pm -	Comprehensive Report on Results of the Battelle-Frankfurt Containment Experiments and Analytical Verification - Invited Paper	G. Hellings, GRS H. Kanzleiter, Battelle/Frankfurt
4:45 pm -	Application of PELE-IC to BWR Containment Issues	C. S. Landram, LLL
5:20 pm -	Adjourn	

WEDNESDAY, NOVEMBER 7, 1979

FUEL BEHAVIOR RESEARCH PROGRAM

MORNING SESSION - GREEN AUDITORIUM

Chairman: W. V. Johnston, NRC

9:15 am	Progress in Fuel Behavior Research	W. V. Johnston, NRC
9:45 am	Recent Results From the NSRR Experiments	M. Ishikawa T. Fujishiro T. Hoshi N. Ohnishi, JAERI
10:15 am	Coffee Break	
10:30 am	Probabilistic Whole Core Damage Analysis Using the SSYST Fuel Behavior Code	H. Borgwaldt R. Meyder W. Sengpiel, KfK/FRG
11:15 am	FRAP-T5 Model Improvements and Uncertainty Analysis Capabilities	M. P. Bohn, EG&G
12:00 pm	Independent Assessment of FRAPCON-1 and FRAP T-5	E. T. Laats, EG&G
12:45 pm	Discussion	
1:00 pm	Lunch	

AFTERNOON SESSION - GREEN AUDITORIUM

Workshop on Modeling of Zircaloy Cladding Properties

Chairman: M. L. Picklesimer, NRC

2:00 pm	Introduction and Status	M. L. Picklesimer, NRC
2:15 pm	Physical Properties of Zircaloy in MATPRO	D. L. Hagrman, EG&G
2:45 pm	Cladding Stress of Failure	D. L. Hagrman, EG&G
3:15 pm	Coffee Break	

WEDNESDAY, NOVEMBER 7, 1979

FUEL BEHAVIOR RESEARCH PROGRAM

AFTERNOON SESSION - GREEN AUDITORIUM

Workshop on Modeling of Zircaloy Cladding Properties (Cont'd)

3:30 pm -	Mechanical Properties of Zircaloy - DILATE	C. L. Mohr, PNL
4:00 pm -	The MATMOD Approach to Modelling of Zircaloy Non-Elastic Deformation	A. K. Miller, Stanford U.
4:30 pm -	Mechanical Properties of Zircaloy - NORA	S. Raff M. Bocek R. Meyder, KfK/FRG
5:00 pm -	Summary and Conclusions	
5:30 pm -	Adjourn	

THURSDAY, NOVEMBER 8, 1979

FUEL BEHAVIOR RESEARCH PROGRAM

MORNING SESSION - GREEN AUDITORIUM

Chairman: R. R. Sherry, NRC

9:15 am -	Fission Product Transport Analysis	J. A. Gieseke, BCL
9:45 am -	Melt/Concrete Interactions: The Sandia Experimental Program, Model Development and Code Comparison Test	D. A. Powers J. F. Muir, SANDIA
10:15 am -	Coffee Break	
10:30 am -	Experimental and Theoretical Results on Long-Term Coolability of a Partially Blocked Core	G. Hofmann W. Baumann, KfK/FRG

THURSDAY, NOVEMBER 8, 1979

FUEL BEHAVIOR RESEARCH PROGRAM

MORNING SESSION - GREEN AUDITORIUM

PBF Program

Chairman: M. L. Picklesimer, NRC

11:00 am -	Overview of Recent PBF Test Results	H. J. Zeile, EG&G
11:15 am -	Influence of Internal Pressure and Prior Irradiation on Deformation of Zircaloy Cladding: LOC-3 Results	T. R. Yackle, EG&G
11:45 am -	An Evaluation of the Effects of Surface Thermocouples on LOCA Rewet: TC-1 Results	J. Broughton, EG&G
12:15 pm -	Light Water Reactor Fuel Response During RIA Experiments	P. E. MacDonald, EG&G
12:45 pm -	Discussion	
1:00 pm -	Lunch	

AFTERNOON SESSION - GREEN AUDITORIUM

Workshop on Plans for In-Reactor Fuel Behavior Experiments

Chairman: R. Van Houten, NRC

2:00 pm -	Introduction - In-Reactor Fuel Testing	R. Van Houten, NRC
2:15 pm -	PBF Experimental Program	P. E. MacDonald H. J. Zeile, EG&G
2:45 pm -	ESSOR Test Program	J. Randles, Ispra
3:10 pm -	Coffee Break	
3:25 pm -	NRU Experiment Plans	C. Mohr, PNL
3:50 pm -	In-Reactor Fuel Transient Fuel Behavior Experiments at CRNL	R. D. MacDonald, AECL
4:15 pm -	In-Reactor Fuel Behavior Tests in the DIDO High Pressure Water Loop	A. Mann, UKAEA
4:40 pm -	French In-Reactor Fuel Behavior Experiments	M. Chagrot, FAR
5:05 pm -	In-Reactor Experiments in Japan	M. Ishikawa M. Ichikawa S. Ohuchi, JAERI
5:30 pm -	Summary and Conclusions	R. Van Houten, NRC
5:45 pm -	Adjourn	

THURSDAY, NOVEMBER 8, 1979

FUEL BEHAVIOR RESEARCH PROGRAM

AFTERNOON SESSION - CONFERENCE ROOM "A"

Workshop on Fission Product Release

Co-Chairmen: R. R. Sherry and G. P. Marino, NRC

2:00 pm -	ANL Fission Gas Release Experiments and Analysis	S. M. Gehl J. Rest, ANL
2:40 pm -	Fission Product Release from Defected LWR Fuel Rods	A. P. Malinauskas R. A. Lorenz J. L. Collins, ORNL
3:15 pm -	Coffee Break	
3:30 pm -	Experimental Investigation of LWR-Core Material Release at Temperatures Ranging from 1500-2800°C	H. Albrecht V. Matschoss H. Wild, KfK/FRG
4:00 pm -	Fission Product Release During the Interaction of Molten Core Materials with Concrete	D. Powers, Sandia
4:30 pm -	Release of Fission Products from Failed Fuel	N. Ishiwatari, JAERI
5:00 pm -	Adjourn	

1600 022

THURSDAY, NOVEMBER 8, 1979

DIVISION OF SAFEGUARDS, FUEL CYCLE AND ENVIRONMENTAL RESEARCH

AFTERNOON SESSION - CONFERENCE ROOM "B"

Systems Performance Research

Chairman: D. Solberg, NRC

2:00 pm -	Atmospheric Degradation of Activated Charcoal	V. R. Deitz, NRL
2:40 pm -	Validation of a Monte Carlo Code for Radiation Streaming Analyses	M. O. Cohen, MAGI
3:15 pm -	Coffee Break	
3:30 pm -	Measurements of Radionuclide Concentrations in Liquid and Gaseous Streams in PWRs	J. W. Mandler, EG&G
4:00 pm -	Impact of Decontamination on Radioactive Waste Treatment Systems	L. D. Perrigo, PNL
4:30 pm -	Analysis of Biological Shield Materials for Elements That Could Produce Long-Lived Activation Products	J. C. Evans, PNL
5:00 pm -	Discussion	
5:15 pm -	Adjourn	

FRIDAY, NOVEMBER 9, 1979

REACTOR OPERATIONAL SAFETY PROGRAM

MORNING SESSION - RED AUDITORIUM

Chairman: G. L. Bennett, NRC

9:15 am	Opening Remarks	G. L. Bennett, NRC
9:20 am	Status of the Qualification Testing Evaluation Program	L. L. Bonzon, SANDIA
9:45 am	Results from Combined and Single Environment Accelerated Aging Studies	K. T. Gillen R. L. Clough E. A. Salazar, SANDIA
10:15 am	Coffee Break	
10:30 am	Status of Research on the Qualification Testing of Wire and Cable Focusing on the Accelerated Aging Test	N. Hayakawa, JAERI
11:00 am	Status of the Fire Protection Research Program	L. J. Klamerus, SANDIA
11:30 am	Fire Suppression Studies - Burning Characteristics of Horizontal Cable Trays	F. R. Krause, SANDIA
12:00 pm	Qualification Testing and Evaluation of Flame-Retardant and Radiation-Resistive Cables in JAPAN	K. Yahagi, Waseda Univ., Japan
12:30 pm	Fire Protection Research for Cables in Swedish Reactors	A. Kjellberg, ASEA-ATOM
1:00 pm	Lunch	

FRIDAY, NOVEMBER 9, 1979

REACTOR OPERATIONAL SAFETY PROGRAM

AFTERNOON SESSION - RED AUDITORIUM

Chairman: G. L. Bennett, NRC

2:00 pm -	Fire Resistance of Cable Penetration Seals- II. Prediction of Trends	L. W. Hunter S. Favin, APL
2:40 pm -	Application of Noise Analysis to Safety-Related Diagnostics and Assessments	D. N. Frij, ORNL
3:15 pm -	Coffee Break	
3:30 pm -	Safety-Related Operator Actions	P. Haas, ORNL
4:00 pm -	Survey of Subcoole[illegible]scharge Flow Through Pressurizer Safety/Relief Valves	E. S. Hutmacher, ETEC
4:30 pm -	Objective, Experimental Results and Analytical Interpretation of Various Valve Tests Performed at the HDR Facility - Invited Paper	T. Grillenberger, GRS/FRG K. H. Scholl, KfK/FRG
5:00 pm -	Discussion	
5:15 pm -	Adjourn	

1600 025

Monday, Nov. 5, 1979	Tuesday, Nov. 6, 1979	Wednesday, Nov. 7, 1979	Thursday, Nov. 8, 1979	Friday, Nov. 9, 1979
RED AUDITORIUM	RED AUDITORIUM	RED AUDITORIUM	RED AUDITORIUM	RED AUDITORIUM
	SEPARATE EFFECTS PROGRAM	ANALYSIS DEVELOPMENT	ANALYSIS DEVELOPMENT	REACTOR OPERATIONAL SAFETY
Introductions Highlights of Achievements Three Mile Island Accident NRC Response to TMI Status in Understanding TMI Radiological Aspects of TMI LOFT PROGRAM Overview of LOFT Program Analysis of LOFT Tests Results Lead Rod Tests Two-Phase Flow Instrumentation Calibration Planning for Small Breaks, Other Future Tests	2D/3D Program Introduction Japanese Programs - ROSA, CCTF, and SCTF Reflood Tests and Analysis FLECHT SEASET Program Gravity Reflood Oscillations in a PWR Experimental Capabilities of HDR Plant, Emphasis on Blowdown Testing	Introduction Code Development Program RELAP-4/MOD 7 Development TRAP-BWR-EM System TRAP-PWR-EM System RAMONA-III and IRT Codes RELAP4 Application to TMI RELAP5 Development and Applications	Development Advanced Codes COBRA-TF Development, Application to Semiscale S-07-6 COBRA-TF Reflood Model Code Assessment-Sensitivity Studies RELAP4/MOD 6 Assessment TRAC Code Dev. Assessment TRAC Code Independent Assessment: Part A TRAC Code Independent Assessment: Part B Statistical Analysis of LOCA Blowdown, RELAP4/MOD6	Opening Remarks Status of OTE Program Combined and Single Environment Accelerated Aging Study Qualification Testing Wire and Cable - Accelerated Aging Test Fire Protection Research Fire Suppression Studies Japanese OTE Program Fire Protection Research, Cables, Swedish Reactors
SEPARATE EFFECTS PROGRAM Semiscale Program Semiscale Tests and Analysis, Nov.78 - Nov.79 Semiscale TMI Experiments Semiscale Small Break Test Instrumentation Programs U.S. Instrumentation Activities Pulsed Neutron Generator for Two-Phase Flow Pulsed Neutron Activation Calibration Technique Instrumentation for Film Dynamics, Two-Phase Flow Advanced Instrumentation for Reflood Studies Advanced Spool Piece Development, Signal Analysis	B&W Safety Research Prog. Introduction - B&W Safety Research Programs B&W BD/ECC Program-System Response with ECC Comparison RELAP with TLTA Test 6406 B&W Core Spray Distribution Improved RELAP-4 Jet Pump Model	Development Advanced Codes Variation of Doppler Coefficient with Depletion TRAC Code Development TRAC Code Hydrodynamics, Heat Transfer TRAC Applications to 2D/3D Facilities Analysis of 2D1 with TRAC Constitutive Modeling for Steam-Water Interactions Numerical Simulation of Hydroelastic Motion, Application to HDR Tests TRAC Code Sensitivity Studies	Containment Analyses and Related Programs BEACON Develop.,Assessment Results of German Containment - Standard Problem Large Scale Pressure Suppression System Expts. at GKSS Facility Hydrogen Released Within Commartmented Containment Battelle-Frankfurt Containment Experiments, Analysis Application of DELE-IC To BWR Containment Issues	Fire Resistance Cable Penetration Seals Application of Noise Analysis to Safety-Related Diagnostics, Assessments Safety-Related Operator Actions Survey Subcooled Discharge Flow Through Pressurizer Safety/Relief Valves Valve Tests at the HDR Facility

MORNING SESSIONS 9:15 am - 1:00 pm

AFTERNOON SESSIONS 2:00 pm - 6:00 pm

Monday, Nov. 5, 1979	Tuesday, Nov. 6, 1979	Wednesday, Nov. 7, 1979	Thursday, Nov. 8, 1979
[illegible] AUDITORIUM	GREEN AUDITORIUM	GREEN AUDITORIUM	GREEN AUDITORIUM
[illegible] AND MATERIAL	METALLURGY AND MATERIALS	FUEL BEHAVIOR RESEARCH	FUEL BEHAVIOR RESEARCH
Ductile Instability and Ductile Shelf Tearing Technology Application of Tearing Instability Analysis to Primary Systems Computer-Interrogative Unloading Compliance Test Method Validation Key Curve Analysis of Ductile Shelf Fracture Toughness Ductile Shelf Crack Toughness of Irradiated Steels	Irradiation Effects and Neutron Dosimetry Notch Ductility Degradation of Low Alloy Steels Pressure Vessel Surveillance Dosimetry Improvement Validation Predictions of Flux and Spectrum, Pressure Vessel Cells Embrittlement Saturation Steam Generator Tube Integrity and Stress Corrosion Feasibility of Studies on a Retired Steam Generator EPR Method for Detection of Sensitization in Stainless Steels Stress Corrosion Cracking Predictability in Steam Generator Tubes	Progress in Fuel Behavior Research Recent Results, NSRR Experiments Probabilistic Whole Core Damage Analysis Using SSYST Code FRAP-T5 Model Improvements and Uncertainty Analysis Independent Assessment FRAPCON-1 and FRAP T-5	Fission Product Transport Analysis Melt/Concrete Interactions Experimental, Theoretical Results on Long-Term Coolability of a Partially Blocked Core PBF Program Overview Recent PBF Test Results Influence Internal Pressure and Prior Irradiation on Deformation Zircaloy Cladding: LOC-3 Evaluation Effects of Surface Thermocouples on LOCA Rewet: TC-1 Results LWR Fuel Response During RIA Experiments
Vessel and Piping Integrity Influence of Critical Parameters on Cyclic Crack Growth Rate Design Rules for Multiple Interacting Nozzles in Vessels Reevaluation of Criteria for Postulating Cold Leg Breaks Two-Phase Jet Loads Development Large-Displacement, Non-Linear, Elastic-Plastic Code for Pipe Dig Analysis Standard Crack Arrest Specimen and Analysis Crack Initiation and Arrest, Deep Flaws Under Thermal Shock Loading Determination K-Factors, Arbitrarily Shaped Flaws at Pressure Vessel Nozzle Corners	Non-Destructive Examination Quantified Flaw Detection and Evaluation During In-Process Welding Acoustic Emission/Material Property Relationships Internal Friction Damping NDE Technique for BWR Piping Improved Ultrasonic Flaw Detection, Characterization Using 3-D Imaging Improved Multi-Frequency Eddy Current Test and Analysis for In-Service Inspection SG Tubes Proposed Improved Test Standard, SG Tube Inspection Ultrasonic Testing Flaw Detection Probability and Reliability of Piping Steels	Workshop on Modeling of Zircaloy Cladding Properties Introduction and Status Physical Properties of Zircaloy in MATPRO Cladding Stress of Failure Mechanical Properties of Zircaloy-DILATE MATHOD Modeling of Zircaloy Non-Elastic Deformation Mechanical Properties of Zircaloy-NORA Summary and Conclusions	Workshop on Plans for In-Reactor Fuel Behavior Experiments Introduction - In-Reactor Fuel Testing PBF Experimental Program EGSOR Test Program NRU Experiment Plans In-Reactor Fuel Transient Behavior Experiments at CRNL In-Reactor Fuel Behavior Tests in the DIDO HP Water Loop French In-Reactor Fuel Behavior Experiments In-Reactor Experiments in Japan Summary and Conclusions

WORKSHOPS AND SPECIAL SESSIONS

Monday, Nov. 5, 1979

CONFERENCE ROOM "A"
SEPARATE EFFECTS PROGRAM

AFTERNOON SESSION - 2:00 - 5:30

Thermalhydraulic Model Development: I. Heat Transfer

Transient CHF Correlations
Low Quality and Subcooled Post-CHF Studies
Non-Equilibrium Post-CHF Heat Transfer
Predictions of Core Rewet Behavior
Cladding Rewets Observed in LOFT Large Break LOCA Tests
Rewetting in Semiscale MOD-1 and MOD-3 Cores

Tuesday, Nov. 6, 1979

CONFERENCE ROOM "A"
LOFT PROGRAM

MORNING SESSION - 9:15 - 1:00

Workshop-Instrumentation Programs

Two-Phase Flow Standards
Video Optical Systems for 2D/3D Refill-Reflood Program
Reactor Noise Applications to Two-Phase Flow Studies
Void Fraction Measurement Using Neutrons
Holographic and Laser Doppler Studies
INEL Advanced Instrumentation

CONFERENCE ROOM "B"
SEPARATE EFFECTS PROGRAM

MORNING SESSION - 9:15 - 1:00

Thermalhydraulic Model Development: II. Interfacial Mass Transfer

Nonequilibrium Phase Change Studies
Steam-Water Mixing Studies
Droplet Entrainment Studies of Dispersed Flow
Droplet Cross Flow Phenomena in an LWR Upper Plenum
Two-Fluid Model and Momentum Interaction Between Phases
Phase Distribution and Separation

CONFERENCE ROOM "B"

AFTERNOON SESSION - 2:00 - 5:30

Thermalhydraulic Model Development: II. Interfacial Mass Transfer

Steam Generator Flow Instabilities and Natural Circulation
HT Modeling for Steam Generators
SG Modeling, Comparisons with PLECHT SEASET Data

Wednesday, Nov. 7, 1979

CONFERENCE ROOM "A"
SEPARATE EFFECTS PROGRAM

MORNING SESSION - 9:15 - 1:00

Workshop on ECC Bypass

Summary of Small Scale ECC Bypass Research Information Letter
Downcomer Flow Topology Results at 2/15 Scale
Flashing Transients and ECC Interactions
Air-Water Flooding Experiments
RSR Data Bank at INEL
RSR Data Repository at ORNL

CONFERENCE ROOM "B"
LOFT PROGRAM

MORNING SESSION - 9:15 - 1:00

Panel Discussion on LOFT Results

CONFERENCE ROOM "A"

AFTERNOON SESSION - 2:00 - 5:30

EPRI R&D PROGRAM

EPRI Safety R&D Program
Pump Two-Phase Performance Results
Analysis of Optional Transients in LWRs Using RETRAN
Human Factors Research & Disturbance Analysis Safety System
BWR Pipe Cracking Research

Thursday, Nov. 8, 1979

CONFERENCE ROOM "A"
FUEL BEHAVIOR RESEARCH

AFTERNOON SESSION - 2:00 - 5:30

Workshop on Fission Product Release

ANL Fission Gas Release Experiments and Analysis
FP Release from Defected LWR Fuel Rods
LWR-Core Material Release at Temperatures from 1500-2800°C.
FP Release During Interaction of Molten Core with Concrete
Release of Fission Products from Failed Fuel

CONFERENCE ROOM "B"
SAFEGUARDS, FUEL CYCLE AND ENVIRONMENTAL RESEARCH

AFTERNOON SESSION - 2:00 - 5:30

Systems Performance Research

Atmospheric Degradation Activated Charcoals
Validation of Monte Carlo Code, Radiation Streaming Analyses
Measurements Radionuclide Concentrations, Liquid and Gaseous Streams in PWRs
Impact of Decontamination on Radioactive Waste Treatment Systems
Analysis of Biological Shield Materials for Elements That Could Produce Long-Lived Activation Products

HIGHLIGHTS OF WPSR ACHIEVEMENTS IN FY-79

L. S. Tong, 11-5-79

As in previous years, this meeting emphasizes research results. I'd like to highlight some of the results in five areas.

I. Accident Detection and Prevention

A. Noise Analysis on Neutron Detectors (ORNL) -
Analytical results indicate that BWR stability can be measured on-line by analyzing the noise signature at 0.5 Hz frequency in the neutron flux power spectral density. This will be useful in measuring the thermal-hydraulic and nuclear stability of a BWR at high fuel burnups.

B. Surveillance of Piping Crack (Daedalean Associates) -
A new non-destructive evaluation technique called internal friction damping, can indicate incipient stress-corrosion cracking in piping. The technique monitors the damping of an output signal resulting from an input vibration to the pipe. The viewgraph is a typical example showing an increase in the specific damping capacity indicating crack initiation. This technique has been demonstrated successfully in four laboratory pipe-loop tests. It is under field test at Dresden Unit II.

C. Quality Assurance of Pipe Welding (GARD) -
The weld-flaw detector developed at GARD is ready for field application. This detector uses acoustic emission to detect and locate flaws during welding. It can distinguish signals between that of cracks and slag inclusions. This technique has been successfully demonstrated to the British at Risley.

D. Quality Assurance of Stainless Steel Against Sensitization (GE)-
A field monitor was developed for detecting sensitization of stainless steel BWR piping by an electrochemical technique. Field tests showed very successful results and it is in process of being adopted by ASTM as a standard method.

II. Separate Effects Understanding and Modeling for Reactor Transients and Accidents

A. Heat Transfer Data in Partially Uncovered Core (W) - In FLECHT SEASET, steam heat transfer and two-phase flow heat transfer were measured in totally and partially uncovered cores, respectively. These data are useful in evaluation of core damage when it is uncovered in a small break LOCA.

B. ECC Penetration in Downcomer, Data and Correlation (BCL & CREARE) - A correlation of ECC penetration in downcomer was developed based on the data obtained from small scale tests (1/15 and 2/15 scale) at BCL and CREARE. This correlation is believed to be conservative for applying to a large scale.

C. Transient Fission Gas Release Data from Irradiated Fuels (ANL) - Data were obtained in out-of-pile tests during very rapid power-cooling mismatch type transients.

D. Elastic-plastic Fracture Toughness of RPV (USNA) - A new technique was established for determination of J-R curve from a single specimen by using the unloading compliance method. This technique will simplify the determination of the elastic-plastic fracture toughness of reactor vessel steels.

III. Reactor System Testing and Evaluation

A. LOFT L2-2 and L2-3 Tests (INEL) -

In the past year, LOFT has run two large break LOCA tests. The first test (L2-2), performed in December 1978, was initiated at a maximum core power density of 8 Kw/ft (two-thirds the value corresponding to full power operation in most commercial PWRs). For the second test (L2-3), performed in May 1979, the maximum core power density was 12 Kw/ft (equal to that for full power operation in commercial PWRs). Both tests simulated full-sized double-ended cold leg breaks with cold leg injection of the emergency coolant and off-site power was assumed to be available to the primary and emergency coolant pumps. Both tests yielded similar results. Where differences were observed, they were only due to the 50% difference in core power being generated at the time of test initiation.

While more large break tests remain to be done, the results of these first two provide confidence in our understanding of large break behavior and in the adequacy of PWR emergency cooling systems intended to cope with large breaks.

Recently, the urgency to study small breaks and anomalous transients was increased. As a result, NRC has advanced small break and transient simulations in its test program. In fact, a zero-powered test

involving depressurization through the pressurizer relief valve was run last May as a preparation for future nuclear power tests. The first nuclear powered small break test is scheduled to be run nine days from now, and several more small break and transient tests will be run during the coming year.

The NRC is proud of the work performed within the LOFT program and give credit for these successes to the staff of EG&G who performed the work and the LOFT Project Office of DOE, which is responsible for the day-to-day management of the project.

B. Fire Protection Tests on Corner Effects (Sandia) -

A series of tests were conducted to test the effect of the presence of walls and ceilings. The results of these tests showed that the presence of walls and ceilings has an adverse effect, i.e., the closer to the walls and ceilings, the faster a fire will propagate.

IV. Analytical Tool Development, Assessment and Application

A. Model Developments (ANL, RPI, NWU, Lehigh, MIT) -

(i) A basic framework for a two-fluid model for flow in a bundle was developed at ANL and incorporated in COBRA.

(ii) Phase separation and distribution data were obtained from "Y", "Tee" and 2D channel geometries at RPI.

(iii) Steam condensation in parallel streams was tested at NWU, and data were sent to LASL for use in K-FIT code.

(iv) Non-equilibrium superheat data were directly measured at Lehigh for validating the existing correlation

(v) Two-phase flow patterns in natural circulation (chimney effect) in a model of slab core were tested at MIT to support 2D/3D program.

B. Thermal-Hydraulic System Codes Released to Public (LASL and INEL) -

(i) TRAC-PIA by LASL - Advanced, detailed, best-estimate analysis of PWR LOCA and other transient/accidents.

(ii) BEACON-MOD 2A by INEL - Best-estimate analysis of inter-compartment loads in PWR containment, during LOCA.

(iii) K-FIX by LASL - PWR core barrel loads and stresses during LOCA.

C. LOCA Codes Completed for Checkout (INEL and PNL) -

(i) RELAP-4/MOD 7-User-convenient code for simplified best-estimate analyses of PWR LOCA and BWR blowdown.

(ii) COBRA-TRAC Link - This link is developed at PNL for evaluating LOCA in a PWR with upper heat injection.

D. Non-NRC Codes Acquired and Installed at BNL -

(i) RAMONA-III - This code was acquired from Norway for calculating BWR transient. This code has 3-D neutron kinetics.

(ii) RETRAN - This code was acquired from EPRI for calculating PWR transients.

E. Fuel Codes Released to Public -

(i) FRAPCON-1 - Steady-state fuel-rod code from INEL and PNL.

(ii) FRAP-T4 - Transient fuel-rod code from INEL.

F. FRAP-T5 - Transient fuel-rod code completed and being assessed at INEL.

V. Accident Consequence Evaluation and Mitigation

A. RIA Tests on Irradiated Fuel at PBF (INEL) -

PBF tests simulating reactivity insertion accidents identified two new fuel mechanisms: In fuel rods preirradiated to 5GWD/T, rapid power increases showed pellet/cladding interaction (PCI) type behavior which could lead to fission product release after rapid energy deposition of 130-170 cal/gm radial average rod enthalpy; and fuel swelling behavior which could lead to post-accident coolant channel blockage at about 270-310 cal/gm radial average rod enthalpy.

B. LOCA Test on Irradiated Fuel at PBF (INEL) -

A nuclear heated LOCA blowdown test (LOC-3) of pressurized fresh and pre-irradiated fuel rods (15 GWD/T) gave peak circumferential expansion range from 20% to 45% (still coolable) for indicated PCTs of 1700-1790°F.

C. Fission Product Release From LWR Fuel (ORNL) -

Fission product release was measured from fuel rod segments with high burnup inductively heated to between 1200°C and 1600°C in a flowing steam environment. The results indicate that above 1350°C, cesium and iodine release increases rapidly.

D. Steam Explosion Test Results (SANDIA) -

In a series of 48 steam explosion experiments at SANDIA where from 1 to 27 Kg of oxidic melts were poured into an open tank of water, the maximum observed thremal-to-mechanical energy conversion efficiency was less than 1.5%, while the maximum theoretical energy conversion efficiency is 30%.

E. Molten Fuel/Concrete Interaction Measurement and Code Corporation (SANDIA) -

To measure the interaction between molten fuel and concrete, a new technique was developed by analyzing the elemental composition of the released aerosols using spark mass spectroscopy. The accumulated interaction data were incorporated in the CORCON code.

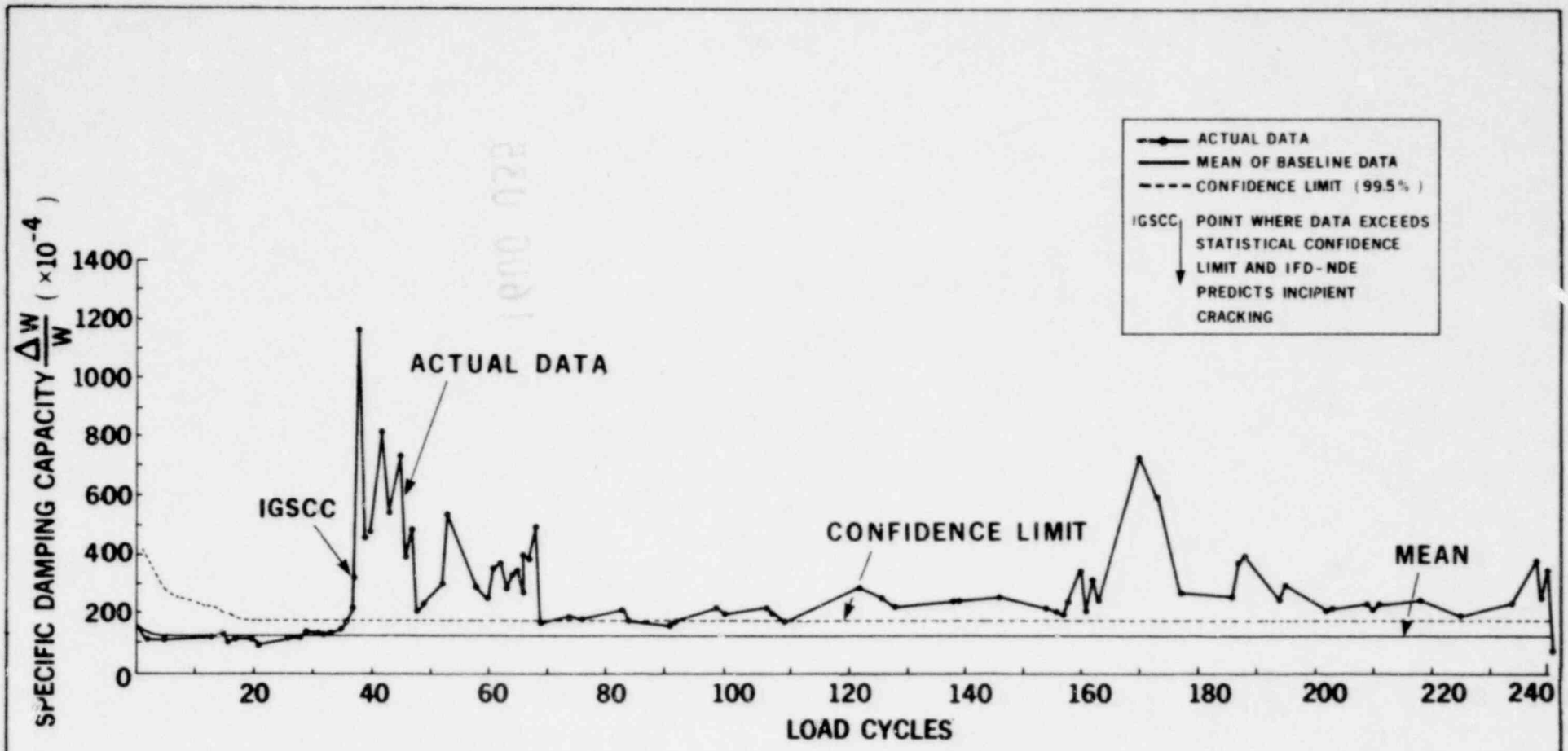

1600 036

SPECIFIC DAMPING CAPACITY VERSUS LOAD CYCLES FOR IGSCC PIPE #2

STATUS IN THE UNDERSTANDING OF TMI

W. V. JOHNSTON
NRC/SIG

INTRODUCTION

As many of you are aware, there are a number of major investigations of the Three Mile Island accident underway. These include the Office of Inspection and Enforcement of the NRC, EPRI, the President's Commission, both houses of Congress, and the Independent Investigation by the NRC.

Both the Nuclear Safety Analysis Center of EPRI and NRC Inspection and Enforcement have published reports containing considerable detail on the sequence of events and radiological aspects, operator actions and the operation, good and bad, of many of the components of the plant. These reports are available as NSAC 1 & 2 and NUREG-0600, respectively. The President's Commission and the NRC are taking a broader look, which include assessment of the utility, and NRC responses to the accident, NRC prior licensing and enforcement practices, and emergency preparedness. Neither group has issued its report as of this writing, however, the President's Commission is due to report very shortly, and if available will be added to this presentation. The Commission sponsored Investigation is not due to report until the end of the year.

The NRC independent investigation, of which I am a part, was organized last May and is being conducted under a contract between the Commission and the law firm of Rogaven, Stern, and Huge. The personnel for the Special Investigation Group consist of lawyers, paralegals, and special consultants retained by the law firm and about 45 NRC staff on special detail to this investigation. We are organized into seven task forces which cover the above mentioned areas. Each task force is monitored by a peer review group which include persons for and against nuclear energy.

As the Task Leader of the group studying the physical aspects of the accident, I am leading an effort to determine and assess the actions of the plant and operating personnel from the time shortly before the beginning of the accident, on March 27, 1979, through to the disapperances of the bubble on April 2, 1979. We are also concerned with the design of the control room and the consequences of alternative courses of action by the operators. Because the Special Investigation Group has not completed its study and prepared its recommendations, I am not at liberty to draw conclusions during this talk. I will, however, present some of the information and facts which we have developed. Of most interest to this technical audience is probably the sequence of events and its implication to core damage and the release of radioactivity.

There are very few differences between the sequence of events which have been developed by the NSAC, I&E, and ourselves. Similar information has been available to all the investigators in the form of reactimeter plots, strip charts, alarm and utility computer printouts and log books, and interviews. In our sequence of events there will be a column listing what information was available to the operators in real time so that a more objective evaluation of their responses and data needs can be made. A simplified chronology of the accident is shown in Table 1. This may be used in conjunction with the pressure and pressurizer level changes in Figure 1.

ACCIDENT NARRATIVE

Initial Period

The accident was initiated by a trip of the main feedwater pumps for the steam generators, probably the result of actions to clear a blockage of resins in the demineralizer tank. The turbine tripped almost simultaneously. The reactor continued to operate in accordance with the protection system design, system temperature, and pressure increase. The electromagnetic operated valve (EMOV) opened at 2255 psi, and the pressure rise continued until at 8 seconds the reactor tripped when the high system pressure trip setpoint was reached at 2355 psi. Reactor trip is normally followed by a pressure and temperature drop resulting in a coolant contraction and a drop of pressurizer level. The operators followed the normal procedures to counteract this drop of pressurizer level by closing off the letdown flow and turning on an additional makeup pump. At approximately 1 minute after the start of the accident, the pressurizer levels stopped decreasing and began to rise. Unknown to the operators, the EMOV did not close when its closure setpoint was reached. This failure was not realized by the plant operators for more than 2 hours. The pressurizer level continued to rise until it went off the scale at about 6 minutes. To slow the level and to avoid this "going solid," operator actions include increasing letdown flow to the maximum extent possible, and throttling the high pressure injection which automatically initiated at 1600 psi at 2 minutes. At this time the RCS temperature was increasing. This increase would also contribute to a mild pressure increase since saturation conditions now existed in the loops. The pressure rise was short lived, however, and the pressure resumed its drop reaching about 100 psi by 20 minutes. The emergency feedwater pumps had come on, as programmed, but flow to the steam generators had not begun when the secondary side water level had dropped to 30 inches at about 30 seconds because the block valves on the emergency feedwater headers were closed. This condition was discovered at about 8 minutes by an operator from Unit 1, who had been called over. Upon opening the block valves, a rapid cooldown of the reactor coolant system (RCS) and corresponding RCS pressure decrease occurred.

At about 14 minutes, the rupture disc burst on the reactor coolant drain tank discharging water and steam into the reactor building. The temperature, pressure, and level alarms on this tank went unnoticed by the operators, because of the multiplicity of alarms actuated at that time and their location in a back panel out of sight of the operators.

Reactor Coolant Pumps Secured

Reactor coolant inventory loss continued with the RCS under saturation conditions. As the fraction of the ACRS volume which was vapor increased, the reactor coolant pumps (RCP) began to vibrate. The B loop pumps were shut off at 73 minutes, and the A loop pumps were secured at 101 minutes with the expection that natural circulation would occur. It has been estimated that nearly two-thirds of the reactor coolant had been lost, and that when the pumps were shut off the coolant level equalized to about a foot above the top of the core. Up to this time, the core has not been damaged, and the accident could still have been averted by the closing of the block valve to the EMOV and increasing the high pressure injection flow.

Temperature Transient

The temperature transient, which damaged the fuel, now began with the boildown of the coolant. The decay heat had reduced to about 1% of full power, but was sufficient to cause the coolant level to drop at a rate of 1 foot every 4-5 minutes. The pressure also continued to drop, reaching a low point of 660 psi at 2 hours and 19 minutes, when the leaking EMOV was diagnosed and the protective block valve closed.

At approximately 2-1/2 hours into the accident, substantial fractions of the core were uncovered and had experienced sustained high temperatures. This condition would be expected to result in fuel damage, substantial releases of core fission products, and hydrogen generation. The magnitude of these conditions were not recognized by the TMI staff. At about this time, the radiation alarms in various parts of the reactor containment building (RB) began to show rapidly increasing radiation levels and a site emergency was declared at 2 hours and 55 minutes. Following the declaration of the site emergency and then general emergency, the operating staff recognized that fuel damage had occurred and presumed that the radiation was due to gap release from perforated cladding, but did not really consider that the core had been uncovered to the extent that much hydrogen had been produced. It was fully recognized that there was superheated steam in the hot legs, that natural circulation was not working, and that their objective was to condense the steam so that a pump could be started.

Attempt to Collapse the Voids

Unsuccessful efforts to collapse the voids continued for approximately 4-1/2 hours at a pressure between 1200 and 2000 psi. During this period, two attempts were made to run a reactor coolant pump, but the effort had to be abandoned after a short time because no fluid was being moved.

During the final portions of this period (6-7-1/2 hours after the start of the accident) a feed and bleed procedure was being utilized with venting of the pressurizer via the block valve. Although rewetting of the hot legs was not successful, it probably inadvertently facilitated the removal of noncondensibles including hydrogen and xenon from the system. In a change of strategy, the decision was made to reduce system pressure and float the core flood tanks on the reactor coolant system as an assurance of core coverage. This depressurization was accomplished in approximately 1 hour using the EMOV and was held for another 5 hours.

Containment Pressure Spike

The extended period of low pressure appears to have facilitated further release of hydrogen from the RCS to the reactor building. Some of this gas ignited at about 10 hours and produced a 28 psi pressure spike in the reactor building initiating containment spray. Although the pressure spike was interpreted by the operators later on as a combustion, it apparently was not attributed to hydrogen until two days later. It is possible that the release of this noncondensible gas from the RCS contributed to the later apparent success in collapsing the voids in the A loop.

Repressurization

Beginning at about 10-1/2 hours, the operators received permission to attempt to form a bubble in the pressurizer using the pressurizer heater. This was accomplished successfully, and for the first time in many hours the A loop hot and cold leg temperatures come on scale and indicated possible natural circulation. The operator has reported that a large amount of water (as much as 20,000 gallons) was added, at this time, to regain pressurizer level. Following some additional venting the pressurizer was again heated. Evidence of a favorable response in the A loop was again developing when the order to repressurize the system to above 2200 psi to collapse the bubbles was given. Following repressurization (during which an additional 30,000 gallons were removed from the borated water storage tank) a reactor coolant pump was successfully started, the loop temperatures dropped to saturation, the system pressure dropped rapidly, and stable heat transfer conditions were obtained at 1000 psi.

The Hydrogen Bubble

There still remained a noncondensible bubble in the system, which until removed threatened to enlarge and once again interrupt heat removal if the pressure were lowered to allow operation of the residual heat removal system. The noncondensible bubble was gradually removed from the RCS, over the next 4 days, by spraying into the pressurizer and venting the gas release to the reactor building and via the letdown line to the makeup tank where the gas was vented to the waste gas compressor. In spite of rising concern at the time, later evaluations of the data taken have shown that the bubble volume was always decreasing. Final agreement has not been reached on the composition of the bubble (was it only hydrogen) and whether radiolytic oxygen could have been produced.

Core Damage

As to the time and extent of core damage, there is substantial agreement that the temperature transient, beginning after the reactor coolant pumps were tripped, caused the initial fission product release and metal water reaction resulting in a very brittle upper half of the core. Furthermore, there are strong indications that thermal shocks or some other event at about 3 hours and 45 minutes caused a substantial change of geometry of the core, possibly forming what has been called a rubble bed in the upper portions of the core. There remains some uncertainty of the highest temperatures reached during this period and whether or not there was some additional periods of core uncovery during the first 12 hours.

FIGURE 1

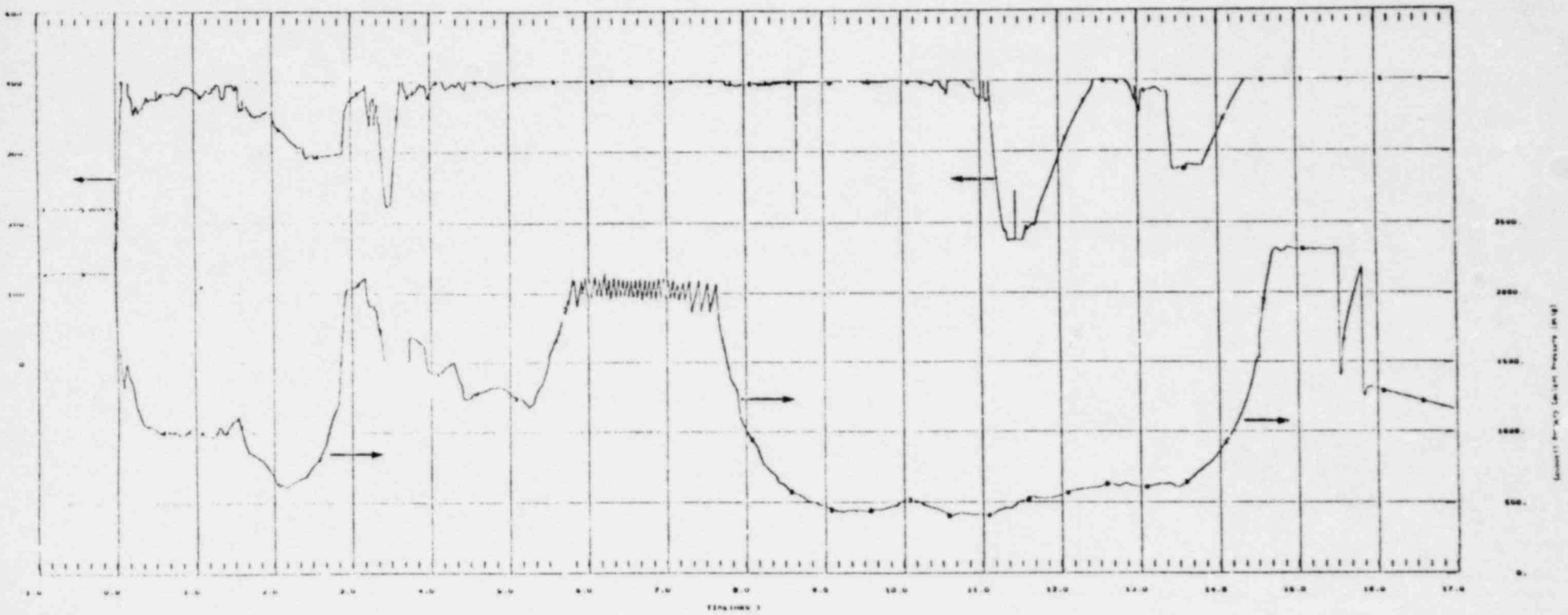

Figure TH6 Composite Primary Coolant Pressure and Pressurizer Level

TABLE 1
SIMPLIFIED TMI-2 CHRONOLOGY

TIME	EVENT
About 4 a.m. (t=0)	Loss of condensate pump; loss of feedwater; turbine trip
t=3-6 sec.	Electromatic relief valve opens (2255 psi) to relieve pressure in RCS (reactor cooling system)
t=[illegible]sec.	Reactor trip on high RCS pressure (2355 psi)
t=13 sec.	RCS pressure decays to 2205 psi (relief valve should have closed)
t=15 sec.	RCS hot leg temperature peaks at 611°F, 2147 psi (450 psi over saturation) Pressurizer peaks, then begins to drop.
t=30 sec.	All three auxiliary feedwater pumps running at pressure (pumps 2A and 2B started at turbine trip); no flow was injected since discharge valves were closed
t=1 min.	Pressurizer level indication begins to rise rapidly
t=1 min	Steam Generators 'A' and 'B' secondary level very low - drying out over next couple of minutes
t=2 min.	ECCS initiation (high-pressure injection) at 1600 psi
t=6 min.	Pressurizer level off scale (high); one HPI pump manually tripped at about 4 min 30 sec. Second pump tripped at~10 min. 30 sec.
t=6 min.	RCS flashes as pressure bottoms out at 1350 psig (hot-leg temperature of 584°F) RCDT pressure rise.
t=7 min., 30 sec.	Reactor building sump pump comes on
t=8 min.	Auxiliary feedwater flow is initiated by opening closed valves.
t=8 min., 18 sec.	Steam Generator 'B' pressure reaches minimum
t=8 min., 21 sec.	Steam Generator 'A' pressure starts to recover
t=10 min.	Pressurizer level indication comes back on scale and decreases
t=11-12 min.	Makeup pump (ECCS HPI flow) restarted by operators
t=15 min.	RC drain/quench tank rupture disk blows at 190 psig (setpoint 200 psig) due to continued discharge of electromatic relief valve
t=16-60 min.	System parameters stabilized in saturated condition at about 1015 psig and about 550°F
t=1 hr.	Steaming to atmospheric dump
t=1 hr. 13 min.	Operator trips RS pumps in Loop 'B'
t=1 hr., 41 min.	Operator trips RS pumps in Loop 'A'
t=1 3/4 - 2 hrs.	Core begins heatup transient -Hot-leg temperature begins to rise to 620° F (off scale within 14 minutes) and cold-leg temperature drops.
t=2.3 hrs.	Eletromatic relief valve isolated by operator after Steam Generator 'B' is isolated to prevent leakage
t=3.0 hrs.	Start Reactor coolant pump - no blow
t=3.2 hrs.	RCS pressure increases to 2150 psi and electromatic relief valve is opened.
t=3.3 hrs.	ECS actuation, Pressurizer level drops, hot leg temp. decrease possible core geometry change
t=3.9 hrs.	ECS actuation
t=5 hrs.	Peak containment pressure of 4.5 psig (EMOV venting)
t=5-6 hrs.	RCS pressure increases from 1250 psi to 2100 psi
t=6-7.5 hrs.	
t=7.5 hrs.	Operator opens electromatic relief valve to depressurize RCS to attempt initiation of RHR (residual heat removal) at 400 psi
t=8-9 hrs.	RCS pressure decreases to about 500 psi; core flood tanks partially discharge.
t=9-13	Atmospheric dump closed on orders
t=10 hrs.	28 psig containment pressure spike; containment sprays initiated and stopped after 500 gal. of NaOH injected (about 2 minutes of operation
t=13 hrs.	Condenser back in operation
t=13.5 hrs.	Electronic relief valve closed to repressurize RCS, collapse voids, and start RC pump
t=13.14.8 hrs.	RCS pressure increased from 650 psi to 2300 psi
t=15.6	Bump RCP
t=15.9 hrs.	RC pump in Loop 'A' started, hot-leg temperature decreases to 560°F, and cold-leg temperature increases to 400°F, indicating flow through steam generator.
Thereafter	Steam Generator 'A' steaming to condenser; condenser vacuum re-established; RCS cooled at about 280°F, 1000 psi renoving H via letdown and vent.
Now (4/4)	High radiation in containment; all core thermocouples less than 460° F; using pressurizer vent valve with small makeup flow; slow cooldown; reactor building pressure negative, no bubble.

RADIOLOGICAL ASPECTS OF THE TMI ACCIDENT

A discussion of the radiological aspects of the TMI accident including:

- release pathways (gaseous and liquid);
- source terms for radioactive materials released; and
- off-site population dose assessments.

Release of Liquids

The only significant release of radioactive liquid occurred through the industrial waste treatment system (IWTS). This system does not normally process radioactive fluids, and there are no installed radiation monitors. The effluent from the system, after dilution, is sampled continually prior to discharge into the Susquehanna River.

Sampling the steam generators after the accident resulted in radioactive liquid being flushed to the contaminated drains tank in the control and service building (as designed). This tank overflowed to the sump in the control and service building, which pumps to the IWTS. The other source of liquid radioactive materials is the turbine sump, with a primary-to-secondary leak in steam generators.

Through midnight on Friday, March 30, 265,000 gallons were released via the IWTS from the time of initiation of the accident. It is estimated that approximately 73 millicuries of I-131 were released through this pathway.

Release of Gases

All releases of gaseous radioactive material from TMI appear to be through the vent stack. The gaseous effluents from the auxiliary and fuel handling buildings, and the releases from the waste gas system all are released through the stack.

Radioactive material entered the auxiliary and fuel handling building air filtration systems via direct gaseous leakage to these buildings, and via offgases from radioactive liquid on the floor of the various levels of the auxiliary building.

Radioactive liquid appeared in the auxiliary building via (1) overflow of auxiliary building sump when it was pumped from the reactor building sump; (2) leaks in the letdown line (makeup and purification system); and (3) leakage from the river water pumps. This added the bulk of the nonradioactive liquid.

Although the presence of radioactive liquid throughout the auxiliary building compounded the contamination problem, the majority of the gaseous activity resulted from leaking gaseous components. The auxiliary building sump tank rupture disc had failed prior to March 28, and gases would be directly released to the building. The Waste Gas Compressor B leaked. The makeup tank removed gases from the letdown (primary coolant) and is vented to the vent header (which leaks) and then to the Waste Gas System (including the compressors). Due to the degassing of the primary coolant, the makeup tank was vented a number of times, resulting in high activity inside the auxiliary building.

The auxiliary and fuel handling building filtration systems prevented the bulk of the radioiodine from escaping. These units contained HEPA filters for particulate removal. Testing of the carbon inplace at the time of the accident showed removal efficiencies of 50 to 70 percent, but carbon installed in mid-April to replace the carbon used during the accident is 80 to 96 percent efficient, even after three months continual operation.

A 4-train supplementary air filtration system was installed on the roof of the auxiliary building to remove additional radioiodines. The stack was capped in late May, thus all ventilation and processed gas from the auxiliary and fuel handling buildings is directed through this filter. These carbon filters, after 60 to 90 days continuation operation, were still 87 to 97 percent efficient in removing radioiodine.

Gaseous radioactive material was released to the environment during the course of the accident. The licensee has calculated 1.0×10^6 curies noble gas (Xe-133) released. The NRC has estimated 1.3×10^6 curies of Xenon -133 released. Radioiodine releases have been estimated to be approximately 15 curies.

Off-Site Population Dose Assessments

Several analyses have been or are being conducted of the off-site population dose as a result of the TMI-2 accident. The initial analyses based upon the TLD's that were in place around the site at the time of the accident and the subsequent NRC dosimeters was performed by the Ad-Hoc Population Dose Assessment Group. The most likely population dose was determined to be 3300 person-rem. The DOE (BNL) also estimated the collective population dose using the data obtained from aerial plume surveys. Their estimate was 2200 person-rem; however, a calibration check of their instrument showed that they were probably high in their estimate by a factor of 3 to 10.* A review conducted for the AIF by Roessler et al did not reassess the population dose estimate but agreed with

*Instruments overresponded by this factor Xe-133. Again, the gas mixture is important.

the health impact assessment of the Ad-Hoc Group, on their population dose. Woodard of Pickard, Lowe and Garrick estimated the population dose to be 3500 person-rem based on the meteorological dispersion models.

Independent analyses of the collective population dose have been performed by the Health Physics and Dosimetry Task Group of the President's Commission. Their analysis will be reported if available.

EPRI is also performing two population dose assessments using the services of an outside contractor organization. EPRI results will also be reported if available.

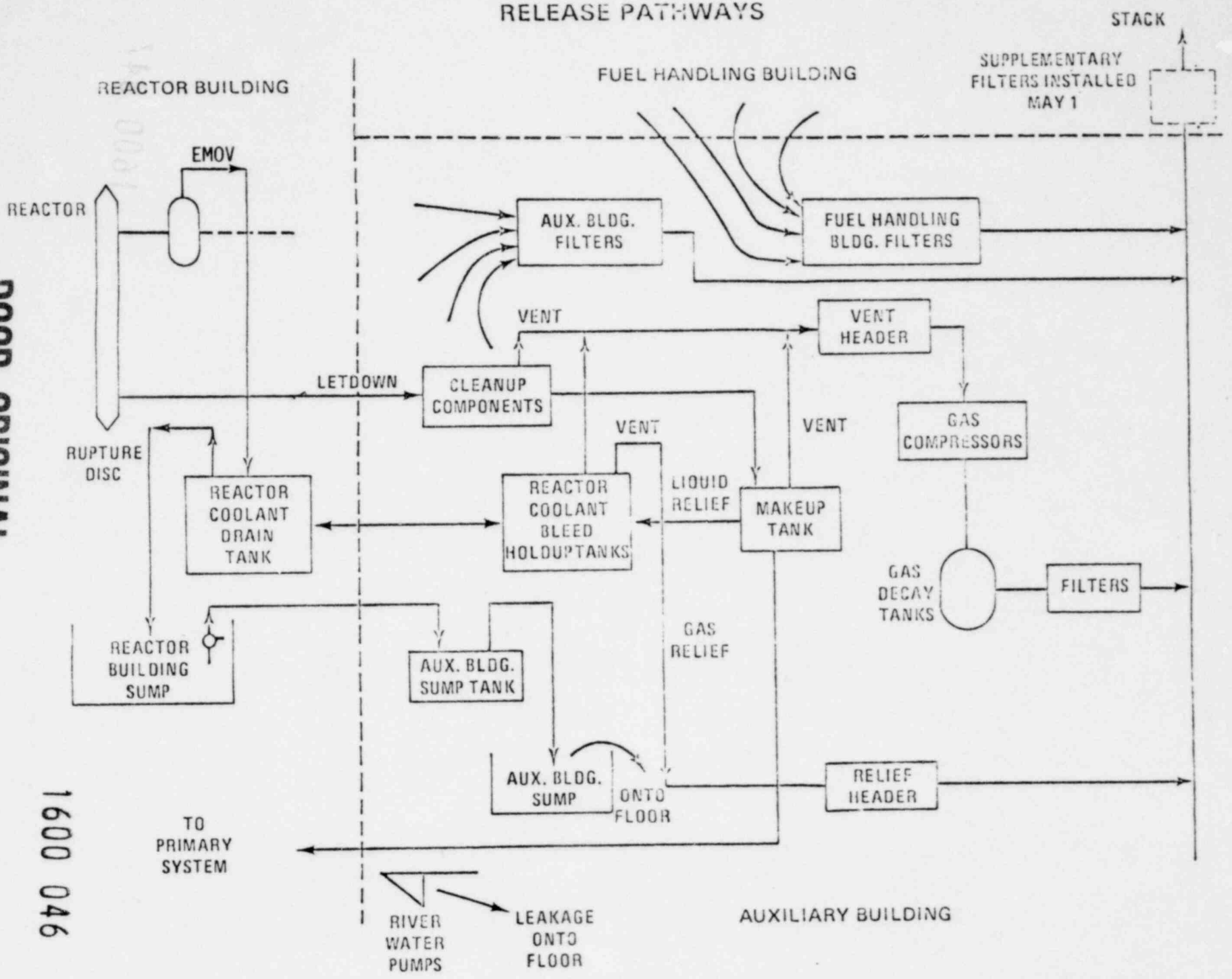

...CHARGES TO THE INDUSTRIAL WASTE TREATMENT SYSTEM

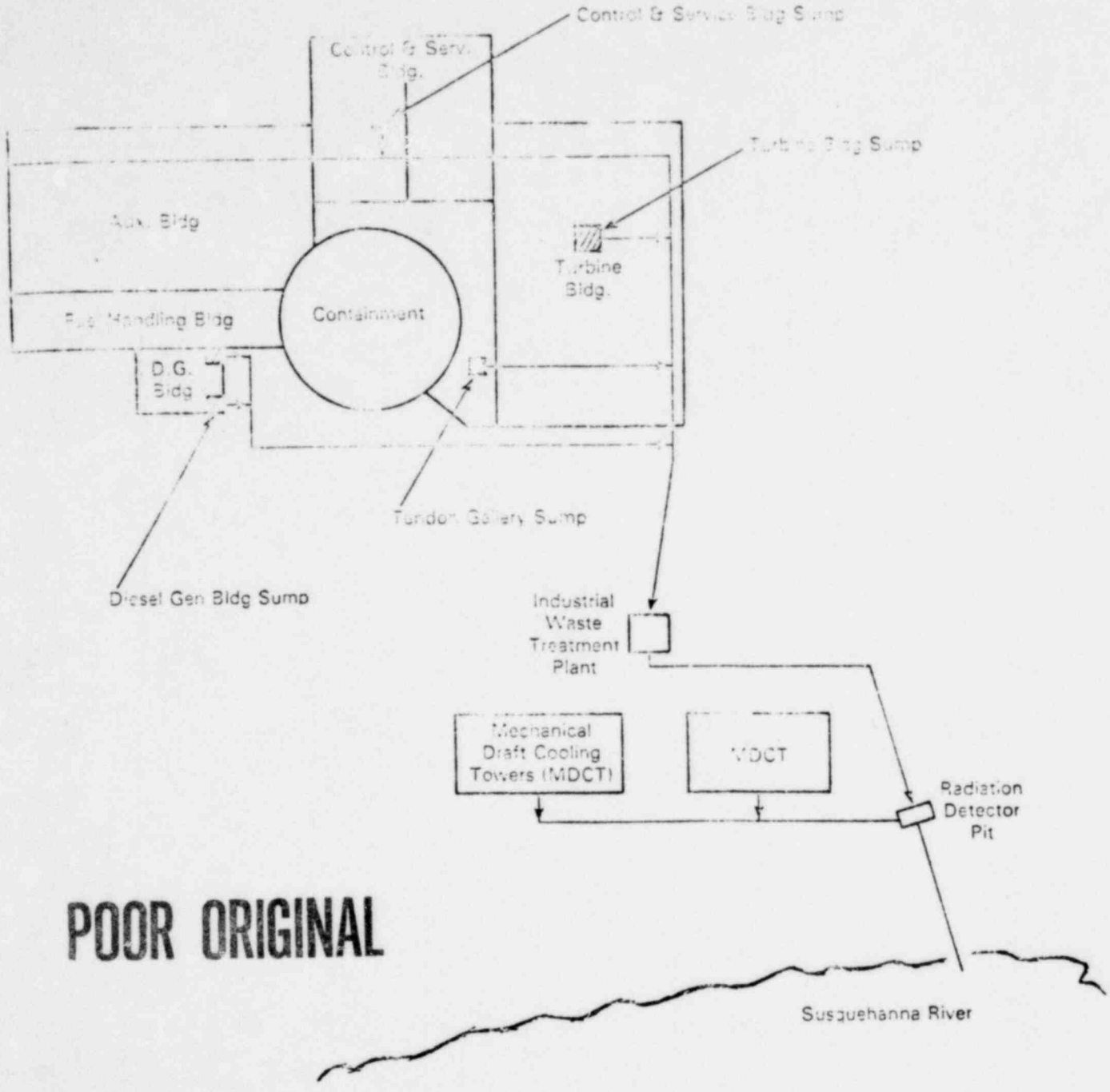

POOR ORIGINAL

1600 047

FIGURE II-3-1

SOURCE: NUREG 0600

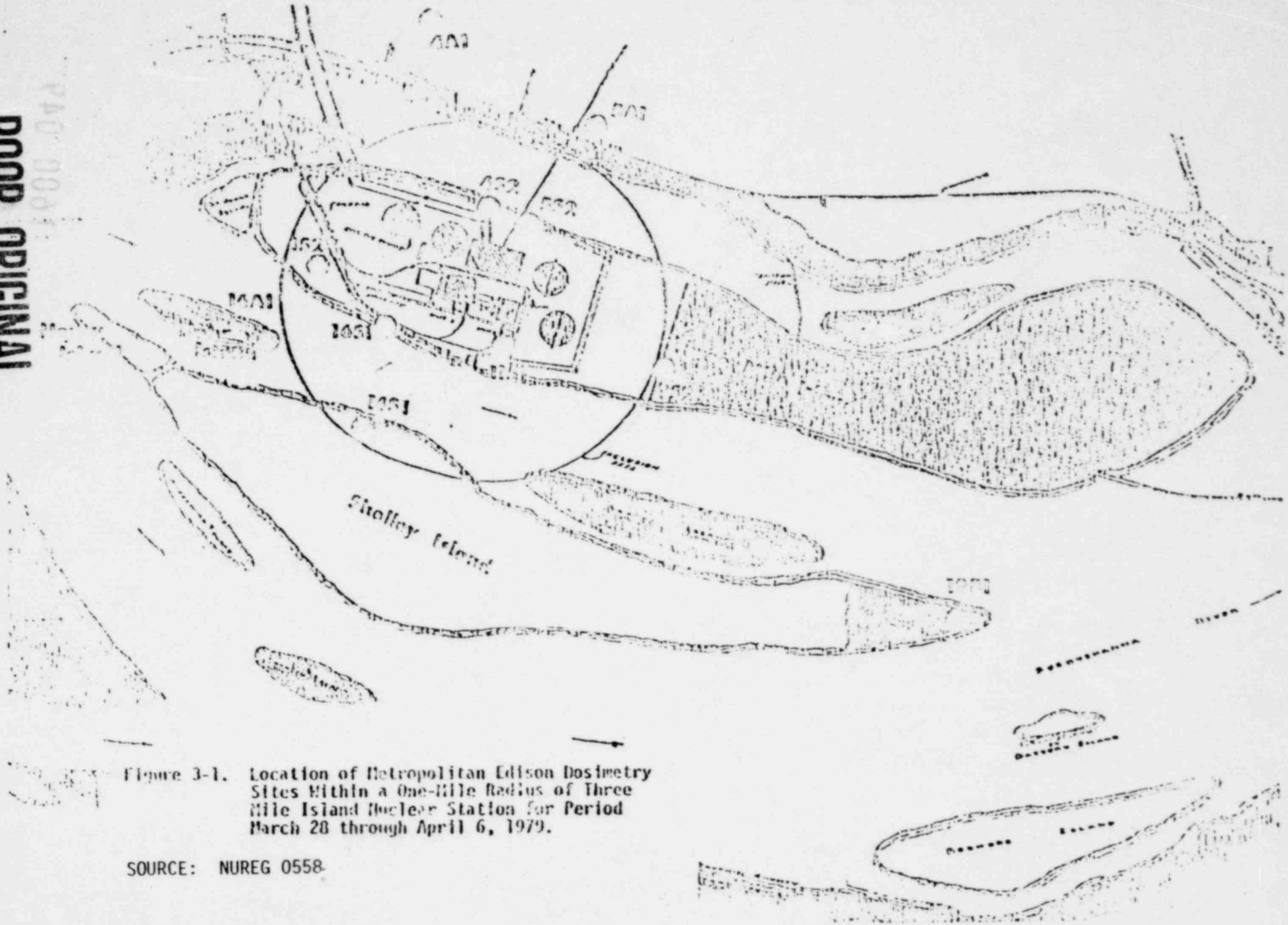

Figure 3-1. Location of Metropolitan Edison Dosimetry Sites Within a One-Mile Radius of Three Mile Island Nuclear Station for Period March 28 through April 6, 1979.

SOURCE: NUREG 0558

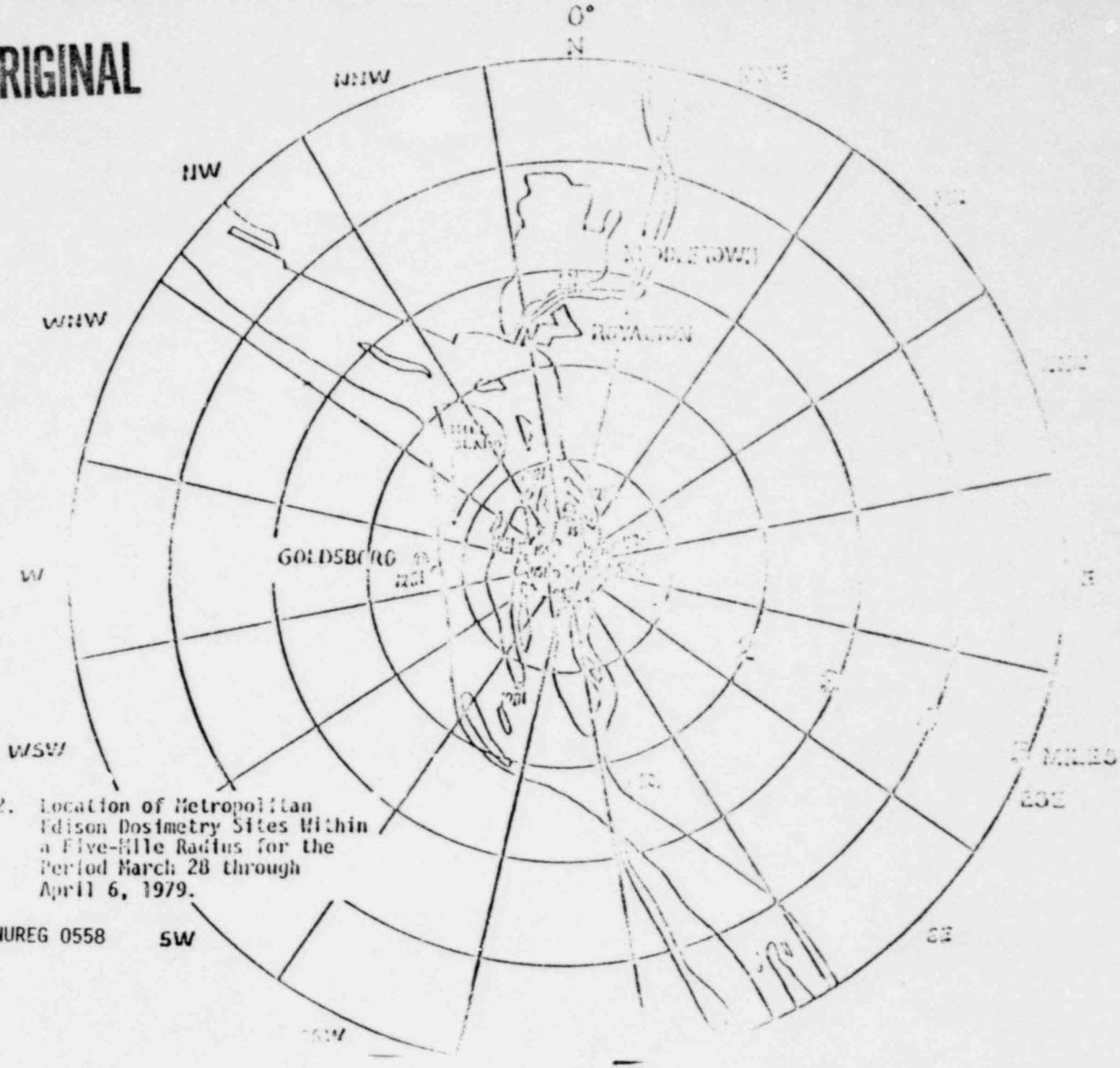

Figure 3-2. Location of Metropolitan Edison Dosimetry Sites Within a Five-Mile Radius for the Period March 28 through April 6, 1979.

SOURCE: NUREG 0558

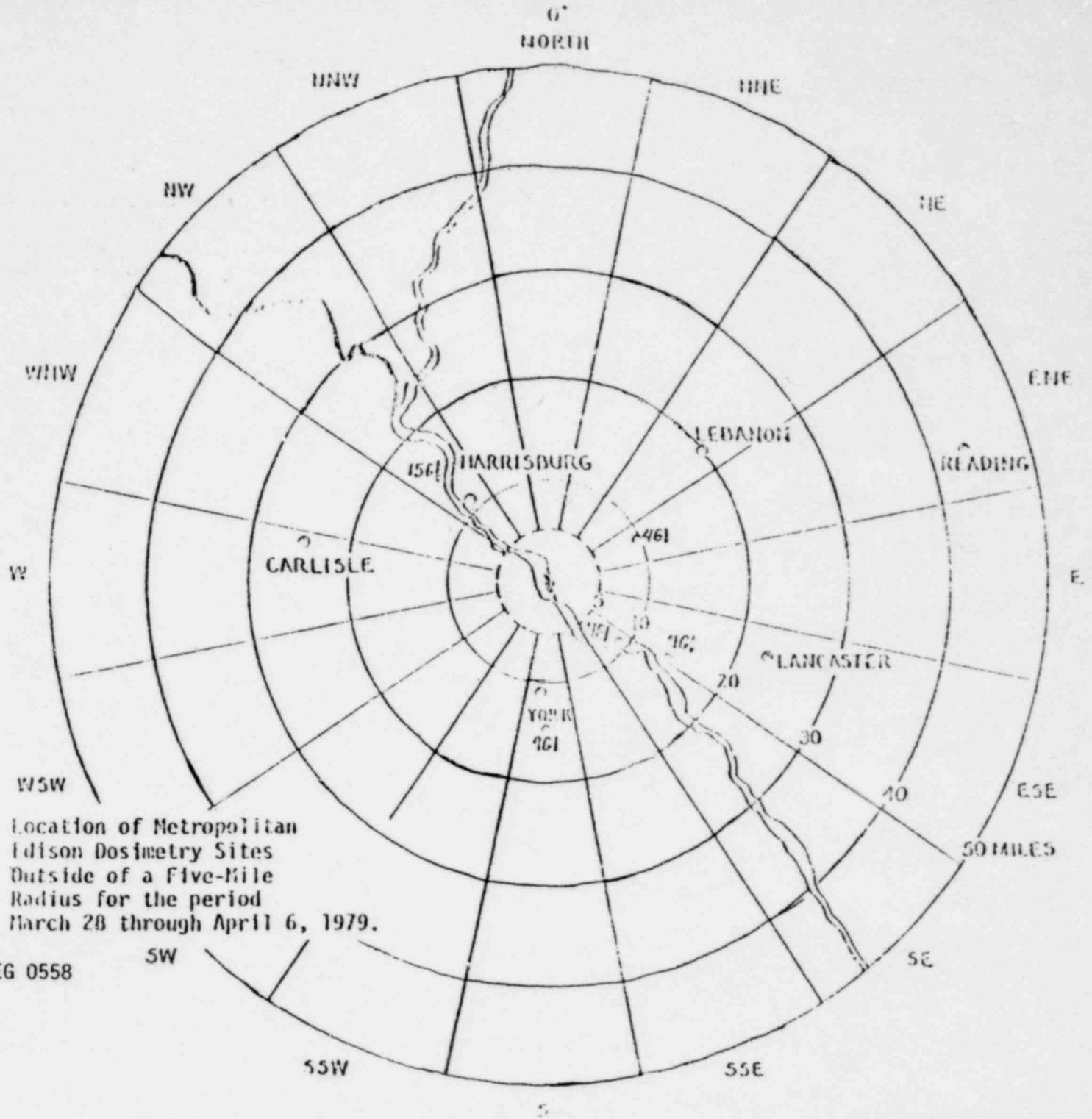

Figure 3-3. Location of Metropolitan Edison Dosimetry Sites Outside of a Five-Mile Radius for the period March 28 through April 6, 1979.

SOURCE: NUREG 0558

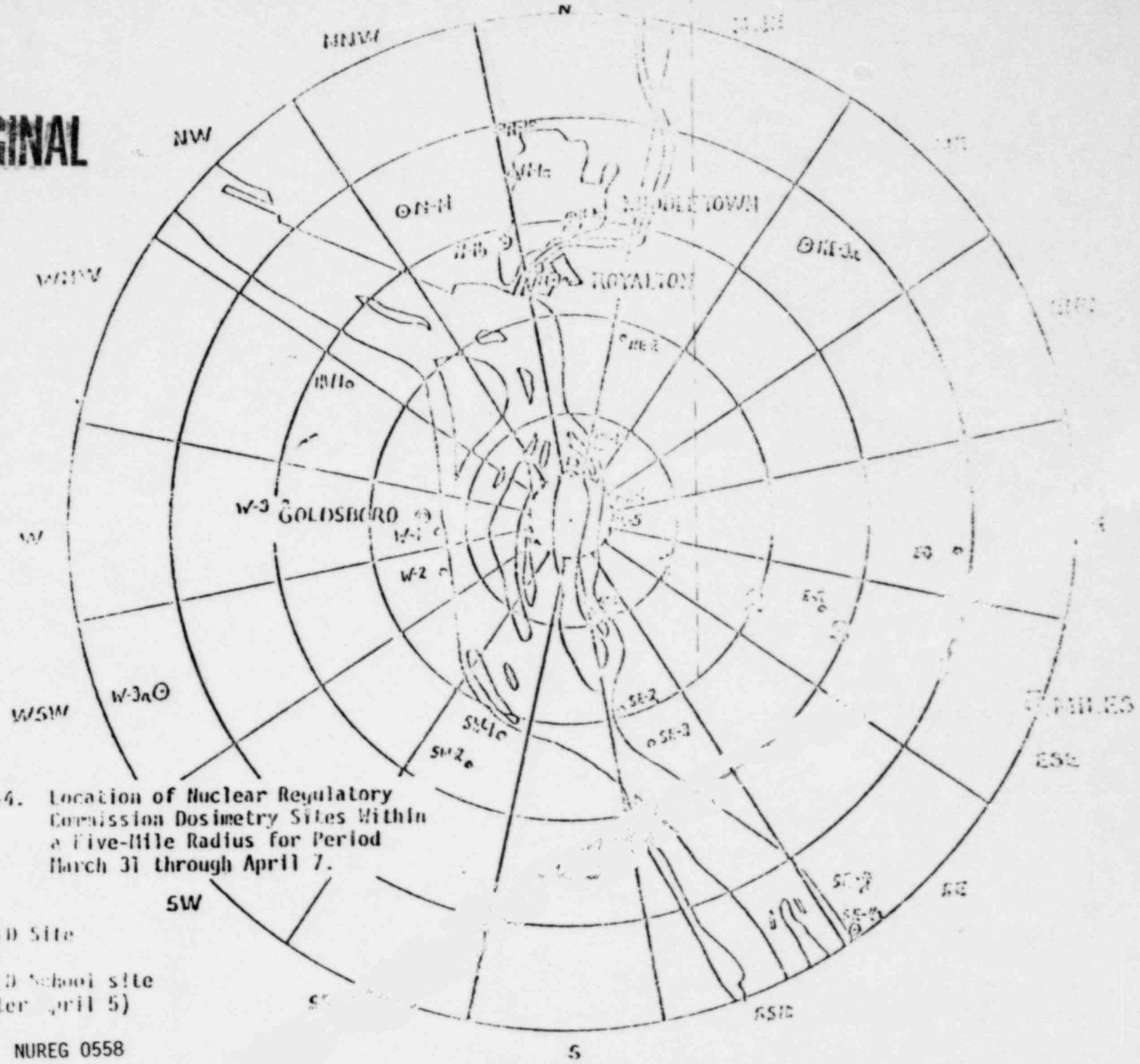

Figure 3-4. Location of Nuclear Regulatory Commission Dosimetry Sites Within a Five-Mile Radius for Period March 31 through April 7.

PEC TLD Site

PEC TLD School site (After April 5)

SOURCE: NUREG 0558

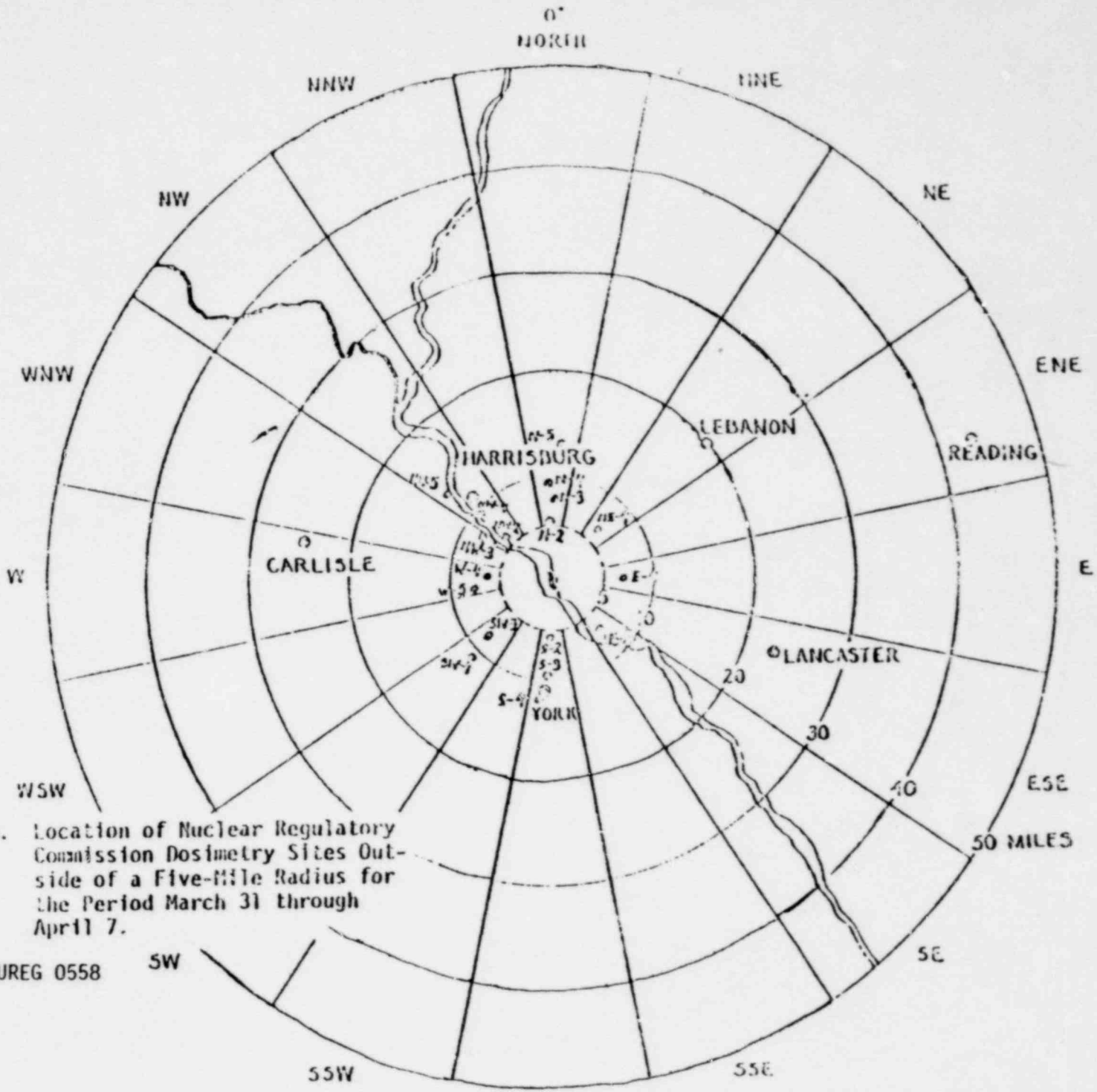

Figure 3-5. Location of Nuclear Regulatory Commission Dosimetry Sites Outside of a Five-Mile Radius for the Period March 31 through April 7.

SOURCE: NUREG 0558

November 5, 1979 Morning Session, Red Auditorium

A. Overview of the LOFT Program

B. Planning for Small Breaks and other Future Tests

By G. D. McPherson, LOFT Program Manager

A

I would like to introduce this overview of the LOFT Program with a reminder of the program objectives.

The primary objective of the program is to provide experimental data from a nuclear reactor scaled to simulate a PWR, for the purpose of developing and assessing LOCA and transient codes.

To achieve this objective LOFT was designed to conserve one central concept: for the PWR accident being simulated the sequence and duration of thermal-hydraulic phenomena should be replicated. This was accomplished by matching fairly closely:

the power/coolant volume ratio,
relative volumes of the primary coolant system components,
power density,
pressures and temperatures.

As a result, flow velocities, flow regimes, system depressurization and heat transfer regimes which occur in LOFT during the course of a simulated accident are approximately the same as those in the PWR. Indeed the thermal-hydraulic codes being assessed for LOCAs and transients do predict this to be the case. It follows that the accuracy with which these codes predict LOFT behavior is, in general, a good indication of the accuracy with which they predict the commercial PWR behavior.

Of importance, therefore is the agreement between the data and the predictions, and this will be addressed in the succeeding presentation.

The secondary objective of the LOFT program is to determine if there exist any significant, unexpected phenomena associated with any stage of a LOCA or transient. While no new phenomena have been identified, it is fair to say that the magnitude and importance of certain phenomena were not predicted accurately, and that the LOFT data have served to point up predictive inadequacies and to improve predictive capabilities. To some extent I believe this situation arose because best-estimate codes were developed from conservative evaluation model codes and consequently preserve some elements of their conversativism. In any event, the following presentation will also focus on phenomena which were not predicted well and our current understanding of these phenomena.

In addition to the first two nuclear large break simulations carried out this past year, the LOFT program has accomplished a first in the field of instrument calibration: a full-size LOFT pipe flow-instrument spool piece has been calibrated in actual blowdown conditions in a test facility replicating the LOFT vessel and piping geometry. The results of these tests, performed at the Wyle Laboratories, in Norco California, under the direction of EG&G personnel will be described briefly later in this session. Together with the full-sized steady-state two-phase flow calibration to be done during the coming year, this will provide a more solid foundation on which to quantify the accuracy of the LOFT data.

In other years I would normally proceed to list the accomplishments expected in the upcoming year; but this year is different. For, while the program in place, up until March 28 of this year, showed a continuation of the large break power ascension series through 1980, the Three Mile Island accident altered this plan and we have brought forward the small break series. In fact the small break tests have already been initiated in LOFT.

However, before we proceed with that part of the story, let us first hear the results of the large break tests and I will return later to report on the small break program. To present the L2-2 and L2-3 results I will first call on Dr. John Linebarger who works in the LOFT Experimental Program Division of EG&G.

In my introduction, I referred to a rearrangement in our test plan so as to bring forward the small break tests. In fact the first small break was done in LOFT on May 31, 1979. This was a zero-powered test initiated at full temperature and pressure, and it involved a depressurization from the pressurizer relief valve. The data from this test has assisted in the planning of the small breaks shown in the revised test sequence in Figure 1.

The small break, L3, series covers the cases of cold leg break flows greater than, equal to, and less than the high pressure safety injection flow, a stuck-open pressurizer relief valve and, in L3-5 and L3-6, it addresses the problem of when the primary coolant pumps should be shut down during a suggested small break accident. The procedures leading into L3-1 have already begun, and we expect this test to be done 9 days from now.

Figure 1 also shows three operational transient tests (the L6 series) to be done this year. Following the last of these, at the end of 1980, we plan to return to the large break series and do the L2-5 test, which is a repeat of the L2-3 test, but assumes a loss of offsite power. Consequently, the core is not predicted to quench during the blowdown as it did in the L2-3 test.

Judging by experience, it could be meaningless to describe our test program any further into the future. It is sufficient to say that we have retained all the elements, including alternate ECC injection, hot leg breaks and steam generator tube ruptures. As the results from this year's testing become available we will decide the details of the future program. Meanwhile I believe we have an ambitious program for the coming year which will provide a very interesting report at next year's meeting.

TABLE 1 LOFT FY 80 TEST SEQUENCE AND TARGET DATES

TEST	TARGET DATE*	POWER LEVEL (MW)	COMMENTS
L3-1	11-14-79	50	SMALL BREAK COLD LEG. BREAK FLOW GREATER THAN HIGH PRESSURE SAFETY INJECTION FLOW.
L3-2	01-16-80	50	SMALL BREAK COLD LEG. HIGH PRESSURE SAFETY INJECTION FLOW GREATER THAN BREAK FLOW.
L3-5	03-07-80	0	SMALL BREAK COLD LEG, PRIMARY COOLANT PUMPS OFF.
L3-6	03-21-80	0	SMALL BREAK COLD LEG, PRIMARY COOLANT PUMPS ON.
L6-1	05-09-80	37	OPERATIONAL TRANSIENT, LOSS OF STEAM LOAD.
L3-4	05-16-80	50	SMALL BREAK, PRESSURIZER RELIEF VALVE.
L6-2	07-01-80	37	OPERATIONAL TRANSIENT, LOSS OF PRIMARY COOLANT FLOW.
L3-3	07-08-80	50	SMALL BREAK COLD LEG. HIGH PRESSURE SAFETY INJECTION FLOW EQUAL TO BREAK FLOW.
L6-3	09-15-80	37	OPERATIONAL TRANSIENT, EXCESSIVE LOAD INCREASE.
L2-5	09-22-80	37	LARGE DOUBLE-ENDED COLD-LEG BREAK AS L2-3 BUT WITH LOSS OF OFFSITE POWER.

1600 056

*TARGET DATES ASSUME NO SIGNIFICANT PROBLEMS

ANALYSIS OF LOFT LOSS-OF-COOLANT EXPERIMENTS

L2-2, L2-3, AND L3-0

Presented at
The Seventh Water Reactor Safety Research Information Meeting
November 5-9, 1979
Gaithersburg, Maryland

L. P. Leach
J. H. Linebarger

EG&G Idaho, Inc.

Idaho National Engineering Laboratory
Idaho Falls, Idaho 83401

ANALYSIS OF LOFT LOSS-OF-COOLANT EXPERIMENTS L2-2, L2-3, AND L3-0

L. P. Leach
J. H. Linebarger

EG&G Idaho, Inc.

ABSTRACT

A summary of results from Loss-of-Coolant Experiments (LOCE) L2-2, L2-3, and L3-0, conducted in the Loss-of-Fluid Test (LOFT) facility, and conclusions from posttest analyses of the experimental data are presented. LOCEs L2-2 and L2-3 were nuclear large break experiments and were dominated by a core-wide fuel rod cladding rewet, which limited the maximum fuel temperature. Analytical models only conservatively predicted the measured fuel rod temperatures and will require improvements to provide best estimate predictions in this area. Analysis of a large commercial pressurized water reactor (PWR) indicates that the cladding rewet observed in LOFT is also likely to occur in a large PWR, and that, therefore, safety analysis calculations of large loss-of-coolant accidents (LOCA) are more conservative than previously thought. LOCE L3-0 was an isothermal small break (top of pressurizer) experiment and illustrated that the pressurizer fills after the primary system fluid saturates someplace other than the pressurizer itself, that the indicated pressurizer level is higher than the actual level, and that additional model development and assessment work is necessary in order to predict small LOCAs as accurately as large LOCAs.

INTRODUCTION

This discussion describes LOCEs L2-2, L2-3, and L3-0, conducted in the LOFT facility, and presents conclusions reached from analyses of these experiments. LOCEs L2-2 and L2-3 were identical, except for core power level, nuclear large break experiments. LOCE L3-0 was an isothermal small break (top of pressurizer) experiment conducted with the same system and core configuration as LOCEs L2-2 and L2-3.

LOCEs L2-2 and L2-3 are part of the LOFT Power Ascension Test Series (Test Series L2), which included six 200% double-ended cold leg break experiments. LOCEs L2-1 through L2-4 were designed to be identical except for step-wise increases in core power for each experiment. These experiments were planned to provide data for comparison to evaluate the effect of core power on system and core cooling behavior. LOCEs L2-5 and L2-6 were designed to provide data for parametric investigations of the effect of loss of offsite power and prepressurized fuel. Prior to starting Test Series L2, it was decided not to perform LOCE L2-1 because the low core power of LOCE L2-1 was not expected to provide data of significant value over that already obtained from the LOFT isothermal experiments and the "lead rod" tests performed in the Power Burst Facility (PBF).

LOCEs L2-2 and L2-3 had the same specific objectives which were to:

1. Determine core-wide spatial variations of fuel rod cladding thermal response

2. Identify thermal-hydraulic phenomena and determine effects of thermal-hydraulic phemomena on fuel rod cladding thermal response

3. Determine emergency core cooling system (ECCS) performance and core reflood characteristics

4. Determine the integrity of the fuel rod cladding

5. Determine principal variables of temperature, pressure, density, mass flow, and mass inventory as functions of time associated with the core, primary coolant system, and emergency core coolant (ECC) sufficient for comparison with and assessment of code predictions.

LOCE L2-2, performed December 9, 1978, and LOCE L2-3, performed May 12, 1979, met these objectives.

LOCE L3-0 was introduced into the LOFT Experimental Program after the occurrence of the Three Mile Island (TMI) accident and the decision to redirect LOFT to accelerate small break testing. Isothermal small break LOCE L3-0 had the following objectives:

1. Provide data to assess the transient pressure, temperature, and density for comparison with predictions from the RELAP4/MOD6, RELAP4/MOD7, RELAP5, and TRAC-P1A small break computer models

2. Determine the break flow from the available pressurizer pressure and level data

3. Determine if chugging occurs in the suppression tank during the small break blowdown

4. Provide operator training in performing small break experiments.

LOCE L3-0 was conducted on May 31, 1979, and met all of these objectives.

This discussion is divided into three major parts. The first part (a) describes the behavior of LOCEs L2-2 and L2-3, (b) presents the most significant results from posttest analyses of LOCEs L2-2 and L2-3 and from comparisons of the experimental data with computer calculations, and (c) presents results and implications of computer calculations on a commercial-size PWR with the same model used for LOFT. The second part of the discussion describes LOCE L3-0 and presents results from posttest analysis of the experimental data. Conclusions reached from the analyses of LOCEs L2-2, L2-3, and L3-0 are presented as the final part of this discussion.

LOCEs L2-2 AND L2-3

LOCEs L2-2 and L2-3 were 200% double-ended cold leg break experiments with ECC injection into the intact loop cold leg. These experiments were

identical except for the core power level and the resultant temperature rise across the core. For this analysis, the data from LOCEs L2-2 and L2-3 were compared with data from nonnuclear isothermal LOCE L1-5 to evaluate the effect of core power on system and emergency core cooling behavior. LOCE L1-5 was identical to LOCEs L2-2 and L2-3 except that the core was at zero power. LOCE L1-5 was used. in some cases, as a baseline and, therefore, is included in the following discussion.

Description of LOCEs L2-2 and L2-3 Behavior

LOCEs L2-2, L2-3, and L1-5 were configured to represent the complete severance of one of the four reactor inlet pipes in a commercial-size four-loop PWR with unobstructed discharge from both sides of the break. Offsite power was assumed available in that the primary coolant pumps were left running at nearly normal speed. ECC was injected from the accumulator and the high-pressure and low-pressure injection systems (HPIS and LPIS) to the intact loop cold leg. The ECC flow rates were adjusted to represent complete loss of ECC injected to the broken loop and failure of one HPIS and LPIS injection train.

The most important plant operating conditions at experiment initiation for LOCEs L2-2, L2-3, and L1-5 are shown in Table 1. Main features of the event sequences for the experiments are listed in Table 2.

The general behavior of the LOFT system during LOCEs L2-2, L2-3, and L1-5 can best be related through consideration of the pressure response of the system shown in Figure 1. On the basis of the pressure response, the experiments may be described in several phases. The first phase, subcooled blowdown, consists of the initial pressure reduction from initial operating pressure to saturation pressure of the reactor outlet fluid. This phase lasted about 50 ms in LOCEs L2-2 and L2-3 and about 80 ms in LOCE L1-5, being shorter in the nuclear experiments due to the lower initial pressure and higher reactor coolant outlet temperature (higher saturation pressure). The subcooled blowdown period is of main interest relative to the structural loading of the system and will not be discussed further here.

TABLE 1. PLANT OPERATING CONDITIONS AT EXPERIMENT INITIATION

Parameter	LOCE L1-5	LOCE L2-2	LOCE L2-3
Primary system:			
Pressure (MPa)	15.45	15.64	15.06
Temperature (K)	555	570	573
Mass flow (kg/s)	175.1	194.2	199.8
Boron (ppm)	3037	838	679
ECC accumulator:			
Pressure (MPa)	4.17	4.11	4.18
Temperature (K)	304	300	307
Boron (ppm)	3155	3301	3281
Injected volume (m^3)	0.97	1.05	0.96
Reactor core:			
Power [MW(t)]	0	24.9	36.7
Average linear heat generation rate (kW/m)	0	10.9	16.0
Maximum linear heat generation rate (kW/m)	0	26.37	39.4
Coolant temperature rise (K)	0	22.7	32.2

The second phase of the pressure response covers the time from initiation of flashing of coolant in the reactor outlet pipes to the time of flashing in the reactor inlet pipes. This time period (milliseconds) was very short for LOCE L1-5, but longer and roughly the same for L2-2 and L2-3 (~3.5 s) and quite important to the response of the core, as will be seen subsequently. During this phase, the pressure in LOCE L2-3 was slightly higher than in LOCE L2-2 due to the higher initial temperature of the reactor outlet fluid. This period may also be thought of as the time of subcooled fluid discharge out of the broken loop inlet pipe.

TABLE 2. CHRONOLOGY OF EVENTS OF NUCLEAR LOCEs L2-2 AND L2-3 WITH NONNUCLEAR LOCE L1-5 COMPARATIVE VALUES

Event	Time after Test Initiation (s)		
	LOCE L2-3	LOCE L2-2	LOCE L1-5
Test initiated	0	0	0
Subcooled blowdown ended[a]	0.06	0.07	0.1
Reactor scram signal received at control room	0.103	0.085	0.087
Earliest departure of cladding temperature from fluid saturation temperature ($T_{clad} > T_{sat}$)	0.96	1.0	25.6
Control rods completely inserted	1.683	1.725	1.85
Subcooled break flow ended[b]	3.0	3.8	0.1
Maximum cladding temperature attained	4.95	5.8	Steady state value at time 0
Earliest core-wide return of cladding temperature to fluid saturation temperature	8.5	8.0	48
HPIS injection initiated	14	12	13
Pressurizer emptied	14	15	14
Accumulator injection initiated	16	18	19
LPIS injection initiated	29	29	34
Lower plenum filled with liquid	35	35	37
Saturated blowdown ended	40	44	47
Accumulator liquid flow ended	45	49	54
Core volume reflooded	55	55	59

1600 063

a. End of subcooled blowdown is defined as the occurrence of the first phase transition in the system other than at the pipe break location.

b. End of subcooled break flow is defined as the completion of subcooled fluid discharge from the break (hot and cold legs) in the broken loop.

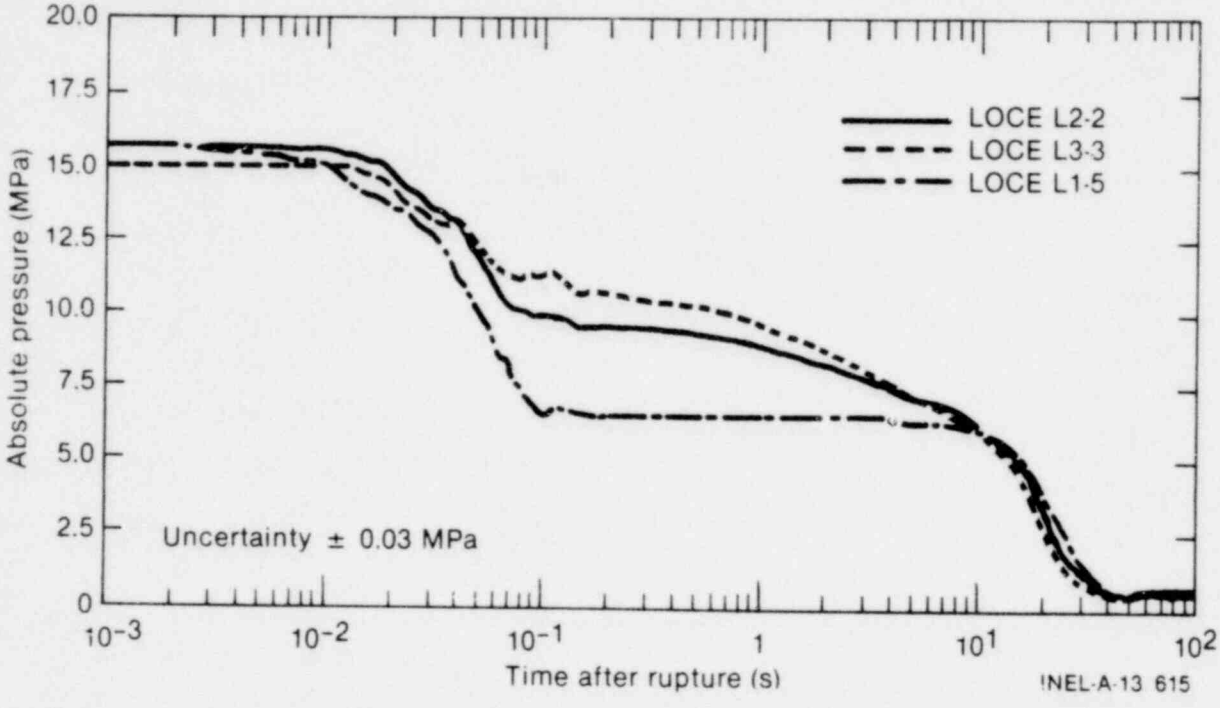

Figure 1. Pressure as a function of time for LOCEs L1-5, L2-2, and L2-3.

1600 064

During the final phase of the depressurization, saturated blowdown, saturated fluid flowed out of both ends of the broken pipe. This phase may be further subdivided to consider the period of break critical flow discharge and break noncritical flow discharge. The later portions of the saturated blowdown phase are very important because, during this time, ECC was effective in reestablishing a stable thermal condition by cooling the core.

During saturated blowdown, LOCE L2-3 depressurized slightly faster than LOCE L2-2 due principally to a higher break discharge flow in the second phase of the blowdown. Later, the depressurization portion of LOCEs L2-2 and L2-3 were identical.

Analysis of LOCEs L2-2 and L2-3 Behavior

The parameter of most interest during the LOFT nuclear powered large break LOCEs is the fuel rod cladding temperature. Figure 2 shows the measured and predicted response of the fuel rod cladding temperature hot spot during LOCE L2-2. The initial increase in cladding temperature was predicted by the calculation; however, the large decrease, or core rewet, measured during LOCE L2-2 was not predicted by the RELAP4/MOD6[a] cladding temperature calculation.

The measured cladding temperature response of LOCE L2-3 was similar to that observed in LOCE L2-2, as shown in Figures 3, 4, and 5. The following observed differences are attributable to core power.

1. The average time of initial departure from nucleate boiling (DNB) was shorter for LOCE L2-3 than for LOCE L2-2, 1.27 and 1.65 s, respectively

2. The peak cladding temperature was higher for LOCE L2-3 than for LOCE L2-2, 914 and 789 K, respectively.

a. The RELAP calculations used in the prediction of LOCEs L2-2 and L2-3 were performed with RELAP4/MOD6, Idaho National Engineering Laboratory Configuration Control Number H001184B.

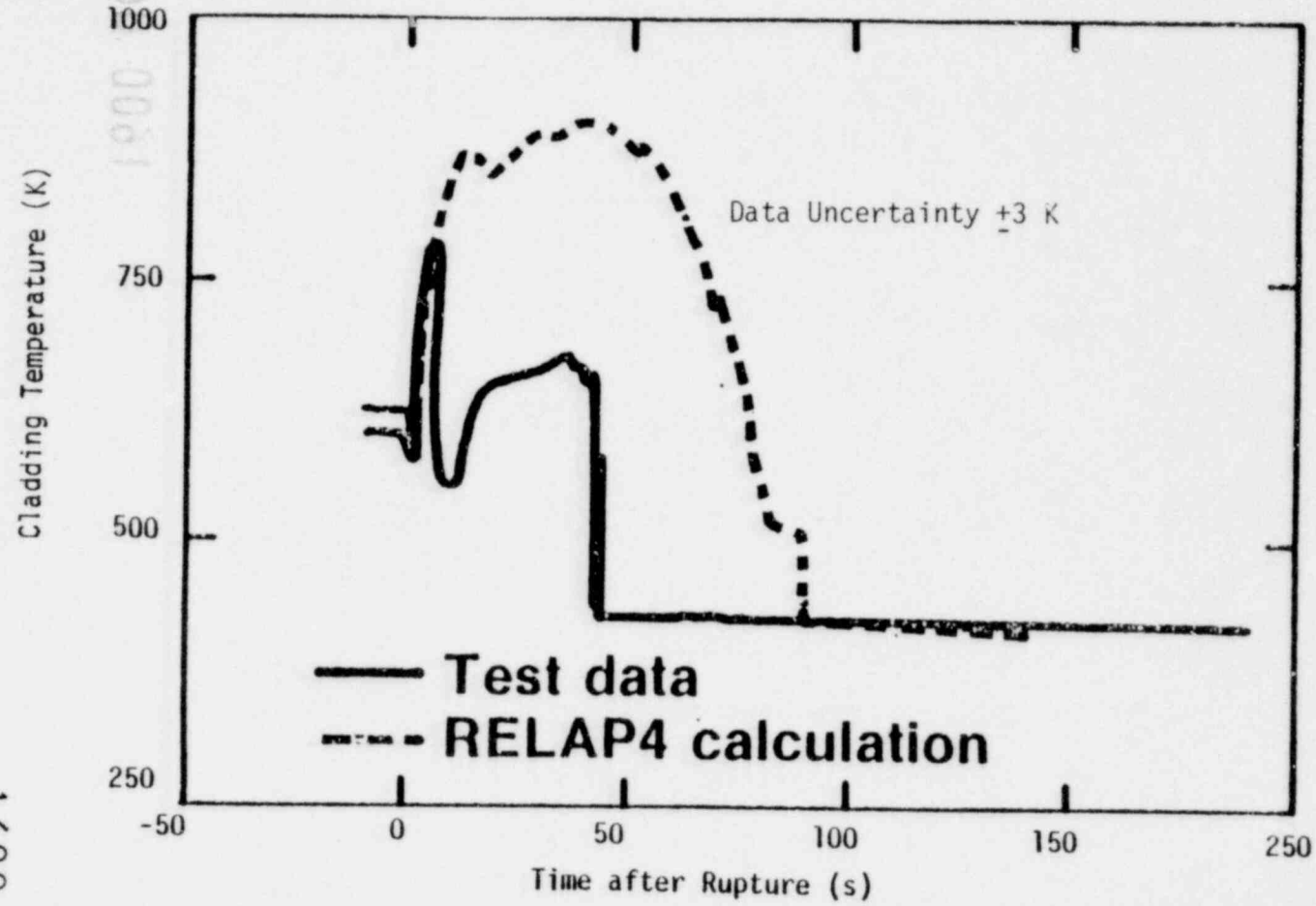

Figure 2. Measured and predicted cladding temperature in center fuel module for LOFT LOCE L2-2.

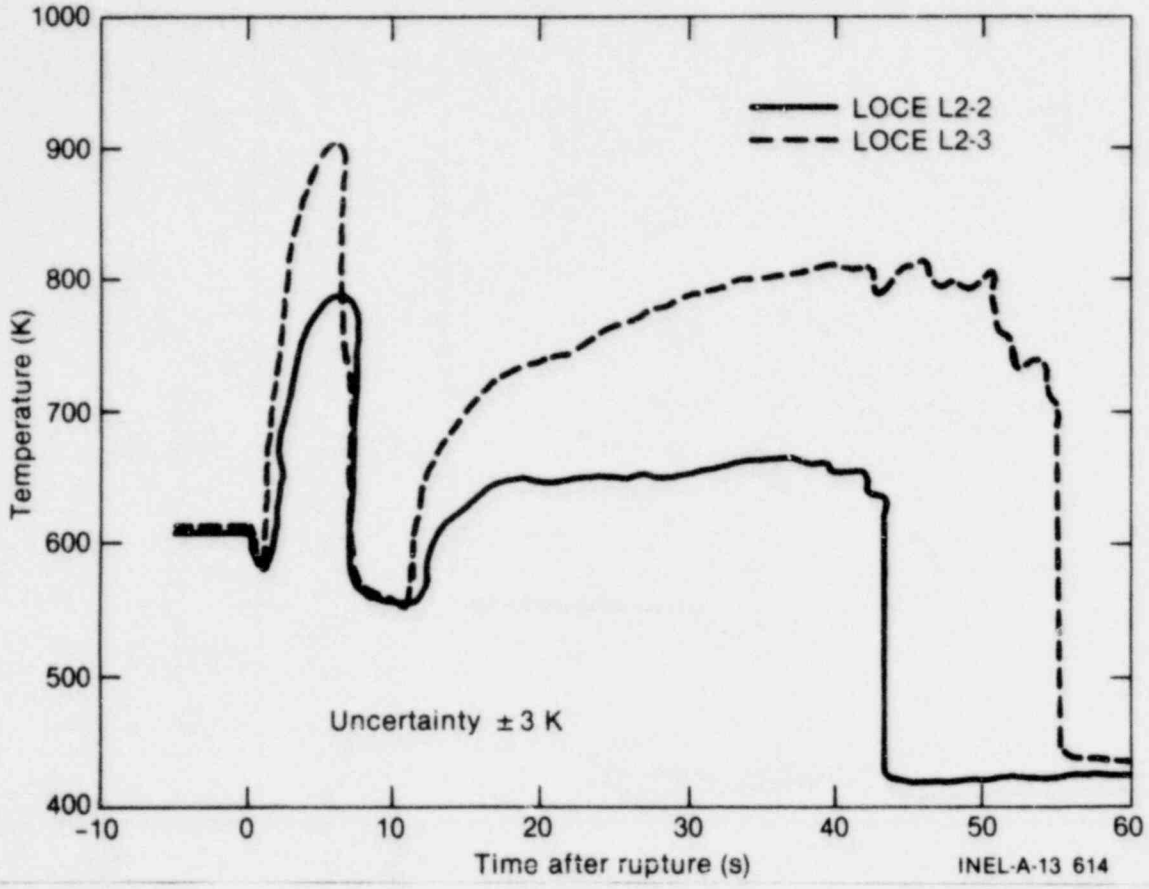

Figure 3. Fuel cladding temperatures for LOCEs L2-2 and L2-3.

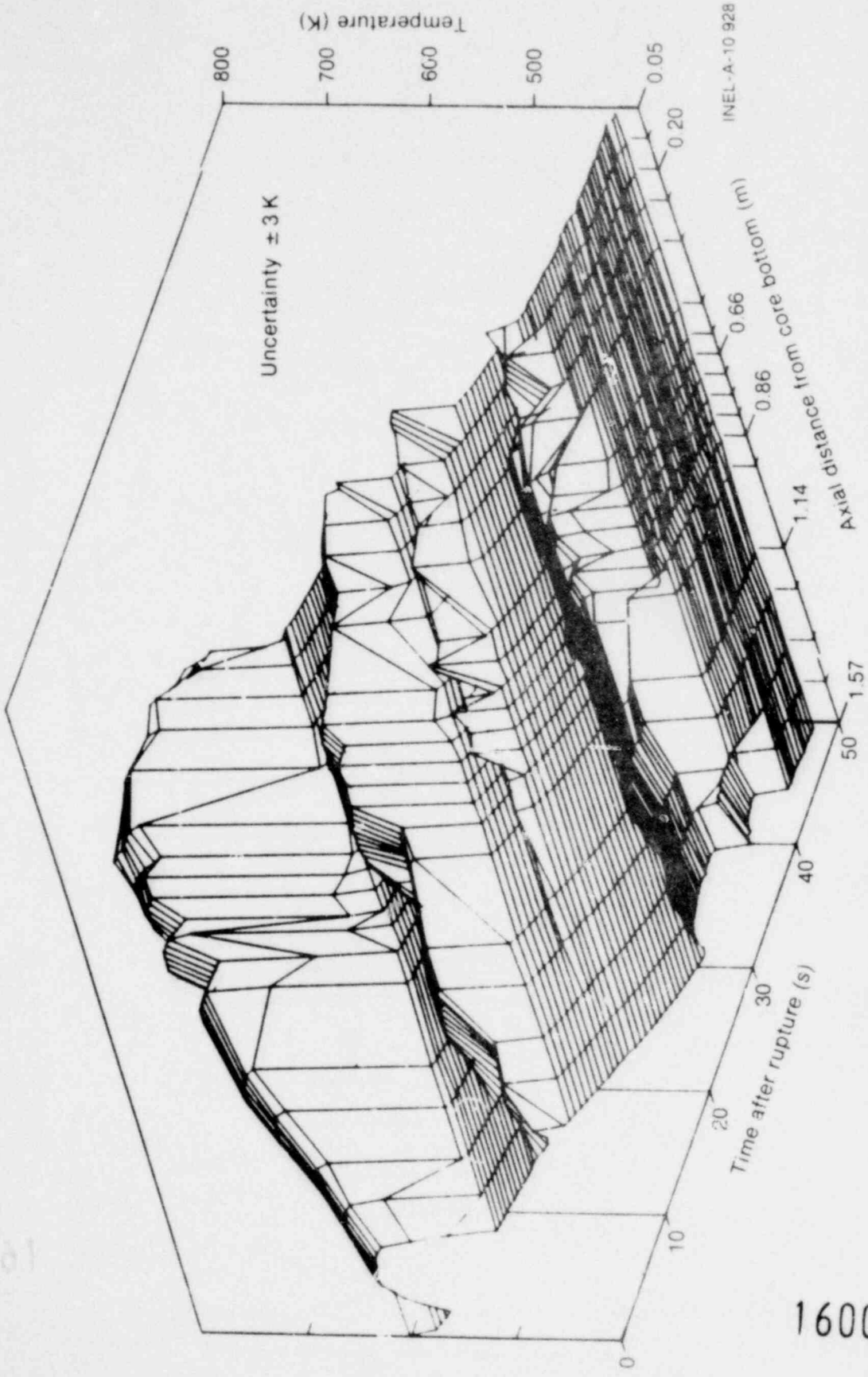

Figure 4. Axial profile of cladding temperature in fuel Module 5 for LOCE L2-2.

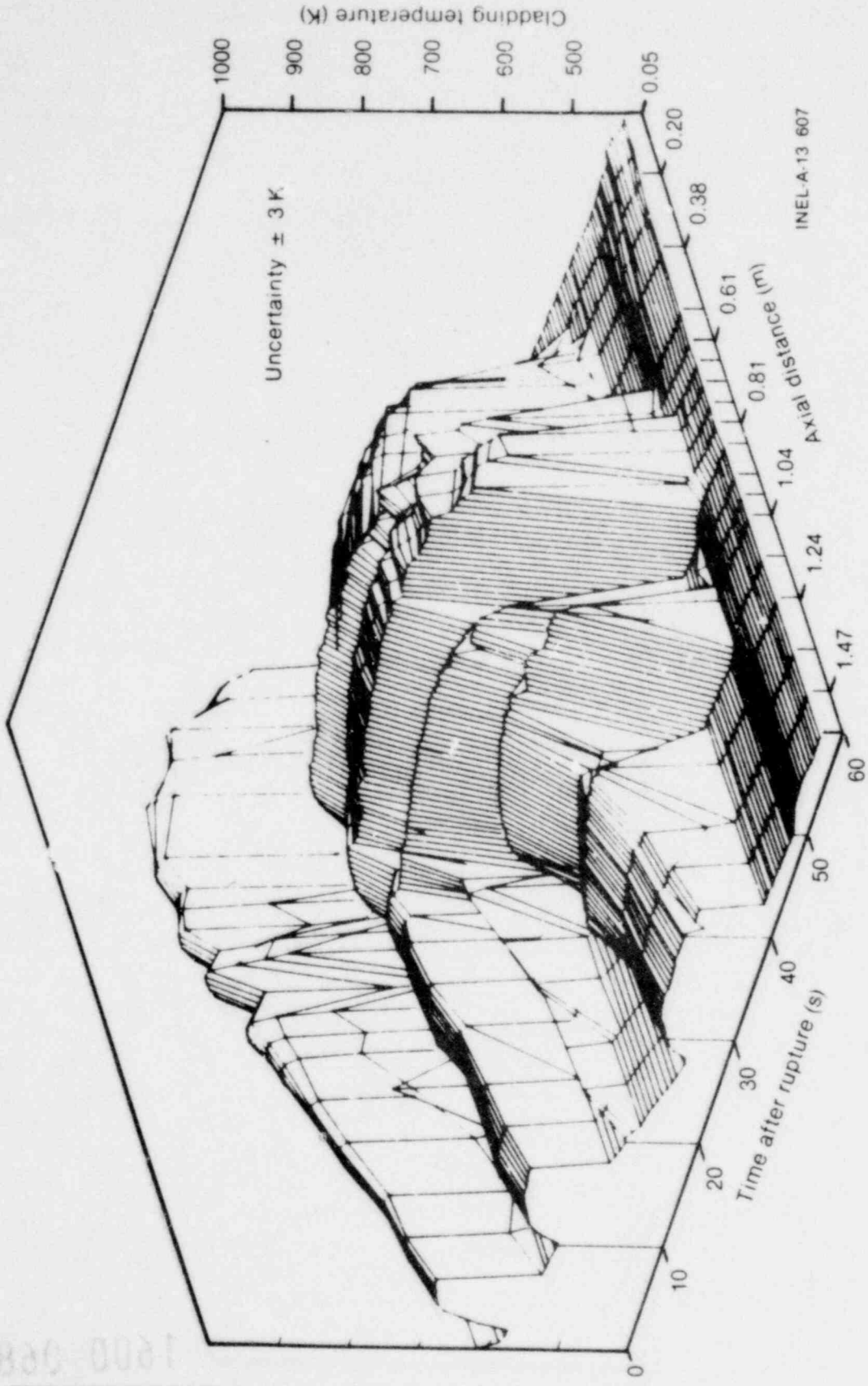

Figure 5. Axial profile of cladding temperature in fuel Module 5 for LOCE L2-3.

3. The pattern of the final rewet, or reflood, in LOCE L2-3 was bottom, top, then middle; whereas, the rewet pattern for LOCE L2-2 was bottom to top.

A revised prediction for LOCE L2-3,[1] based on a computer model that described the rewet of LOCE L2-2,[2] did not predict the rewet observed in LOCE L2-3.

The analysis effort to describe the cause of the disparity between measured and predicted cladding temperature in LOFT LOCE L2-2[3] considered several possible contributors as follows:

1. The thermocouples rewet, but the cladding did not
2. Differences between actual and planned initial conditions
3. The initial fuel rod stored energy
4. The heat transfer correlations in the analytical model
5. The hydraulic calculation.

Investigations into the possibility that the cladding did not rewet concluded that, while additional data on the cladding thermocouple performances are needed, the core did rewet during LOCE L2-2. This conclusion was reached based on data taken in the LOFT nonnuclear isothermal LOCEs, in PBF LOCA tests, from REBECCA tests, detailed thermal analysis, and investigation of other LOFT data. For example, Figure 6 shows the measured fluid temperature and the saturation temperature (determined from pressure) above the LOFT core. The termination of the superheated steam indication at 8 s corresponds to the cladding temperature rewet indication. Additional testing is now being performed at KfK in Germany and at the Idaho National Engineering Laboratory (INEL) to further evaluate the effect of the thermocouples.

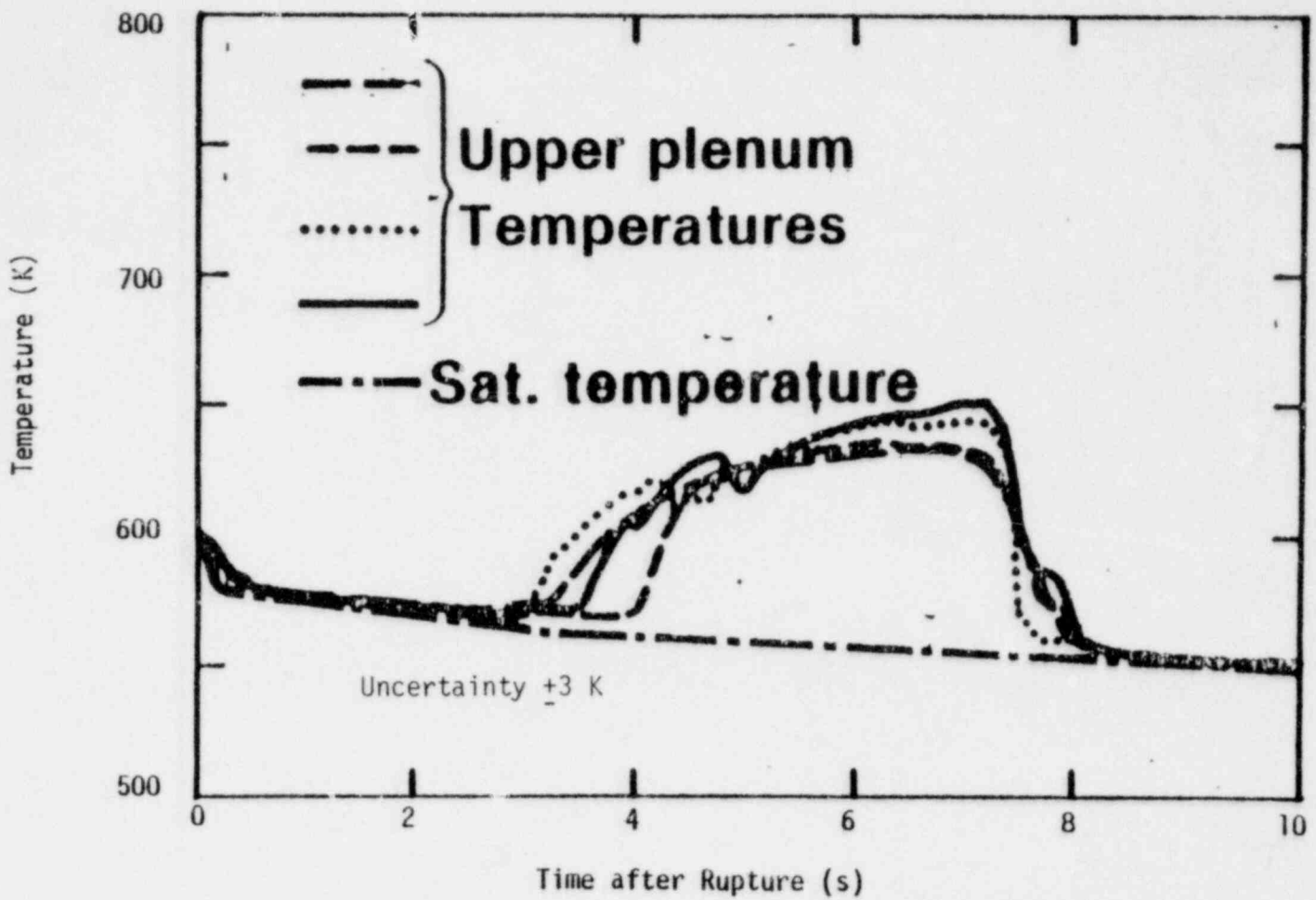

Figure 6. Fluid and saturation temperature above core for LOCE L2-2.

The effect of actual initial conditions on the test was determined by rerunning the prediction model with measured initial conditions. As shown in Figure 7, changing the initial conditions in the calculation did not provide a prediction of rewet.

The stored energy in the fuel rods was correlated to rod experimental and calculated heat-up rates, at times during the transient when fluid cooling effects were negligible. The correlation indicates that the stored energy in the rods is properly calculated. The analysis is currently being refined to include significant parameter uncertainties.

The effect of the heat transfer correlations was evaluated by running analyses with both the specified and measured initial conditions and two different film boiling correlations (new Groeneveld versus Condie-Bengston). Figure 8 indicates that while a better estimate of the peak cladding temperature was obtained with the Condie-Bengston correlation, the rewet was still not predicted.

Evaluation of the system hydraulics indicated generally good comparison between measured and predicted performance, with the exception of the flow in the broken loop cold leg shown in Figure 9. The analytical model for break flow consists of a subcooled discharge model, saturated discharge model, transition quality at which the model changes from subcooled to saturated discharge, and discharge coefficients. Table 3 lists a number of parametric evaluations of these variables. Figure 9 shows how these changes affected break flow, with the last run labeled "Best PT" (posttest) giving the best agreement.

The information in Figure 10 indicates that the changes in critical flow choice did not greatly affect early pressure response, but Figure 11 shows a significant change in core upflow. Figure 12 shows that the Best PT case did predict a cladding rewet, whereas all the others did not. (Note: Figure 12 is not a "cladding hot spot" prediction; therefore, it shows low temperatures.) Thus, the failure to predict the rewet in LOCE L2-2 was due mostly to the core hydraulic calculation.

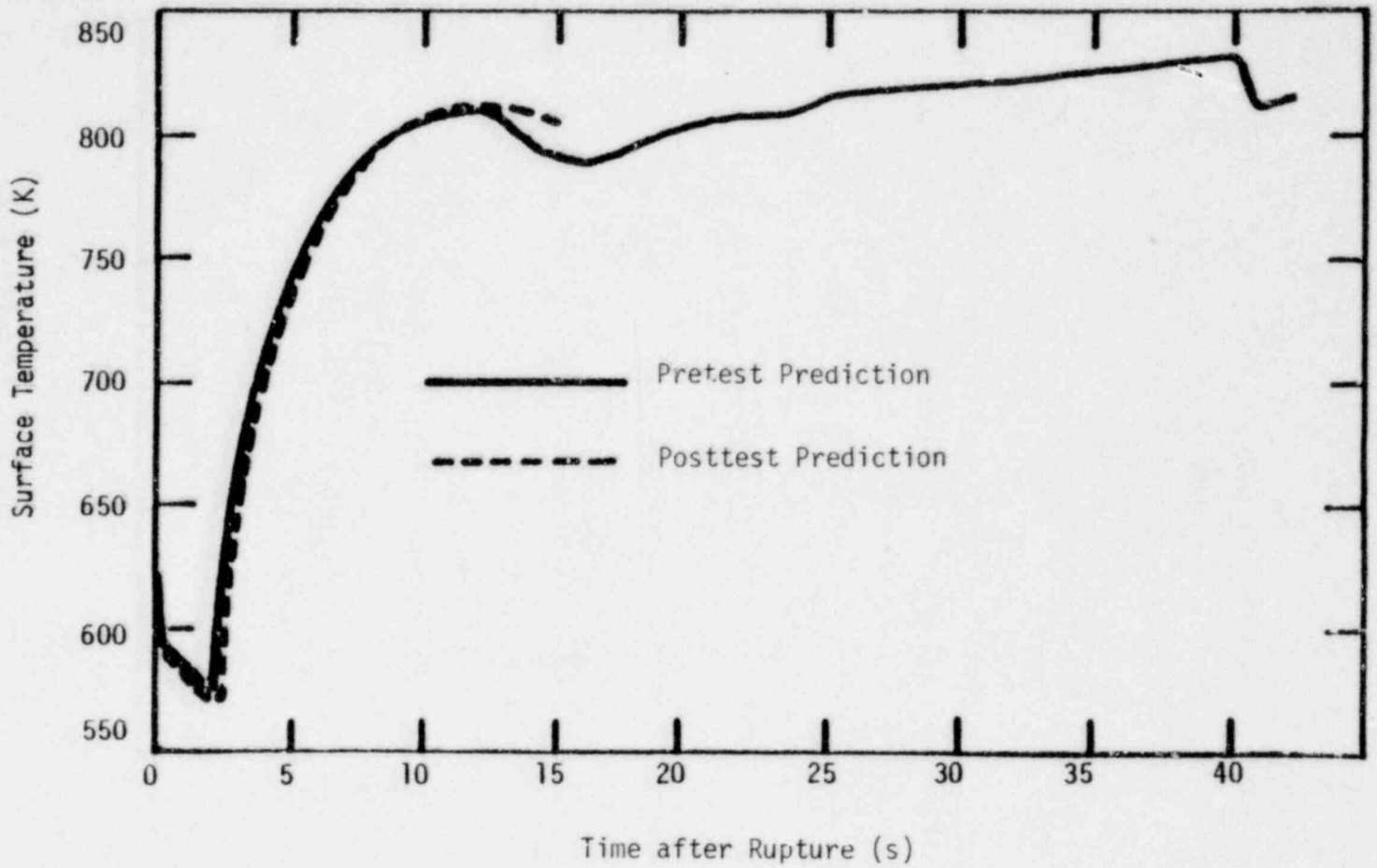

Figure 7. Effect of initial conditions on LOCE L2-2 prediction.

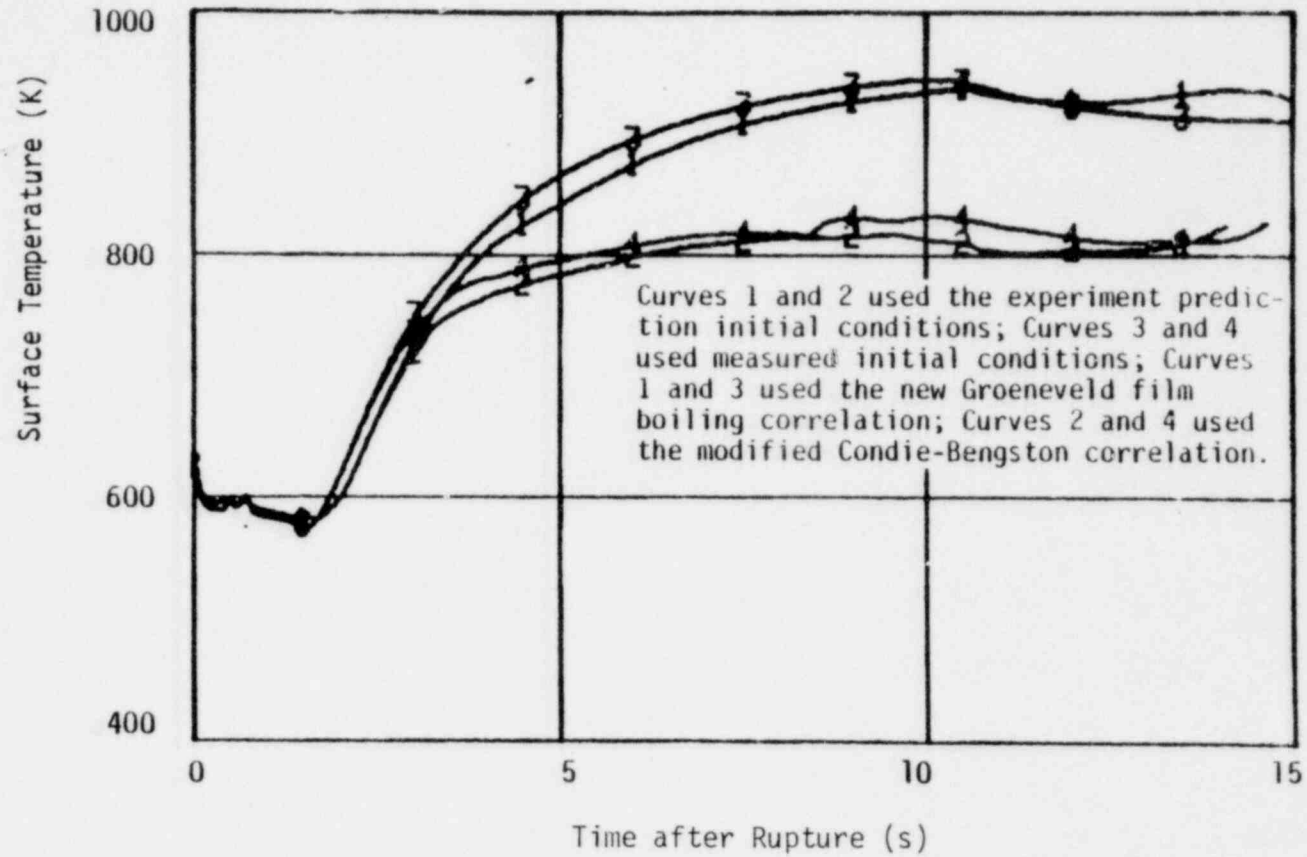

Figure 8. Cladding temperature on highest-powered fuel rod showing sensitivity to both film boiling correlation choice and initial conditions for LOCE L2-2.

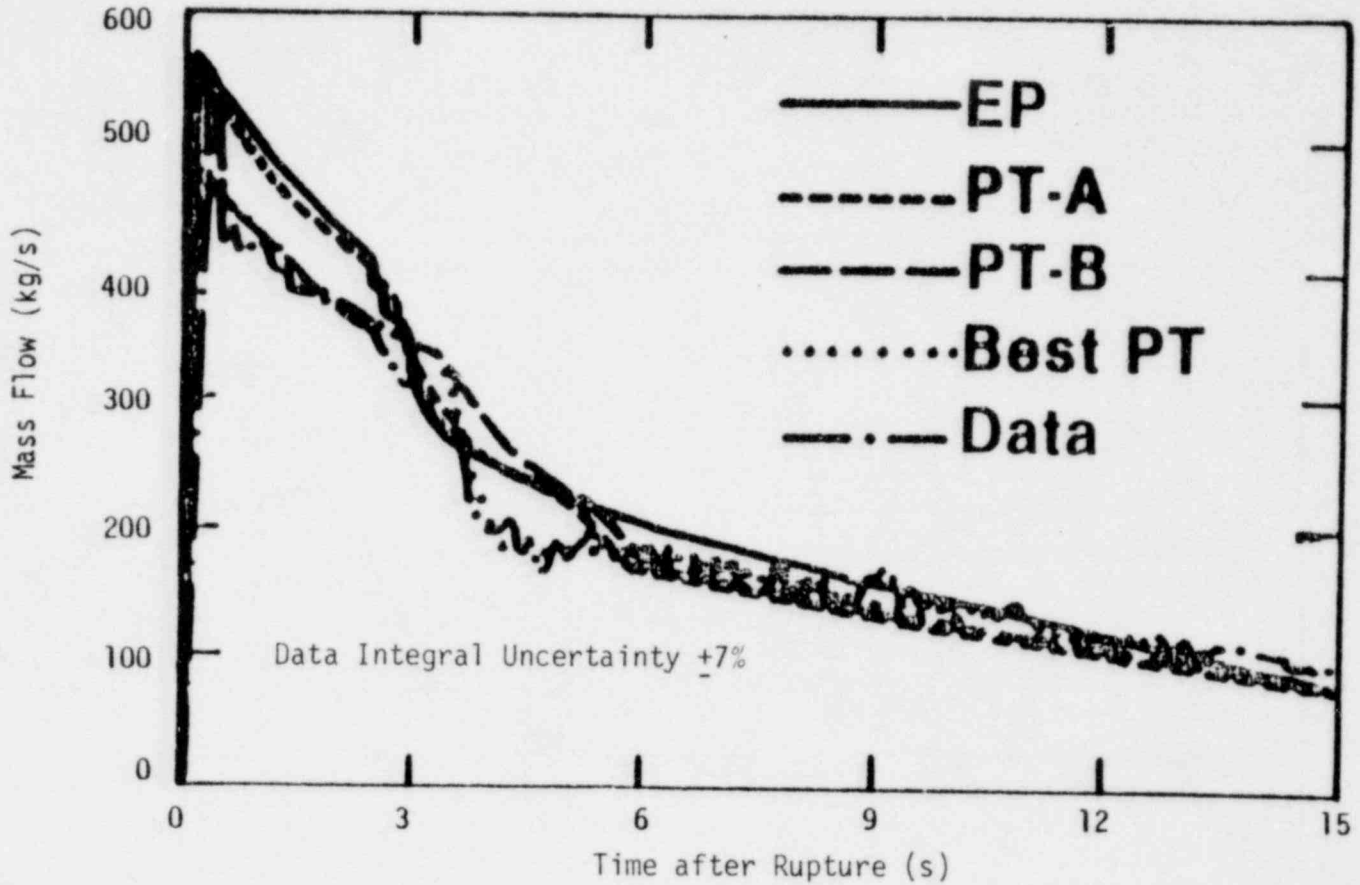

Figure 9. Broken loop cold leg flow for various critical flow choices for LOCE L2-2.

TABLE 3. CRITICAL FLOW SENSITIVITIES

Run	Multipliers		
	Henry-Fauske (Subcooled)	Homogeneous Equilibrium (Saturated)	Transition Quality
Experiment prediction	1.0	1.0	0.02
PT-A[a]	1.0	0.848	0.02
PT-B[a]	0.848	0.848	0.02
Best PT[b]	0.848	0.848	0.0025

a. PT-A and PT-B are posttest break flow sensitivity calculations.

b. Best PT is the posttest calculation which best predicted the LOCE L2-2 results.

The relatively abrupt transition between subcooled and saturated discharge at the break was traced to the progression of hot fluid from the core to the break, as shown in Figure 13. This type of behavior is difficult to calculate with a discrete model of the system, but using a very low value of transition quality allows for the abrupt transition even though the transmission of the temperature increase and consequent fluid density decrease are damped by the discrete model.

The net result of the broken loop cold leg mass flow transition is to enhance positive core flow and force fluid down the downcomer and into the core. This can be seen in Figure 14, which compares the measured intact and broken loop cold leg mass flows for LOCE L2-2. The overlap between 4 and 6 s after rupture represents the fluid forced down the downcomer and through the core. The data in Figure 15 indicate that the same phenomena occurred in LOCE L2-3.

As previously mentioned, a reprediction of LOCE L2-3 was made with the Best PT model that did predict the rewet for LOCE L2-2. Figure 16 shows the comparison between the original RELAP4/MOD6 prediction[3] (RELAP A) and the revised model[2] (RELAP B). Although the revised model

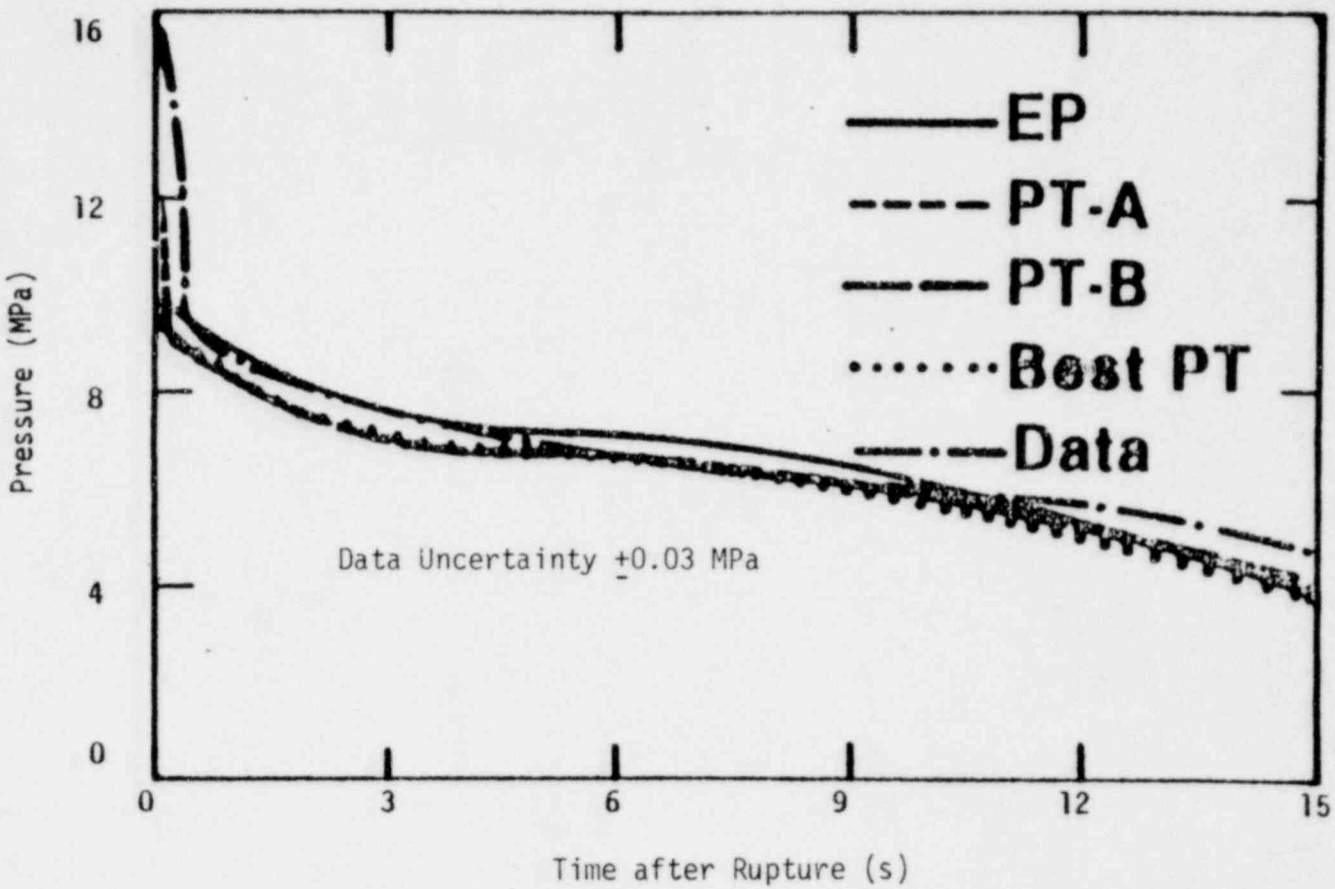

Figure 10. Posttest analysis of system depressurization for various critical flow choices for LOCE L2-2.

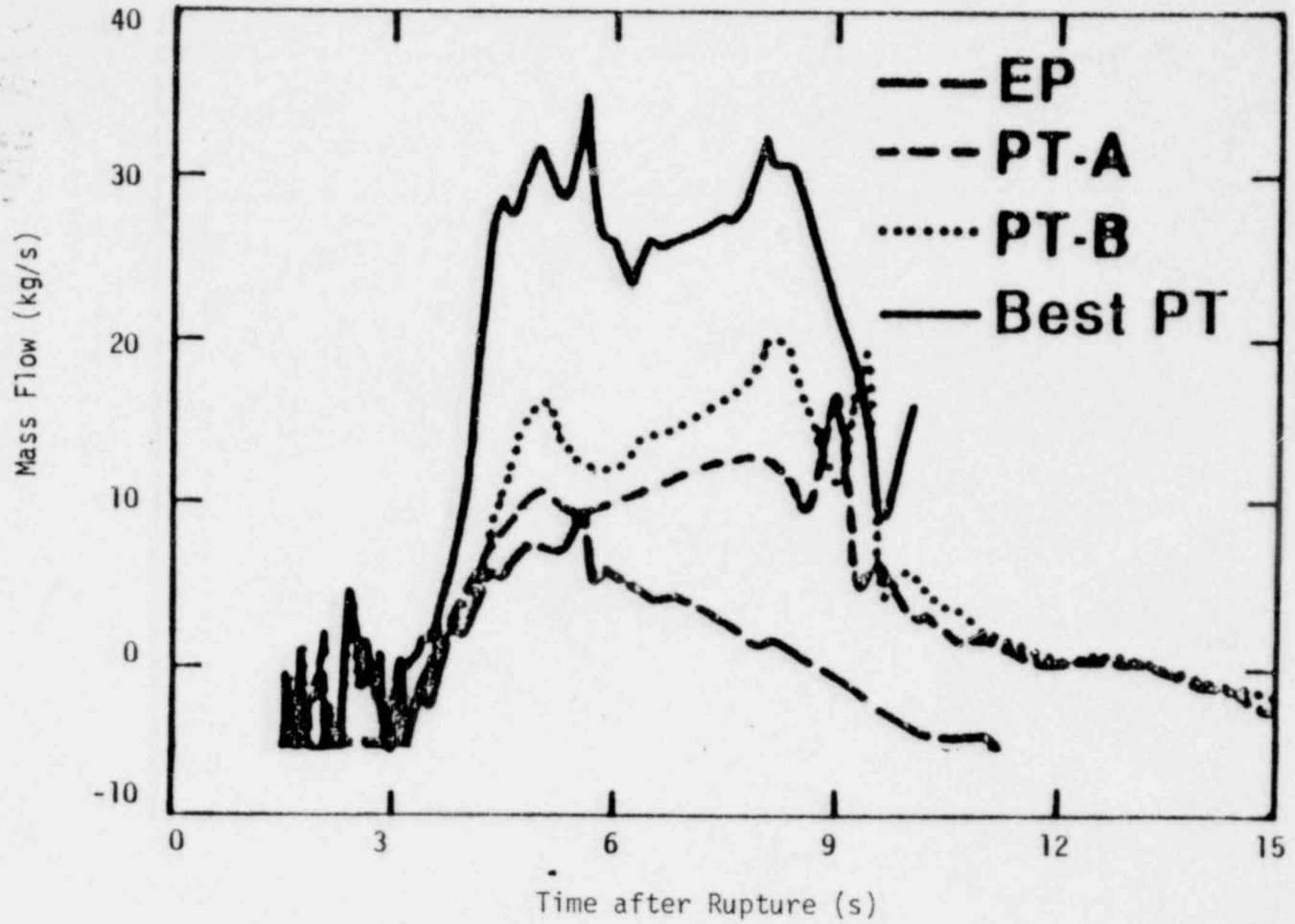

Figure 11. Posttest analysis of core inlet upflow for various critical flow choices for LOCE L2-2.

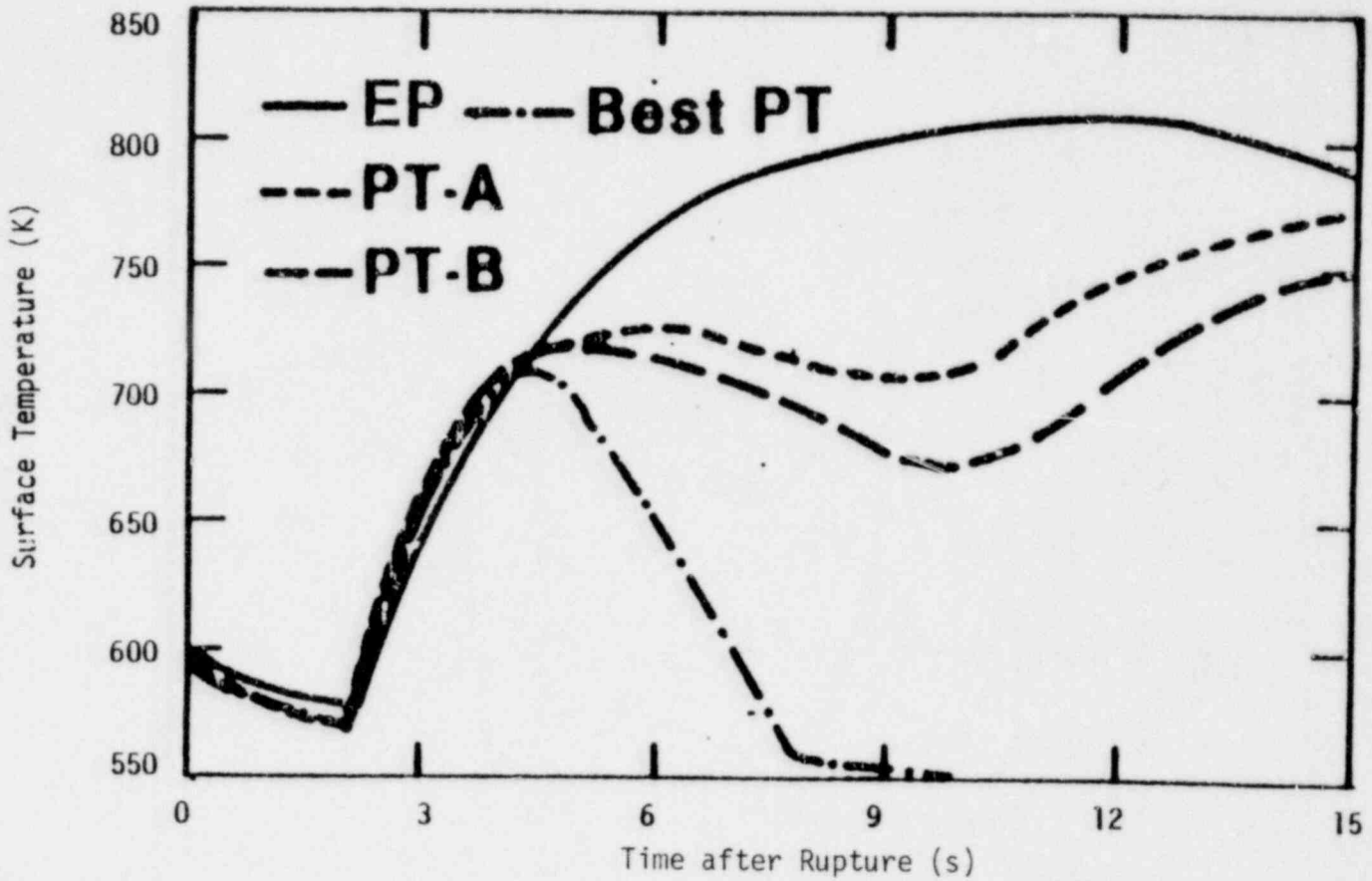

Figure 12. Posttest analysis of system model cladding temperature for various critical flow choices for LOCE L2-2.

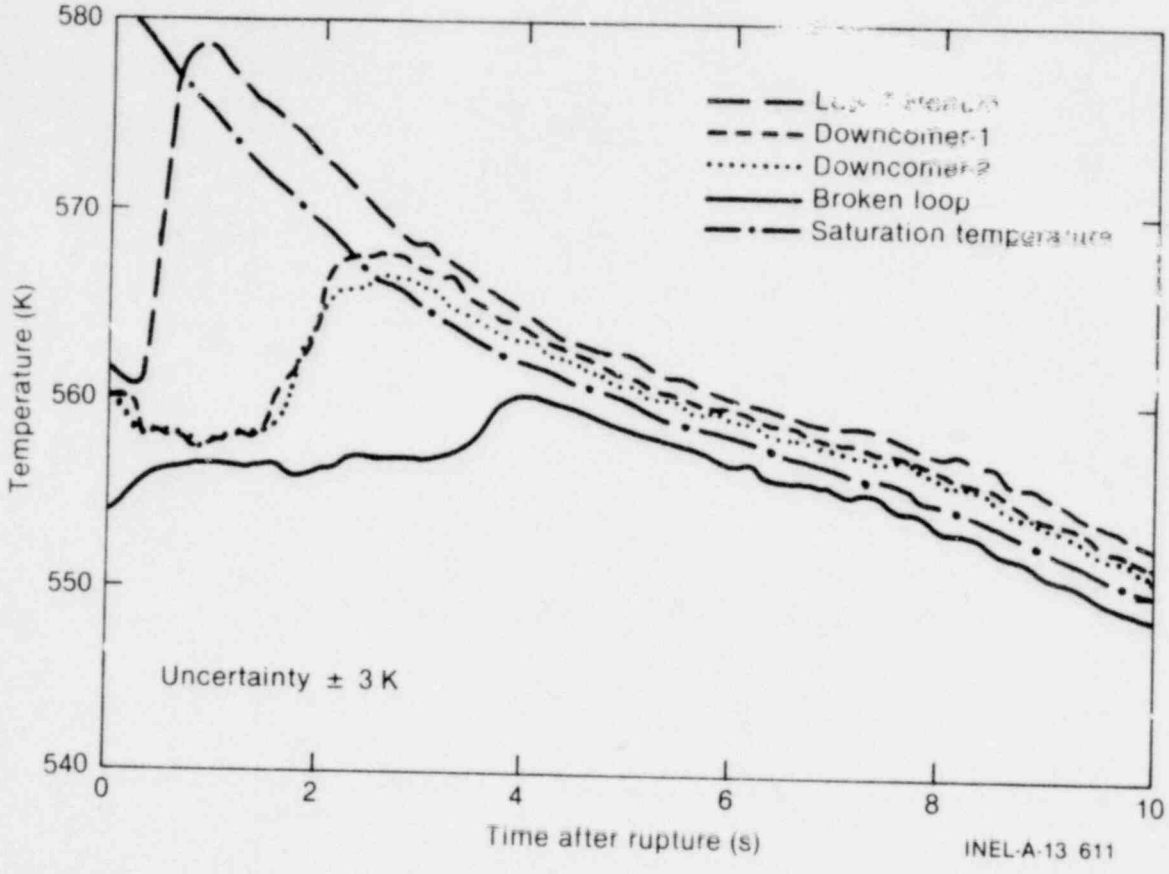

Figure 13. Fluid temperatures at various locations for LOCE L2-2.

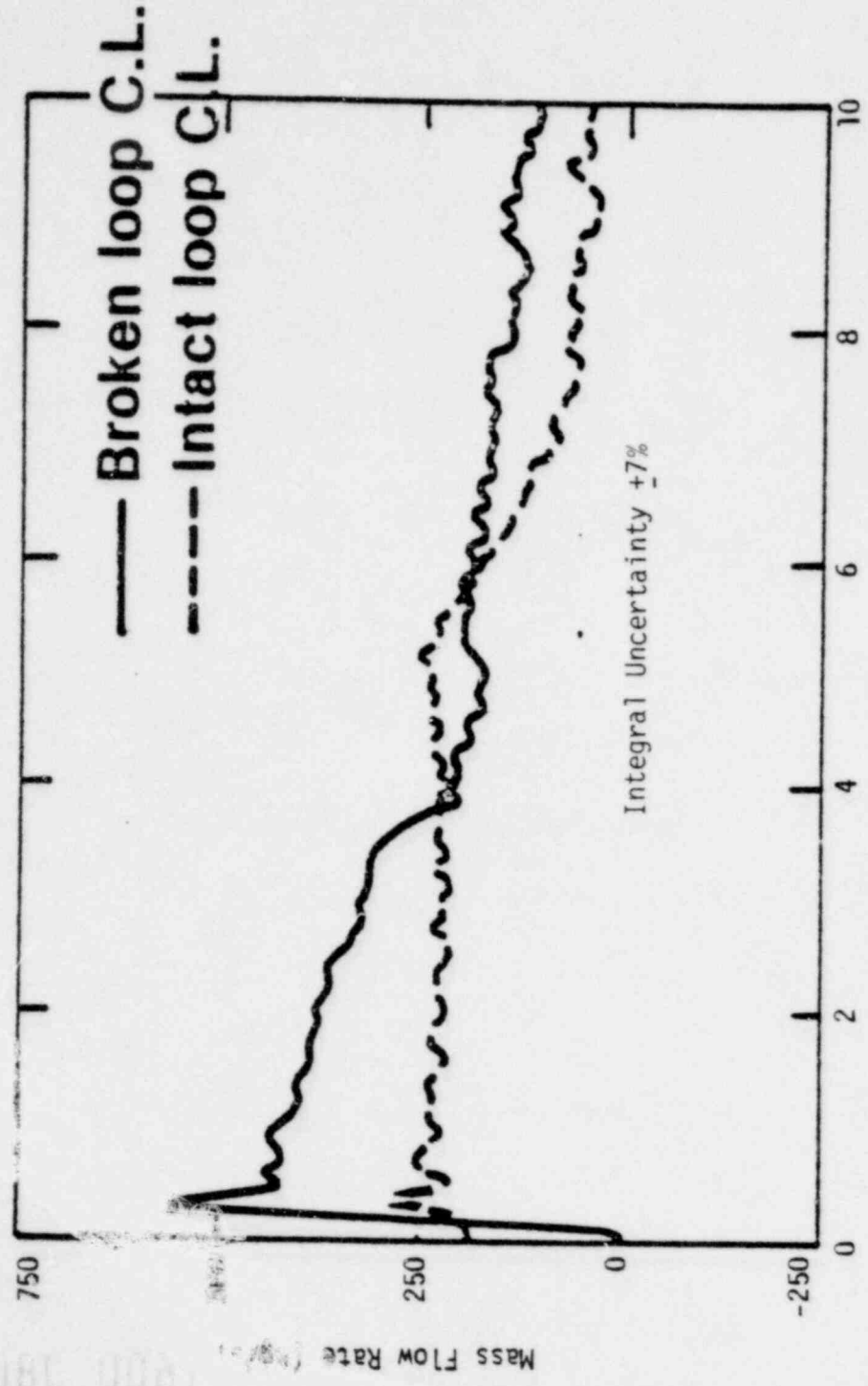

Figure 14. Measured mass flow rates for LOCE L2-2.

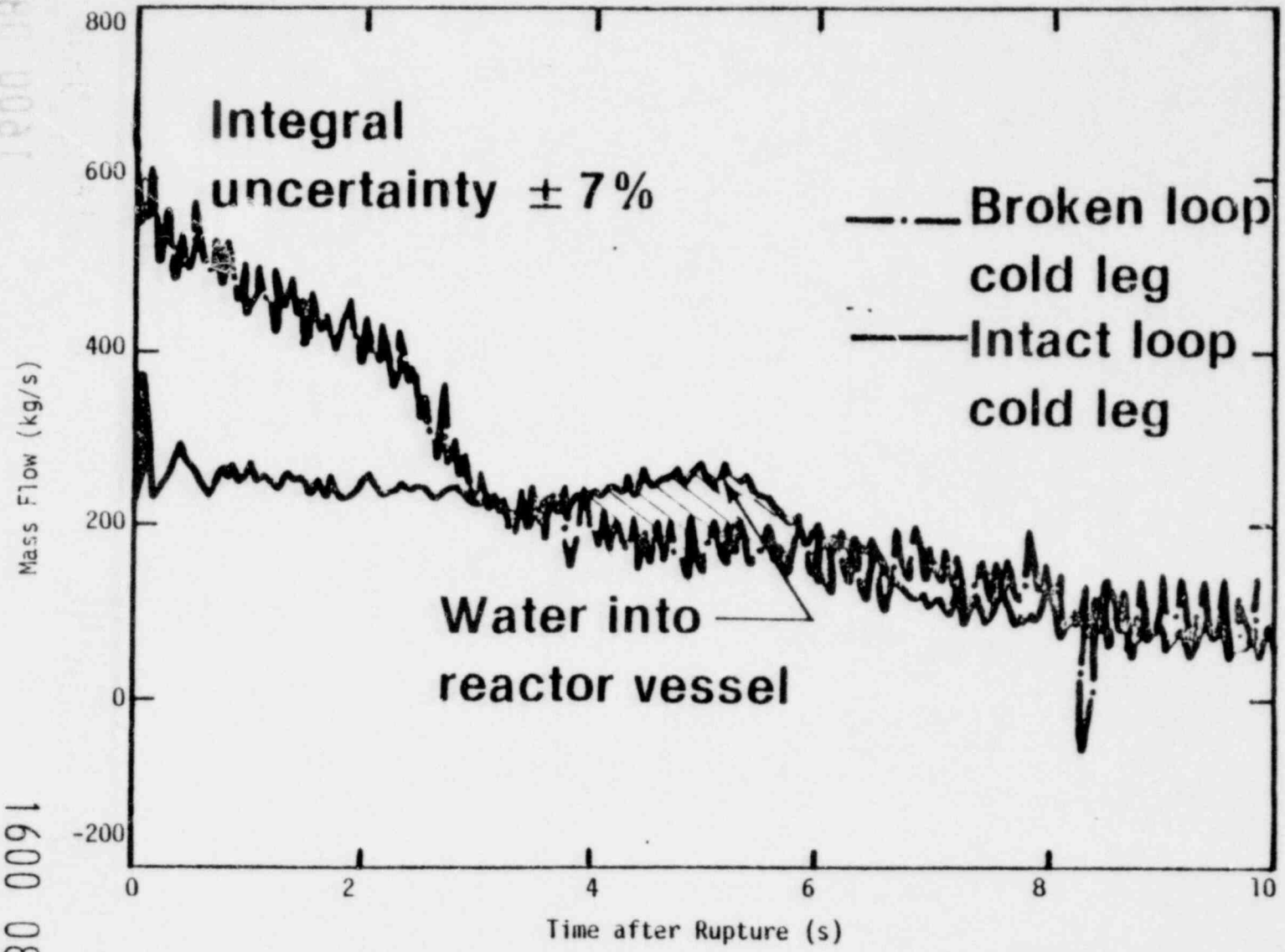

Figure 15. Measured cold leg mass flows for LOCE L2-3.

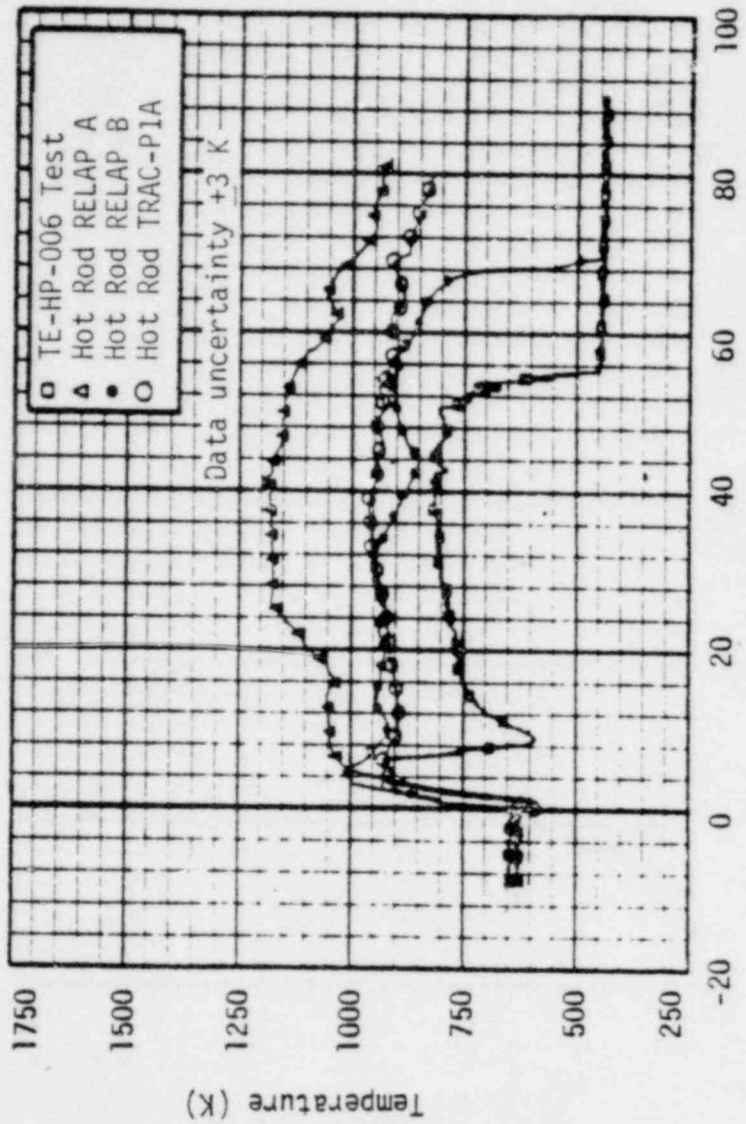

Figure 16. Comparison of measured and calculated hot rod cladding temperatures for LOCE L2-3.

did not predict rewet, the peak cladding temperature was better predicted. Also, review of the system hydraulics compared with the revised prediction showed excellent agreement. Figure 16 includes the cladding temperature prediction made with TRAC-P1A. This prediction does not show the rewet either. An alternate TRAC-P1A prediction with a revised rewet criteria, however, did predict the rewet. Posttest analysis of LOCE L2-3 is continuing, but it now appears that additional work on the heat transfer models is required in order to obtain best estimate calculations of cladding temperature in large PWRs.

Relationship to a Large PWR

In order to evaluate the relationship of the LOFT results to large commercial PWRs, a RELAP4/MOD6 analysis of a large PWR was made using the same model options as applied in the LOFT LOCE L2-2 Best PT model and the initial conditions for LOCEs L2-2 and L2-3. That is, the large PWR in both cases was run at a power sufficient to reproduce the core fluid temperature rise (core ΔT) forecast for LOCEs L2-2 and L2-3.

Figures 17 and 18 are comparisons of the best estimate predictions for the large PWR with the LOFT data for LOCEs L2-2 and L2-3, respectively. The excellent agreement shown implies the following:

1. The LOFT system is a good model of expected large PWR behavior (that is, scaling is accurate) during a large LOCA

2. The large PWR LOCA consequences are much less than previously thought

3. The peak cladding temperatures that would occur in the large PWR are probably less than occurred in LOFT, since the LOFT prediction with the same model yields higher cladding temperatures.

This information has been transmitted to the licensing portion of the NRC and is currently under evaluation.

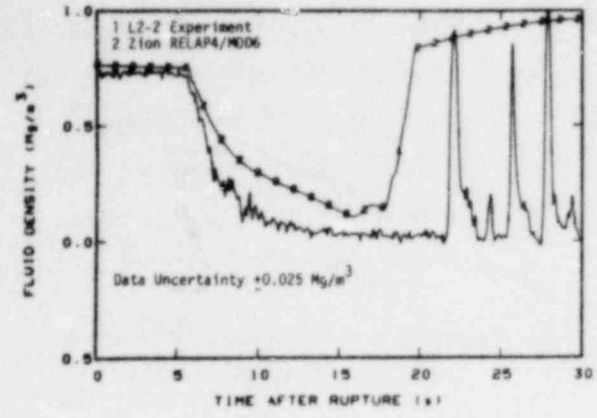

INTACT LOOP COLD LEG DENSITY

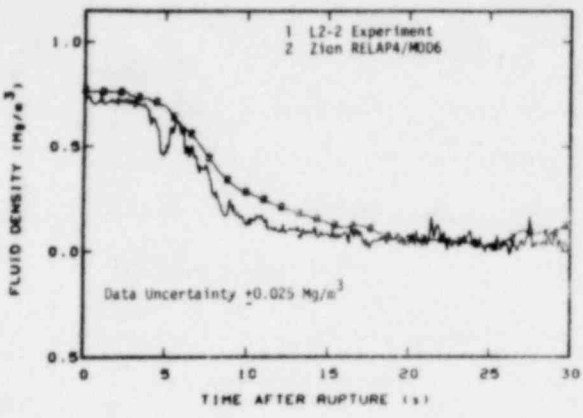

BROKEN LOOP COLD LEG DENSITY

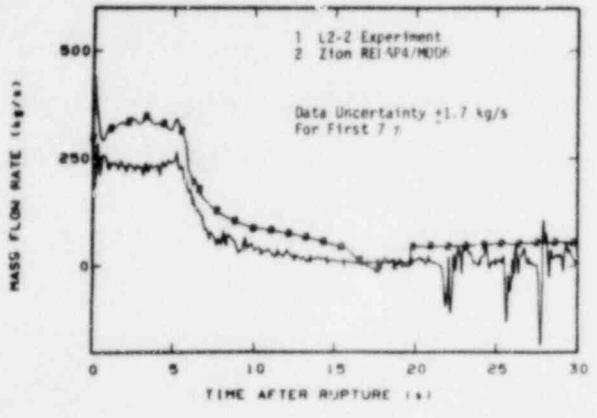

INTACT LOOP COLD LEG MASS FLOWRATE

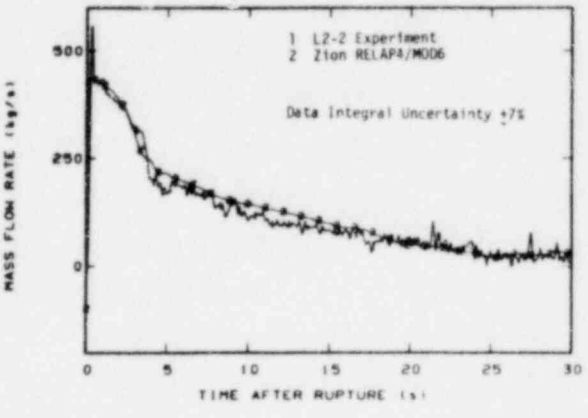

BROKEN LOOP COLD LEG MASS FLOWRATE

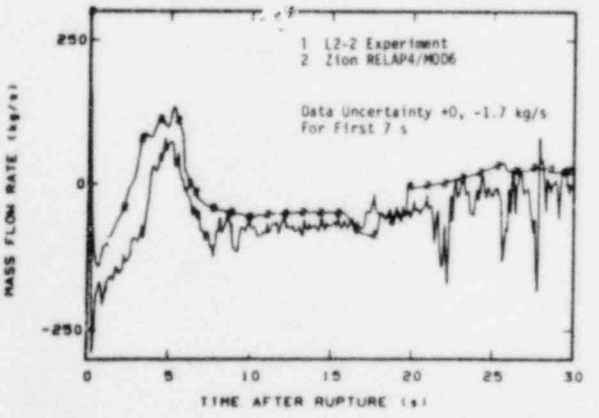

DIFFERENCE BETWEEN INTACT LOOP AND
BROKEN LOOP COLD LEG MASS FLOWRATES

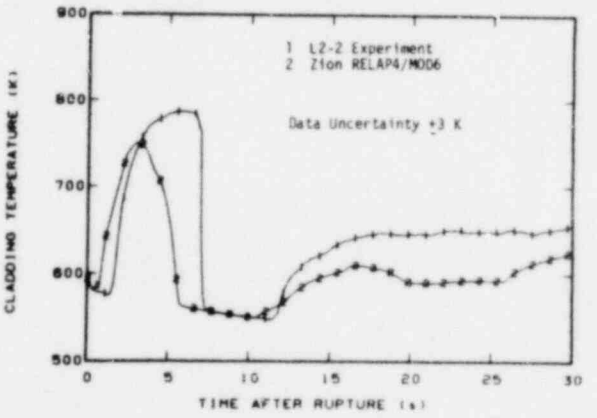

CLADDING TEMPERATURE IN THE PEAK
POWER REGION

Figure 17. LOFT data and Zion prediction comparisons for LOCE L2-3 initial conditions.

1600 085

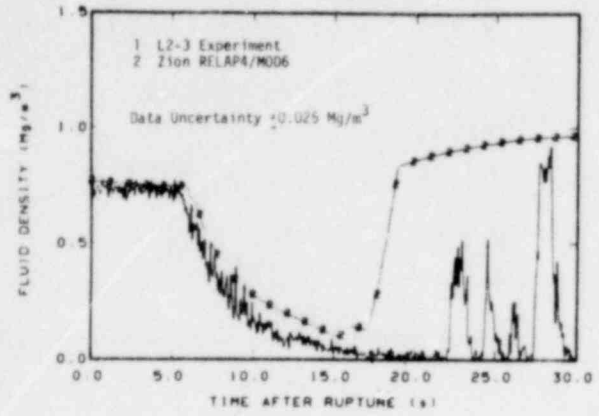

INTACT LOOP COLD LEG DENSITY

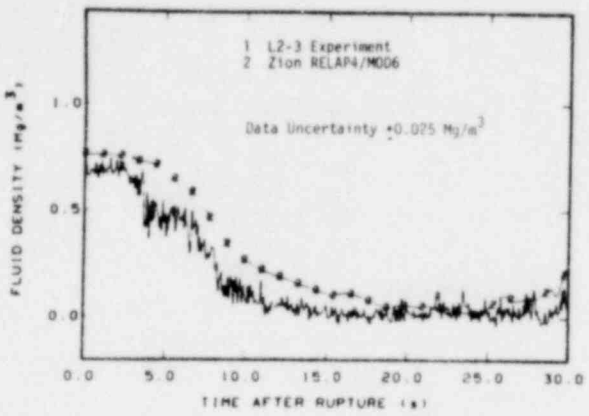

BROKEN LOOP COLD LEG DENSITY

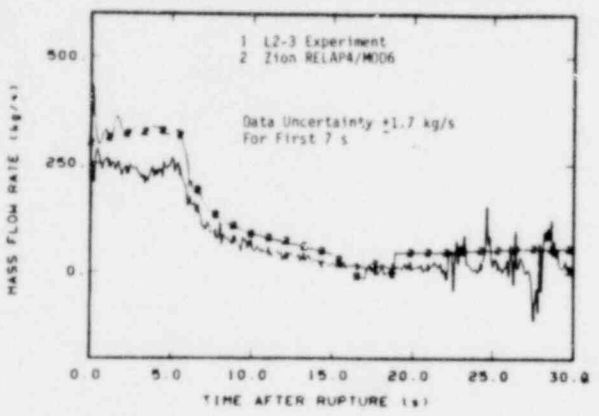

INTACT LOOP COLD LEG MASS FLOWRATE

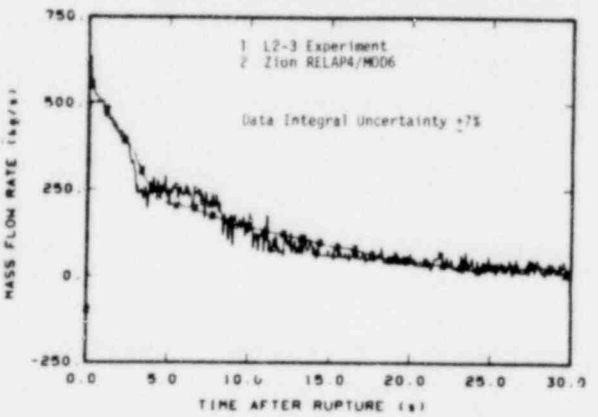

BROKEN LOOP COLD LEG MASS FLOWRATE

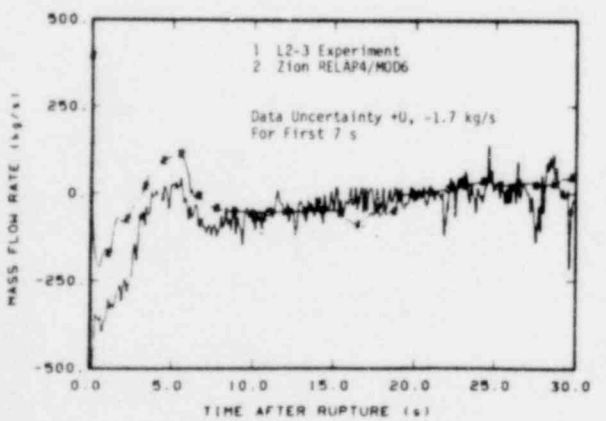

DIFFERENCE BETWEEN INTACT LOOP AND
BROKEN LOOP COLD LEG MASS FLOWRATES

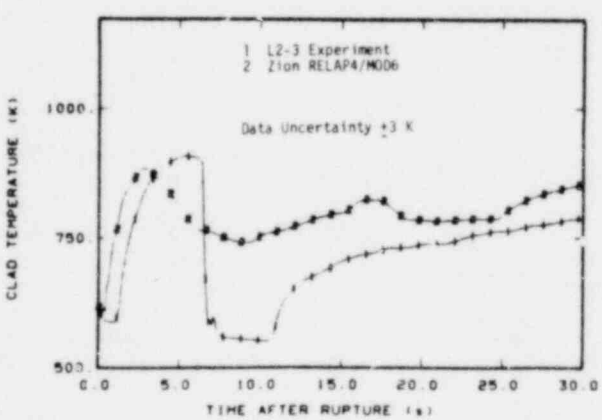

CLADDING TEMPERATURE IN THE PEAK
POWER REGION

Figure 18. LOFT data and Zion prediction comparisons for LOCE L2-3 initial conditions.

1600 086

LOCE L3-0

LOCE L3-0 was conducted with the same system and core configuration as LOCEs L2-2 and L2-3. Only minor instrumentation changes were made in order to record data for a longer time. LOCE L3-0 was an isothermal experiment with negligible nuclear decay heat power. The primary coolant pumps were tripped at the initiation of the transient. No ECC was used in LOCE L3-0. Initial conditions are given in Table 4. The experiment was initiated by opening the power operated relief valve (PORV), rather than the quick-opening blowdown valves. The experiment was terminated by opening the quick-opening valves after the pressure had reduced below normal accumulator pressure, and the LPIS was used to refill the system. The sequence of events for LOCE L3-0 is given in Table 5.

TABLE 4. LOCE L3-0 INITIAL CONDITIONS

Parameter	Measured Value
Primary system mass flow (kg/s)	201
Pressurizer pressure (MPa)	14.7
Primary system fluid temperature (K)	557
Decay heat level (kW)	4.2
Steam generator pressure (MPa)	6.8

The data from LOCE L3-0 were not processed for 3 weeks following the experiment in order to complete computer calculations of experiment performance without the benefit of the experimental data. Since the flow characteristics of the PORV were relatively uncertain, it was necessary to use data from the early portion of the transient to determine a valve coefficient for steam flow. The valve steam flow characteristics and experiment initial conditions data were incorporated into the computer

TABLE 5. CHRONOLOGY OF EVENTS FOR LOCE L3-0

Event	Time After LOCE Initiation (s)
LOCE initiated	0
PSMG[a] power tripped	11
PCP[b] coastdown completed	15
Pressurizer reached minimum indication	48
Primary system reached saturation pressure	48
Pressurizer indicated full	73
Pressurizer returned to indicating range	1420
Broken loop isolation valves opened	2416
Quick-opening blowdown valves opened	2460
End of saturation blowdown	2490
LPIS initiated	2535

a. PSMG - primary system motor generator.

b. PCP - primary coolant pump.

calculations performed with the RELAP4/MOD6[a], RELAP4/MOD7[b], RELAP5[c], and TRAC-P1A[d] computer codes. (Only 87 s of transient time were calculated with RELAP4/MOD7.)

The measured and calculated pressure response are shown in Figure 19. While all of the computer models accurately calculated the steam depressurization phase, none of the models were accurate for the long-term

a. RELAP4/MOD6, Idaho National Engineering Laboratory Configuration Control Number H007561B.

b. RELAP4/MOD7, Idaho National Engineering Laboratory Configuration Control Number H013382B.

c. RELAP5, Update Cycle 102, Idaho National Engineering Laboratory.

d. TRAC-P1A, Los Alamos Scientific Laboratory.

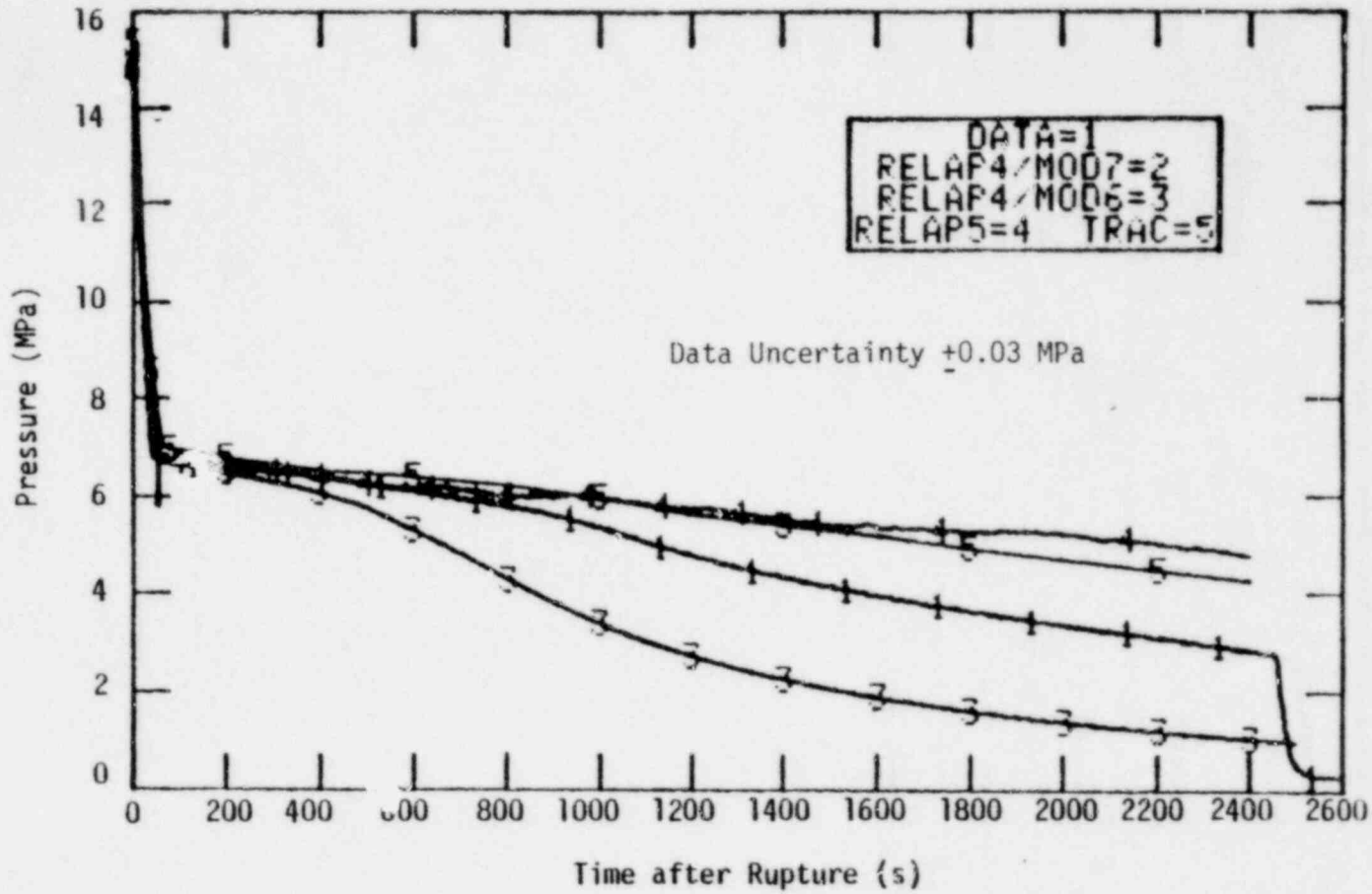

Figure 19. Calculated and measured primary system pressure for LOCE L3-0.

pressure response where saturated liquid and/or two-phase flow was passing through the PORV. The valve characteristics in two-phase flow and/or liquid discharge are unknown, so this result is not surprising.

Figure 20 exhibits the measured and predicted pressurizer liquid level response. The data show the pressurizer rapidly filled after the system pressure reached system saturation and remained full until 1400 s. The indicated level shown was not compensated for fluid temperature and, thus, does not assure that the pressurizer was completely full for the whole time it was indicated full. In fact, correcting the indicated level for temperature makes it almost match the RELAP4/MOD6 calculation. While all the calculations showed the initial decrease and rapid increase in pressurizer level, neither TRAC-P1A (not shown) nor RELAP5 calculated a full pressurizer; whereas, RELAP4/MOD6 and RELAP4/MOD7 calculations did.

The measured density in the intact loop hot leg near the top of the pipe is shown in Figure 21. These data indicate stratified flow in the pipe with steam at the top. The surge line, which connects the pressurizer to the intact loop hot leg, connects to the top of the hot leg pipe. The LOFT surge line does not contain a loop seal; that is, the pipe from the hot leg to the pressurizer first rises, is horizontal, and then rises again. The pressurizer may have remained full after the time that steam was known to exist in the intact loop hot leg. However, this conclusion cannot be confirmed with measured data from LOCE L3-0.

CONCLUSIONS

The main conclusions reached from analysis of the LOFT LOCEs L2-2 and L2-3 are as follows:

1. The behavior of LOCEs L2-2 and L2-3 was dominated by the occurrence of a core-wide early rewet of the fuel rod cladding. This rewet occurred from a rereversal of core flow caused by a critical flow transition at the broken loop cold leg piping.

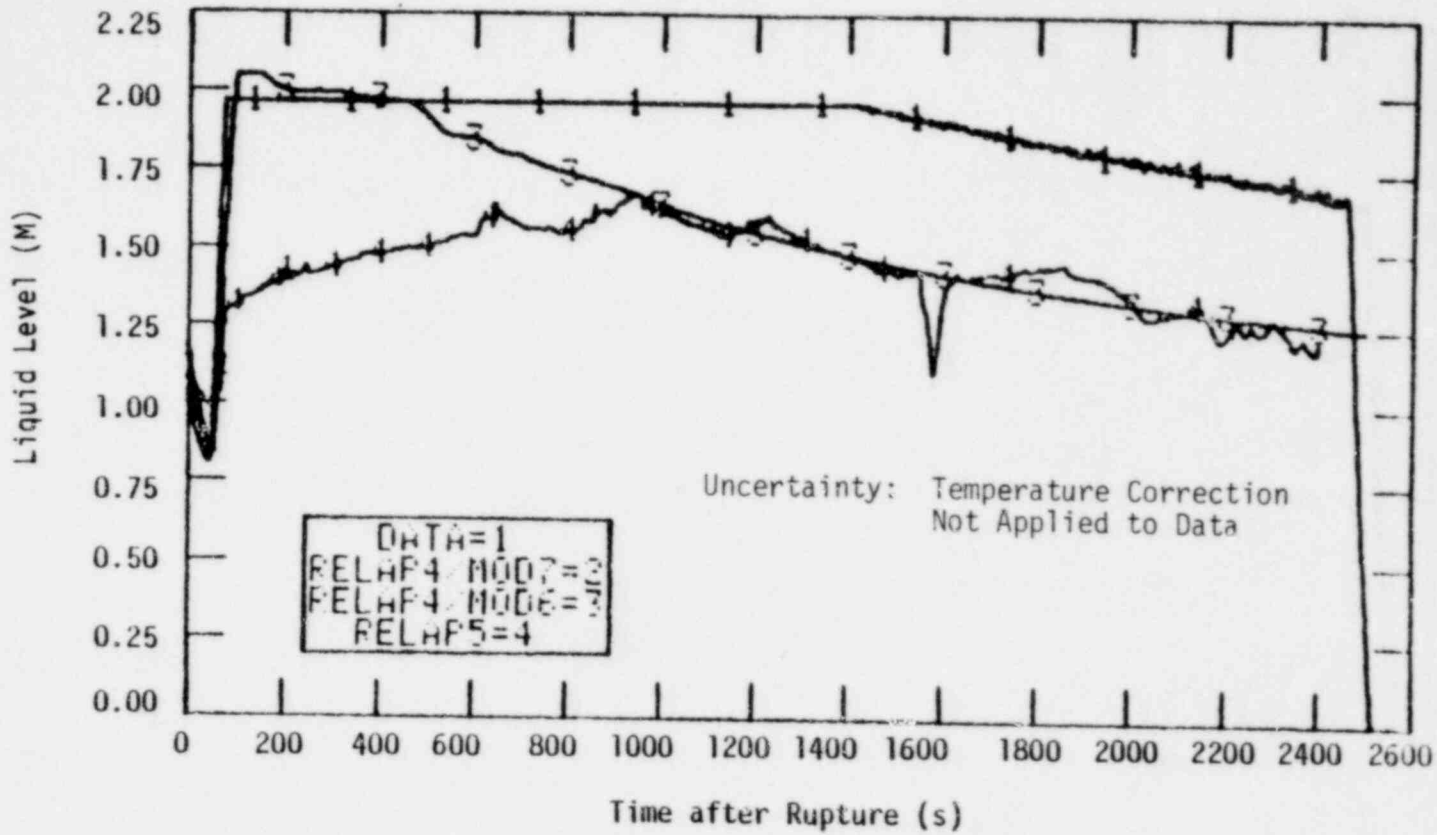

Figure 20. Calculated and measured liquid level in pressurizer for LOCE L3-0.

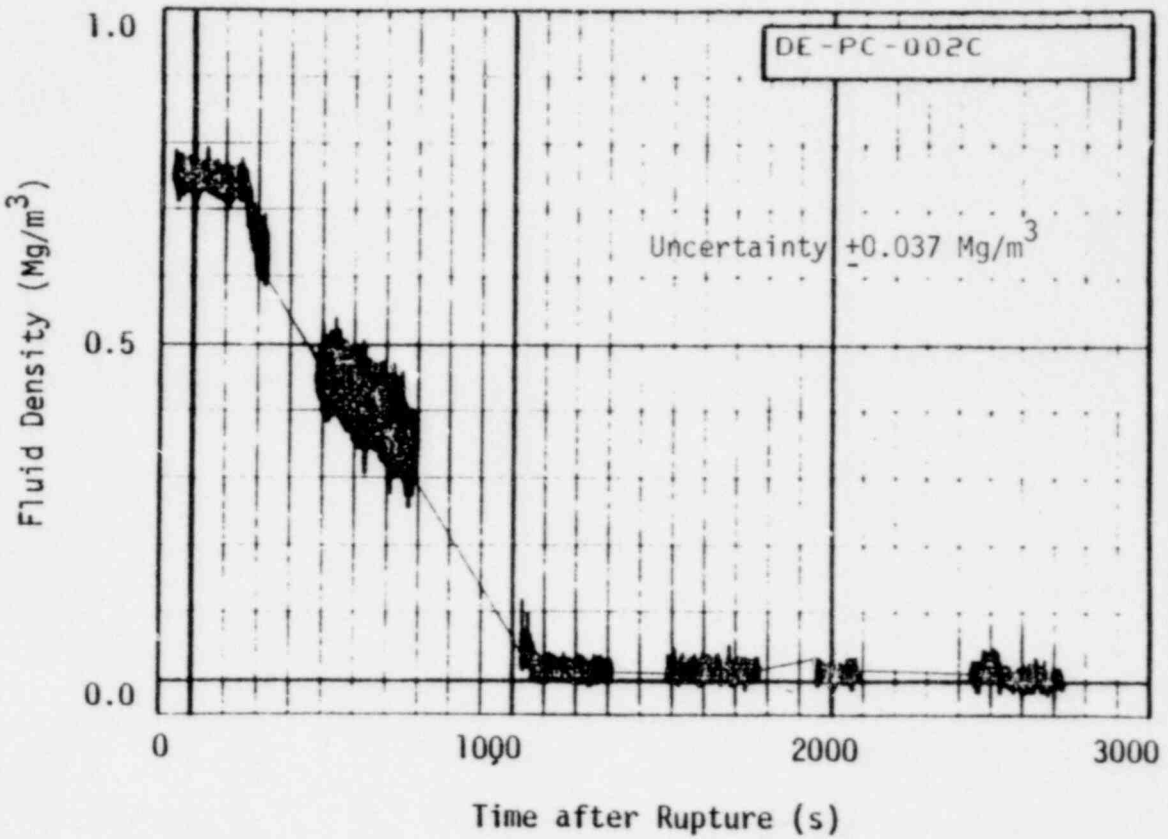

Figure 21. Fluid density in intact loop hot leg (chordal density) for LOCE L3-0.

2. Analytical model predictions of LOCEs L2-2 and L2-3 provided a good prediction of system hydraulics but did not predict the core-wide rewet. The model "deficiencies" identified as needing further work in order to improve the best estimate predictive capability (the original models are conservative) are as follows:

   a. Critical flow in the transition region from subcooled discharge to saturated discharge

   b. Wave transport of density variations, particularly as they affect discharge flow and rewet

   c. High pressure (≈6 MPa), low quality (0.1 to 0.3), low flow film boiling, and rewet heat transfer.

3. Analysis of a commercial PWR with the models that best predict LOFT behavior indicate the same expected response as observed in LOFT which means that LOFT is scaled correctly to represent commercial PWR behavior. Therefore, commercial PWRs are likely to experience the same cladding rewet in the event of a large LOCA which implies there is significantly more conservatism in the reactor safety analysis requirements of 10 CFR 50.46, Appendix K than previously envisioned.

The main conclusions reached to date from analysis of LOCE L3-0 are as follows:

1. During a LOCA caused by a break at the top of the pressurizer, for example, a PORV stuck open, the pressurizer starts filling when the primary system fluid saturates someplace other than the pressurizer itself. The pressurizer fills and may remain full even though steam exists in the hot leg piping and there is no loop seal in the pressurizer surge line.

2. The pressurizer level indication indicates a higher level than occurs in the pressurizer, as the indicated level is not compensated for fluid temperature.

3. The RELAP4/MOD6 model of LOCE L3-0 small break predicted the trends of the observed behavior, but more testing and modeling experience are needed to make the predictive capability for the small break as good as for the large break.

REFERENCES

1. E. J. Kee and W. H. Grush, Best Estimate Prediction for LOFT Nuclear Experiment L2-3, EG&G Idaho, Inc., internal report EP-L2-3, April 1979.

2. J. R. White, W. H. Grush, C. D. Keeler, Preliminary Posttest Analysis of LOFT Loss-of-Coolant Experiment L2-2, EG&G Idaho, Inc., internal report LTR 20-103, June 1979.

3. W. H. Grush et al, Best Estimate Experiment Predictions for LOFT Nuclear Experiments L2-2, L2-3 and L2-4, EG&G Idaho, Inc., internal report LOFT-TR-101, November 1978.

RELATED REFERENCES

1. W. H. Grush et al, Experiment Prediction for LOFT Nonnuclear Experiment L1-5, TREE-NUREG-1209, March 1978.

2. P. G. Prassinos, Quick Look Report on LOFT Nonnuclear Experiment L1-5, May 1978.

3. M.S. Jacoby, Isothermal Test With Core 1 Installed, June 1978.

4. D. L. Reeder, LOFT System and Test Description (5.5 ft Nuclear Core 1 LOCEs), NUREG/CR-0247, TREE 1208, July 1978.

5. P. A. Harris, T. K. Samuels, H. J. Welland, LOFT Experiment Operating Specification, Vol. 2 Power Ascension Test Series L2, Rev. 2, July 1979.

6. J. R. White et al, Best Estimate Experiment Predictions for LOFT Nuclear Experiments L2-2, L2-3, and L2-4, November 1978.

7. E. J. Kee and W. H. Grush, Best Estimate Prediction for LOFT Nuclear Experiment L2-3, April 1979.

8. D. L. Batt, Quick Look Report on LOFT Nuclear Experiment L2-2, December 1978.

9. M. McCormick-Barger, Experiment Data Report for LOFT Power Ascension Test L2-2, NUREG/CR-0492, TREE-1322, February 1979.

10. D. L. Reeder, Quick Look Report on LOFT Nuclear Experiment L2-3, May 1979.

11. P. G. Prassinos et al, Experiment Data Report for LOFT Power Ascension Experiment L2-3, NUREG/CR-0792, TREE-1326, July 1979.

12. C. W. Solbrig, "Current Capabilities of Transient Two-Phase Flow Instruments," ISA Conference, Anaheim, California, May 7-10, 1979.

13. G. D. Lassahn et al, "LOFT Advanced Densitometer for Nuclear LOCE," ISA Conference Anaheim, California, May 7-10, 1979.

14. L. D. Goodrich, "LOFT Two-Phase Flow Data Integrity Analysis," ISA Conference, Anaheim, California, May 7-10, 1979.

15. L. D. Goodrich and D. L. Batt, "LOFT Liquid Level Transducer Application Techniques and Measurement Uncertainty," ISA Conference, Anaheim, California, May 7-10, 1979.

16. R. R. Good, "Interpreting Two State Instruments for Intermediary Values," ISA Conference, Anaheim, California, May 7-10, 1979.

17. R. R. Good, "Binary Signal Processing," ISA Conference, Anaheim, California, May 7-10, 1979.

18. C. W. Solbrig, "Current Capabilities of Transient Two-Phase Flow Instruments," ISA Conference, Anaheim, California May 7-10, 1979.

19. J. H. Linebarger et al, "LOFT Experiment L2-2 Analysis of First Ten Seconds of Blowdown," ASME Conference, San Francisco, California, June 25-29, 1979.

20. W. C. Phoenix, "Third U.S. National Congress on Pressure Vessels and Piping LOFT Power Range Testing Program," ASME Conference San Francisco, California, June 25-29, 1979.

21. W. H. Grush and J. R. White, "RELAP4 Posttest Analysis of LOFT LOCE L2-2," ASME Conference, San Francisco, California, June 25-29, 1979.

22. M. A. Langerman and E. A. Harvego, "An Analysis of LOFT Scaling Distortions," ASME Conference, San Francisco, California, June 25-29, 1979.

23. D. A. Niebruegge et al, "An Evaluation of EVEL Performance During LOFT Test L2-2 and Comparison with Predictions," International Colloquium on Irradiation, Petten, Netherlands, June 25-28, 1979.

24. J. D. Burtt, "Overview of the LOFT Experimental Program," International Colloquium on Irradiation, Petten, Netherlands, June 25-28, 1979.

25. D. A. Niebruegge, "Nuclear Fuel Rod Behavior During LOFT Experiment L2-2," International Colloquium on Irradiation, Petten, Netherlands, June 25-28, 1979.

26. C. L. Nalezny et al, "Performance Evaluation of a Drag-Disc Turbine Transducer and Three Beam Gamma Densitometer Under Transient Two-Phase Flow Conditions," International Colloquium on Two-Phase Flow Instrumentation, Idaho Falls, Idaho, June 11-14, 1979.

27. L. D. Goodrich et al, "INEL Conductivity Liquid Level Transducer," International Colloquium on Two-Phase Flow Instrumentation, Idaho Falls, Idaho, June 11-14, 1979.

28. A. G. Stephens and G. D. Lassahn, "X-Ray and Gamma Ray Densitometer," International Colloquium on Two-Phase Flow Instrumentation, Idaho Falls, Idaho, June 11-14, 1979.

29. M. L. Russell, "LOFT Fuel Design and Operating Experience," ANS Conference, Atlanta, Georgia, June 3-8, 1979.

30. K. Tasaka, "Sensitivity of Decay Powers of Uncertainty," ANS Conference, Atlanta, Georgia, June 3-8, 1979.

31. T. H. Howell and H. S. Selcho, "LOFT Reactor Advanced Instrumented Center Fuel Bundle," ANS Conference, Atlanta, Georgia, June 3-8, 1979.

32. E. L. Tolman and D. A. Niebruegge, "LOFT Nuclear-Fuel Rod Behavior," ANS Conference, Portland, Oregon, April 29 - May 2, 1979.

33. J. C. Lin et al, "Experiment Predictions of LOFT Reflood Behavior Using the RELAP4/MOD6," ANS Conference, Williamsburg, Virginia, April 23-25, 1979.

34. T. H. Chen and C. L. Nalezny, "Performance Evaluation of a Drag-Disc Turbine Transducer and Gamma Densitometer Under Transient Conditions," Multi-Phase Flow Heat Transfer Symposium, Miami, Florida, April 16-18, 1979.

35. D. L. Reeder et al, "The Loss-of-Fluid Test (LOFT) Facility," 14th Intersociety Energy Conversion Engineering Conference, Boston, Massachusetts, August 5-10, 1979.

36. J. H. Linebarger et al, "LOFT Isothermal and Nuclear Experiment Results," 14th Intersociety Energy Conversion Engineering Conference, Boston, Massachusetts, August 5-10, 1979.

37. G. G. Neff et al, "Instrumentation for Localized Measurements in Two-Phase Flow Conditions," 14th Intersociety Energy Conversion Engineering Conference, Boston, Massachusetts, August 5-10, 1979.

38. C. W. Solbrig and J. Riemann, "Calibration of Drag Disc Turbine Transducer and a Gamma Beam Densitometer to Measure the Mass Flow Rate in Separated Horizontal Two-Phase Flow," 14th Intersociety Energy Conversion Engineering Conference, Boston, Massachusetts, August 5-10, 1979.

Results of LOFT Loss-of-Coolant Experiments

Presented by
J.H. Linebarger

EG&G Idaho, Inc.

LOFT System Configuration

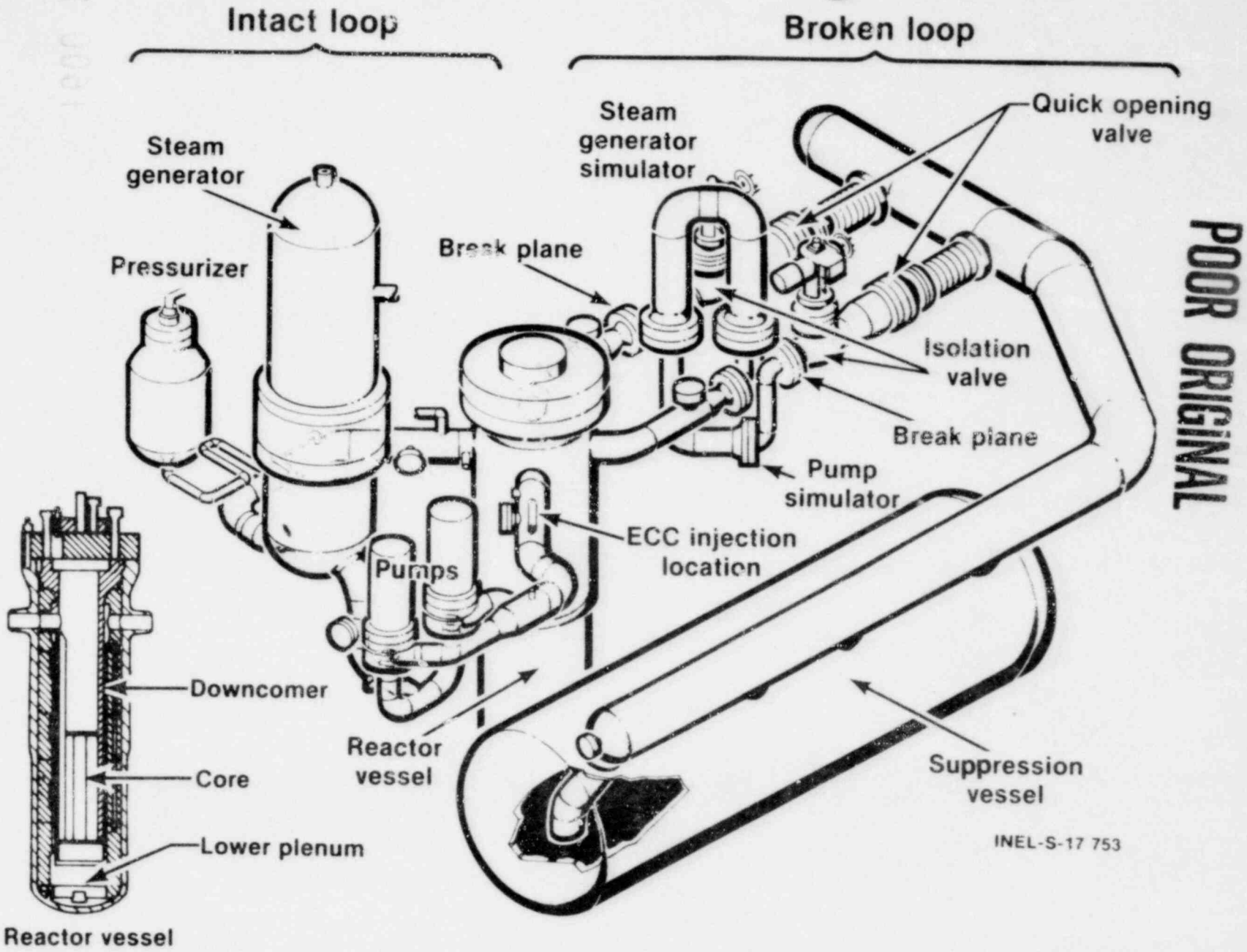

LOCEs Completed Since October 1978

Designation	Type	Date
L2-2	Nuclear, 200% DECL	Dec. 9, 1978
L2-3	Nuclear, 200% DECL	May 12, 1979
L3-0	Isothermal, Small Break, PORV	May 31, 1979

INEL-S-21 846

Contents

- L2-2/L2-3 Results and Analysis
- Blowdown Prototypic Study
- L3-0 Results and Analysis
- Summary Conclusions

L2-2/L2-3 Initial Conditions

	LOCE L2-2	LOCE L2-3
MLHGR (kW/m)	26.4	39.4
Power (MW)	24.9	36.7
Mass flow (kg/s)	194.2	199.8
ΔT (K)	22.7	32.2
P (MPa)	15.64	15.06

INEL-S-21 854

L2-3 Replica of L2-2

- Blowdown dominated
- Core thermal response tightly coupled to hydraulics
- Same event sequence

INEL-S-19 883

L2-2/L2-3 Cladding Temperature Comparison

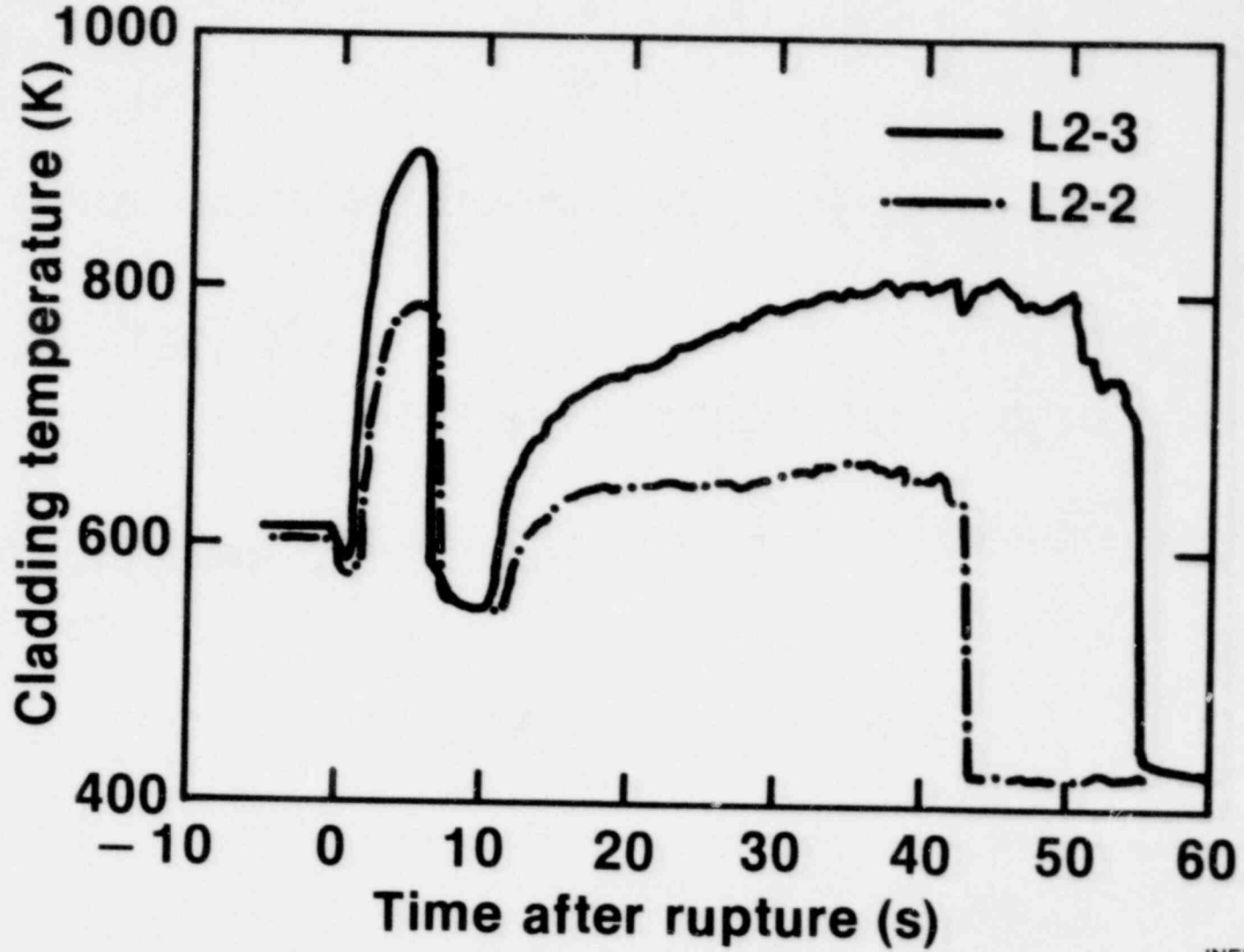

INEL-S-19 871

Thermocouples Clustered About Rod 5J8

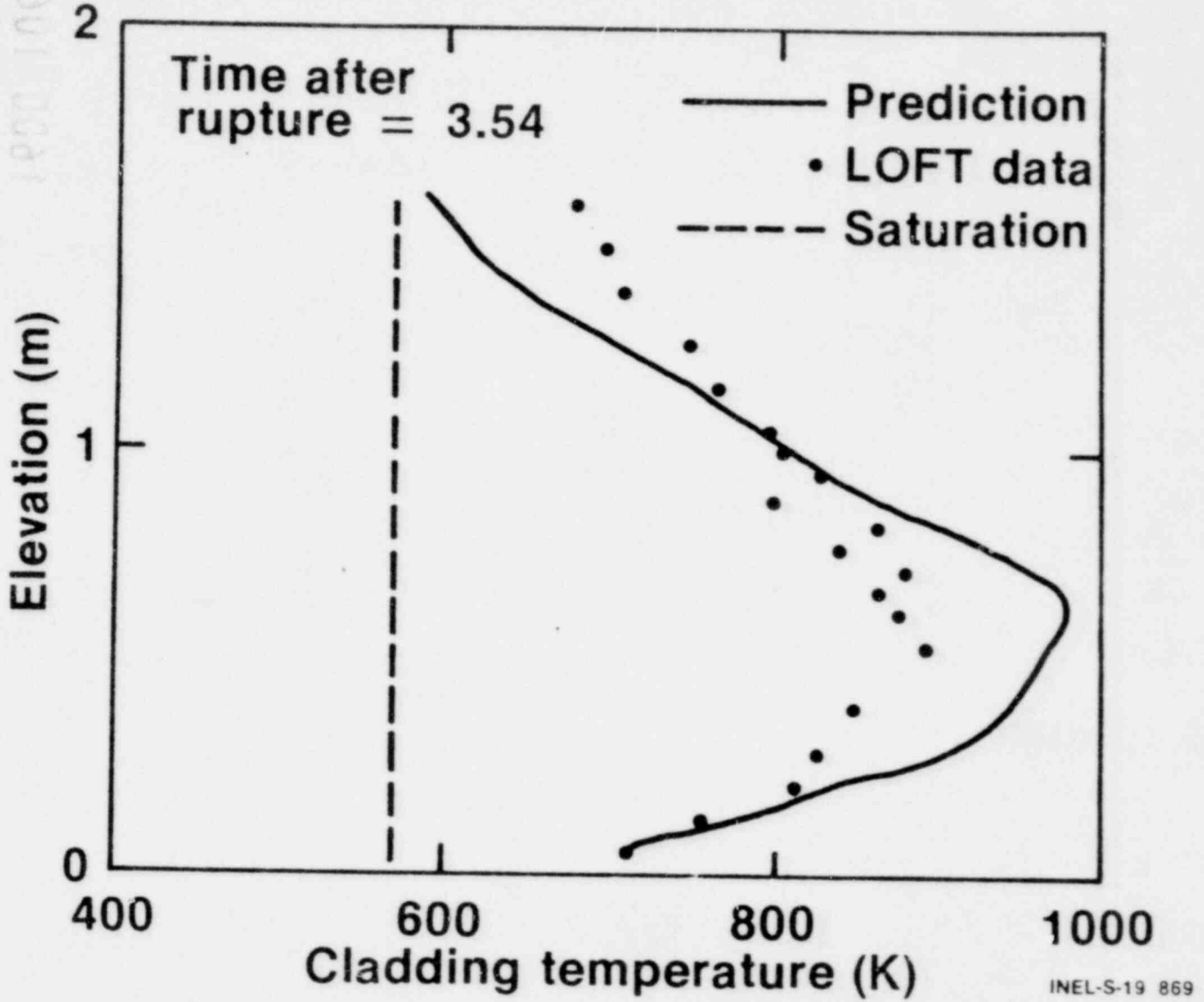

Simplified Primary Coolant System

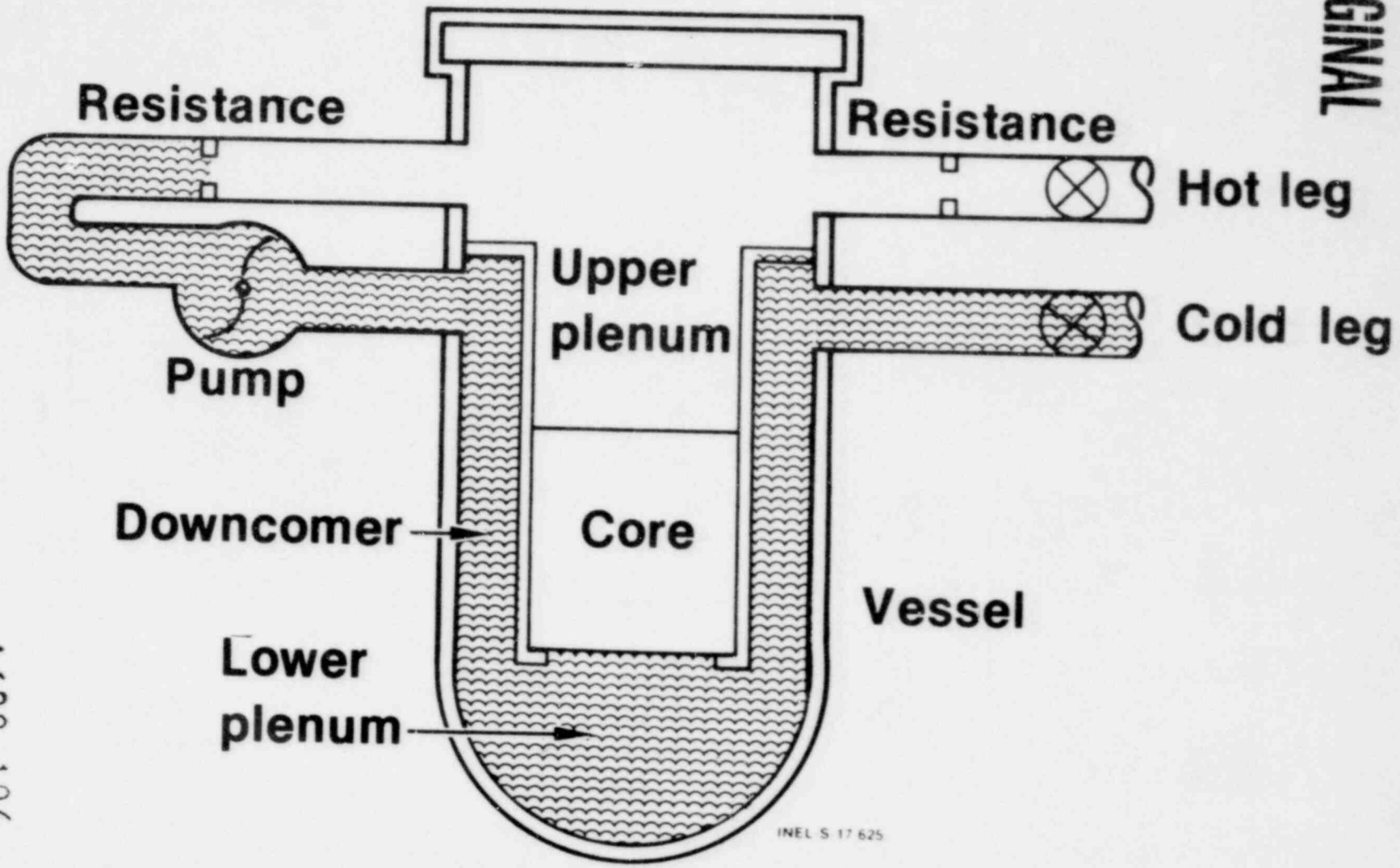

L2-3 Cold Leg Mass Flows

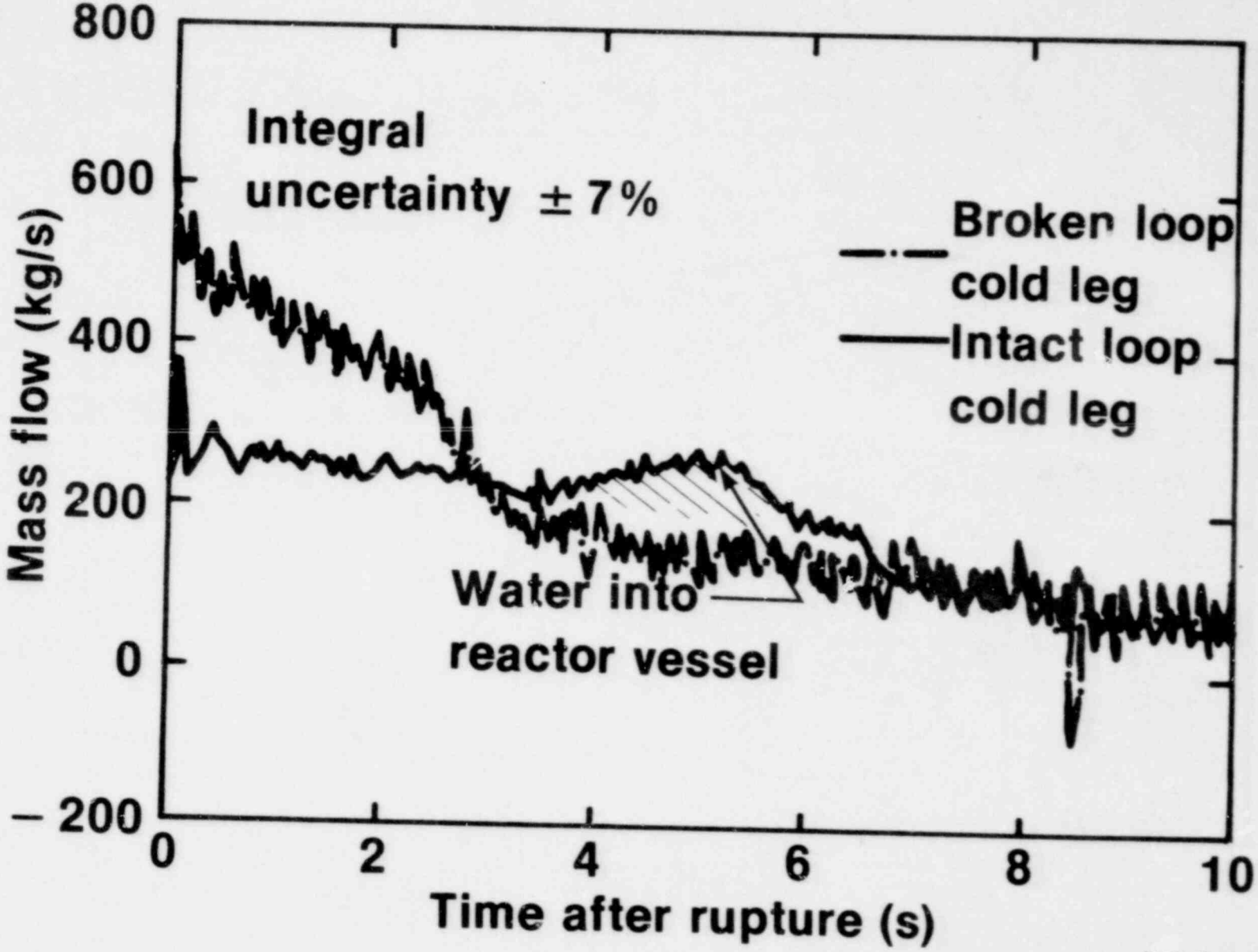

INEL-S-19 393

L2-3 Cladding Temperature vs SPND Output

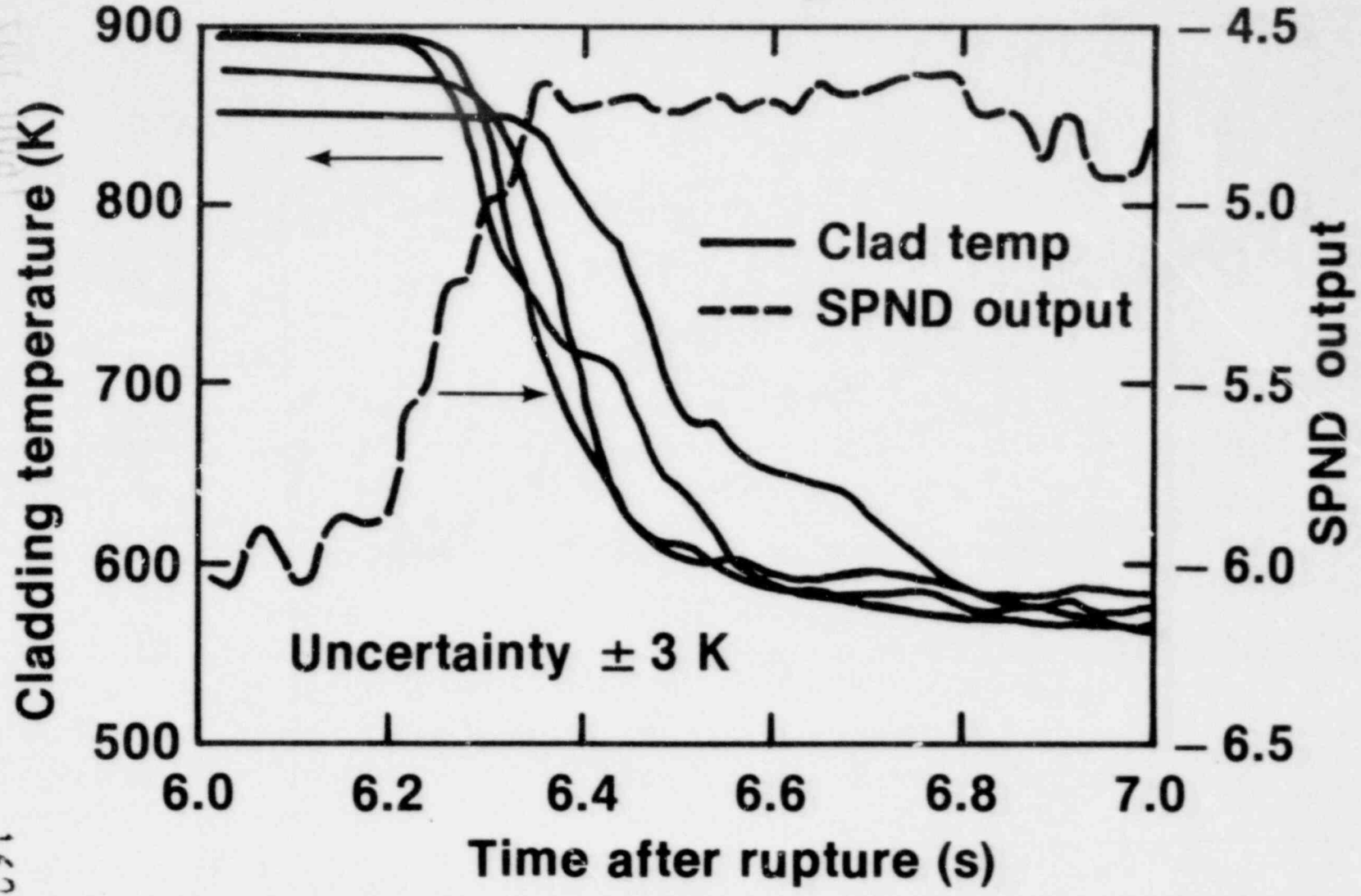

INEL-S-19 877

Conclusions

L2-2/L2-3 Results:

- **LOCES - blowdown dominated and self-limiting.**
- **During blowdown — thermal tightly coupled to hydraulics**
- **During blowdown — phenomena relative magnitudes/timing consistent with initial power/core ΔT.**

Conclusions (cont'd)

L2-2/L2-3 results: (cont'd)

- ECC fluid delivery not significantly different from L1-5
- Core rewetting during L1-5 and L2-2 virtually identical. However transient time increased 22% during L2-3
- Best-estimate calculations conservative and developmental areas are known

INEL-S-21 852

Initial Conditions

	L2-2	ZION	L2-3	ZION
Mass flow (kg/s)	194.20	18395	199.80	18395
ΔT (K)	22.70	23.90	32.20	35.80
Power (MW)	24.88	2296.60	36.70	3540.0
MLHGR (kW/m)	26.40	25.60	39.40	39.40
Tc (K)	557.70	549.80	560.70	549.80
P (MPa)	15.64	15.42	15.06	15.43

INEL-S-21 856

Fuel Cladding Temperature Comparison

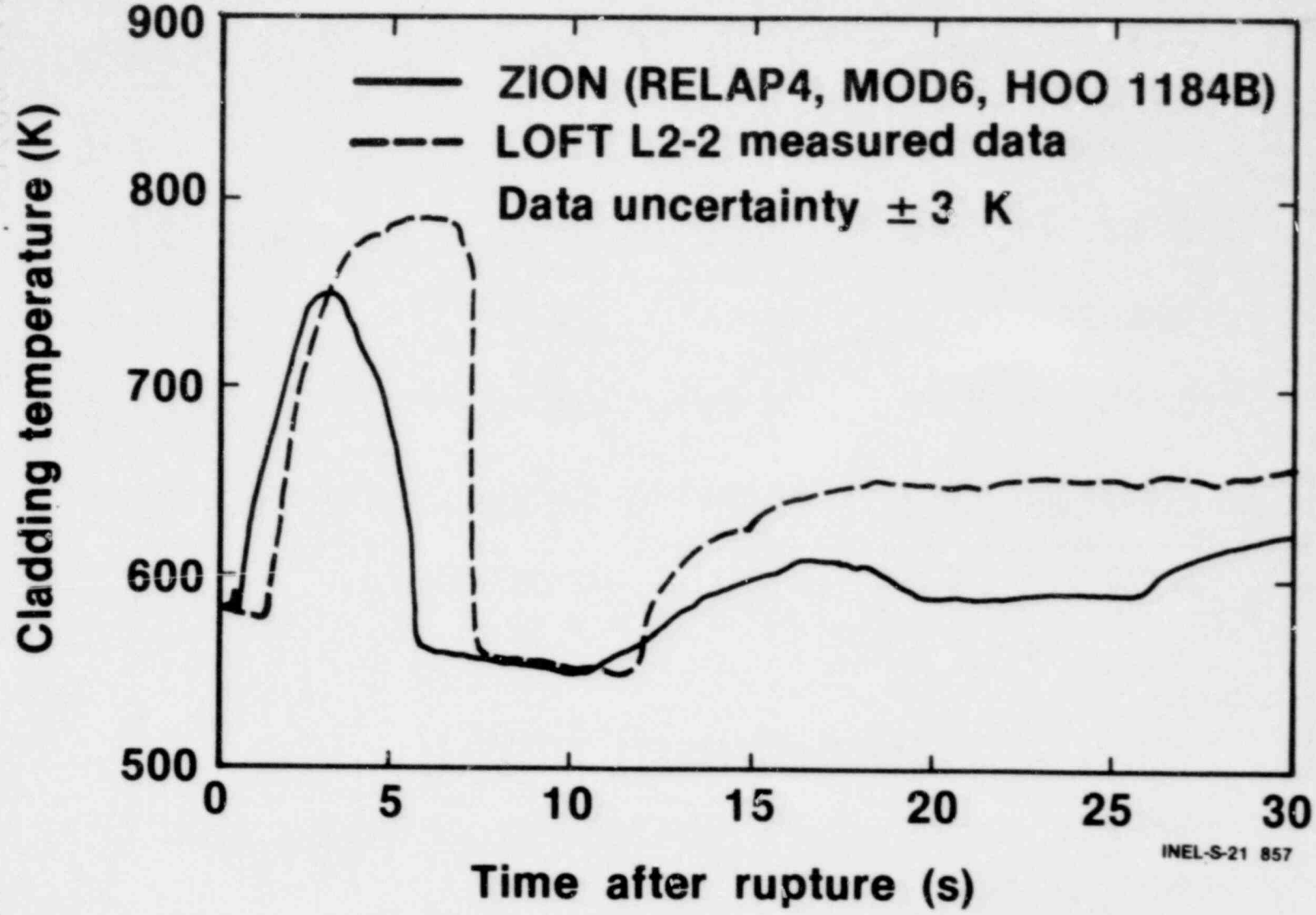

Fuel Cladding Temperature Comparison (L2-3)

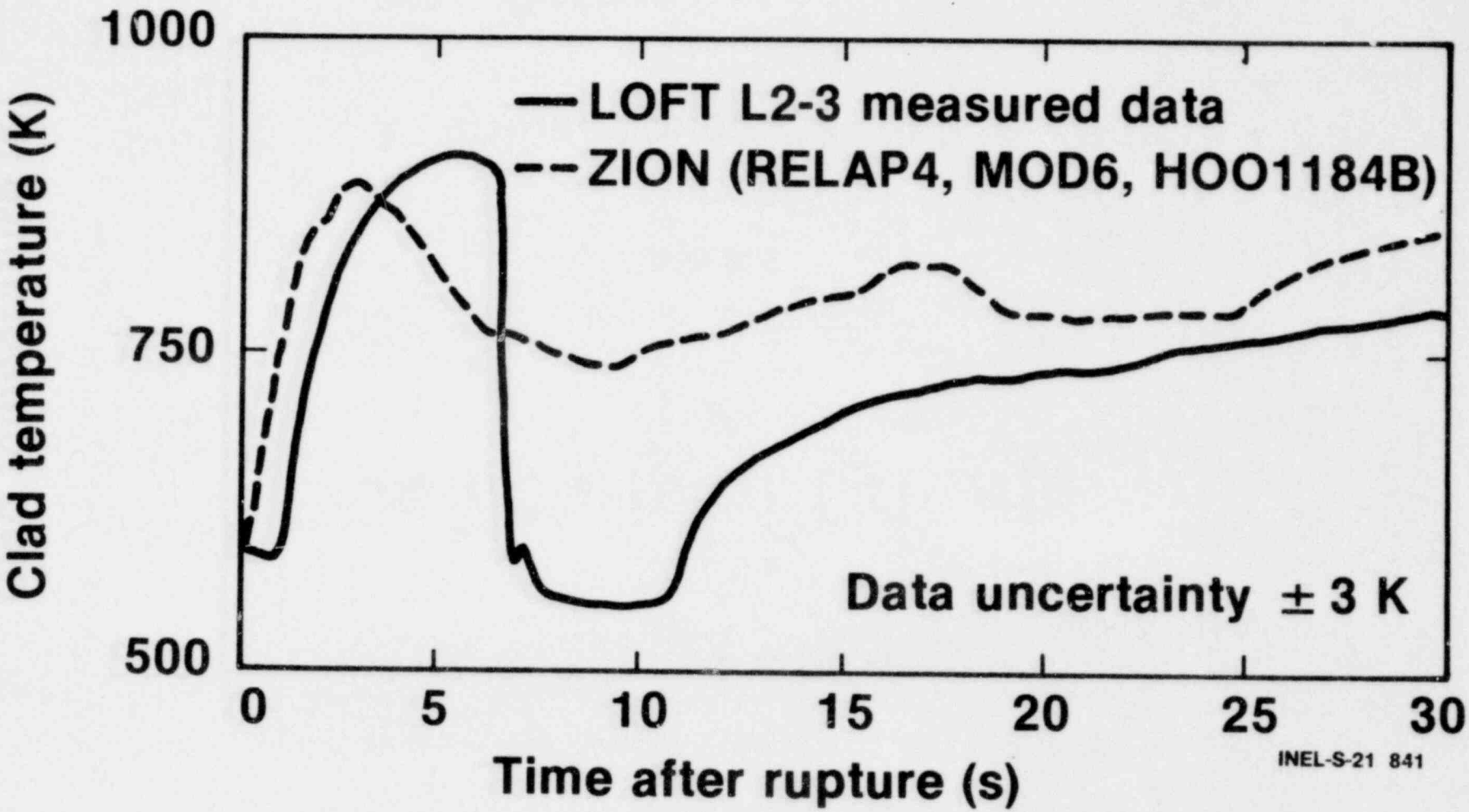

Comparison Criteria

- LOCE results
- Initial conditions
- Difference in scale

Broken Loop Cold Leg Mass Flow Comparison (L2-2)

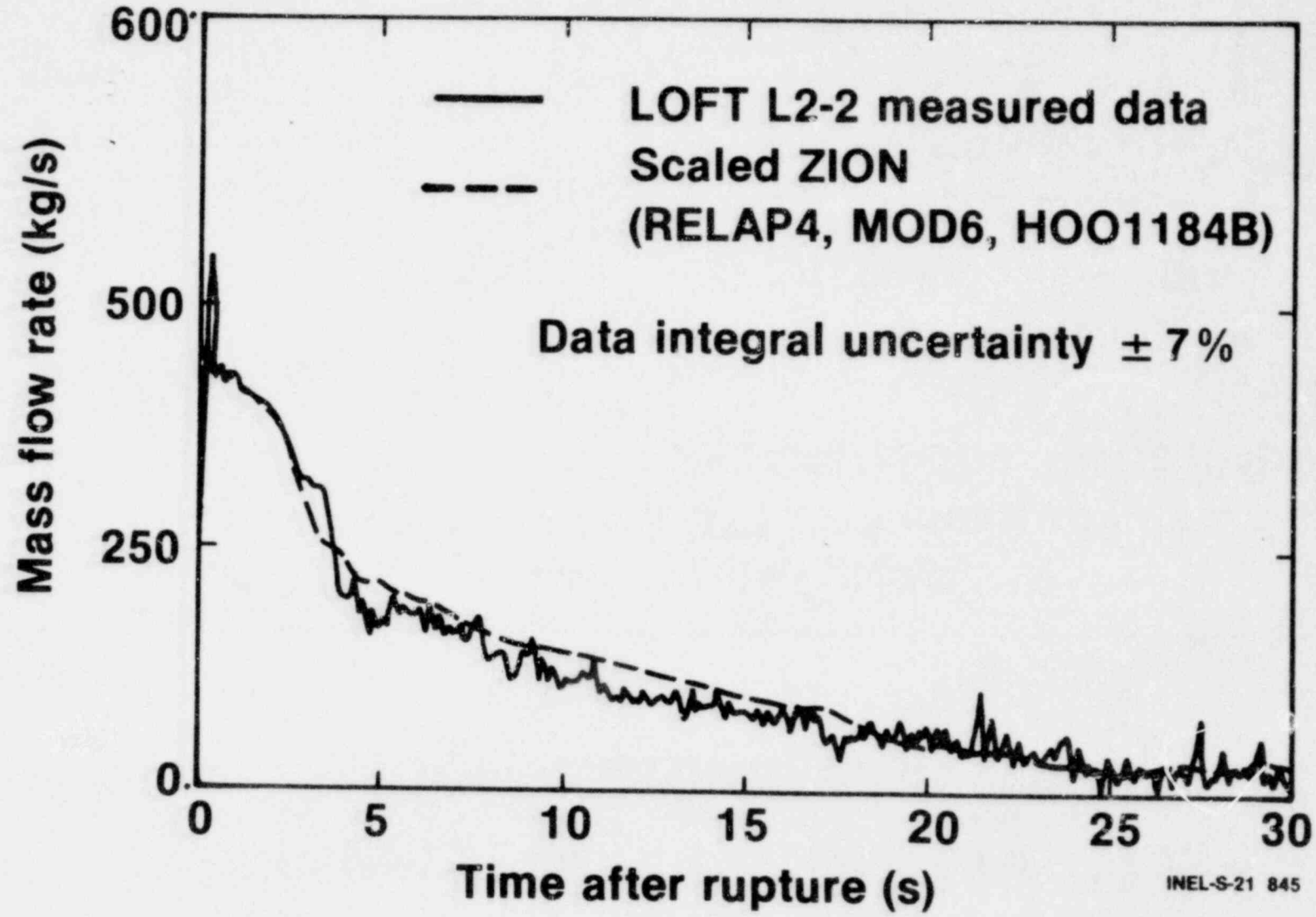

Intact Loop(s) Cold Leg Mass Flow Comparison (L2-2)

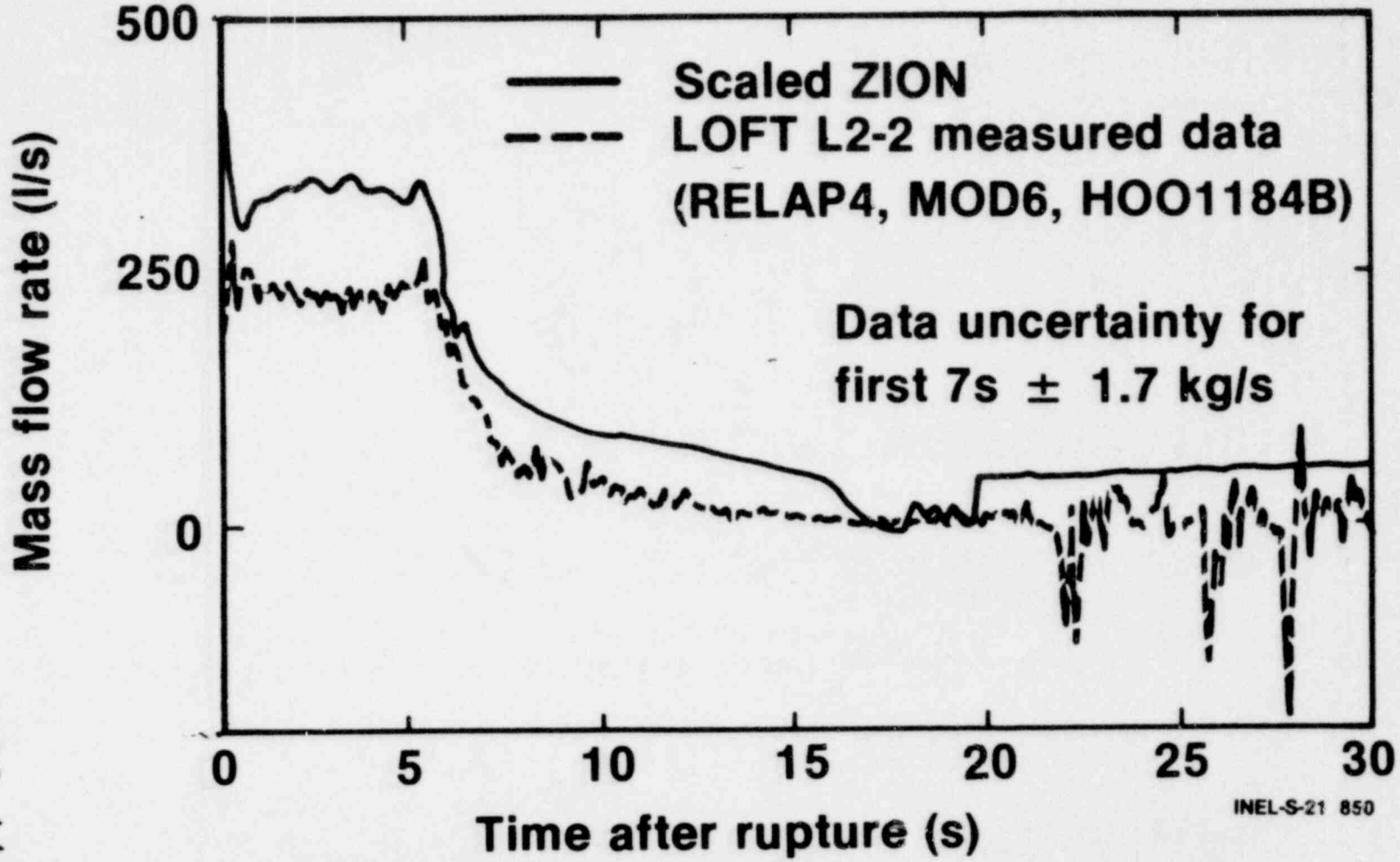

Cold Leg Mass Flow Balance (L2-2 Intact-Broken)

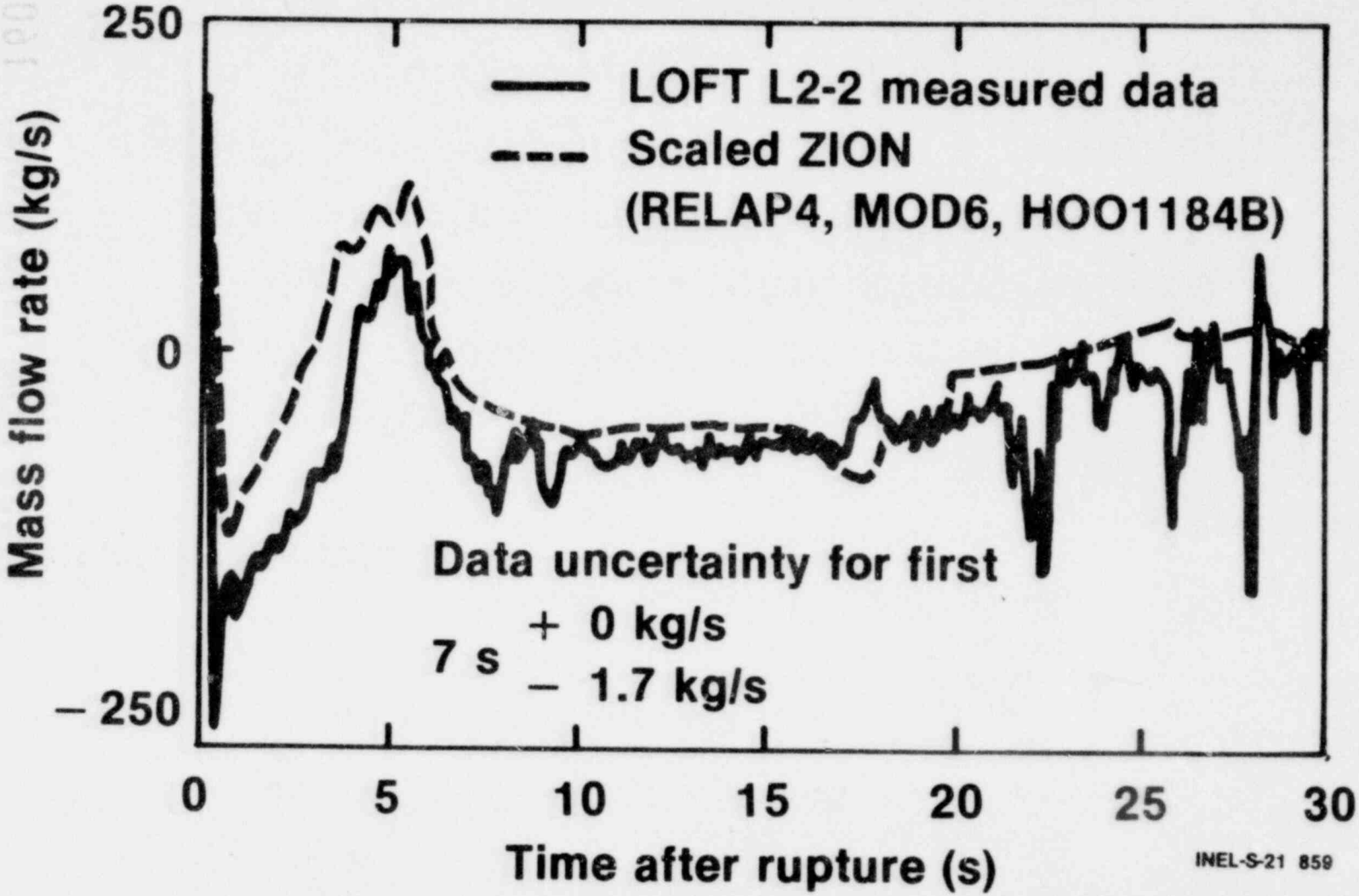

Conclusions (cont'd)

Blowdown prototypic study:

For the tests to run to date the LOFT results, relative to a commercial pressurizer water reactor, conservatively scale the dominant hydraulic phenomena during blowdown resulting in a realistic, if not conservative, indication of fuel cladding temperatures.

L3-0 Initial Conditions

P (MPa)	14.74 ± 0.07
Mass flow (kg/s)	201.0 ± 6.3
T_H (K)	556.7 ± 3.0
T_C (K)	559.7 ± 3.0

INEL-S-21 842

L3-0 Transient Conditions

Pumps tripped (s)	0 ± 0.5
Decay heat (kW)	4.2 ± 1.0
Ambient heat loss, pumps off (kW)	140.0 ± 20.0
Auto. accumulator injection control	Disabled
HPIS injection	Logic unsatisfied

INEL-S-21 839

L3-0 Primary System Pressure

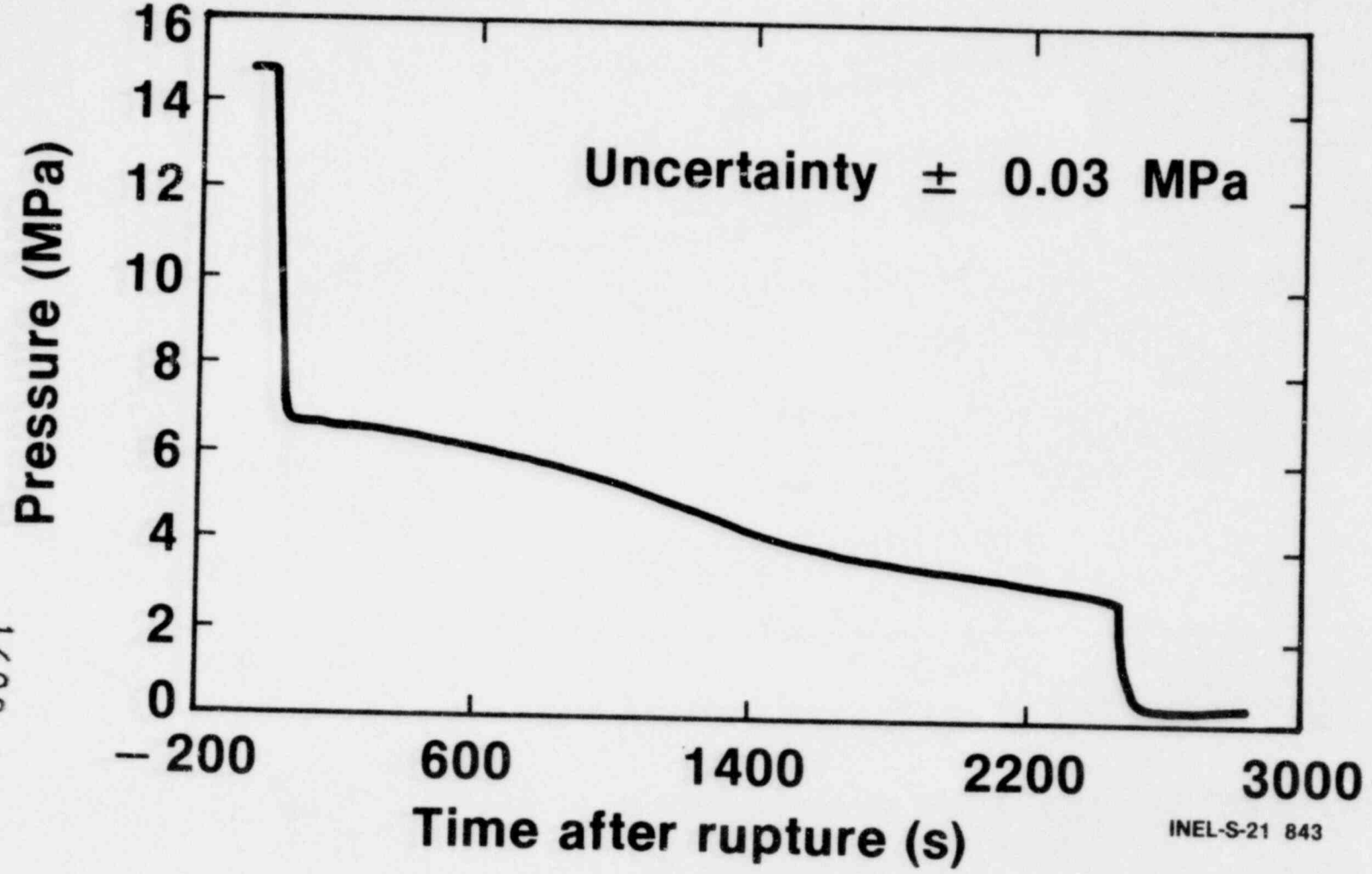

L3-0 Predicted and Measured Primary System Pressure

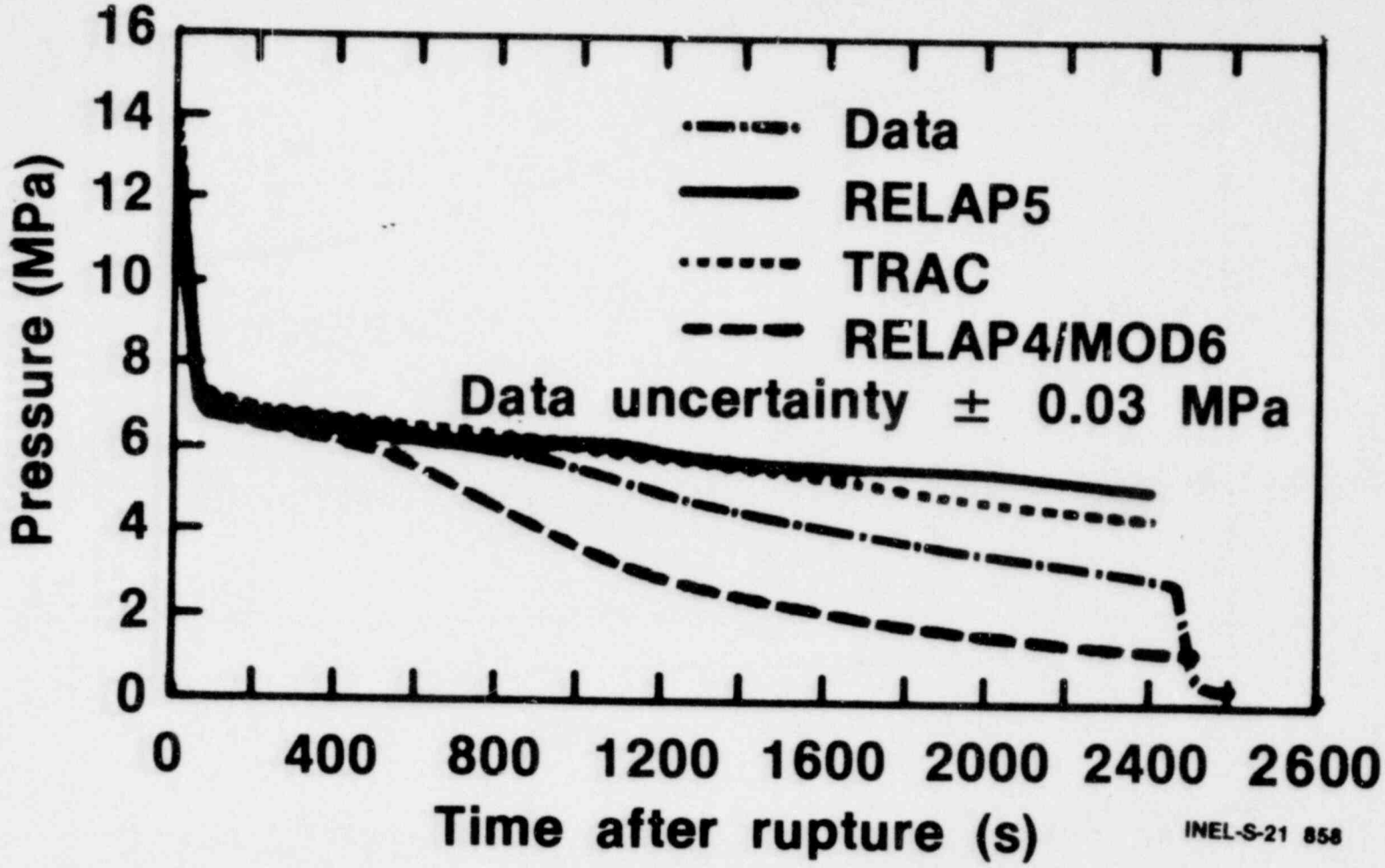

L3-0 Pressurizer Level Comparison and Intact Loop Hot Leg Fluid Density

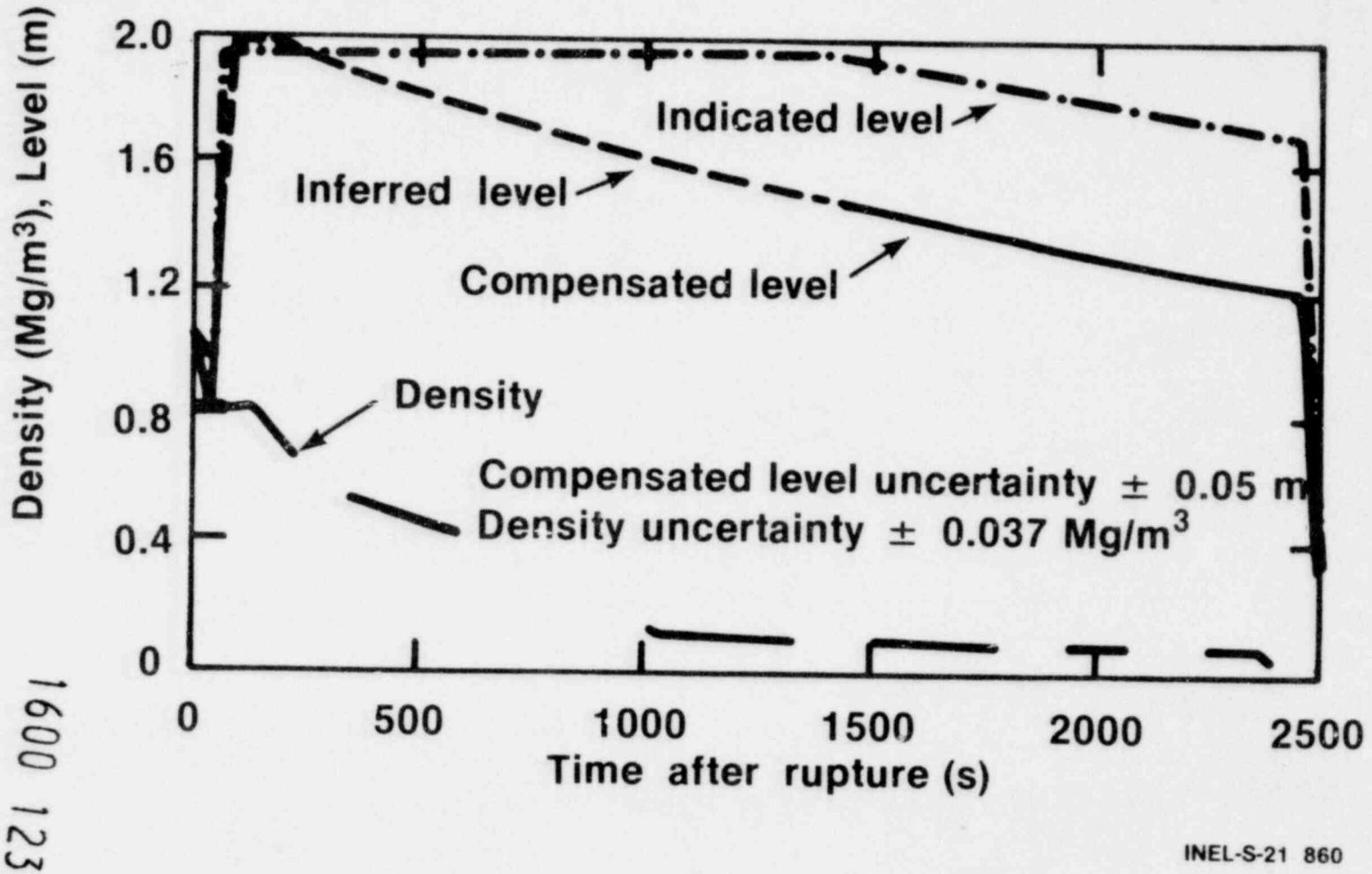

INEL-S-21 860

L3-0 Predicted and Measured Pressurizer Liquid Level

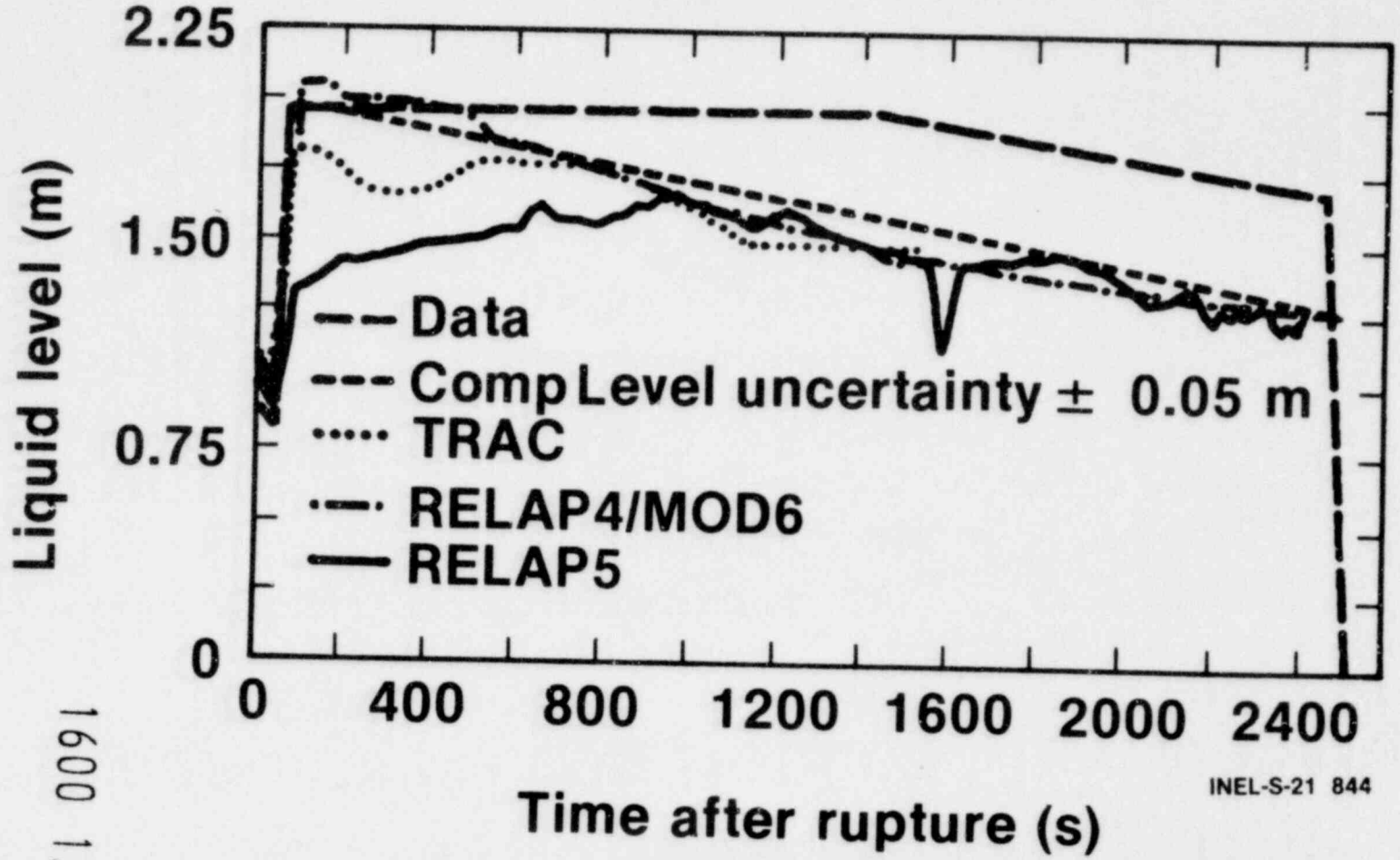

Conclusions (cont'd)

L3-0 test results:

- **Pressurizer filled after vapor generated elsewhere in system**
- **Pressurizer fluid did not return to operational level**
- **Pressurizer indicated level uncompensated for fluid temperature -indicated high**
- **Calculations predicted data trends but experience needed to upgrade capability**

Summary Conclusions

- Large break LOCEs self-limiting
- Self-limiting mechanisms understood
- Large break cladding temperatures are prototypic
- Large break calculations conservative -- developmental areas known
- Data for small break code development
- Small break code development not as advanced as large breaks

INEL-S-21 848

RESULTS OF THE PBF/LOFT LEAD ROD TEST PROGRAM

Presented at
The Seventh Water Reactor Research Information Meeting
November 5-9, 1979
Gaithersburg, Maryland

D. J. Varacalle, Jr.
EG&G Idaho, Inc.

Idaho National Engineering Laboratory
Idaho Falls, Idaho 83401

RESULTS OF THE PBF/LOFT LEAD ROD TEST PROGRAM

D. J. Varacalle, Jr.
EG&G Idaho, Inc.

The PBF/LOFT Lead Rod (PBF/LLR) Test Series consisted of four sequential, nuclear blowdown experiments (Tests LLR-3, LLR-5, LLR-4, and LLR-4A). The primary objective of the test series was to evaluate the extent of mechanical deformation that would be expected to occur to low pressure (0.1 MPa) light water reactor design fuel rods subjected to a series of nuclear blowdown tests, and to determine if subjecting deformed fuel rods to subsequent testing would result in rod failure. The results of the PBF/LLR tests have direct application to evaluating the extent of fuel rod deformation that would be expected to occur during the LOFT L2 Power Ascension Test Series[1], and the consequences of continued operation of the LOFT core with deformed fuel rods.

The extent of mechanical deformation (buckling, collapse, or waisting of the cladding) was evaluated by comparison of cladding temperature versus system pressure response with out-of-pile experimental data (Olsen[2]) and by posttest visual examinations and cladding diametral measurements.

Tests LLR-3, LLR-5, LLR-4, and LLR-4A were performed at system conditions of 595 K coolant inlet temperature, 15.5 MPa system pressure, and 41, 46, 57, and 56 kW/m test rod peak linear powers respectively, at initiation of blowdown. Mechanical deformation of the cladding was expected to occur during the early part of the blowdowns when cladding temperatures were near their maximum values and system pressure was still relatively high. During this time, the system thermal-hydraulic response was similar for all the PBF/LLR tests since the initial conditions at the time of blowdown (except rod power) were essentially the same.

Test LLR-3 was performed with four, fresh, separately shrouded LOFT design fuel rods which reached peak measured cladding temperatures from 870 to 1005 K. One rod was determined to have failed during the blowdown transient, apparently due to water-logging that resulted in subsequent ballooning and rupture. On the basis of measured temperatures no mechanical deformation is expected to have occurred to the other three fuel rods.

Two rods were replaced for Test LLR-5, and peak measured cladding temperatures ranged from 995 to 1015 K. It is possible that the cladding could have experienced some two-point buckling during this test.

Test LLR-4 was the first test of the series during which post-irradiation examination confirmed that cladding surface temperatures were sufficiently high (ranging from measured values of 1060 to 1170 K) to result in significant cladding deformation. One rod was removed following the test and visual examination revealed that the rod had indeed reached the waisting regime of mechanical deformation.

The final test, Test LLR-4A, was performed to investigate the effects of successive preconditioning cycles and LOCA transients on deformed fuel rods. Peak measured cladding temperatures ranged from 1075 to 1260 K for this test. None of the previously deformed fuel rods failed during Test LLR-4A, and visual examination of the rods after the test revealed that all four rods had reached the waisting regime of mechanical deformation.

In summary, the PBF/LLR Test Series fuel rods experienced the maximum mechanical deformation that would be expected to occur to the LOFT fuel rods during the LOFT L2 Power Ascension Test Series. The program demonstrated that deformed, low pressure, light water reactor design fuel rods, and specifically LOFT design fuel rods, will be able to withstand successive LOCA tests to the extent that will be required for completion of the planned LOFT program.

REFERENCES

1. D. L. Reeder, "LOFT System and Test Description," NUREG/CR-0247, TREE-1208, July 1978.

2. C. S. Olsen, "Zircaloy Cladding Collapse Under Off-Normal Temperature and Pressure Conditions," TREE-NUREG-1239, April 1978.

Results of the PBF/LOFT Lead Rod Test Program

Presented by
D.J. Varacalle

EG&G Idaho, Inc.

INEL-S-21 588

Outline

- PBF/LLR Program Objectives
- Experiment Description
- System Thermal-Hydraulics
- Fuel Rod Behavior
- Conclusions

PBF/LLR Test Objectives

- Experimentally evaluate the anticipated behavior of the LOFT core during the L2 Power Ascension Test Series
  - Extent of cladding collapse and waisting during the LOCA transients
  - Effects of PCI during preconditioning cycles
- Benchmark the fuel rod analysis package (FRAP) used to requalify the LOFT core after each test.

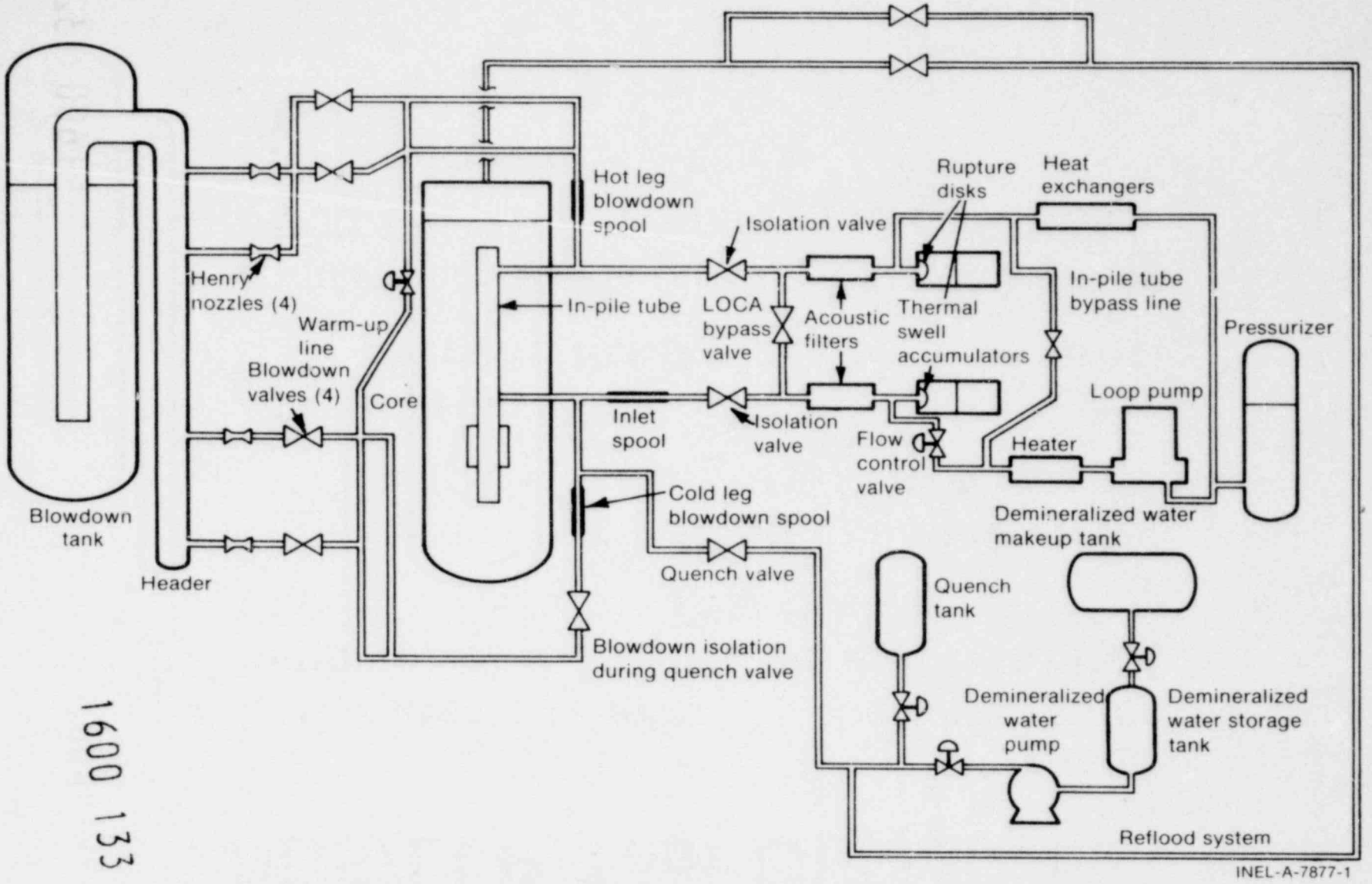
Hot leg blowdown spool
Isolation valve
Rupture disks
Heat exchangers
Henry nozzles (4)
Warm-up line
Blowdown valves (4)
Core
In-pile tube
LOCA bypass valve
Acoustic filters
Thermal swell accumulators
In-pile tube bypass line
Pressurizer
Loop pump
Inlet spool
Isolation valve
Flow control valve
Heater
Cold leg blowdown spool
Demineralized water makeup tank
Blowdown tank
Header
Quench valve
Quench tank
Blowdown isolation during quench valve
Demineralized water pump
Demineralized water storage tank
Reflood system
INEL-A-7877-1

1600 133

PBF Inpile Tube and LLR Test Train

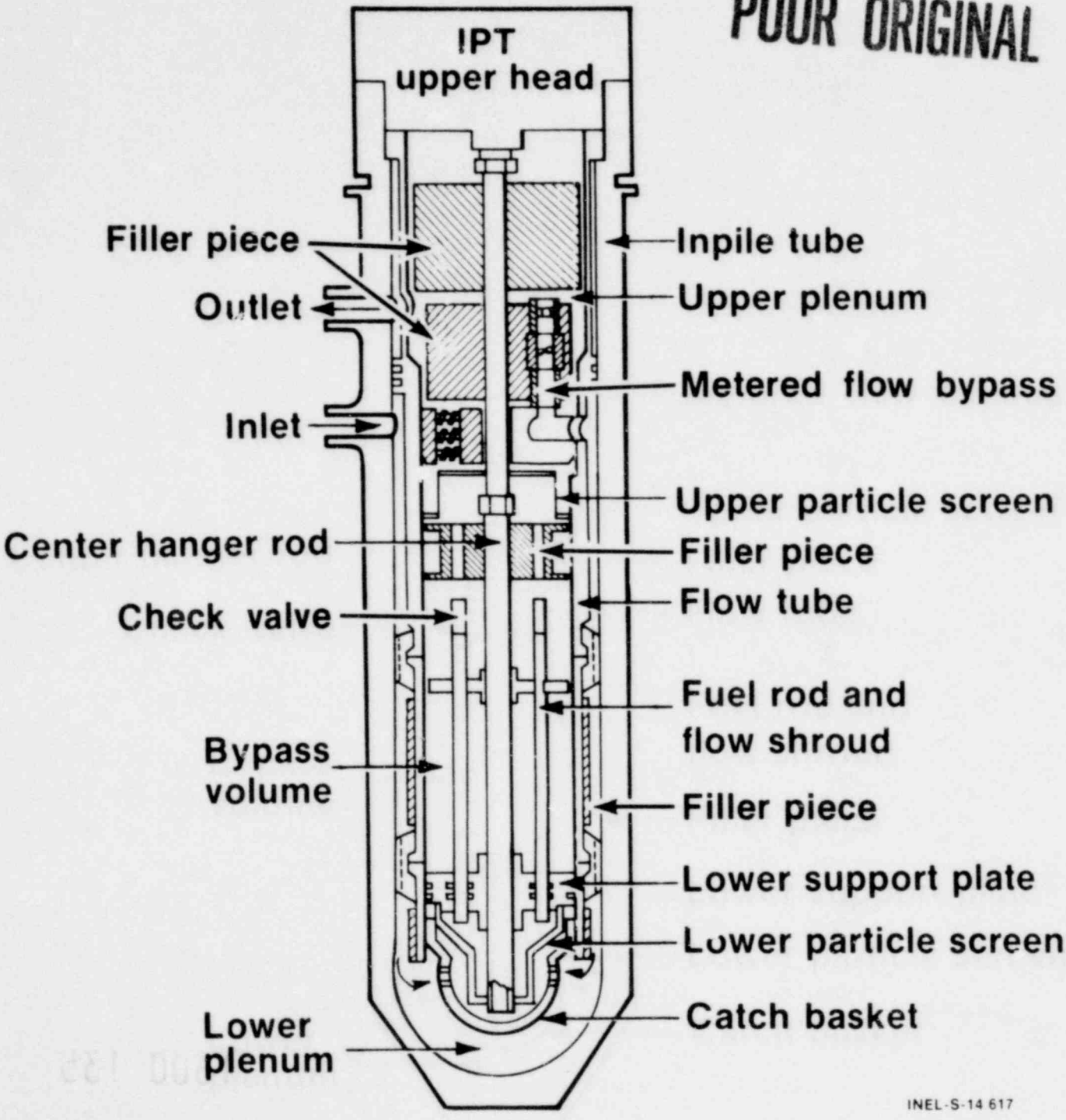

INEL-S-14 617

Nominal LLR Test Conditions

- **Pressure** — **15.5 MPa**
- **IPT inlet temperature** — **600 K**
- **Shroud flow** — **0.6 - 0.8 l/s**

INEL-S-21 590

PBF/LLR Test Initial Conditions

Test	Rod Power kW/m	Fission Heat s
LLR-3	40.5	0
LLR-5	47.4	2.0
LLR-4	56.6	2.6
LLR-4A	55.6	2.85

INEL-S-21 591

Summary LLR Tests

Test	Measured Cladding Temperatures (K)	Comments
LLR-3	870-1005	Four fresh rods Rod 312-3 failed (waterlogged) No mechanical deformation
LLR-5	995-1015	Two rods replaced Possible deformation
LLR-4	1060-1170	Mechanical deformation incurred
LLR-4A	1075-1260	One rod replaced Mechanical deformation incurred

INEL-S-21 592

Test LLR-5
System Depressurization

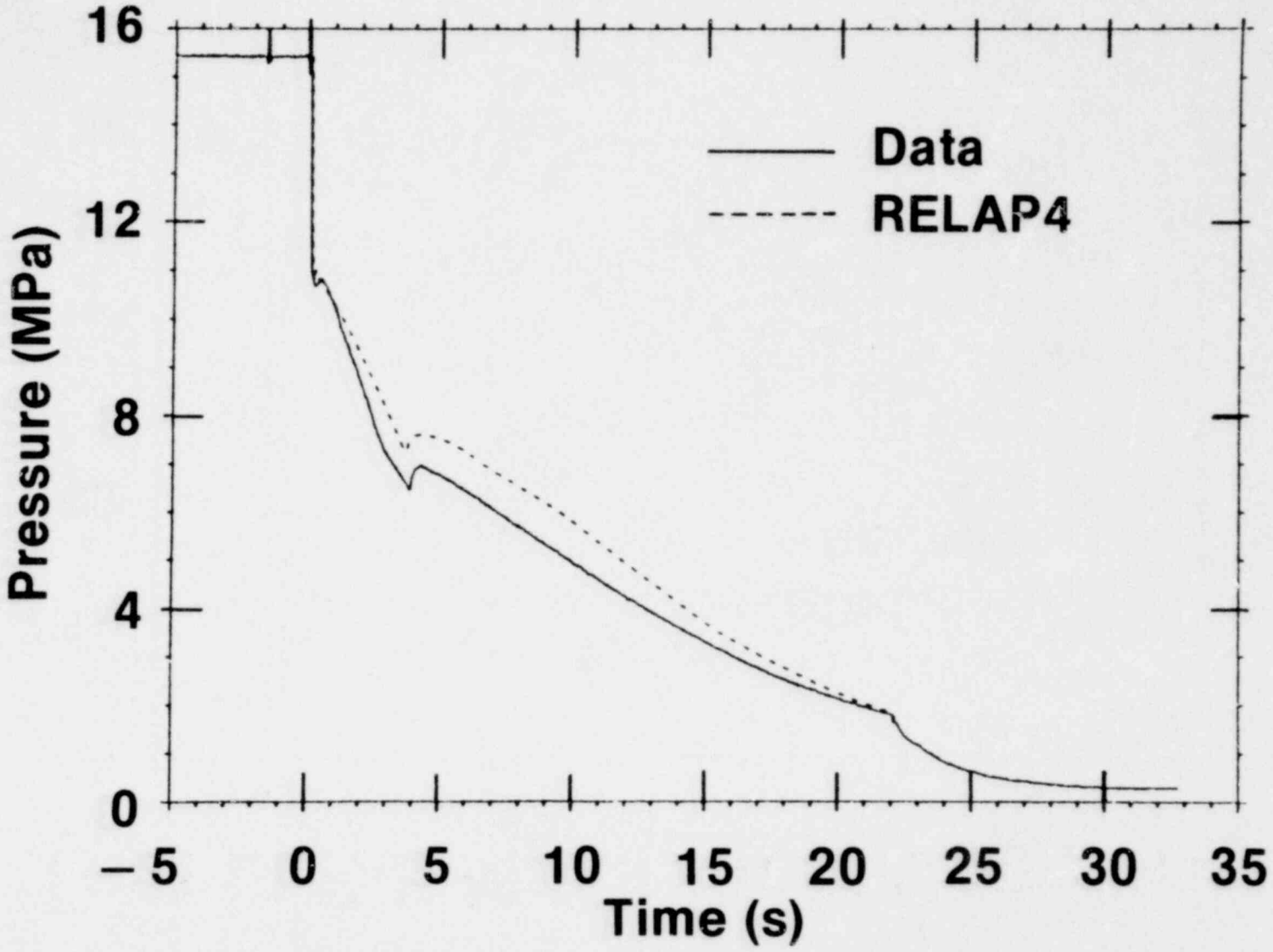

INEL-S-19 368

Test LLR-5 Mass Flow Comparison

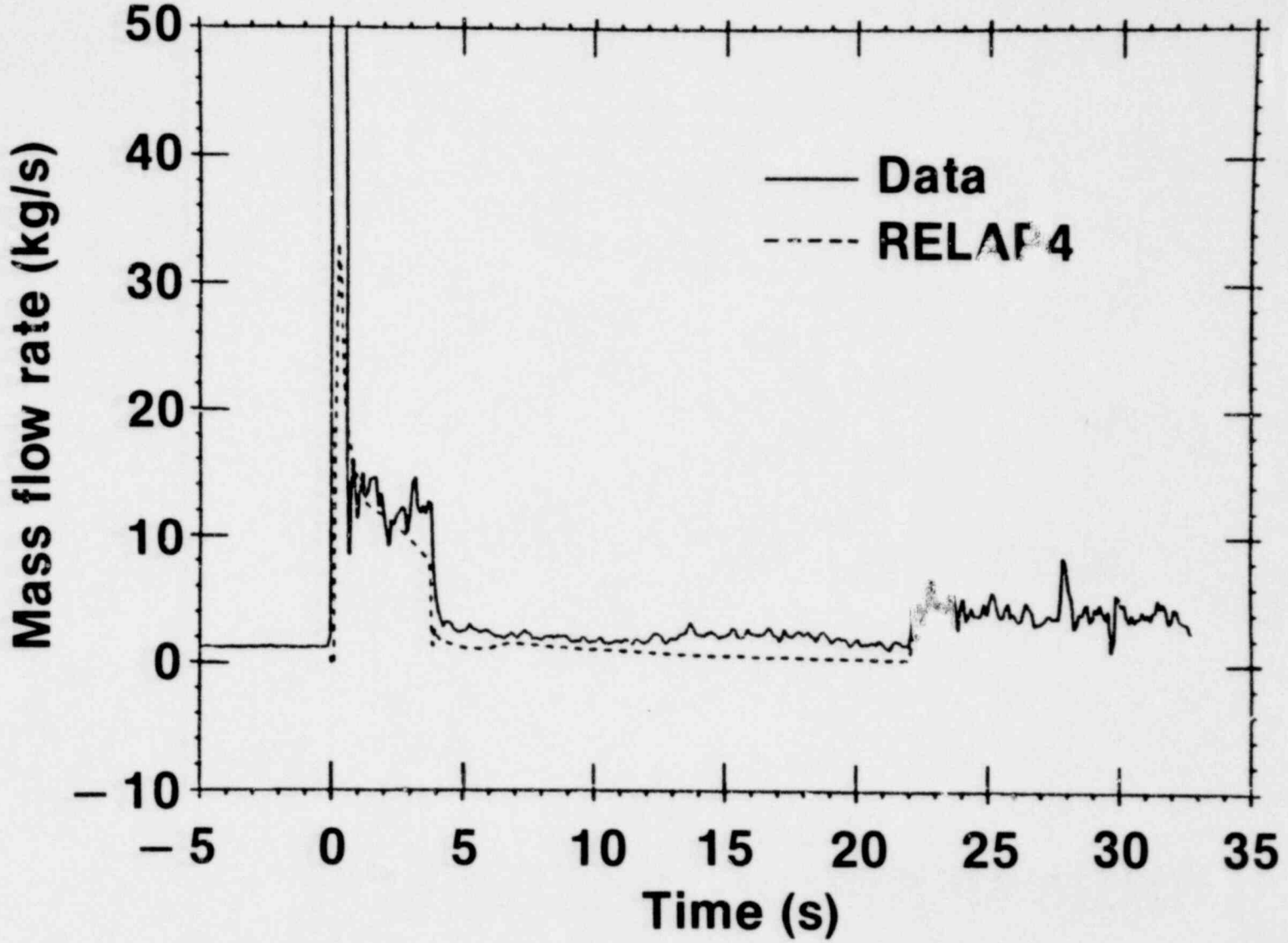

INEL-S-19 364

Test LLR-5
Lower Turbine Flowrate

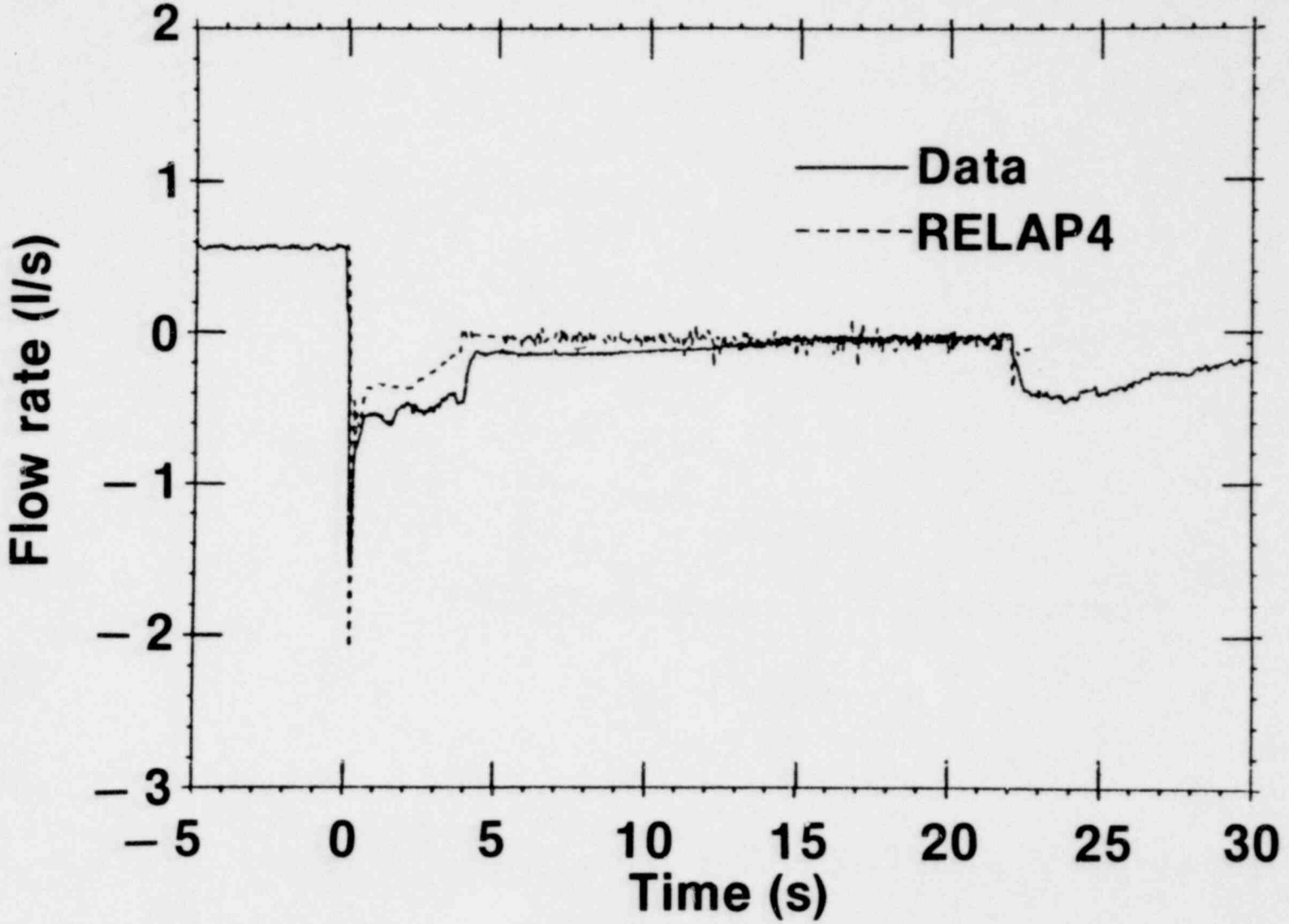

INEL-S-19 363

Test LLR-3 Thermal and Mechanical (Rod 312-1) Behavior

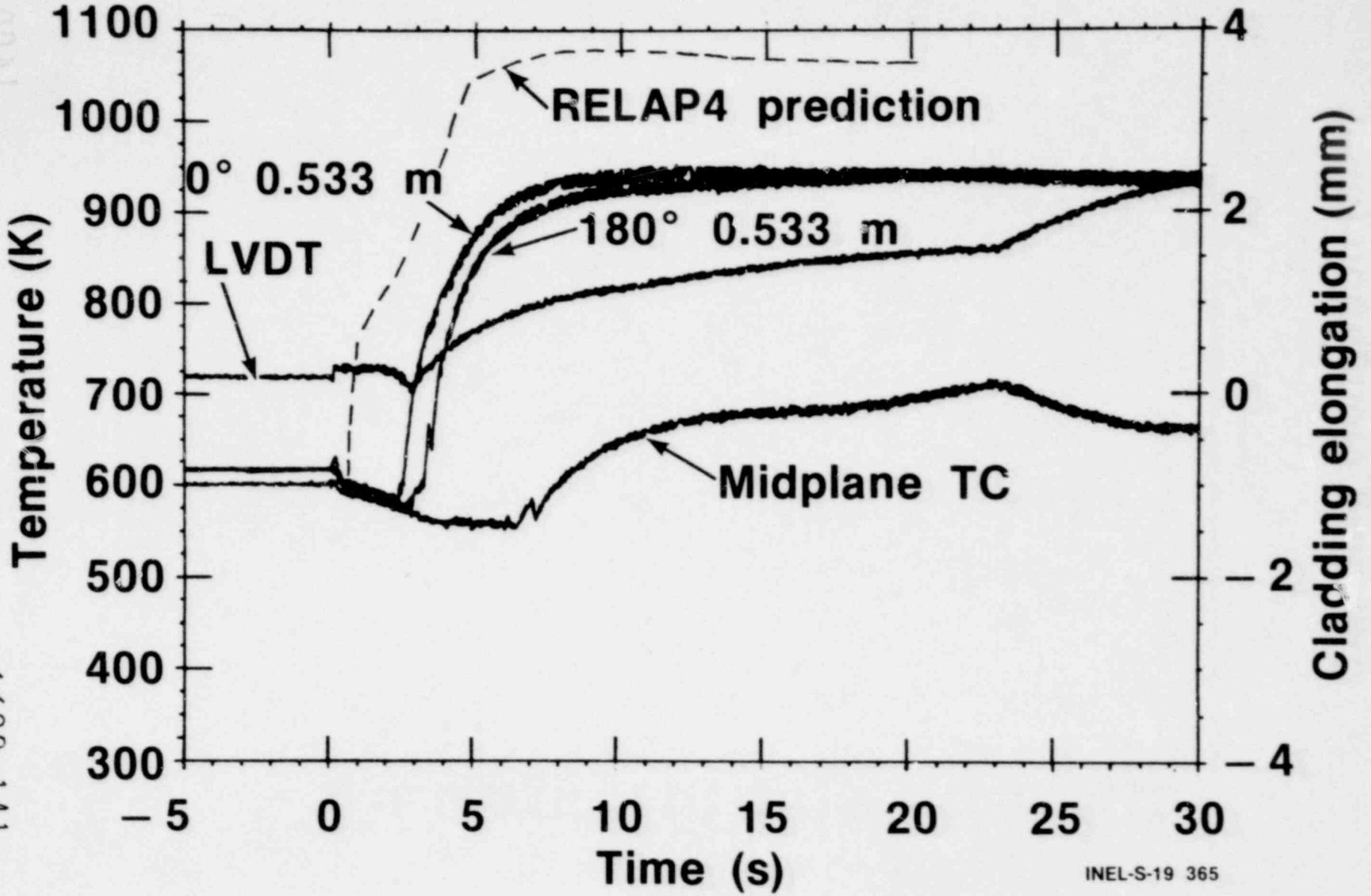

Summary Fuel Rod 312-1

Test	Peak Clad T 0°0.53 m	Max Estimated T 0° 0.31 m	Mechanical Deformation Predicted (Olsen)
LLR-3	950	1010	Incipient buckling
LLR-5	1000	1060	Incipient collapse
LLR-4	1130	1225	Waisting

INEL-S-21 593

Test LLR-4 Rod 312-1 Surface Temperature vs Pressure Response

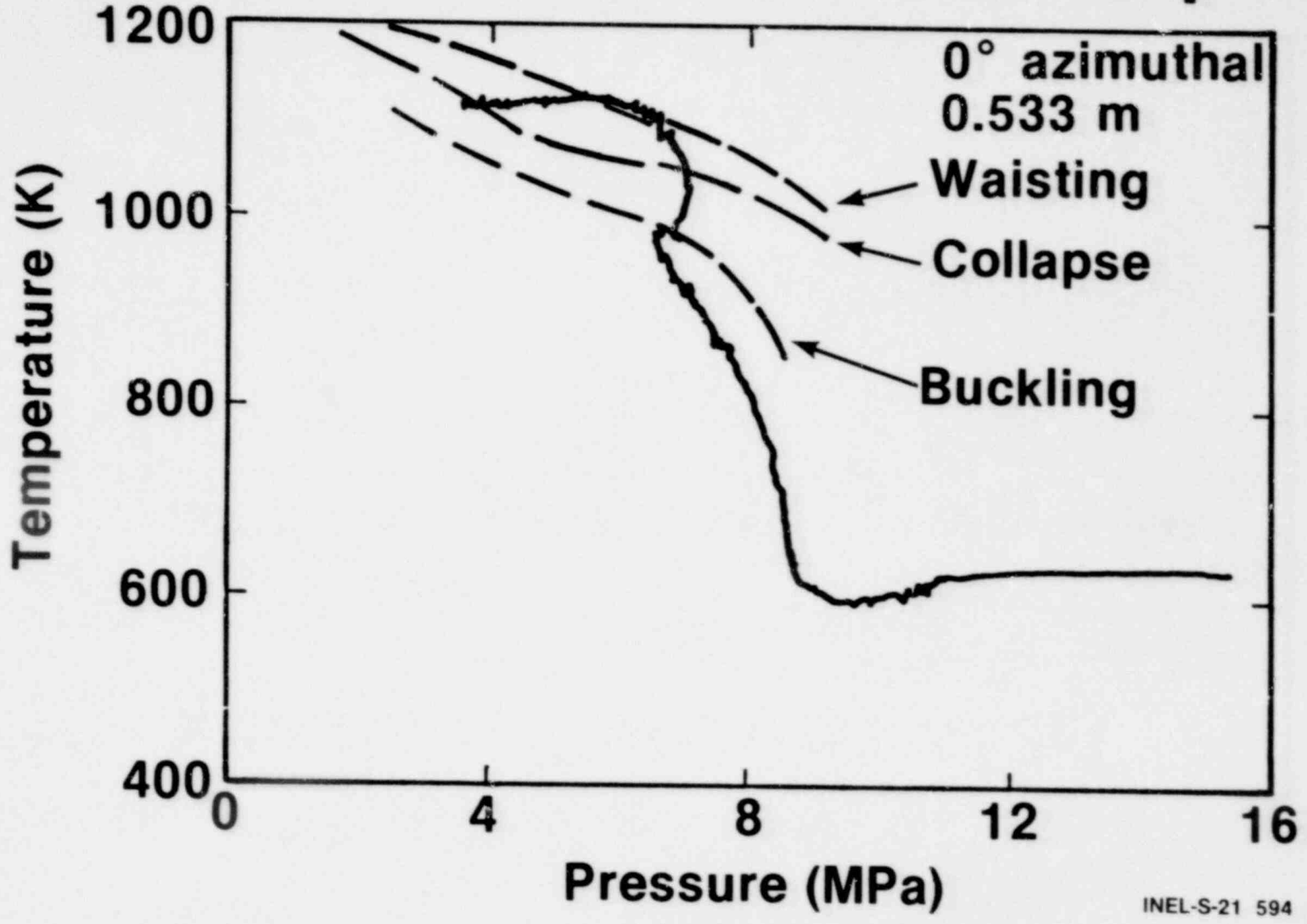

Post Irradiation Examination Results of Rod 312-1

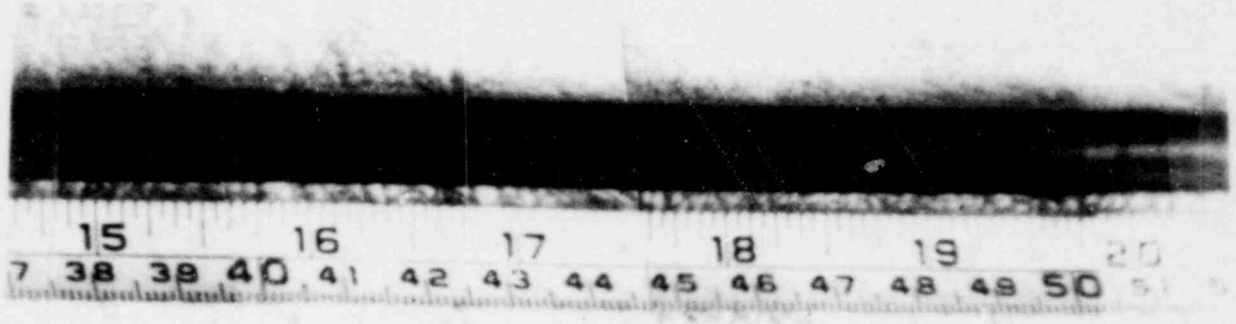

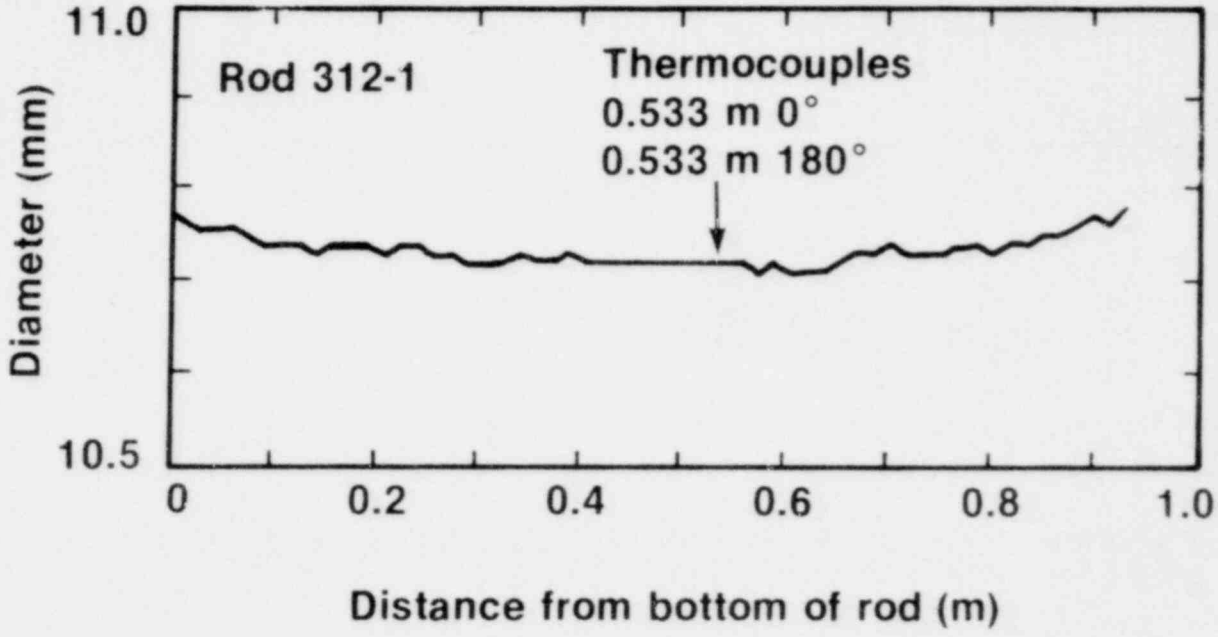

INEL-S-21 595

Test LLR-5 Thermal and Mechanical (Rod 312-2) Behavior

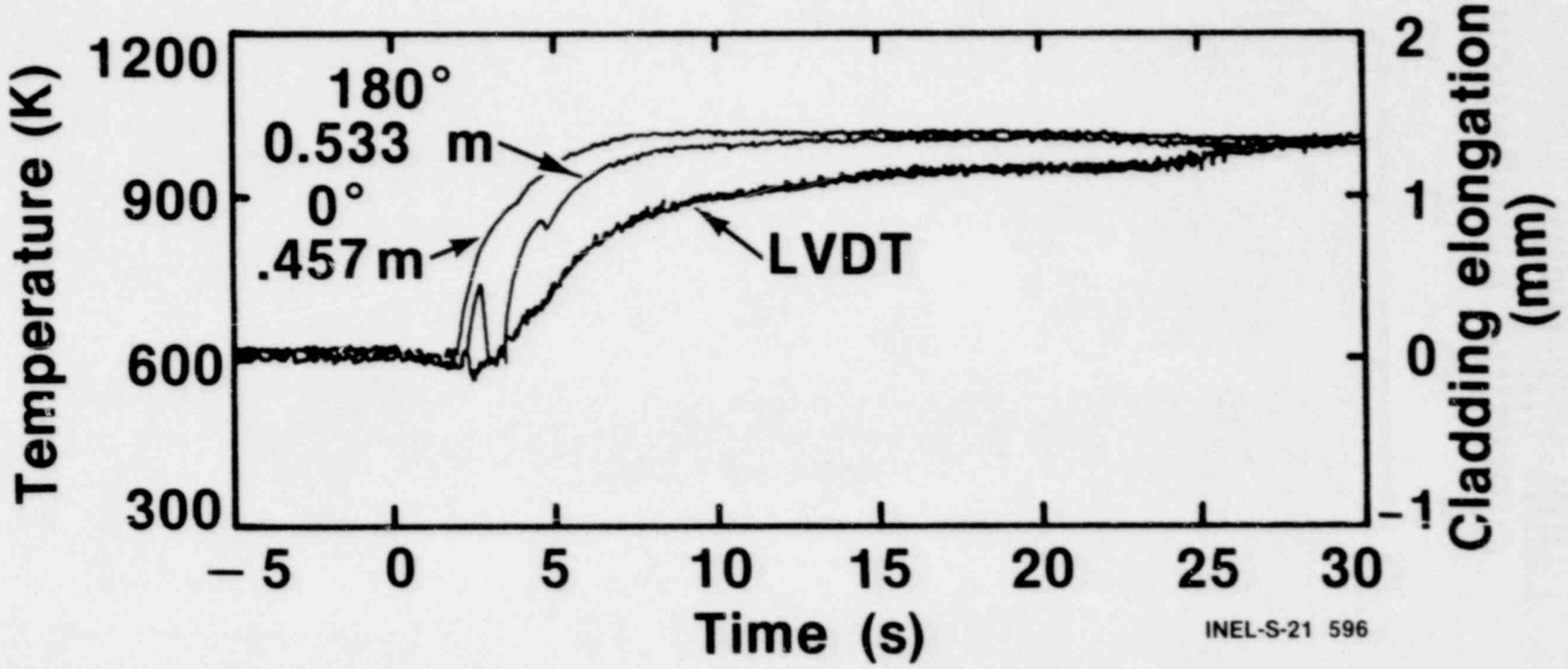

Test LLR-4A Rod 312-2
Thermal Response

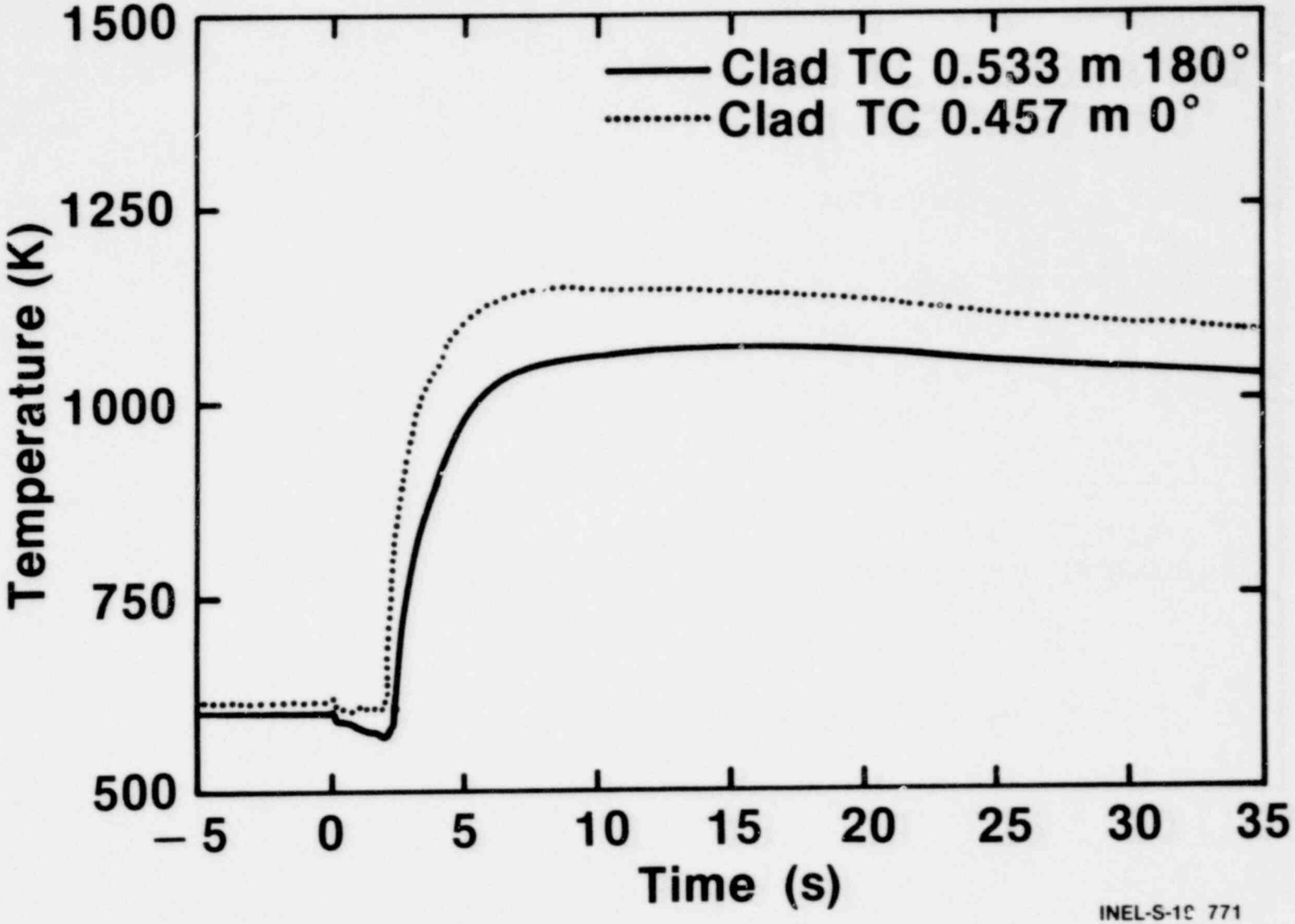

INEL-S-10 771

Summary Fuel Rod 312-2

Test	Peak Clad T 0°0.46 m	Max Estimated T 0° 0.31 m	Mechanical Deformation Predicted (Olsen)
LLR-3	925	960	None
LLR-5	1015	1050	Probable buckling Possible collapse
LLR-4	1170	1225	Waisting
LLR-4A	1150	1205	Waisting

INEL-S-21 597

Test LLR-4A Rod 312-2 Surface Temperature vs Pressure Response

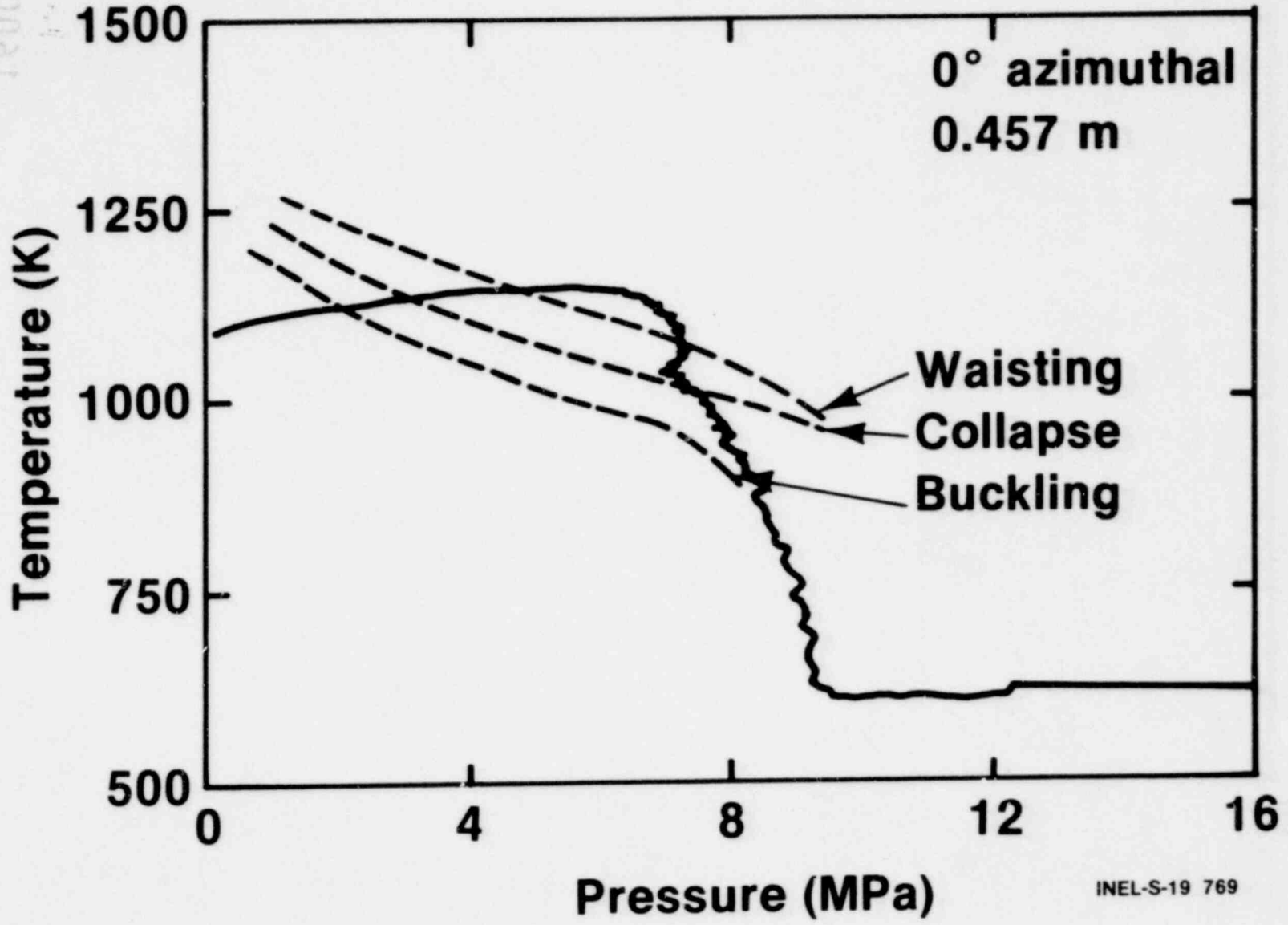

Post Irradiation Examination Results of Rod 312-2

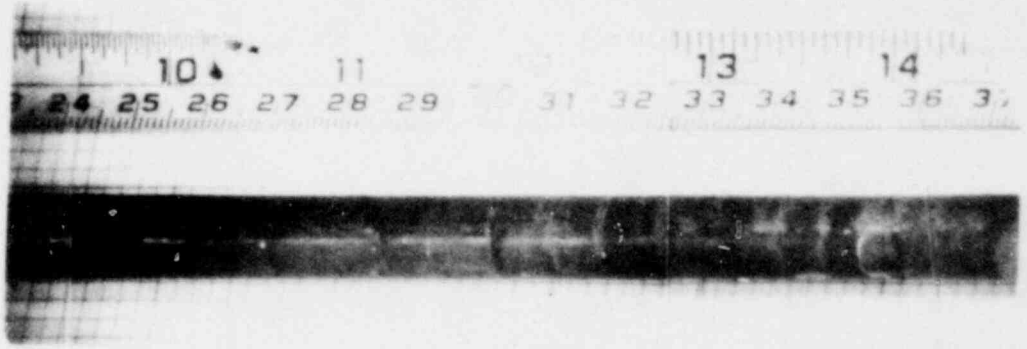

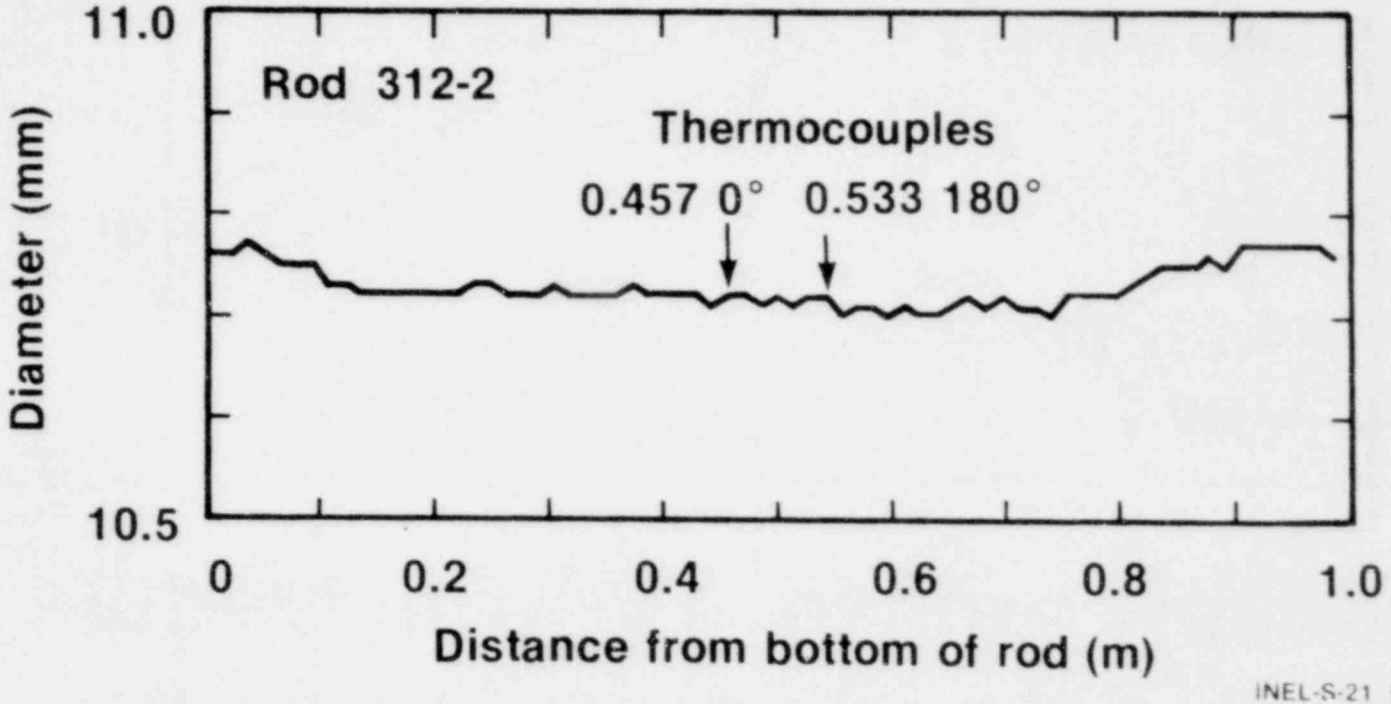

INEL-S-21 598

Program Conclusions

- Objectives of tests were met
  - LLR fuel rods experienced maximum mechanical deformation expected in the LOFT L2 tests
  - Deformed LLR rods subjected to subsequent preconditioning ramps and LOCA transients did not fail

Test Conclusions

- Observed deformation was consistent with Olsen's criteria
- DNB was first observed at lower elevations
- Lower elevations achieved higher clad temperatures
- RELAP4 well predicted system thermal-hydraulic behavior
- RELAP over predicted the cladding temperatures

STATUS OF LOFT TWO-PHASE FLOW INSTRUMENTATION CALIBRATION

Presented at

The Seventh Water Reactor Safety Research Information Meeting

November 5-9, 1979

Gaithersburg, Maryland

W. J. Quapp

EG&G Idaho, Inc.

Idaho National Engineering Laboratory

Idaho Falls, Idaho 83401

STATUS OF LOFT TWO-PHASE FLOW INSTRUMENTATION CALIBRATION

W. J. Quapp
EG&G Idaho, Inc.

The key to understanding the system behavior during any loss-of-coolant experiment (LOCE) is suitably located and calibrated instrumentation. In the LOFT system, the coolant instrumentation is located throughout the primary system piping (broken and intact loops) and, to a lesser extent, in the plena above and below the core region. This paper deals with the progress in calibrating the LOFT piping instruments (Slide 3).

The key instruments in the LOFT piping are the three-beam gamma densitometers, arrays of three drag disc turbine flowmeters (Slide 4), arrays of eight pitot tubes (Slide 5) and numerous pressures and temperatures. The measurements from these instruments are used with mathematical models to arrive at mass flow rates in the LOFT piping. The details of these models have been reported elsewhere. The locations of these instruments are shown in Slide 6.

Calibration of the LOFT instrumentation has up to now been limited to small scale air-water and steam-water testing or large scale single phase testing. No suitable facility has previously existed which could provide the steam-water testing environment in the size required for LOFT instrumentation. Consequently, during the last year, the Nuclear Regulatory Commission (NRC) authorized EG&G Idaho, Inc. to proceed with construction of two large facilities which could provide the needed full scale testing

environment for both transient and steady-state tests of LOFT piping instrumentation. Both facilities were needed in order to resolve questions related to the effects of installation and piping geometry and transient versus steady-state testing. Full-scale facilities are required to resolve the uncertainties related to free field versus full flow calibration.

The steady state two-phase loop is a high pressure (7MPa) steam-water loop which is being constructed at the Idaho National Engineering Laboratory (INEL) near the location of the existing large single phase loop and small blowdown loop at the LOFT Test Support Facility (LTSF) area.

The two-phase loop is illustrated in Slide 10 in the horizontal piping instrument calibration configuration which will be used for testing LOFT piping instruments. Design modifications are underway to allow testing of LOFT core instrumentation in a vertical positive flow configuration as shown in Slide 11. The test section will consist of a single LOFT fuel assembly mock up with the core flow instrumentation planned for later center fuel assemblies in the LOFT core.

The two-phase loop consists of separate steam and water subsystems brought together in a mixing tee upstream of the test section. The liquid side of the loop is driven by a diesel powered pump.

The steam is supplied by a 4500 Kg/hr high pressure boiler which is used to charge the large tanks shown on Slide 12. These tanks are then discharged in a controlled blowdown to the test section to supply the steam. Total tank volume is approximately 85 cubic meters and will provide sufficient steam for up to approximately four minutes of operation at full steam flow

and proportionally longer at lower steam flow. The loop operating conditions are summarized on Slide 13 for the current horizontal test section, high flow rate capability and the future vertical test section, low flow rate capability. The maximum flow rate capability represents the maximum flow obtained in LOFT during a 200% LOCE. The planned reference instrumentation is listed on Slide 14.

Construction is underway and scheduled for completion by December 1, 1979 followed by a two-month period of startup operations testing. Calibration of LOFT piping instruments is scheduled to begin in February 1980.

The two-phase flow loop will initially be used for calibration testing of LOFT piping and core instruments but will later support testing needs of other NRC programs at the INEL and elsewhere.

The Transient Flow Calibration Facility (TFCF) has been constructed for EG&G by Wyle Laboratories in Norco, California. The system basically consists of a large pressure vessel and a single pipe leg which can be configured to approximately represent either the hot or cold side of the LOFT intact or broken loops. The TFCF system has been scaled to approximate the key dimensions of the LOFT system in order to produce discharge mass flows similar to the LOFT system.

The facility and test program is designed around the four pipe penetrations entering or leaving the LOFT pressure vessel (Slide 6). An isometric of the TFCF is shown in Slide 17.

The main characteristics of the reference mass flow system (Slide 18) consist of load cells whose output is differentiated to get a mass flow

rate. The static cold fill calibration of the vessel yielded a load cell accuracy of better than ±1%. The dynamic mass flow rate accuracy has not yet been fully established but is expected to be better than ±10%. A backup system consisting of differential pressure measurements on the vessel is used to provide additional reference mass flow measurement.

The test matrix, Table 1, is organized to test the various instruments installed on the hot and cold legs of the broken and intact loops. The primary variables are listed on Slide 3. The other information in Table 1 relates to the break size or LOFT nozzle as the controlling break area.

Since the end of July 1979, twenty-three tests have been conducted. In the following few slides, examples of the data obtained at the TFCF are presented. The tests are initiated by rupturing a disc at the end of the test spool piping when the vessel and test leg are filled with water nominally at 15 MPa and 565K. A typical test will be shown in a short movie. A photograph of the facility during a test is snown on Slide 20. The vessel is supported on three load cells which are electronically summed to yield a total mass record of the vessel plus liquid contents. An example of this data is shown in Slide 21. The reference mass flow rate is derived by differentiating and filtering the data shown in Slide 21 to yield the mass flow rate data found in Slide 22.

The measured data are combined as shown on Slide 23 to yield the calculated mass flow rates shown in Slide 24 which present the comparative mass flow rate data derived from the load cell and calculations using combinations of: 1) a gamma densitometer and a rake of three drag discs; and 2) a gamma densitometer and a rake of flow turbines. Comparing the data in these slides it can be seen that both derived mass flow measurements

compare very well in magnitude and timing to the reference load cell data. These data result from only the first simple data processing efforts and consequently are quite preliminary.

The data are taken under the homogeneous flow conditions of the LOFT broken loop cold leg as evidenced by the similarity in the density traces from the three-beam gamma densitometer as shown in Slide 25, which shows almost identical conditions along the three chordal regions of the pipe.

This test program is providing previously unavailable information on the LOFT instrument performance and measurement uncertainty. The test program at Wyle will be completed by the end of November 1979, with reporting to continue over the next year.

TABLE I

TEST MATRIX

Test Description	Test ID	No. of Tests Instr.	Primary Flow Instr.	Sec. Flow	Orifice Diam.	Spool Orient	Pipe Geom.	LOFT Nozzle
Cold Fill (Load Cell Test)	IACF	1	-	-	-	0°	Elbow	Yes
Broken Loop Cold Leg Single Phase	IBISP	1	DTT	No	-	0°	Elbow	Yes
Broken Loop Cold Leg Single Phase	IB2SP	1	Pitot	No	2"	0°	Elbow	Yes
Broken Loop Cold Leg	IA1	3	DTT	No	-	0°	Elbow	Yes
Broken Loop Cold Leg	IA2	2	Pitot	No	-	0°	Elbow	Yes
Intact Loop Cold Leg	IAIIA1	2	DTT	ECC	4"	90°	Elbow	No
Intact Loop Cold Leg	IAIIA2	2	No	ECC	4"	90°	Elbow	No
Intact Loop Hot Leg	IVA1	2	DTT Reversed	ECC	2"	90°	Elbow	No

TABLE I (Con't)

TEST MATRIX

Test Description	Test ID	No. of Tests Instr.	Primary Flow Instr.	Sec. Flow	Orifice Diam.	Spool Orient	Pipe Geom.	LOFT Nozzle
Broken Loop Hot Leg	IIA1	2	DTT	No	2"	0°	Elbow	Yes
Broken Loop Hog Leg	IIA2	2	Pitot	No	2"	0°	Elbow	Yes
Broken Loop Hot Leg	IIB1	1	DTT	No	2"	0°	Straight	Yes
Broken Loop Hot Leg	IIB2	1	Pitot	No	2"	0°	Elbow	Yes
Broken Loop Cold Leg	IB1	2	DTT	No	-	0°	Straight	Yes
Broken Loop Cold Leg	IB2	1	Pitot	No	-	0°	Straight	Yes
Small Break Orifice Test	WSB01	2	-	-	0.6824"	0°	Straight	Yes
Small Break Orifice Test	WSB03	2	-	-	0.6374"	0°	Straight	Yes
Small Break Orifice Test	WSB05	2	-	-	0.1593"	0°	Straight	Yes

Presentation Outline

- Instruments used in LOFT piping
- Two-phase flow calibration status
- Need for additional calibration facilities
- Transient versus steady-state calibration
- INEL two-phase loop
- Wyle transient calibration test facility

Key LOFT Instruments

- Drag disc turbine flowmeter rake
- Pitot tube rake
- Three-beam gamma densitometers
- Numerous system pressures and temperatures

INEL-S-21 880

1600 161

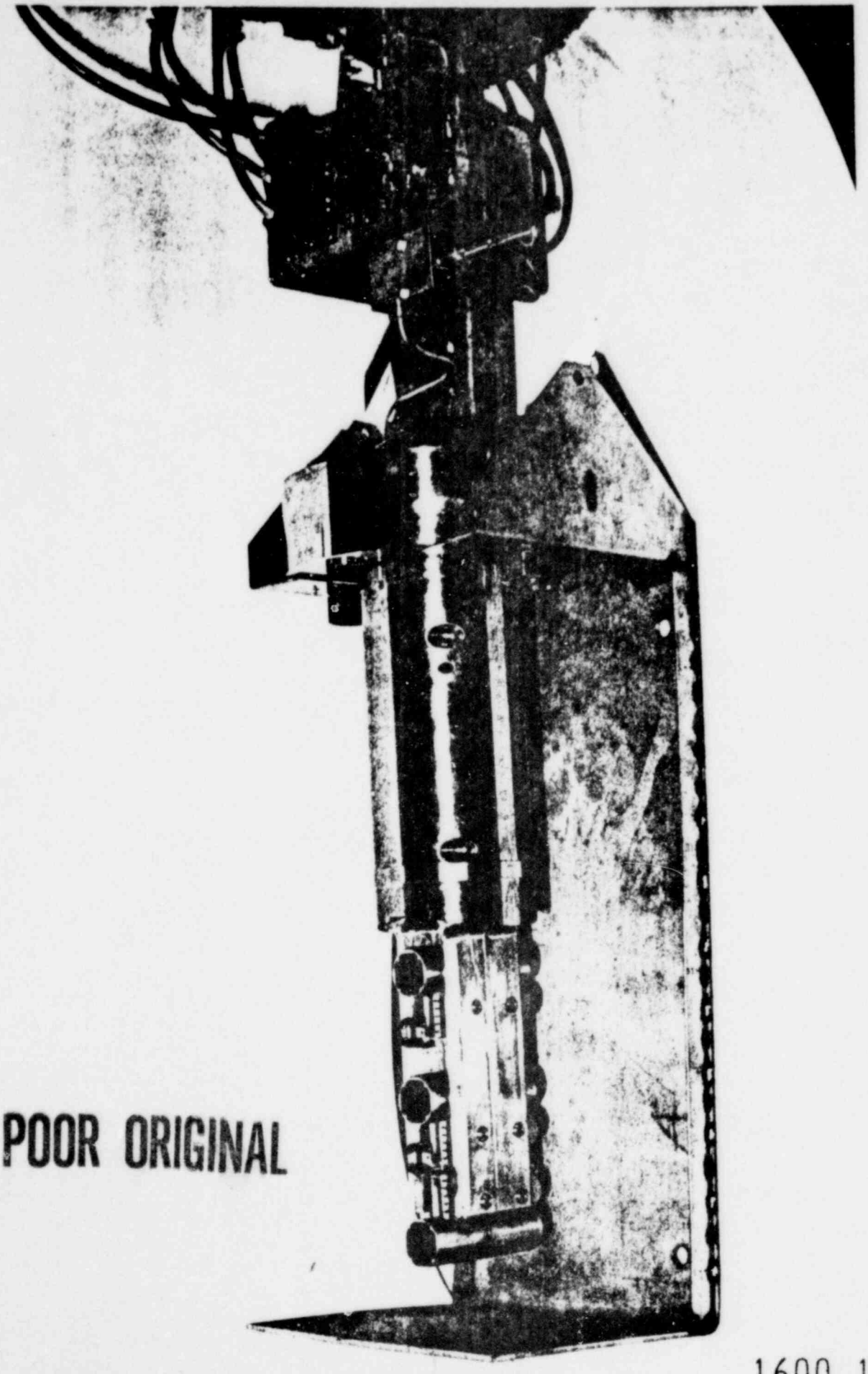

Slide 4

POOR ORIGINAL

LOFT TC Pitot-Probe Rake

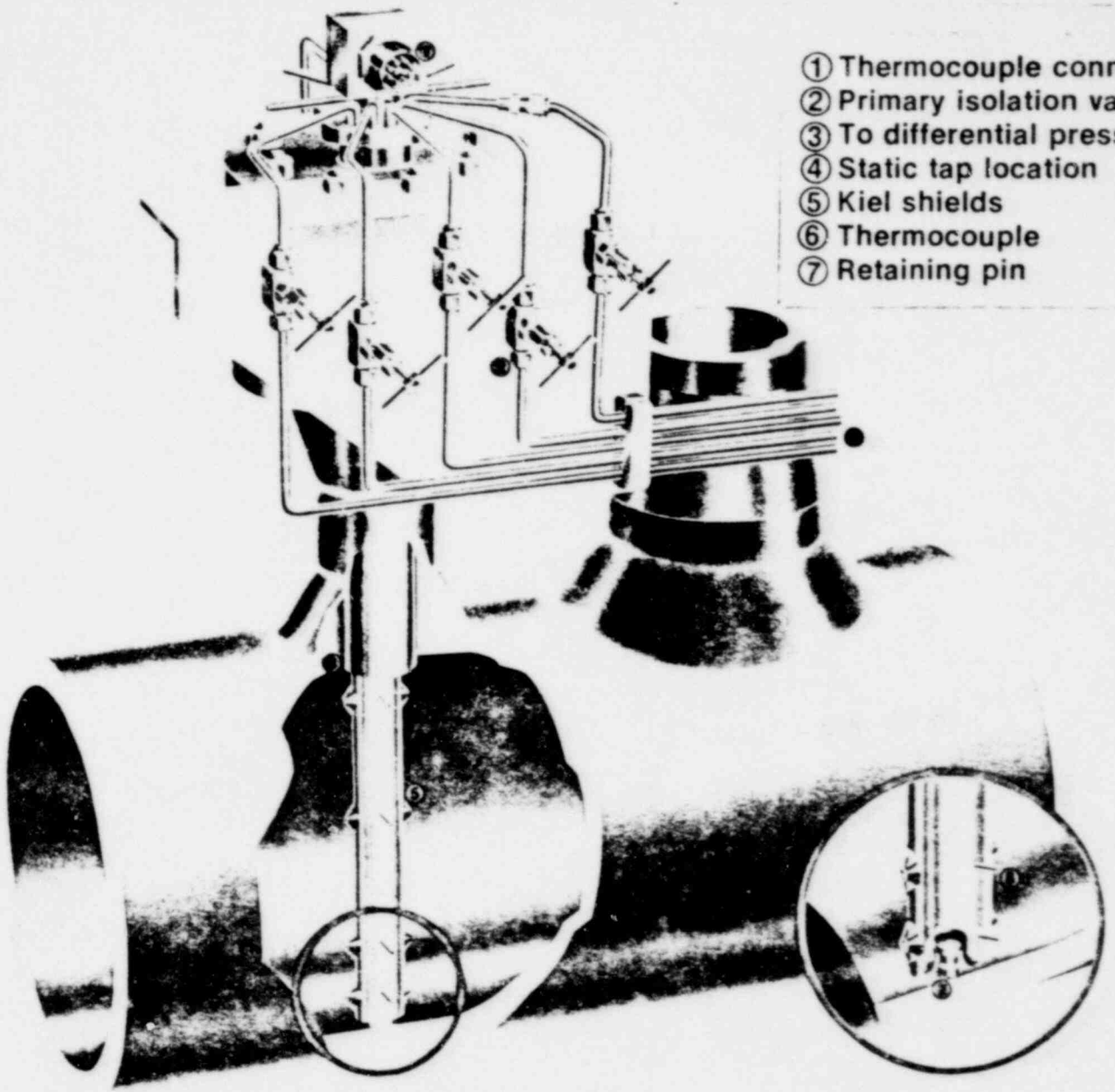

① Thermocouple connector
② Primary isolation valves
③ To differential pressure transducers
④ Static tap location
⑤ Kiel shields
⑥ Thermocouple
⑦ Retaining pin

LOFT Intact and Broken Loop Piping and Instrumentation

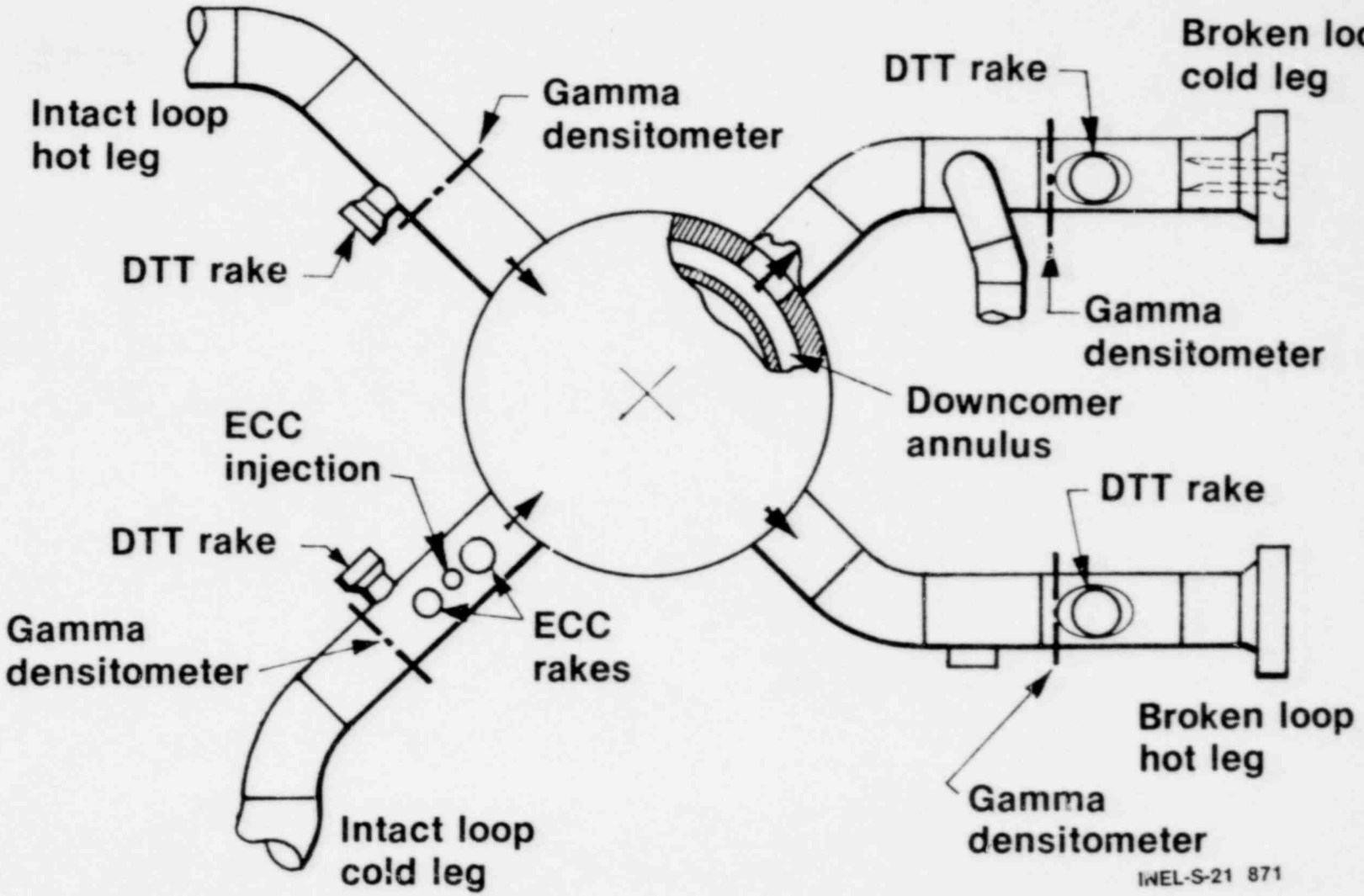

1600 164

Current Calibration Limitations

- Small scale air-water testing
- Small scale steam-water testing
- Hot full scale single-phase testing

INEL-S-21 881

Unresolved Calibration Concerns

- Effect of geometry on measurement
- Adequacy of free-field versus full flow calibration
- Transient versus steady-state calibration

INEL-S-21 878

New Two-Phase Calibration Facilities

- INEL steady-state two-phase loop
- Wyle transient flow calibration facility

INEL-S-21 879

INEL Large Steady State Facility

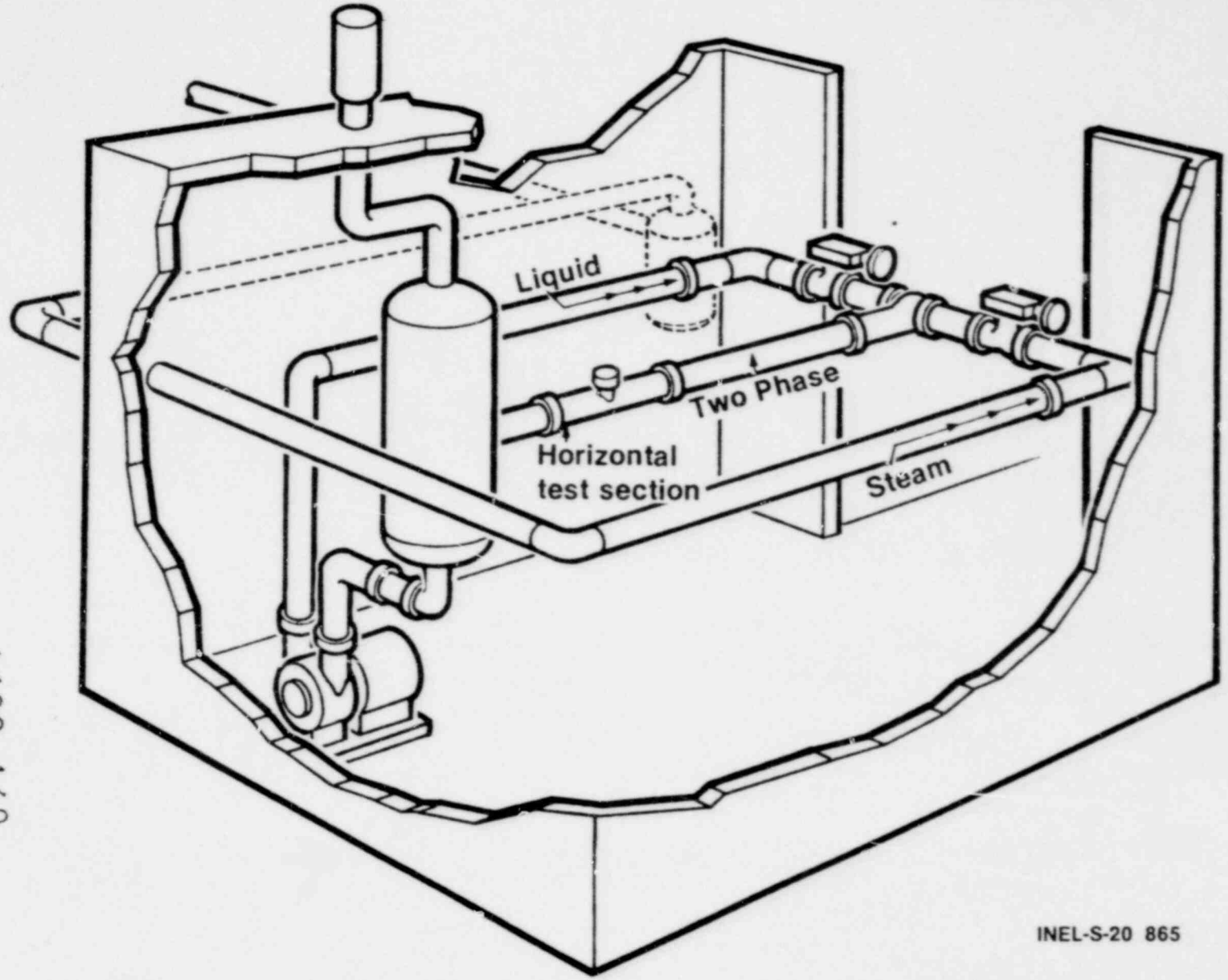

Modified with Vertical Test Section

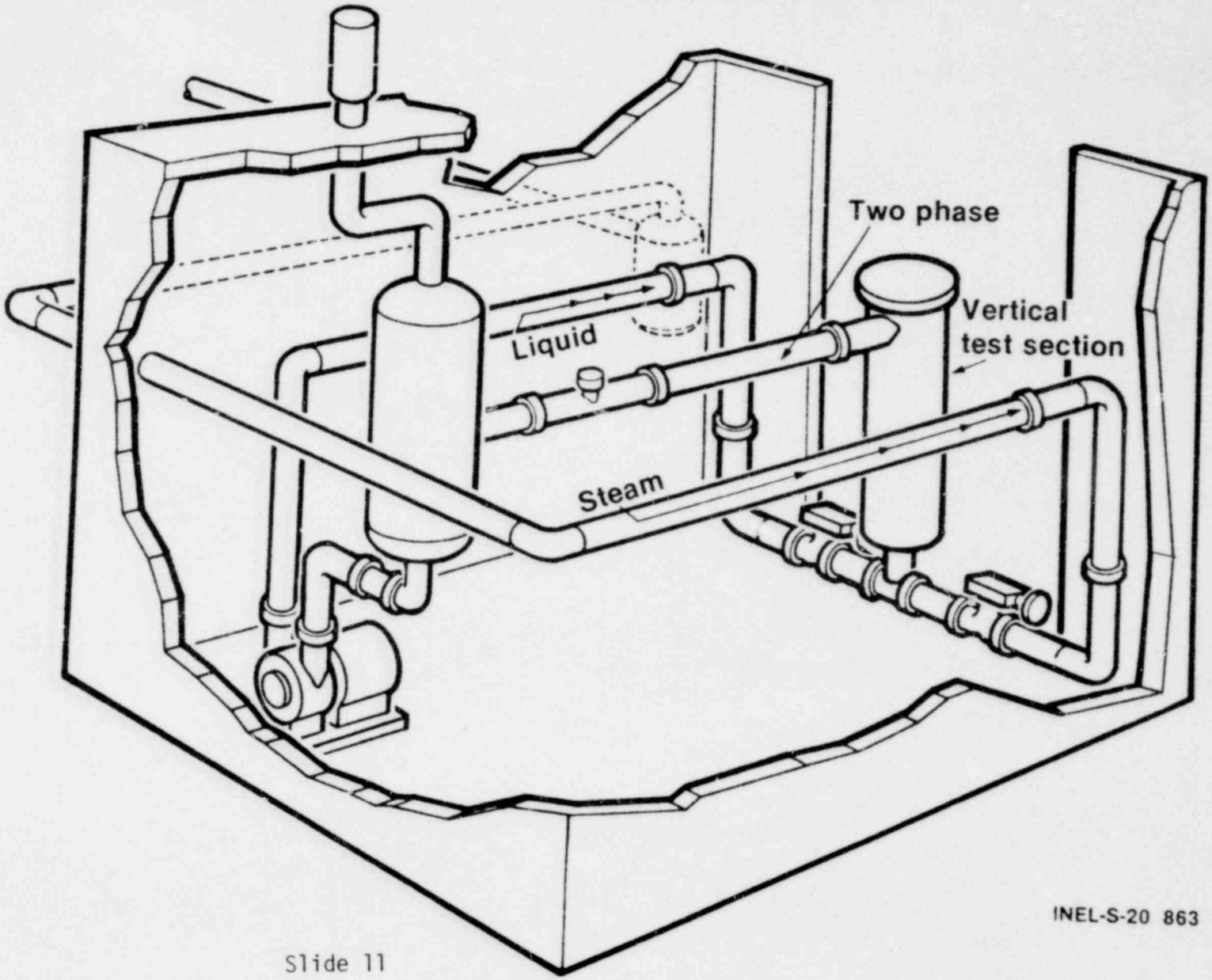

INEL-S-20 863

Slide 11

Slide 12

INEL Two-Phase Operating Loop Characteristics

High Flow Range Configuration

• Liquid mass flow	42	—	420 kg/s
• Steam mass flow	2.5	—	25 kg/s
• Pressure	2.07	—	6.9 MPa

Low Flow Range Configuration

• Liquid mass flow	4	—	40 kg/s
• Steam mass flow	0.28	—	2.8 kg/s
• Pressure	2.07	—	6.9 MPa

INEL-S-21 876

1600 171

Two-Phase Flow Loop Reference Instrumentation

- Orifice flow meters in steam and water legs
- Pressures and temperatures
- Three-beam gamma densitometers
- Tomagraphic gamma densitometer
- Traversing turbine
- Traversing pitot tube
- Traversing impedance probe

INEL-S-21 877

1600 172

Two-Phase Flow Loop Schedule

- Complete construction — December 1, 1979
- Complete startup operations — February 1, 1979
- Testing planned for FY 1980
  - Drag disc turbine rake
  - ECC pitot tube rake
  - Calibration of LOFT small break spool piece instruments

INEL-S-21 875

1600 173

Wyle Transient Flow Calibration Facility

- System design features
- Reference mass flow rate system
- Test program
- Movie of test
- Preliminary results
- Conclusions

INEL-S-21 874

Wyle Transient Flow Calibration Facility

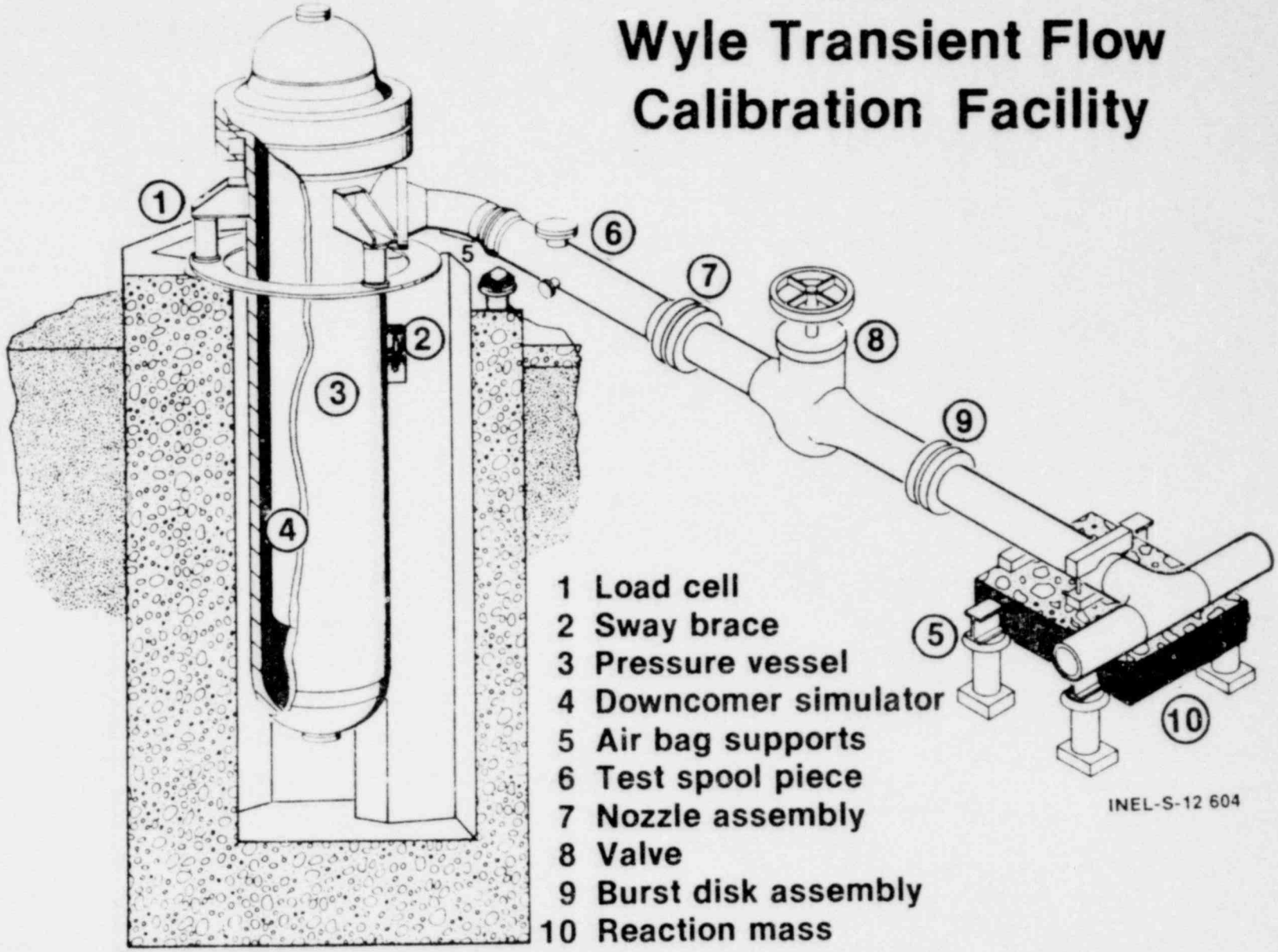

1 Load cell
2 Sway brace
3 Pressure vessel
4 Downcomer simulator
5 Air bag supports
6 Test spool piece
7 Nozzle assembly
8 Valve
9 Burst disk assembly
10 Reaction mass

Wyle TFCF Reference Mass Flow Rate System

- Based on total vessel and contents weight measurement using load cells (uncertainty based on static fill $< \pm 1\%$)
- Time derivative of vessel weight change gives mass flow rate (Expected uncertainty $< \pm 10\%$)
- Limited in some periods of the transient due to system dynamic response
- Backup system using differential pressure transducers

Test Program Variables

- Hot and cold leg of intact and broken loops
- Drag disc turbine and emergency core cooling pitot tube rakes
- System discharge rate
- System initial conditions

INEL-S-21 872

1600 177

POOR ORIGINAL

1600 178

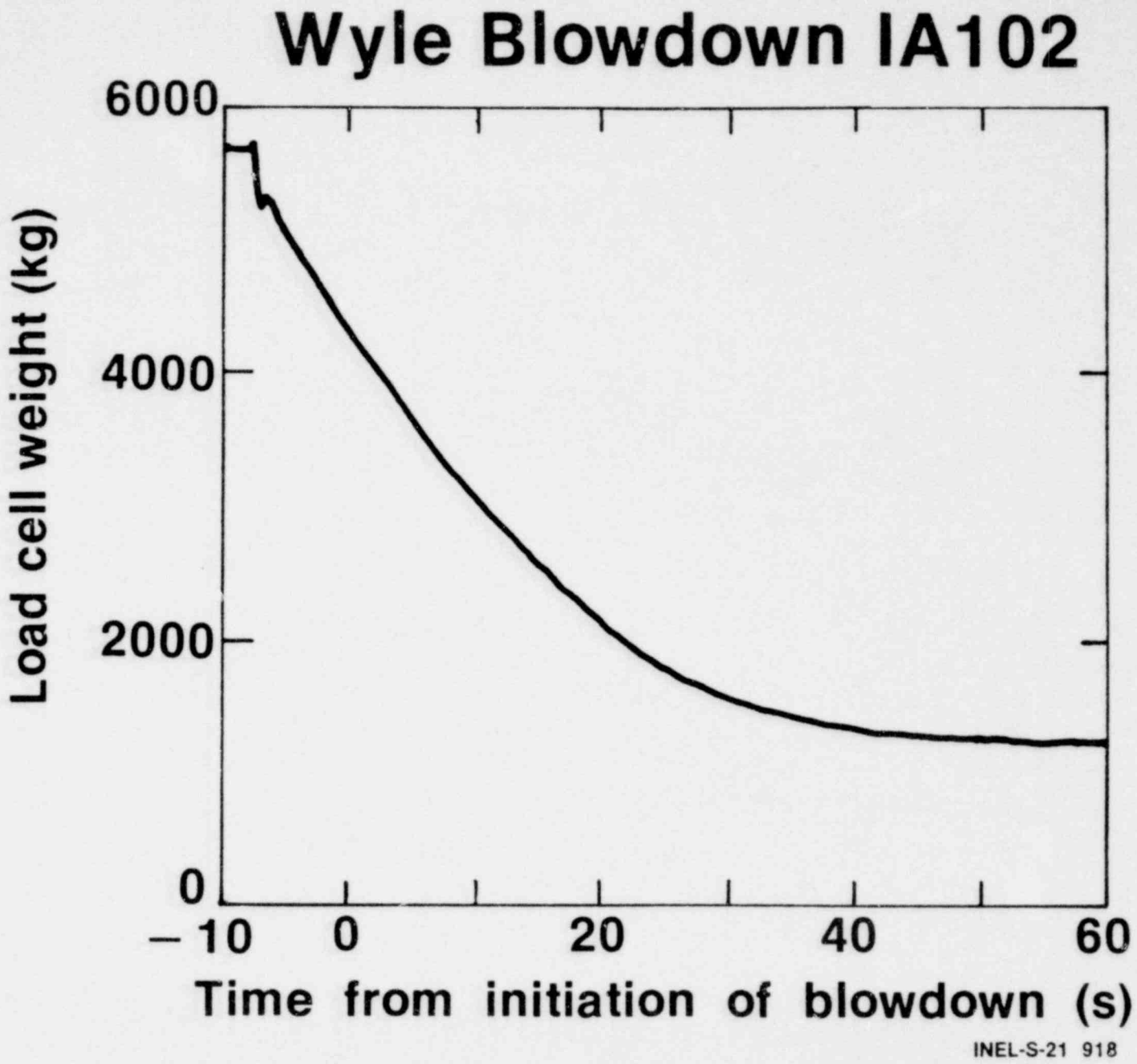

1600 179

Slide 21

Wyle TFCF Test Number 1A1-02

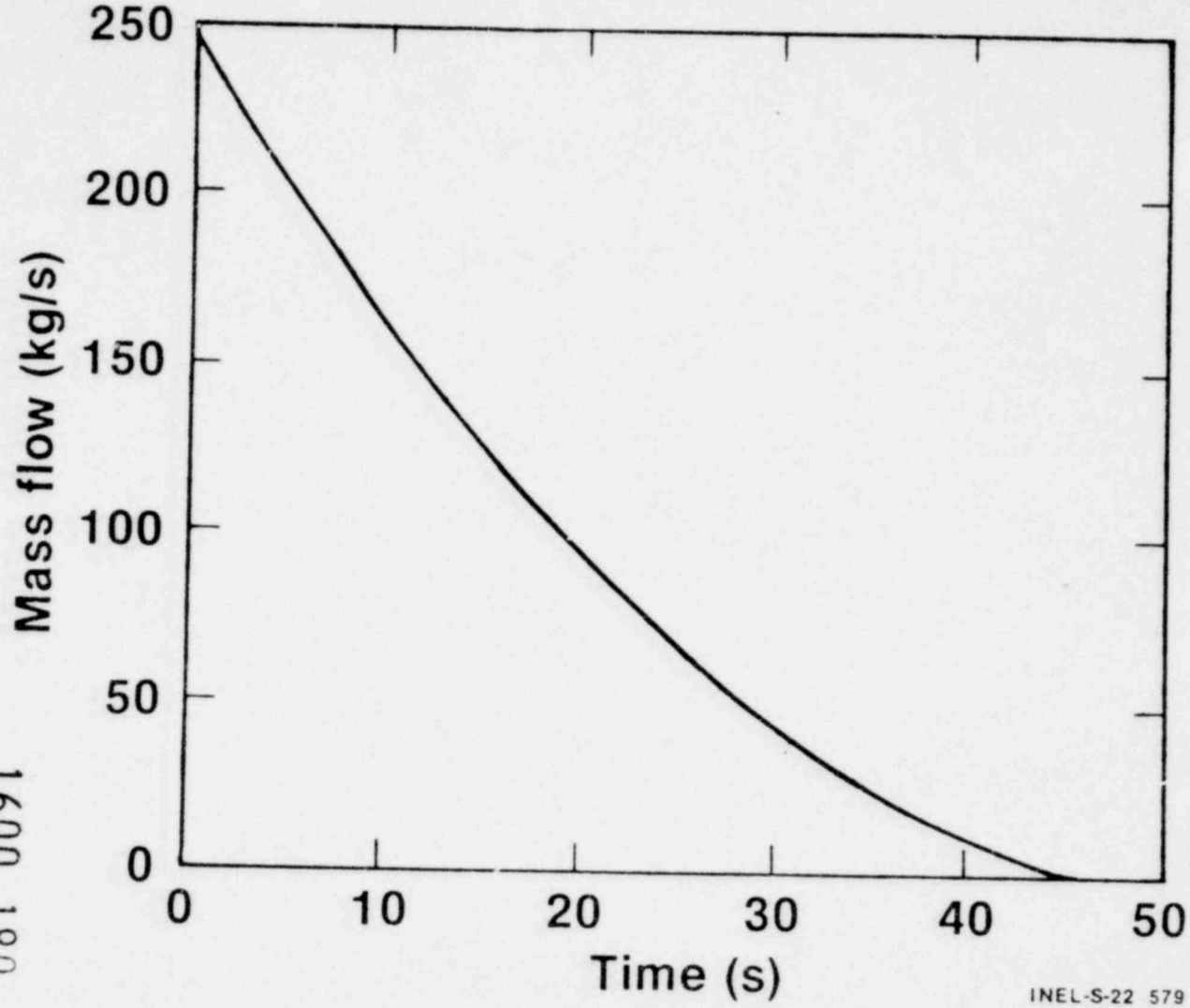

1600 180

SLIDE 22

Determination of Mass Flux

Densitometer and Turbine

$$G = f\left[\rho_{DENS} \cdot V_{TURBINE}\right]$$

Densitometer and Drag Disc

$$G = f\left[\left(\rho_{DENS} \cdot \left(\rho V^2\right)_{DD}\right)^{1/2}\right]$$

Drag Disc and Turbine

$$G = f\left[\frac{\left(\rho V^2\right)_{DD}}{V_{TURBINE}}\right]$$

1600 181

INEL-S-22 354

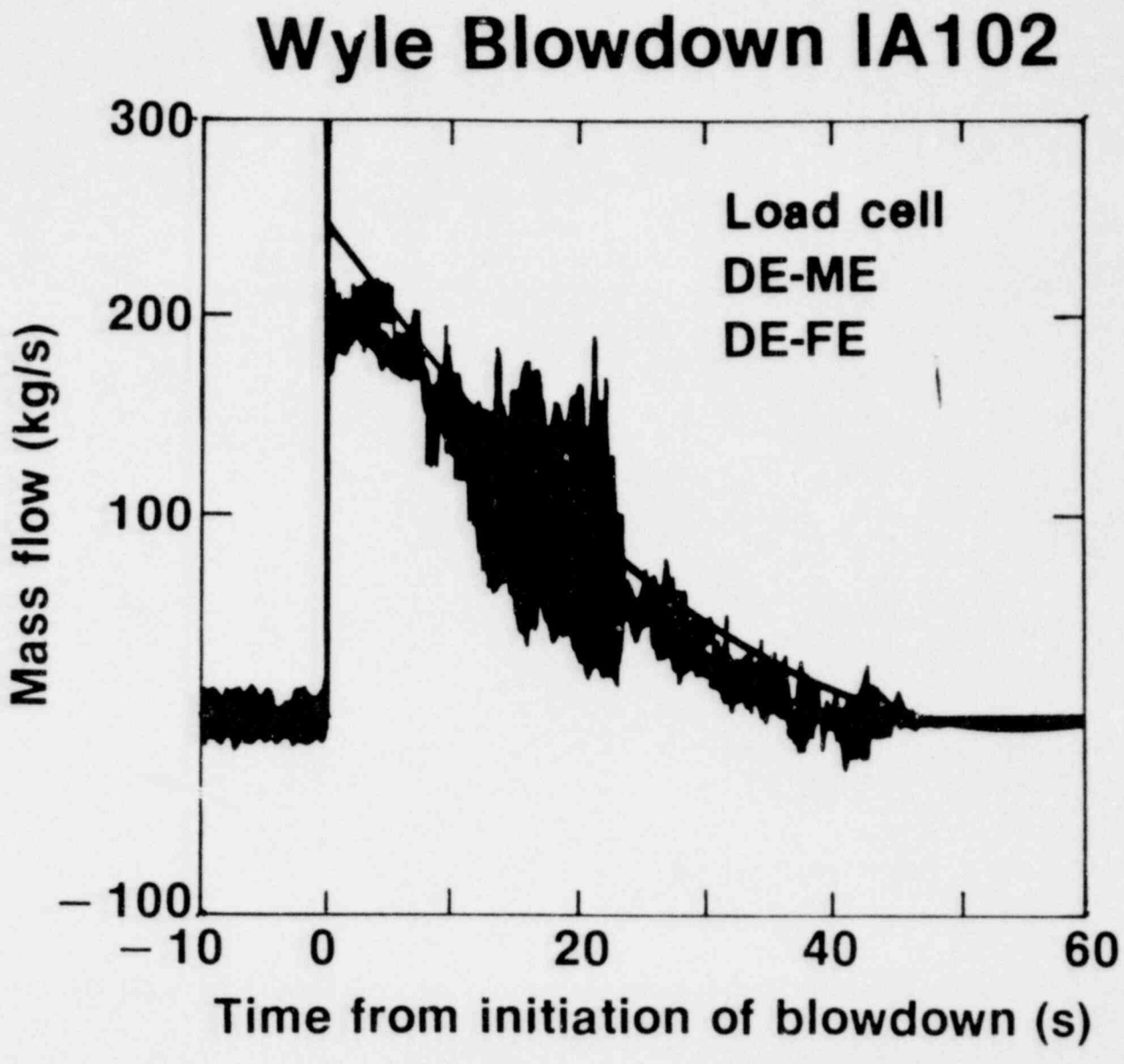
Wyle Blowdown IA102
300
200
100
−100
Mass flow (kg/s)
Load cell
DE-ME
DE-FE
−10
0
20
40
60
Time from initiation of blowdown (s)
INEL-S-21 914

1600 182

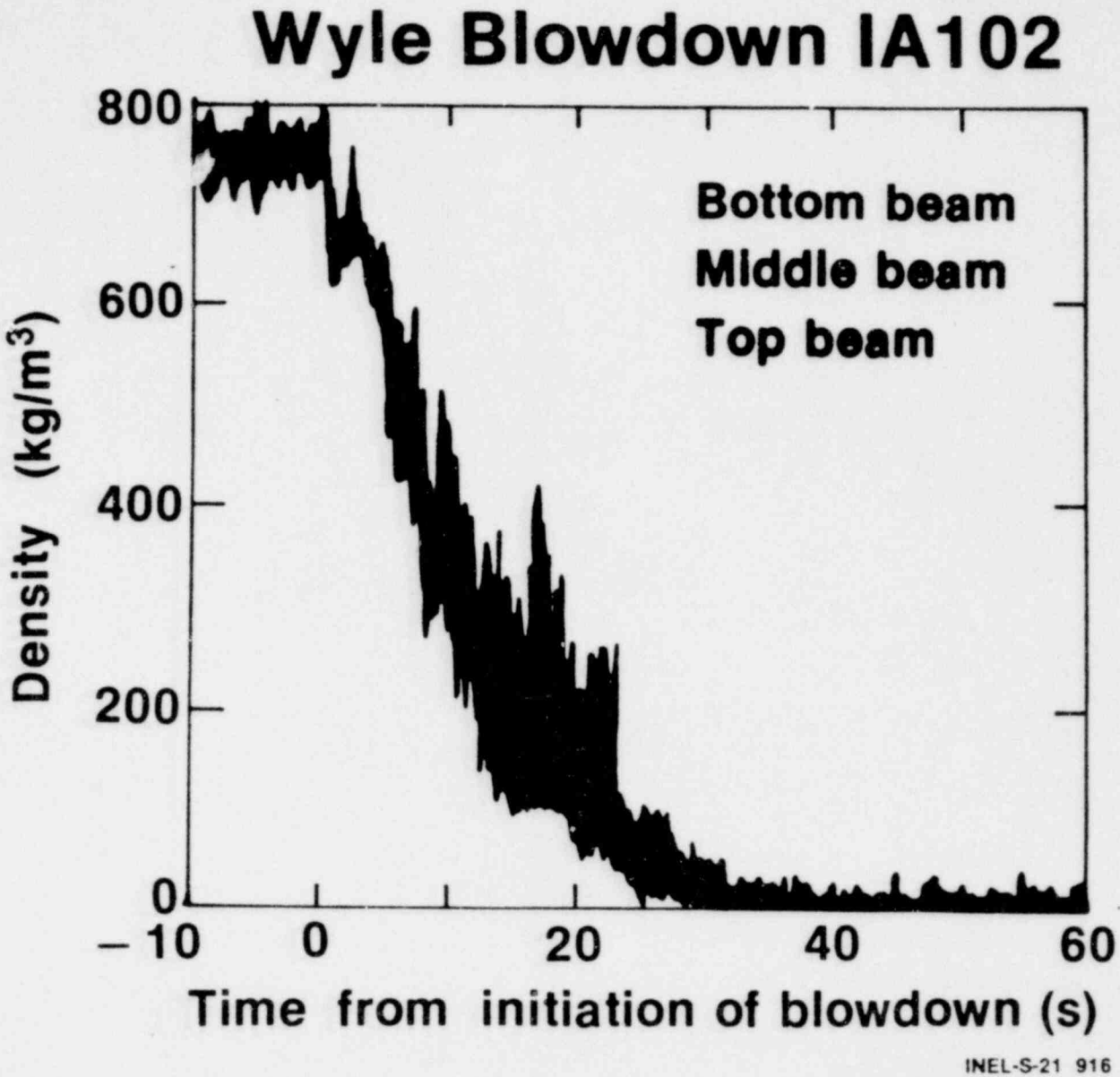

1600 183

SLIDE 25

Conclusions

- Capability for transient testing LOFT instruments in full scale LOFT geometry is now operational
- Agreement of techniques using densitometer, drag disc and flow turbine in homogeneous flow
- TFCF met its design criteria with respect to load cell mass flow rate performance and the duplication of the LOFT response
- Based on observations to date, total mass flow error can be reduced to less than $\pm 10\%$

Conclusions (cont'd)

- Steady-state two-phase calibration facility to be operational early 1980
- Simulated core calibration facility option to be available late 1980
- Expect to be able to improve calibrations and models and define total measurement uncertainty

INEL-S-21 921

STATUS OF TWO-PHASE FLOW STANDARDS SELECTION

Presented at
The Seventh Water Reactor Safety Research Information Meeting
November 5-9, 1979
Gaithersburg, Maryland

J. R. Fincke
EG&G Idaho, Inc.

Idaho National Engineering Laboratory
Idaho Falls, Idaho 83401

STATUS OF TWO-PHASE FLOW STANDARDS SELECTION

J. R. Fincke
EG&G Idaho, Inc.

The nuclear community faces a particularly difficult problem relating to the calibration of instrumentation in a two-phase steam/water environment. The rationale of the approach to water reactor safety questions in the United States demands that accurate measurements of mass flow during loss-of-coolant experiments (LOCE) be made. An accurate measurement dictates an accurate calibration.

To date, two meetings, the first an instrumentation review group meeting held by the NRC in Silver Springs, Maryland, in 1977 and the second in 1978 at Dartmouth, England, provided the forum for presentations and discussions relating to the problem of methods and standards for the calibration of instrumentation for the measurement of two-phase flow. At these meetings, a number of proposals were made concerning the selection of standards. These proposals have been reviewed and evaluated by EG&G Idaho, Inc., with particular reference to the steady-state two-phase flow test facility being built at the Idaho National Laboratory (INEL).

The two-phase flow test facility at the INEL will include a flow loop with a test section made up of 14-inch Schedule-160 piping. Reference instrumentation will be installed including orifice flowmeters to measure liquid and gas mass flow rate before mixing along with a calorimeter to determine steam quality before mixing. The two-phase reference instrumentation will consist of multibeam densitometry and density distribution imaging through the use of reconstructive tomography (RT). Local void fraction information will also be obtained through use of local needle-type impedance probes of

the type developed at Karlsruhe in Germany. Local velocity and profile information will be obtained through the use of pitot tubes; swirl and three dimensional effects will be quantified through the use of a five-point stagnation probe. The center of mass velocity information will be provided by a pulse neutron activation (PNA) system.

In the future it is hoped that additional flow instrumentation will be provided by the Storz lens system, sophisticated laser velocimetry, and single- and double-pulsed holography. The development of these techniques is currently under way at the INEL.

At this point in time it is difficult to refer to any of the two-phase measurement schemes as standards; they are references only. They represent the types of measurements required to characterize a two-phase flow for the purpose of understanding and calibrating other instrumentation for use in LOCEs.

REFERENCE

1. M. L. Stanley, "State of the Art - Two-Phase Flow Calibration Techniques," NRC Two-Phase Flow Instrumentation Meeting at Silver Springs, Maryland, January 13, 1977.

JRF3

Status of Two Phase Flow Standards Selection

Presented by
J.R. Fincke
EG&G Idaho, Inc.

EG&G Idaho, Inc.

Introduction

- History
- Status
- Ref Inst.
- Conclusions

INEL-S-21 516

History

- STDS proposed 1977
- 1978 Dartmouth Meeting

INEL-S-21 517

STDS Proposed 1977

Global mass flow rate	- Measure before mixing
Void fraction	- Gamma densitometers
Phase velocity	- Tracers, local probes

INEL-S-21 518

1978
Dartmouth Meeting
Recommendations

INEL-S-21 519

Summary of Method Selection

Property	Primary	Secondary	Potential
Global mass	Two streams	PNA	Tracers
Flux	Separate flow (meas. before mix)	TM FM	

INEL-S-21 523

Summary of Method Selection

Property	Primary	Secondary	Potential
Void, global	Quick C.V. (T)	Gamma scanning (T)	NMR
	($\Delta\rho$) gravity (S)	PNA (S,T)	Tracers
			Neutron scattering
Void, local	Gamma scattering	Multi-beam	Digital interference meter
		Transmission (attenuation)	Local probes
		Tomography	

INEL-S-21 521

Summary of Method Selection

Property	Primary	Secondary	Potential
Velocity, local (instrusive)	Stagnation Probe (T,S) Isokenetic sample	Stero lens	Hot film Anemometer
Phase velocity	Tracer, PNA	———	Local Probes

INEL-S-21 524

References to be used on the INEL 14-Inch Two-Phase Test Facility

INEL-S-21 515

Global Mass Flow Rate

- Orifice flow measurement of each phase before mixing

Local Void Fraction

1. Tomographic reconstruction of multibeam densitometer data

2. Local Karlsruhe type impedance probe

INEL-S-21 522

Global Void Fraction

- **Multibeam Scanning Densitometer**

INEL-S-21 525

Square Plot

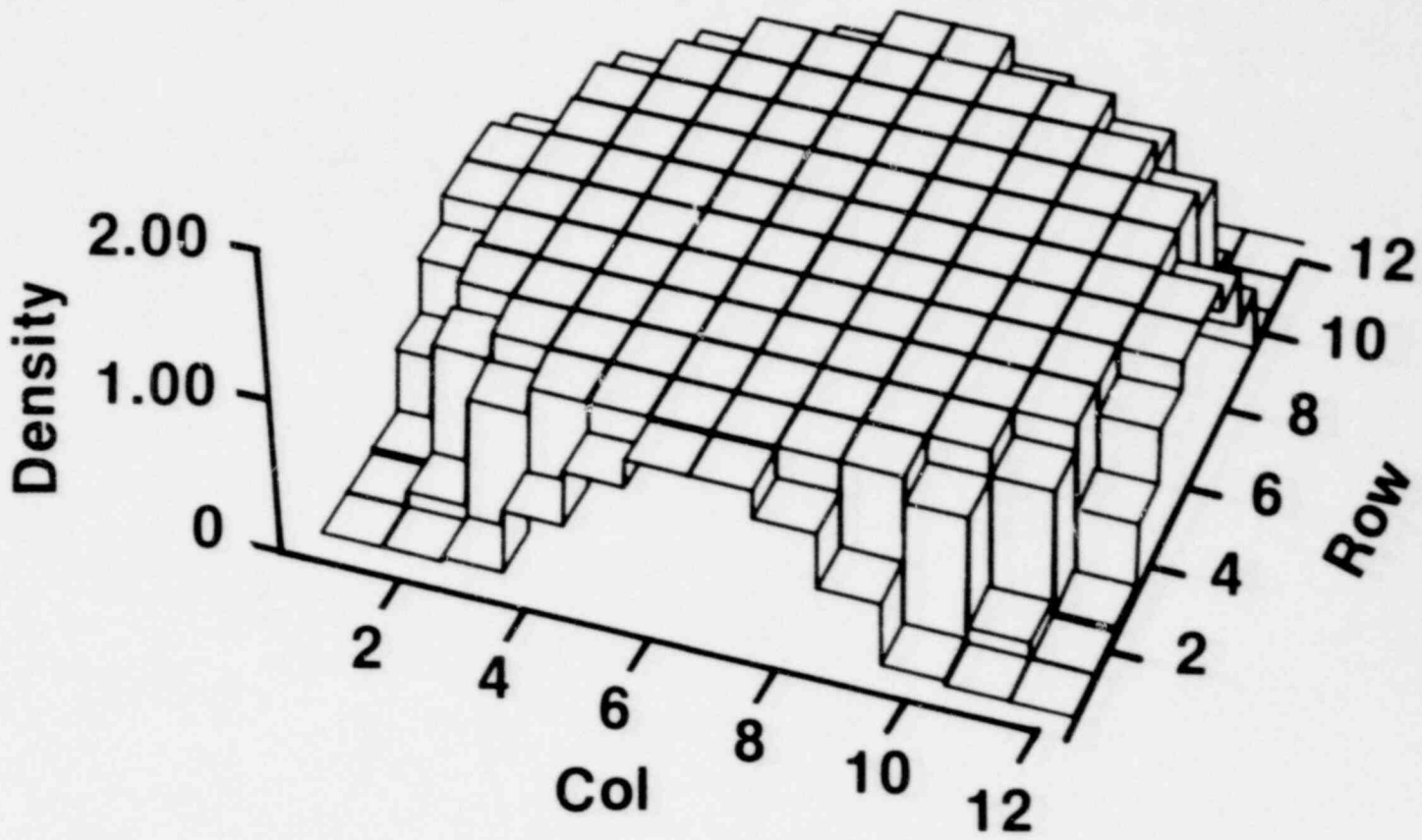

INEL-S-21 677

Square Plot

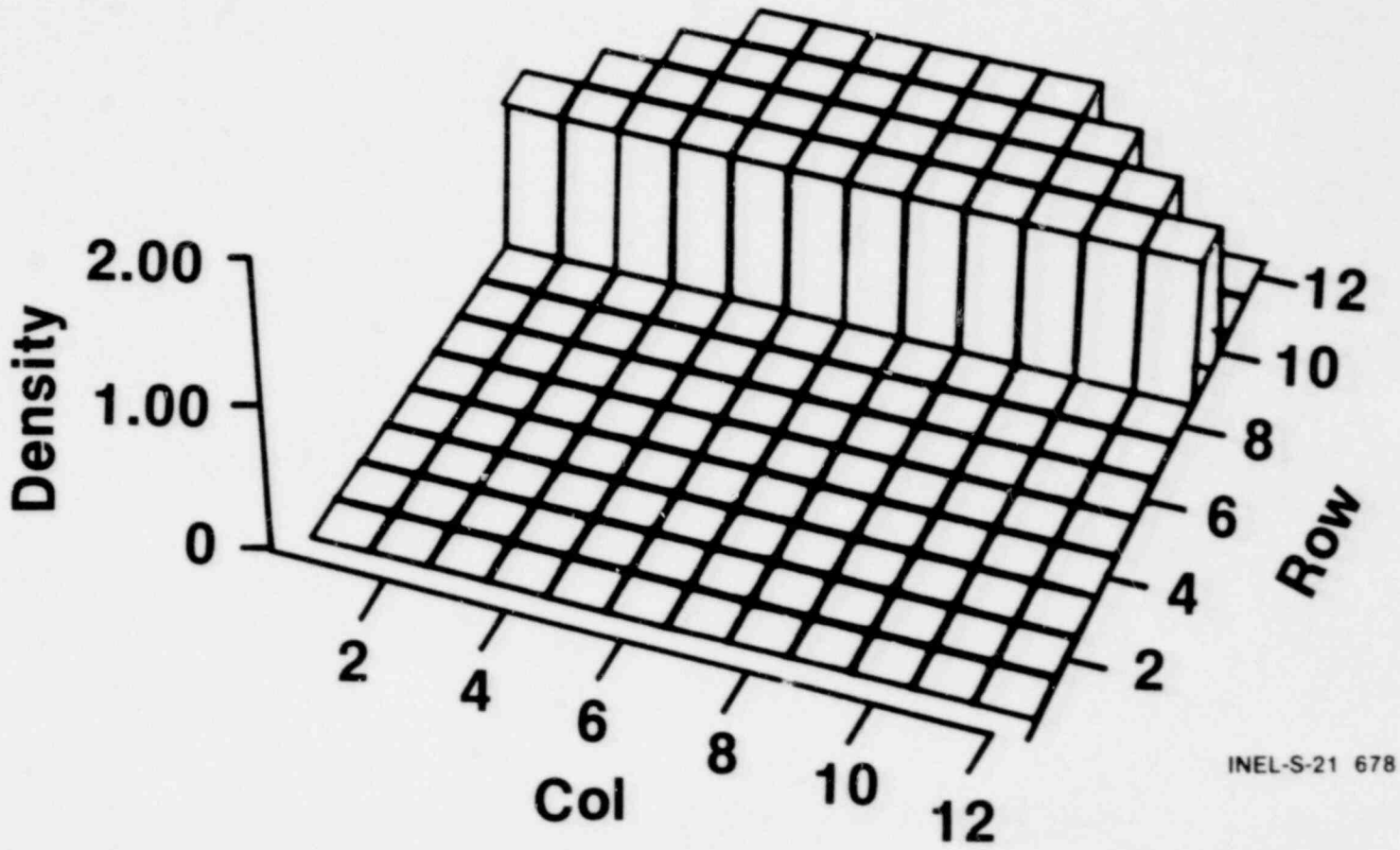

Digitized Test Phantom
10 Bubbles in Pipe

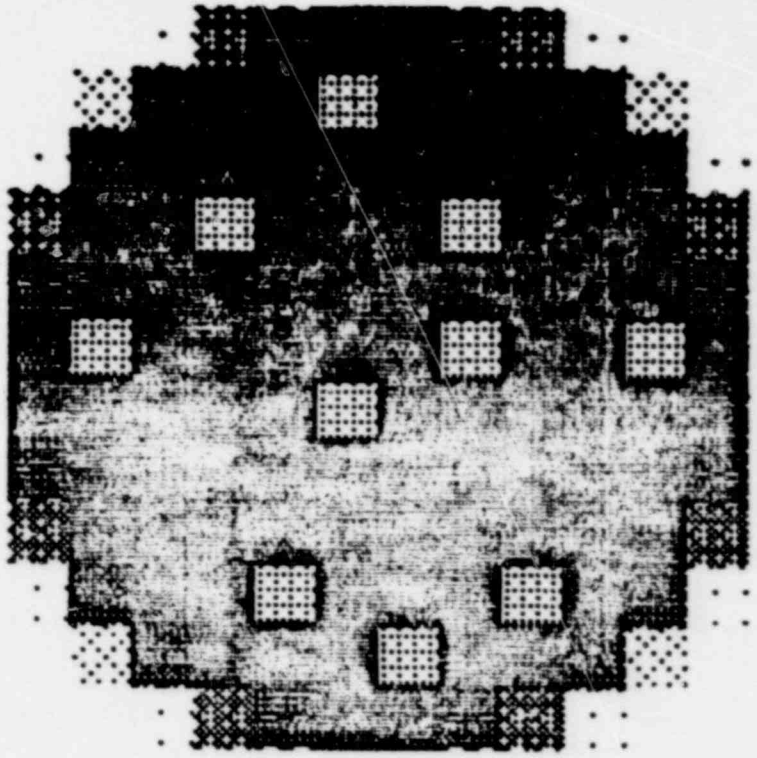

INEL-S-21 676

Reconstruction after 5 Iterations (30 Views - 9 Detectors/View)

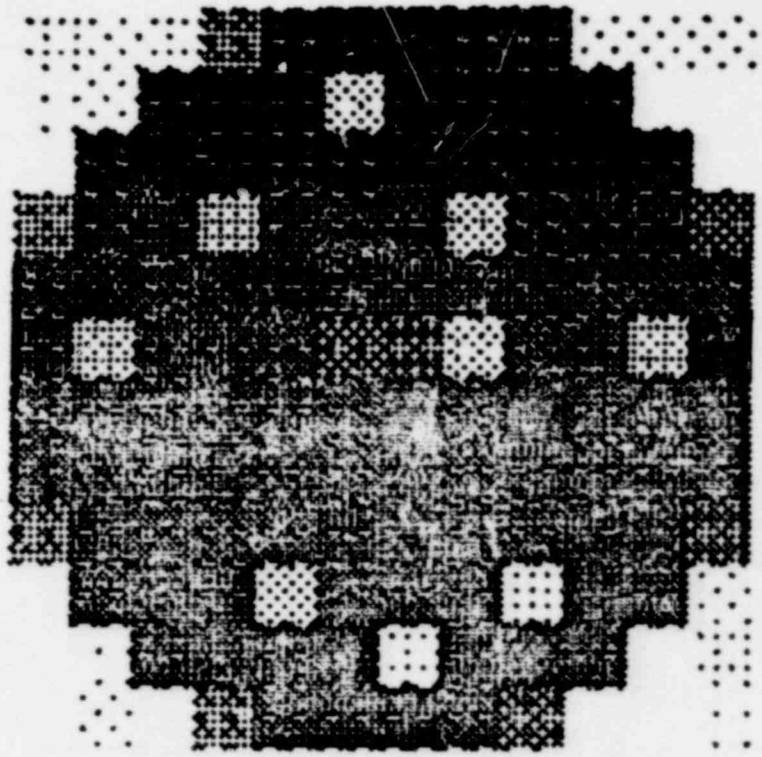

INEL-S-21 675

Local Phase Velocity

1. Stagnation probes

    a. Pitot tube

    b. 5-point stagnation probe to determine vector components

Global Phase Velocity

- Velocities calculated from input mass flow rates, system heat balance, and global void fraction.

INEL-S-21 526

Center of Mass Velocity

Pulsed neutron activation

INEL-S-21 528

Laser Technology

- Holography
  - Imaging
  - Interfacial area mapping
  - Void fraction
- Light scattering void fraction
- Doppler velocity
  - LDV - 1Ø
  - FOLDA probe - 2Ø

POOR ORIGINAL

FOLDA Probe

1600 210

Conclusions

- At best, a standard for global mass flow rate, pressure, and temperature (sat. cond.) presently exists.

INEL-S-21 529

1600 211

LA-UR 79-

TITLE: VIDEO OPTICAL SYSTEMS FOR THE 2D/3D MULTINATIONAL REFILL-REFLOOD PROGRAM

AUTHOR(S): Walter L. Kirchner
Wilfred G. Hansen
Charles R. Mansfield
John F. Spalding

PRESENTED AT: Seventh Water Reactor Safety Research Meeting
Gaithersburg, MD
November 6, 1979

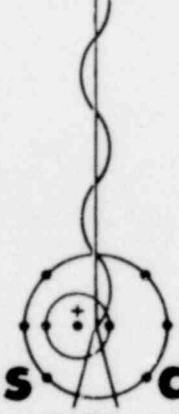

los alamos
scientific laboratory
of the University of California
LOS ALAMOS, NEW MEXICO 87544

1600 212

Form No. 836
St. No. 2629
1/75

UNITED STATES
ENERGY RESEARCH AND
DEVELOPMENT ADMINISTRATION
CONTRACT W-7405-ENG. 36

Video Optical Systems for the 2D/3D Multinational Refill-Reflood Program

W. Kirchner, W. Hansen, C. Mansfield, and J. Spalding
Energy Division
Los Alamos Scientific Laboratory

ABSTRACT

Video optical systems are under development at the Los Alamos Scientific Laboratory for installation in the participating reactor safety experiment facilities of the Multinational 2D/3D Refill-Reflood Program. The purpose of these systems is to provide high quality visual images of two-phase flow phenomena in the upper plena of these facilities. A long range objective is to develop supporting analysis software to convert the recorded visual images to digital information containing ensemble and discrete particle size and velocity data.

INTRODUCTION AND APPLICATION

The Los Alamos Scientific Laboratory is participating in a multinational program to investigate refill and reflood phenomena in simulated loss-of-coolant-accident (LOCA) experiments. As part of this effort, video imaging systems are under development in the Reactor Safety Experiments Group at LASL. These systems are designed to provide high quality video images of the two-phase flow phenomena in the upper plena of the facilities. This information is extremely valuable for use in interpreting the results of the

experiments. It will provide the analysts and experimentalists with flow regime information to evaluate instrumentation response, develop phenomenological models, and assess code predictions. On a long term basis, the systems show much promise for digitization of the images and subsequent conversion to liquid phase velocity and size information. Table I lists the systems development schedule.

SYSTEM DEVELOPMENT

To date, two systems have been constructed and tested: one for the German PKL reflood facility and one for the Japanese Cylindrical Core Test Facility (CCTF). Both systems were based on a stereo viewing design concept. Rod lens (commercially manufactured in Germany by Stortz) optical trains were built up by disassembling short probes made for medical applications. By stacking these relay lens to the necessary lengths, an optical path to relay the image from the probe tip within the facility to the video TV units exterior to the facility pressure boundary is constructed. The TV signal is then recorded on tape for subsequent playback and analysis. Since most of the probe is immersed in a hostile environment, an environmental envelope is used to house the optics trains and light source. Sapphire windows are used for viewing at the probe tip and a heat pipe is used to maintain the optics at a uniform low temperature (about 35 C). Lighting in the viewing region at the probe tip is provided by fiber optics illumination in the PKL probe and by a built-in light source at the probe tip of the CCTF unit. Figure 1 illustrates schematically the general probe design. Figure 2 shows the completed PKL probe and associated support electronics. The system is self-powered by batteries and a

DC/AC inverter to run with US standards equipment. Figure 3 displays the contents of the support electronics box.

CURRENT EFFORT

Based on available data from the experimental facilities, it appears that the two-phase droplet flow regimes expected to dominate these experiments are of relatively short duration. Hence, the emphasis of this program has been shifted to providing high quality video images instead of droplet flow data. As a result, future systems no longer need be stereo. To meet this new objective the system design has been substantially altered. Space constraints in the old units required transmitting stereo images via relay lens, but it is now possible to install a miniature TV camera at the probe tip within the same environmental envelope. Figure 4 shows a typical commercially available miniature TV camera (diameter slightly greater than 1 inch). Future units will use the miniature TV camera design where possible. The elimination of the relay lens optic trains is desirable when possible because it has been found that stacking long lengths of relay lenses results in degradation of image quality due to light losses (transmission and scattering) and distortion. A new relay lens design of much larger diameter (1/2 inch vs. less than 1/4 inch for Stortz) and length with superior optical coatings has been contracted for manufacture. This design will serve as a backup for situations where the TV camera cannot be cooled adequately.

TABLE I

ROD LENS DEVELOPMENT SCHEDULE

FACILITY	UNIT #	LOCATION	MOUNTING/ VIEW ANGLE	FOV	LENGTH	MONO/ STEREO	DATE REQUIRED	STATUS/COMMENTS
PKL	PRL-1	Broken HL nozzle	Vertical/45°	45°	1 m	S	2/79	Shipped 3/79 Tested in PKL 4/79
	PRL-2	UCSP	Vertical/45°	30°	1 m	M	1/80	Design
CCTF	CRL-1	Broken HL nozzle	Vertical/90°	40°	3 m	S	7/79	Shipped 7/79 Tested 10/79
	CRL-2	UCSP	Vertical/45°	30°	4 m	M	5/81	Design
SCTF	SRL-1	End box	Horizontal/0°	30°	1 m	M	5/80	Design
	SRL-2	HL nozzle	Horizontal/0°	30°	1 m	M	5/80	Design
UPTF	URL-1	Broken HL nozzle	Vertical/90°	30°	4 m	S/M	6/81	Design
	URL-2	Intact HL nozzle	Vertical/90°	30°	4 m	M	6/81	Design
	URL-3	Middle UP internals	Vertical/90°	30°	4.5 m	M	6/81	Design
	URL-4	UCSP	Vertical/90°	30°	5 m	M	6/81	Design

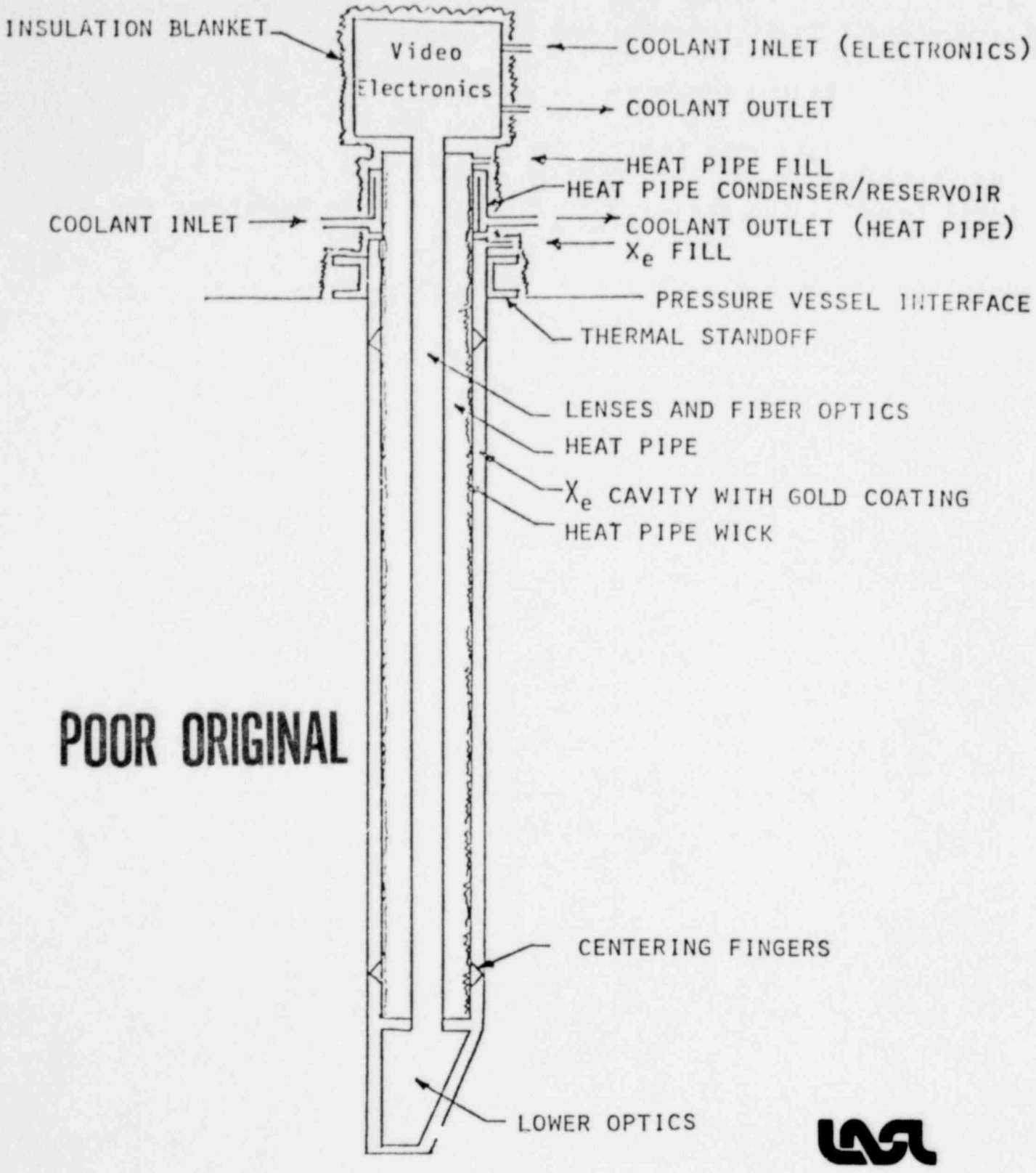

FIGURE 1 - SCHEMATIC OF ROD LENS PROBE UNIT.

POOR ORIGINAL

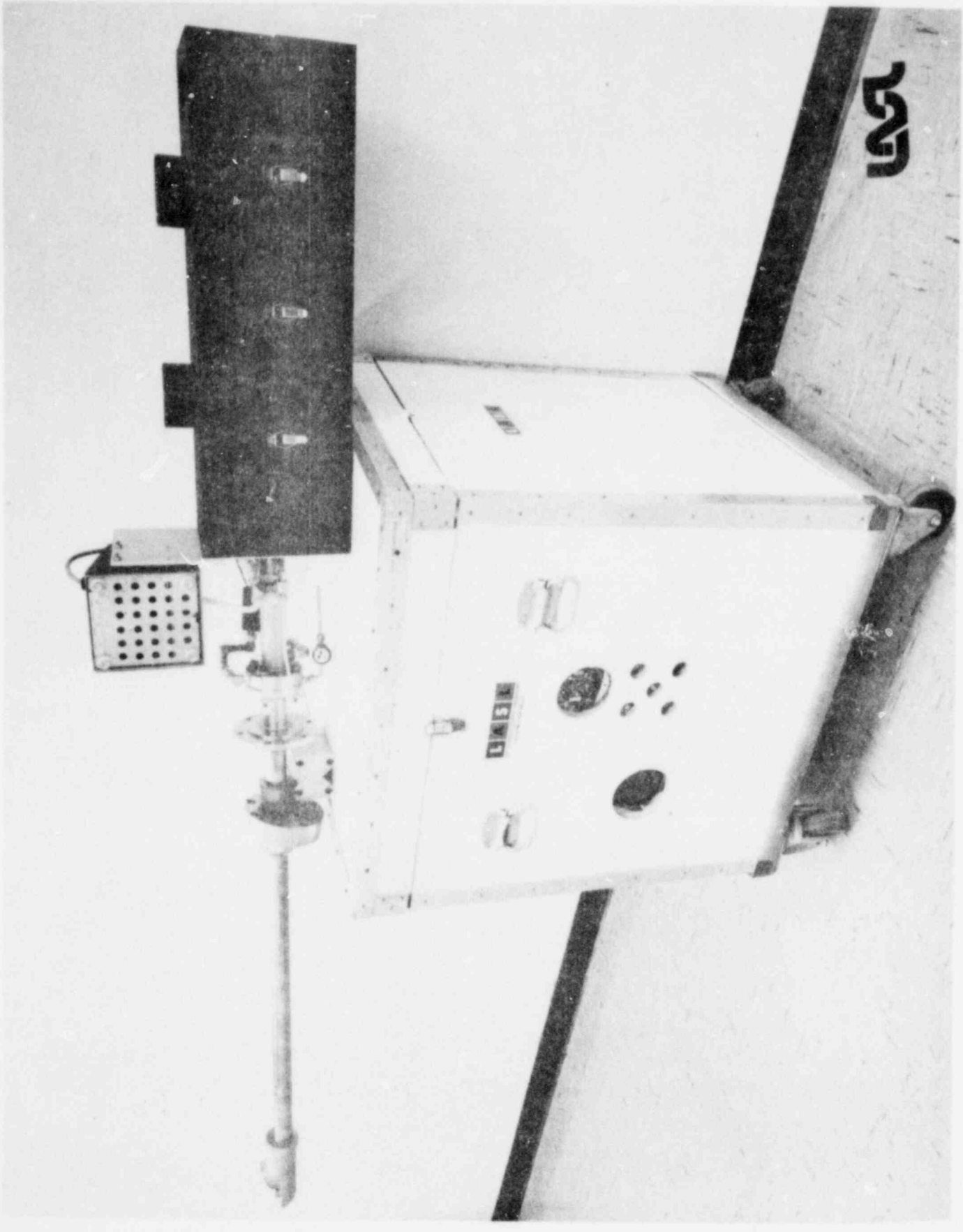

FIGURE 2 - PKL ROD LENS SYSTEM.

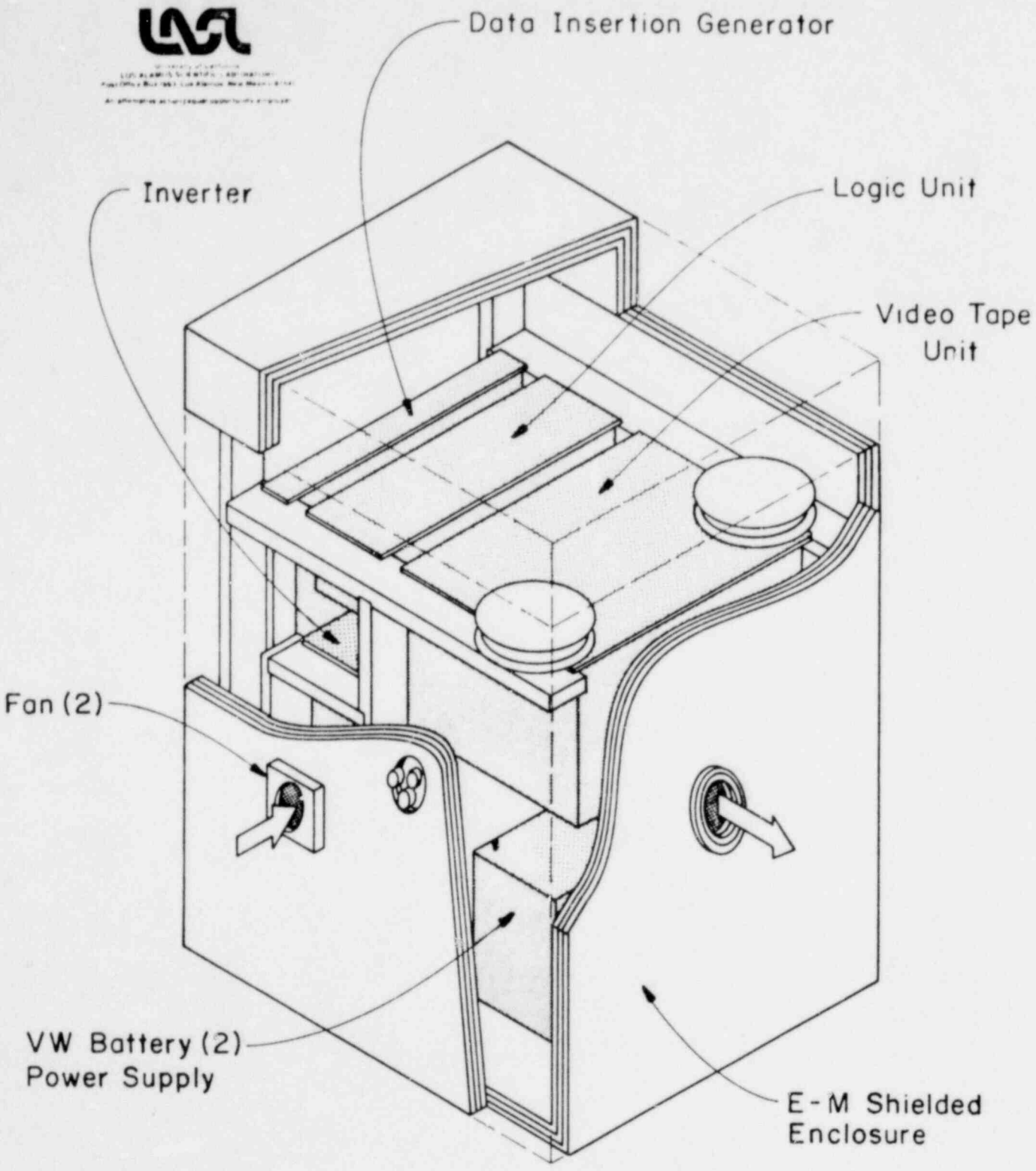

FIGURE 3 - ROD LENS SYSTEM SUPPORT ELECTRONICS.

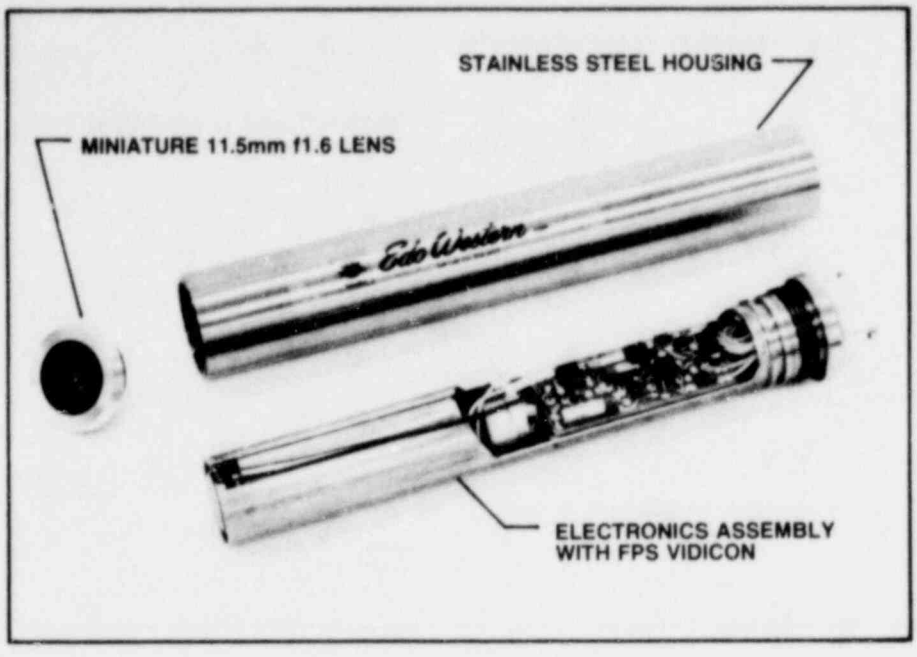

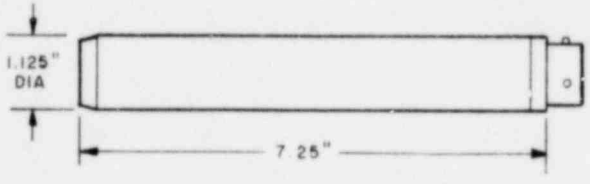

FIGURE 4 - MINIATURE TV CAMERA FOR VIDEO PROBE (Edo-Western).

REACTOR NOISE APPLICATIONS TO TWO-PHASE FLOW STUDIES

Robert W. Albrecht
Dept. of Nuclear Engineering
University of Washington
Seattle, Washington

SUMMARY AND VISUALS

for

presentation at the

SEVENTH WATER REACTOR SAFETY RESEARCH INFORMATION MEETING

(workshop on instrumentation programs)

November 5-9, 1979

National Bureau of Standards

Washington, D. C.

Summary of Results and Technical Achievements

(1) Drag disc dynamic response

The dynamic response of LOFT drag discs was tested in air, water, and air/water mixtures. Figure 1 shows the impulse response of one of the drag discs in air. Figure 2 shows the impulse response of the same drag disc in water. It is found that the resonant frequency in water is significantly lower than in air and that the 'Q' is higher in air than in water. Figure 3 shows the spectrum of the drag disc response in an air/water mixture. The resonance is at an intermediate frequency and the 'Q' is lower than in either the pure air or pure water case. The spectrum of the two-phase flow is seen to peak at 12 Hz. Figure 4 shows a zoom of the resonance with two phase flow present. Distinct responses due to air and water are not evident. Figure 5 summarizes responses observed for two drag discs. It is concluded that drag disc resonant response is weakly related to two-phase flow conditions.

(2) Global two-phase flow measurements

Figure 6 shows the PSD of neutronic fluctuations measured with two phase bubbly flow in the core by ex-core detectors. The PSD follows a model derived from purely random fluctuations. The sink frequency at 10 Hz is evident ($f_s = 2v/H$). The lower figure shows the ratio of the measured to modelled PSD. Deviations are generally less than a factor of two but some structure is seen at 2 - 4 Hz. Figure 7 is for a case dominated by slug flow. Resonant deviations show the frequency content of slugging. The sink frequency shows a lower flow velocity (down flow). These results show the potential for flow regime classification using global neutronic methods. Figure 8 shows the measured flow velocities from sink frequencies vs. air flow rate at constant water flow. The difference in slip between up and down flow is evident. It is concluded that global neutronic methods can determine average perturbation velocities.

(3) Acoustic-neutronic cross correlation

Figure 9 summarizes the conditions and results for an experiment that cross correlated neutronic and acoustic signals in a flowing system. The experiment is shown schematically in figure 10 and typical results of the phase of the cross spectra are shown in figure 11. With pure local boiling present the linear phase with frequency is clearly

evident. The presence of undisolved gas destroys this coherence.

(4) Local-global two-phase flow measurements

These type of experiments will be performed for the first time this autumn. Figure 12 lists the flow configurations and measurements. Figure 13 lists expected results and applications. Figure 14 shows the configuration of the experiments. It is known that global neutronic responses contain flow characterization information. Local neutronic responses also contain two-phase flow characterization information of a different type. The combination of both types of data together with auxillary instruments is expected to be rich in two phase flow classification information.

(5) LOFT SPND behavior during reflood

Data from four LOFT SPNDs was examined to determine regions of interesting signal characteristics that meet the following requirements:

1. signal structure ammenable to dynamic/stochastic analysis
2. signal response susceptable to phenomenological explanation
3. signal not under intense study by others

The portion of the SPND signals that met these three requirements occurs during the reflood stage in the L2-2 tests. The SPNDs exhibit the following characteristics during the time period from 36 seconds after blowdown to 150 seconds:

1. a generally decreasing (negative) trend
2. oscillations of about 0.5 Hz
3. spikes that appear to be in common between detectors and are occasionally time delayed

Figure 15 shows a typical amplified signal with trend, oscillations, and blips identified. Signals from the four SPNDs are being processed to extract their significant characteristics and a preliminary investigation into the causes of the major features of the SPND data during reflood is being actively pursued.

EGG-DTT # 1 (LARGE DISC)
IN AIR
⅛ IN. BALL BEARING IMPACTING
116.1 HZ RESONANCE

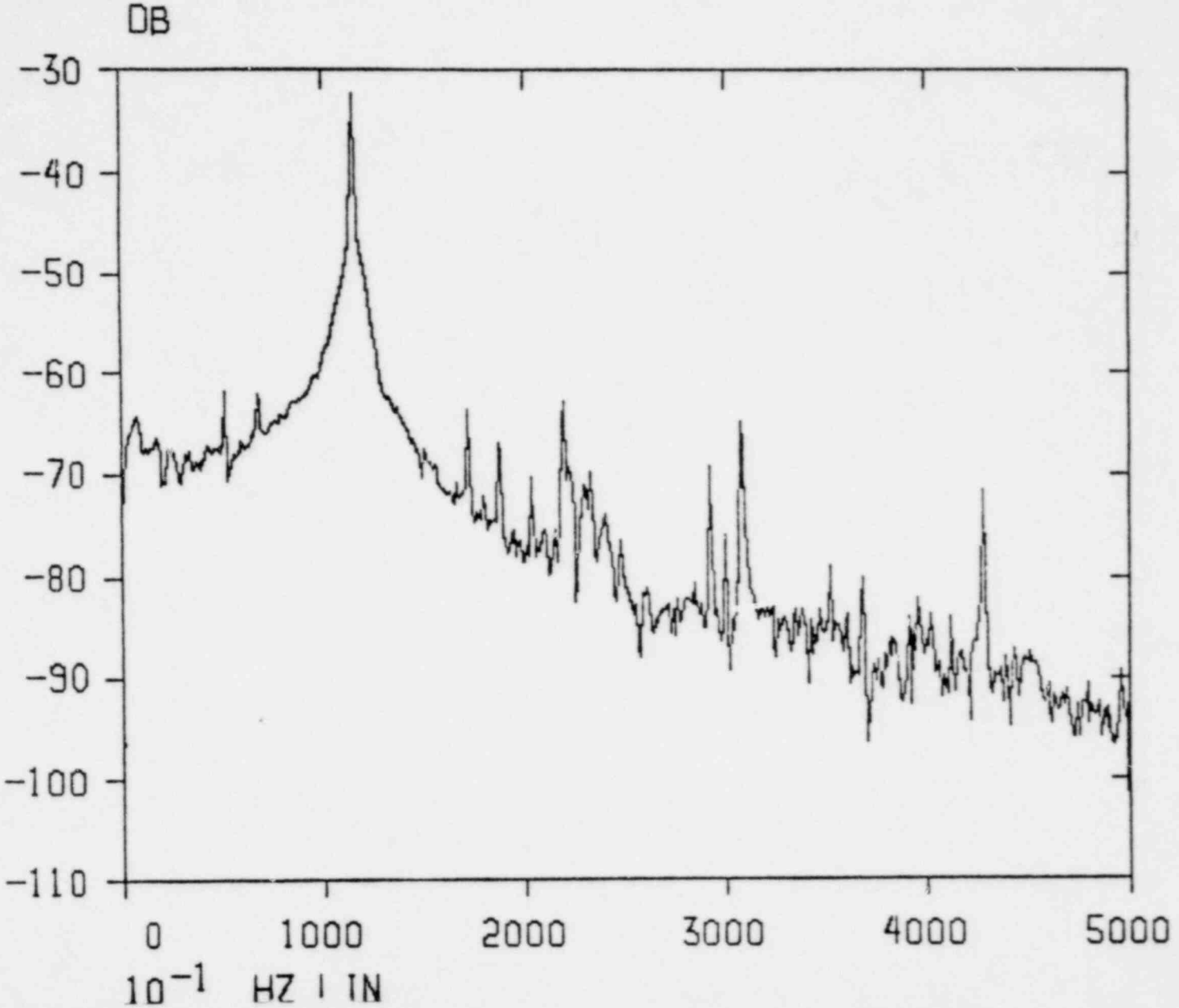

FIGURE 1

EGG-DTT #1
UNDER WATER-COLD
1/8 IN. BALL BEARING IMPACTING
98.5 HZ RESONANCE

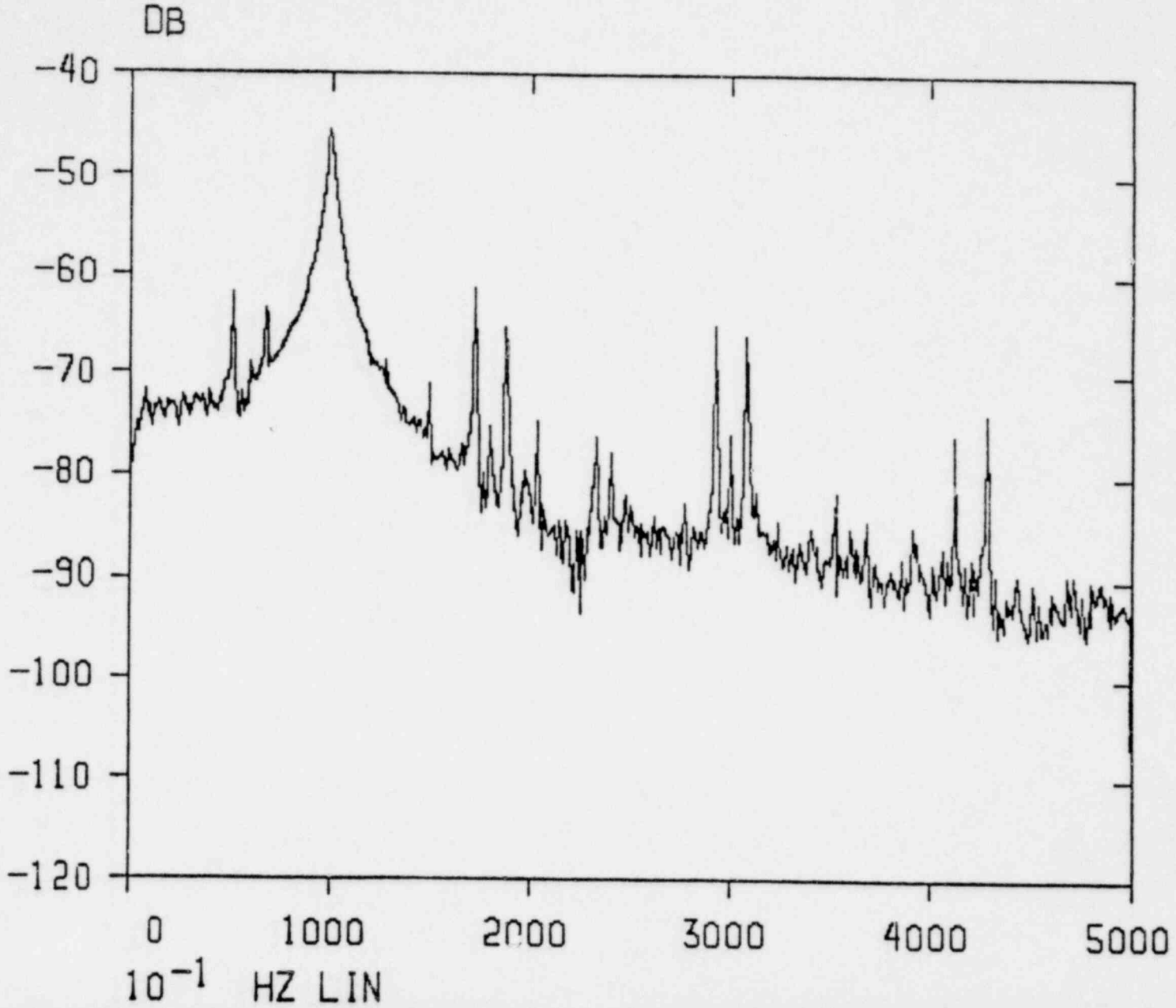

FIGURE 2

EGG-DTT #1 (LARGE DISC)
2 PHASE FLOW-REVERSE DIRECTION
102.5 HZ RESONANCE
≈12 HZ BUBBLE FORCING FUNCTION FREQUENCY

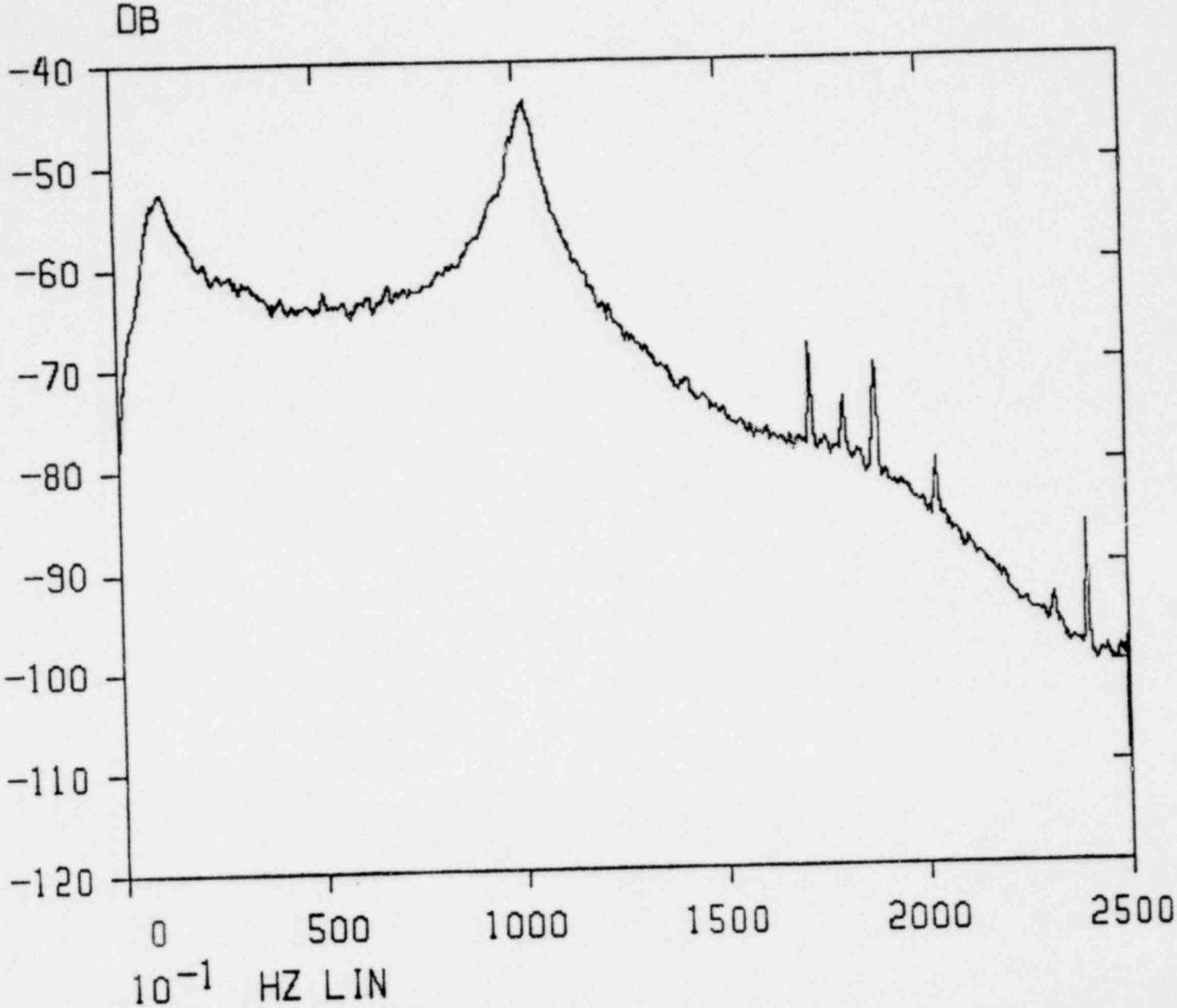

FIGURE 3

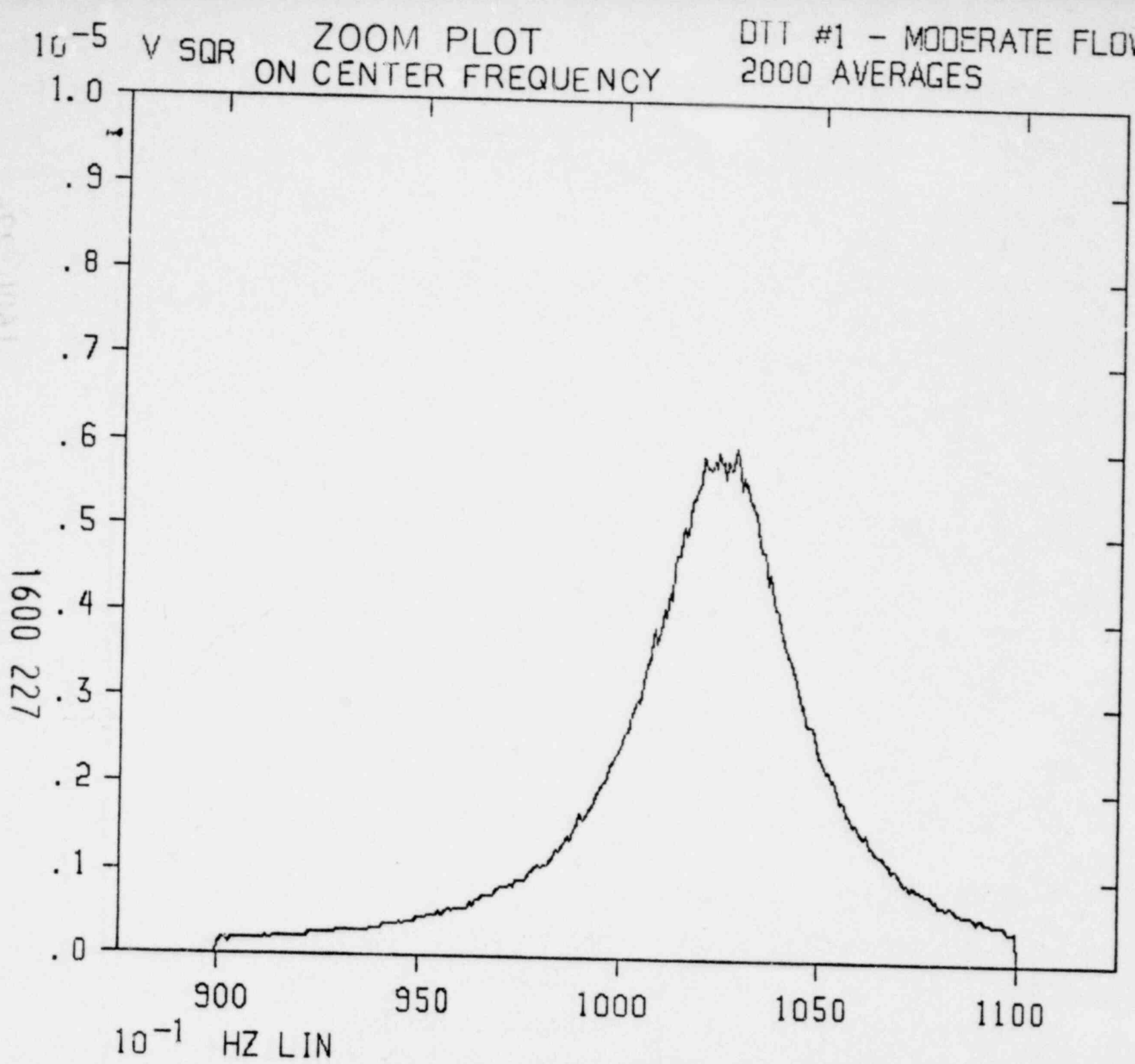
10^{-5} V SQR
ZOOM PLOT
ON CENTER FREQUENCY
DTT #1 - MODERATE FLOW
2000 AVERAGES
1.0
.9
.8
.7
.6
.5
.4
.3
.2
.1
.0
1600 227
900
950
1000
1050
1100
10^{-1} HZ LIN

FIGURE 4

FIGURE 5

EGG DTT PEAK FREQUENCY RESPONSE

	LARGE DTT	SMALL DTT
AIR	116.1 HZ	122 HZ
WATER	98.5 HZ	117 HZ
LARGE $\frac{\text{AIR}}{\text{WATER}}$	102.5 HZ	115 HZ
LESS $\frac{\text{AIR}}{\text{WATER}}$	103 HZ	115 HZ

1600 228

FIGURE 6

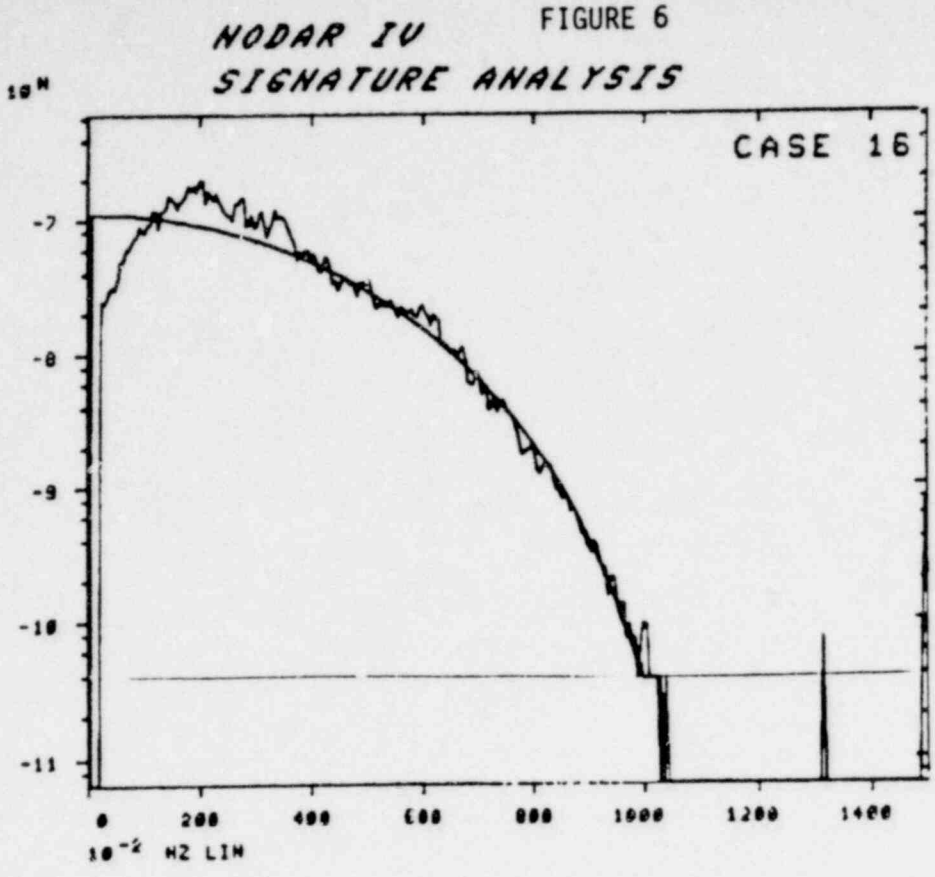

UNIVERSITY OF WASHINGTON NUCLEAR ENGINEERING DEPARTMENT

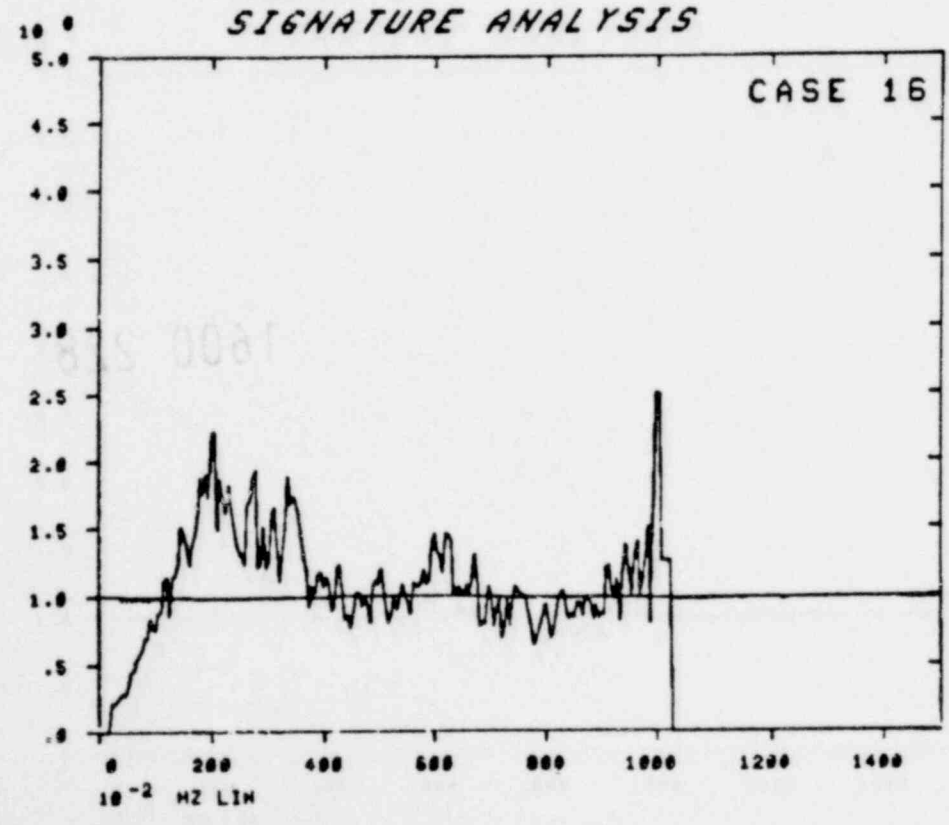

1600 229

UNIVERSITY OF WASHINGTON NUCLEAR ENGINEERING DEPARTMENT

FIGURE 7

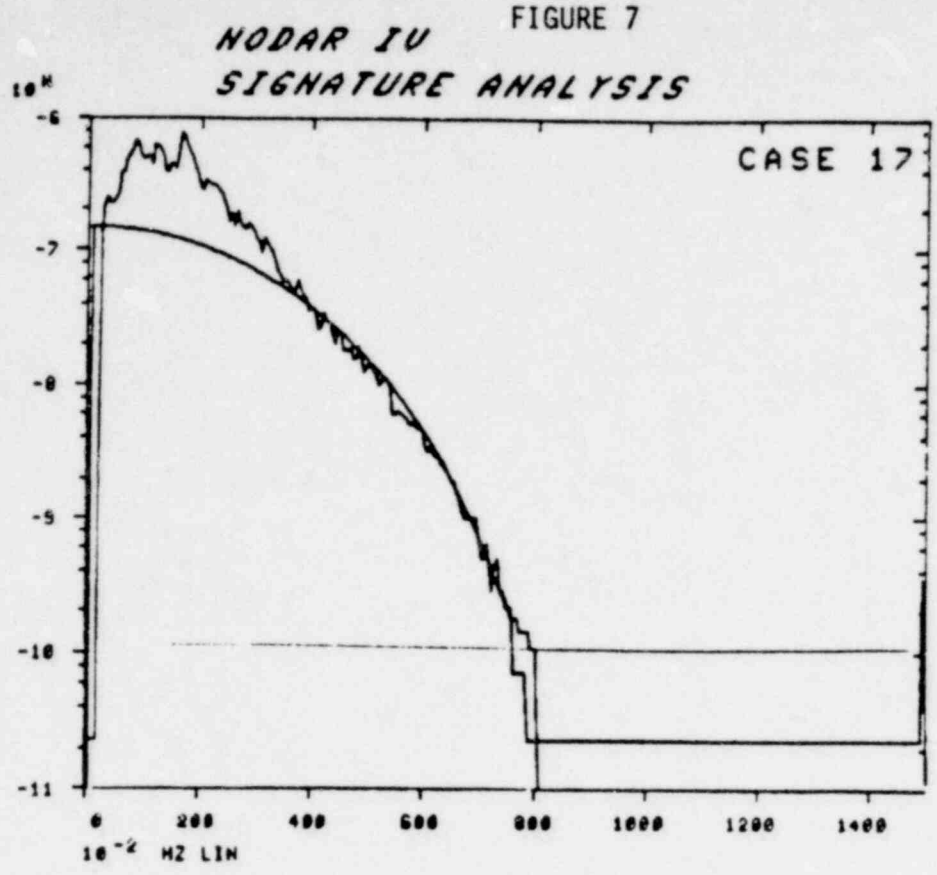

UNIVERSITY OF WASHINGTON NUCLEAR ENGINEERING DEPARTMENT

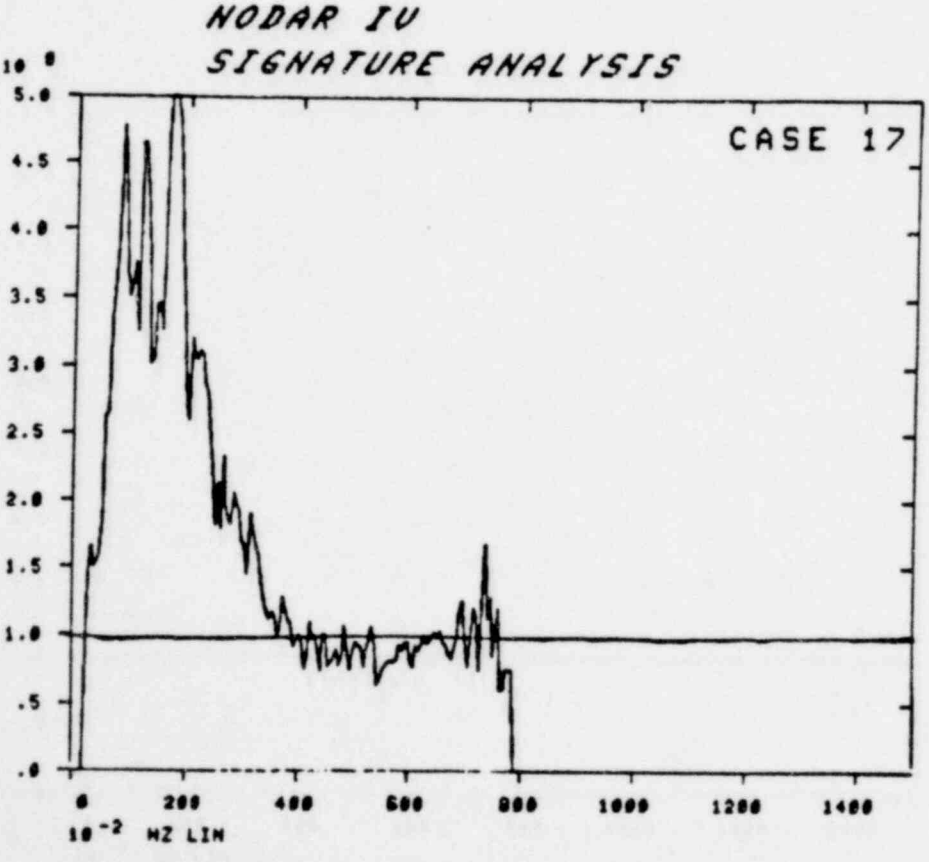

1600 230

UNIVERSITY OF WASHINGTON NUCLEAR ENGINEERING DEPARTMENT

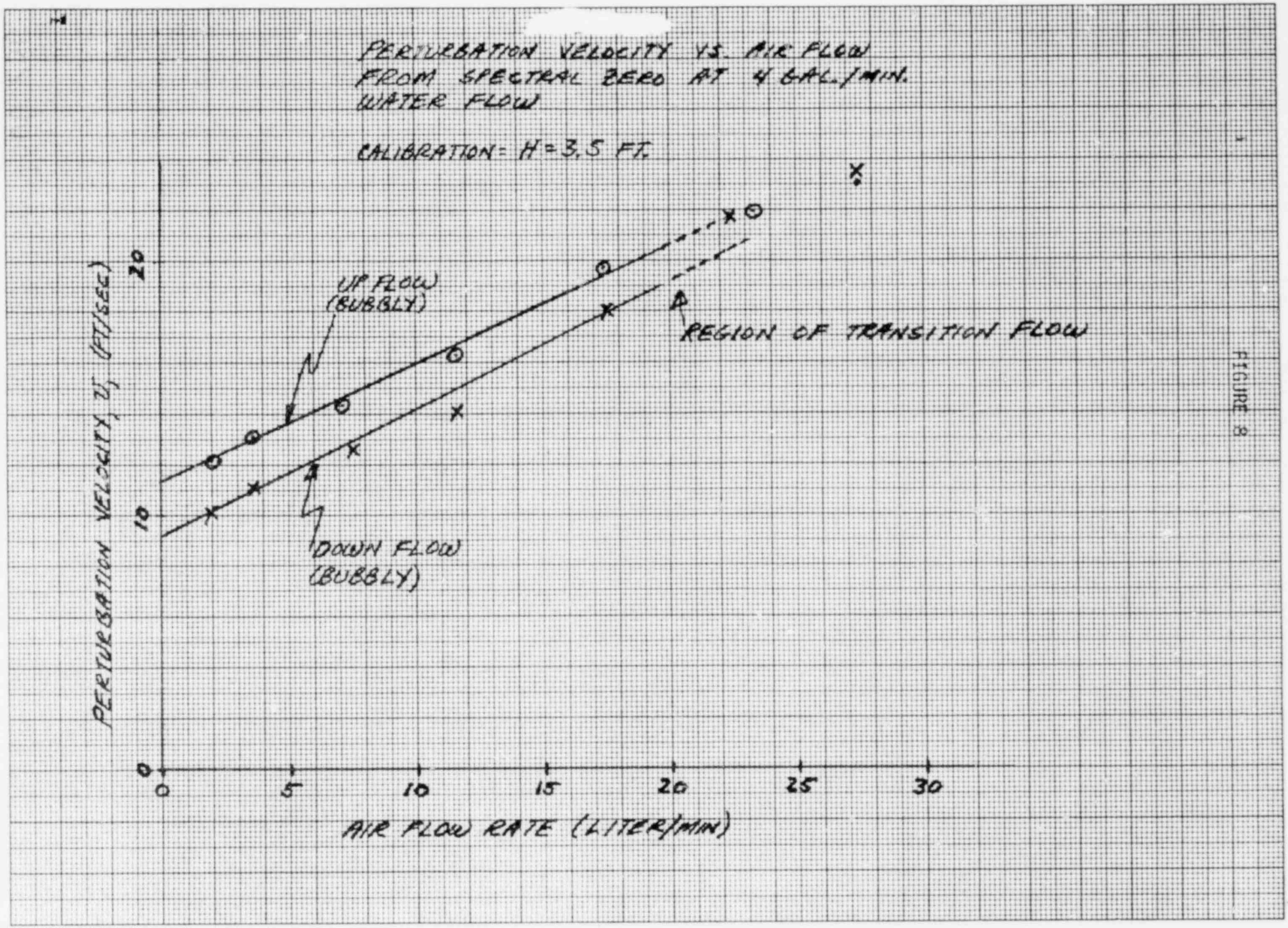

FIGURE 8

FIGURE 9

NODAR III
STEAM INJECTION EXPERIMENT

FLOW CONFIGURATIONS

FLUID: WATER, WATER AND AIR
GEOMETRY: VERTICAL, CYLINDRICAL
FLOW REGIMES: PURE LIQUID, BUBBLY
FLOW DIRECTION: UP

MEASUREMENTS

GLOBAL (OUT OF CORE) NEUTRON DETECTOR
PLENUM TANK MICROPHONE
ACOUSTIC NEUTRONIC CROSS POWER SPECTRUM

RESULTS

PHASE SHIFT OF CPSD LINEAR WITH FREQUENCY
IN CASES WITHOUT AIR IN SYSTEM
NO DISCERNABLE PHASE FREQUENCY RELATIONSHIP
IN CASES WITH AIR PRESENT

APPLICATIONS

SODIUM BOILING DETECTION

FIGURE 10

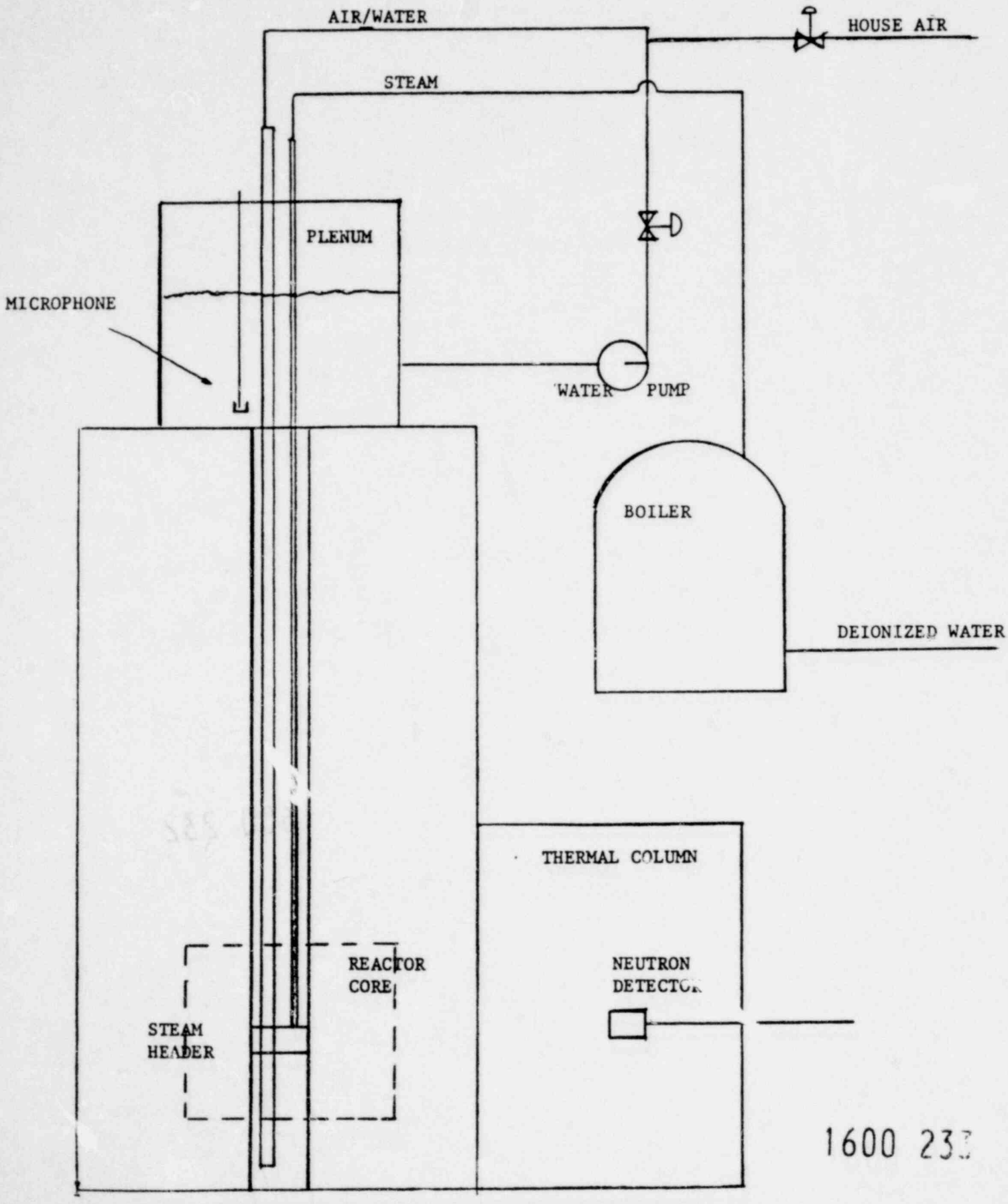

1600 23

FIGURE 11

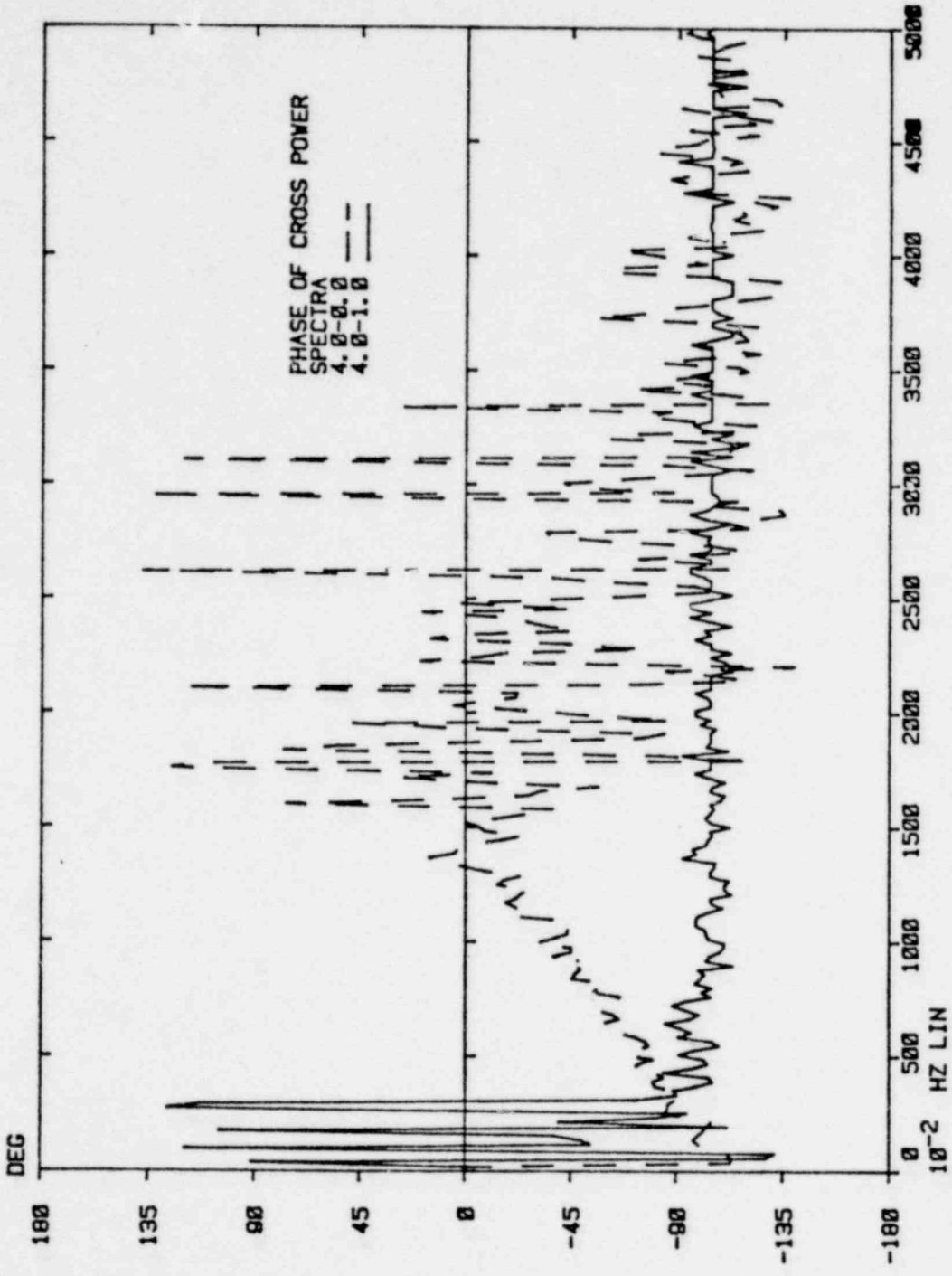

1600 234

FIGURE 12

2ΦC - NODAR V

TWO PHASE FLOW EXPERIMENT

FLOW CONFIGURATIONS

FLUID: TWO PHASE AIR AND WATER
GEOMETRY: VERTICAL, CYLINDRICAL (Ø.745" ID)
FLUID SUPERFICAL VELOCITIES:
WATER - Ø TO 4 M/SEC
AIR - Ø TO 3 M/SEC
FLOW REGIMES: LIQUID, BUBBLE, SLUG, ANNULAR, MIST, GAS
FLOW DIRECTION: UP OR DOWN

MEASUREMENTS

ONE PHASE: LIQUID AND GAS BULK FLOWS
(MASS FLOW, PRESSURE)
TWO PHASE: PHOTOGRAPHY (FLOW REGIMES)
DRAG DISC (MOMENTUM FLUX)
TURBINE (VELOCITY)
PITOT TUBE (VELOCITY)
PRESSURE DROP
LOCAL (IN-CORE) NEUTRONICS
(CPSD & TF)
GLOBAL (OUT-OF-CORE) NEUTRONICS
(APSD)

1600 235

FIGURE 13

2ΦC - NODAR V
TWO PHASE FLOW EXPERIMENT

EXPECTED RESULTS

BULK MASS FLOWS
PHOTOGRAPHIC CHARACTERIZATION
LOCAL MOMENTUM FLUX
LOCAL VELOCITY
LOCAL PERTURBATION VELOCITY
GLOBAL PERTURBATION VELOCITY
GLOBAL VOID FRACTIONS
STOCHASTIC CHARACTERIZATION

APPLICATIONS

TWO PHASE FLOW CHACTERIZATION
CALIBRATION OF TWO PHASE DTT
BWR SURVEILLANCE AND DIAGNOSTICS
PBF EXPERIMENTS FOR SUBASSEMBLY FLOW
LOFT SPND INTERPRETATION (PRE-BLOWDOWN)

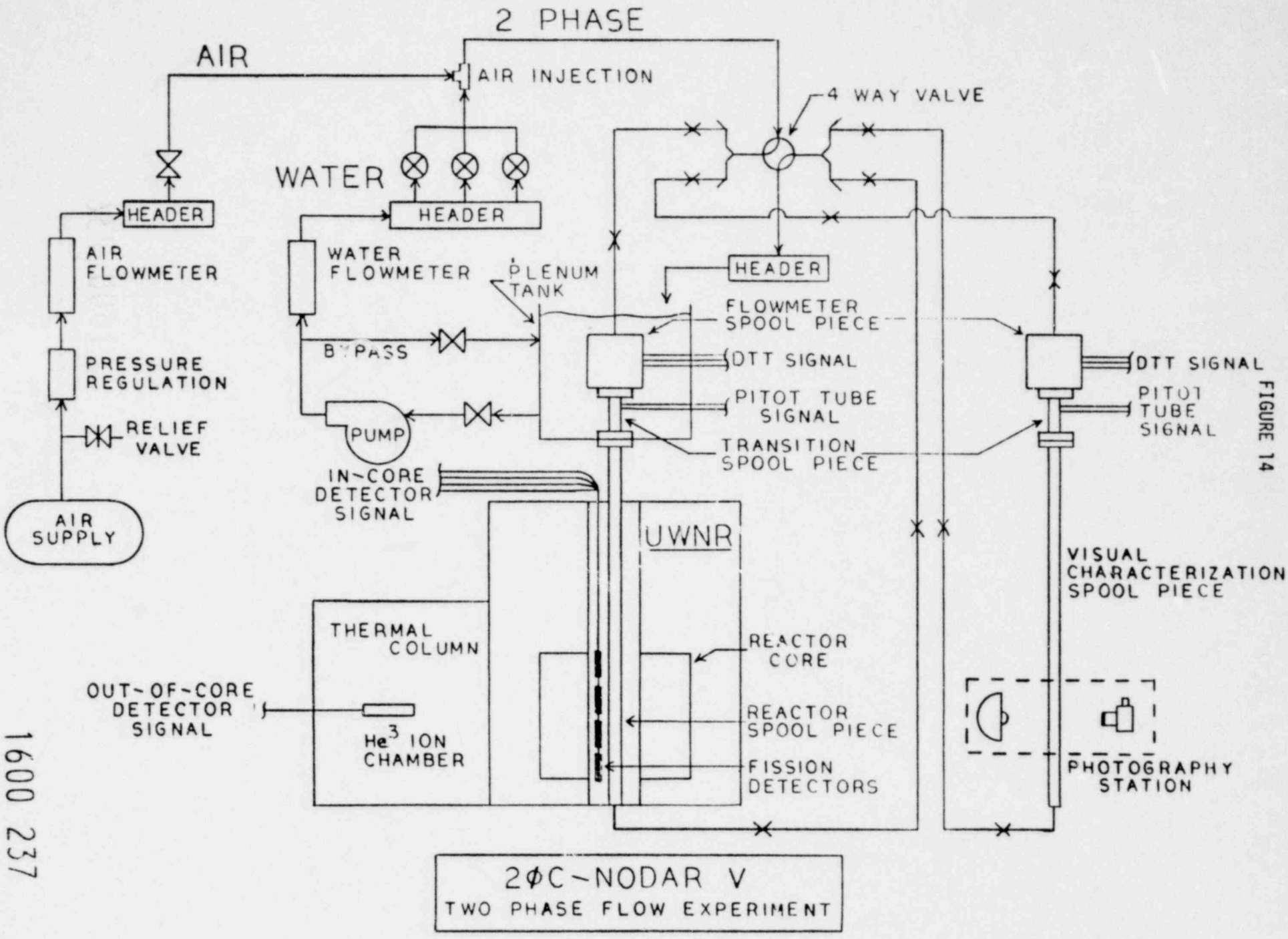

FIGURE 14

1600 237

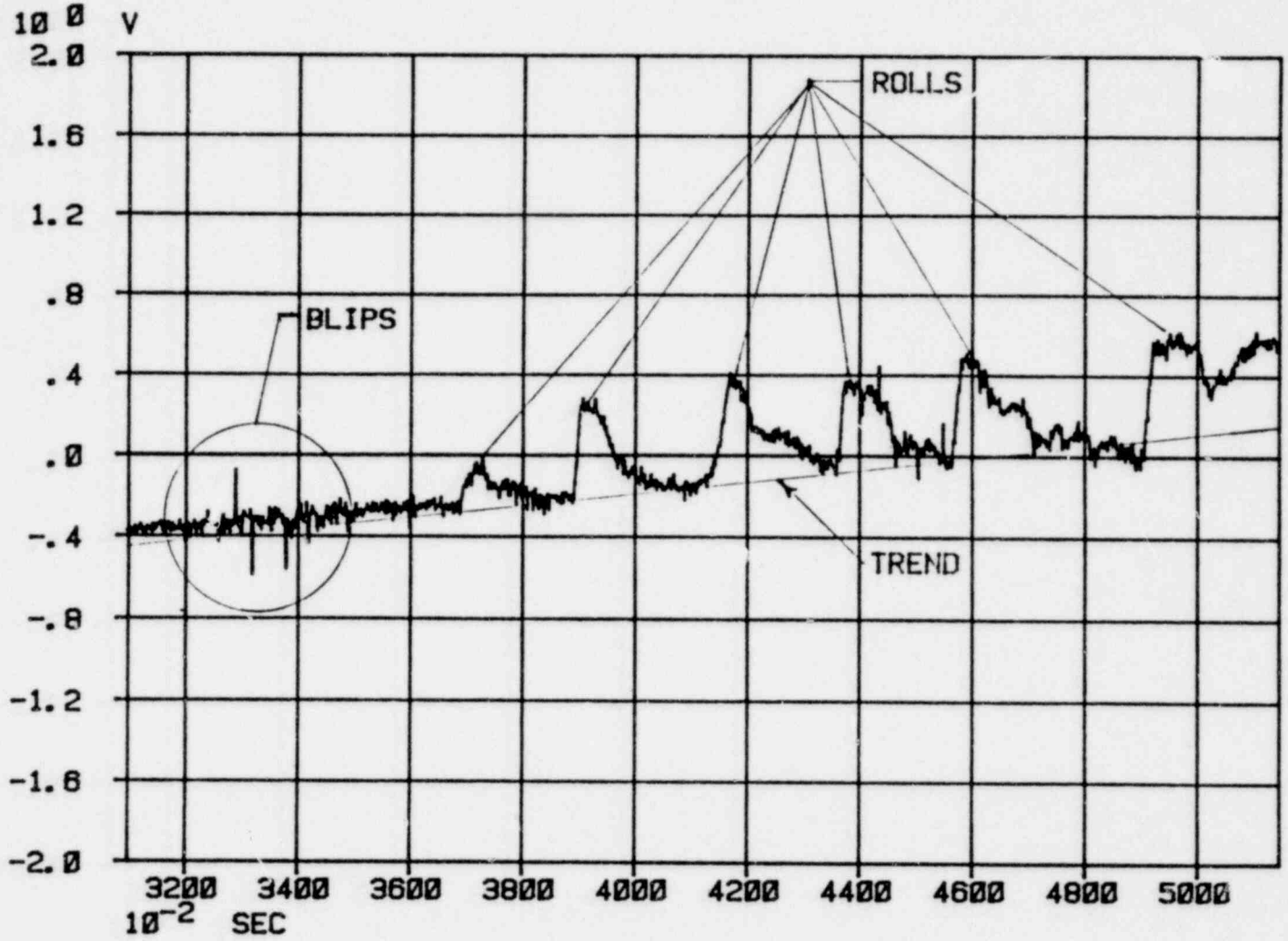

Figure 15

Void Fraction Measurement Using Neutrons

S. Banerjee - McMaster University

The presentation will discuss the experimental setup and measurements made of void fraction using fast/epithermal neutron transmission and scattering. The enclosed figures describe the experimental setup, void simulation using aluminum pieces, results for static calibration using aluminum water systems, and calibrations in two-phase flow against quick-closing valves. The results are for vertical downward flow in tubes and in 37-element rod bundles. It has been found that the scattered neutron count rate is proportional to the cross section averaged void fraction and is only weakly dependent on phase distribution. This has been confirmed by Monte Carlo calculations. On the other hand, the transmitted neutron flux is sensitive to phase distribution and can be used to indicate flow regimes. Results regarding the Monte Carlo calibrations and flow regime determination using the transmitted neutron beam will also be presented.

Reference List

1. "Fast Neutron Scattering and Attenuation Technique for Measurement of Void Fractions and Phase Distributions in Transient Flow Boiling", S. Banerjee, A. M. C. Chan, N. Ramanathan, P. Yuen, Sixth International Heat Transfer Conference, 1978, Vol. 1, 351-355, Hemisphere Press, Washington, 1978.

2. "Calibration of a Fast Neutron Scattering Technique for Measurement of Void Fraction in Rod Bundles", S. Banerjee, P. Yuen, M. A. Vandenbroek, Trans. ASME Journal of Heat Transfer, 101, 295-299, May, 1979.

3. "Simulation of a Neutron Scattering Method for Measuring Void Fraction in Two-Phase Flow", S. Banerjee, E. Hussein, D. Meneley, Nuclear Engineering and Design, 53, 393-405, August, 1979.

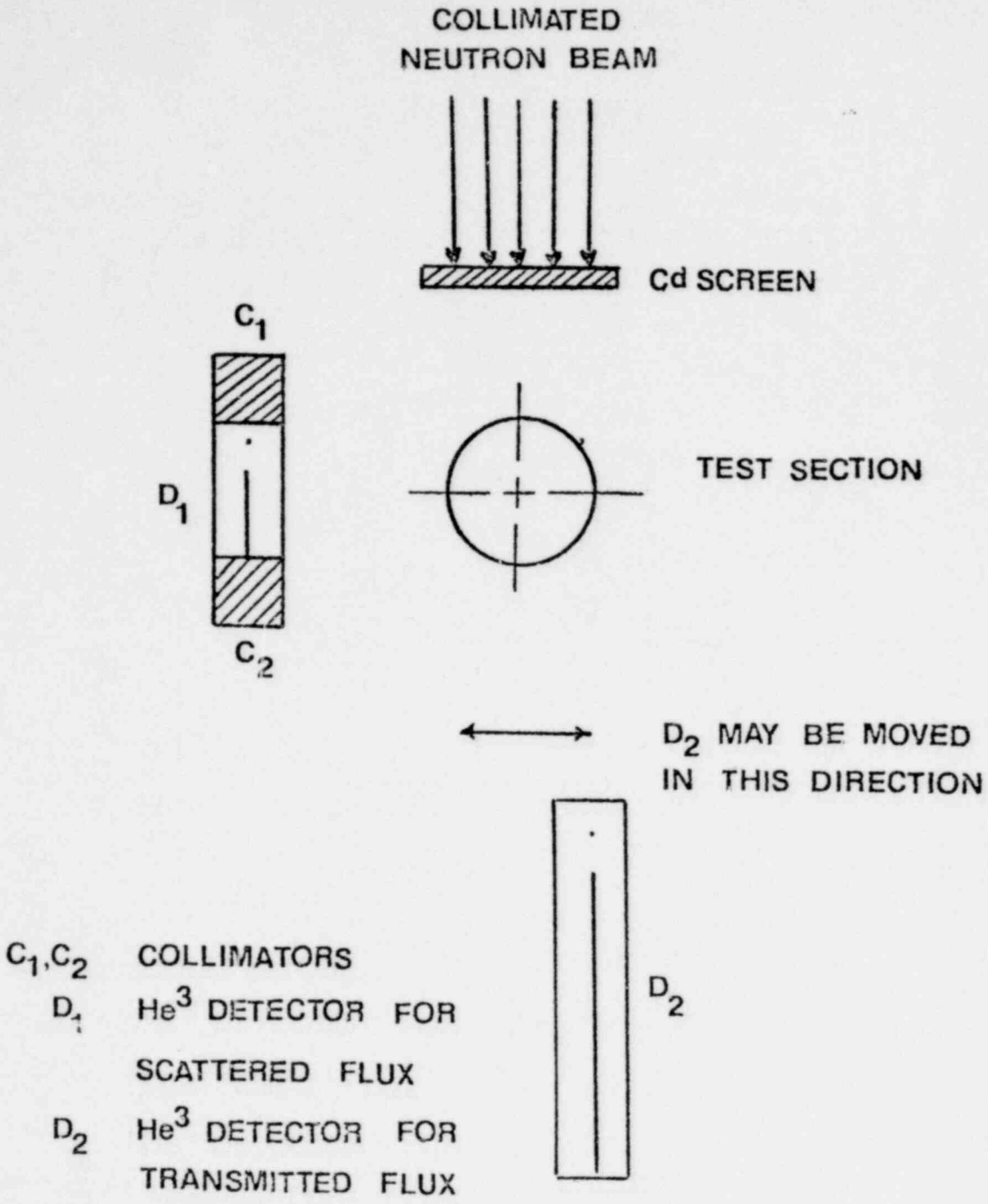

Figure 1- Plan view of experimental setup showing position of detectors, test section and neutron beam. The transmitted beam detector can be moved in the direction shown.

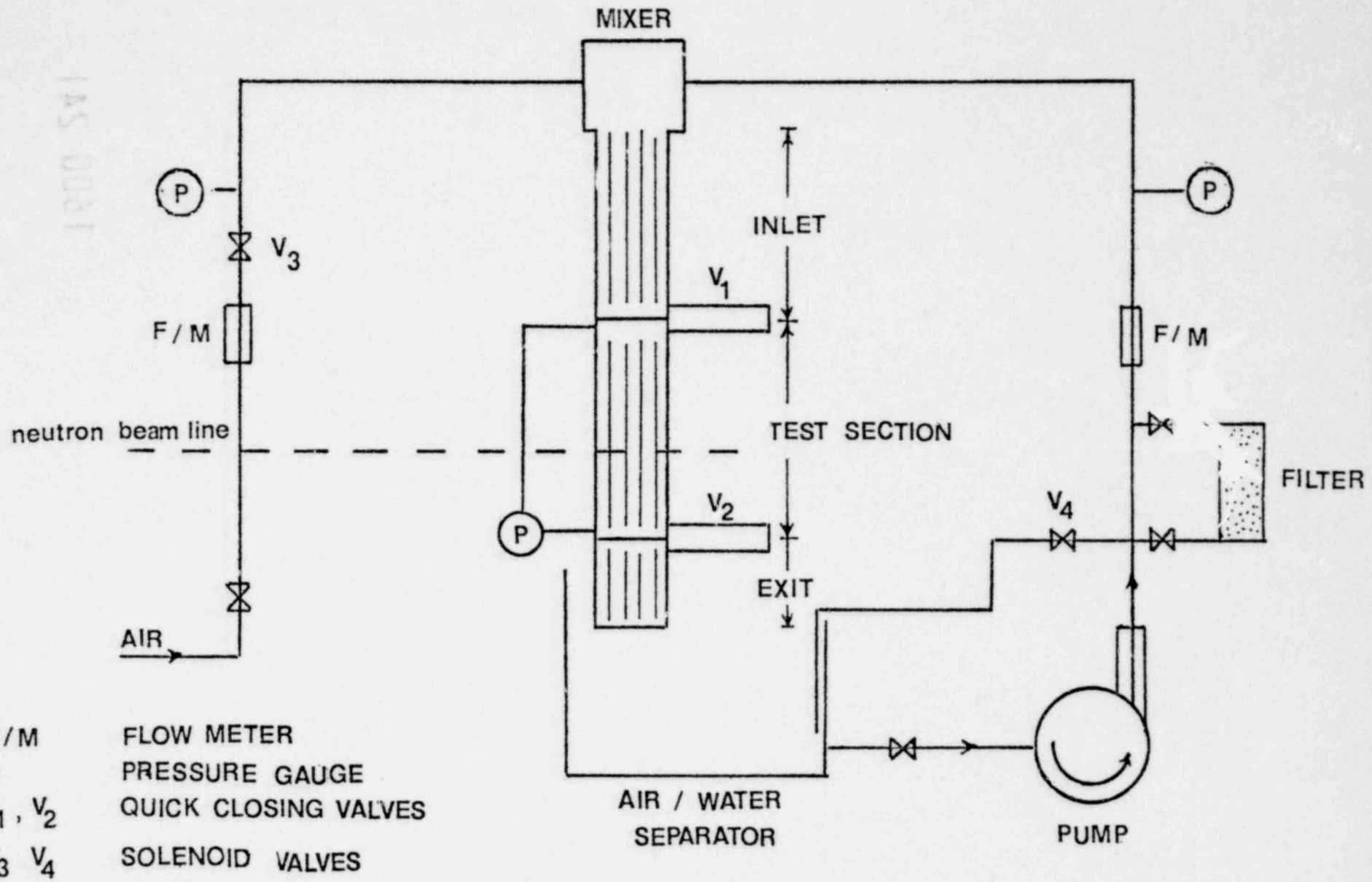

Figure 2 - Diagram of air-water loop

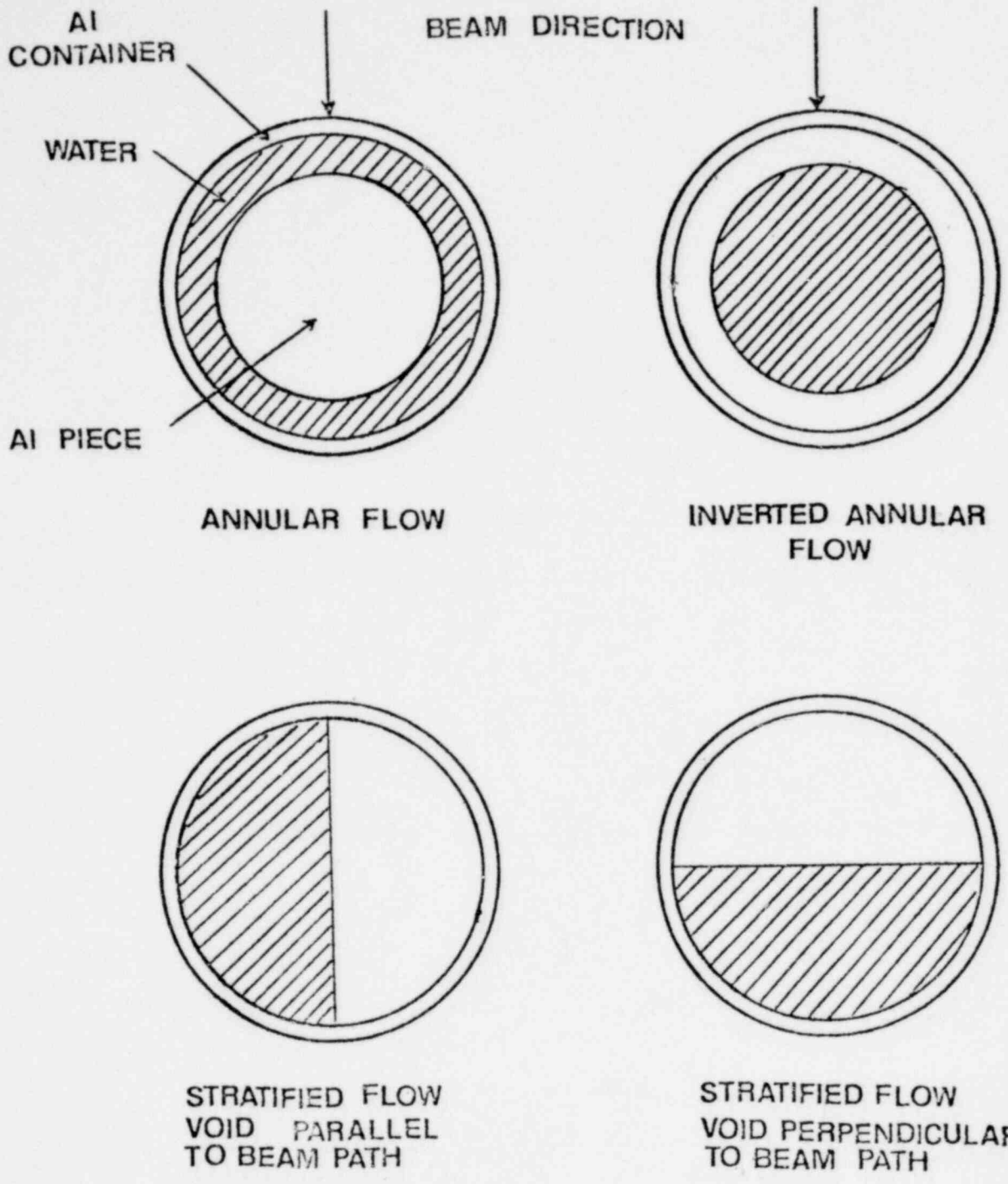

Figure 3 Cross-sectional view of aluminum shapes for void fraction of 0.5

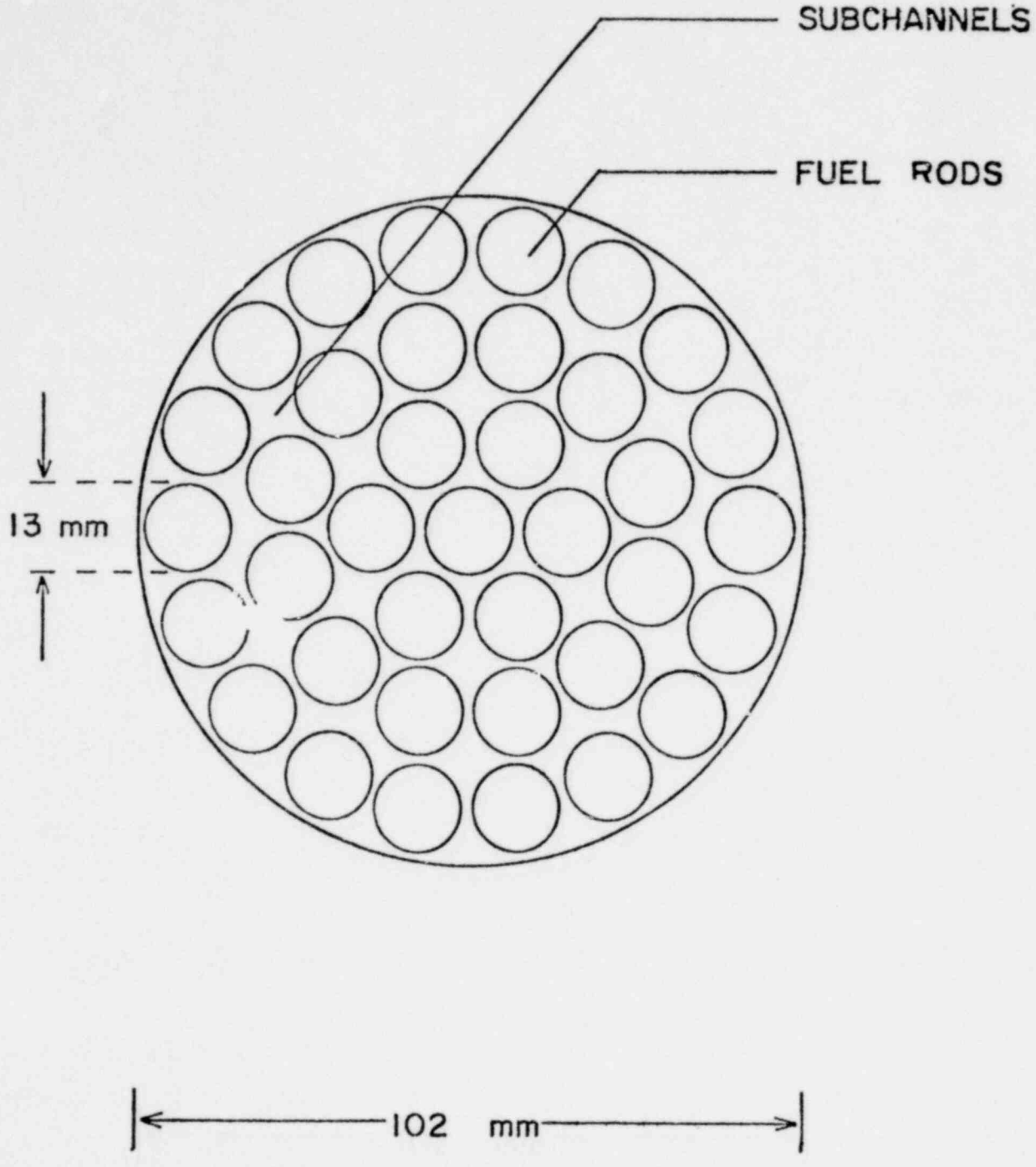

Figure 4 - Cross section of rod bundle test section.

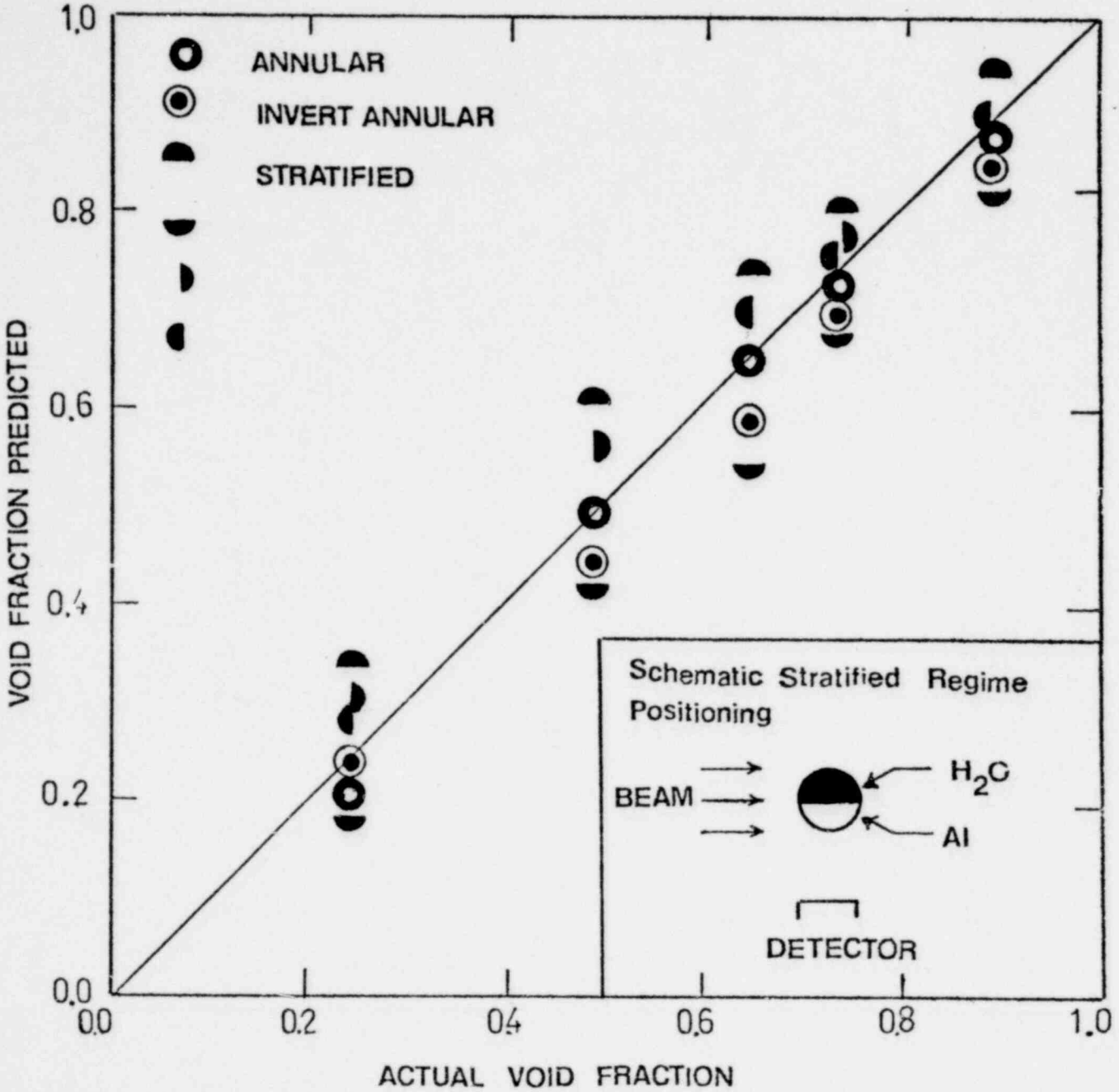

Figure 5 - Void fraction predicted by neutron scattering experimental measurements compared to actual void fraction for 50.8 mm containers. STRT denotes stratified flow pattern simulation.

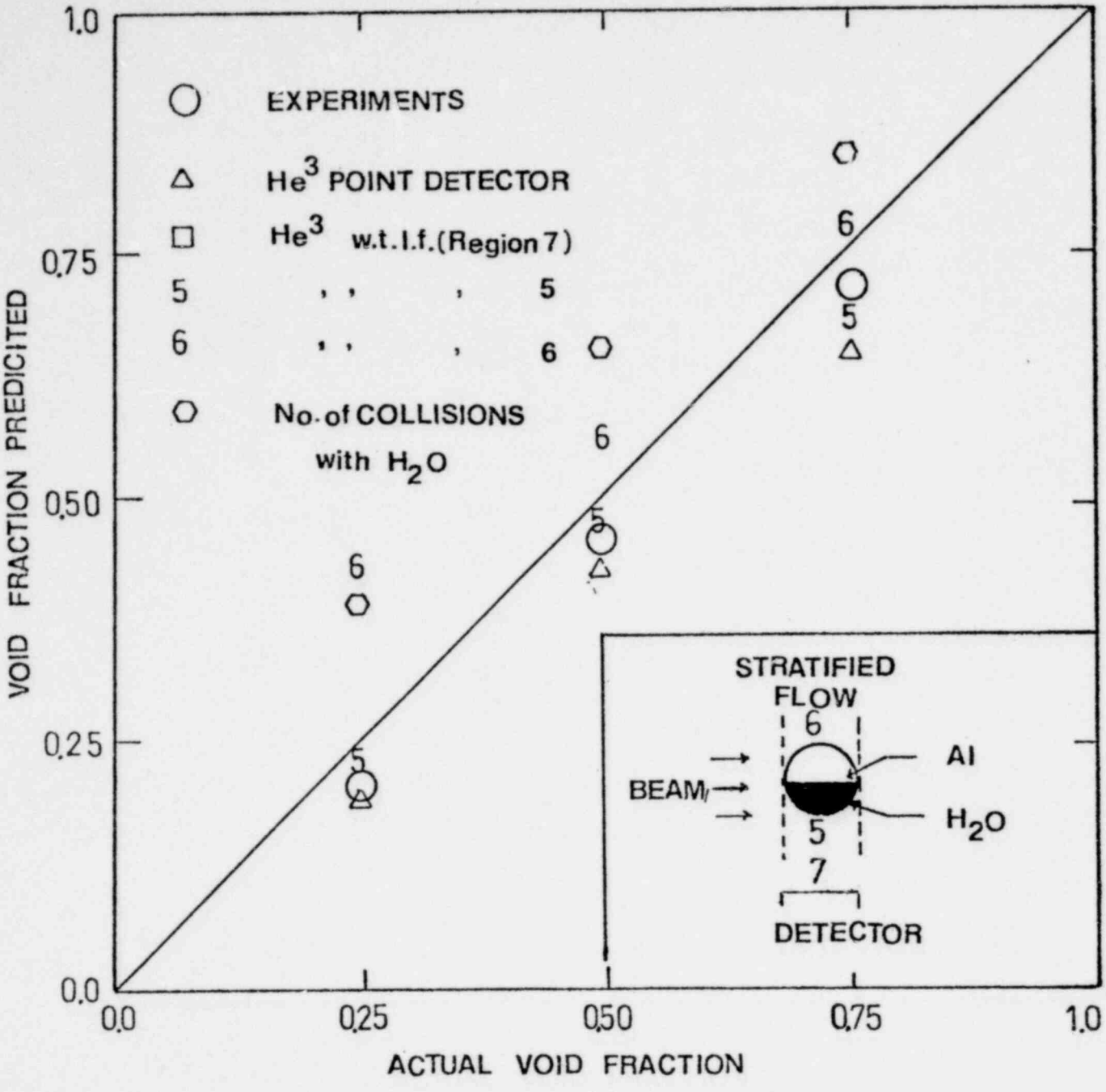

Figure 6 -Void fractions predicted for the shown stratified flow regime. w.t.l.f. denotes weighted track length fluence. These are results of Monte Carlo calculations for various detectors compared against experiment.

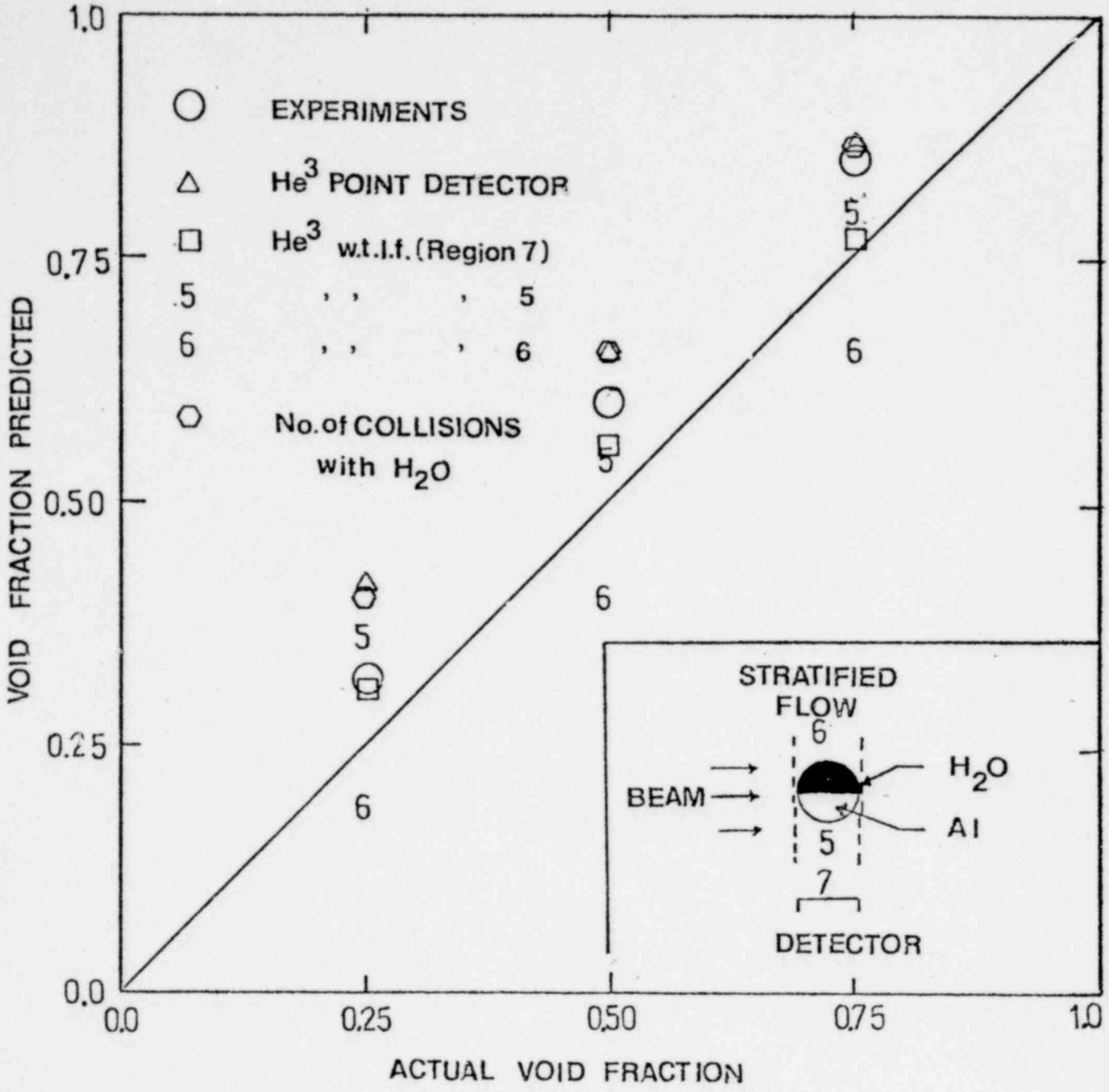

Figure 7 - Void fractions predicted for the shown stratified flow regime. w.t.l.f. denotes weighted track length fluence. These are results of Monte Carlo calculations for various detectors compared against experiment.

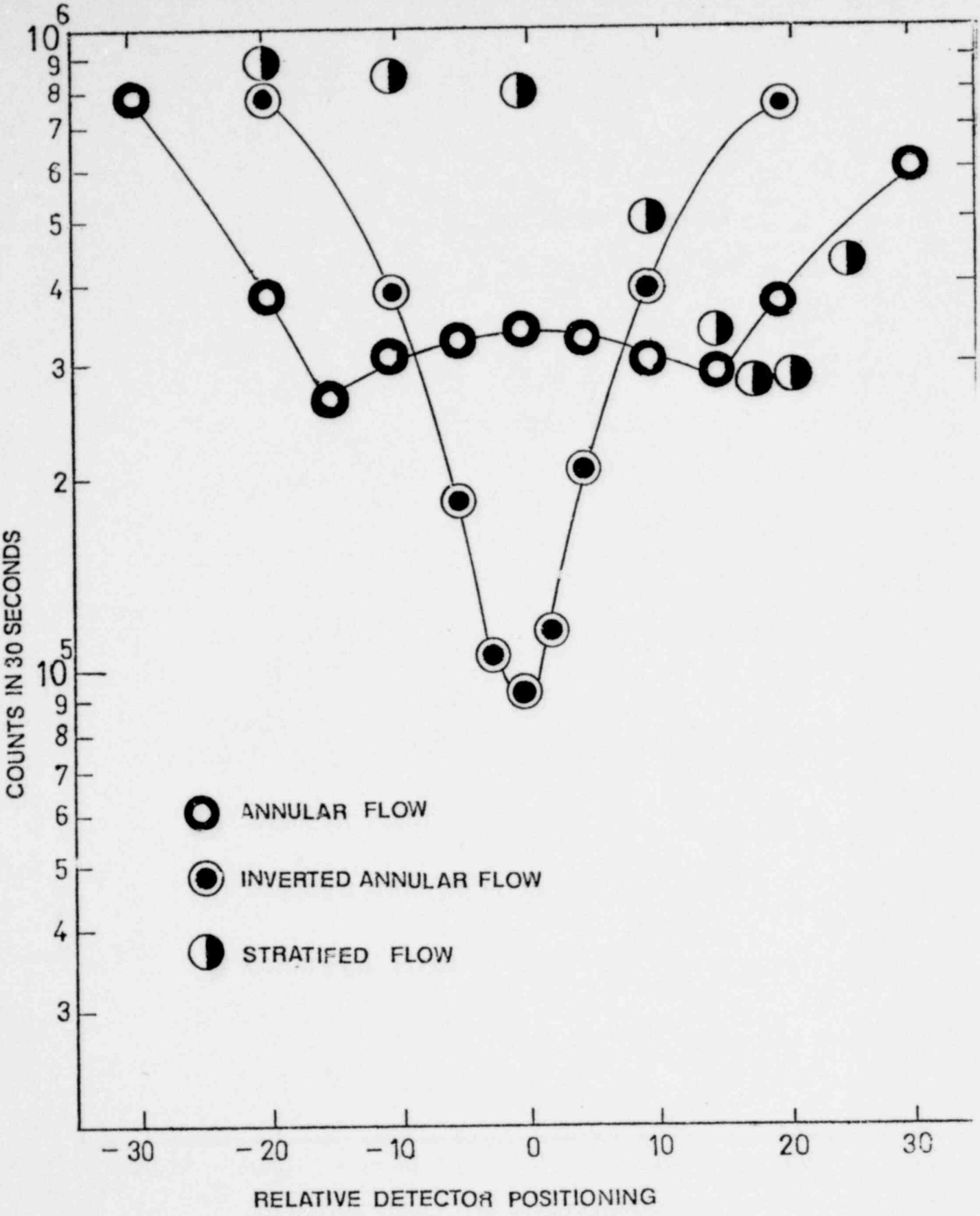

Figure 8 - Transmitted flux profile for various void distribution at void fraction of 0.75

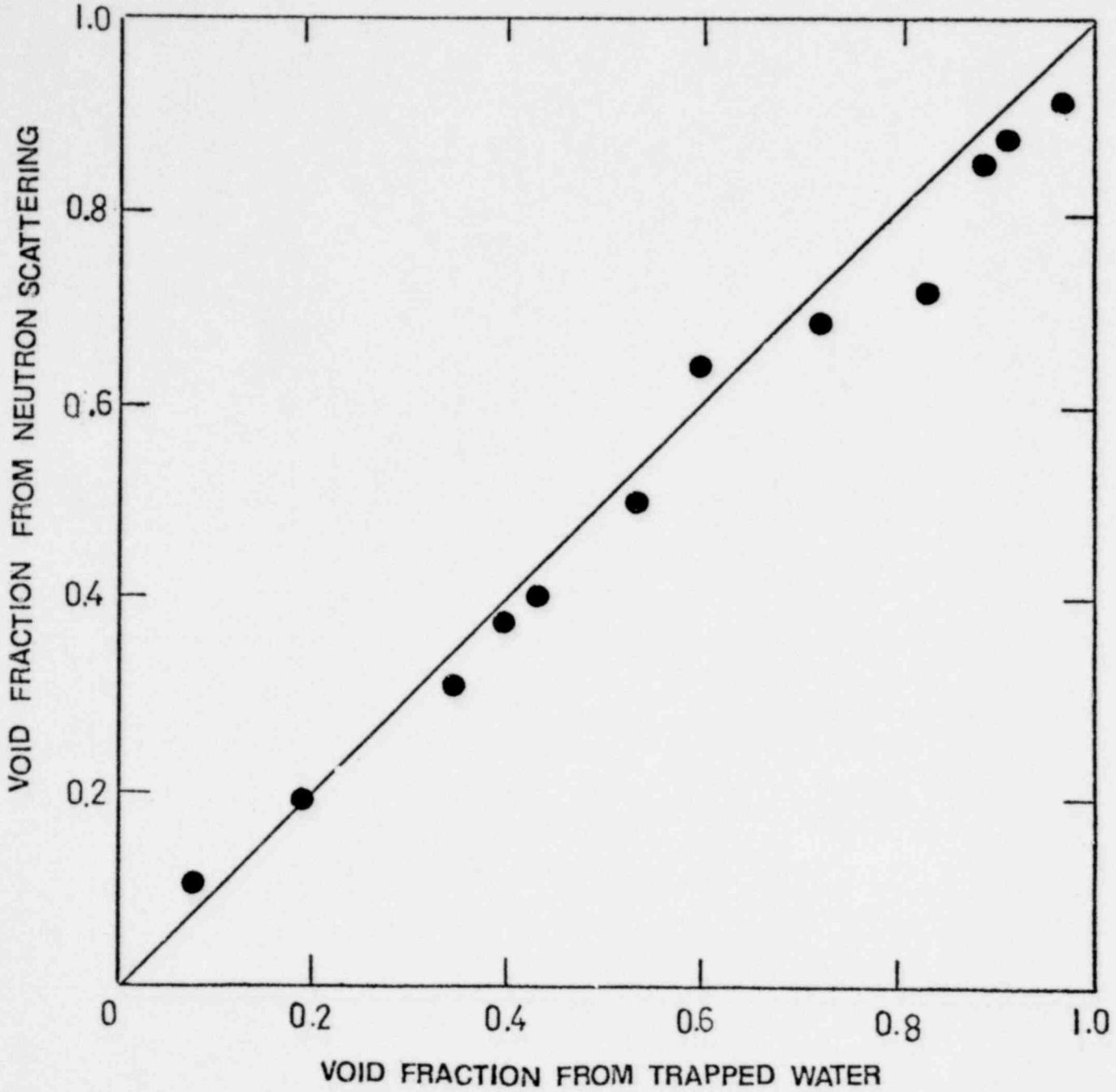

Figure 9 - Comparison of void fractions determined by neutron scattering method and values measured by trapping air-water flow between two quick closing gate valves

Figure 10 - Void fraction predicted by neutron scattering experimental measurements compared to actual void fractions in the rod bundle test section.

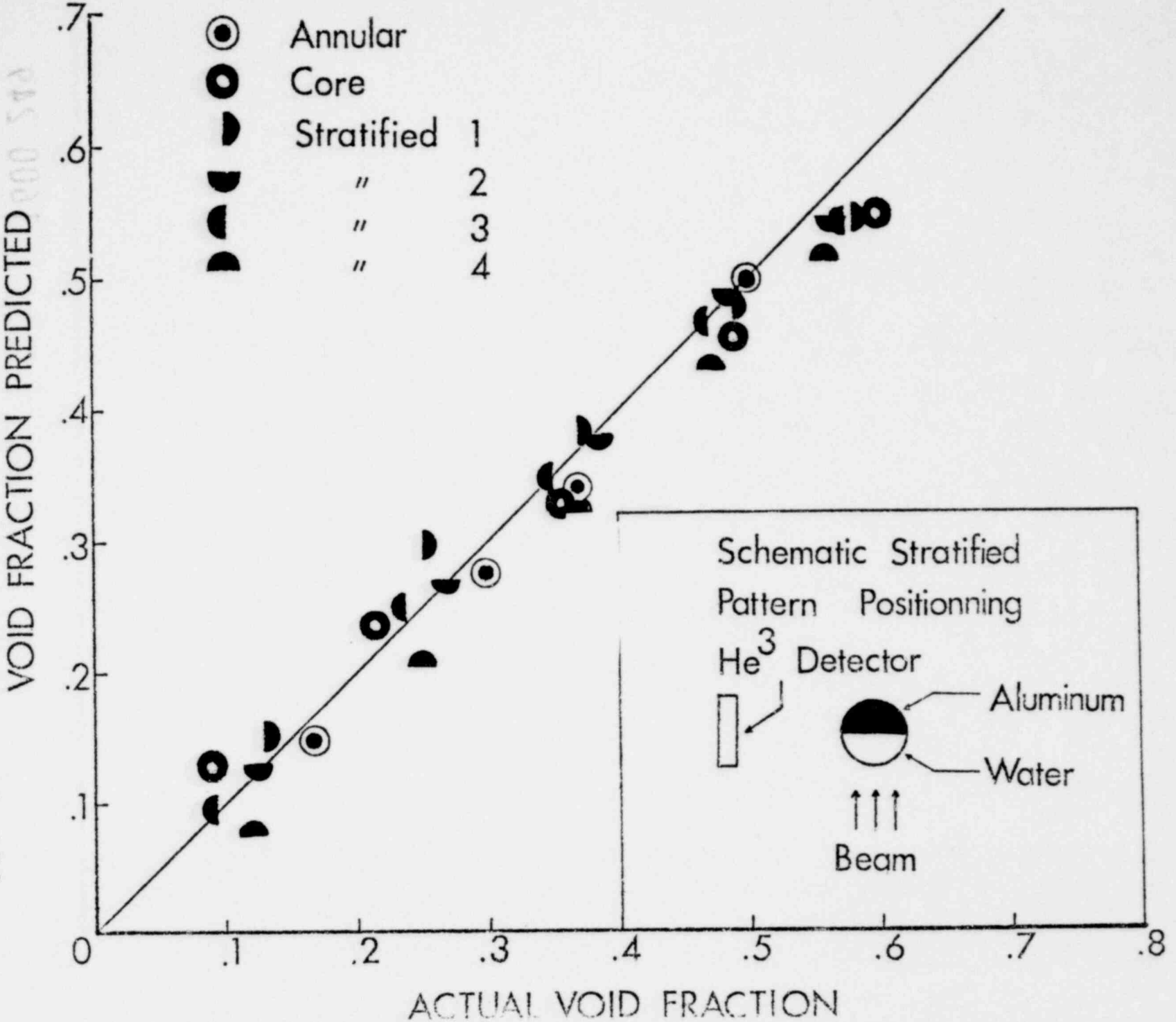

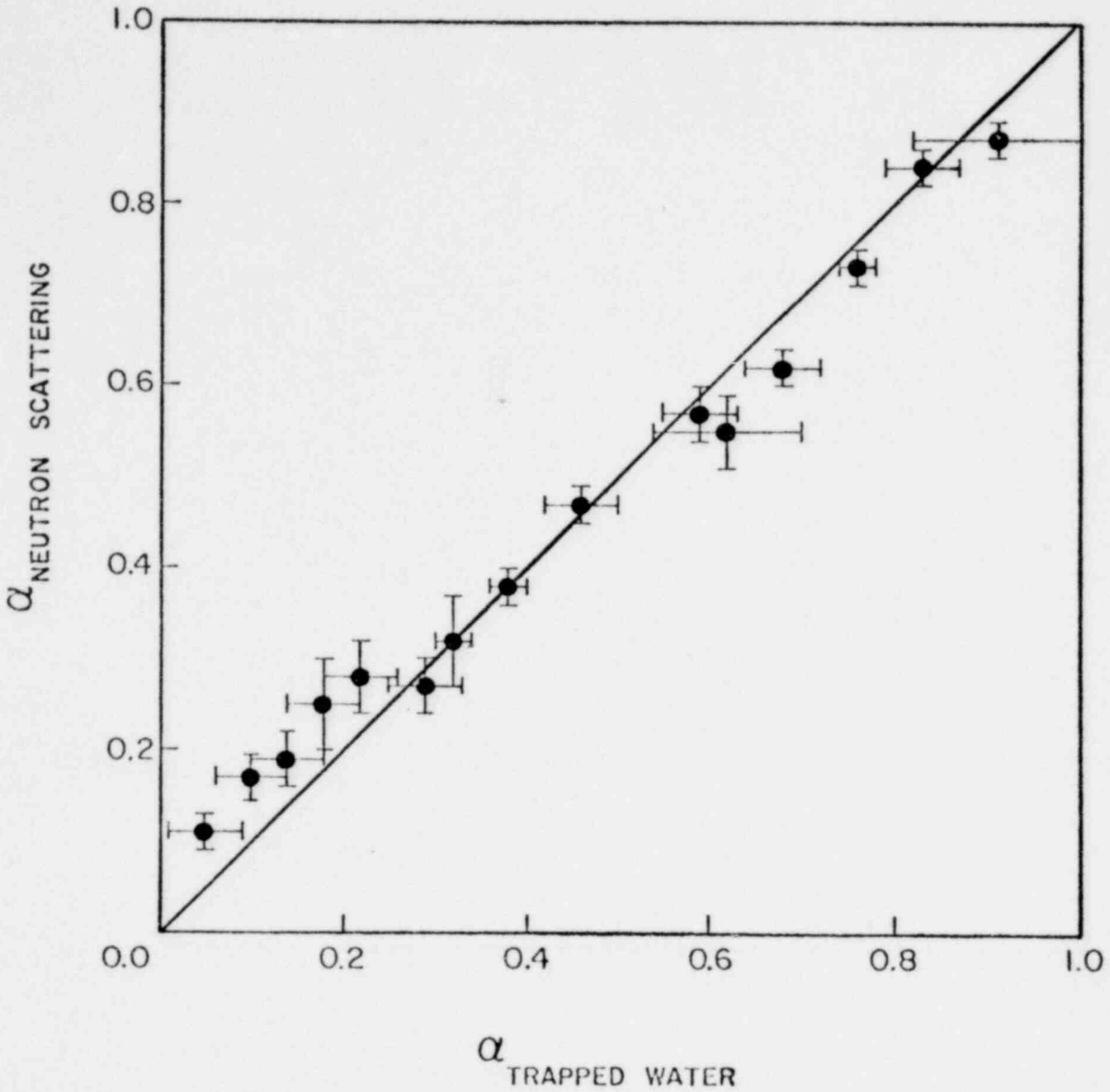

Figure 11- Comparison of void fractions determined by neutron scattering method and measured by trapping air-water flow between two quick-closing gate valves in rod bundles.

SURVEY OF INEL ADVANCED INSTRUMENTATION

Presented at
The Seventh Water Reactor Safety Research Information Meeting
November 5-9, 1979
Gaithersburg, Maryland

R. D. Wesley
EG&G Idaho, Inc.

Idaho National Engineering Laboratory
Idaho Falls, Idaho 83401

SURVEY OF INEL ADVANCED INSTRUMENTATION

R. D. Wesley
EG&G Idaho, Inc.

Instrumentation development, design, and analysis were accomplished during this past fiscal year by Advanced Instrumentation, Instrument Systems Engineering, 3-D Measurement Engineering, and Measurement Engineering and Experimental Instrumentation Branches of EG&G Idaho, Inc., at the Idaho National Engineering Laboratory (INEL). Instrumentation related topics included are categorized as applied, recently developed, improvements in basic understanding, small break instrumentation, and future measurement goals.

The applied technologies include gamma densitometers, drag bodies, ultrasonic densitometers, LOFT pitot tube/thermocouple rakes, optical probes, and small diameter zircaloy sheathed thermocouples. There are 74 gamma densitometers and 63 drag bodies either installed and operating at INEL or delivered as spool piece components to the multi-national 3-D Program. Additional instruments have been supplied to private industry and other national laboratories. LOFT core inlet/outlet ultrasonic densitometers have been produced for inclusion on the LOFT assembly and the pitot tube/thermocouple rakes have been installed. The 343^{o}C, 15.2 MPa optical probe using the Storz lens has been routinely used during this past fiscal year at the Semiscale Facility. The ability to video record and visualize steam-water conditions in the downcomer and pump discharge locations for blowdown reflood studies has aided in analysis and code assessment. Small diameter (to 0.61 mm) zircaloy sheathed thermocouples have been used at the LOFT Test Support Facility (LTSF) and the Thermal Fuels Behavior Program Power Burst Facility during temperature and re-wet studies. These applications are results of earlier development activities as sponsored by the U.S. Nuclear Regulatory Commission through the support of programs at INEL.

Instruments which reflect recently developed technologies include the water cooled pitot tube rake, mist phase and five hole stagnation probes, 600°C, 15.2 MPa optical probe, local ultrasonic densitometer, and differential thermocouple liquid level probe. Testing of the water cooled pitot tube rake and subsequent testing of the LOFT pitot tube/thermocouple rake at Wyle Laboratories proved the viability of these instruments in the measurement of momentum flux profile. The mist phase and five hole stagnation probes stem from the reference instrumentation effort and will be utilized to characterize two-phase flow in the LTSF steady state loop as part of a continued reference/calibration effort. As part of a three-step effort directed towards flow visualization and code assessment, a 600°C, 15.2 MPa probe has been constructed and tested. Basic structure is similar to the 343°C, 15.2 MPa probe, but it uses an evacuated silvered channel filled ceramic insulation. Successful testing at a surface temperature of 540°C in a 0.3-m length indicates the usefulness of this technique to longer lengths. Development of the local ultrasonic densitometer provides an instrument for downcomer and core measurement of density and density profile. Like the LOFT inlet/outlet ultrasonic densitometer, the local ultrasonic densitometer uses all stainless steel interfaces and radiation environment proven components. An extension of the heated/unheated thermocouple technology led to the differential thermocouple liquid level probe. A three-mode controller has been added to enhance the air-to-water and water-to-air responses as a liquid level indicating device. Currently, response is limited to 20 ms by available devices but like ultrasonic densitometers and zircaloy sheathed thermocouples, these devices are suitable for power water reactor adaptation.

Additional basic understanding has been gained in several areas. Included are the Mach Number and Reynolds Number dependence on large hole drag discs and analysis techniques as applied to 3-D Program spool pieces.

1600

As a result of TMI-2, a change in emphasis has been reflected in new low velocity measurement needs. The Advanced Instrumentation Branch has been active in determination and implementation of suitable small break instrumentation planned for LOFT and Semiscale.

Future measurement goals continue to include distributed measurements, reference two-phase flow measurements, calibration standards, and instrumentation for advanced code assessment. These needs commonly serve the programs at INEL.

REFERENCE SOURCES

V. A. Deason, J. R. Fincke, "Velocity Determination Using Stagnation Probes," NRC Instrumentation Review Group Meeting, Silver Spring, Maryland, July 24-26, 1979.

A. E. Arave, "Ultrasonic Densitometer Development," NRC Instrumentation Review Group Meeting, Silver Spring, Maryland, July 24-26, 1979.

A. G. Baker, "Horizontal Two-Phase Flow Transit Time Measurements," NRC Instrumentation Review Group Meeting, Silver Spring, Maryland, July 24-26, 1979.

M. R. Donaldson, R. E. Pulfrey, "Imaging Optical Probe for pressurized Steam-Water Environment," NRC Instrumentation Review Group Meeting, Silver Spring, Maryland, July 24-26, 1979.

J. R. Fincke, V. A. Deason, "Mass Flow Rate Measurement in Two-Phase Mixtures with Stagnation Probes," NRC Instrumentation Review Group Meeting, Silver Spring, Maryland, July 24-26, 1979.

J. R. Wolf, "The Linear Variable Differential Transformer and Its Use In-Core Fuel Rod Behavior Measurements," International Colloquium on Irradiation Tests for Reactor Safety Programmes, Petten, The Netherlands, June 25-28, 1979.

J. V. Anderson, R. D. Wesley, S. C. Wilkins, "Zircaloy-Sheathed Thermocouples for PWR Fuel Rod Temperature Measurements," International Colloquium on Irradiation Tests for Reactor Safety Programmes, Petten, The Netherlands, June 25-28, 1979.

A. G. Stephens, D. B. Wood, D. J. Taylor, G. D. Lassahn, "X-Ray and Gamma Ray Transmission Densitometry," International Colloquium on Two Phase Flow Instrumentation, Idaho Falls, ID, June 11-14, 1979.

J. L. Anderson, "Drag Devices for Two-Phase Mass Flow Measurements," International Colloquium on Two Phase Flow Instrumentation, Idaho Falls, ID, June 11-14, 1979.

J. R. Fincke, and V. A. Deason, "Mass Flow Rate Measurements in Two-Phase Mixtures with Stagnation Probes," International Colloquium on Two Phase Flow Instrumentation, Idaho Falls, ID, June 11-14, 1979.

A. E. Arave, "Reactor Vessel and Core Two-Phase Flow Ultrasonic Densitometer," International Colloquium on Two Phase Flow Instrumentation, Idaho Falls, ID, June 11-14, 1979.

M. R. Donaldson and R. E. Pulfrey, "Imaging Optical Probe for Pressurized Steam-Water Environment," International Colloquium on Two Phase Flow Instrumentation, Idaho Falls, ID, June 11-14, 1979.

R. H. Averill, and L. D. Goodrich, "Design and Performance of the Drag Disc Turbine Transducer," International Colloquium on Two Phase Flow Instrumentation, Idaho Falls, ID, June 11-14, 1979.

D. L. Batt, G. L. Biladeau, L. D. Goodrich, and C. M. Nightingale, "LOFT Liquid Level Transducer Application Techniques and Measurement Uncertainty,"

J. B. Colson, and J. B. Gilbert, "JAERI Instrumented Spool Piece Performance In Two-Phase Flow," International Colloquium on Two Phase Flow Instrumentation, Idaho Falls, ID, June 11-14, 1979.

J. M. Cozzuol, and R. W. Shumway, "Measurement of Two-Phase Flow Conditions in a Horizontal Pipe Aided by Multibeam Gamma Densitometers," International Colloquium on Two Phase Flow Instrumentation, Idaho Falls, ID, June 11-14, 1979.

A. G. Stephens, "Local Density Measurements in a Steam-Water Mixing Zone using the Photon Attenuation Technique," ASME Annual Winter Meeting, San Francisco, CA, December 10-15, 1978.

G. L. Biladeau, R. Y. Maughan, P. A. Quinn, LOFT Experimental Measurements Uncertainty Analysis, Volume V, LOFT External Accelerometer Uncertainty Analysis, NUREG/CR-0169, Vol. V., TREE-1089 (October 1978).

S. C. Wilkins, High-Temperature, Tungsten-Rhenium Thermocouple with Molybdenum-Rhenium Sheaths, TFBP-TR-285 (October 1978).

S. C. Wilkins, Miniature Zircaloy-Sheathed Fuel Rod Cladding Surface Thermocouples, TFBP-TR-286 (December 1978).

J. R. Fincke, V. A. Deason, Performance Testing of the LOFT Modular Drag Disc Turbine, LTR 141-102 (May 1979).

A. G. Stephens, Experiment Data for Determination of Uncertainty of Two-Phase Mass Flow Rate in a Semiscale MOD-3 System Spool Piece at Karlsruhe Kernforschungzentrum, SEMI-TR-006 (June 1979).

J. L. Anderson, Air-Water Testing of a Full Flow Perforated Drag Plate (Beveled-Small Hole) for Mass Flow Rate Measurements, SEMI-TR-009 (July 1979).

M. W. Dacus, V. A. Deason, J. R. Fincke, "Pitot Tube and Drag Body Measurements in Transient Steam-Water Flows," 25th ISA International Instrumentation Symposium, Anaheim, CA, May 7-10, 1979.

V. A. Deason, J. R. Fincke, C. E. Winsel, "Drag-Disc Turbine Transducer Data Evaluation Methods for Dynamic Steam-Water Mass Flow Measurements," 25th ISA International Instrumentation Symposium, Anaheim, CA, May 7-10, 1979.

J. R. Fincke, R. S. Flemons, J. R. Soltvold, "Conductivity Probes for Void and Velocity Measurements in High Temperature Steam-Water Flow," 25th ISA International Instrumentation Symposium, Anaheim, CA, May 7-10, 1979.

M. R. Donaldson, R. E. Pulfrey, S. K. Merrill, "Imaging Optical Probe for Pressurized 620 K Steam-Water Environment," 25th ISA International Instrumentation Symposium, Anaheim, CA, May 7-10, 1979.

A. E. Arave, "Ultrasonic Density Detector for Vessel and Reactor Core Two-Phase Flow Measurements," International Colloquium on Irradiation Tests for Reactor Safety Programs, Petten, the Netherlands, June 25-28, 1979.

Survey of INEL Advanced Instrumentation

Seventh Water Reactor Safety Research Information Meeting

Presented by
R.D. Wesley

November 6, 1979

EG&G Idaho, Inc.

Outline

- **Developed technologies now applied**
  - **Gamma densitometers**
  - **Drag bodies**
  - **Other**
- **Technologies recently developed**
- **Improved understanding**
- **Small break instrumentation**
- **Future goals**

INEL-S-21 756

Densitometers

	Pipe size cm	Strength	Source	Operating
High energy	5-36	15-30 Ci	Cs^{137}	25 △
Nuclear hardened	15-36	11-60 Ci	Co^{60}, Cs^{137}	6 ◇ ○
Low energy	3-15	0.05-0.2 Ci	Cd^{109}, Am^{241} Gd^{153}, Fe^{55}	41 △ □
Scanning	3-15	0.05 Ci	Cd^{109}	2 ▽

○ LOFT
△ Semiscale
□ 3-D
◇ PBF
▽ Air-water loop

INEL-S-19 436

Drag Bodies

	Use	Operating
Disc	Piping	18△○◇□
Hinged-multihole	Piping and core outlet	4△
3-point-multihole	Piping and downcomer	37△□
Diamond arm	Guide and support tubes	3△
Lattice	Core inlet	1△

○ LOFT ◇ PBF
△ Semiscale □ 3-D

INEL-S-21 757

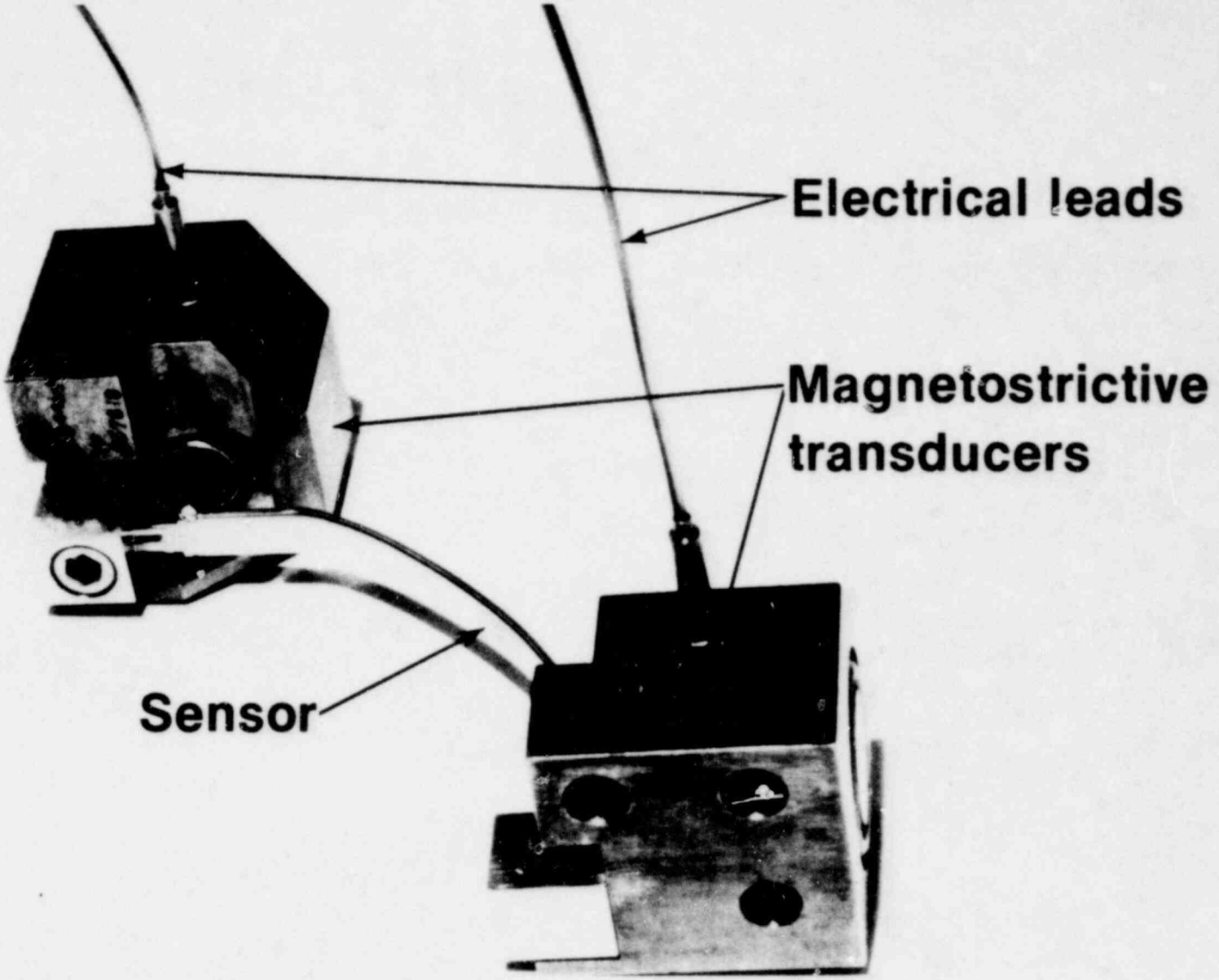

LOFT Core Inlet Ultrasonic Densitometer

INEL-S-18 970

POOR ORIGINAL

LOFT Pitot Tube
Thermocouple Rake

Zircaloy/Stainless Steel Explosion Bonded Transition Junction

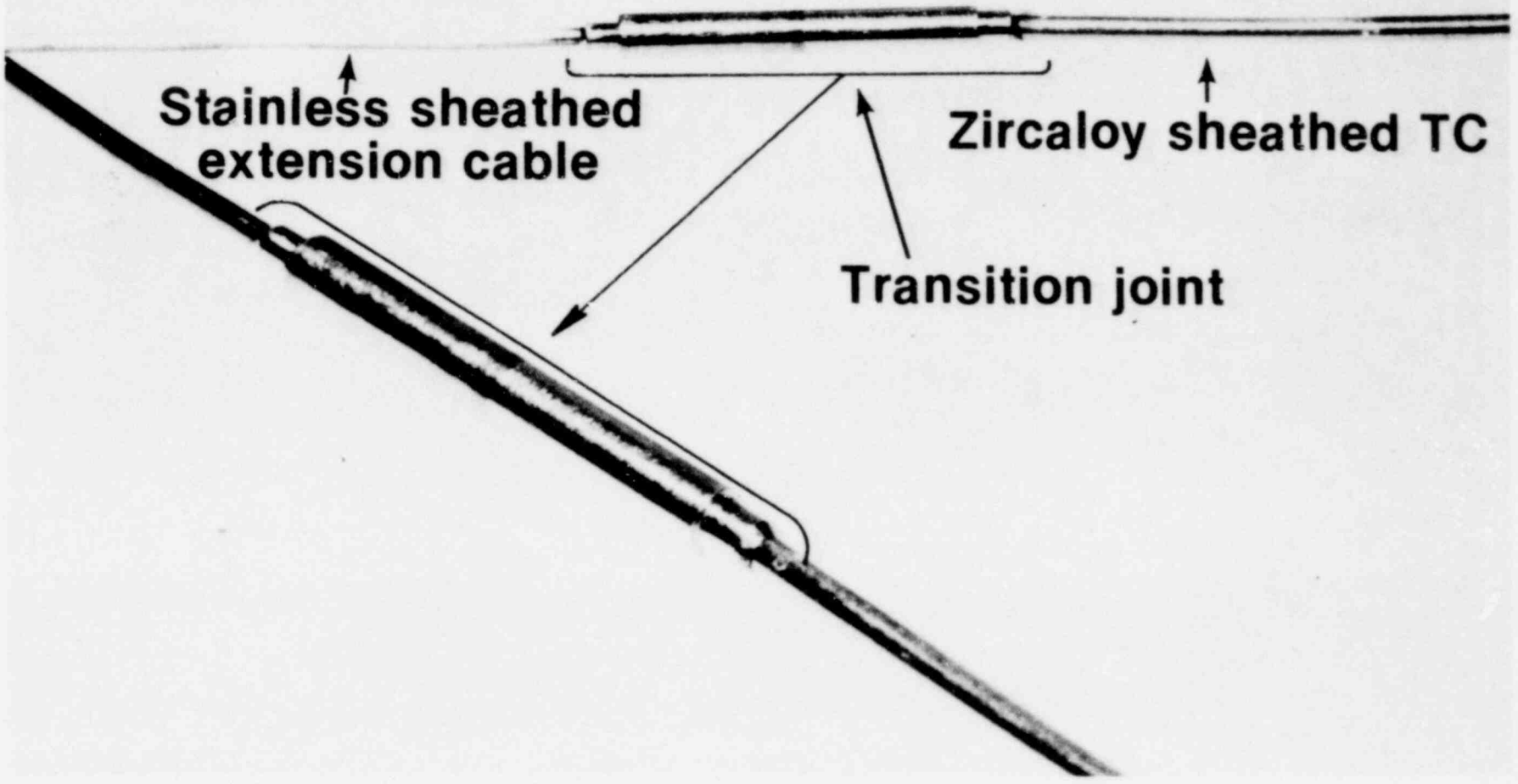

Outline

- Developed technologies now applied
- Technologies recently developed
  - Stagnation probes
  - HPHT optical probe
  - Local ultrasonic densitometer
  - Differential TC liquid level
- Improved understanding
- Small break instrumentation
- Future goals

INEL-S-21 758

Stagnation Probes

	Water Cooled Pitot	Mist Phase	Five Hole
Use	Total flow momentum flux	Separate phase momentum flux	Vector velocity
Void fraction range	0-1	0.9-1	0-0.5
Test conditions	PWR conditions Transient Steady state	Low temperature Low Pressure Steady state	PWR conditions Steady State

INEL-S-20 439

POOR ORIGINAL

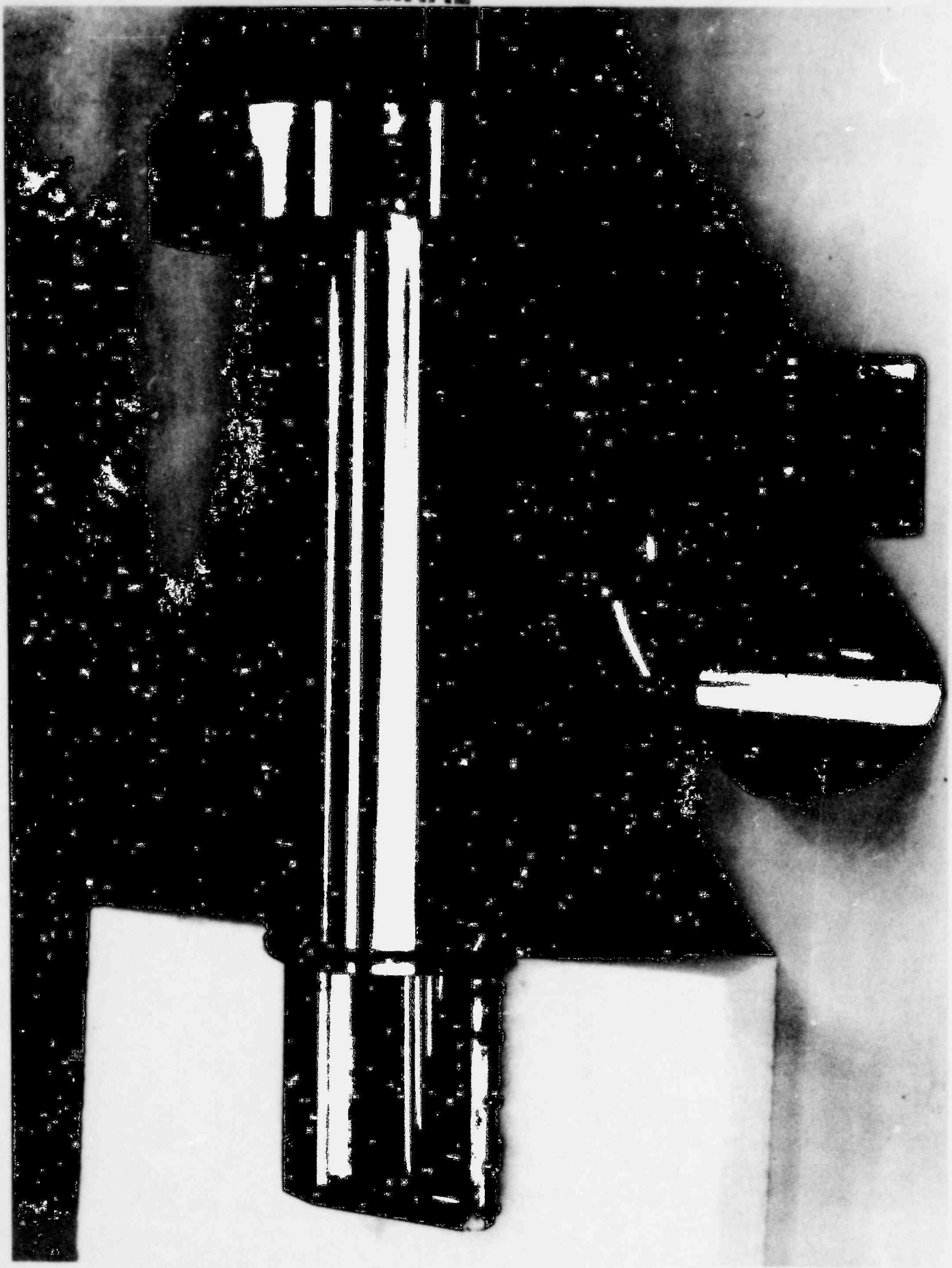

1600 270

Transient Profile Data

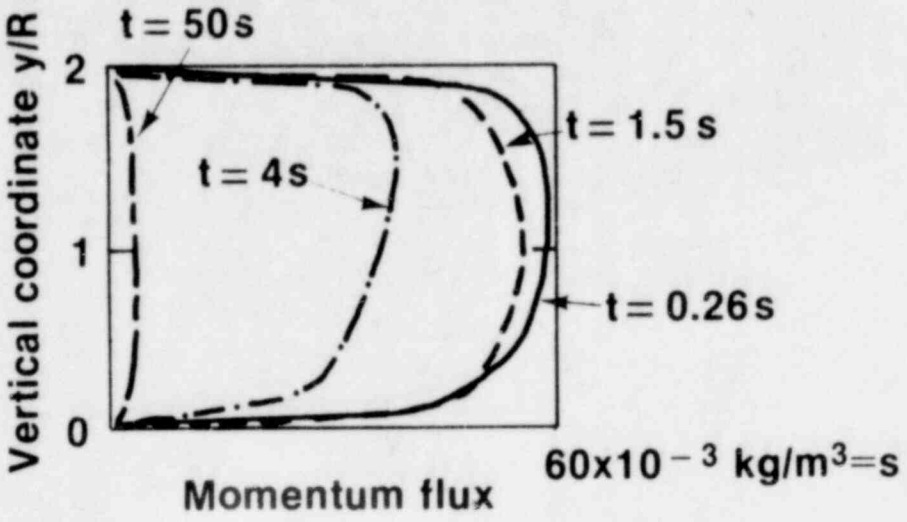

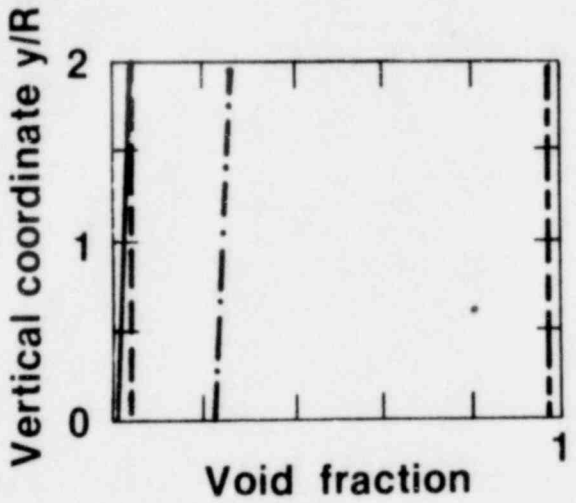

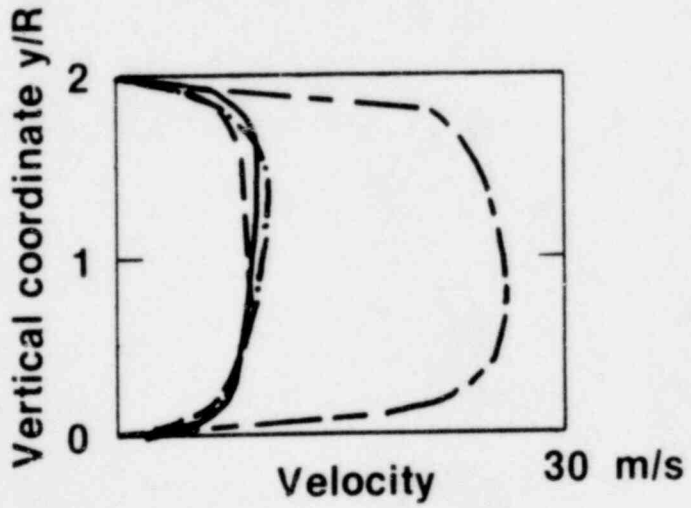

INEL-S-21 760

Mist Phase Stagnation Probe

INEL-S-19 130

Mist Flow Stagnation Probe

$$P_t = \tfrac{1}{2}\alpha\ \rho_g V_g^2 + (1-\alpha)\ \rho_\ell V_\ell^2$$

$$P_g = \tfrac{1}{2}\alpha\ \rho_g V_g^2 + C\,\rho_g V_g^2\ \frac{\dot{m}_\ell}{\dot{m}_g}$$

$$\dot{m}_\ell = (1-\alpha)\ \rho_\ell V_\ell A$$

$$\dot{m}_g = \alpha\ \rho\ g\ V_g\ A$$

INEL-S-13 874

Mist Flow VSG = 80 m/s

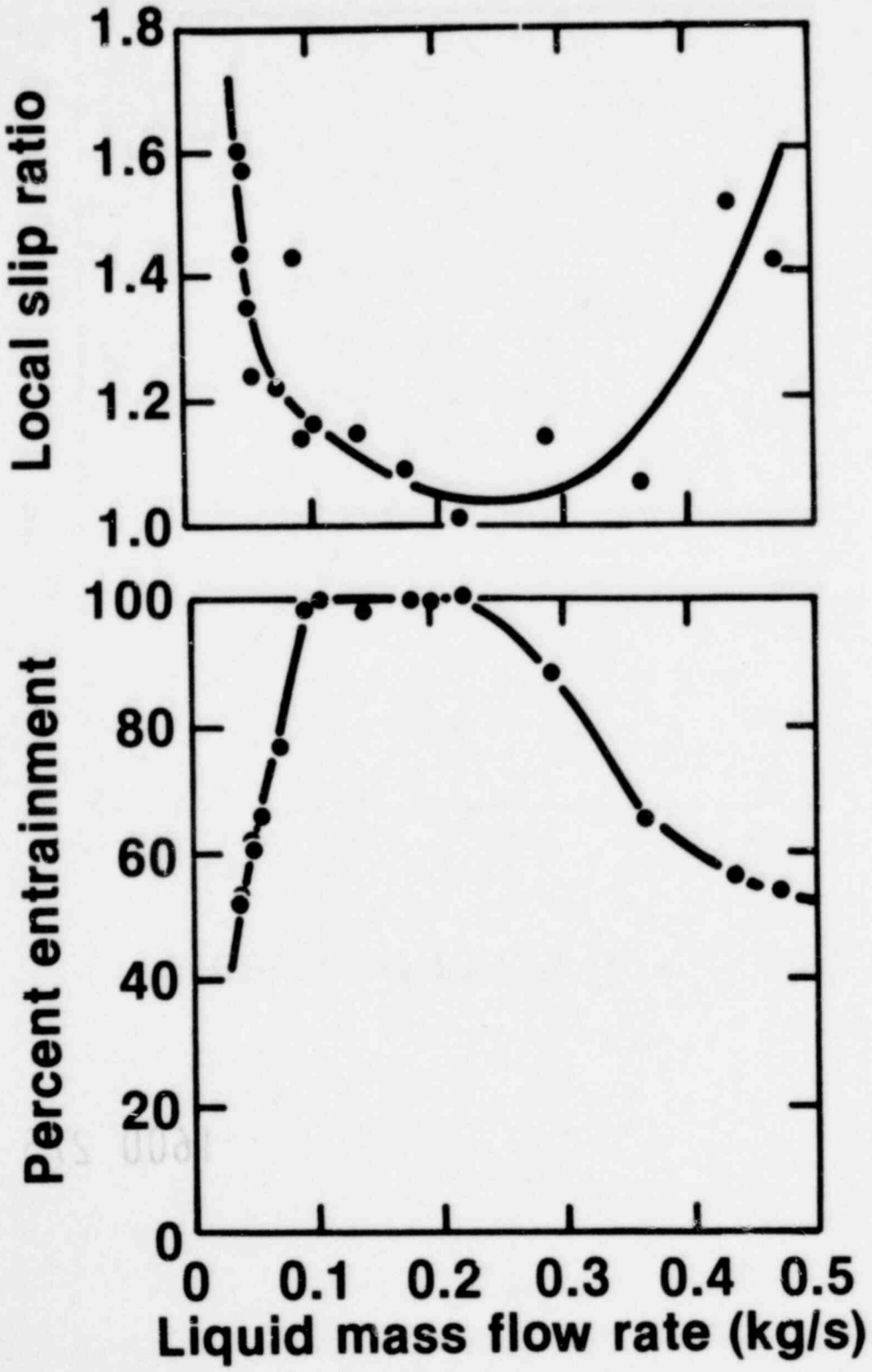

INEL-S-19 122

Gas Mass Flow Rate

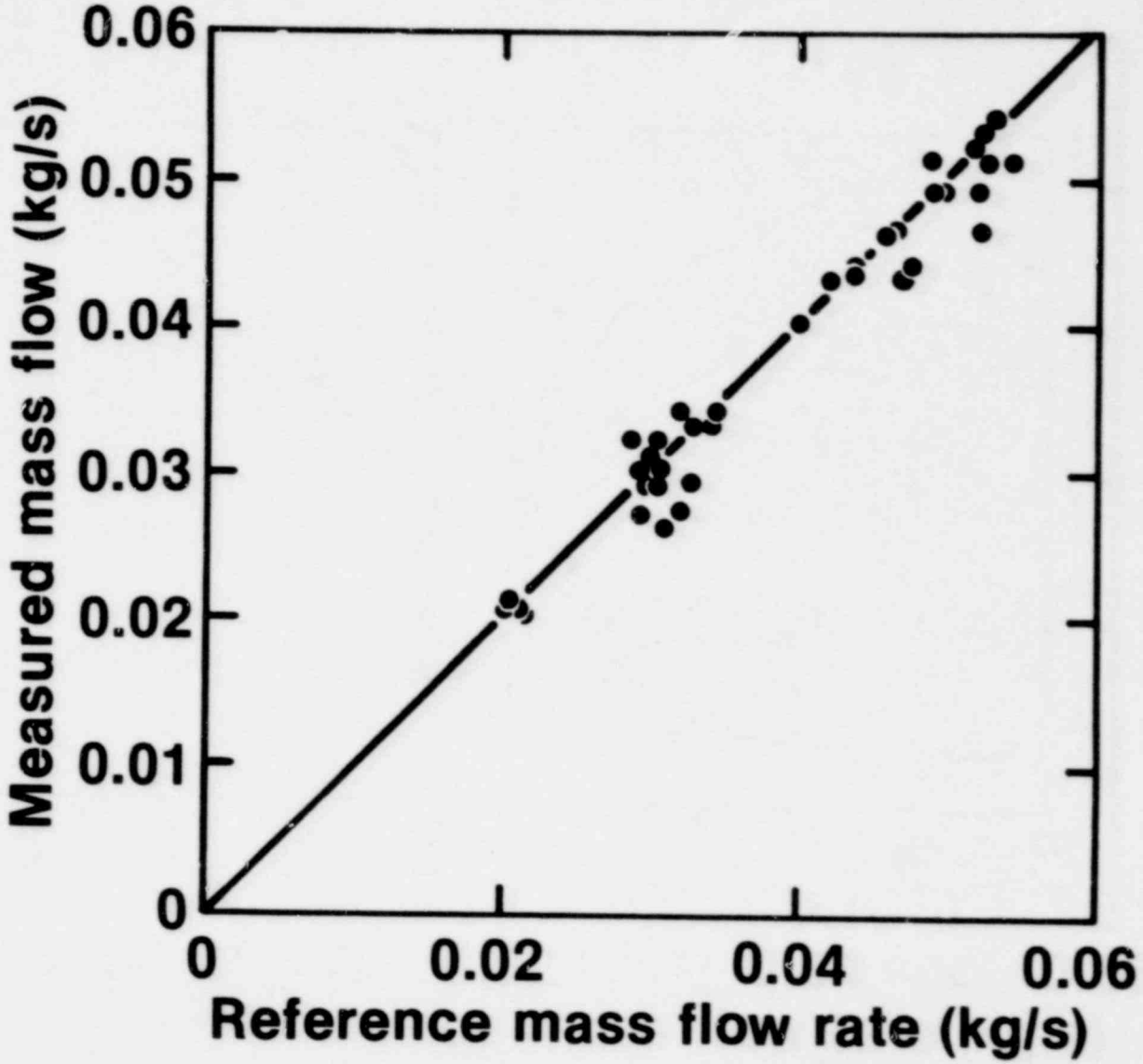

INEL-S-19 119

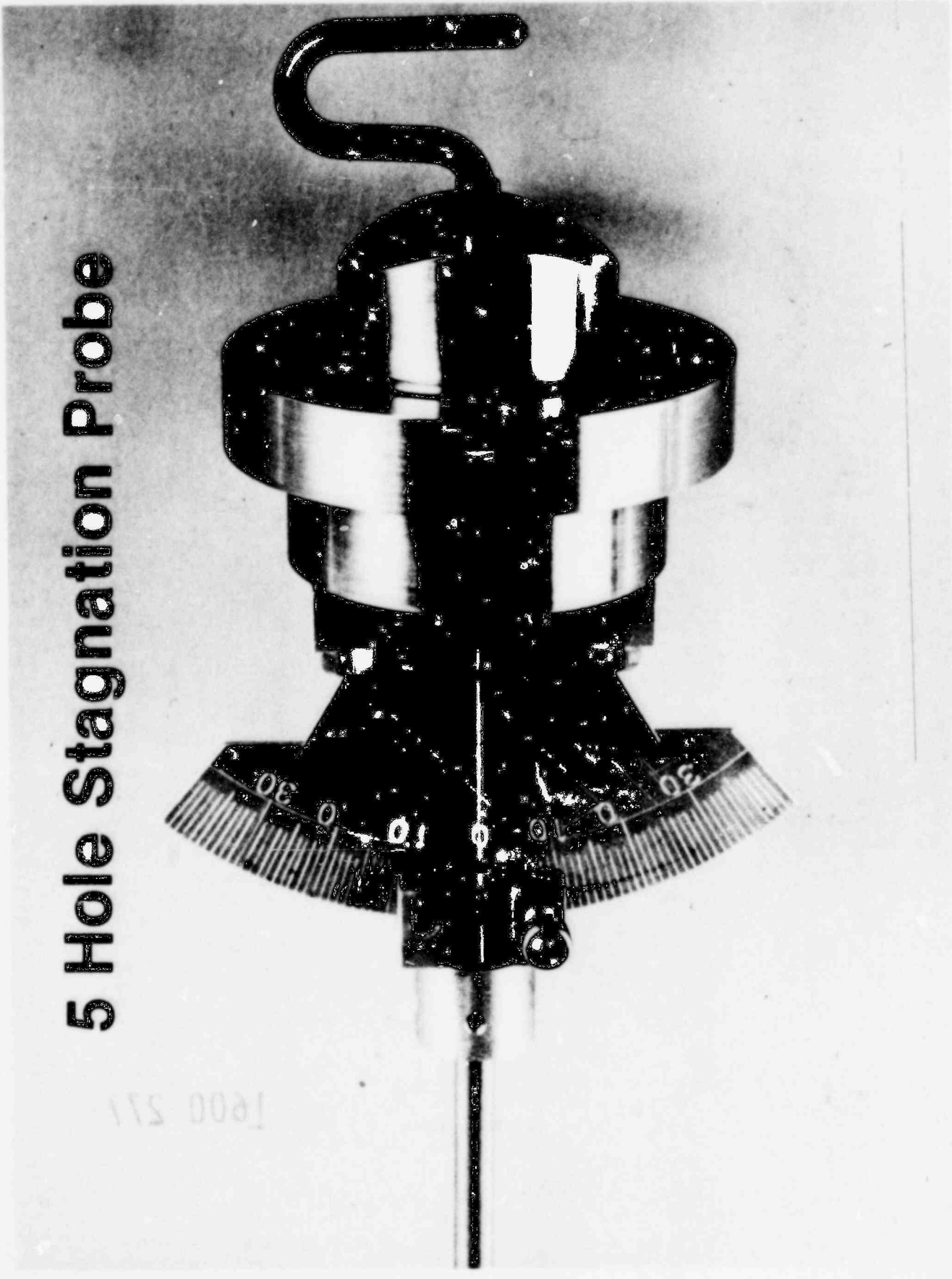

5 Hole Probe Geometry

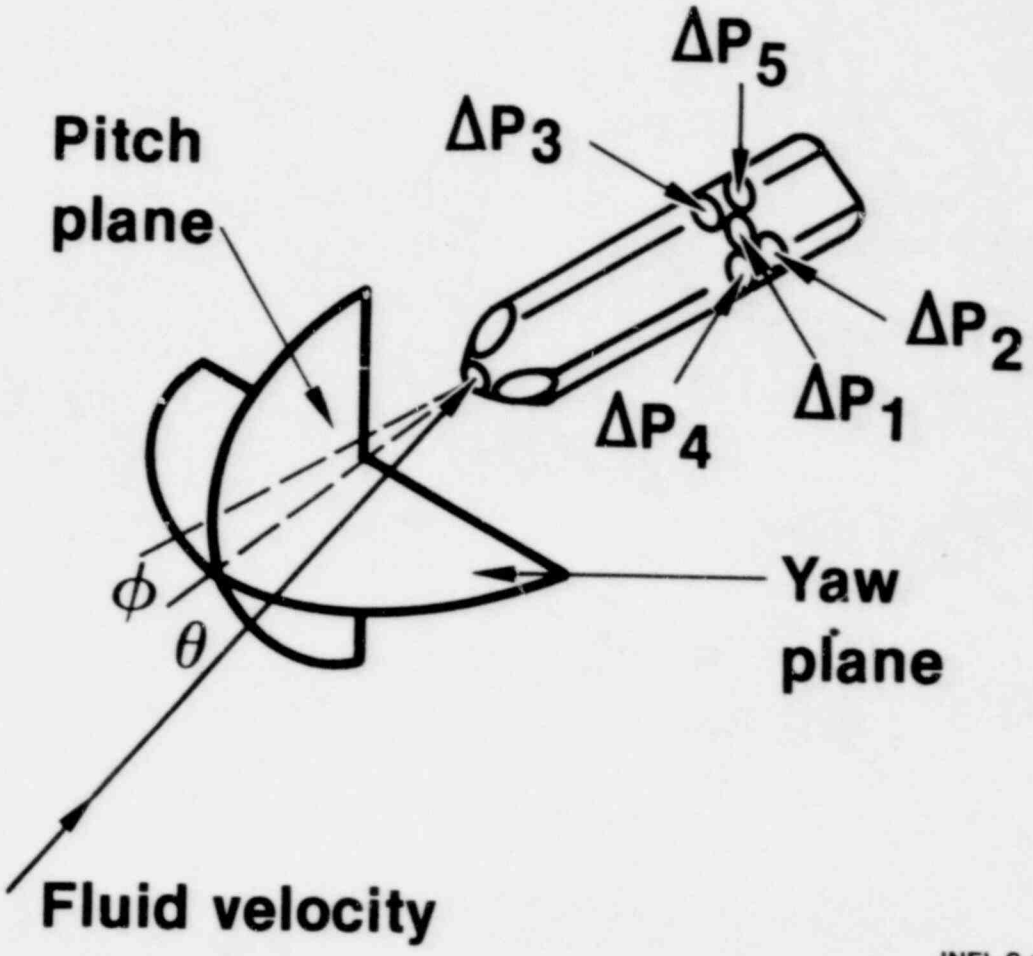

INEL-S-19 317

Calibration Coefficients

$$\text{CP PITCH} \equiv \frac{\Delta P_4 - \Delta P_5}{\Delta P_1 - \overline{\Delta P}}$$

$$\text{CP YAW} \equiv \frac{\Delta P_2 - \Delta P_3}{\Delta P_1 - \overline{\Delta P}}$$

$$\text{CP TOTAL} \equiv \frac{\Delta P_1 - \Delta P_{\text{Total}}}{\Delta P_1 - \overline{\Delta P}}$$

$$\overline{\Delta P} = \frac{\Delta P_2 + \Delta P_3 + \Delta P_4 + \Delta P_5}{4}$$

Model
Bernoulli's Equation

$$\bar{U} = \left[\frac{2\left(\Delta P_1 - (\text{CP TOTAL})(\Delta P_1 - \overline{\Delta P})\right)}{\text{Density}}\right]^{1/2}$$

INEL-S-21 759

Single Phase Calibration Data (Water)

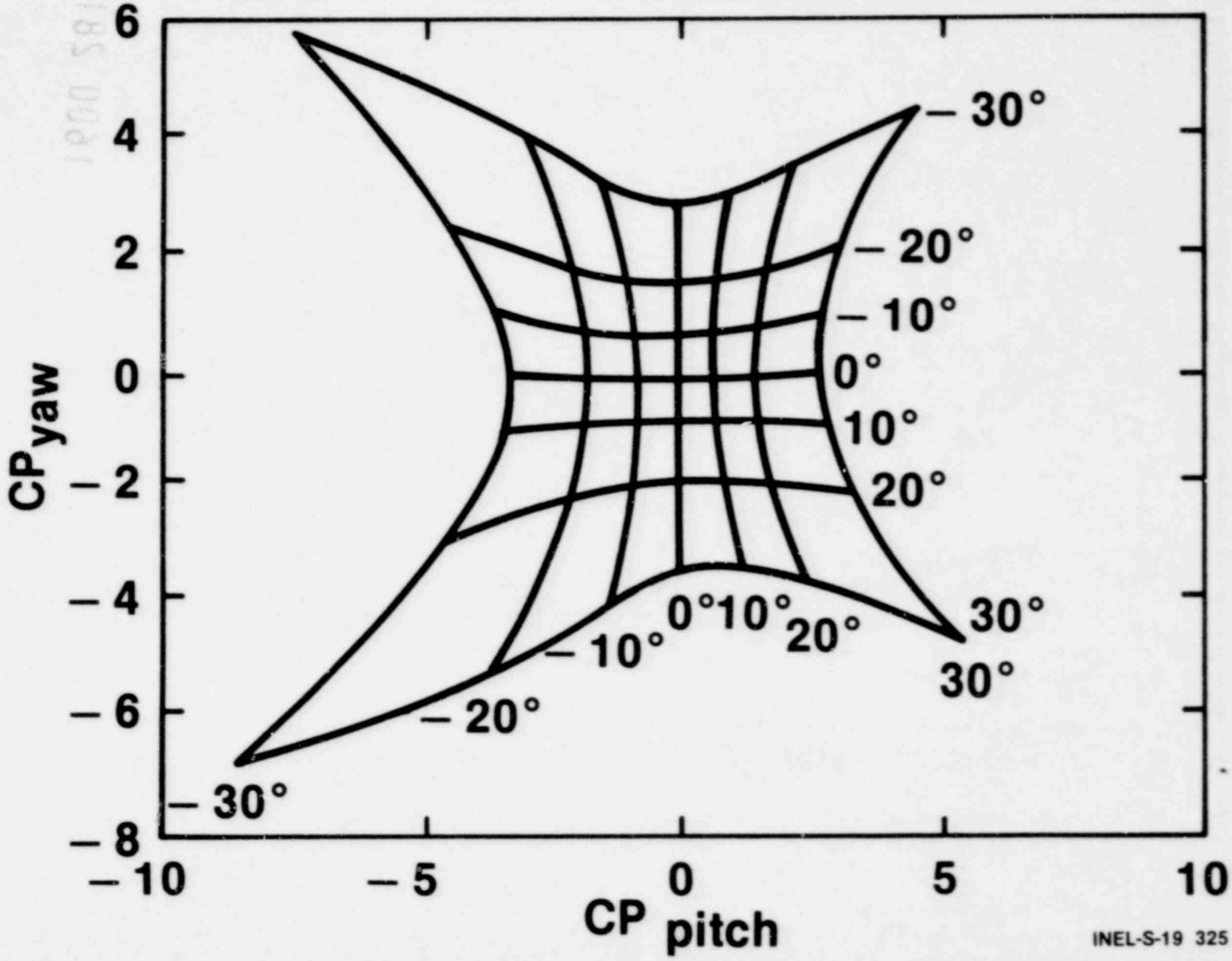

All-Water Data; CP Total vs Pitch Angle

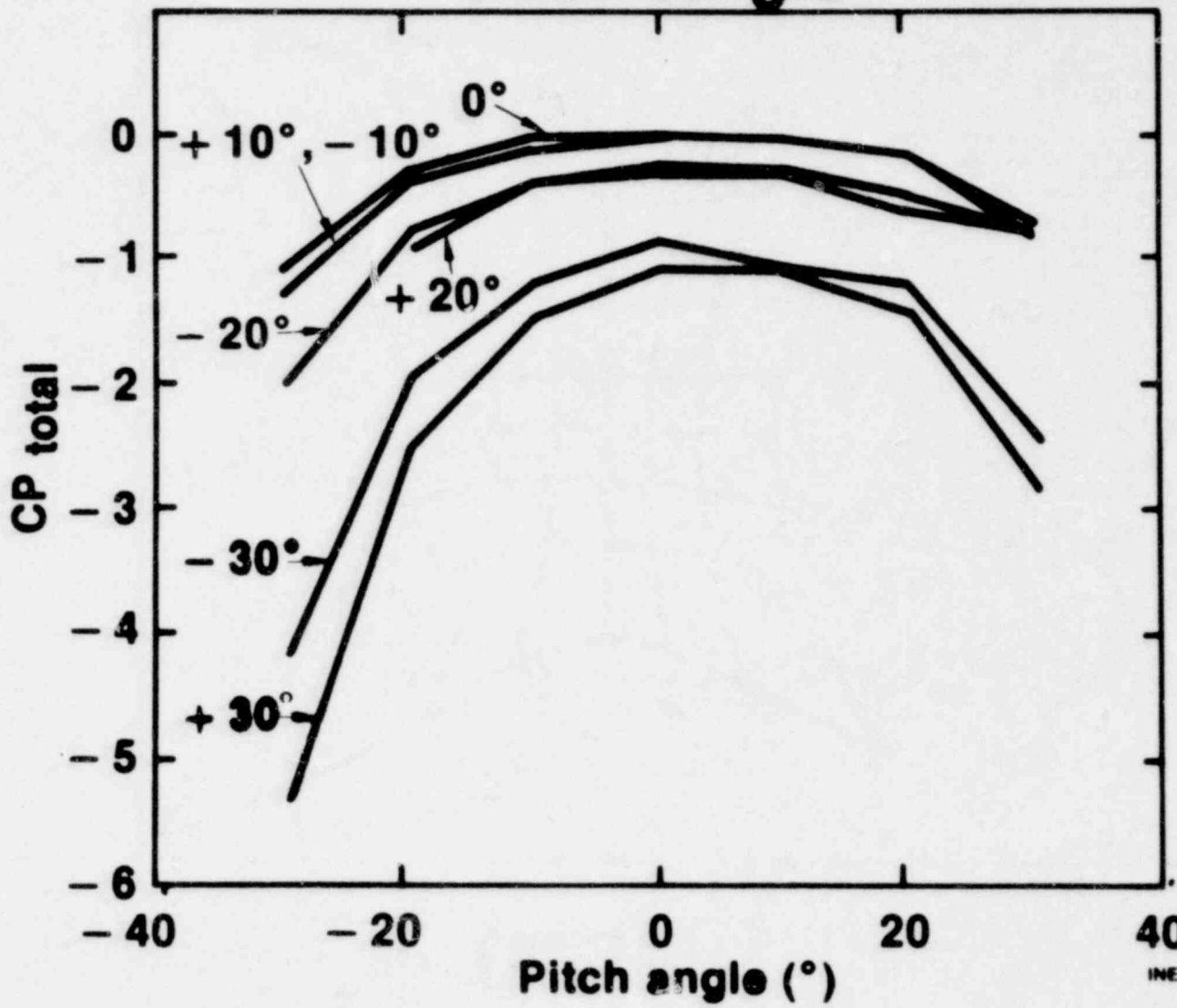

INEL-S-19 324

Outline

- Developed technologies now applied
  - Stagnation probes
- Technologies recently developed
  - HPHT optical probe
  - Local ultrasonic densitometer
  - Differential TC liquid level
- Improved understanding
- Small break instrumentation
- Future goals

INEL-S-21 758

Imaging Optical Probe

	Phase 1	Phase 2	Phase 3
Use	Piping	Piping and electrically heated core	Nuclear
Test conditions	15.2 MPa 343°C MTHP	15.2 MPa 600°C HTPH	15.2 MPa 600°C
Dimensions	0.3-m to 3-m lengths 25.4-mm diameter		

INEL-S-20 442

Flow Regime Viewing Using Endoscope and CCTV

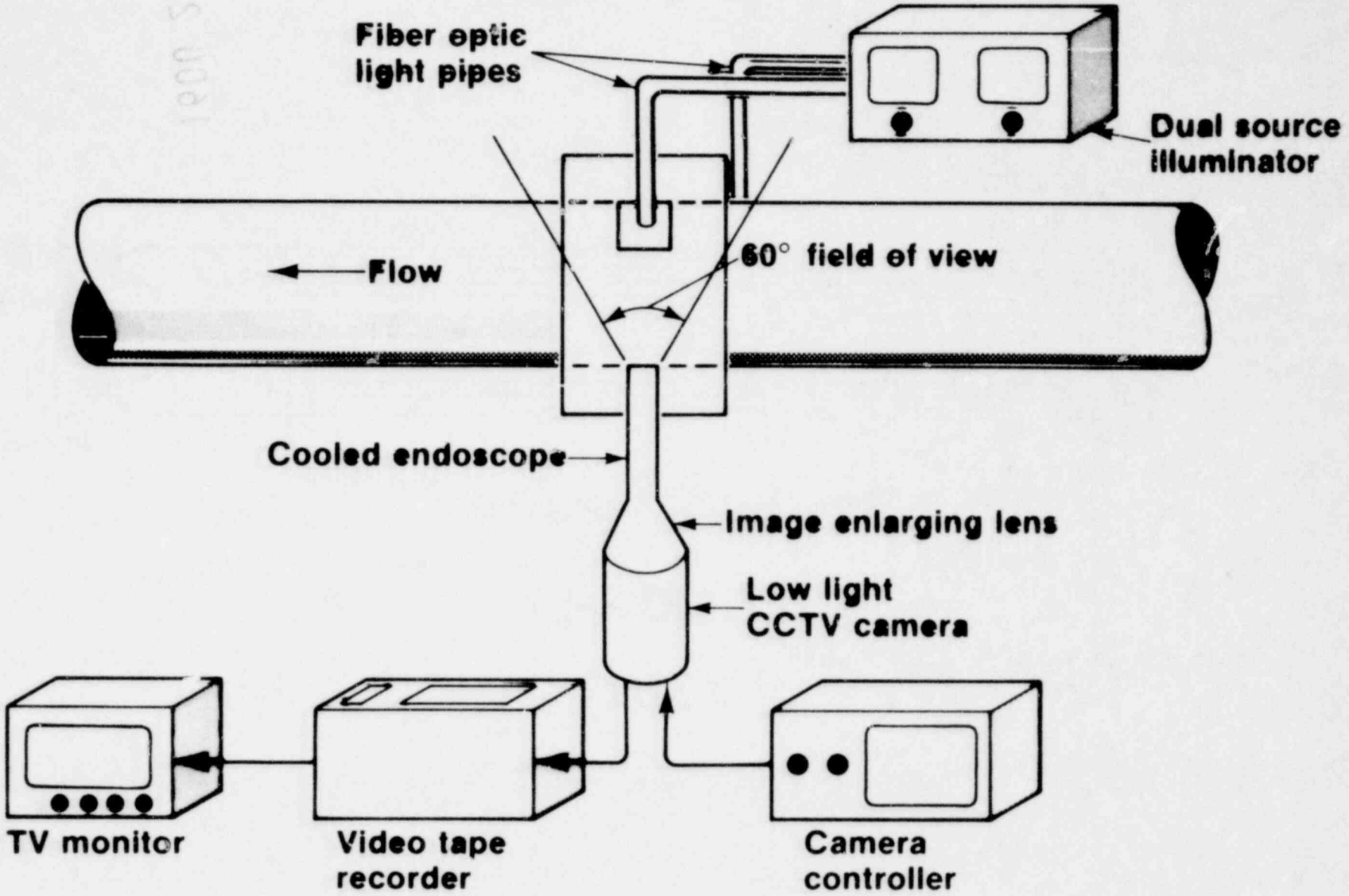

Air Cooled Imaging Optical Probe

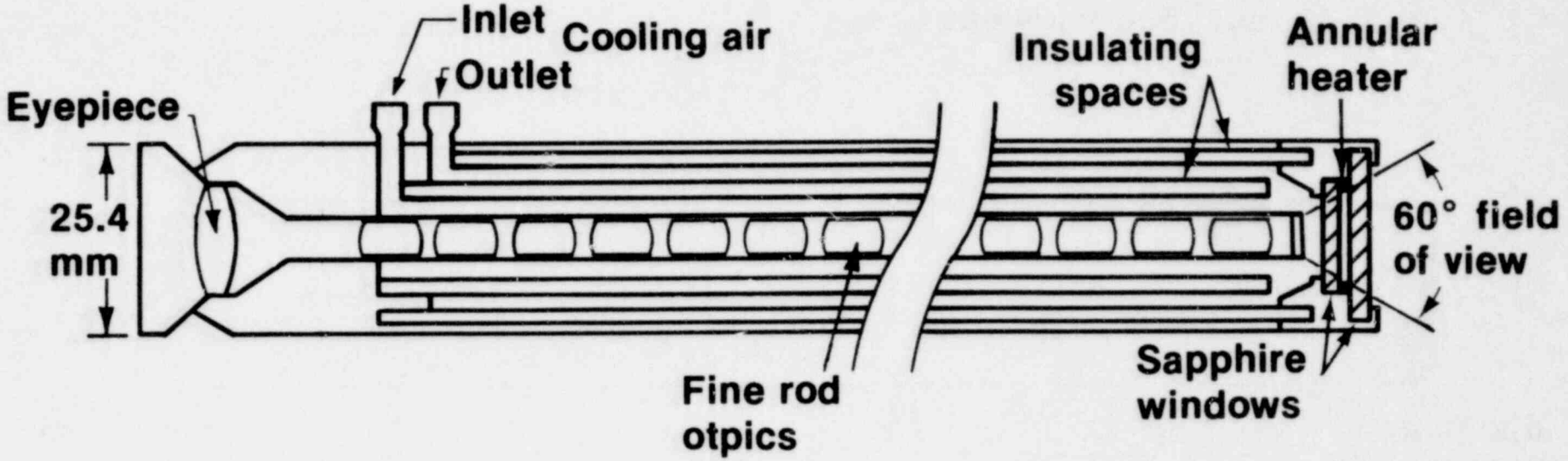

INEL-S-17 648

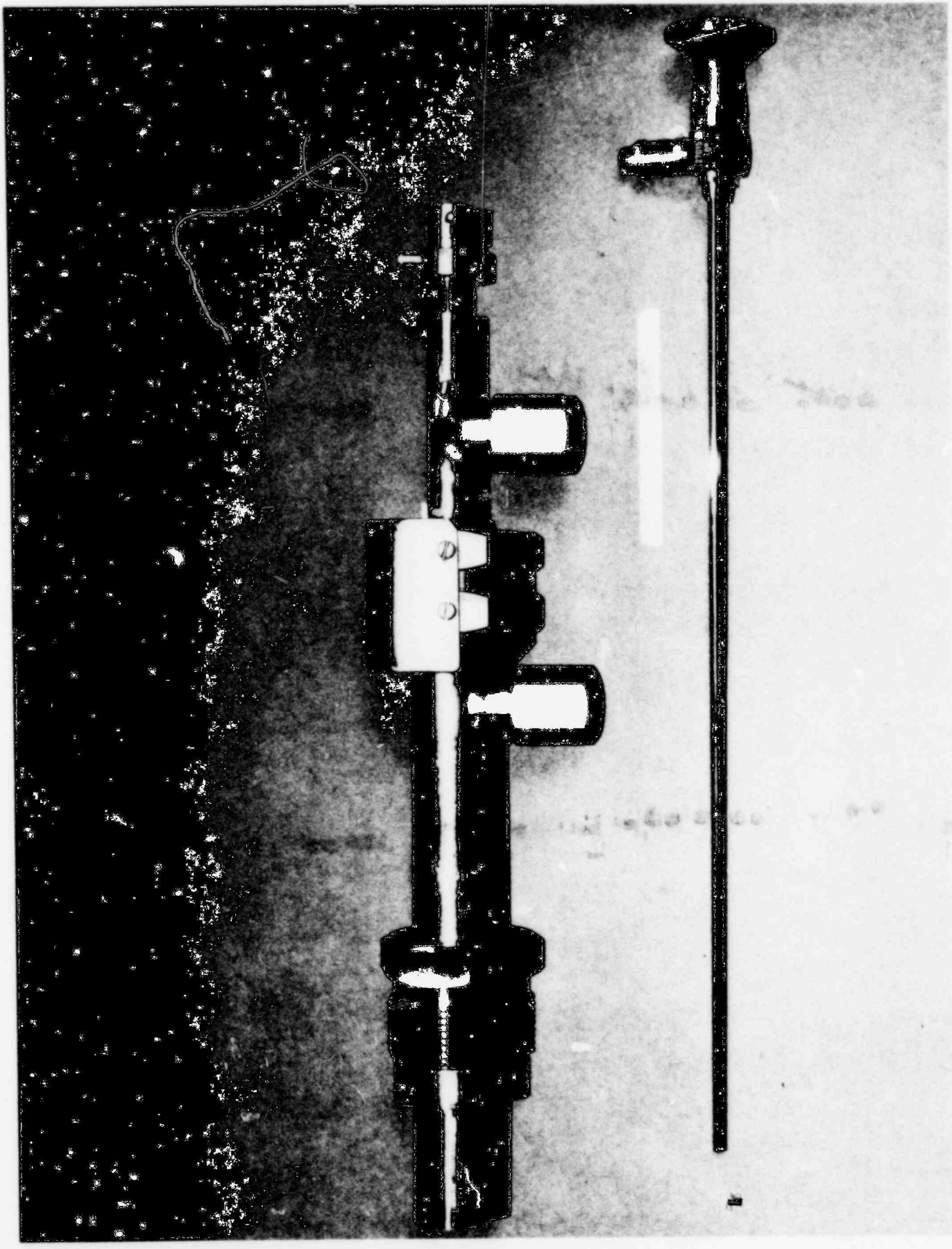

POOR ORIGINAL

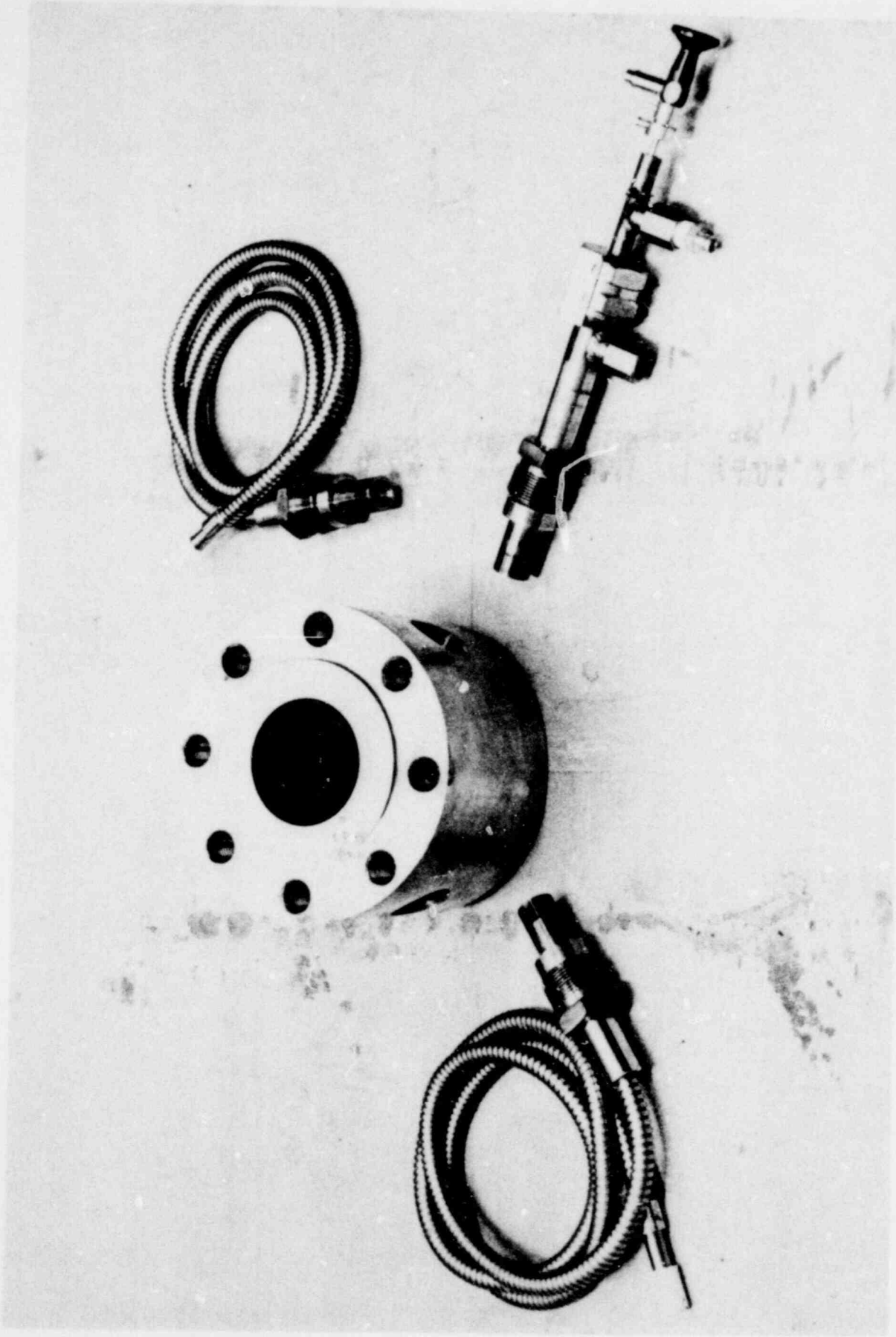

Ultrasonic Densitometer

	Ultrasonic Densitometer Detector (UDD)	Local Ultrasonic Detector (LUD)
Use	Core inlet and outlet density	Local density
Principle	Propagation time	Pulse/reflection
Test conditions	PWR conditions Transient Steady state	PWR conditions Steady state

INEL-S-20 444

Basic Configuration

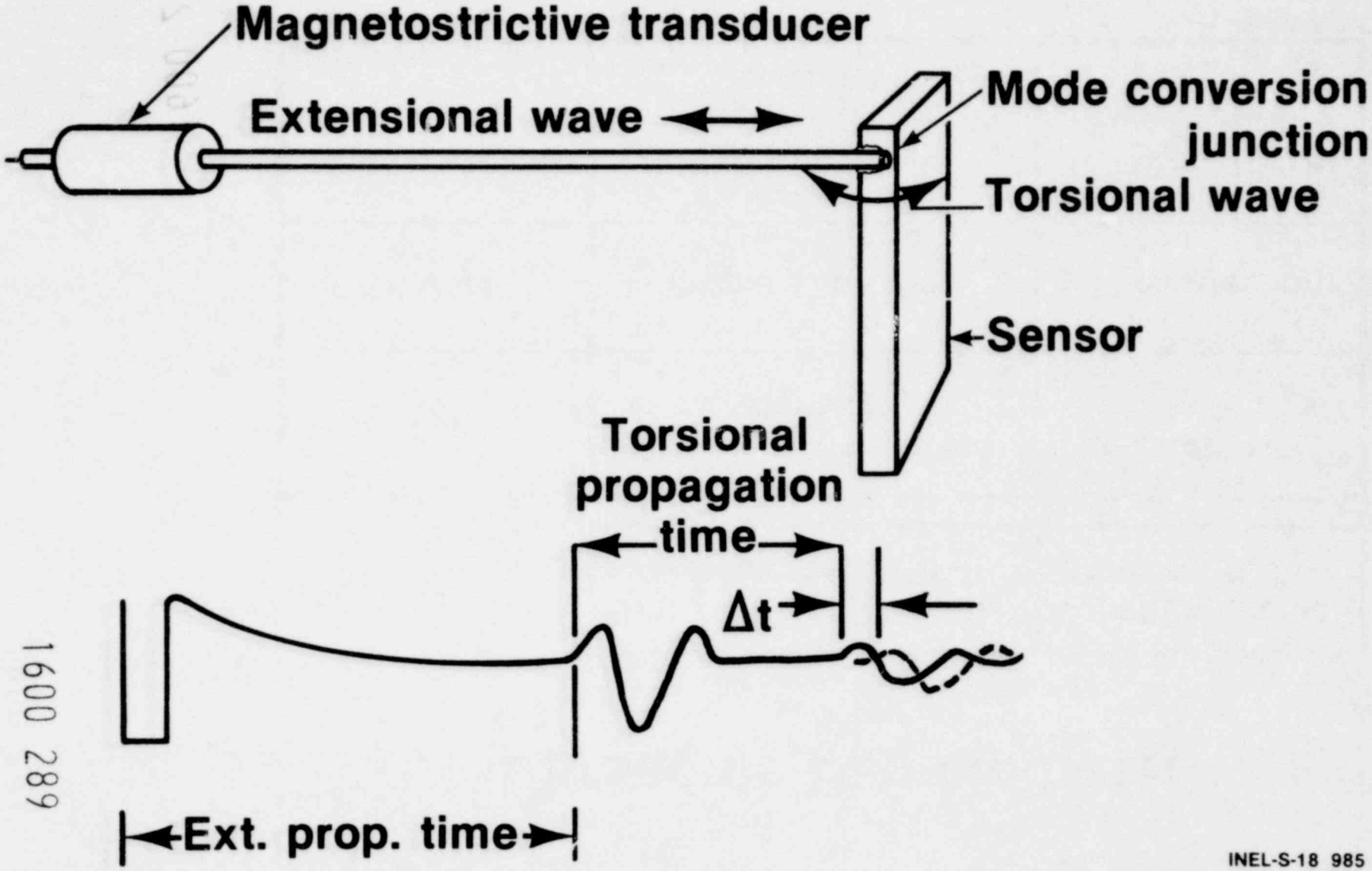

1600 289

INEL-S-18 985

Air-Water Test Ultrasonic Densitometer

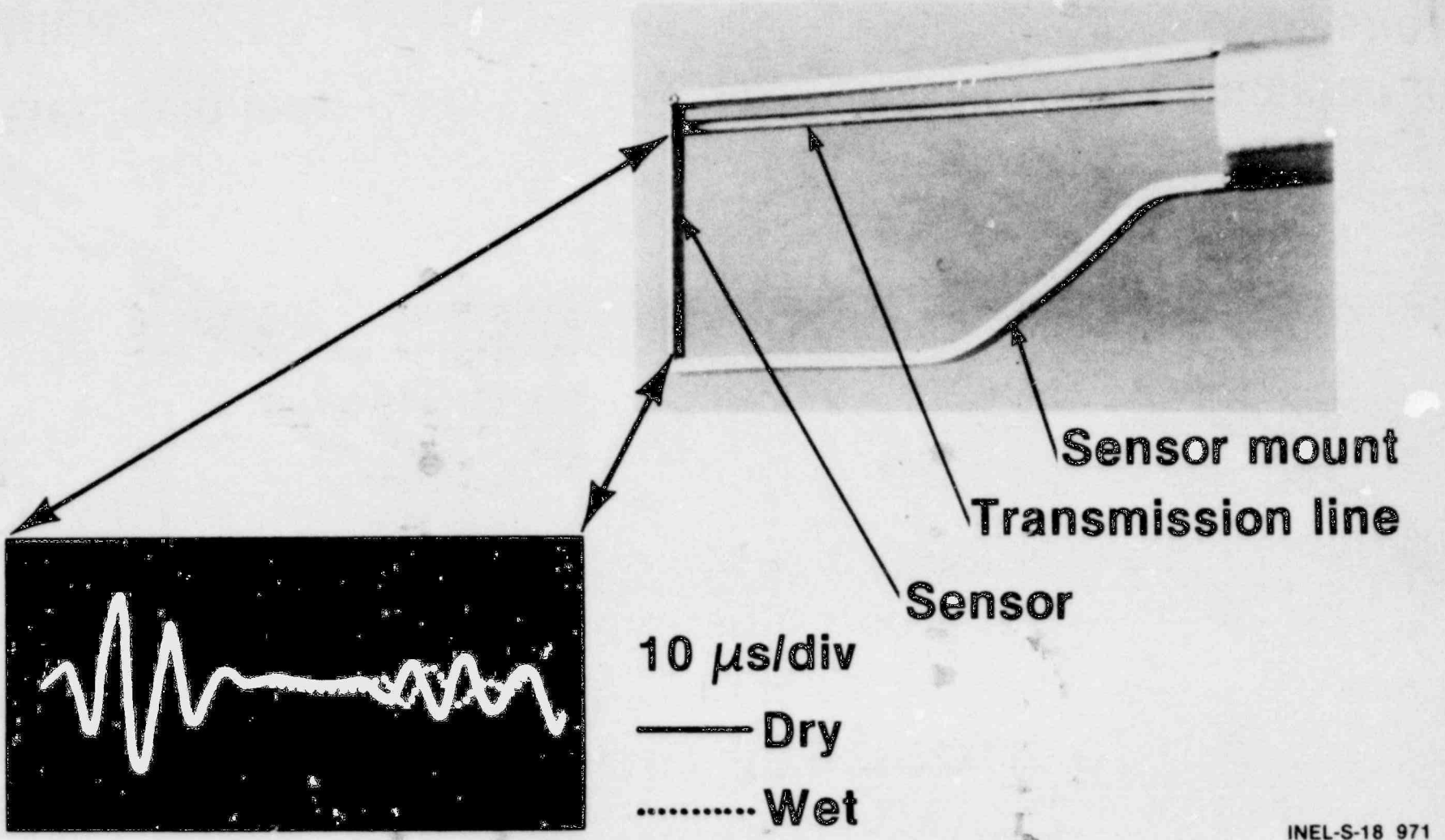

A Typical Magnetostrictive, Ultrasonic Transducer

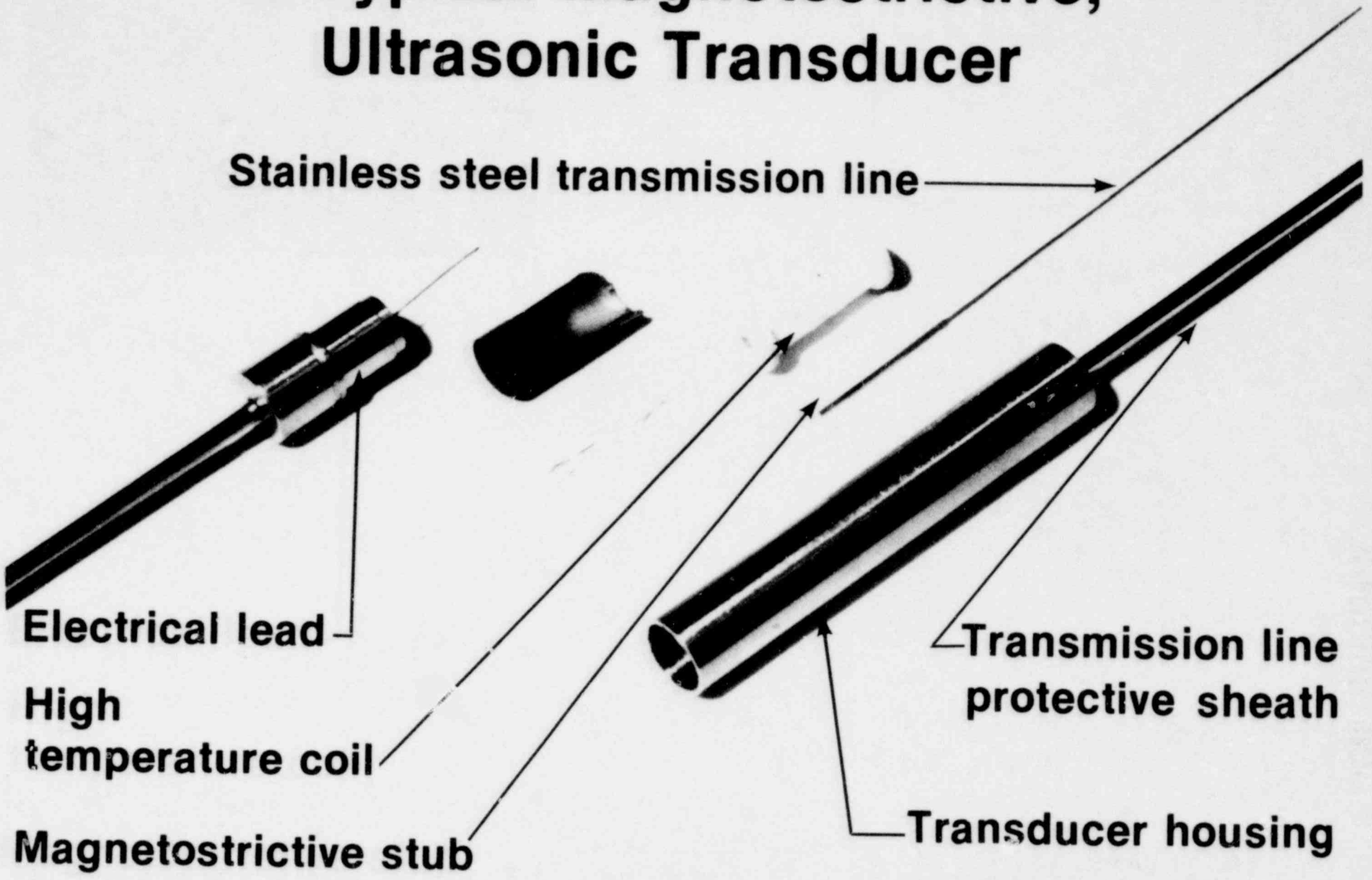

INEL-S-19 006

Reference vs Ultrasonic Density

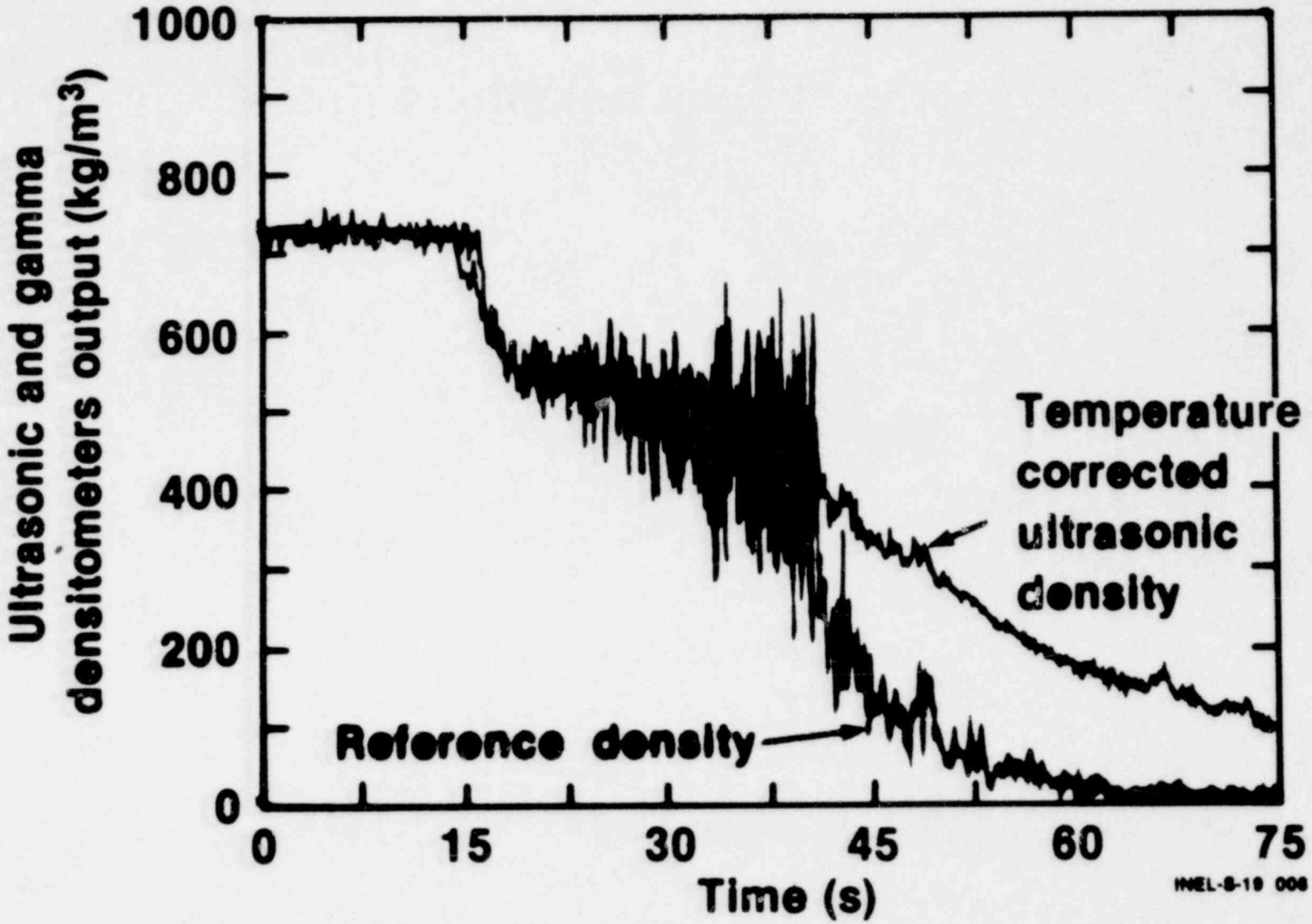

Differential TC Liquid Level Probe

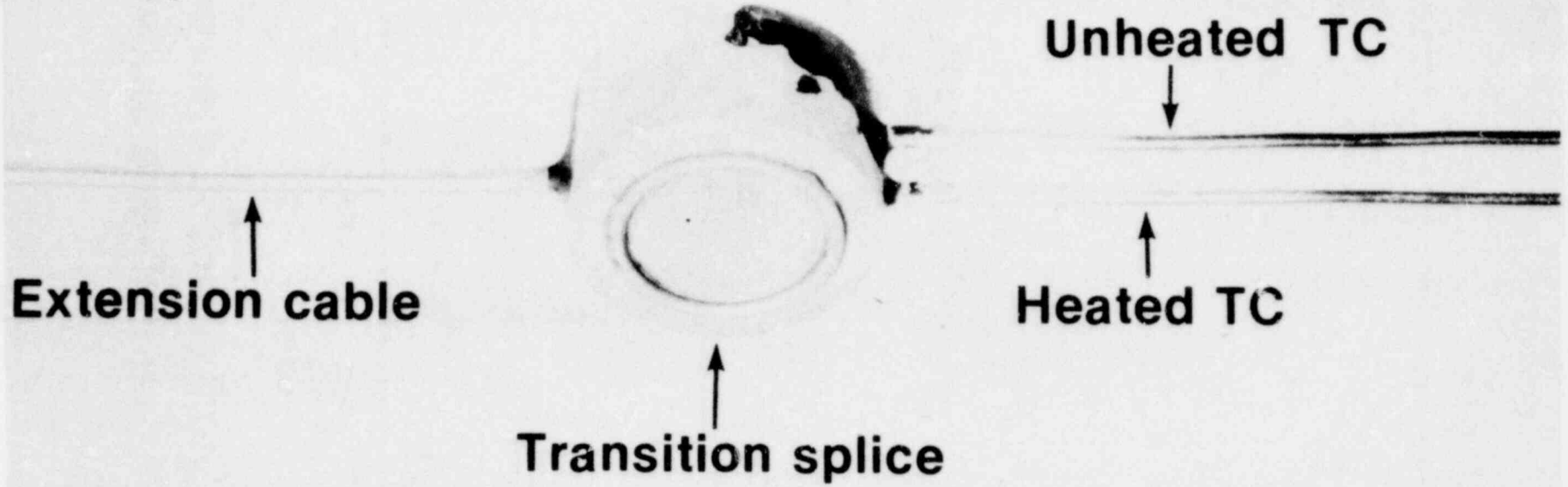

Liquid Level System

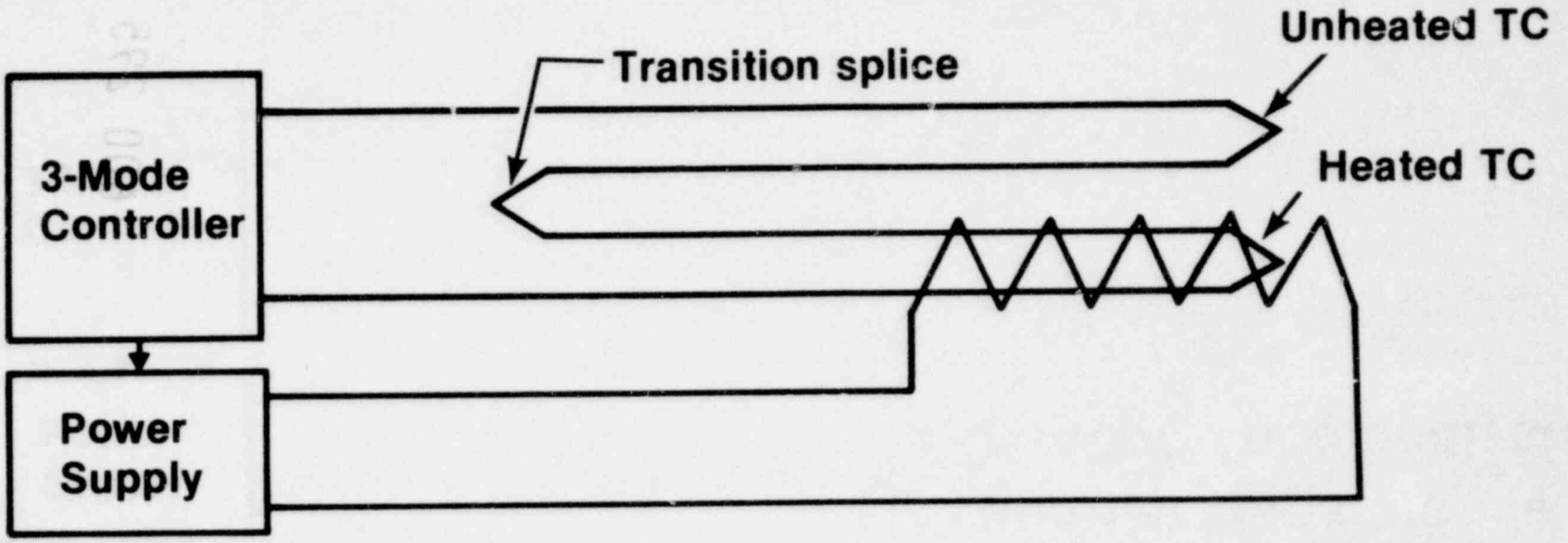

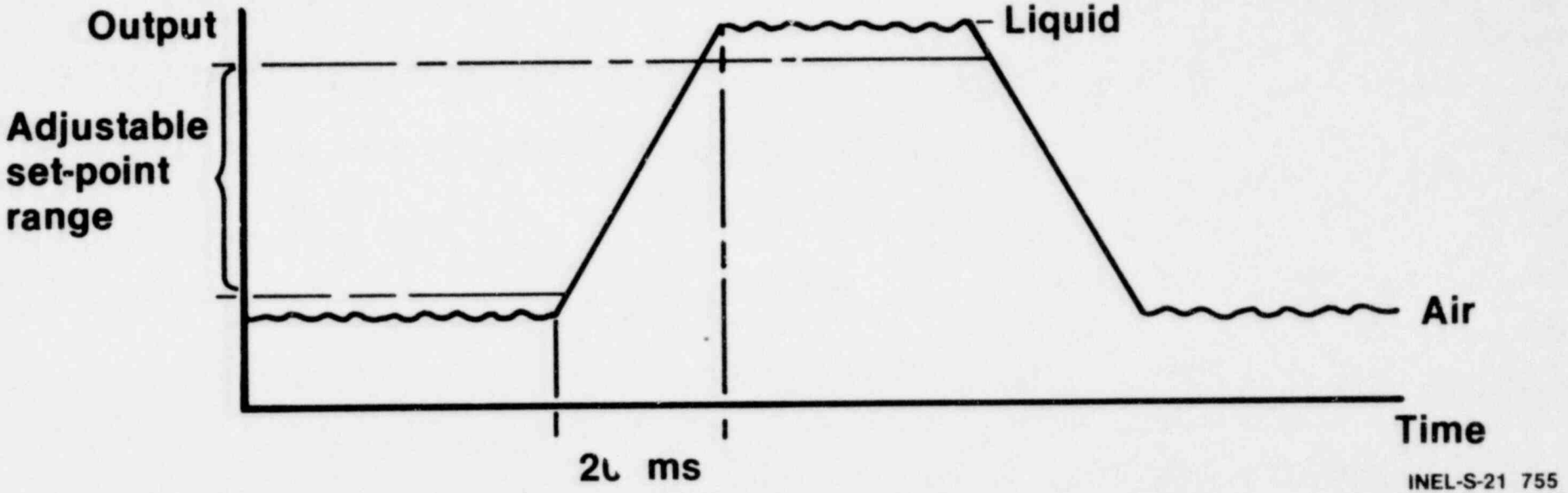

INEL-S-21 755

Outline

- Developed technologies now applied
- Technologies recently developed
- Improved understanding
  - Drag body
    - Reynolds and Mach Number dependence
  - 3-D spool piece analysis
- Small break instrumentation
- Future goals

Single Phase Drag Coefficients

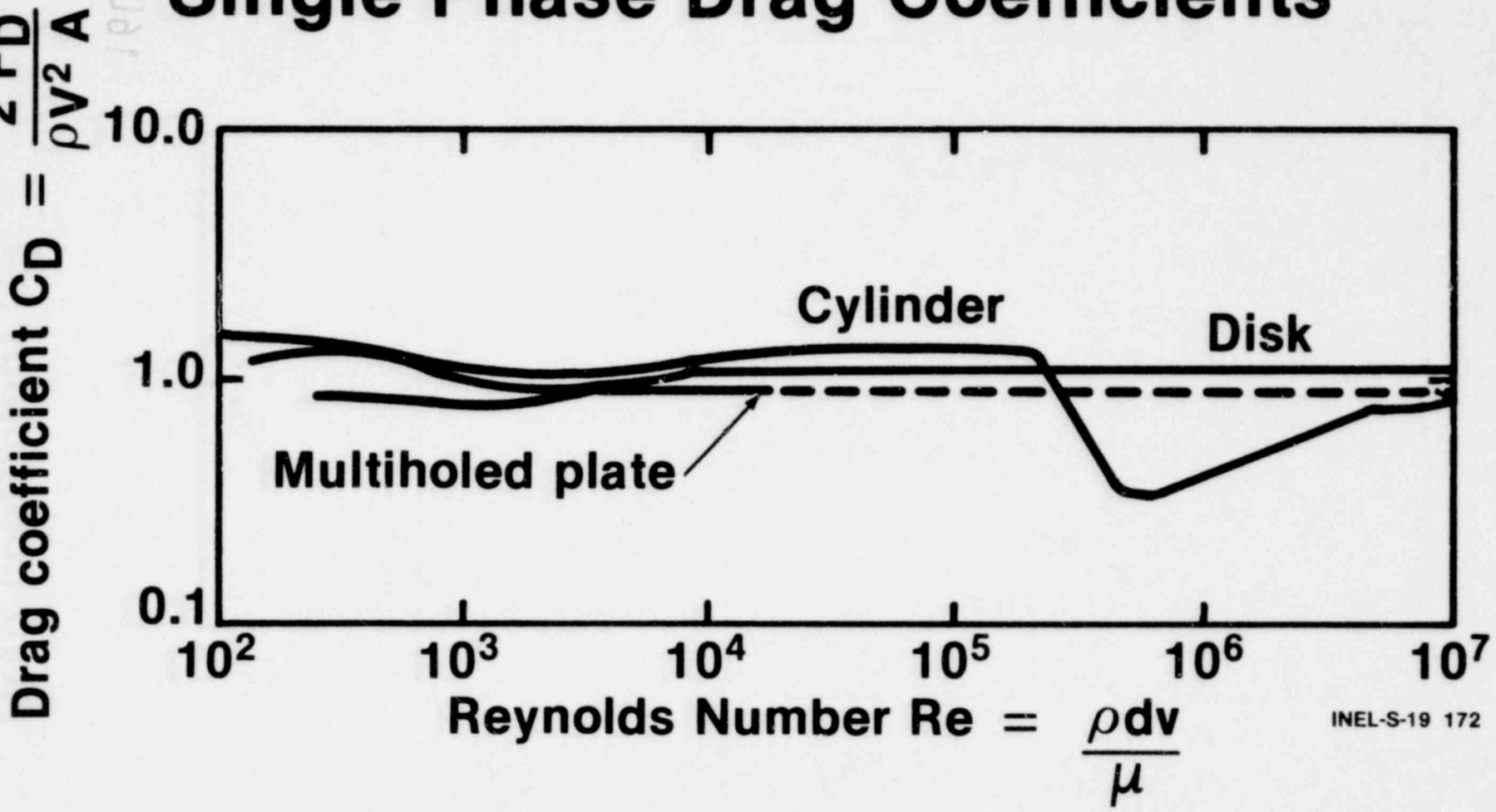

Drag Coefficient for Water Flows

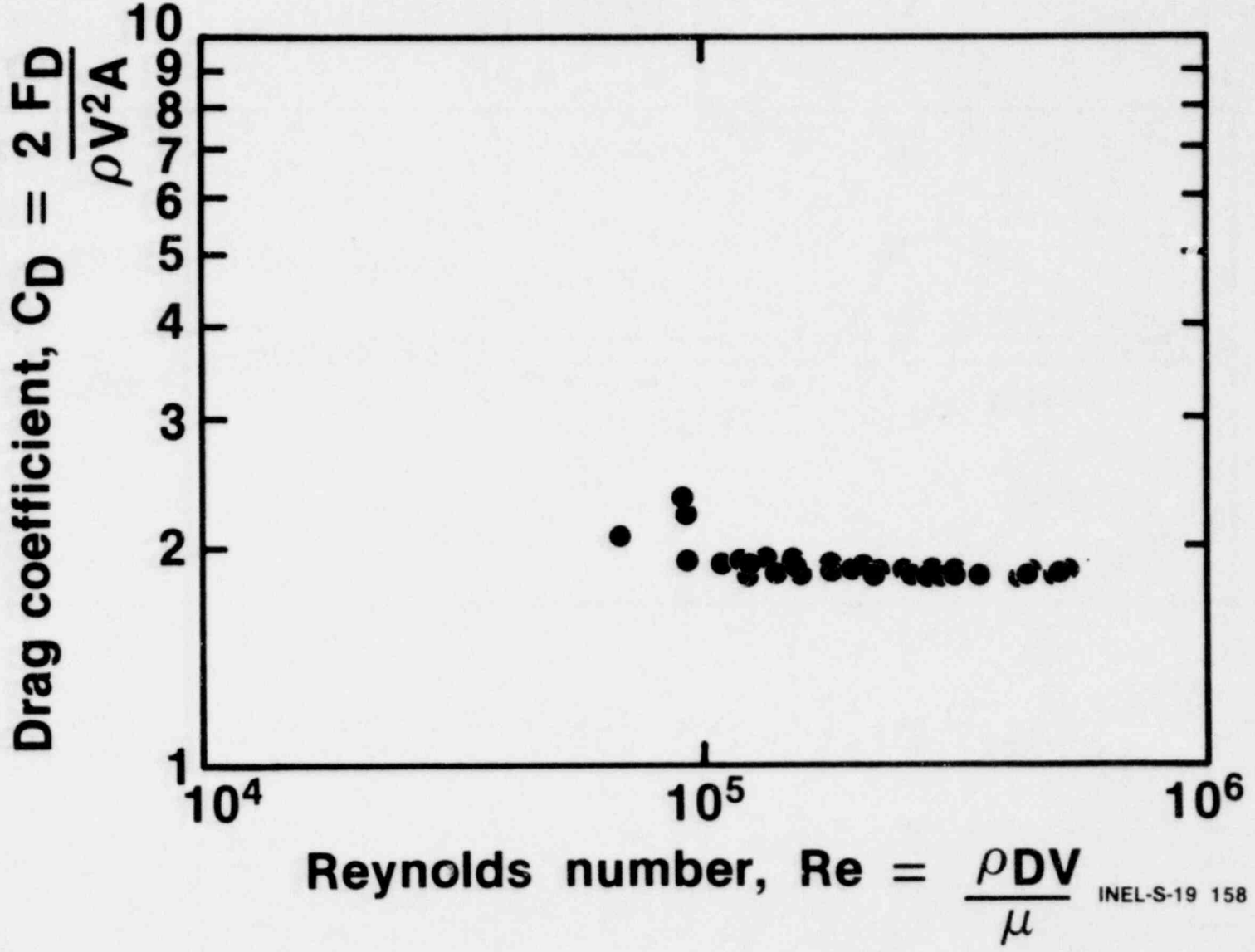

Drag Coefficient for Air Flows

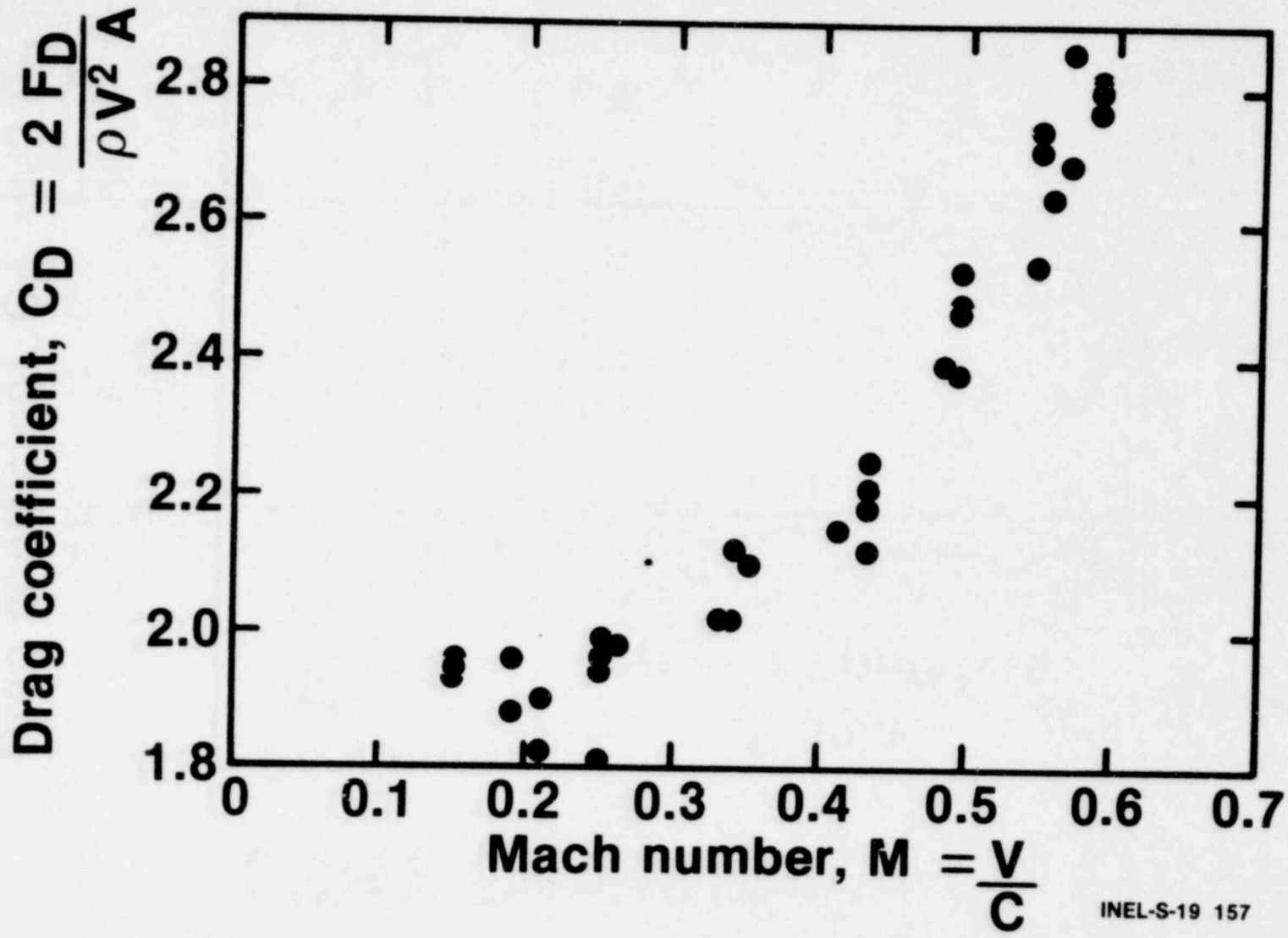

JAERI
LSRT Spool Piece

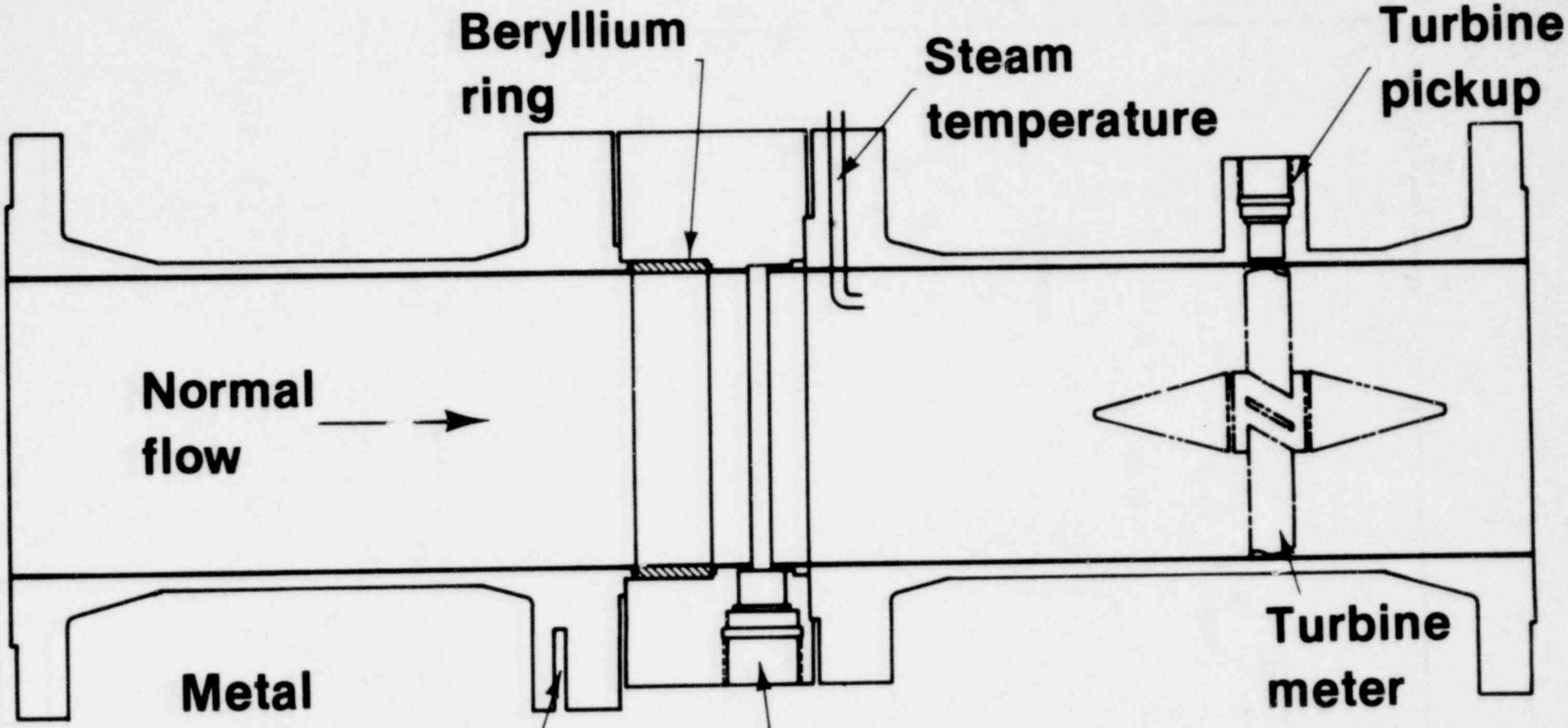

Hot Leg Spool Turbine Flowmeter

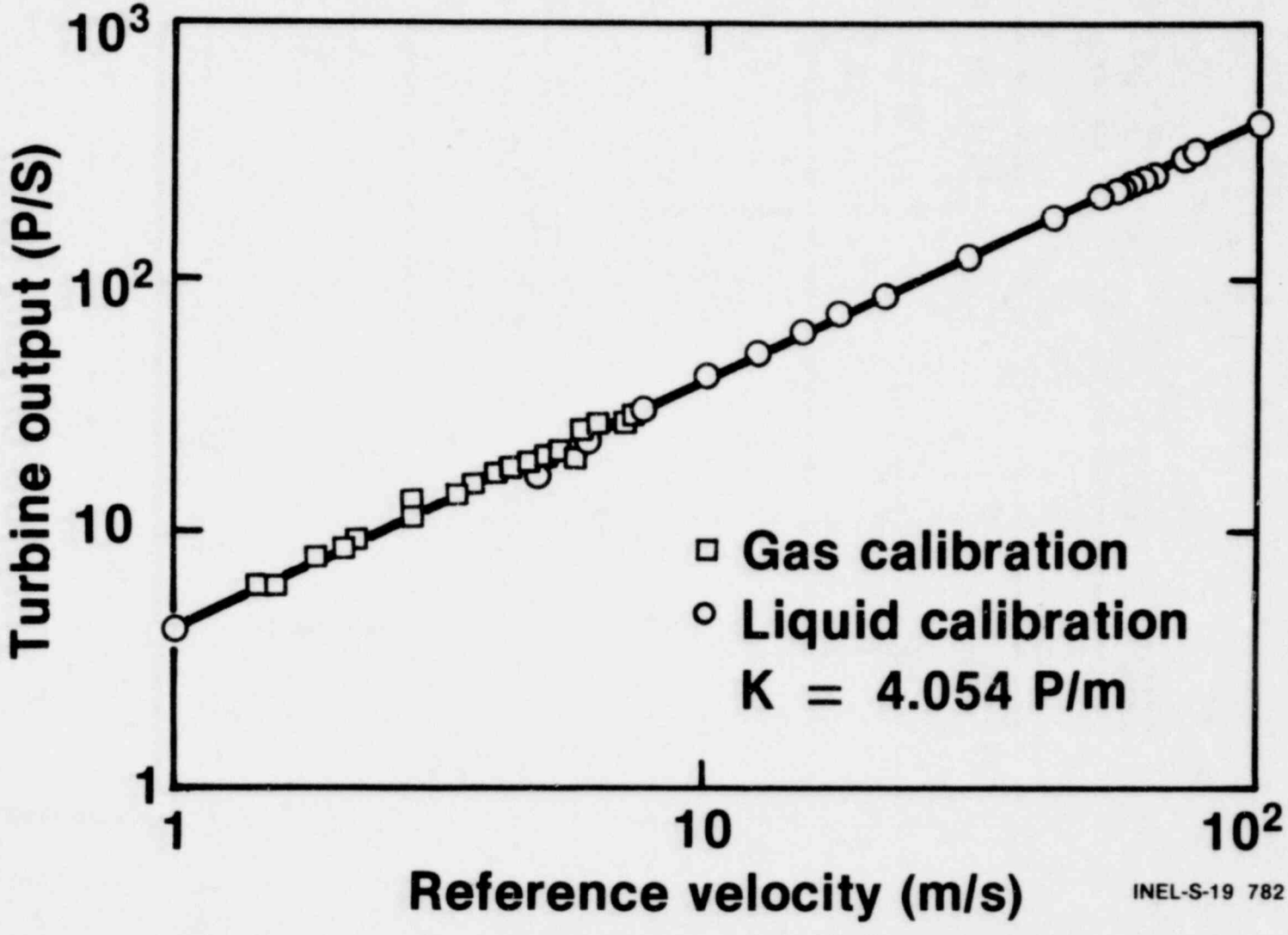

Analysis Techniques

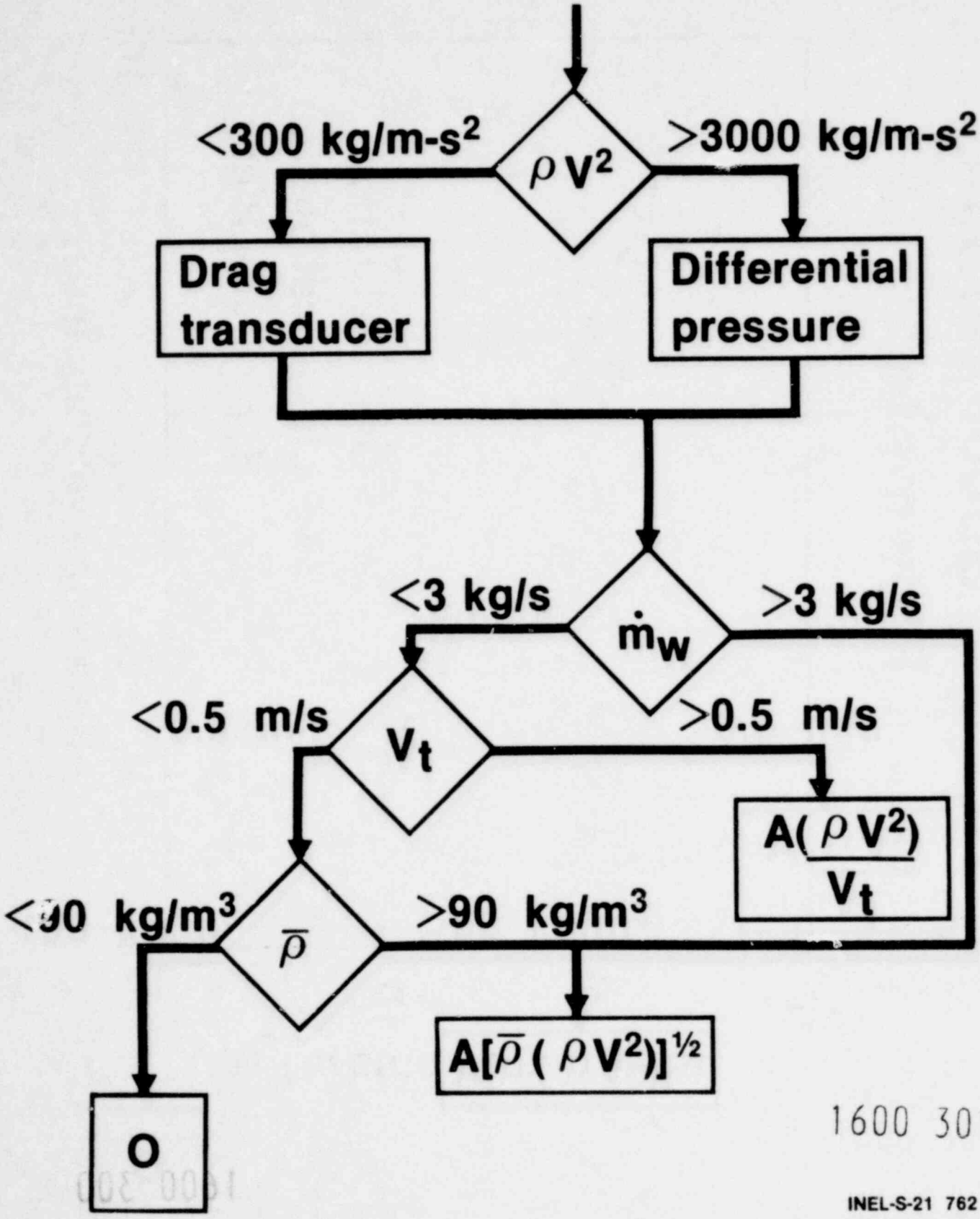

1600 301

INEL-S-21 762

Combined Results

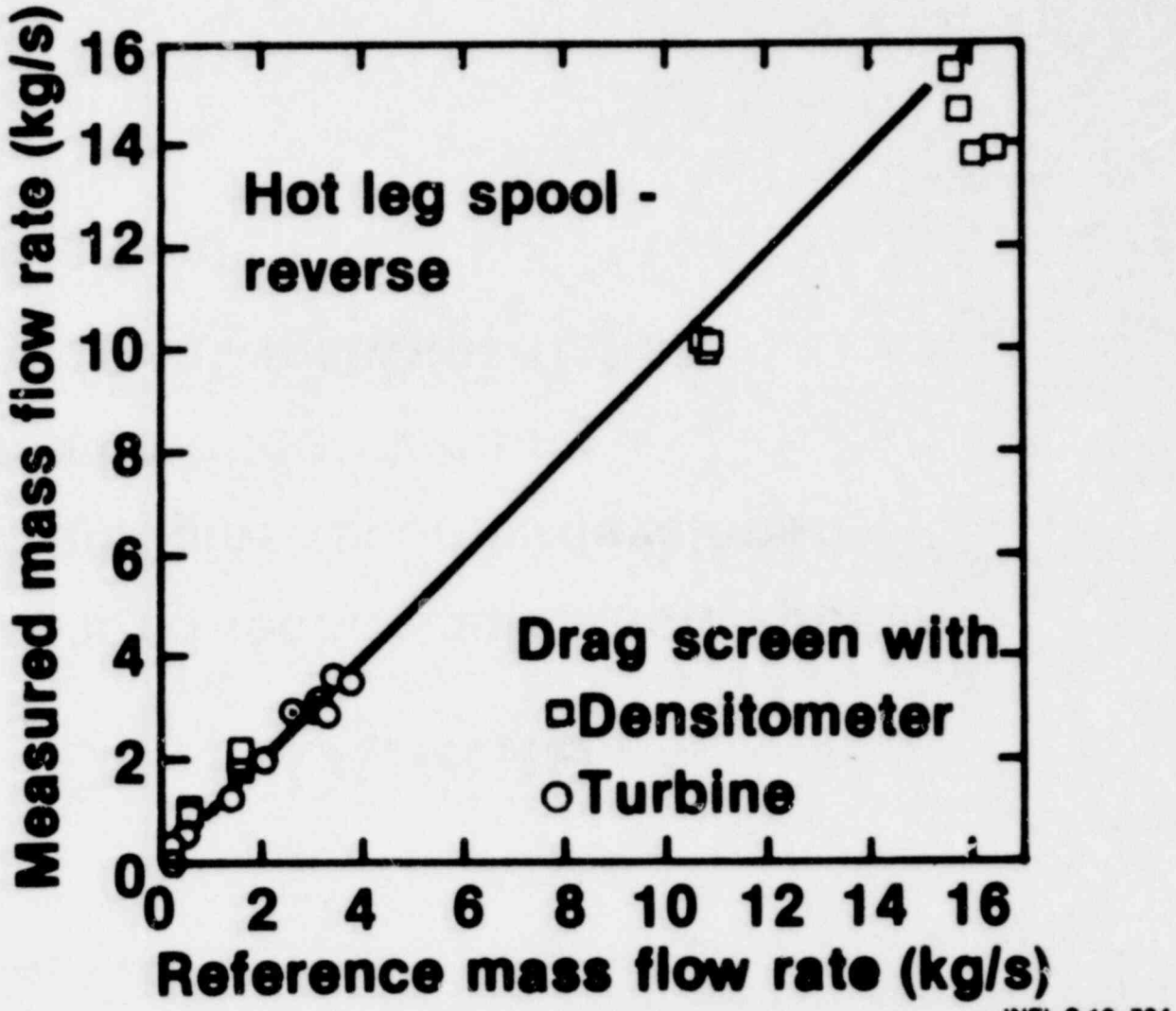

INEL-8-19 784

Outline

- Developed technologies now applied
- Technologies recently developed
- Improved understanding
- Small break instrumentation
- Future goals

INEL-S-21 763

Small Break Instrumentation

Type	LOFT	Semiscale
Thermocouple transit - time flowmeter	X	X
Pulsed neutron activation	X	X
Drag bodies	X	X
Low Energy Densitometer	X	X
Turbines	X	X
Thermionic flowmeter		X
Dual Optical Probes		X

INEL-S-21 784

Outline

- Developed technologies now applied
- Technologies recently developed
- Improved understanding
- Small break instrumentation
- Future goals

INEL-S-21 765

Future Goals

- Reference two-phase flow instrumentation
- Two-phase calibration standards
- Local velocity, density, and void fraction instruments
- Advanced code verification instrumentation
- High temperature, high pressure, radiation hardened optical probe

INEL-S-13 157

RESULTS FROM SEMISCALE THREE MILE ISLAND EXPERIMENTS

Presented at
The Seventh Water Reactor Safety Research Information Meeting
November 5-9, 1979
Gaithersburg, Maryland

T. K. Larson
EG&G Idaho, Inc.

Idaho National Engineering Laboratory
Idaho Falls, Idaho 83401

RESULTS FROM SEMISCALE THREE MILE ISLAND EXPERIMENTS

T. K. Larson
EG&G Idaho, Inc.

The occurrence of the Three Mile Island (TMI) Unit 2 loss-of-coolant accident (LOCA) incident has stimulated increased interest in the simulation, understanding, and calculation of thermal-hydraulic phenomena associated with extremely slow off-normal transients in nuclear power generating systems. To help examine proposed TMI recovery procedures, to assist in analysis of the TMI transient, and to investigate the capabilities of the Semiscale facility with regard to small break simulation, a series of experiments was conducted in the Semiscale Mod-3 system.

System Description

The Semiscale facility is operated by EG&G Idaho, Inc., for the Department of Energy and the United States Nuclear Regulatory Commission. The Semiscale Mod-3 system is essentially a small-scale model of a typical four-loop nuclear reactor system. The system contains most of the hardware found on large nuclear systems including a pressure vessel, two active coolant loops with associated pumps and steam generators, and associated systems, such as, the pressurizer and emergency core cooling (ECC) subsystems. The pressure vessel has a full-length upper plenum and upper head and an external downcomer. A full-length (3.65-m) electrically heated 25-rod bundle is contained within the pressure vessel to provide a simulation of a nuclear core. The pressure vessel, loops, and core are extensively instrumented in order to provide information on pressure drop, volumetric flow, momentum flux, fluid density, and fluid and metal temperatures.

The Semiscale system was basically volume-scaled from a four-loop Westinghouse reactor design. In order to improve simulation of the TMI plant, which is a Babcock and Wilcox Company (B&W) 2 x 4 design,

that is, two hot legs and four cold legs, several significant changes to the Mod-3 system hardware and operating procedures were made. These changes included addition of hardware required to more closely simulate the B&W pressurizer (relief valves and surge line geometry), valves and piping required to simulate the B&W upper plenum-to-inlet annulus vent valve, and coolant loop hydraulic resistance modifications. Despite these modifications, the fact that Semiscale was scaled from a system different than the B&W reactor and problems inherent in small-scale systems such as Semiscale will influence the experimental results. The more significant limiting factors include system heat losses to the environment, steam generator design and elevations, and loop pump degradation.

Noncondensible Gas Venting Experiments

Two experiments (gas venting tests) were conducted to investigate the behavior of a noncondensible gas bubble in the Semiscale pressure vessel upper head and upper plenum during system depressurization through the pressurizer power operated valve (POV).[1] The initial conditions for these experiments were based on measurements taken at TMI several days after the accident. Saturated conditions at 6.89 MPa were established in the system, and nitrogen gas was introduced into the pressure vessel upper head and plenum regions. The experiments were initiated by opening the pressurizer POV and allowing the system to depressurize.

In the first Semiscale gas venting test conducted (Test S-TMI-1), a nitrogen bubble volume of 0.0142 m^3 was used to represent the estimated TMI noncondensible gas volume of 21.54 m^3. Results from this test showed that by venting through the POV, the Semiscale system could be depressurized to a point where the residual heat removal (RHR) system could have been activated without significant shock to the core. Noncondensible gas movement was determined to be primarily from the vessel into the upper elevations of the loops, and minimal gas escaped from the system through the POV.

In the second venting test (Test S-TMI-2), the initial nitrogen gas volume was increased to 0.017 m^3 to investigate the influence of bubble size on system response. Results similar to those obtained on Test S-TMI-1 were obtained during the depressurization phase of Test S-TMI-2. Following depressurization to 1.86 MPa, the POV was closed and the high-pressure injection (HPI) pumps were used to refill and repressurize the system, demonstrating the ability to recover from operations attempted to depressurize and activate the RHR system. A return to stable conditions was successful although it was found that, due to shifting gas volumes in the loops, only one loop pump at a time could be started to provide forced circulation.

TMI Transient Simulations

Eight Semiscale experiments[2] were conducted to examine system thermal-hydraulic response to a sequence of events similar to that which occurred during the first 2 hours of the TMI transient. These experiments focused primarily on determining those variables that had an influence on the system response. The test results showed that the early system response was strongly influenced by the steam generators and HPI flow. In general, the Semiscale results showed trends very similar to those observed in the TMI data. Core heater rod cladding temperature excursion occurred shortly after the loop pumps were shut off. Superheated steam was observed in the Semiscale coolant piping hot legs in the same time frame as it was observed in the TMI piping hot legs which suggests that the cores in the two systems uncovered at about the same time. The pressurizer was noted to fill early in the transient and remain full even though the core and vessel were voiding. This result indicated that pressurizer liquid level was not an appropriate indication of the core and system mass inventory when the system was operating in a saturated two-phase state. After the core uncovered in the Semiscale system, the rod heat transfer coefficients were found to be primarily a function of the collapsed liquid level in the core. These heat transfer coefficients, when

combined with an estimate of the TMI collapsed core level, suggest that significant core damage could have occurred in the TMI core above the 2.9-m elevation.

The complete simulations of the TMI transient that were conducted in the Semiscale system have provided considerable insight into the basic phenomena associated with slow transient LOCAs and have provided an indication of the ability of the Semiscale facility to provide meaningful data in this area. In particular, information has been obtained regarding component interaction (steam generator influence and pressurizer response), partially uncovered core heat transfer, and Semiscale facility limitations.

REFERENCES

1. D. J. Clafin and E. L. Wills (eds.), Quarterly Technical Progress Report on Water Reactor Safety Programs Sponsored by the Nuclear Regulatory Commission's Division of Reactor Safety Research, April-June 1979, NUREG/CR-0871, TREE-1300, July 1979.

2. R. W. Shumway et al, Semiscale Simulations of the Three Mile Island Transient - A Summary Report, SEMI-TR-10, July 13, 1979.

Results from Semiscale Three Mile Island Related Experiments

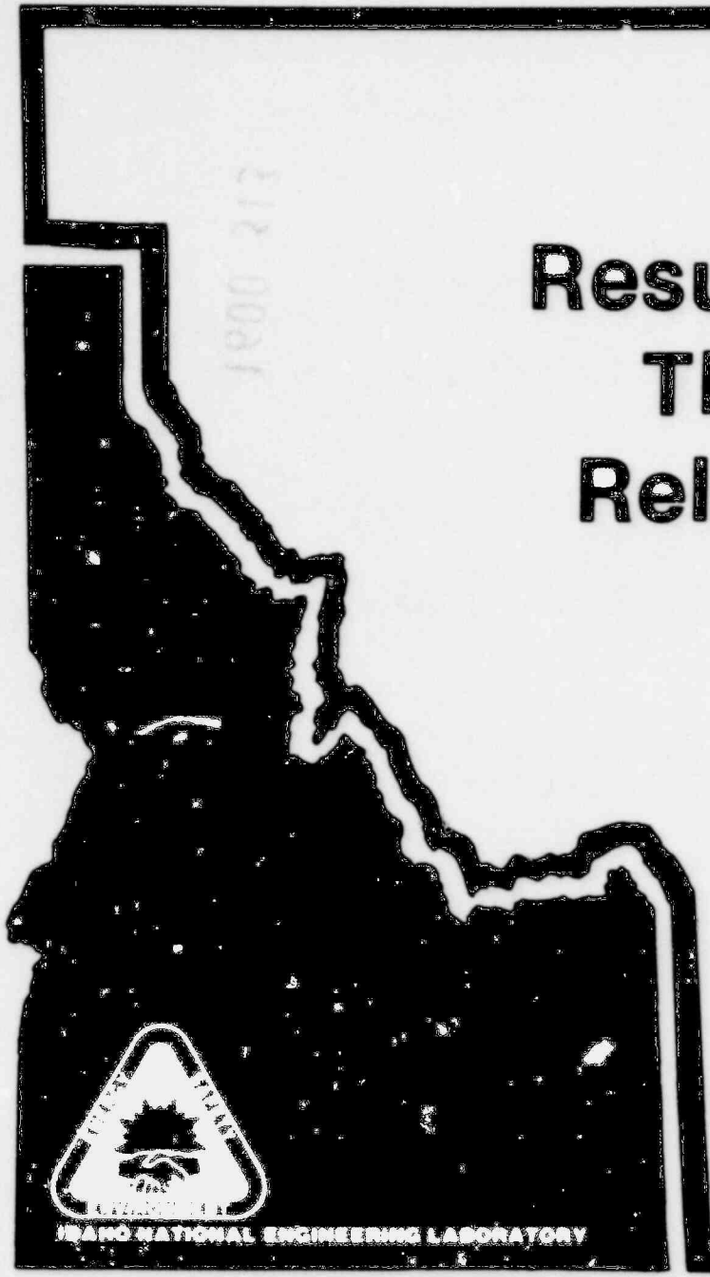

Presented by
T.K. Larson

EG&G Idaho, Inc.

Semiscale Simulations Done in Support of TMI Transient

- Noncondensible gas bubble vent tests (2 experiments)
- Complete simulations of TMI transient (8 experiments)

Objectives

- Investigate noncondensible gas bubble behavior during pressurizer venting and qualify system recovery procedures

- Establish system thermal-hydraulic response to TMI sequence of events
  - Quantify pressurizer liquid level behavior
  - Identify Semiscale hardware and configuration limitations

Hardware Changes Made to Semiscale System

- Pressurizer surge line elevation and resistance modified
- Addition of pressurizer safety valves and power operated valve
- Addition of upper plenum to inlet annulus vent line and valve
- Reduced loop resistance
- Added orifice in hot leg vessel nozzle to promote symmetric loop response

Semiscale System Operating Limitations

- External heat loss
- Steam generator design
- PCP degradation

Noncondensible Gas Bubble Vent Experiments

INEL-S-21 734

Significant Results from Venting Tests

- System was depressurized to low pressure without core uncovery
- Gas moved primarily from plenum to the upper elevations of the loops
- The pressurizer and surge line remained liquid full
- System could be recovered and repressurized
- After recovery, shifting gas volumes allowed operation of only one loop pump at a time

Semiscale Complete Simulations of the TMI Transient

INEL-S-21 732

Sequence of Events for Complete Simulation

Approximate time (s)	Event
0	Isolate steam generator and initiate drain
8	Pressurizer heaters off
12	Scram core when pressure =2355 psig
40	Open POV on top of pressurizer
120	Initiate HPIS when pressure = 1600 psig
180	Terminate HPIS
6000	Terminate pump power
7000	Terminate core power when rod temperature = 1600°F

INEL-S-21 731

Comparison of System Pressure

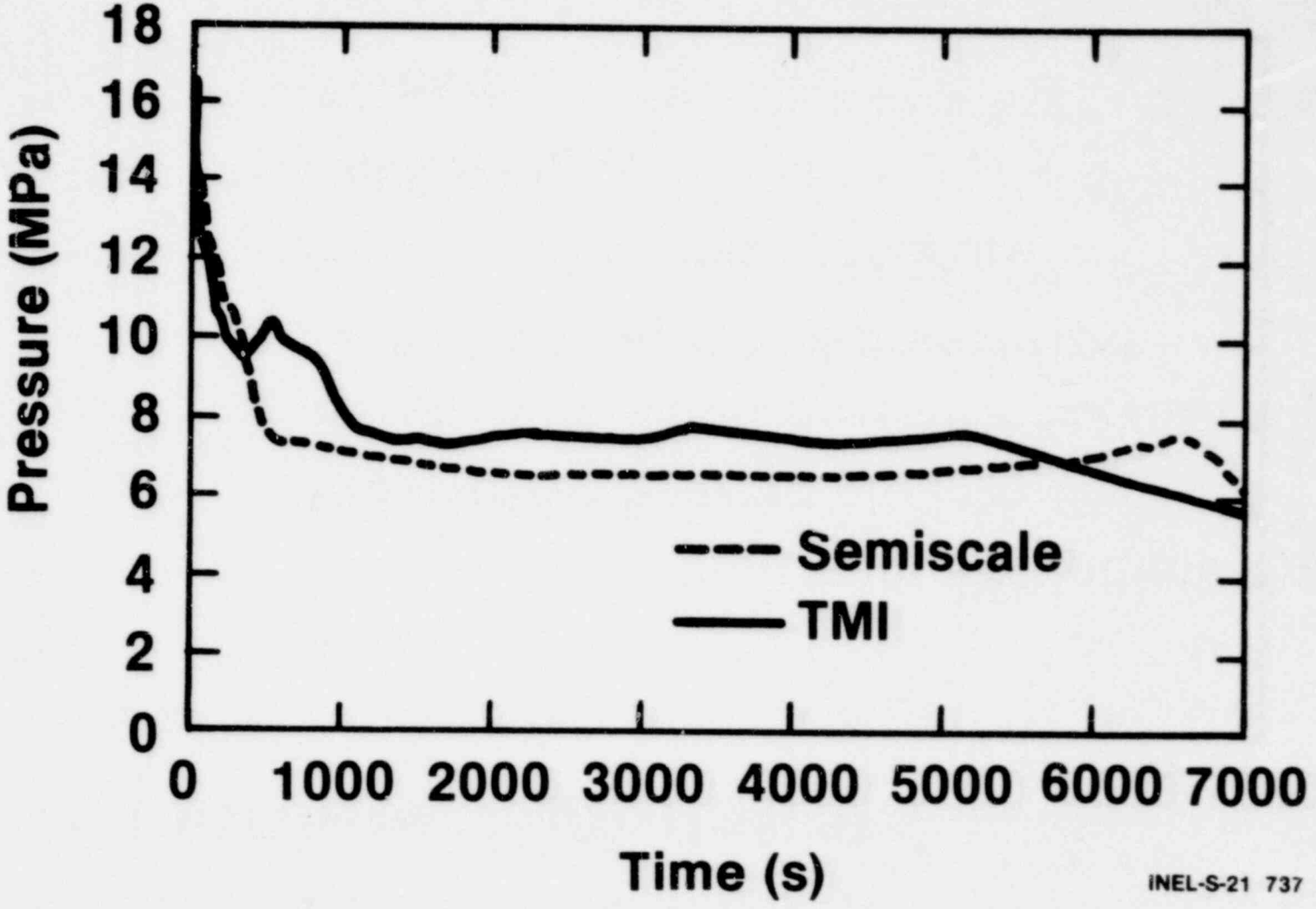

Comparison of Pressurizer Level

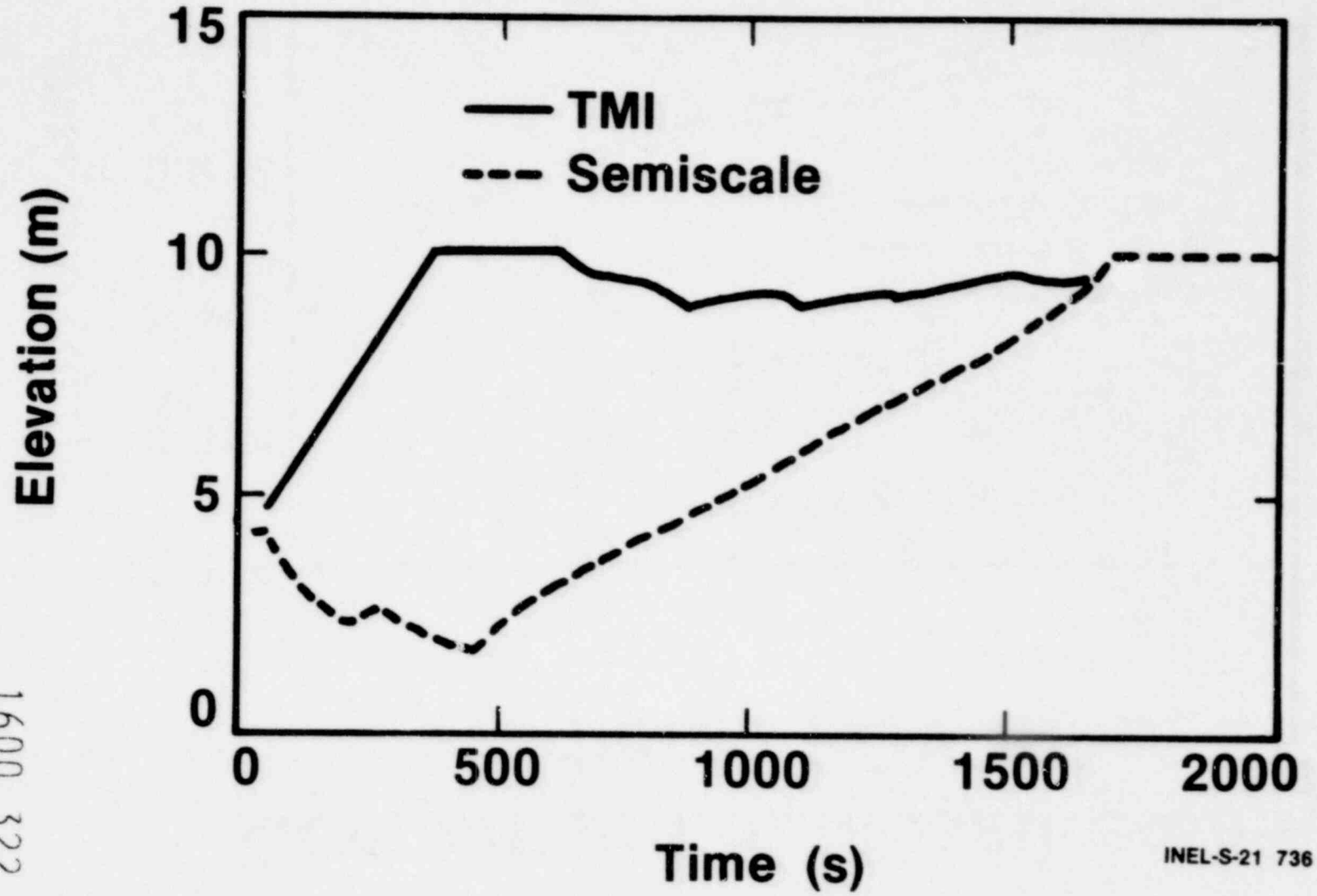

Comparison of Measured and Predicted POV Flow

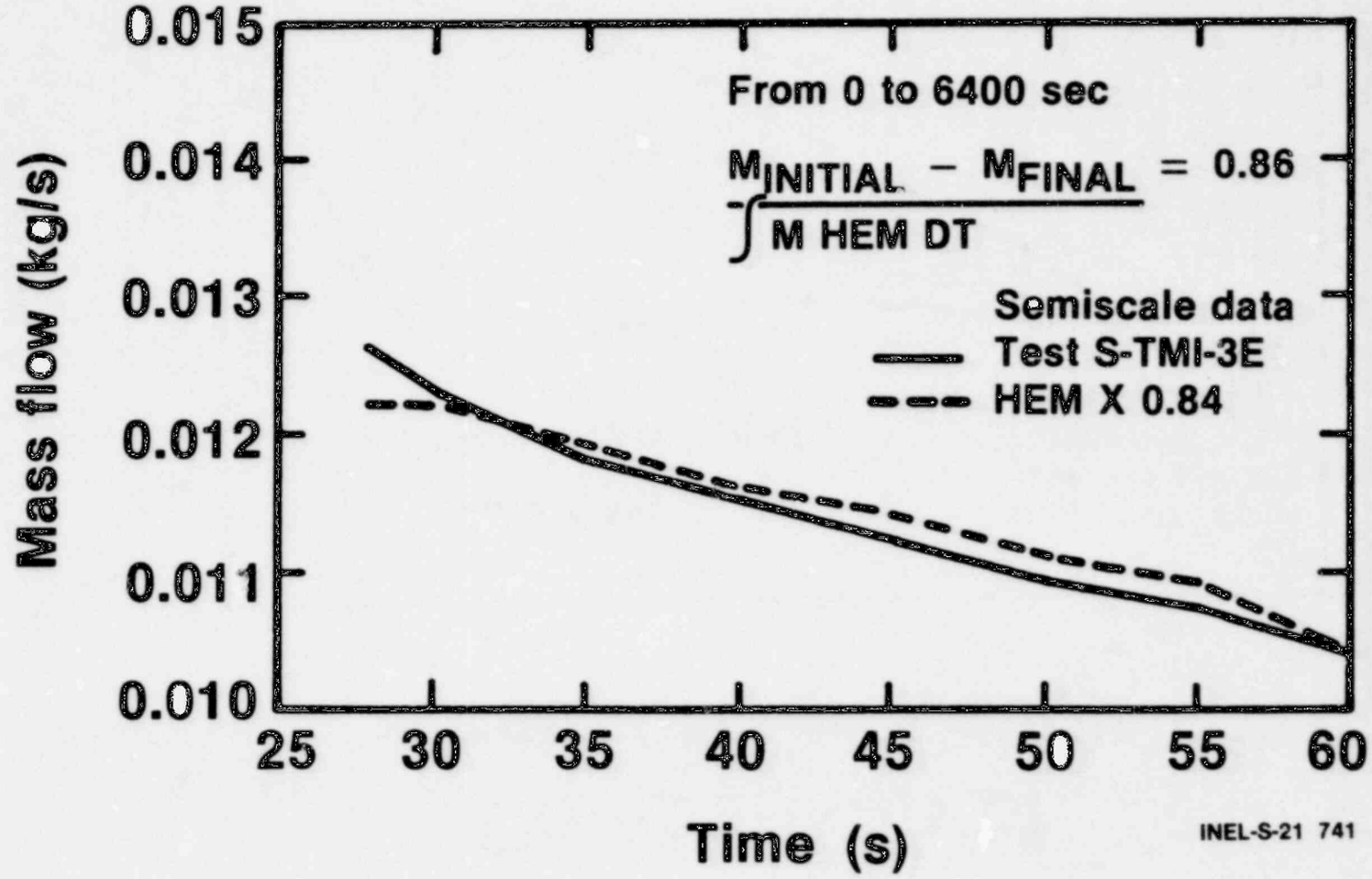

Comparison of Normalized Loop Flows

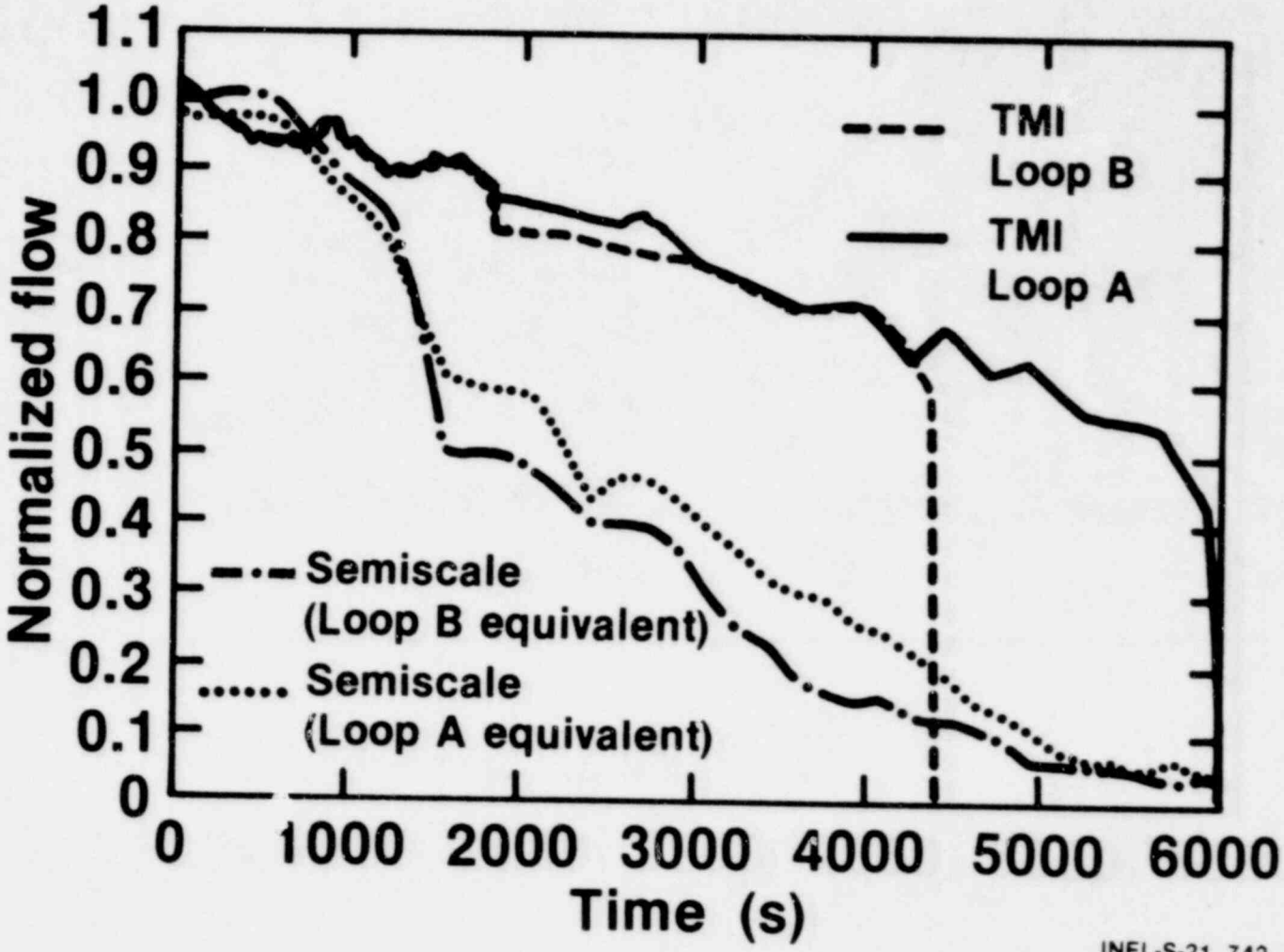

INEL-S-21 742

Intact Loop Density Distribution (Test S-TMI-3I)

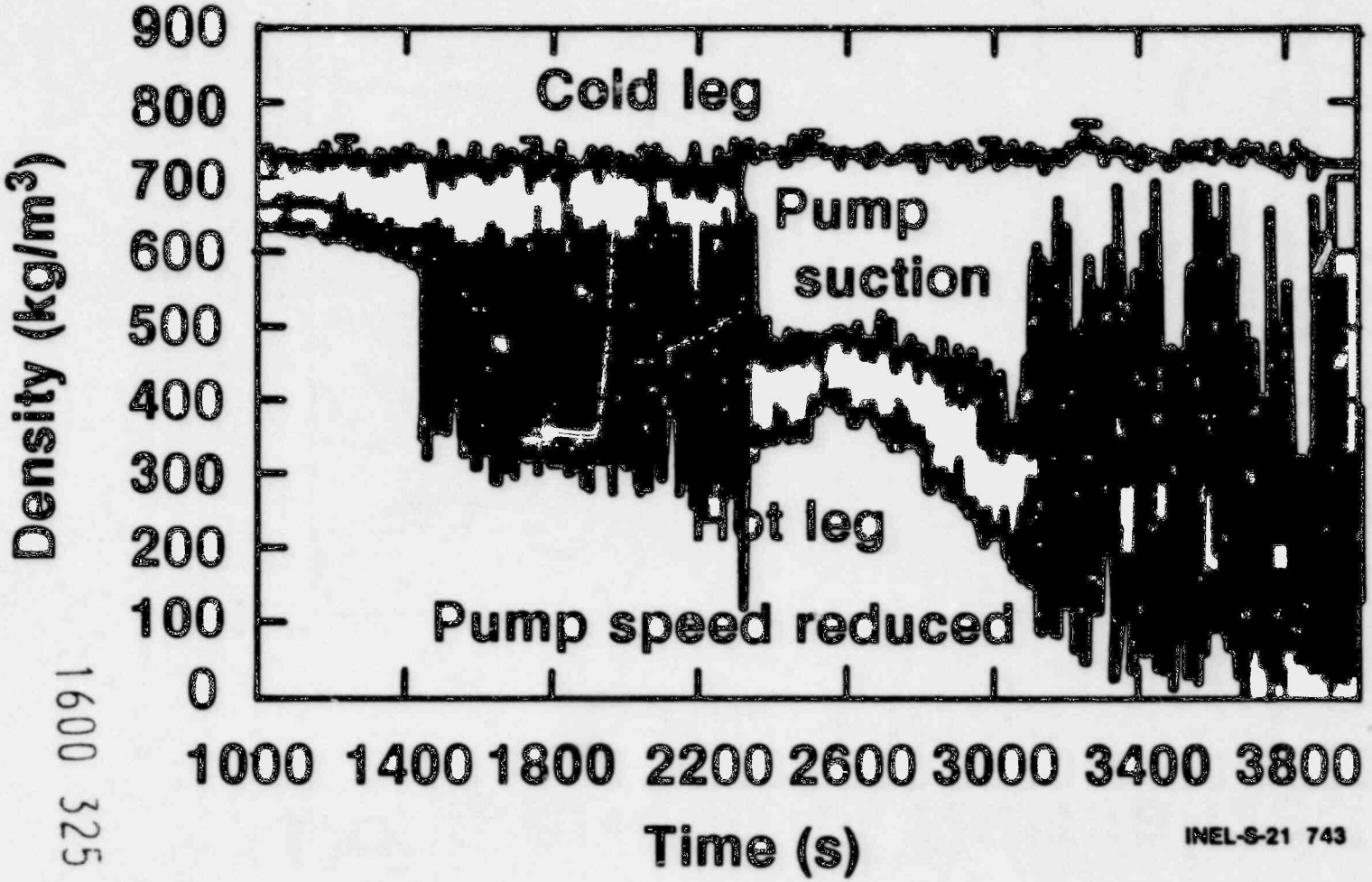

Summary of System Hydraulics

- Response is influenced by steam generator heat transfer, pressurizer venting characteristics, and core power
- Semiscale and TMI pressurizer level showed similar trends
- Semiscale POV flow was predicted reasonably well
- Semiscale coolant pumps degraded earlier than the TMI pumps
- A significant density distribution existed in the Semiscale loops before pump shutdown

Core Thermal Hydraulics

INEL-S-21 729

Downcomer and Core Collapsed Liquid Levels (Test S-TMI-3I)

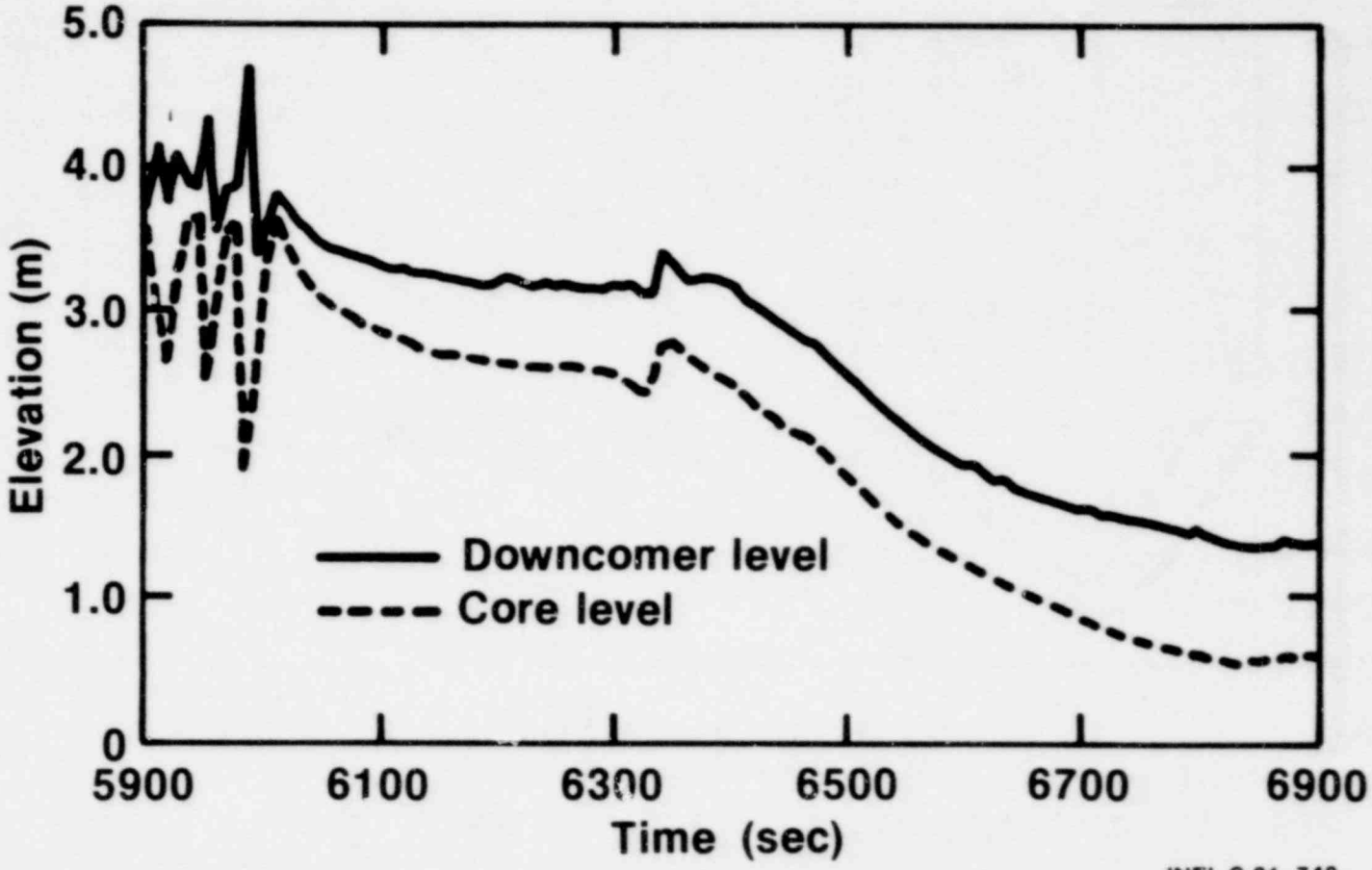

INEL-S-21 748

Incore Fluid Density and Heater Rod Thermocouple Response (Test S-TMI-3i)

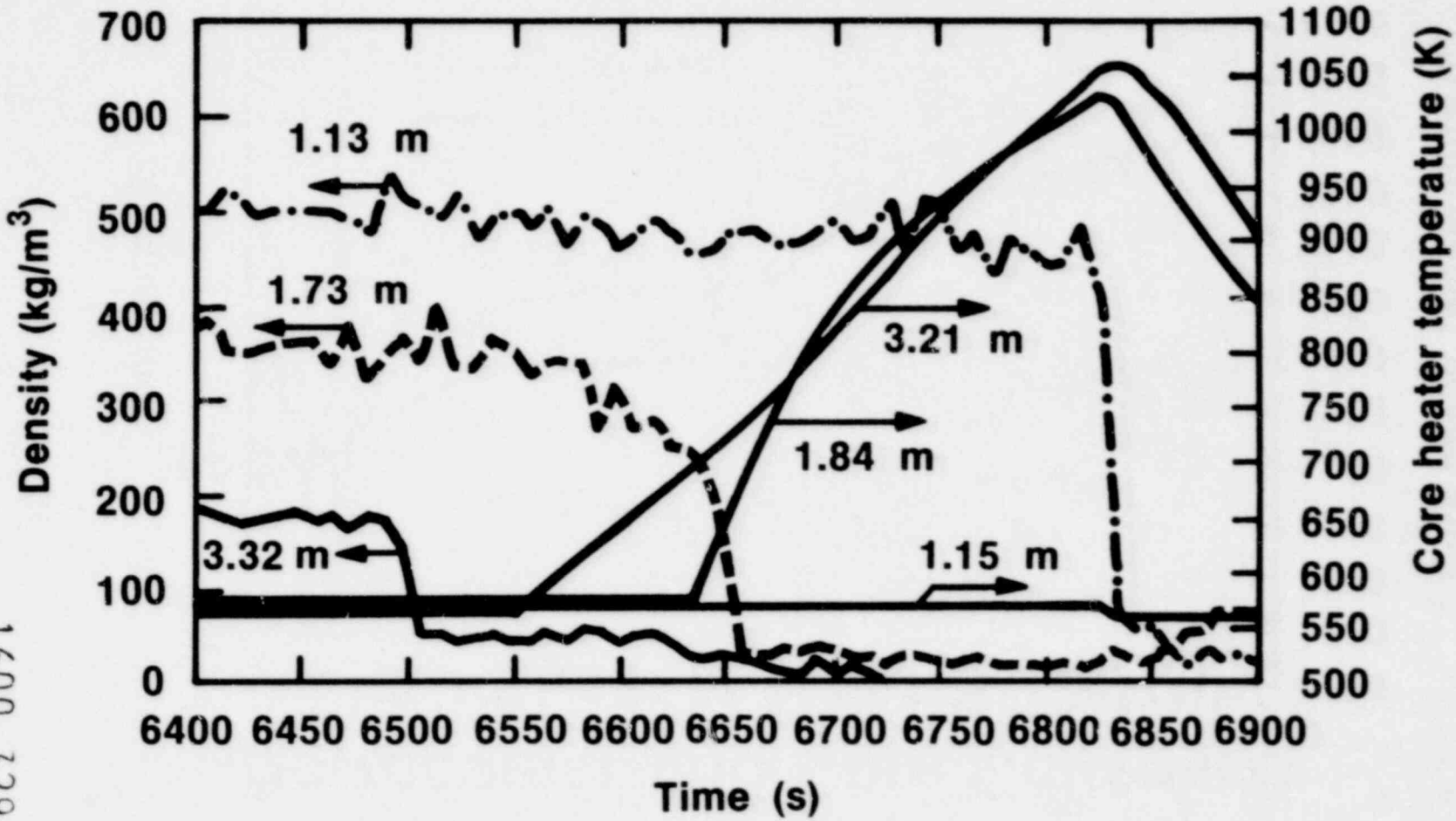

INEL-S-21 746

Pressurizer Level, Core Level and Rod Clad Temperature (Test S-TMI-3I)

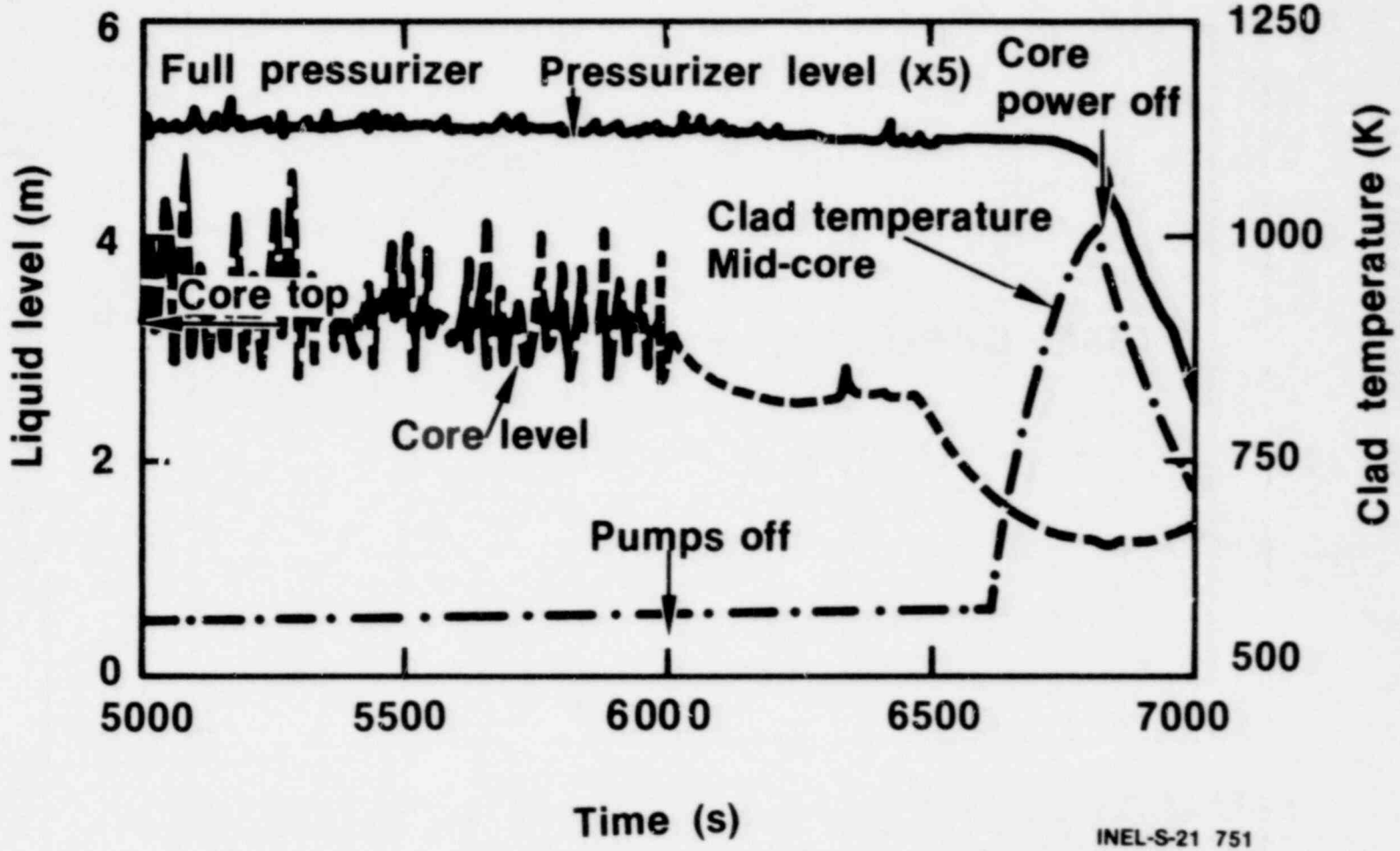

INEL-S-21 751

Core Froth and Collapsed Liquid Levels (Test S-TMI-3I)

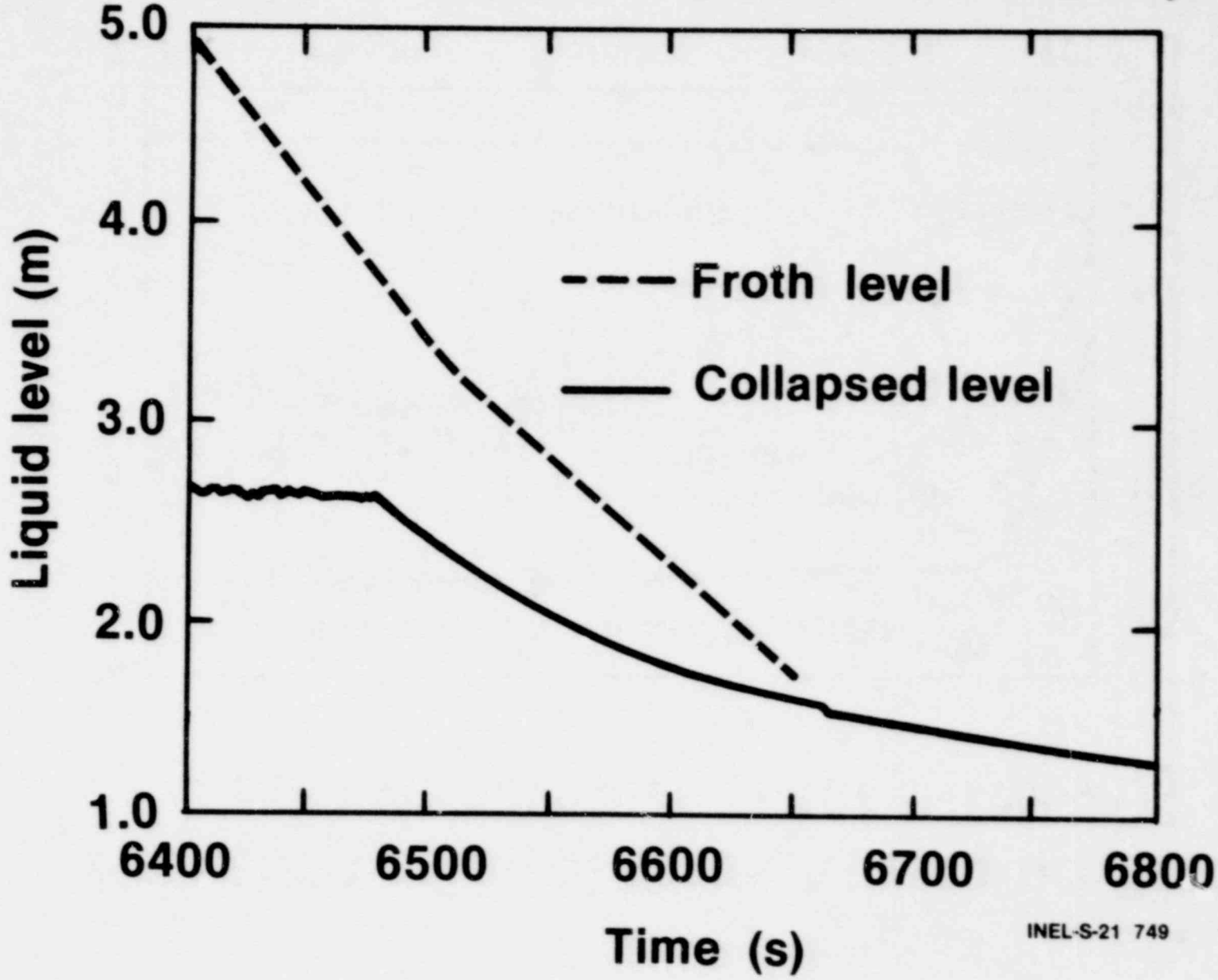

Calculated Heat Transfer Coefficient Versus Liquid Level (Test S-TMI-3C)

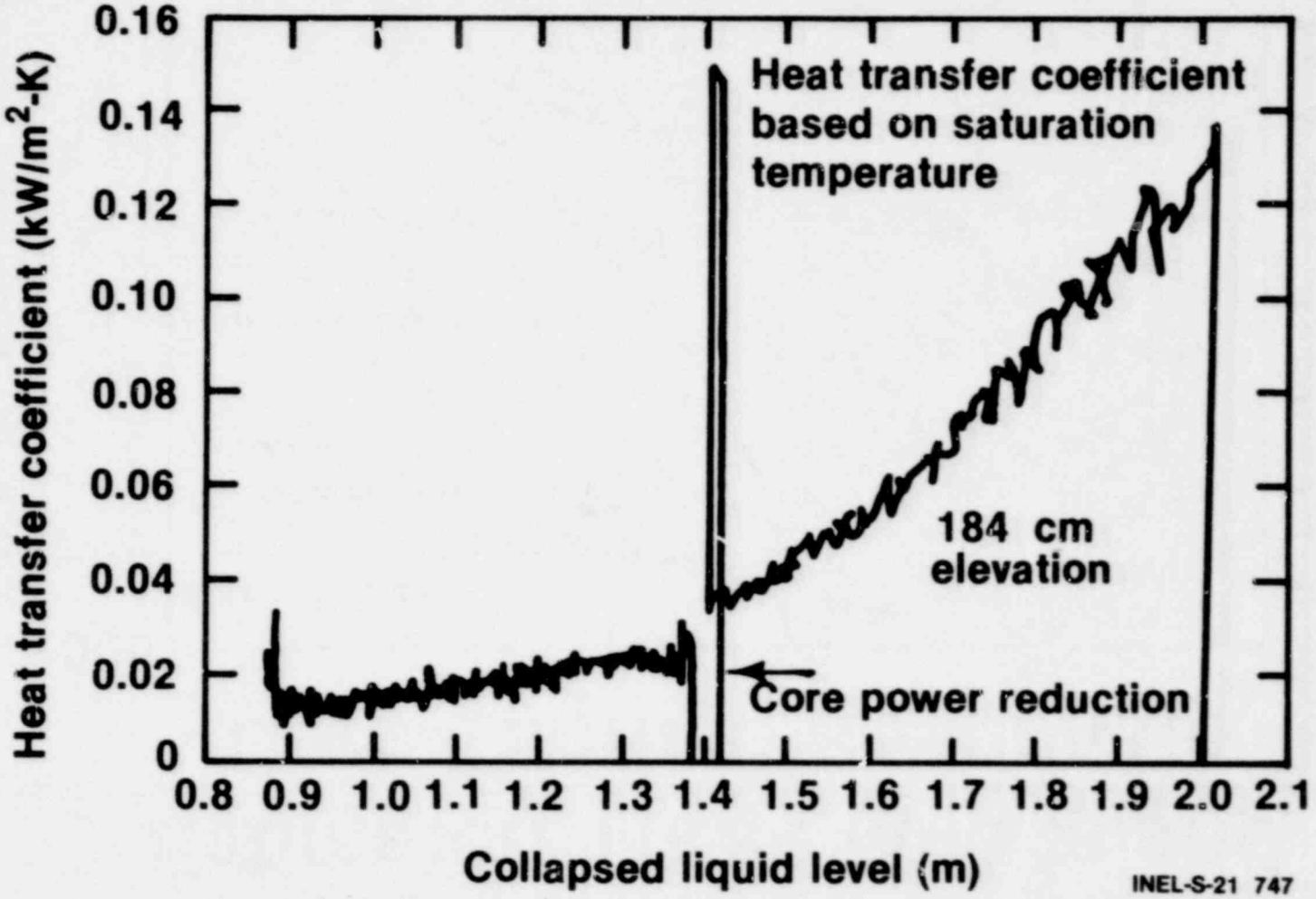

Estimated Three Mile Island Core Thermal Response

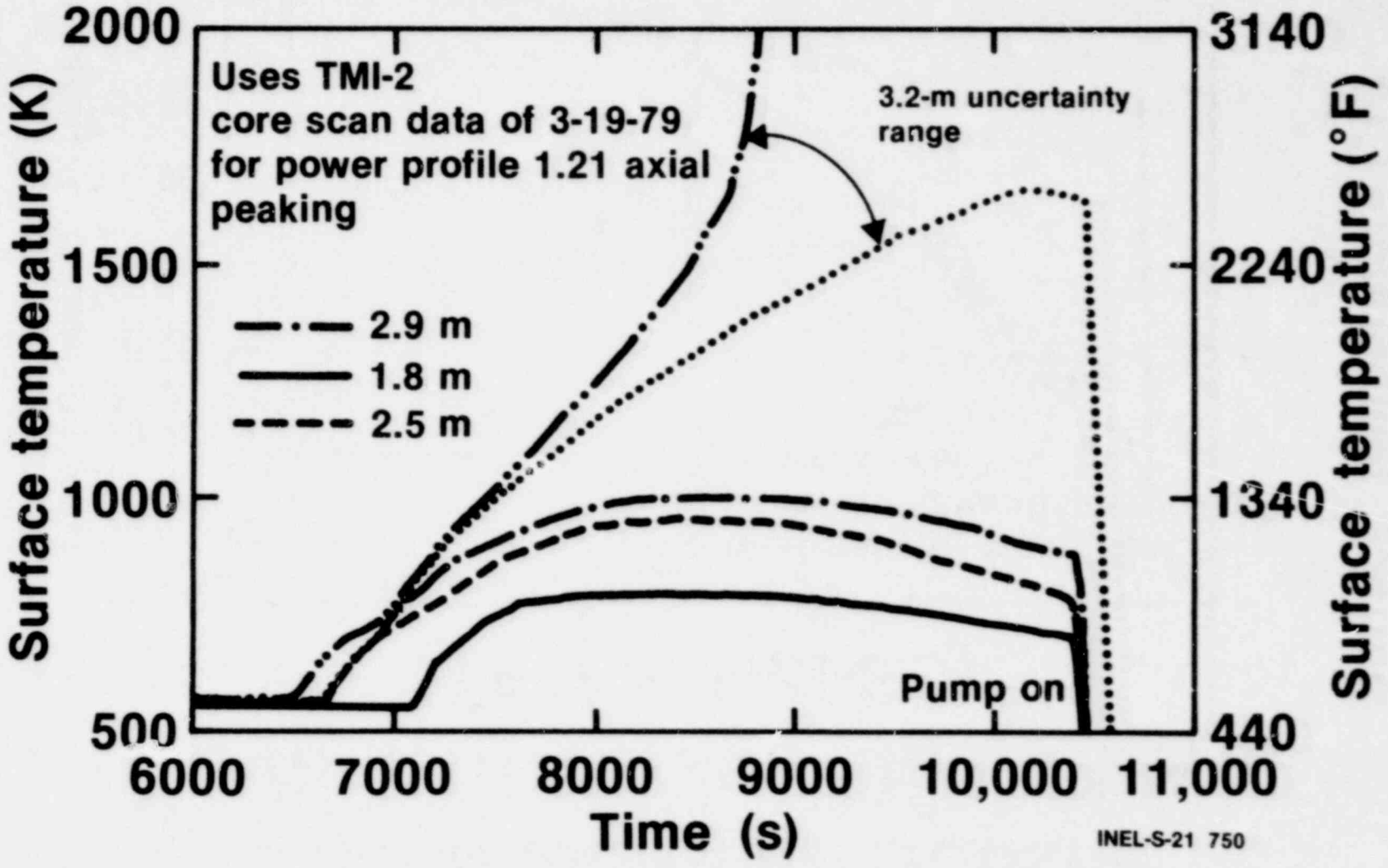

Summary of Core Thermal Hydraulics

- Core froth region provided good cooling in Semiscale prior to loop pump shutdown
- Rod high power zone cladding heatup occurred when the froth level approached the collapsed liquid level
- Hot leg draining maintained core cooling for about 500 seconds after pump shutdown
- Superheated steam was observed in the Semiscale hot legs in the same frame as was observed in the TMI transient
- Semiscale core heat transfer coefficients were correlated to the core collapsed liquid level

INEL-S-21 745

Summary of Core Thermal Hydraulics (cont'd)

- Measured Semiscale heat transfer coefficients, when applied in the TMI core, suggest cladding temperatures in excess of 1500 K above the 2.9 m elevation. Excessive temperatures were not calculated to occur below the 2.9 m elevation.

DEVELOPMENT OF A PULSED NEUTRON GENERATOR FOR TWO-PHASE FLOW MEASUREMENT

Gary E. Rochau
Generator Development Division 2351
Sandia Laboratories, Albuquerque, New Mexico 87185

Introduction

A high-output, unclassified, transportable neutron generator has been under development at Sandia Laboratories for use with pulsed neutron activation (PNA) techniques since April 1977. The PNA neutron generator has the capability of generating outputs in excess of 10^{10} neutrons in a pulse of 1.2 milliseconds duration.

The neutron generator is designed for maximum flexibility and can be modified and repaired. The modular construction allows the physical configuration of the generator to be changed to accommodate the particular environment in which it is to be used.

The generator has demonstrated an average output of 1.2×10^{10} neutrons/pulse for 1010 pulses. It has also demonstrated a pulse repetition rate of up to 13.3 pulses/minute. The generator power supply has been operated for more than 12,000 operations without failure.

Apparatus

The pulsed neutron activation (PNA) neutron generator, currently in development, is being designed to meet the requirements listed in Table I. The objective of the design is to develop a transportable, unclassified neutron generator which would generate 10^{10} neutrons/pulse. A more complete description of the development is given in References 1, 2, and 3.

The generator is designed to be easily repaired and modified. The generator is self-sufficient such that no additional equipment is required to operate it and determine its output. The generator is expected to have a minimum operational life of 1000 pulses for pulse repetition rates less than 1 pulse per minute. When the end of operational life is reached, the neutron tube will require minor servicing before it can be used again.

The PNA neutron generator will be segmented into the three major components shown in Figure 1. Each major component contains the individual components, listed in Table II, which are required to operate the unit. These components, interconnected by long cables, will allow the experimenter to conveniently place them in the available space of the experimental area. This design allows

components to be tailored to meet the specific requirements of the experiment without redesign of the unit. A general electrical schematic of the PNA neutron generator is shown in Figure 2. A conceptual design of the PNA generator is shown in Figure 3.

The PNA neutron generator utilizes the millisecond pulse (MSP) neutron tube (Figure 4) which was specifically developed for this application. This unclassified neutron tube utilizes a focused deuterium ion beam produced by a specially modified occluded gas ion source (Reference 3). The deuterium beam impinges a 100% tritium-loaded scandium target to produce an isotropic distribution of neutrons with an energy of approximately 14 million electron volts.

Eighty-three variations of the MSP neutron tube have been constructed to study the operational characteristics of the tube. The final tube design (Figure 5) has demonstrated the capability of producing an average output of 1.2×10^{10} neutrons/1.2 ms pulse for 1010 pulses and a neutron production efficiency of 4.3×10^{7} neutrons/A-us at an accelerating voltage of 116 kV. The tube is completely demountable to allow for servicing and requires a small vacuum appendage pump for operation.

The MSP neutron tube is housed in the tube-transformer assembly (TTA) which is placed at the position where the source of neutrons is desired. The TTA, shown in Figure 6, contains the high-voltage transformer, the MSP neutron tube, and the neutron monitor. The TTA design represents a package for these components.

The TTA is enclosed in a stainless steel cylinder 12.75 inches in diameter and 26 inches long. The cylinder is pressurized to 50 psi with sulfur hexafluoride, a dielectric gas, to provide high-voltage insulation. All electric connections are made at the rear of the cylinder, and the neutrons are provided to the experiment at the front. The TTA has been designed so that it can be completely disassembled for repair or replacement of components in the field.

The high-voltage pulse transformer contained in the TTA provides the accelerating voltage required for operation of the MSP neutron tube. This 18 kg transformer, Figure 7, has a turns ratio of 1:64 and converts the 165-joule pulse from the pulse-forming network (PFN) to a pulse capable of delivering 300 mA at 160 kV.

The TTA also contains a neutron detector to monitor the output of the MSP neutron tube. The detector, Figure 8, consists of a silicon photodetector. Neutrons are detected when they interact with the paraffin radiator which is placed on the front surface of the detector. Protons created by the H(n,p)n reaction deposit their energy in the photodetector. The signal from the photodetector is integrated to give an output proportional to the actual neutron output of the generator. The detector is inefficient for detecting neutrons and requires very large neutron fluxes to obtain an appreciable signal. This inefficiency is advantageous for this application since the detector can be placed very close to the neutron tube and is insensitive to the experimental geometry and to scattered neutrons from outside the TTA.

The TTA is driven by two PFNs. One PFN, Figure 9, drives the high-voltage pulse transformer. The second PFN, Figure 10, supplies a 160-joule pulse to drive the occluded gas ion source at 80 A of arc current. This second PFN supplies all the power required to operate the ion source and determines the length of the neutron pulse

The PFNs are switched with silicon-controlled rectifier (SCR) switch circuits. These circuits, Figure 11, were developed specifically for this application. These battery-powered circuits are reliable and noise-free compared to gas-filled switch tubes. The switches are capable of switching up to 300 A for pulse durations of up to 1.6 ms. This switch design has been used for over 12,000 operations without failure.

The PFNs are charged with 6 kV, 20 mA dc power supplies which are isolated from the PFNs by safety interlocks. The PFNs are allowed to be charged only when a valid "arm" signal is issued by the experimenter. The unit must then be operated within a specific period of time or the PFNs will be discharged and the unit returns to the "safe" mode. After a "fire" signal has been received, the unit will not recharge the PFNs until another "arm" signal is received.

Test Results

One development tube has been life-tested for 1010 operations, and an average output of 1.2×10^{10} neutrons/pulse with a standard deviation of 10.9% was observed. The results of the life test are summarized in Figure 12. The points plotted represent the average of 100 operations plotted at the median operation number. The solid line represents the average output for all operations, and the dotted lines represent the average output plus or minus 1, 2, or 3 times the standard deviation. There appears to be no apparent change in output after 1010 operations. A typical neutron pulse is shown in Figure 13. The amplitude of the pulse is expressed in units of neutrons per microsecond.

Also tested during this test were all components required to operate the tube. No failures occurred, and the components are still in use for tube testing.

Tests have also been performed at high repetition rates. Figure 15 shows the results of testing a tube at a repetition rate of 4.5 seconds.

Program Schedule

The program schedule is shown in Figure 16. The program calls for the delivery of up to 5 neutron generators by June 1980. Figure 17 shows the fabrication schedule to meet this requirement. Evaluation of the MSP neutron tube has been completed, and an evaluation TTA has been constructed. A prototype power supply has been tested, and an evaluation power supply is under construction.

References

1. R. C. Dougherty, G. E. Rochau, R. W. Bickes, Jr., R. J. Walko, and R. S. Berg, "Neutron Generator For Two-Phase Flow Calibration: Annual Progress Report," NUREG/CR-0480, SAND78-2030, November 1978.

2. G. E. Rochau, "Development of a Pulsed Neutron Generator For Two-Phase Flow Measurement," Review Group Meeting on Two-Phase Flow Instrumentation, July 24-27, 1979.

3. K. W. Ehlers, et al., "Development of an Occluded Gas Ion Source," Rev. Sci. Inst. 29, 7, July 1958.

Table I

PNA NEUTRON GENERATOR

SPECIFICATIONS

Neutron Output:	$>10^{10}$ Neutrons/Pulse
Pulse Duration:	1.2 Milliseconds
Pulse Repetition Rate:	$\leq$12 Pulses/Minute
Lifetime:	$\geq$1000 Pulses (Low Repetition Rate) $\geq$100 Pulses (High Repetition Rate)
Life-Limiting Mechanism:	Neutron Tube
Exclusive Lifetime:	$\geq$10,000 Pulses
Neutron Monitor:	Integral Part of Generator. Sensitive to High Neutron Fluxes, Insensitive to Experimental Geometry.

FEATURES

Repairability:	Completely Demountable
Flexibility:	Easily Modified
Portability:	Two People Required
Safety:	Cannot be Triggered Accidentally
Completeness:	Requires AC Line Power Only
Availability:	Most Parts Commercially Available

Table II

PNA NEUTRON GENERATOR COMPONENTS

POWER SUPPLIES & INTERFACE:

- PFN Charging Power Supplies
- Neutron Monitor Power Supply
- Trigger Conditioning
- Safety Interlocks
- Data Interface

PULSE-FORMING NETWORKS:

- Ion Source Drive
- Accelerating Voltage Drive
- PFN Control Switches
- Pulse Phasing

TUBE-TRANSFORMER ASSEMBLY:

- Neutron Tube
- Accelerating Voltage Transformer
- Neutron Monitor

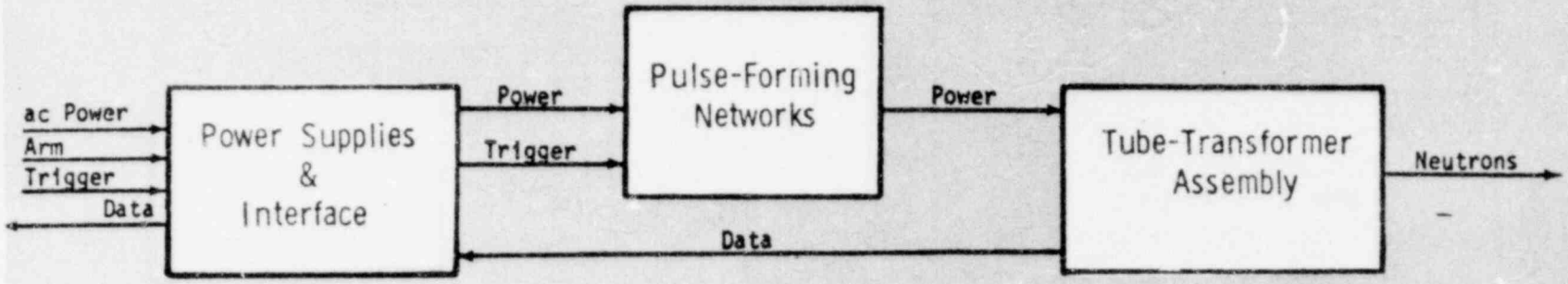

PNA NEUTRON GENERATOR
MAJOR COMPONENT ASSEMBLY

Figure 1

Figure 2

PNA NEUTRON GENERATOR
ELECTRICAL SCHEMATIC

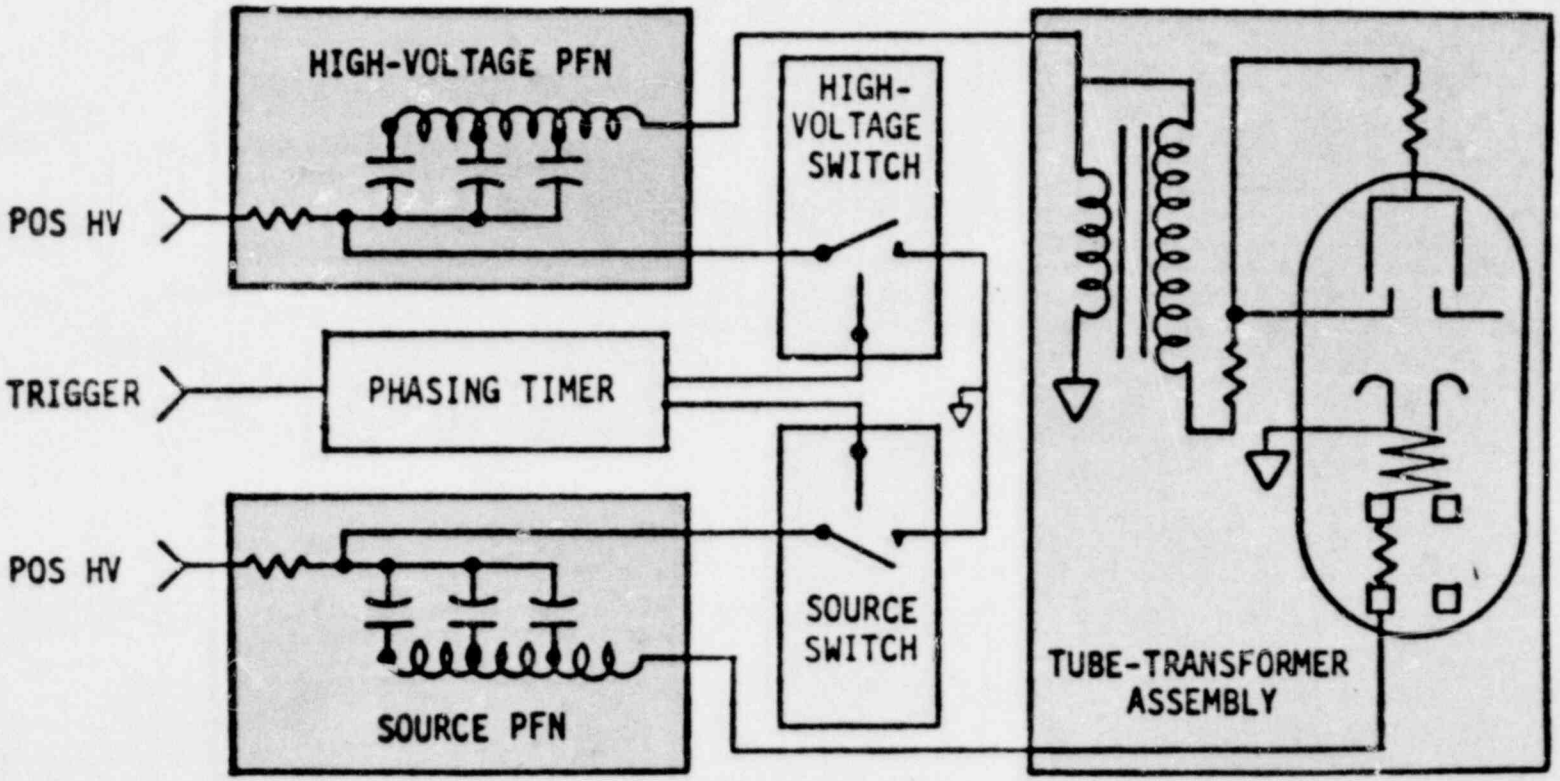

PNA NEUTRON GENERATOR CONCEPTUAL UNIT DESIGN

Figure 3

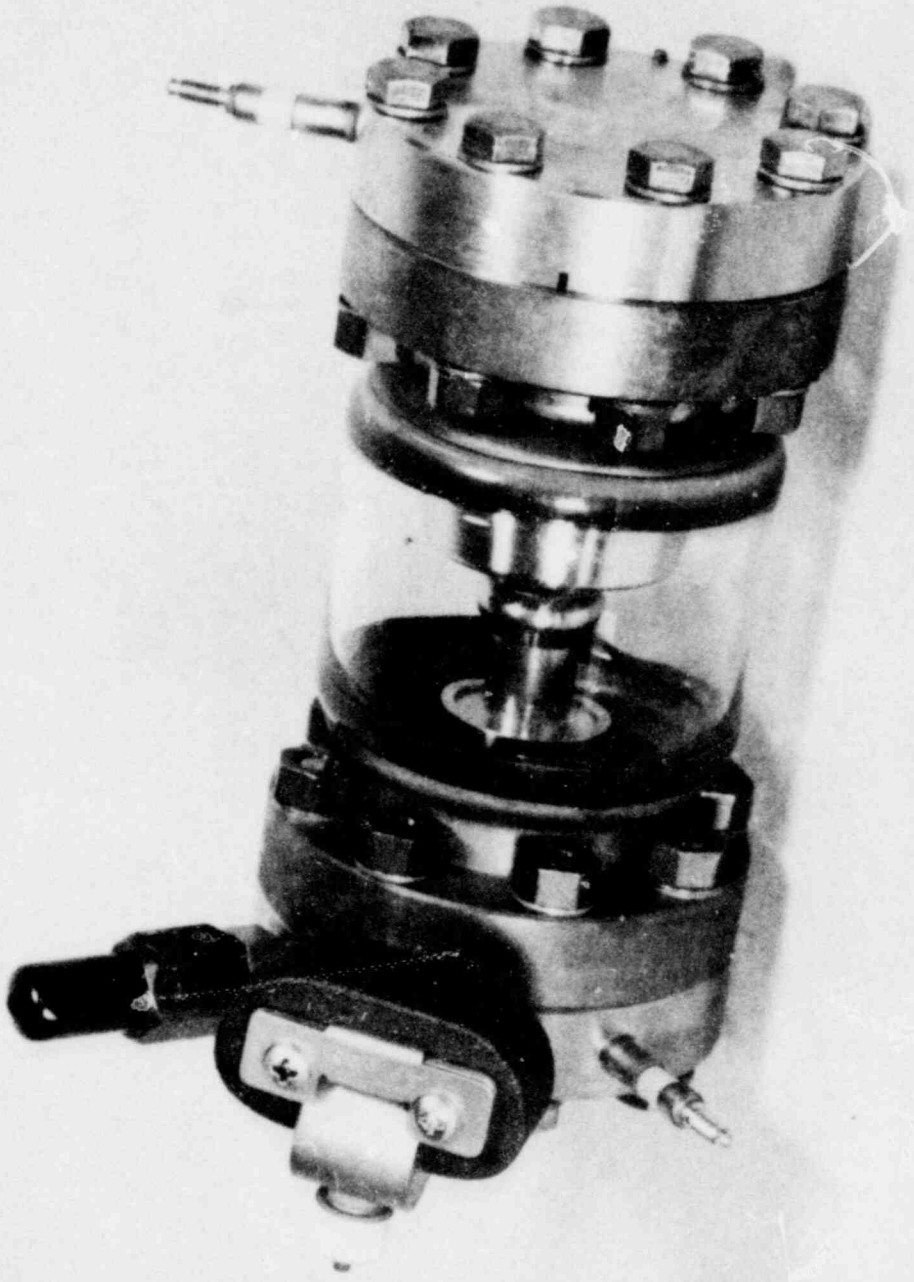

Figure 4

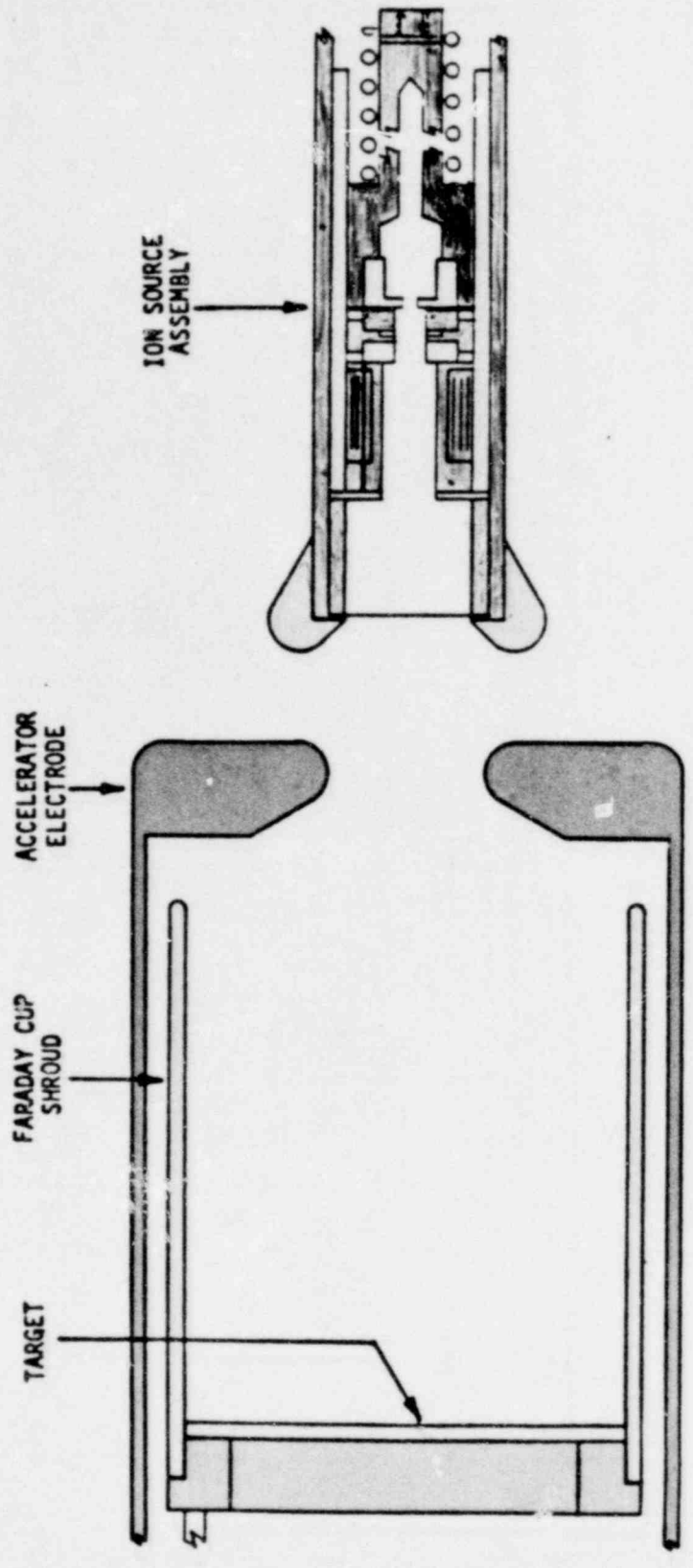

MSP NEUTRON TUBE

Figure 5

Figure 6

PNA NEUTRON GENERATOR
TUBE-TRANSFORMER ASSEMBLY (TTA)

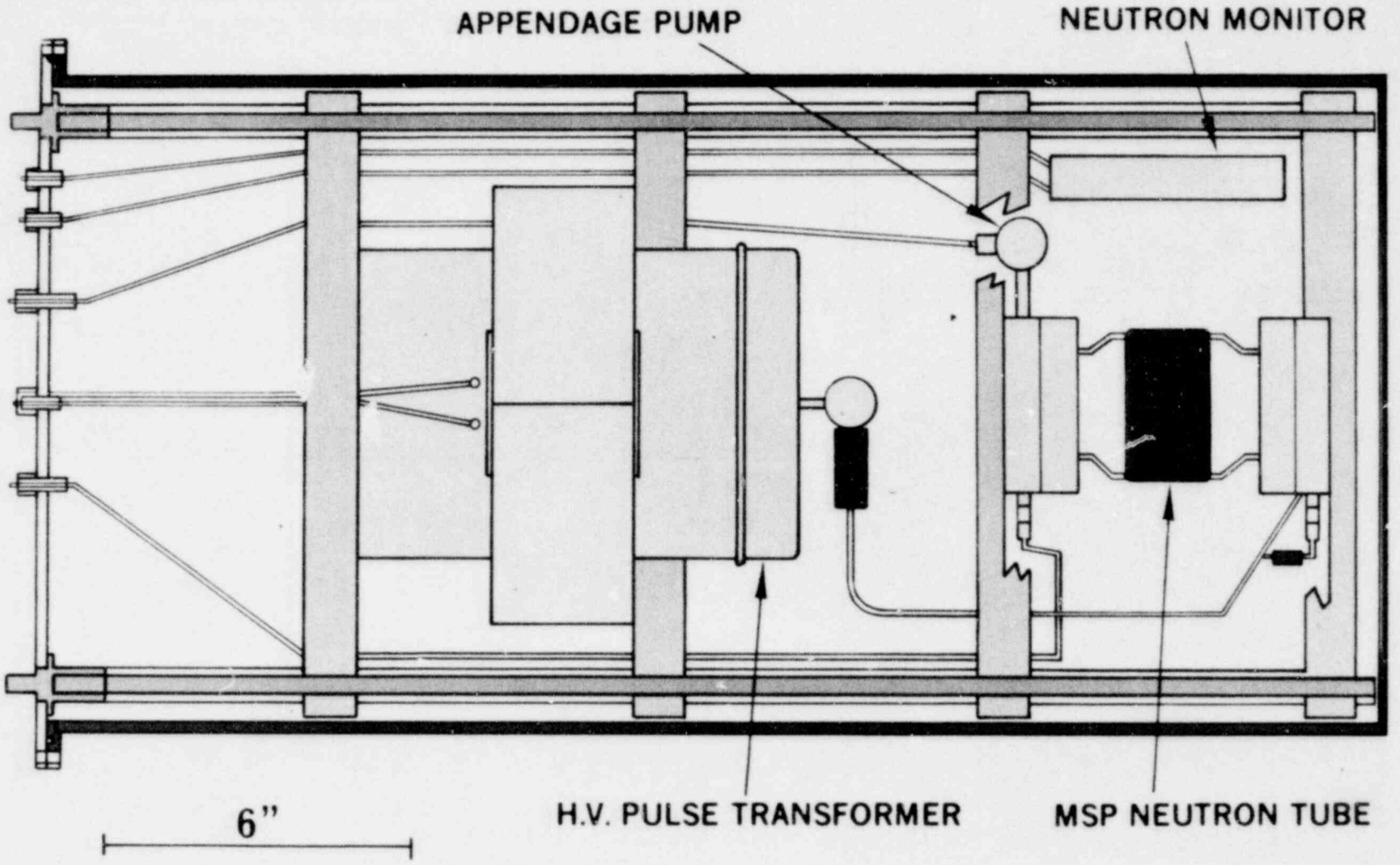

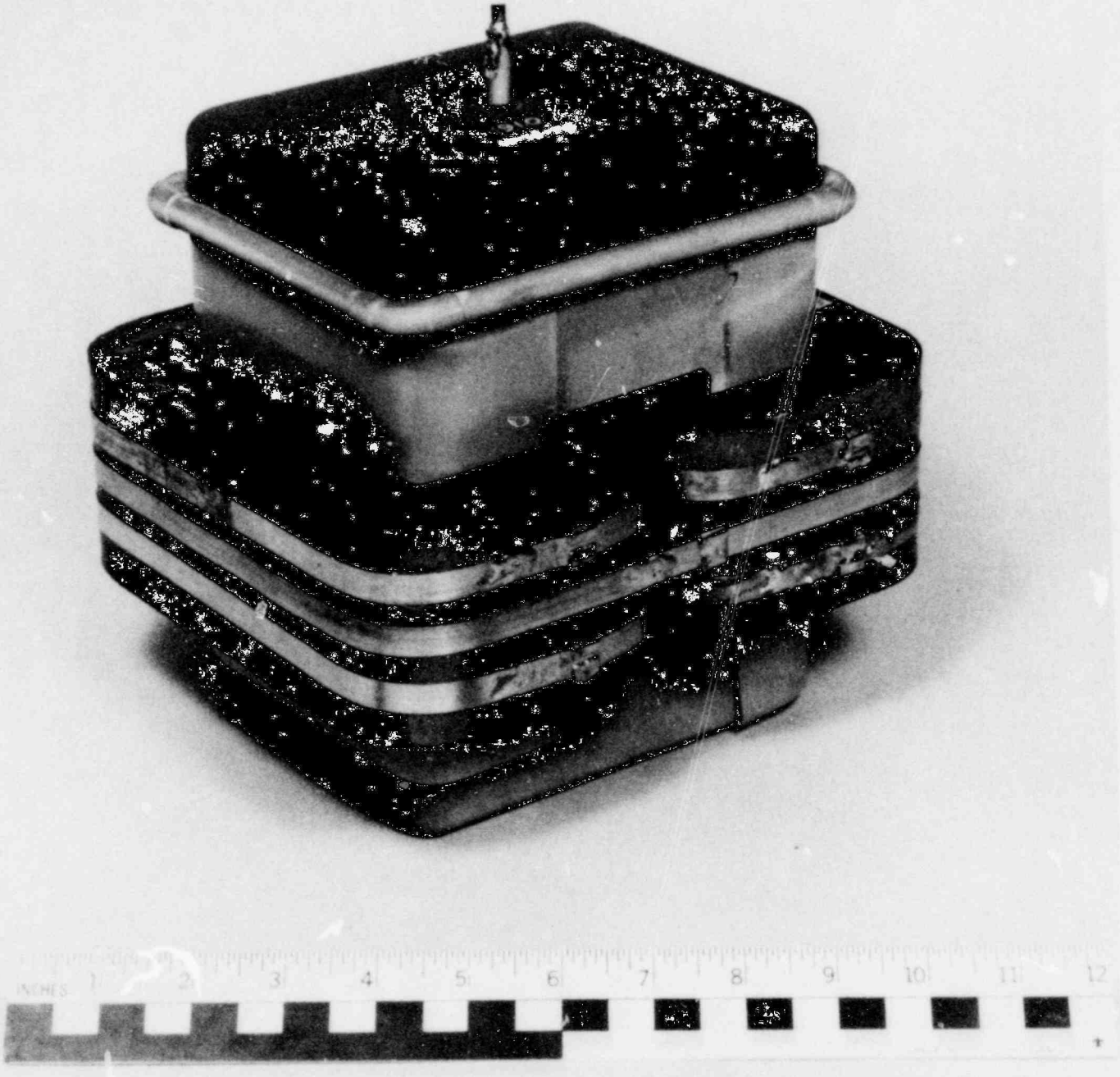

Figure 7

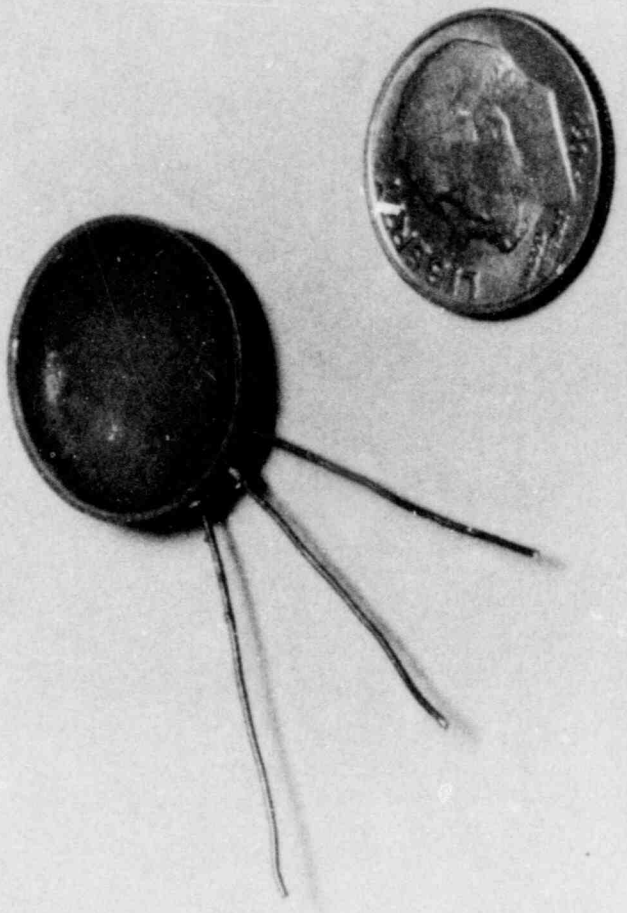

Figure 8

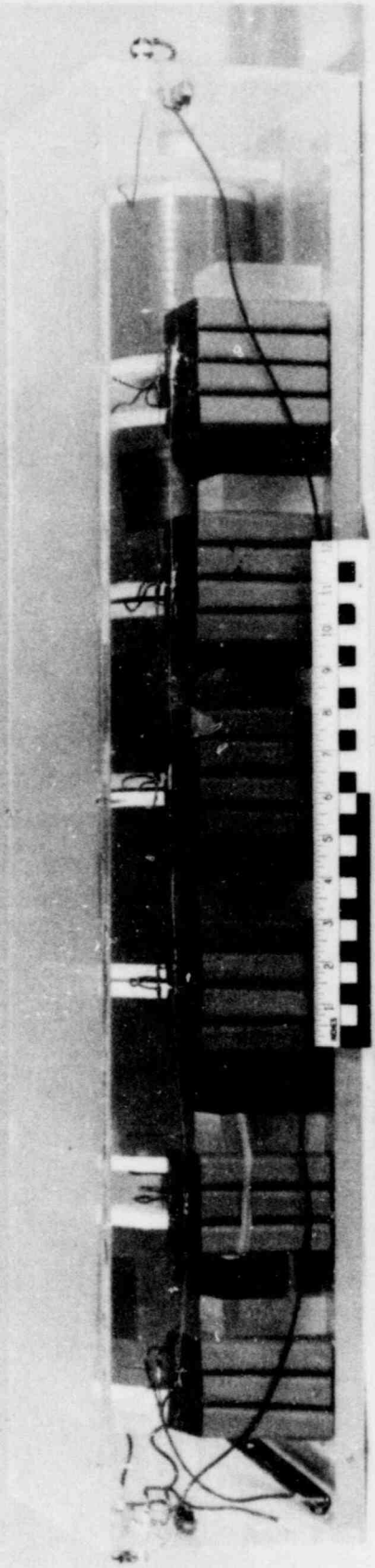

Figure 9

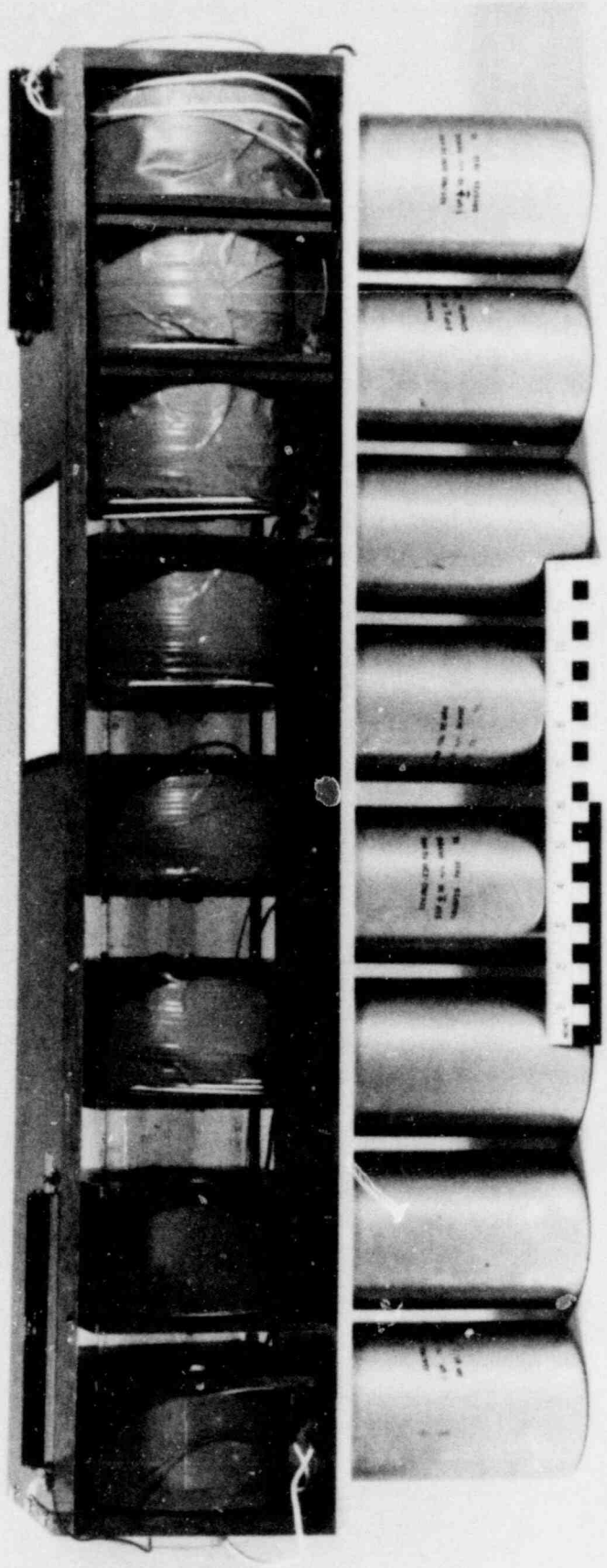

Figure 10

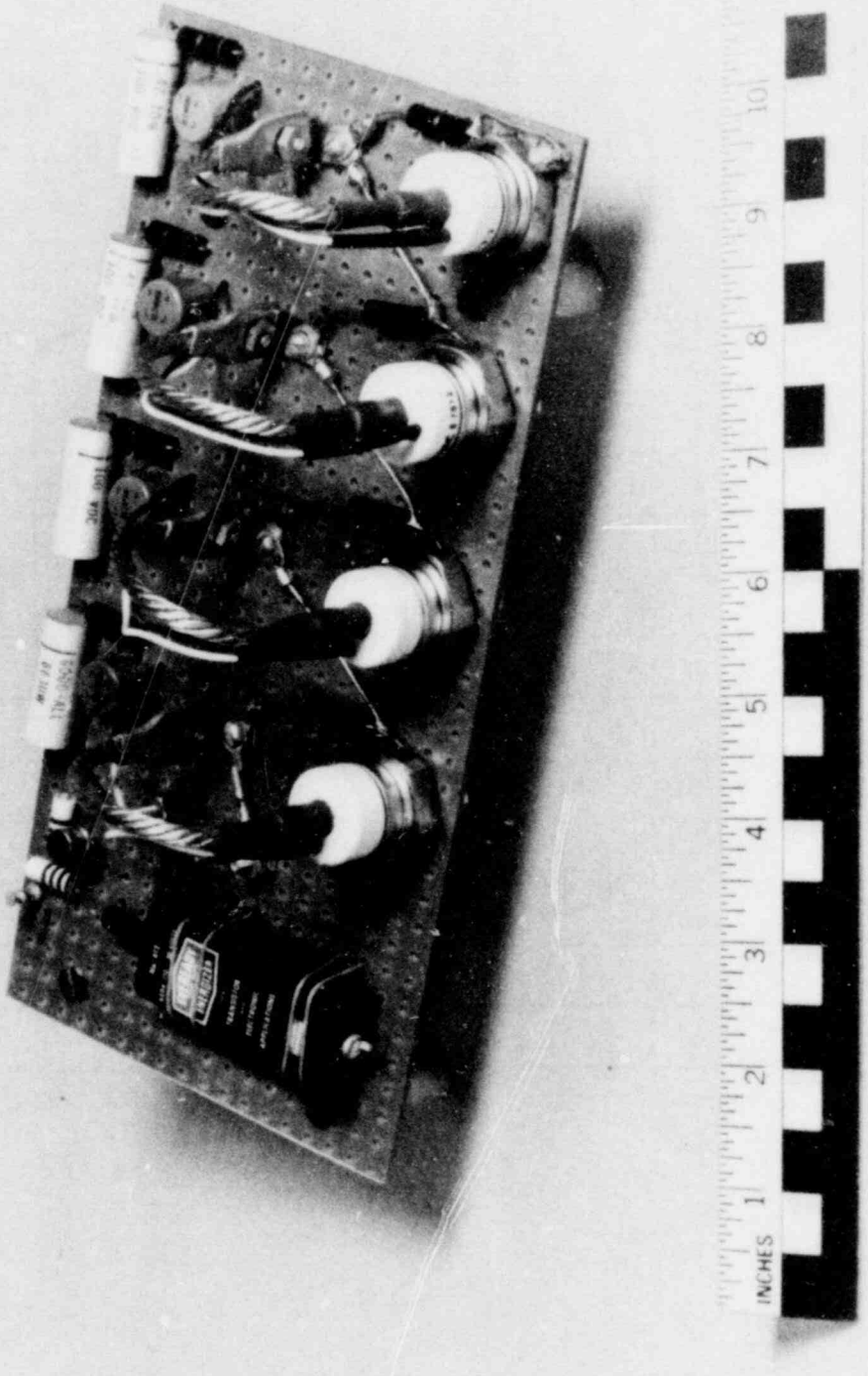

Figure 11

Figure 12

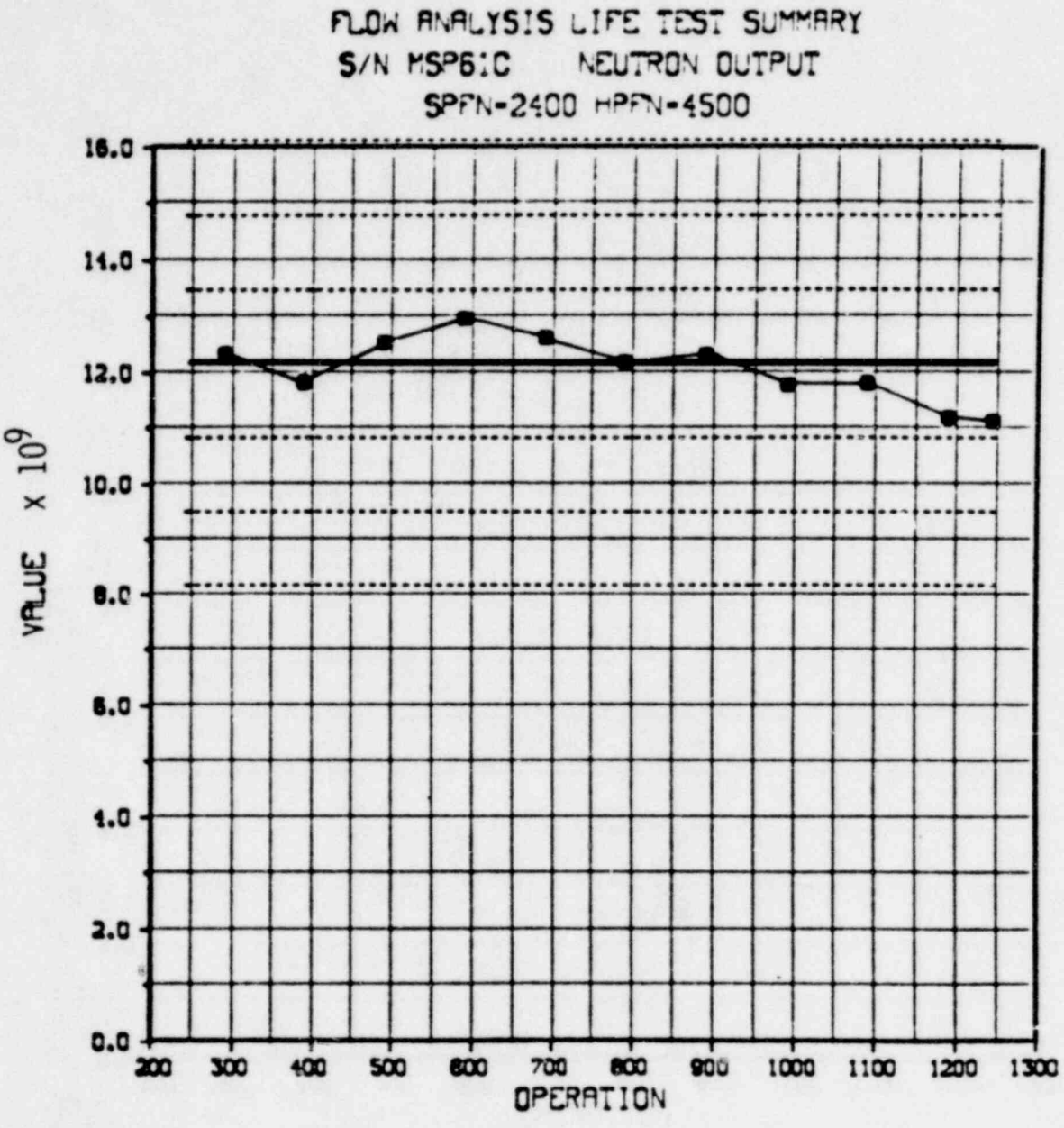

Figure 13

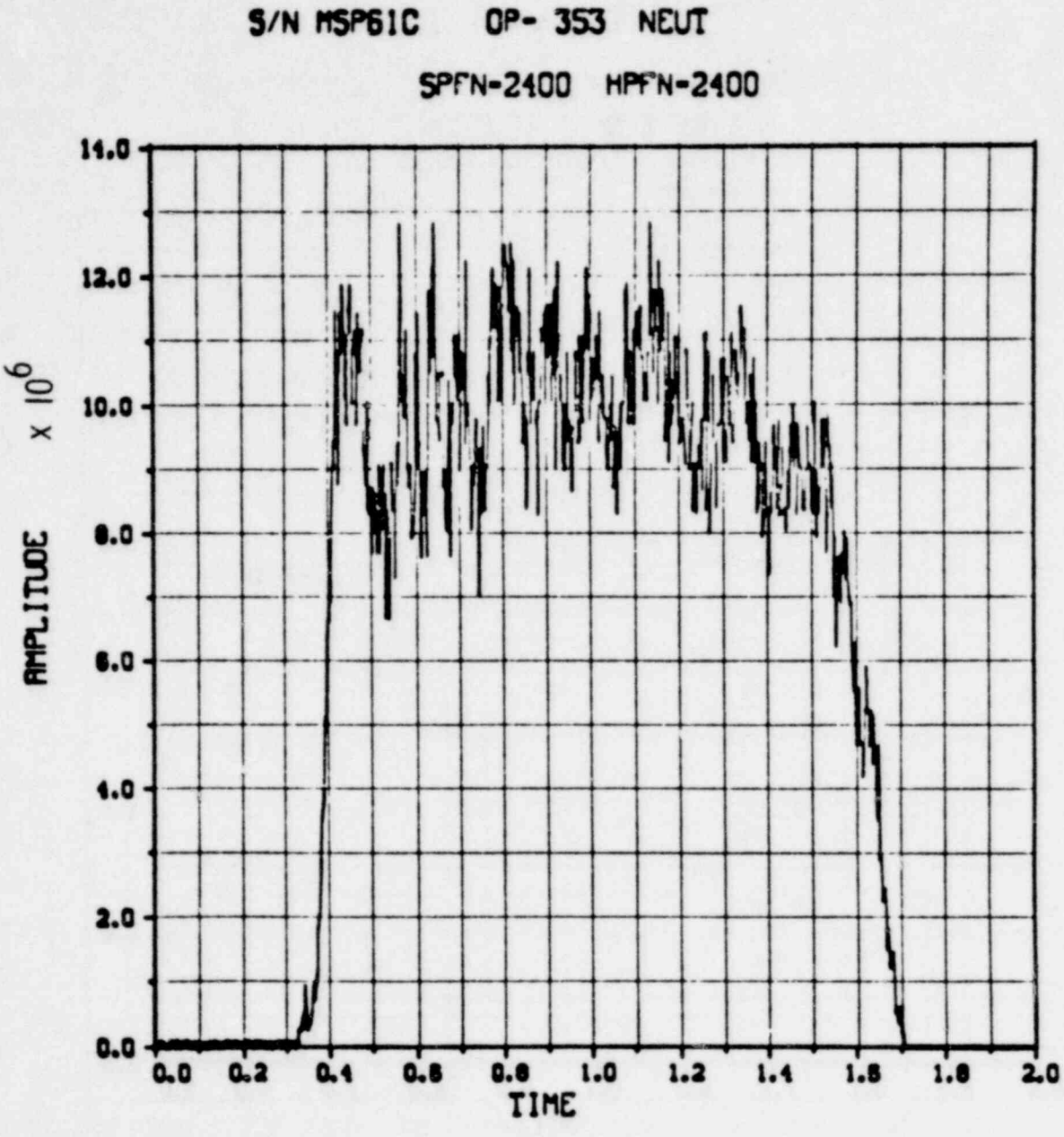

Figure 14

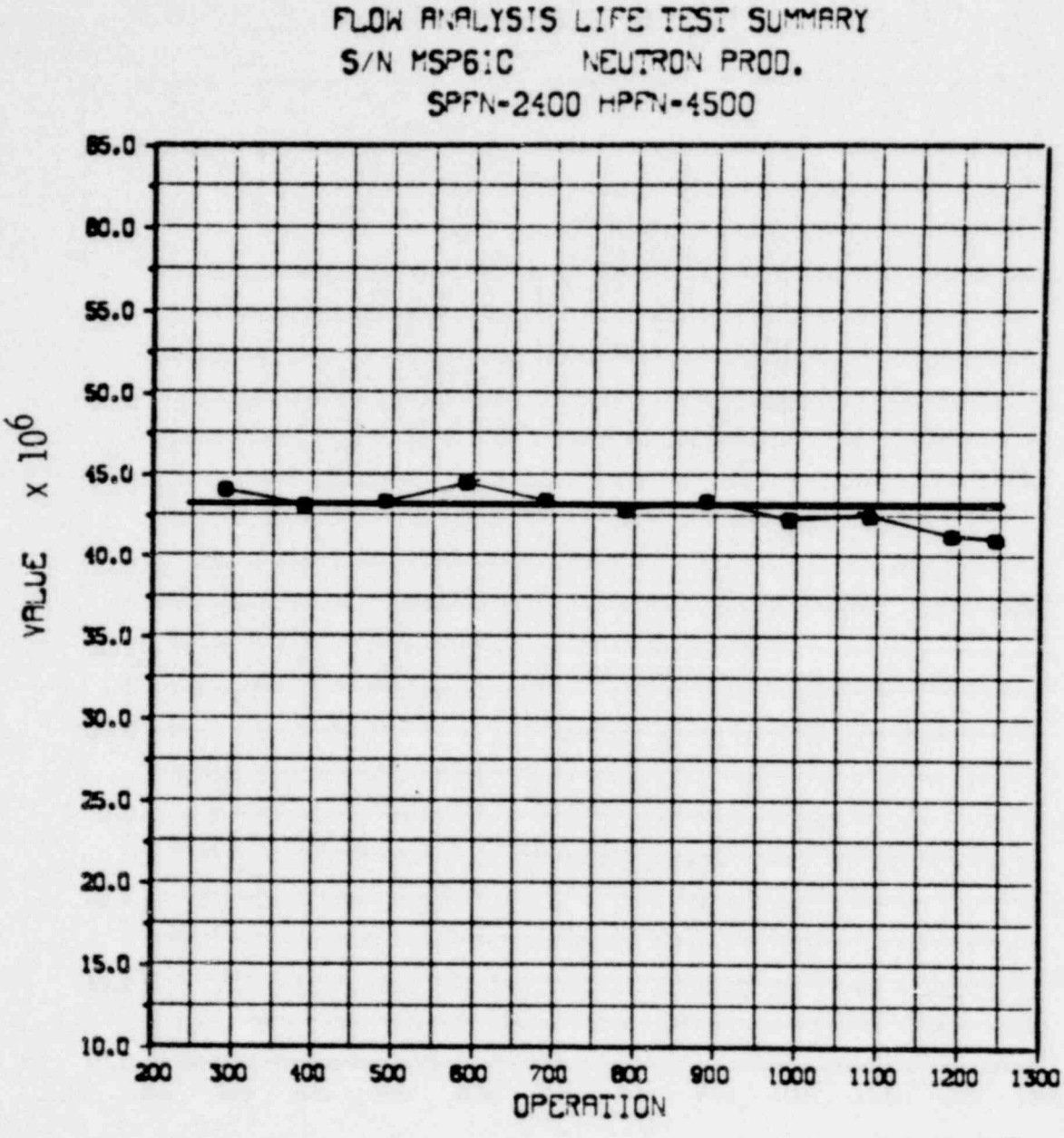

Figure 15

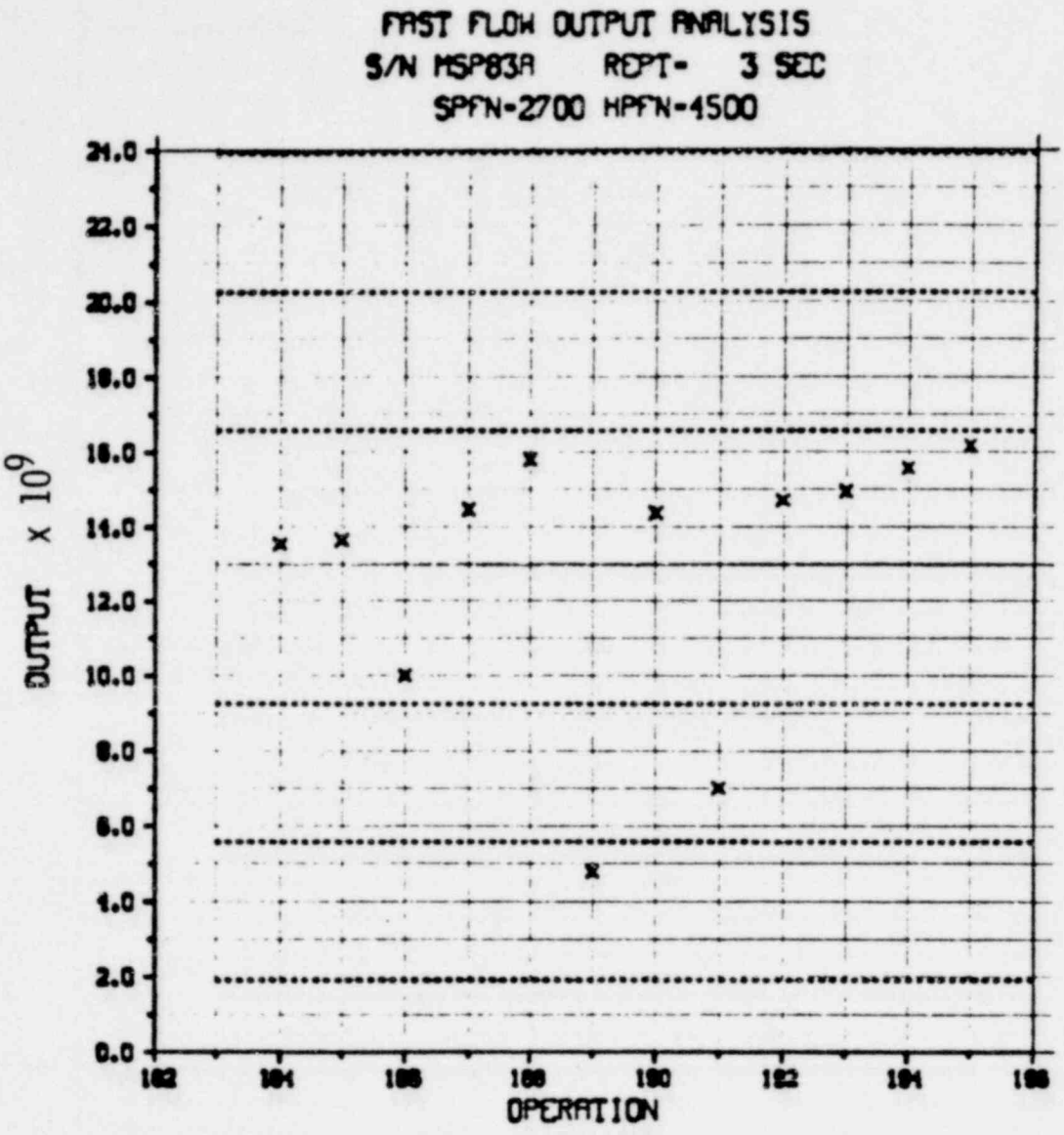

Figure 16

NEUTRON GENERATOR FOR TWO-PHASE FLOW CALIBRATION
PROGRAM SCHEDULE

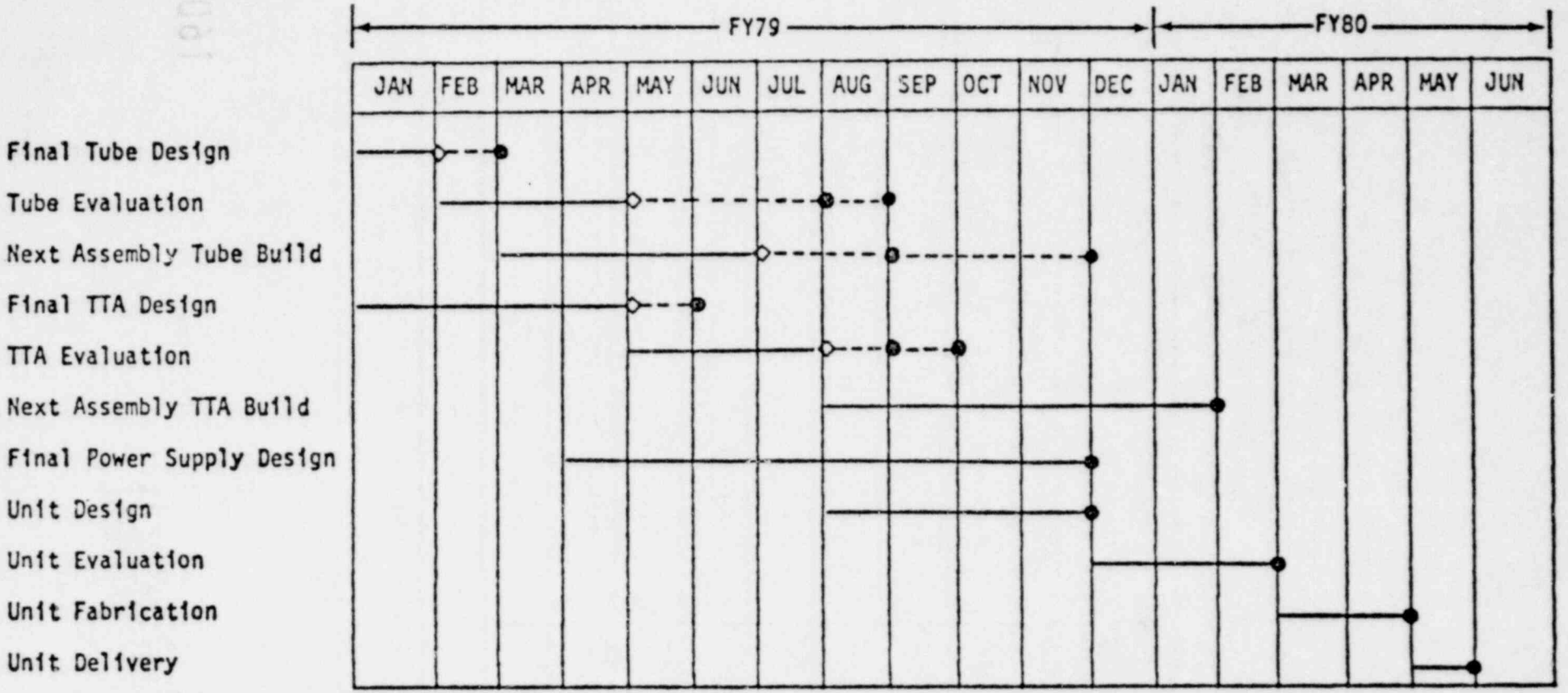

Figure 17

PNA NEUTRON GENERATOR FABRICATION SCHEDULE

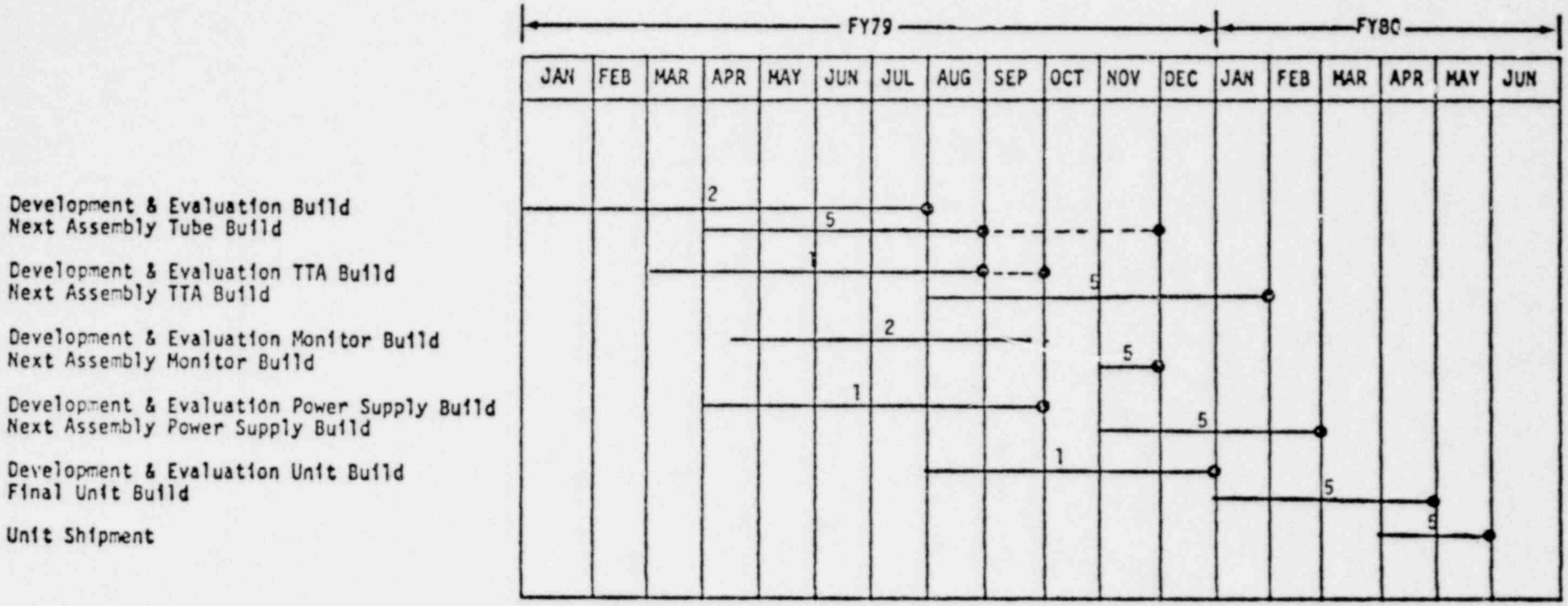

PULSED NEUTRON ACTIVATION

CALIBRATION TECHNIQUE

PAUL KEHLER

COMPONENTS TECHNOLOGY DIVISION

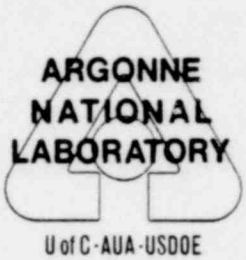

PRESENTATED AT THE

SEVENTH

WATER REACTOR SAFETY RESEARCH

INFORMATION MEETING

NATIONAL BUREAU OF STANDARDS
GAITHERSBURG, MARYLAND

NOVEMBER 5-9, 1979

THIS WORK PERFORMED UNDER THE AUSPICES OF THE USNRC.

Pulsed Neutron Activation Calibration Technique

Paul Kehler

Components Technology Division
Argonne National Laboratory
9700 S. Cass Avenue
Argonne, Illinois 60439

Introduction

Fig. 1 shows a schematic diagram of a Pulsed Neutron Activation (PNA) setup for the measurement of two-phase flow: A pulsed source of fast neutrons (E_n = 14 MeV) is used to activate the oxygen in a steam-water mixture by the O^{16} (n,p) N^{16} reaction, and the activity introduced into the flow is measured downstream of the source by a NaI detector. The measured counts are sorted by a multiscaler into different time channels. A counts vs. time distribution typical for two-phase flow with slip between the two phases is shown in Fig. 1. Proper evaluation of this counts/time distribution leads to flow-regime independent equations for the average of the inverse transit time, $(\overline{1/t})$, and the average density ρ (Fig. 2). After calculation of the average mass flow velocity U_m, the true mass flow is derived as $\dot{\rho} = U_m \rho F$, where F = cross sectional area of the pipe.

Using the PNA technique, the velocity measurement is reduced to measurement of distance and time, and the density measurement is reduced to measurements of ratios of numbers of counts. Measurements of distance and time can be performed absolutely with great accuracy, and the errors normally associated with the measurement of numbers of counts are eliminated by the ratio used for the derivation of density. Sensitivity of the detectors, gain of the electronic equipment and collimation angles of the source and the detectors need not to be known as long as they are kept constant during an experiment. Gain-stability of the electronic equipment is assured by locking it on the Cs^{137} peak. Thus using the PNA technique, two-phase mass flow measurements can be reduced to measurements of distance and time only, a feature that makes very attractive the use of PNA techniques for the calibration of other, more indirect two-phase flow measuring devices.

All parameters effecting the registered number of counts can be summarily described by the "K-value", a calibration constant that is derived by measuring the activity A of water flowing at a known average velocity in a completely filled pipe (ρ = 1 g/cm^3). Although the correct determination of the K-value must be performed according to the equations shown in Fig. 2, it can be approximated by the total number of counts, C_o, measured on a water-filled pipe (ρ_o = 1 g/cm^3) in which the water is flowing at a velocity of U_o = 1 m/sec (See Fig. 3). Experimentally determined K-values for various conditions are tabulated in Fig. 3. The detectors used in these tests were NaI scintillation detectors, with dimensions as shown. The TC-655 neutron source has an output of 3 x 10^9 neutrons/pulse. The K-values listed in Fig. 3 are a valuable aid in planning PNA tests, since K-values for other sources and detectors can be estimated from those listed by proportionating them to the new source strengths and detector areas. Once the K-value of

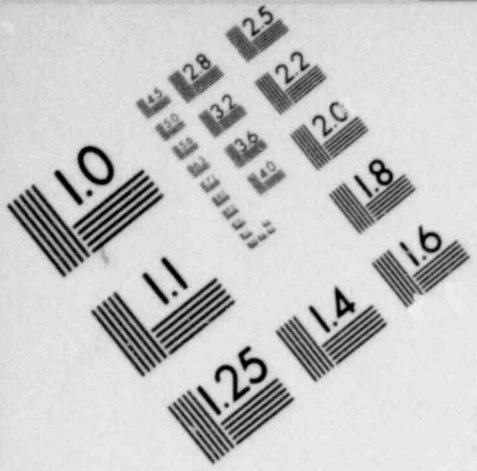

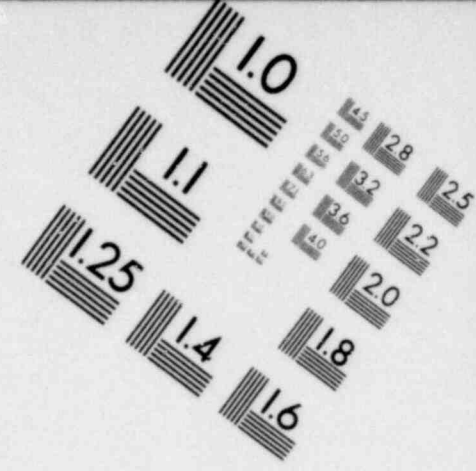

IMAGE EVALUATION TEST TARGET (MT-3)

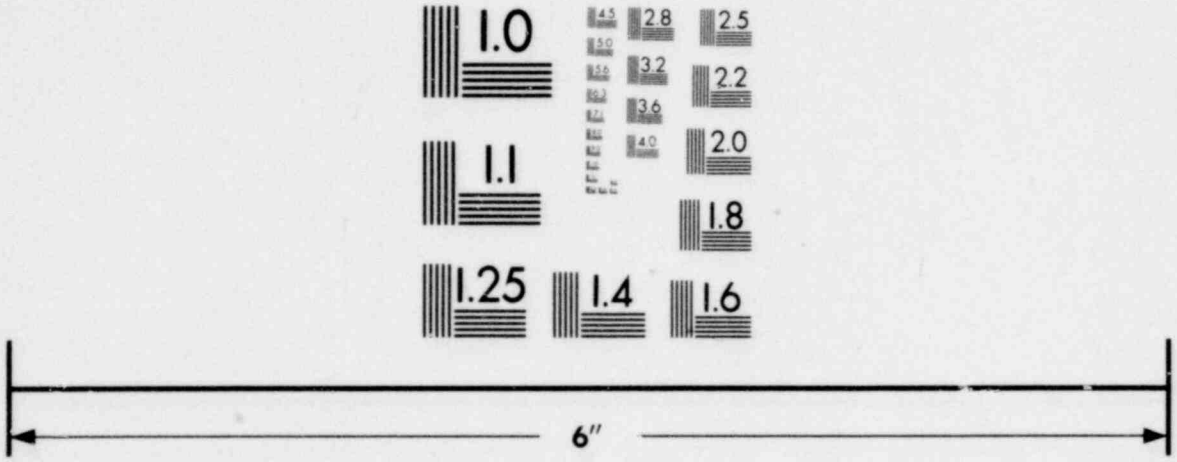

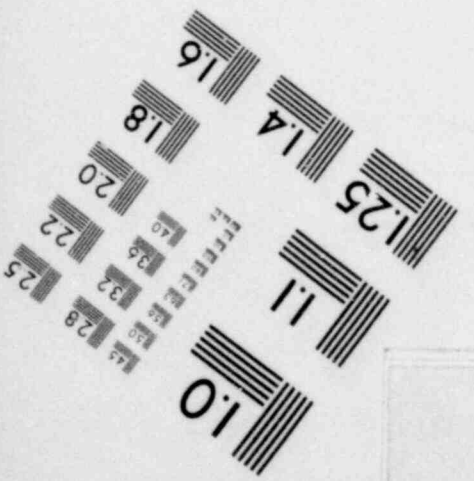

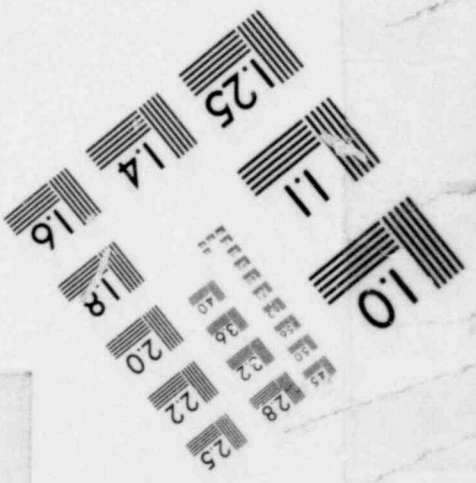

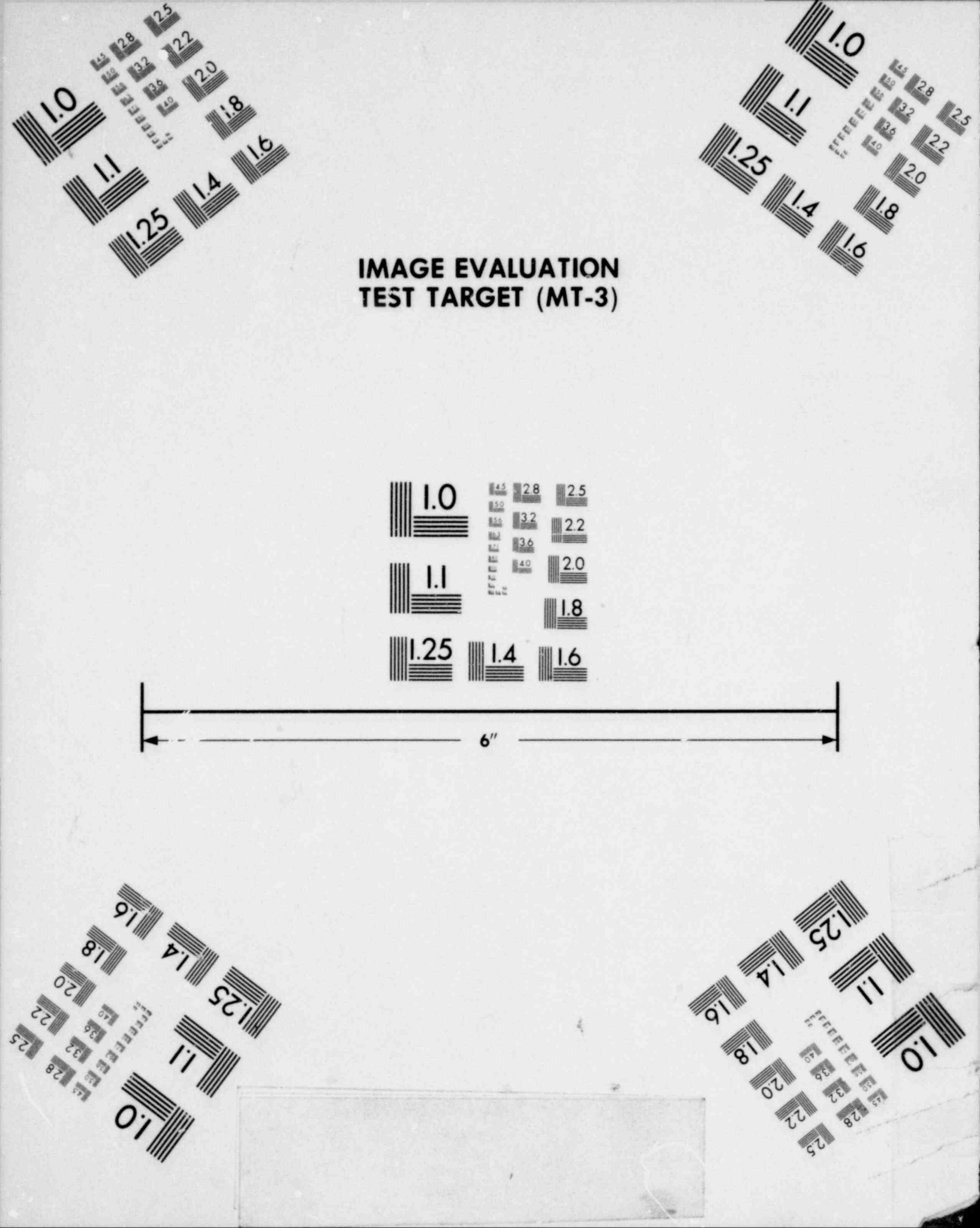
IMAGE EVALUATION
TEST TARGET (MT-3)
1.0
1.1
1.25
1.4
1.6
1.8
2.0
2.2
2.5
2.8
3.2
3.6
4.0
4.5
5.0
5.6
6"

IMAGE EVALUATION
TEST TARGET (MT-3)

6"

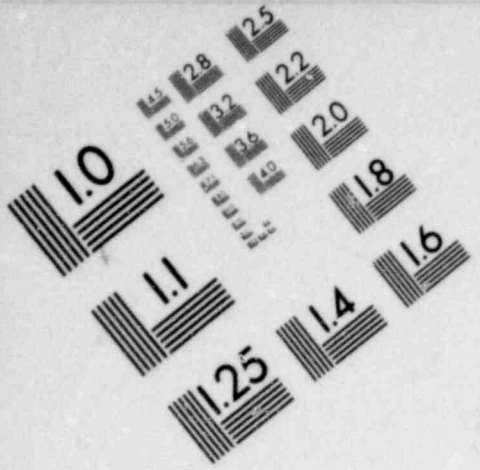

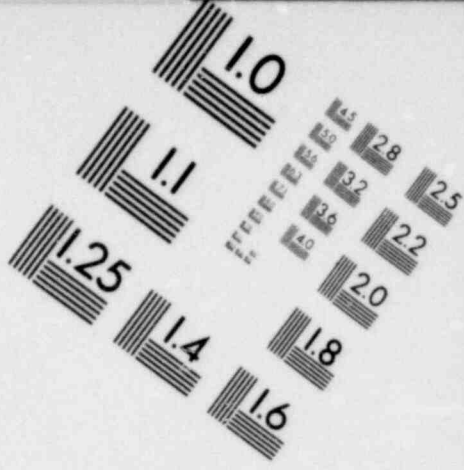

IMAGE EVALUATION TEST TARGET (MT-3)

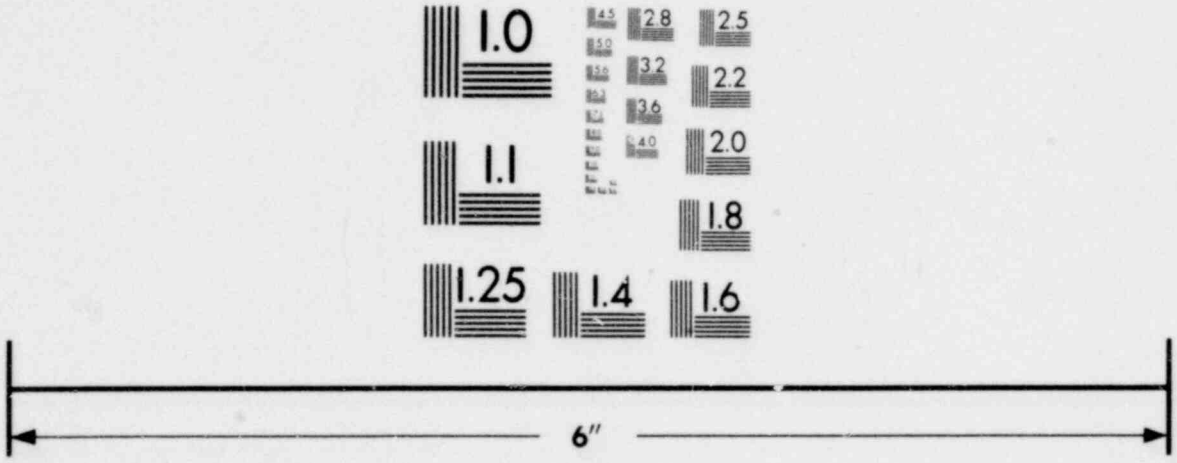

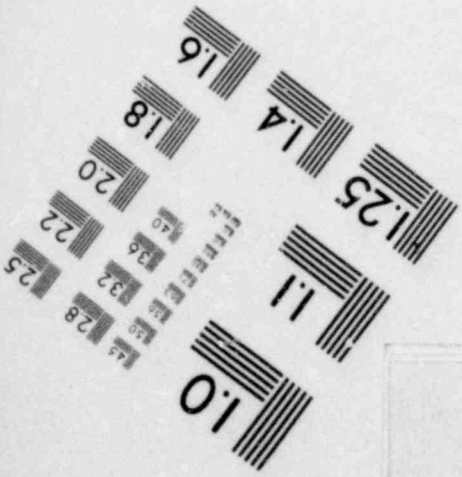

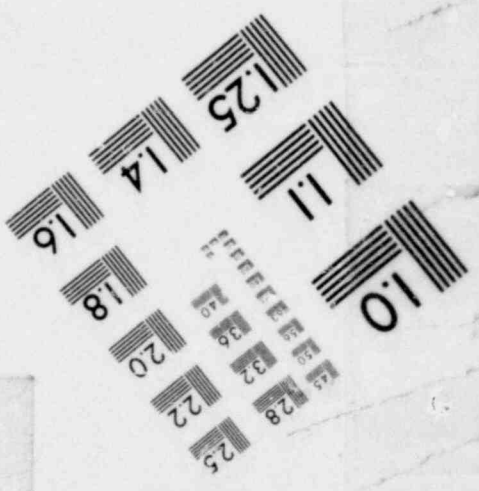

a PNA setup is estimated, the total number of counts, C, expected for any flow conditions can be estimated by $C = K \rho/U$. The number of counts, C, should be $C \geq 1000$ if the average density is to be measured with an error of $\leq 3\%$, and the mass flow velocity is to be measured with an error of $\leq 4\%$.

Application of PNA Technique

Figure 4 lists those fields where application of PNA techniques was found to be useful. First of all, the PNA technique is more accurate than any other two-phase flow measuring device for the measurement of mass flow in small pipes (with diameters $D \leq 10$ cm), and can be used for calibration of these devices. The basic equations for velocity and density measurements (Fig. 2) are rigidly valid only if the neutron fluence and the sensitivity of the detectors can be assumed to be constant over the whole cross section of the pipe. These conditions are sufficiently met for pipe diameters $D \leq 10$ cm. For larger pipes, a correction must be applied to the density reading, considering the attenuation of neutrons and gammas in the fluid as well as geometric attenuation ($1/r^2$ law). Although these effects can be easily modeled, and correction factors for the density reading can easily be derived for large pipe diameters, the PNA technique can not be considered as an absolute two-phase flow calibration tool for large pipes. However, relative measurements can be made even on large-diameter pipes, and gain changes of permanently installed flowmeters can be detected and calibrated by portable and non-intrusive PNA equipment.

The PNA technique is a non-intrusive radioactive tracer technique and, therefore, can be used like any other tracer technique for the measurement of flow distributions in large flow systems. We have measured the ECC bypass ratio in the LOFT reactor and plan to measure flow distributions in the 3-D test facility.

A unique capability of the PNA technique is the measurement of slow flows. This capability is usefully applied to tests simulating slow breaks. TMI related PNA flow measurements are planned for the LOFT reactor (EG&G Idaho, Inc.) and for the PKL (Erlangen, Germany).

Progress in 1979

PNA work performed at the Argonne National Laboratory (ANL) in 1979 is listed in Fig. 5. The PNA technique is now believed to have been developed to a point when it is prudent to disseminate it to other users. A number of publications (Fig. 6) was written with this in mind. ANL assembled PNA equipment is now installed at the LOFT facility for use on the L3-1 test. EG&G Idaho, Inc., will use their own PNA equipment in future small-break tests (L3 series). Another set of ANL assembled PNA equipment will be used at the PKL (at Erlangen, Germany), in the small-break tests planned there for the first quarter of 1980.

Progress was also made in the areas of testing, analysis, and instrumentation development.

Tests

The PNA technique was used for the measurement of the Emergency Core Cooling (ECC) bypass ratio at the LOFT reactor. The geometric arrangement of PNA equipment (Fig. 7) as well as the preliminary results of this test were presented at last year's meeting. After this meeting, a more detailed analysis of the test data was performed, which can be nummerized as follows:

Transient flow in the broken cold leg during the L1-5 Loss Of Coolant Experiment (LOCE) lasted for less than 50 sec (Fig. 8). During this time, fluid in the ECC line was activated by pulsed neutrons three times: at the beginning of the ECC flow, well within the flow, and at a time when the ECC flow was mixed with the pressurant that expels it from the storage tanks. Figure 8 shows the ECC flow through the ECC injection line. The times at which the three PNA tests were made are indicated by arrows in Fig. 8. The ECC bypass ratio is defined as that amount of ECC fluid that went out through the broken cold leg (Fig. 7), and was found to be 0.4 for the two PNA measurements taken while liquid was flowing through the ECC line, and 0.8 at the third PNA measurement, where the ECC liquid was mixed with the pressurant. A detailed analysis of the time distribution of the activities measured in the broken cold leg (by the Detectors 1 and 2 in Fig. 7) led to the conclusion that the flow conditions in the reactor vessel were different for each of the three PNA measurements:

The ECC fluid activated by the first neutron burst bypassed the core and left the broken cold leg in one coherent slug (Fig. 9). LOFT instrumentation data support the interpretation that, at this time, the water level in the reactor vessel was below the core barrel, that the ECC fluid went down the downcomer on one side of the core barrel, passed under the barrel, and that about 40% of the liquid went up the downcomer on the other side of the core barrel and out through the broken cold leg. 60% of the ECC fluid went up into the core assembly.

At the time of the second neutron burst, the reactor vessel was partially filled with water. The ECC fluid injected into the vessel fell on the existing water surface, mixed with the surface layers, went around the core barrel on different paths, and 40% of it went out through the broken cold leg in several small and poorly defined slugs (Fig. 9). The remainder mixed with the water in the partially filled vessel and stayed there.

The two-phase mixture flowing is the ECC injection line during the third neutron burst resided in the reactor for a very short time only. At this time, the vessel was almost filled with water, and most of the ECC fluid (80%) only skimmed the surface of the liquid in the vessel and went out, through the broken cold leg in one well defined slug.

PNA tests were also performed at the FAST loop, a large diameter (30 cm) test loop operated by EG&G at the INEL. The objective of this test was to evaluate the performance of a water pump when operating under two-phase flow conditions, and to compare readings from a LOFT spool spiece with PNA

measurements. The geometric arrangement of PNA equipment on the loop is shown schematically in Fig. 10. The pump failed when the void fraction went up to 20%. The distribution of counts measured at this void fraction (Fig. 11) indicated that the flow was homogeneous without measurable slip between the velocities of the two phases. The flow regimes found at the lower void fractions were similar to the one shown in Fig. 11.

The detailed analysis of the PNA data taken at the FAST loop is still in progress. This analysis is more complicated due to the need to model two-phase flow for the large-pipe correction of the density readings. The K-value for 30 cm-pipes, needed for test planning for the L3-1 test at the LOFT reactor, was measured experimentally during this FAST-loop test.

Analyses

The K-value of a particular PNA setup depends not only on the diameter of the pipe, but also on its wall thickness. Source characteristics effecting the K-value are neutron output, collimation, and distance from the pipe. Detector size, collimation, nuclear efficiency as well as the distance of the detector from the pipe also enter into the K-value. Even the electronic equipment used for data processing effects the K-value of a PNA setup, through the setting of the gamma ray energy discriminator. All these parameters are constant during a particular PNA test and the K-value of any particular setup can be determined experimentally by performing PNA measurements on a water-filled pipe in which the water is flowing with a known velocity.

In large pipes, the number of counts registered by PNA equipment is effected not only by the parameters mentioned above but also by geometric and nuclear attenuations. These effects can be best formalized by using corrected K-values for large pipes. In the absence of geometric and nuclear attenuations, the K-value should be proportional to the cross sectional area of the pipe, $K \propto D^2$. Deviations from this ideal relation are shown in Fig. 12. Relations between the density readings obtained from non-corrected K-values and the true density, are shown in Fig. 13 for several pipe diameters.

The Figures 12 and 13 were computed by use of the FORTRAN program PNA-SIMulation, which is an advanced version of the program ACTivation OPTimization written previously for single-phase flow (Paul Kehler, "Feasibility of Calibration of Liquid Sodium Flowmeters by Neutron Activation Techniques", ANL-CT-76-17, July 1976). The PNASIM program models all the parameters effecting the K-value as discussed above, as well as various regimes of two-phase flow. Presently, it is written in polar coordinates and models homogeneous and annular flows, with tabulated inputs of velocity and density distributions. Rectangular coordinates will be used to model stratified flow. The accuracy of the models used in PNASIM was verified by experimentally determined K-values (Fig. 3) and flow distributions (Fig. 11). It is planned to improve the PNASIM program by improving its mixing model and by using analytically expressed void and velocity distributions.

Instrumentation Development

The geometric effects on the K-value can be reduced by using a multiplicity of sources and detections, arranged circumferentially around the pipe. A torus detector (Fig. 1) fully encircling pipes with dameters $D \leq 15$ cm, was built to increase the total number of counts and to reduce the geometric effect on the K-value. Using this torus detector, the correction to be applied to the K-value for pipe diameters $D \leq 15$ cm is much smaller than that shown in Fig. 12, which was calculated for input parameters representative of the PNA setup now used on the LOFT reactor. The only variable in Fig. 12 is the diameter of the pipe.

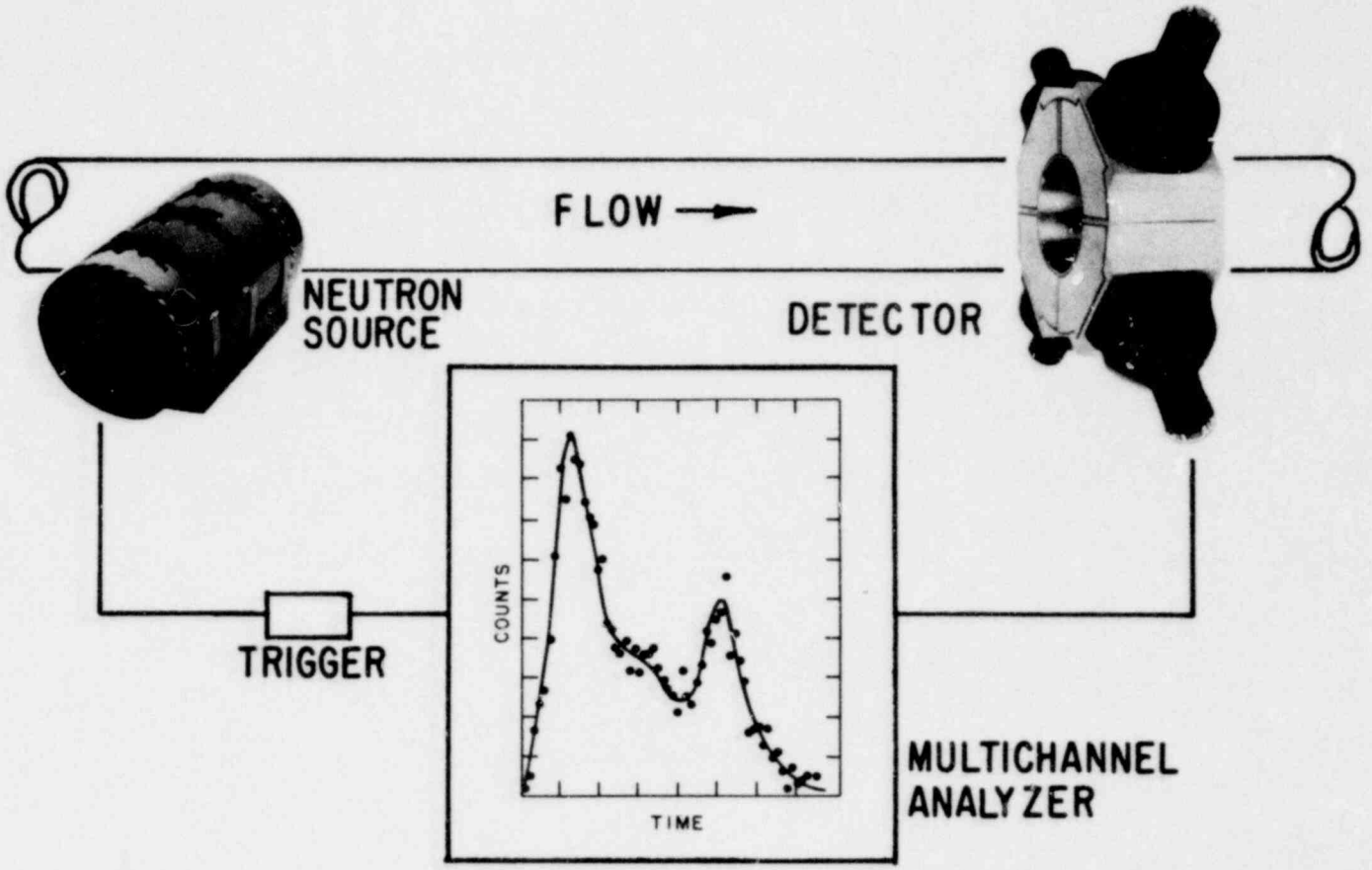

Fig. 1

PNA EQUATIONS

- MASS FLOW VELOCITY U_M FROM THE MASS WEIGHTED AVERAGE OF THE INVERSE OF THE TRANSIT TIME DISTRIBUTION:

$$U_M = \left(\overline{\frac{1}{\tau}}\right) Z$$

Z = SOURCE - DETECTOR SPACING

$$\left(\overline{\frac{1}{\tau}}\right) = \frac{\sum \frac{1}{\tau^2} C\, e^{\lambda T}}{\sum \frac{1}{\tau} C\, e^{\lambda T}}$$

C = NUMBER OF COUNTS AT TIME τ

λ = DELAY CONSTANT OF ACTIVATED O^{16}

- AVERAGE DENSITY ρ FROM THE TOTAL AMOUNT OF ACTIVITY A INJECTED INTO THE FLUID BY ONE NEUTRON PULSE:

$$\rho = \frac{A}{K}$$

K = CALIBRATION CONSTANT

$$A = \frac{1}{\tau} \sum C\, e^{\lambda T}$$

Fig. 2

EXPERIMENTALLY DETERMINED K-VALUES

$$K = \frac{U_Q C_Q}{\rho_Q}$$

SOURCE: TC 655	DETECTOR:				
PIPE DIAMETER (CM)	DIAMETER (CM)	HEIGHT (CM)	PIPE DIAMETER (CM)	K	TEST LOCATION
7.5	7.5	7.5	7.5	1280	A/W LOOP
7.5	12.5	7.5	7.5	2480	A/W LOOP
12.5	7.5	7.5	12.5	1050	A/W LOOP
12.5	12.5	7.5	12.5	2670	A/W LOOP
10.0	12.5	7.5	35.0	280	LOFT
35.0	12.5	7.5	35.0	640	FAST

NOTE: WHEN K IS KNOWN, THE TOTAL NUMBER OF COUNTS IS ESTIMATED BY:

$$C = \frac{K\rho}{U}$$

Fig. 3

APPLICATIONS OF PNA TECHNIQUE

- CALIBRATION OF TWO-PHASE FLOW INSTRUMENTATION IN TEST LOOPS.
- IN-SITU RE-CALIBRATION OF TWO-PHASE FLOW INSTRUMENTATION INSTALLED IN LARGE TEST FACILITIES.
- MEASUREMENT OF FLOW DISTRIBUTIONS.
- MEASUREMENT OF SLOW FLOW VELOCITIES (TMI-RELATED SLOW-BREAK TESTS).

Fig. 4

SUMMARY OF PROGRESS

1979

- DISSEMINATION OF PNA TECHNIQUE
  - PUBLICATIONS
  - TRANSFER OF TECHNOLOGY (LOFT, PKL)
- TESTS
  - PERFORMED: LOFT L1-5 (ANALYSIS OF DATA)
    FAST LOOP
  - PLANNED:

LOFT L3-1	Nov.	79
ORNL	Dec.	79
PKL	Jan.	80
3-D		80
SLAB CORE		80 ?

- ANALYSIS
  - PERFORMED: MODELING OF TWO-PHASE, HOMOGENEOUS AND ANNULAR FLOW (PROGRAM PNASIM)
  - PLANNED: MODELING OF STRATIFIED FLOW, PHASE CHANGE, IMPROVEMENT OF MIXING MODEL
- DEVELOPMENT OF INSTRUMENTATION
  - PERFORMED: TORUS DETECTOR
  - PLANNED: GLOBAL GAMMA DENSITOMETER

Fig. 5

PUBLICATIONS SINCE LAST MEETING

1) PAUL KEHLER: "USE OF PULSED NEUTRON SOURCES FOR FLOW MEASUREMENTS IN REACTOR RESEARCH", TRANS. AM. NUCL. SOC. 30, 14 (NOV 1978).

2) PAUL KEHLER: "TWO-PHASE FLOW MEASUREMENT BY PULSED NEUTRON ACTIVATION TECHNIQUES", MEASUREMENTS IN POLYPHASE FLOW, P. E. STOCK EDITOR, ASME PUBLICATION H00121I (DEC 1978).

3) PAUL KEHLER: "PULSED NEUTRON MEASUREMENT OF SINGLE- AND TWO-PHASE LIQUID FLOW", IEEE TRANS. NUCL. SC. NS-26 (1), 1627 (FEB 1979).

4) M. KONDIC, P. KEHLER, S. MAFF: "REACTOR VESSEL BLOWDOWN: DETERMINATION OF EMERGENCY CORE COOLING PARAMETERS", ASME PUBLICATION 79-HT-83 (JUNE 1979).

5) PAUL KEHLER AND C. W. SOLBRIG: "MEASUREMENT OF THE EMERGENCY CORE COOLANT BYPASS FLOW ON THE LOFT REACTOR", NUREG/CR-0208 (IN PRINT).

6) PAUL KEHLER: "ACCURACY OF TWO-PHASE FLOW MEASUREMENTS BY PULSED NEUTRON ACTIVATION TECHNIQUES", PRO. 2ND MULTI-PHASE FLOW AND HEAT TRANSFER SYMP. WORKSHOP, MIAMI BEACH, FL (APRIL 79).

7) PAUL KEHLER: "TWO-PHASE FLOW MEASUREMENT BY PULSED NEUTRON ACTIVATION TECHNIQUES", PROC. (Y. Y. HSU, EDITOR), REVIEW GROUP MTG. ON TWO-PHASE FLOW INSTRUMENTATION, NUREG/CP-0006 (MAY 1979).

Fig. 6

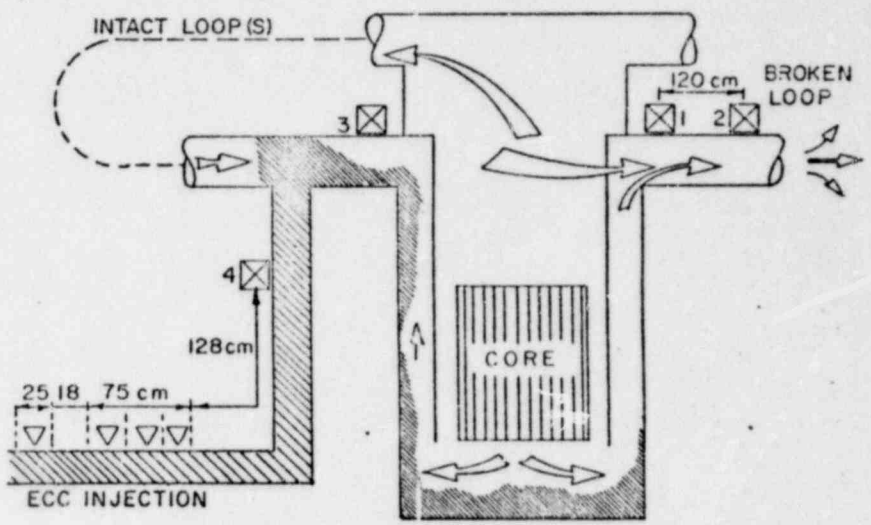

Fig. 7

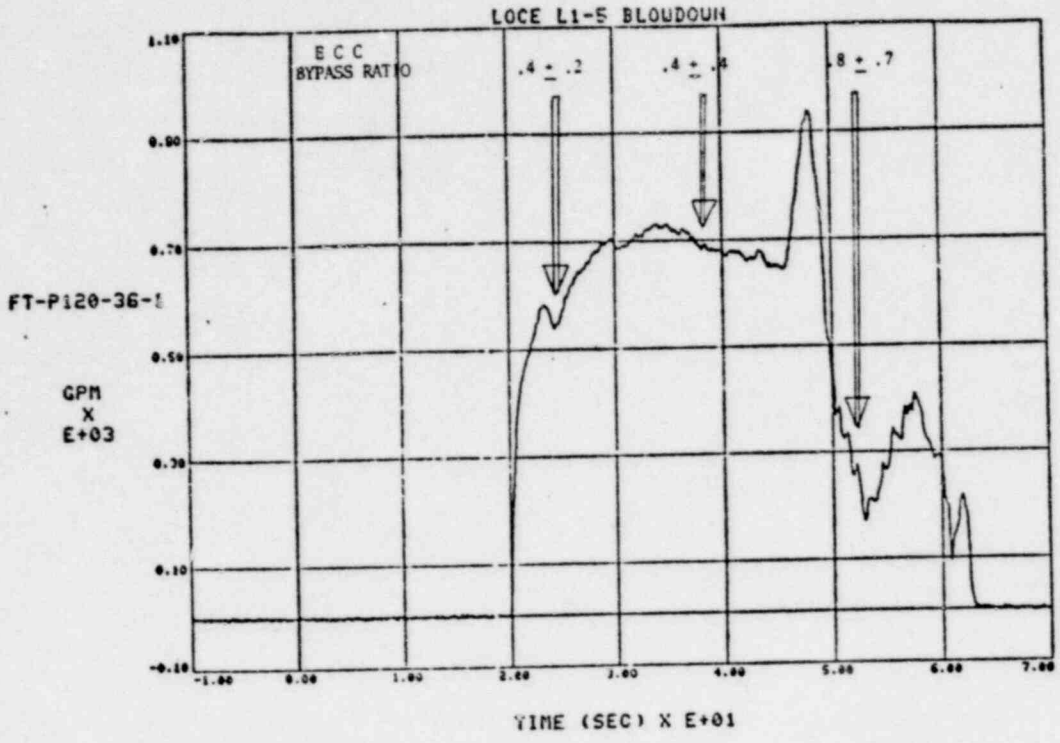

Fig. 8

POOR ORIGINAL

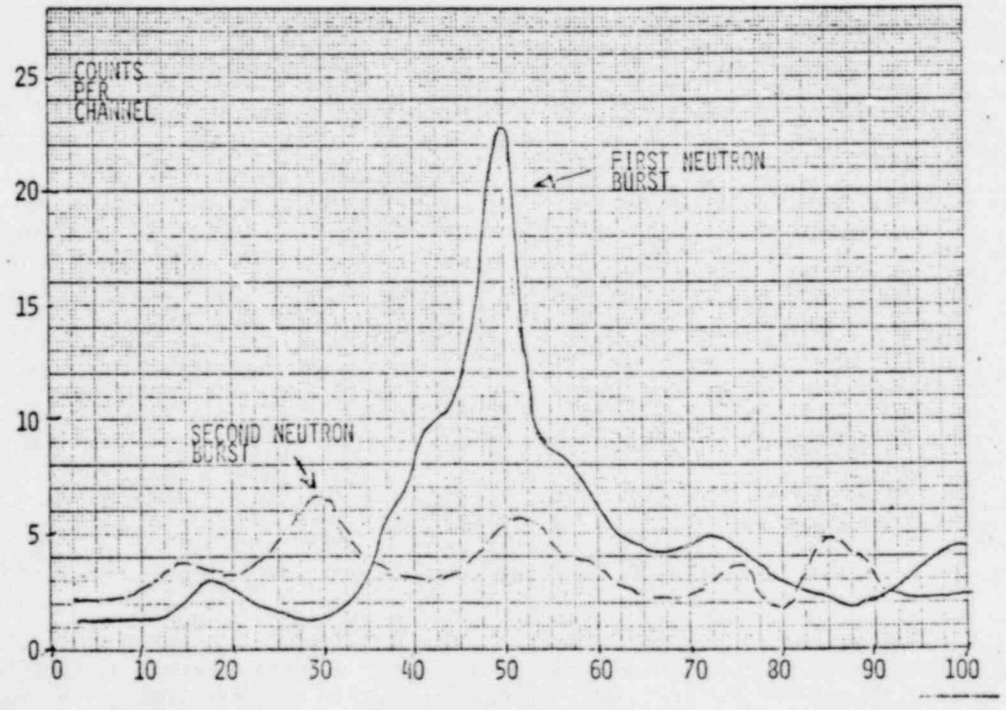

Fig. 9

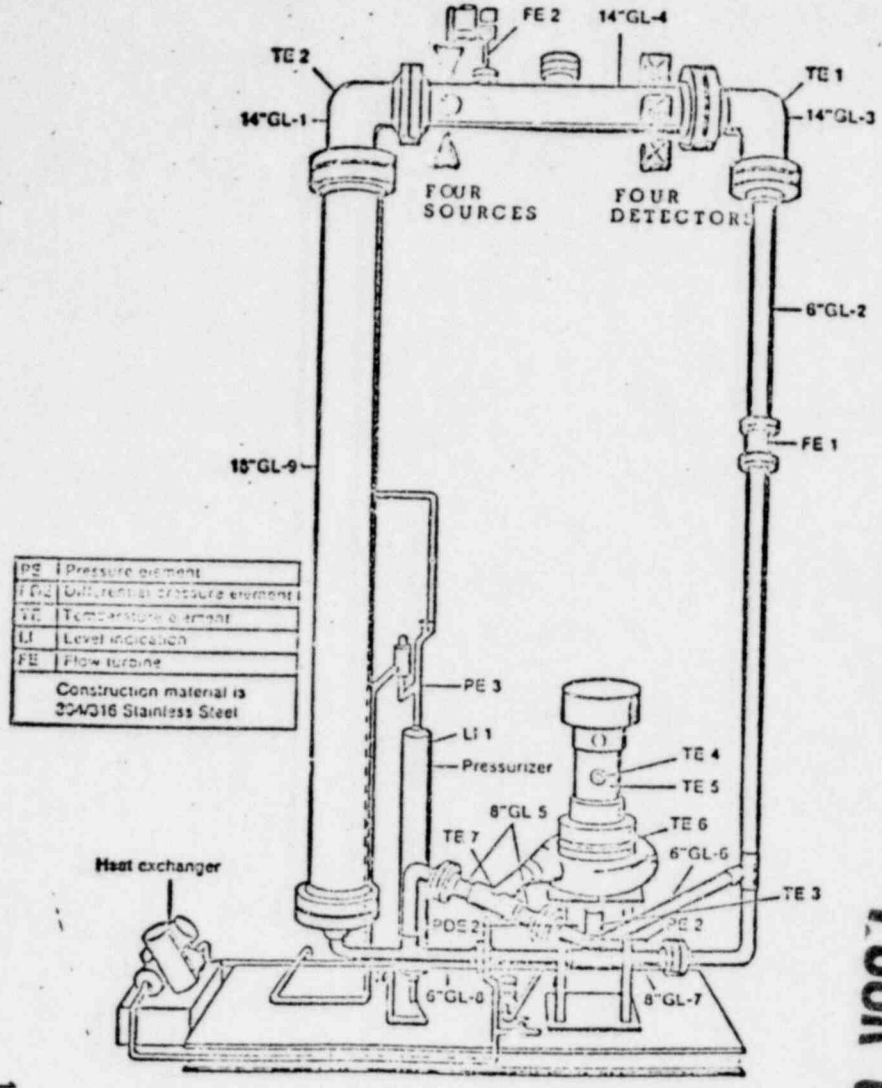

Fig. 10

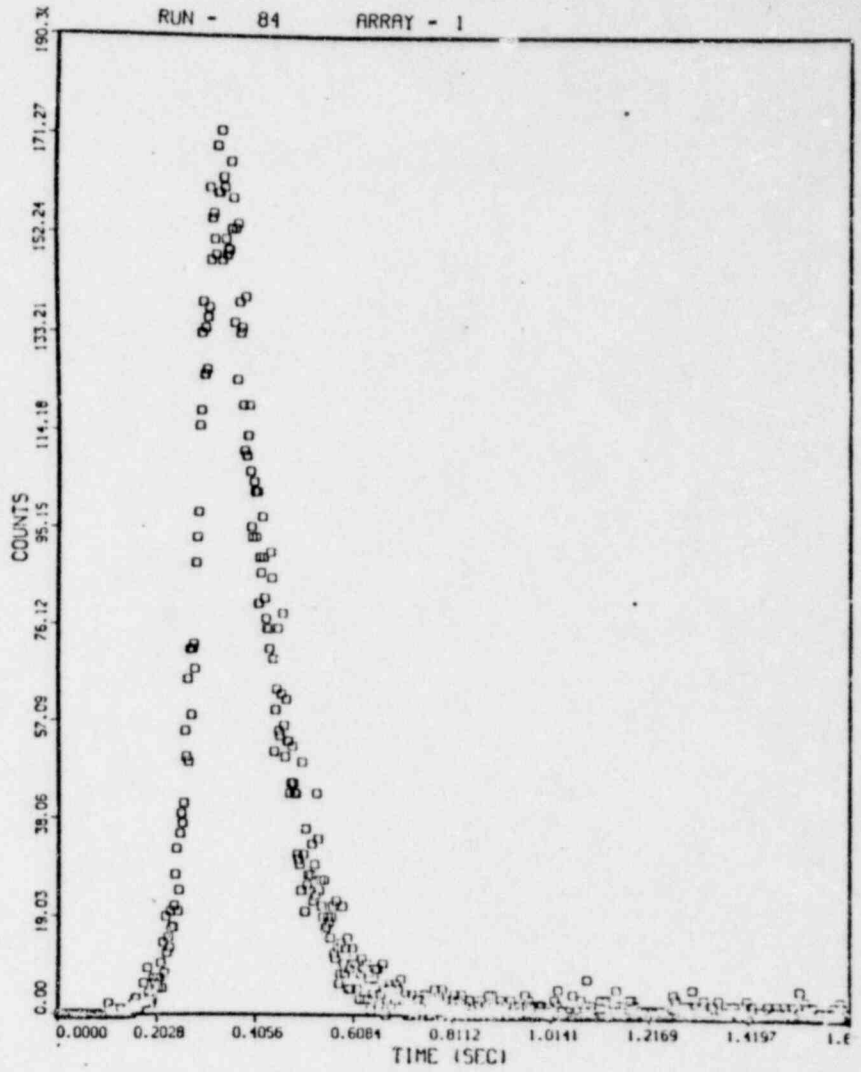

Fig. 11

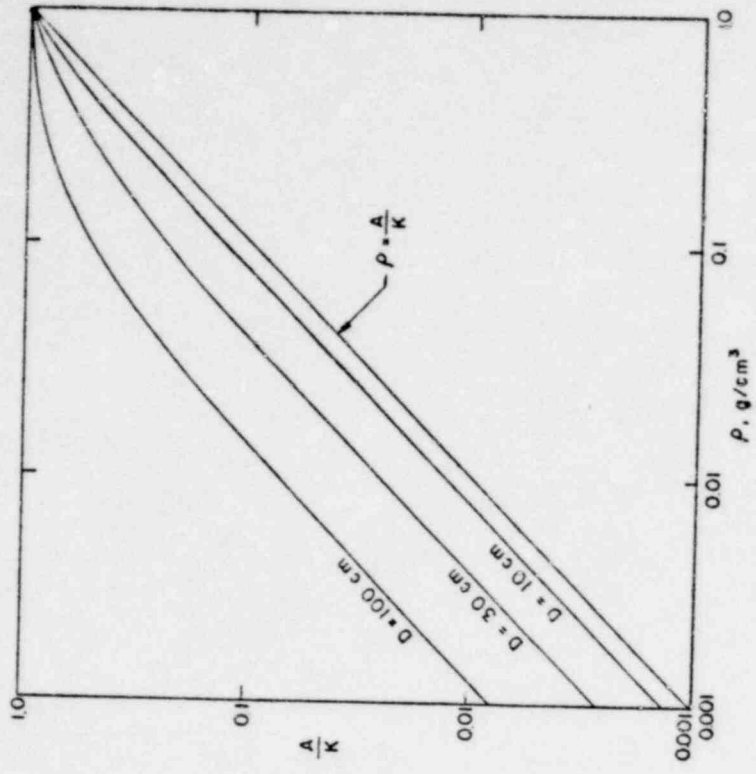

Fig. 13

POOR ORIGINAL

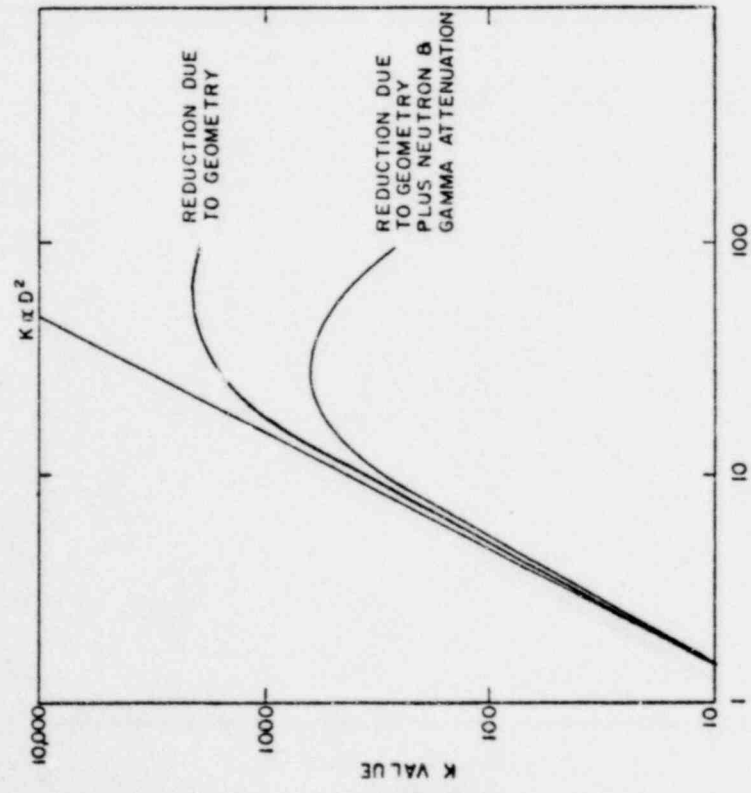

Fig. 12

1601 011

INSTRUMENTATION FOR FILM DYNAMICS IN TWO-PHASE FLOW

by

Ramu K. Sundaram
Assistant Professor

John C. Chen
Professor

E. J. London
Research Engineer

A. T. Fei
Research Assistant

Institute of Thermo-Fluid Engineering and Science
Lehigh University
Bethlehem, PA 18015

For Presentation
at

Seventh Water Reactor Safety
Research Information Meeting
U.S. Nuclear Regulatory Commission
November 5-9, 1979, Washington, D.C.

SCOPE

The objective of the program was to develop instruments that would be of help in understanding the dynamics of liquid films in two-phase flows. An immediate concern was film behavior on unheated surfaces in the upper plenum of reactors during the reflood phase of loss-of-coolant accidents. The instrumentation techniques described in this report deal with the measurement of film thickness and film flow rate. Also described in an extension of the thickness measurement technique to the measurement of liquid holdup on rod surfaces. Initial application of these instruments is envisioned to be in reflood tests in a non-radioactive stream-water environment at pressures up to 115 psia (saturation temperature 338°F/170°C).

FILM THICKNESS MEASUREMENT

Electrical impedance probes, mounted flush on the surface, are used for measuring film thickness. The probes can be operated in the capacitive or conductive mode. A typical probe configuration, consisting of three electrodes, is shown in Figure 1. The normalized capacitance ratios across two different pair of probes is also shown as a function of film thickness (δ). It is desirable that the probe be operated in its most sensitive range ($\delta/d \leq 0.5$). This can be attained by suitably designing the electrode gap 'd' for any estimated range of expected film thickness.

A similar result can be obtained by operating the probe in the conductive mode. In this case, the conductance ratio between the two

electrode pairs behaves similar to the normalized capacitance shown in Figure 1.

FILM FLOW RATE MEASUREMENT

The measurement of film flow rate is much more difficult than film thickness measurement. One technique that was found to be promising was the use of electrolysis potential (EP). A typical EP probe, mounted flush on the surface over which the film flows, consists of 2 Pt wires (0.005" diameter). At a fixed applied d.c. voltage, the electrolytic current between the electrodes was found to be a function of the film flow rate and the ohmic resistance between the electrodes (which is a function of water electrical resistivity, electrode length and diameter, gap between electrodes and the film thickness). A typical test in closed channel flow between two parallel plates (constant film thickness) yields the data shown in Figure 2. The data are over a wide range of water electrical resistivities (ρ_o = 20 - 200 kΩ - cm). It can be seen that the data can be correlated approximately as:

$$i \cdot R_p = Ae^{-BV} \qquad (1)$$

where i = electrolysis current, mA

R_p = ohmic resistance between electrodes, kΩ

V = average film velocity, cm/s

A,B = correlational function, dependent on the film thickness (δ) and applied voltage (V_o)

Thus if δ is known, for a given v_o, A and B can be determined from calibration tests and by measuring i and R_p, the average film velocity V can be found from equation (1).

The data shown in Figure 2 have been obtained in a closed channel, where a constant film thickness could be maintained. It is possible that the EP probe behavior could be affected by the film velocity profile, which would be different in bounded film as compared to free surface films experiencing varying amounts of interfacial shear at the free surface due to counter current vapor flow. Initial tests have shown that the EP probe behavior in free surface films with no interfacial shear can be characterized by an equation similar to equation (1), although the correlational functions are different. Further tests are in progress to resolve this question.

LIQUID HOLDUP ON VERTICAL RODS

These measurements are carried out using band-type capacitance probes. The technique is to measure the electrical capacitance between two band electrodes (width d, gap d) mounted flush on the surface over which the liquid film flows. It can be shown that the capacitance is directly proportional to the volume of liquid over the probe surface irrespective of the length of coverage and the nonuniformity of the film as long as the condition:

$$\frac{\delta}{d} < 0.5 \qquad (2)$$

1601 015

is met along the l[illegible] probe. In this case, it is possible to show that:

$$\frac{\Delta C}{(\delta L_c)} = A_1 = \text{Constant for Probe} \qquad (3)$$

Here, L_c is the length of [illegible] f the electrodes and (δL_c) provides a measure of the average area of cross section of the flowing film and is directly proportional to the volume of liquid (holdup) over the probe surface.

A 4" diameter [illegible]od was instrumented with 3 band probes at various axial locations and installed in an assembly at LASL which can produce air-water cross-flow over the rod surface over a wide range of air and water flow rates. Figure 3 shows typical data from the top most probe on the rod. In the figure, the local liquid holdup (δL_c) is plotted versus the incident total water flow rate (Q_L^o) for various air velocities. It can be seen that at a given Q_L^o, the holdup decreases as air flow increases. This can be expected physically as higher air velocities would lead to higher reentrainment and hence thinner films. Also, at a given air velocity, the increase in holdup with increasing Q_L^o is similar to laminar film theory prediction (film thickness proportional to cube root of flow rate). In these experiments, the liquid usually covered about 60% of the probe length.

Since the probes can yield holdup information in the presence of non-uniform as well as discontinuous films (rivulets), it is believed that they would be useful tools for film drainage studies and

investigations of deentrainemnt/reentrainment mechanisms. Preliminary analysis of the data obtained in the LASL experiments support this contention.

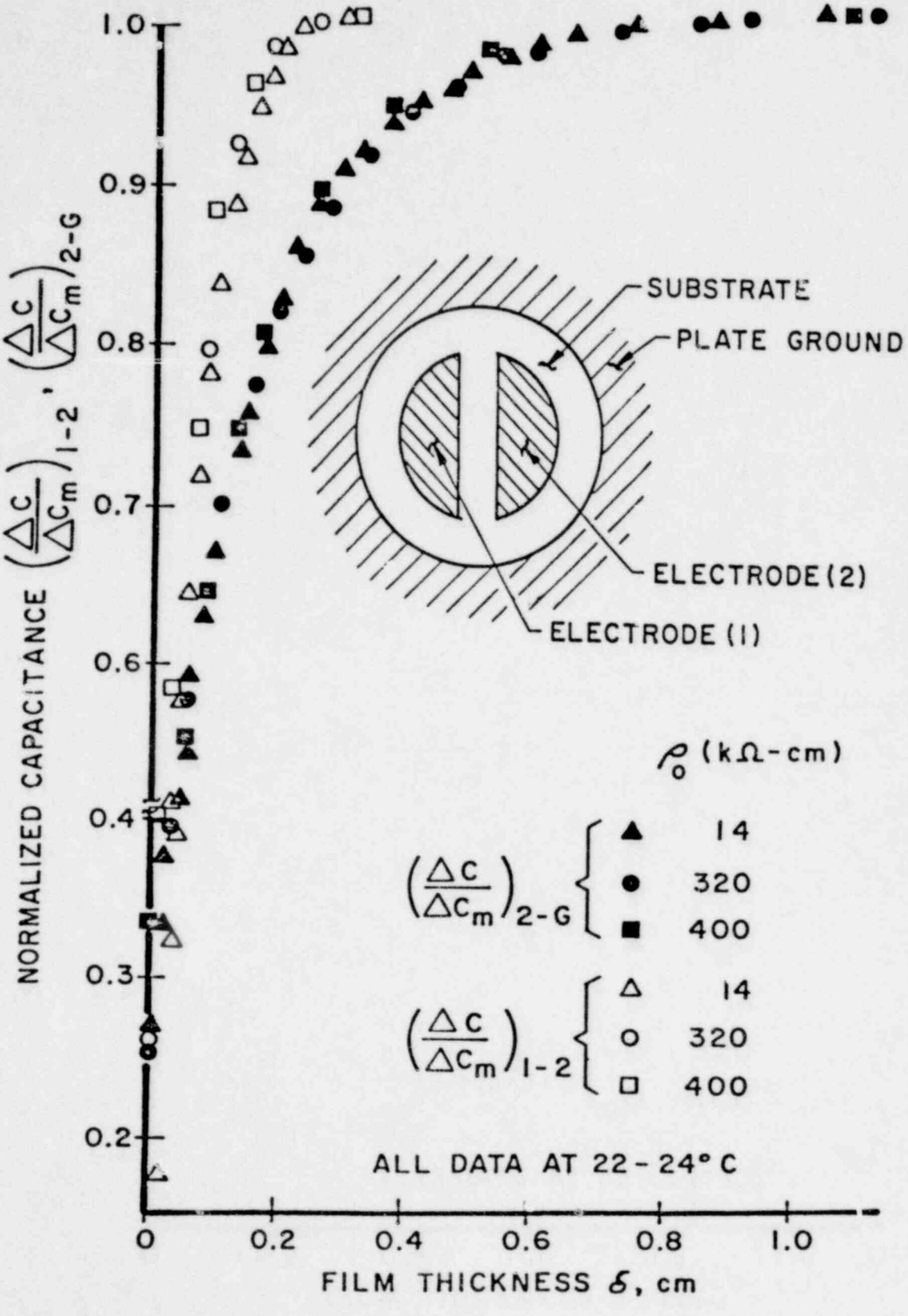

Figure 1 Capacitance probe for film thickness measurement

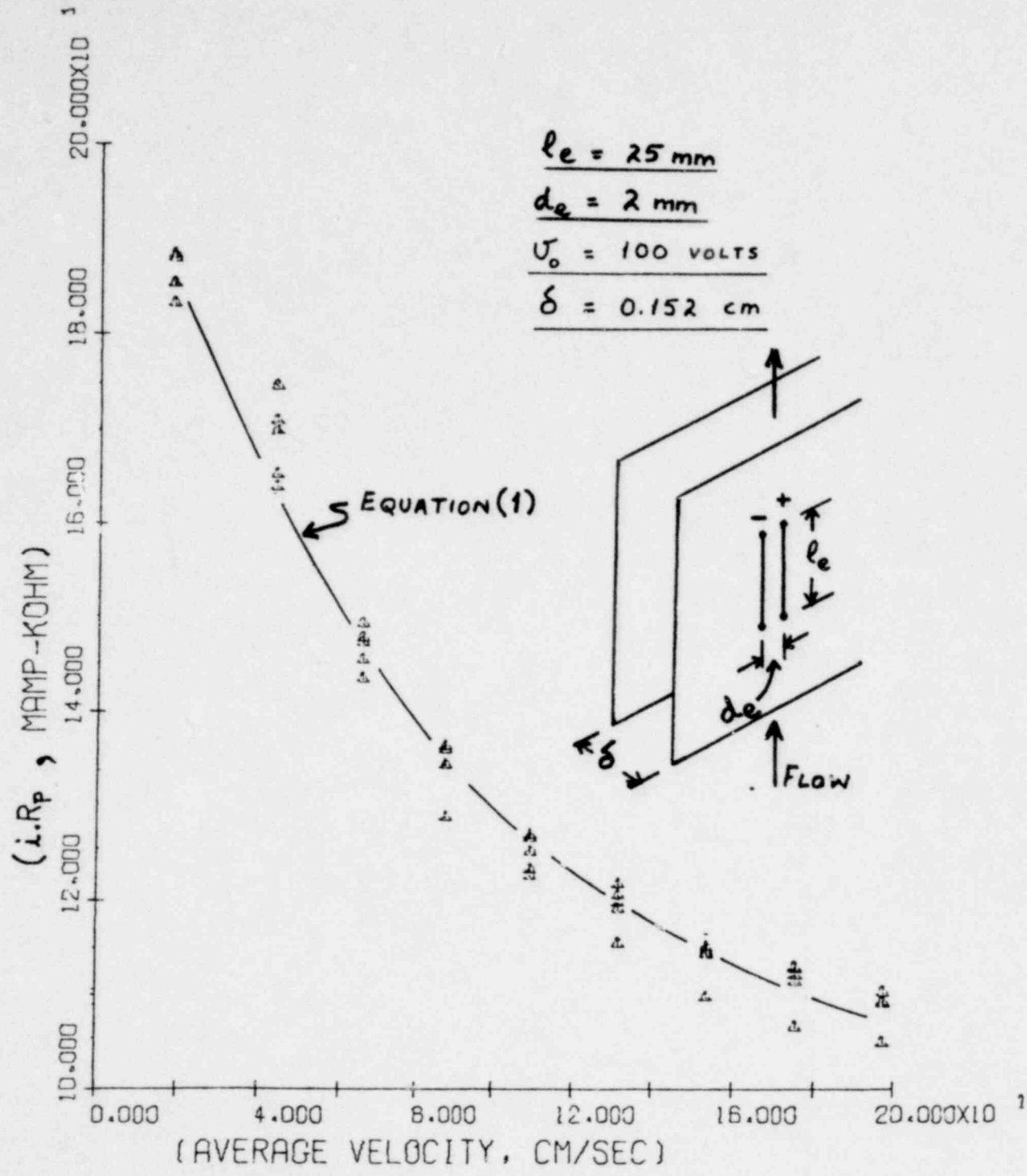

Figure 2 Typical EP probe response

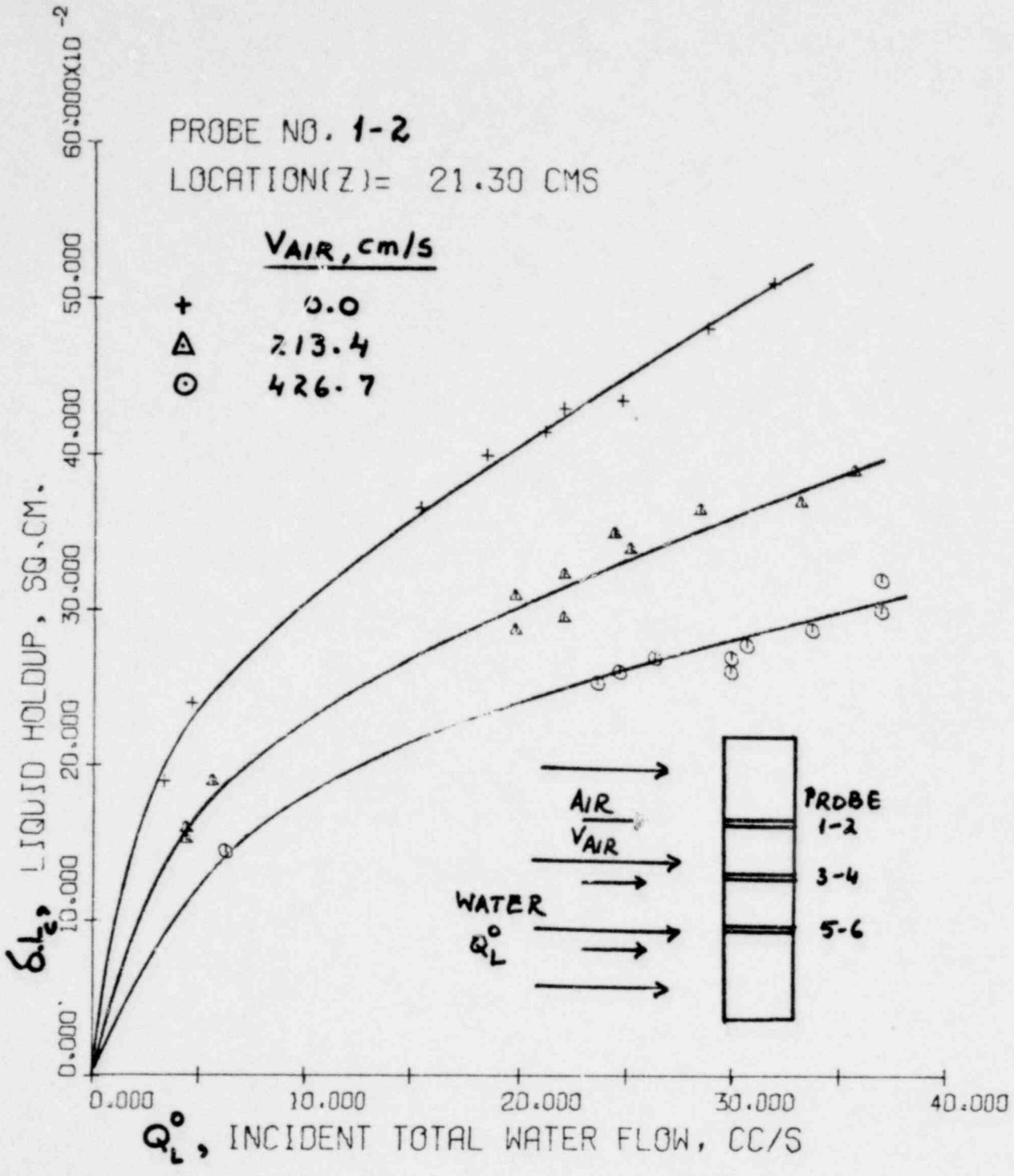

Figure 3 Liquid holdup data from Probe 1-2

ornl
10/30/79

B. G. EADS AND J. O. HYLTON

ADVANCED INSTRUMENTATION
FOR REFLOOD STUDIES
PROGRAM

DEVELOPMENT OF IMPEDANCE SENSORS AT ORNL: FOR MEASUREMENT OF TWO-PHASE FLOWS

PRESENTED AT
SEVENTH WATER REACTOR SAFETY RESEARCH
INFORMATION MEETING
GAITHERSBURG, MARYLAND
NOVEMBER 5-9, 1979

DEVELOPMENT OF IMPEDANCE SENSORS AT ORNL FOR MEASUREMENT OF TWO-PHASE FLOWS

INTRODUCTION

A program under the sponsorship of the United States Nuclear Regulatory Commission (USNRC) was initiated in 1977 at the Oak Ridge National Laboratory (ORNL) to develop instrumentation for application in PWR safety experimental facilities. The program, Advanced Instrumentation for Reflood Studies (AIRS), is specifically to develop instrumentation for measurement of in-vessel local fluid phenomena in safety experiments designed to investigate the refill and reflood phases of the PWR loss-of-coolant accident. However, the technology being developed has general applicability to the measurement of two phase fluid flow. The objective of the ORNL program is to develop techniques and systems for measuring fluid flow in-core, deentrainment in the upper plenum, and liquid fallback from the upper plenum into the core. To attain this objective, liquid film thickness and velocity and two-phase flow velocity and void fraction must be measured. Liquid film thickness and film velocity measurement systems are being implemented utilizing concepts developed at Lehigh University.[1,2] The major portion of the ORNL effort is devoted to the development of impedance sensors for measurement of two-phase flow local velocities and void fractions with emphasis on high void fraction flow regimes. Film sensor development at ORNL is limited to adaptation of the present techniques to the environment of a refill/reflood facility. As the development progresses on the measurement techniques, ORNL will fabricate and supply instrument systems to facilities which are included in the international (West Germany, Japan and the U. S.) 2D/3D Refill/Reflood Program.

---

*Research Sponsored by the Office of Nuclear Regulatory Research, U. S. Nuclear Regulatory Commission, under Interagency Agreements DOE 40-551-75 and 40-552-75 with the U. S. Department of Energy under Contract W-7405-eng-26 with the Union Carbide Corp.

At this time some instrument systems, which could be regarded as the first generation, have been fabricated. The term first generation implies that these systems are probably not yet optimum; therefore, a significant development effort is continuing to provide improvements and to develop other systems.

This presentation is to provide a brief overview of the program and to highlight some of the recent development results. Primary emphasis is given to the "string probe" and "flag probe" test results in a variety of two-phase flow environments.

IMPEDANCE PROBE OPERATING PRINCIPLES

The principle of operation of the impedance probes is based on measurement of the electrical impedance of the fluid mixture in the vicinity of a set of electrodes, as shown in Fig. 1. The impedance varies with the relative amounts of liquid and vapor present and with the changing distribution of the phases. Measured impedance can be used to estimate the void fraction of a two-phase mixture and the velocity of the mixture or of one of the phases. Velocities are determined from the phase shift of the transfer function of signals from two spatially separated probes. The velocity measured by this procedure is referred to as the "noise velocity" later in this report. This term is used because statistical signal analysis techniques, often referred to as "noise analysis", are used in determining a velocity estimate. This technique is often referred to as the "transit time" method of determining velocity. Figs. 2 and 3 illustrate the "transit" time method.

Two basic methods are used to determine void fraction from impedance sensor signals. If the sensor is very small (a point probe) it is likely that at any instant in time the sensing region will contain either all liquid or all vapor. Sensors of this type are designed so that the sensing region is smaller than the majority of the droplets or bubbles; thus the sensor will seldom be exposed to a mixture of the phases. In this case the sensor signal alternates between the "wet" and "dry" levels. The fraction of the time spent at the dry level or the "residence time" is used as a measure of the void fraction.

For larger sensors where the sensing volume contains both phases most of the time, the "residence time" method may not work well. In this case, one technique used relates the average impedance of the mixture to the void fraction. Most of the sensors being developed at ORNL are of the latter type. The relationship between mixture impedance and void fraction is dependent upon the electrode geometry and the distribution of the phases as shown in Figs. 4 and 5. In many cases a linear calibration based on admittance or capacitance yields good results. This is called the "relative admittance" method and was used with all of the void fraction results presented later in this report. Another method of analyzing the mixture impedance signal utilizes the "amplitude histogram" or "amplitude probability density." The mean value of impedance determined by the histogram method is equal to the inverse of the value obtained by the relative admittance method. The histogram has the added advantage of giving an indication of flow regime by observing the pattern or shape of the histogram.

All the proposed methods for velocity and void fraction are dependent upon some type of time averaging; therefore, the following constraints on the analysis must be made:

- Steady-state is assumed between data points.
- The time steps between data points must be small enough to resolve a reflood transient.
- The time steps must be large enough to reduce the statistical errors to an acceptable value.

SENSOR GEOMETRY

The primary consideration in the design of sensors for in-vessel local measurements in a reflood test facility is the proper geometry to sense two-phase flow parameters in the region of interest. For instance, the geometry best suited for in-core subchannel measurements is not as suitable for upper plenum application and vice versa. The application of various forms of impedance sensors to the measurement of two-phase flow has spanned over thirty years,[3] and efforts are continuing to understand and optimize sensor geometries.[4] The most successful applications reported in the

literature are based on the use of small needle shaped sensors which give a highly local measurement. This type of sensor requires relatively simple electronics which gives a binary output signal; zero for vapor and one for liquid. The sensors being developed are based on obtaining localized area or volume measurements as contrasted to the point measurement of the needle sensor.

The environmental conditions, high temperature and thermal shock, are the next most important influence on sensor geometry. Development at ORNL has resulted in significant strides toward design and application of sensor assemblies which can survive a severe environment; however, the empnasis of this report is on the measurement results obtained to date rather than on the fabrication techniques.

Sensors have been developed in a guide tube configuration for in-core subchannel measurements. Several sensor electrode configurations have been considered (Shown schematically in Fig. 7), but to date the greatest overall success has been with the "flag probe" configuration shown in Fig. 8. For application in the upper plenum, the downcomer, and other locations of larger cross sectional area the "string probe" configuration has given very useful results in both air-water and steam-water tests. This configuration has been adapted from the work of Carrard and Ledwidge[5] who applied it to low void fraction (α <25%) two-phase air-water flows. As shown later in this report, its use has been successfully extended to the high end of the void fraction range.

IN-CORE GUIDE TUBE FLAG PROBE TESTS

Steam-water testing in 9-rod bundle. A prototype guide tube assembly like the one in Fig. 9 has been tested in a 3 x 3 heated rod bundle where the central heater rod was replaced by the instrumented guide tube. The purpose of the tests was to determine survivability and operability in an environment and with flows similar to the reflood facilities of the 2D/3D Program. The heated length of the core is 1.9 meters (6.23 ft.). The heater rod flux, grid spacer locations, flag probe and other sensor locations are shown in Fig. 10. The flag probe assembly is approximatley 4.3 meters (14 ft.) in length; thus, as indicated in Fig. 11, the upper

portion of the guide tube extended outside the top of the bundle and test vessel.

The flag probe assembly used for the test was one which had been intended for use in an actual reflood test facility but had failed during fabrication. In the desire to have one assembly which could be tested in a reflood-like environment an attempt was made to repair the rod. On the second attempt, repair was successful. The initial fabrication failure and the necessity for multiple attempts to repair the assembly would cause one to assign a lower probability of success in a reflood test and this should be considered in evaluating the test results.

Test Description. A total of ten tests were conducted with the flag probe assembly in the 9-rod bundle. For these tests the flooding rate, rod power and injection point were varied. The first nine tests were conducted with the heater rod initial clad temperature at a nominal 600°C. Test No. 10 had an initial guide tube clad temperature of 700°C but was aborted mid-way through the test due to a leak in the test vessel housing.

Survivability. The survivability of the probe was a key issue in this test with the integrity of the probe itself and of its ceramic-to-metal seals being of greatest concern. Following each test, electrical tests of the integrity of the sensor cables were made. Also, the guide tube vent line was observed for discharge of steam or condensate which would indicate a leak in the ceramic-to-metal seals. The results of the test series relative to survivability are as follows:

1. Electrical measurements following each test showed that 7 of the 8 sensor leads remained intact through all 10 tests. One lead indicated an open circuit after Test No. 7.
2. Ceramic-to-metal seal leakage was minimal. A few drops of condensate water were observed at the vent line discharge following Tests 7 and 9. Also, during Test No. 9 a few small puffs of steam were discharged.

Experimental tests have shown that the effects of small leaks through the ceramic-to-metal seals have little, if any, detrimental effect on the impedance measurement. The break in sensing leads obviously results in the loss of data.

The analysis of signals from the tests is continuing but preliminary indications are as follows:

1. An impedance measurement is possible during the major portion, and perhaps all, of the reflood transient (Figs. 12 and 13). Arrival of the quench front with the attendant quantity of water causes a step reduction in impedance and results in reduced sensitivity to flow in the subchannel.
2. Velocity measurements were obtained for Tests No. 2 and No. 3 which are in the range of expected values. Figs. 14 and 15 show noise analysis velocity results from Test No. 2 on two different scales for the vertical axis.
3. Further development and confirmation is needed of the void fraction analytical method. There was no other void fraction measurement in these tests with which to compare the flag probe results. The data appears to have the correct trend but some of the measurement amplitudes are questionable. Tests must be conducted where a local independent measurement of void fraction can be made. Such tests are planned.
4. Interference from the electrical power supply was of such magnitude in all tests following Test No. 3 that analysis of the data was impossible. A change in behavior of the system or the probes seems to have occurred during Test No. 3 which apparently caused this problem. The change in behavior is not understood at this time. It is felt that improvements in the filtering in the electronics which were made subsequent to the tests would have greatly reduced or eliminated the interference problem.

The performance criteria for such an instrument assembly is survival of 25 such reflood tests. The prototype tested did not meet this criteria; however, it should again be noted that this particular rod was considered at the outset to be marginal at best, due to the repairs made during fabrication.

Air-Water Droplet Tests. In order to gain an understanding of the transit time velocity measurements obtained from the impedance sensors, other tests have been and are being conducted. A series of simple experiments were conducted with a flag probe using a vibrating capillary to generate a single stream of gravity accelerated droplets. In these tests the droplet

flow passing between the sensor electrodes was well controlled and made it possible to know all the flow parameters, i.e., droplet size, velocity and spacing. These tests simulate the very high void fraction dispersed droplet flow regime except that a single stream of droplets is involved. As indicated in Fig. 16, the flag probe gave an accurate reporting of the droplet velocities.

STRING PROBE TESTING AND RESULTS

The basic configuration of a string probe is as shown in Fig. 17 which is an early developmental geometry tested in air-water. Three different prototype designs have been tested in air-water and steam-water. These tests are discussed in the following paragraphs.

Steam-Water Test Description. Steam-water tests were conducted in the AIRS Steam-Water Test Stand at ORNL shown in Fig. 18. The probes were installed in a vertical 6-inch (152 mm) ID test section as shown in Fig. 19. Flow entered the test section from a 3 1/2 inch ID pipe with approximately 20 feet of straight length upstream of the test section. A spool piece containing a drag disk, a three-beam gamma densitometer and a turbine meter was located just downstream of the test section. The steam and water flowrates were measured separately before being mixed and injected into the 3 1/2 inch pipe at the upstream end of the 20 feet long straight section. All tests were conducted in the vertical upflow mode covering a void fraction range of approximately 40% to 99+% and flow regimes; bubbly, slug, churn, and annular.

Probe Description. The probes that were tested are called the Large and Intermediate Model II and the Large Model III. The Mod II design, Fig. 20, contains two planes of electrodes which are attached to insulator spools mounted on the top and bottom of the stainless steel probe frame. The Mod III design, Fig. 21, represents some reduction in flow blockage and provides some streamlining by installing the insulator spools in the side-walls of the probe frame.

Tests Conditions. Each of the probes was subjected to a series of 15 steady state test runs. The pressure and temperature in the test section

were approximately 90 psi (6.2 bar) gauge and 165°C (330°F). The measured inlet flows and void fractions for the test runs were:

RUN NO.	STEAM FLOW LBM/HR	WATER FLOW LBM/HR	VOID FRACTION BY GAMMA-DEN
1	3380	2600	.99
2	4590	3400	.99
3	1660	2500	.88
4	2530	6000	.82
5	1740	4000	.79
6	2410	8480	.60
7	1720	6000	.40
8	4080	6000	.98
9	4570	5000	.98
10	4570	4000	.98
11	4570	3000	.99
12	4620	3000	.99
13	2250	4000	.93
14	3420	6000	.97
15	3920	8300	.96

The liquid phase velocity in the 3.5 inch pipe was calculated from the separated flow model using the void fraction as measured by the gamma densitometer. The quality is determined from an energy balance assuming saturated conditions in the test section. The string probe "noise velocity" and void fraction measurement results are shown in Figs. 22 through 28.

Air-Water Test Results. The string probes were also tested in the air-water Instrument Development Loop (IDL) which was built at ORNL to test instrumentation schemes for measurement of the mass flow across the core and upper plenum interface. These tests are regarded as a particularly good check on the ability of the string probe to measure void fraction because a low energy gamma densitometer is installed inside the vessel near the probe location. A view of the probe installed in the IDL is shown in

Fig. 21. Fig. 29 shows that both the Mod II and Mod III probes agree quite well with the local gamma densitometer in both core spray and hot leg injection tests in the IDL over a wide range of flow conditions.

SUMMARY

In summary, techniques and equipment have been developed to measure in-vessel local void fraction and velocity in a reflood transient test facility. The two impedance sensors highlighted in this report, the flag probe and the string probe, have been tested (prototype sensors) in a variety of air-water and steam-water facilities and in all cases acceptable measurement results were obtained.

Further development is needed and is continuing in the following areas:

1. Development of methods to interpret the impedance sensor void fraction and velocity measurements.
2. Quantification of the statistical and other error mechanisms.
3. Improvements in the signal analysis method to obtain void fraction, particularly for in-bundle sensors.
4. Improvements in present sensor geometries and development of others.

REFERENCES

1. Chen, Jonn C., et al, "Investigation of Post-CHF Heat Transfer for Water-Cooled Reactor Application and Development of Two-Phase Flow Instrumentation, Progress Report April 1, 1977 to June 30, 1977," LU-NUREG-PR771.
2. Chen, John C., et al, "Investigation of Post-CHF Heat Transfer for Water-Cooled Reactor Application and Development of Two-Phase Flow Instrumentation, Progress Report January 1, 1978 to March 31, 1978," LU-NUREG-PR781.
3. Bergles, A. E., "Electrical Probes for Study of Two-Phase Flow," in Two-Phase Flow Instumentation, ASME, New York, pp. 70-81, 1969.
4. Del Tin, G. and Negrini, A., "Development of the Electrical Impedance Probes for Void Fraction Measurements in Air-Water Flow," 2nd Multi-Phase Flow and Heat Transfer Symposium-Workshop, Miami Beach, Florida, April 16-18, 1979.
5. Carrard, G. and Ledwidge, T. J., "Measurements of Slip Distribution and Average Void Fraction in an Air-Water Mixture," Progress in Heat and Mass Transfer, Vol. 6, (Proceedings of the International Symposium on Two-Phase Systems 1971), Hetsroni, et al, Editor, pp. 405-418, Pergamon Press, Oxford 1972.

ORNL-DWG 79-9581

TWO-PHASE FLOW IS SENSED BY MEASURING IMPEDANCE

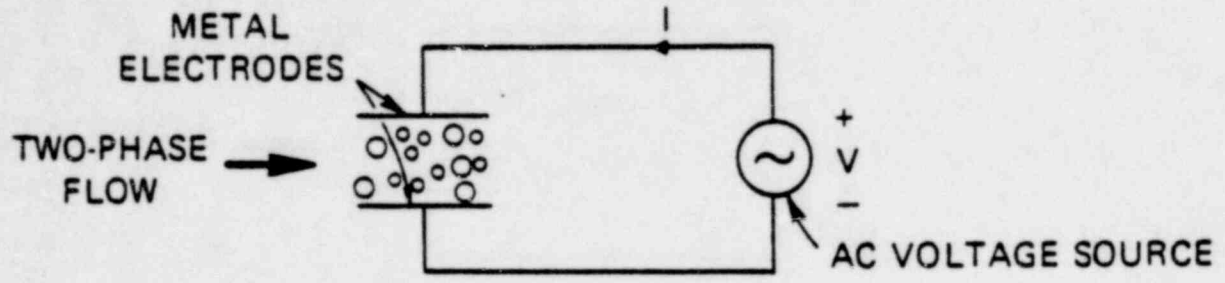

$$\text{IMPEDANCE, } Z = \frac{V}{I}$$

$$Z = R + \frac{1}{jwC}$$

$$R = f(\text{CONDUCTIVITY, GEOMETRY})$$

$$C = f(\text{PERMITTIVITY, GEOMETRY})$$

Fig. 1

ORNL-DWG 79-9579

TWO-PHASE FLOW VELOCITY IS MEASURED BY ANALYSIS OF RANDOM SIGNALS FROM TWO PROBES

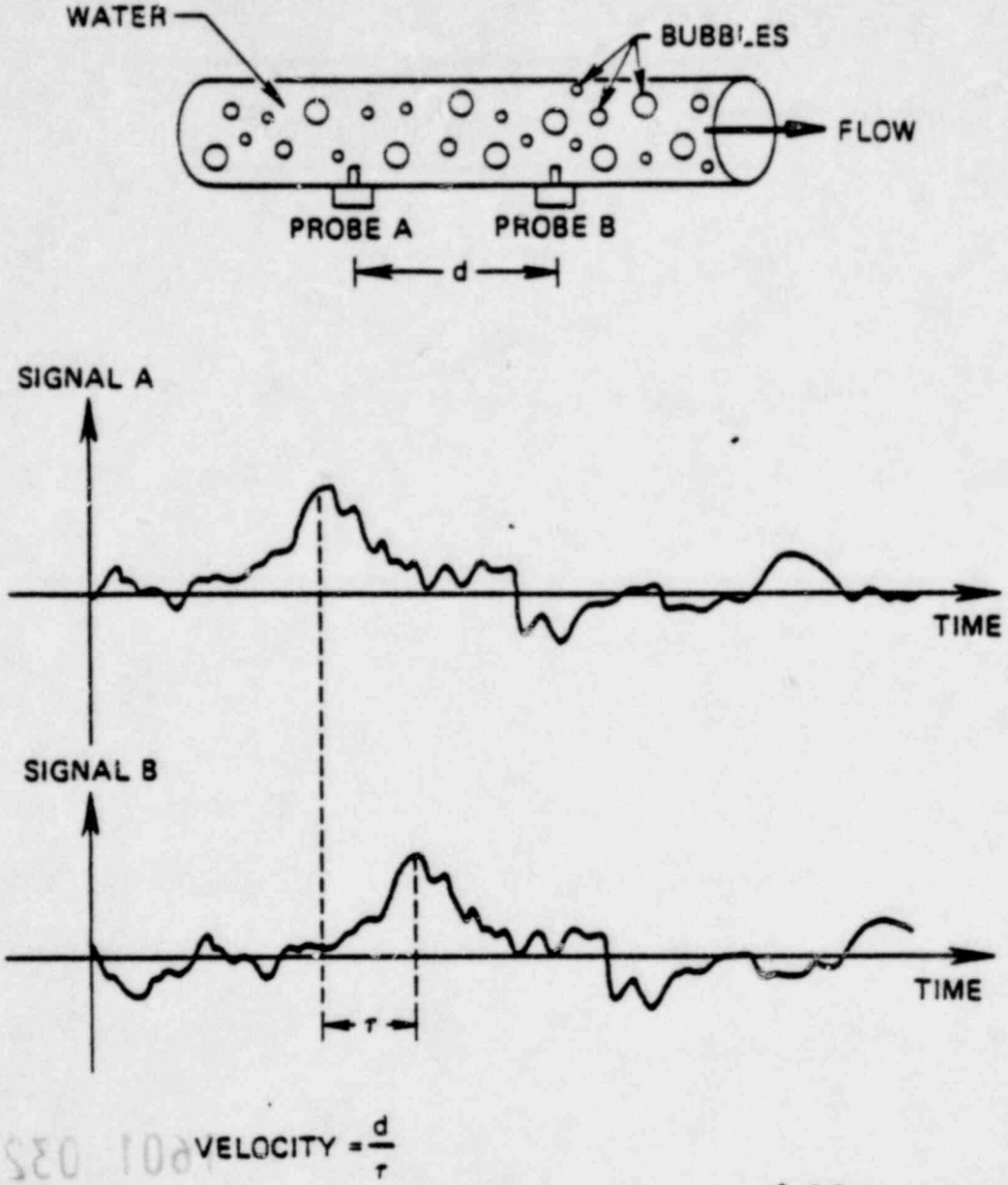

Fig. 2

TIME DELAY BETWEEN SIGNALS IS CALCULATED FROM THE TRANSFER FUNCTION FROM SIGNAL A TO SIGNAL B

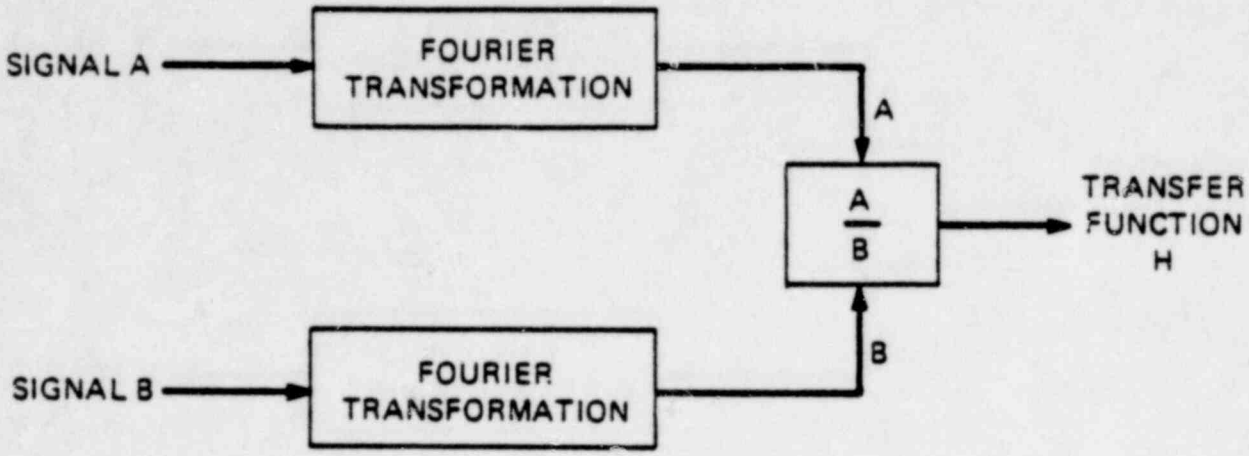

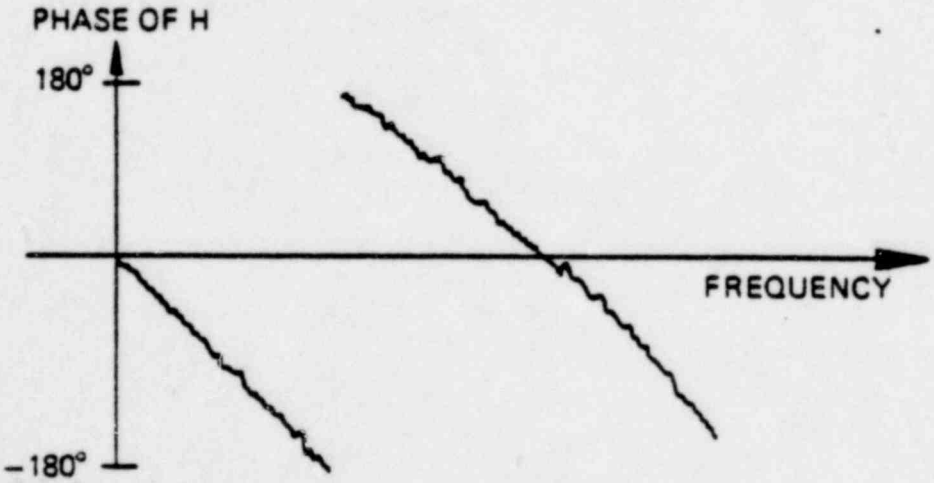

$d/df[\text{PHASE OF } H] = -\tau$

Fig. 3

ORNL-DWG 79-9581

THE RELATIONSHIP BETWEEN IMPEDANCE AND
VOID FRACTION DEPENDS ON THE "FLOW REGIME"

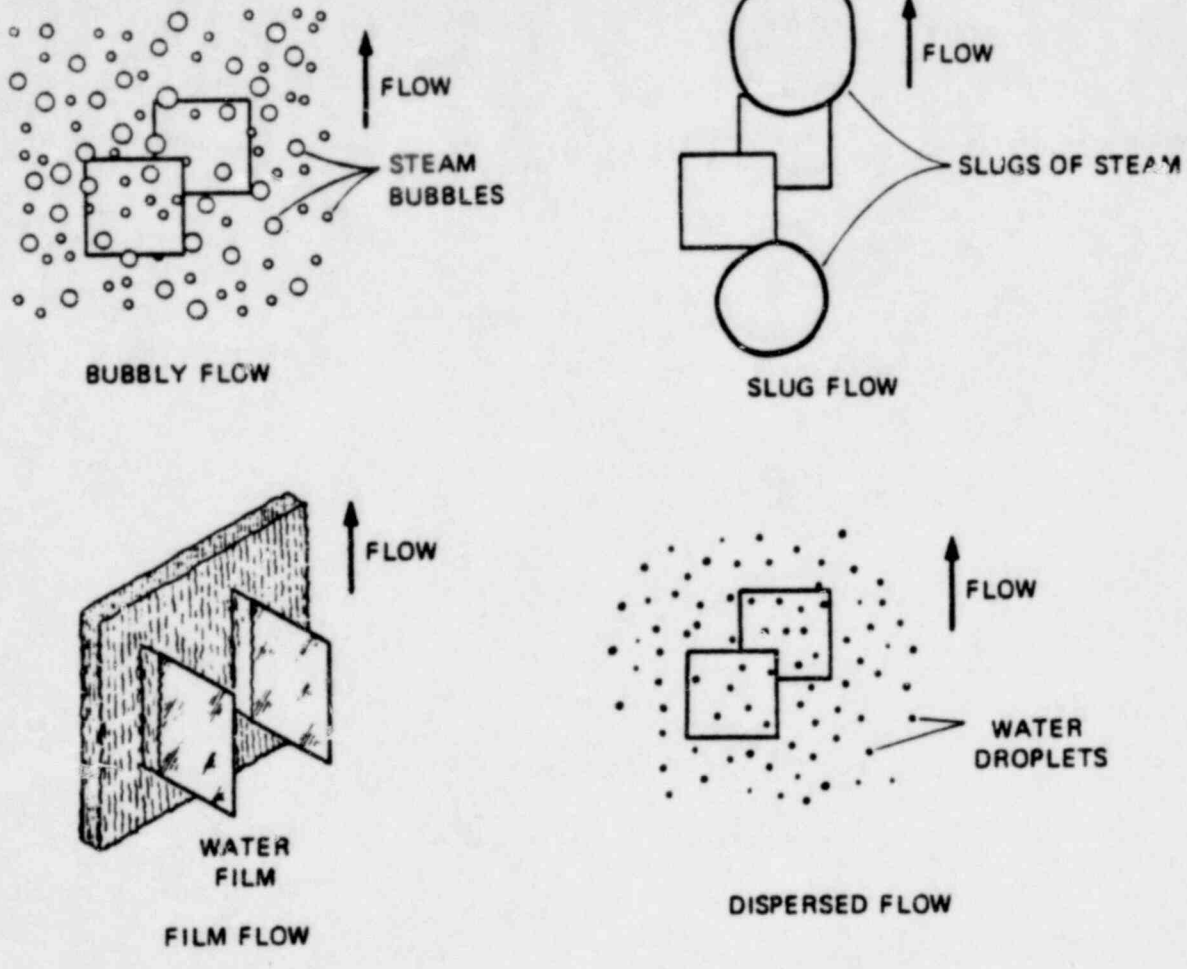

Fig. 4

1601 035

ORNL–DWG 79-9583

FOR THE AIRS "FLAG" PROBE THE CAPACITANCE VARIATION WITH VOID FRACTION IS SIGNIFICANTLY DIFFERENT FOR DIFFERENT FLOW REGIMES

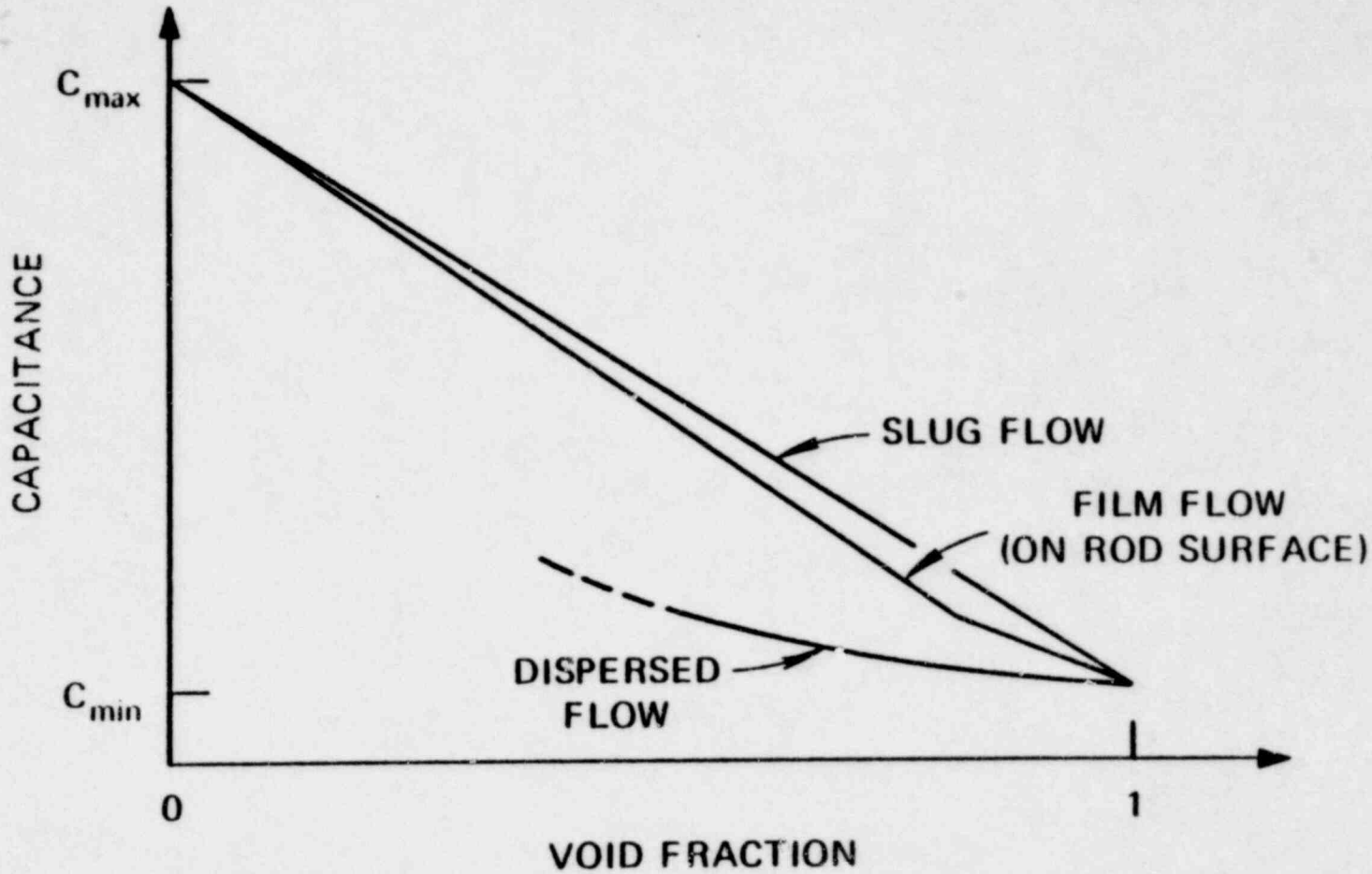

Fig. 5

ornl
10/30/79

DATA PROCESSING METHODS FOR TRANSIENT VELOCITY AND VOID FRACTION ARE SUBJECT TO THE FOLLOWING CONSTRAINTS

* BETWEEN DATA POINTS STEADY STATE CONDITIONS ARE ASSUMED TO EXIST.

* TIME STEPS BETWEEN DATA POINTS MUST BE SHORT ENOUGH TO RESOLVE A REFLOOD TRANSIENT.

* TIME STEPS BETWEEN DATA POINTS MUST BE LONG ENOUGH TO REDUCE THE STATISTICAL ERRORS TO AN ACCEPTABLE VALUE.

Fig. 6

ORNL-DWG 78-16899

A VARIETY OF SENSOR CONFIGURATIONS ARE UNDER DEVELOPMENT

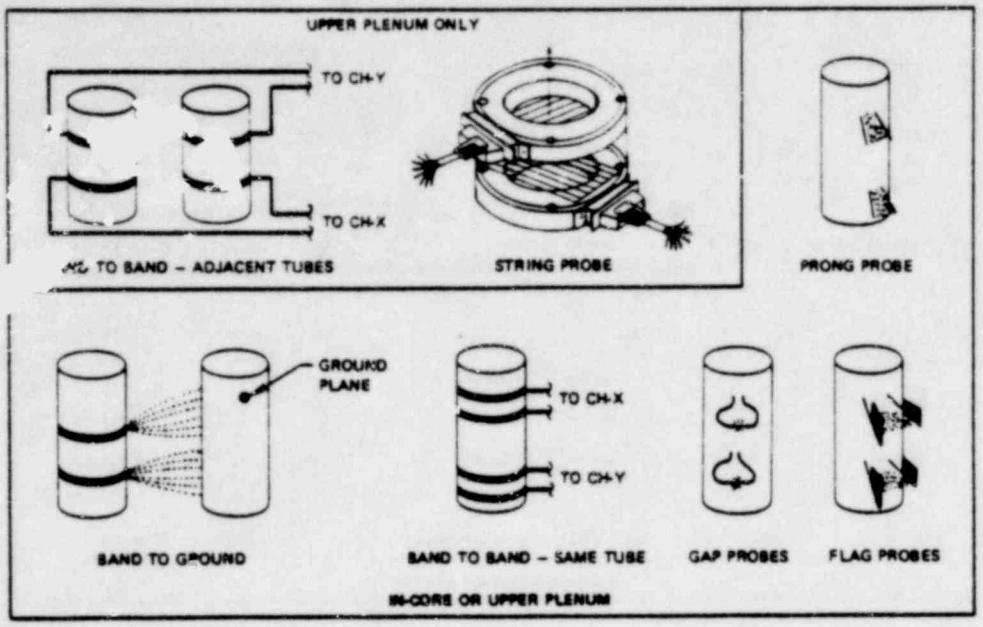

2/8/78

ornl

Fig. 7

ORNL-DWG 78-19763

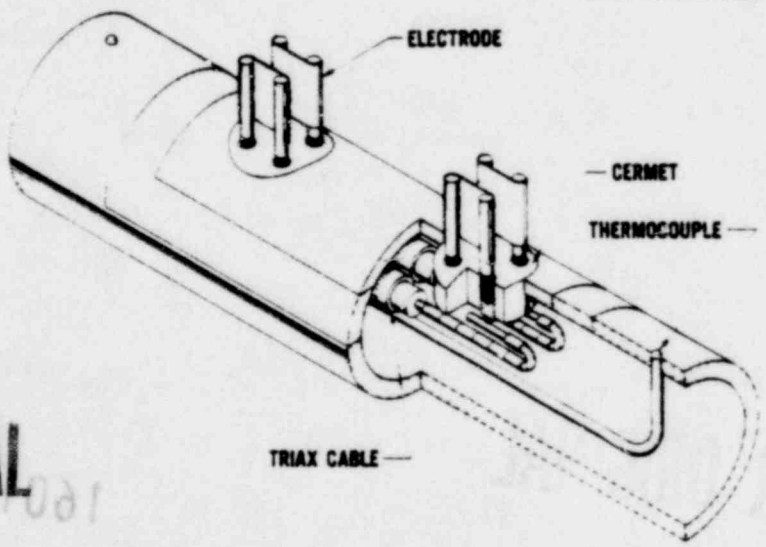

In-Core Guide Tube
Impedance Measurement Assembly
Flag Probe Sensor

10/24/78

ornl

Fig. 8

ORNL–DWG 78-19802

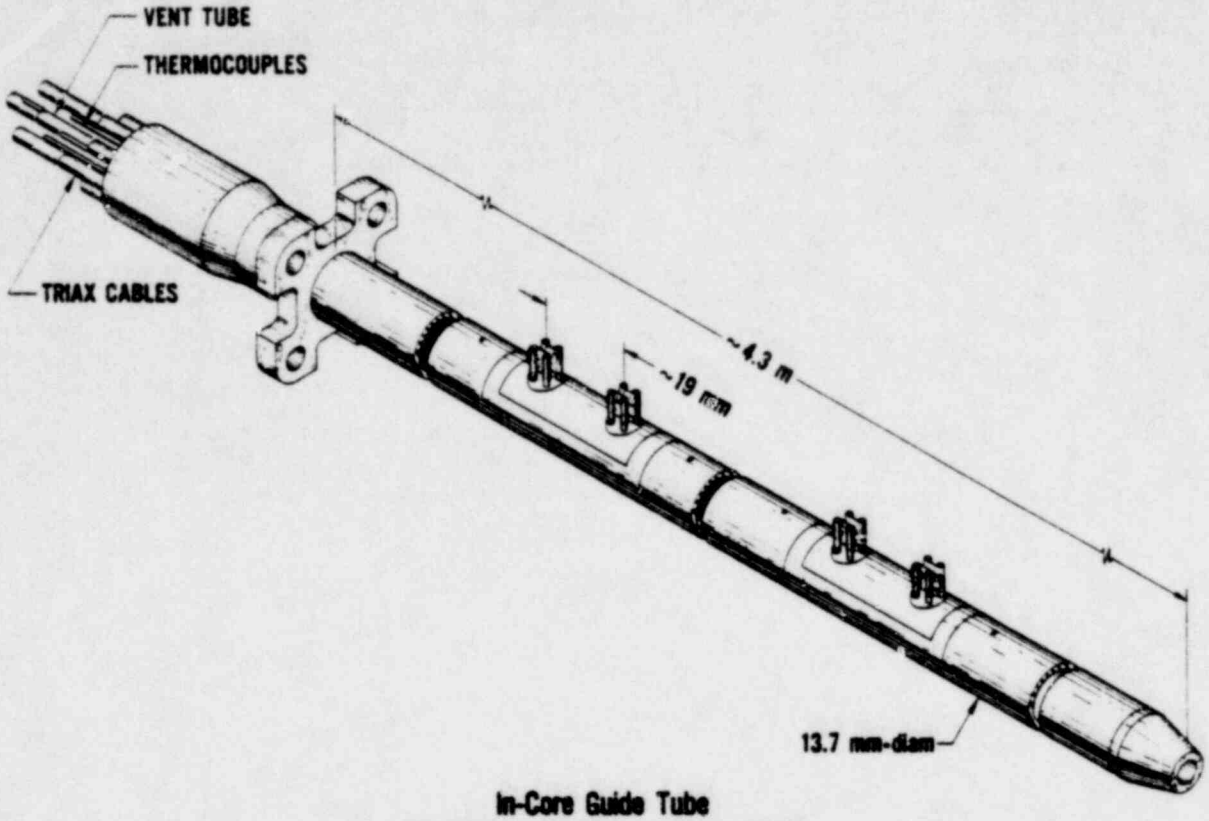

In-Core Guide Tube
Impedance Measurement Assembly
Flag Probe Type

10/24/78

ornl

Fig. 9

LOCATIONS OF THE IMPEDANCE AND OTHER SENSORS IN THE 9-ROD BUNDLE TEST FACILITY
(ALL DIMENSIONS IN MILLIMETERS)

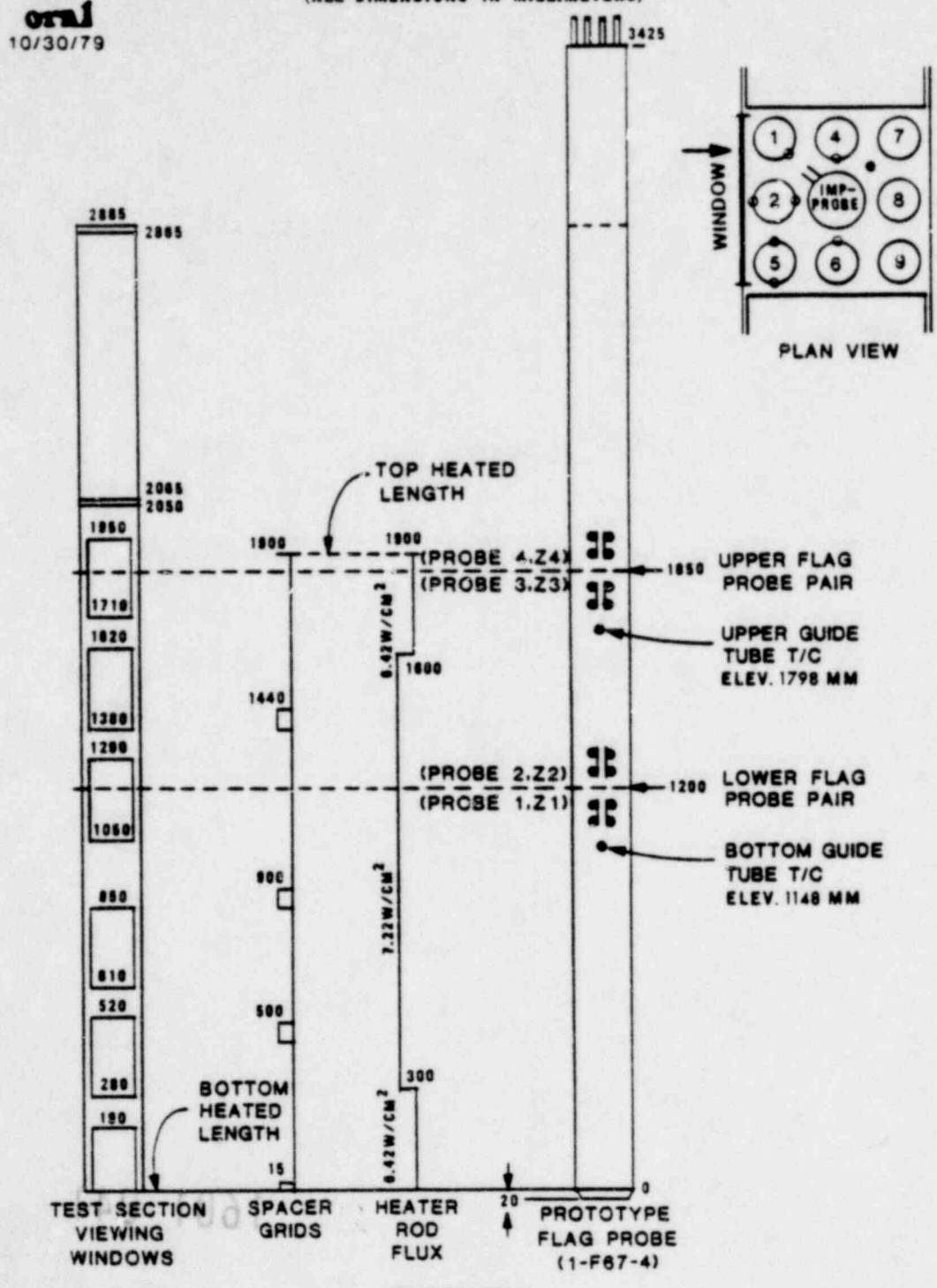

Fig. 10

ornl
10/30/79

A PROTOTYPE FLAG PROBE WAS TESTED IN THE 3X3 ROD BUNDLE FACILITY TO DETERMINE OPERABILITY AND SURVIVABILITY

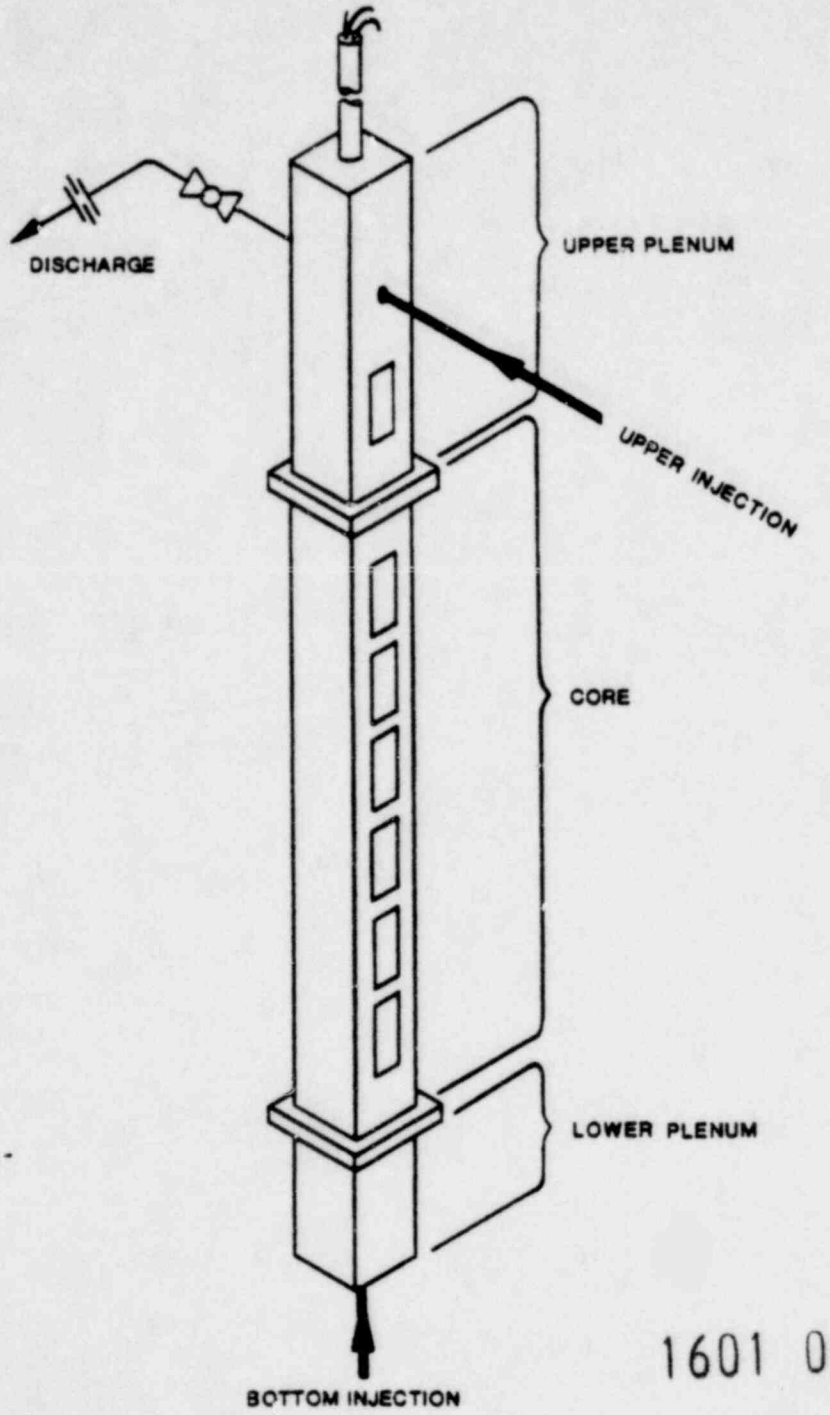

1601 041

Fig. 11

TIMING OF QUENCH OF VARIOUS SENSORS--TEST #2

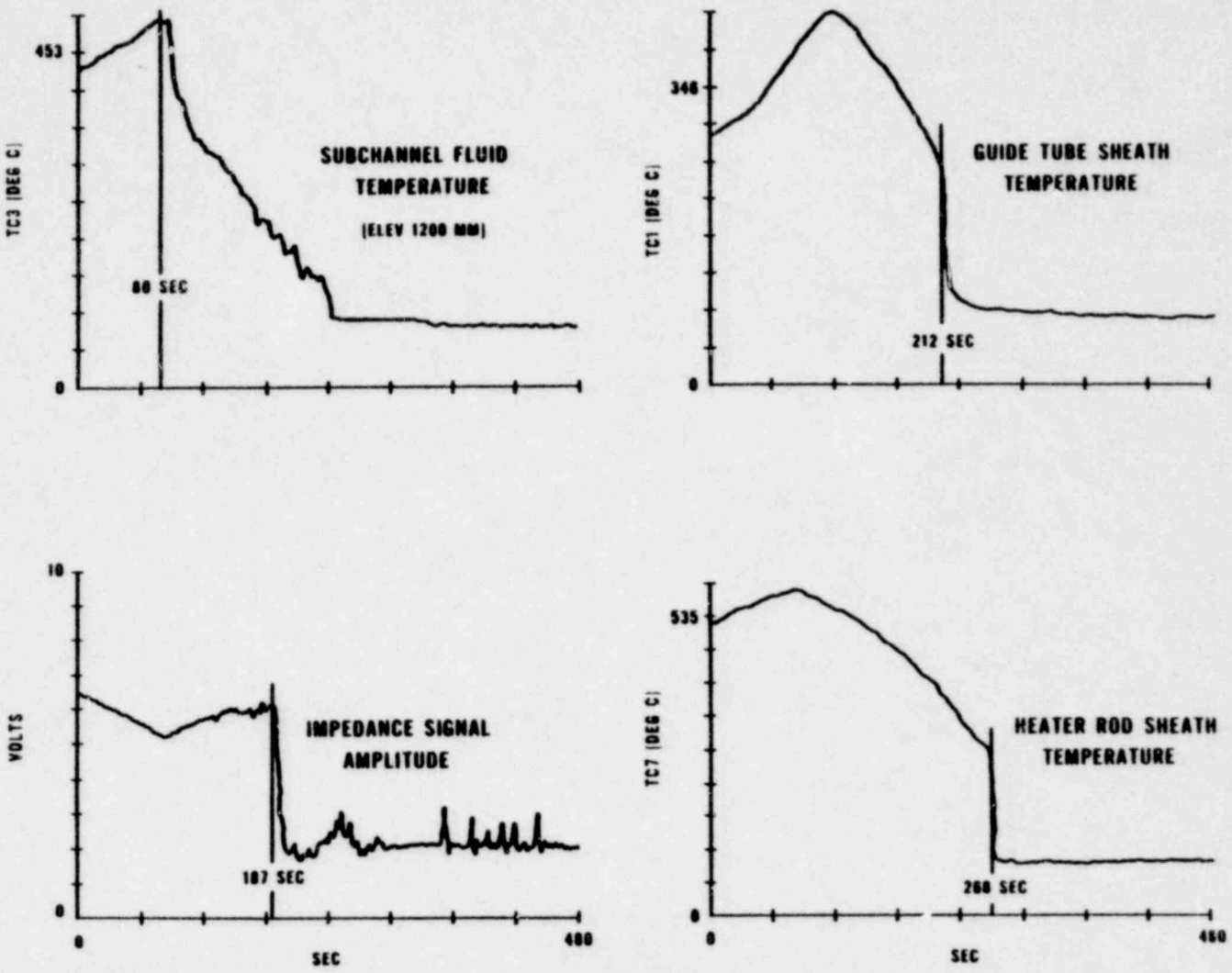

Fig. 12

ornl
10/30/79

TIMING OF QUENCH OF PROTOTYPE FLAG PROBES RELATIVE TO THE HEATER RODS IN THE 3x3 ROD BUNDLE INDICATES THAT IMPEDANCE MEASUREMENTS CAN BE MADE FOR THE MAJOR PORTION OF THE REFLOOD TEST PERIOD.

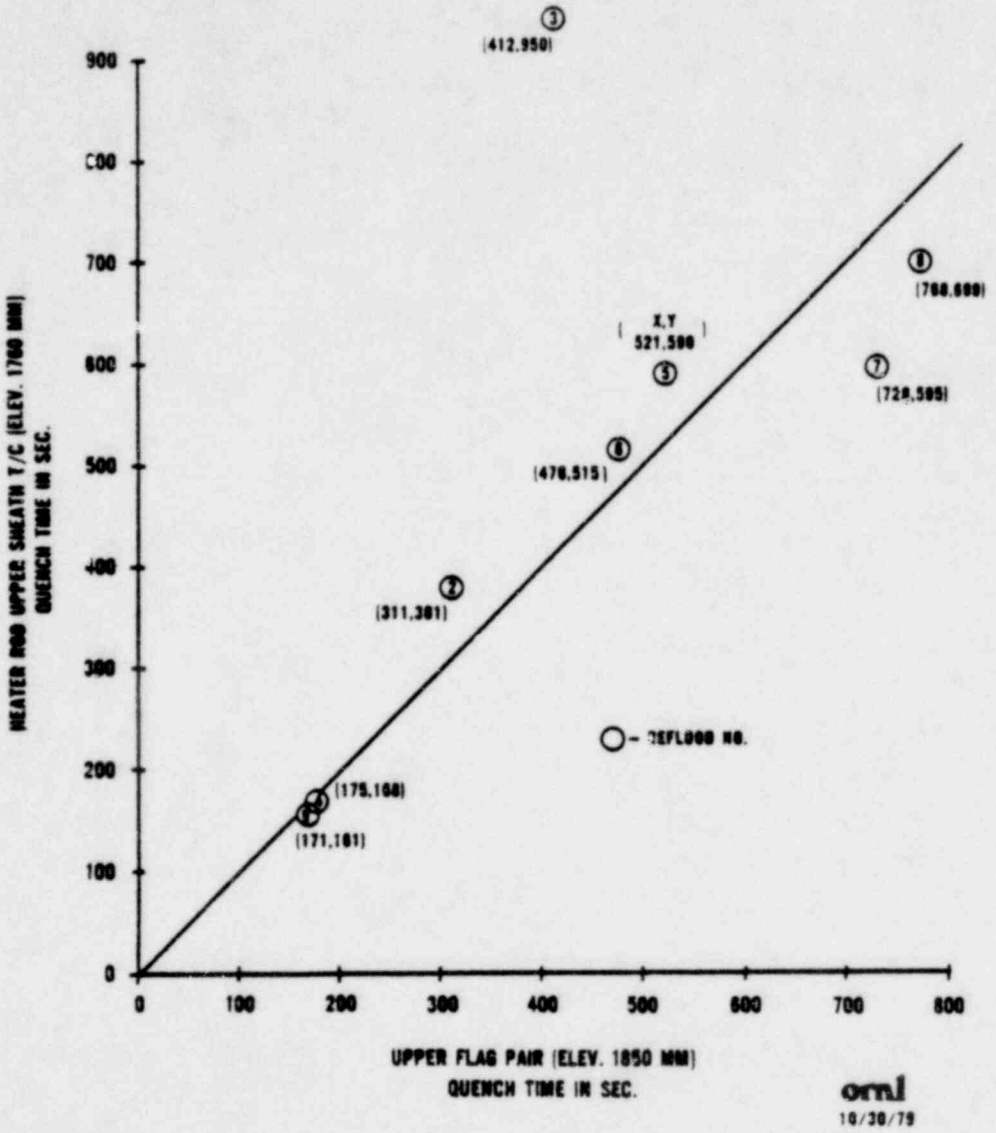

Fig. 13

1601 043

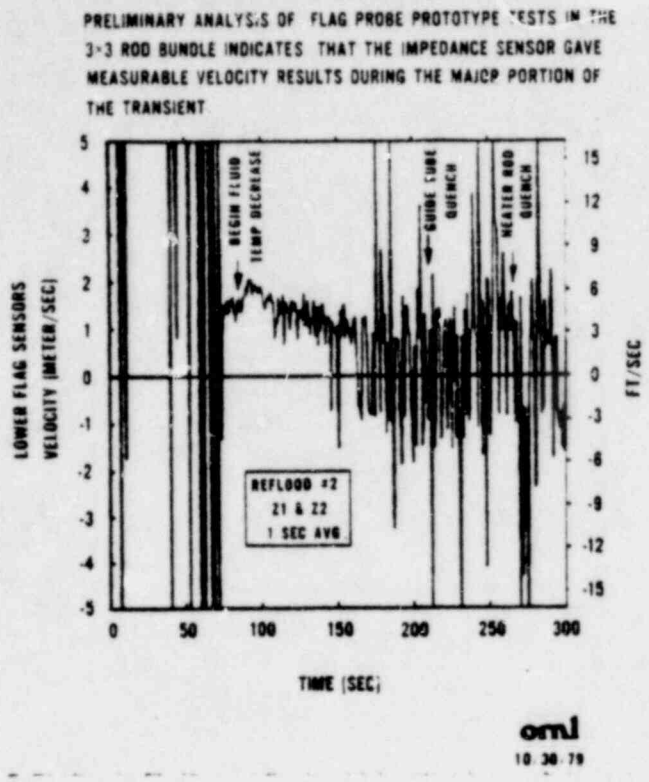

Fig. 14

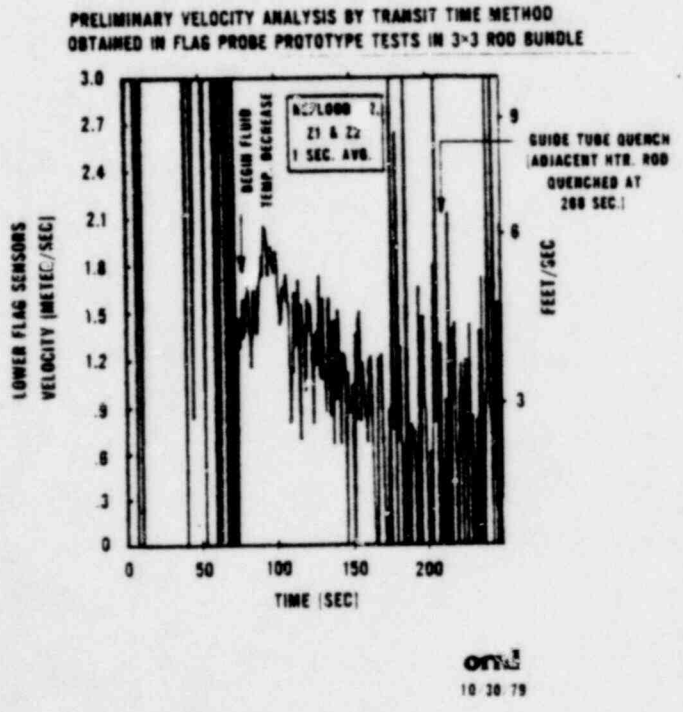

Fig. 15

FLAG PROBE MEASURED VELOCITY AGREED WELL WITH INDEPENDENTLY ESTIMATED VELOCITY OF FREE- FALLING DROPLETS (TIME-AVERAGED VOID FRACTION 0.988 TO 0.995)

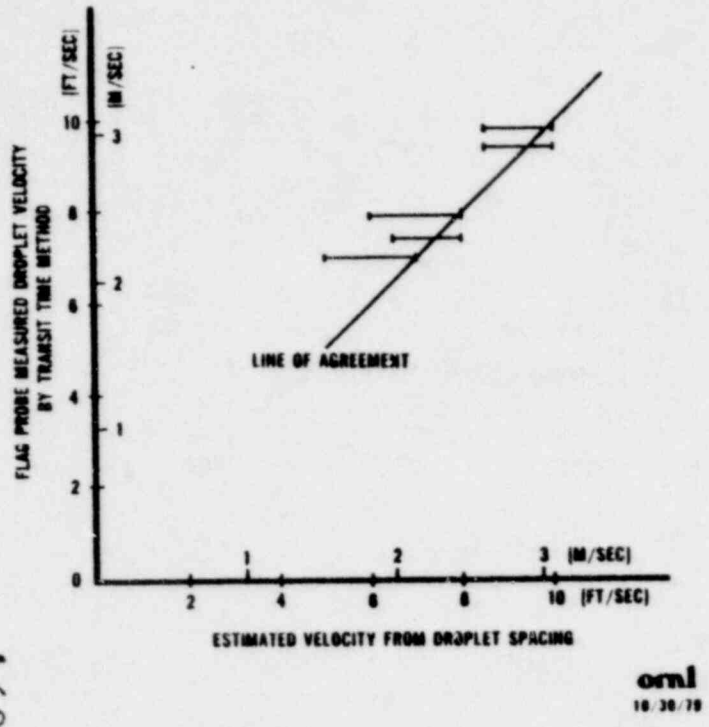

orni
10/30/78

Fig. 16

ORNL DWG 78-8272

orni

A VARIETY OF UPPER PLENUM AND IN-BUNDLE INSTRUMENTS TESTED TO DATE

UPPER PLENUM

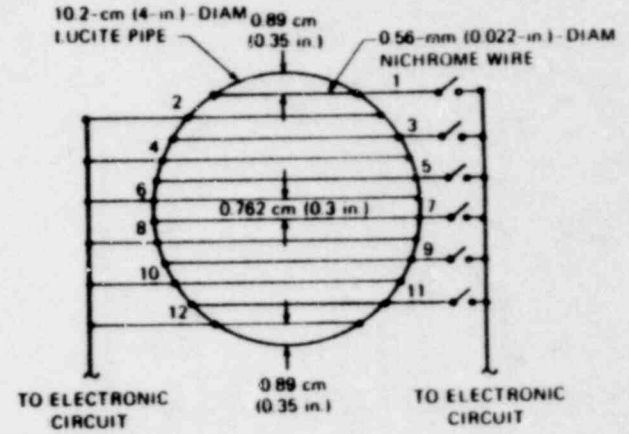

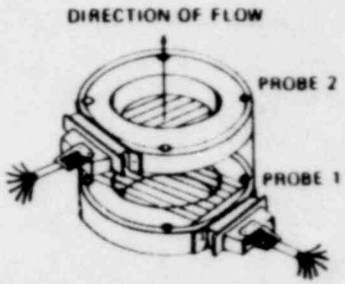

Fig. 17

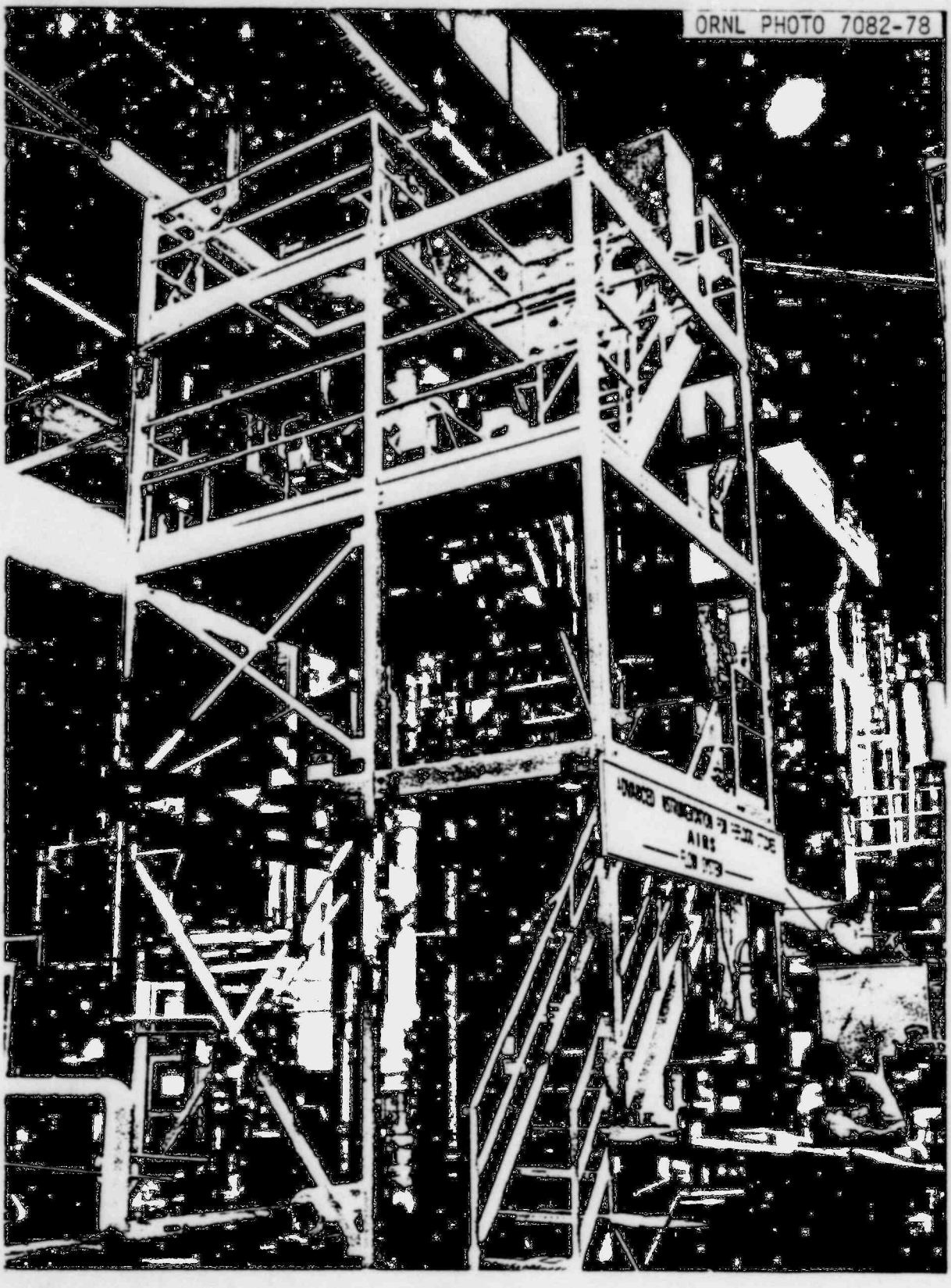

Fig. 18

ornl
10/30/79

CONFIGURATION FOR STEAM/WATER TESTING OF STRING PROBES

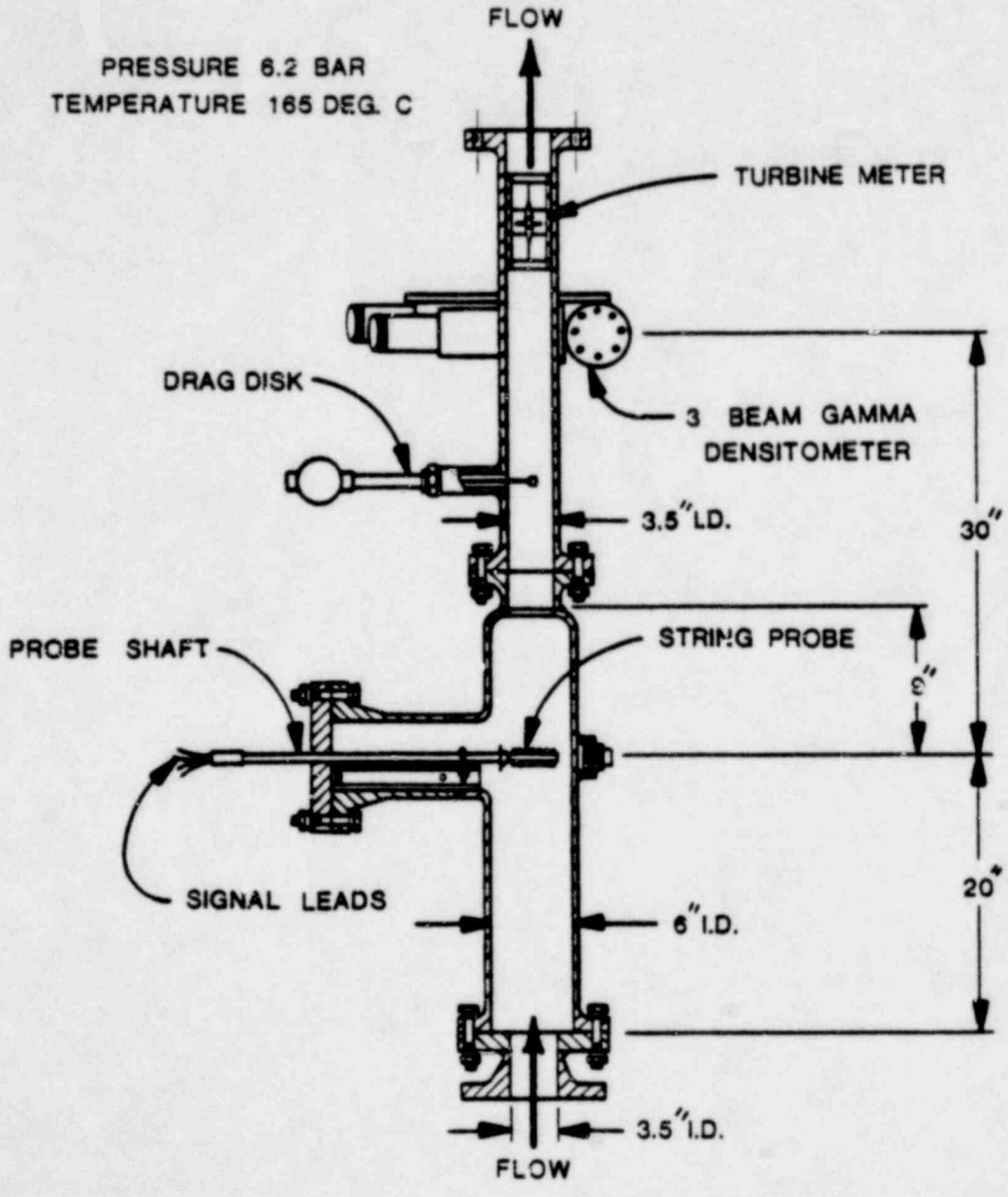

Fig. 19

1601 047

ORNL-PHOTO 2720-79

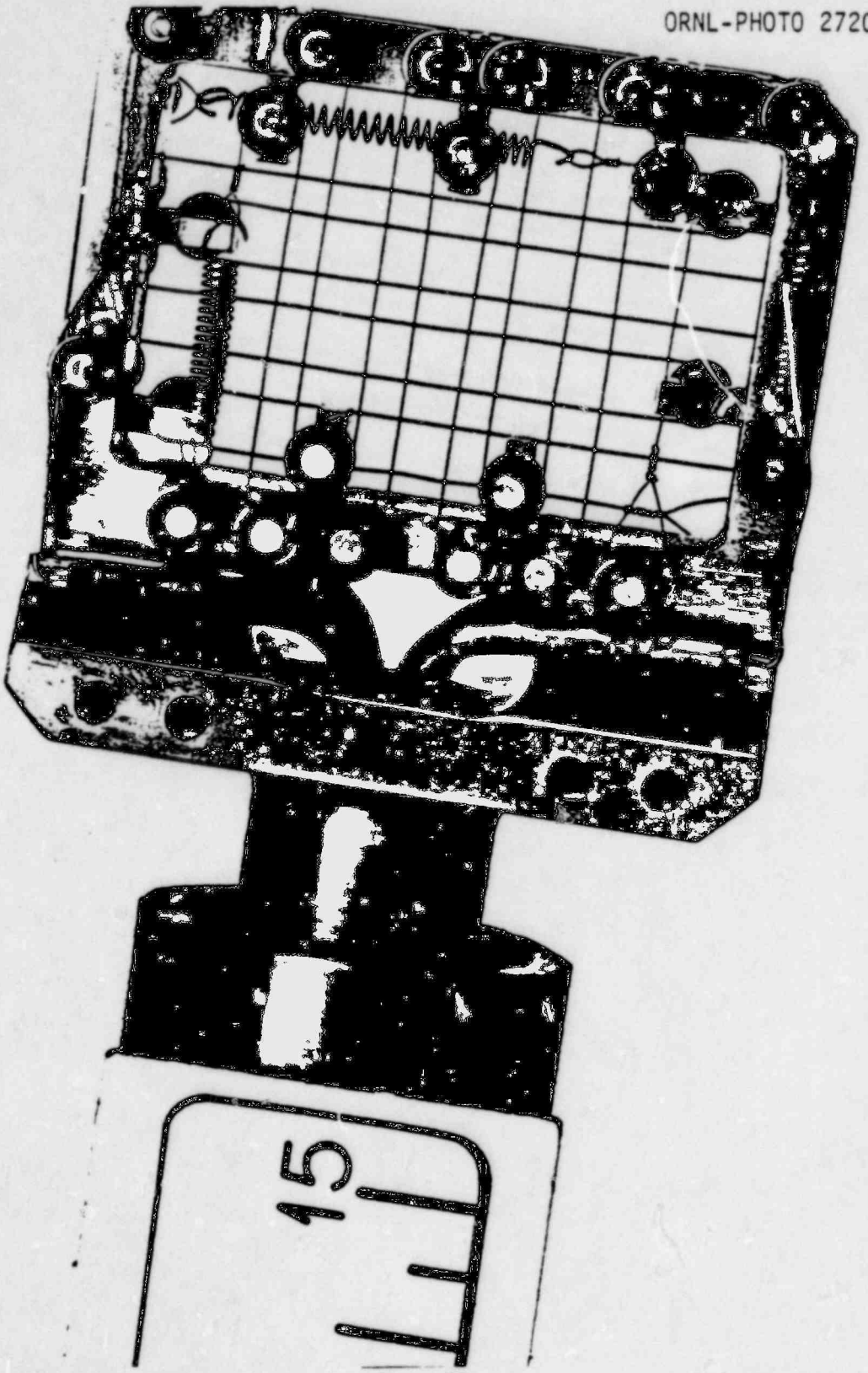

Fig. 20

Fig. 21

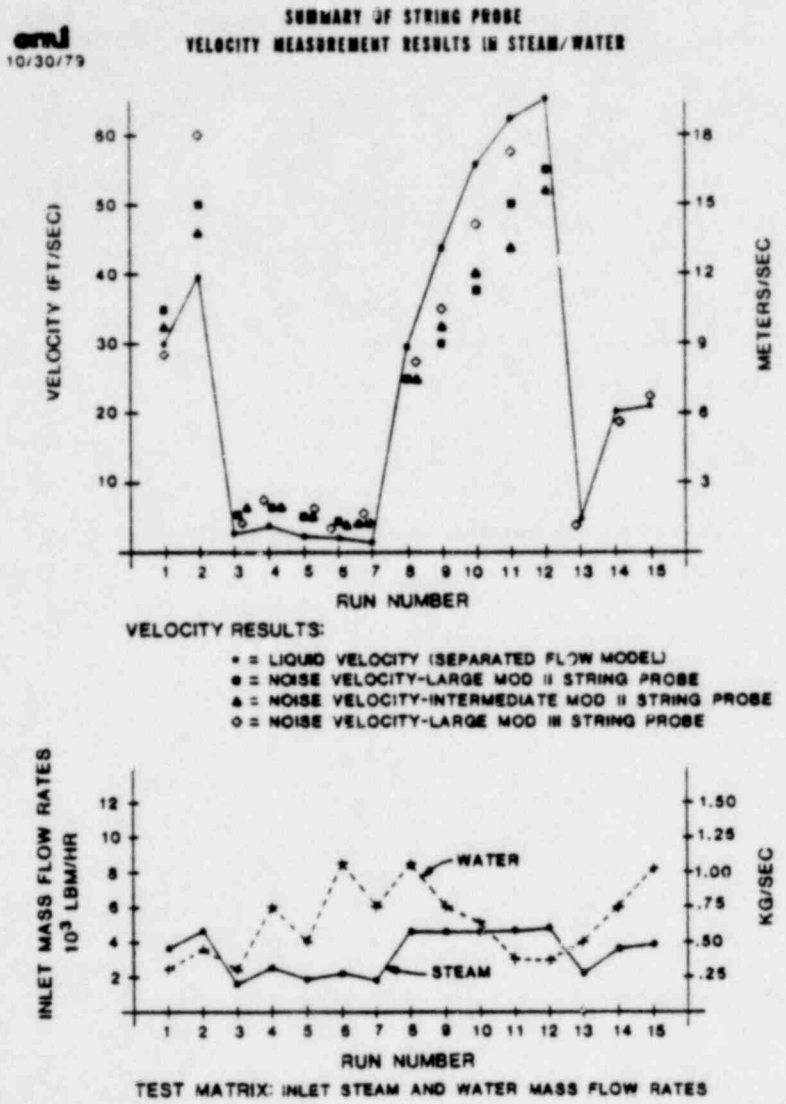

Fig. 22

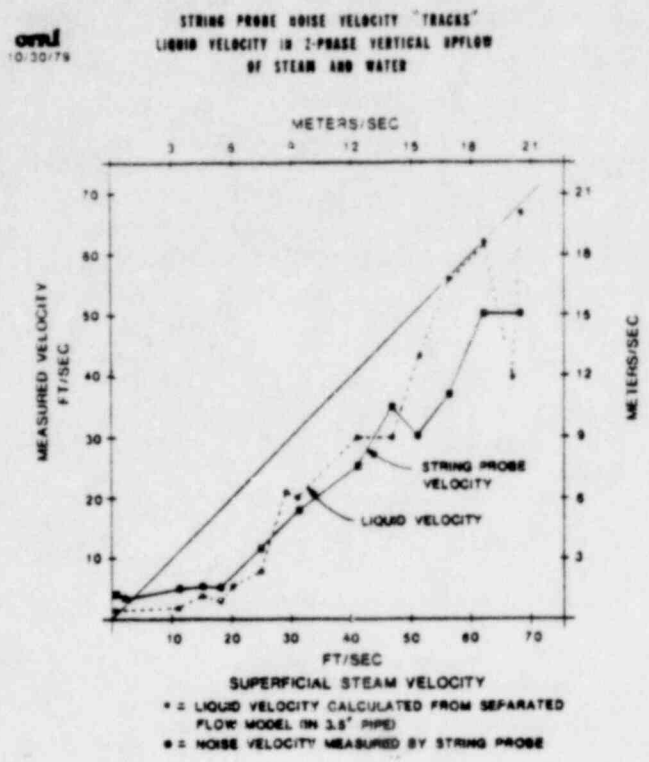

Fig. 23

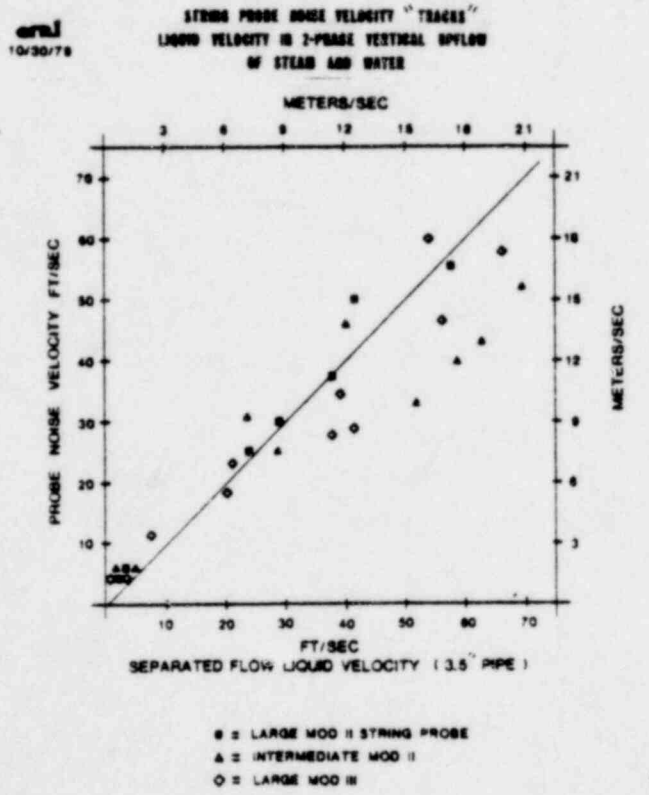

1601 051

Fig. 24

STRING PROBE VOID FRACTION MEASUREMENT BY RELATIVE ADMITTANCE METHOD IN HIGH VOID FRACTION STEAM-WATER VERTICAL UPFLOW SHOWS GOOD AGREEMENT WITH GAMMA DENSITOMETER VOID FRACTION.

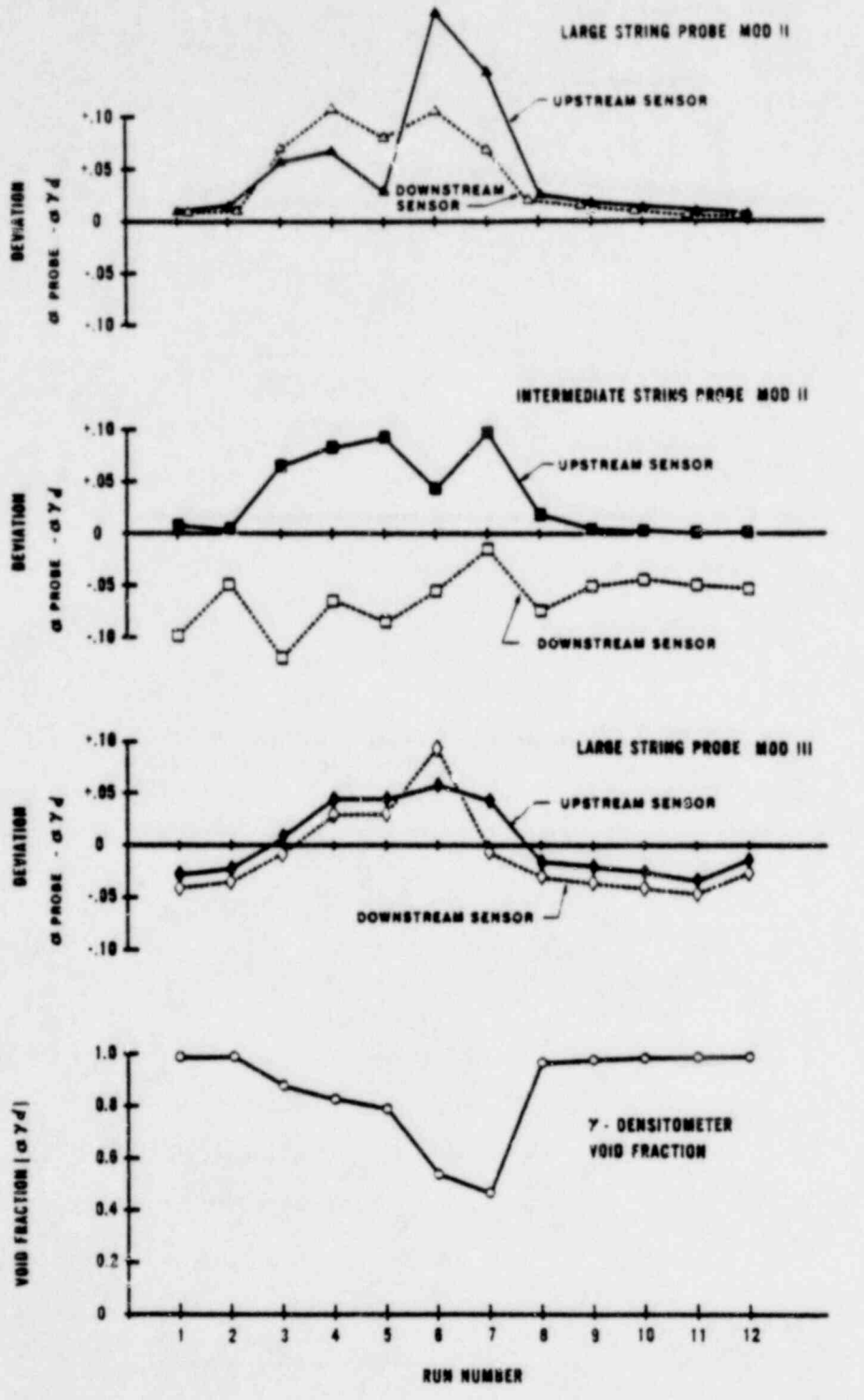

ornl
10/30/79

Fig. 25

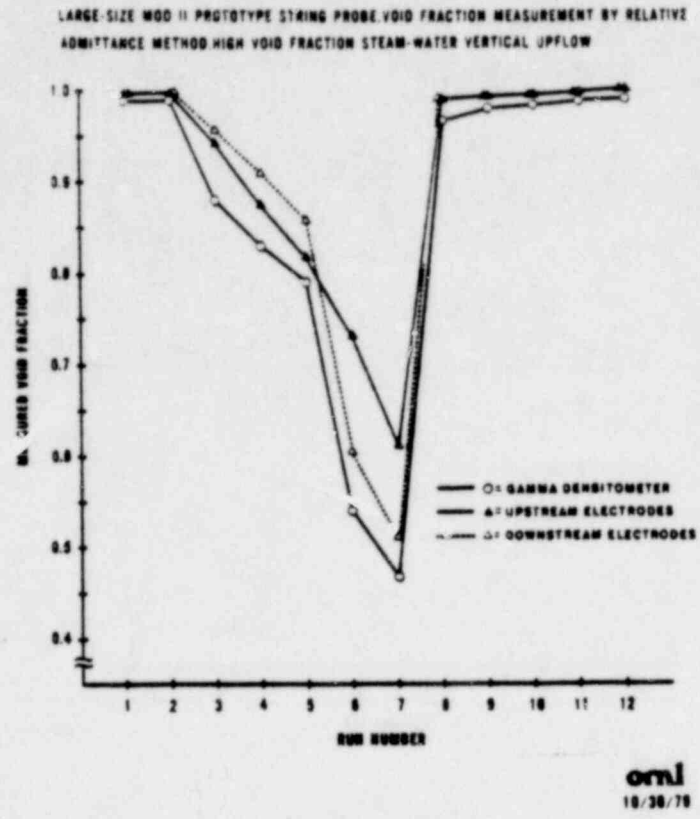

Fig. 26

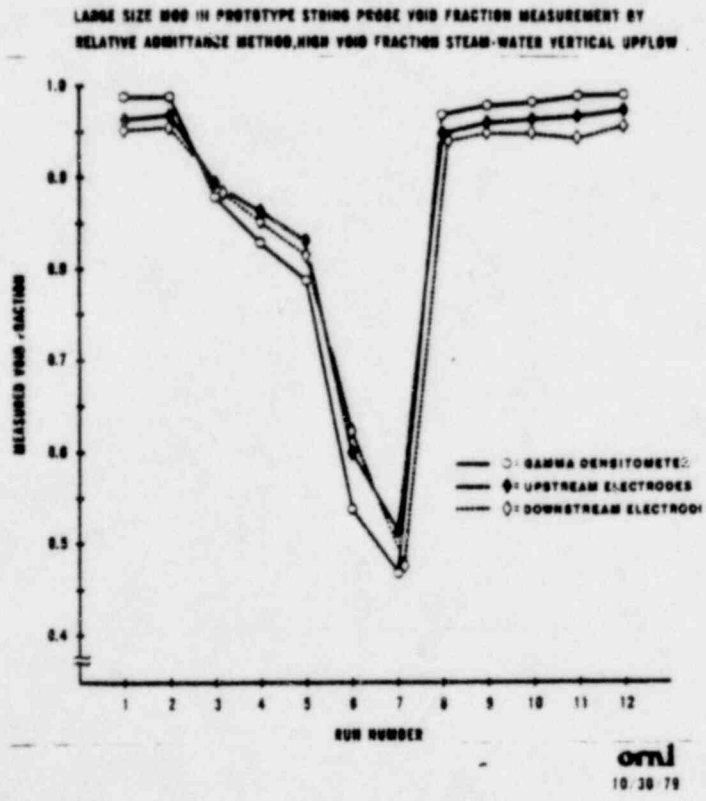

Fig. 27

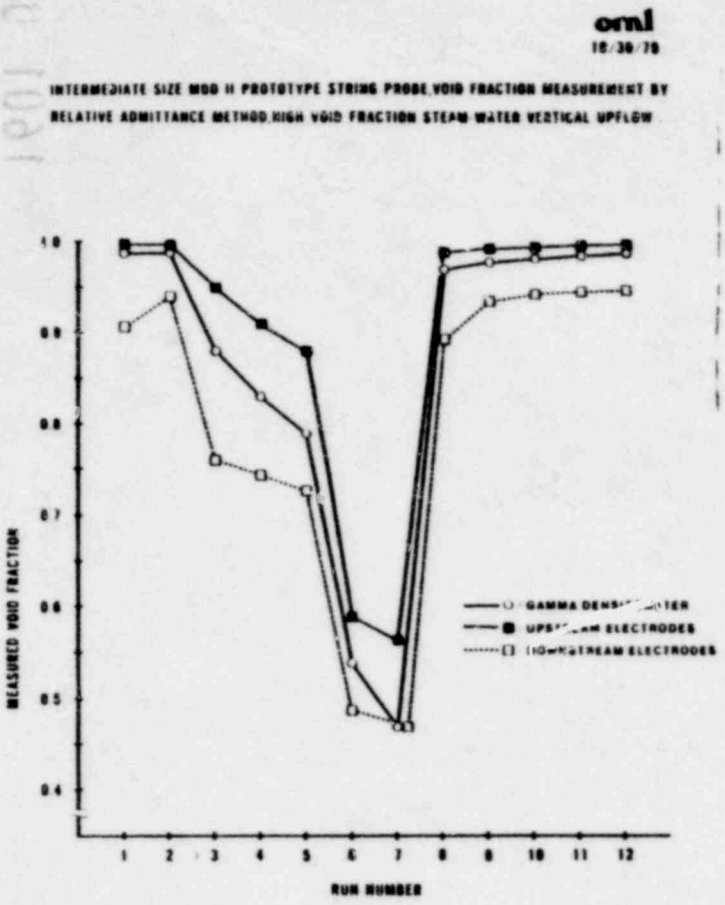

Fig. 28

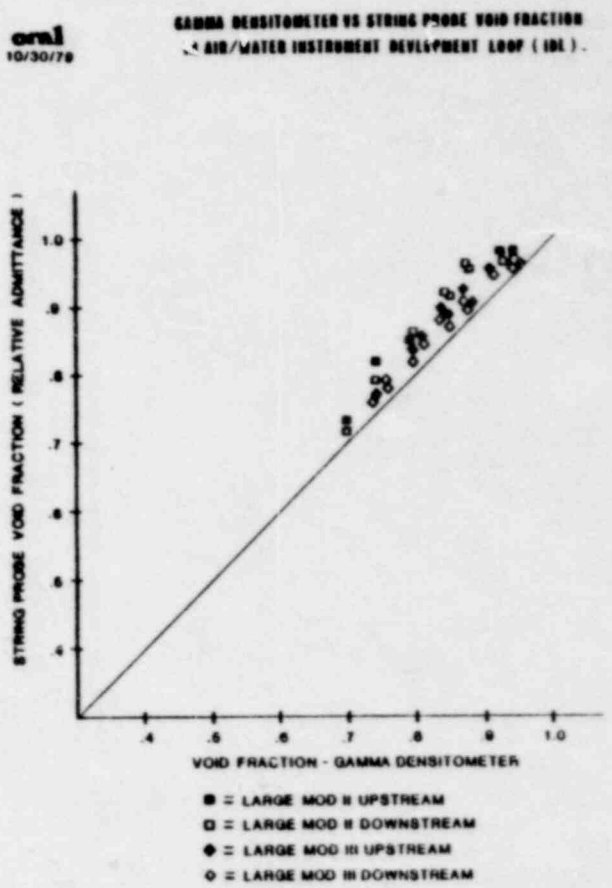

Fig. 29

ornl
10/30/79

SUMMARY

- IN-VESSEL LOCAL IMPEDANCE SENSORS
  - -TRANSIT TIME VELOCITY
  - -VOID FRACTION
- FLAG PROBE RESULTS
  - -PRELIMINARY RESULTS ENCOURAGING IN REFLOOD ENVIRONMENT
  - -SUCCESSFUL DROPLET VELOCITY MEASUREMENT AT VERY HIGH VOID FRACTION
- STRING PROBE RESULTS
  - -EXCELLENT AGREEMENT WITH GAMMA DENSITOMETER
  - -"TRACKS" LIQUID VELOCITY
- DEVELOPMENT CONTINUING
  - -INTERPRETATION
  - -ERROR ANALYSIS
  - -SIGNAL ANALYSIS METHODOLOGY
  - -SENSORS

Fig. 30

ADVANCED SPOOL PIECE DEVELOPMENT AND SIGNAL ANALYSIS*

K. G. Turnage and C. F. Davis

Oak Ridge National Laboratory
Oak Ridge, TN 37830

Presented at the Seventh Water Reactor Safety Research Information Meeting, November 5, 1979

Gaithersburg, Maryland

---

*Research sponsored by Division of Reactor Safety Research, U.S. Nuclear Regulatory Commission under Interagency Agreements DOE 40-551-75 and 40-552-75 with the U.S. Department of Energy under contract W-7405-eng-26 with the Union Carbide Corporation.

Advanced Spool Piece Development and Signal Analysis

Flow measurements in loss-of-coolant experiments are often derived from data obtained with turbine meters, drag flowmeters and gamma attenuation densitometers, which may be located on a short piping segment called a spool piece. This paper describes experiments performed at ORNL using air-water and steam-water two-phase flow facilities to evaluate improved instrumented spool pieces and to develop techniques for measuring two-phase flow parameters, including mass flux. As another part of the effort to understand the behavior of spool piece and impedance-type reflood instrumentation, signal analysis studies were performed in the air-water and steam-water loops with conductivity probes obtained from Canadian General Electric and Atomic Energy of Canada Limited (AECL).

The instrumented spool piece used in the air-water studies incorporates several design improvements: (1) the upstream drag flowmeter (normal flow direction), the densitometer, and the turbine are located within 46 cm (18 in.) of each other, (2) location of a drag flowmeter on either end allows one drag meter to always be upstream of the turbine in case of bidirectional flow, (3) the "full-flow" turbine rotor and drag flowmeter targets used sample the fluid flow in the pipe to within 3.2 mm (0.125 in.) of the pipe wall, and (4) fast response, high sensitivity turbine monitor electronics developed at ORNL were used with the turbine meter. The spool piece was tested with two-phase horizontal flow, vertical downflow and vertical upflow. Superficial velocities ranged from 0.3 to 38 m/sec (1 to 128 ft/sec) for air and from 0.1 to 5 m/sec (0.3 to 17 ft/sec) for water; all flow regimes were included.

Comparisons of data calculated using three mass flow models with the spool piece instrumentation to the actual two phase mass fluxes have suggested the following (ρ_a = density from densitometer, V_t = turbine speed and I_d = drag flowmeter reading):

1. $G_1 = \rho_a V_t$ and $G_2 \sqrt{\rho_a I_d}$ are reliable at relatively low void fractions, but tend to seriously overpredict the correct mass flux at high void fractions.
2. $G_3 = I_d/V_t$ gave reasonable results for nearly all flow rates and was clearly the best model at higher void fractions.
3. Steam water spool piece tests, limited to vertical upflow at void fractions above 50%, tend to confirm indications regarding instrument performance observed in the air-water loop. That is, of the models tried, $G_3 = I_d/V_t$ is the most accurate mass flux model for use at high void fractions.

Two types of local conductivity probes were tested in vertical upflow in the ORNL air-water loop, concurrently with the spool piece testing. The AECL velocity probes, positioned along the pipe center line, gave cross correlation velocities which generally agreed with the turbine speed in the bubble, slug and froth flow regimes. The turbine velocity was higher in annular flow. Composite void fractions obtained with the five-point void fraction probe always agreed with the void fraction from the densitometer within 20% of reading. Radial void profiles obtained with the void probe were characteristic of particular flow regimes and generally had a symmetric shape about the pipe axis.

For the steam-water tests, a salt solution was injected into the liquid input stream so that liquid phase conductivity in the test section would be adequate for probe operation (k_ℓ must be $\gtrsim$ 40 μs for adequate signal-to-noise ratio with the signal analysis method used). Results obtained with the five

point void fraction probe in the steam-water tests were difficult to interpret, largely due to variations in the water conductivity during the tests. Cross correlation with the velocity probe in steam-water flow was successful, however. The indicated probe velocities, for the most part, approximated the mean liquid phase velocities determined with the aid of gamma densitometer measurements.

References

1. K. G. Turnage, et al., Advanced Two-Phase Instrumentation Program Quarterly Progress Report for April-June 1978, ORNL/NUREG/TM-279 (January 1979).

2. K. G. Turnage, et al., Advanced Two-Phase Instrumentation Program Quarterly Progress Report for July-September 1978, ORNL/NUREG/TM-309 (May 1979).

3. K. G. Turnage, et al., Advanced Two-Phase Flow Instrumentation Program Quarterly Progress Report for October-December 1978, ORNL/NUREG/TM-313 (May 1979).

4. K. G. Turnage and C. E. Davis, "An Improved Spool Piece for LOCE Blowdown Flow Measurements," ANS Transactions, Vol. 32, pp. 813-14 (June 1979).

5. K. G. Turnage, et al., Advanced Two-Phase Flow Instrumentation Program Quarterly Progress Report for January-March 1979, ORNL/NUREG/TM-331 (September 1979).

6. K. G. Turnage, et al., Advanced Two-Phase Flow Instrumentation Program Quarterly Progress Report for April-June 1979, ORNL/NUREG/TM- (in press).

TWO-PHASE FLOW MEASUREMENTS WITH ADVANCED INSTRUMENTED SPOOL PIECES AND LOCAL CONDUCTIVITY PROBES

K. G. TURNAGE

- AIR-WATER TESTING WITH ADVANCED SPOOL PIECE 1
- STEAM-WATER SPOOL PIECE TESTING
- SIGNAL ANALYSIS STUDIES USING AECL CONDUCTIVITY PROBES

ORNL-DWG 79-12578

UNION CARBIDE ORNL

EXPERIMENTAL EQUIPMENT

THE SPOOL PIECE TESTED INCORPORATES SEVERAL DESIGN IMPROVEMENTS

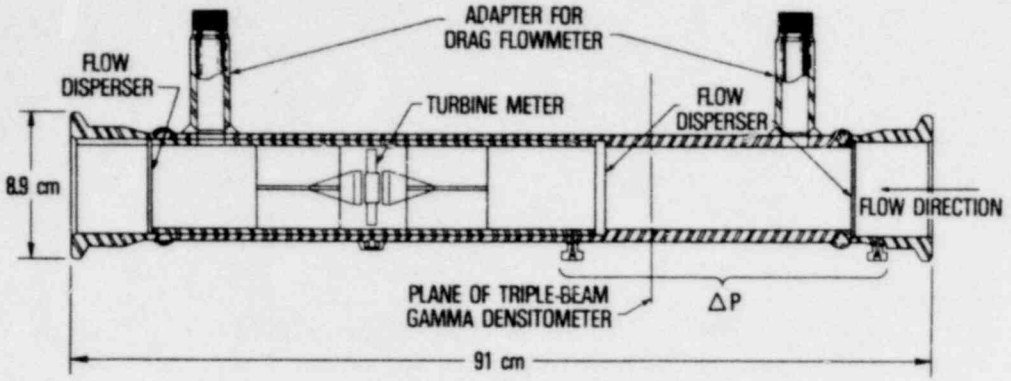

- THREE PRIMARY INSTRUMENTS LOCATED WITHIN 46 cm OF EACH OTHER
- TWO DRAG FLOWMETERS
- FULL-FLOW DRAG BODIES
- FAST-RESPONSE TURBINE METER ELECTRONICS

ORNL-DWG 79-12582

UNION CARBIDE ORNL

EXPERIMENTAL EQUIPMENT

THE SPOOL PIECE WAS TESTED IN TWO-PHASE HORIZONTAL FLOW, DOWNFLOW, AND UPFLOW IN THE ORNL AIR-WATER LOOP

1601 061

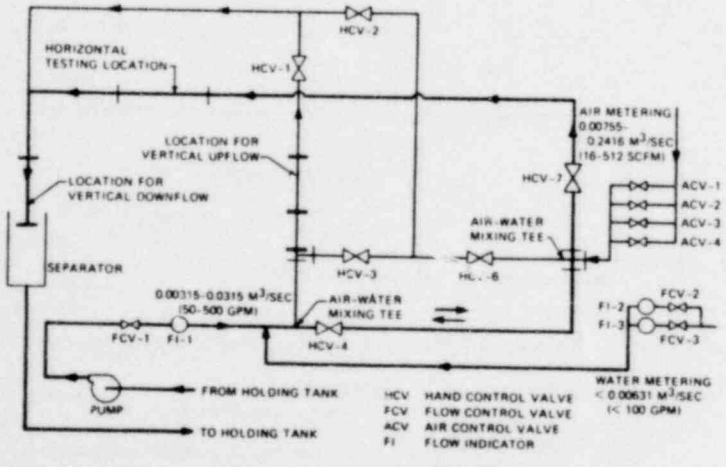

ORNL-DWG 79-12575

UNION CARBIDE ORNL

EXPERIMENTAL METHODS

THE AIR AND WATER FLOW RATES USED FOR THE HORIZONTAL TESTS PRODUCED SEVERAL TWO-PHASE FLOW REGIMES

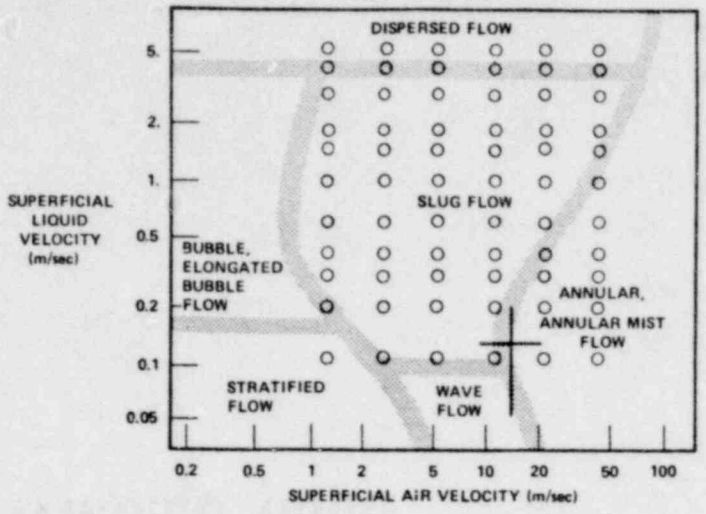

FLOW REGIME MAP OF MANDHANE AND AZIZ (1974)

ORNL-DWG 79-12576

UNION CARBIDE ORNL

EXPERIMENTAL METHODS

THE AIR AND WATER FLOW RATES USED FOR THE VERTICAL DOWNFLOW TESTS PRODUCED MANY FLOW REGIMES

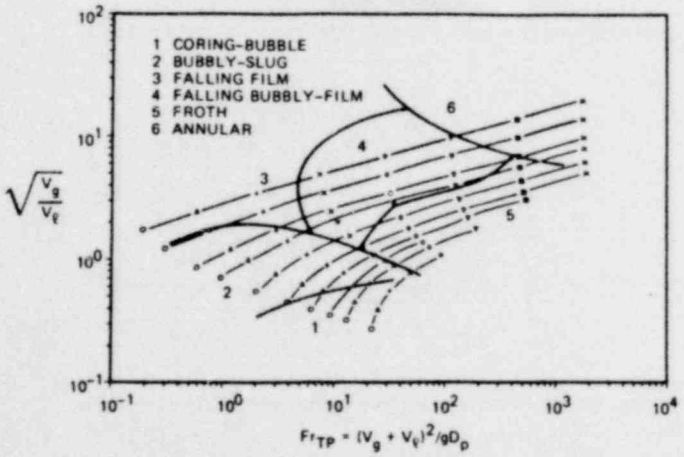

FLOW REGIME MAP OF OSHINOWO AND CHARLES (1974)

1601 062

UNION CARBIDE ORNL

ANALYSIS METHODS

USING THE IMPROVED TURBINE ELECTRONICS, AIR-WATER SPOOL PIECE DATA WERE USED TO EVALUATE THREE TURBINE MODELS

- VOLUMETRIC
  $V_t = \alpha V_g + (1 - \alpha)\, V_f$
- AYA
  $C_f \rho_f\, (1 - \alpha)(V_t - V_f)^2 = C_g \rho_g\, \alpha (V_g - V_t)^2$
- ROUHANI
  $C_f \rho_f\, (1 - \alpha)\, V_f\, (V_t - V_f) = C_g \rho_g\, \alpha V_g\, (V_g - V_t)$

UNION CARBIDE ORNL

RESULTS

IN HORIZONTAL TWO-PHASE FLOW, THE AYA AND THE ROUHANI MODELS ACCURATELY PREDICT THE TURBINE VELOCITY. THE VOLUMETRIC MODEL DOES POORLY

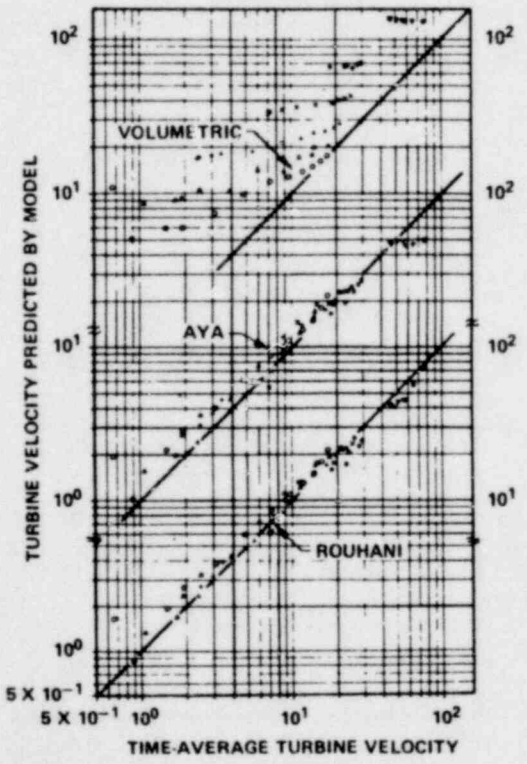

IN AIR-WATER VERTICAL UPFLOW, THE AYA AND THE ROUHANI MODELS PREDICT THE TURBINE SPEED WELL, EXCEPT AT HIGH GAS FLOW RATES WITH LOW LIQUID FLOW RATES. THE VOLUMETRIC MODEL OVERESTIMATES THE TURBINE VELOCITY.

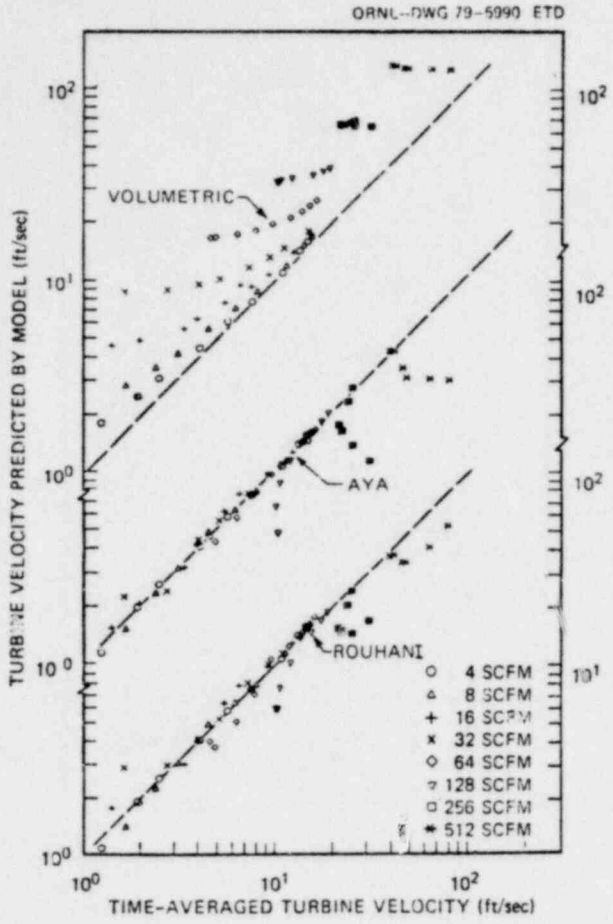

ORNL-DWG 79-12724

UNION CARBIDE ORNL

RESULTS

IN VERTICAL DOWNFLOW, THE AYA AND THE ROUHANI MODELS ADEQUATELY PREDICT TURBINE VELOCITY, WHEN $S > 0.75$. WHEN $S < 0.75$, THE VOLUMETRIC MODEL PERFORMS BEST

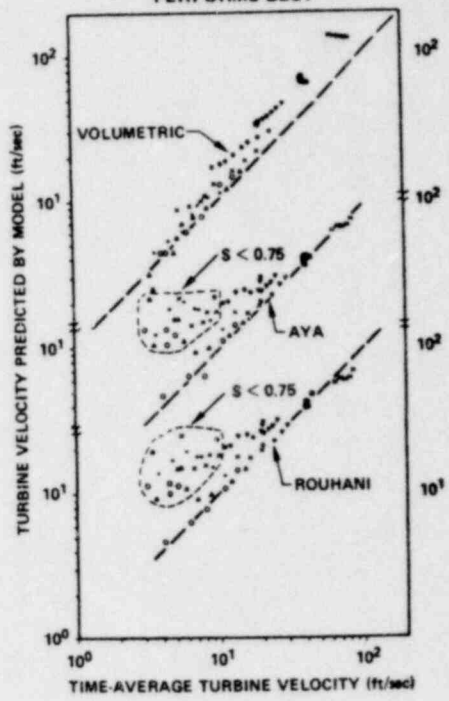

UNION CARBIDE ORNL

ANALYSIS METHODS

THE DRAG FLOWMETER READINGS WERE COMPARED TO TWO-VELOCITY MOMENTUM FLUXES DETERMINED USING THE METERED INPUT FLOW RATES Q_f AND Q_g, THE MEASURED VOID FRACTIONS α AND THE RECORDED TURBINE VELOCITIES V_t

$$\rho\hat{V}^2 = (1 - \alpha)\rho_f V_f^2 + \alpha\rho_g V_g^2$$

$$\alpha = \alpha_a \text{ (FROM DENSITOMETER)}$$

METHOD 1: V_f AND V_g ARE $f(\alpha, Q_f, Q_g)$

METHOD 2: V_f AND V_g ARE $f(V_t, Q_f, Q_g)$

ORNL-DWG 79-12723

UNION CARBIDE ORNL

RESULTS

AIR-WATER TESTS WITH THE FULL FLOW DRAG TARGETS SUGGEST THAT THE TARGETS' C_D's IN TWO-PHASE FLOW ARE LESS THAN THE C_D's IN SINGLE PHASE FLOW

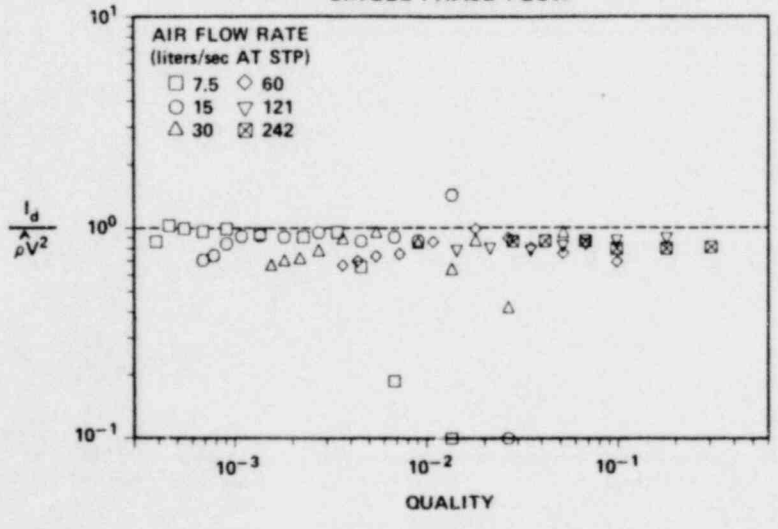

ORNL–DWG 79-12720

UNION CARBIDE ORNL

RESULTS

THE MASS FLOW MODEL $G_1 = \rho_a V_t$ INCREASINGLY OVERPREDICTS THE CORRECT MASS FLUX AT HIGH VOID FRACTION

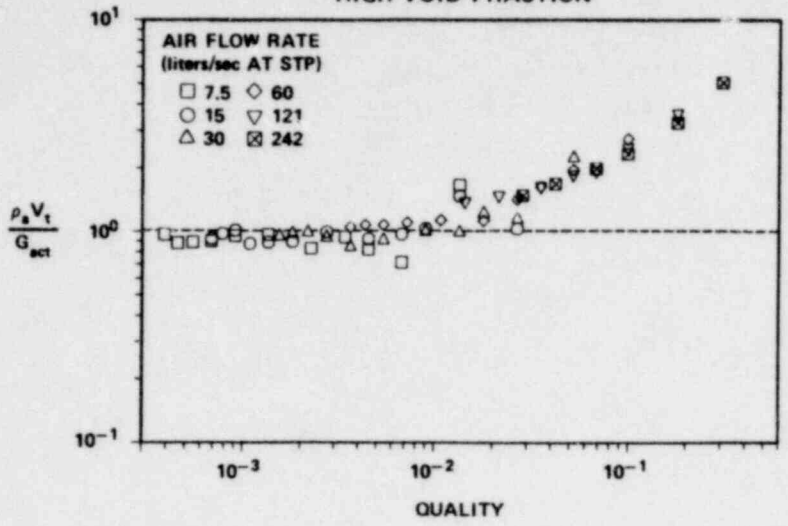

ORNL–DWG 79-12722

UNION CARBIDE ORNL

RESULTS

THE MEAN TURBINE VELOCITY INCREASINGLY EXCEEDS THE MEAN LIQUID-PHASE VELOCITY AT HIGH VOID FRACTIONS

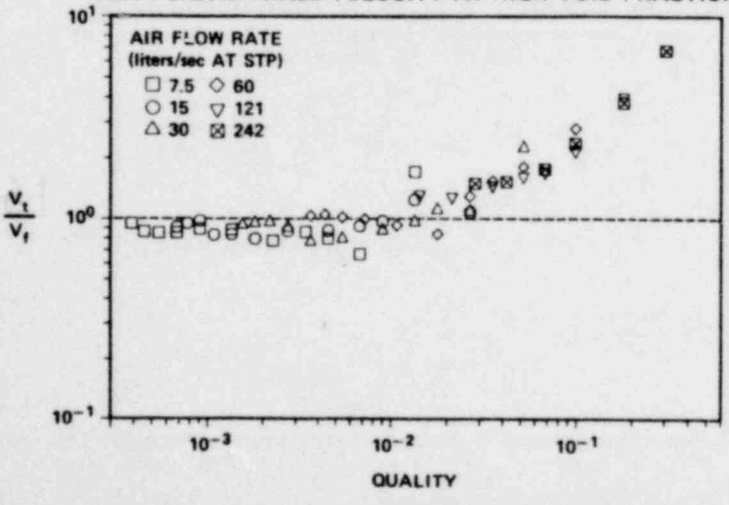

UNION CARBIDE ORNL

RESULTS

THE MASS FLOW MODEL $G_2 = \sqrt{\rho_s I_d}$ TENDS TO OVERPREDICT THE TRUE MASS FLUX AT HIGH VOID FRACTIONS

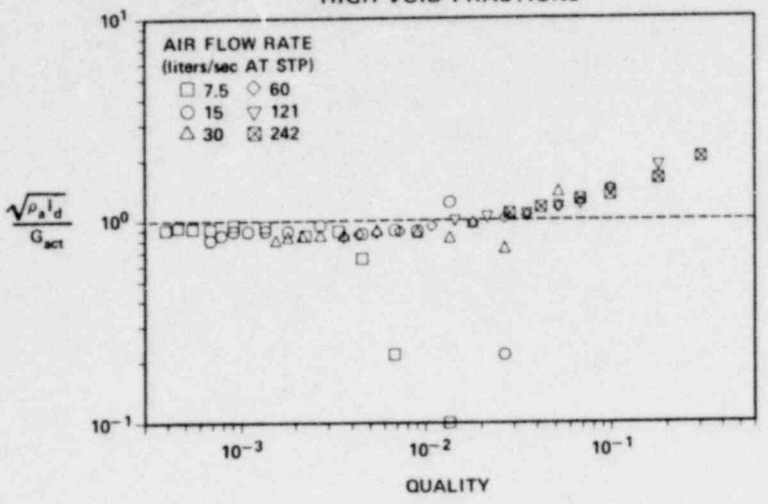

ORNL WS-6136

UNION CARBIDE ORNL

ANALYSIS METHODS

ROUHANI TURBINE MODEL:

$$\rho_f(1-\alpha)\,V_f(V_t - V_f) = \rho_g \alpha V_g(V_g - V_t)$$

SOLVING FOR V_t

$$V_t = \frac{(1-\alpha)\rho_f V_f^2 + \alpha\rho_g V_g^2}{(1-\alpha)\rho_f V_f + \alpha\rho_g V_g}$$

TWO-VELOCITY DRAG MODEL:

$$I_d = (1-\alpha)\rho_f V_f^2 + \alpha\rho_g V_g^2$$

ALSO,

$$G = G_f + G_g = (1-\alpha)\rho_f V_f + \alpha\rho_g V_g$$

$$\therefore V_t = \frac{I_d}{G}$$

AND

$$\boxed{G_3 = \frac{I_d}{V_t}}$$ TWO-VELOCITY MASS FLUX MODEL

UNION CARBIDE ORNL

RESULTS

THE MASS FLOW MODEL $G_3 = \frac{I_d}{V_t}$ WAS FOUND TO GIVE RESULTS WHICH WERE USUALLY LESS THAN THE METERED MASS FLUXES, BY APPROXIMATELY 20 PERCENT

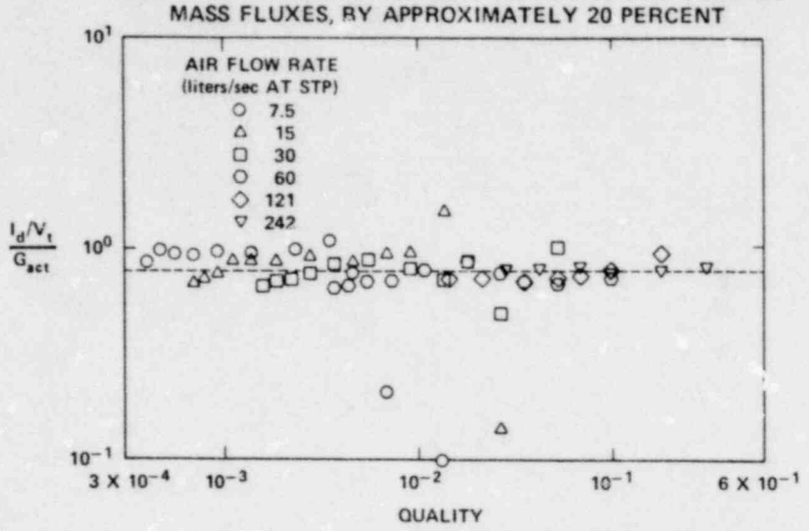

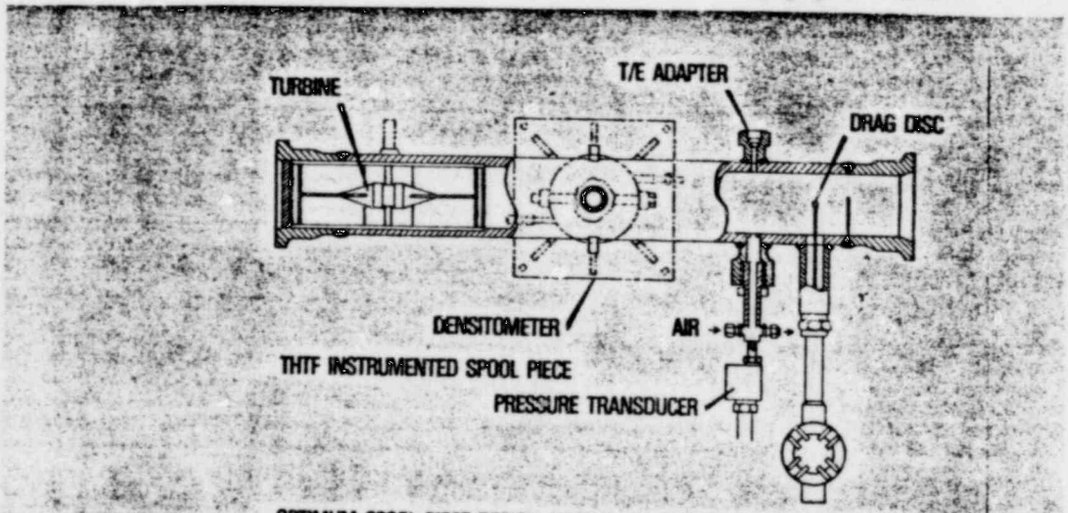

OPTIMUM SPOOL PIECE DESIGN ALLOWS CLOSE SPACING OF INSTRUMENTS, YET MINIMIZES THE INSTRUMENTS' EFFECTS ON EACH OTHER.

INSTRUMENTED SPOOL PIECE USED IN STEADY STATE STEAM WATER TESTS.

AIRS STEAM WATER TEST STAND.

ORNL DWG 78 12753

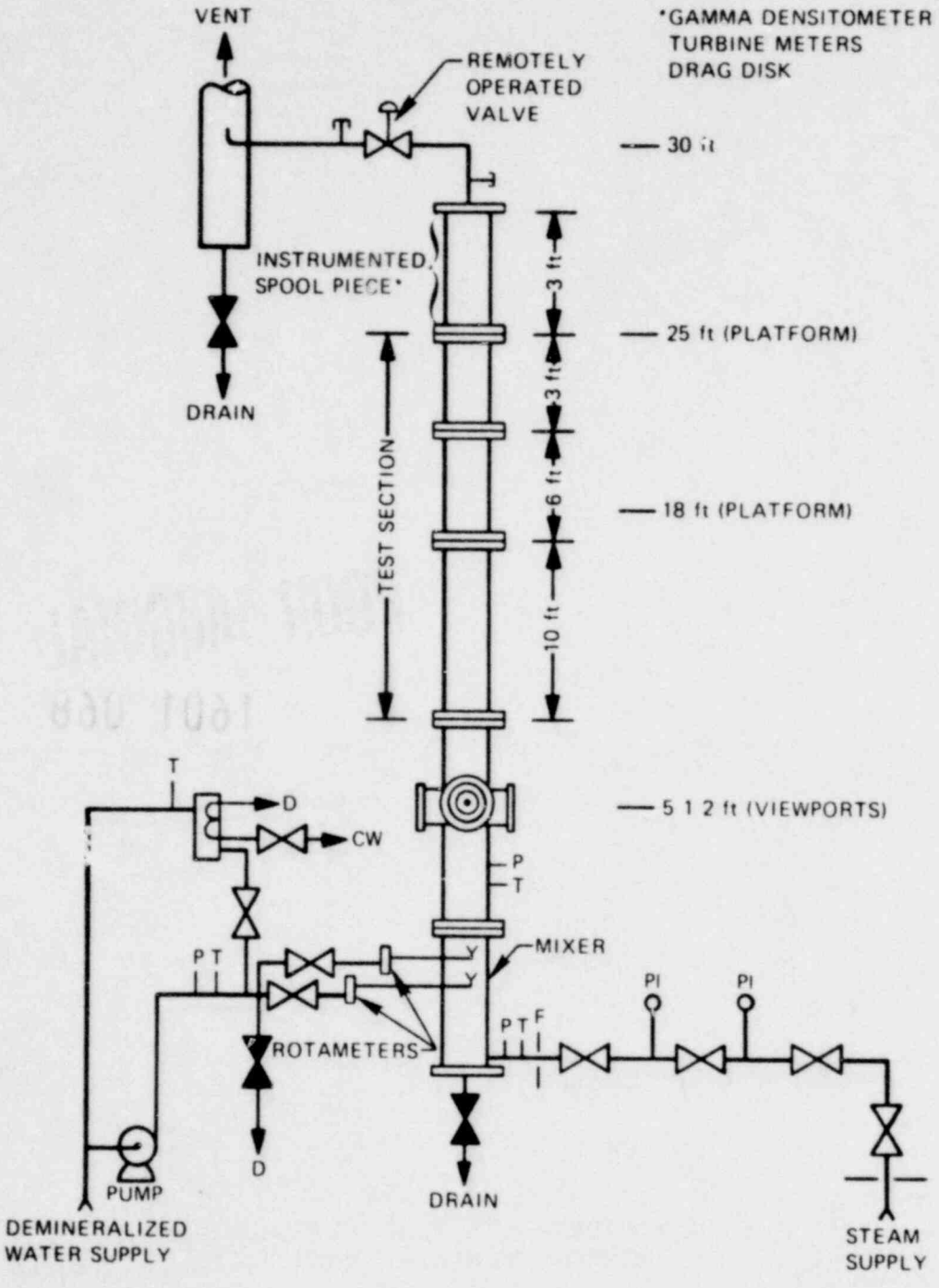

1601 069

MASS FLUXES OBTAINED USING THE TURBINE AND THE DENSITOMETER
IN STEAM-WATER TWO-PHASE FLOW (VOID FRACTION >50%)
GROSSLY OVERESTIMATED THE METERED MASS FLUX

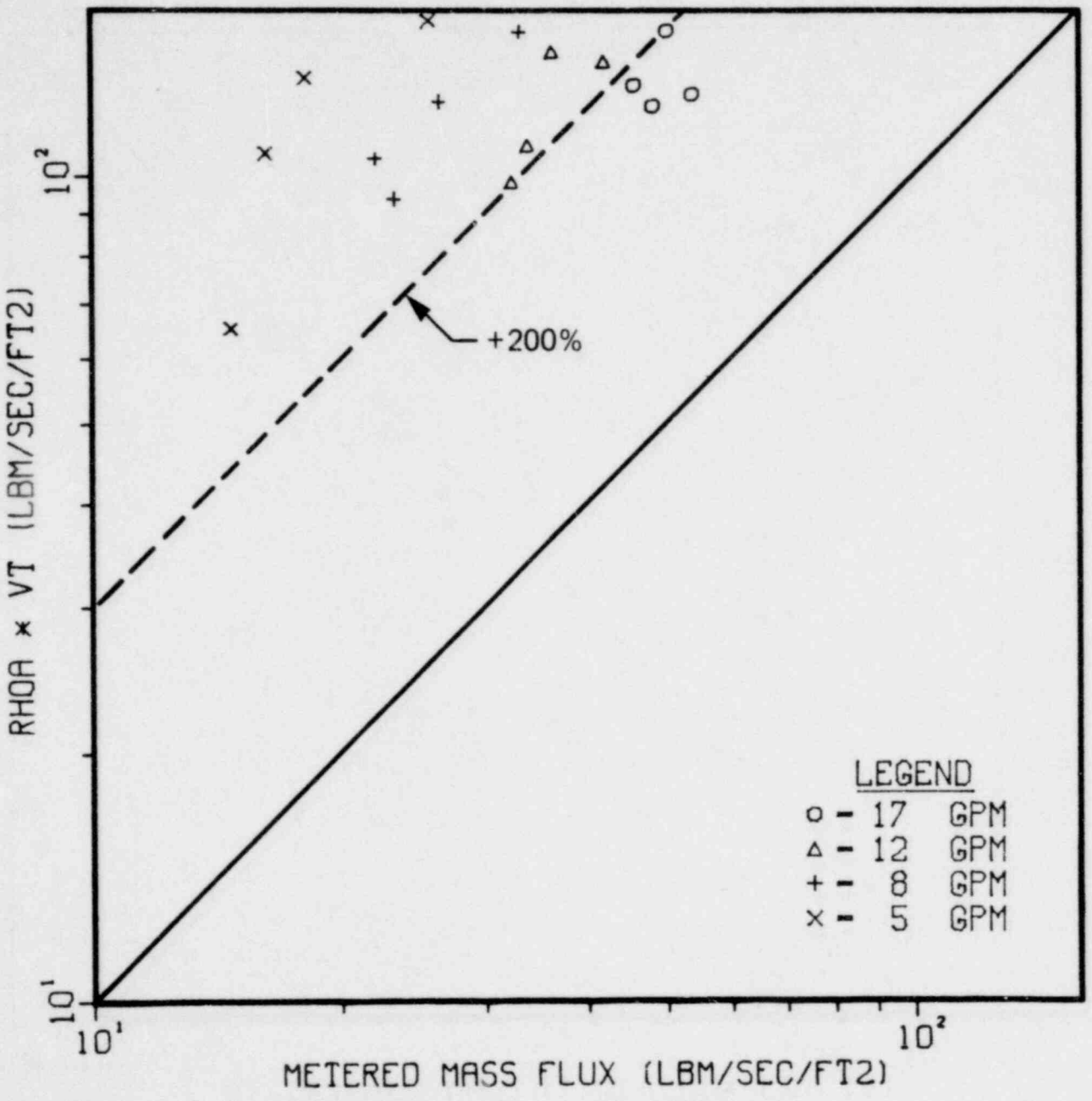

1601 070

MASS FLUXES OBTAINED USING THE DRAG FLOWMETER AND THE DENSITOMETER
IN STEAM-WATER TWO-PHASE FLOW (VOID FRACTIONS >50%)
EXCEEDED THE METERED FLUXES BY SOME 50%

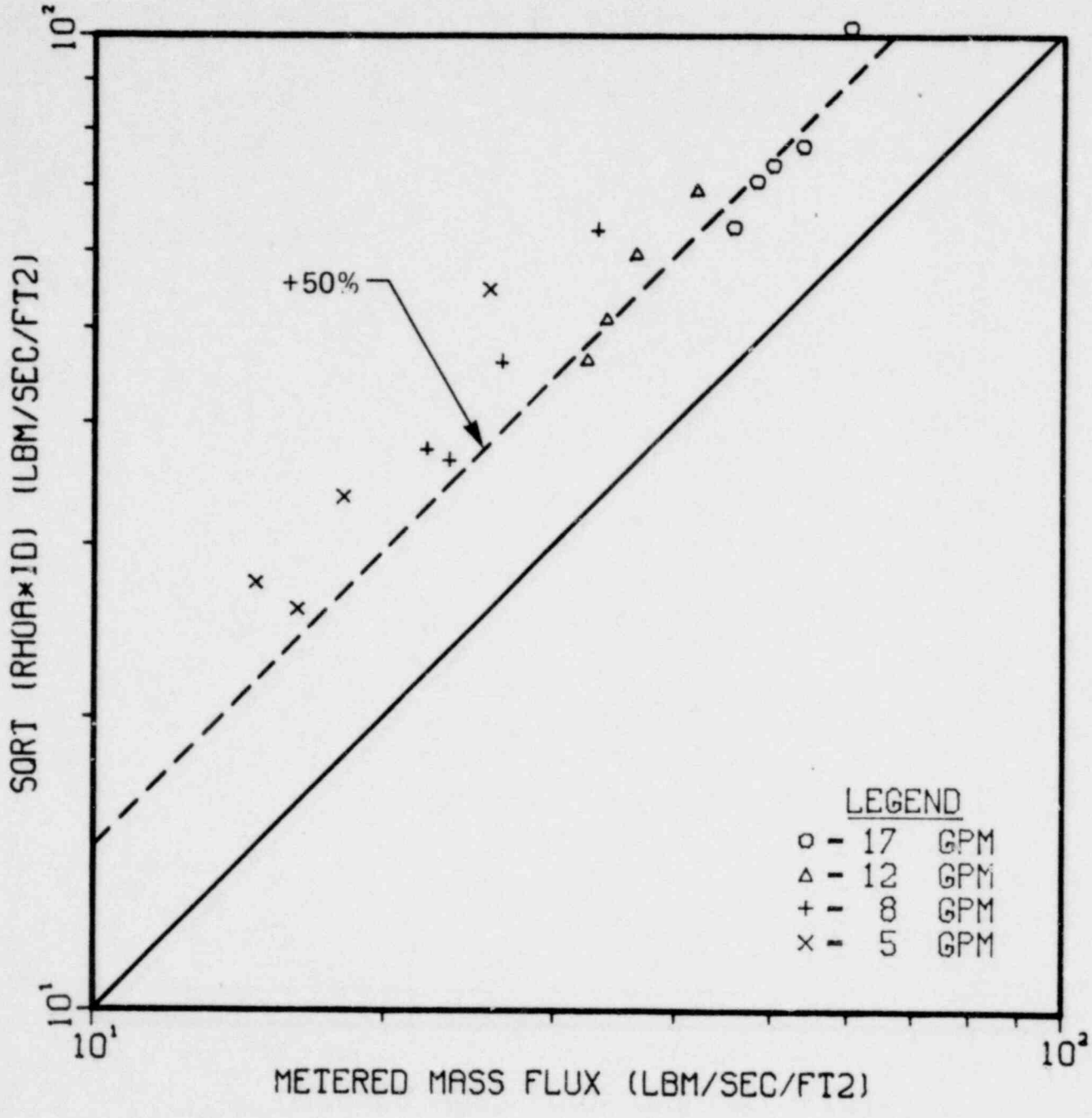

1601 071

MASS FLUXES OBTAINED USING THE DRAG FLOWMETER AND THE TURBINE IN STEAM-WATER TWO-PHASE FLOW (VOID FRACTIONS >50%) WERE SOME 20% BELOW THE METERED MASS FLUXES

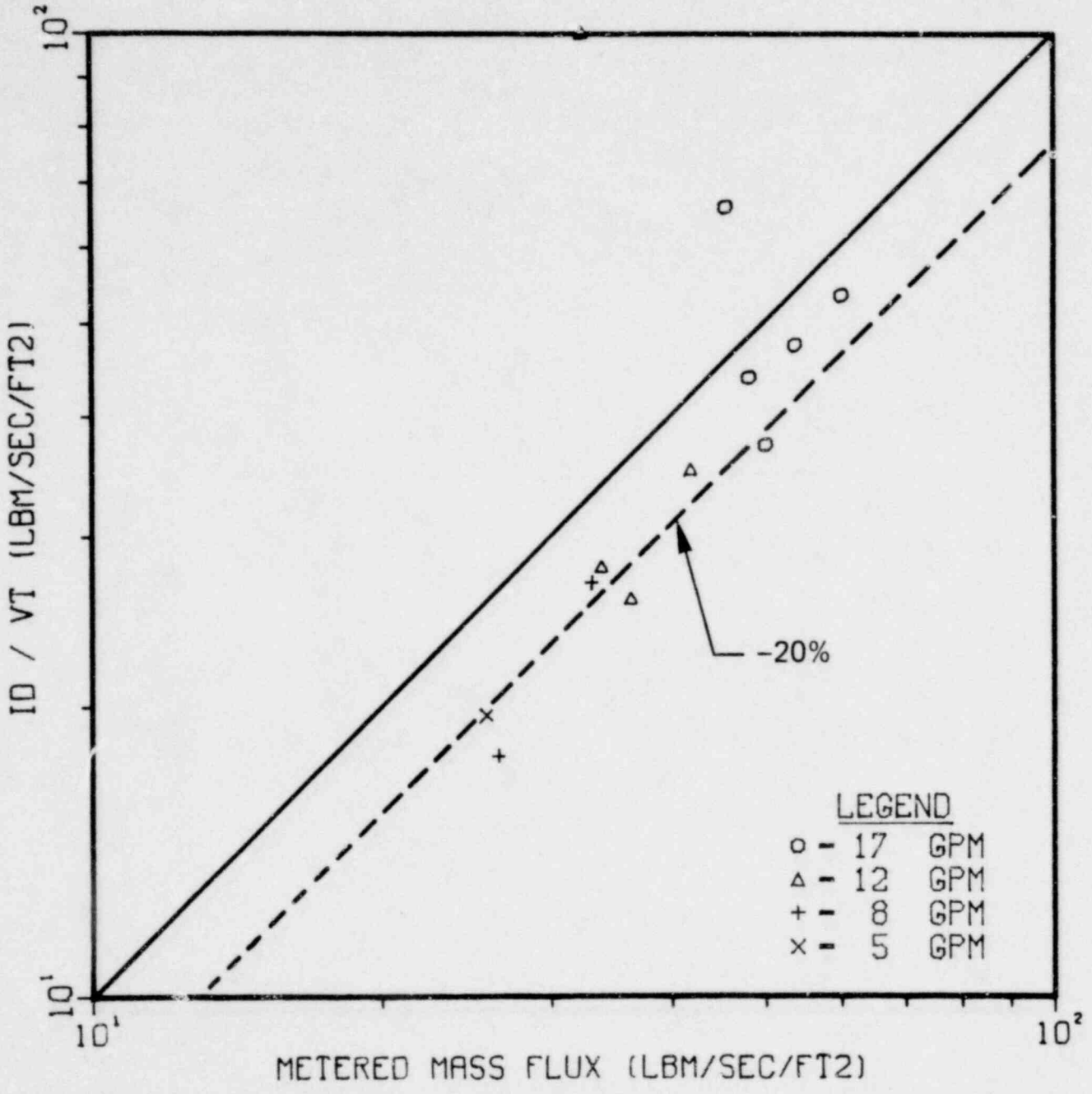

1601 072

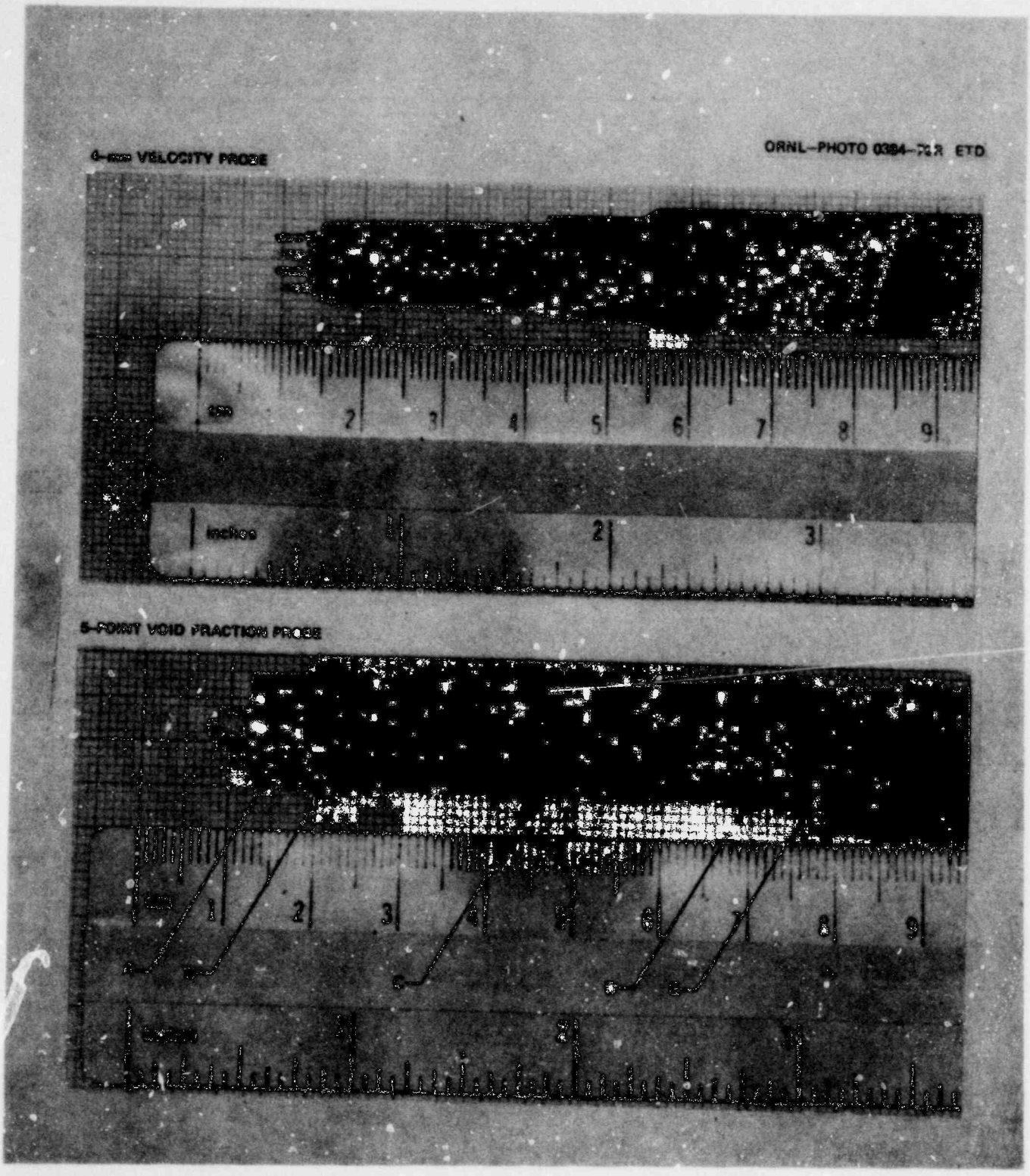

UNION CARBIDE

ORNL

VELOCITIES DERIVED FROM THE TWO-PRONG PROBE SIGNALS, USING CROSS CORRELATION ANALYSIS, APPEAR TO APPROXIMATE V_f RATHER THAN V_g

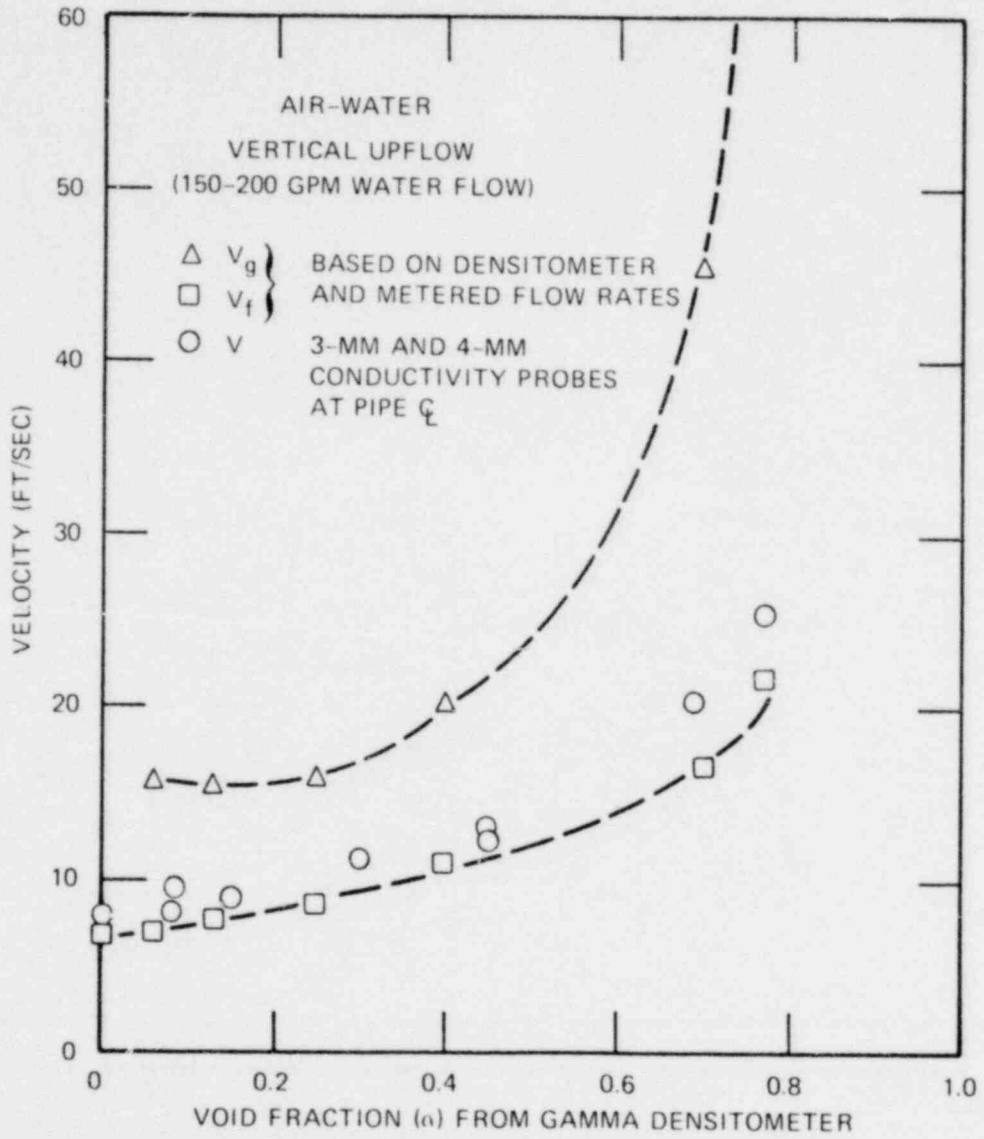

PIPE-AVERAGE VOID FRACTIONS DERIVED FROM THE CONDUCTIVITY PROBE DATA AGREE WELL WITH VOID FRACTIONS INDICATED BY THE THREE-BEAM DENSITOMETER.

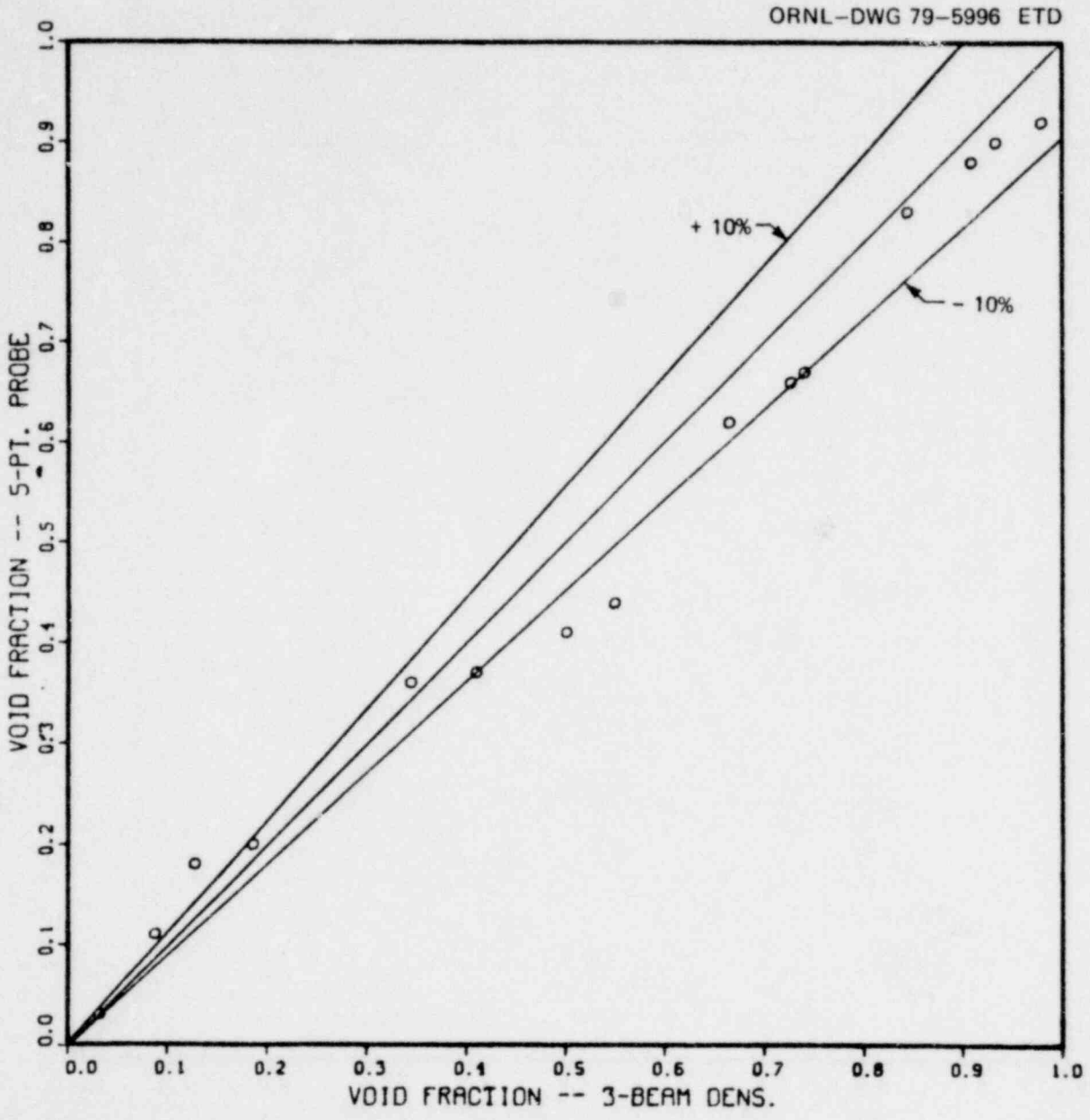

LOCAL VOID DATA FROM ANALYSIS OF FIVE-POINT A.E.C.L. PROBE SIGNALS

AIR-WATER VERTICAL UPFLOW.

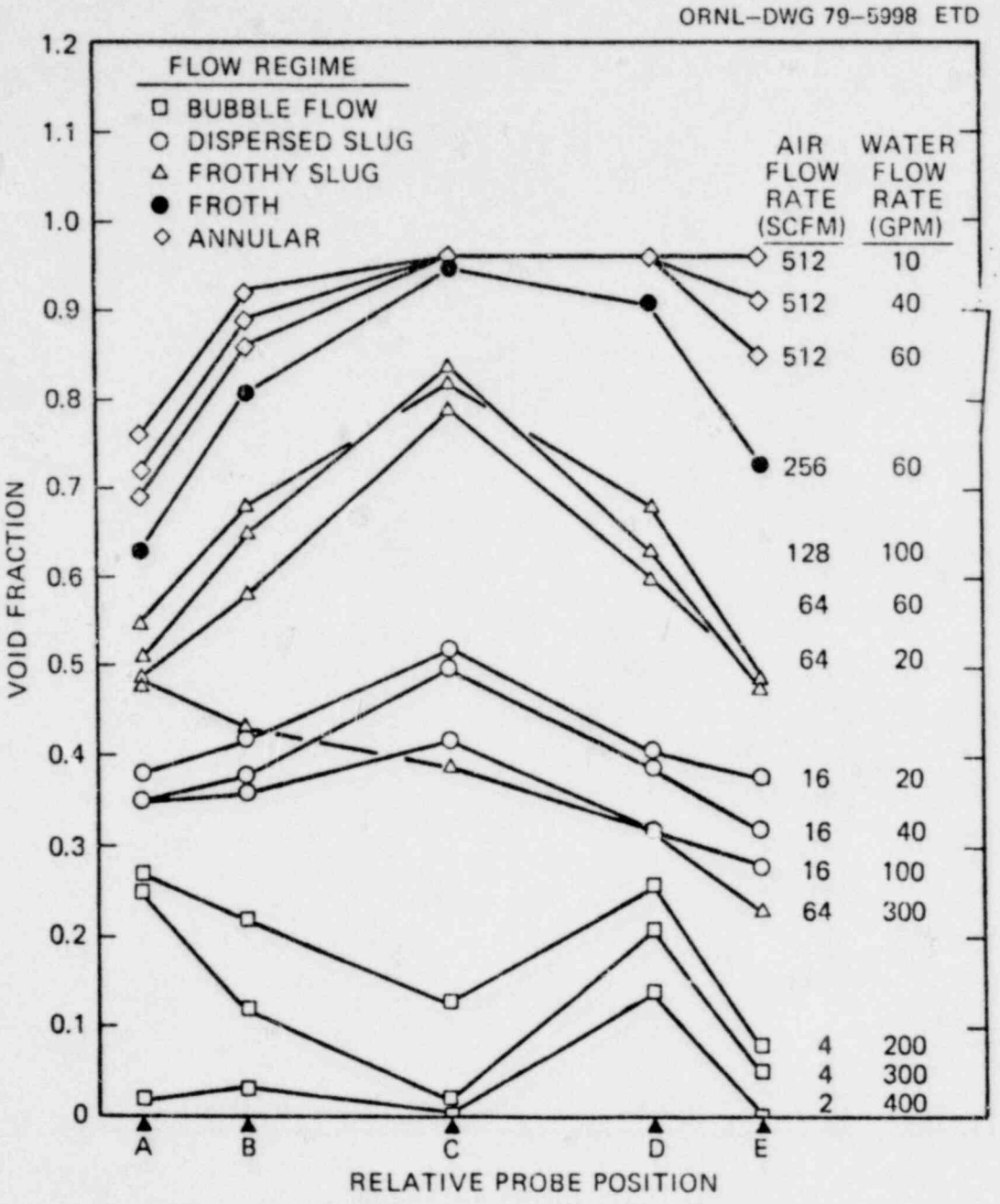

1601 076

IN THE STEAM-WATER TESTS, CHANGES IN THE WATER CONDUCTIVITY INVALIDATED THE VOID PROBE CALIBRATION. BUT VOLTAGE HISTOGRAMS SUGGEST THAT THE PROBE CORRECTLY RESPONDED TO THE PRESENCE OF EACH PHASE

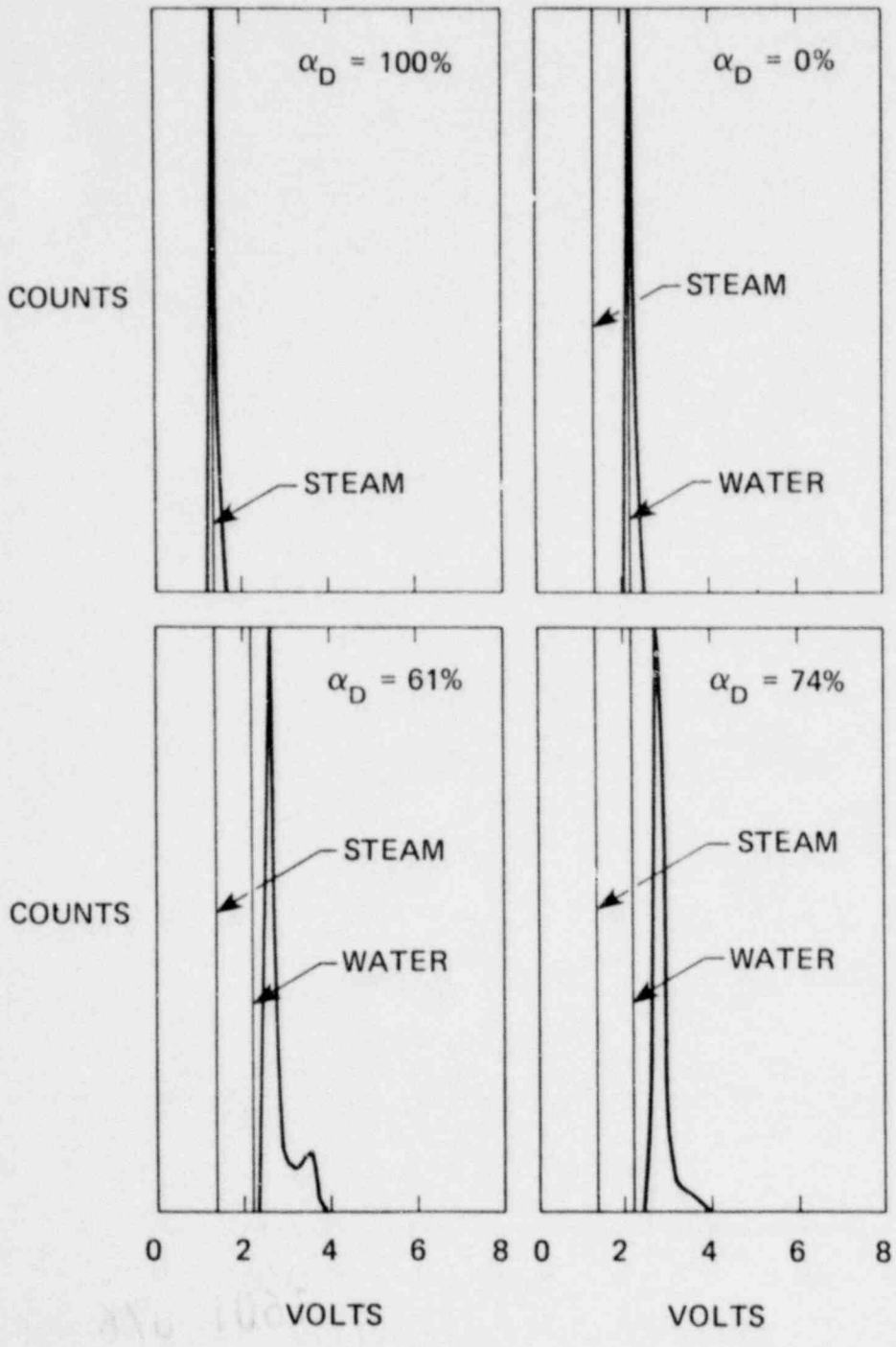

IN STEAM–WATER TWO–PHASE FLOW, THE VELOCITIES DERIVED BY SIGNAL ANALYSIS FROM THE CONDUCTIVITY PROBE APPROXIMATED THE MEAN LIQUID PHASE VELOCITIES DERIVED USING DENSITOMETER DATA

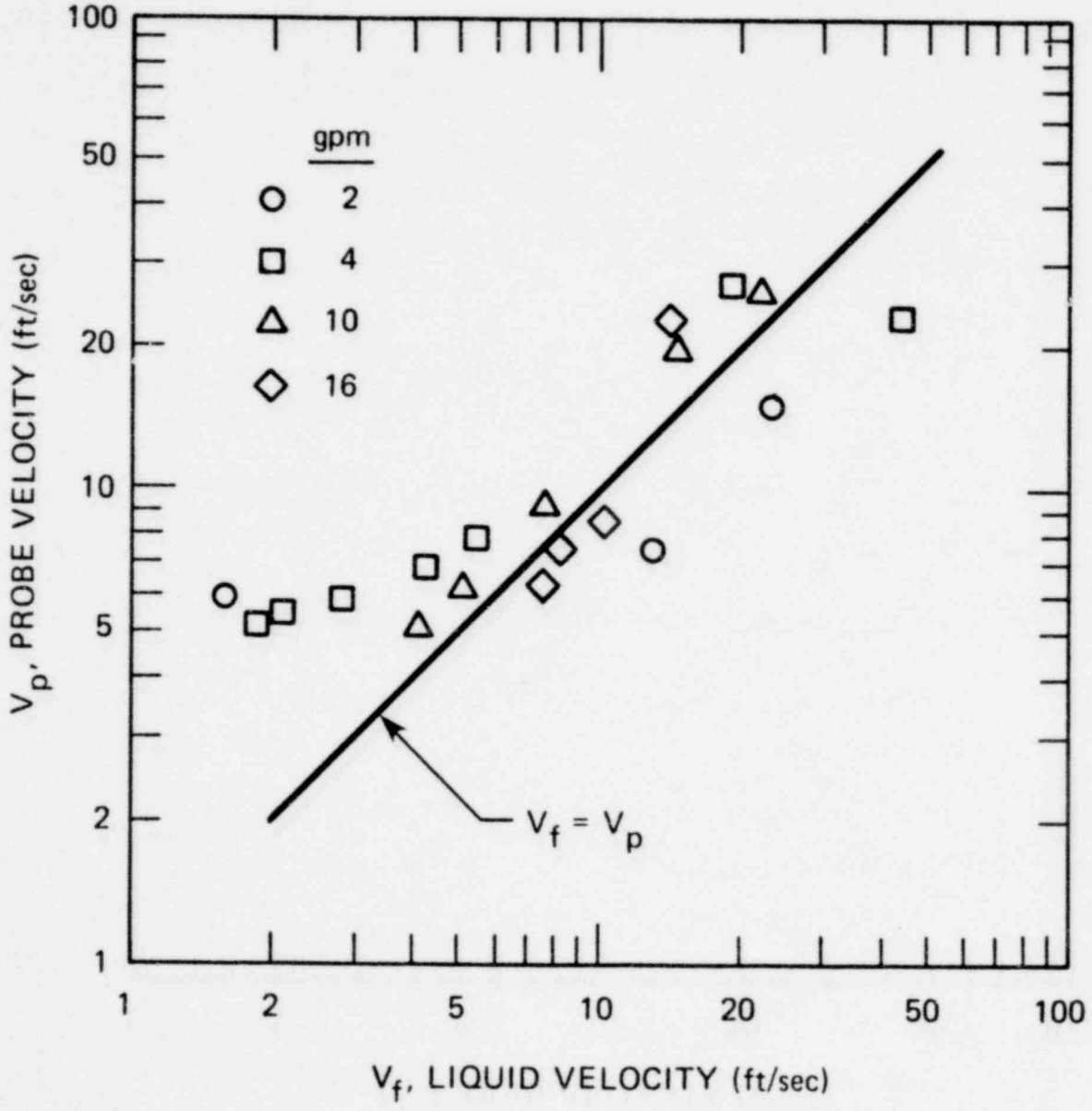

UNION CARBIDE
ORNL

SUMMARY AND CONCLUSIONS

- IN THE AIR-WATER SYSTEM, THE MASS FLUX MODELS $G_1 = \rho_a V_t$ AND $G_2 = \sqrt{\rho_a I_d}$ PERFORM WELL WITH SPOOL PIECE DATA AT LOW VOID FRACTIONS, BUT THE MODELS SERIOUSLY OVERPREDICT THE CORRECT MASS FLUX AT HIGHER VOID FRACTIONS
- THE MODEL $G_3 = I_d/V_t$ YIELDS RESULTS WHICH ARE USUALLY LESS THAN THE METERED MASS FLUXES BY APPROXIMATELY 20 PERCENT
- RESULTS FROM VERTICAL UPFLOW, HIGH VOID FRACTION STEAM-WATER EXPERIMENTS WITH SPOOL PIECE INSTRUMENTATION CONFIRMED TRENDS OBSERVED IN THE AIR-WATER LOOP.
- VELOCITY AND VOID FRACTION INFORMATION DERIVED USING SIGNAL ANALYSIS WITH CONDUCTIVITY PROBES IN THE AIR-WATER AND STEAM-WATER TESTS SHOWED THAT THE VOID PROBE DATA GENERALLY AGREED WITH THAT FROM THE GAMMA DENSITOMETER. VELOCITIES OBTAINED BY CROSS CORRELATION APPROXIMATED THE MEAN LIQUID PHASE VELOCITIES, PARTICULARLY AT HIGH VOID FRACTIONS.

PROGRESS IN LOW QUALITY AND SUBCOOLED POST-CHF STUDIES

by

D.C. Groeneveld
Chaik River Nuclear Laboratories
Atomic Energy of Canada Limited
Chalk River, Ontario, Canada KUJ 1JO

S.C. Cheng
Associate Professor
Department of Mechanical Engineering
University of Ottawa
Ottawa, Ontario, Canada K1N 6N5

and

K.K. Fung
Research Associate
Department of Mechanical Engineering
University of Ottawa
Ottawa, Ontario, Canada K1N 6N5

Paper to be presented at the USNRC's
Seventh Water Reactor Safety Research Information Meeting
Gaithersburg, Maryland
1979 November 5 - 9

PROGRESS IN LOW QUALITY AND SUBCOOLED POST-CHF STUDIES

by

D.C. Groeneveld, S.C. Cheng and K.K. Fung

1.0 LOW QUALITY AND SUBCOOLED FILM BOILING

1.1 General

Low quality and subcooled film boiling data were obtained using the "hot patch" technique was reported previously [1,2]. This technique, which was originally developed at Chalk River, permits film boiling conditions to be maintained in a heat flux controlled sy tem at heat flux levels well below the CHF, thus minimizing the possibility of a heater failure.

The test section is shown schematically in Fig. 1. It consists of a high thermal inertia copper "hot patch" (equipped with eight 250 W cartridge heaters) which is brazed to the Inconel test section tube.

The test section formed part of a loop through which water was circulating at atmospheric pressure. Initially the test section and hot patch were heated separately, while the desired flow conditions were established in a bypass leg having the same hydraulic characteristics as the test section leg. When the test section and hot patch temperature exceeded the minimum temperature required to maintain film boiling (usually in the range of 350 - 550°C), the flow was diverted from the bypass to the test section. As soon as the first test section thermocouple showed a decrease in temperature (indicating that water had arrived at that location) the test section power was increased rapidly to prevent the heated section from being quenched. The presence of the hot patch at the entrance created a vapor annulus around the circumference, which could be maintained downstream in the heated tube at heat flux levels as low as one-tenth of CHF.

1.2 Recent Results

During the past year the investigation has concentrated on

(a) measurement of axial profile of void fraction by means of γ-attenuation technique, and

(b) obtaining lower equilibrium qualities inside the film boiling section, thus lengthening the test section in the inverted annular flow region by using a shorter hot-patch (2.5 cm instead of 6.35 cm used previously).

The arrangement of the γ-densitometer is shown in Fig. 1. The theoretical predictions of attenuation were found to agree with measurement on cylindrical plexiglass inserts of different diameters to simulate inverted annular flow. Some of the data are plotted in Fig. 2 as measured void fraction vs. axial location. It can be seen that the void fraction at a fixed axial location increases with a decrease in inlet subcooling and an increase in heat flux. When the data are replotted in Fig. 3 against equilibrium quality these effects can no longer be discerned. This suggests that the local phase and velocity distribution is primarily a function of equilibrium quality.

The data of Fig. 3 were combined with a large number of other void fraction measurements (obtained over a wide range of flow, subcooling and heat flux) in Fig. 4. It can be seen that a 40 - 50% void fraction was encountered at zero equilibrium quality. At such high void fraction the flow regime could be in a transition to dispersed flow.

Fig. 5 compares the measured void fraction to that calculated based on constant slip and either saturated or film temperature for the vapor. It is shown that a large slip ratio (≈ 10) is required in order to match the data. This is not surprising for an accelerating flow and a high density ratio ($\rho_\ell/\rho_g \approx 1600$). At the highest void fraction the liquid will be broken up in small droplets which are easier to accelerate; this agrees with the measurements as here the slip ratio is reduced considerably.

Our earlier results showed a strong effect of heated length on the film boiling heat transfer coefficient (e.g., Fig. 6). Tests were subsequently carried out with a shorter hot patch to obtain film boiling data at (i) a higher inlet subcooling, and (ii) a shorter film boiling

length. (Film boiling was assumed to start at the upstream face of the copper hot-patch.) The shorter hot-patch results confirm the exponential increase in heat transfer coefficient with decreasing film boiling length.

1.3 Further Studies

The low pressure data are being analyzed using two approaches

(i) Empirical: To correlate the data in terms of equilibrium conditions.

(ii) Post-CHF Model: A model is being developed for the inverted annular flow regime which is similar in structure to the M.I.T. and Harwell post-dryout models for the dispersed flow regime. Both the void fraction and the surface temperature measurements will be used to verify this model.

Subcooled film boiling data will also be obtained at higher pressures in Chalk River's FLARE loop (maximum pressure: 12 MPa). These data will fill the final existing gap in the post-CHF data bank.

2.0 TRANSITION BOILING

2.1 General

Forced convective transition boiling data were obtained at the University of Ottawa for water at atmospheric pressure. The test section used consists of a high thermal inertia cylindrical copper block having a flow tube along its centerline (Fig. 7). The copper block is heated by cartridge heaters located in a concentric ring at some distance from the center of the flow tube. Transition boiling data were obtained either from steady-state measurements or from transient measurements by differentiating the temperature-time cooling curve. Details of the experimental technique have been reported previously [3,4].

2.2 Recent Results

During the past year much emphasis has been put on studying the effect of heated surface materials on the boiling curve. Three techniques were used:

(a) A centrally cooled cylindrical test section was constructed of a single material. This technique is only suitable for materials having a relatively high thermal conductivity (Fig. 7a).

(b) The central flow tube was brazed to the cylindrical copper block using high temperature silver solder. This technique is not suitable for aluminum or Zircaloy flow tubes (Fig. 7b).

(c) Same as (b) except that thermal contact between the copper block and the flow tube was provided by a liquid metal gland (Wood's metal) instead of a brazing material. This technique is suitable for any flow tube material (Fig. 7c).

Fig. 7 shows a schematic of the three setups. A comparison of experimental results for Inconel, brass, aluminum, copper and Zircaloy heated surfaces is shown in Figs. 8 to 10 for standard test conditions: $G = 136\ kg \cdot m^{-2} \cdot s^{-1}$ and $\Delta T_{in} = 13.9°C$. The results show a strong effect of thermal conductivity (or $k \cdot \rho \cdot Cp$) on the boiling curve;

(i) An increase in k decreased the transition boiling heat transfer coefficient.

(ii) The effect of heated surface material on CHF is small.

(iii) An increase in k (or $k \cdot \rho \cdot Cp$) decreased the wall superheat at CHF and at rewetting (this is in agreement with experiments carried out elsewhere [5,6]).

Caution should be exercised in using the results quantitatively as the wall thickness, δ, and the finish of the tube bore were not identical. Also, axial conduction heat losses were different because of the large differences in thermal conductivity.

A tentative empirical correlation has been proposed by Cheng [3] to include the effects of inlet subcooling, ΔT_{sub}, G and $k \cdot \rho \cdot Cp$ (units: kg, m, s, kJ, K):

$$\phi = 9.27 \times 10^{7} \left(\Delta T_{sat}\right)^{-1.189 - 0.226 \times 10^{-5} \sqrt{k \cdot \rho \cdot Cp}} \exp\left[0.02\ \Delta T_{sub} + 0.00393\ G + \frac{5770}{\sqrt{k \cdot \rho \cdot Cp}}\right] \quad \ldots \quad (1)$$

This correlation was derived based on 601 data points with an rms error of 12.65%. It should be noted that this correlation is limited to a narrow range of conditions and strictly speaking is only valid for the test sections used in this study. A more general phenomenological correlation with correct asymptotic trends is being derived at the present time.

2.3 Further Studies

The atmospheric pressure data obtained during the past three years are being reanalyzed to isolate the effects of: test section geometry, heated surface properties (k, ρ, Cp, roughness, wall thickness), method of analysis (1-D, 2-D conduction model), method of operation (steady state vs. transient) etc. In addition, further tests will be carried out to study the effect of heated length.

The derivation of a phenomenological correlation, having the correct asymptotic trends, is in progress. Much emphasis is placed on correct prediction of the transition boiling boundaries: CHF and Leidenfrost point.

The construction of a pressurized system is in progress and is almost completed. Transition boiling tests will be carried out at pressures up to 1.3 MPa and a much wider range of subcooling.

REFERENCES

1. D.C. Groeneveld et al., "Post-CHF Studies at Low Pressures", paper presented at the 6th USNRC Water Reactor Safety Research Information Meeting, Gaithersburg, Md., 1978 November.

2. D.C. Groeneveld and S.R.M. Gardiner, "A Method of Obtaining Flow Film Boiling Data for Subcooled Water," Int. J. of Heat & Mass Transfer, Vol. 21, pp 664-665, 1978.

3. S.C. Cheng et al., "Transition Boiling Heat Transfer in Forced Vertical Flow," Final Report for Period June 1978 - June 1979, University of Ottawa, Department of Mechanical Engineering.

4. S.C. Cheng et al., "Transition Boiling Heat Transfer in Forced Vertical Flow," Final Report for the Period June 1977 - June 1978, NUREG/CR-0357, ANL-78-75.

5. R.E. Henry, "A Correlation for the Minimum Film Boiling Temperature," AIChE Symposium Series No. 138, Vol. 70, pp 81-90, 1974.

6. V. Magrini and E. Nannel, "On the Influence of Thickness and Thermal Properties of Heating Walls on the Heat Transfer Coefficient in Nucleate Boiling," J. of Heat Transfer, Vol. 77, pp 173-178, 1975.

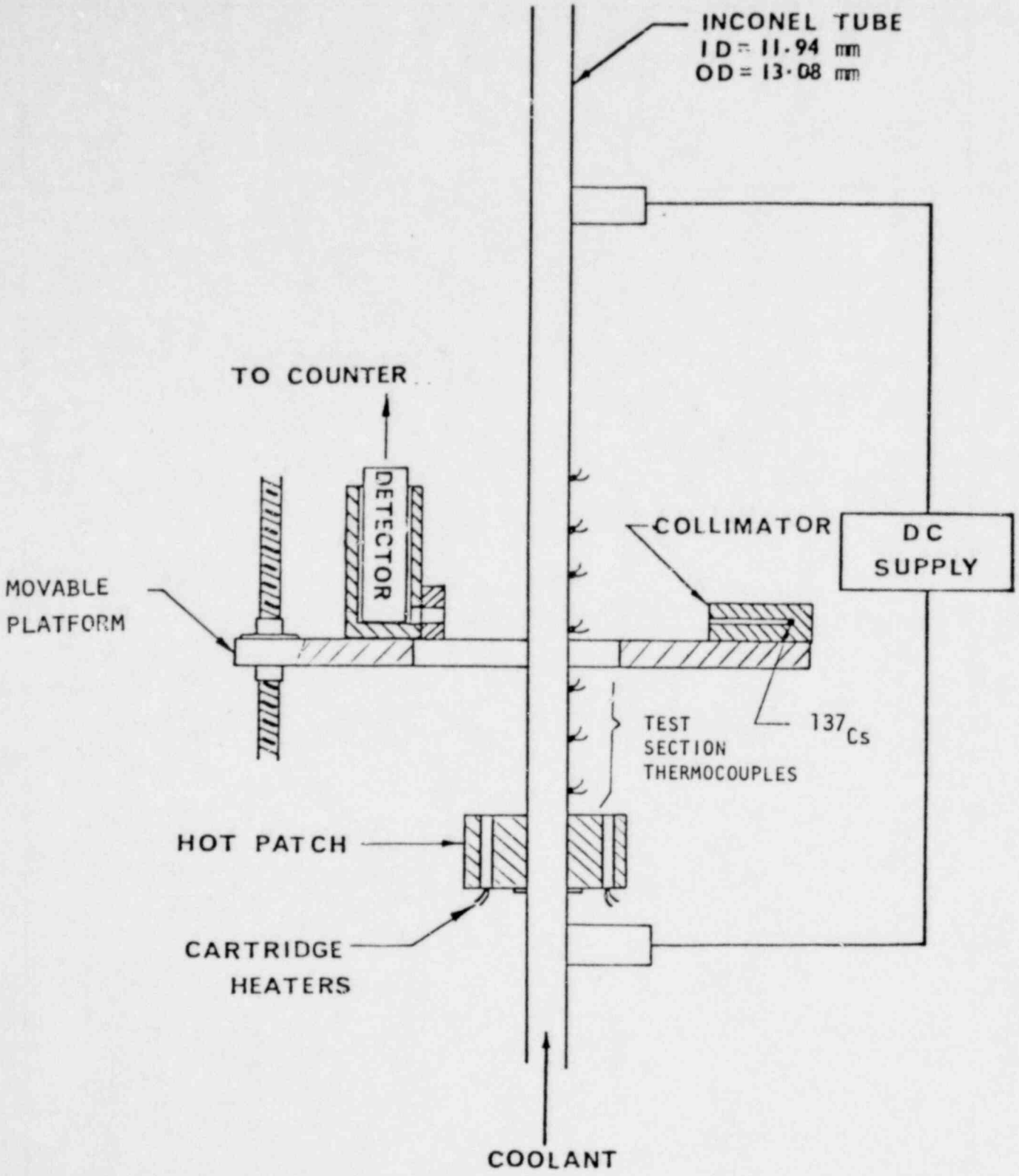

FIGURE 1 SCHEMATIC OF TEST SECTION AND γ-DENSITOMETER

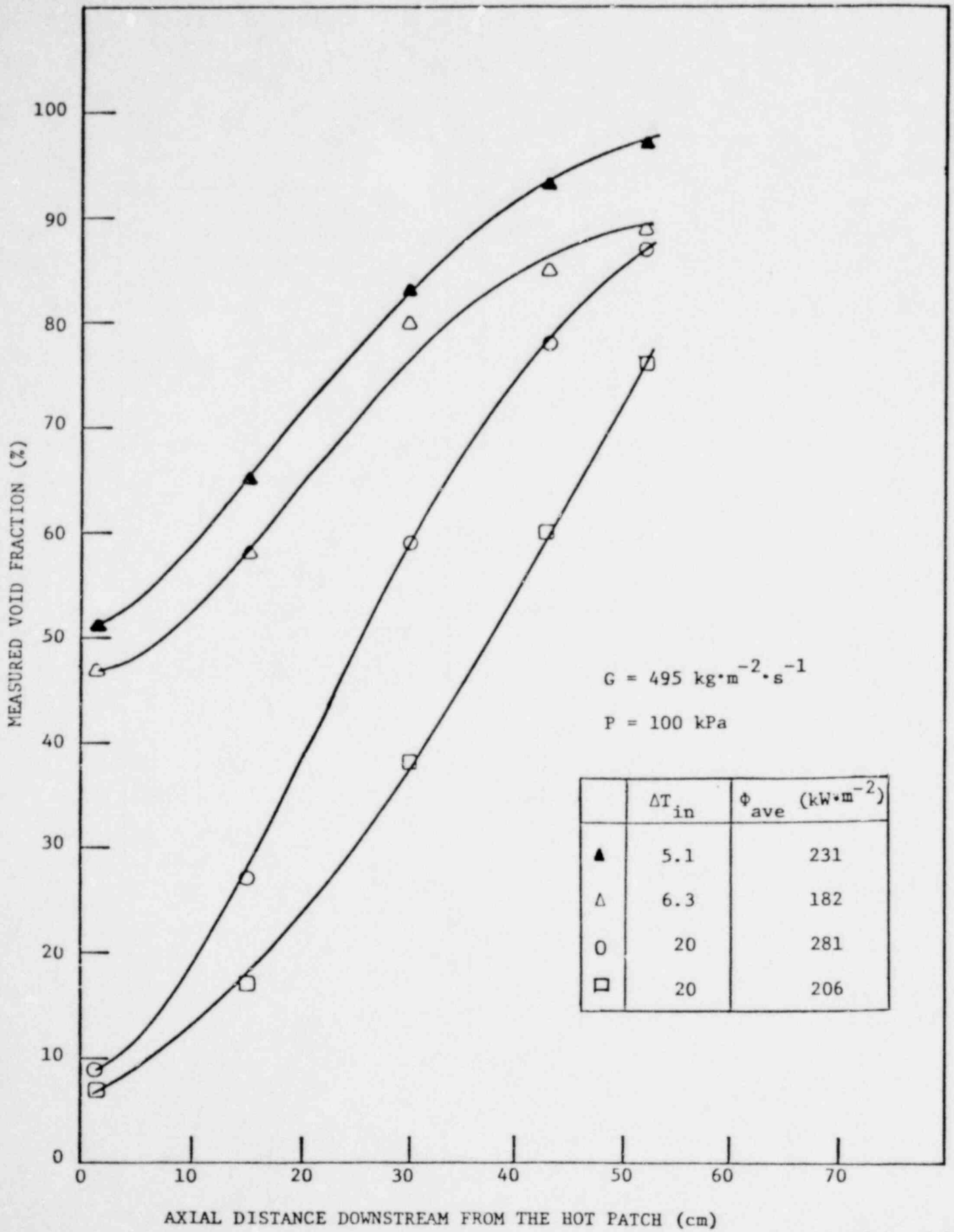

FIGURE 2 AXIAL VARIATION OF VOID FRACTION

1601 088

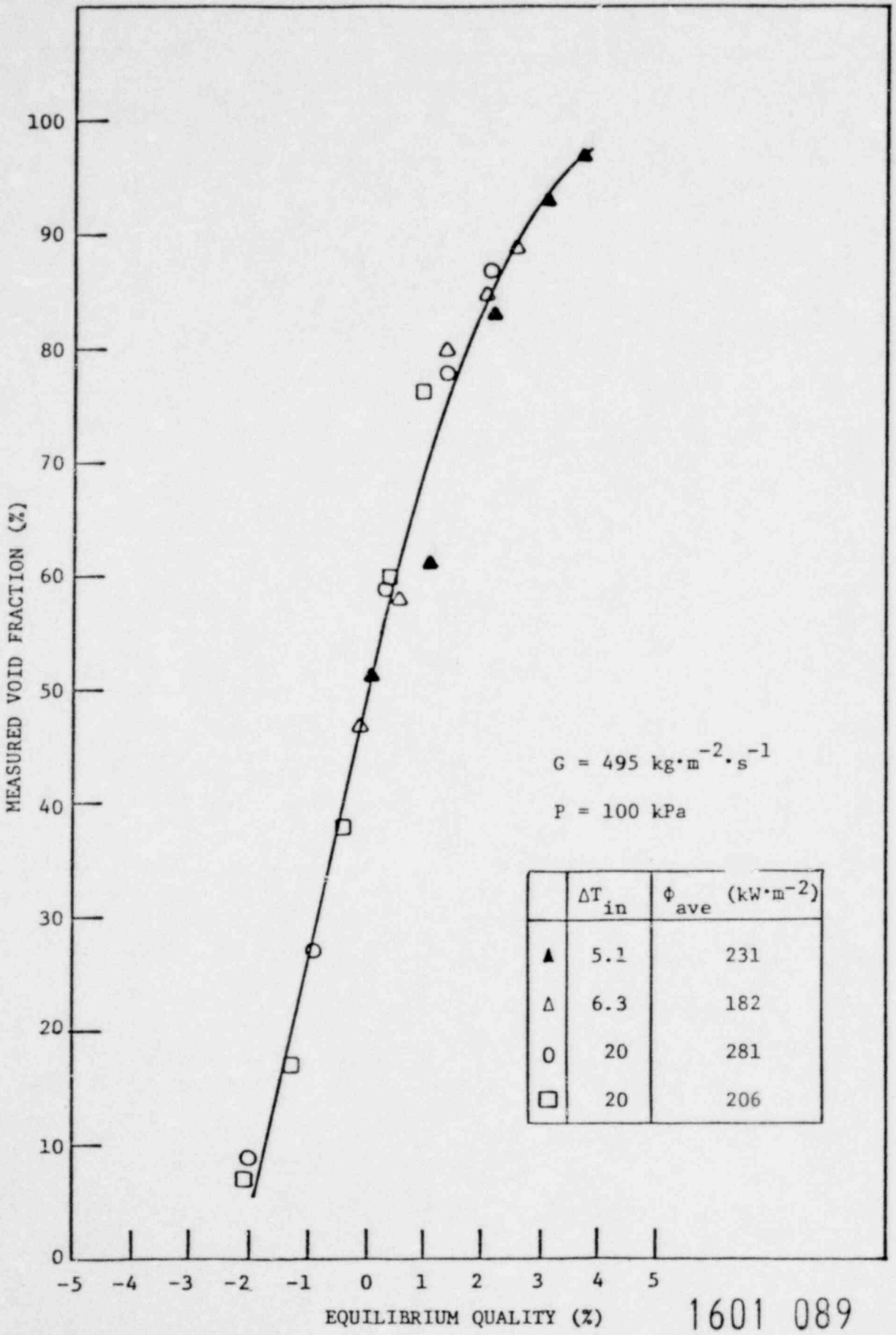

1601 089

FIGURE 3 VOID FRACTION AS A FUNCTION OF EQUILIBRIUM QUALITY

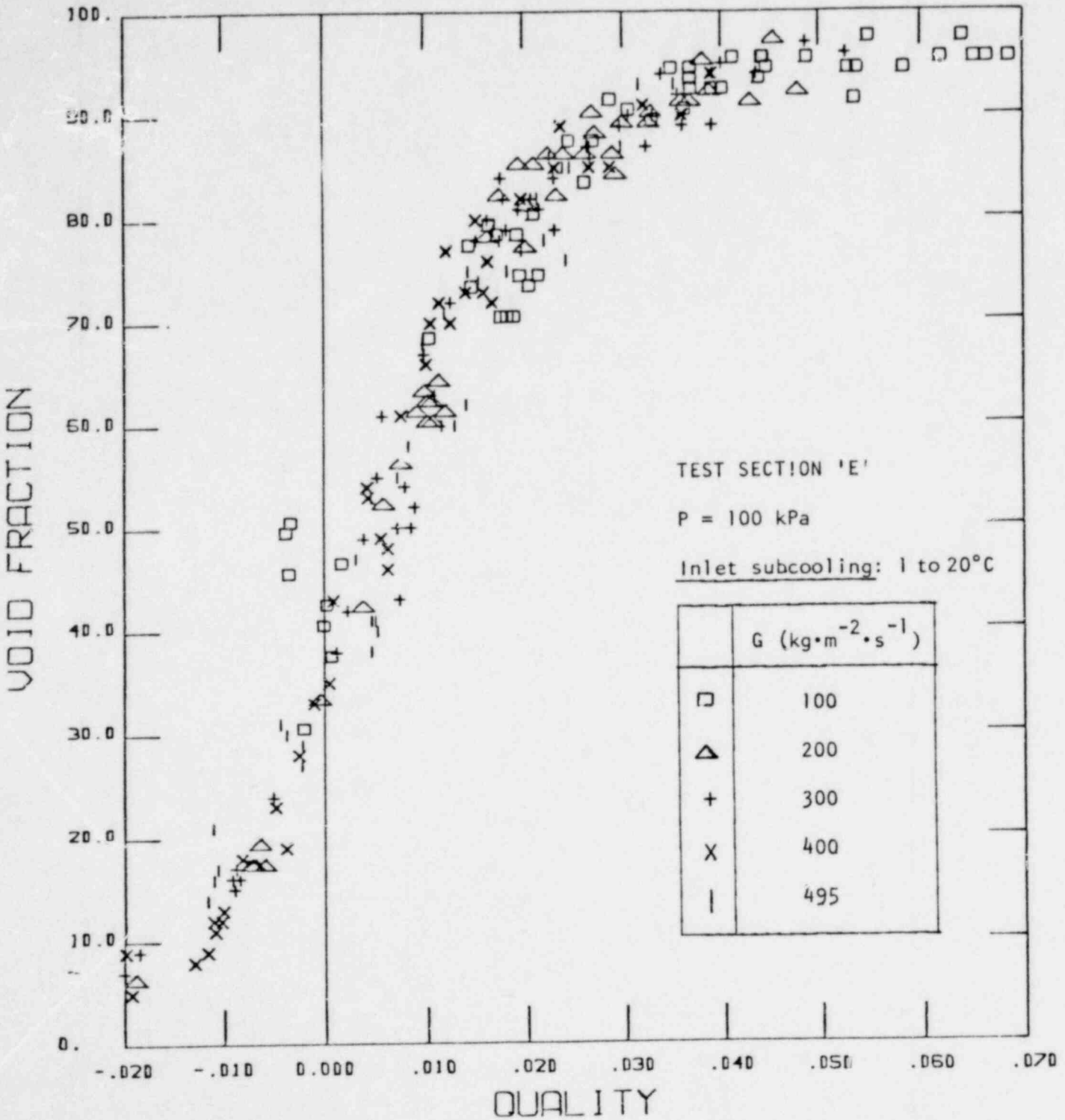

FIGURE 4 VOID FRACTION AS A FUNCTION OF EQUILIBRIUM QUALITY FOR VARIOUS FLOWS, SUBCOOLINGS, HEAT FLUX LEVELS AND WALL TEMPERATURES

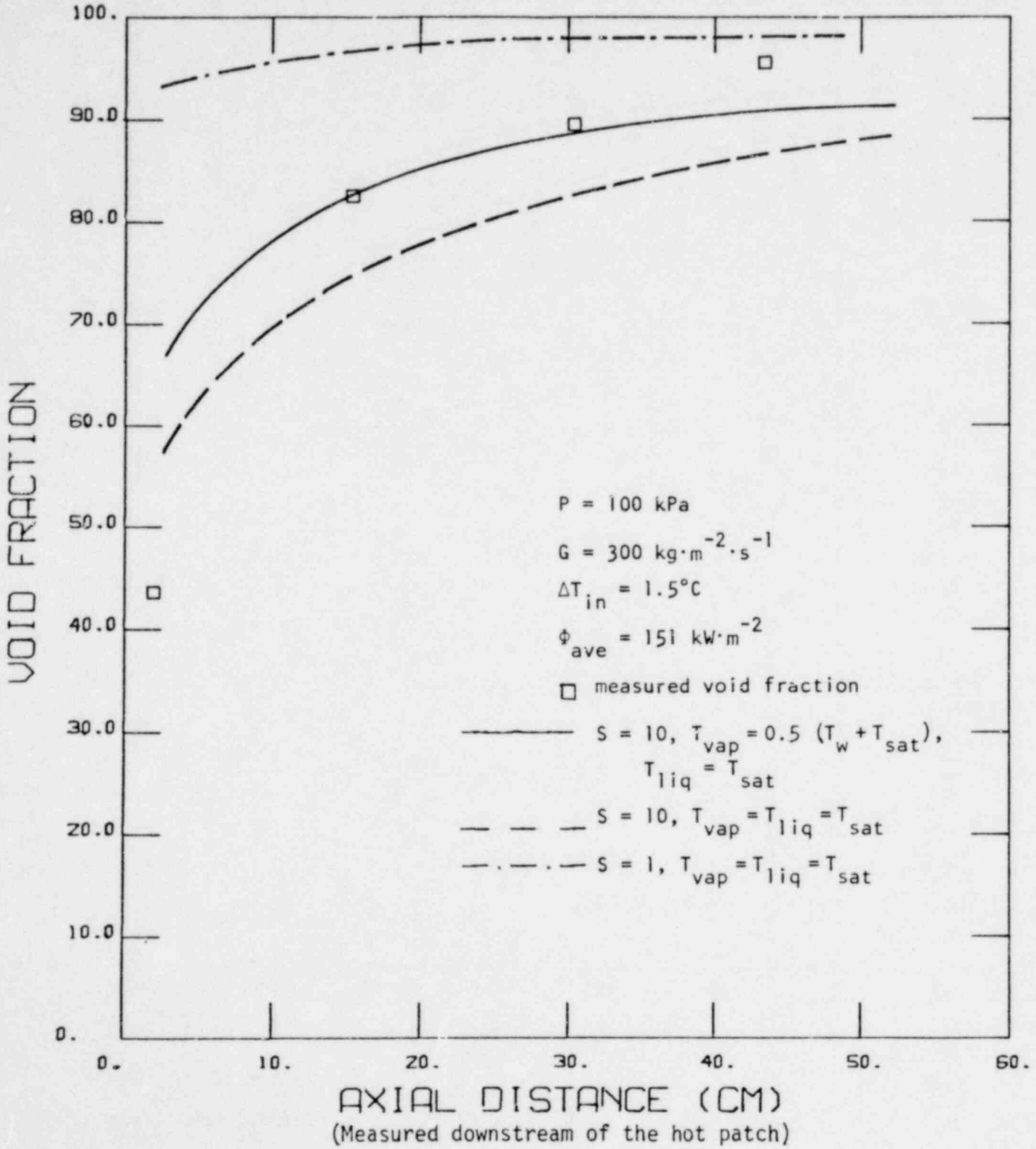

FIGURE 5 COMPARISON OF MEASURED AND PREDICTED VOID FRACTION PROFILE

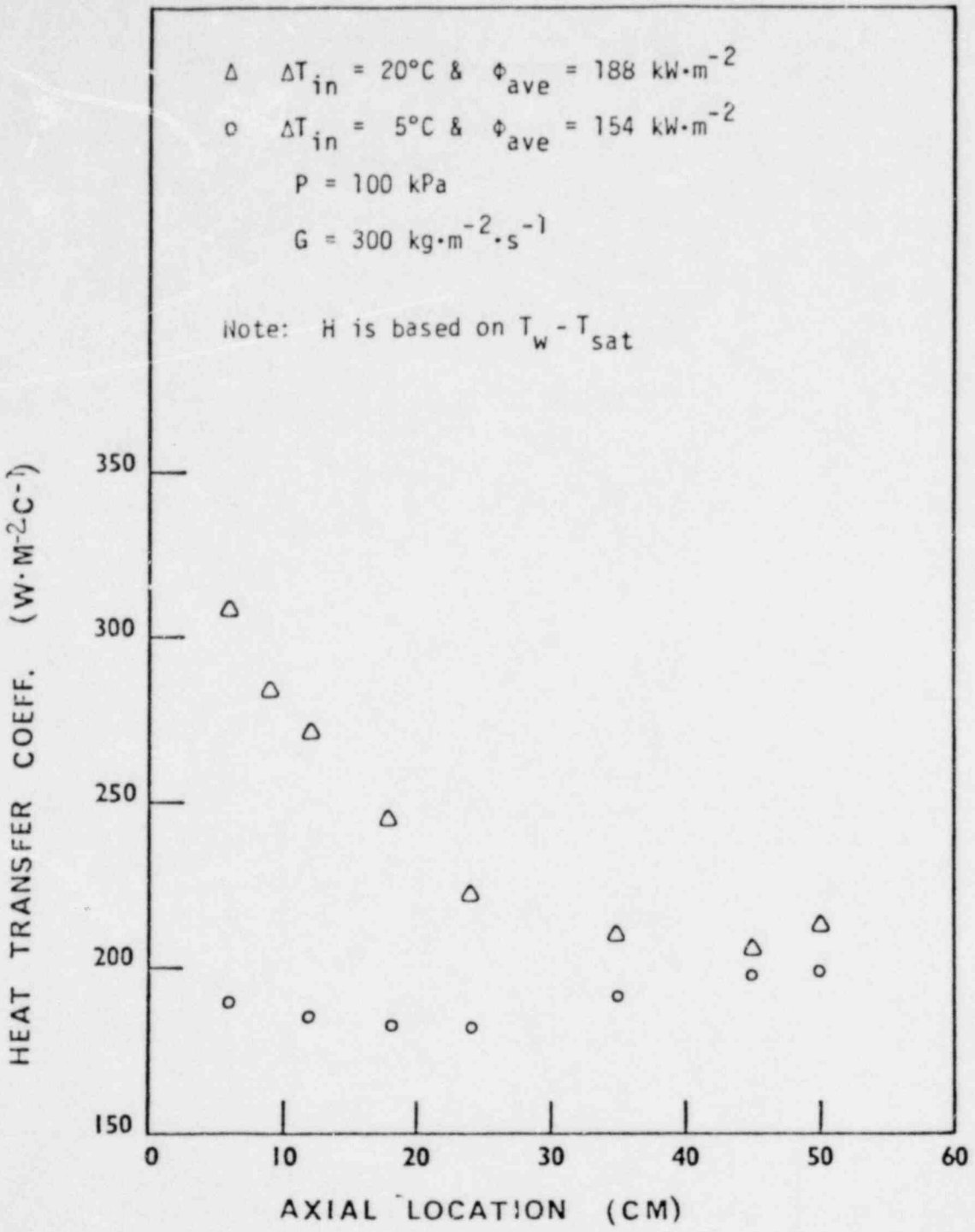

FIGURE 6 VARIATION OF HEAT TRANSFER COEFFICIENT ALONG HEATED LENGTH

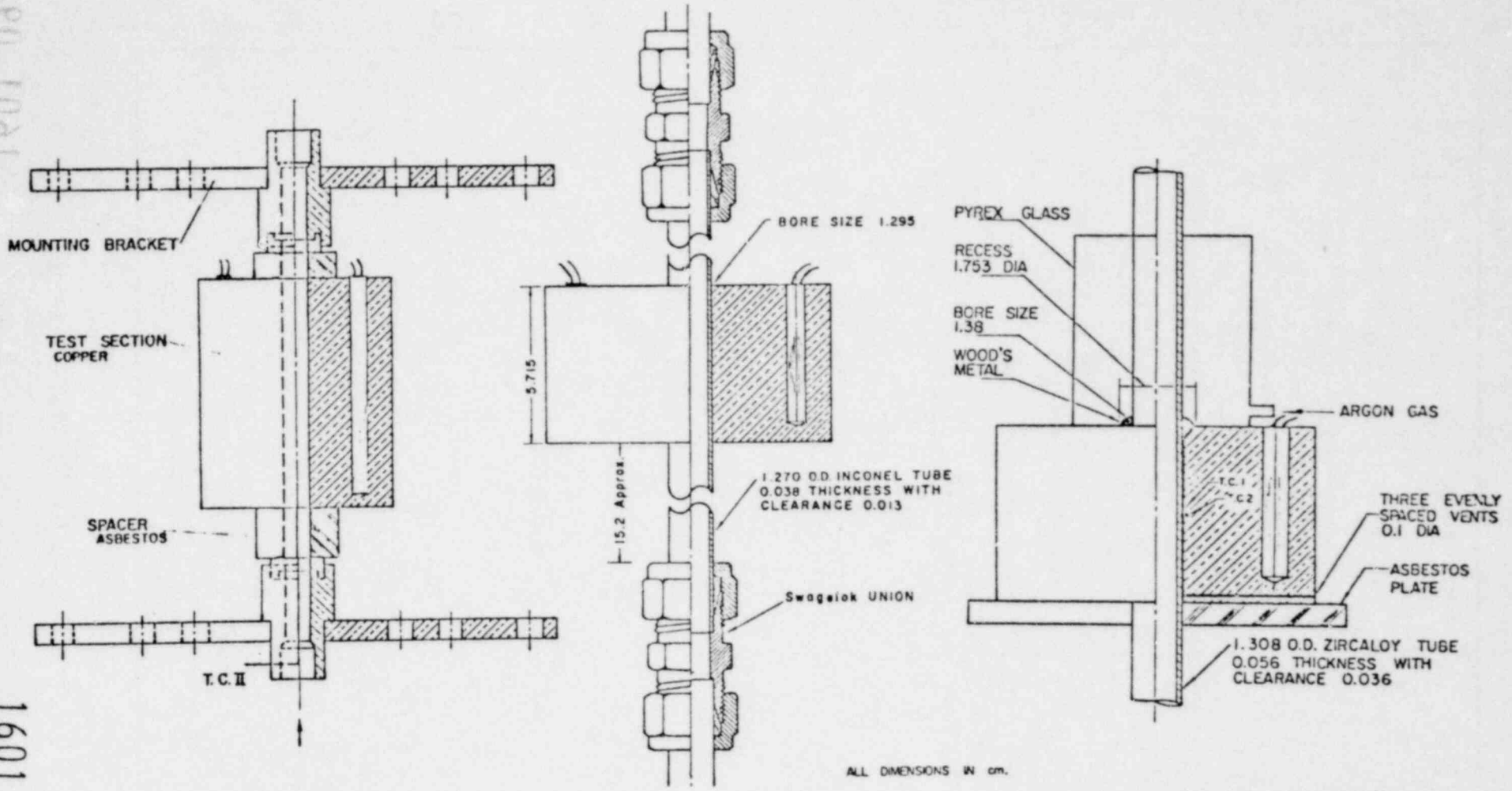

(a) CYLINDRICAL BLOCK, CENTRAL COOLING

(b) FLOW TUBE BRAZED TO BLOCK

(c) LIQUID METAL GLAND BETWEEN COPPER BLOCK AND FLOW TUBE

FIGURE 7 TEST SECTION DESIGNS FOR TRANSITION BOILING STUDY

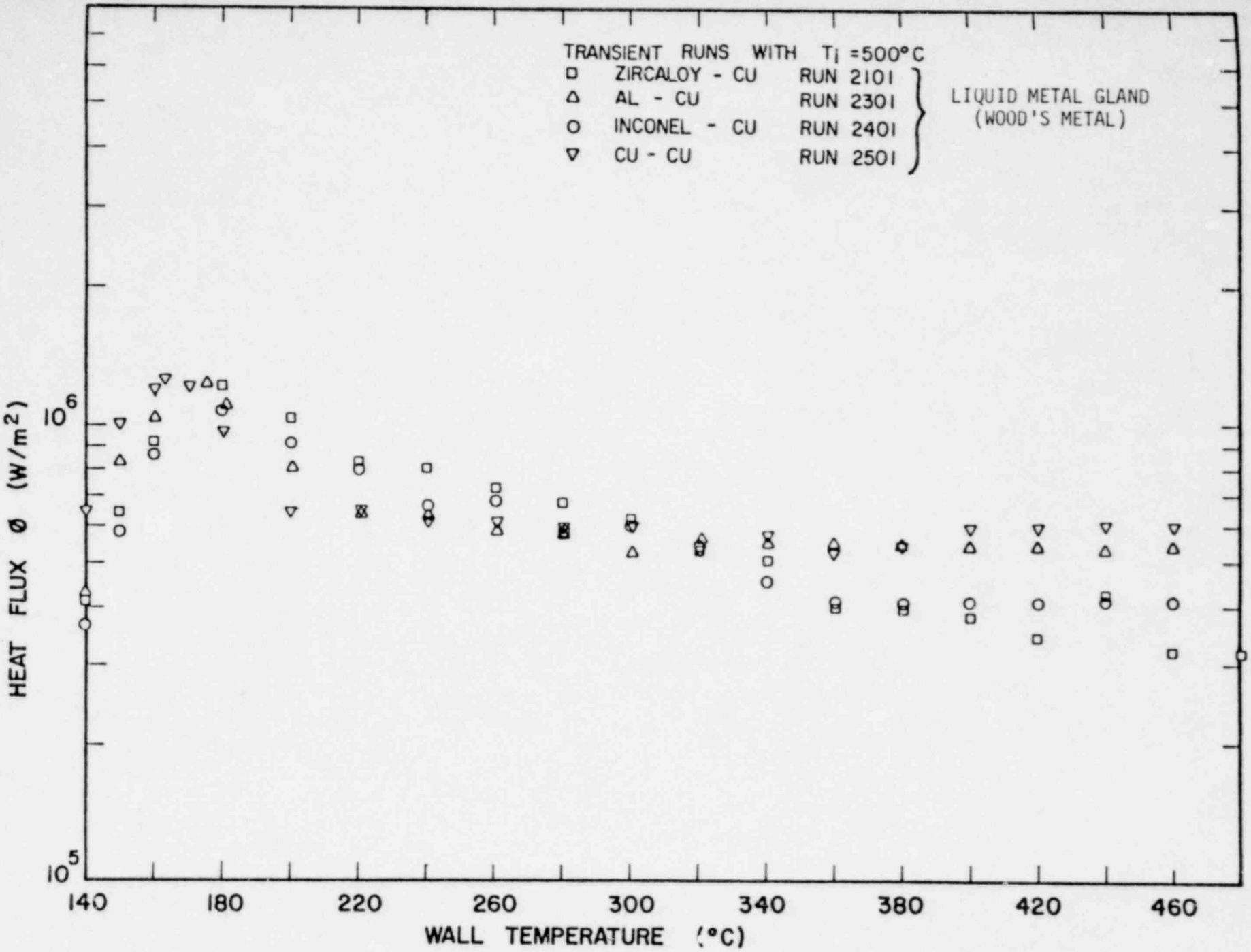

FIGURE 8 COMPARISON OF BOILING CURVES FOR VARIOUS HEATED SURFACES AT G=136 kg/m²s & ΔT_{SUB} = 13.9°C, USING 1-D MODEL

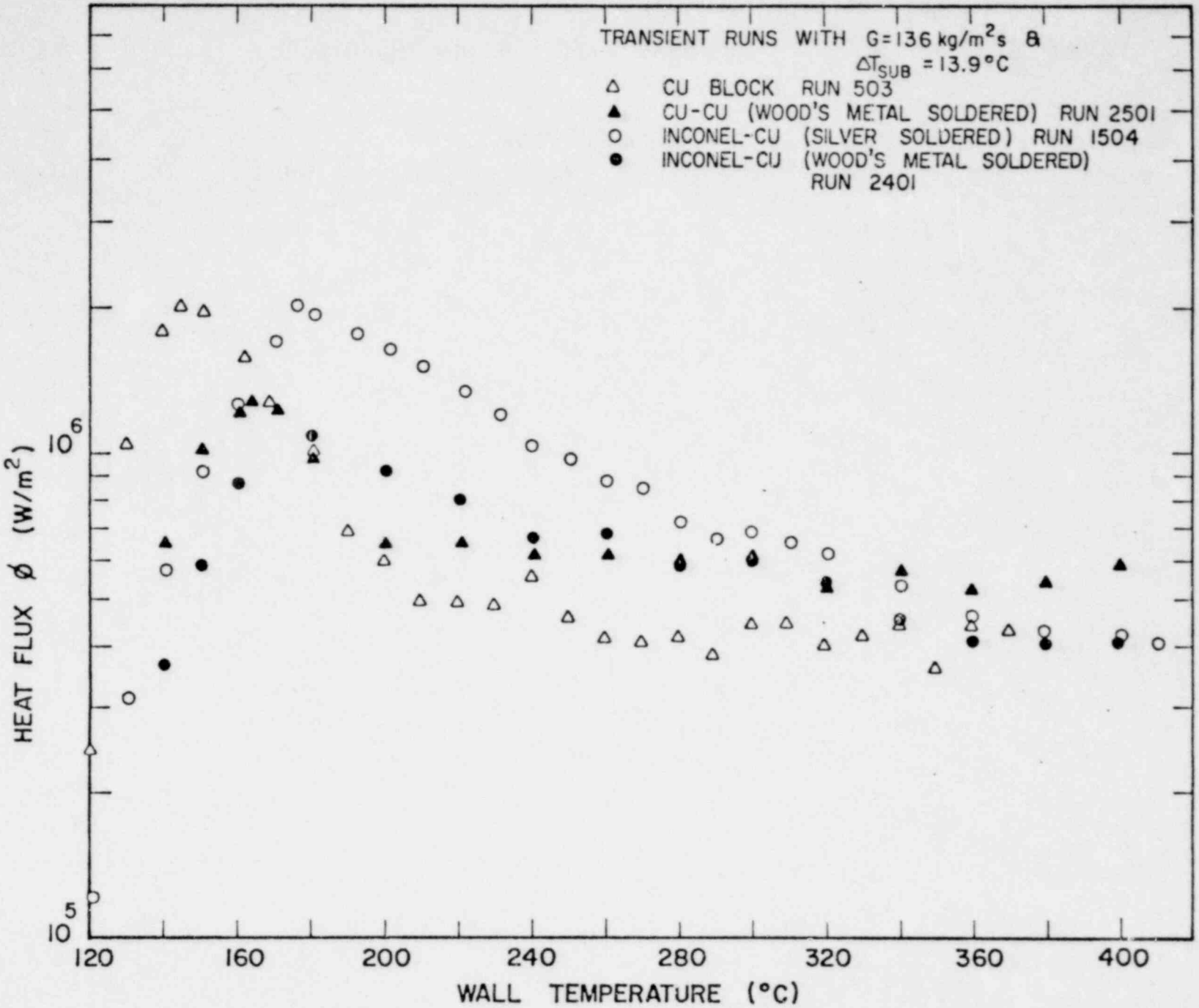

FIGURE 9 COMPARISON OF BOILING CURVES FROM WOOD'S METAL SOLDERED COMPOSITE TEST SECTIONS WITH OTHER DATA

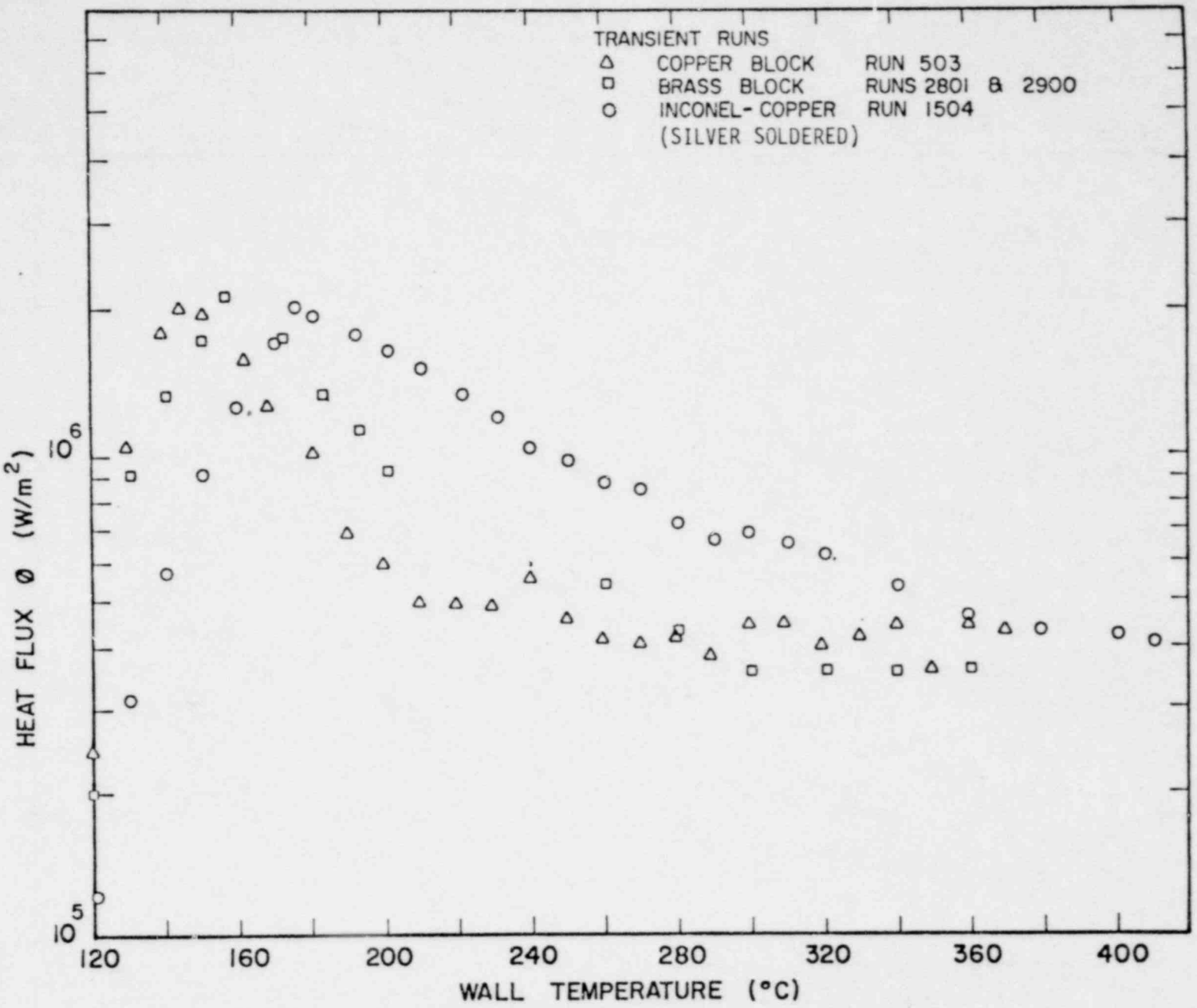

FIGURE 10 COMPARISON OF BOILING CURVES FOR COPPER, BRASS & INCONEL HEATED SURFACES AT $G = 136\ kg/m^2s$ & $\Delta T_{SUB} = 13.9°C$

PREDICTION OF CORE REWET BEHAVIOR

Presented at
The Seventh Water Reactor Safety Research Information Meeting
November 5-9, 1979
Gaithersburg, Maryland

R. A. Nelson
EG&G Idaho, Inc.

Idaho National Engineering Laboratory
Idaho Falls, Idaho 83401

PREDICTION OF CORE REWET BEHAVIOR

R. A. Nelson
EG&G Idaho, Inc.

The core rewet phenomena observed in recent LOFT Loss-of-Coolant Experiments (LOCE) L2-2 and L2-3 were not adequately predicted by either RELAP4/MOD6[a,b] or TRAC-P1A. The experimentally observed rewet phenomena have been predicted, however, by modifying RELAP4/MOD6 with the TRAC-P1A critical heat flux (CHF) correlation[c] and by modifying TRAC-P1A to include the Iloeje minimum film boiling correlation. A study is currently underway to determine what physical phenomena must be accounted for to obtain a correct analytical technique to accurately predict the core rewet phenomena observed in experiments such as LOFT LOCEs L2-2 and L2-3. The first phase of that study involves determining the reasons why RELAP4/MOD6 and TRAC-P1A did or did not predict the experimentally observed rewets. This discussion explains what has been learned to date, during this first phase of the study.

---

a. RELAP4/MOD6, Idaho National Engineering Laboratory Configuration Control Number C0010006.

b. RELAP4/MOD6, versions used for the experiment prediction for LOCE L2-3, Idaho National Engineering Laboratory Configuration Control Numbers H0003384B and H0003284B.

c. RELAP4/MOD6, as modified with the TRAC CHF correlation, Idaho National Engineering Laboratory Configuration Control Number H0072284B.

Three calculational aspects of the codes are postulated to have caused the disparity between predicted and measured fuel rod cladding temperature response for LOCEs L2-2 and L2-3:

1. The calculated initial fuel rod stored energy
2. The hydraulic calculation
3. The calculated heat transfer surface.

The RELAP4/MOD6 fuel rod stored energy and hydraulic calculations have been examined and determined to be reasonable. Although TRAC-P1A did not predict the system hydraulics as well as RELAP4/MOD6, its core hydraulics were similar enough to those of RELAP4/MOD6 to not affect the material presented here. The conclusion reached is that further investigation on core rewet behavior should be concentrated on gaining an understanding of methods of calculating the basic heat transfer processes. To obtain this understanding, the initial process is to determine how the CHF boiling curves are constructed in the two codes.

Heat transfer surfaces are constructed in RELAP4/MOD6 and TRAC-P1A in different ways. The RELAP4/MOD6 post-CHF portion of the boiling curve is constructed by summing transition and film boiling correlations. This approach allows a minimum film boiling point to be implied which can be calculated, although it is not generally evaluated.

The post-CHF portion of the boiling curve is constructed in TRAC-P1A by linear interpolation between the departure from nucleate boiling point and the minimum film boiling point. A specific correlation is used to define the minimum film boiling correlation.

When the Iloeje minimum film boiling correlation is used to replace the correlation in TRAC-P1A, the code predicts the rewets observed in LOFT LOCEs L2-2 and L2-3. The reason is that the modified

version of TRAC-P1A now predicts transition instead of film boiling at the fluid conditions of interest. For similar reasons, RELAP4/MOD6, when modified with the TRAC-P1A CHF correlation, predicts the rewets observed in LOCEs L2-2 and L2-3.

In order to evaluate which technical approach is appropriate for predicting the rewet observed in LOCE L2-3, the available (approximately 4500) post-CHF data points, with respect to their mass flux and quality were examined, and the RELAP4/MOD6 prediction of the hot spot hydraulics for LOCE L2-3 was superimposed. The conclusion reached was that no (or minimal) data are available to determine which technical approach is most correct. Also the conclusion was reached that additional separate effects tests are needed to broaden the data base, especially in the area of low flow, low quality post-CHF heat transfer.

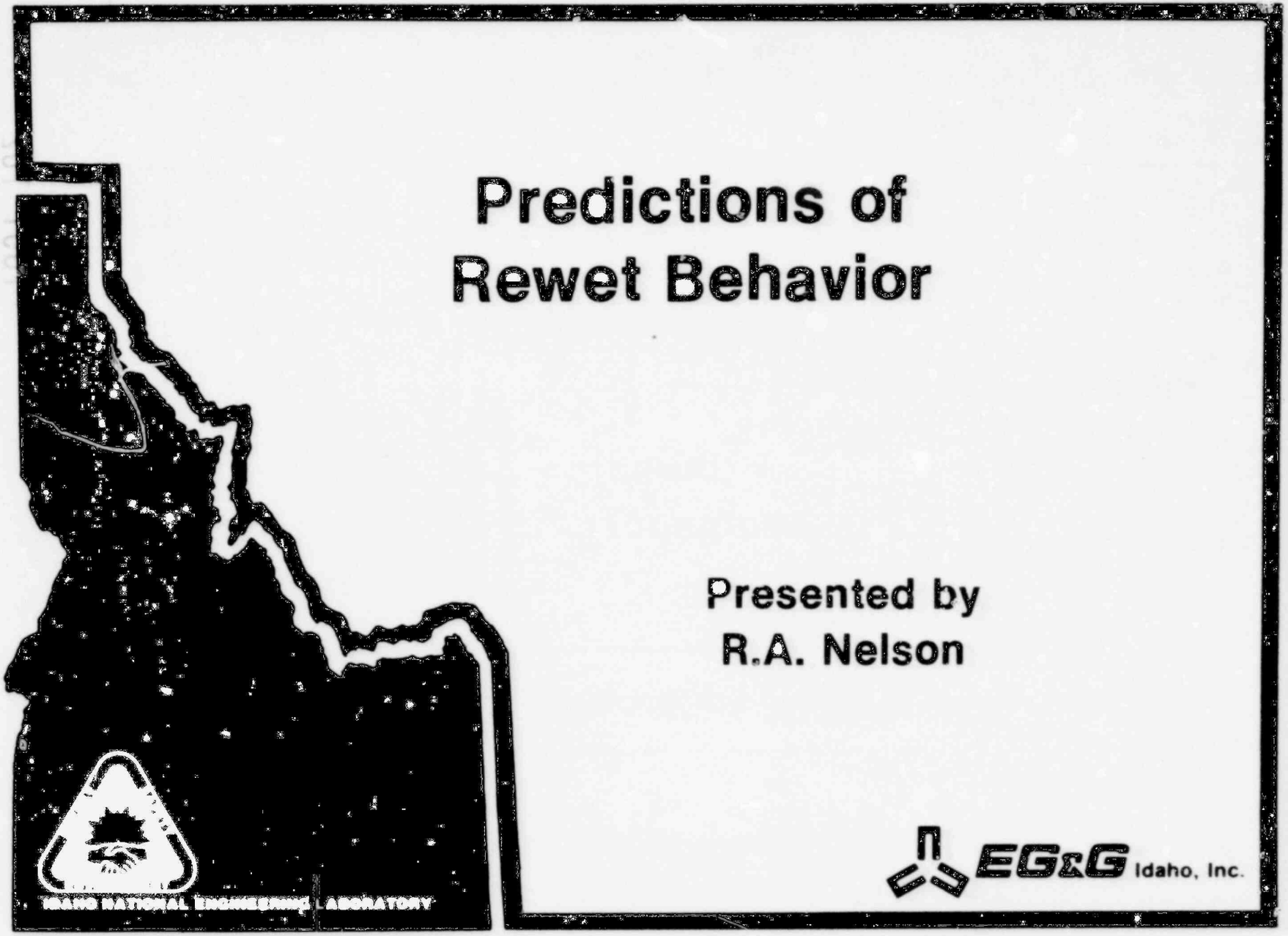

Predictions of Rewet Behavior

Presented by
R.A. Nelson

EG&G Idaho, Inc.

1601 101

RELAP4/MOD6
Boiling Curve

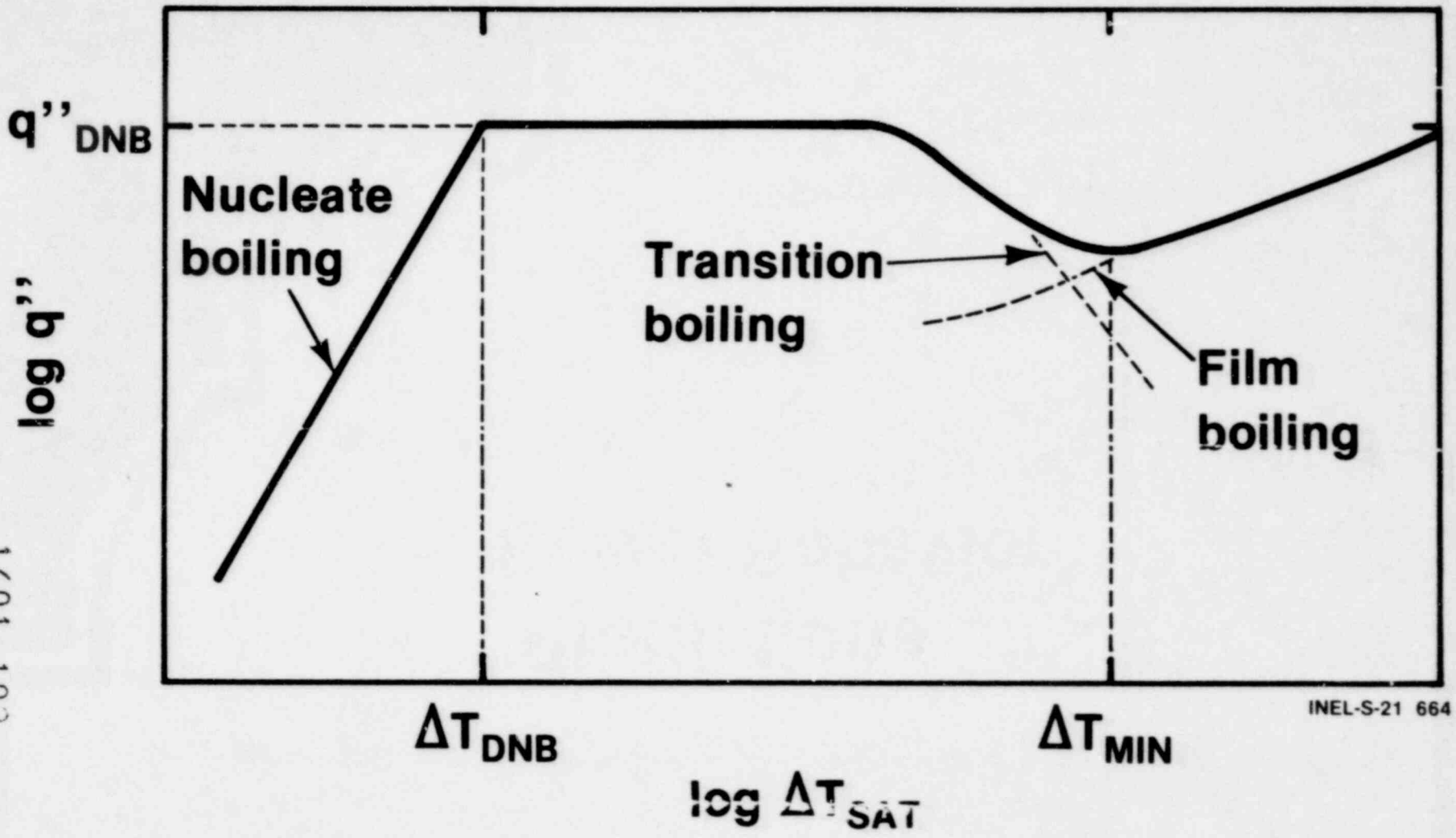

RELAP4/MOD6 Blowdown Heat Transfer Surface

INEL-S-21 665

RELAP4/MOD6 Calculated Mass Flux

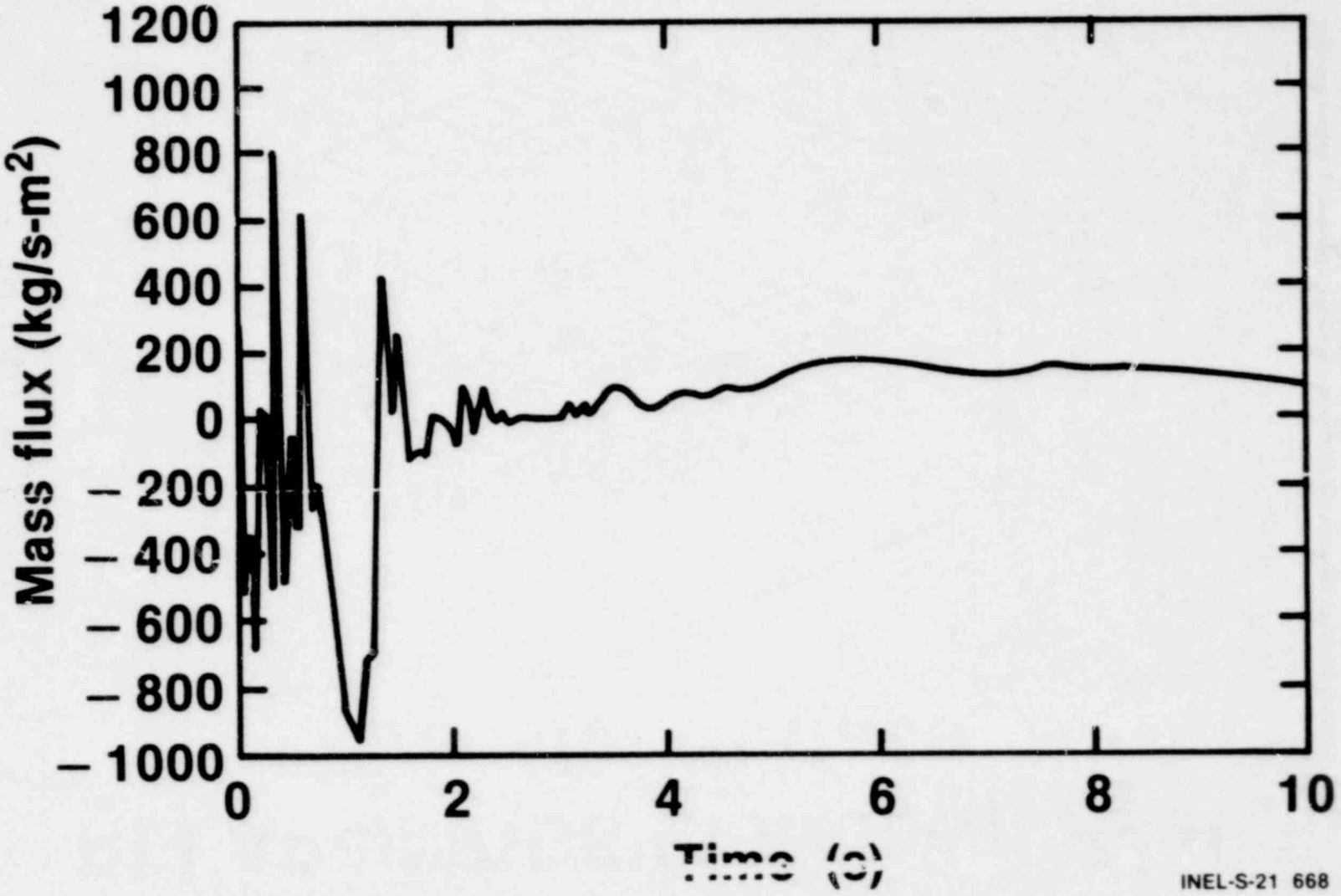

INEL-S-21 668

RELAP4/MOD6 Calculated Quality

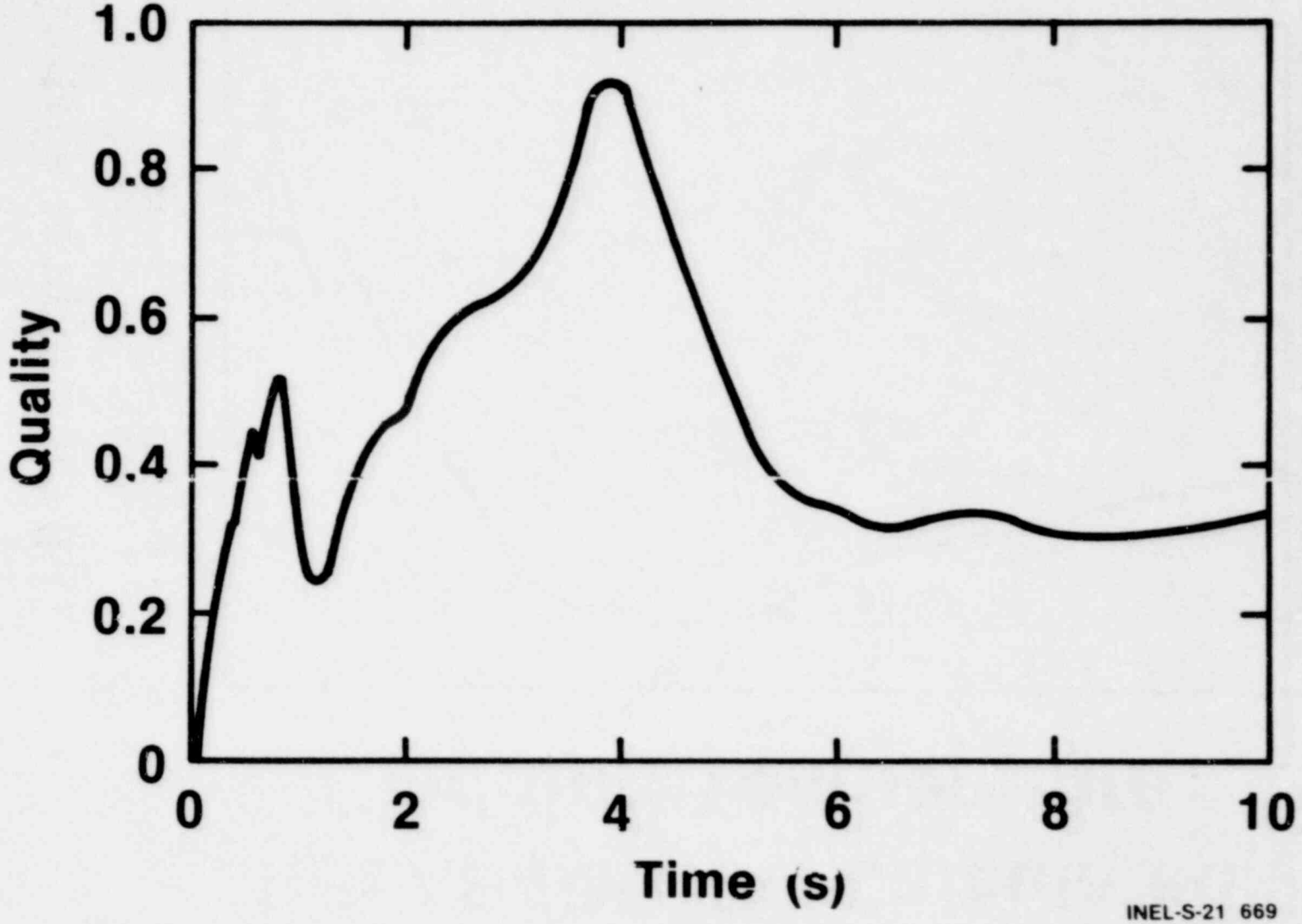

INEL-S-21 669

RELAP4/MOD6 Calculated Cladding Temperature

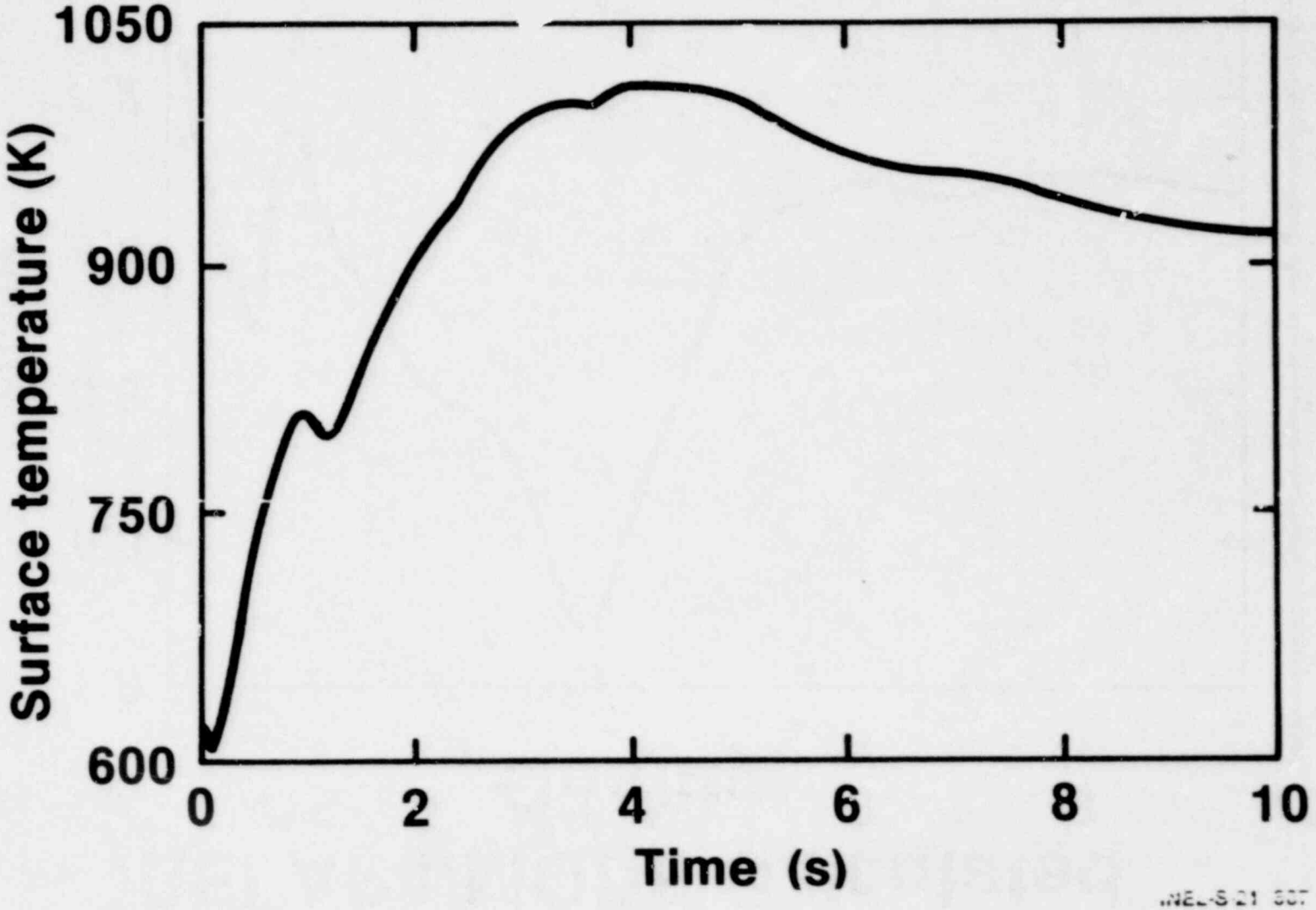

TRAC Boiling Curve

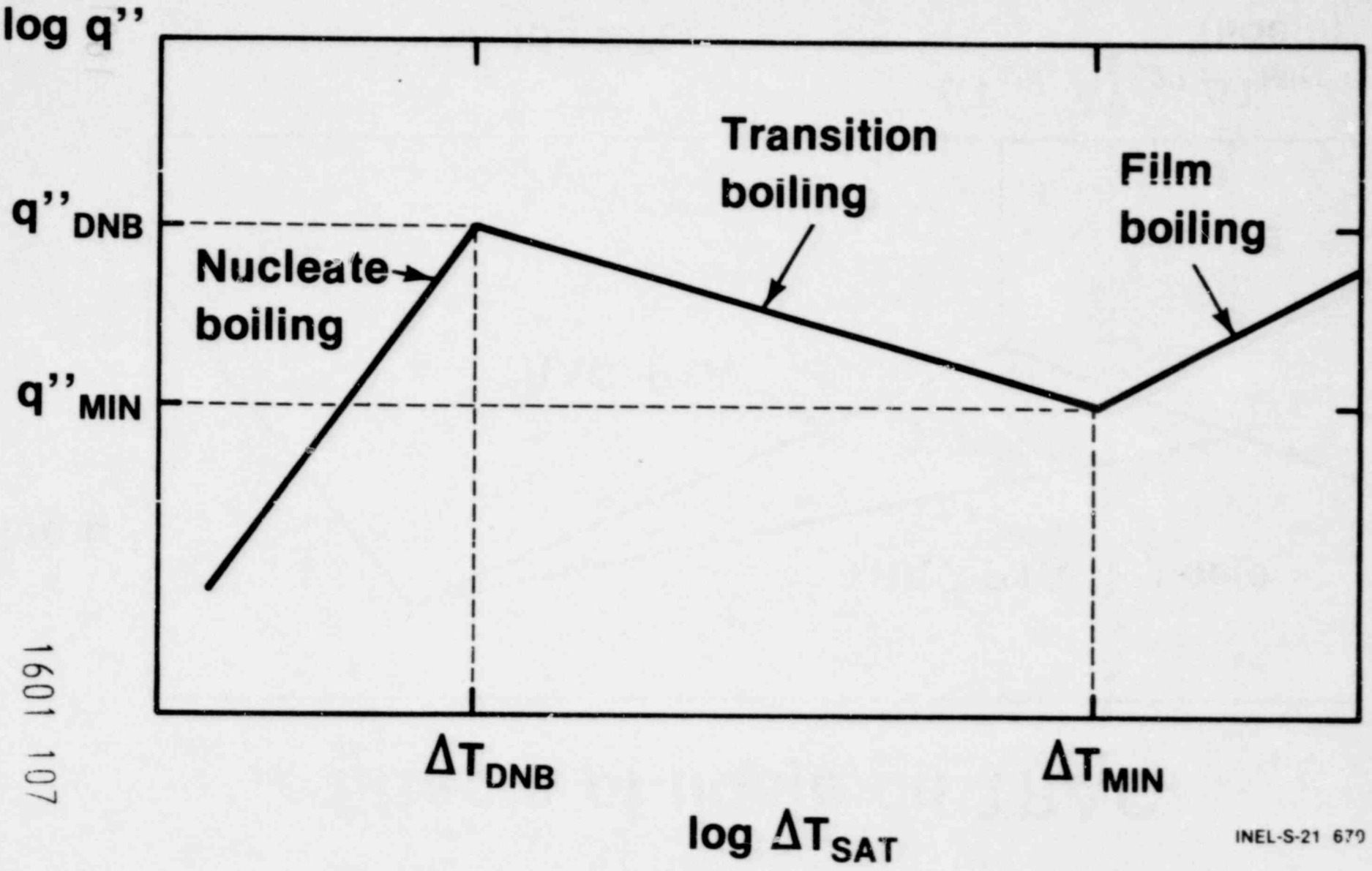

INEL-S-21 679

1601 107

Effects of Iloeje on TRAC

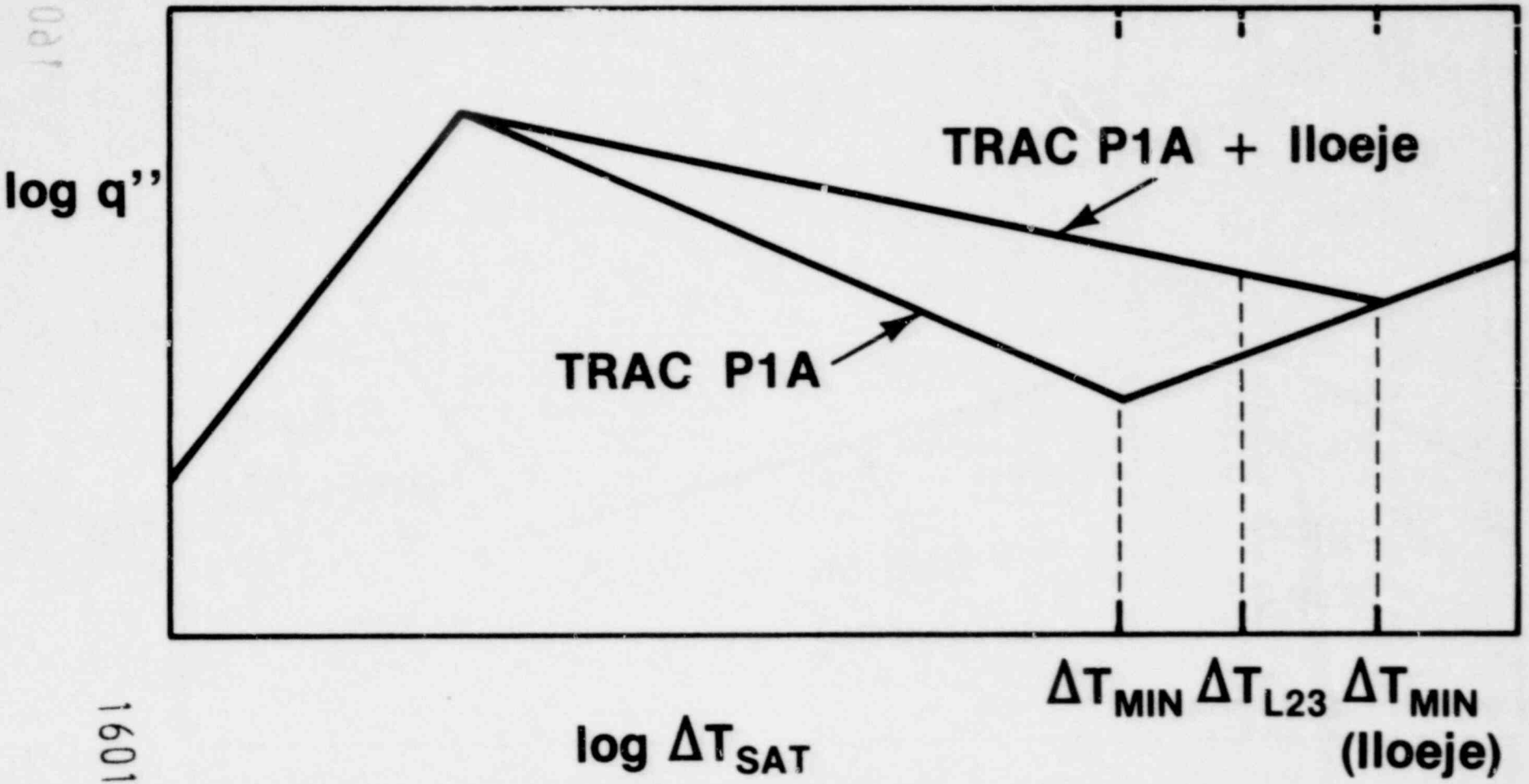

INEL-S-21 671

Effect of CHF Correlation on TRAC

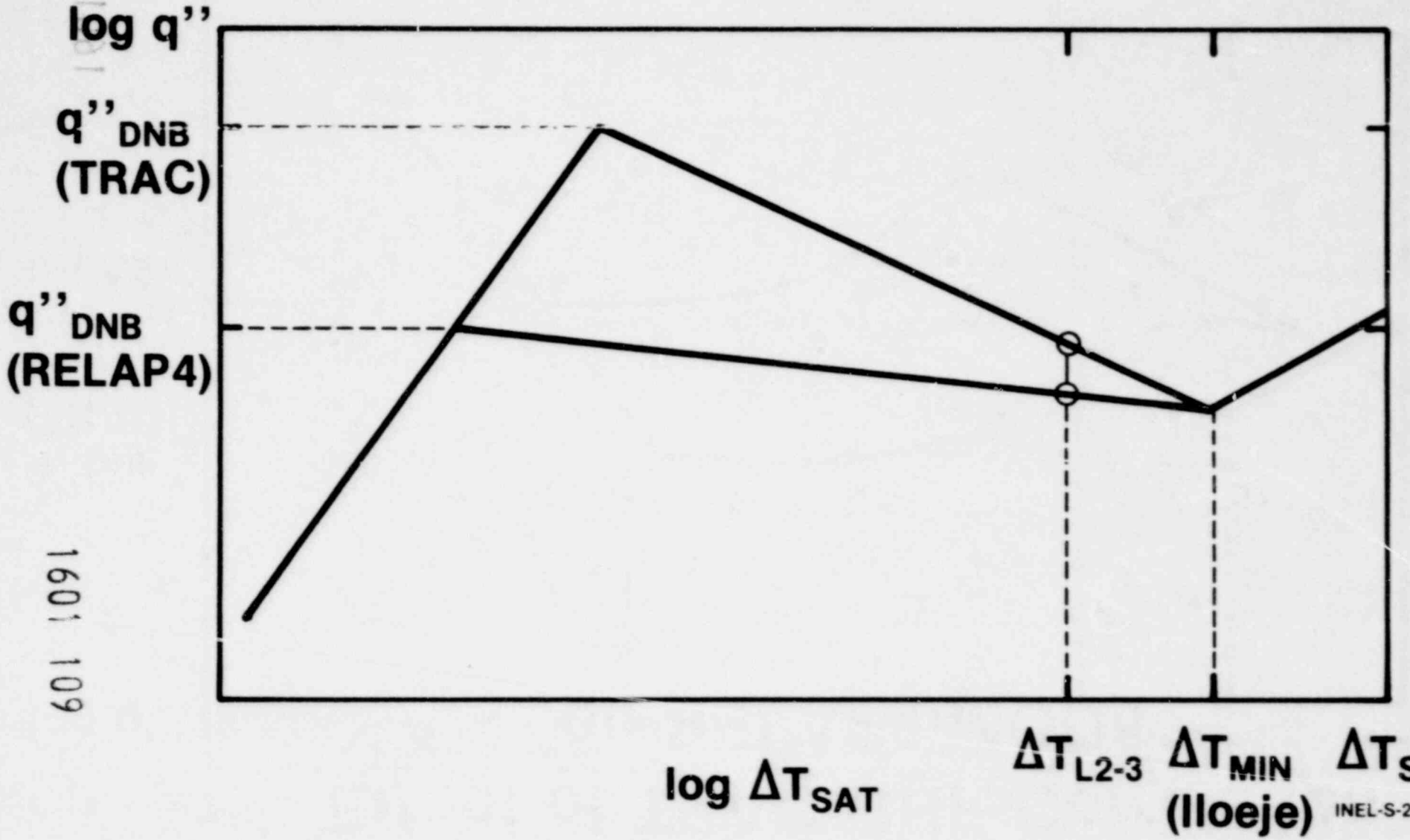

Effect of TRAC CHF Correlation on RELAP4/MOD6

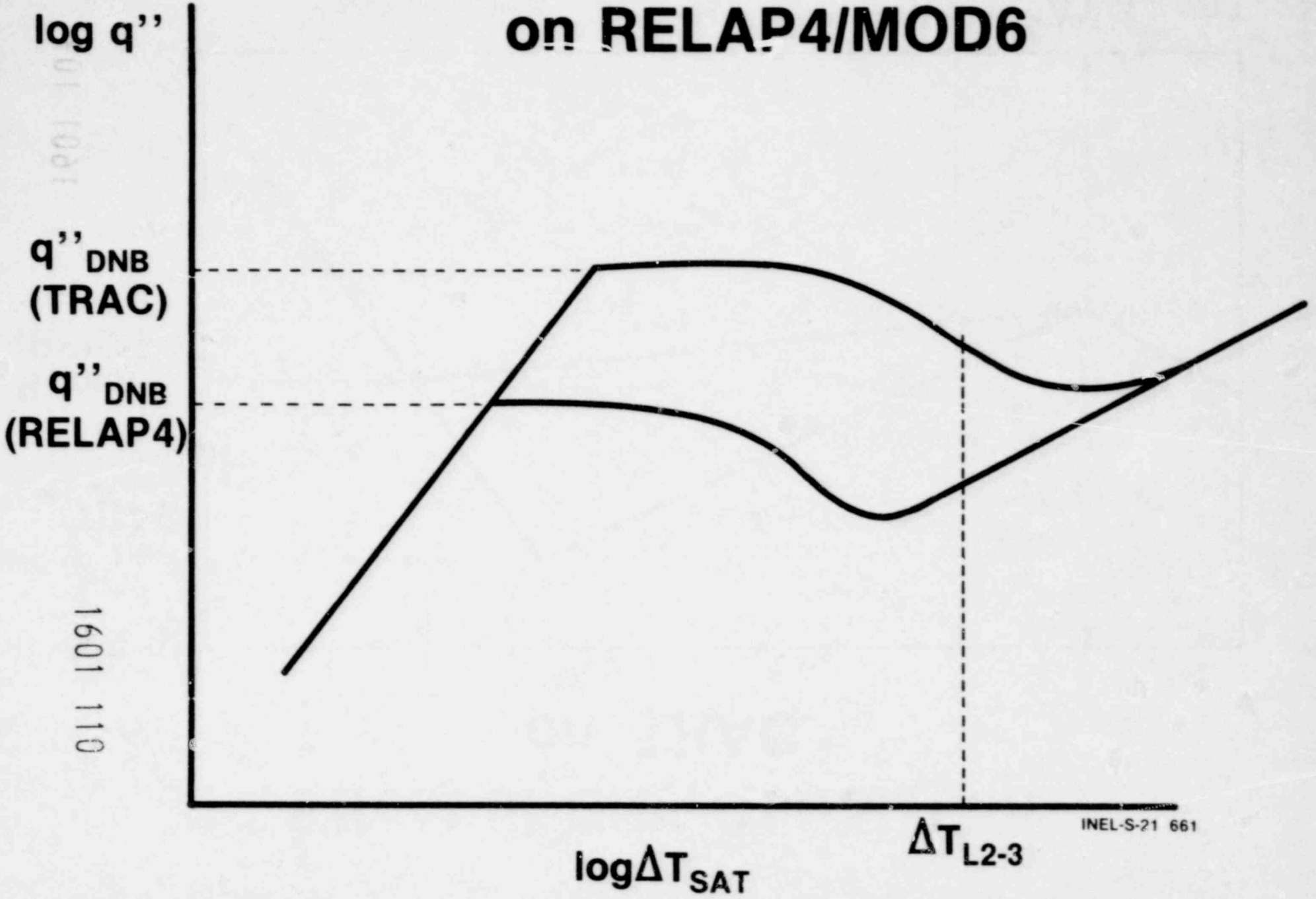

Effect of TRAC CHF Correlation on RELAP4

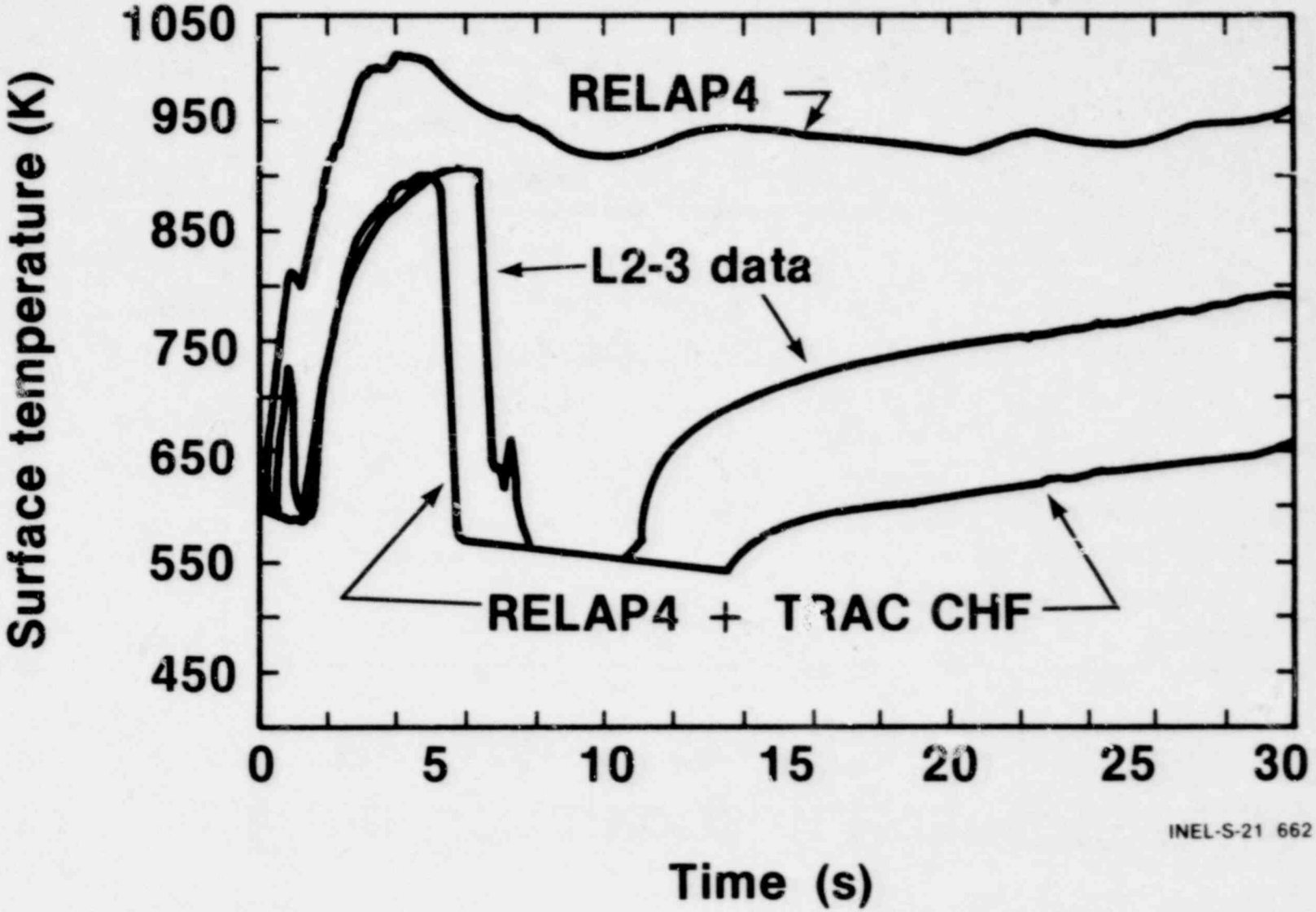

Fluid Conditions in Post-CHF Data Base and LOFT Calculations

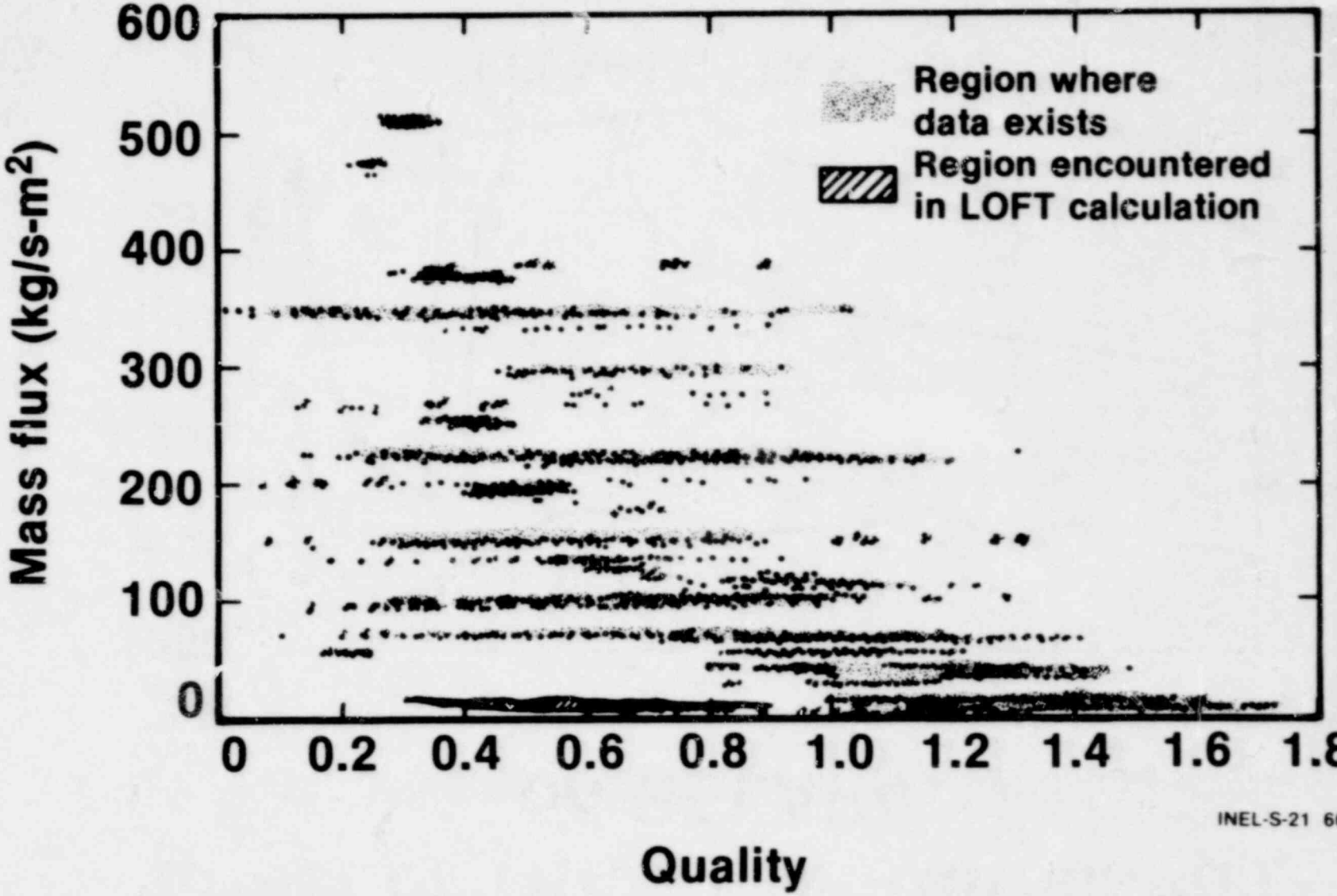

Conclusions

1. Neither RELAP4/MOD6 or TRAC-P1A properly predict high pressure rewet

2. Both codes can predict rewet when their heat transfer surfaces are changed

3. An inadequate data base exists for post-CHF heat transfer in area of interest

CLADDING REWETS OBSERVED IN THE LOFT LARGE BREAK LOSS-OF-COOLANT ACCIDENT TESTS

Presented at
The Seventh Water Reactor Safety Research Information Meeting
November 5-9, 1979
Gaithersburg, Maryland

E. L. Tolman

EG&G Idaho, Inc.

Idaho National Engineering Laboratory
Idaho Falls, Idaho 83401

CLADDING REWETS OBSERVED IN THE LOFT LARGE BREAK LOSS-OF-COOLANT ACCIDENT TESTS

E. L. Tolman
EG&G Idaho, Inc.

During FY 79, two large break loss-of-coolant-experiments (LOCEs) were conducted in the Loss-of-Fluid-Test (LOFT) reactor. The tests designated L2-2 and L2-3 differed only in core linear heat generation of 26 and 39 kW/M respectively. The test results are summarized in References 1-4. Of particular interest during both tests was the dominant cladding rewet and temperature quench which occurred between 5 and 10 seconds during the blowdown phase of the experiment. This paper summarizes the current understanding of the observed rewet behavior in LOFT tests, particularly in regard to the strong correlation between cladding rewets and core thermal hydraulic conditions, the consistency of the cladding thermocouple data, and the ability of the cladding thermocouples to accurately measure cladding temperatures.

The LOFT core consists of 1300 fuel rods of nominal PWR design except for length (1.67 m) and internal prepressurization (0.10 MPa). The rods are assembled in nine fuel rod assemblies with the center assembly producing the maximum power. The cladding surface temperature is measured at 186 locations on 76 fuel rods located throughout the core and provide the only measurement of fuel rod response during the experiments. The measured peak cladding temperatures were 780 and 910 K for L2-2 and L2-3 respectively.

The cladding temperatures for both experiments show the same general trends and correlate directly to the core thermal-hydraulic behavior which was similar for both tests. Initial departure from

nucleate boiling and resulting rapid cladding temperature increase occurred between 0.9 and 2.20 s (all times are with respect to the initiation of the break) as a result of core flow stagnation which continued until upward core flow was reestablished at about 2.5 s. The upward flow continued for several seconds and resulted in significant cooling of the fuel rods; for example, between 3 and 5.5 seconds the maximum cladding temperature increase was less than 125 K. The timing of the very rapid cladding temperature quench which progressed from the bottom to top of the core between 5.5 and 7.5 s, is coincident with a redistribution of lower quality coolant flow (150 cm/sec) in the reactor vessel as indicated by the measured mass flow in the downcomer, increased sensitivity of the core neutron detectors, core liquid level detectors, core upper plenum coolant thermocouples, and the increased coolant density in the broken hot leg. The cladding remained quenched for 2 - 8 s (depending on thermocouple location) after which the higher power locations experienced dryout as a result of decreasing core flows. Finally the reactor was rapidly flooded by emergency core cooling (ECC) water between 40 - 50 s.

The emergency core cooling (ECC) reflood rates were very rapid for L2-2 (10 cm/s) and L2-3 (12 cm/s) indicating insignificant nuclear stored energy in the core at the time of reflood. In fact, for the lower power L2-2 test, the core reflooding rate was identical to a similar test (L1-5, Reference 5) with zero nuclear power. By comparison, pretest RELAP4/MOD6 predictions in which cladding temperatures were not quenched (high nuclear stored energy at reflood initiation) indicates reflood rates less than 2 cm/s. These observations imply that the cladding temperature quench occurred corewide (as opposed to only the 76 rods instrumented with thermocouples) and resulted in significant stored energy removal from the fuel rods. FRAP-T4 energy balance calculations using the measured peak cladding temperature indicate 30 to 40% of the initial nuclear stored energy is removed during the several second quench period for both tests.

Evaluation of the center module thermocouple data prior to and during the temperature quench shows remarkable consistency. The thermocouples at identical axial elevations in the three instrumented rod clusters measure the same peak cladding temperature to within 10 to 40 K and comparison of the cladding temperature turnaround time at each axial elevation as a result of the quench is consistent to within 0.1 to 0.2 seconds. The time required to quench the cladding temperatures to the coolant saturation point ranges from 0.5 to 3.0 seconds being maximized at axial elevations corresponding to the rod peak power zone (0.61 to 0.76 m).

The measured cladding temperatures indicate the importance of the local thermal-hydraulic conditions along the axial length of the rod both before and during the temperature quench. Comparison of the quench rate between the single rods (next to control rod guide tubes) and clustered rods, show the single rods to quench faster. Also, faster cooling rates are observed in the regions of the fuel rod spacer grids. Changing thermal-hydraulic differences axially along the fuel rod explain the more rapid quench observed near the bottom of the rod compared to equal power producing regions at higher elevations.

The potential perturbation effects and accuracy of the cladding surface thermocouples have been questioned and several test programs are providing data to better establish conditions under which the thermocouples could result in atypical cooling of the fuel rod.

The ability of the thermocouples to accurately measure cladding temperatures has been evaluated at INEL by comparing the response of LOFT surface thermocouples to very small surface embedded thermocouples on zircaloy clad heater rods under simulated LOFT blowdown and reflood conditions (References 6 and 7). The results showed temperature agreement to within 30 K and reflood quench times to within 1.0 second. These tests did not compare rod response with

and without surface thermocouples and therefore do not provide a basis for estimating the selective interference of the thermocouple sheath attachment (axially along the fuel rod) with the test hydraulics. Tests are currently being conducted in the INEL Blowdown Facility and the German COSIMA facility using electric heater rods (with and without LOFT thermocouples) and in the Power Burst Facility (PBF) test reactor utilizing nuclear rods (with and without LOFT thermocouples) to study the effects of surface thermocouples during simulated blowdown and reflood temperature quenches. Low pressure reflood tests will be conducted this fiscal year in the Swiss NEPTUN and German REBEKA facilities to evaluate thermocouple response in larger rod clusters.

The most significant insight relating to the atypical cooling effects of surface thermocouples during a LOCA sequence has been obtained from the LOFT Lead Rod Tests conducted in the PBF reactor during FY 79 (References 8 and 9). The purpose of these tests was to quantify the mechanical behavior of the LOFT fuel rods during LOCE tests simulating the first LOFT nuclear series in which cladding deformation could be expected. The comparison of cladding elongation measurements with cladding temperature measurements on rods with and without surface thermocouples during quench events allow an evaluation of the potential cooling effects of LOFT type cladding surface thermocouples. The results indicate, (1) very rapid (1.0 - 2.0 s) cladding temperature quench can occur for nuclear rods during fast, high pressure, cooling transients, (2) during low pressure reflood, for rapid reflooding rates (10 cm/s), differences in reflood quench as indicated by surface thermocouples and cladding elongation measurements can be 3-4 s, (3) during low pressure reflood, for slower reflooding rates (< 1.0 cm/s), the difference between quench measurements was less than 1.0 s, and (4) the cladding elongation measurements showed the same relative response for rods with and without surface thermocouples. Also post-test visual observation of the rods with and without thermocouples indicate no significant

difference in the oxidation characteristics which indicates the surface thermocouples do not appreciably affect the overall thermal behavior of the rod prior to quench.

The LOFT data from Tests L2-2 and L2-3 indicate cladding temperature quench can occur on a nuclear fuel rod during the blowdown phase of a Loss-of-coolant-experiment. The tests provide a basis for a better understanding of the thermal-hydraulic behavior which influences fuel rod cladding temperatures.

REFERENCES

1. D. L. Batt, Quick Look Report on LOFT Nuclear Experiment L2-2, EG&G Idaho, Inc., LOFT-TR-103, December 1978.

2. M. L. McCormick-Barger, Experiment Data Report for LOFT Power Ascension Test L2-2, TREE-1322, NUREG/CR-0492, February 1979.

3. D. L. Reeder, Quick Look Report on LOFT Nuclear Experiment L2-3, EG&G Idaho Inc., QLR-L2-3, May 1979.

4. P. G. Prassinos et al, EDR for LOFT Power Ascension Experiment L2-3, TREE-1326, NUREG/CR-0792, July 1979.

5. M. S. Jacoby, Experiment Data Report for LOFT Nonnuclear Test L1-5 (Isothermal Test With Core 1 Installed), TREE-NUREG-1215, June 1978.

6. A. M. Eaton et al, LOFT Fuel Rod Thermocouple Calibration Test - Rod IH-8029-1, EG&G Idaho, Inc., LTR 141-87, September 1978.

7. A. M. Eaton et al, LOFT Cladding Surface Thermocouple Calibration Test Results for Zircaloy Clad Rod IH-8029-2, EG&G Idaho, Inc., LTR 141-88, January 1979.

8. D. J. Varacalle, Jr., R. W. Garner, PBF/LOFT Lead Rod Program Tests LLR-3, -4, -5 Quick Look Report, EG&G Idaho Inc. Report TFBP-TR-315, April, 1979.

9. D. J. Varacalle Jr., R. W. Garner, PBF/LOFT Lead Rod Program Test LLR-4A Quick Look Report, EG&G Idaho Inc. Report TFBP-TR-320, June 1969.

Cladding Rewet Experience from the LOFT Program

Presented by
E. Tolman

EG&G Idaho, Inc.

LOFT Core Cross Section

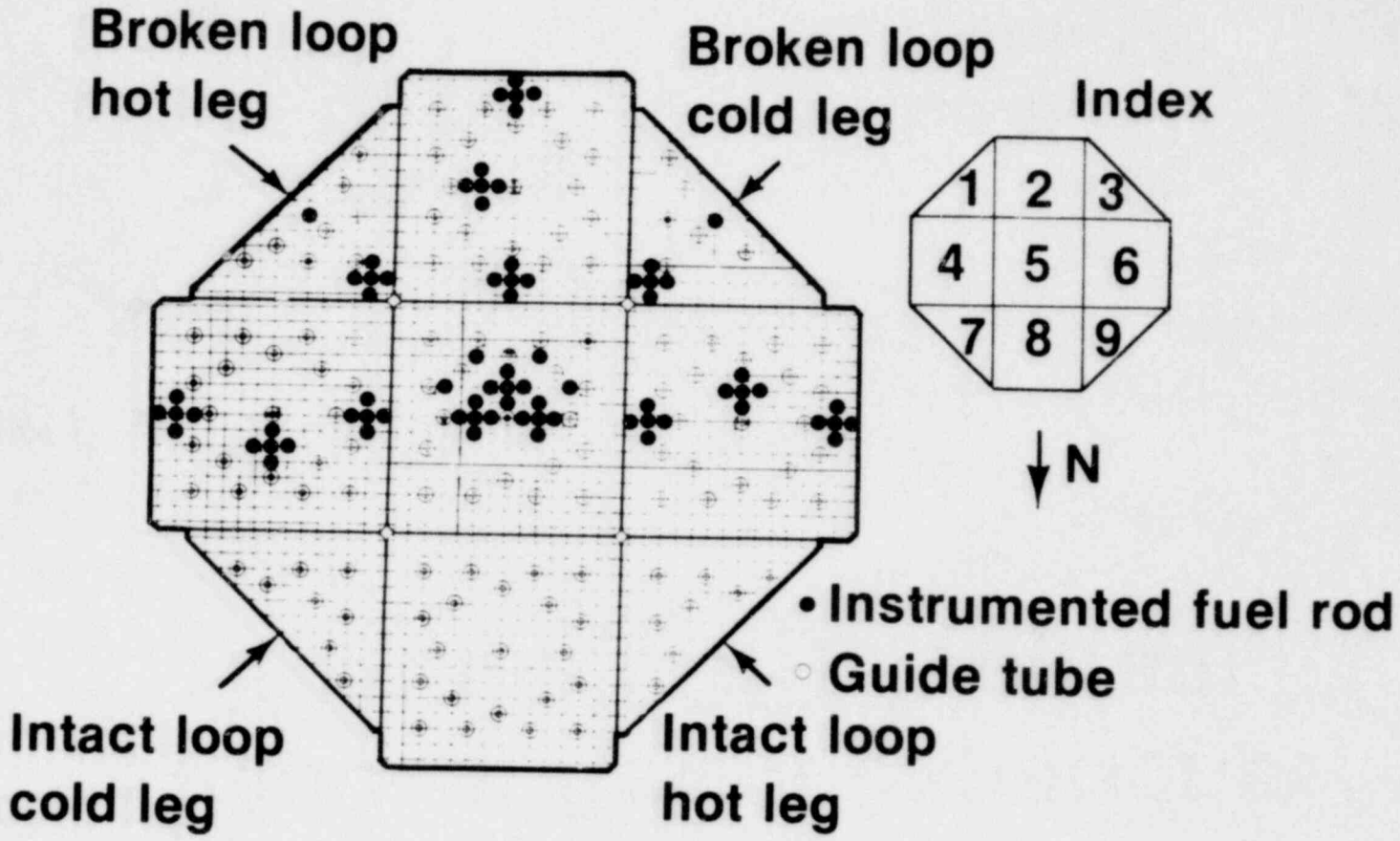

INEL-A-11 835
REVISION 1

L2-2/L2-3 Cladding Temperature Comparison

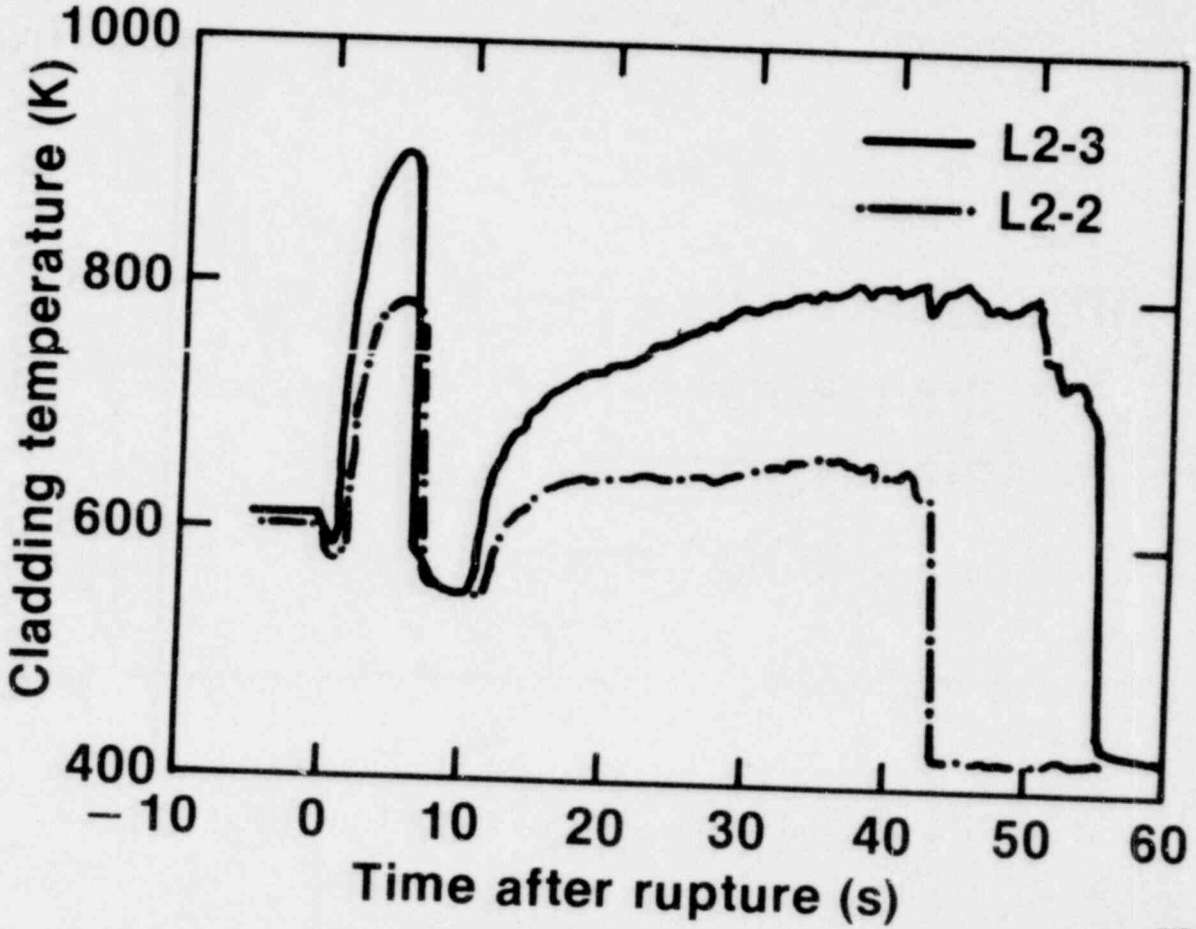

:NEL-S-19 871

Core Reflood Characteristics

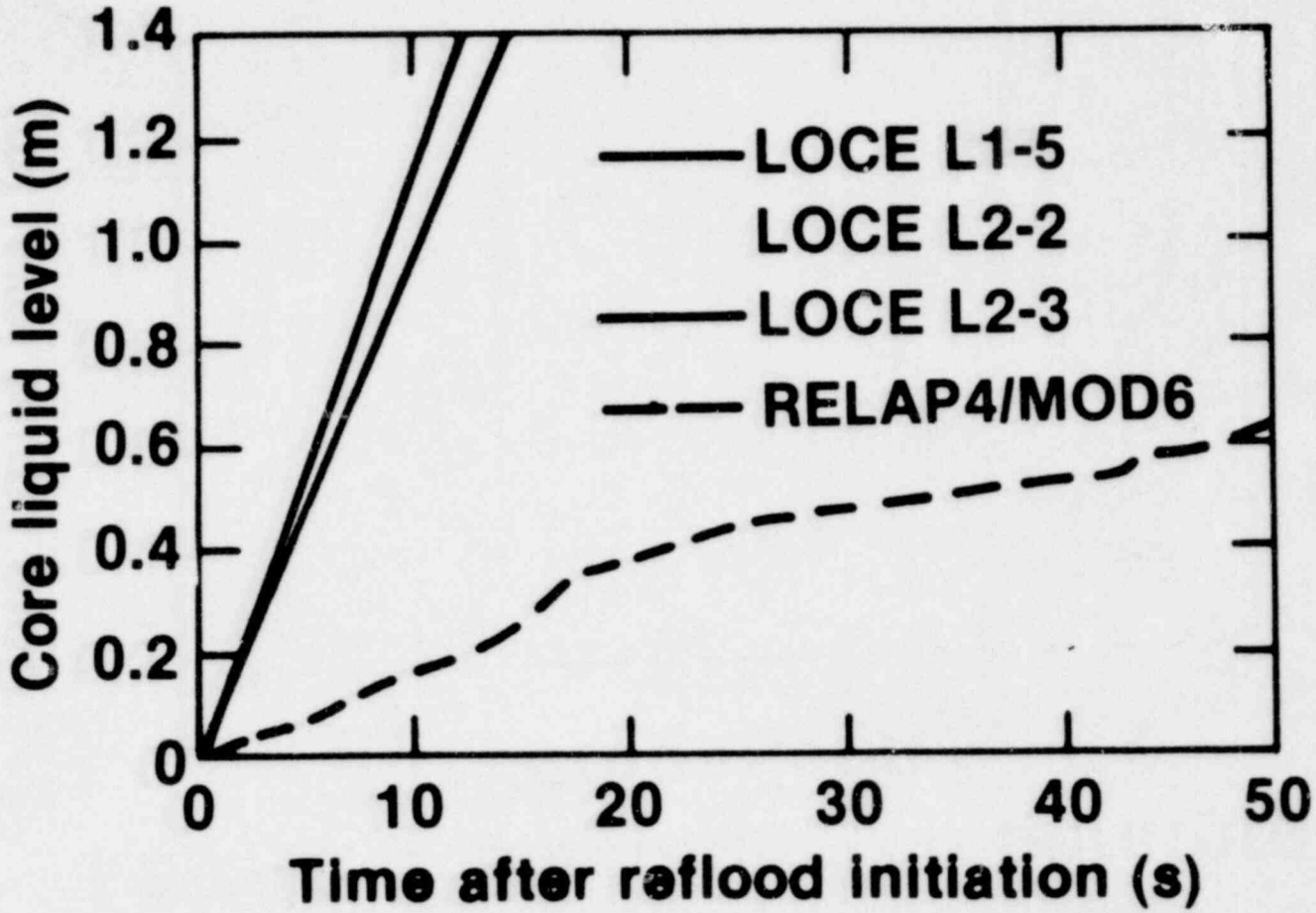

INEL-S-18 317

Fuel Rod Stored Energy

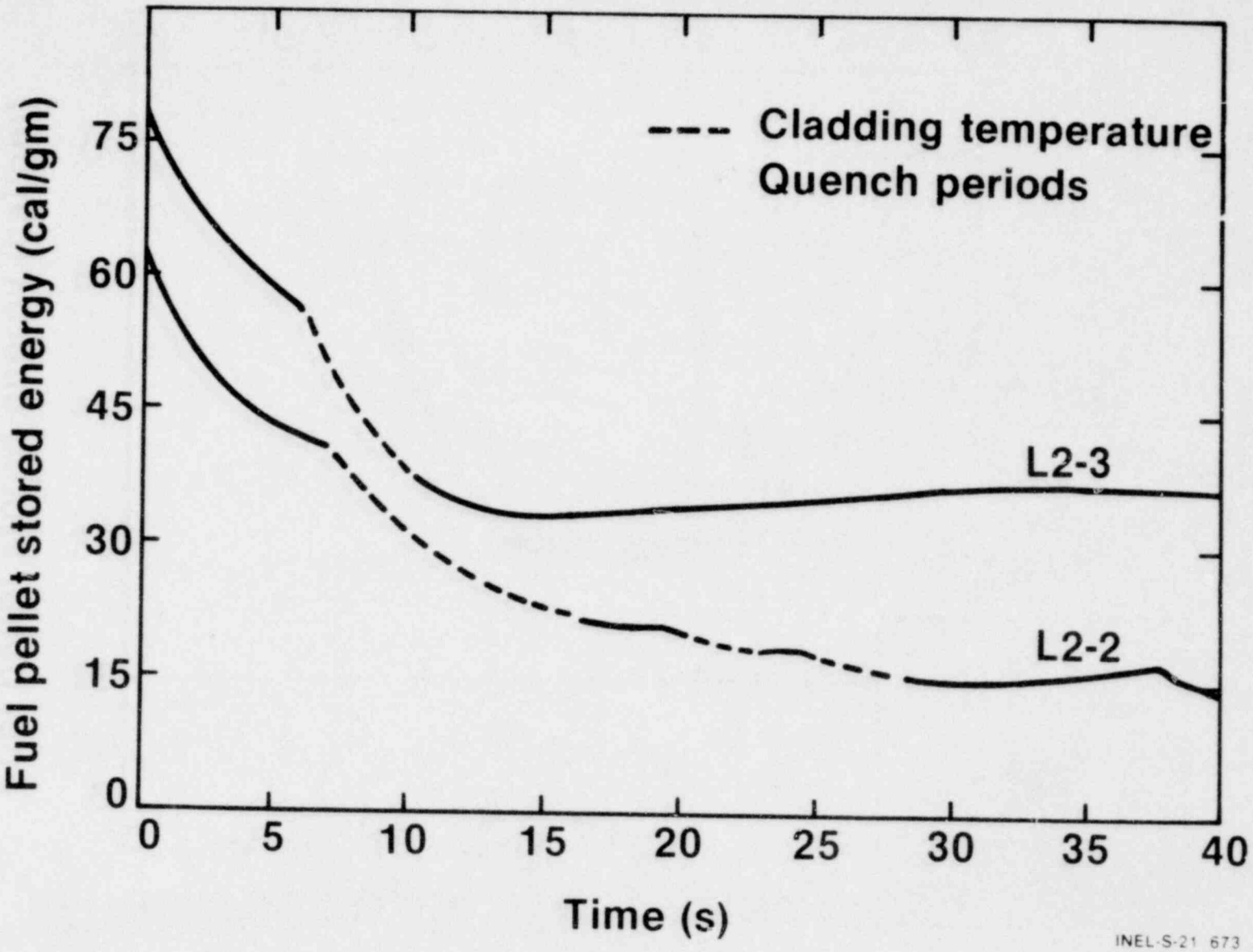

INEL-S-21 673

Thermocouple Response
0.2 m (L2-3)

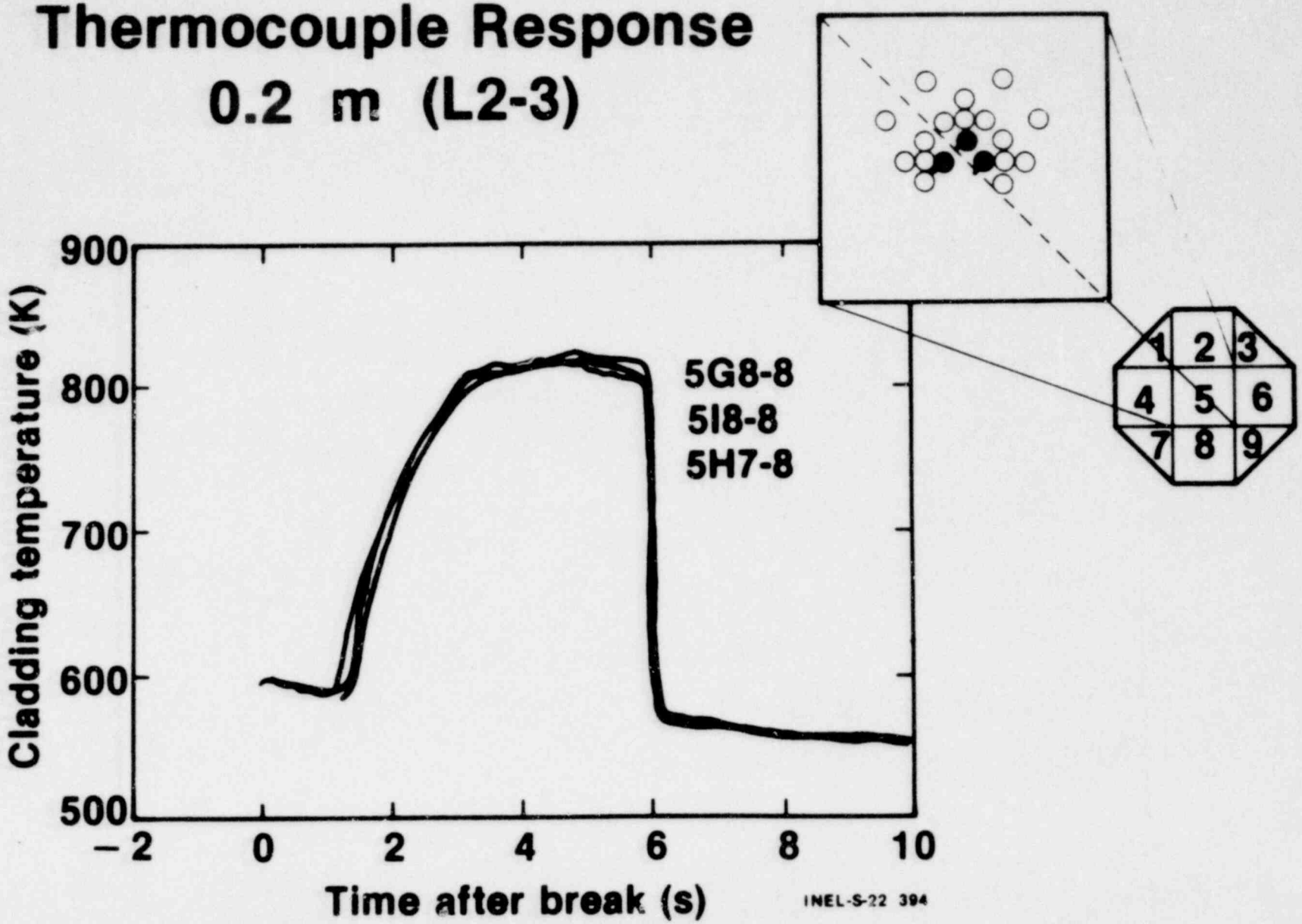

Thermocouple Response
0.81 m (L2-3)

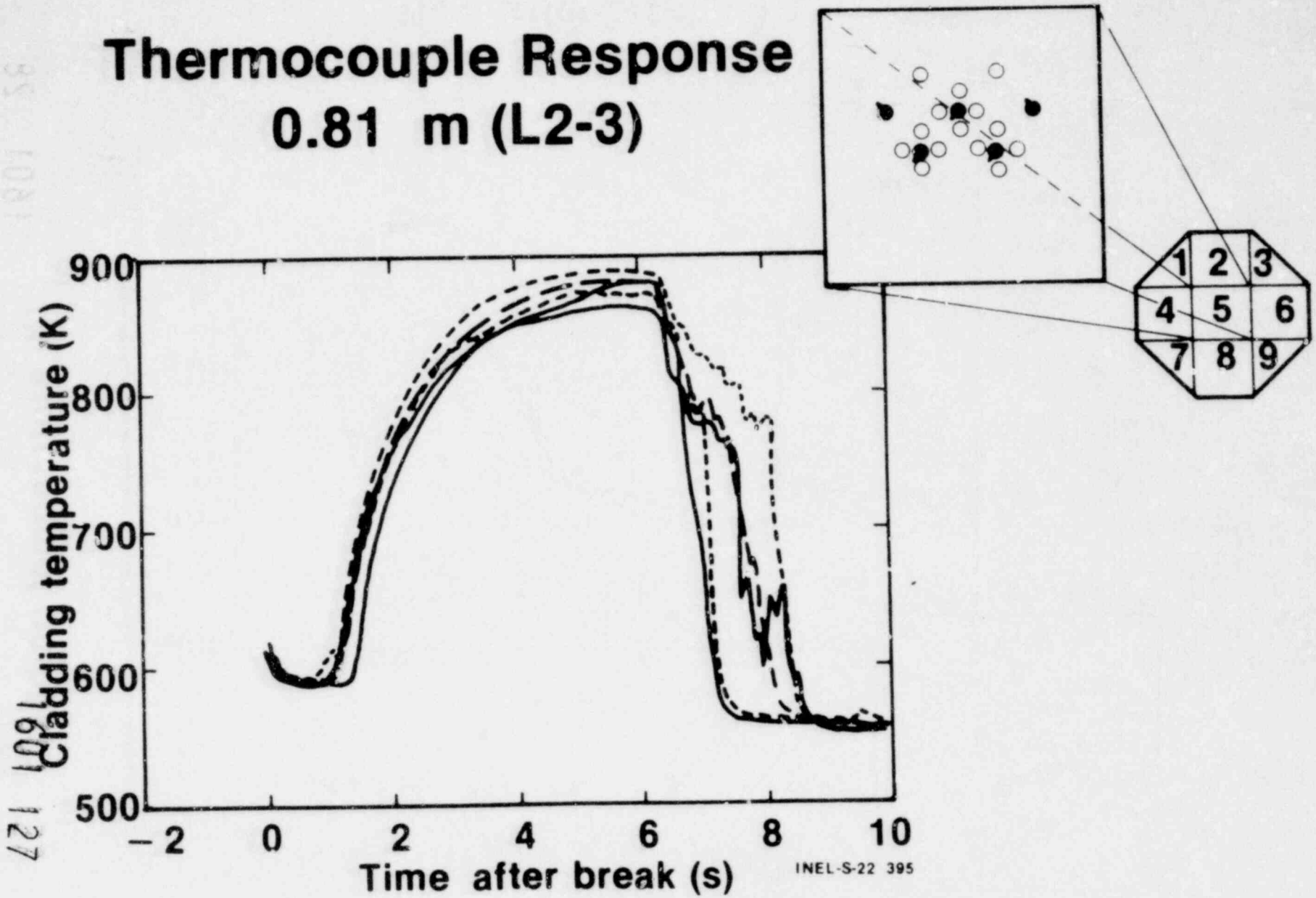

Thermocouple Response
1.14 m (L2-3)

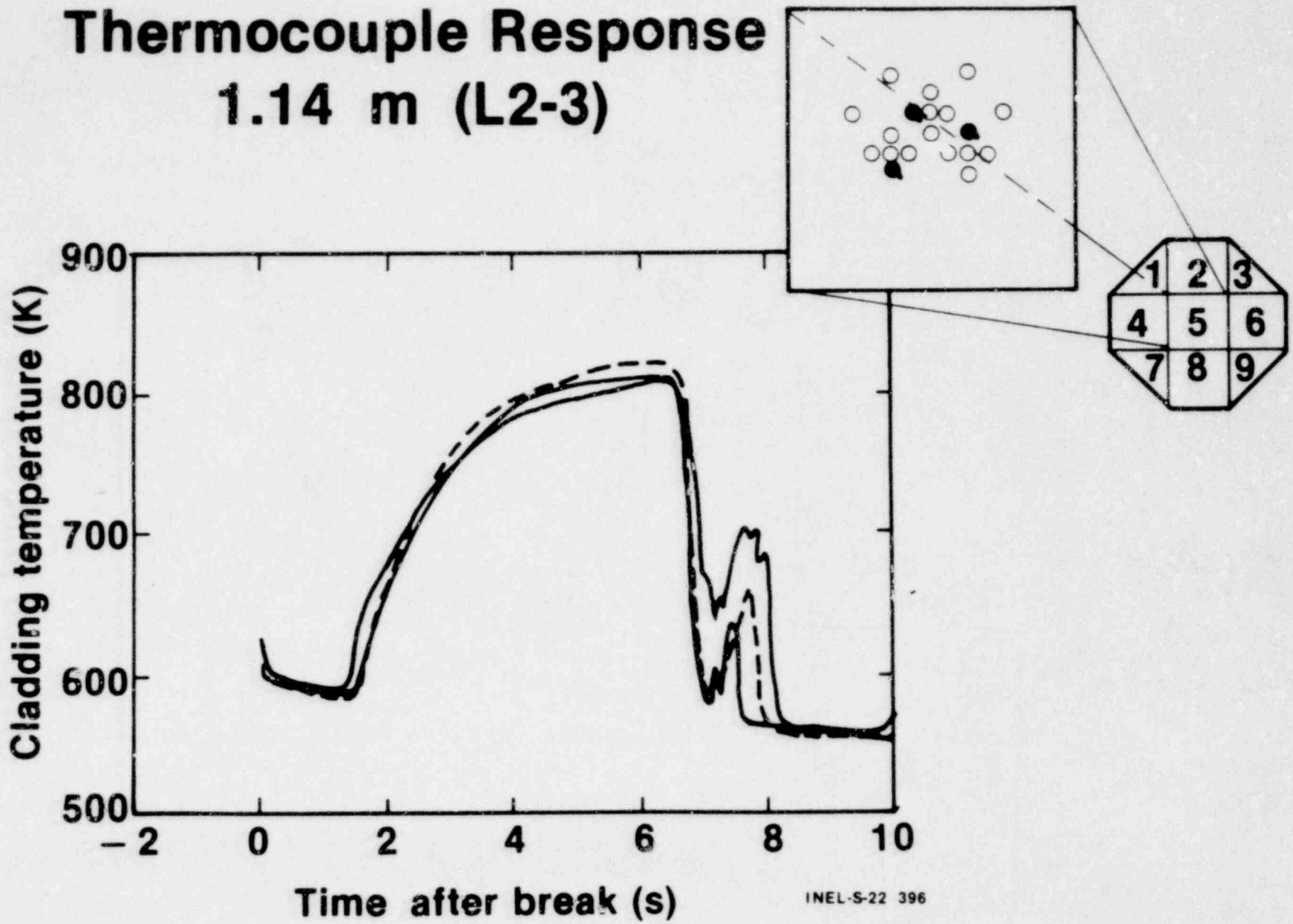

Comparison of Temperature Turnaround and Quench Times from Center Fuel Module Clusters (L2-3)

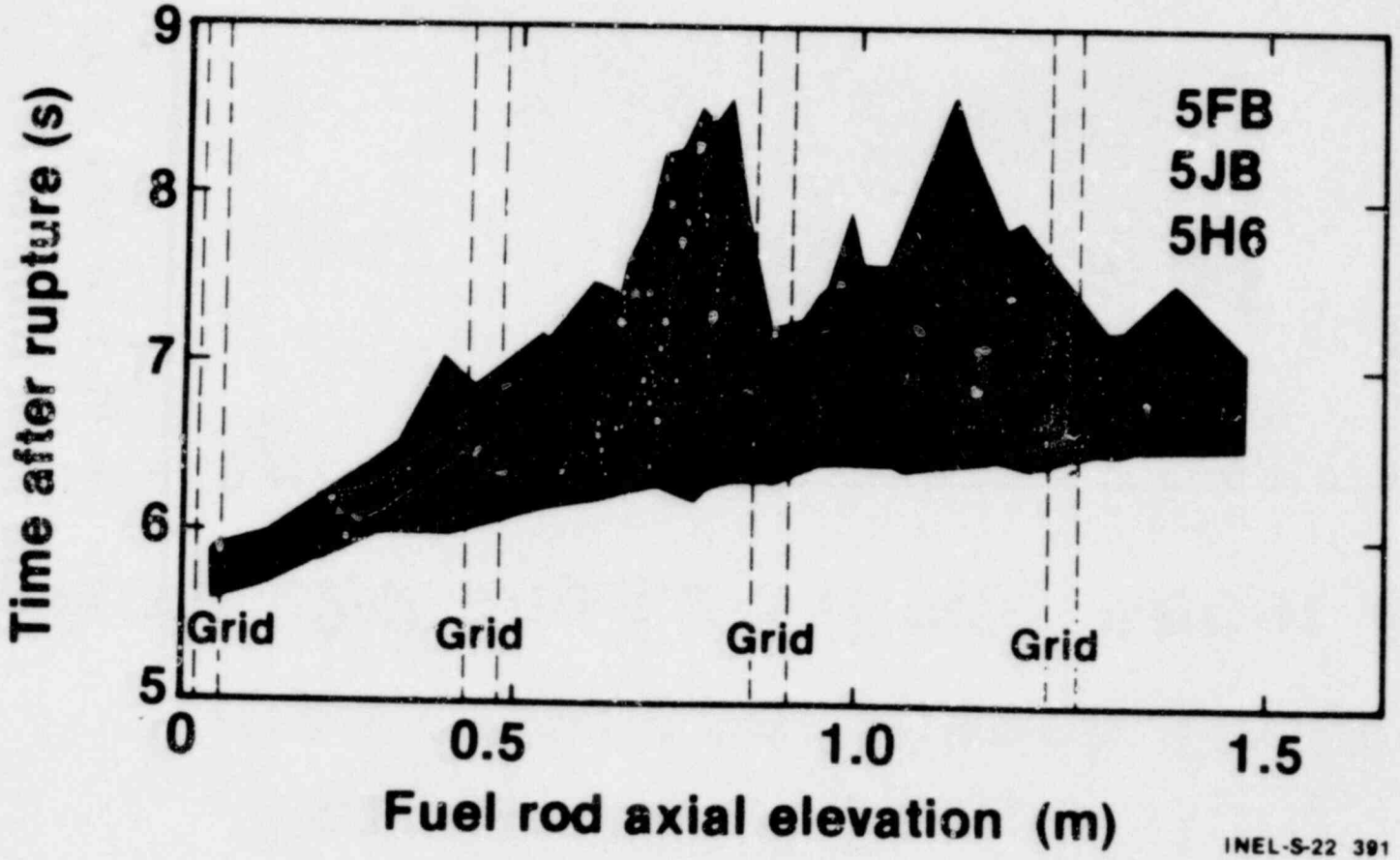

Comparison of Temperature Turnaround and Quench Times from L2-2 and L2-3 (Rods About 5F8)

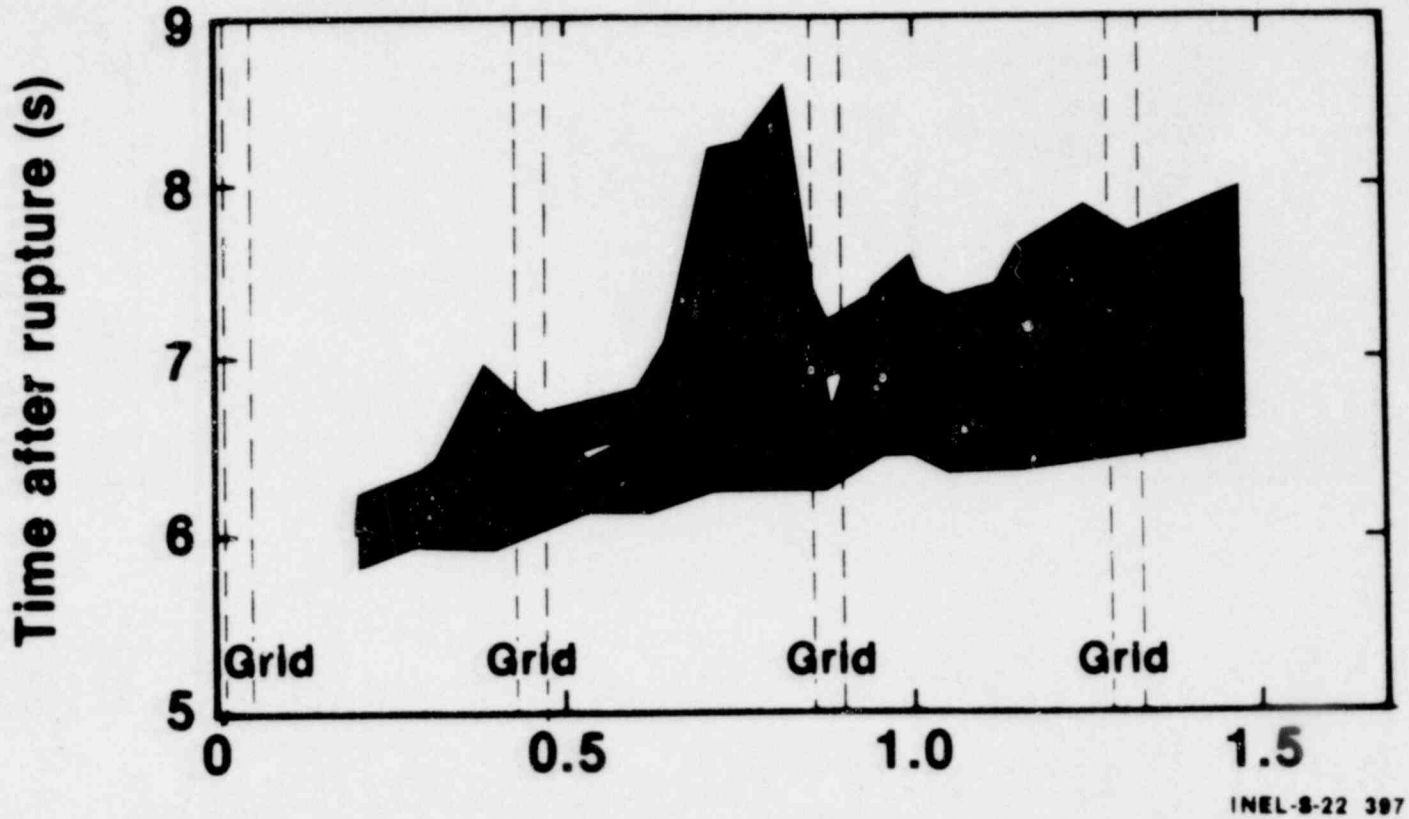

Thermocouple Barrier Junction

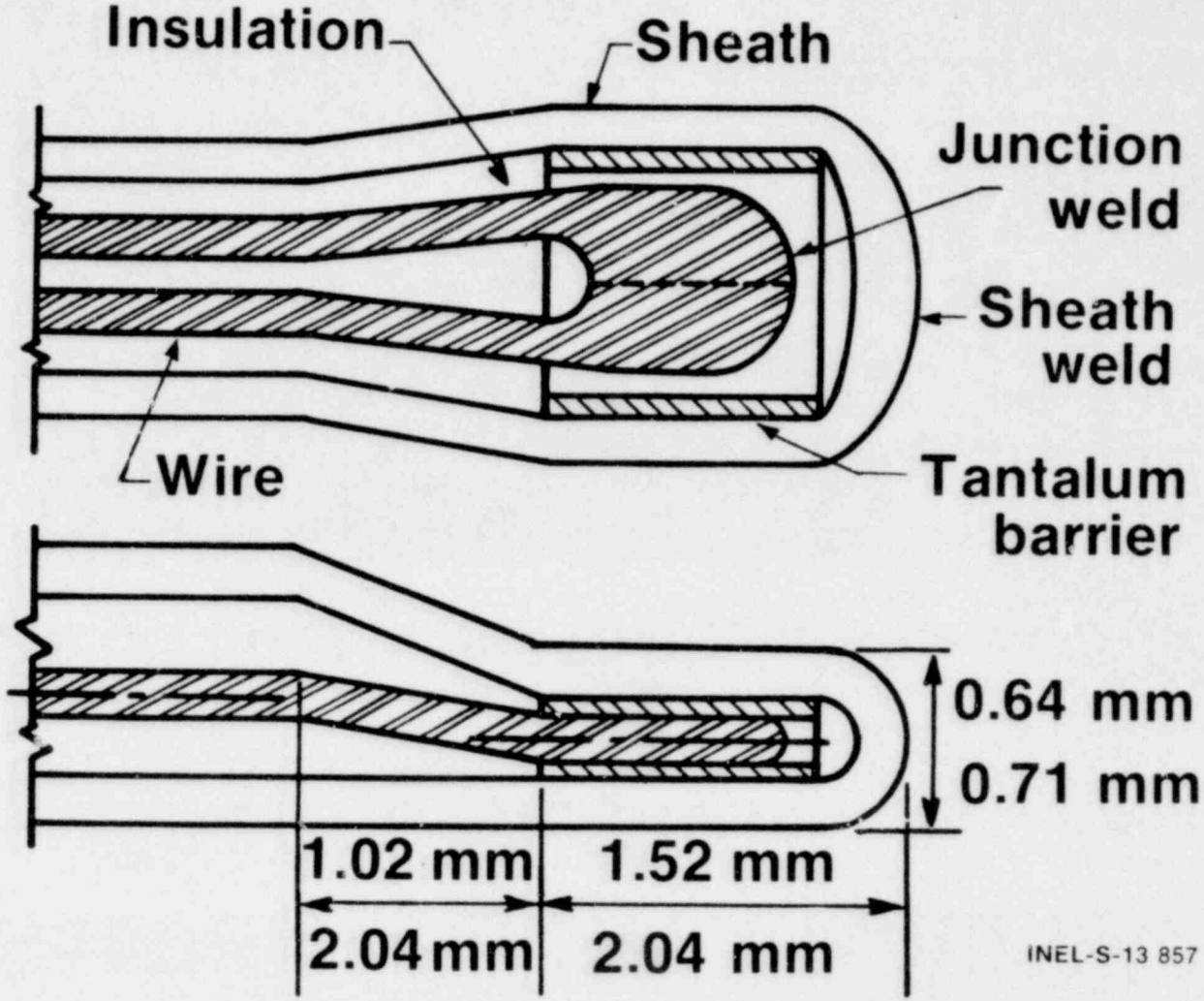

Cross-Section of LOFT Cladding Thermocouple

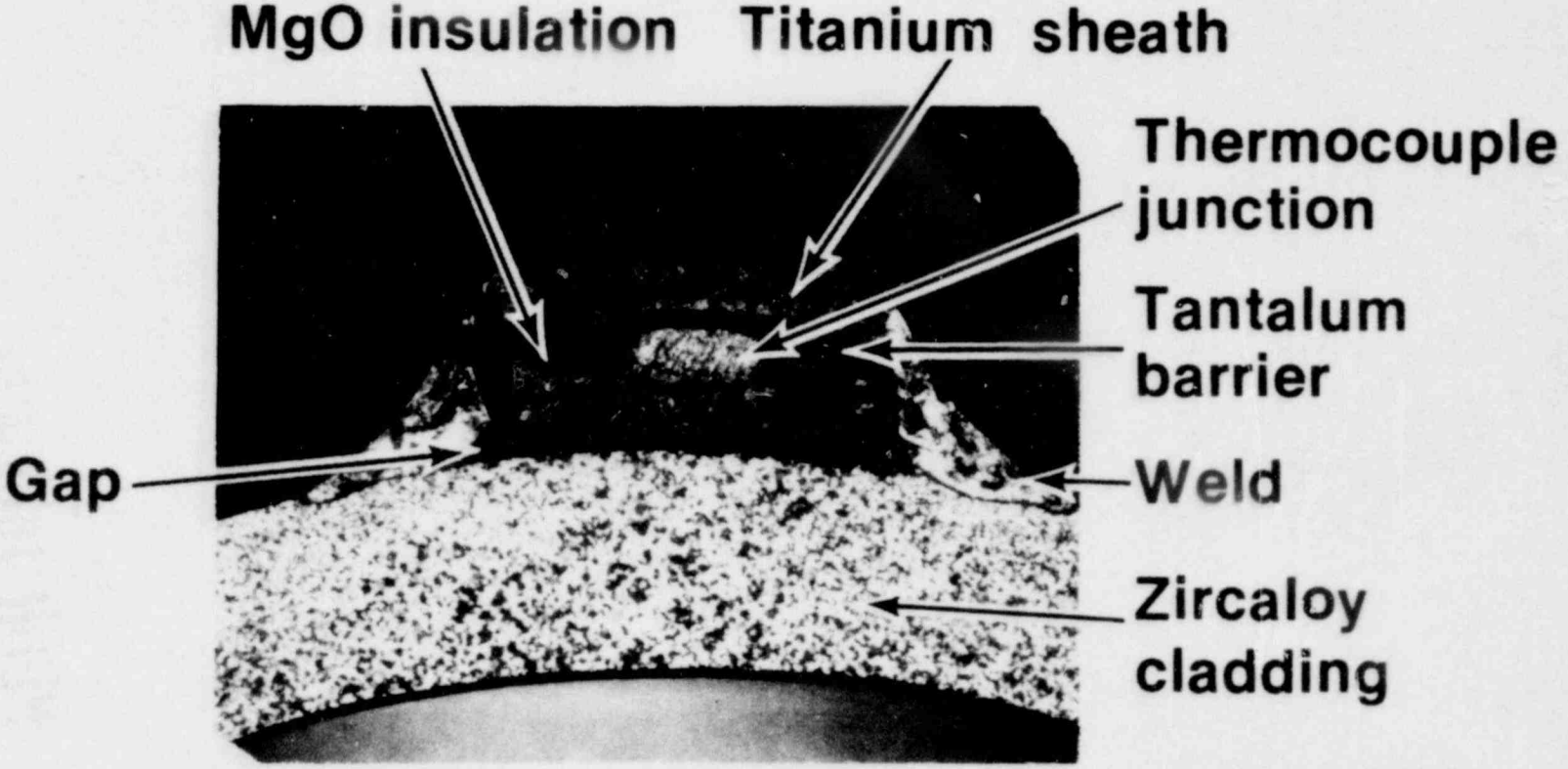

Cross-Section of Zircaloy Clad Heater Rod

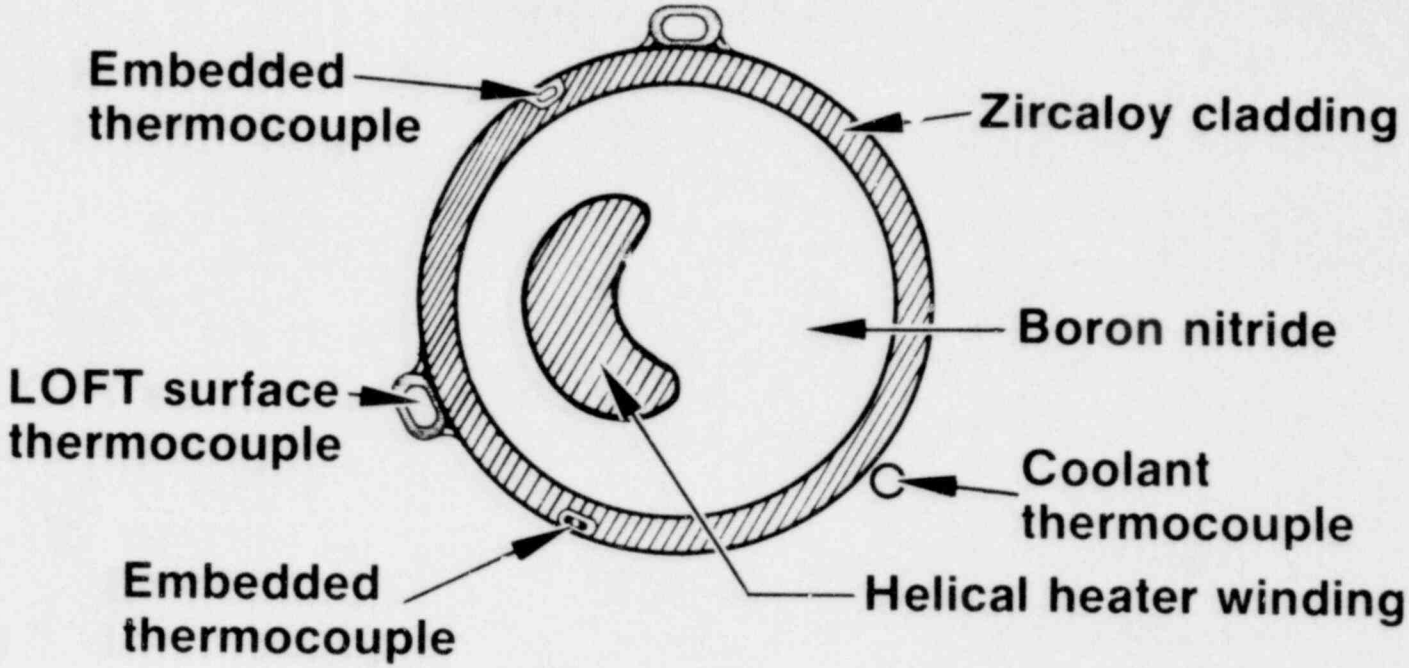

INEL-S-16 420

Zircaloy Heater Rod Response (IH-8029-1, Blowdown 2)

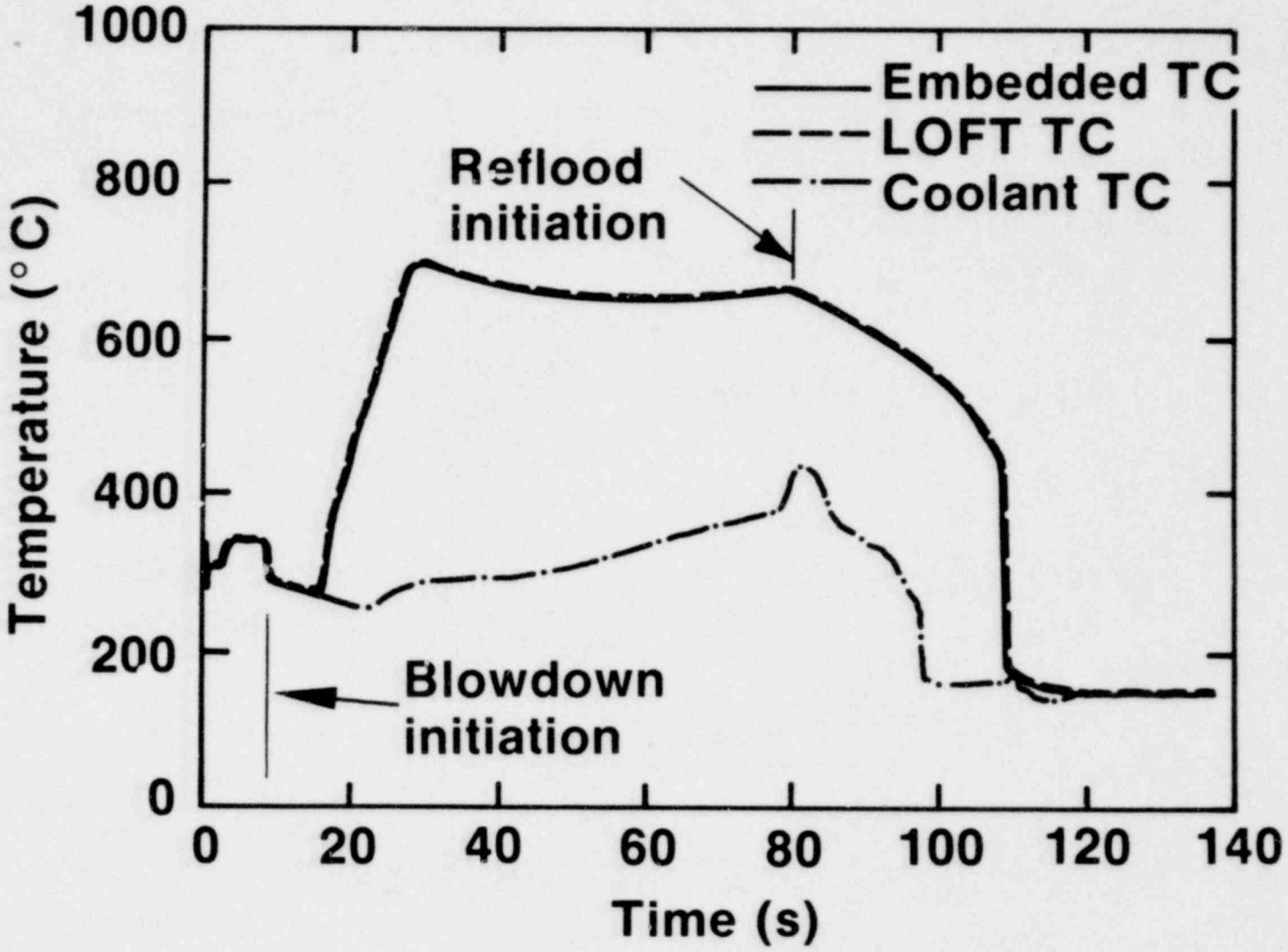

INEL-S-16 422

Difference Between Embedded and LOFT Thermocouples (IH-8029-1, Blowdown 2)

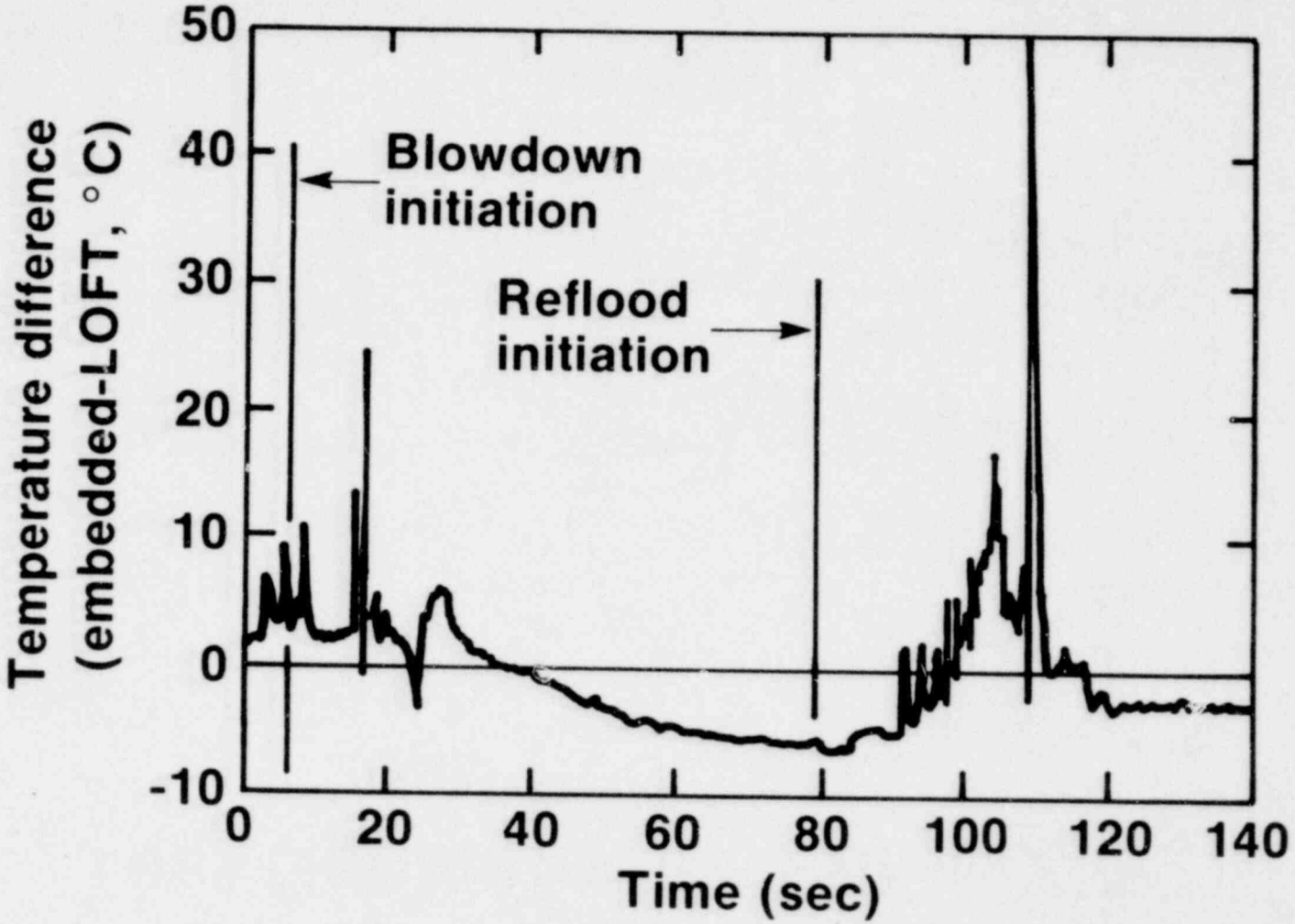

INEL-S-16 417

Test Geometry for PBF-LOFT Lead Rod Tests

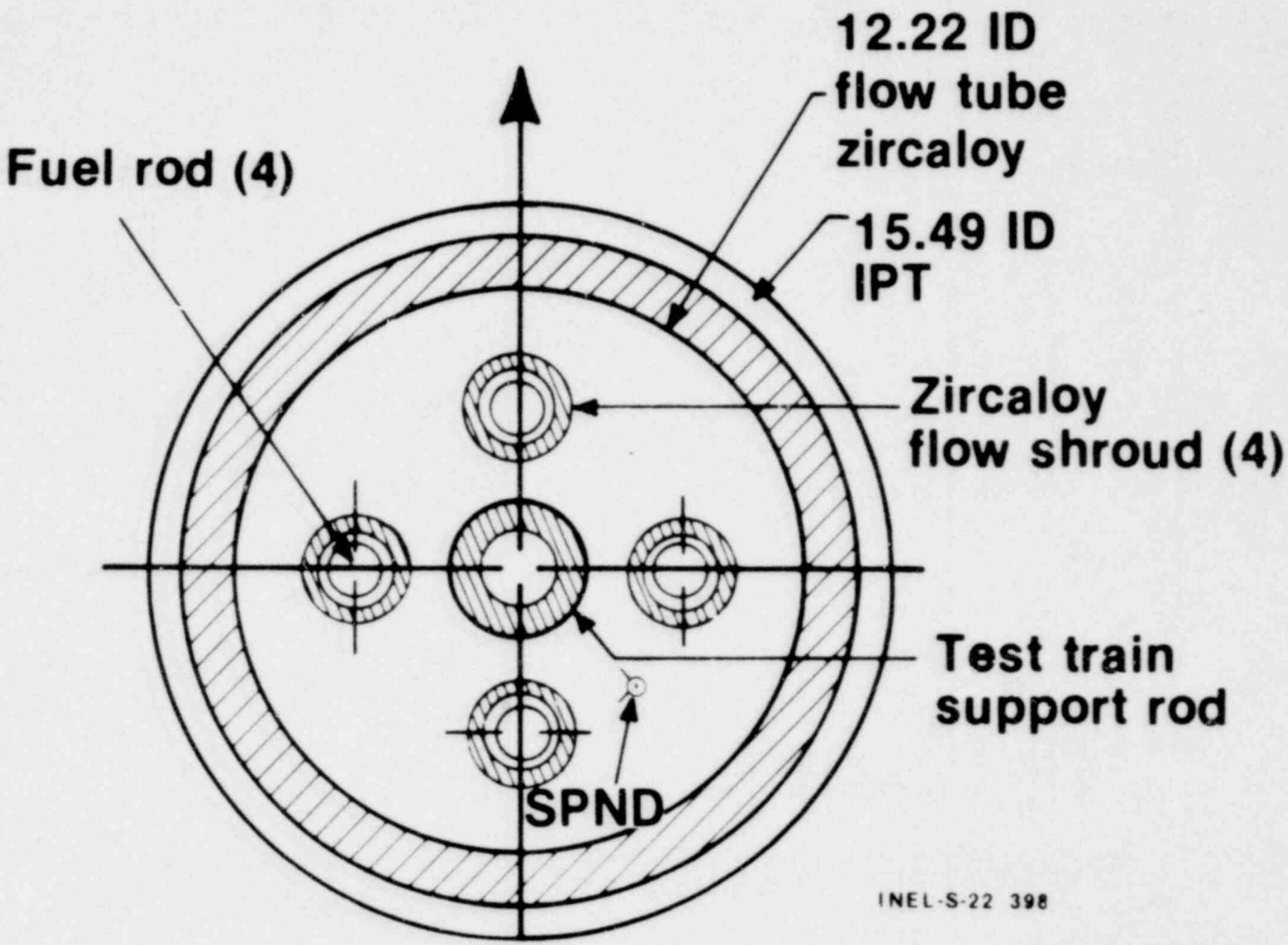

LOFT Lead Rod Individual Test Rod Configuration

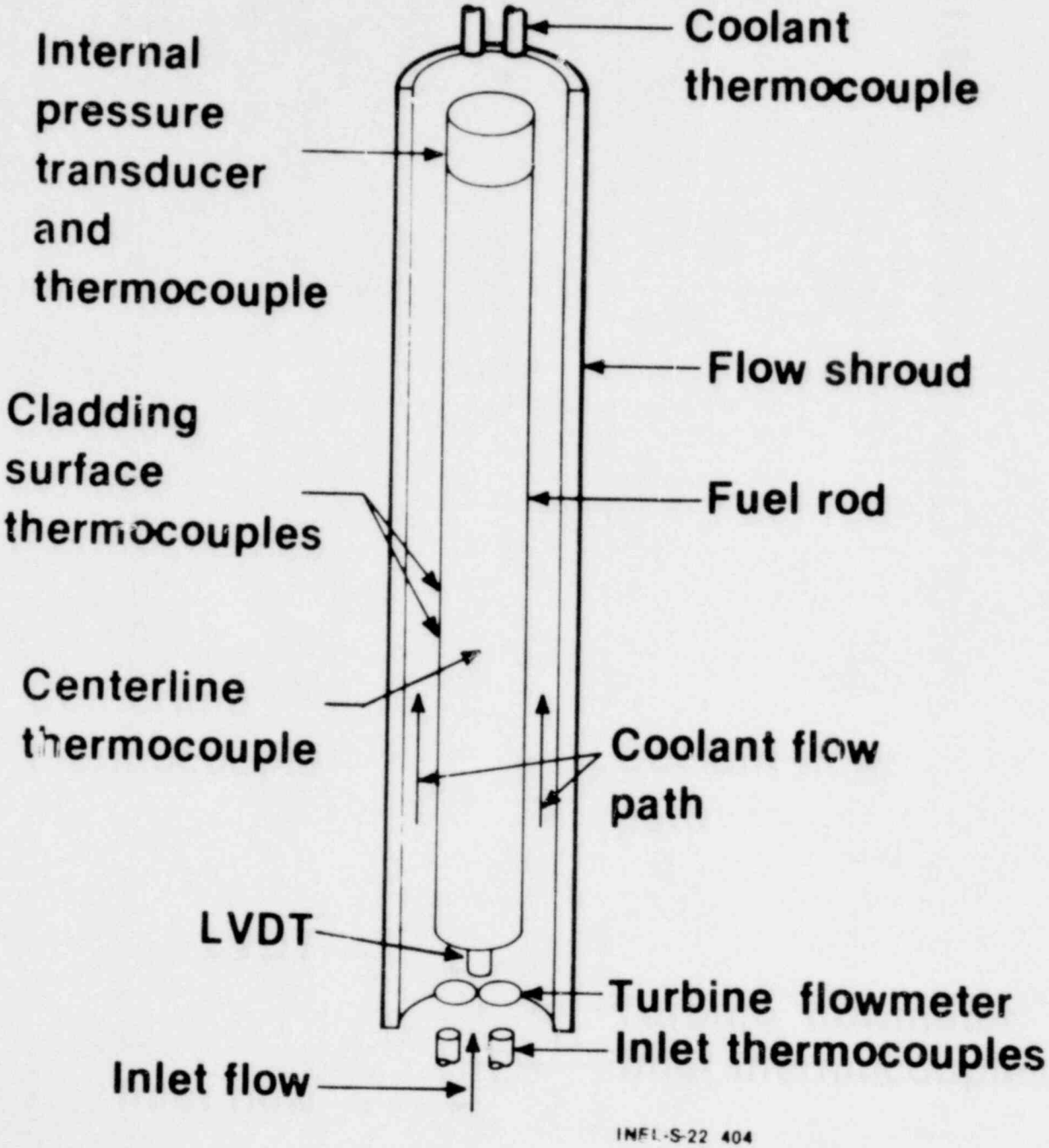

Preliminary Summary of Quench Characteristics from PBF-LOFT Lead Rod Tests

Test	Peak Clad Temperature (K)	Rod Cooling Characteristics	Conclusions
LLR-4	1040-1160	Valve cycling* during blowdown	Rapid response by LVDT & TC's T/C quenched ~ 1.0 s earlier than LVDT LVDT response same for rods with and without TC
LLR-4A	1060-1260	Reflood (~ 7 cm/s)	T/C quench ~ 1.5-2.0 s earlier than LVDT LVDT response same for rods with and without TC

INEL-S-22 393

*Test similar to blowdown quench conditions during LOFT L2-2 and L2-3 tests.

General Test Response for LLR-4
(Rod 312-1, Valve Cycling During Blowdown)

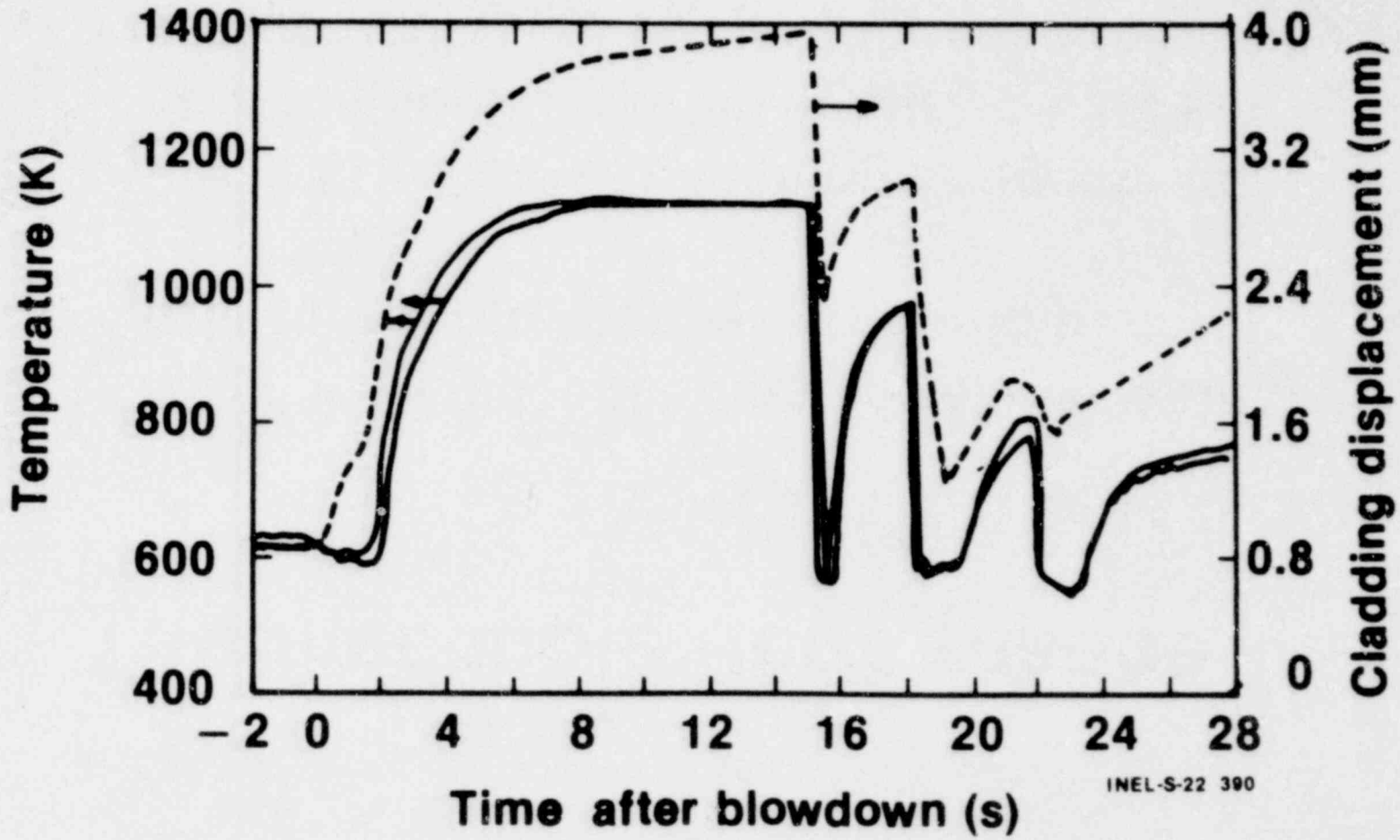

Thermocouple Performance

1. LOFT thermocouple data correlates well with measured thermal-hydraulic behavior

2. Rapid LOFT core reflooding suggests total core temperature quench during L2-2 and L2-3 as indicated by the thermocouple measurements.

INEL-S-22 389

Thermocouple Performance (cont'd)

3. Blowdown facility tests show LOFT thermocouples accurately measure cladding surface temperature (<30 K) during blowdown and reflood. Measured reflood quench times are within 1.0 s of cladding quench as measured by embedded thermocouples

INEL-S-22 388

Thermocouple Performance (cont'd)

4. PBF tests show cladding surface thermocouple quench ~1.3 s earlier than indicated by total cladding elongation measurements

5. PBF tests indicate rod quench times from cladding elongation measurements are the same for rods with and without surface thermocouples

INEL-S-22 387

Conclusions

1. Cladding rewet can occur for several seconds during the blowdown phase of a LOCA.

2. Cladding rewets are correlated to thermal-hydraulic behavior (low quality, steam flow through core)

3. 30-40% of the steady-state nuclear stored energy can be transferred from the rod during the several seconds rewetting period.

REWET IN THE SEMISCALE MOD-1 AND MOD-3 CORES

Presented at
The Seventh Water Reactor Safety Research Information Meeting
November 5-9, 1979
Gaithersburg, Maryland

D. M. Snider
EG&G Idaho, Inc.

Idaho National Engineering Laboratory
Idaho Falls, Idaho 83401

REWET IN THE SEMISCALE MOD-1 AND MOD-3 CORES

D. M. Snider
EG&G Idaho, Inc.

The rewetting behavior of the electrically heated rods in the Semiscale Mod-1 and Mod-3 systems during loss-of-coolant accident (LOCA) simulation experiments is described. The Mod-1 and Mod-3 systems use many of the same components and are close in size. However, there are some significant hardware differences between the two systems which lead to considerably different rewet behavior. The Mod-1 system[1] was scaled to the Loss-of-Fluid Test (LOFT) system, had a 1.68-m-long heated core and used orifices to simulate the pump and steam generator in the broken loop. The Mod-3 system[2] is scaled to a pressurized water reactor with an upper head injection system, contains a 3.66-m-long heated core, and is equipped with an active steam generator and pump in the broken loop. These configuration differences produce significantly different rewet behavior between the two systems. In particular, the Mod-1 system core experienced rewet shortly after attaining critical heat flux (CHF) while no rewets occur in the Mod-3 system core.

From examining measured hydraulic data and from analysis of the core behavior[3], it has been determined that in the Mod-1 system, rewet is a result of an influx of coolant into the top of the heated core. The source of this coolant is the 1.83-m core section encompassing unheated rods above the heated core and the upper plenum. In the Mod-3 system no large influx of coolant into the core was noted. The Mod-3 system core fluid quality remained high (above 0.4) and rewetting did not occur.

The differences in rewet behavior between Semiscale Mod-1 and Mod-3 systems brings to light two considerations. First, if only data from the Semiscale Mod-1 system and LOFT[4] system were examined, where rewets significantly reduced core temperatures, it might be concluded that rewet is an important phenomena in power reactors. However, with significant rewet differences between the two Semiscale systems, which have much in common but which also have differences in

some of the major components, it is apparent that the extrapolation of data from small scale experiments directly to large reactors must be tempered with judgement and analysis. A second consideration, which may be obvious, is that a change in an important hardware section, for example core length, may lead to the gain or loss of beneficial phenomena. However, the phenomena that may change and the manner of change may not be obvious prior to testing.

An attempt was made to quantify the criterion for rewet in the Mod-1 system core. Two important parameters controlling rewet are the cladding wall temperature and the amount of liquid available to wet the rod surface. By multiplying the wall-to-saturation temperature difference (ΔT_{sat}) by the void fraction (α) and normalizing with respect to the saturation temperature, a nondimensional parameter $(\Delta T_{sat}\ \alpha)/T_{sat}$ can be defined. This parameter intuitively has the potential for describing the onset of rewet. As ΔT_{sat} or α increases, rewet is not likely to happen; as ΔT_{sat} or α decreases, rewet is more likely to occur. By examining this parameter for three Semiscale blowdown experiments, it was found that of the 46 rewets that occurred following CHF, 80% of them occurred at values of $(\Delta T_{sat}/T_{sat})\alpha$ less than 0.35, with an average value being 0.31. The value of 0.31 for the nondimensional parameter is consistent with the value of 0.25[5] used to define top down quench based on reflood experiments performed in the FLECHT and Semiscale systems.

This simple empirical relation is considered to be only an approximate approach to describing the complex rewet phenomena occurring during blowdown. However, the initial study using this nondimensional parameter has shown the parameter to have some utility in describing the onset of rewet in Semiscale and is worthy for consideration in other experiments.

REFERENCES

1. L. J. Ball et al, Semiscale Program Description, TREE-NUREG-1210, May 1978.

2. M. L. Patton, Semiscale Mod-3 Test Program and System Description, TREE-NUREG-1212, July 1978.

3. D. M. Snider, "The Thermal-Hydrualic Phenomena Resulting in Early Critical Heat Flux and Rewet in the Semiscale Core", Journal of Heat Transfer, 101, February 1979.

4. M. L. McCormick-Barger, Experiment Data Report for LOFT Power Ascension Test L2-2, TREE-NUREG-1322, February 1979.

5. R. W. Shumway, Core Reflood Dynamics Code - FLOOD4, SEMI-TR-12, September 1979.

Rewet in the Semiscale Mod-1 and Mod-3 Cores

Presented by
D.M. Snider

EG&G Idaho, Inc.

INEL-S-21 577

Semiscale Mod-1 System

- Scaled to LOFT/TROJAN
- 1.68 m heated core
- Inactive broken loop components
- Annular downcomer
- 40 electrical rod core

INEL-S-21 578

Semiscale Mod-3 System

- Scaled to UHI plant
- Full length 3.66 m heated core
- Active broken loop pump and steam generator
- Pipe external downcomer
- 25 electrical rod core

Heater Rod Thermocouples D4-29 and D5-29 During Test S-02-7

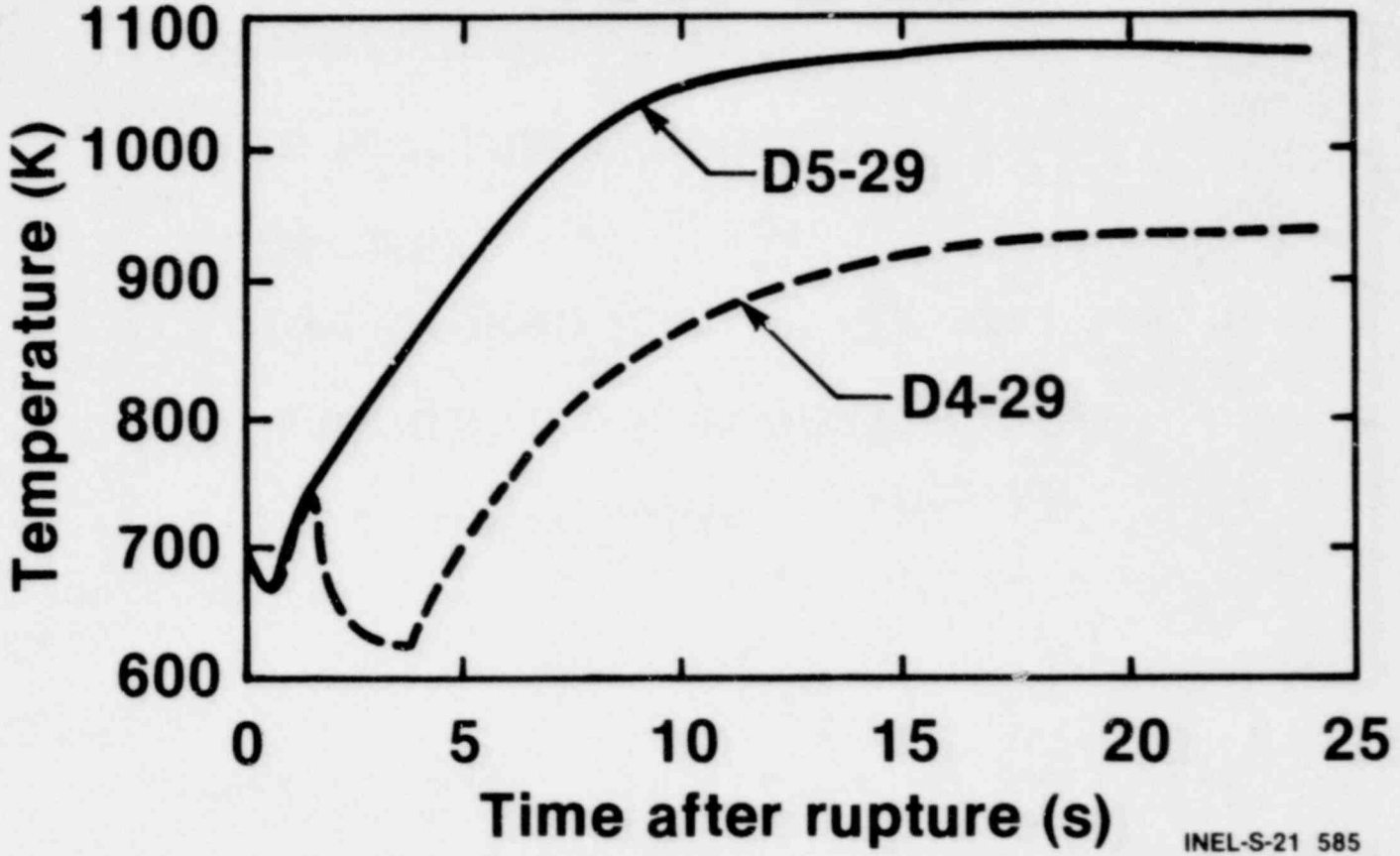

Mod-1 Rewet Behavior

- Rewet happened shortly after CHF
- Rewet significantly reduced core temperature
- Repeatable
- Varied from rod to rod at axial level
- Influenced by grid spacers
- Influenced by dead rods

INEL-S-21 580

Calculated Quality and Rod Surface Temperature — Mod-1

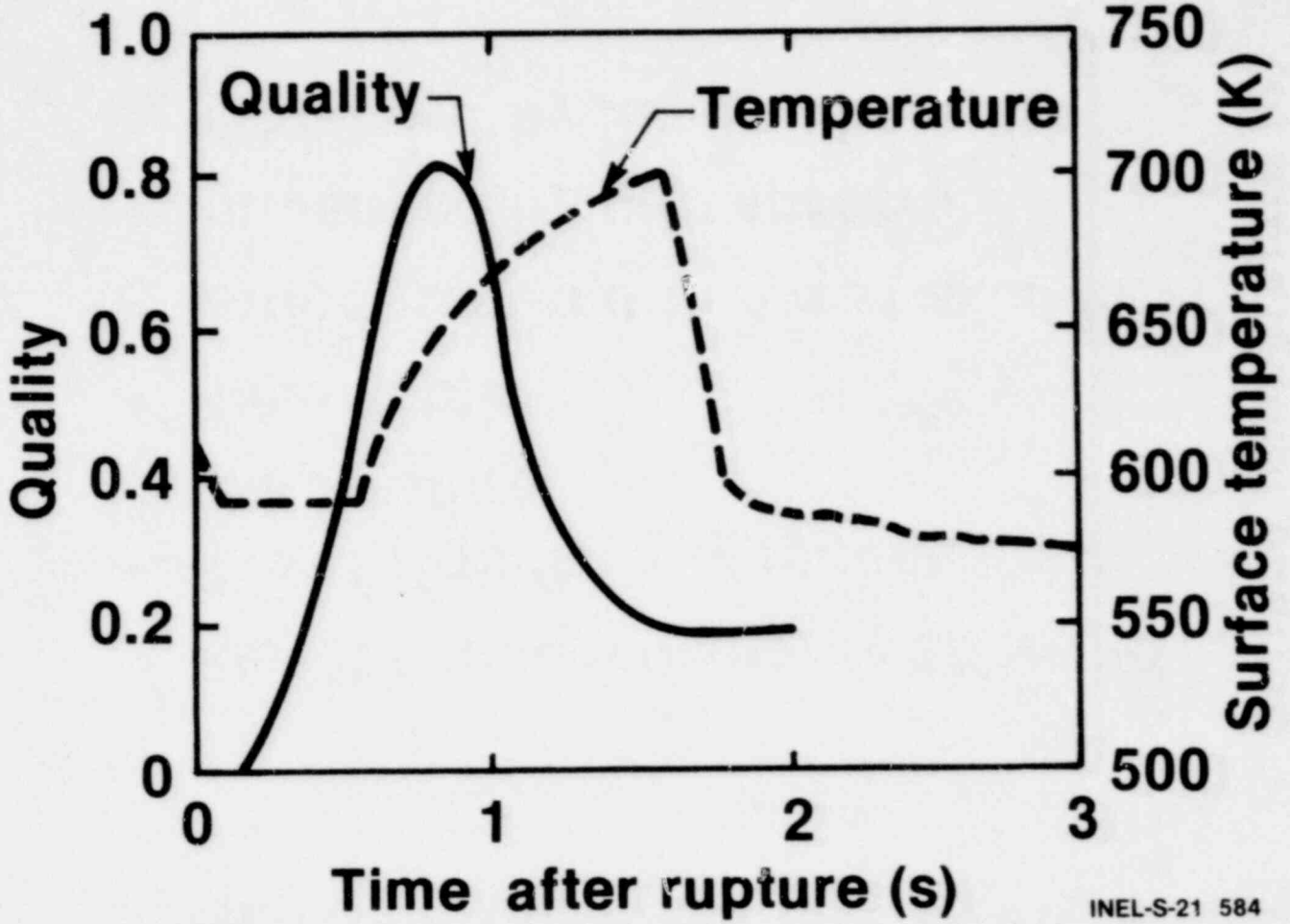

Number of Rewets per Surface Temperature

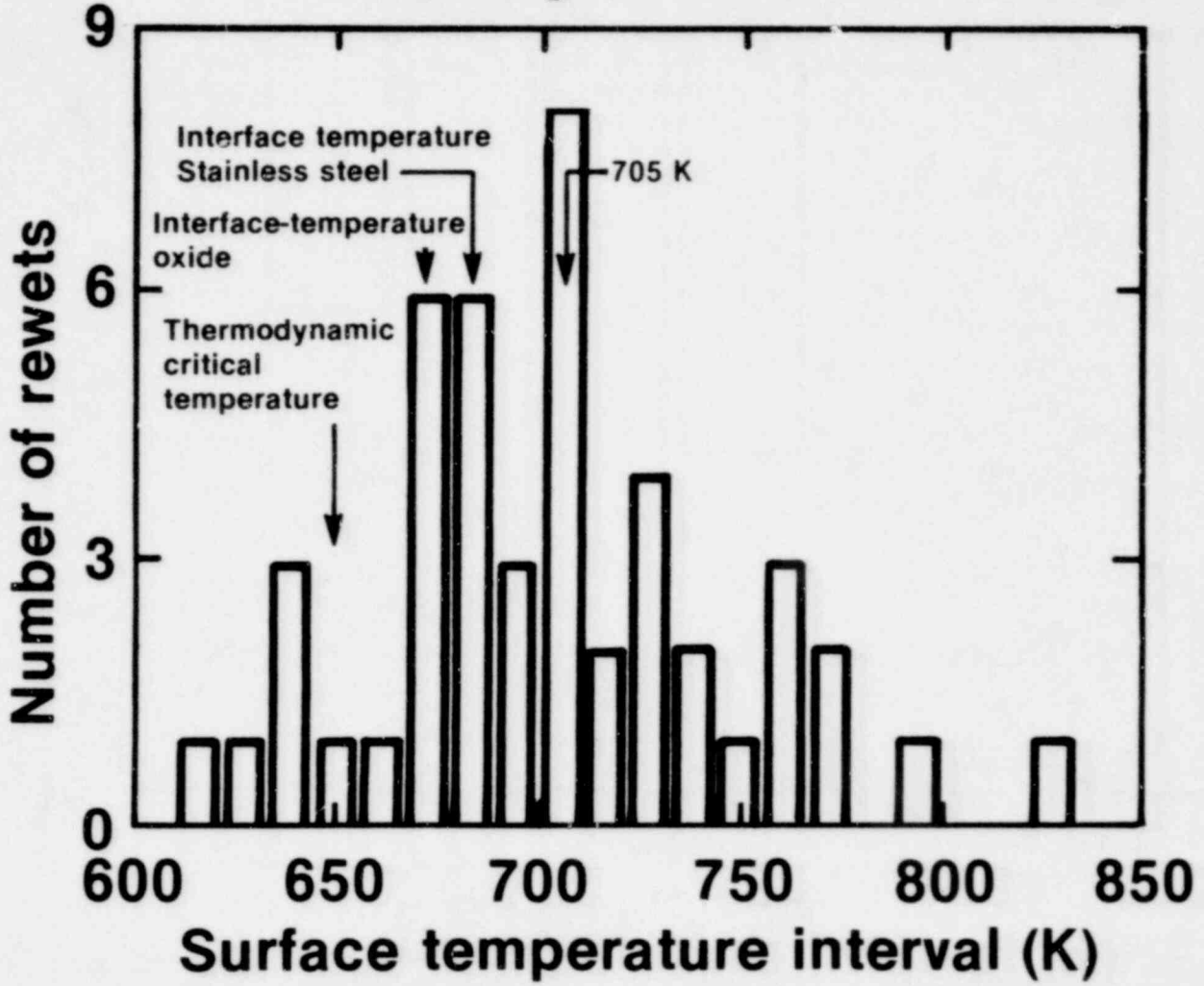

INEL-S-21 582

Number of Rewets per Rewet Parameter

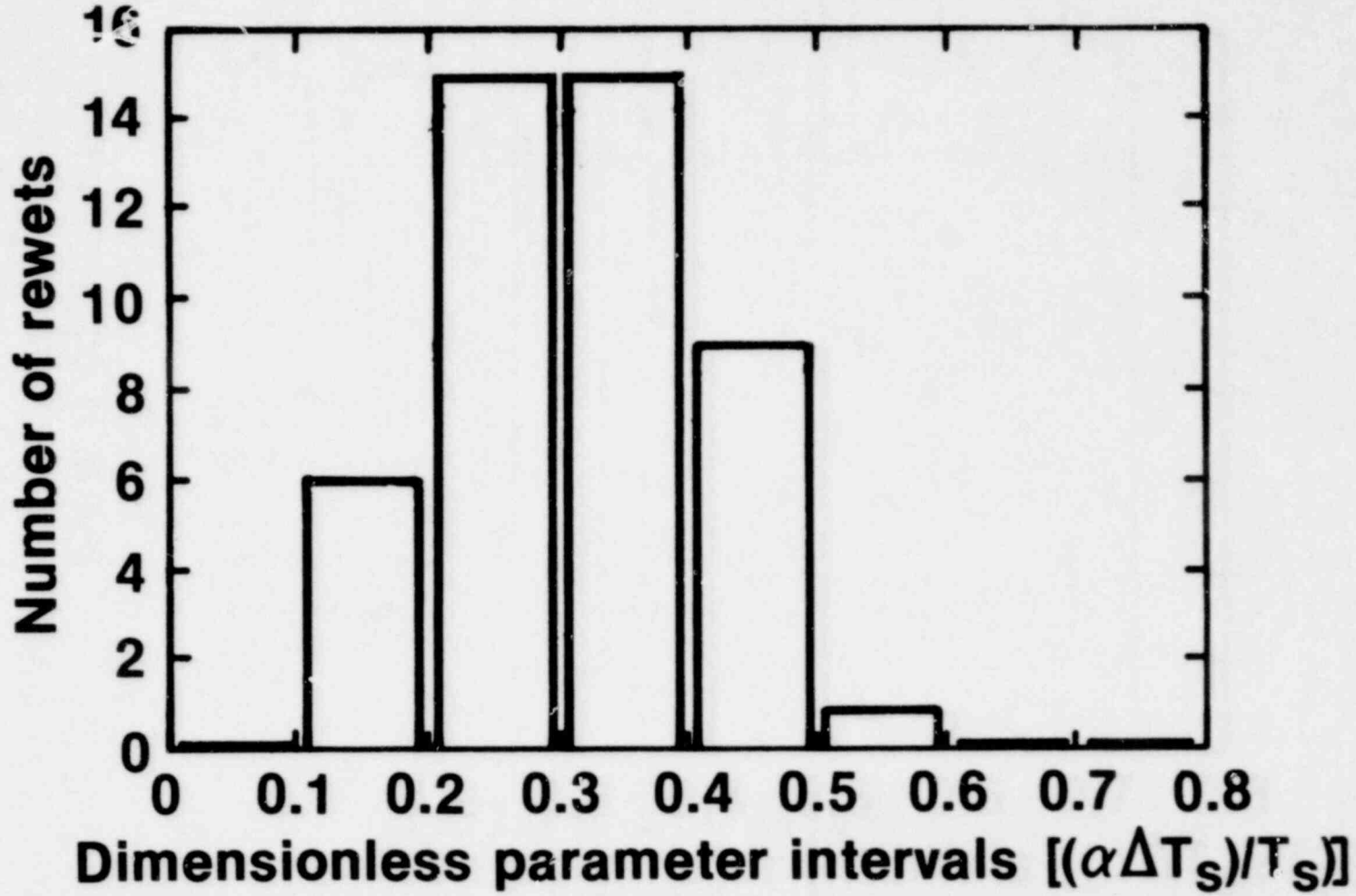

INEL-S-21 581

Rewet Number for Mod-1 Core

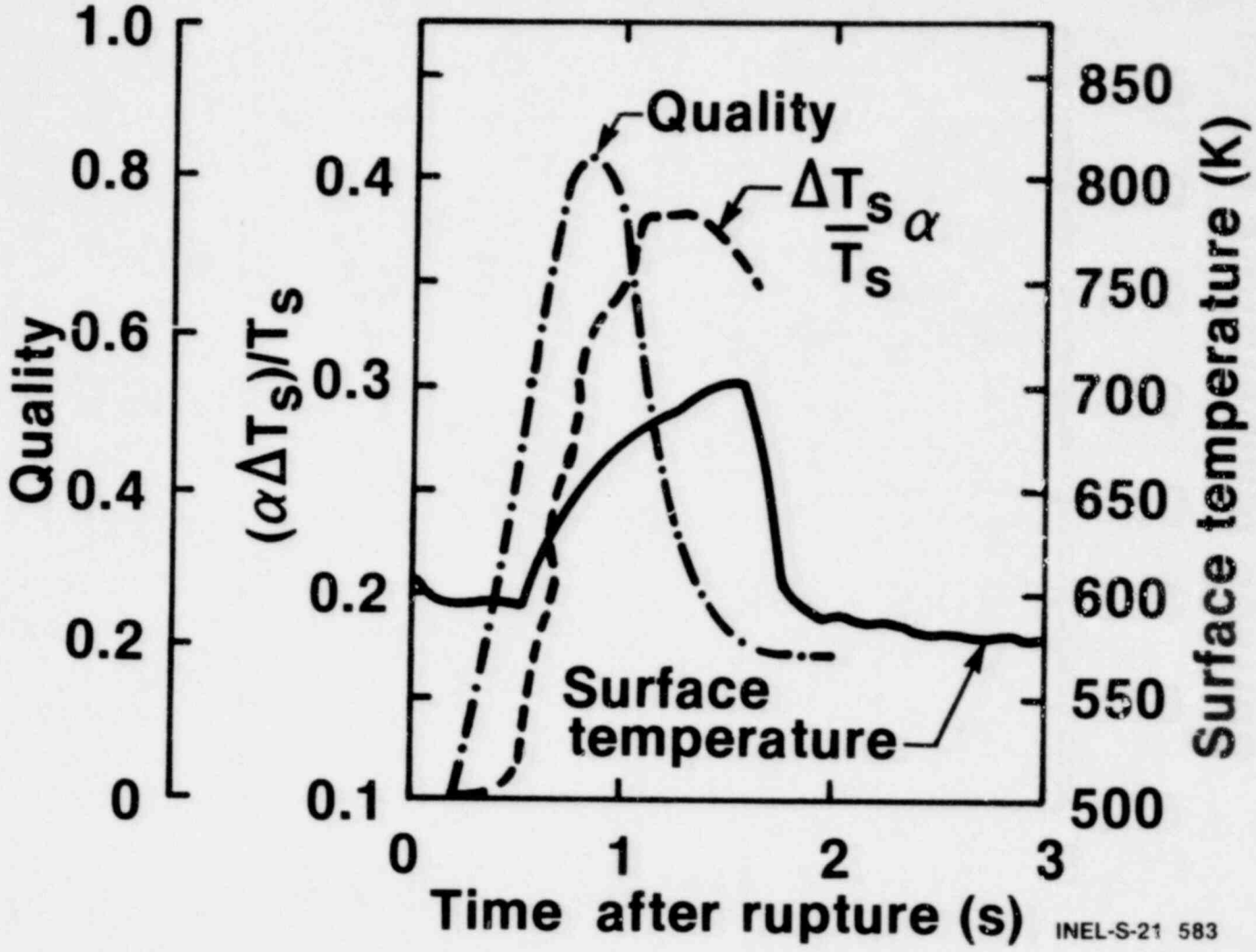

COBRA-IV Calculated Quality at Peak Power Zone

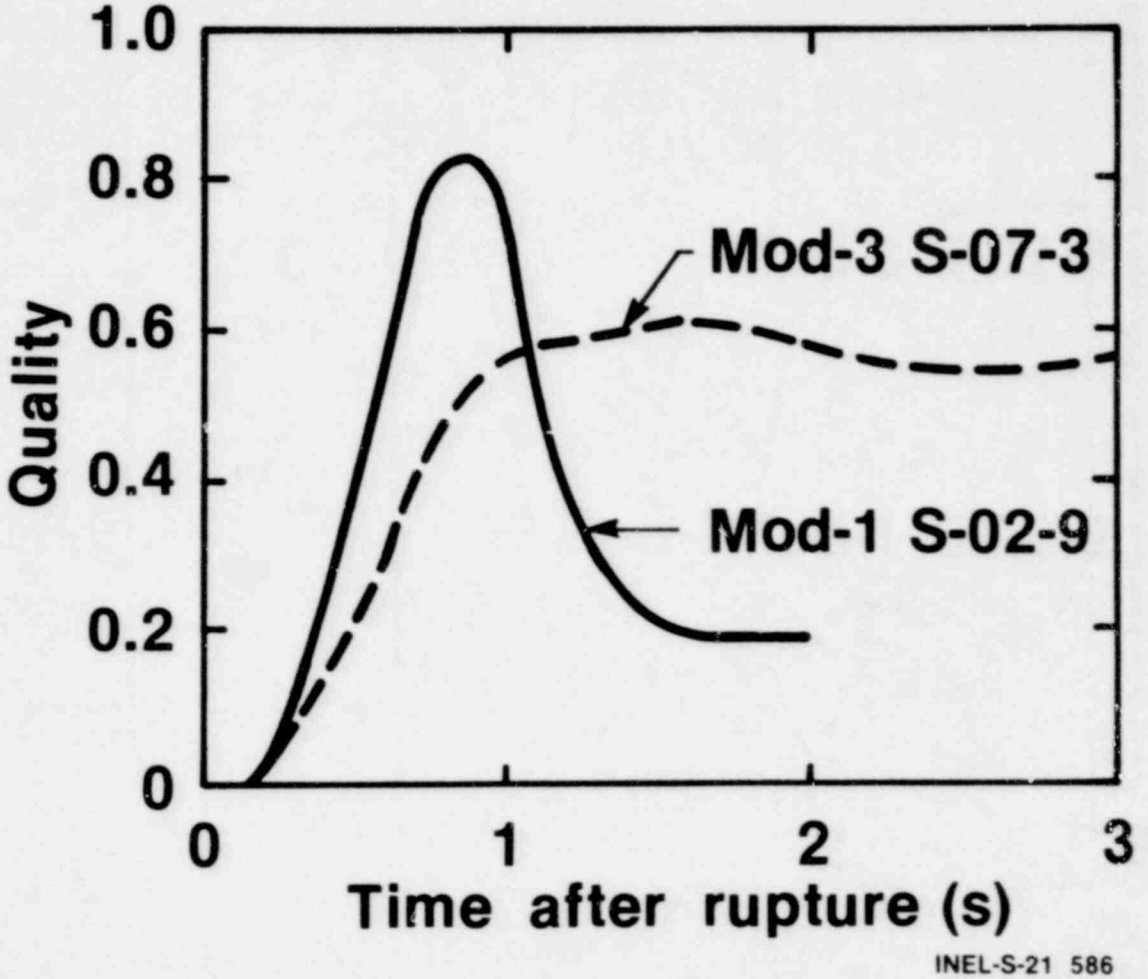

Summary

- Rewet happened in Semiscale Mod-1 core
- Rewet in Mod-1 happened below 800 K
- Rewet in Mod-1 caused from influx of coolant from top of core
- Mod-3 core did not experience the strong influx of coolant and did not rewet

INEL-S-21 587

STATUS REPORT OF 2D/3D PROGRAM

L. S. Tong, 11-5-79

This report will be a short update on the status of the 2D/3D Program since the Water Reactor Safety Meeting last year. The 2D/3D Program is an international program of reflood research involving the supply of advanced two-phase instruments and analytical calculational support for tests to be run in research facilities to be built in Japan and Germany. Dr. Nozawa of JAERI, the guest speaker today, will describe and discuss the results of Japanese 2000 rod cylindrical core test facility. Unfortunately, Professor Mayinger of Germany could not make this meeting to discuss the German 2D upper plenum test facility. However, I will provide a short presentation in my talk of progress on the design of that facility for your information.

Significant progress has been made this year on all phases of the 2D/3D Program. The Japanese cylindrical core test facility was completed in February and shakedown tests were finished by May of this year. A few of the initial base core reflood system effects tests have been run and testing is continuing. The preliminary design of the German upper plenum test facility (UPTF) and the Japanese Slab Core Test Facility (SCTF) were recently completed. The USNRC, through its DOE laboratory contractors, has delivered four large 4" instrumented spool pieces to Germany for testing in the German PKL facility and six large 6" instrumented spool pieces to Japan for use in the Japanese cylindrical core test facility. In addition, other advance instrumentation, including conductivity liquid level probes, downcomer drag disks and advance flag probes for local velocity measurement, have been

delivered to the CCTF and PKL. The TRAC Code has been used extensively for calculating the design features of both the SCTF and UPTF and is currently being run to provide pretest predictions and post-test analysis for the CCTF experiments.

I would like to digress now and briefly describe the slab core test facility and upper plenum test facility. The first slide on the screen is a cross-section of the design of the 2000 heater rod slab core test facility. The facility will have 8 full scale heater rod simulated PWR fuel bundles arranged in a line inside a flat walled vessel. This represents a simulated radial cut through a PWR core. A rectangular downcomer is provided on one side of the vessel. Both lower and upper plenum of a PWR are simulated, including typical control rod guide tubes and support columns in the upper plenum. A single cold leg and single hot leg nozzle are shown. Significant mechanical and thermal design problems have had to be solved by JAERI and its contractor IHI for this uniquely designed vessel. The vessel and internals will be built in CY-1980 and testing is to be initiated in CY-1981. Initial tests with Core I will be used to study flow blockage, followed by reflood tests with Core II.

The next slide is a cross-section of the German Upper Plenum Test Facility vessel. This vessel represents a full-scale reactor vessel in both diameter and height. The core is to be simulated by nozzles which will inject a programmed mixture of steam and water equivalent to that from a fuel rod core. Seventeen radial zones of spray nozzles will be provided to permit matching the core radial power distribution. Above the core spray nozzles, there is a length of simulated dummy fuel rods to provide

for proper flow distribution to the tie plates in the simulated fuel element end boxes. The true upper plenum of a PWR, including core support plate, control rod guide tube columns, structural supports and upper support plate, are replicated in the vessel. Four hot and four cold legs are provided, as well as a full-scale downcomer.

Fabrication of components and facility construction are scheduled to start in CY-1980, with construction to be completed in CY-1982. Both upper plenum entrainment and de-entrainment tests are to be run using both ECC cold leg injection according to US design philosophy and combined hot and cold leg ECC injection as employed in German PWR design philosophy. Provisions are included in the vessel design for testing a simulation of the significant CE upper plenum internals feature and also the B&W vent valves. The test program includes as well an extensive series of tests of ECC bypass behavior.

Finally, I would like to take a minute to discuss some of the more recent discussions concerning small break tests that have taken place between the Japanese, German and US 3D participants. As a result of the TMI-2 accident, a review was made by the 3D Program of how the facilities involved might contribute to understanding small break behavior. As a result of discussions in June between Professor Mayinger of Germany, Dr. Nozawa of Japan and myself, it was agreed that a program of small break integral tests would be proposed to our respective governments. The BMFT of Germany has agreed to continue the PKL Core I testing series through this fall and coming winter to perform 25 small break tests. The PKL has 340 heater rods and can operate at up to 35 bar pressure. It has

a full height core and steam generators. The USNRC is having its DOE laboratory contractors modify two of the 4" spool pieces for use in measuring the low flow for small breaks and is providing several turbines and a pulse neutron activation device for additional PKL flow measurements. Small break tests will also be run later in the larger Japanese CCTF test facility.

In conclusion, I am looking forward next year to an increased data flow from the 3D program and expect to be able to report further on the status of construction of the 3D facilities.

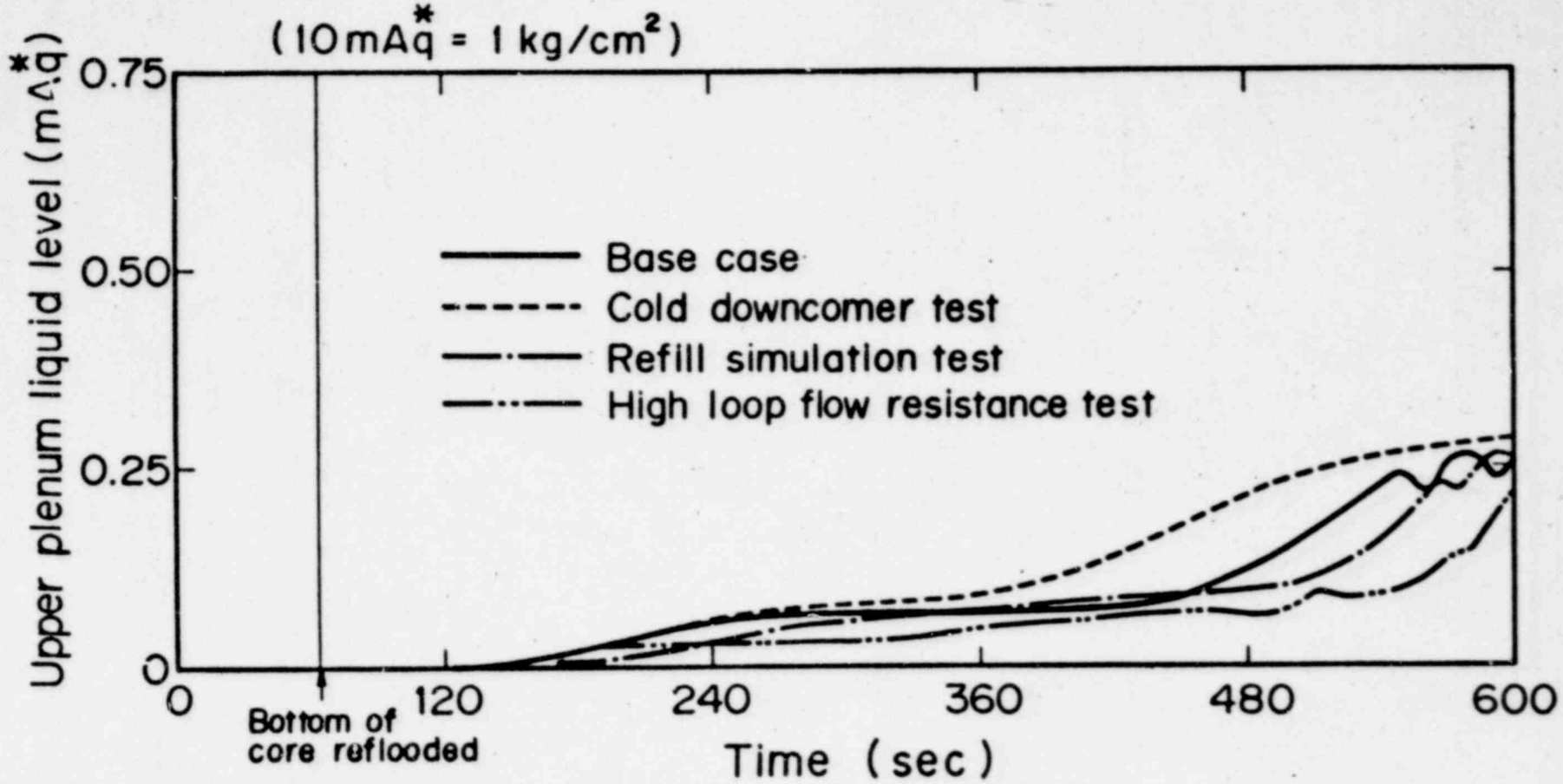

Fig. 12 Water accumulation in upper plenum (CCTF)

Japanese Safety Research Programs——ROSA, CCTF, and SCTF

M. Nozawa

Japan Atomic Energy Research Institute

The JAERI's investigation of thermo-hydraulic behavior of primary coolant during a large break LOCA is comprised of two kinds of programs, i.e. an integral test and partial effect tests. The ROSA program is an integral test series and now it is its third phase. The ROSA-III program is simulated ECCS tests which cover blowdown, refill and reflood phases of a BWR LOCA. It has four simulated 8 x 8 fuel assemblies of half length in the core, provided with a broken and an intact loop with two externally installed jet pumps and appropriate ECCS functions. The 2D-3D program is a partial effect test which covers a part of refill phase and reflood phase of a PWR LOCA. This program is now carried out as a three-party, F.R.G., U.S.A. and Japan, coordinated study program. Federal Republic of Germany is responsible to make experiments using a full scale 3-D upper plenum test facility (UPTF). United States of America is responsible to make development of 3-D analysis code and advanced two-phase flow instrumentations and experimental analysis. JAERI is responsible to make experiments using two scaled-down facilities having 2000 simulated fuel rods of full length in cores. One facility is a cylindrical core test facility (CCTF) which has one broken loop and three intact loops provided with steam generator and pump simulator in each loop. Another facility is a slab core test facility (SCTF). It is in designing stage and has only one loop provided with no steam generator but various capability of ECC injections.

Major results of ROSA-III are as follows. The BWR LOCA standard test series started in May, 1978, and seven experiments Runs 701 ∿ 706, 721 were done before April, 1979. Run 701 is a scoping LOCA experiment at low power. Runs 702 and 703 are split break experiments. Runs 704, 705 and 706 simulate 200% double-ended breaks at the recirculation pump inlet side with the initial system pressure of 7.2 MPa. Run 704 is a standard BWR LOCA experiment with ECC injection. Run 705 is an isothermal blowdown experiment without heat generation in the core. Run 706 is an experiment with power in the core but without ECC

injection. Run 721 is a scoping experiment with the radial power distribution in the core. It is confirmed from the experimental results that the ROSA-III facility can simulate qualitatively the major aspects of a BWR LOCA, such as pressure increase by the closure of main steam line, pressure decrease by the uncovery of the downcomer outlet to the recirculation loop, core cooling effect by the lower plenum flashing, and the final quenching of the whole core by reflooding after the start of the low-pressure coolant injection system. Therefore, the facility is useful as the rig for producing the integral test data of BWR LOCAs to assess the computer codes. The calculated system pressure by the RELAP4J computer code agreed well with the experimental results, however, the fuel surface temperature was not in good agreement with the experimental results. Improvement of the calculation model in the two-phase counter current flow and the heat transfer correlations is necessary for the accurate calculation of the fuel surface temperature during a BWR LOCA.

Major results of CCTF are as follows. Four main tests have been completed and test conditions are as follows;

(1) High loop flow resistance test, K factor = $\sim$ 35,

(2) Base case, K factor = $\sim$ 25, wall temp. of downcomer Twd = 198°C, system pressure P = 2 kg/cm^{2}a,

(3) Cold downcomer test, Twd = 118°C, and

(4) Refill simulation test, P = 6-2 Kg/cm^{2}a.

Main results are as follows;

(1) Except the case of the refill simulation test, the attained maximum clad temperatures were nearly the same but the heat transfers after turnaround time were slightly different. The lower heat transfer was obtained in the case of the high loop flow resistance test than base case and is thought to be caused by low flooding rate. In the case of the cold downcomer test, the higher heat transfer was obtained and is due to higher subcooling at the core inlet. In the case of the refill simulation test, the maximum clad temperature was higher and the heat transfer was lower than the others. That is due to lower subcooling at the core inlet.

(2) In spite of lower head of water in downcomer, the effective driving head of the base case with hot downcomer was higher than that of the cold downcomer test in the earlier half of reflood phase. That was caused by the pressure drop at the broken cold leg nozzle by the presence of the two-phase flow.

(3) Symmetry of flow was found in intact loops and the core and the downcomer were observed to have symmetry of thermal behavior to the center axis.

(References)

(1) M. Shiba, et. al., ROSA-II Data Report·1 (Runs 202, 203, 303, 304, 306), JAERI-M-6240 (1975).

(2) M. Shiba, et. al., ROSA-II Data Report·2 (Runs 307, 308, 309), JAERI-M-6241 (1975).

(3) M. Suzuki, et. al., ROSA-II Data Report·3 (Runs 204, 301, 302), JAERI-M-6512 (1976).

(4) M. Sobajima, et. al., ROSA-II Data Report·4 (Runs 401, 403, 404), JAERI-M-6513 (1976).

(5) M. Sobajima, et. al., ROSA-II Data Report·5 (Runs 310, 311, 312, 313, 317), JAERI-M-6709 (1976).

(6) M. Suzuki, et. al., ROSA-II Data Report·6 (Runs 411, 314, 315, 316), JAERI-M-6849 (1976).

(7) M. Sobajima, et. al., ROSA-II Data Report·7 (Runs 318, 320, 321, 322, 323), JAERI-M-7106 (1977).

(8) M. Suzuki, et. al., ROSA-II Data Report·8 (Runs 324, 325, 326), JAERI-M-7236 (1977).

(9) M. Sobajima, et. al., ROSA-II Data Report·9 (Runs 418, 419, 420, 423), JAERI-M-7239 (1977).

(10) M. Sobajima, et. al., ROSA-II Data Report·10 (Runs 415, 417, 421, 422), JAERI-M-7437 (1977).

(11) M. Suzuki, et. al., ROSA-II Data Report·11 (Runs 327, 328, 329, 330), JAERI-M-7505 (1978).

(12) M. Suzuki, et. al., ROSA-II Data Report·12 (Runs 332, 413, 425), JAERI-M-7944 (1978).

(13) M. Sobajima, et. al., ROSA-II Data Report·13 (Runs 502, 505, 506, 507), JAERI-M-7737 (1978).

(14) M. Shiba, et. al., "Experiment on Performance of Upper Head Injection System with ROSA-II", JAERI-M-6707 (1976).

(15) K. Tasaka, et. al., "ROSA-II UHI Tests in JAERI", Trans. Am. Nucl. Soc., 26, 407 (1977).

(16) K. Tasaka, et. al., "Performance Test of the Upper Head Injection System at the ROSA-II Test Facility", Nuclear Technology, 45, 121 (1979).

(17) K. Tasaka, et. al., "Study on the Similarity between ROSA-III Experiment and BWR LOCA (Pre-Analysis of ROSA-III)", JAERI-M-6703 (1976).

(18) H. Kitaguchi, et. al., "Preliminary Analysis of ROSA-III Experiment (II)", JAERI-M-7488 (1978).

(19) H. Kitaguchi, et. al., "Preliminary Analysis of ROSA-III Experiment (III)", JAERI-M-7791 (1978).

(20) H. Kitaguchi, et. al., "LOCA Analysis of BWR/6 for the ROSA-III Test", JAERI-M-8185 (1979).

(21) K. Soda, "Prediction of ROSA-III Experiment RUN 701", JAERI-M-7712 (1978).

(22) Y. Koizumi, et. al., "Prediction of ROSA-III Experiment RUN 702", JAERI-M-7970 (1978).

(23) Y. Koizumi, et. al., "Prediction of ROSA-III Experiment RUN 703", JAERI-M-8300 (1979).

TABLE I Primary Characteristics of BWR-6 and ROSA-III

	BWR-6	ROSA-III	BWR/ROSA
No. of Recirc. Loops	2	2	1
No. of Jet Pumps	24	4	6
No. of Separators	251	1	251
No. of Fuel Assemblies	848	4	212
Active Fuel Length (m)	3.76	1.88	2
Total Coolant Volume (m^3)	623	1.37	455
Power (MW)	3800	4.24	896
Pressure (MPa)	7.23	7.23	1
Core Flow (kg/sec)	1.39×10^4	36.4	382
Recirculation Flow (l/sec)	2970	7.01	424
Feedwater Flow (kg/sec)	2060	4.86	424
Feedwater Temp (°K)	489	489	1

Table 2 Experimental Conditions

RUN	Core No.	Break	Power			ECCS
			P_0 (MW)	P(t)	Distribution	
701	No.1	200% double ended	3.7	n+d	No	Yes
702	No.1	200% split break	3.7	n+d+s*)	No	No
703	No.1	100% split break	3.7	n+d+s	No	Yes
704	No.2	200% double ended	3.3	n+d+s	No	Yes
705	No.2	200% double ended	0.0	—	—	No
706	No.2	200% double ended	3.3	n+d+s	No	No
721	No.2	200% double ended	4.2	n+d+s	Yes	Yes

*) n = delayed neutron fission power
d = decay power of FPs and actinides
s = stored heat in the nuclear fuel rods

Table 3 Test Condiiton (CCTF)

RUN (M:Main test)	M.1	M.2	M.3	M.4
DATE (1979)	June 21	July 4	July 13	July 27
System Pressure (kg/cm^2a)	2.0	2.0	2.0	6.0 → 2.0
Averaged Linear Power (kw/m)	1.40	1.40	1.40	1.40
Radial Power Ratio	←	1.15 : 1.10 : 0.89		→
ACC Injeciton Rate (m^3/h)	83.8x3	83.8x3	83.8x3	83.8x3
ACC Injection Period (sec)				
Total Time	26	26	26	26
From Lower Plenum	15	15	15	0
From Cold Leg	11	11	11	26
Total Time after flood	14	14	14	-
ACC Water Temp. (°C)	35	35	35	35
LPCI Injeciton Rate (m^3/h)	10x3	10x3	10x3	10x3
LPCI Water Temp. (°C)	35	35	35	35
Initial Peak Clad Temp. (°C)	600	600	600	600
Downcomer Wall Temp. (°C)	198	198	119	198
K factor of loop (NOMINAL)	~35	~ 25	~ 25	~ 25
Note	HIGH FLOW RESISTANCE	BASE	COLD DOWNCOMER	REFILL

SG secondary side water temp. = 265°C

Structure temp. = ~ Tsat
2kg/cm^2a : 119°C
4.9 : .44°C6 : 158°C

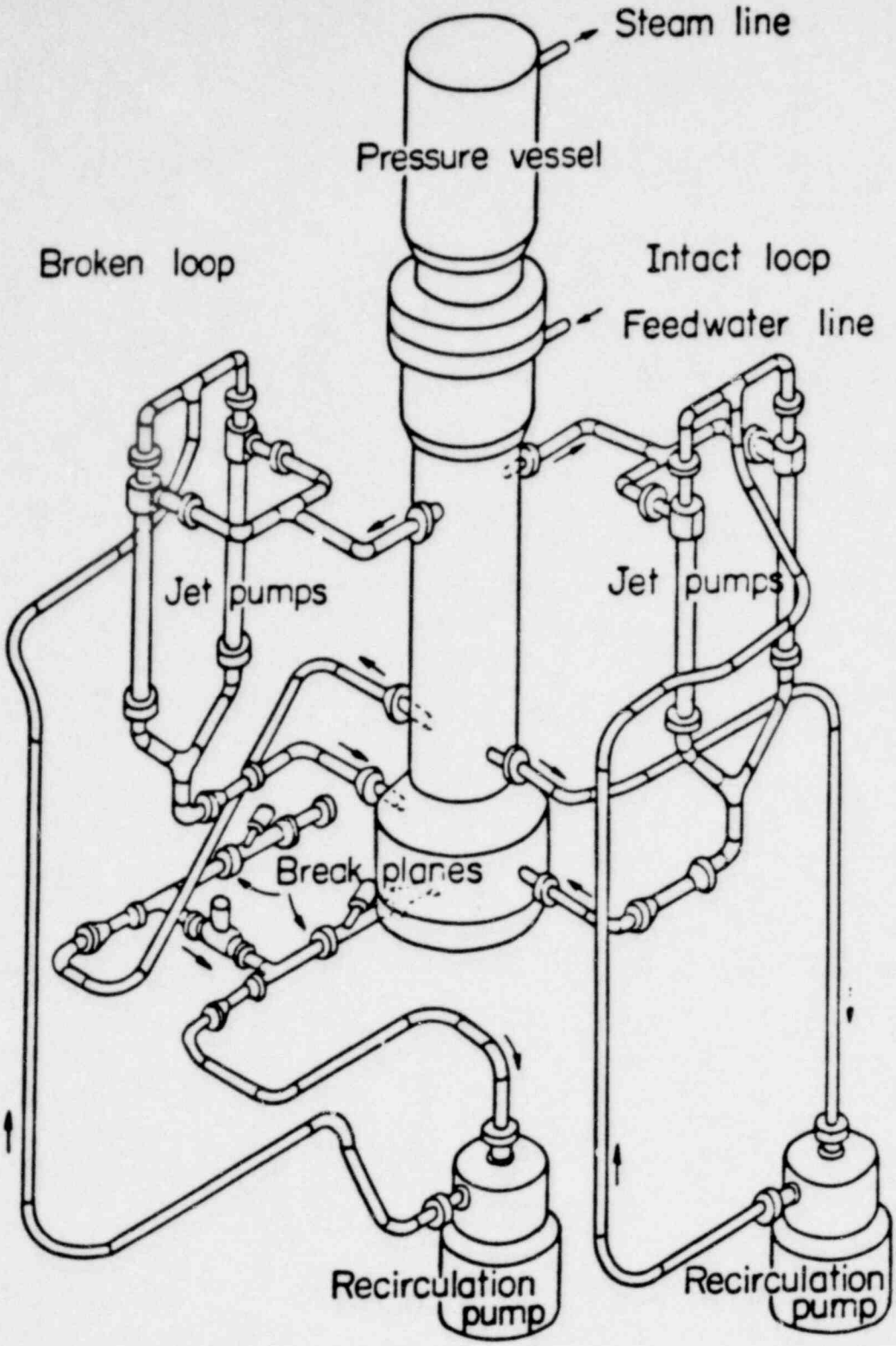

Fig. 1 Schematic Diagram of ROSA-III Test Facility

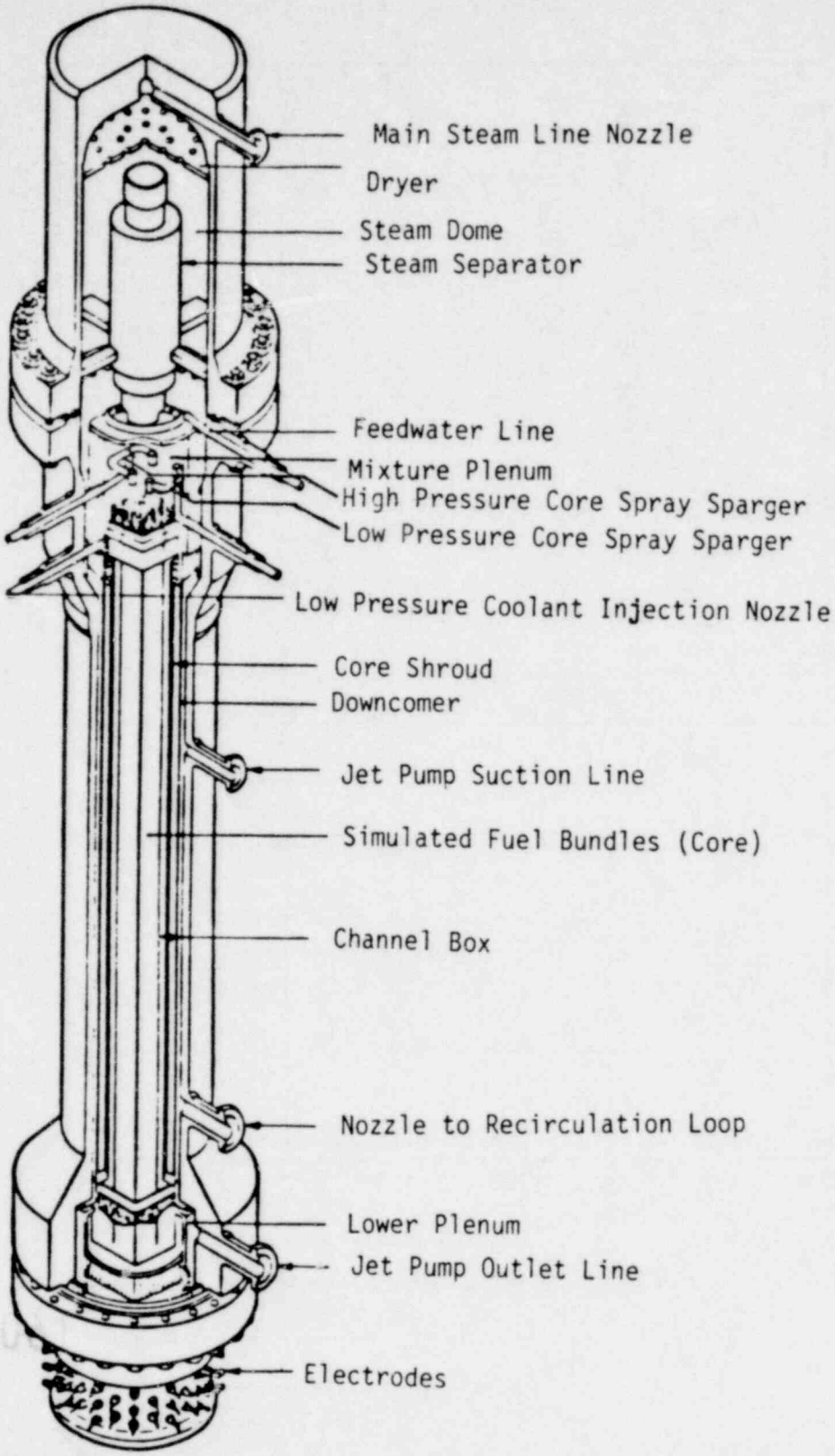

Fig. 2 Internal Structure of Pressure Vessel of ROSA-Ⅲ

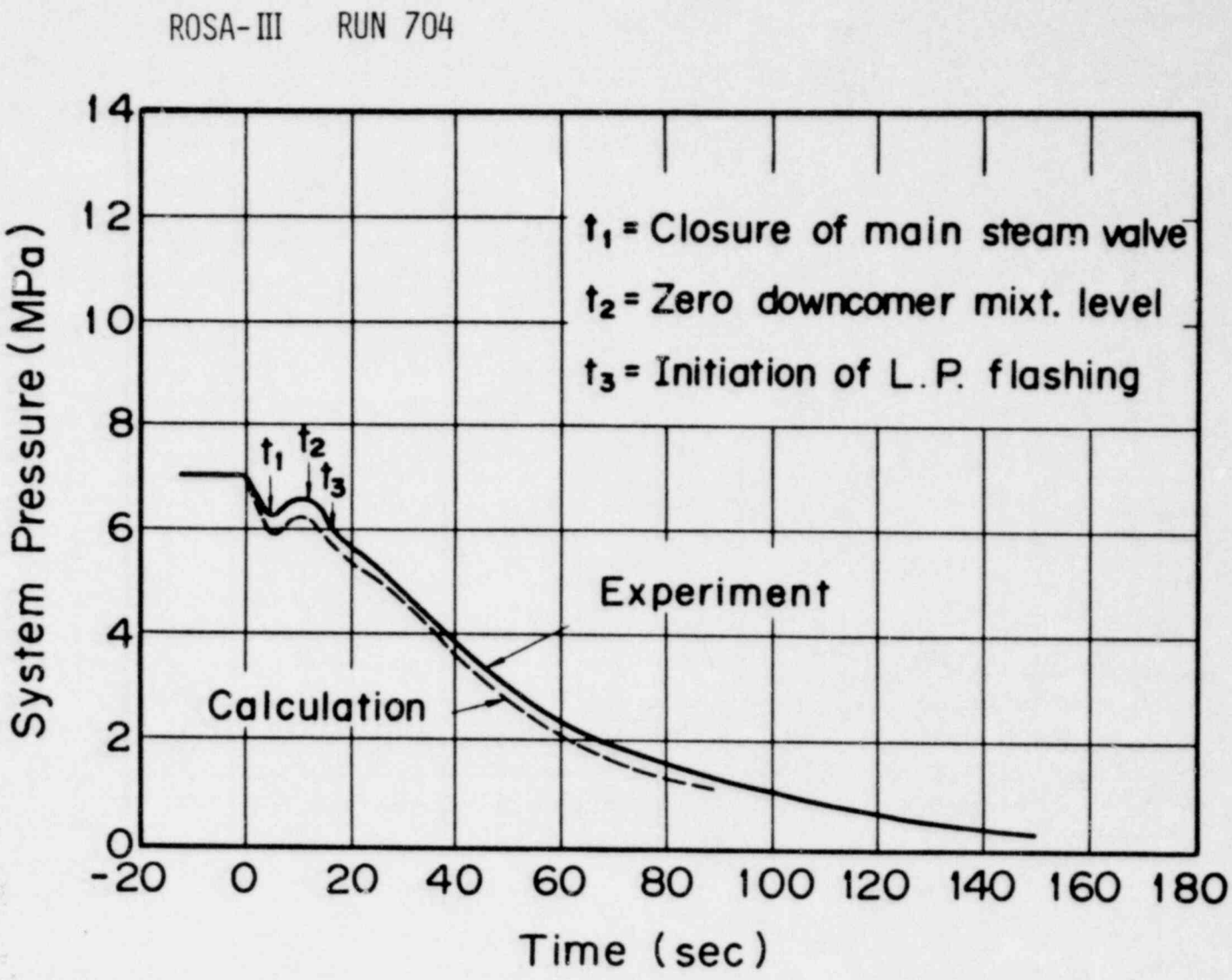

Fig. 3 System Pressure Transient in RUN 704

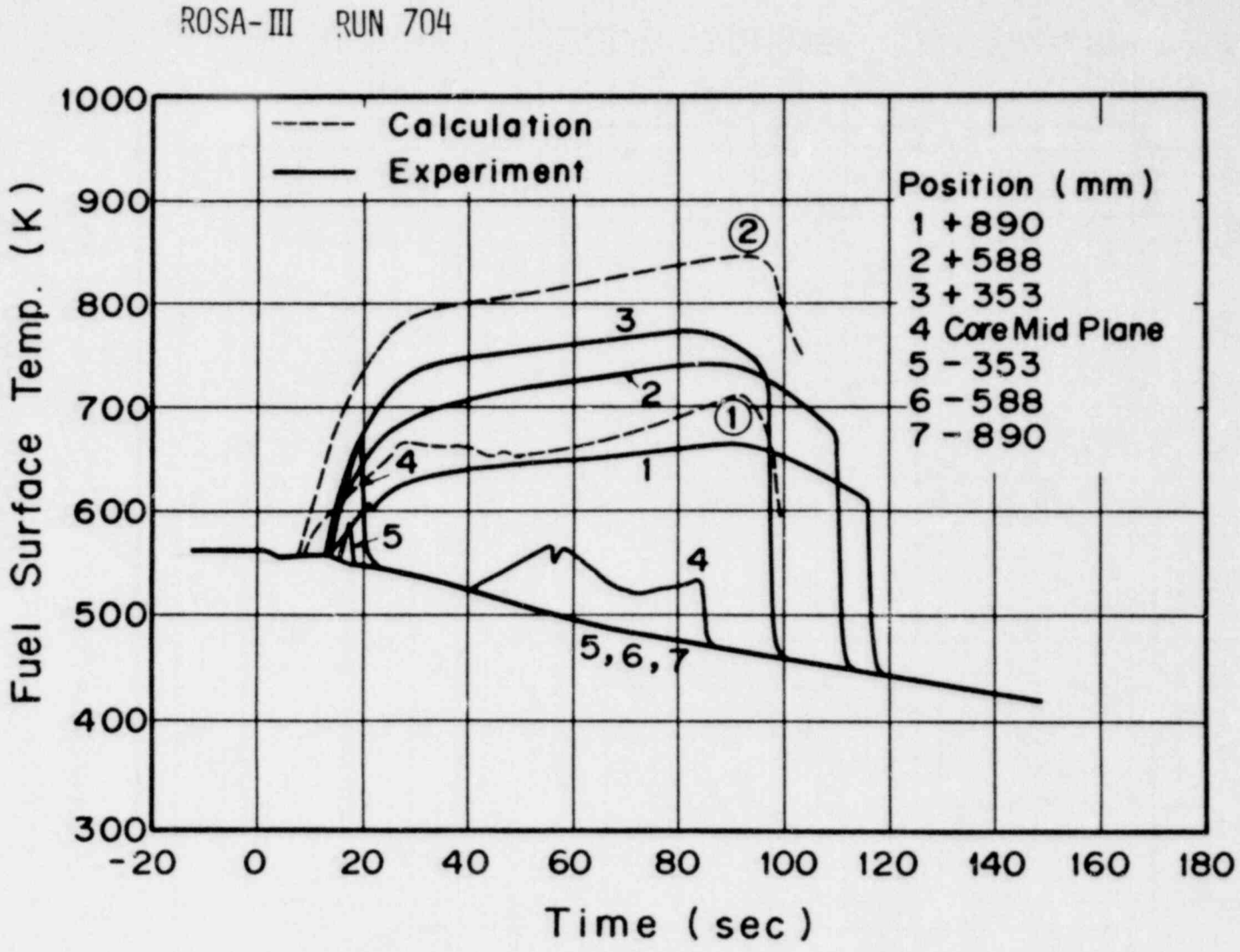

Fig. 4 Fuel Surface Temperature Transient in RUN 704

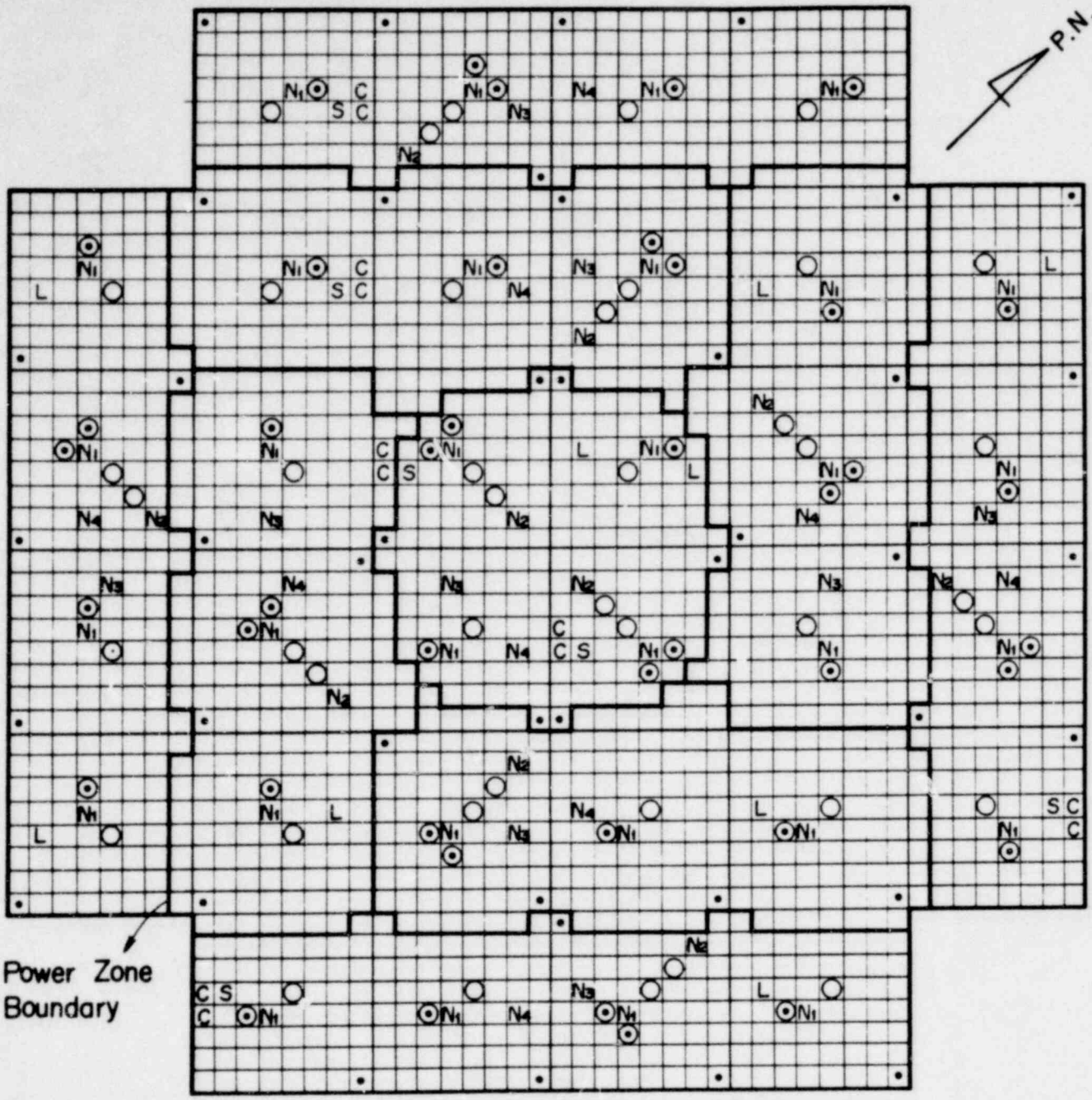

Symbols

- ⊙ : High Power Heater Rod (42)
- ○ : Medium Power Heater Rod (42)
- • : Low Power Heater Rod (42)
- C : Low Power Heater Rod US NRC Requested (12)
- S : Superheated Steam Probe (6)
- N_1, N_2 : Non-Heated Rod, Rod Surface Temp. (42)
- N_3 : Non-Heated Rod, Fluid Temp. (9)
- N_4 : Non-Heated Rod, Top & Bottom Temp. of Rod Surface (9)
- L : Liqud Level Detector (9)

Fig. 5 Location of Instrumented Rods (CCTE)

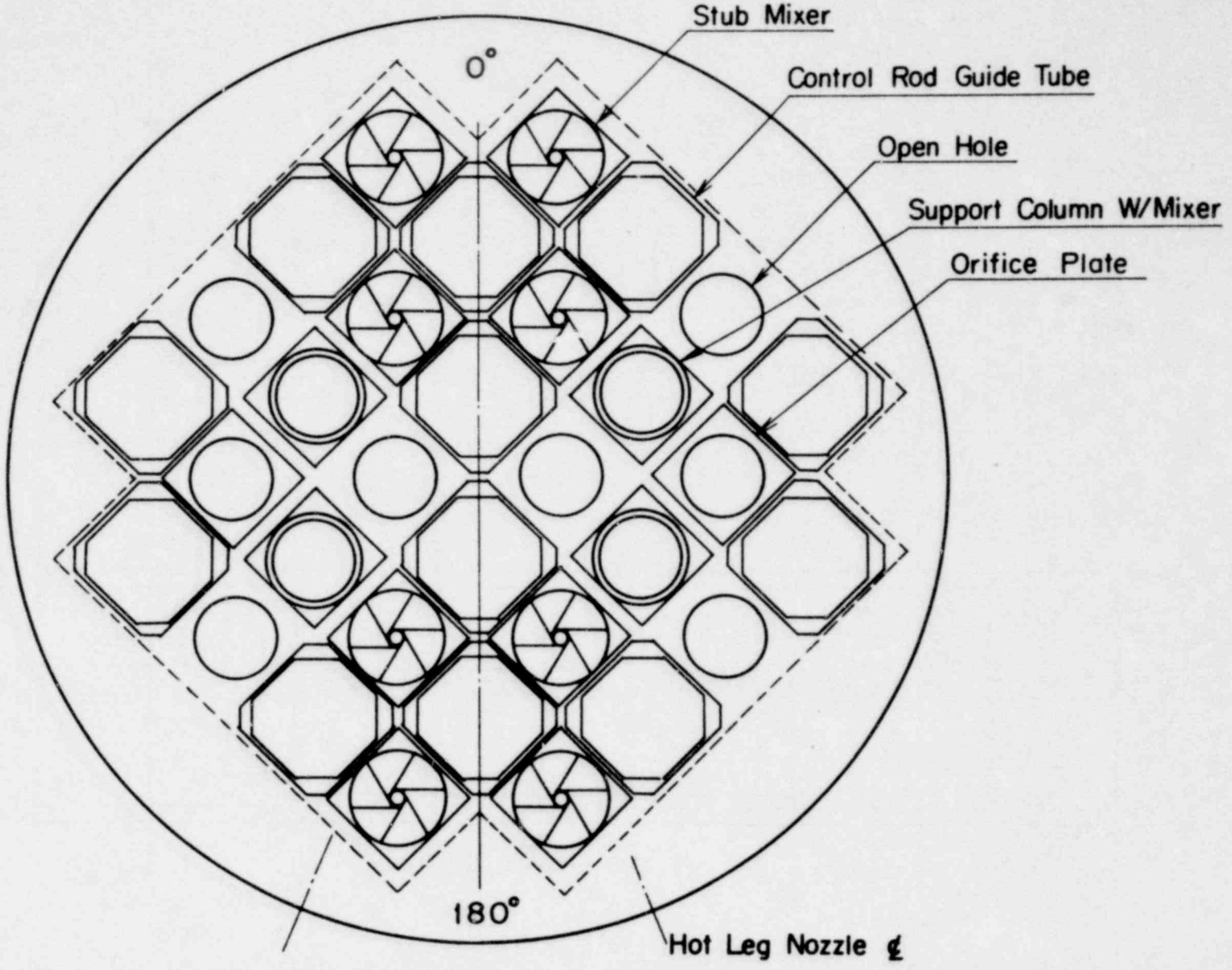

Fig. 6 ARRANGEMENT OF INTERNALS (CCTF)

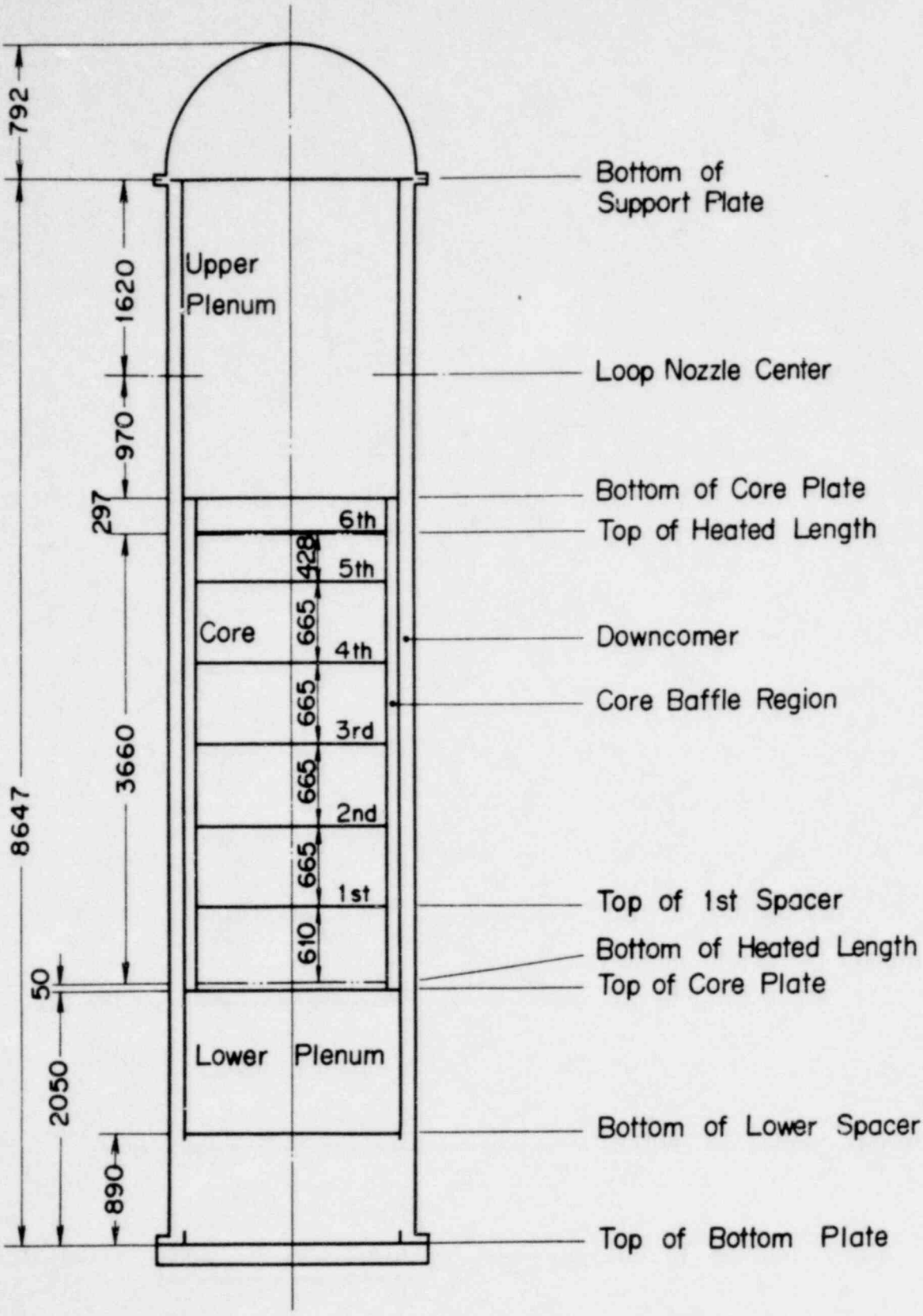

Fig. 7 DIMENSION OF PRESSURE VESSEL (CCTF)

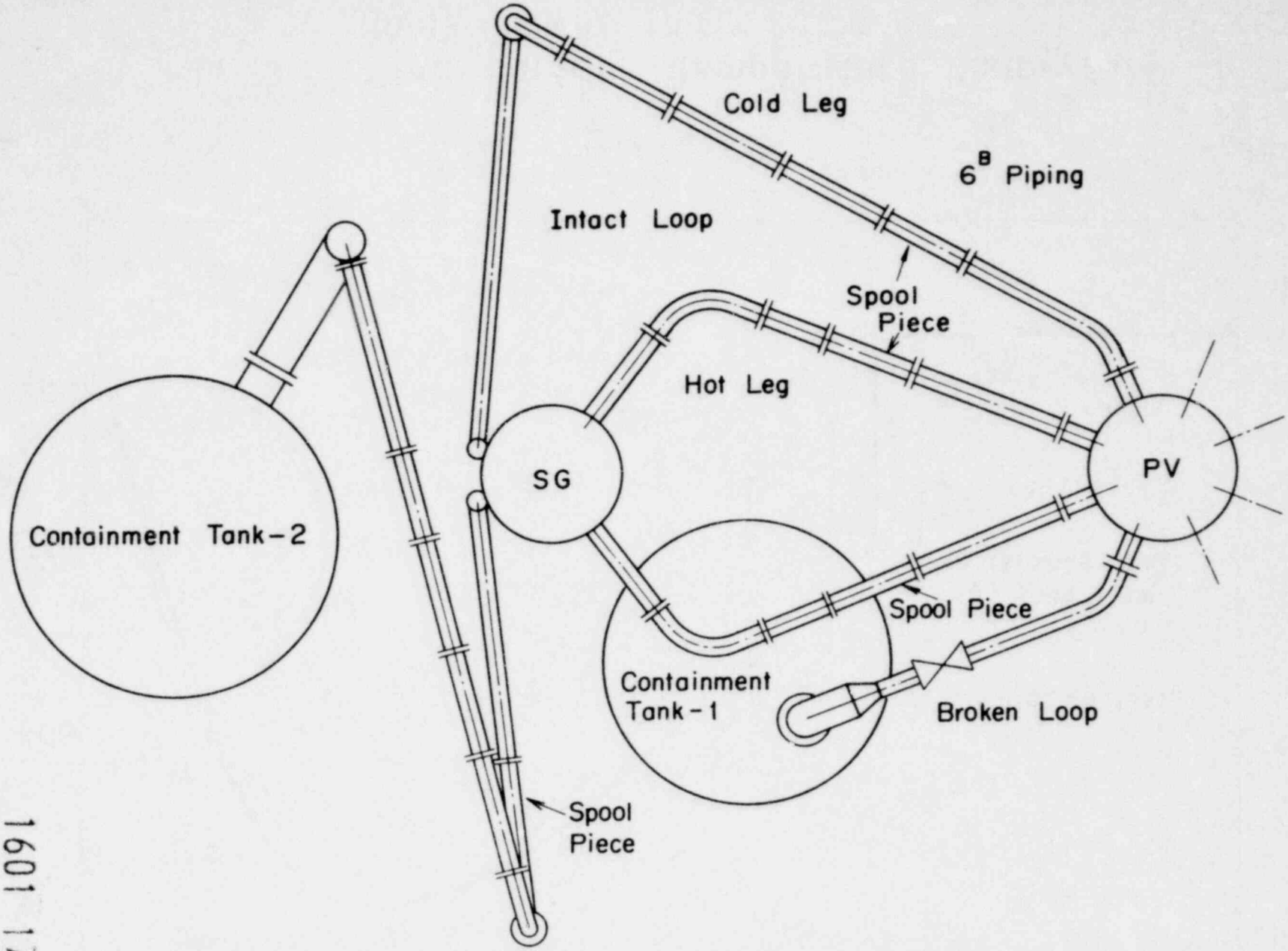

Fig. 8 PRIMARY LOOP PIPING (half part)
(CCTF)

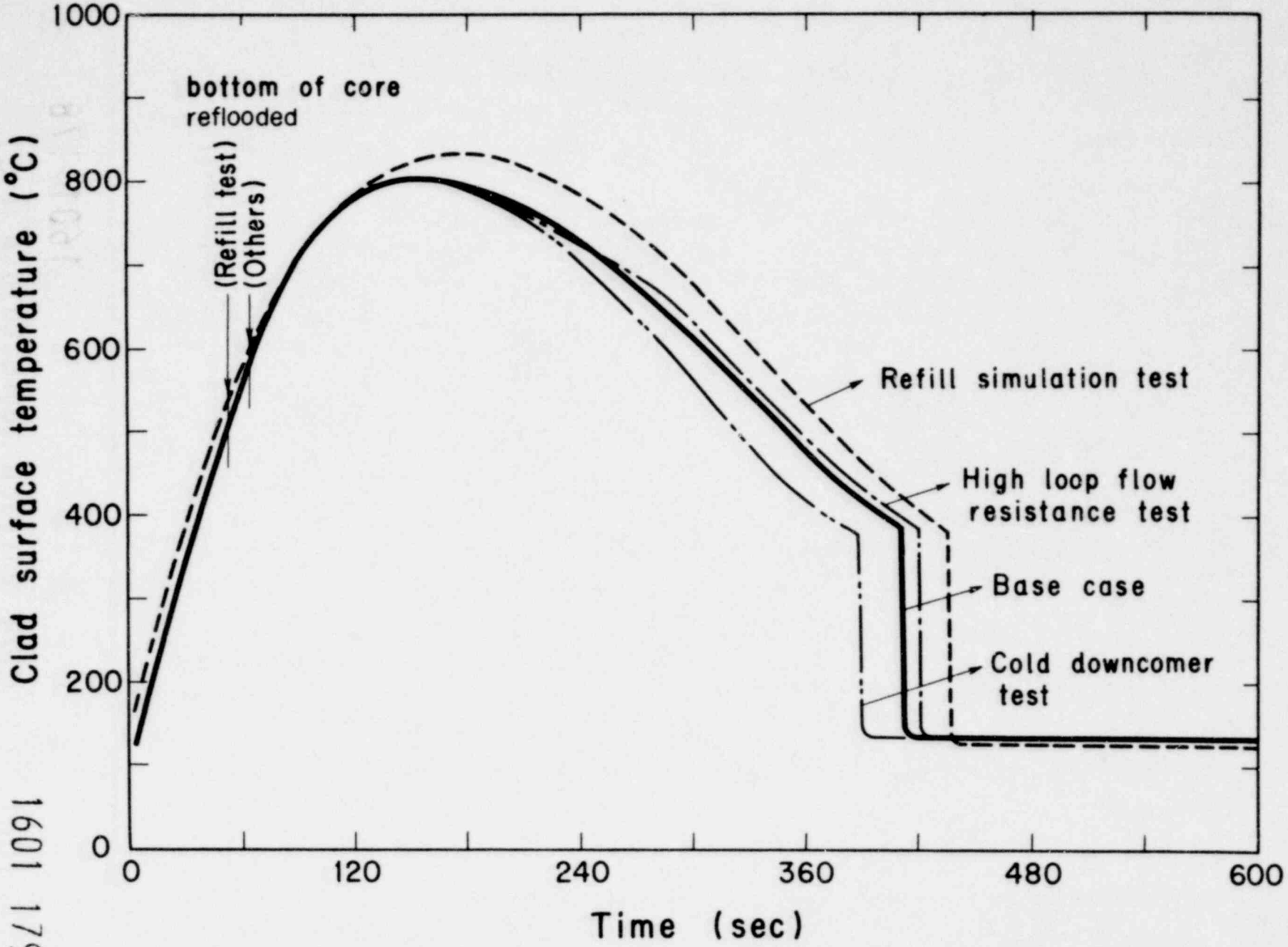

Fig. 9 Clad surface temperature history of peak power rod (CCTF)

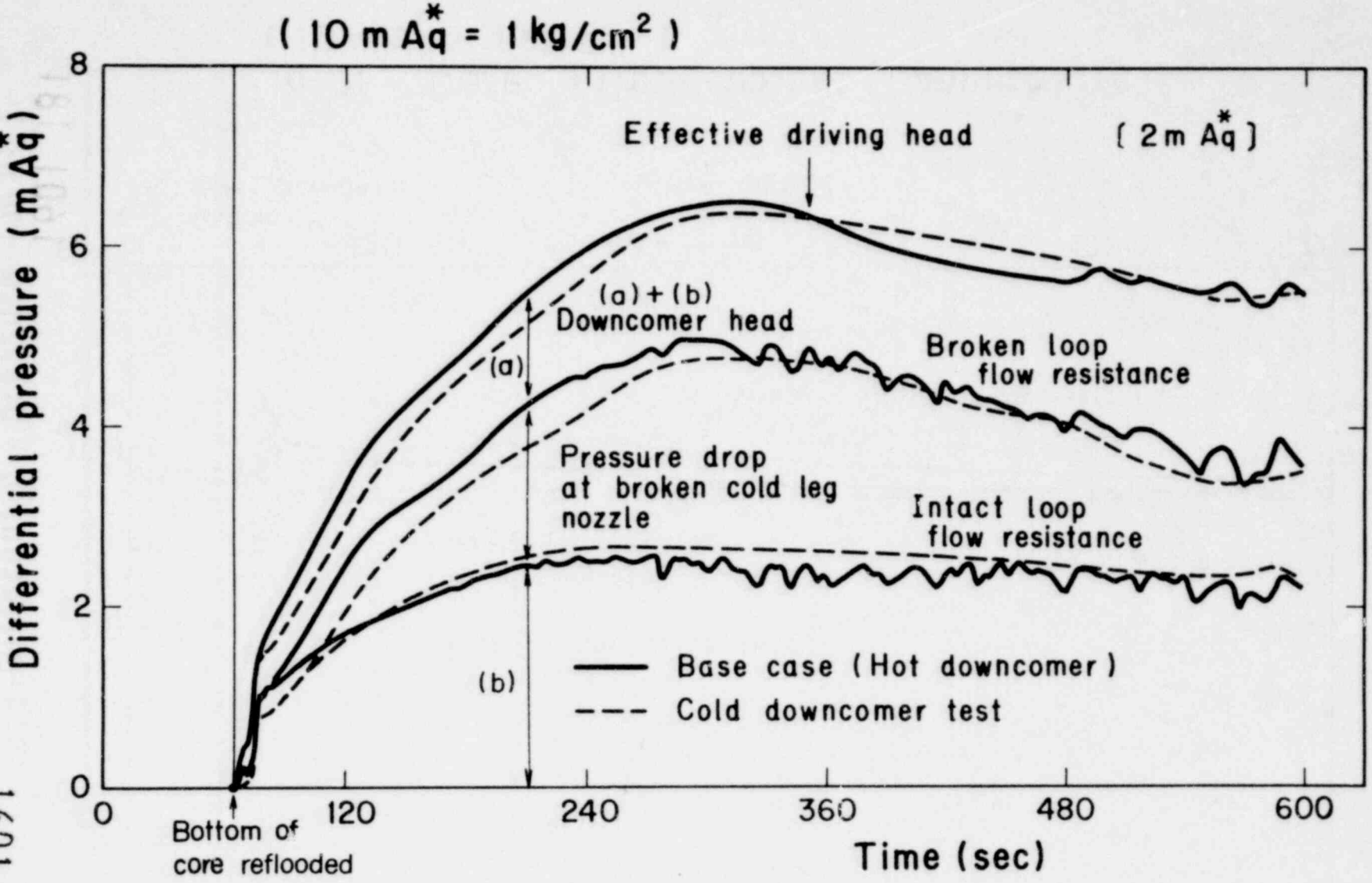

Fig. 10 Loop flow resistance
(effect of downcomer wall temperature)
(CCTF)

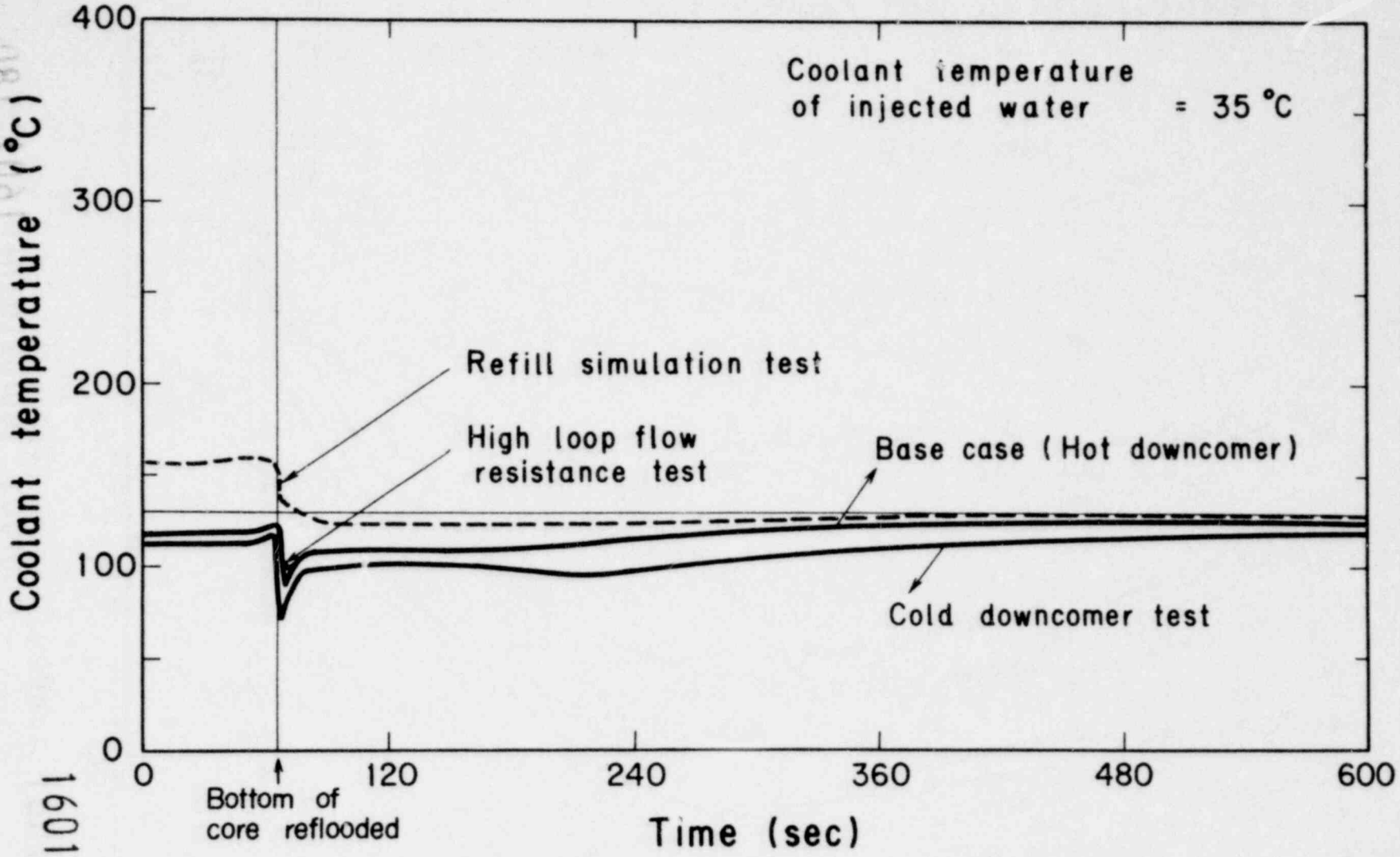

Fig. 11 Core inlet coolant temperature (CCTF)

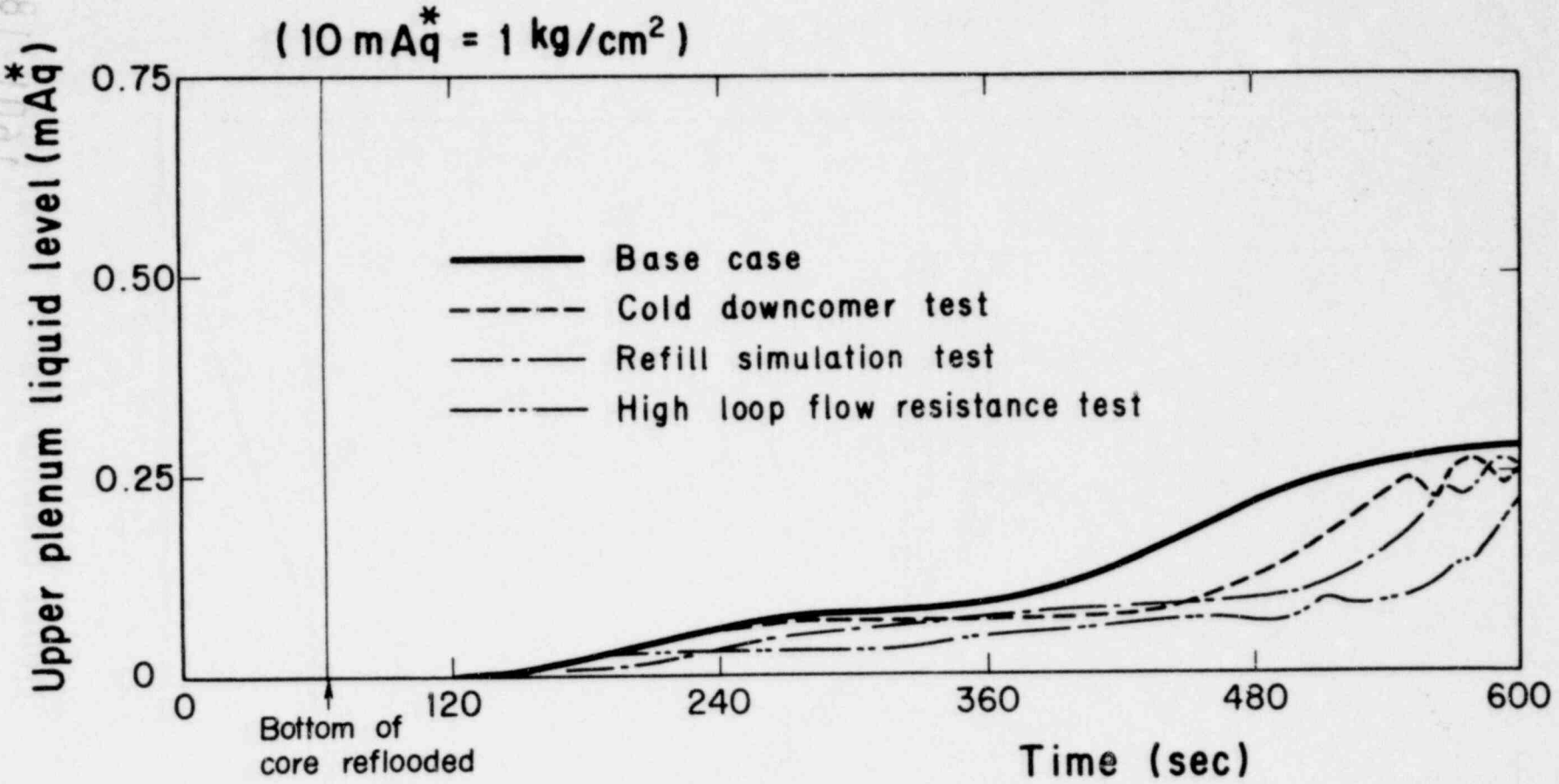

Fig. 12 Water accumulation in upper plenum (CCTF)

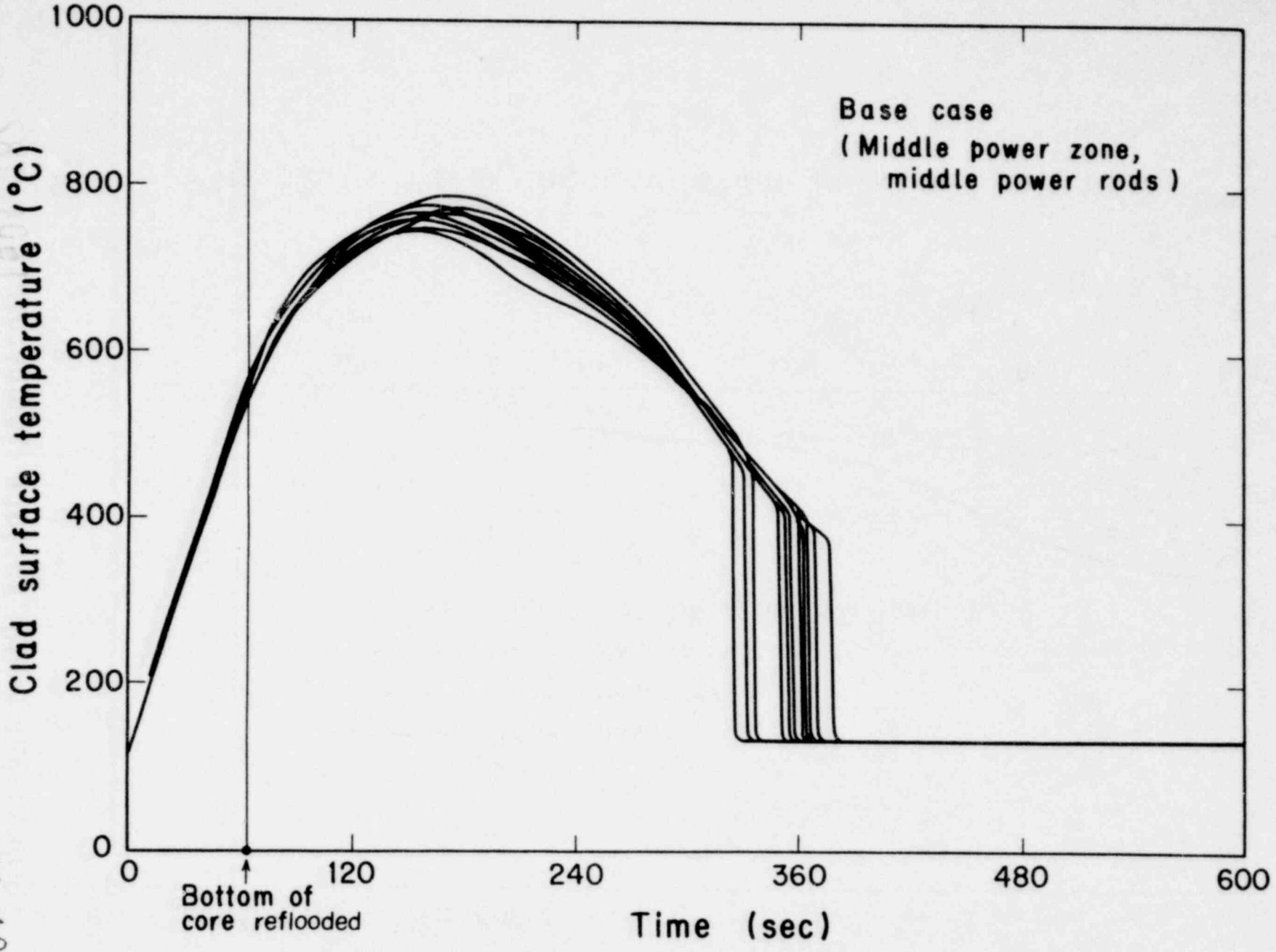

Fig. 13 Symmetry of clad surface temperature histories to the center axis (CCTF)

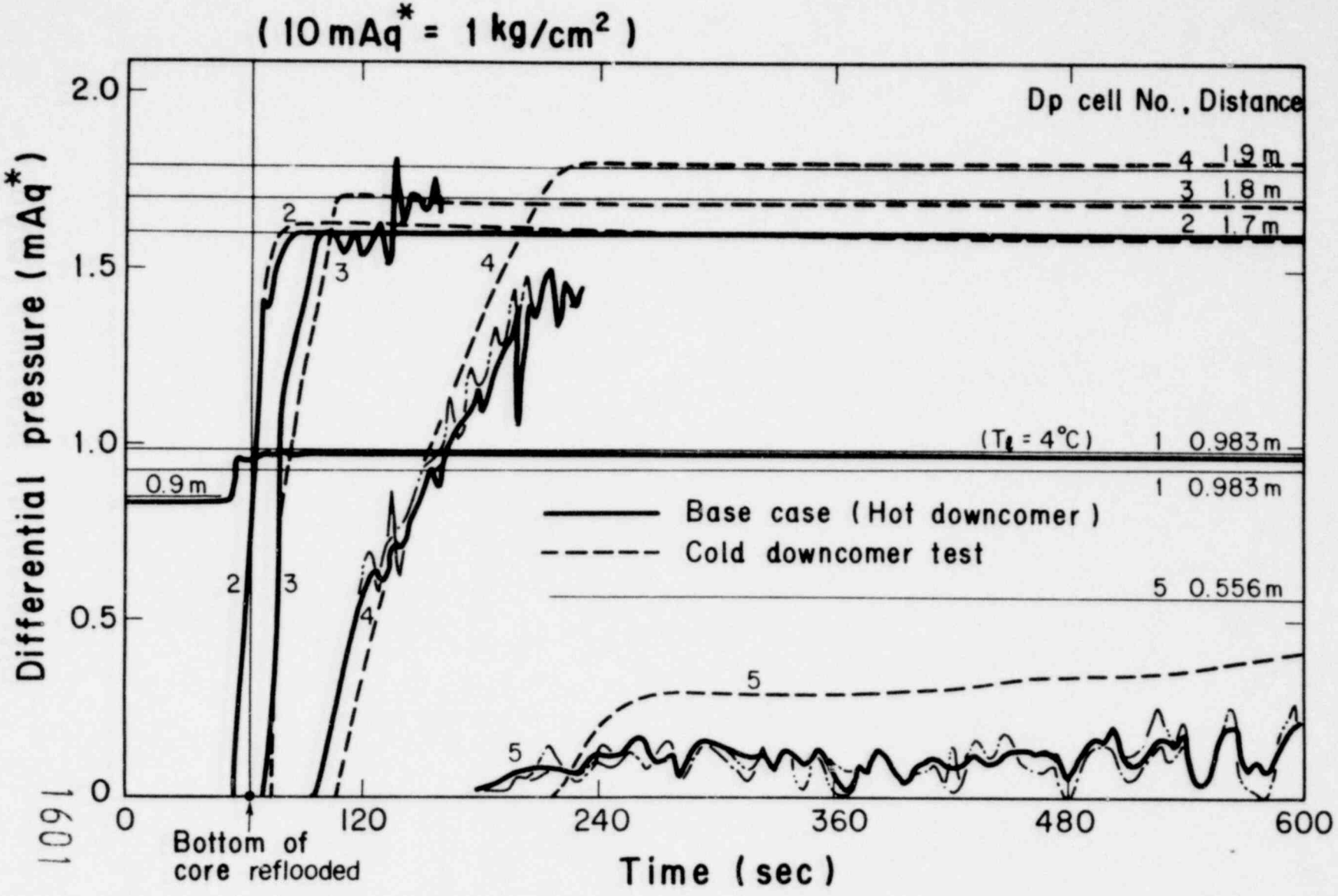

Fig. 14 Water accumulation in downcomer (effect of downcomer wall temperature)

(CCTF)

NRC EPRI/WESTINGHOUSE
FULL LENGTH EMERGENCY CORE HEAT TRANSFER
SEPARATE EFFECTS AND SYSTEMS EFFECTS TESTS

(FLECHT-SEASET):
PROGRAM STATUS/RESULTS

Presented by

L. E. Hochreiter

Westinghouse Nuclear Safety Dept.
Nuclear Technology Division

At

Seventh Water Reactor Safety Information Meeting,
November 6, 1979

INTRODUCTION

The Westinghouse/NRC/EPRI Full Length Emergency Core Heat Transfer Separate Effects And System Effects Tests (FLECHT-SEASET) is designed to examine the reflood portion of a calculated hypothetical Loss of Coolant Accident for a PWR. A list of some of the key individuals from different organizations who are participating in the FLECHT-SEASET program is shown in Figure 1.

The objectives of the program are given in Figure 2 and are to:

1. enhance the understanding of the physics of reflood phenomena in PWRS,

2. aid in the improvement or further the development of thermal hydraulic models and computer codes for reflood

3. aid in the validation of best estimate thermal hydraulic models and/or computer codes for reflood and aid in improving the understanding of safety margins associated with current licensing criteria.

4. broaden the data base for PWR LOCA-ECCS safety evaluations to permit a coordinated reappraisal of existing licensing criteria.

To accomplish these objectives, the program is divided into several different tasks. The interrelationship between these different tasks is shown in Figures 3 and 4. In Figure 3, the 17 x 17 unblocked FLECHT tests will examine rod bundle configuration effects through comparison of the 17 x 17 rod geometry (0.374-inch rod OD, 0.496-inch rod pitch) with the previously tested 15 x 15 geometry (0.422-inch OD, 0.563-inch pitch). These tests will also provide a basis for reflood code development and or assessment since detailed fluid properties such as vapor temperature, void fraction, real quality, and equilibrium quality will be measured or calculated from the data. The unblocked bundle will also serve as a basis to evaluate flow blockage effects.

The 21-rod bundle will serve as a small scale test which will be used to assess the heat transfer effects of different blockage shapes and distributions and to aid in the development of a flow blockage model. Both coplanar and non-coplanar blockage distributions will be examined. Short concentric sleeve blockages simulating beta bursts and longer non-concentric sleeve shapes simulating alpha phase burst will be examined to determine heat transfer effects at and downstream of the blockage zone. A total of ten configurations of concentric, non-concentric sleeves, bypass, no bypass flow, coplanar, and non-coplanar blockage will be tested in the 21-rod bundle. This data will then serve as a basis to develop a flow blockage analysis method.

The 161 rod blocked bundle FLECHT tests will utilize the blockage shape which gave the poorest heat transfer in the 21-rod bundle and will test that shape in a larger bundle (161 rods) with flow bypass. The objective in these tests is to provide ample flow area for the two-phase mixture to bypass the blockage zone which could result in lower heat transfer. The blockage distribution will be non-coplanar since the multi-rod burst test data indicates non-coplanar distributions. The 161-rod blocked bundle data will also be used to assess the blockage analysis method developed from the 21-rod bundle test program.

The combination of the three tasks and associated analysis given in Figure 3 will be used to reassess the flow blockage-steam cooling portion of the Appendix K safety analysis rule for low flooding rates. The objective will be to identify the amount of conservatism in the existing rule and to provide a basis for a rule change. The FLECHT-SEASET flow blockage program is also being planned in such a manner that its results can help with the interpretation of the three country 2D/3D slab core blockage tests which will be performed in Japan.

The systems effects portion of the FLECHT-SEASET program is also subdivided into several tasks as shown in Figure 4. The steam generator tests will be used to examine steam generator heat release characteristics during reflood to see if all the entrained two-phase flow is evaporated in the steam generator. This data can also be used

for development and or assessment of reflood steam generator models. A steam generator model for the FLECHT-SEASET steam generator will be developed from this task.

The upper plenum task is similar in nature to the steam generator task in which the FLECHT-SEASET upper plenum will be studied separately to characterize the plenum separation, de-entrainment, re-entrainment and fallback characteristics. These experiments will permit thermal-hydraulic characterization of the FLECHT-SEASET upper plenum. This task is currently being reassessed by the PMG.

After completion of the steam generator and upper plenum tests, the entire system will be coupled together to perform integrated system reflood tests. By performing the separate steam generator and upper plenum tests before the systems tests, interpretation of the systems effects data should be easier and more precise such that an improved data base for reflood systems code assessment will be possible. The systems tests will also examine the loop feedback effects, the steam generator feedback on the flooding rate, and the downcomer behavior; all of which influence the core flooding rate and heat transfer.

The end result of all the systems effects tasks will be to provide a data base and models for the FLECHT-SEASET system which can then be used to develop and verify reflood system codes.

PROGRAM STATUS

The status of each of the tasks and representative data from the unblocked bundle and steam generator tasks will be discussed.

The status of the unblocked bundle task is shown in Figure 5 and the loop flow schematic for the test facility is given in Figure 6. Reflood testing program was shortened due to heater rod and thermocouple problems. However the most important reflood tests were conducted. In addition to forced and gravity reflood tests, a series of TMI-related low temperature steam cooling tests were conducted as well as three low pressure bundle boil-off tests.

The original reflood test matrix was shortened due to heater rod and heater rod thermocouple problems. A much greater heater rod thermocouple failure rate was observed in the rod bundle test as compared to the single rod prototype tests which were conducted before bundle construction. In addition some rods showed unacceptable low isolation resistance. Heater rods were replaced in the FLECHT-SEASET unblocked bundle to extend its useful testing life without bundle disassembly.

A heater rod development-improvement program has been formulated with ORNL and the Rama Corporation to develop an improved heater rod with a longer thermocouple life which is suitable for high temperature operation ($\sim$2000^{o}F). ORNL had determined that the main problem is the cold work put into the thermocouples during the swagging operation. A low temperature annealing procedure developed by ORNL will be tested on annealled rods to see if improved thermocouple performance occurs. Also a lighter swagged rod is being developed by Rama Corporation in conjunction with Westinghouse and ORNL to investigate improved thermocouple lifetime.

Examples of the forced flooding reflood data are shown in Figures 7 and 8. A very preliminary review of the data indicates that the smaller rod diameter and pitch rod array shows the same overall characteristics as previous FLECHT rod bundle reflood data. That is, increasing flooding rate, pressure, and inlet subcooling improve heat transfer while increasing rod power and initial temperature decrease heat transfer.

A comparison of overlap tests between the smaller rod diameter and pitch fuel bundle (0.496-inch rod pitch with a 0.374-inch rod diameter) and the older FLECHT data (0.563 rod pitch and 0.422-inch rod diameter) is shown in Figures 9 and 10. In these figures a power/flow scaling was used such that the same power would be generated in a fuel assembly for each type of rod. These figures indicate that with this scaling basis there does not appear to be any significant rod geometry effects.

Significant progress has been made on an improved predictive dispersed flow heat transfer model. The FLECHT-SEASET program has also developed a model for dispersed flow heat transfer in rod bundles during reflood. The key features of the model are shown in Figure 11 and include using the rod bundle geometry, simulation of the guide tube thimbles, inclusion of a droplet flow, thermodynamic non-equilibrium; and solution of the vapor energy equation which includes radiation to vapor, drops and surfaces. The model requires input conditions at the quench front as a function of time, droplet size information at the quench front, and the initial rod and vapor temperature distribution in the bundle. Typical comparisons of quality and vapor temperature with older FLECHT data are shown in Figures 12 and 13. The transient rod temperature histories for a skewed axial profile and cosine axial profile FLECHT test are shown in Figures 14 and 15. The over predictions for the upper elevations maybe due to a top down quench which is observed in the tests but not accounted for in the model. This model will be evaluated with the recently obtained FLECHT-SEASET unblocked bundle data.

A series of steam cooling and core uncovery tests were performed in the unblocked bundle in light of the TMI incident. The purpose of these tests was to obtain data on low Reynolds number steam cooling convective heat transfer in a rod bundle geometry. This data spans the Reynolds number range of approximately 300 to 20,000 with the lowest Reynolds number data being obtained from the bundle uncovery tests. The reduced heat transfer data will be correlated in a forced convection heat transfer correlation for use in rod bundle analyses.

The status of the 21 rod bundle program and the 161 rod bundle program is shown in Figure 16. The task plan for the 21 rod bundle program has been completed and construction of that facility is underway with testing to be initiated in the first quarter of 1980. Experiments have also been conducted on a single rod facility to test the blockage sleeve

attachment method, a self-aspirating steam probe design, and a method of attaching blockage sleeve thermocouples. The sleeve attachment and self-aspirating steam probes work reasonably well, but attaching thermocouples to the blockage sleeves promotes early sleeve quench. We are presently investigating sleeve thermocouples with the Karlsrule FEBA group. The 161-rod blocked bundle task is currently in the design stage and the task plan for this test will be issued shortly.

The status of the steam generator separate effects tests which is part of the system effects tests is shown in Figure 17. The current activity is developing a steam generator heat transfer model and preparing the data and analysis reports. The picture one obtains from examining the data with two-phase primary side inlet conditions is:

1. the primary tubes and secondary side are initially at or above the Lidenfrost temperature and film boiling to a dispersed two-phase inlet mixture occurs.

2. non-equilibrium is present in the two-phase region

3. a climbing film quench occurs on the tube as it is cooled below the Lidenfrost temperature

4. as the tube quenches, it removes the stored energy from the secondary fluid

5. reverse heat transfer (primary to secondary) can occur at the steam generator exit due to secondary side stratification.

Examples of the steam generator data for a reference test with 80% inlet quality are shown in Figures 18 and 19. A summary of the data analyzed to date is given in Figure 20. Liquid is observed to flow through the U-tube steam generator, however the exit drop size is usually quite small and appears almost as a mist flow.

A predictive model for the steam generator heat transfer is being developed using the approach by El-Shanawany et. al. reported in the Int. Journal Heat Mass Transfer, Vol 21, 1978. The key model assumptions are given in Figure 21, and a prediction of the axial tube quench (rewetting) behavior is shown in Figure 22 where a dryout CHF correlation has been used for a rewet criteria. This model and resulting analysis will be reported in the analysis and evaluation report on this task.

The status of the systems effects reflood tests is given in Figure 23. The draft task plan for this test program has been issued and a design review of the proposed test facility has occurred. Currently task redirection is being conducted by the three sponsoring parties to obtain TMI and long term cooling related data. The types of tests, in addition to the system reflood tests are single phase natural circulation, two-phase natural circulation, and reflux condensation tests in which the uphill side of the steam generators are the heat sink for the rod bundle. A proposal for such tests is currently under evaluation by all three parties.

In conclusion it is felt that the FLECHT-SEASET program will:

1. extend the existing PWR reflood data to new rod geometries

2. provide data and analysis to address the Appendix K rule

3. provide separate effects and reflood systems effects data and analysis for best estimate reflood code assessment

4. be responsive to current long term cooling and post TMI needs.

NRC/W/EPRI FULL LENGTH EMERGENCY CORE HEAT TRANSFER SEPARATE EFFECTS AND SYSTEMS EFFECTS TESTS (FLECHT-SEASET):

PROGRAM STATUS/RESULTS

PRESENTED BY
L. E. HOCHREITER
W NUCLEAR SAFETY DEPT.
NUCLEAR TECHNOLOGY DIVISION

PRESENTED AT
SEVENTH WATER REACTOR SAFETY
INFORMATION MEETING
NOVEMBER 6, 1979

FIGURE 1

KEY PERSONNEL ON FLECHT-SEASET PROGRAM

Westinghouse	EPRI	EG&G	NRC
R. C. Howard	K. H. Sun	G. Wilson	H. L. Sullivan
N. Lee	R. B. Duffey	D. Odgen	L. Thompson
M. J. Loftus			W. Hodges
E. R. Rosal			M. Pickesimer
A. E. Tome			
H. C. Yeh			
T. E. Sobek			
M. A. Emery			
K. M. Beatty			
D. P. Kitzmiller			
D. Dixon			
L. R. Katz			
C. E. Conway			
W. M. Kavalkovich			
M. F. McGuire			
B. R. Sinwell			
M. M. Valkovic			
C. E. Fuchs			
R. P. Vijuk			
L. E. Hochreiter			
H. W. Massie, Jr.			
L. Chajson			
Test Operations Personnel			
Calibration Lab Personnel			
Quality Assurance Personnel			

THE GOALS OF THE PROGRAM ARE TO:

- ENHANCE THE UNDERSTANDING OF THE PHYSICS OF REFLOOD PHENOMENA IN PWRS.

- AID IN THE IMPROVEMENT OR FURTHER DEVELOPMENT OF THERMAL-HYDRAULIC MODELS AND/OR COMPUTER CODES FOR THE REFLOOD PHASE IN PWRS.

- AID IN THE VALIDATION OF BEST ESTIMATED THERMAL-HYDRAULIC MODELS AND/OR COMPUTER CODES FOR THE REFLOOD PHASE IN PWRS AND AID IN IMPROVING THE UNDERSTANDING OF SAFETY MARGINS ASSOCIATED WITH CURRENT LICENSING EVALUATION MODELS AND CRITERIA.

- BROADEN THE DATA BASE FOR PWR LOCA-ECCS SAFETY EVALUATIONS TO PERMIT A COORDINATED REAPPRAISAL OF EXISTING LICENSING CRITERIA.

1601 195

FIGURE 2

FLECHT-SEASET TASKS

- 17 x 17 UNBLOCKED FLECHT TESTS
  - GEOMETRY EFFECTS, DATA BASE FOR BLOCKAGE
  - PROVIDE DATA FOR REFLOOD CODE DEVELOPMENT / VERIFICATION (TRAC, RELAP MOD-6)
- 21 - ROD BUNDLE TESTS
  - ASSESS BLOCKAGE GEOMETRY AND CONFIGURATION EFFECTS
  - PROVIDE DATA FOR BLOCKAGE ANALYSIS METHOD
- 17 x 17 BLOCKED BUNDLE FLECHT TESTS
  - BLOCKAGE AND BYPASS EFFECTS
  - ADDRESS CURRENT LICENSING CRITERIA
  - ASSESS BLOCKAGE ANALYSIS METHOD

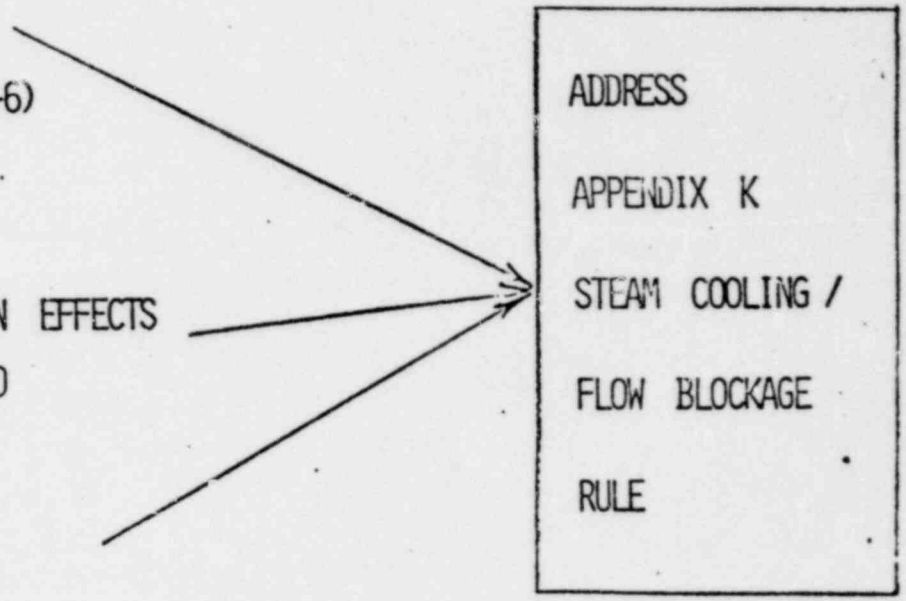

1601 196

FIGURE 3

FLECHT-SEASET TASKS

- **STEAM GENERATOR TESTS**
  - OBTAIN SG HEAT RELEASE CHARACTERISTICS
  - PROVIDE DATA FOR STEAM GENERATOR MODEL DEVELOPMENT/VERIFICATION (TRAC, RELAP-MOD 6)
- **FLECHT-SEASET (F/S) UPPER PLENUM TESTS**
  - OBTAIN F/S UPPER PLENUM SEPARATION / FALLBACK CHARACTERISTICS
- **FLECHT-SEASET SYSTEMS EFFECTS TESTS**
  - TWIN BUNDLE EFFECTS
  - SYSTEM RESPONSE DURING REFLOOD
  - REFLOOD SYSTEM CODE ASSESSMENT

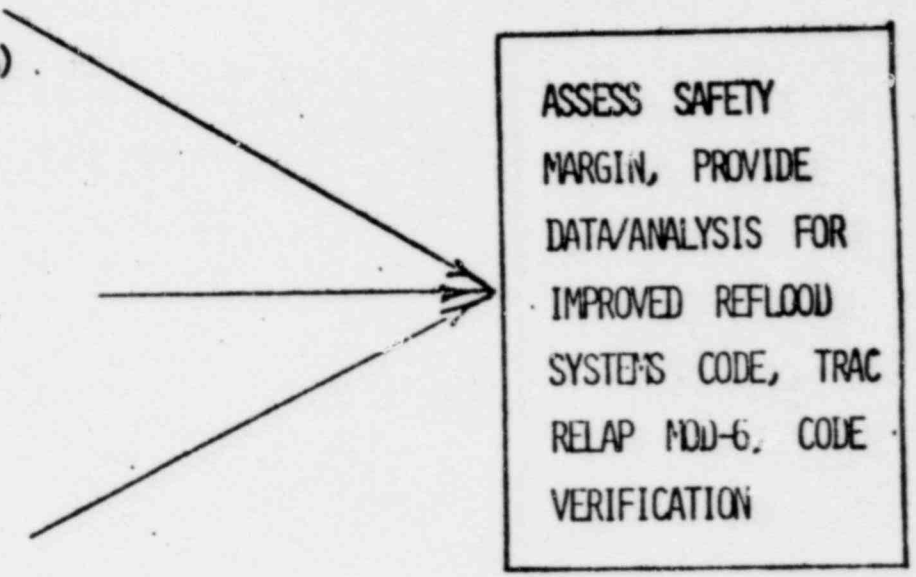

1601 197

FIGURE 4

FIGURE 5

UNBLOCKED BUNDLE TASK STATUS

- TESTING IS COMPLETE
- HEATER ROD PROBLEMS OCCURRED, A NEW HEATER ROD TYPE IS BEING DEVELOPED
- KEY REFLOODING TEST WERE OBTAINED
- AN IMPROVED DISPERSED FLOW REFLOOD MODEL HAS BEEN DEVELOPED
- A SERIES OF STEAM COOLING TESTS WERE PERFORMED
- A SERIES OF CORE BOIL OFF TESTS WERE PERFORMED

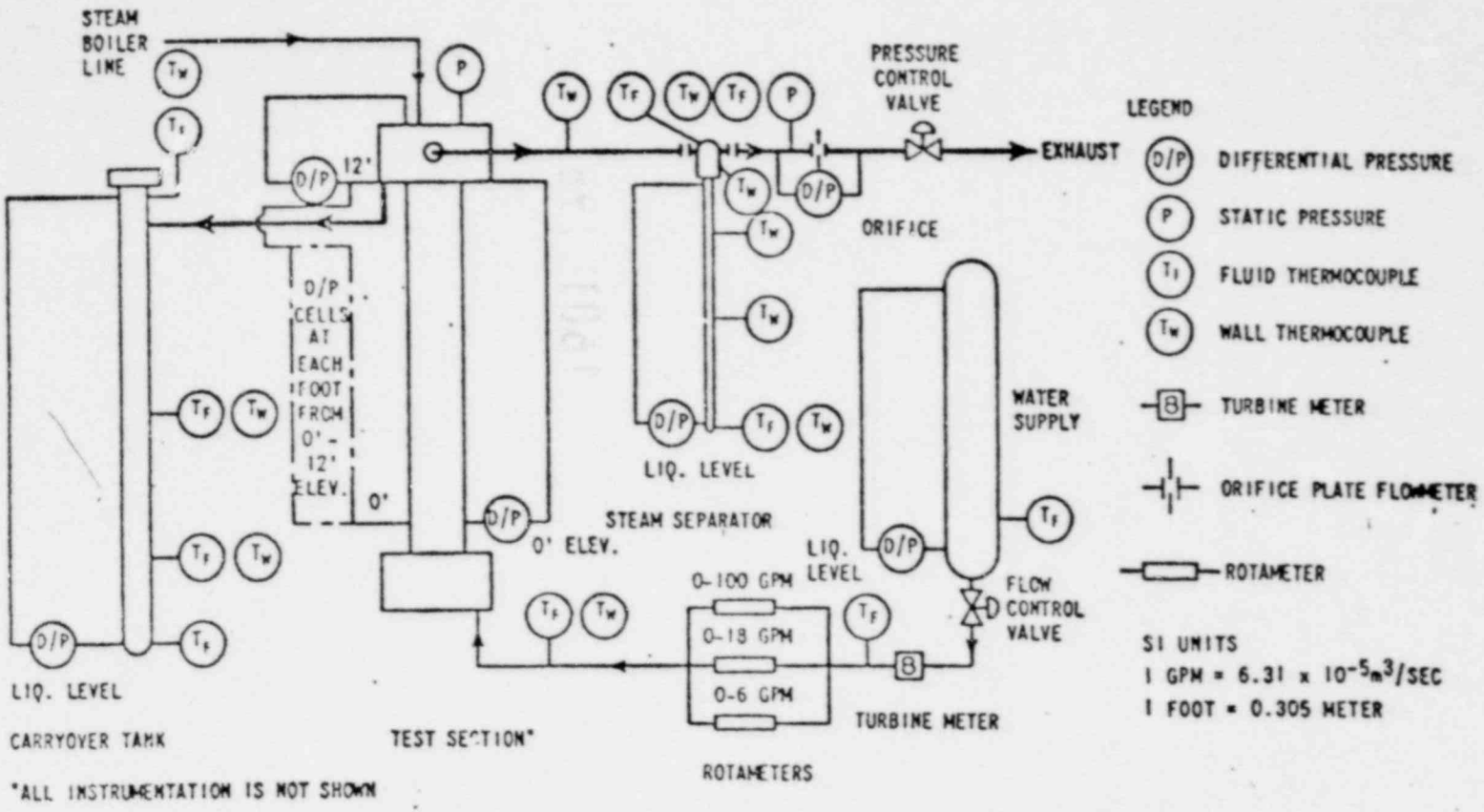

1601 199

FLECHT-SEASET TEST CONFIGURATION (UNBLOCKED BUNDLE TASK)

FIGURE 6

FIGURE 7

UNBLOCKED BUNDLE QUENCH FRONT

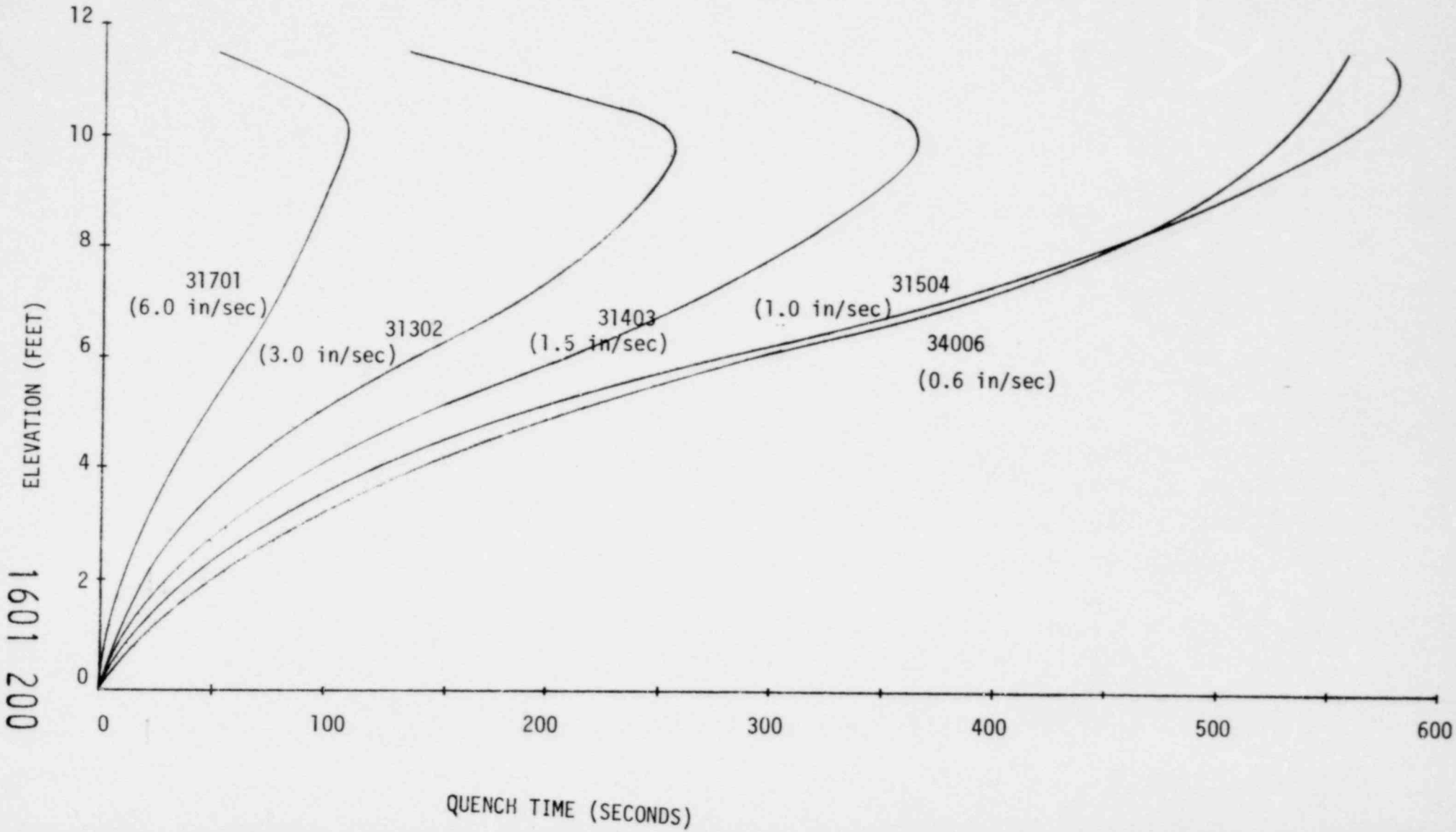

FIGURE 8
UNBLOCKED BUNDLE HEAT TRANSFER

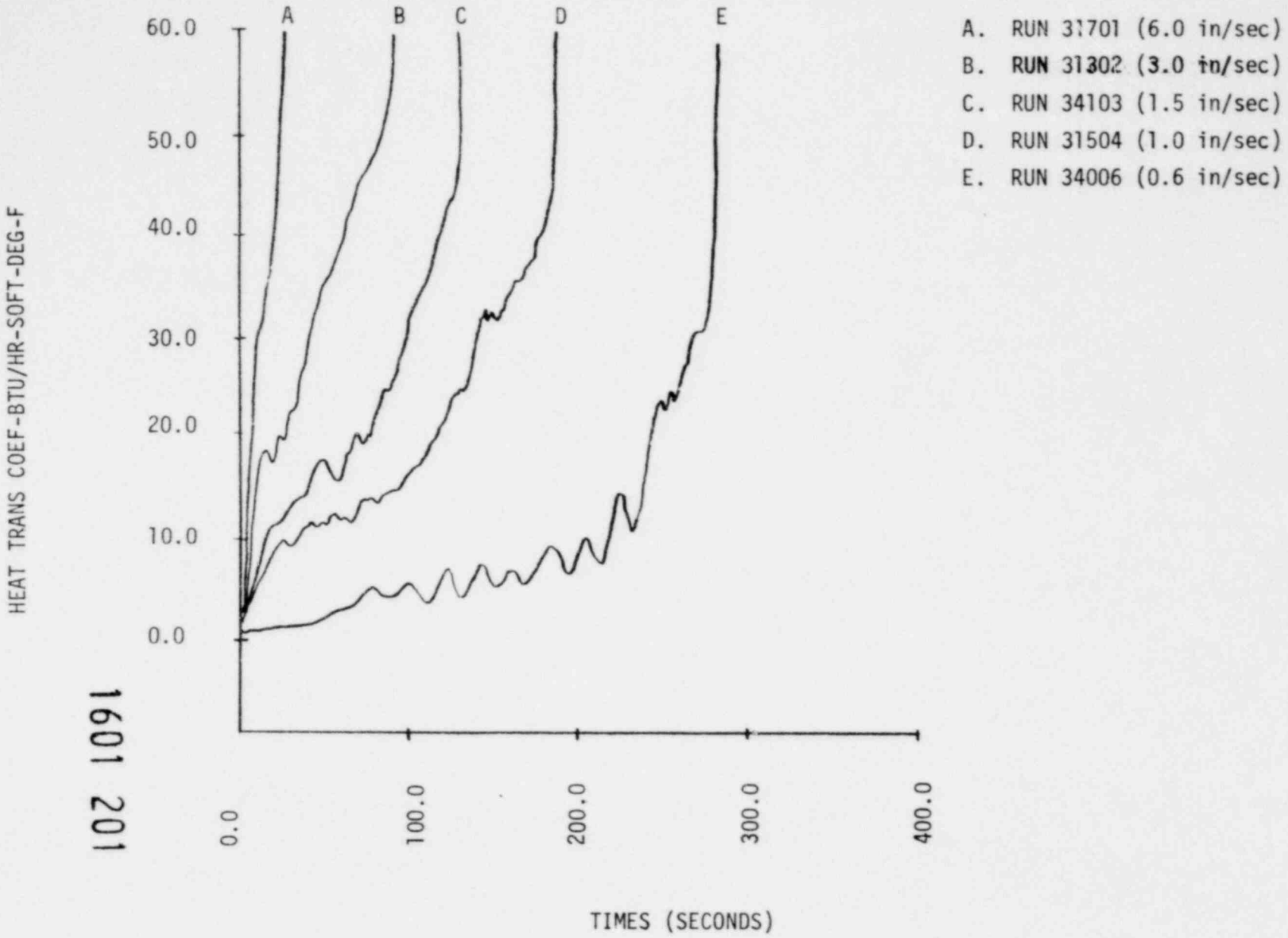

A. RUN 31701 (6.0 in/sec)
B. RUN 31302 (3.0 in/sec)
C. RUN 34103 (1.5 in/sec)
D. RUN 31504 (1.0 in/sec)
E. RUN 34006 (0.6 in/sec)

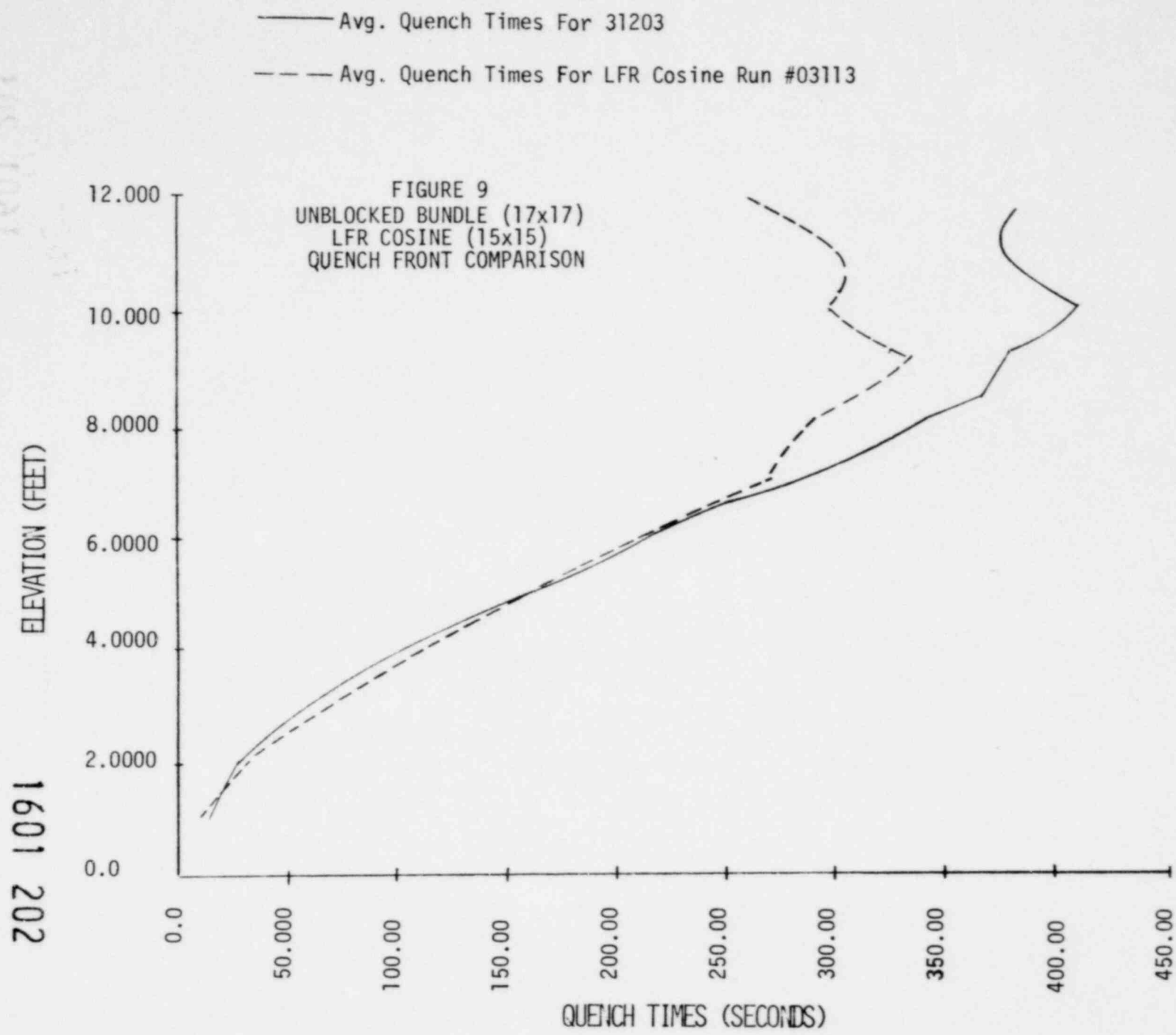
Avg. Quench Times For 31203
Avg. Quench Times For LFR Cosine Run #03113
FIGURE 9
UNBLOCKED BUNDLE (17x17)
LFR COSINE (15x15)
QUENCH FRONT COMPARISON
12.000
10.000
8.0000
6.0000
4.0000
2.0000
0.0
ELEVATION (FEET)
0.0
50.000
100.00
150.00
200.00
250.00
300.00
350.00
400.00
450.00
QUENCH TIMES (SECONDS)

FIGURE 10
UNBLOCKED BUNDLE (17x17)
LFR COSINE (15x15)
HEAT TRANSFER COMPARISON

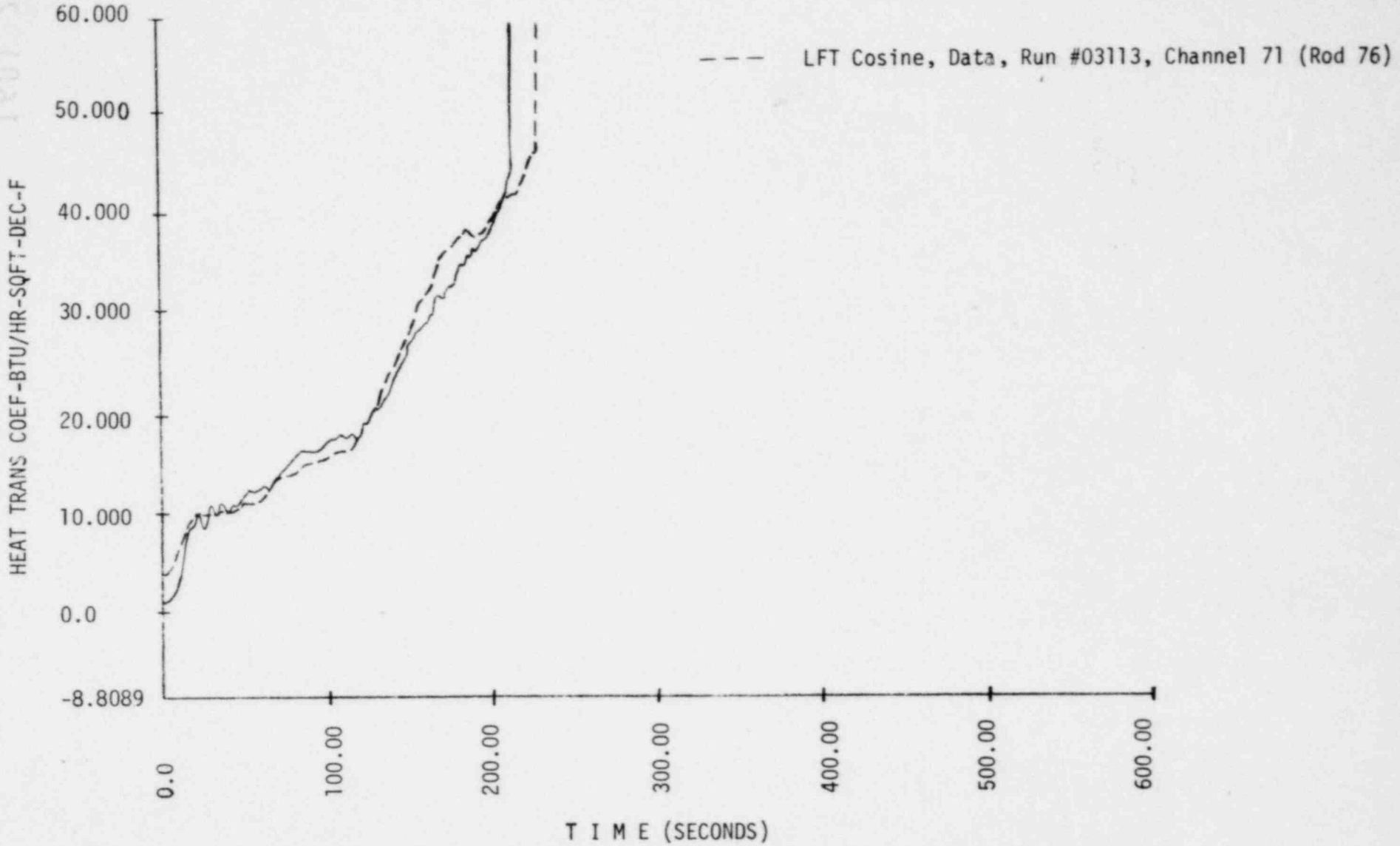

FIGURE 11

KEY FEATURES OF DISPERSED FLOW REFLOOD HEAT TRANSFER MODEL

- USES ROD BUNDLE GEOMETRY, CAN REPRESENT THIMBLE TUBES
- TREATS NON-EQUILIBRIUM DROPLET FLOW
- DEVELOPS A VAPOR ENERGY EQUATION AND SOLVES FOR VAPOR TEMPERATURE DISTRIBUTION $T_v(r,\phi,z,t)$
- CALCULATES q''_{w/v_c}, q''_{w/ℓ_r}, q''_{w/w_r}, q''_{w/v_r}, $q''_{v/\ell}$
- HAS A TRANSIENT ROD MODEL COUPLED TO FLUID MODEL

Figure 12 Comparison of Steam Quality Predicted by Dispersed Flow Model With FLECHT Data

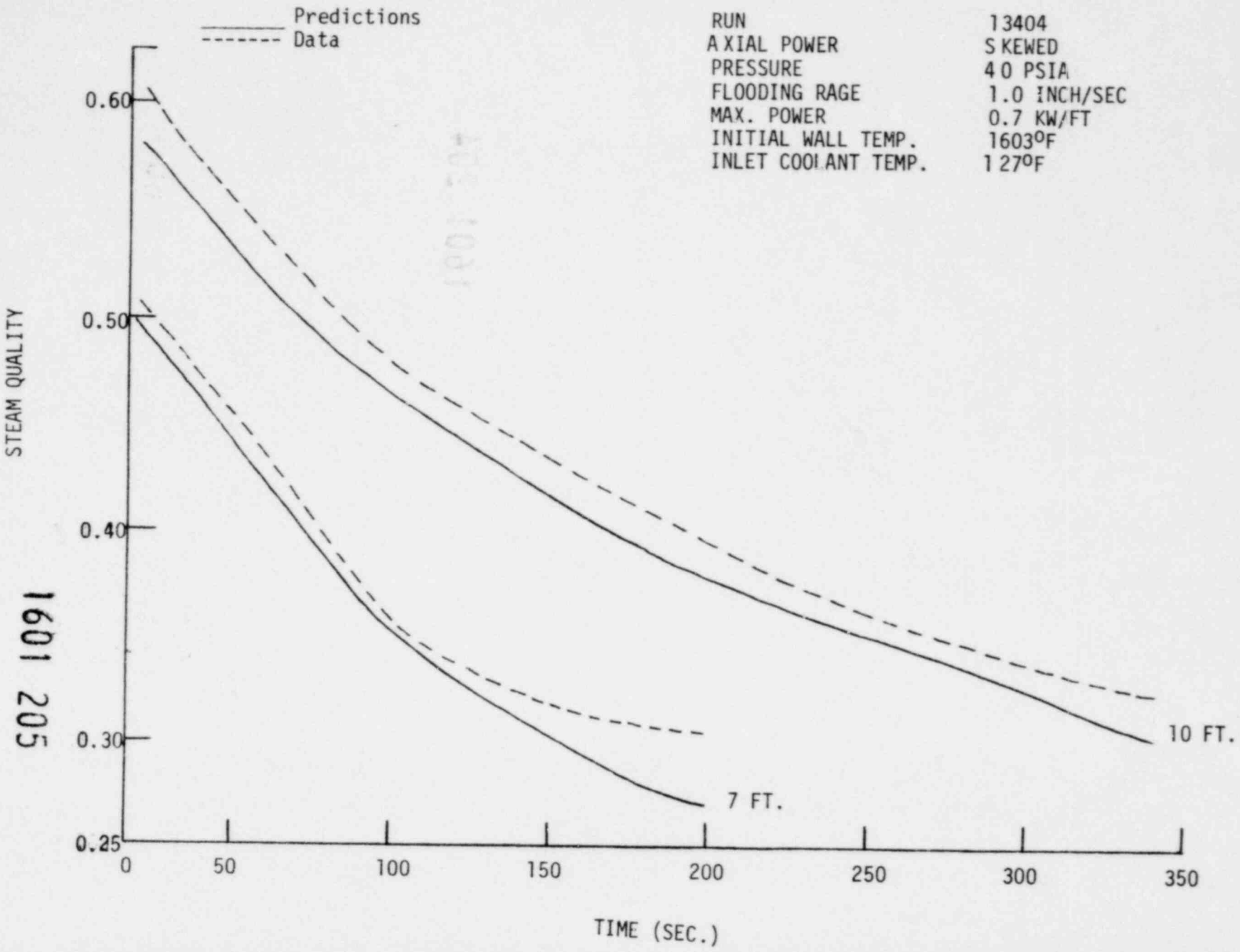

Figure 13 Comparisons of Steam Temperature Predicted By Dispersed Flow Model With Data

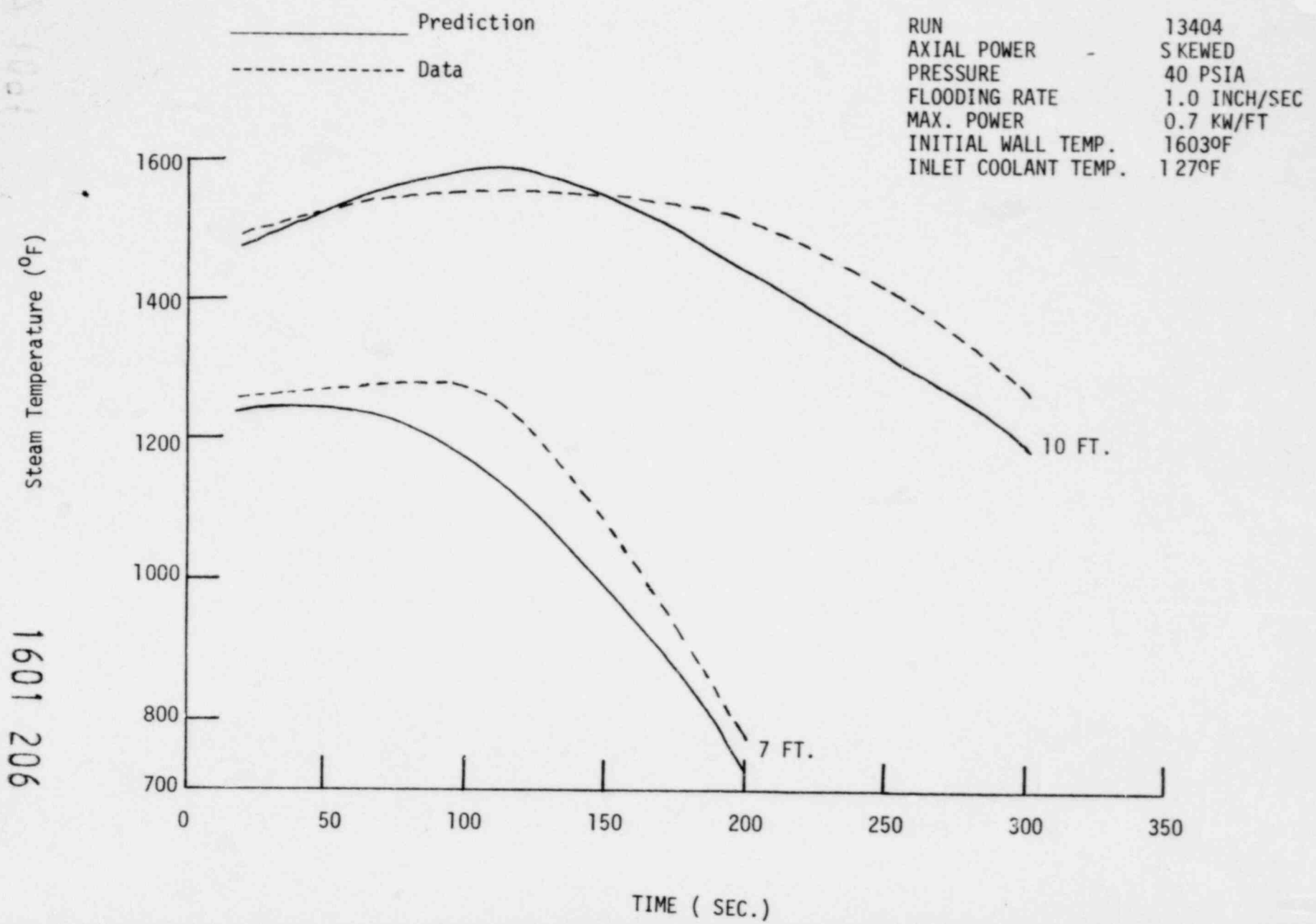

Figure 14 Comparison of Wall Temperature Predictions By Dispersed Flow Model With FLECHT Data

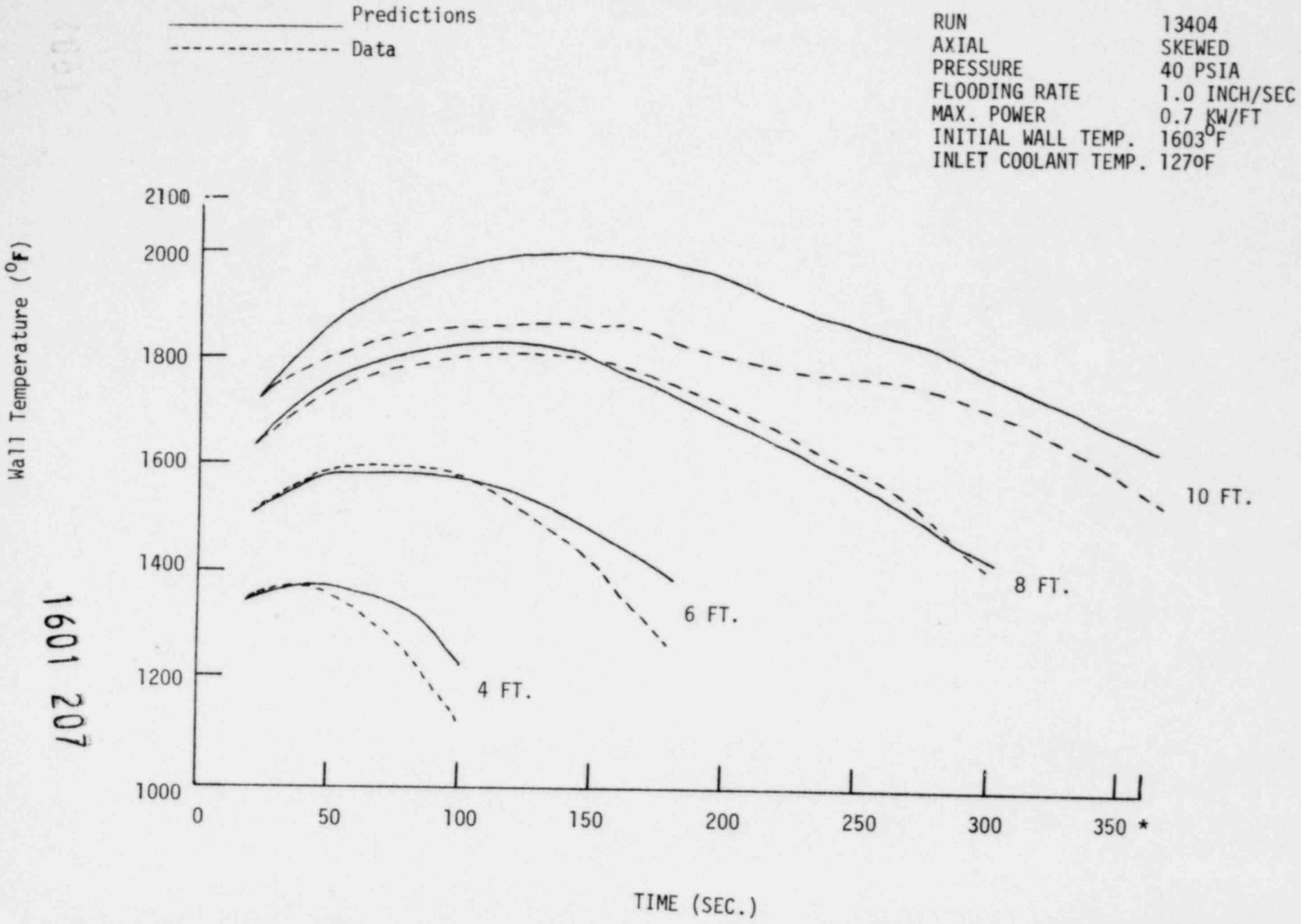

Figure 15 Comparison of Wall Temperature Predictions By Dispersed Flow Model With FLECHT Data

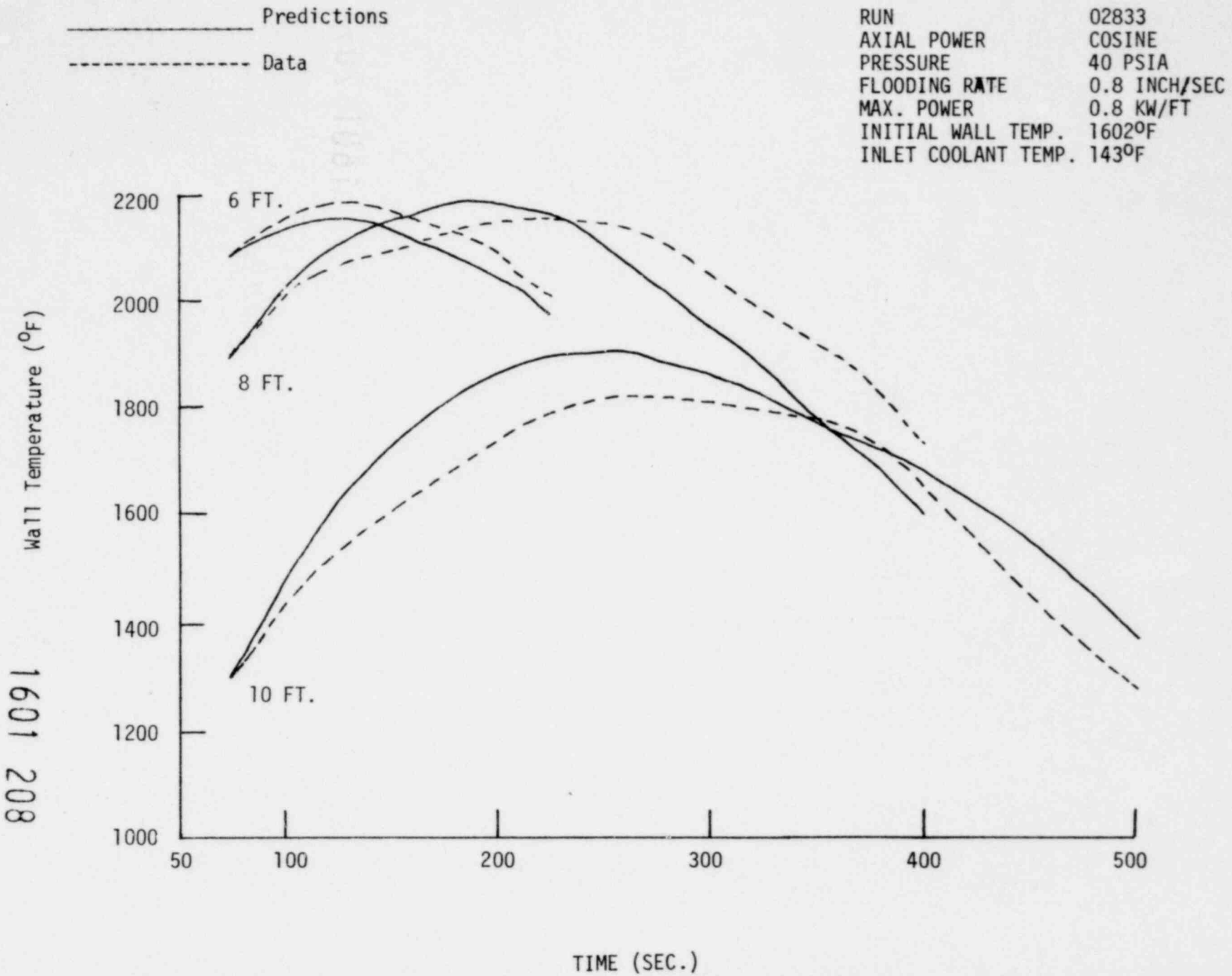

FIGURE 16

STATUS OF 21 ROD BUNDLE TASK

- TASK PLAN ISSUED
- DESIGN COMPLETE CONSTRUCTION STARTED
- TESTING BEGINS FIRST QUARTER 1980
- SINGLE ROD TESTS WITH BLOCKAGE SLEEVE T/C's SHOW EARLY QUENCH

STATUS OF 161 ROD BLOCKED TASK

- DRAFT TASK PLAN TO BE ISSUED
- DESIGN AND PROCUREMENT INITIATED
- TESTING BEGINS FIRST QUARTER 1982

FIGURE 17

STEAM GENERATOR SEPARATE EFFECTS TASKS STATUS

- AIR/WATER INLET PLENUM TESTS ARE COMPLETE
- TWO-PHASE STEAM GENERATOR TESTS ARE COMPLETE
- DRAFT DATA REPORT ISSUED
- A MULTI-TUBE TRANSIENT HEAT TRANSFER MODEL TO PREDICT THE STEAM GENERATOR RESPONSE IS BEING DEVELOPED

FIGURE 18

STEAM GENERATOR SEPARATE EFFECTS TEST
STEAM PROBE TUBE WALL & SECONDARY FLUID TEMP. VS TIME

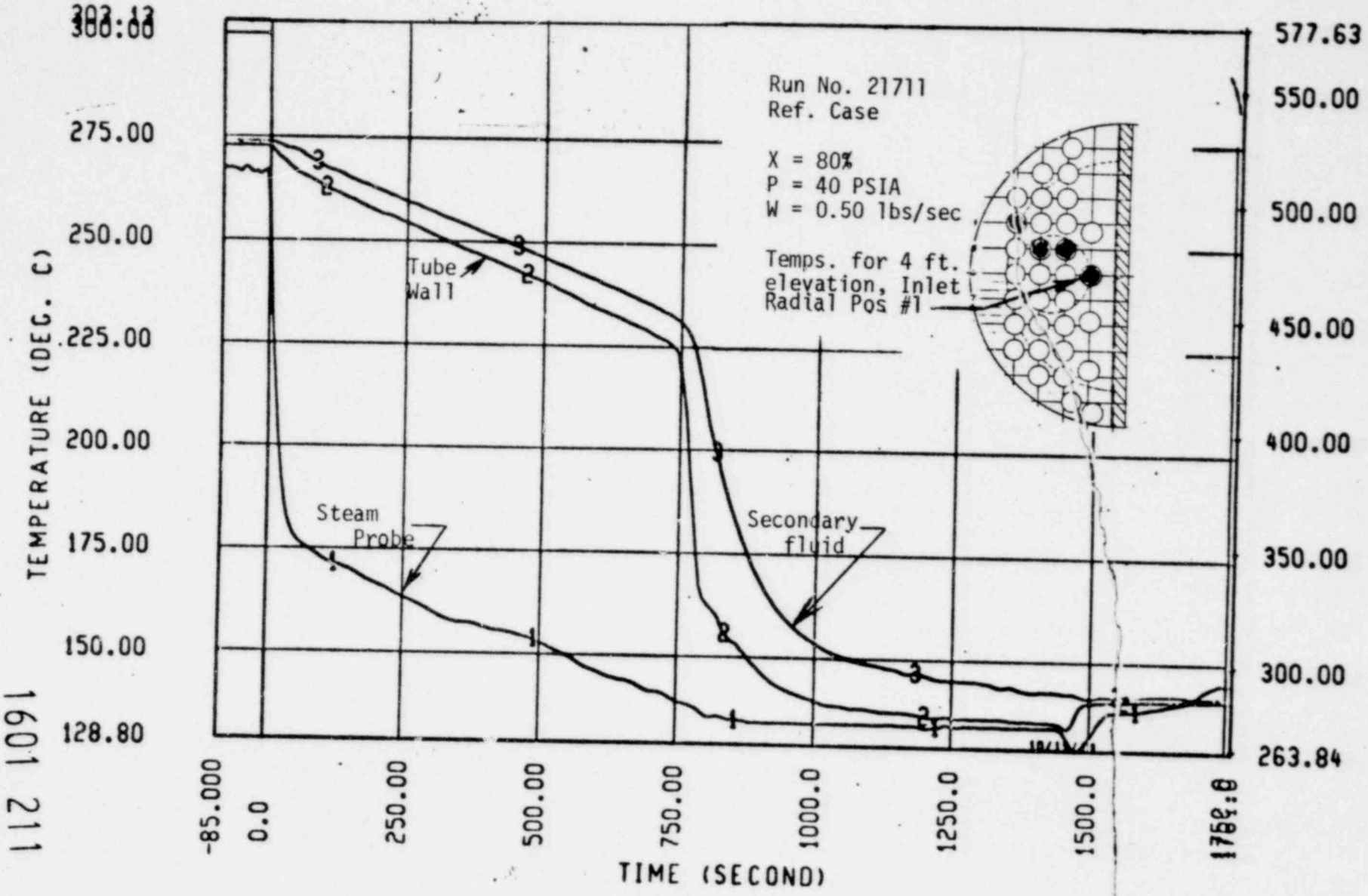

1601 211

POOR ORIGINAL

FIGURE 19

STEAM GENERATOR SEPARATE EFFECTS TEST

STEAM PROBE TUBE WALL & SECONDARY FLUID TEMP. vs TIME

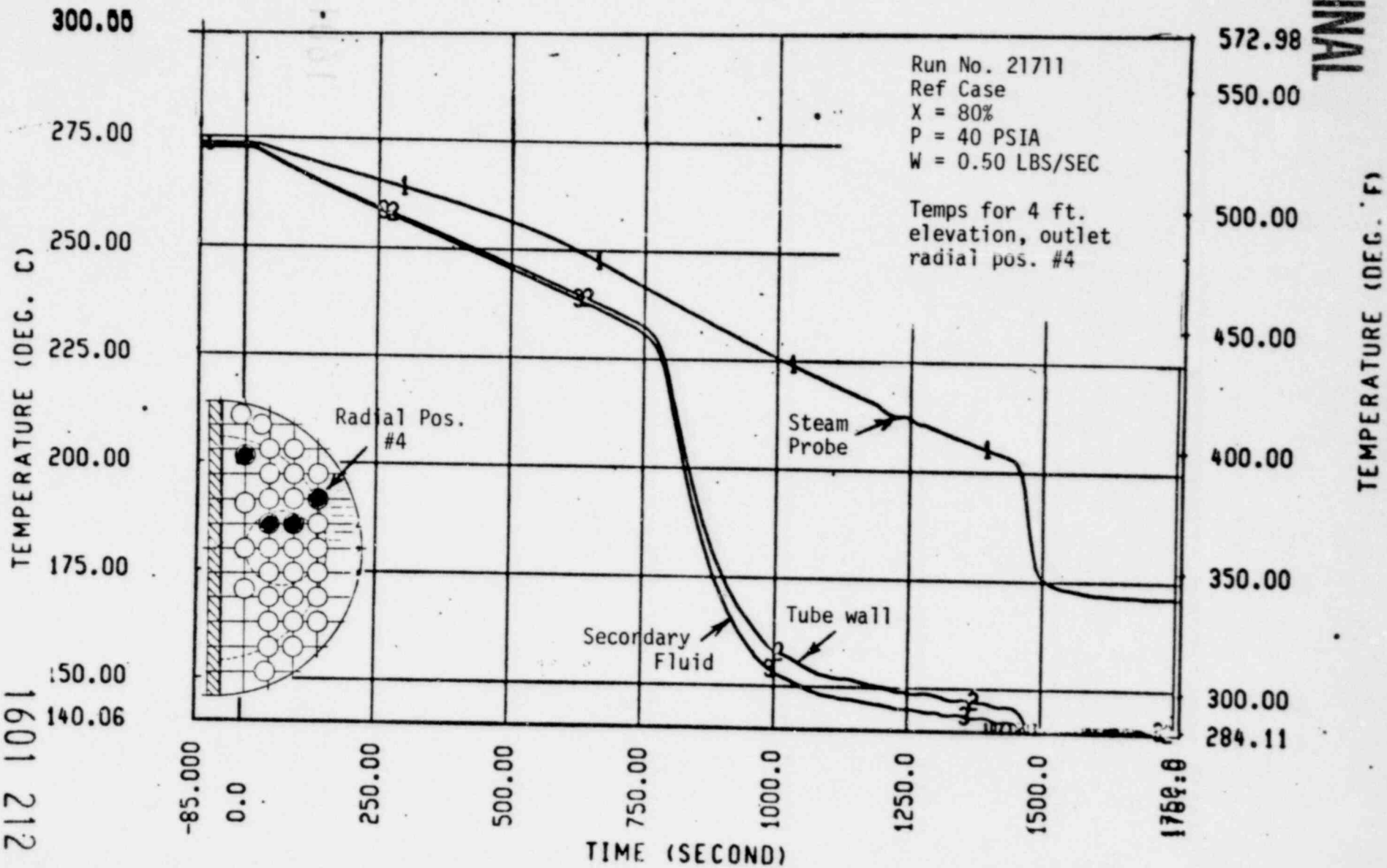

FIGURE 20

STEAM GENERATOR SEPARATE EFFECTS
TASK SUMMARY RESULTS

- NEARLY TOTAL LIQUID EVAPORATION
  (OUTLET PLENUM QUALITY 99%)

- THE VAPOR TEMPERATURE INCREASES IN THE UPFLOW REGION AND COOLDOWNS SIGNIFICANTLY IN THE DOWNFLOW REGION OF THE TUBE BUNDLE AFTER AN AXIAL TEMPERATURE GRADIENT IS ESTABLISHED IN THE SECONDARY FLUID

- ALMOST NO RADIAL VARIATION IN SECONDARY FLUID TEMPERATURE

- A NON-EQUILIBIUM MIXTURE OF DISPERSED DROPS AND SUPER HEATED STEAM EXISTS OVER ALMOST THE ENTIRE TUBE LENGTH

FIGURE 21

STEAM GENERATOR SEPARATE EFFECTS TEST PREDICTIVE MODEL ASSUMPTIONS

- PREDICT DRYOUT ELEVATION USING CHF CORRELATION OF BIASI
- ASSUME ANY LIQUID AT THE CHF ELEVATION IS ENTRAINED IN STEAM
- ASSUME HEAT TRANSFER BASED ON TWO PHASE FORCED CONVECTION BELOW DRYOUT, SINGLE PHASE CONVECTION TO STEAM ABOVE DRYOUT WITH DROPLET EVAPORATION AND WALL TO DROPLET RADIATION AND TURBULENT FREE CONVECTION ON THE SECONDARY SIDE OF THE TUBE BUNDLE
- ASSUME SECONDARY FLUID MIXES COMPLETELY IN THE RADIAL DIRECTION BUT NO MIXING AXIALLY

FIGURE 22

POOR ORIGINAL

STEAM GENERATOR
SEPARATE EFFECTS TEST
QUENCH ELEVATION VS.
QUENCH TIME

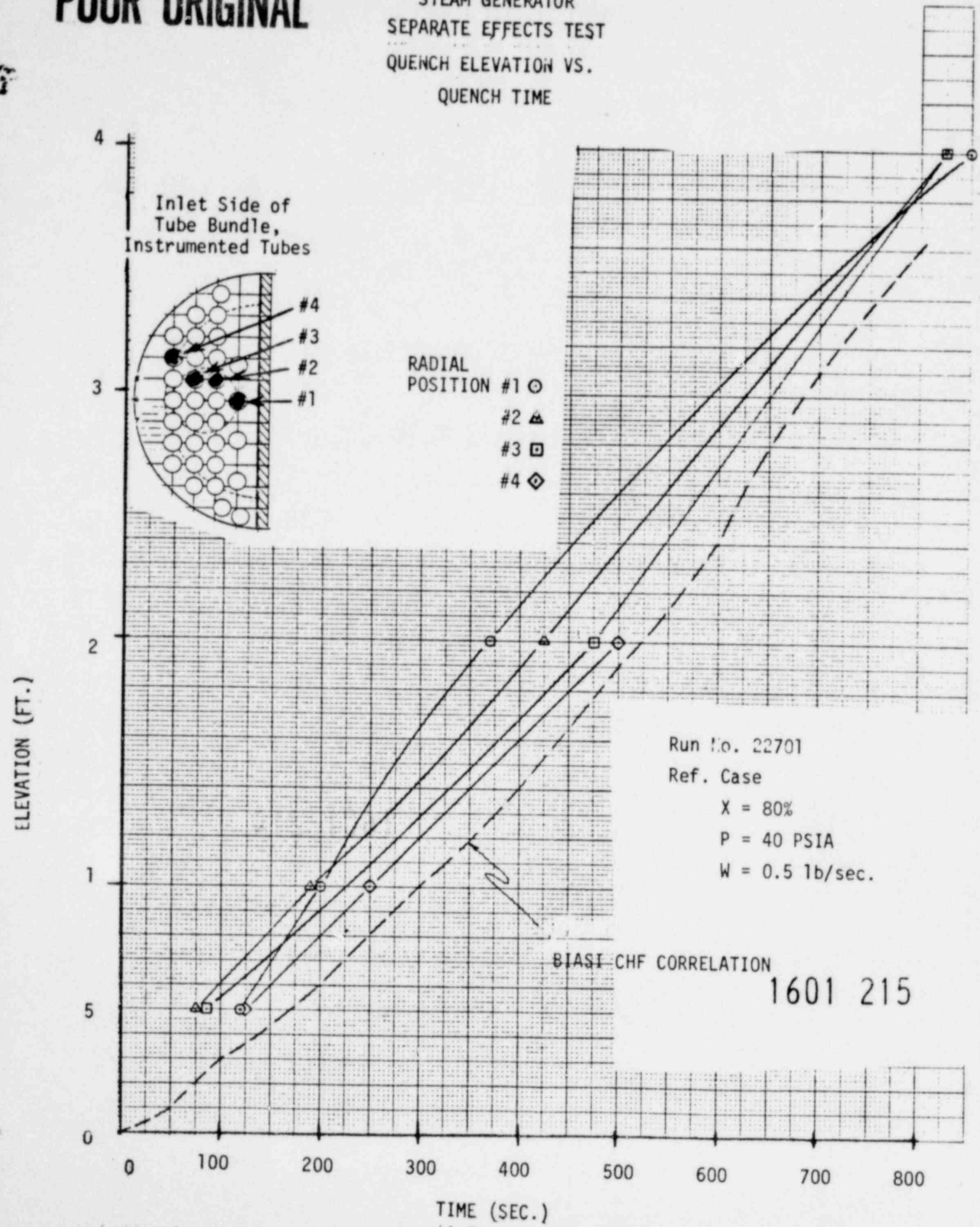

1601 215

FIGURE 23

STATUS OF SYSTEMS EFFECTS REFLOOD TASK

- DRAFT TASK PLAN ISSUED
- DESIGN REVIEW WAS HELD
- PROGRAM REDIRECTION IS BEING CONSIDERED TO:
  - PERFORM SYSTEMS EFFECTS TESTS
  - PERFORM LONG TERM COOLING AND TMI RELATED TESTS INCLUDING
    - NATURAL CIRCULATION
    - 2Ø NATURAL CIRCULATION
    - POSSIBLE REFLUX COOLING MODE

FIGURE 24

CLOSING REMARKS

- FLECHT-SEASET WILL EXTEND REFLOOD DATA BASE TO NEW PWR GEOMETRIES.

- FLOW BLOCKAGE/STEAM COOLING APPENDIX K RULE WILL BE ASSESSED.. WIDE RANGE OF INPUT HAS BEEN FACTORED INTO THESE TESTS.

- IMPROVED INSTRUMENTATION AND DATA ANALYSIS WILL ASSIST MECHANISTIC REFLOOD CODE MODEL DEVELOPMENT AND ASSESSMENT OF ADVANCED REFLOOD CODES.

- REFLOOD SYSTEM EFFECTS TESTS ARE PLANNED USING A BUILDING BLOCK APPROACH SUCH THAT COMPONENT BEHAVIOR IS UNDERSTOOD AND REFLOOD SYSTEM RESPONSE MAY BE ANALYZED.

- PROGRAM IS RESPONSIVE TO POST TMI NEEDS.

MULTI-FACILITY TEST PROGRAM FOR PWR LOCA HEAT TRANSFER

FLECHT-SEASET PROGRAM

EXECUTIVE SUMMARY • NOVEMBER 1979

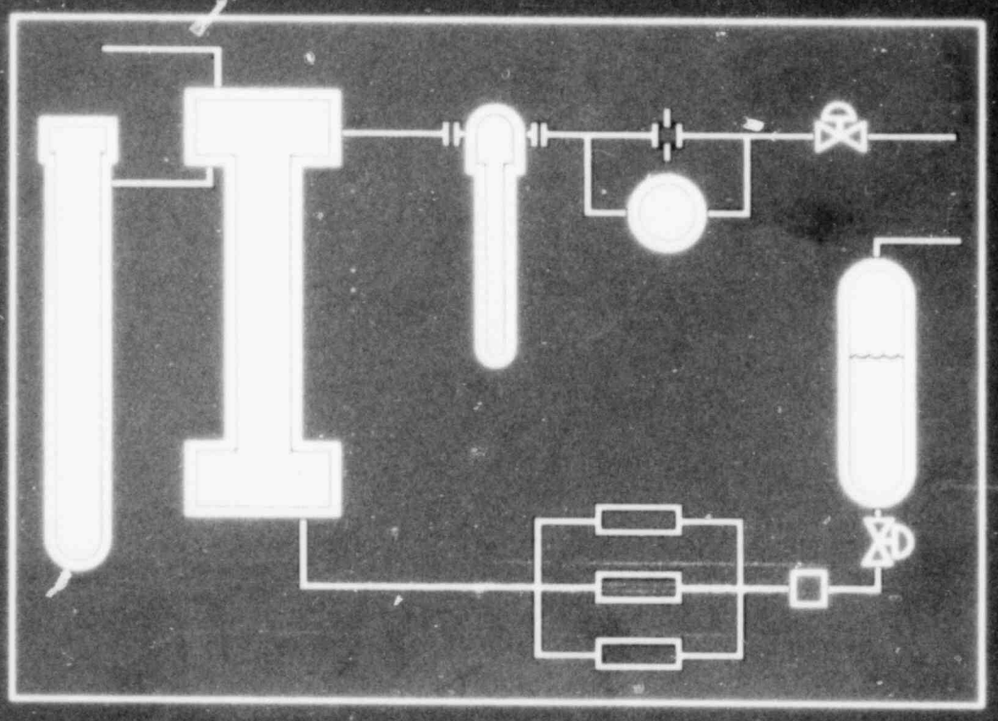

Program jointly sponsored by
USNRC, EPRI, and Westinghouse
under contract number NRC-04-77-127

EPRI

FLECHT-SEASET PROGRAM

This Executive Summary reports on the technical progress of the Full Length Emergency Core Heat Transfer-System Effects and Separate Effects Test (FLECHT-SEASET) Program, a multi-facility five year test program for generating PWR LOCA heat transfer data and correlations. The FLECHT-SEASET program is jointly managed and funded by the U.S. Nuclear Regulatory Commission (NRC), Electric Power Research Institute (EPRI), and Westinghouse Electric Corporation and is conducted by the Westinghouse Nuclear Technology Division. Recently, the program has been responsive to post TMI needs by performance of bundle boil-off tests and bundle steam cooling tests.

PROGRAM DESCRIPTION

The overall purpose of the FLECHT-SEASET program is to provide experimental reflood heat transfer and two-phase flow data in simulated PWR geometries for postulated LOCA conditions. The test parameters will cover a spectrum of conditions that encompass both best estimate and current licensing calculations. The test bundle simulates a full-length portion of PWR cores with fuel rod geometry typified by a Westinghouse 17x17 fuel assembly design (0.374 inch rod diameter and 0.496 inch fuel rod pitch).

The FLECHT-SEASET program consists of two major subprograms each with experimentation and analysis efforts: A Flow Blockage Program (Figure 1A) to address safety and licensing requirements for steam cooling/flow blockage effects specified in the Appendix K (10CFR50) rule and a System Effects Program (Figure 1B) to examine system and bundle reflood response for a postulated LOCA. Both programs have flexibility to address TMI-related phenomena as may be desired by the program sponsors. This work is closely coordinated as as appropriate with other international research programs in the reflood heat transfer area.

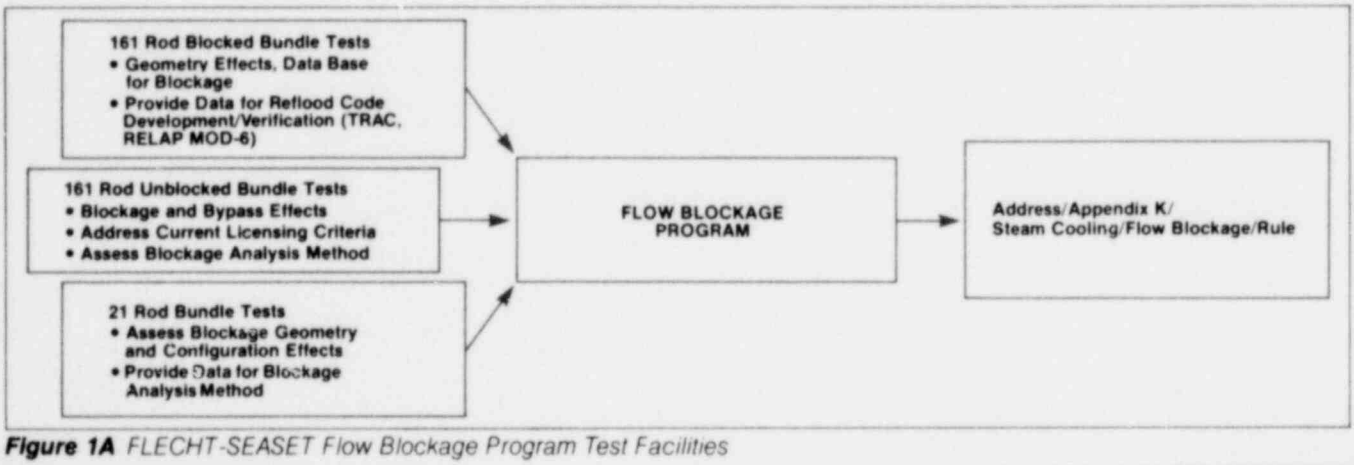

Figure 1A *FLECHT-SEASET Flow Blockage Program Test Facilities*

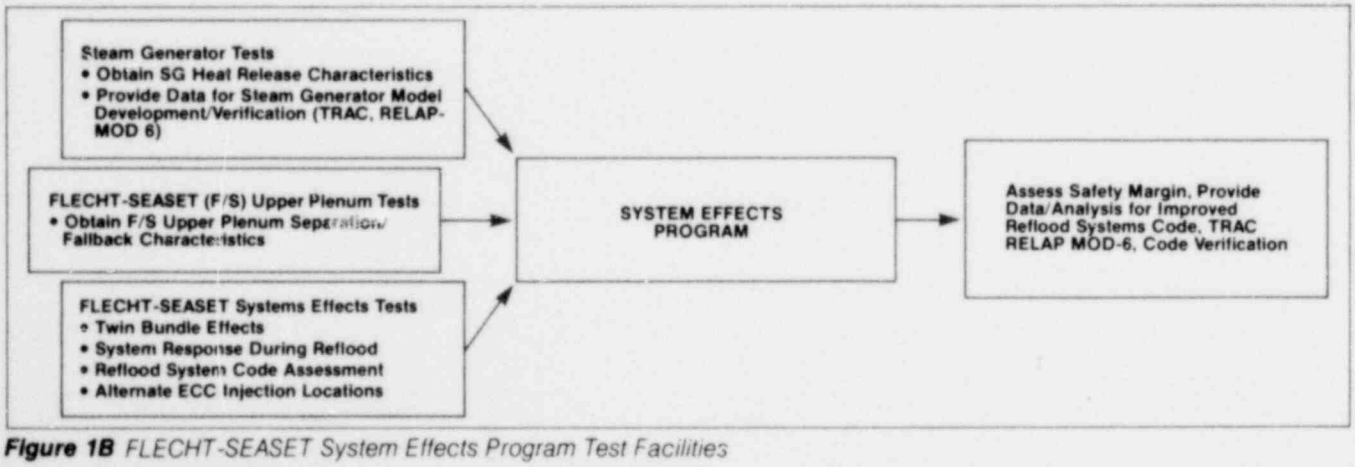

Figure 1B *FLECHT-SEASET System Effects Program Test Facilities*

FLOW BLOCKAGE PROGRAM

The Flow Blockage Program consists of the following major program Tasks, each with a separate test facility and data analysis and evaluation efforts:

- 161 Rod Unblocked Bundle
- 21 Rod Blocked Bundle
- 161 Rod Blocked Bundle

The prime objective of the Flow Blockage Program is to assess the effects of flow blockage through the full range of cladding temperatures, flooding rates, and system pressures typical of calculated PWR reflood conditions, as required by Appendix K ECCS regulations and for model development. The reflood heat transfer effects of flow blockage caused by ballooned fuel rods, will be determined primarily at flooding rates of one inch per second (2.54 cm/sec) or less through comparison of the 161 Rod Unblocked Bundle Test Series and the 161 Rod Blocked Bundle Test Series. The 21 Rod Blocked Bundle Test Series serves as a flexible test vehicle for examining many blockage shapes and configurations and hence guides the model development efforts in the larger 161 Rod Blocked Bundle Test Series. The 161 Unblocked Bundle Test Series serves as the reference test series and hence has no flow blockage simulation. The 161 Rod Unblocked Bundle tests were completed in September, 1979.

Figure 2 presents the heater rod bundle assembly for the 161 Rod Unblocked Bundle Test Series prior to installation into the test facility. The heater rods are 0.374 inch in diameter with a kanthal coil heater element, BN insulation, and stainless steel sheath. The heater rods are designed for high temperature operation as calculated in ECCS safety analyses.

An example of 161 Rod Unblocked Bundle test data is presented in Figure 3. Also, as part of the Unblocked Bundle Test Series, several TMI-related tests relevant to very low core flows were performed including steam cooling tests with Reynolds numbers of 2,000 to 15,000 and three bundles boil-off tests were performed. A special report on these tests will be completed at the end of 1979 for publication in the first quarter of 1980.

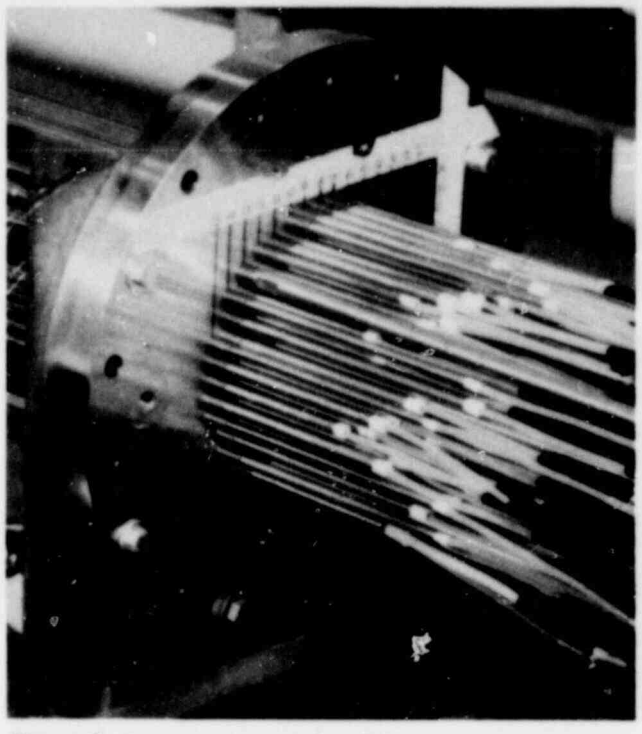

Figure 2 *(Portion of) Heater Rod Bundle for the Unblocked Bundle Test Facility*

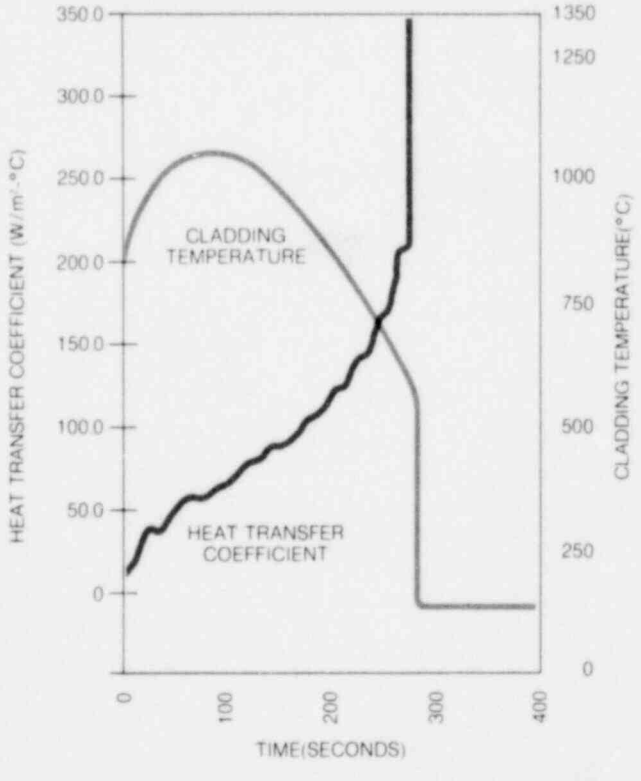

Figure 3 *FLECHT-SEASET Unblocked Bundle Data from Matrix Run No. 4 (0.276 MPa, 25.4 MM/s, 2.3 Kw/M and 871 °C Test Initial Conditions)*

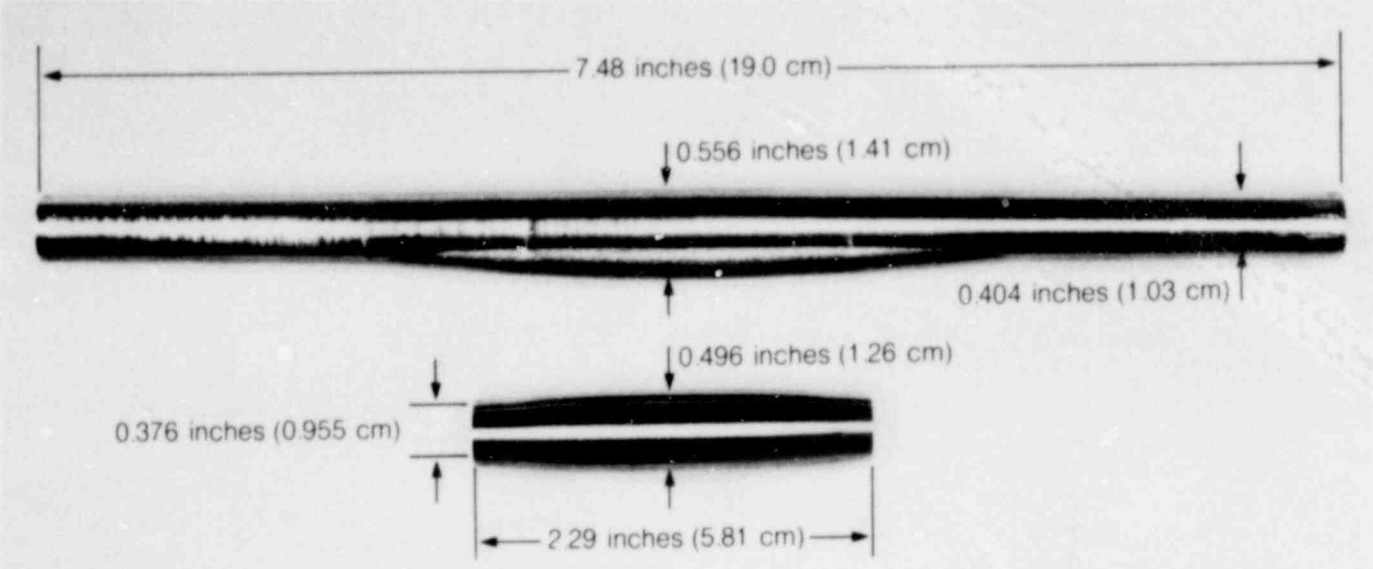

Figure 4 *FLECHT-SEASET Flow Blockage Sleeves for Simulated Flow Blockage in the 21 Rod Blocked Bundle Facility*

The 21 Rod Blocked Bundle test facility will be used to test and examine various blockage shapes and configurations (coplanar and non-coplanar) and to help develop a flow blockage heat transfer model. The flow blockage is simulated with manufactured blockage sleeves attached to individual heater rods. Figure 4 presents the two basic blockage sleeve shapes representing alpha and beta phase rod burst found in zircaloy tube burst tests. These two shapes can be modified by increasing or reducing the simulated blockage strain as represented by the sleeve diameters.

Seven (7) bundle test series will be performed on the 21 Rod Blocked Bundle to select an appropriate blockage sleeve for use in the 161 Rod Blocked Bundle Test Series. The remaining three (3) bundle test series will be performed with the selected blockage sleeve shape with higher and lower strains than depicted in Figure 4 and a "burst" lip configuration. The large 161 Rod Blocked Bundle tests will address flow blockage with flow bypass effects.

SYSTEM EFFECTS PROGRAM

The second major FLECHT-SEASET program is the System Effects Program and consists of the following major Tasks, each a separate test facility with data analysis and evaluation efforts:

- Steam Generator Separate Effects Task
- Upper Plenum Separate Effects Task
- System Effects Task

The System Effects Program focuses on the simulated thermal-hydraulic response of a bundle, upper plenum and steam generator tested both separately and in combination. In system effects tests, the bundle inlet flooding rate is dependent upon the hydraulic and heat transfer behavior of the bundle and system components. In order to understand the performance of the simulated primary system, the behavior of the components must first be better understood.

The thermal-hydraulic behavior of the bundle is examined in the 161 Rod Unblocked Bundle tests and previous FLECHT tests. The steam generator and upper plenum are examined in separate tests, each a separate test loop.

The Steam Generator Separate Effects testing was completed in April 1979 and data reports are being prepared. The key objective was to determine the heat release rate for various known inlet fluid conditions and secondary side fluid conditions and to develop a corresponding model. The test was performed with a full-length 33 tube steam generator which was instrumented with over a hundred thermocouples for the tube walls and secondary fluid, 6 pressure probes and 47 steam probe primary measurements. Figures 5 to 8 present a summary of the complex instrumentation utilized on the Steam Generator Separate Effects Test Facility.

A series of twenty tests were performed on the Steam Generator Separate Effects Test Facility to measure the tube bundle heat transfer under postulated large break LOCA conditions.

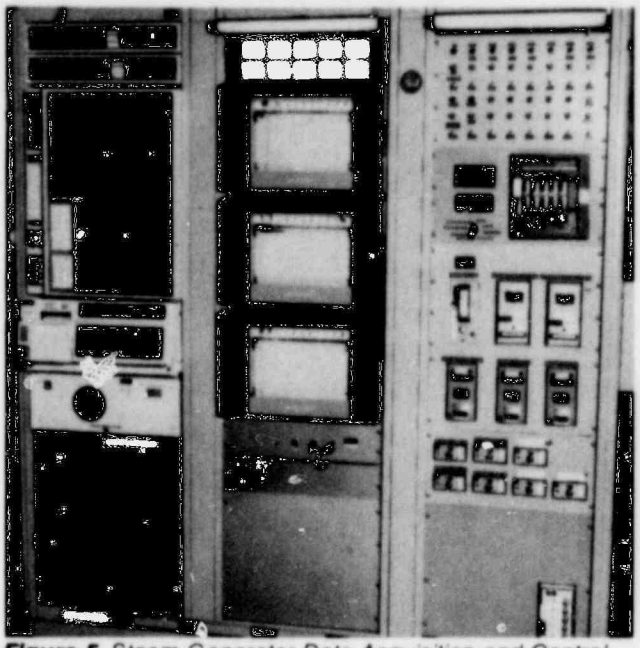

Figure 5 *Steam Generator Data Acquisition and Central Test Control Station*

Figure 6 *Steam Generator Tube Bundle Thermocouple Installation Detail*

Figure 7 *Steam Generator Flange and Bundle Instrumentation Ports*

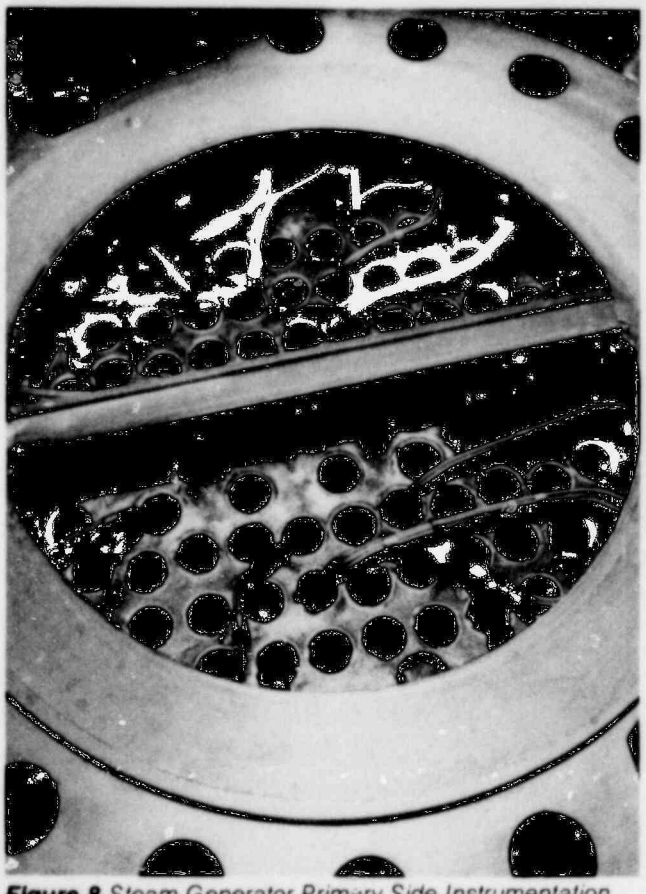

Figure 8 *Steam Generator Primary Side Instrumentation (Steam Brakes and Pressure Probes)*

The test results show that most of the liquid component of the two phase flow entering the tube bundle evaporates, but a small residual amount of liquid migrates through the tube bundle without evaporating.

The primary liquid is in the form of small drops entrained in steam. The steam phase may be superheated by over 200°F (110°C). On the inlet side of the tube bundle, the tube wall is quenched by the primary side liquid. This quench front migrates slowly up the tube. Figures 9A and 9B illustrate the measured secondary fluid, tube wall and steam probe temperatures on the inlet and outlet side of the tube bundle at the 4 ft. elevation above the tube sheet.

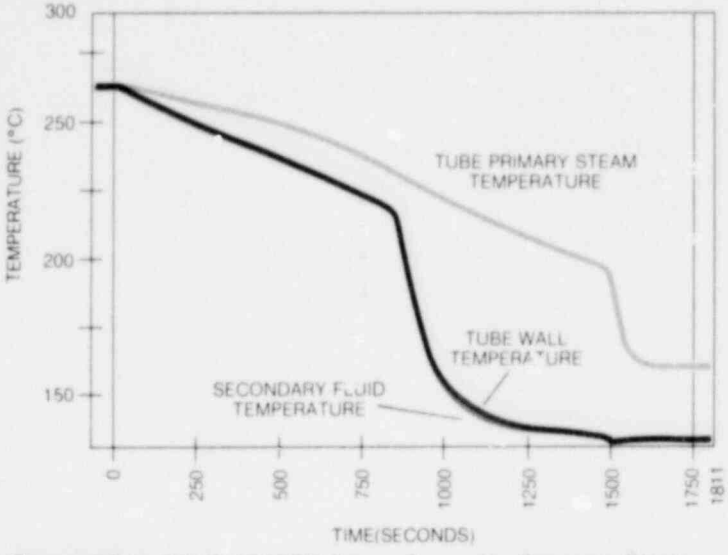

Figure 9A *FLECHT-SEASET Steam Generator Separate Effects Test Data at 4 feet tube elevation near inlet of steam generator (Test Matrix Run No. 1)*

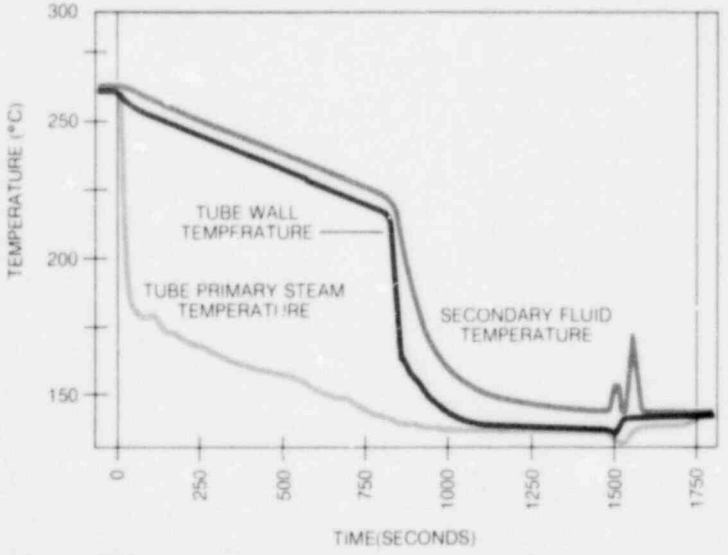

Figure 9B *FLECHT-SEASET Steam Generator Separate Effects Test Data at 4 feet tube elevation near outlet of steam generator (Test Matrix Run No. 1)*

A similar test facility, to characterize the upper plenum simulation, is currently under evaluation. The System Effects Test Facility is in the conceptual design stage with substantial effort expected in 1980.

ORGANIZATION

The FLECHT-SEASET program is a three party cooperative research and development effort funded by NRC, EPRI, and Westinghouse. Program technical direction and guidance is provided by the Program Management Group (PMG), presently consisting of Dr. Loren B. Thompson (NRC), Dr. K. H. Sun (EPRI), and Mr. Lee Chajson (Westinghouse).

The FLECHT-SEASET program is implemented by the contractor, Westinghouse Electric Corporation, under the following structure:

Program Management: L. Chajson, Manager of Strategic Projects; H. W. Massie, Jr., FLECHT-SEASET Project Engineer, Strategic Projects

Test Planning and Analysis: Dr. L. E. Hochreiter, FLECHT-SEASET Principal Investigator
R. P. Vijuk, Manager of Safeguards Development

Facility Preparation and Testing: L. R. Katz, Manager of Facilities Engineering; C. E. Fuchs, Manager of Test Operations

The above structure is supported by a team of experienced engineers and technicians to design, build, and operate the test facilities, and to perform data analysis and evaluation activities. Each test facility or Task has a lead technical engineer for test planning and analysis activities and a lead design engineer to direct the design, hardware fabrication and testing effort.

1979/1980 PLANNED WORK EFFORT

Over the next 14 months the following work is planned under the FLECHT-SEASET program as reflected in the schedule.

- Complete and publish Unblocked Bundle technical reports
- Complete and publish Steam Generator Separate Effects technical reports
- Complete construction of 21 Rod Bundle Test Facility and perform several bundle test series
- Complete design of 161 Rod Blocked Bundle facility and initiate construction
- Finalize design of the System Effects Test Facility

FLECHT-SEASET PROGRAM MANAGEMENT SUMMARY SCHEDULE

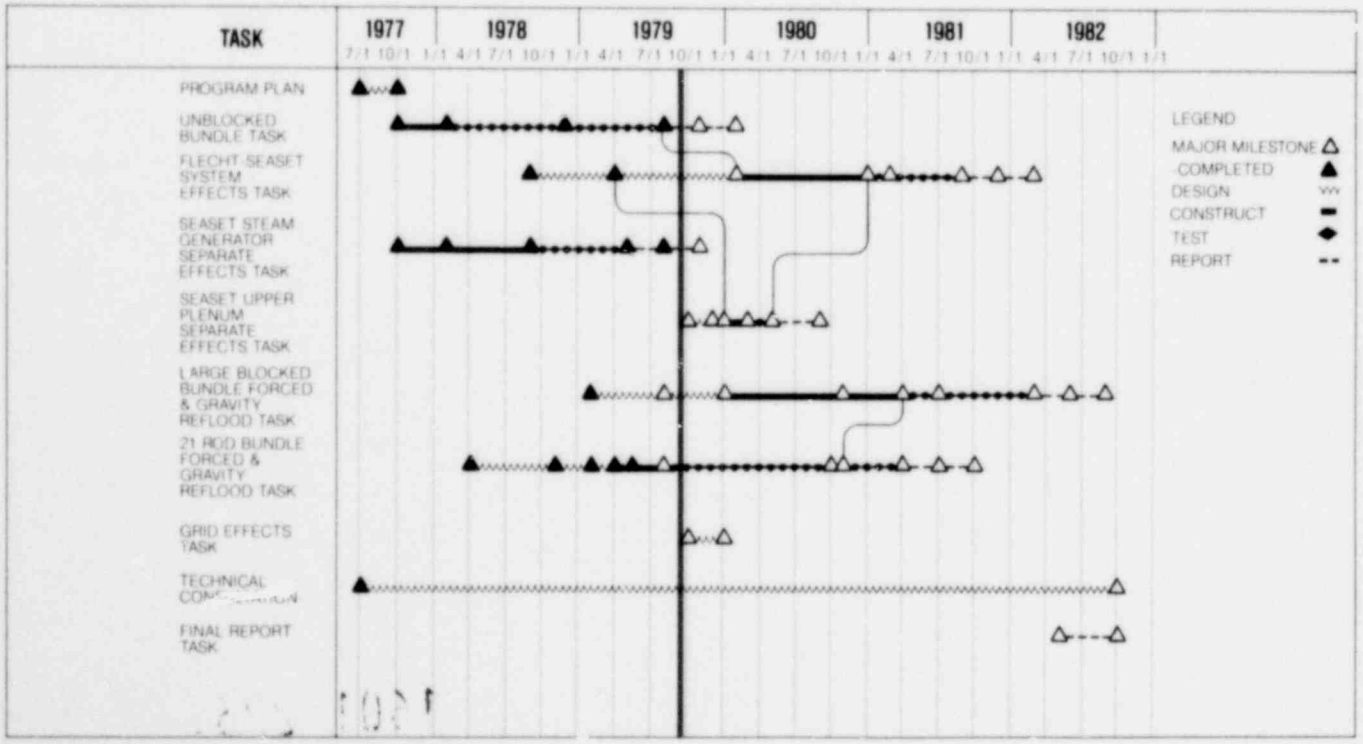

1601 225

Westinghouse Electric Corporation, P.O. Box 355, Pittsburgh PA 15230 November, 1979

Gravity Reflood Oscillations in a PWR*

Peter Griffith
Yin L. Cheung

Massachusetts Institute of Technology

Presented at 7th Water Reactor Safety Research Information Meeting, November 6, 1979

*USNRC Report, to be published.

Gravity Reflood Oscillations in a PWR

Summary

Oscillations in core and downcomer coolant levels are possible during the reflood process. U-tube type oscillations have been observed in gravity-feed reflood experiments such as FLECHT-SET[1] and Semi-scale[2]. The frequencies of the observed oscillations correlate closely to the natural frequencies (about 0.3 Hz) of the systems under test.

This study proposes a mechanism by which the U-tube type oscillations can be driven. When emergency coolant rushes into the hot core, it overshoots the quench front, where rod heat flux is highest. When the coolant flow stagnates, subcooling is rapidly removed and violent boiling begins at some point beneath the free surface of the liquid.

If the rate of vapor generation is so high that the vapor cannot vent fast enough, the liquid trapped above the vapor pocket will be accelerated upwards. Simultaneously, the resulting pressure pulse pushes core coolant downwards. After the vapor has vented, the coolant rushes back up the core and the process repeats.

Based on this driving mechanism and a simple thermal-hydraulics model, a computer program, REDY[3], has been developed. Core and downcomer coolant dynamics is modeled as single-phase, one-dimensional flow with lumped fluid resistance, inertia, and capacitance. Rod heat transfer coefficients as a function of rod surface temperatures only are derived from a boiling curve. The vapor generation rate, calculated from a heat balance assuming thermodynamic equilibrium between liquid

and vapor phases, provides the disturbance input to the dynamic equations. It determines the system back pressure as well as when liquid expulsion occurs.

Calculations with REDY are performed on selected FLECHT-SET and Semiscale Mod-3 runs. In general, frequencies and amplitudes of the oscillations compare favorably with the experiments. The calculated vapor flow rates at the core exit also exhibit cyclical variations. When exit flow rates are low, liquid that is stored in the upper plenum should be able to drain back into the core, although the present model does not allow for this.

The core and downcomer heads cannot be predicted with accuracy because of two areas of uncertainty: the amount of liquid carry-over, and the pressure drop across the hot and cold legs.

All the liquid thrown up by the driving mechanism is assumed to reach the upper plenum and stay there. In reality, only a fraction of the liquid reaches the upper plenum. Furthermore, liquid in the upper plenum may drain into the core. Thus, the model tends to underestimate the liquid inventory, and therefore the gravity head, of the core.

In the scaled experiments, the loop piping provides large metal surface areas on which evaporation and condensation, not modeled here, can take place. This, together with uncertain two-phase flow conditions in the hot leg, make the calculation of the pressure drop across the loop inaccurate.

Despite its shortcomings, the model adequately demonstrates reflood oscillations while its simplicity reduces mathematical complexity to a minimum.

References

1. Blaisdell, J.A. et al, "PWR FLECHT-SET Phase A Report," WCAP-8238, Westinghouse Electric Corp., Dec. 1973.

2. Gillins, R.L. et al, "Experimental Data Reports for Semiscale Mod-3 Reflood Heat Transfer Test S-07-4," NUREG/CR-0254, TREE-1224, Aug. 1978.

3. Cheung, Y.L. and P. Griffith, "Gravity Reflood Oscillations in a PWR," USNRC Report, to be published.

4. Hsu, Y.Y., "A Tentative Correlation for the Regime of Transition Boiling and Film Boiling During Reflood," presented at 3rd WRSR Information Meeting, USNRC, October 1, 1975.

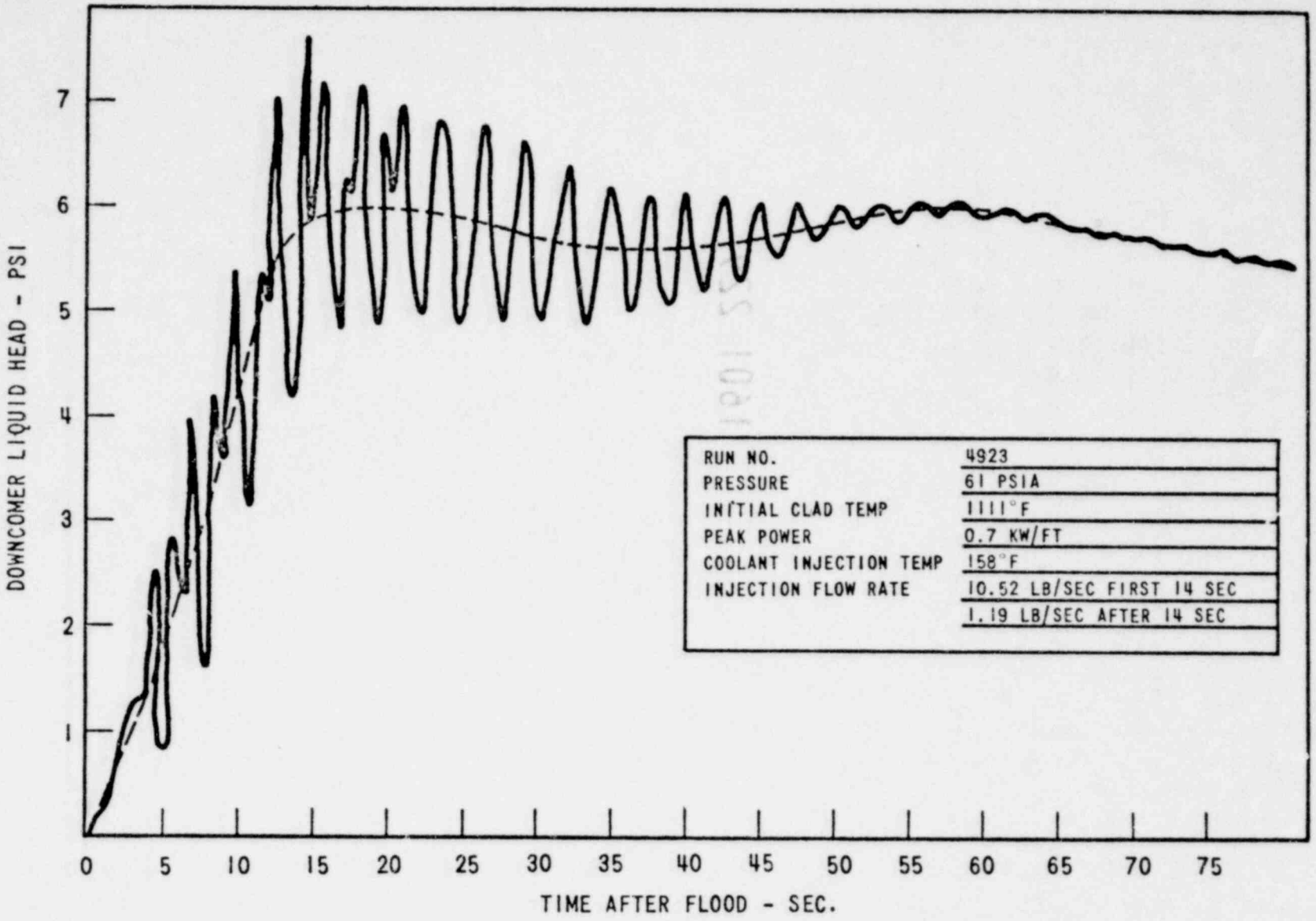

Figure 1. Oscillations in Downcomer Head during Reflood Test
(FLECHT-SET Run #4923, Ref. 1)

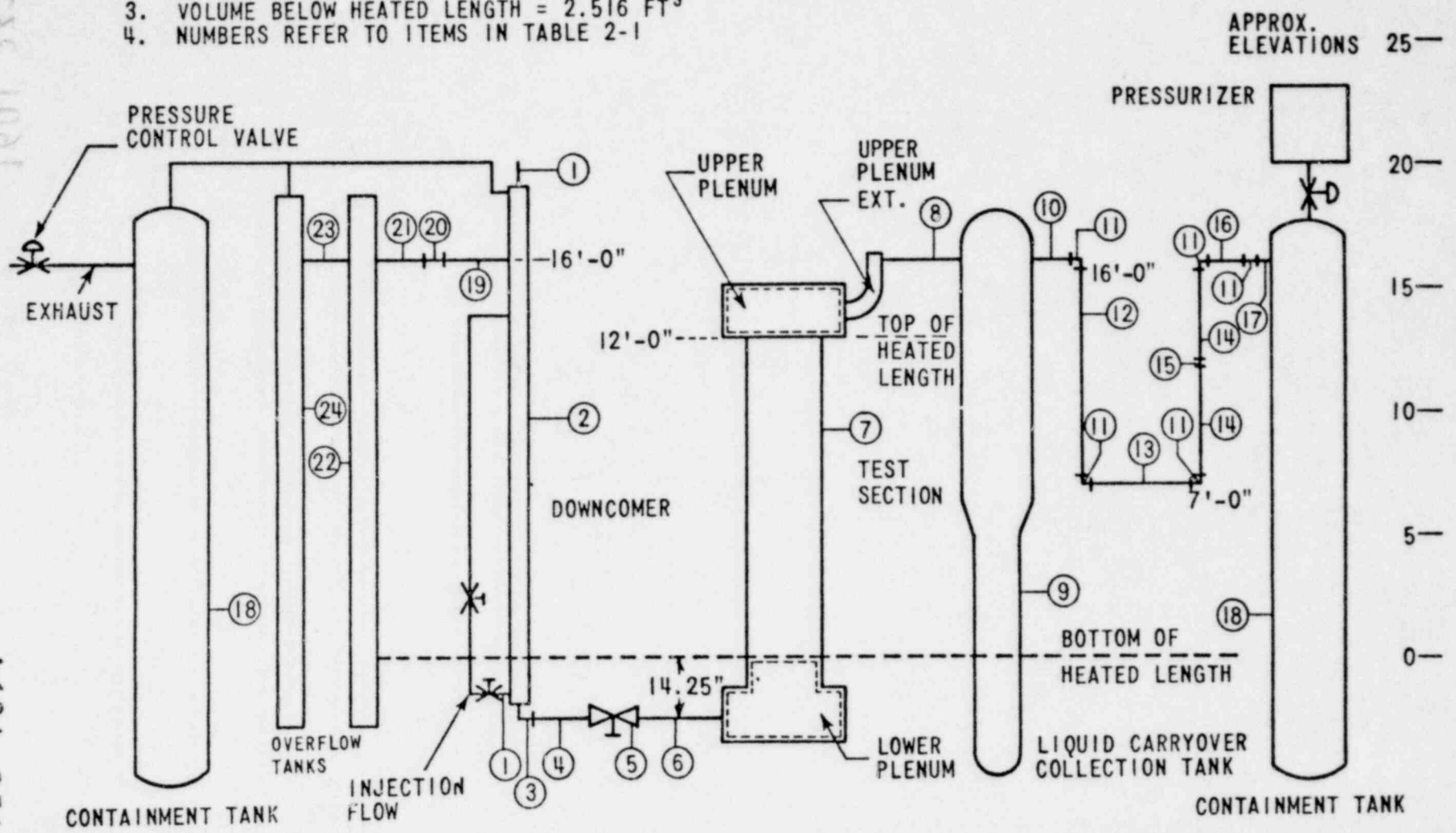

Figure 2. Schematic of FLECHT-SET Phase A Test Facility (Ref. 1)

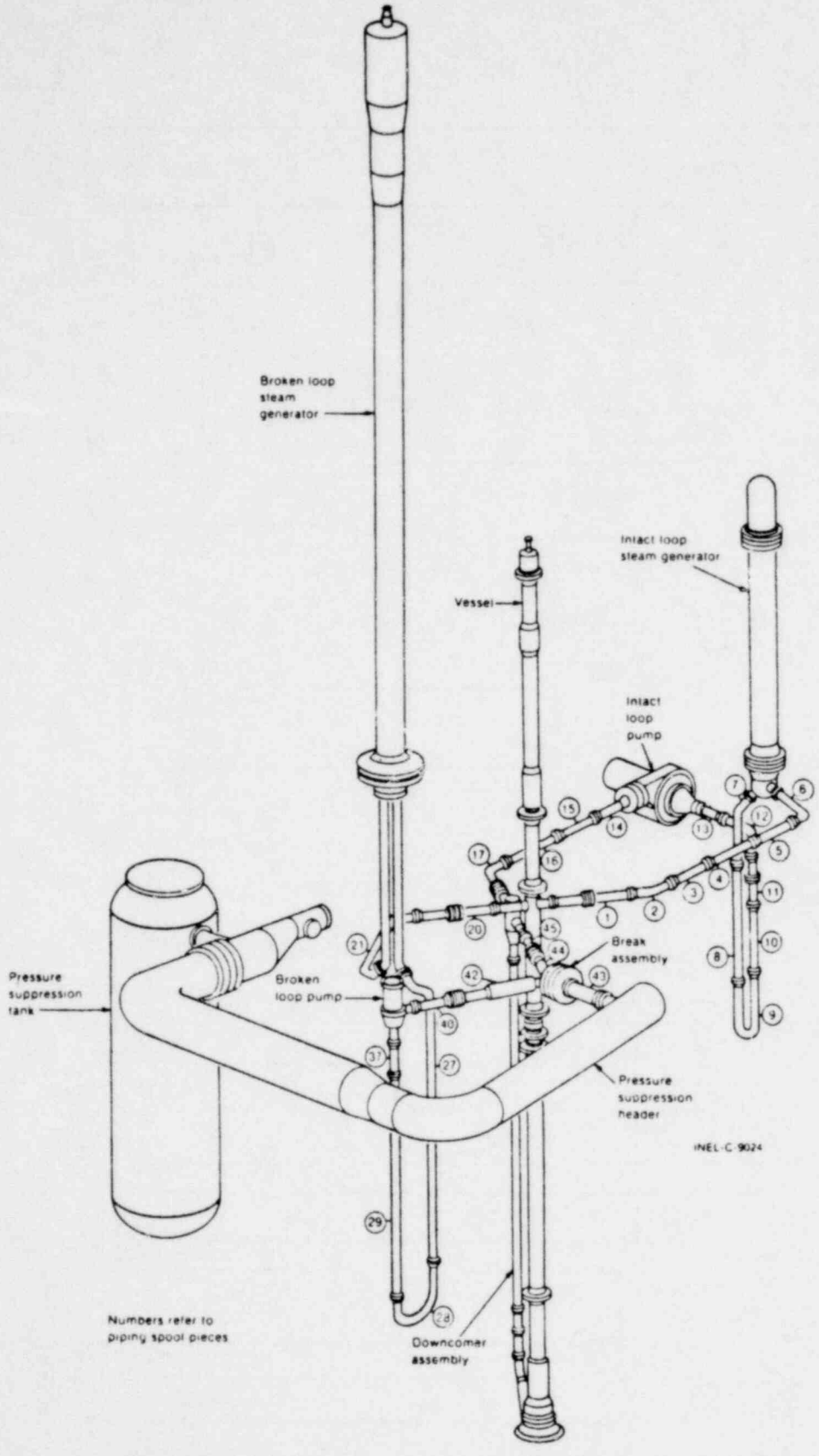

Fig. 3. Semiscale Mod-3 system for cold leg break configuration – isometric. (Ref. 2)

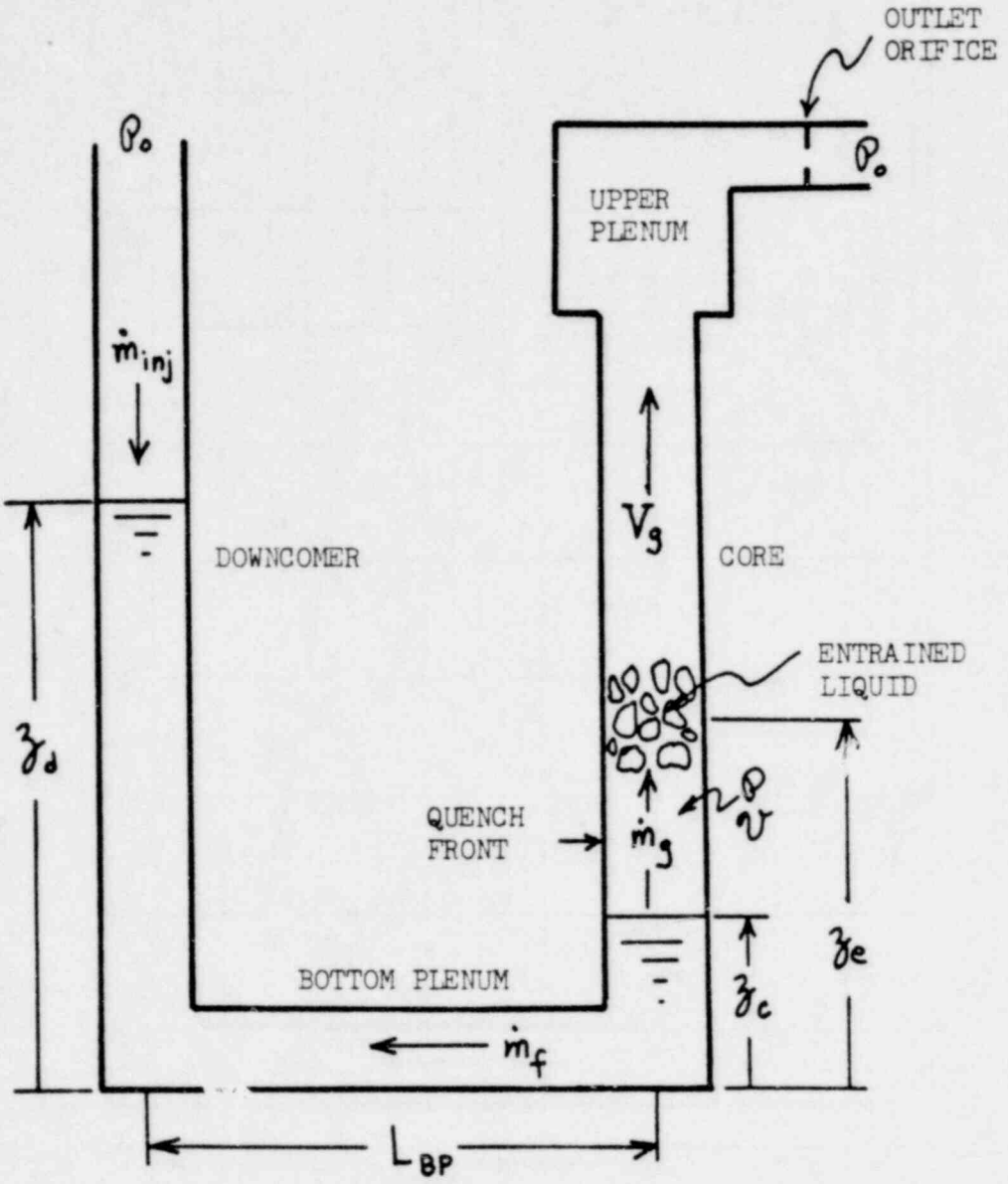

Fig. 4. Schematic of Gravity Reflood Model

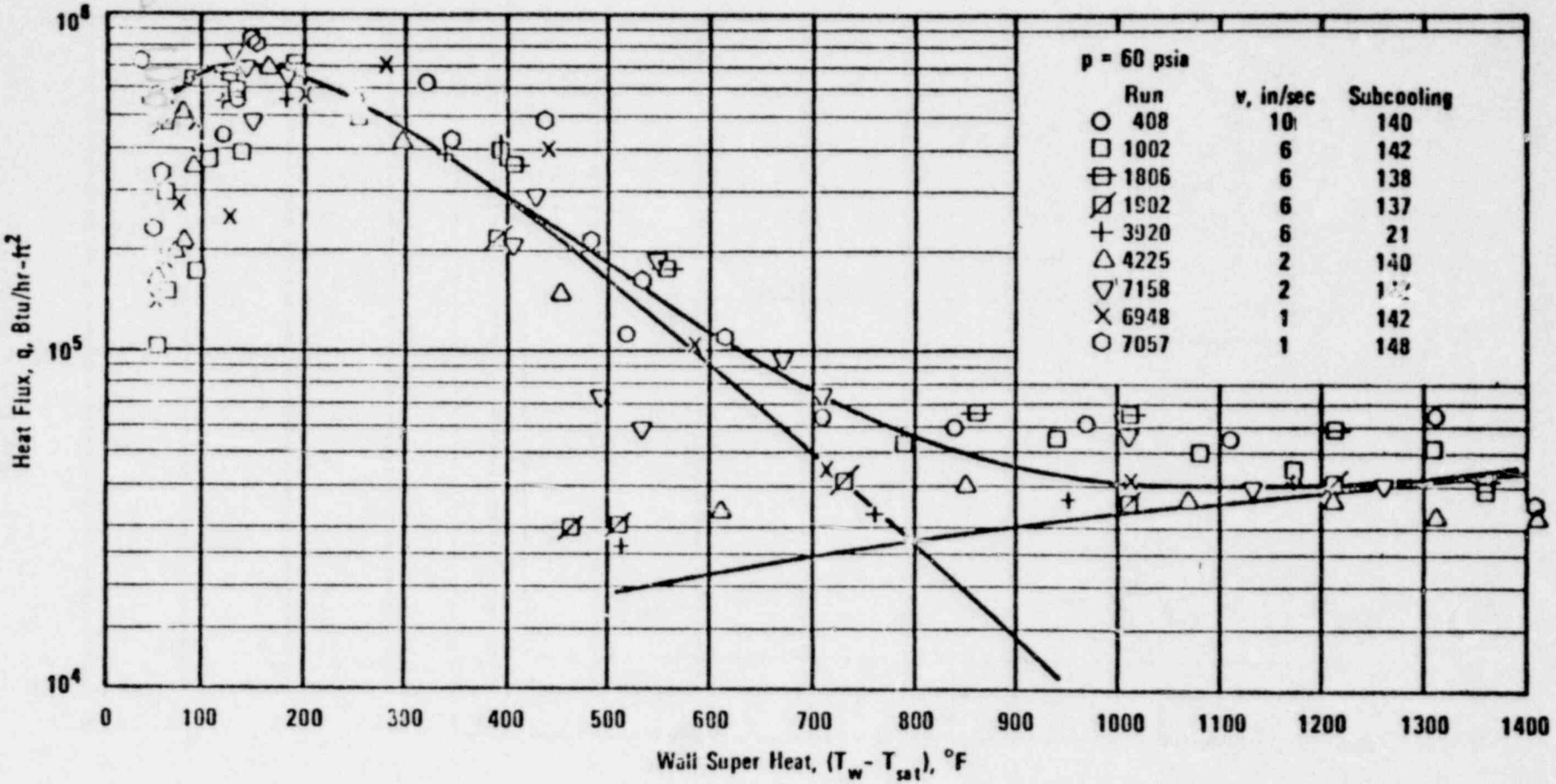

FIG. 5. HEAT FLUX AS FUNCTION OF SUPERHEAT FOR TRANSITION AND FILM BOILING AT 60 PSI (Ref. 4)

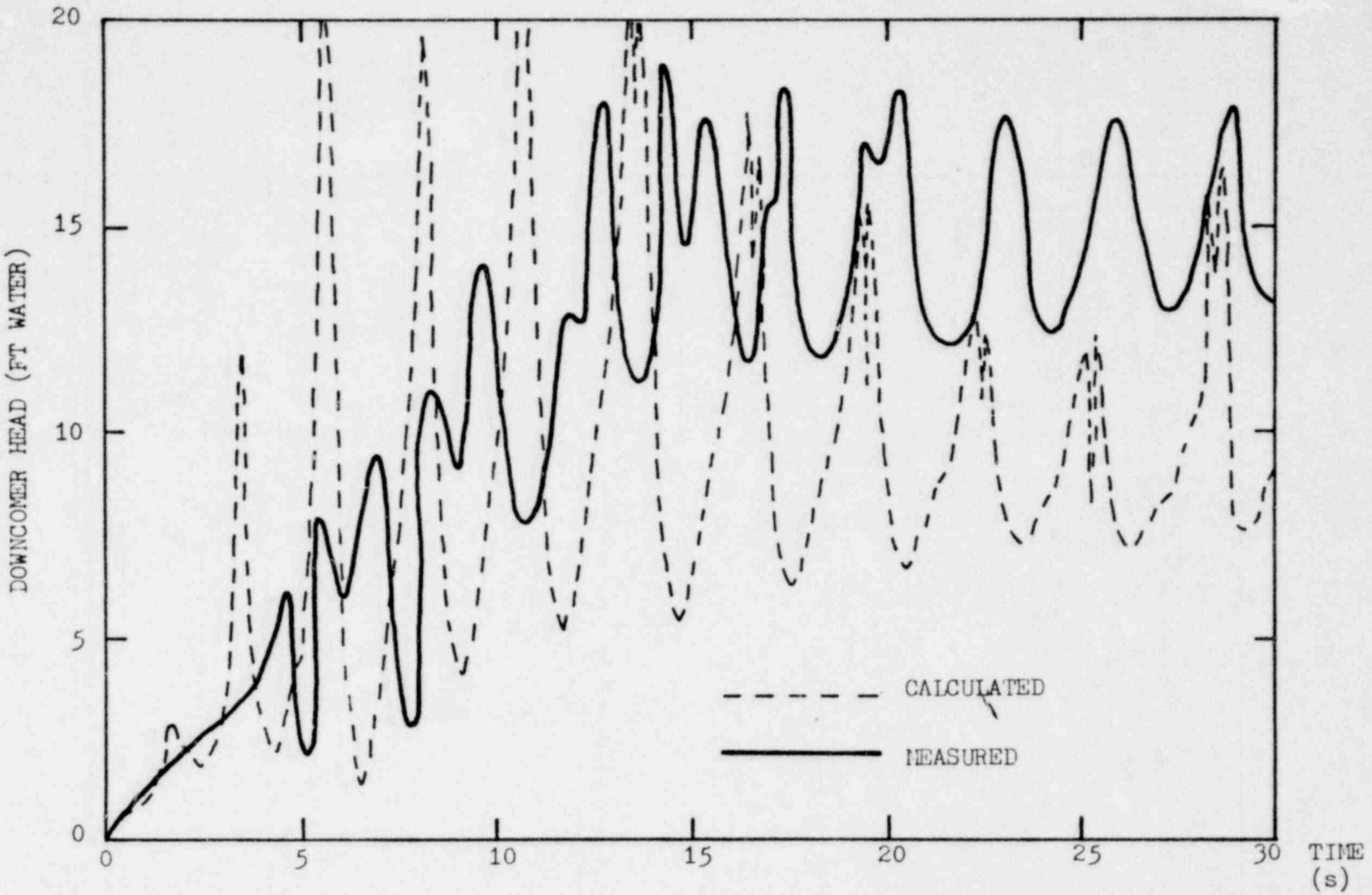

Fig. 6. Measured and Calculated Downcomer Head for FLECHT-SET Run #4923 (61 psia)
Initial Clad Temp.: 1111 F, Peak Power: 0.7 kW/ft, Injection Temp.: 158 F
Injection Flow Rate: 10.52 lb/s First 14 s, 1.19 lb/s thereafter

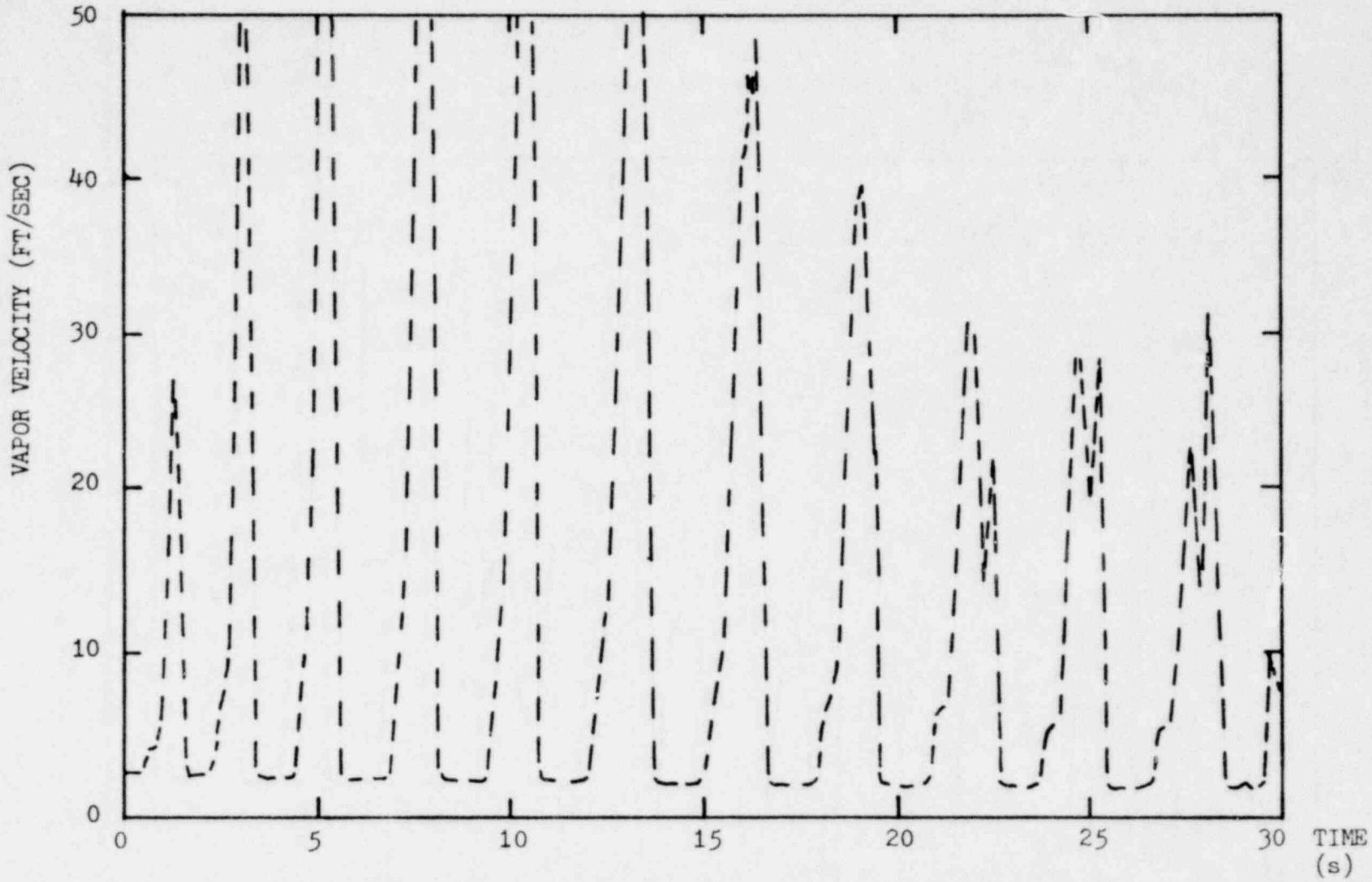

Fig. 7. Calculated Vapor Velocity at Core Exit for FLECHT-SET Run #4923

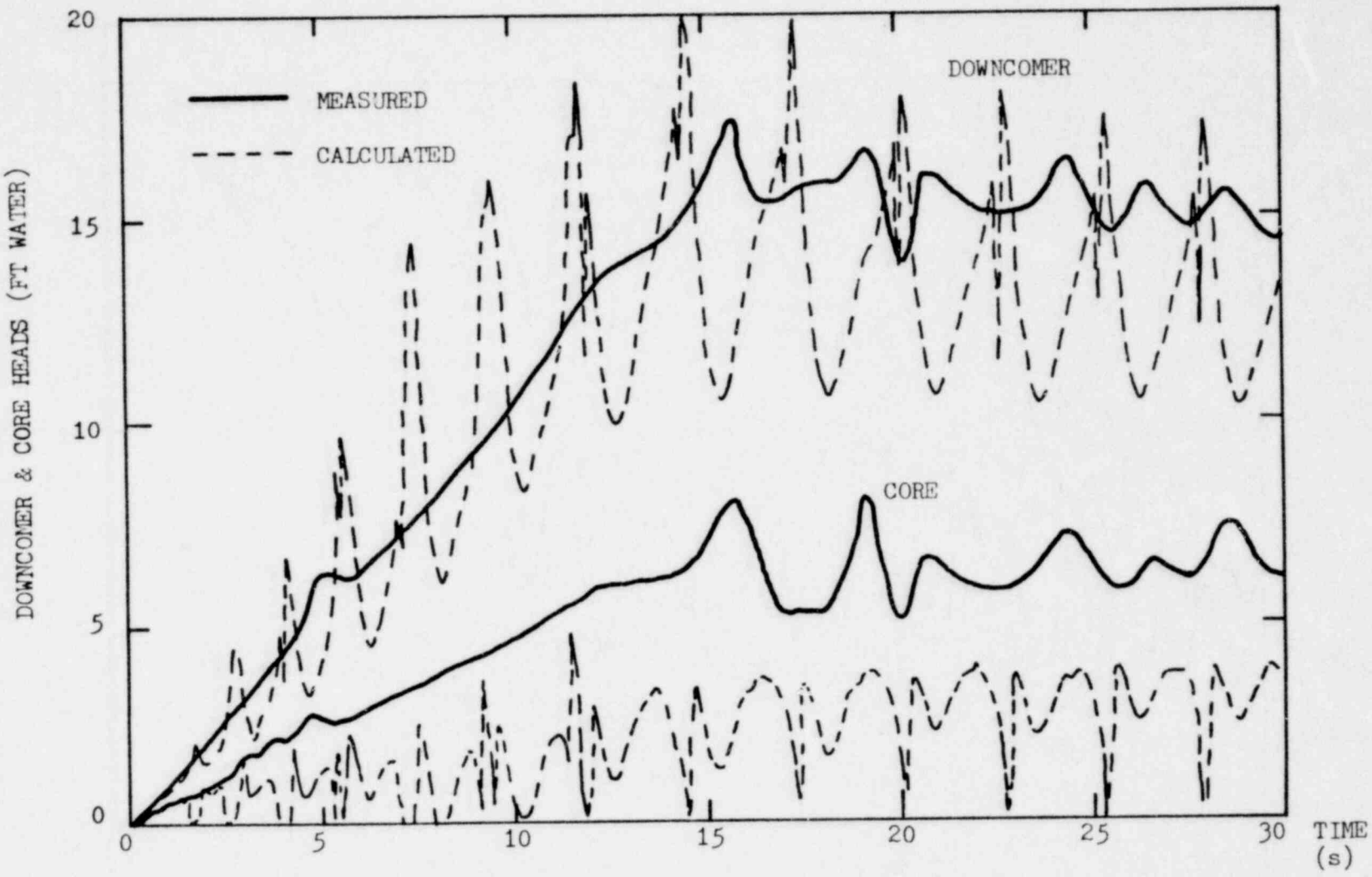

Fig. 8. Measured and Calculated Downcomer and Core Heads for Semiscale Test S-07-4 (60 psia)
Initial Clad Temp.: 980 F, Peak Power: 0.63 kW/ft, Injection Temp.: 141 F
Injection Flow Rate: 2.69 lb/s First 16 s, 0.21 lb/s thereafter

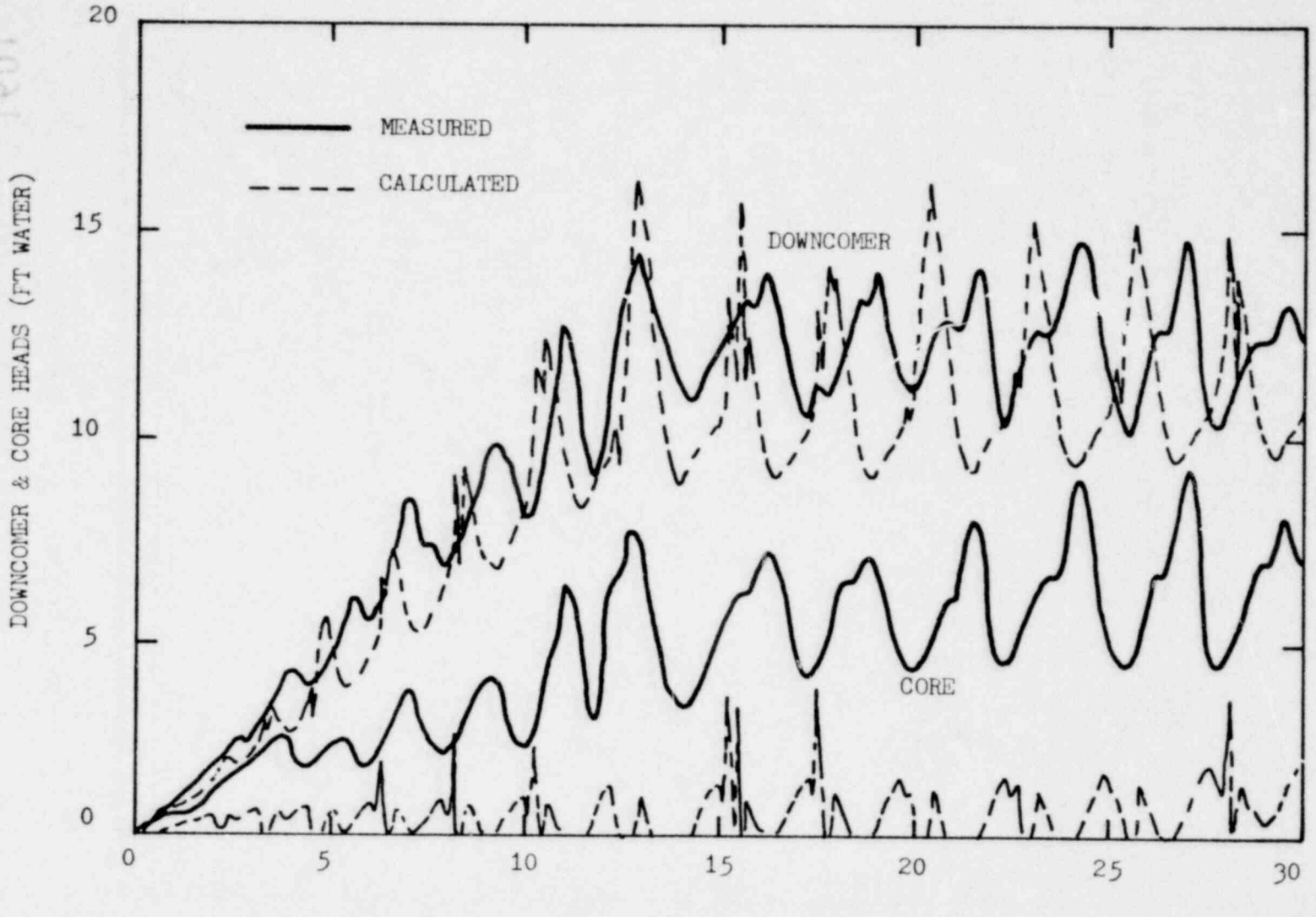

Fig. 9. Measured and Calculated Downcomer and Core Heads for Semiscale Test S-07-5 (18.4 psia)
Initial Clad Temp.: 1268 F, Peak Power: 0.405 kW/ft, Injection Temp.: 170 F
Injection Flow Rate: 2.55 lb/s First 12 s, 0.34 lb/s thereafter

Appendix

Equations for Dynamics Model

The equations which describe the mechanisms forcing the gravity feed reflood oscillations will be presented in this section. Figure 4 shows the reflood system and defines some of the symbols used below. Consider the case when the quench front is below the core water level and net vapor generation starts at the quench front. If the vapor generation rate is high enough, the water trapped above the quench front will be pushed up and into the upper plenum. The pressure of the generated vapor can be approximated by the ideal gas law:

$$P\mathcal{V} = (m_g - m_v)RT \tag{1}$$

where M_g is the mass of steam generated and M_v is the mass of steam vented through the entrained water. Also

$$\mathcal{V} = A_c(z_e - z_c) \tag{2}$$

where A_c is the core flow area.

Differentiating and rearranging:

$$\dot{P} = \frac{[(\dot{m}_g - \dot{m}_v)\cdot RT - PA_c(\dot{z}_e - \dot{z}_c)]}{A_c(z_e - z_c)} \tag{3}$$

A force balance on the continuous reflood column yields:

$$\frac{1}{g_c}\left[z_c \frac{d(\rho AV)_c}{dt} + L_{BP}\frac{d(\rho AV)_{BP}}{dt} + z_d \frac{(d(\rho AV)_d}{dt}\right]$$

$$= (\rho A_c - \rho_o A_d) - K_c \frac{\rho_f A_c V_c^2}{g_c} - \rho_f (A_d z_d - A_c z_c)\frac{g}{g_c} \qquad (4)$$

or $$(z_c + L_{BP} + z_d)\frac{d\dot{m}_f}{dt} = (\rho A_c - \rho_o A_d) g_c - \frac{K_c \dot{m}_f^2}{\rho_f A_c}$$

$$- \rho_f (A_d z_d - A_c z_c) g \qquad (5)$$

where $\dot{m}_f$ is the actual mass flooding rate.

Conservation of mass: $$\rho_f A_d \dot{z}_d = \dot{m}_{inj} - \dot{m}_f \qquad (6)$$

$$\rho_f A_c \dot{z}_c = \dot{m}_f \qquad (7)$$

A force balance on the entrained liquid and the vapor downstream of the quench front yields approximately:

$$\frac{m_e}{g_c}\ddot{z}_e = (\rho - \rho_o) A_c - \frac{K_f \rho_g V_g^2 A_c}{g_c} - m_e \frac{g}{g_c} \qquad (8)$$

where m_e is the mass of liquid entrained, and K_f is the effective friction coefficient of the flow path from the quench front to the outlet orifice.

Assuming that the acceleration of the vapor is negligible, a force balance on the vapor alone yields V_g:

$$0 = (\beta - \beta_0) - \frac{K_d \rho_g (V_g - j_e)^2}{g_c} - \frac{K_f \rho_g V_g^2}{g_c} \qquad (9)$$

where K_d is an effective drag coefficient for the entrained liquid.

The resulting system of equations (3),(5)-(9) is fifth order.

Heat Transfer

Heat transfer in nucleate boiling is calculated from McAdam's equation; critical heat flux is calculated from Zuber's pool boiling CHF equation. Heat transfer in the post-CHF regimes are calculated from Hsu's correlation [4]:

$$h = h_{HSU} + h_{MOD\ BROMLEY}$$

$$= 1456\, p^{0.558} \exp(-0.003758\, p^{0.1733}\, \Delta T_{sat})$$

$$+ 0.62 \left[\frac{g k_g^3 \rho_g (\rho_\ell - \rho_g) H_{fg}}{\Delta T_s \mu_g} \frac{1}{2\pi} \sqrt{\frac{g(\rho_\ell - \rho_g)}{\sigma}} \right]^{1/4} \qquad (10)$$

Figure 5 shows heat flux calculated from the equation plotted against some reflood data.

BOILING WATER REACTOR
SAFETY RESEARCH PROGRAMS

PRESENTED BY
WILLIAM D. BECKNER
U.S. NUCLEAR REGULATORY COMMISSION

U.S. NUCLEAR REGULATORY COMMISSION
SEVENTH WATER REACTOR SAFETY RESEARCH
INFORMATION MEETING
GAITHERSBURG, MARYLAND
NOVEMBER 6, 1979

Fiscal year 1979 resulted in a significant advancement in boiling water reactor (BWR) safety research both in terms of information obtained in existing programs and in terms of major new programs initiated. The ongoing BWR Blowdown/Emergency Core Cooling (BD/ECC) Program is continuing and a new program, Countercurrent Flow Limiting (CCFL) Reflood/Refill Program, was started in fiscal year 1979. These programs, which are jointly sponsored by the U.S. Nuclear Regulatory Commission, the Electric Power Research Institute and the General Electric Company, represent a major upgrading of BWR safety research.

Research in the BD/ECC program involved the study of the effect of ECC injection during the early blowdown phase of a hypothetical loss of coolant accident (LOCA). Testing is performed using the Two Loop Test Apparatus (TLTA) which is a model of a BWR incorporating a single full sized electrically simulated fuel bundle. Papers later in this session will summarize this work. A scoping test to study a small break LOCA is also planned in the very near future. Testing in the TLTA will be terminated in early CY 1980 to allow an upgrade of the experimental facility. A multiple bundle facility capable of simulating the entire LOCA transient through reflood is currently under consideration.

The CCFL Refill/Reflood Program involves several different tasks designed to investigate multidimensional phenomena that could occur during a LOCA. The major facility used by this program is the Sector Steam Test Facility (SSTF), as shown in Figure 1. The SSTF is a full sized model of a 30° "pie shaped" sector of a BWR using steam injection to simulate core generated steam. Core spray distribution tests investigating the distribution of the ECC spray over the simulated core are underway and will be described in a paper later in this session. Later transient tests will simulate the LOCA blowdown and refill and will investigate the multiple dimensional breakdown of CCFL and penetration of the ECC fluid into the core region. Other tests will investigate any compromises in simulation due to the 30° sector and due to using injected steam to simulate core generated steam. A task to assist in the development of a BWR version of TRAC is also included in the CCFL Refill/Reflood Program.

POOR ORIGINAL

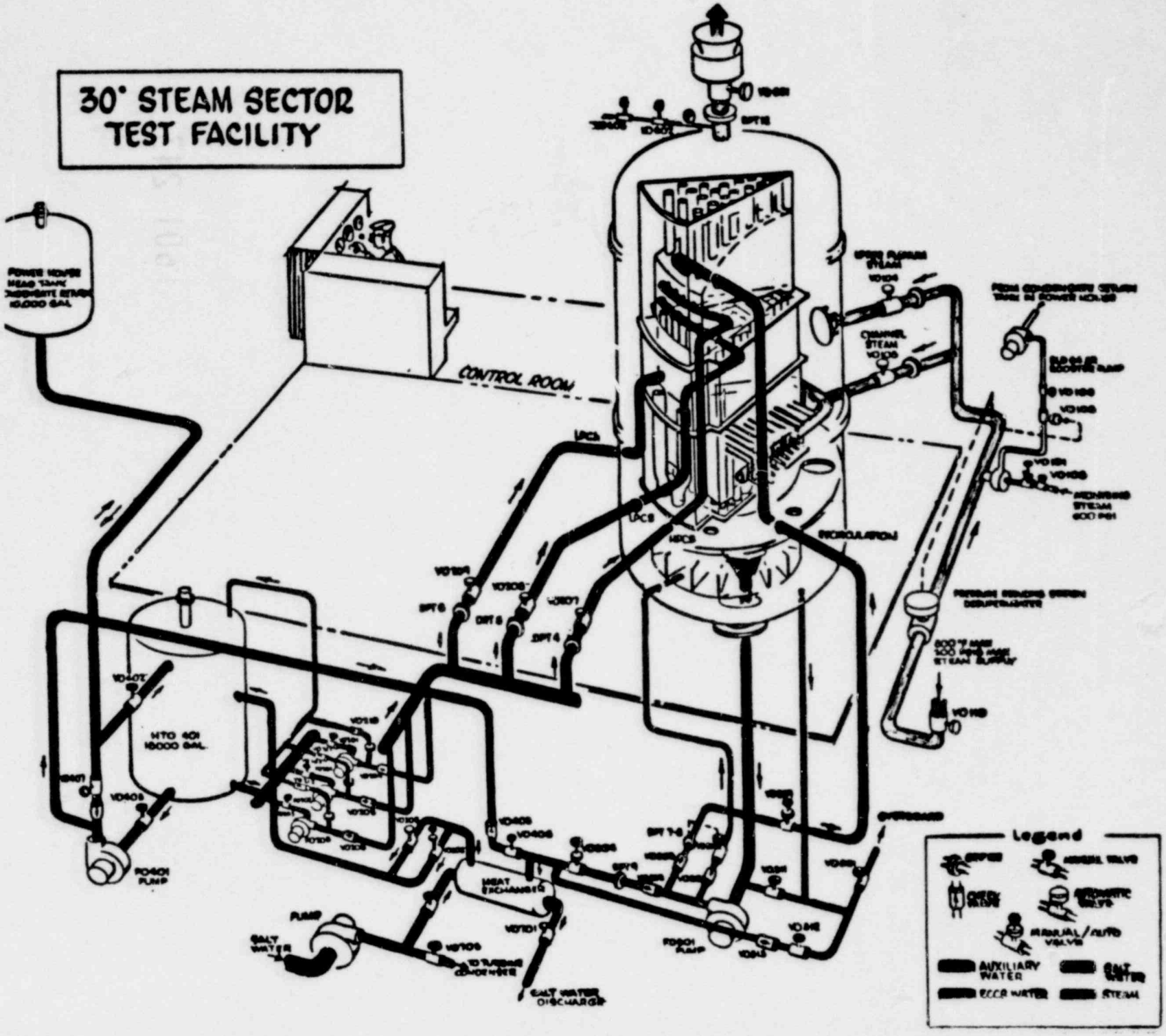

1601 244

A COMPARISON OF RELAP CALCULATIONS WITH TLTA TEST 6406

Presented at
The Seventh Water Reactor Safety Research Information Meeting
November 5-9, 1979
Gaithersburg, Maryland

G. E. Wilson
EG&G Idaho, Inc.

Idaho National Engineering Laboratory
Idaho Falls, Idaho 83401

A COMPARISON OF RELAP CALCULATIONS WITH TLTA TEST 6406

G. E. Wilson
EG&G Idaho, Inc.

To assess the capabilities of RELAP4/MOD6 an analysis was performed to calculate boiling water reactor (PWR) emergency core cooling (ECC) type transients. The analysis was performed comparing RELAP4/MOD6 calculations to experimental data from the Two-Loop Test Apparatus (TLTA) Test 6406, Run 1 as part of the INEL technical support to the Nuclear Regulatory Commission (NRC) in the surveillance of NRC/industry cooperative programs.

TLTA is an integral blowdown refill test facility for evaluating potential BWR loss of coolant accidents. The facility consists of a single bundle electrically heated core simulator and the major components of a BWR pressure vessel. Test 6406, Run 1 is a 200% recirculation break test with average core power and average ECC flows. Initial conditions are a steam dome pressure of 7.28 MPa and core inlet temperature of 557 K.

The base case results show that during the early transients (before 40 seconds) calculated system pressure agrees with the data. However, the calculated depressurization is high by as much as 0.70 MPa during the later portions of the transient. For this same RELAP calculation the upper plenum mass inventory is increasingly high after 30 seconds, whereas the lower downcomer mass inventory is low, starting at 15 seconds. Although flow rates exiting the upper plenum are not measured, it can be inferred that the code underpredicted the mass flow from the upper plenum to the lower downcomer. An increased mass inventory in the lower plenum would lead to a reduced volumetric break flow and result in a lower calculated depressurization rate in the later part of the transient.

Experimentally determined flow data for the jet pumps, core inlet, and guide tubes are only valid over the first 10 to 12 seconds when the flow is single phase. During this period the calculated flows agree both in trend and magnitude with the experimentally derived values.

Calculated core temperatures show that code predicted DNB occurs as much as 20 seconds early in the upper core region. Lower core calculated DNB times agree well with the experimental data. Because the code predicted early DNB and did not calculate rewets the calculated core temperatures are higher than measured values

REFERENCE

E. E. Ross, RELAP4/MOD6 Data Comparison for TLTA Test 6406, Run 1, CAAP-TR-056, EG&G Idaho, Inc. (September 1979)

A Comparison of RELAP4/MOD6 Calculations with TLTA Test 6406

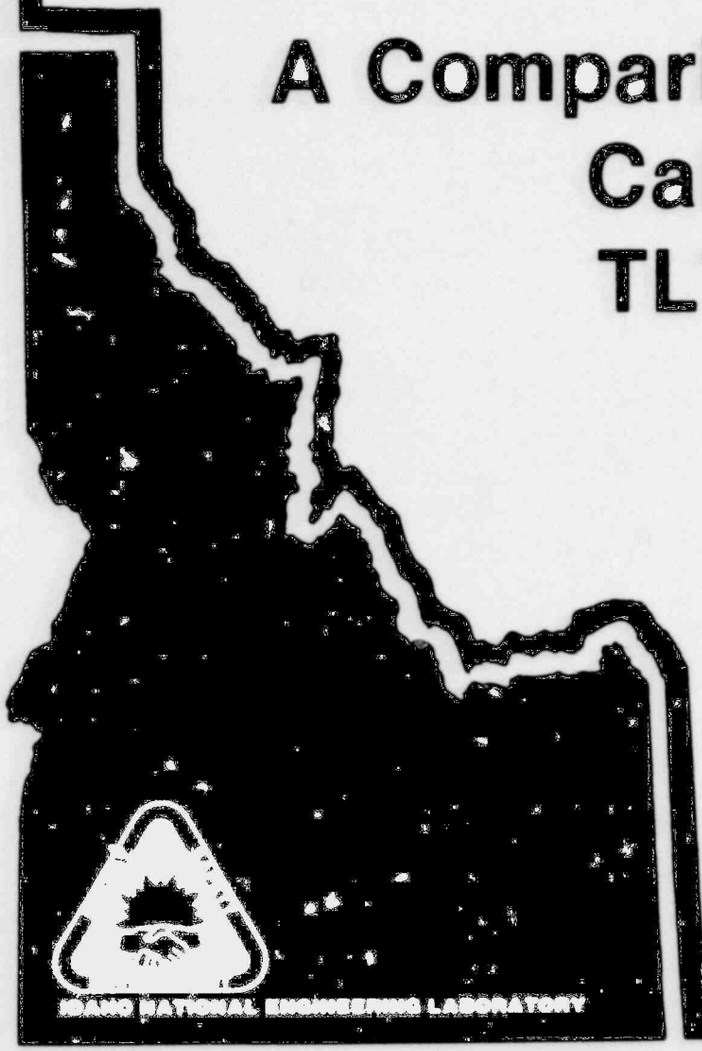

Presented by
G.E. Wilson

EG&G Idaho, Inc.

Two-Loop Test Apparatus Schematic

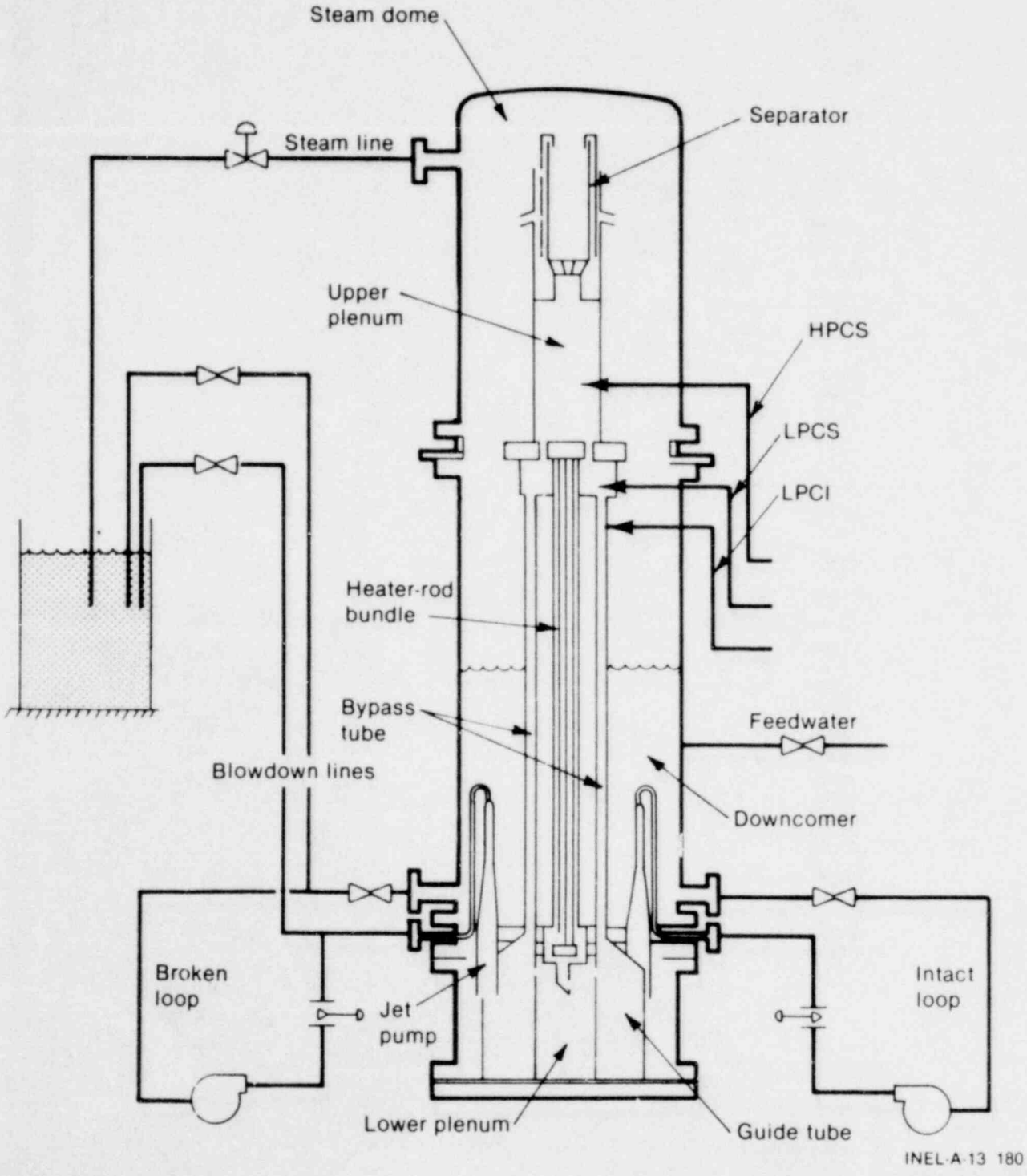

Initial Conditions

- 200% recirculation line break
- Steam dome pressure - 7.28 MPa
- Bundle inlet flow - 16.1 kg/s
- Outlet steam flow - 2.86 kg/s
- Bundle power:
  - Symetrical chopped cosine
    5.04 MW - 1.39 P.F.

INEL-S-21 556

1601 250

Core Power History

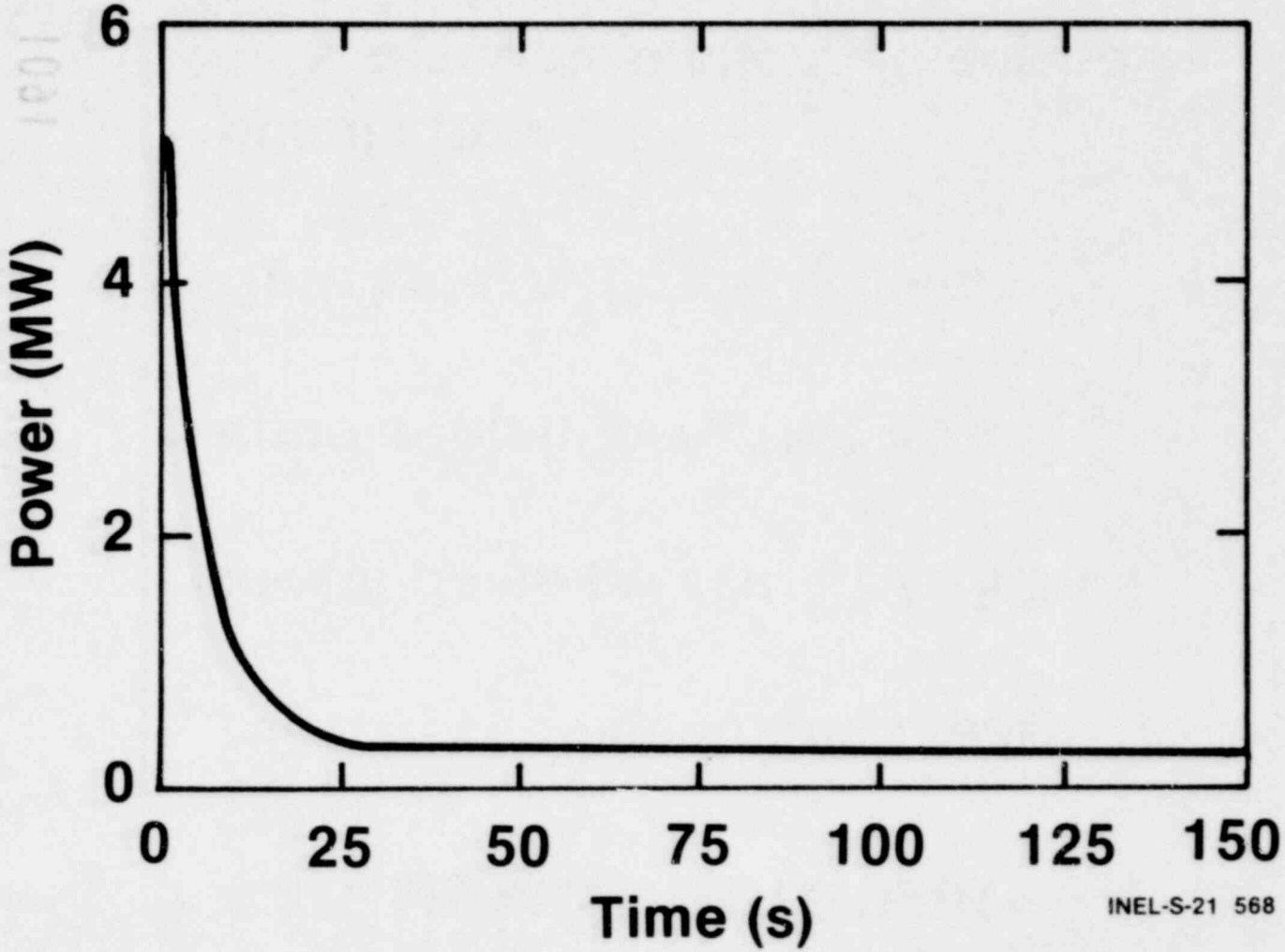

Emergency Core Cooling Flow Rate

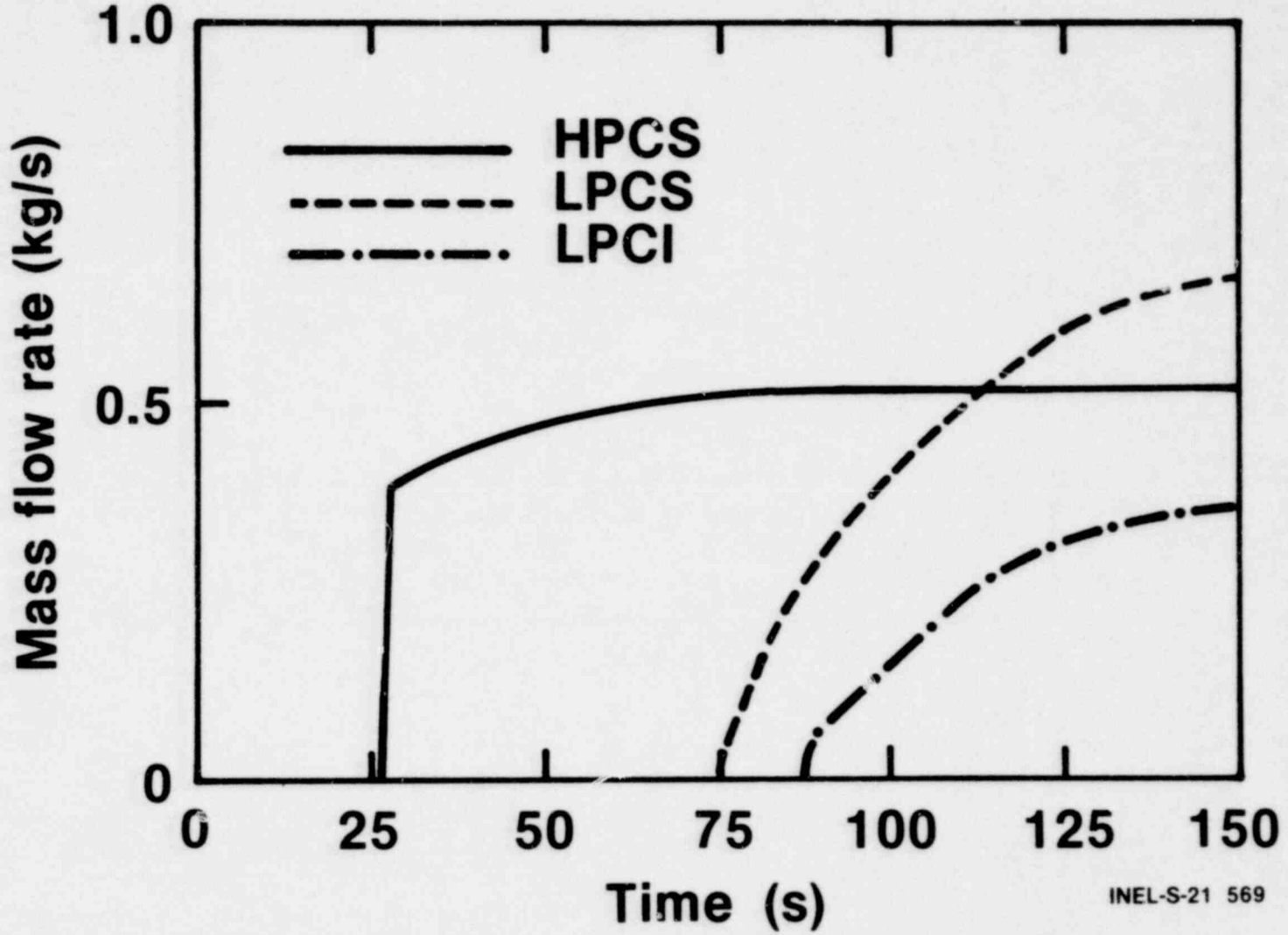

RELAP4/MOD6 TLTA System Nodalization Diagram

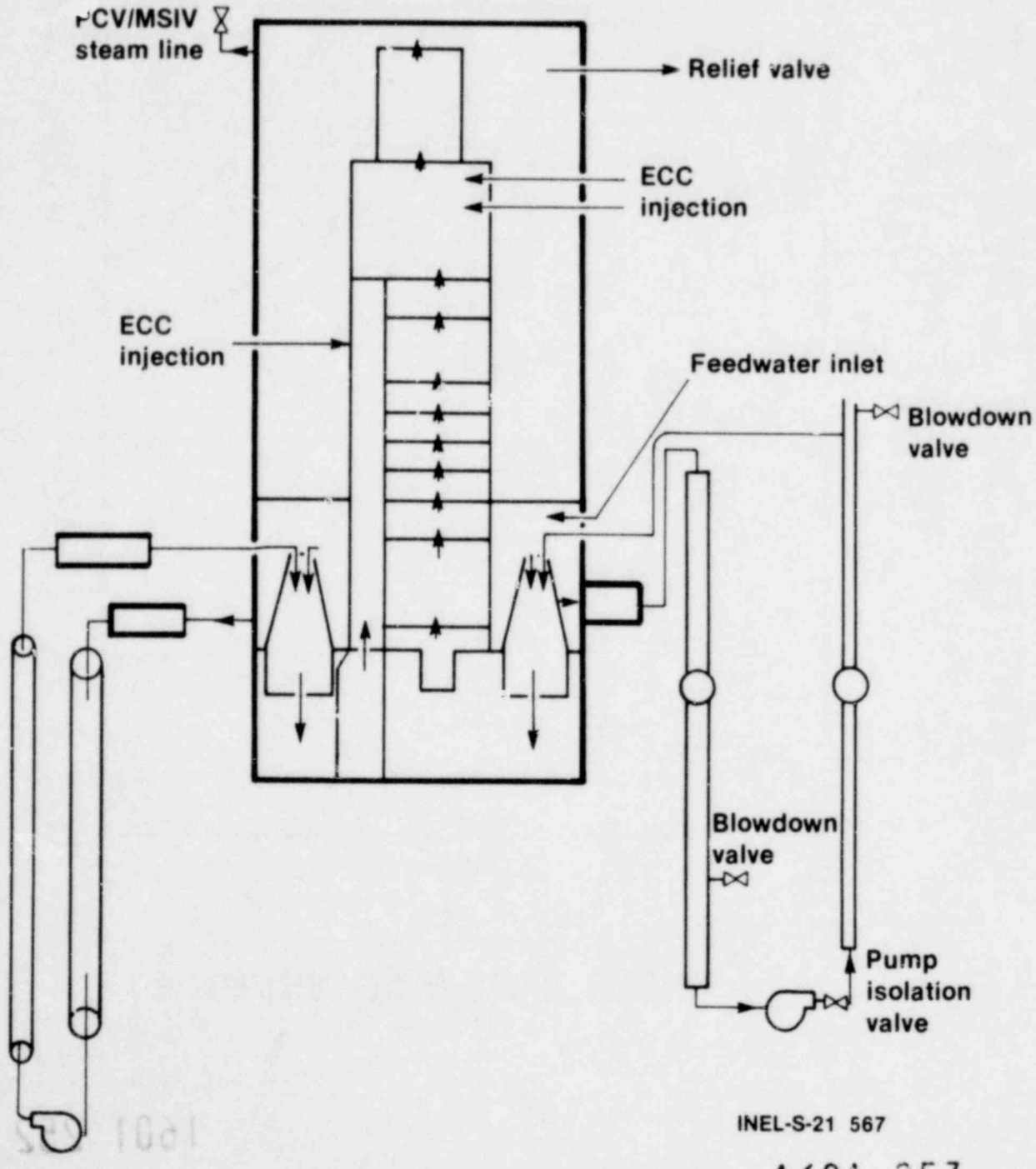

INEL-S-21 567

Major Code Options

- Slip
- Bubble rise
- Critical flow multipliers
- Heat transfer package

Junction Slip Models

- Used in:
  - Bundle
  - Bypass
  - Guide tube
  - Upper plenum
- Default values

Bubble Rise Models

- Downcomer:
  - Slope parameter - 0
  - Velocity - 0.91 m/s
  - Tripped off at 10 s

- Lower plenum:
  - Slope parameter - 0.8
  - Velocity - 0.61 m/s

Recirculation Pump Suction

Critical flow model

- **Subcooled:**
  - **Modified Burnell**
  - **Multiplier - 0.83**
- **Saturated:**
  - **HEM**
  - **Multiplier - 1.00**
  - **Transition quality - 0.02**

Jet Pump Drive

Critical flow model

- **Subcooled:**
  - Henry-Fauske
  - Multiplier - 0.95

- **Saturated:**
  - HEM
  - Multiplier - 1.00
  - Transition quality - 0.01

Heat Transfer Package

- Standard blowdown package with:
  - W-3
  - HSU-BECKNER
  - Modified Zuber DNB

INEL-S-21 562

Steam Dome Pressure

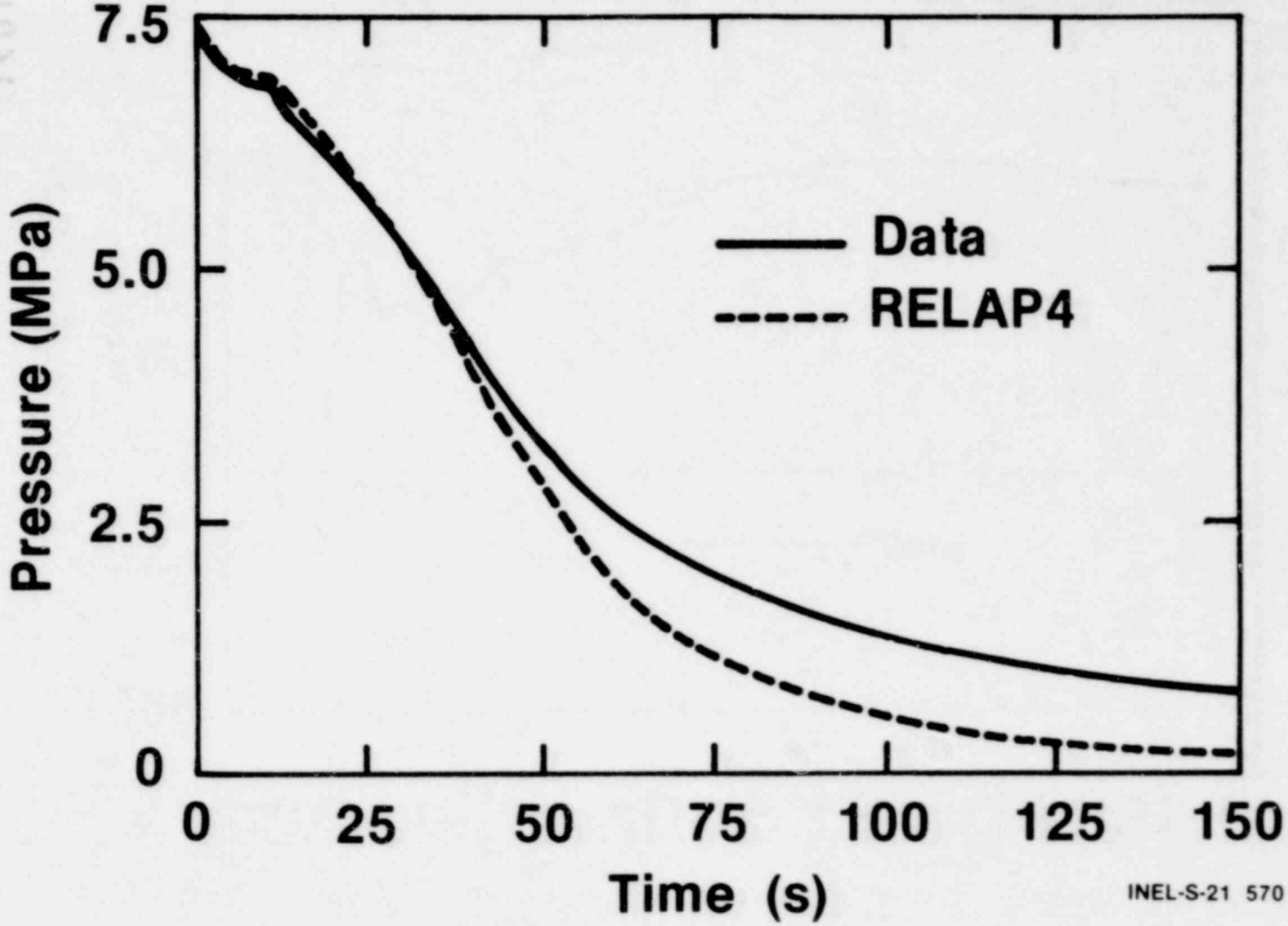

Lower Downcomer Density

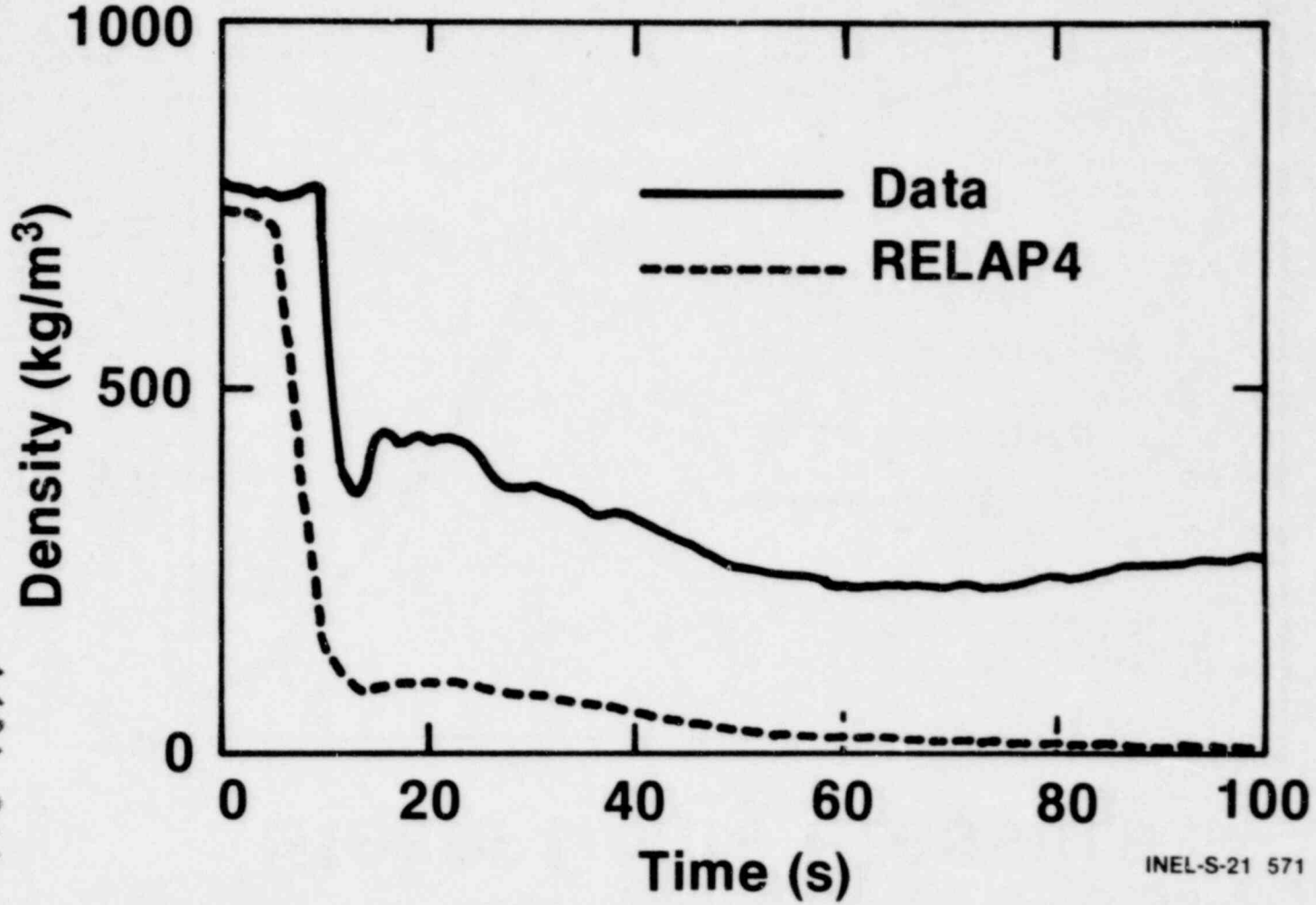

Lower Plenum Mass Inventory

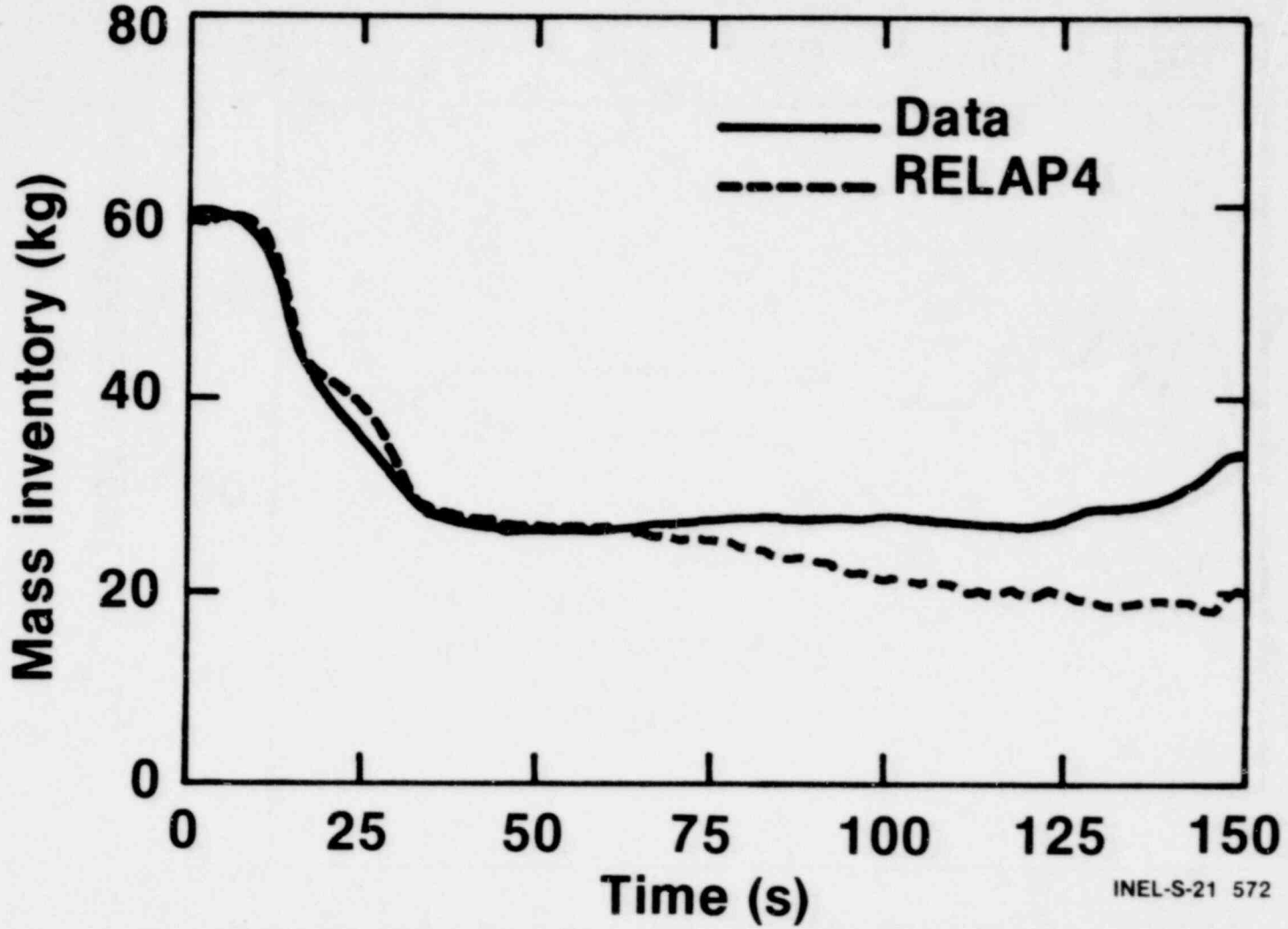

Upper Plenum Mass Inventory

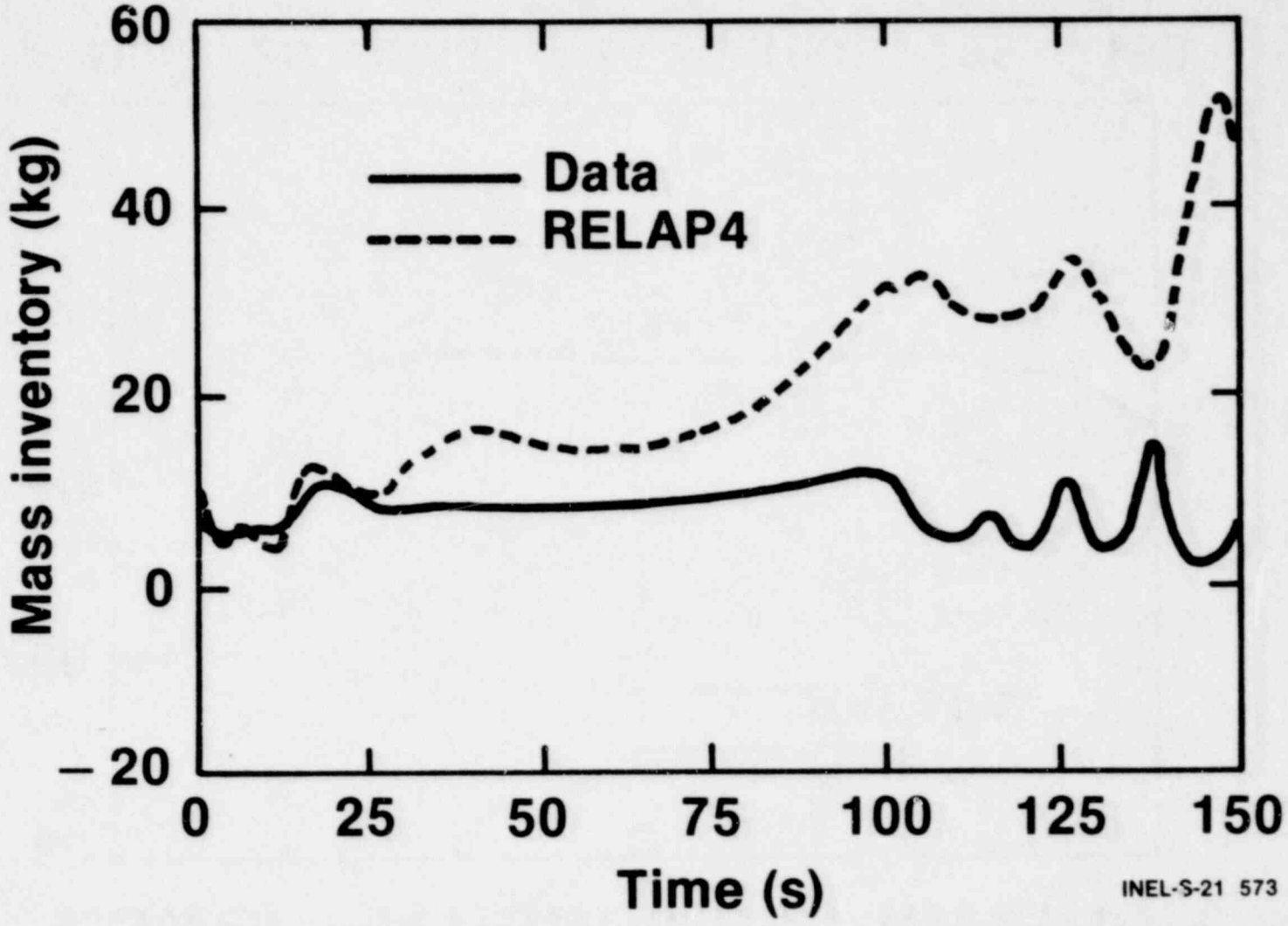

Recirculation Break Volumetric Flow Rate

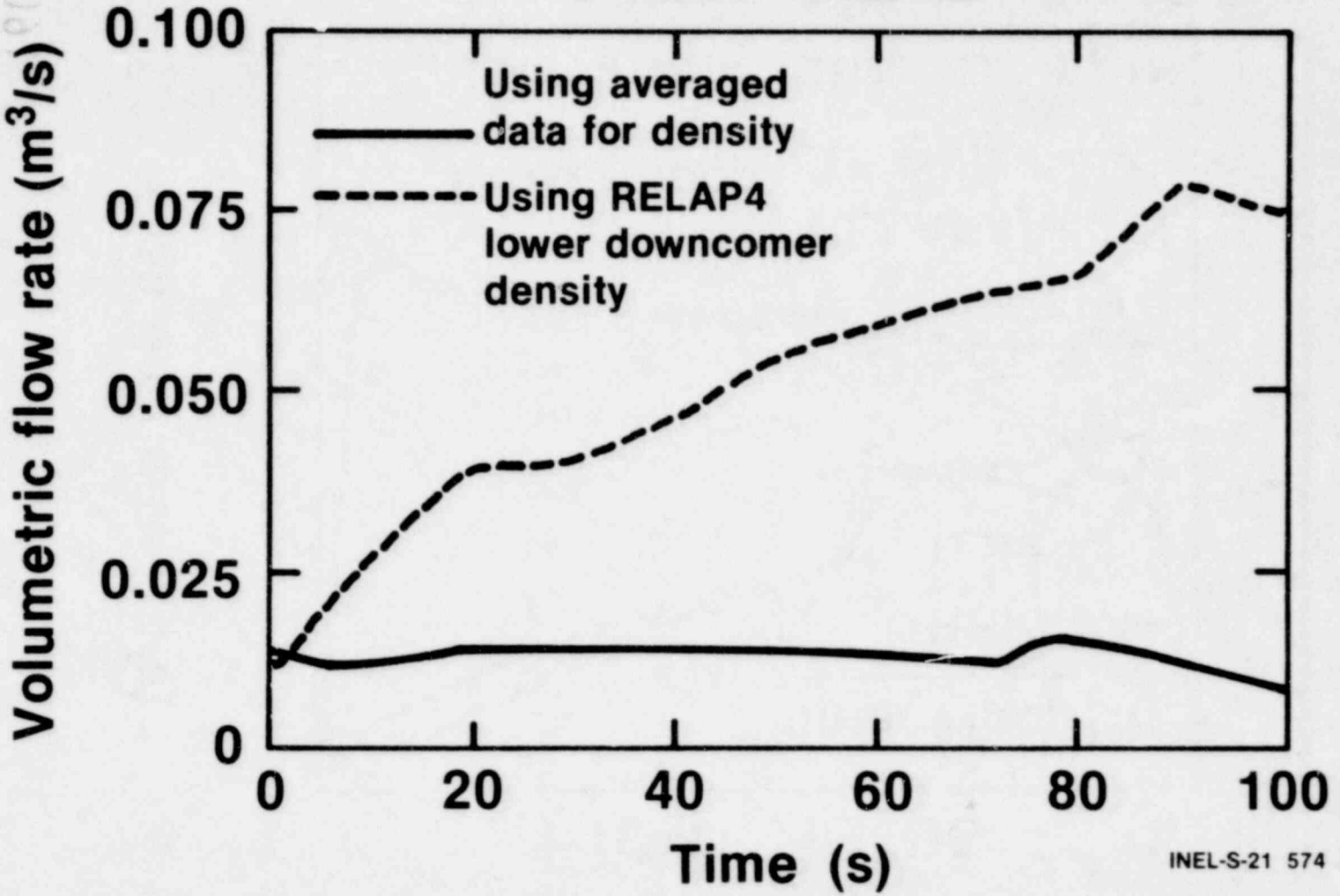

Jet Pump Discharge Mass Flow Rates

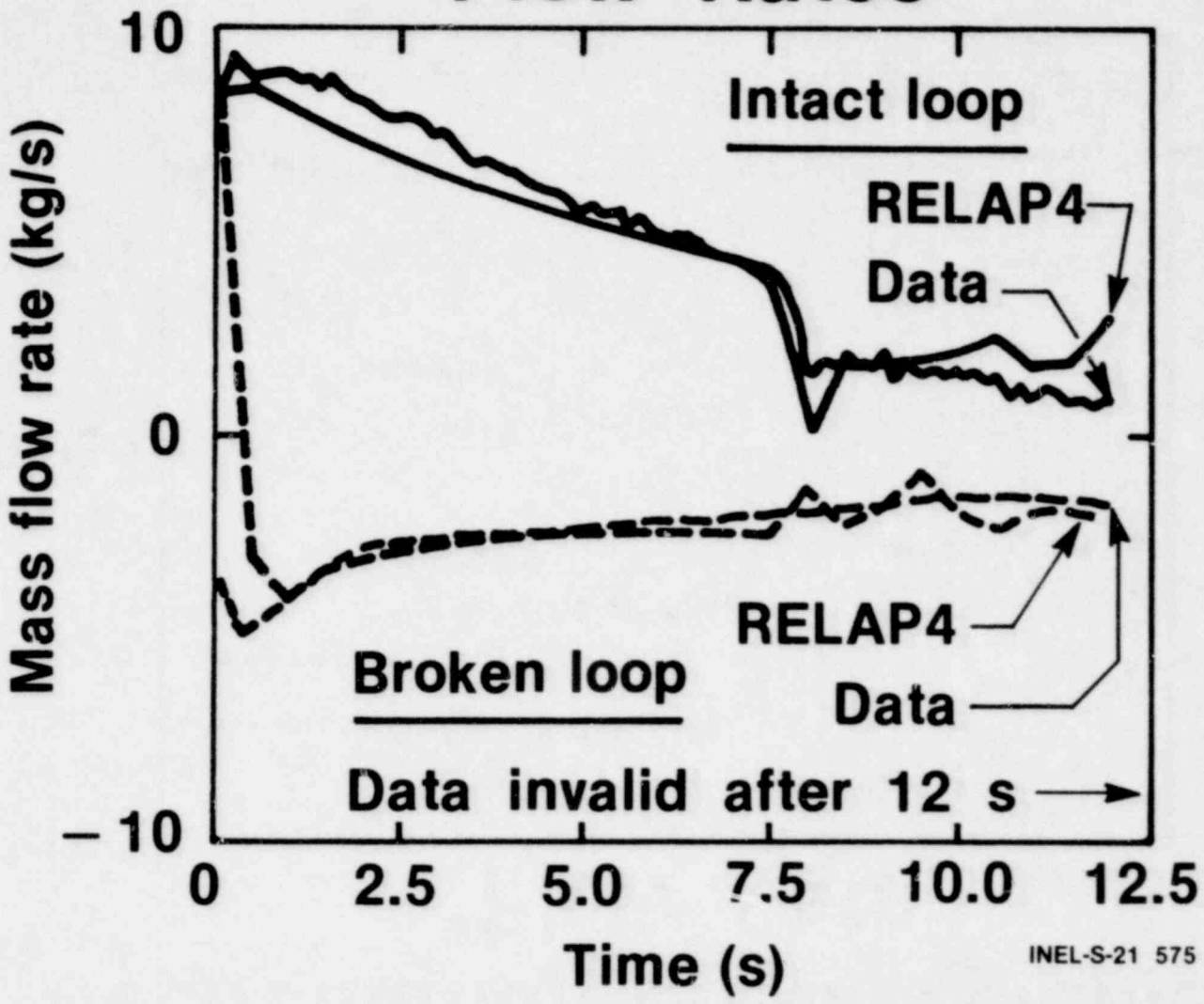

Bundle Surface Temperature 2.00-m Elevation

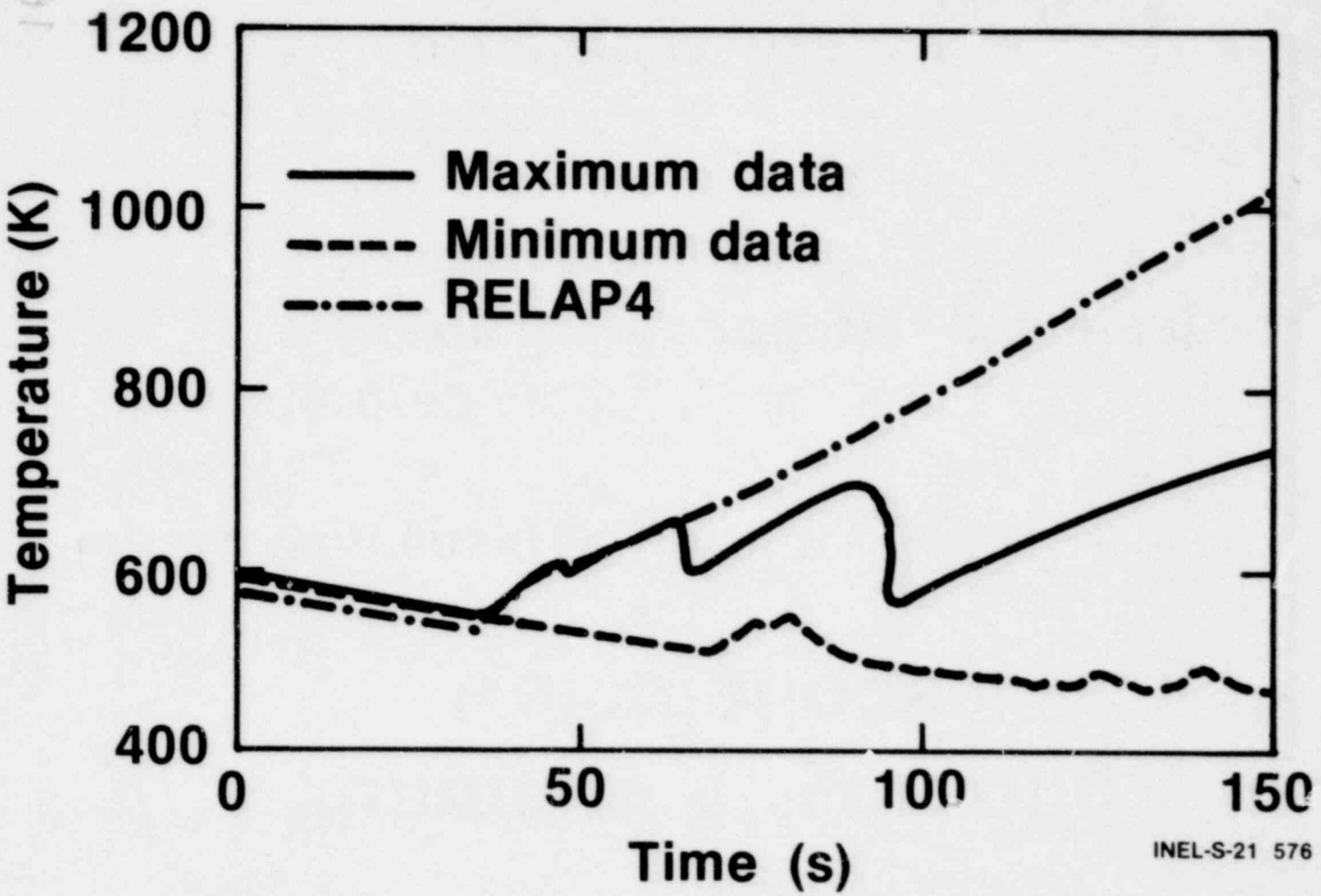

Summary - Hydraulic Calculations

- Good-measured flows
- Underpredicted:
  - Downcomer and lower plenum mass
  - System pressure
- Overpredicted:
  - Upper plenum mass

INEL-S-21 563

Summary - Temperature Calculations

- DNB:
  - Early
  - Core slip
- Rewet not calculated
- Temperatures overpredicted

INEL-S-21 564

Improvements

- Measurements:
  - Break flow/quality
  - Major hardware temperatures
  - Upper plenum flows:
    - Bypass, downcomer,
    - Lower plenum

INEL-S-21 565

Improvements

Code:

- **Slip:**
  - **Multiple models**
  - **Assessment - upper plenum junction**

INEL-S-21 566

Improvements

Code:

- **Slip:**
  - **Multiple models**
  - **Assessment - upper plenum junction**

BWR CORE SPRAY DISTRIBUTION

G. E. Dix

September 1979

General Electric Company
Nuclear Energy Engineering Division
San Jose, California, USA

For presentation at the 7th Water Reactor Safety Research Information Meeting, November 5-9, 1979, National Bureau of Standards.

SUMMARY

The General Electric core spray technology program was initiated in 1974 to obtain understanding of steam environment effects on core spray distribution and develop procedures to include these effects in ECCS design.

The influence of steam on single spray nozzle performance was first examined. This influence was found to be consistent and reproducible for a specific nozzle type, but varied from one nozzle type to another. The spray distribution changes result from the interaction of the condensing steam and the spray jet as it exits the nozzle. Further studies revealed that the changes in spray distribution were a result of a very rapid steam condensation on the spray near the nozzle exit. This rapid condensation has been previously reported by Weinberg[1], Lekic[2], and Takahashi[3]. This rapid condensation causes the subcooled spray to approach saturation temperature within a few inches of the nozzle.

---

[1] Weinberg, S. *Heat Transfer to Low Pressure Sprays of Water in a Steam Atmosphere.* Inst. of Mech. Engrs. Proc., Vol. 1B, No. 7, P240, 1952.

[2] Lekic, A. *Direct Contact Condensation of Vapour on a Spray of Subcooled Drops.* Ph.d Dissertation, University of Waterloo, Ontario, Canada, 1976.

[3] Takahashi, Y; M. Masuda; K. Aikawa; and M. Tahara. *A Basic Study of Mixture Type Steam Condensers.* Mitsubishi Heavy Industries Technical Report, Vol. 9, No. 1, PP 15-20 (1972).

The spray distribution results for each nozzle type of interest were individually measured and modelled empirically, leading to the ability to calculate single nozzle spray distribution patterns.

In a multi-nozzle ECC System, the spray distribution results from a combination of the initial single nozzle distribution and the interactions between the nozzle sprays. The interactions start at some distance from the nozzles, where the spray patterns begin to overlap. In this region, the steam condensation on the spray is negligible because the water temperature is very near saturation. Therefore, the interactions between sprays are hydrodynamic, and can be determined with tests of spray performance without condensation effects. This allows the large scale multiple nozzle interaction experiments to be conducted in economical air-environment facilities.

The method developed by GE to predict ECC spray distribution involves the combination of single nozzle test data obtained in steam with multiple nozzle interaction effects obtained in air. This method has been successfully confirmed with multiple-nozzle tests in a Steam Sector Test Facility (SSTF). Pre-test predictions were made for these tests before the steam test facility was completed. Subsequent comparisons showed agreement of the prediction and test results within the pre-determined acceptance limits[4], thus confirming the use of air-environment tests for multiple nozzle interaction evaluations.

---

[4] Sandoz, S. A.; L. L. Myers; W. A. Sutherland; D. G. Schumacher; and G. E. Dix. *Core Spray Design Methodology Confirmation Tests.* NEDO-24712, August 1979.

WATER REACTOR SAFETY RESEARCH

INFORMATION MEETING

BWR CORE SPRAY DISTRIBUTION

G. E. DIX

NOVEMBER 6, 1979

CORE SPRAY TECHNOLOGY

OBJECTIVES

UNDERSTAND STEAM ENVIRONMENT PHENOMENA

DEVELOP PREDICTION METHOD

QUALIFY PREDICTION CAPABILITY

- CONFIRM ASSUMPTIONS

GED
11/6/79

CORE SPRAY SYSTEM

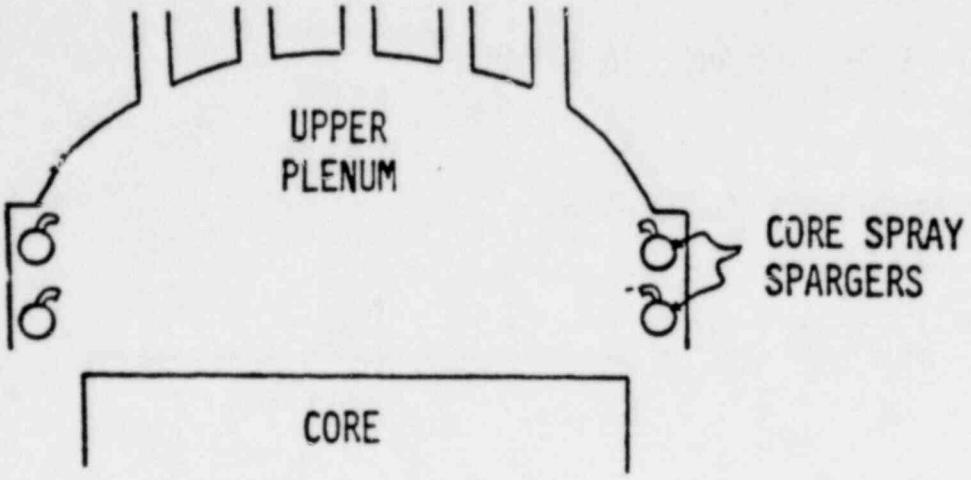

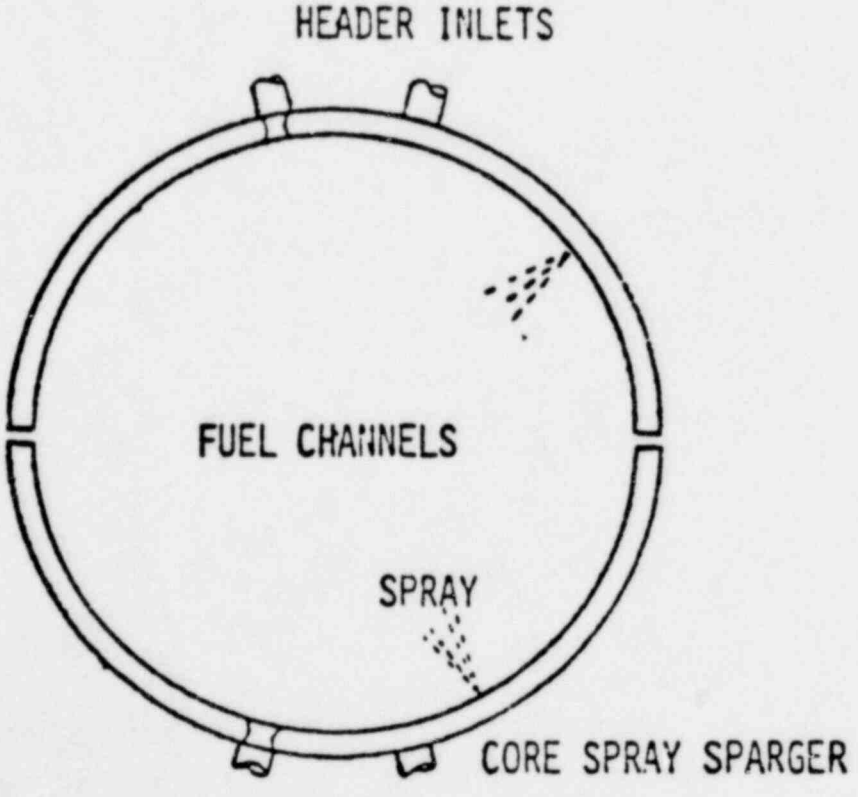

1601 276

CED
11/6/79

- NOZZLE PERFORMANCE IN STEAM

VERTICAL NOZZLE TESTS

CONDENSATION EFFECTIVENESS STUDIES

GED
11/6/79

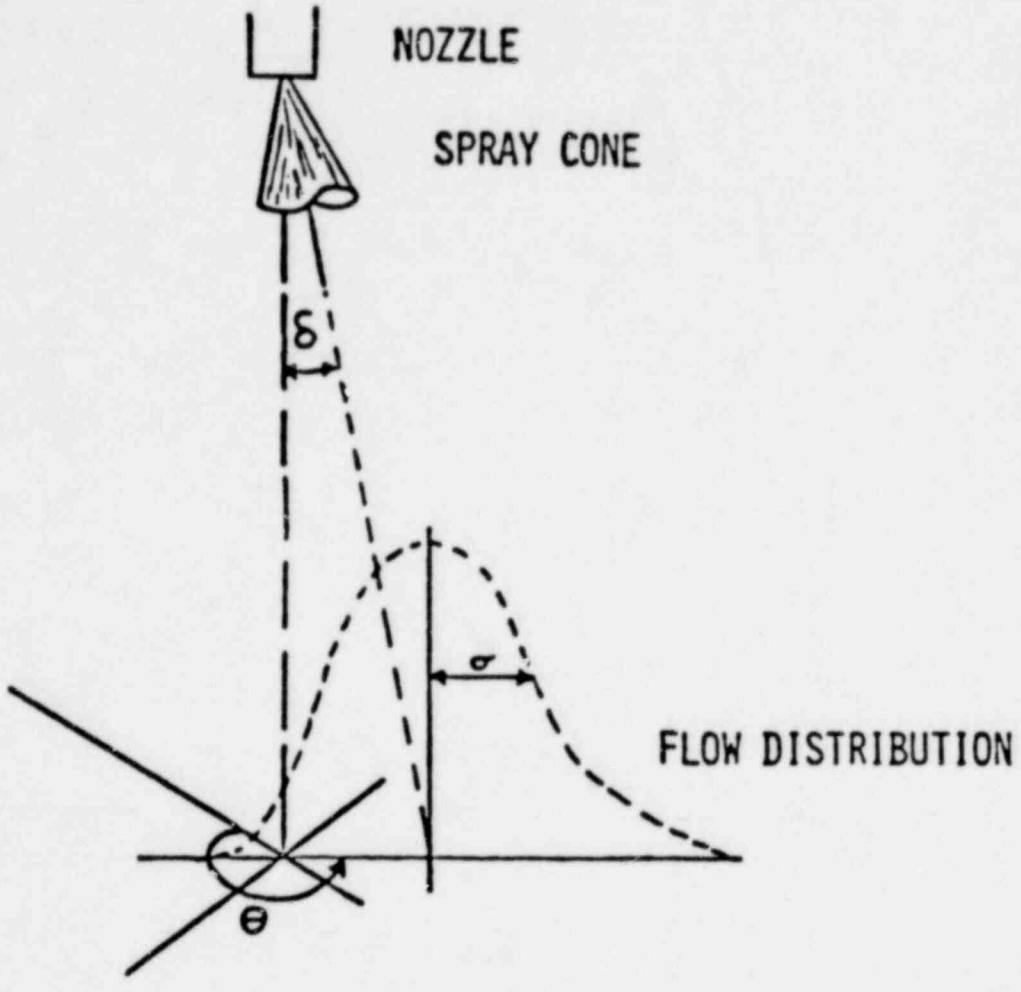

1601 278

GED
11/6/79

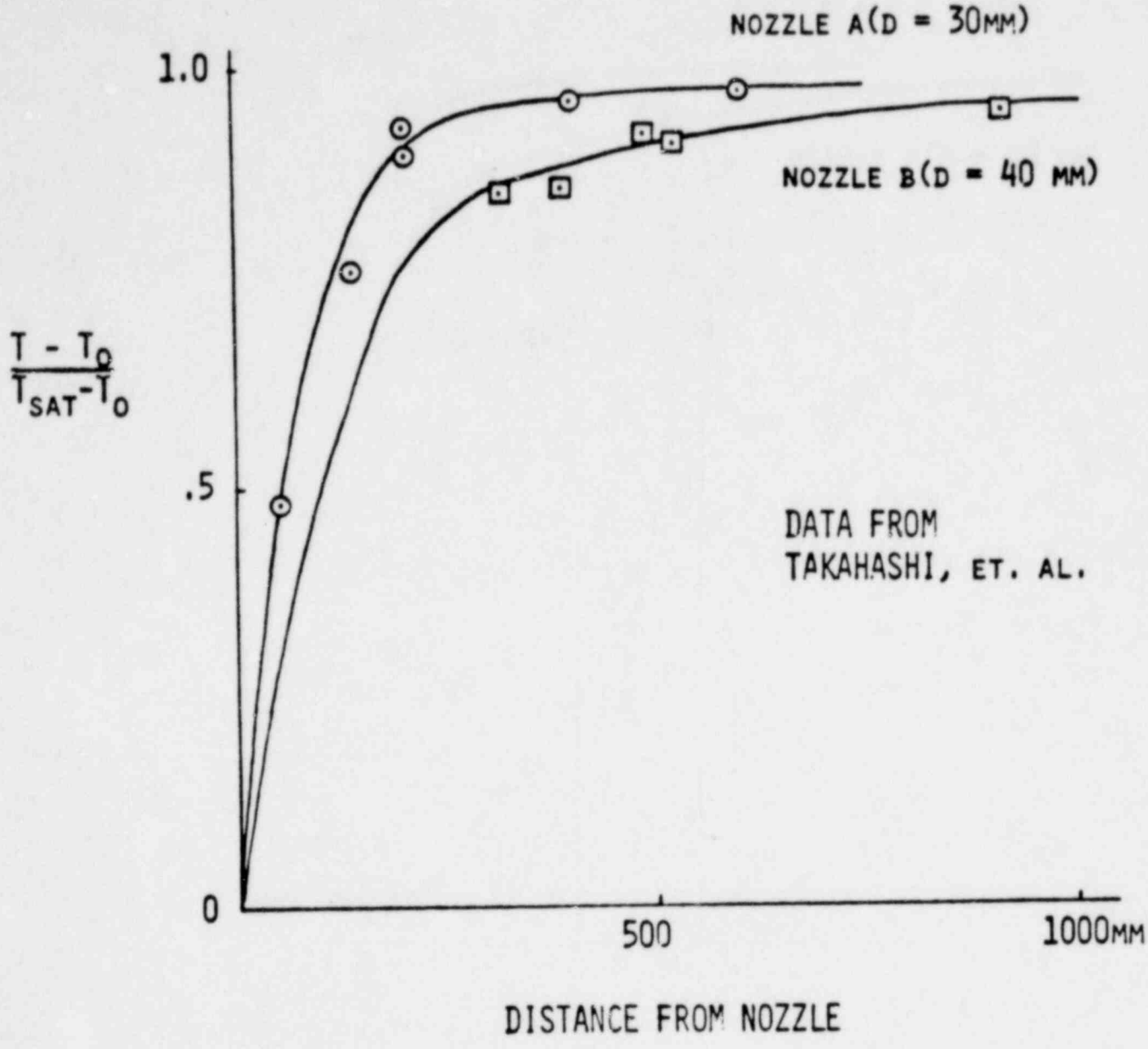

1601 279

GED
11/6/79

NEAR-NOZZLE

BEHAVIOR IN STEAM

- CONSISTENT
- REPRODUCIBLE
- CORRELATES AS A FUNCTION OF SUBCOOLING
- CONDENSING CLOSE TO NOZZLE

1601 280

GED
11/6/79

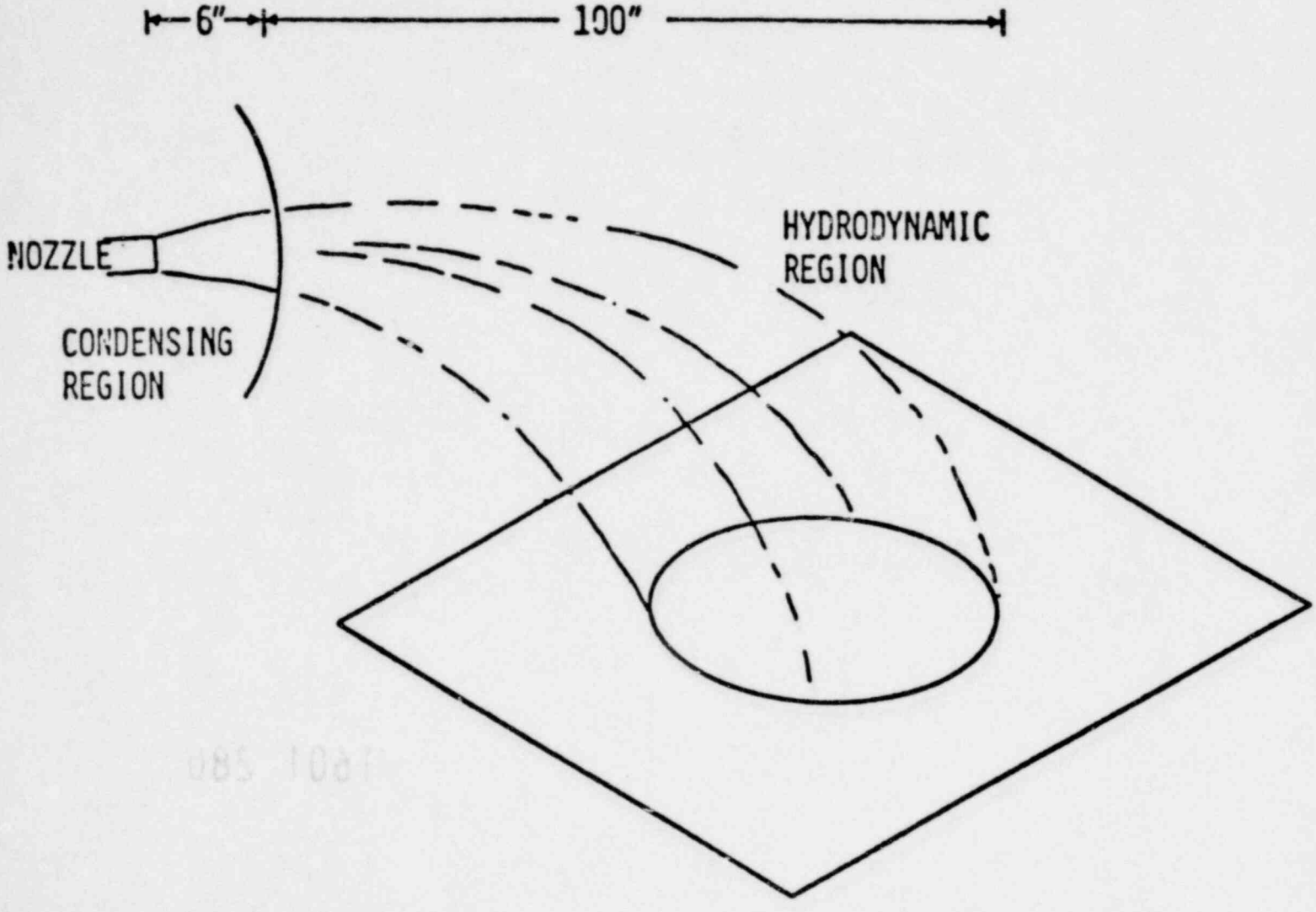

1601 281

GED

11/6/79

- NOZZLE MODEL

  TRAJECTORY ANALYSIS

  CORRELATION FROM VERTICAL RESULTS

  PROVIDES BASIS FOR EXTRAPOLATION

    ORIENTATION

    FLOW RATE

GED

11/6/79

CORE SPRAY PREDICTION METHOD

POOR ORIGINAL

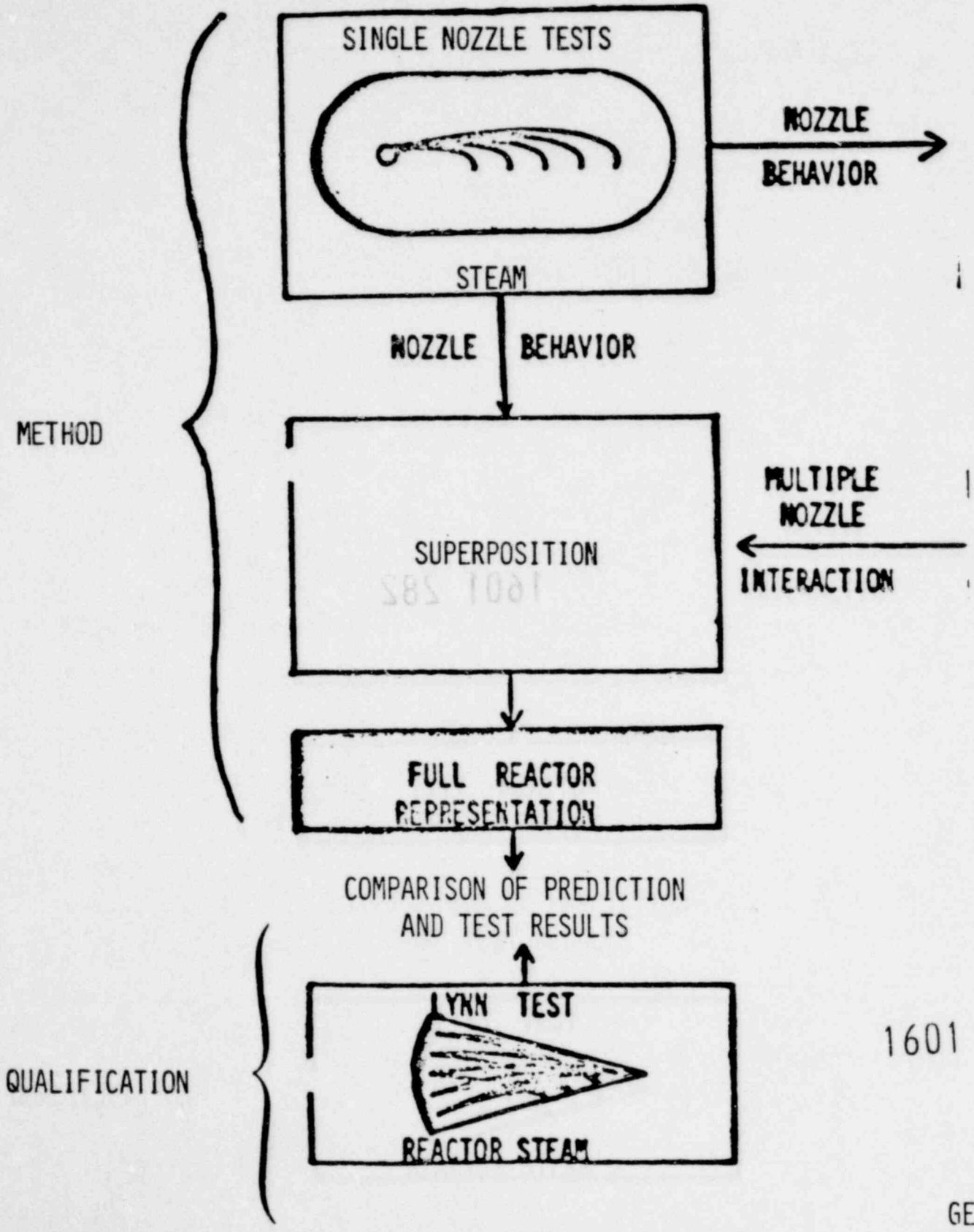

1601 283

GED
11/6/79

QUALIFICATION TEST REQUIREMENTS

- SPRAY NOZZLES
- LIQUID AND VAPOR FLOW PATHS
- REACTOR-TYPICAL HARDWARE

GED
11/6/79

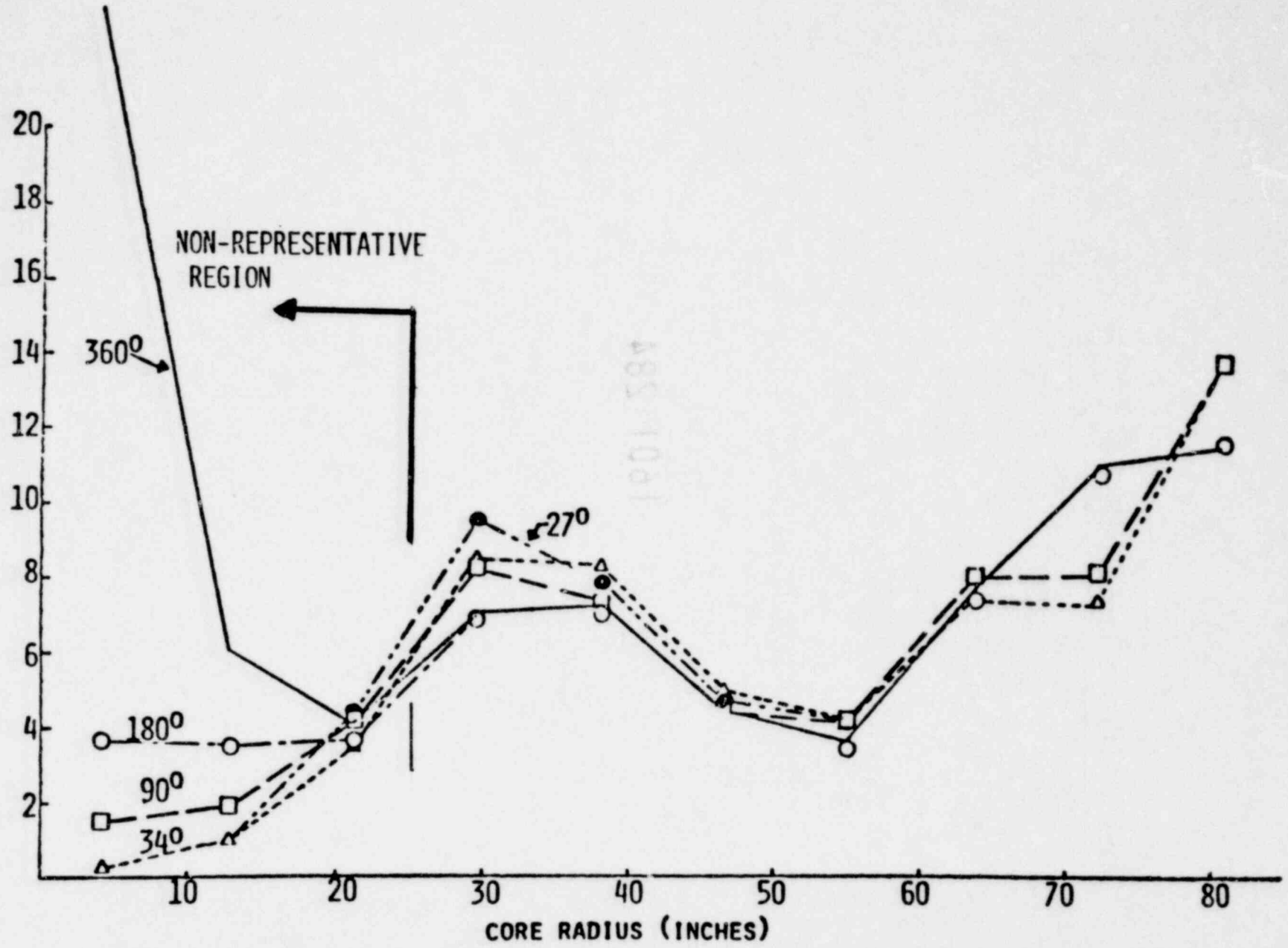

CORE SPRAY DISTRIBUTION AS A FUNCTION OF SECTOR SIZE

GEC
11/6/79

COMPARISON OF SSTF DATA TO PRE-TEST PREDICTION FOR LPCS OPERATION

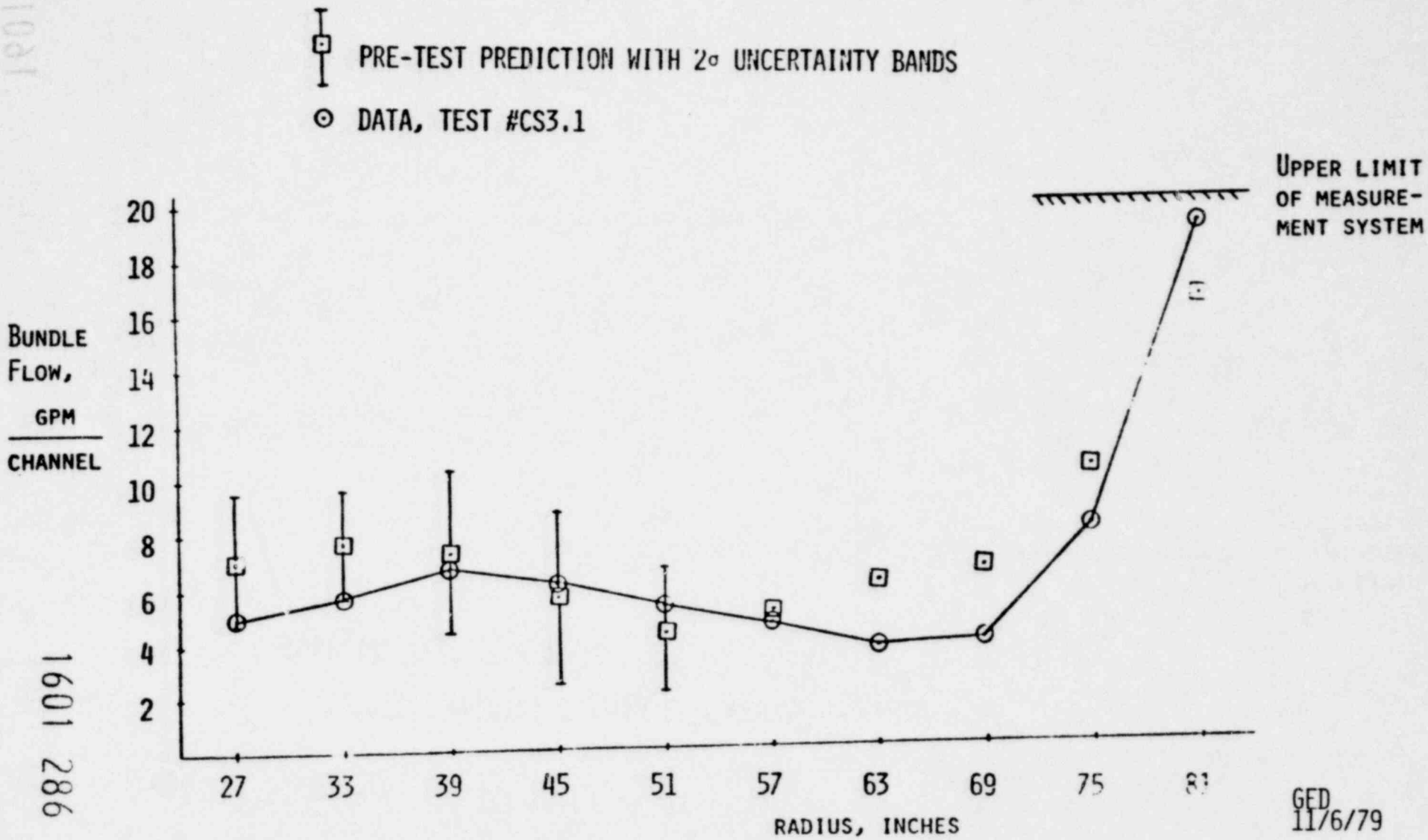

GED
11/6/79

COMPARISON OF SSTF DATA TO PREDICTION FOR HPCS OPERATION

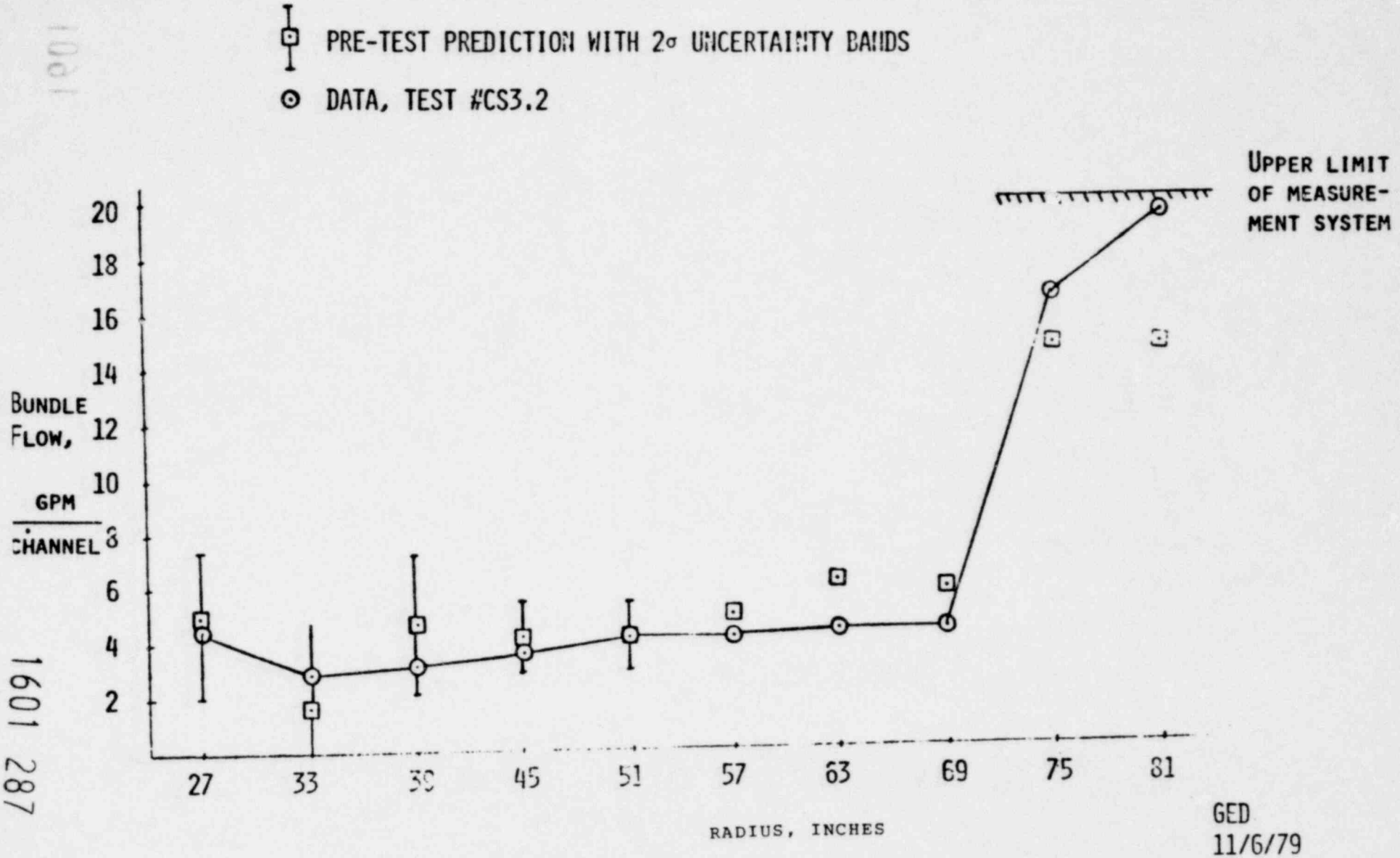

CONCLUSIONS

- KEY PHENOMENA UNDERSTOOD
- EMPIRICALLY-BASED MODEL DEVELOPED
  - NEAR NOZZLE CONDENSATION EFFECTS
  - FAR REGION INTERACTION EFFECTS
- QUALIFICATION TESTS SUCCESSFUL

GED
11/6/79

AN IMPROVED RELAP4 JET PUMP MODEL

Presented at
The Seventh Water Reactor Safety Research Information Meeting
November 5-9, 1979
Gaithersburg, Maryland

T. R. Charlton
EG&G Idaho, Inc.

Idaho National Engineering Laboratory
Idaho Falls, Idaho 83401

AN IMPROVED RELAP4 JET PUMP MODEL

T. R. Charlton
EG&G Idaho, Inc.

A RELAP4 boiling water reactor (BWR) jet pump model development effort was conducted to attain a new RELAP4 BWR jet pump model from test data. Results from the Jet Pump Test and Model Development Program conducted at the Idaho National Engineering Laboratory (INEL) are being used. The overall program consisted of three phases: subscale testing, model development, and model evaluation. This summary briefly describes the program and model, and also provides a model evaluation.

Since little off-design (operational conditions outside the range considered during normal operations) jet pump behavior data was available for model development and evaluation, 1/6 scale tests were performed in the LOFT Tests Support Facility at the INEL to supplement the data base. Both subcooled steady state and two-phase transient tests were performed for a wide range of environmental conditions. During steady state tests, the jet pump was operated extensively for on- and off-design flow patterns, providing over 200 data points. The transient tests approximated flow patterns found in BWR jet pumps during a loss-of-coolant accident. Model evaluation was performed using data from this program, the General Electric Company Two-Loop Test Apparatus, and full scale on-design data.

For two-stream mixing, as occurs in a jet pump, a momentum exchange term is used in the RELAP4 momentum equation. The model development goal was to rectify the two-stream momentum exchange term using knowledge gained from the steady state test data. Where possible, the original form of these terms was to be retained, thereby maintaining RELAP4 two-phase and scaling calculational capabilities.

Briefly, the procedure was to compare the original exchange term with an analogous value calculated from the data and to then correct discrepancies as required. Although these calculated values are biased by wall effects, turbulence, and other phenomena, trends and approximate magnitudes can be determined.

Although numerous flow patterns and associated exchange terms occur, only the suction terms with positive drive flow are presented. Both RELAP4 and data values are presented in Figure 1. For normal positive flow, the exchange term is fairly well understood and, in general, the original model represents the data. However, for reversed suction flow there is little similarity between the RELAP4 equation and the calculated value. Better agreement is achieved by extending the positive suction flow equation into the negative flow region as shown in Figure 1.

The performance of the new model is evaluated by performing RELAP4 jet pump calculations with that model and comparing the results to data. This comparison is shown in Figure 2 as a four-quadrant jet pump characteristic curve. Plotted are the improved model, the original model, and data from this program. The improvements are particularly evident in the second quadrant, the region of particular interest in model evaluation.

The improved jet pump model has also been compared to data from the General Electric Company Two-Loop Test Apparatus and full scale steady state data. The results of these comparisons have shown that the improved jet pump model provides better calculations of data than does the original model.

In summary, an improved RELAP4 jet pump momentum exchange model has been developed. The model is based on pump behavior observed in subscale tests. Although the improved model is of the same form as the original model, discrepancies between the original model and data have been rectified. Jet pump calculations with the improved model show substantial improvements over the original model.

REFERENCES

1. E. E. Ross, Jet Pump Test and Model Development Program Requirements and Plan, PG-R-77-33, (March 1978).

2. E. E. Ross, An Improved RELAP4 Jet Pump Model, CAAP-TR-046, (April 1979).

3. H. S. Crapo, One-Sixth Scale Model BWR Jet Pump Test, LTR-20-105 (August 1979).

4. RELAP4/MOD5 - A Complete Program for Transient Thermal-Hydraulic Analysis of Nuclear Reactors and Related Systems - User's Manual, Volume I ANCR-NUREG-1335 (September 1976).

5. G. W. Burnette and G. L. Sozzi, Two-Phase Pump Performance During Steady State Operation and During a Simulated LOCA Blowdown, NEDE-13239 (November 1971).

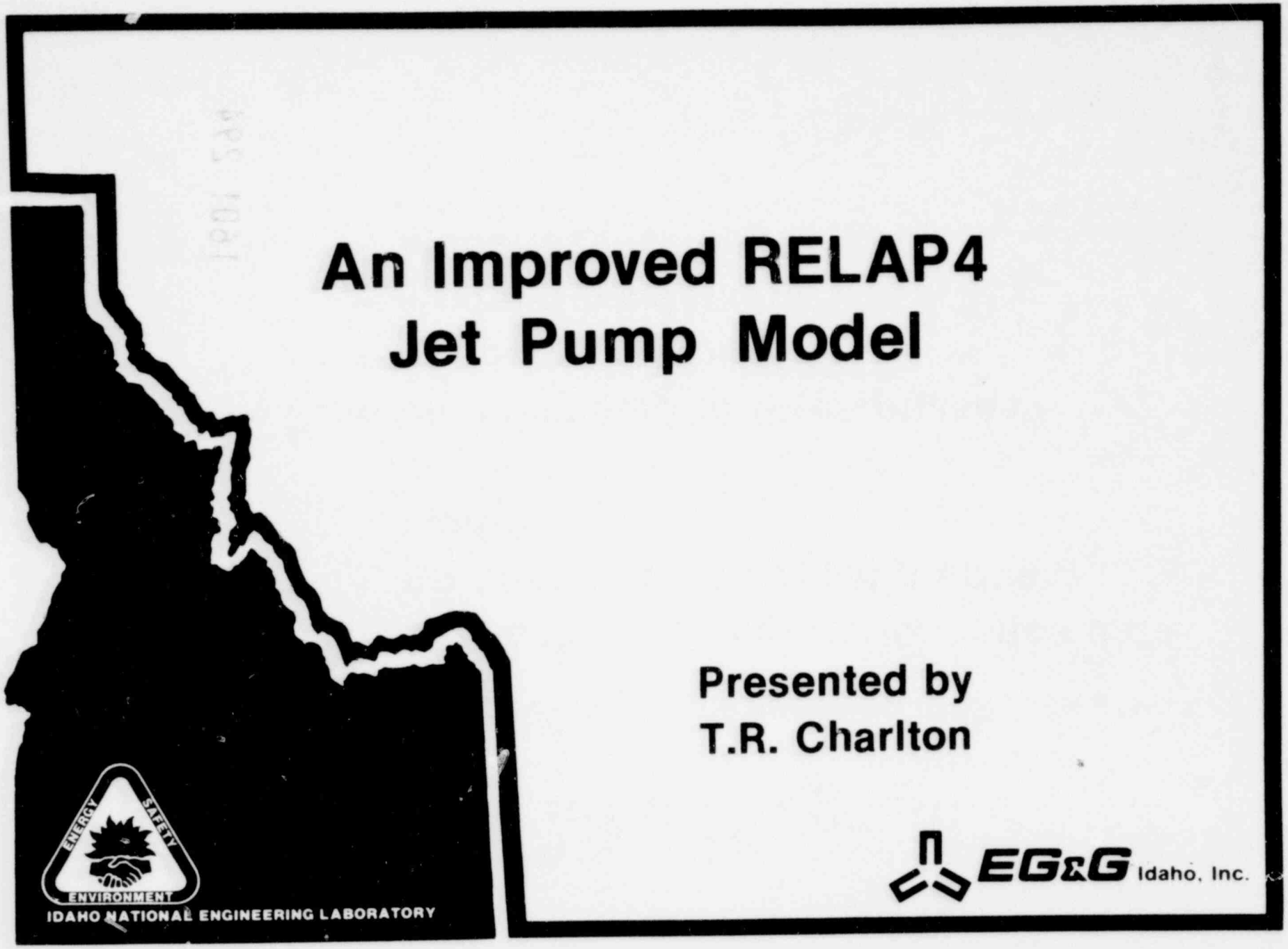

An Improved RELAP4 Jet Pump Model

Presented by
T.R. Charlton

EG&G Idaho, Inc.

Jet Pump Program

- Objectives
  - Subscale jet pump performance data
  - An improved analytical jet pump model

- Program consisted of three phases
  - Jet pump testing
  - Model development
  - Model assessment

INEL-S-21 476

Steady State Jet Pump Tests

- Over 200 data points were obtained
- Environmental variation from ambient to reactor operating conditions.
- Positive and negative flow through drive nozzle, suction nozzle, and discharge

INEL-S-21 475

Transient Jet Pump Tests

- One test to simulate the intact loop during a LOCA
- One test to simulate the broken loop during a LOCA

INEL-S-21 474

Jet Pump Test Assembly

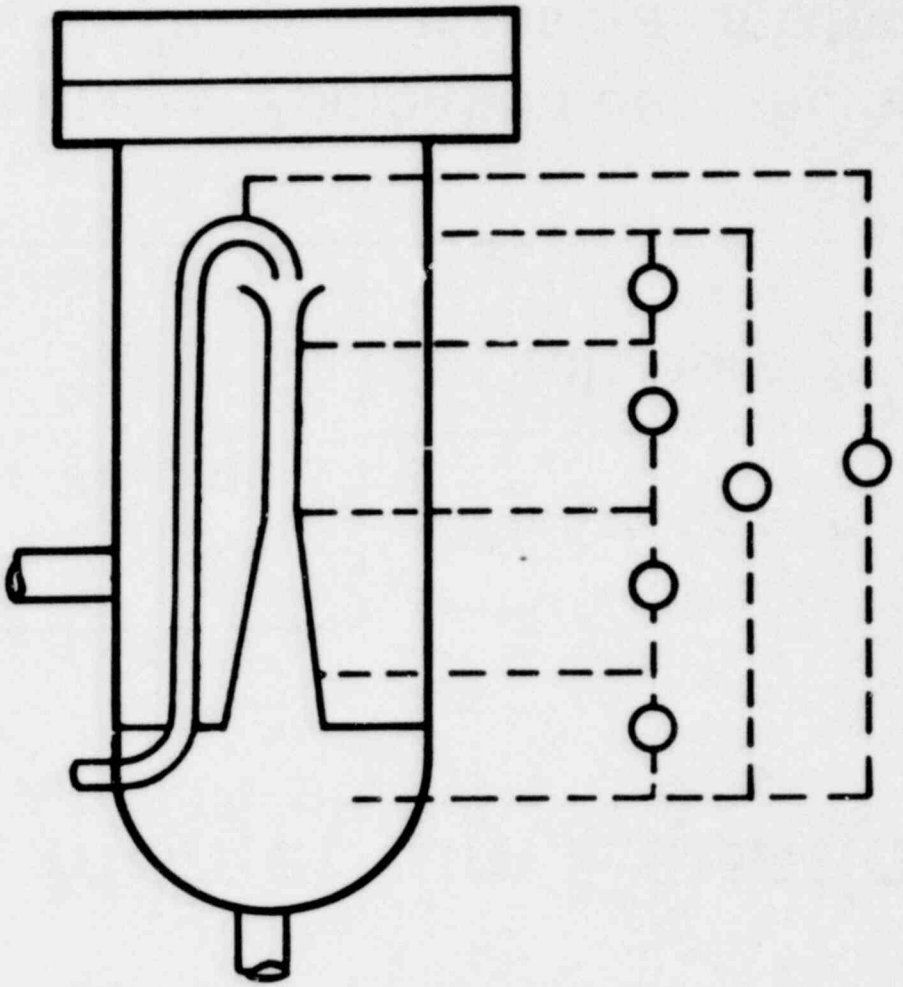

INEL-S-18 551
REVISION 1

RELAP4 Momentum Equation

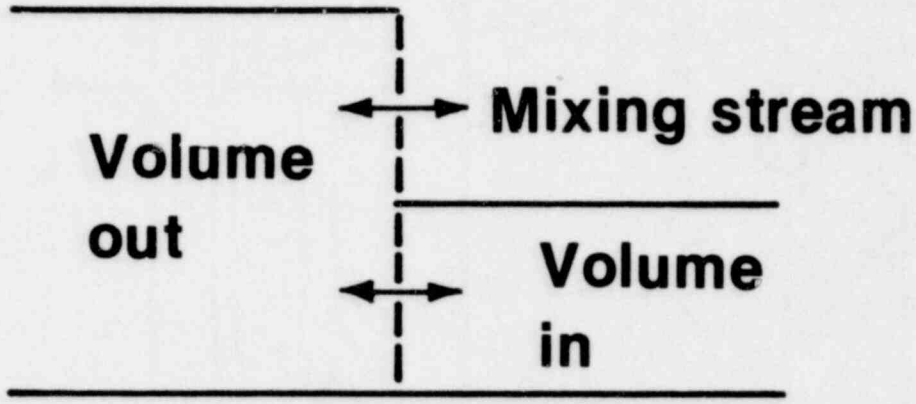

Transient terms = Momentum out - momentum in − losses + mixing term

INEL-S-18 552

Definition of M and N Ratios

$$M = \frac{W_2}{W_1}$$

$$N = \frac{\bar{P}_3 - \bar{P}_2}{\bar{P}_1 - \bar{P}_3}$$

$$\bar{P} = \frac{P}{\rho} + \frac{V^2}{2g_c}$$

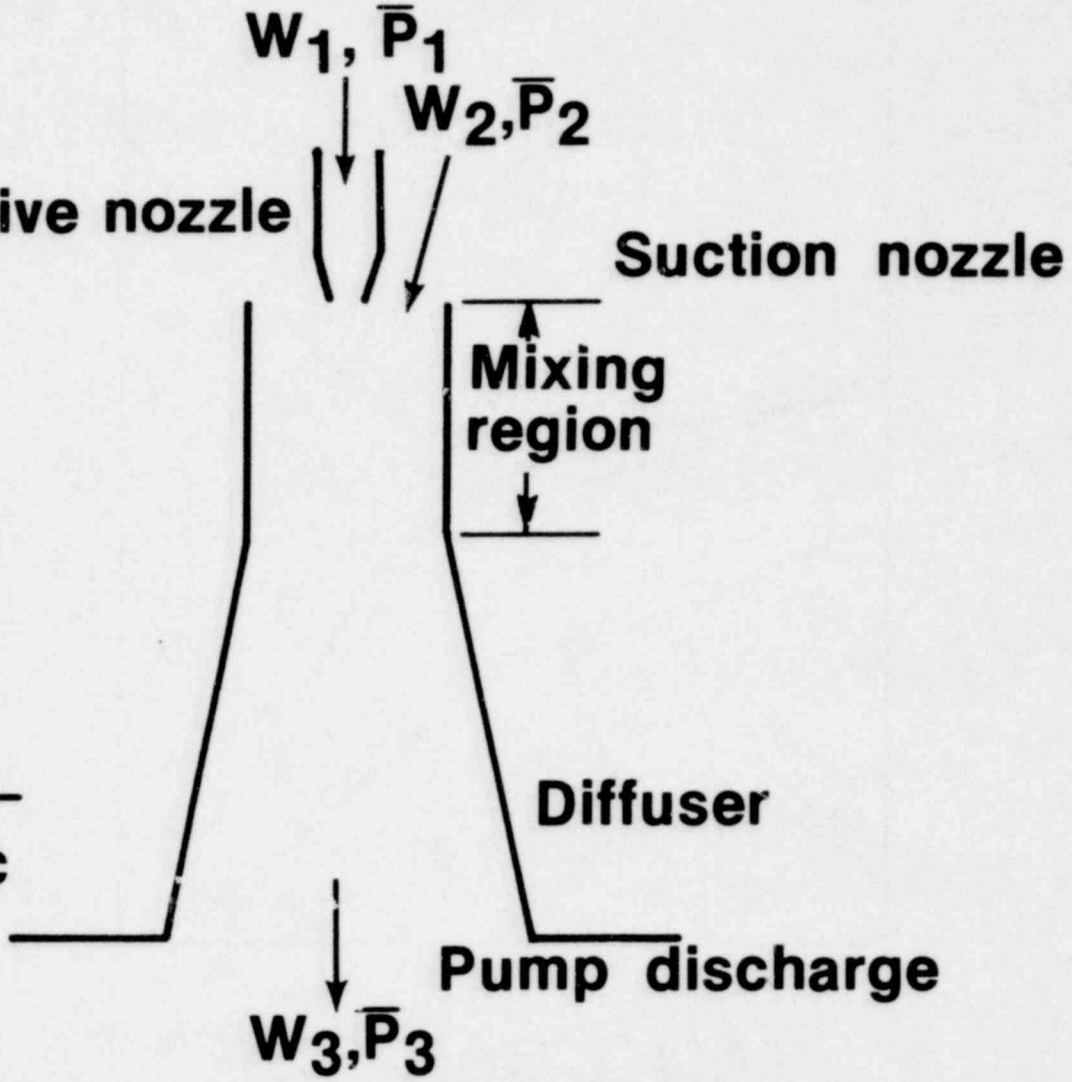

INEL-S-21 478

Suction Mixing Term
Positive Drive

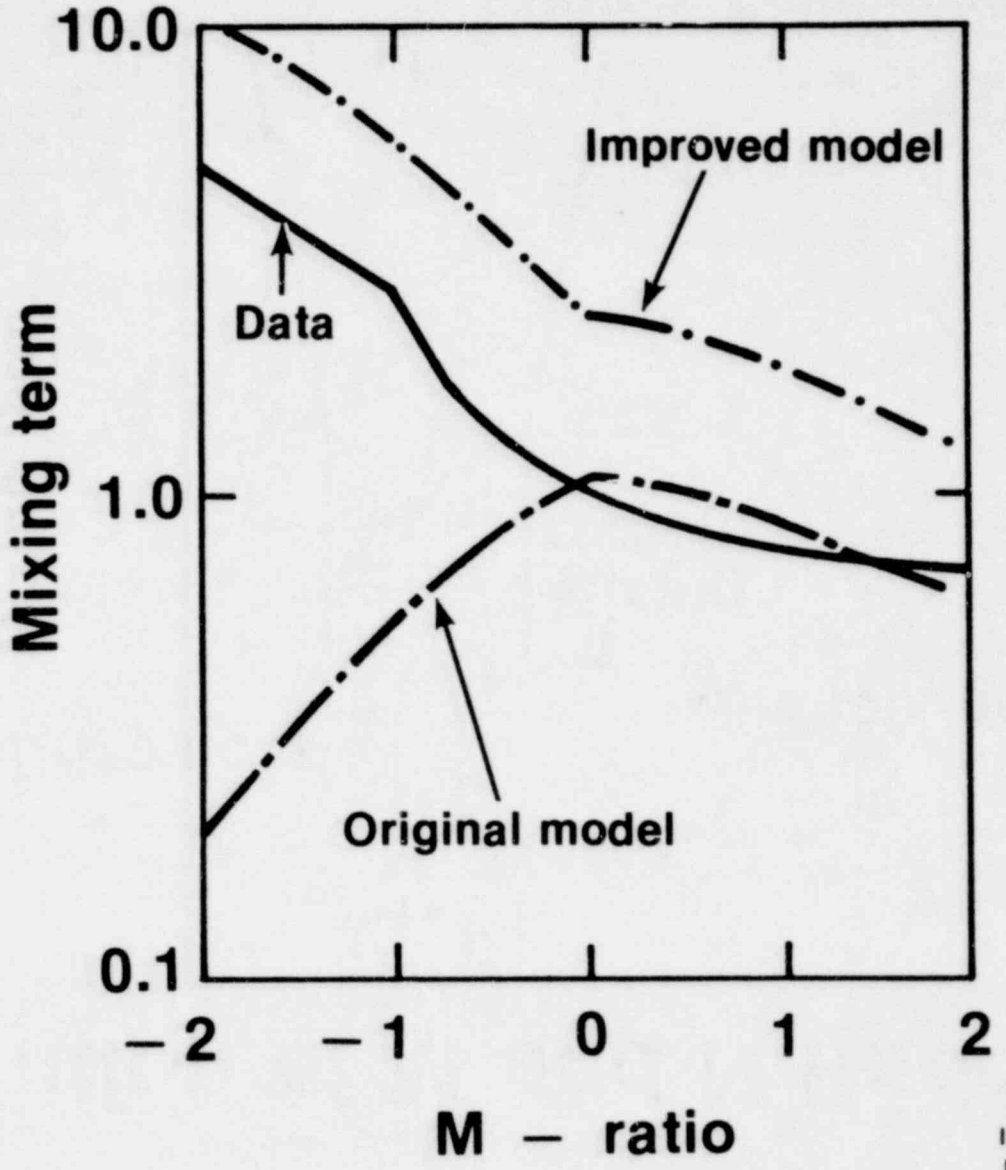

INEL-S-18 550
REVISION 1

M-N Curve — Original Model

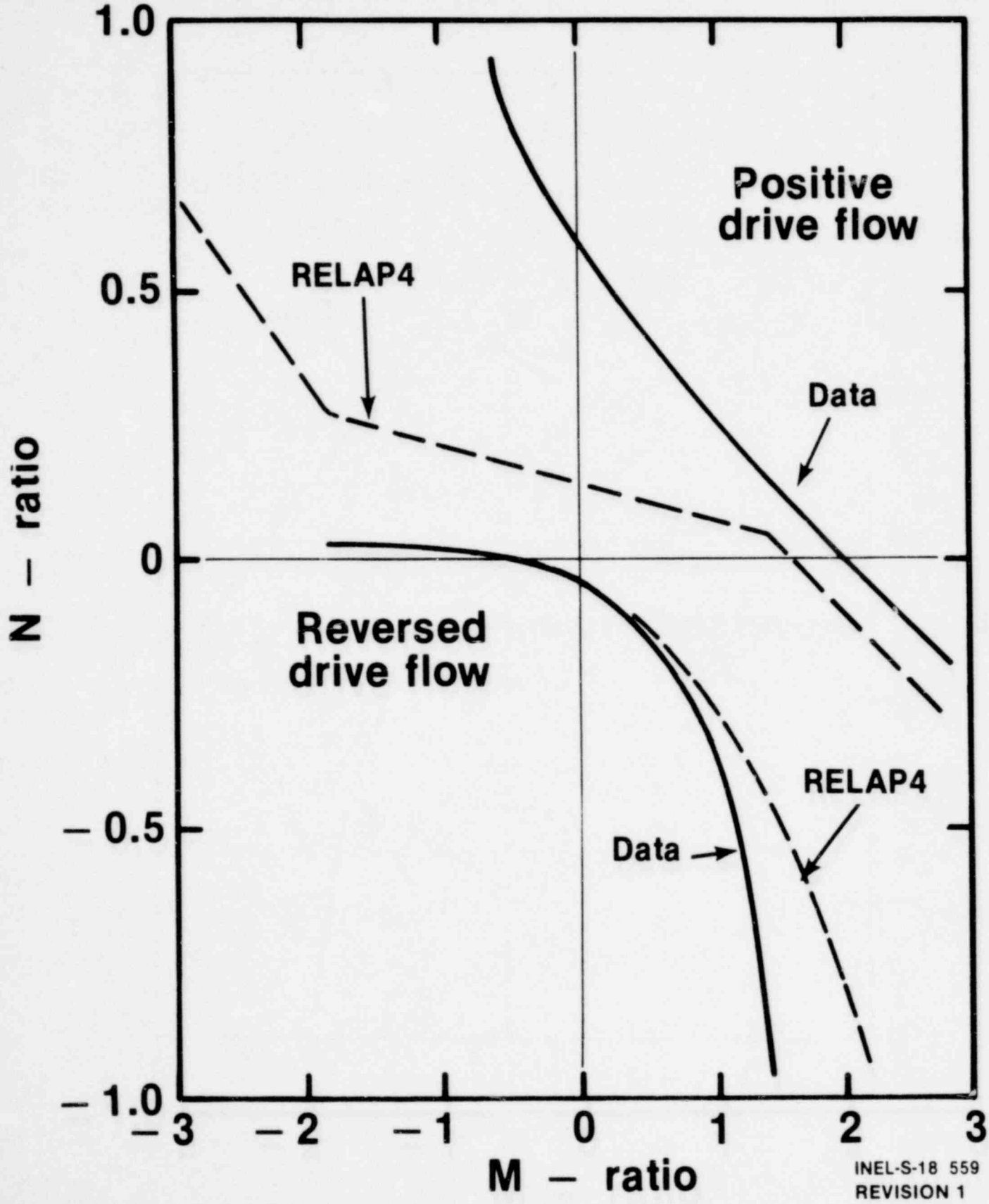

INEL-S-18 559
REVISION 1

M-N Curve — Improved Model

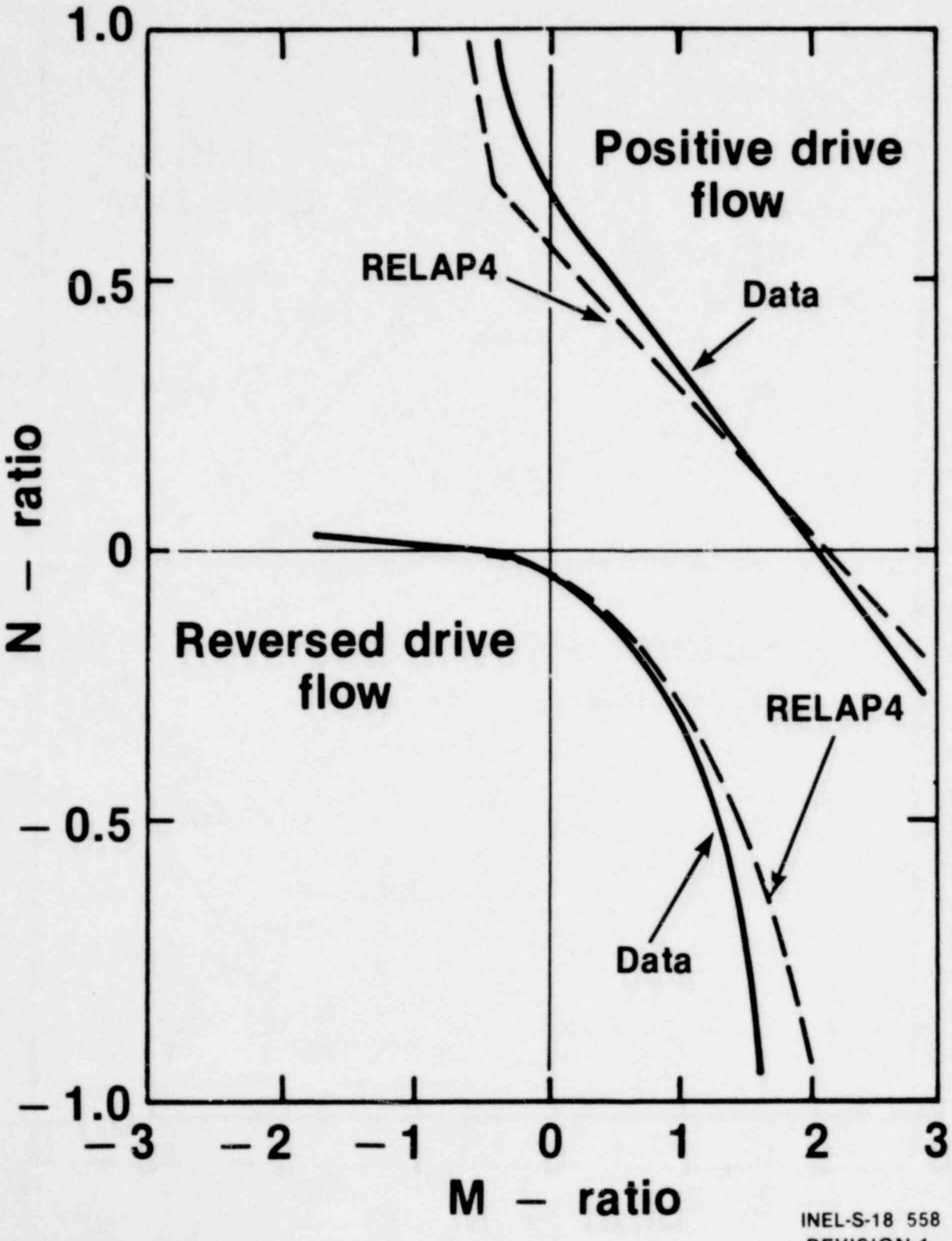

INEL-S-18 558
REVISION 1

Drive and Suction Flow for Intact Loop Simulation

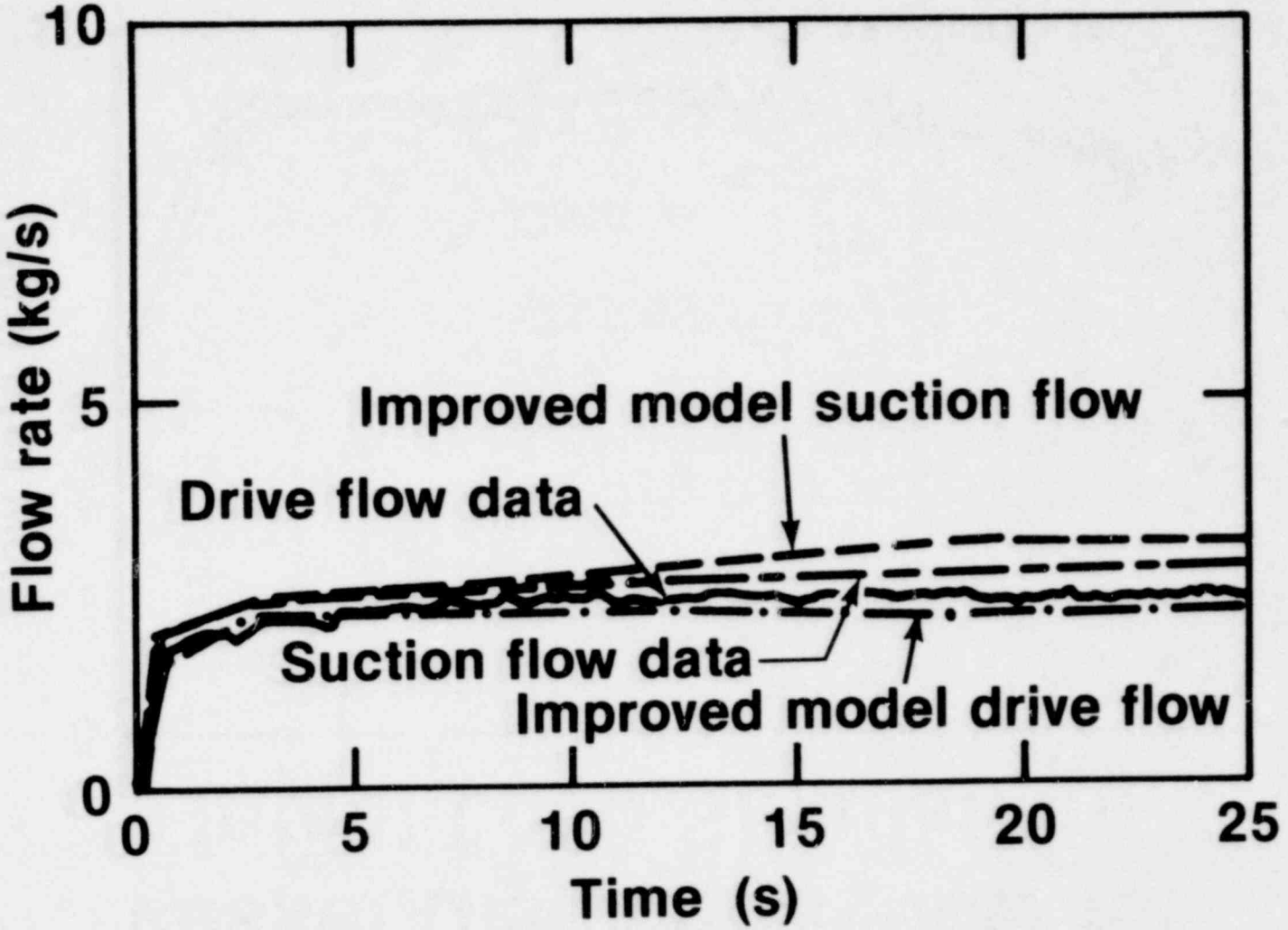

INEL-S-21 485

Vessel Discharge Flow for Intact Loop Simulation

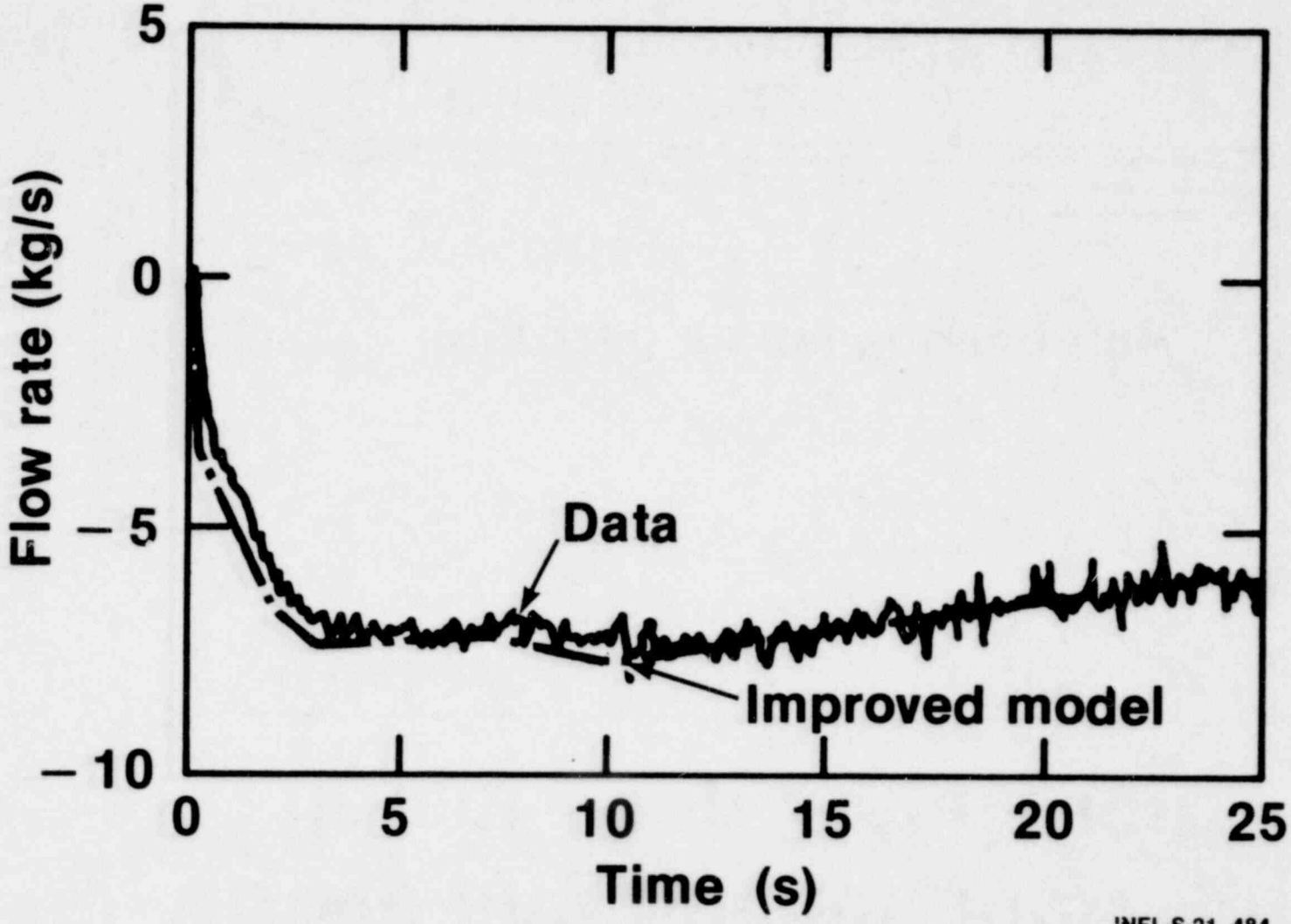

INEL-S-21 484

Suction and Discharge Flow for Broken Loop Simulation

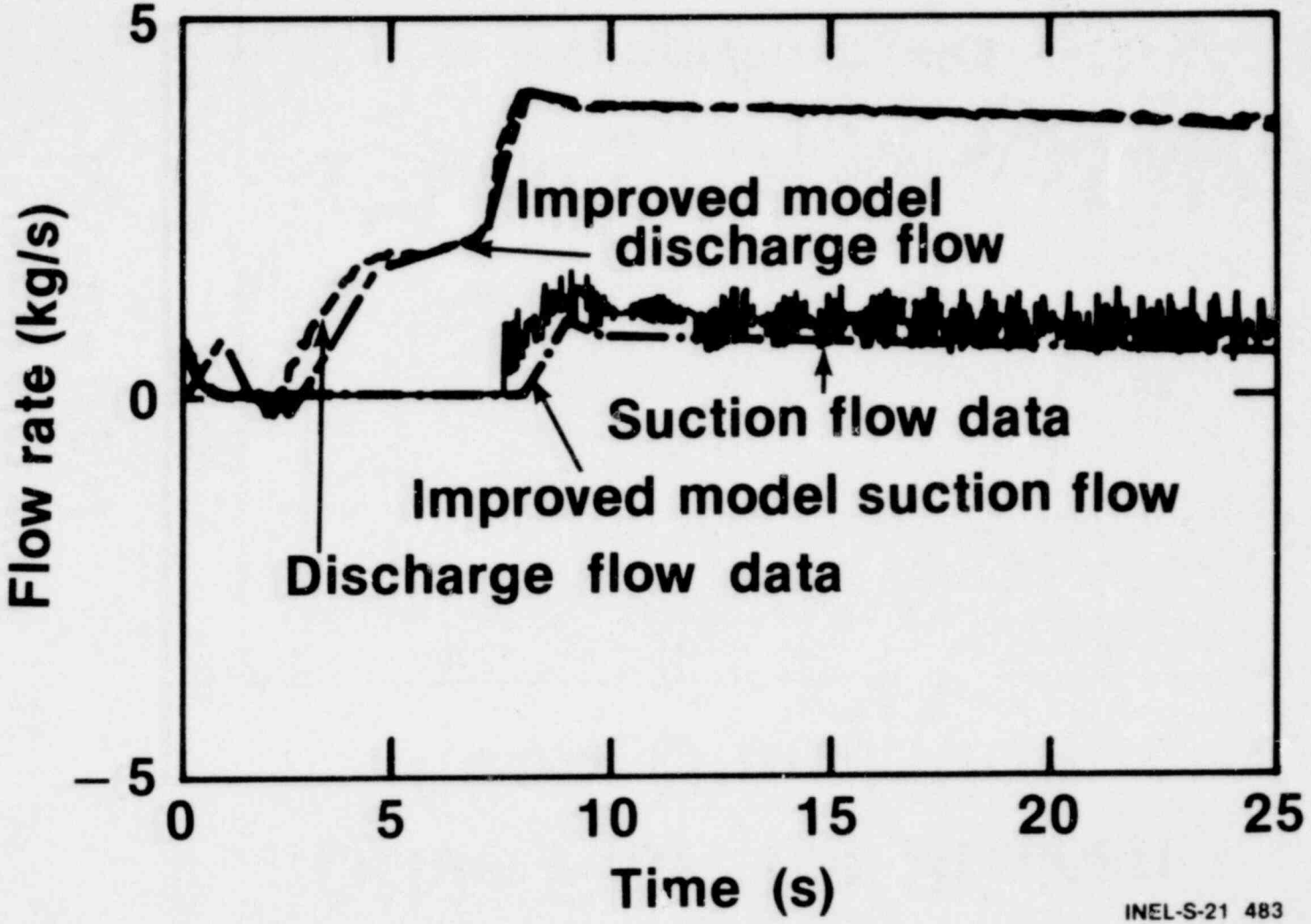

Drive Flow for Broken Loop Simulation

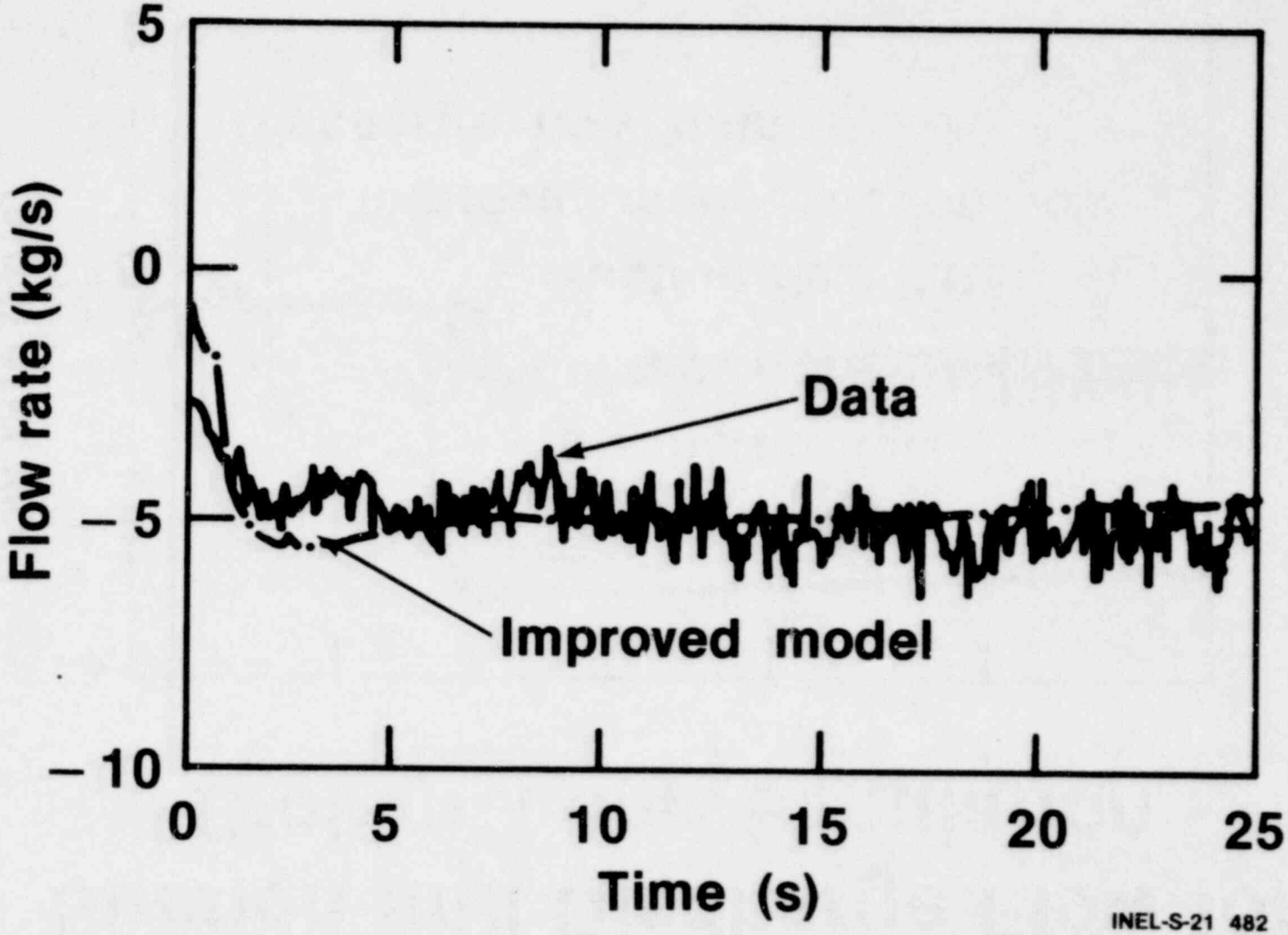

TLTA Intact Loop Jet Pump Flows

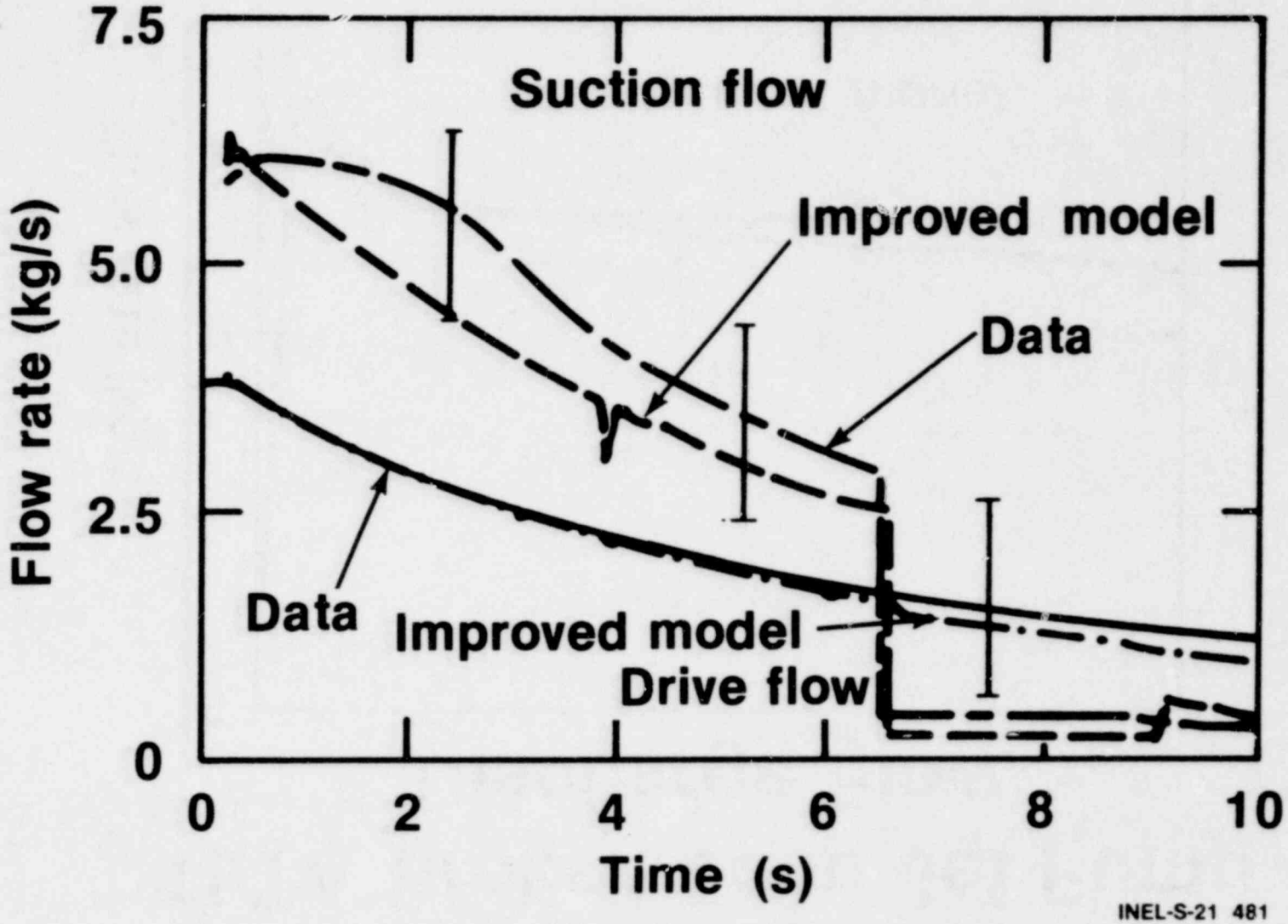

INEL-S-21 481

TLTA Broken Loop Jet Pump Discharge Flow

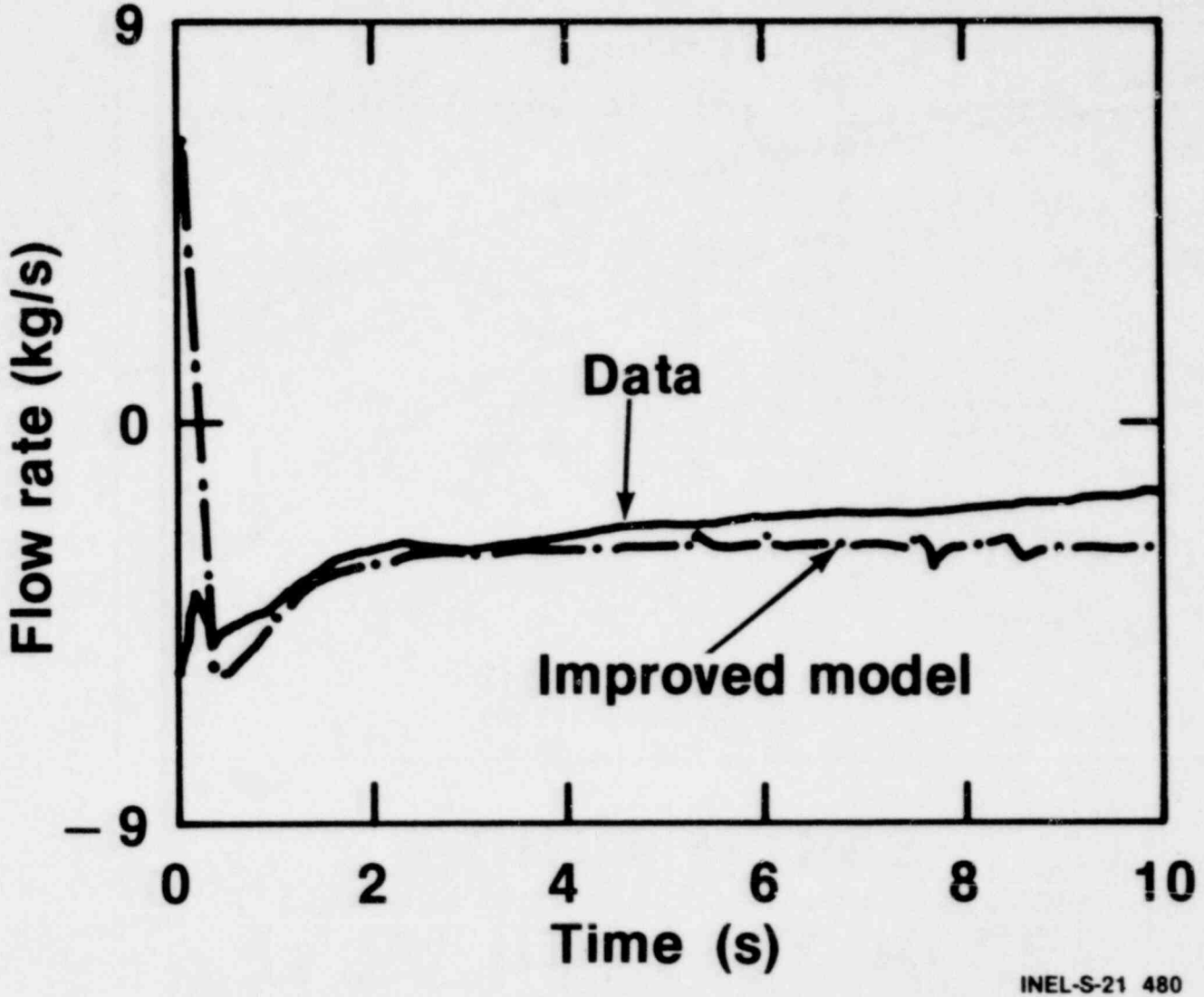

Improved Model Performance for Full Scale Pump

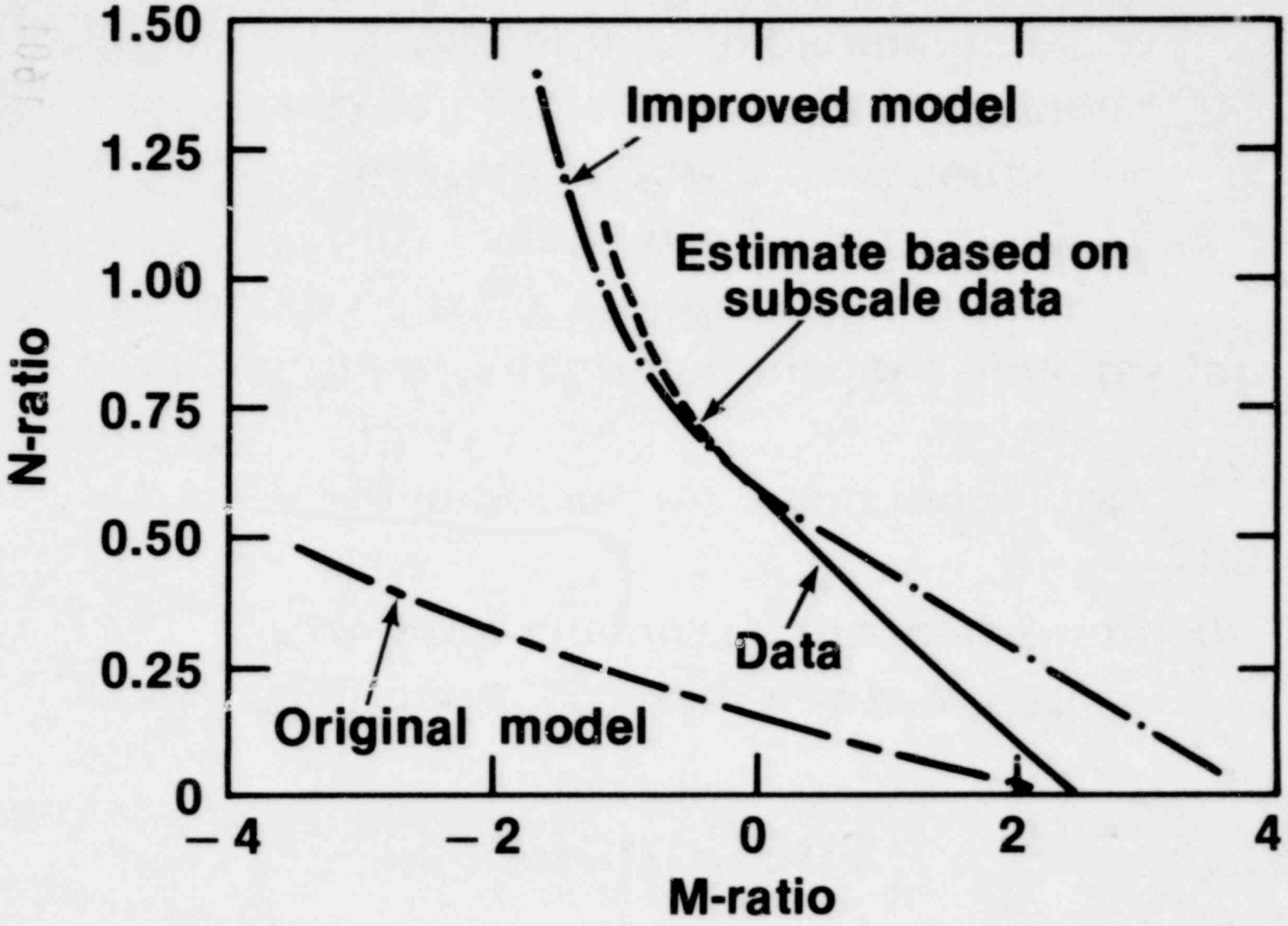

INEL-S-21 479

Conclusions

- The jet pump program has provided:
  - A large amount of subscale jet pump data
  - An improved jet pump model for RELAP4
- The RELAP4 jet pump model calculates jet pump behavior well for:
  - Small scale, two phase, transient, separate effects experiments
  - Small scale, two phase, transient, system effects experiments
  - Large scale, steady state, separate effects experiments

Summary Report Prepared for Light Water Reactor Safety Information Meeting
NBS, Gaithersburg, MD, November 5-9, 1979

NONEQUILIBRIUM PHASE CHANGE STUDIES

by
N. Abuaf, G. A. Zimmer, B.J.C. Wu, and O. C. Jones, Jr.
Brookhaven National Laboratory
Upton, New York 11973

OVERVIEW

A steady water loop with well-controlled flow and thermodynamic conditions (1500 ℓ/min, 100-1000 kPa, 20-150 °C) was made operational to measure the net vapor generation rates under nonequilibrium conditions. The test section consists of a converging-diverging nozzle (5 cm - 2.5 cm - 5 cm in diameter, 55.9 cm long) with 49 pressure taps along the nozzle and observation windows at the exit.

First the test section was calibrated hydrodynamically by static pressure measurements along the nozzle. Second, a set of flashing experiments were performed where pressure distributions and photographic observations were recorded under various flashing conditions. During these preliminary experiments, the effects of the various parameters on the pressure distributions and flashing regimes in the nozzle were investigated. For low back pressures or high mass fluxes a constant pressure region was observed all along the diverging section. For high back pressure or low flow rates, a recondensation zone was observed downstream of the flashing onset.

Using a single channel low activity γ-densitometer a third set of flashing experiments were conducted, where in addition to the pressure distributions, the chordal averaged void fraction profiles were also recorded. With flashing inception close to the nozzle throat, and for a given inlet temperature, a wide range of void profiles was observed by varying the inlet mass flux. For flows with a constant pressure distribution in the diverging section, a linear variation in the void profiles coupled with a linear variation of the diameter suggested the presence of a nearly constant area liquid jet at the core surrounded by a steam envelope.

Using a five beam high activity γ densitometer, a fourth set of flashing experiments were conducted where the pressure distributions and radial chordal void fractions at several axial locations, as well as area-averaged void fraction profiles were recorded under various flashing conditions.

For the previously reported flashing experiments, the measured wall static pressure distributions were combined with both the centerline axial void fraction profiles and the area-averaged void fraction profiles to calculate the volumetric vapor generation rates under nonequilibrium flashing conditions.

MODELING OF FLASHING INCEPTION

In Pipes The superheat at flashing inception in the experiments of Reocreux and Seynhaeve seemed to vary inversely with the mass flux. It was assumed that decompressive flashing inception can be characterized by initial temperature, decompression rate and degree of liquid turbulence. This implies that turbulent pressure fluctuations may lower the instantaneous local fluid pressure below the mean value thus ocasionally reaching pressures capable of

causing flashing inception. By estimating an appropriate band on the turbulent velocity fluctuations, an adequate representation of the inverse mass flux effect on the dynamic flashing inception for existing data was obtained.

In Nozzles In addition to our experimental data, the data of Brown, Sozzi and Sutherland and Simoneau were also analyzed and investigated for the flashing inception under various subcooled inlet flow conditions. Assuming that the liquid remained liquid all the way from the inlet of the nozzle to the throat independent of its inlet subcooling, the inlet to throat pressure difference divided by the throat kinetic energy was correlated to the throat mass flux through the single phase discharge coefficient concept. This fact implies that once the inlet conditions are subcooled in a nozzle, the flashing, even if it occurred upstream of the throat, does not cause a major change in the density and has little effect on the static pressure measurements in the converging section from inlet to throat. When the local superheat pressures are plotted as a function of the local depressurization rates and compared to the onset correlation of Alamgir and Lienhard one observes that onset occurs always between the pressure taps before the nozzle throat and the throat.

PRESSURE DISTRIBUTION, VOID PROFILES, AND VAPOR GENERATION RATES

The experimental results were also compared with TRAC-P1A steady-state predicitons. Here the inlet mass flux is underpredicted by TRAC. The pressure distributions in the nozzle do not show as large a pressure drop as the ones observed experimentally. This discrepancy decreases as the onset of flashing in the nozzle is close to the equilibrium saturation state. The area averaged void fraction profiles calculated by TRAC were compared to chordal-averaged experimental results. During the presentation, the area-averaged profiles that are being obtained now will be compared to TRAC predictions. The vapor generation rates were also calculated from the TRAC output.

Flashing flow of an intially subcooled liquid in a converging-diverging nozzle may be considered as a combination of three regions: a frozen expansion from the entrance to the flashing inception point, followed by a nonequilibrium transition zone at the end of which the fluid returns to thermodynamic equilibrium, and finally, an equilibrium expansion region. Conservation laws across the transition zone are valid regardless of the actual transition process, and may be used to relate the states across this zone with two different equations of states. A one-dimensional treatment of this problem has been undertaken, and "jump" conditions, Rankine-Hugoniot relations and the Hugoniot curves have been obtained. However, preliminary results indicate the maximum wave speed (corresponding to the Chapman-Jouguet point) to be too low compared with the experimental value.

Publications:

Abuaf, N., Feierabend, T. P., Zimmer, G. A., and Jones, O. C., Jr. Radio frequency (r-f) probe for bubble size and velocity measurements, BNL-NUREG-50997, March 1979; Rev. Sci. Instrum. (in press).

Abuaf, N., Jones, O. C., Jr., Zimmer, G. A. Response characteristics of optical probes, BNL-NUREG-24479, December 1978; ASME paper 78-WA/HT-3, 1978.

Abuaf, N., Jones, O. C., Jr., and Zimmer, G. A. Optical probe for local void fraction and interface velocity measurements, BNL-NUREG-50791, March 1978; Rev. Sci. Instrum., 49(8), 1978.

Abuaf, N, Zimmer, G. A., and Jones, O. C., Jr., BNL instrumentation research program, BNL-NUREG-26-51, April 1979.

Jones, O. C., Abuaf, N., Zimmer, G. A., and Feierabend, T., Void fluctuation dynamics and measurement techniques, BNL-NUREG-26466, paper presented at the Joint U. S. Japan Exchange on Two-Phase Flow Dynamics, Osaka, Japan, August 1-3, 1979.

Jones, O. C. Inception and development of voids in flashing liquids, BNL-NUREG-26464, paper presented at the Joint U. S. Japan Exchange on Two-Phase Flow Dynamics, Osaka University, Osaka, Japan, August 1-3, 1979.

Jones, O. C., Saha, P., Wu, B.J.C., and Ginbserg, T. Condensation induced water hammer in steam generators, to be published, paper presented at the Joint U. S. Japan Exchange on Two-Phase Flow Dynamics, Osaka University, Osaka, Japan, August 1-3, 1979.

Jones, O. C., Jr., et al. Reactor Safety Research Program Quarterly Progress Report, January 1-March 31, 1978, BNL-NUREG-50820.

Jones, O. C., Jr. and Saha, P. Nonequilibrium aspects of water reactor safety, BNL-NUREG-23143, July 1977.

Jones, O. C., Jr. Flashing inception in flowing liquids, BNL-NUREG-April 1979; Nonequilibrium Interfacial Transport Processes, ASME, 1979.

Jones, O. C., Jr. et al. Reactor Safety Research Program. Quarterly Progress Report, April-June 1978, BNL-NUREG-50883; July-September 1978, BNL-NUREG-50931; October-December 1978, BNL-NUREG-50978; January-March 1979, BNL-NUREG-51015; April-June 1979, BNL-NUREG-

Saha, P. A review of two-phase steam-water critical flow models with emphasis on thermal nonequilibrium, BNL-NUREG-50907, September 1978.

Publications: (Cont'd)

Wu, B.J.C., Saha, P., Abuaf, N., and Jones, O. C., Jr. A one dimensional model of vapor generation in steady flashing flow, BNL-NUREG-25709, March 1979; ANS Trans., 32, 1979.

Zimmer, G. A., Wu, B.J.C., Leonhardt, W. J., Abuaf, N., and Jones, O. C., Jr. Pressure and void distributions in a converging-diverging nozzle with nonequilibrium water vapor generation, BNL-NUREG-26003, April 1979.

Zimmer, G. A., Wu, B.J.C., Leonhardt, W. J., Abuaf, N., and Jones, O. C., Jr. Experimental investigations of nonequilibrium flashing of water in a converging-diverging nozzle, BNL-NUREG-25716, April 1979; Nonequilibrium Interfacial Transport Processes, ASME, 1979.

NONEQUILIBRIUM PHASE CHANGE STUDIES

BY

N. ABUAF, G. A. ZIMMER, B.J.C. WU AND O.C. JONES, JR.

BROOKHAVEN NATIONAL LABORATORY

UPTON, NEW YORK 11973

OBJECTIVES

- Investigate Nonequilibrium Vapor Generation in Flashing Flows
  - Inception
  - Interfacial Transfer
  - Interfacial Area Density
- Compare Results With Analytical Expressions for Nonequilibrium Vapor Generation Rates
  - Analytical Models
  - Code Modeling

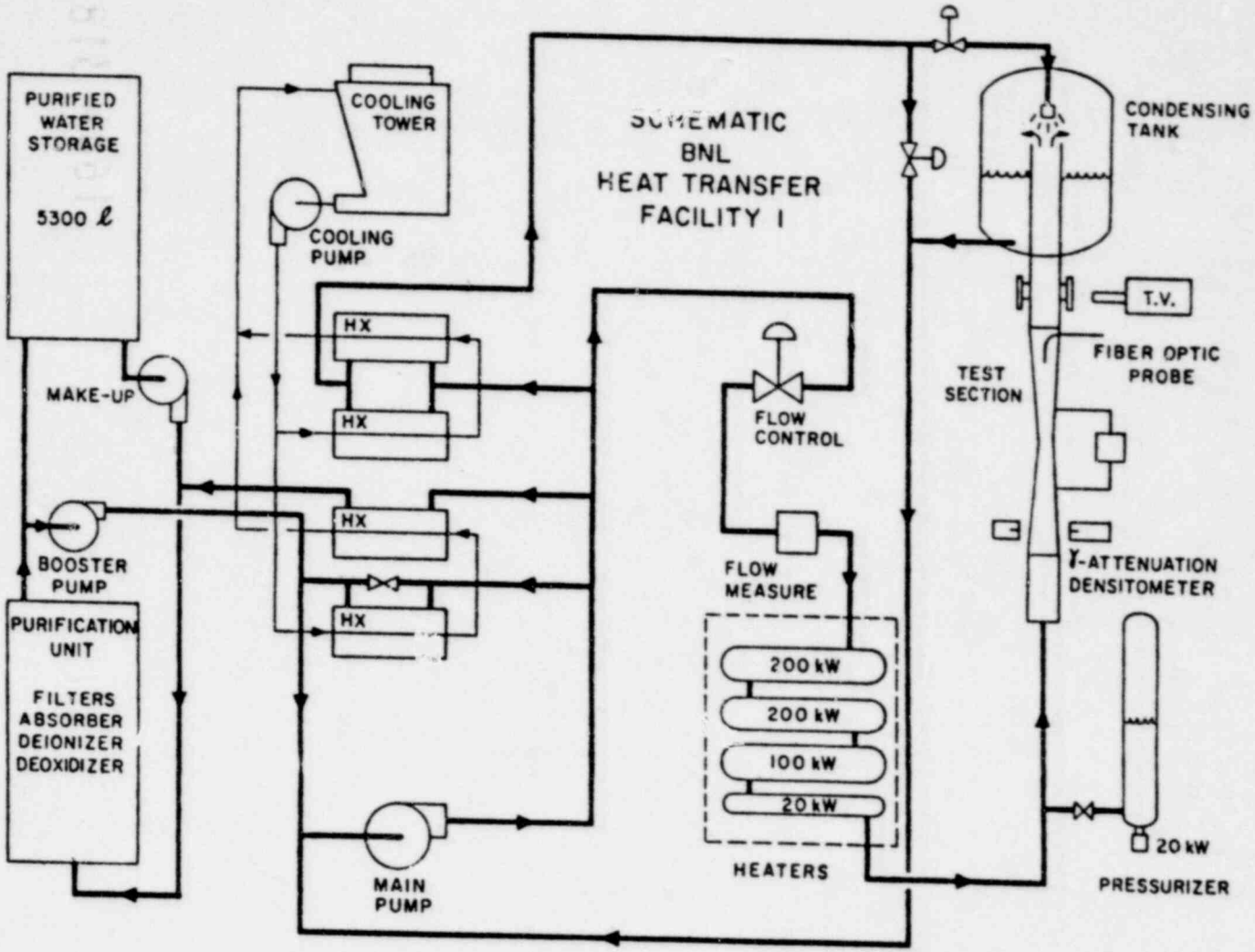

TEST FACILITY

TS-2 TEST SECTION

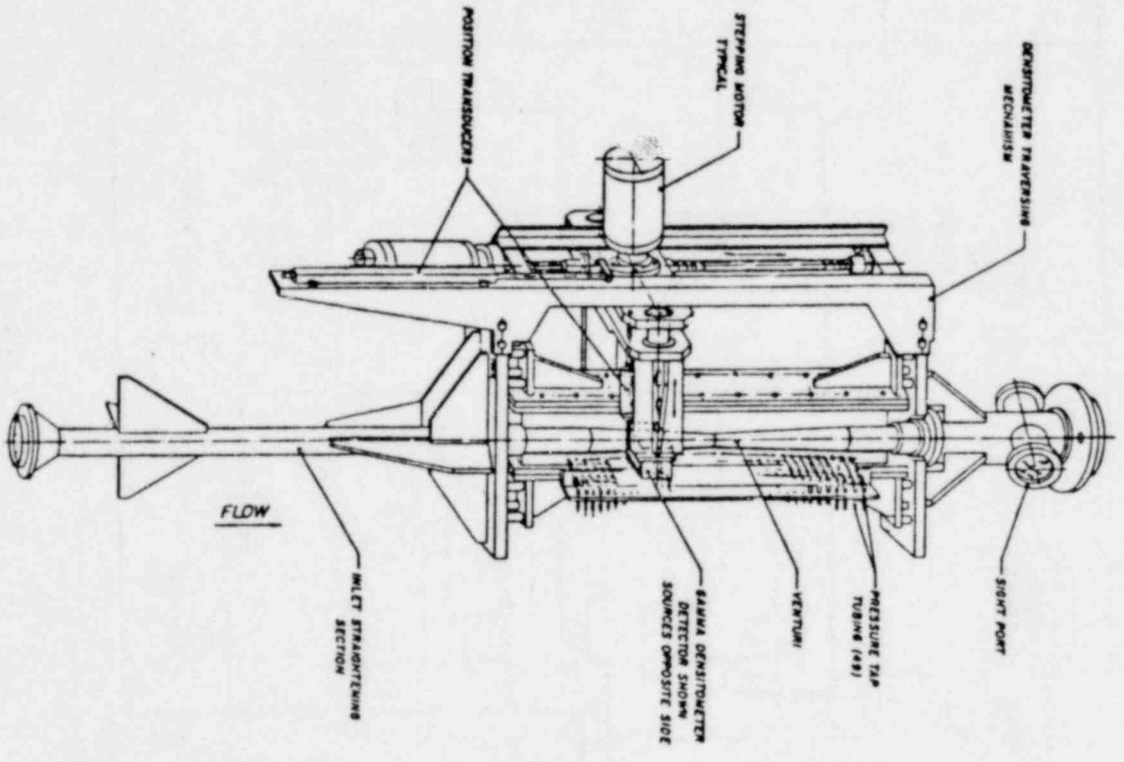

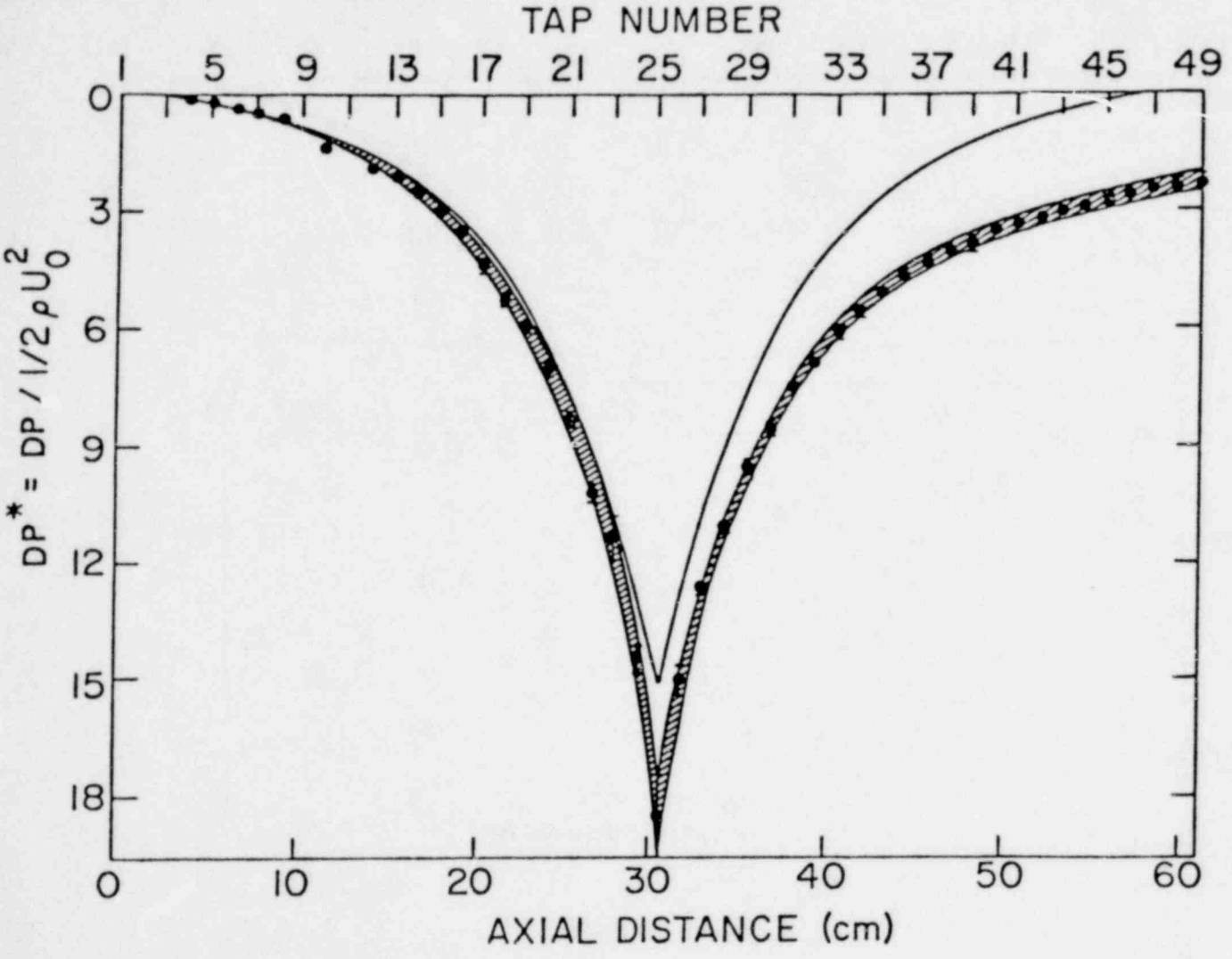

SINGLE-PHASE VENTURI CALIBRATION EFFECTIVE AREA (MOMENTUM DEFECT)

TYPICAL EXPERIMENTAL RESULTS

TWO-PHASE PRESSURE PROFILES

SYMBOL	RUN	G(MG/M^{2}S)	P_{IN}(KPA)	T_{IN}(C)	P_{CT}(KPA)
◇	23	1.81	130	99.4	121
□	22	3.04	170	100.2	125
△	20	4.90	281	98.3	245
○	21	6.01	393	100.6	136

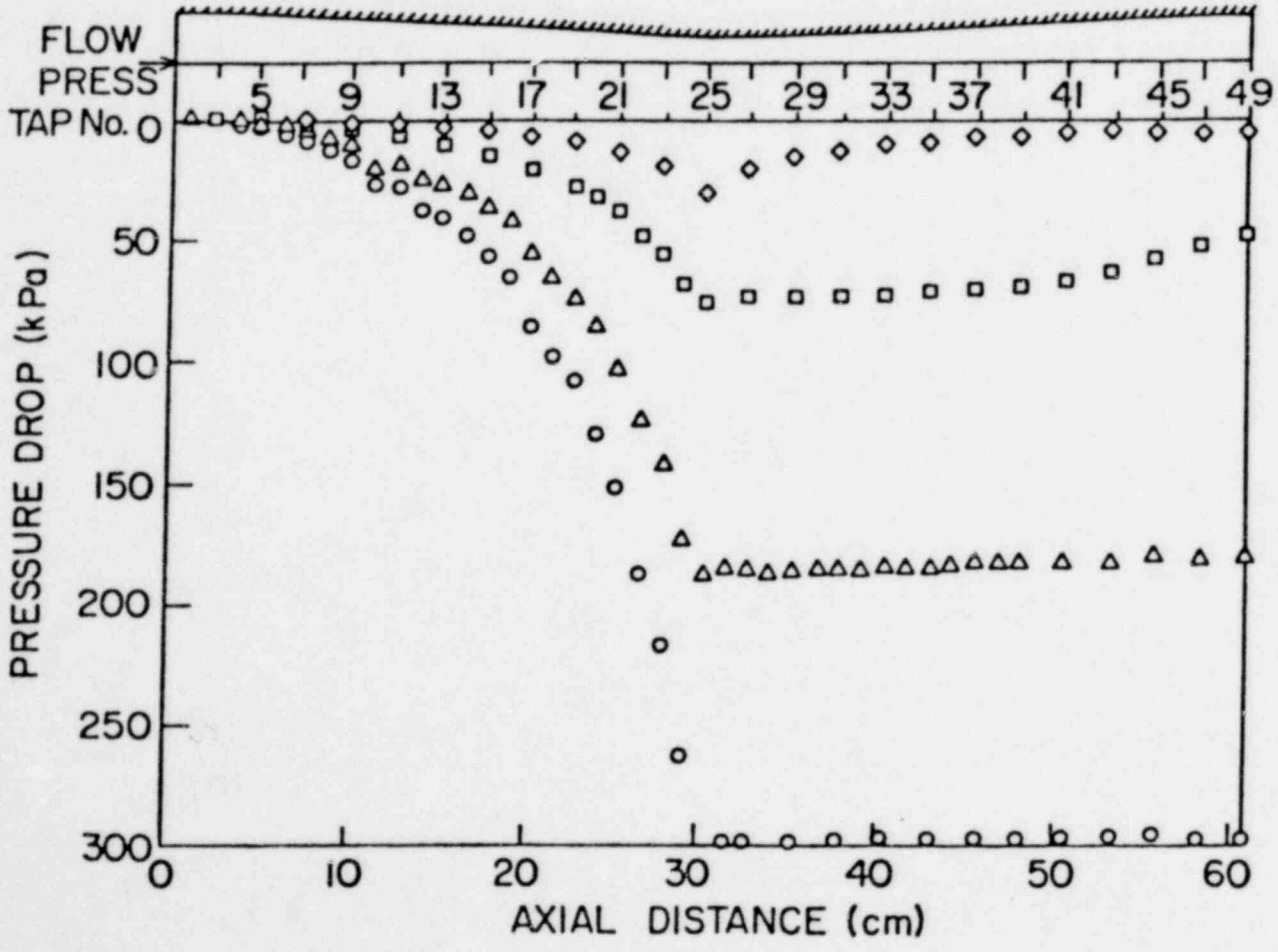

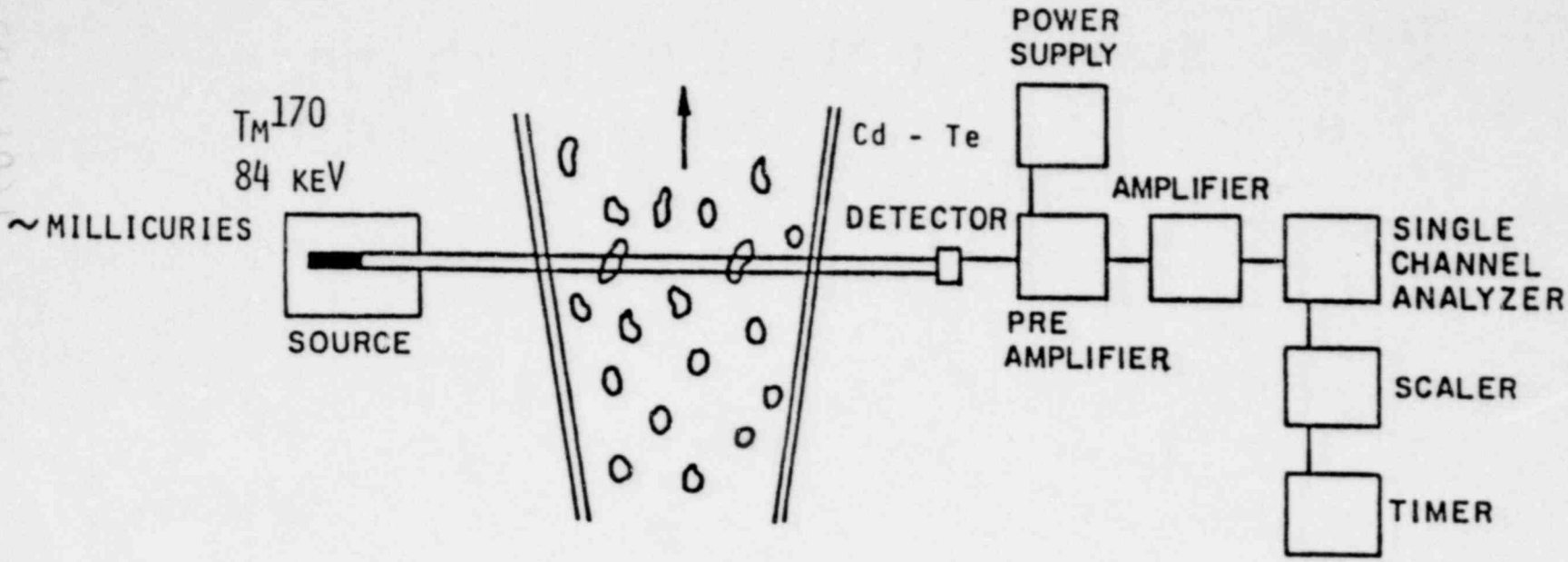

$$\alpha = 1 - \frac{\rho_{\ell c}}{\rho_{\ell m}} \frac{\ell n(I_{2\phi}/I_e)}{\ell n(I_f/I_e)}$$

GAMMA DENSITOMETER

PRESSURE AND PRESSURE DEVIATION RESULTS TOGETHER WITH VOID FRACTION RESULTS

FLASHING WITH CONDENSING

1601 322

PRESSURE AND PRESSURE DEVIATION RESULTS TOGETHER WITH VOID FRACTION RESULTS

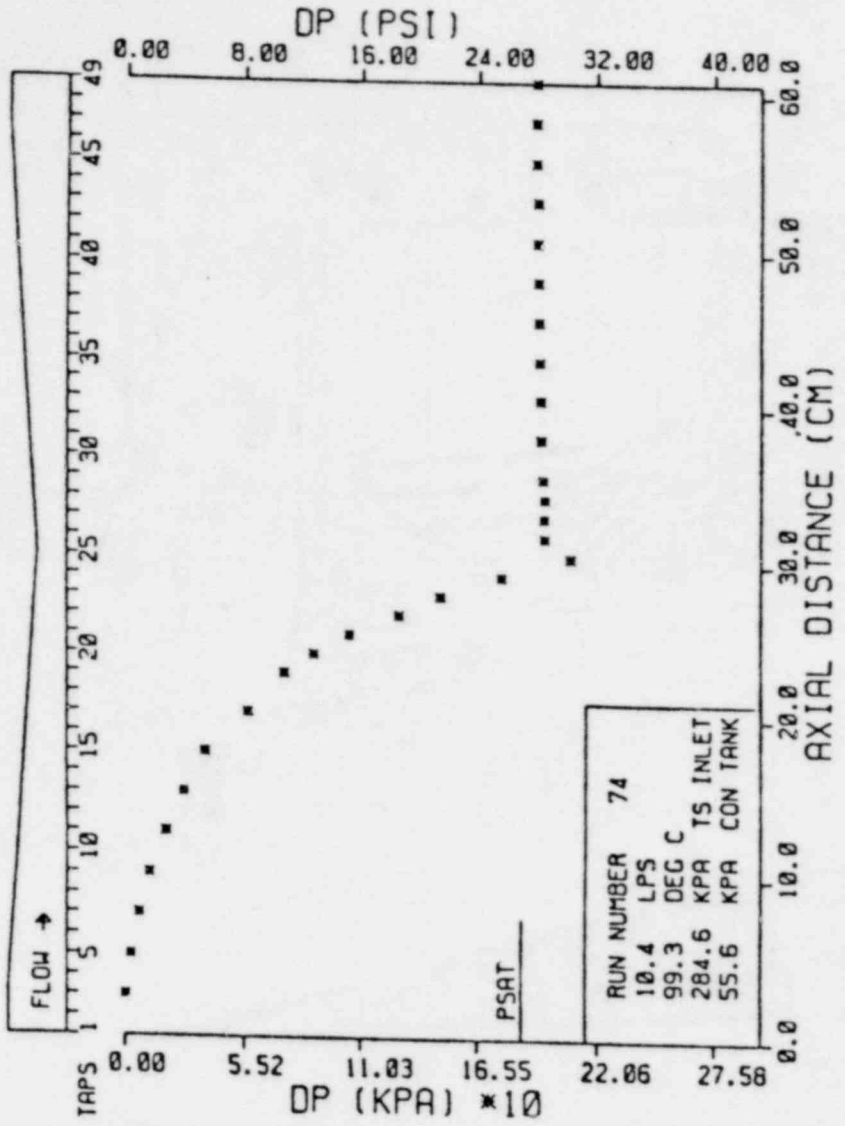

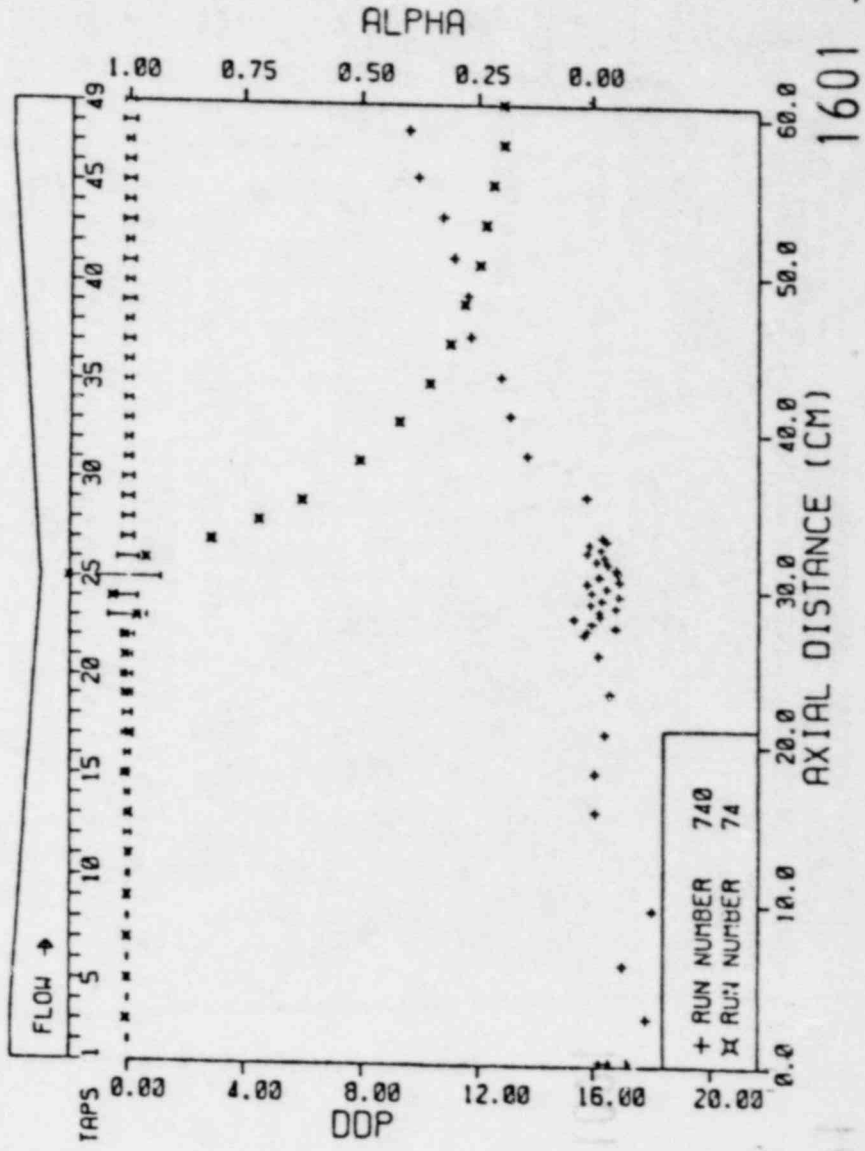

1601 523

FLASHING ONLY

MULTI-BEAM GAMMA DENSITOMETER

1601 32

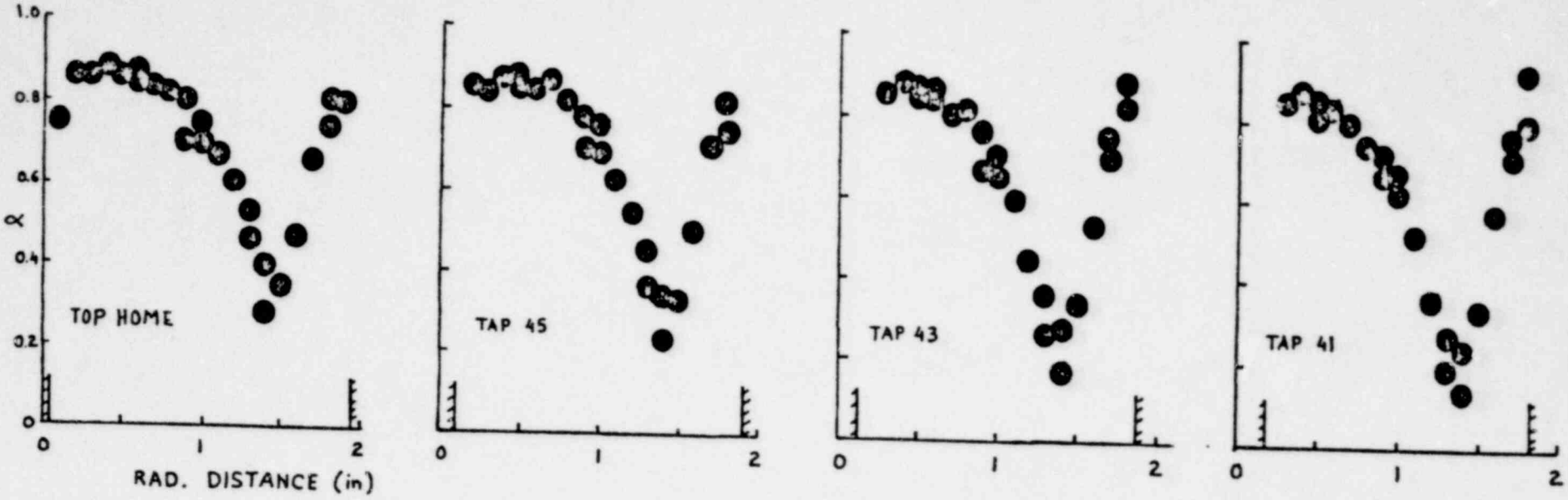

RUN 130 P_{IN}= 382 KPA T_{IN}=100 c G=6.04 MG/M^2S

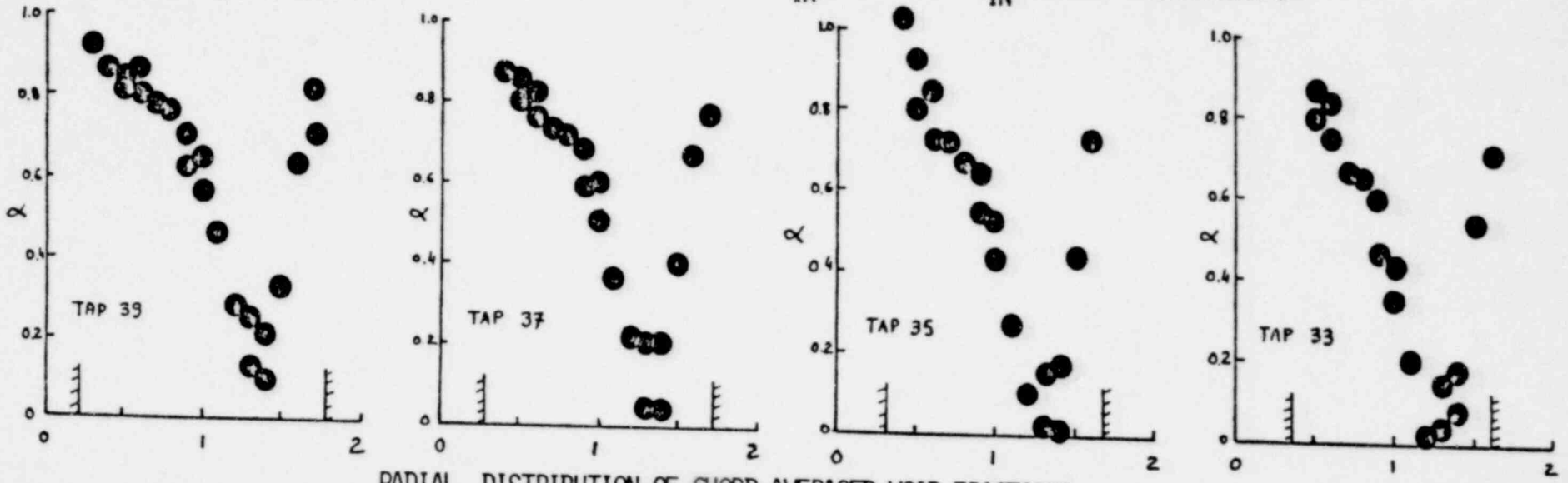

RADIAL DISTRIBUTION OF CHORD AVERAGED VOID FRACTIONS

1601 325

FLASHING INCEPTION

IN PIPES

HYPOTHESIZE

- Static Flashing underpressure is a function Only of initial temperature and decompression Rate (Lienhard)

- Dynamic Flashing underpressure is subject to the effects of turbulence

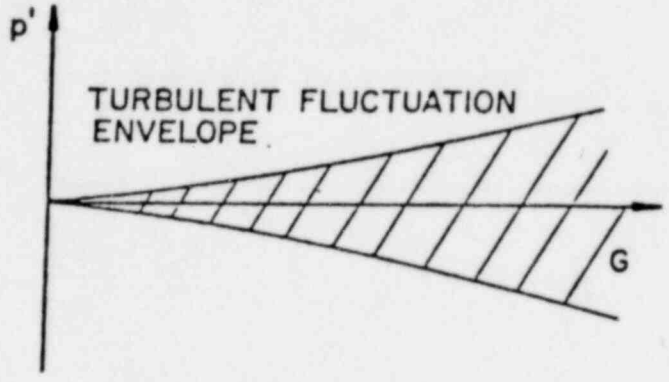

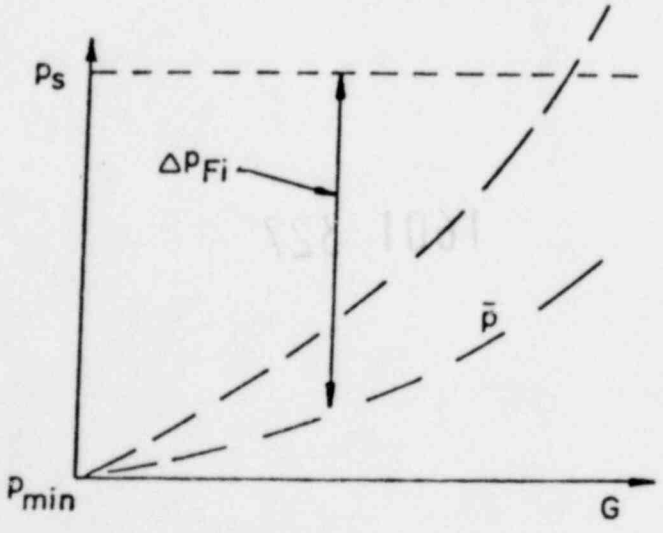

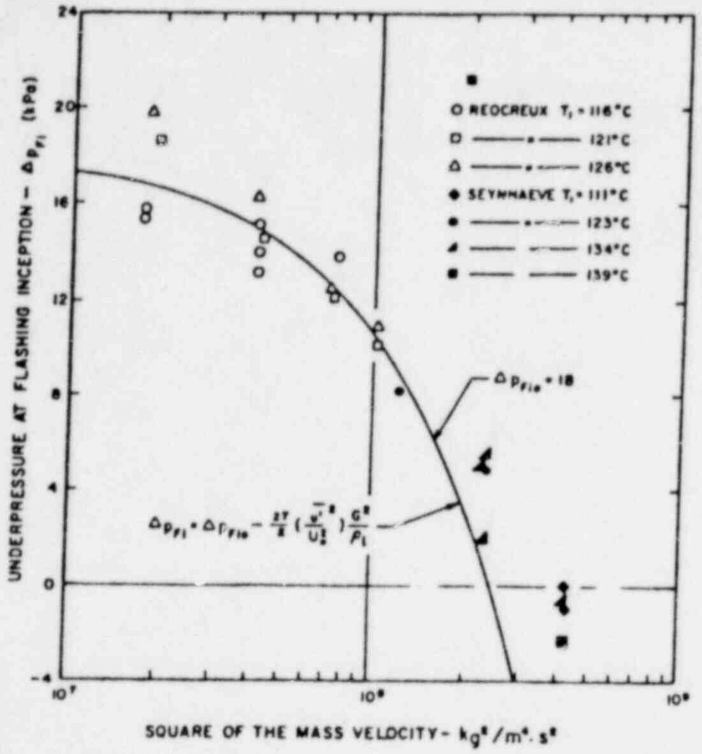
UNDERPRESSURE AT FLASHING INCEPTION – Δp_Fi (kPa)
SQUARE OF THE MASS VELOCITY – kg²/m⁴·s²
REOCREUX T_i = 116°C
121°C
126°C
SEYNHAEVE T_i = 111°C
123°C
134°C
139°C
Δp_Fio = 18

1601 329

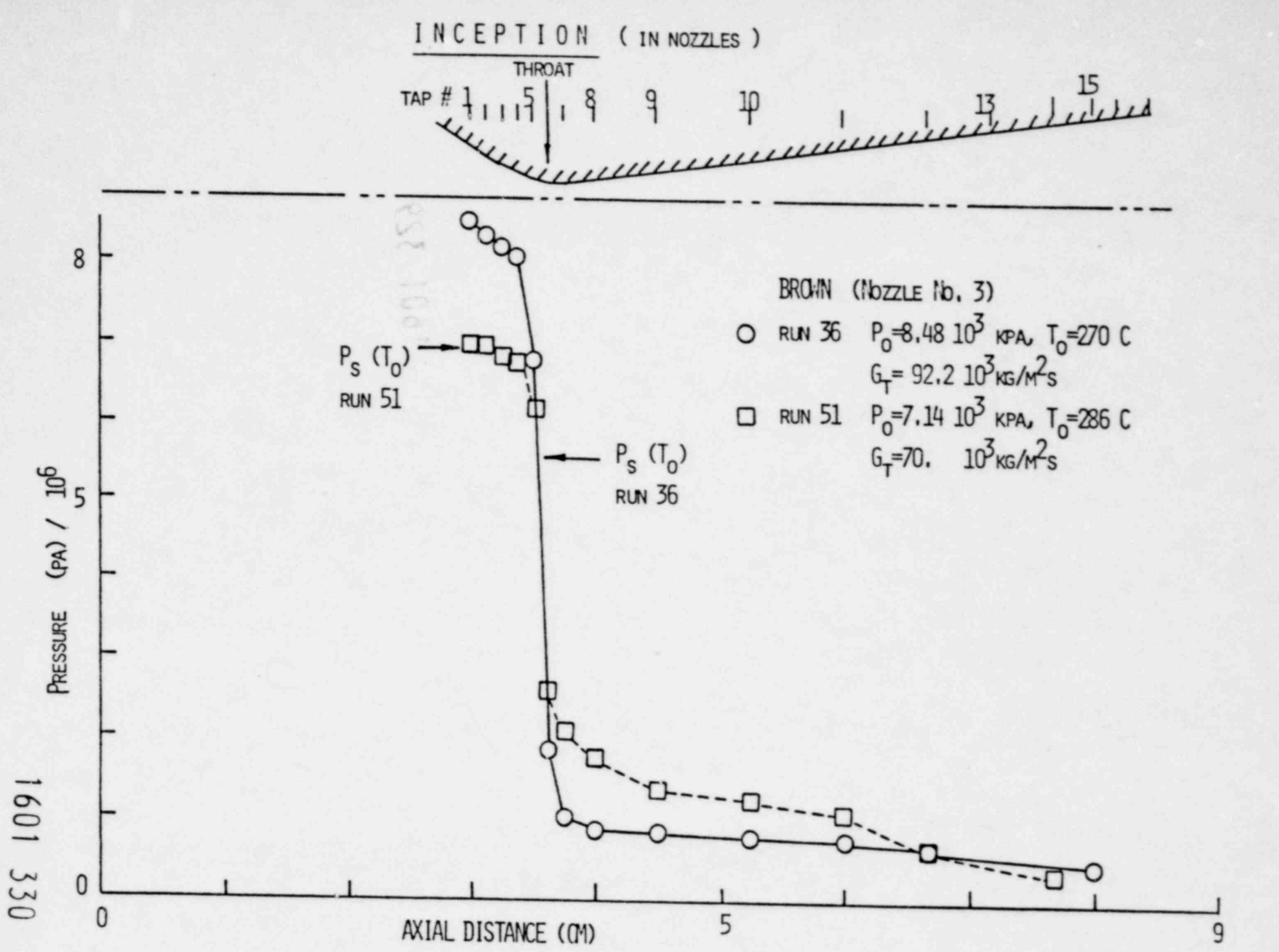
INCEPTION (IN NOZZLES)
THROAT
TAP # 1 5 8 9 10 13 15
BROWN (NOZZLE No. 3)
RUN 36 P_0=8.48 10^3 KPA, T_0=270 C
G_T= 92.2 10^3 KG/M^{2}S
RUN 51 P_0=7.14 10^3 KPA, T_0=286 C
G_T=70. 10^3 KG/M^{2}S
P_S (T_0) RUN 51
P_S (T_0) RUN 36
PRESSURE (PA) / 10^6
8
5
0
0
5
9
AXIAL DISTANCE (CM)

1601 330

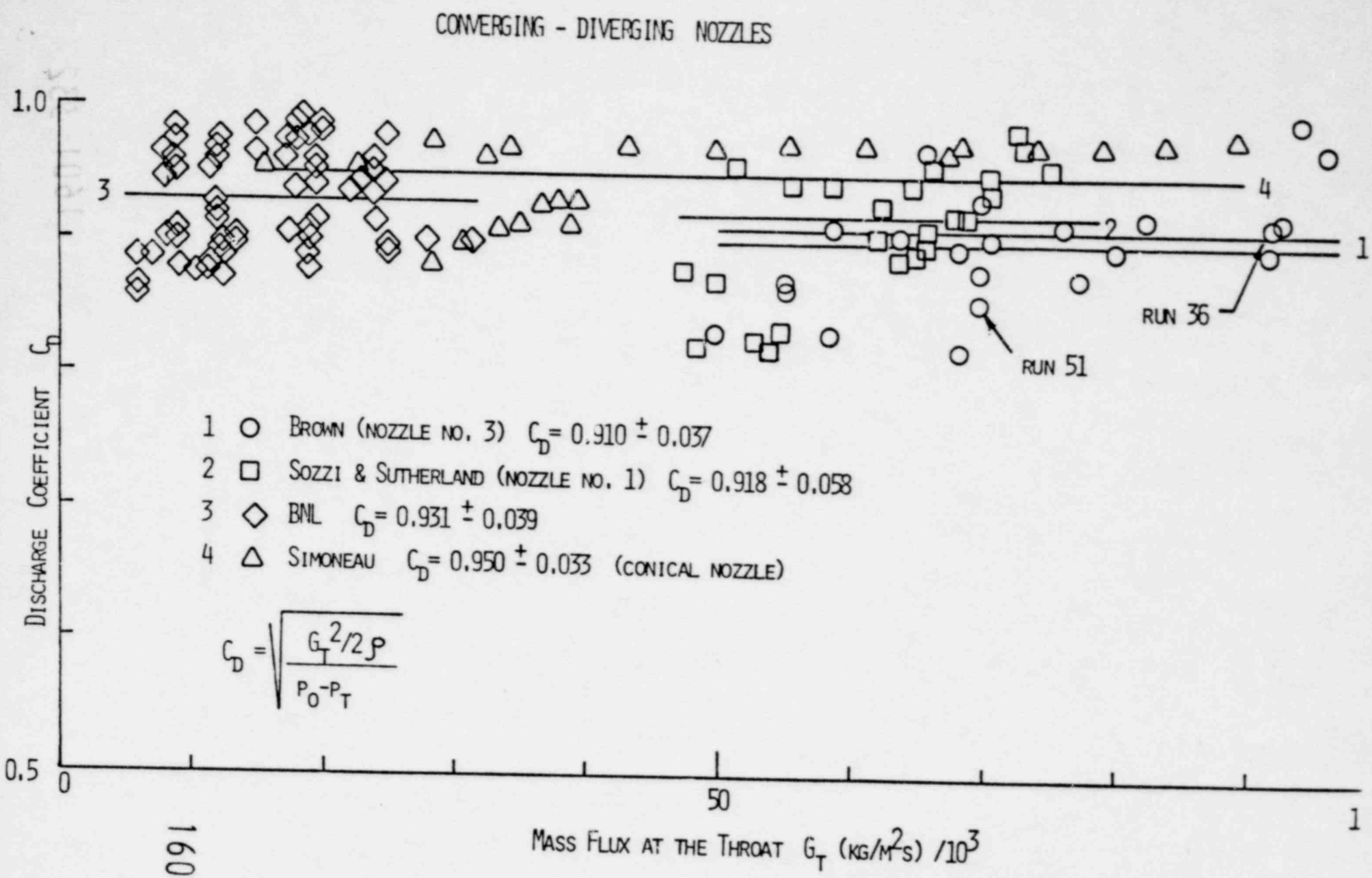
CONVERGING - DIVERGING NOZZLES
1.0
0.5
0
50
1
3
4
2
1
RUN 36
RUN 51
DISCHARGE COEFFICIENT C_D
1 ○ BROWN (NOZZLE NO. 3) $C_D = 0.910 \pm 0.037$
2 □ SOZZI & SUTHERLAND (NOZZLE NO. 1) $C_D = 0.918 \pm 0.058$
3 ◇ BNL $C_D = 0.931 \pm 0.039$
4 △ SIMONEAU $C_D = 0.950 \pm 0.033$ (CONICAL NOZZLE)
$C_D = \sqrt{\frac{G_T^2/2\rho}{P_0 - P_T}}$
MASS FLUX AT THE THROAT G_T (KG/M^{2}S) /10^3

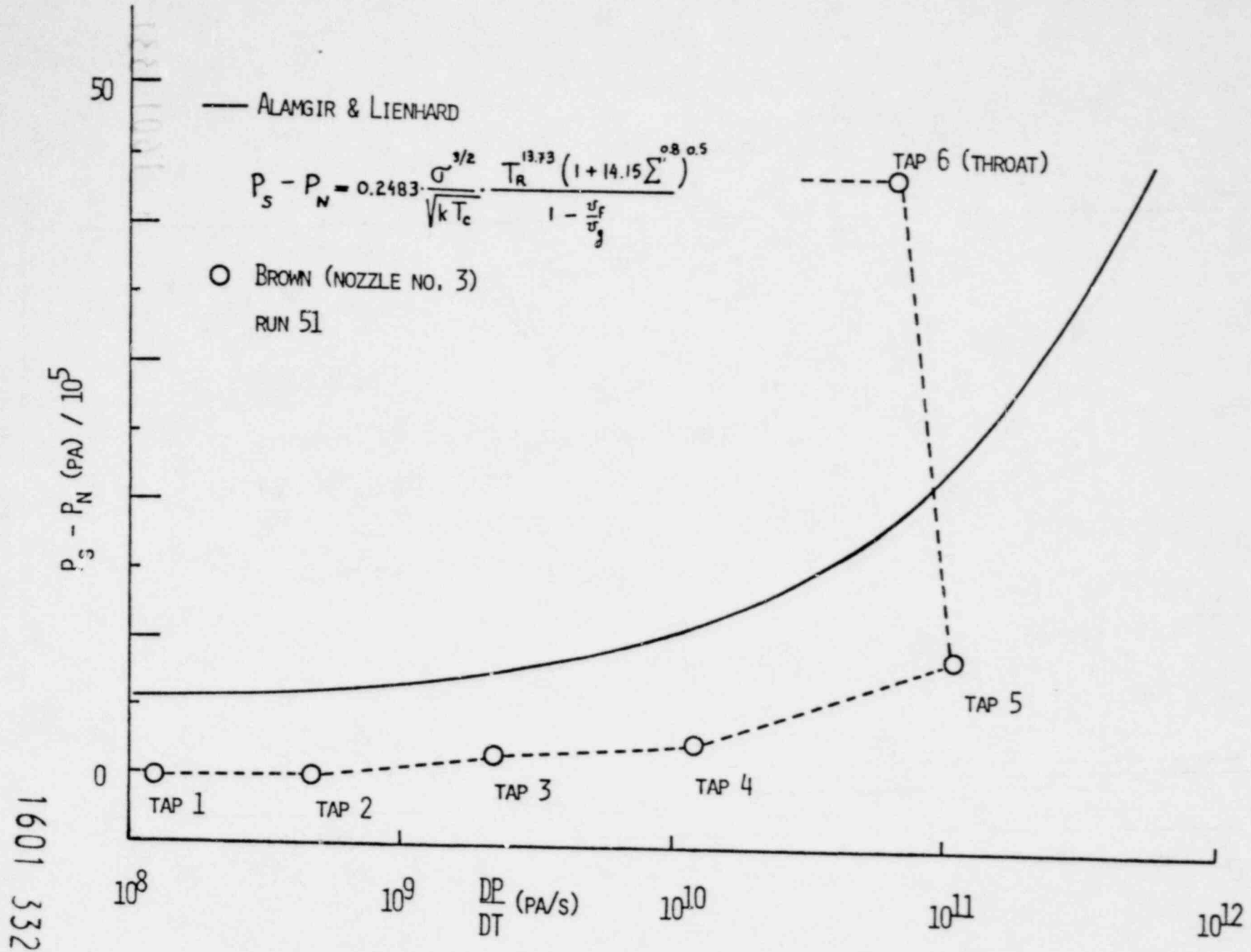
50
0
ALAMGIR & LIENHARD
$P_S - P_N = 0.2483 \cdot \frac{\sigma^{3/2}}{\sqrt{k T_c}} \cdot \frac{T_R^{13.73}\left(1 + 14.15 \Sigma^{0.8}\right)^{0.5}}{1 - \frac{v_f}{v_g}}$
BROWN (NOZZLE NO. 3)
RUN 51
TAP 6 (THROAT)
TAP 5
TAP 4
TAP 3
TAP 2
TAP 1
$P_S - P_N$ (PA) / 10^5
10^8
10^9
$\frac{DP}{DT}$ (PA/S)
10^{10}
10^{11}
10^{12}

1601 332

PRESSURE DISTRIBUTIONS, VOID PROFILES AND VAPOR GEN. RATES

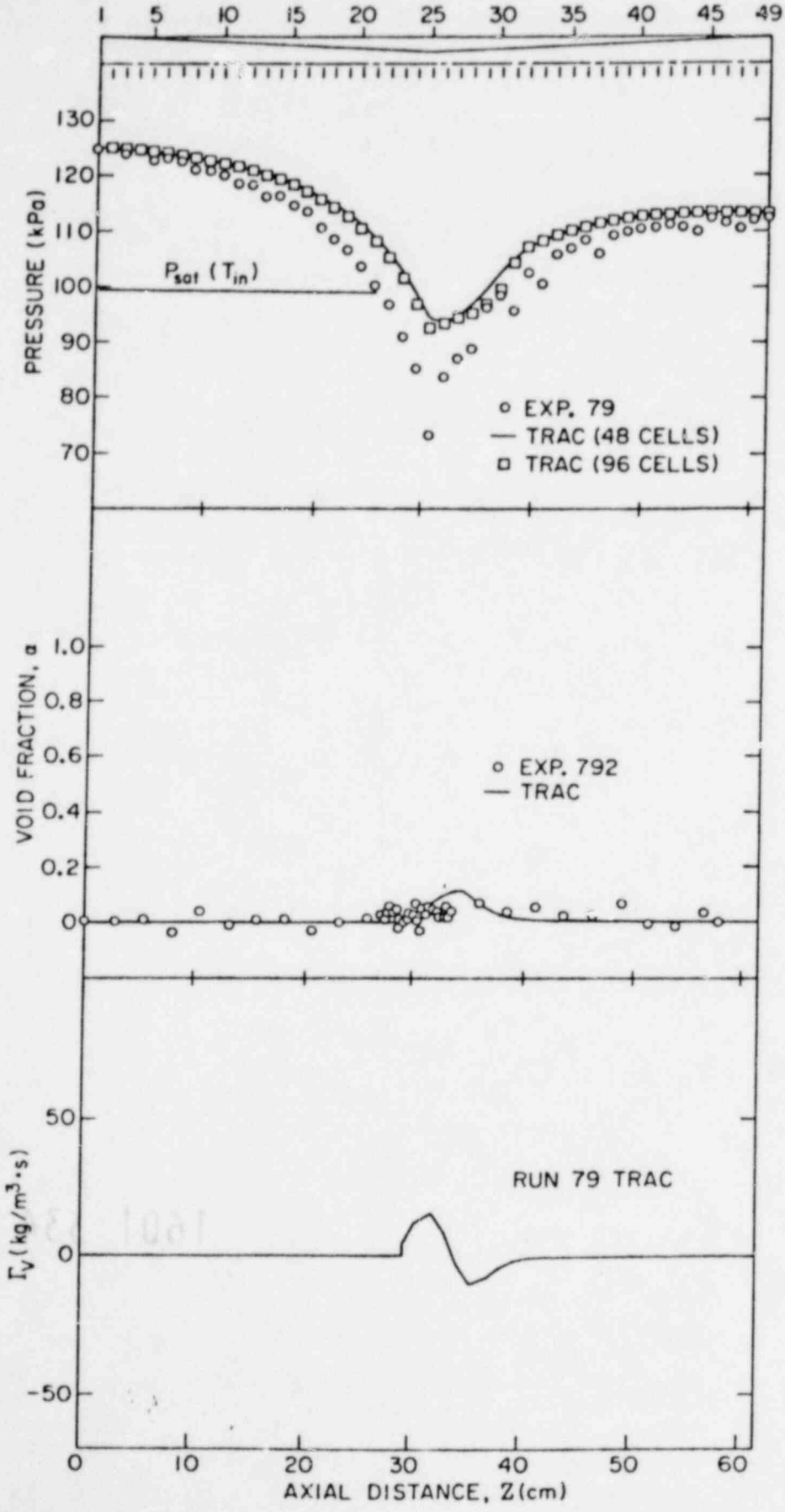

RUN 79

P_{IN}=124 KPA

T_{IN}=99.4 C

G=2.27 MG/M^{2}S

1601 333

PRESSURE DISTRIBUTIONS, VOID PROFILES AND VAPOR GEN. RATES

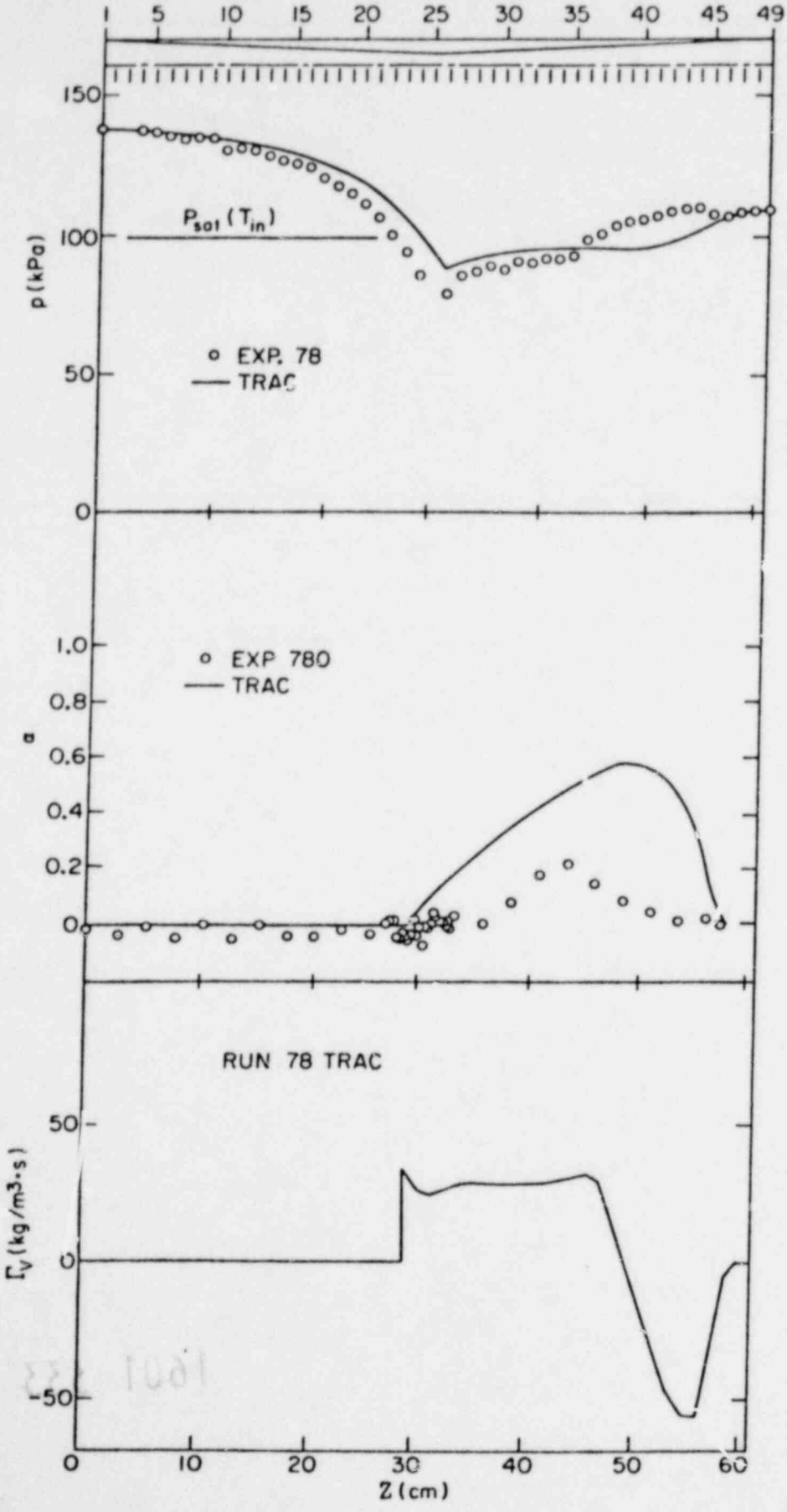

RUN 78

P_{IN}=138 KPA

T_{IN}=99.3 C

G=2.61 MG/M^{2}S

1601 334

PRESSURE DISTRIBUTIONS, VOID PROFILES AND VAPOR GEN. RATES

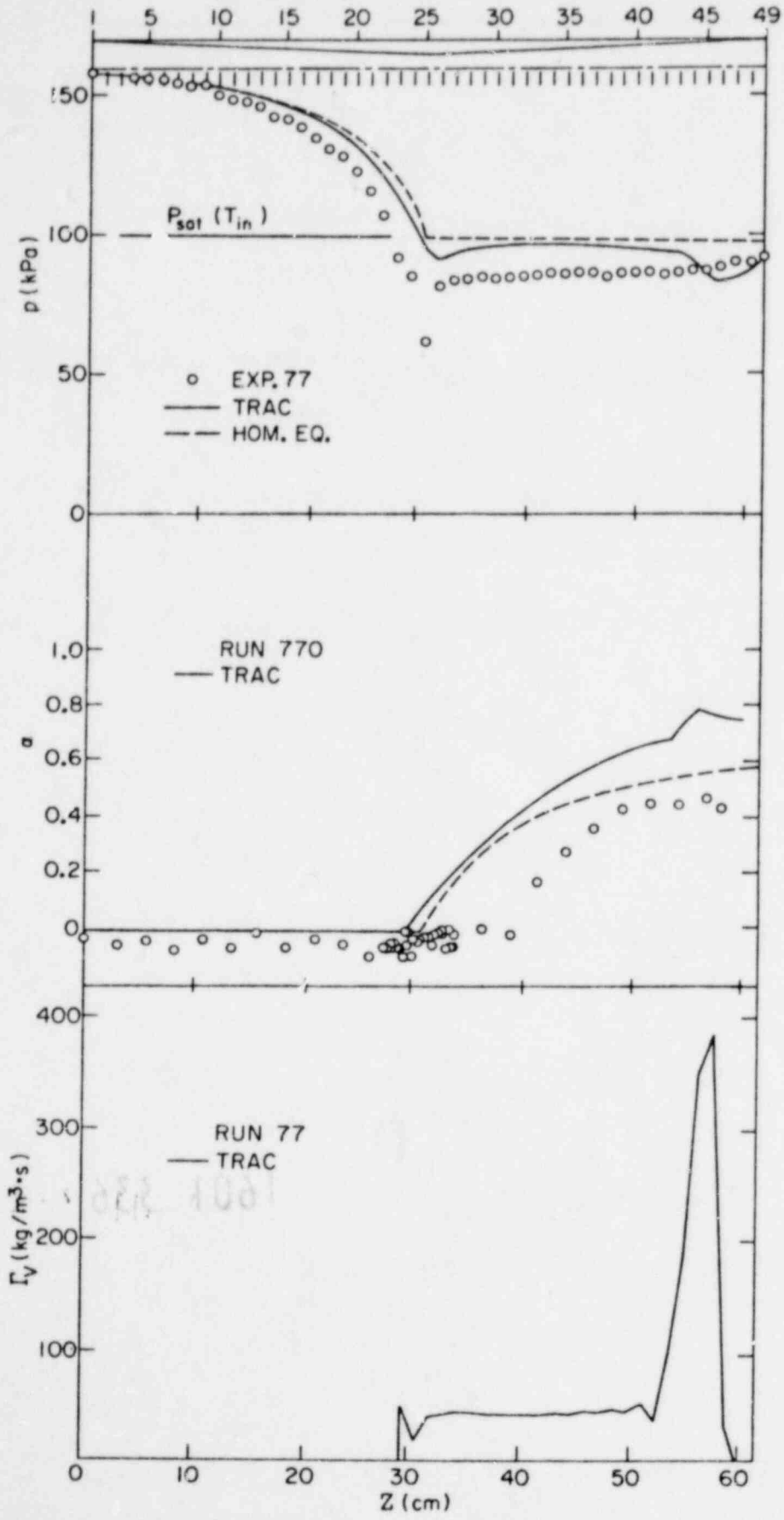

RUN 77

P_{IN}=157 KPA

T_{IN}=99.3 C

G=3.06 MG/M²S

1601 335

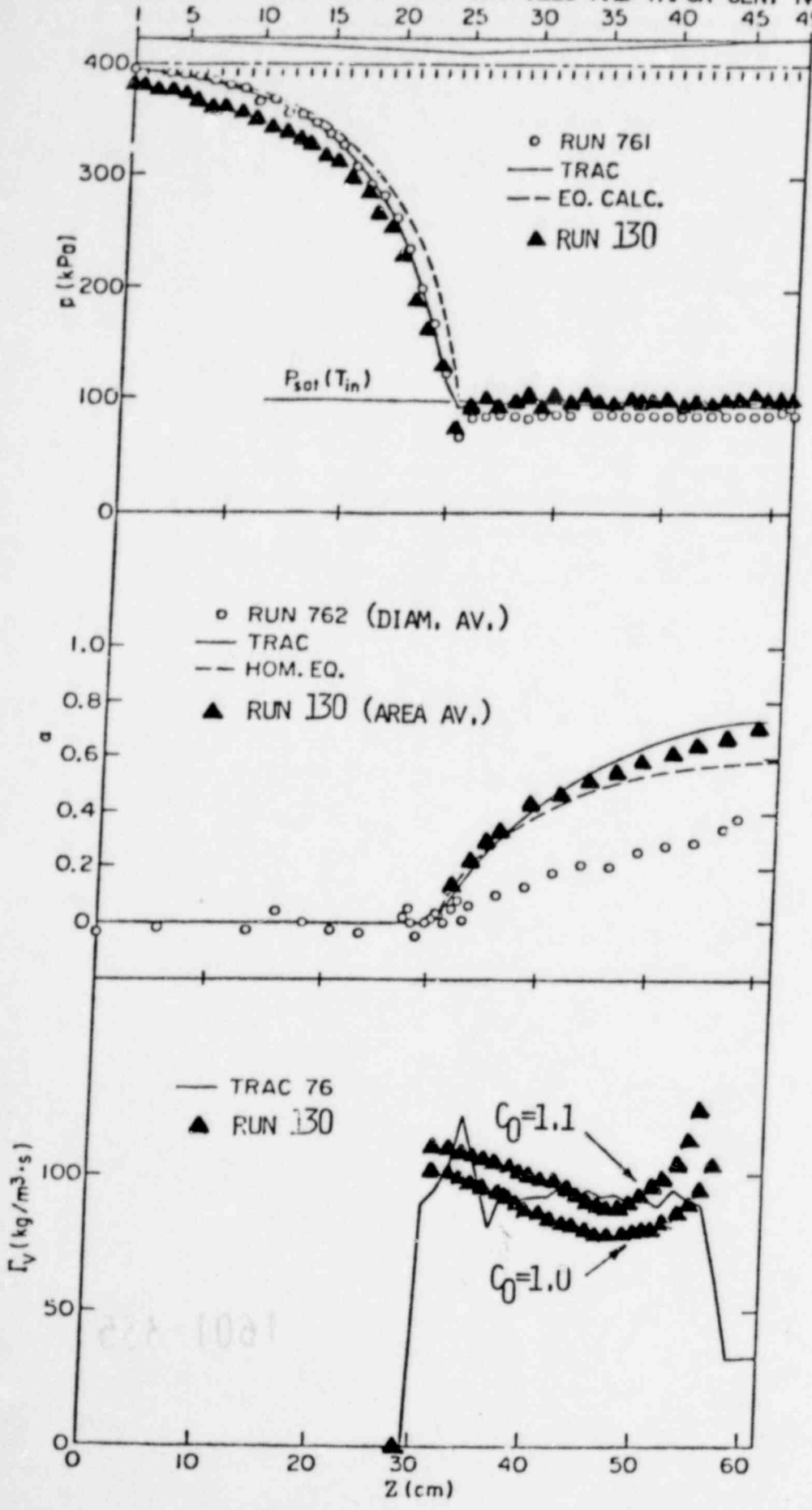

RUN 76

P_{IN}=395 KPA

T_{IN}=99.3 C

G=6.04 MG/M²S

RUN 130

P_{IN}=382 KPA

T_{IN}=100 C

G=6.04 MG/M²S

1601 336

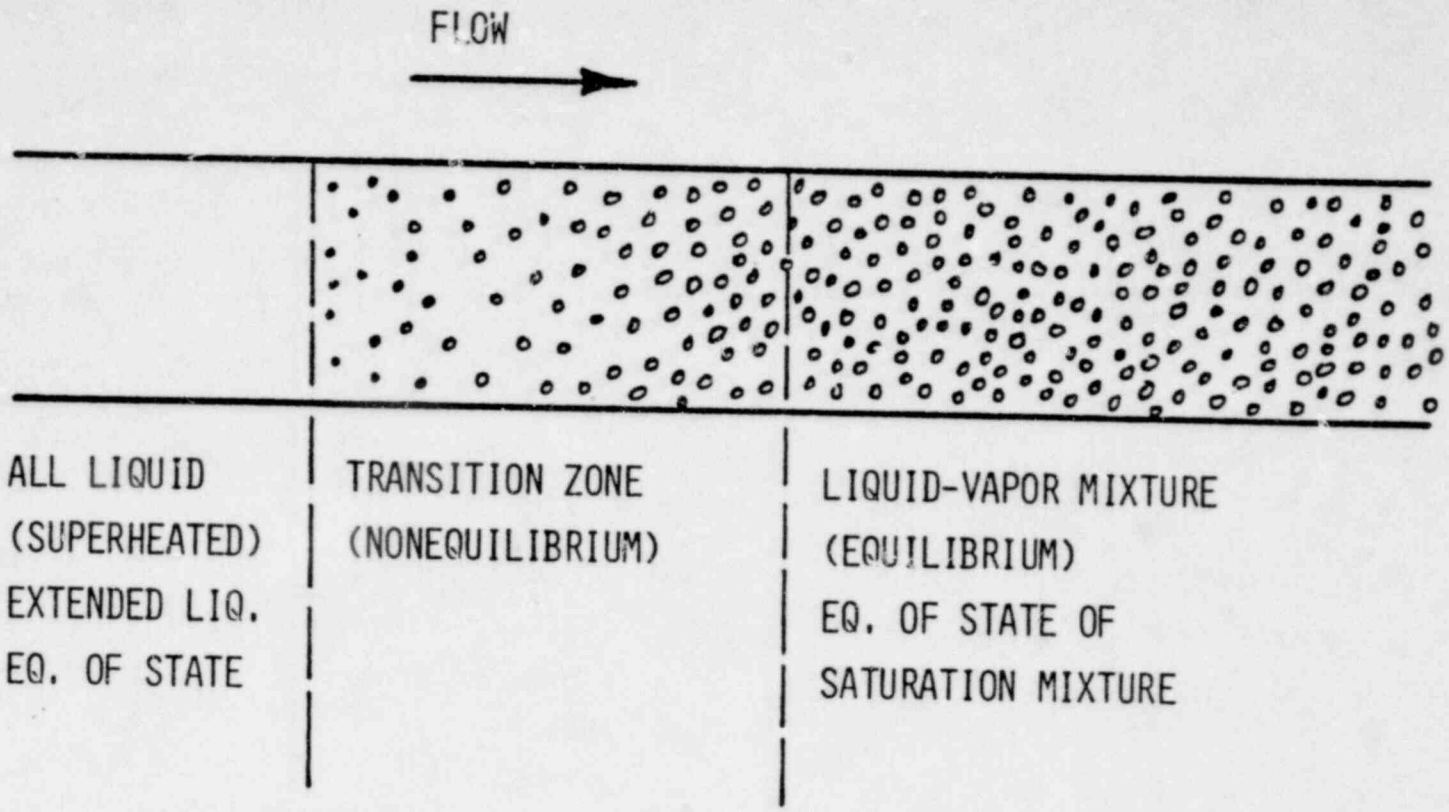
FLOW
ALL LIQUID
(SUPERHEATED)
EXTENDED LIQ.
EQ. OF STATE
TRANSITION ZONE
(NONEQUILIBRIUM)
LIQUID-VAPOR MIXTURE
(EQUILIBRIUM)
EQ. OF STATE OF
SATURATION MIXTURE
JUMP CONDITION

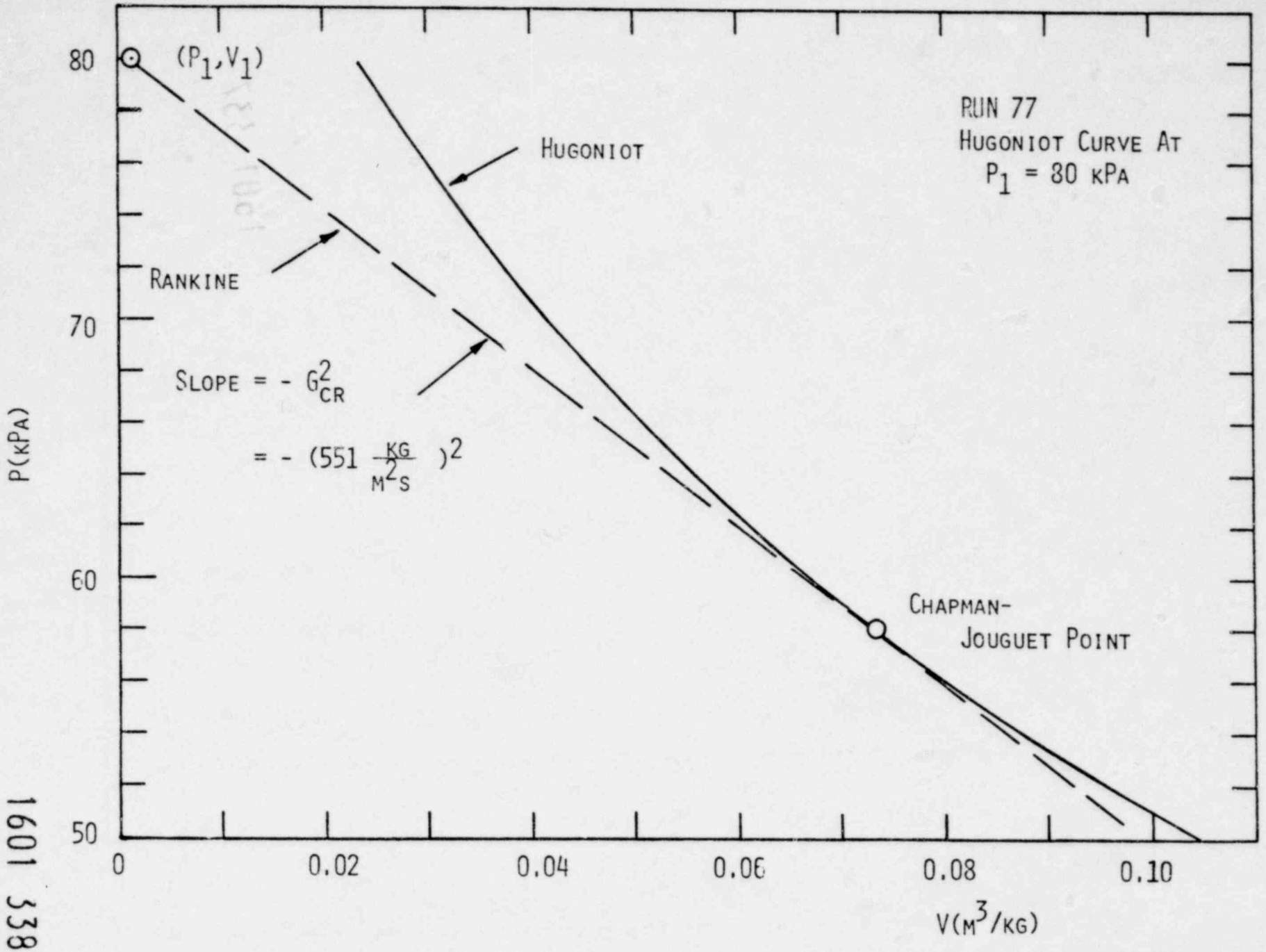
RUN 77
HUGONIOT CURVE AT
P_1 = 80 KPA
(P_1, V_1)
HUGONIOT
RANKINE
SLOPE = $- G_{CR}^2$
$= - (551 \frac{KG}{M^2 S})^2$
CHAPMAN-
JOUGUET POINT
P(KPA)
80
70
60
50
0
0.02
0.04
0.06
0.08
0.10
V(M^3/KG)

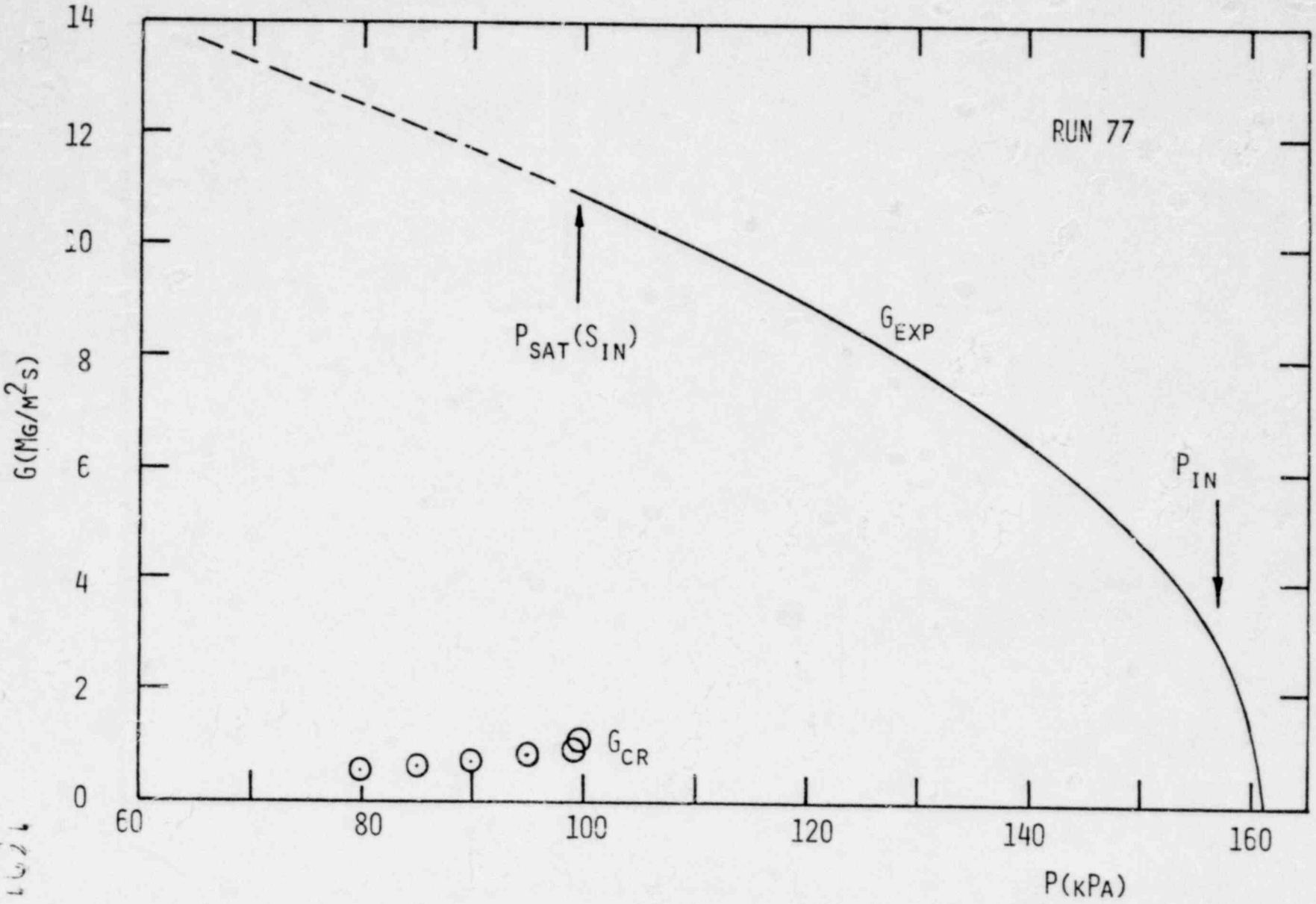
RUN 77
$P_{SAT}(S_{IN})$
G_{EXP}
P_{IN}
G_{CR}
G(MG/M²S)
P(KPA)
0
2
4
6
8
10
12
14
60
80
100
120
140
160

To be presented at the LWR Safety Information Meeting, Gaithersburg, Md. in November 1979.

Steam-Water Mixing Studies

S. G. Bankoff, R. S. Tankin and M. C. Yuen
Technological Inst., Northwestern Univ., Evanston, Ill. 60201

1. Introduction

Three separate studies are being performed of steam-water mixing:

1. Transition from bubbling to downflow in a water pool as a function of steam flow rate, steam superheat, and number and location of support plate holes.
2. Countercurrent flow of steam and water in a nearly vertical flat-plate geometry, with local condensation and flooding inception measurements.
3. Horizontal co-current stratified flow of steam and cold water, with measurements of local condensation rates by heated Pitot tube traverses in the steam space; and of liquid velocities and turbulent intensities by LDA.

Typical data from the first two studies will be presented; the third study will be discussed elsewhere.[1]

2. Transition to Downflow in a Bubbly Pool[2]

The flow system (Fig. 1) allowed either saturated or superheated steam, or air to be introduced below a perforated plate. Cold water enters above the plate from an adjustable-height tube with horizontal spray holes, and overflows to drain. Various perforation geometries were tested (Fig. 2); the 15-hole geometry corresponds to the KKU upper tie plate. The plate dimensions were 71.5 x 42.9 mm by 20 mm thick.

2.1 Air-Water CCFL

195 data points were taken with air-water, using seven perforation geometries and two inlet water tube elevations. As shown in Fig. 3, J^* scaling, using the hole diameter as the characteristic length, does not collapse the data, although the expected slope of -1 is obtained. K^* scaling brings the data somewhat closer (Fig. 4). Here

$$J_i^* = j_i \left[\rho_i / g\, D_h\, (\rho_f - \rho_g)\right]^{\frac{1}{2}} \qquad i = g \text{ or } f \qquad (1)$$

$$K_i^* = j_i\, \rho_i^{\frac{1}{2}} / (g\, \sigma\, (\rho_f - \rho_g))^{\frac{1}{4}} \qquad i = g \text{ or } f \qquad (2)$$

Following to some extent the work of Liu and Collier[3], a new scaling is introduced

$$H_i^* = j_i \left(\rho_i / g\, w\, (\rho_f - \rho_g)\right)^{\frac{1}{2}} \qquad i = g \text{ or } f \qquad (3)$$

where the characteristic length w is given by

$$w = D_h^{1-\alpha} \left[\sigma / g\, (\rho_f - \rho_g)\right]^{\alpha/2} \qquad (4)$$

For $\alpha \to 0$ $H_i^* \to J_i^*$ and for $\alpha \to 1$ $H_i^* \to K_i^*$. A function with the required properties is

$$\alpha = \tanh \left[(k\, D_h)\ (A_n / A_T)\right] \qquad (5)$$

where D_h = hole diameter; k = critical wave number = $2\pi/t_p$; t_p = plate thickness; A_n = area of holes; A_T = total plate area. As suggested by Sun[4], the intercept C is a function of the Bond number $L^* = n\pi D_h \left[g(\rho_f - \rho_g)/\sigma\right]^{\frac{1}{2}}$, where n is the number of holes:

$$C = 1.07 + 4.33 \cdot 10^{-3}\, L^* \qquad L^* < 200 \qquad (6)$$
$$= 2 \qquad L^* > 200$$

as shown in Fig. 5, which includes the available simulated BWR bundle data[5,6].

The correlation equation

$$H_g^{*\frac{1}{2}} + H_f^{*\frac{1}{2}} = C \qquad (7)$$

collapses our air-water data, as well as the saturated steam-water data of Naitoh et al.[5] and of Jones[6] reasonably well. The effects of the inlet water elevation and of the lower plenum volume were both found to be negligible.

2.2 Steam-Water End-of-Complete-Bypass (EOCB)

In these experiments a steam-supported water pool was established above the plate, and the steam flowrate was then slowly decreased until liquid penetration through the plate (end of complete bypass or, in chemical engineering terms, onset of weeping) was observed. Test ranges were: T_g = 373-421 K; T_f = 285-359 K; number of holes (Fig. 2) 3-15; H_{in}, water inlet height above plate 5-710 mm.

Fig. 7 shows the effect of ΔT_{sub} on EOCB for the 15-hole (KKU geometry) plate with inlet spray above the pool surface. The line $R_T \equiv C_f(T_g - T_f)W_f/h_{fg}W_g \equiv \dot{h}_f/\dot{h}_g = 1$, which represents thermodynamic equilibrium between the entering steam and water flows to produce only saturated water, is uncorrelated with these data. There are two regions, corresponding to $\dot{h}_f \equiv W_f C_f \Delta T_{sub} \lesssim 120$ kw. For $\dot{h}_f < 120$ kw the slope f = 0.24 can be considered a mixing efficiency for bringing cold water to the plate. For $\dot{h}_f > 120$ kw this linear mixing process becomes saturated, and excess water simply bypasses to drain. As $\dot{h}_f$ increases the EOCB changes from a continuous leakage to oscillatory weeping, with a frequency ~ 1 s, as shown in Fig. 8. Similar data were taken with the 9-hole plate (Fig. 9), showing a similar slope in the (f = 0.24), but a lower intercept, in the linear range, but the same limiting value of $\dot{h}_g$ ~ 71 kw for the saturation range. This suggests that the vapor velocity through the holes, j_g', may be important in the linear range, which is verified by replotting the data in Fig. 9. An effective dimensionless steam flowrate can be defined as

$$H_{g,e}^* = H_g^* - \frac{fC_f \Delta T_{sub}}{h_{fg}} \left(\frac{\rho_f}{\rho_g}\right)^{\frac{1}{2}} H_f^* \qquad (8)$$

which differs from the analogous quantity for PWR annulus flows[7] by the fact that f represents an efficiency for transport of cold water into the plate bubble boundary layer. The EOCB point is now given by

$$H_{g,e}^{*\frac{1}{2}} = C \qquad (9)$$

As shown in Fig. 10 the steam-water data agree with the air-water data correlation for EOCB.

Similar runs were made with plates with smaller perforation ratios (Fig. 11) and T_f = 285 K, giving similar results, except that f = 0.49 and $\dot{h}_{g,max}$ = 62 kw for 5 holes and 47 kw for 3 holes. The explanation for the improved mixing efficiency is believed to be the presence of large vertical standing eddies above the plugged-off regions, which help bring cold water down to the plate. This is shown by Fig. 12, where the EOCB point is no longer determined only by the steam velocity entering the holes, but now also depends on $\dot{h}_f$ and the perforation ratio. These data can also be correlated by Eq. (9), as shown in Fig. 13, although the spread is somewhat larger, in view of the great variation in plate geometry.

These data may be representative of EOCB behavior of the upper-head pool with elevated ECCS injection. To investigate the effect of bringing ECCS directly down to the tie plate, data were taken with the closed end of the inlet water tube 5 mm. above the plate, with horizontal injection through holes drilled in the tube side wall. The effects of T_f are shown in Fig. 14.

A marked improvement in liquid penetration ability is seen with T_f = 285 K, and for h_f > 150 kw two distinct modes of EOCB are observed. The higher, called oscillatory weeping, lies close to R_T = 1, which means that f ~ 1 for mixing of steam and cold water in the vicinity of the plate holes. Vapor-rich regions grow and collapse above the plate, resulting in inertial penetration of the holes. As the steam flowrate is reduced, the large scale growth and collapse ceases, and so does inertial penetration. Further reduction of steam flow leads to a nearly all-liquid pool, with high-speed bubble (or vapor jet) collapse in a thermal boundary layer near the plate. This is a stable region with no liquid penetration. Still further reduction of steam flow results in dumping of the entire pool into the lower plenum. The behavior at higher water temperatures was not investigated at these high values of h_f, due to equipment limitations, but does not appear to follow the line R_T = 1 closely, indicating much less effective condensation at the holes.

This phenomenon with T_f = 385 K was explored more fully with different perforation ratios (Fig. 15). Here the R_T = 1 line (f = 1) is followed more closely with f ~ 0.85 for h_f < 9 kw, and f ~ 0.63 for h_f > 9 kw with m < 15. This shows again the powerful effect of the standing eddies above the blocked-off regions of the plate in bringing cold water back to the plate, and inducing excellent mixing in a thin layer above the holes. These eddies are very weak for the reference plate (n = 15), so that with low water flows (h_f < 4 kw) most of the steam-water mixing takes place away from the plate, even with H_{in} = 5-15 mm. Hence for this plate, the EOCB behavior in the R_T < 1 region is similar both for the high and low water inlet positions. In the R_T > 1 region the two-mode behavior (oscillatory weeping at a high h_g and dumping for a low h_g, both for the same value of h_f, with a region of zero leakage in between, was exhibited at the low perforation ratios (n = 3 or 5). A simple calculation of the heat transfer coefficient on a hemispherical bubble at the mouth of the hole in the stable intermediate region (no weeping) gives a range of condensation heat transfer coefficients of 1.1 x 10^6 to 1.8 x 10^6 w/m^2K for these data for n = 3, 5, 9 and 15. This range agrees with condensation heat transfer coefficients measured by Bankoff and Mason[8] for single steam bubbles injected into a high-shear cold water region, and estimated by Merilo, Colah and Duffey[9] from data for transition to downflow for a steam-water bubbly pool.

It follows therefore that direct injection of cold water at the plate has a strong effect on EOCB, while water injected at higher elevations is much less effective. This is also shown by Fig. 16, where the 45° diagonal line (R_T = 1) is approximated only by cold water injected at the reference plate (n = 15). The situation is somewhat better for n = 9 (Fig. 17), since cold water can penetrate down along the walls more effectively.

2.3 Discussion and Conclusions

1. An extended CCFL scaling equation has been presented, which employs scaling which varies smoothly from J^* scaling for small tubes to K^* scaling for large flow passages. The transition between these two limits is determined by two geometric factors, consisting of the perforation ratio, A_p/A_T, and the hole diameter/thickness ratio. The "constant" C, which physically can be related to a critical relative velocity between the gas and liquid, is in fact a smooth function of a Bond number, L^*, and varies from one to two as L^* increases from zero. This scaling equation correlates all the present data for different perforated plates, as well as the available BWR simulated tube bundle data. As expected, this equation also agrees with our steam-water EOCB (end of complete bypass or weep point) data in the low inlet water flowrate limit.

2. The EOCB data show the importance of bringing cold water down to the plate, and agree with the air-water correlation if an effective vapor volumetric flux is used, in which the efficiency factor f is now an efficiency for steam-water mixing at the plate.

3. In general, unless very cold water is injected directly at the plate, $f < 0.5$, so that the line $R_T = 1$ (which corresponds to $f = 1$) does not describe the behavior. However, for tube bundle data in the "water-first" mode, the choke point is within the tube bundle, so that $R_T = 1$ describes CCFL (end of complete delievery) in view of the large steam-water contact area within the bundle[5,6]. However, it should be pointed out that the available simulated tube bundle data have been taken with unheated "fuel" pins. With hot dry metal surfaces the choke point will be significantly higher, and may be expected to be at the upper tie plate.

3. Local Condensation Coefficients in Vertical Steam-Water Separated Flow[10]

A PWR-annulus scaled flat-plate vertical test section, of gap 38.1 mm, depth 381 mm and height 0.965 m, was constructed for measurement of local heat transfer coefficients in separated countercurrent flow of steam and cold water (Fig. 18). Electrically-heated Pitot tube traverses could be made in the steam space at four elevations, in order to compute condensation rates. Typical steam velocity profiles are shown in Fig. 19. Because of unstable growth of surface waves in the vertical position, it was necessary to tilt the test section slightly to 7^o with the vertical. Even so, instabilities and entrainment at the lowest Pitot tube (0.08 m from the plate bottom) caused these readings to be less reliable than the others. The effect of the inlet steam flowrate, $W_g(0)$ at nearly constant water flow rates is shown in Fig. 20, where $x = 0$ is the plate bottom, and $x < 0$ represents the lower plenum. Similar data for different inlet water temperatures and flow rates are shown in Figs. 21-24. Second-order polynomials were fitted to these data by least squares, and local slopes taken in order to calculate the local heat transfer coefficients, h_x. These are shown in Figs. 25-28. These are replotted in Figs. 29-32 as local Stanton numbers, $St_x = h_x/c_f G$, where $G = G(x)$ is the local liquid mass flux vs. distance, x. It is seen that the steam flow rate varies almost linearly with distance, and the local heat transfer coefficients are generally within the expected range of 20-100 kw/m^2K. The highest heat transfer coefficient is always at the bottom of the plate, but the measurement technique in this region needs further refinement. No correlation is offered at this time.

The range of water and steam flows was limited by the desire to have less than total condensation on the one hand, and to prevent flooding at the bottom of the plate on the other. Quantitative measurements of the change in flow regime associated with flooding were not made in these preliminary runs, but some interesting qualitative observations can be reported at this time. The instabilities were definitely not of the form of solitary waves whose growth is determined by quasi-static Bernoulli equations in the gas and liquid phases, as has been successfully employed in horizontal air-water flow. Instead, the instabilities were characterized by three-dimensional waves, which gave the water surface a pebbly texture 0.5m from the top, and which resulted in strong entrainment of drops at the bottom. The new feature here is that the drops tended to concentrate into a steady fluidized region near the bottom, in which entrained droplets would rise up to a critical location where the steam velocity is barely sufficient to levitate the droplet, and would therefore oscillate around that point. Such behavior is not observed with air/water flows, and is indicative of the important qualitative, as well as quantitive, differences between steam/water and air/water separated flows.

4. Application to Reactor Flooding

Although the present perforated plate steam-water data deal only with EOCB (minimum $W_{g,in}$ such that $W_{fd} = 0$, where $W_{g,in}$ and W_{fd} are the mass flow rates of steam in and liquid delivered), it is interesting to consider the reactor flooding problem by UHI in conjunction with the data of Naitoh et al.[5]

and Jones[6]. The latter investigators measured W_{fd} vs. $W_{g,in}$ at constant $W_{f,in}$ in unheated simulated BWR tube bundles, the steam being introduced at the bottom of the bundle. With saturated steam/water a delivery curve was obtained as a function of $W_{g,in}$, which has been correlated by a Wallis-type equation[4], using K^* scaling and Bond number dependence of C. As shown above, we are able to correlate all their data, plus our own air/water data in a variety of perforated plate geometries, by a new scaling (H^*). In their cold water steam experiments the line $R_T = 1$, corresponding to marginally complete condensation of all the steam in a perfectly mixed system, signals an important change in water delivery. Typical data by Jones are shown in Fig. 33, where W_{fd} and $W_{g,in}$ are measured at constant $W_{f,in}$. In the "water-first" mode, delivery is complete as the steam flow is increased until the line $R_T = 1$ is reached. At this point some steam can reach the upper tie plate and reduces the downward water flow. However, any slight reduction in downward flow increases the steam flow reaching the plate, since the large tube bundle area guarantees excellent contact between the steam and water. This has an autocatalytic effect, resulting in a jump to the CCFL line. Further increases in steam flow decrease W_{fd} until at the EOCB point, $W_{fd} = 0$. On reversing the direction of traverse (steam-first mode) a hysteresis loop is obtained, since the jump point is now at $R_T > 1$. This is because the delivery through the holes in the neighborhood of $R_T = 1$ is saturated water, and it is not until the water delivery and the pool subcooling both increase, as $W_{g,in}$ decreases further, to some critical value that subcooled water is drawn through the holes, producing a jump to full delivery.

On the other hand, the present EOCB data consist of measurements of $W_{g,in}$, $T_{f,in}$ and $W_{f,in}$ at which W_{fd} begins to be nonzero. A flow map for the 15 hole data with water inlet not at the plate is shown in Fig. 34, which simulates the KKU geometry. The line $R_T = 1$ is not followed, but instead the EOCB boundary is given by Eq. (9). Below this point, data were not taken, but probably follow a modified Eq. (7), in which $H^*_{g,e}$ is used instead of H^*_g (Eq. (8)). An estimated line for complete delivery ("dumping") is also shown with region $R_T > 1$, corresponding to cold water being drawn through the holes. EOCB data have been taken at water mass fluxes well above those previously studied, and include the KKU range of interest.

It is thus clear that a two-dimensional flow map is inadequate, and a three-dimensional representation must be constructed for any particular flow system. We now define an additional thermodynamic quantity system:

$$R_{T,d} = \dot{h}_{fd} / \dot{h}_g = W_{fd} C_f \Delta T_{sub} / h_{fg} W_g \qquad (10)$$

No steam reaches the holes in a simulated tube bundle experiment if $R_{T,d} > 1$, and hence there is complete delivery in this region. In the CCFL region a modified Eq. (7) applies:

$$H^{*\frac{1}{2}}_{g,e} + H^{*\frac{1}{2}}_{fd} = C \qquad (11)$$

where $H^*_{g,e}$ is defined by Eq. (8). The complete bypass region is

$$H^{*\frac{1}{2}}_{g,e} \geq C \qquad (12)$$

For $H^{*\frac{1}{2}}_{g,e} < C$ and $R_T < 1$ Eq. (11) holds, and at $R_T \gtrsim 1$ a jump to complete delivery occurs in the steam-first mode, while at $R_T = 1$ a jump from complete delivery to Eq. (11) occurs in the steam-first mode. These equations are sufficient to construct a three-dimensional water delivery surface H^*_{fd} as a function of $H^*_{f,in}$ and H^*_g.

Some words of caution should be expressed at this point. In the unheated tube bundle studies as well as our own studies, W_g, and hence H_g^*, is a fixed input variable. With hot dry surfaces below the tie plate, however, water penetrating down no longer has an autocatalytic effect of reducing the steam flow to the plate. Instead, there is a feedback between W_{fd} and W_{gu}, where W_{fd} is the water flowing downwards from the plate, and W_{gu} is the steam flowing upwards to the plate. When the EOCB point is reached, ($W_{fd} > 0$) water penetrating downwards results in an increased steam flow upwards, so that complete bypass is re-established. One can therefore expect the system to oscillate around the EOCB point for some time, unless delivery incoherencies are established due to scale effects, radial non-uniformities of rod temperatures, and/or ECCS inlet design.

References

1. R. S. Tankin, M. C. Yuen and S. G. Bankoff, "Electrically-Heated Pitot Tubes, Laser-Doppler Anemometer and Holography in Steam-Water Flow", this Information Meeting.

2. C. L. Hsieh, "Countercurrent Air/Water and Steam/Water Flow Above a Perforated Plate", M.S. Thesis, Chem. Eng. Dept., Northwestern Univ. (1979).

3. R. P. Collier, et al., "Steam-Water Mixing and System Hydrodynamics Program, Quarterly Progress Report, Jan-Mar. 1979", NUREG/CR-0897, BMI-2029, Battelle Columbus Laboratories (1979).

4. K. H. Sun, "Flooding Correlations for BWR Bundle Upper Tieplates and Bottom Side-Entry Orifices", Second Multi-Phase Flow and Heat Transfer Symposium-Workshop, Miami Beach, Florida, April (1979).

5. M. Naitoh, K. Chino and R. Kawabe, "Restrictive Effect of Ascending Steam on Falling Water During Top Spray Emergency Core Cooling", J. of Nuclear Science and Technology, 15, 11, pp 806 (1978).

6. D. D. Jones, "Test Report TLTA Components CCFL Tests", General Electric Company, NEDG-NUREG-23732 (1977).

7. J. A. Block, "Condensation-Driven Fluid Motion", EPRI Workshop on Basic Two-Phase Modeling, Tampa, Florida, March 1, (1979).

8. S. G. Bankoff and J. P. Mason, AIChE J., 8, 30 (1962).

9. M. Merilo, M. Colah and R. B. Duffey, "Condensation Induced Transition from Bubbling to Liquid Downflow in a Turbulent Two-Phase Pool", 18th Nat. Heat Transfer Conf., San Diego (1979).

10. D. H. Cook, "Local Condensation Rates for the Countercurrent Stratified Flow of Steam and Water in a Vertical Channel", Mech. Eng. Dept., Northwestern Univ., (1979).

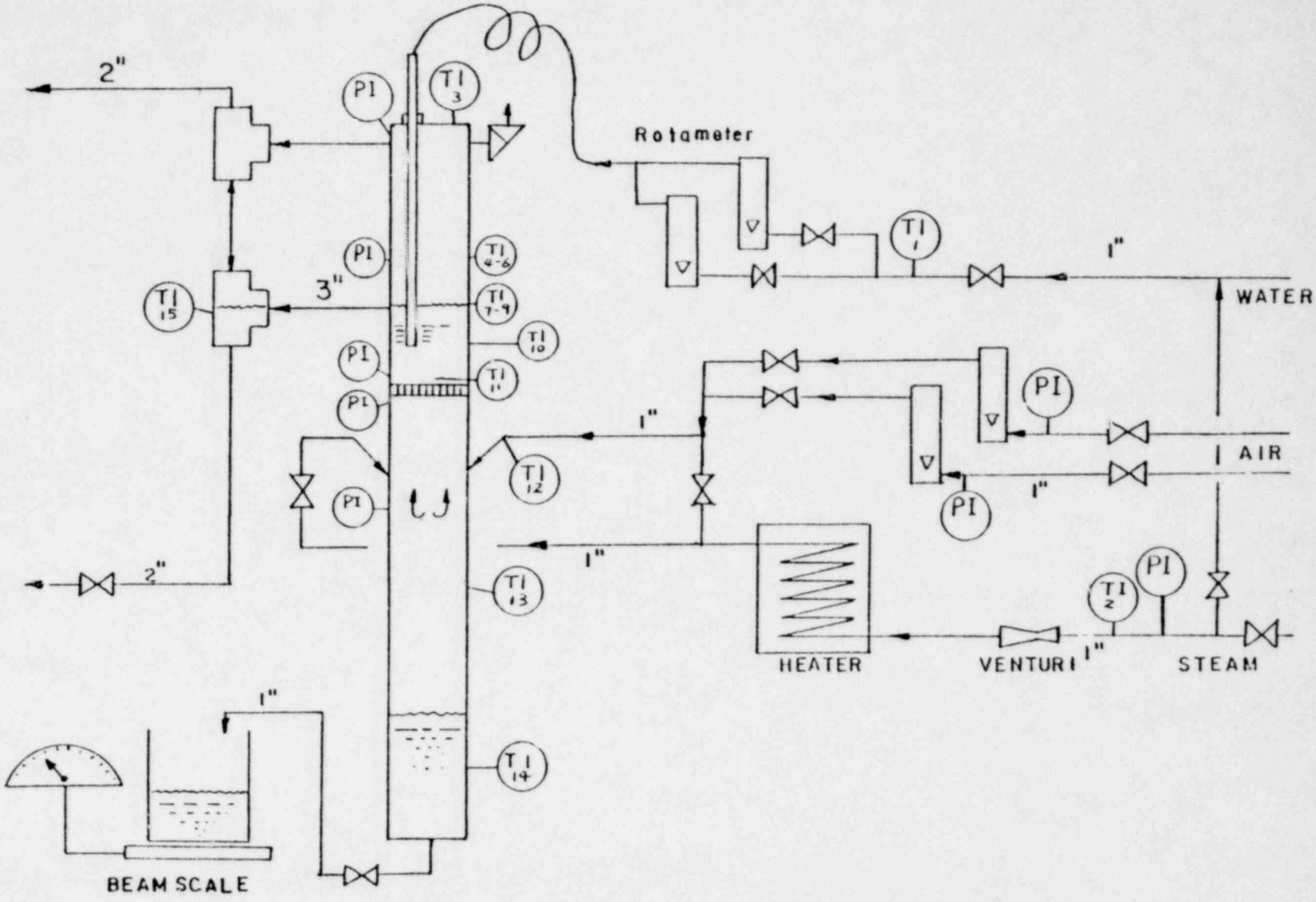

FIGURE 1. Schematic diagram of experimental apparatus.

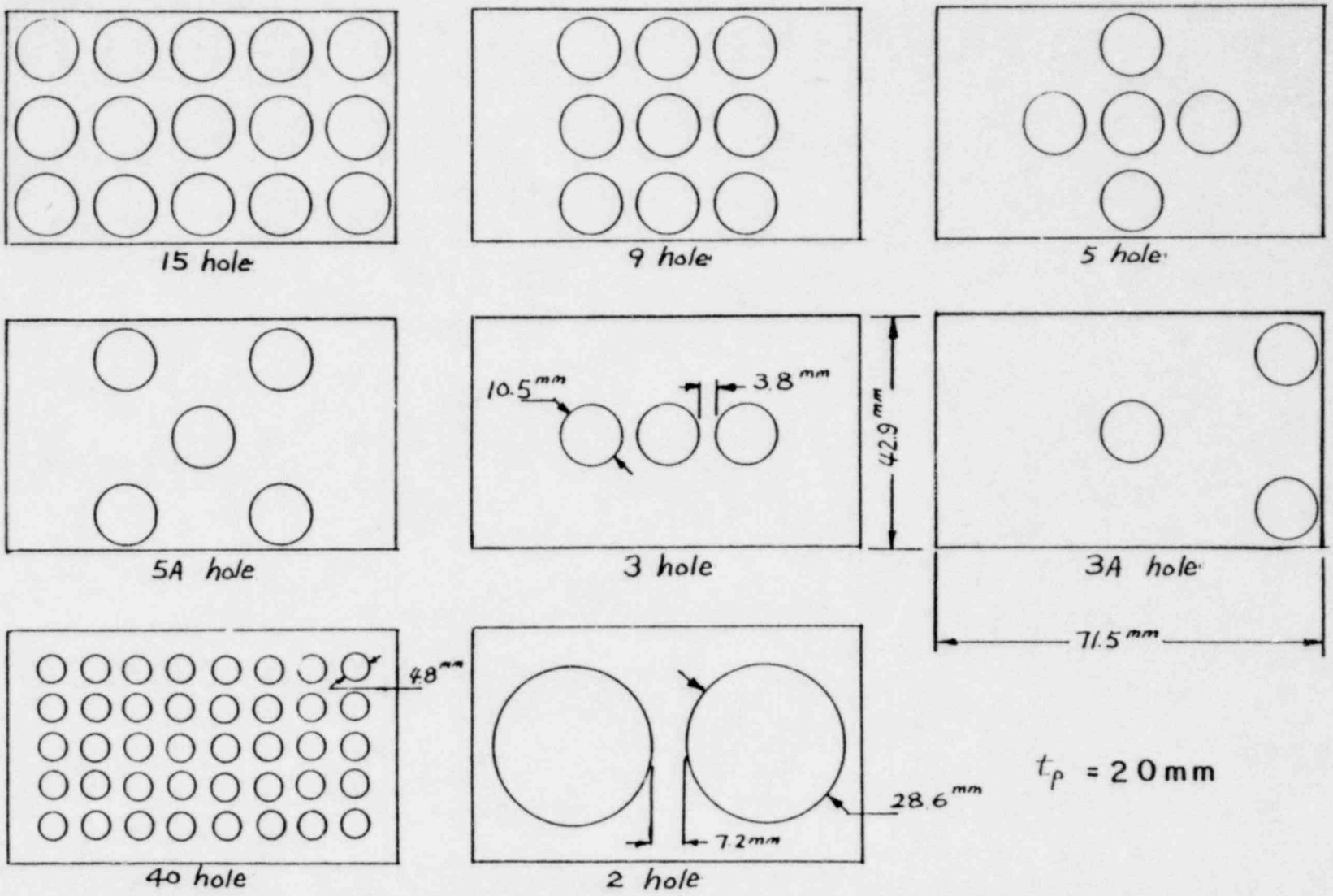

FIGURE 2. Geometries of the test perforated plate.

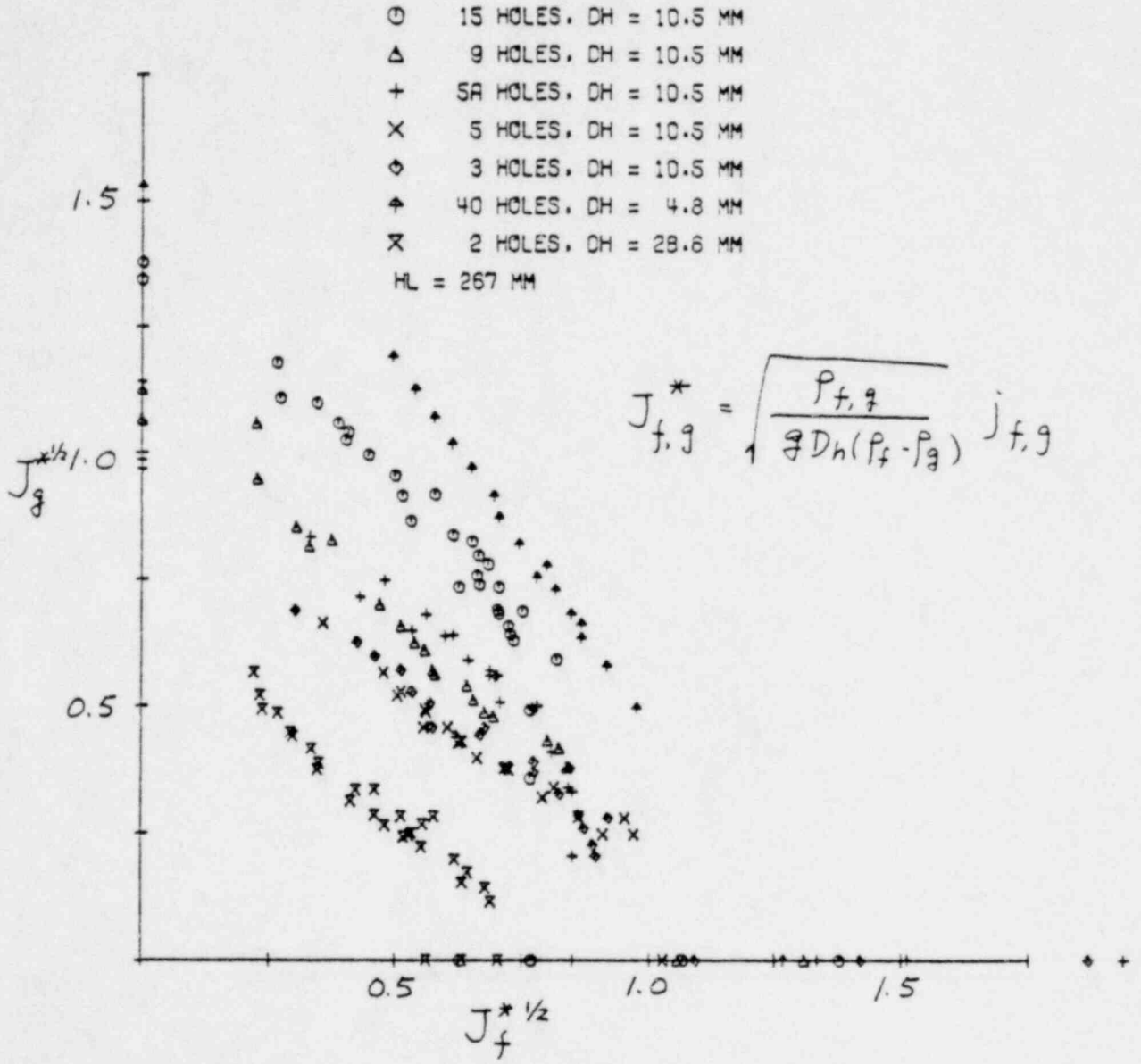

Figure 3. Data Correlation with Equation (1), w = D_h.

$$J_g^{*1/2} + J_f^{*1/2} = C$$

1601 348

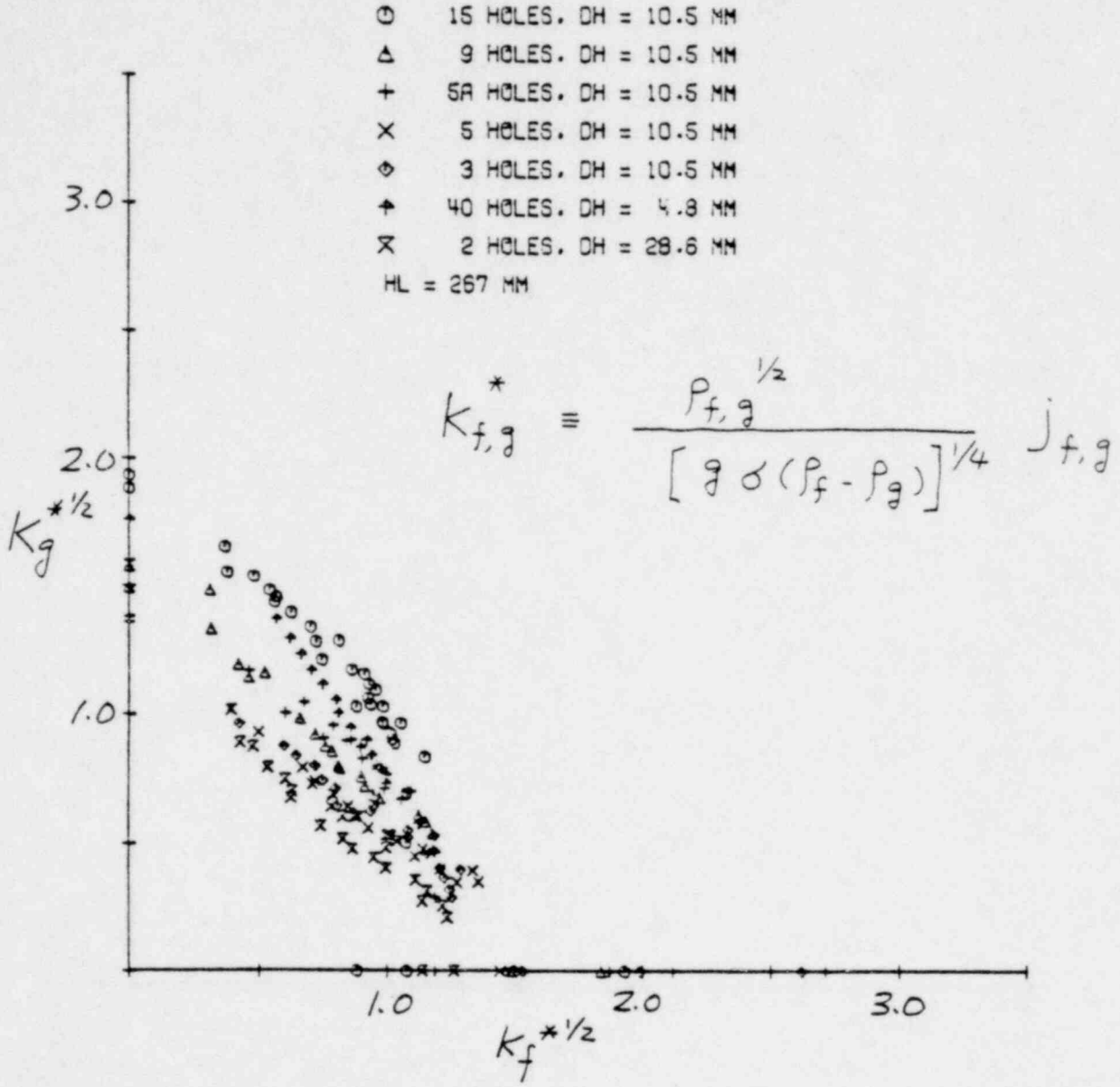

Figure 4. Data Correlation with Equation (2).

$$K_f^{*1/2} + K_g^{*1/2} = C$$

1601 349

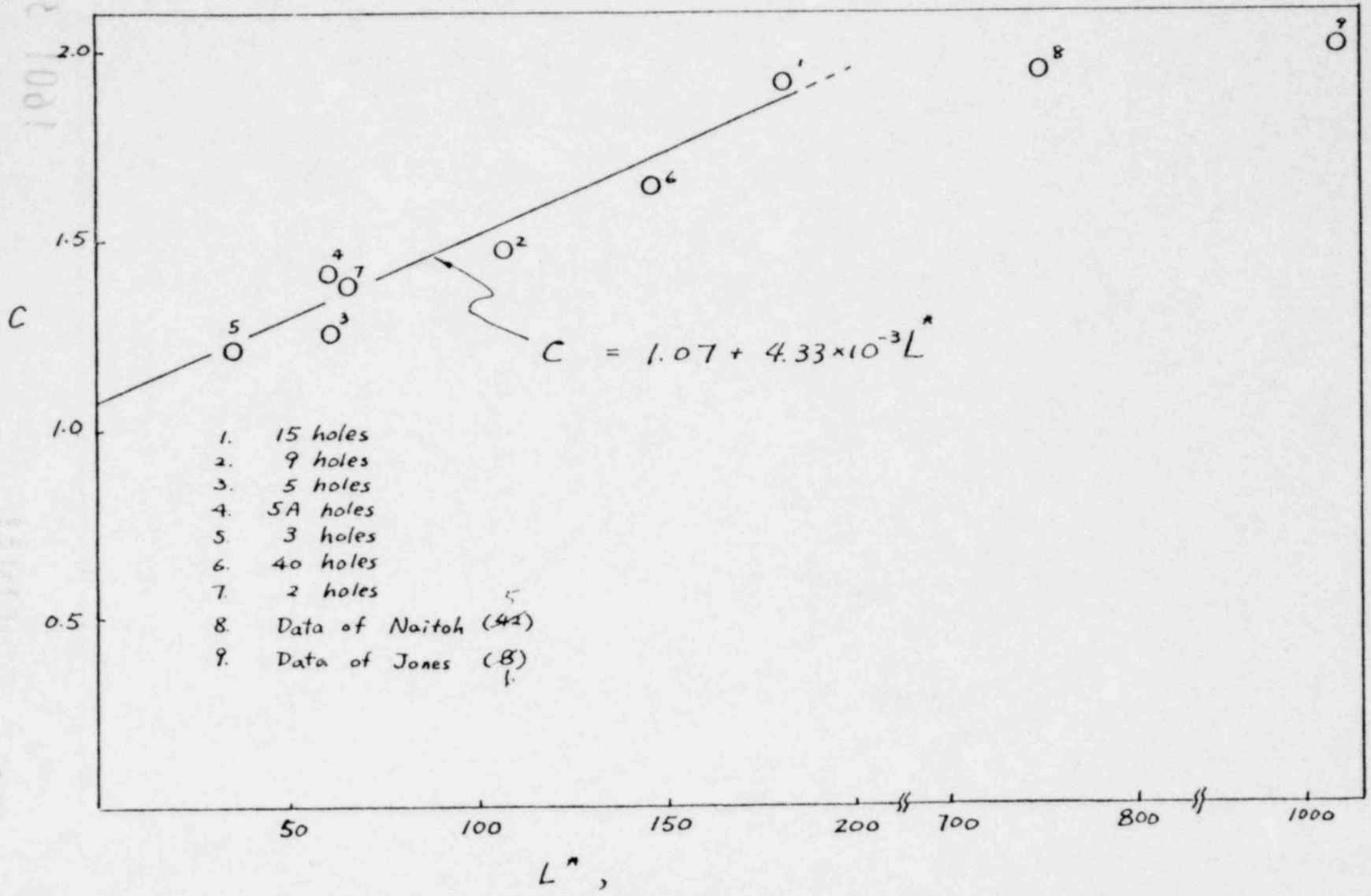

Figure 5 Intercept C in equation (7) as a function of L^*.

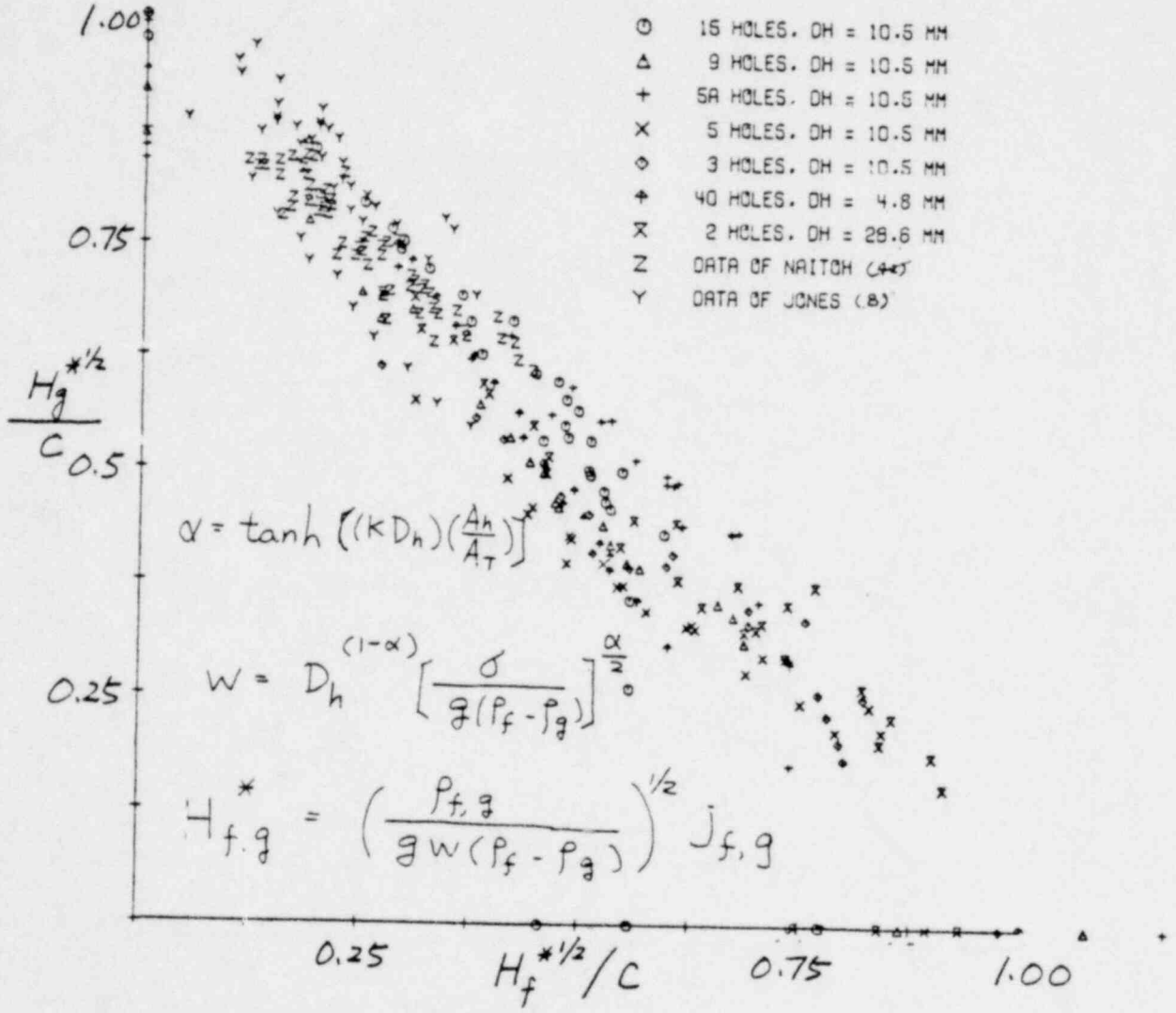

Figure 6 Data Correlation with Equation (7).

$$\frac{H_g^{*1/2}}{C} + \frac{H_f^{*1/2}}{C} = 1$$

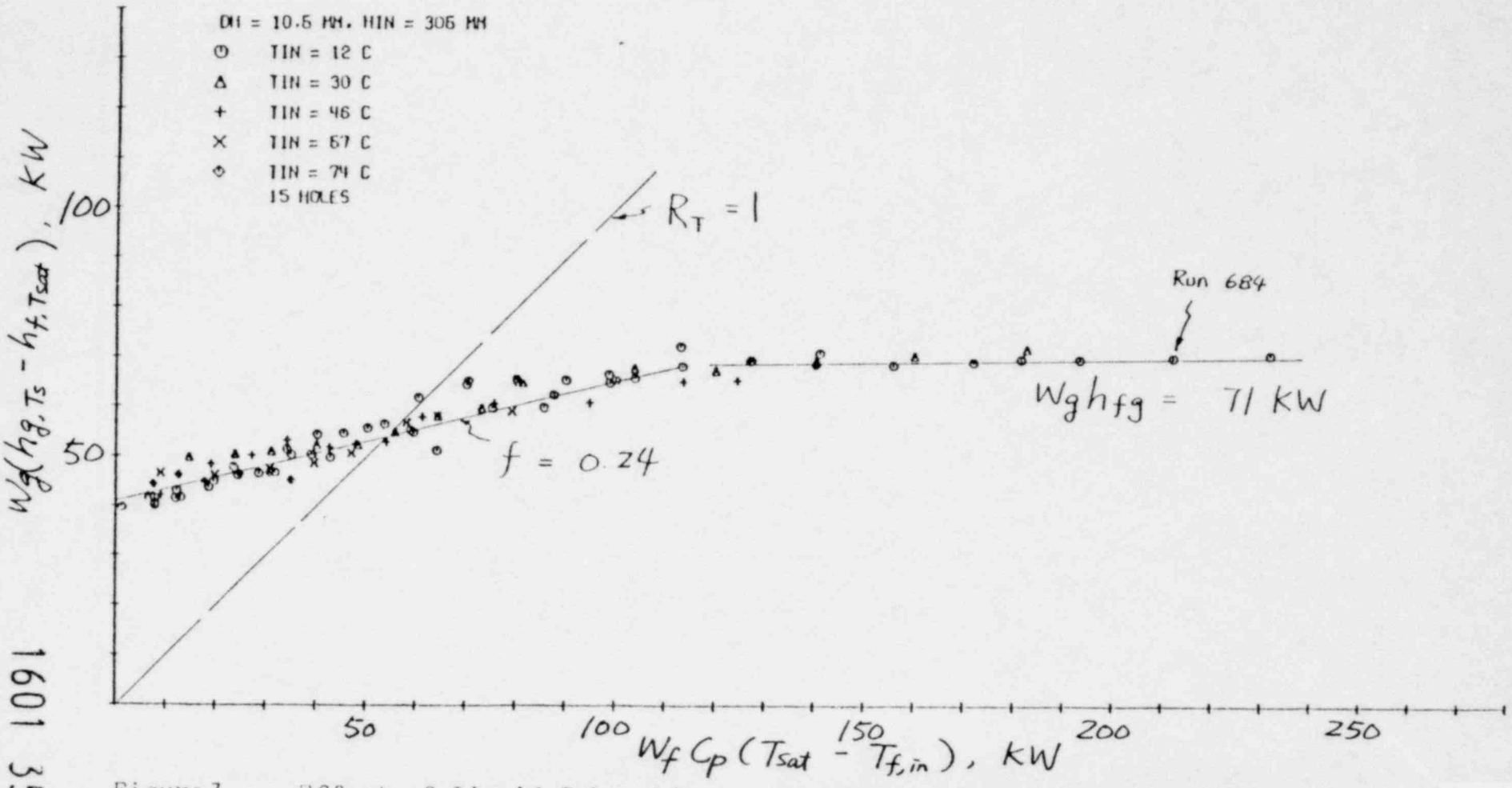

Figure 7 . Effect of Liquid Subcooling on EOCB (End of Complete Bypass, 15 Hole Data.

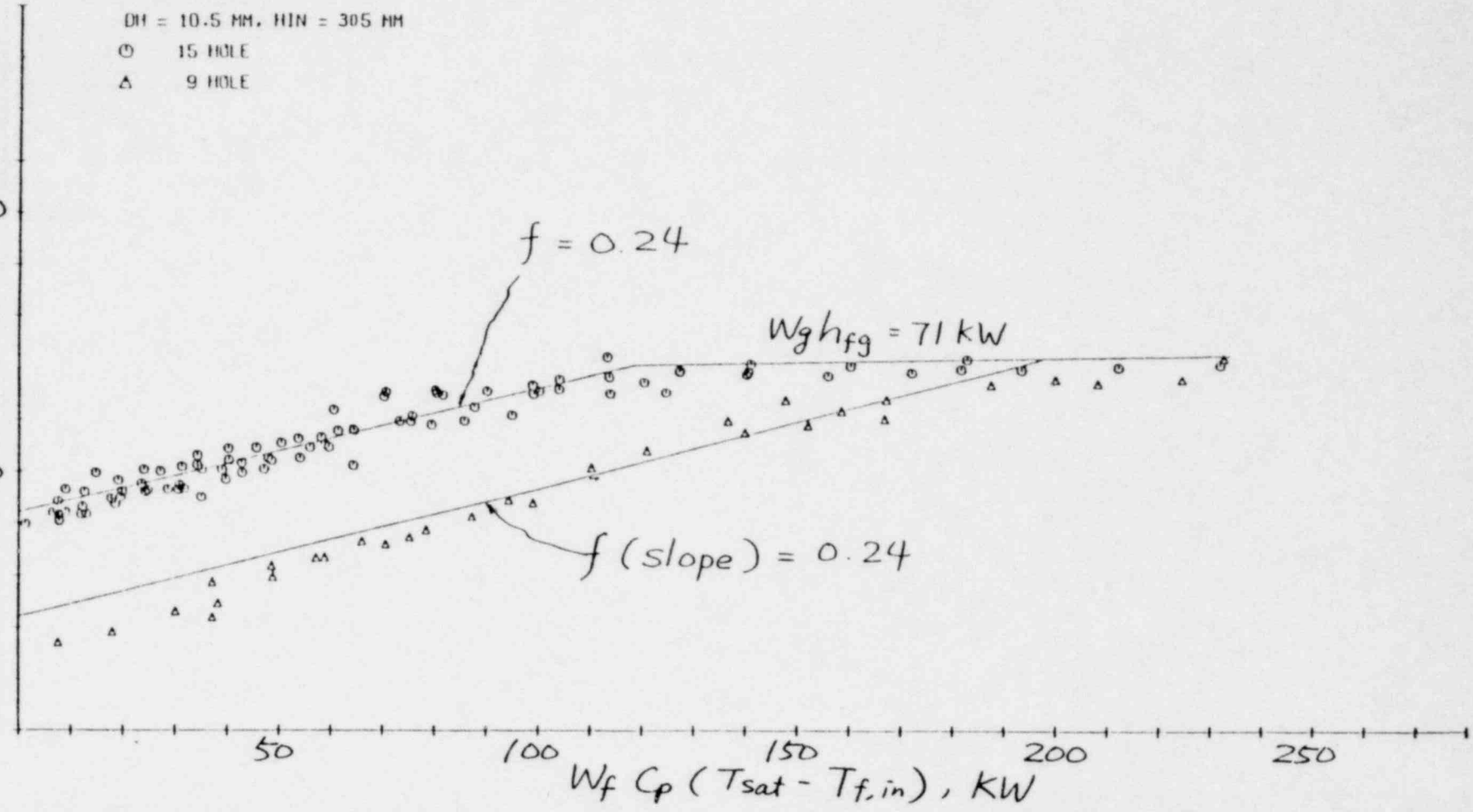

Figure 8 . Total Enthalpy Flux at EOCB 15 Hole and 9 Hole Data, H_{in} = 305 mm.

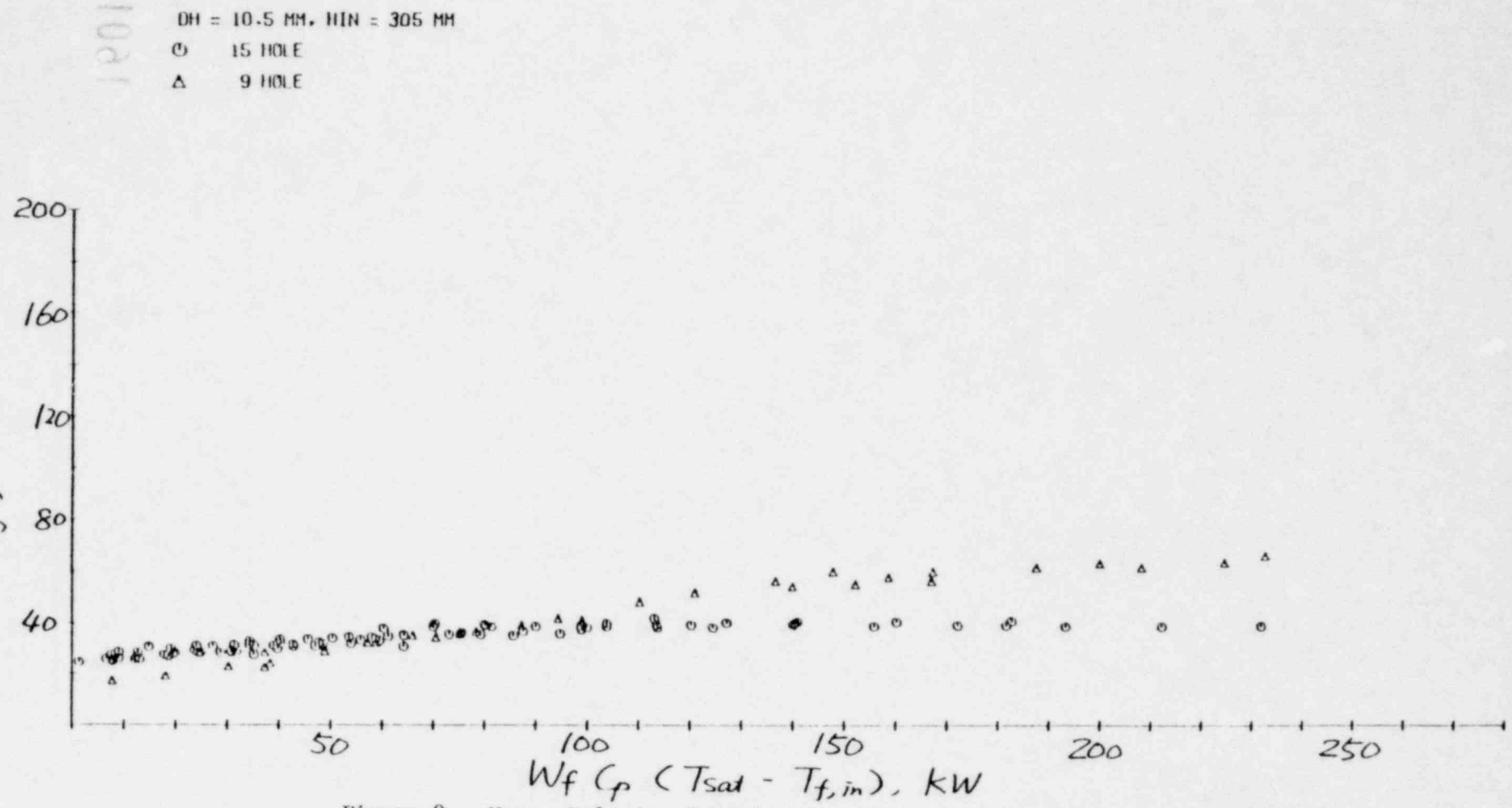

Figure 9. Vapor Velocity Entering the Holes, 15 Hole and 9 Hole Data, h_{in} = 305 mm.

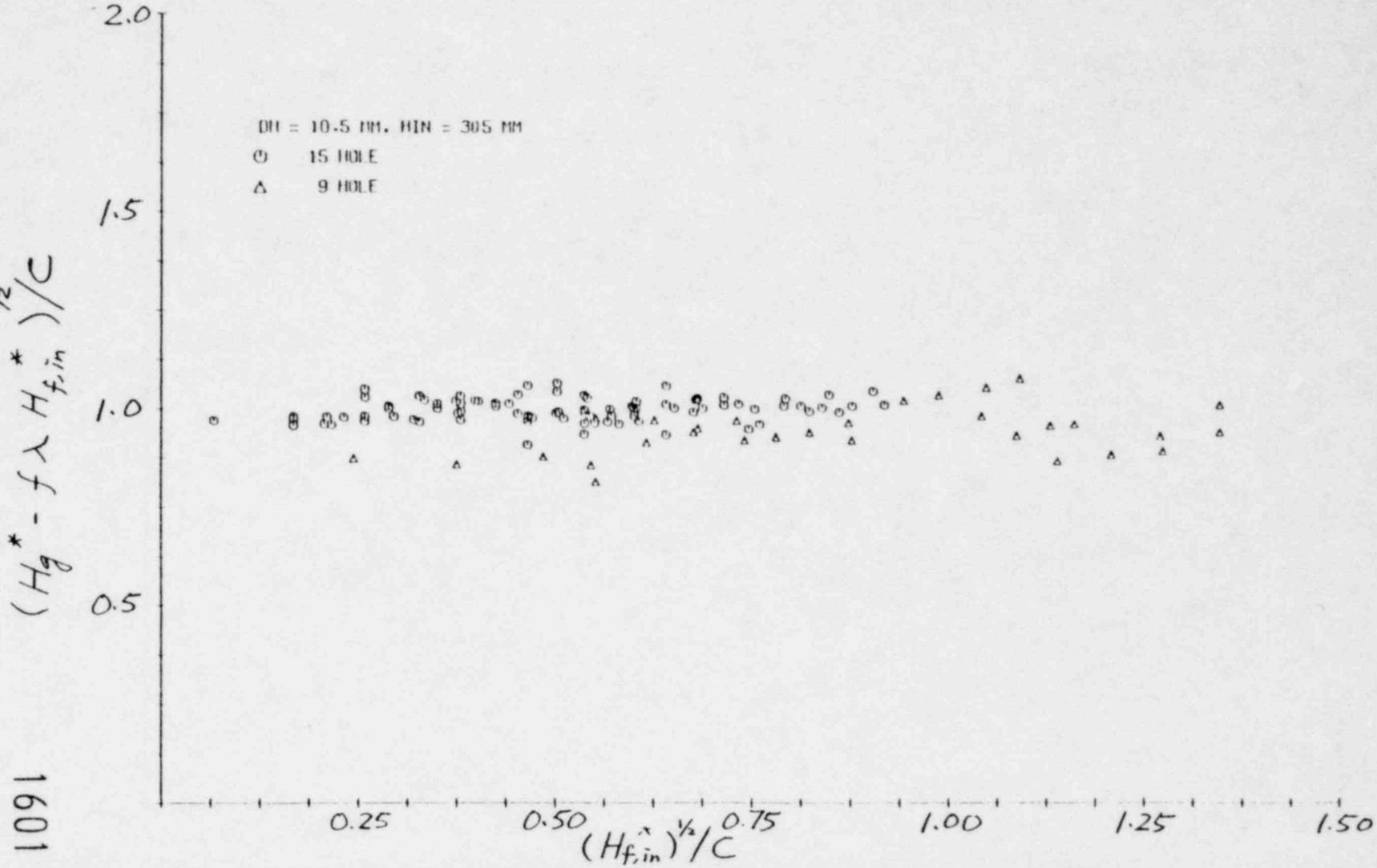

Figure 10 . Comparison of 15 Hole and 9 Hole Data with EOCB Correlation Corrected for Condensation, (Eq. 9).

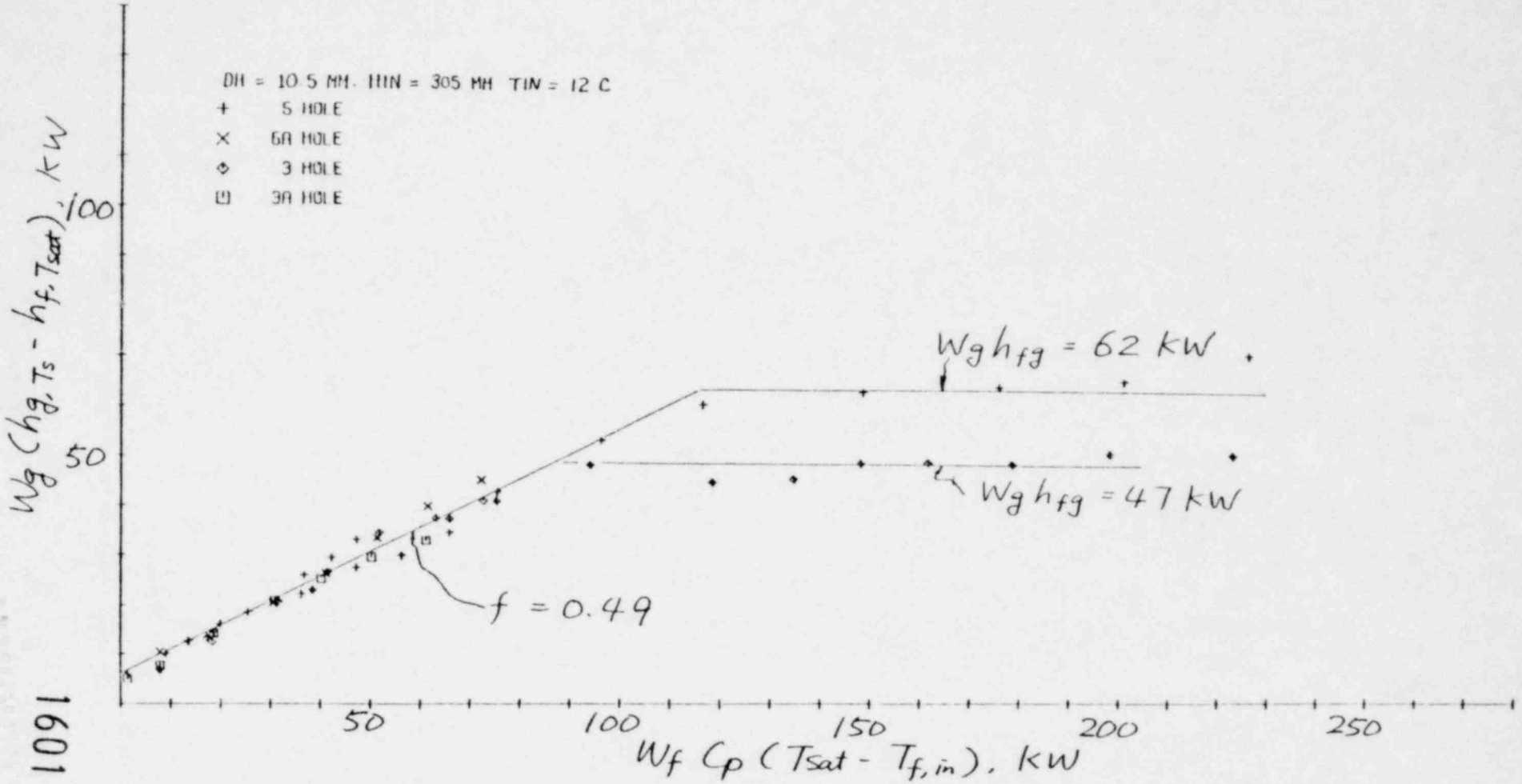

Figure 11. EOCB Data for 5 Hole, 5A Hole, 3 Hole and 3A Hole Geometries.

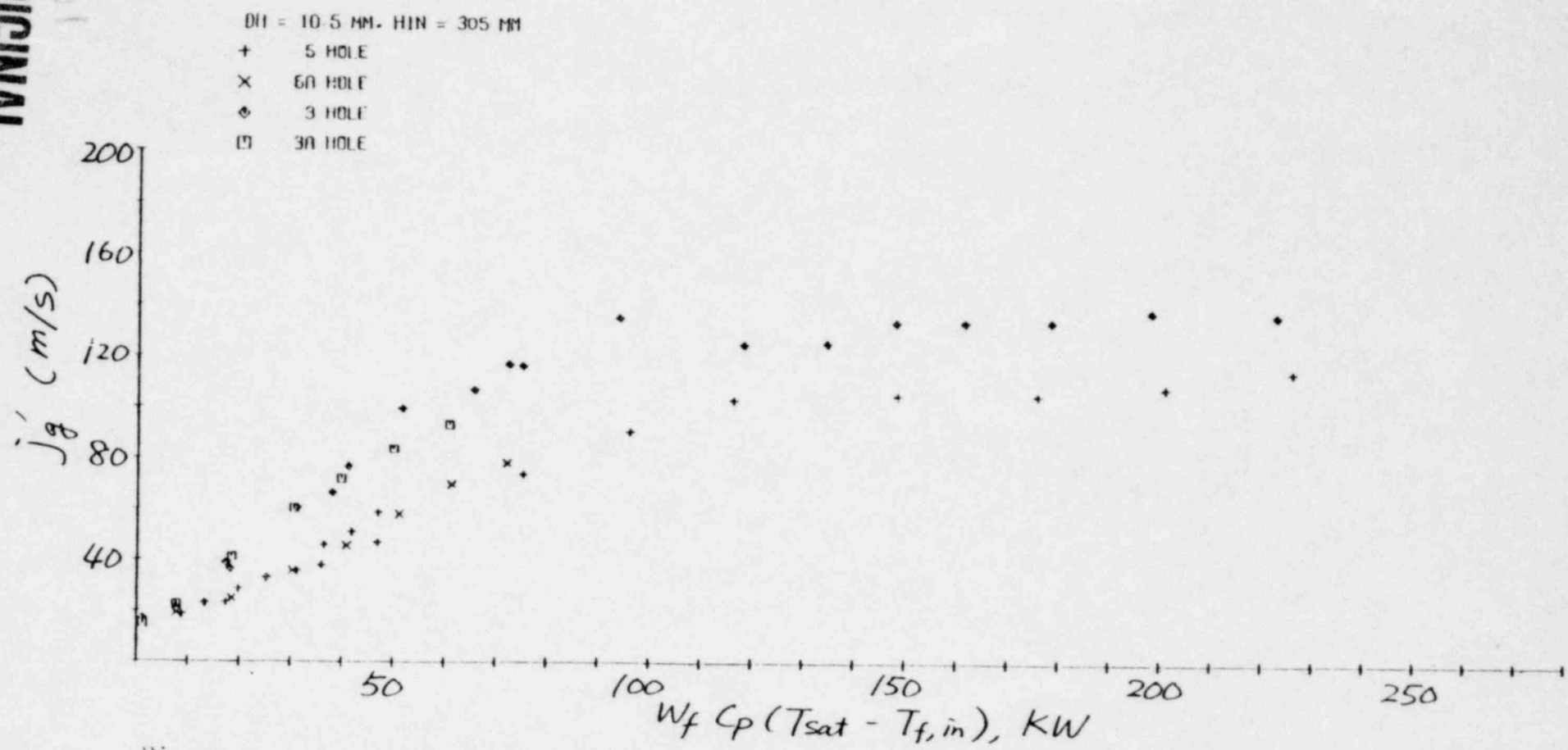

Figure 12 Steam Velocity Entering Holes for 5 Hole, 5A Hole, 3 Hole, and 3A Hole Data.

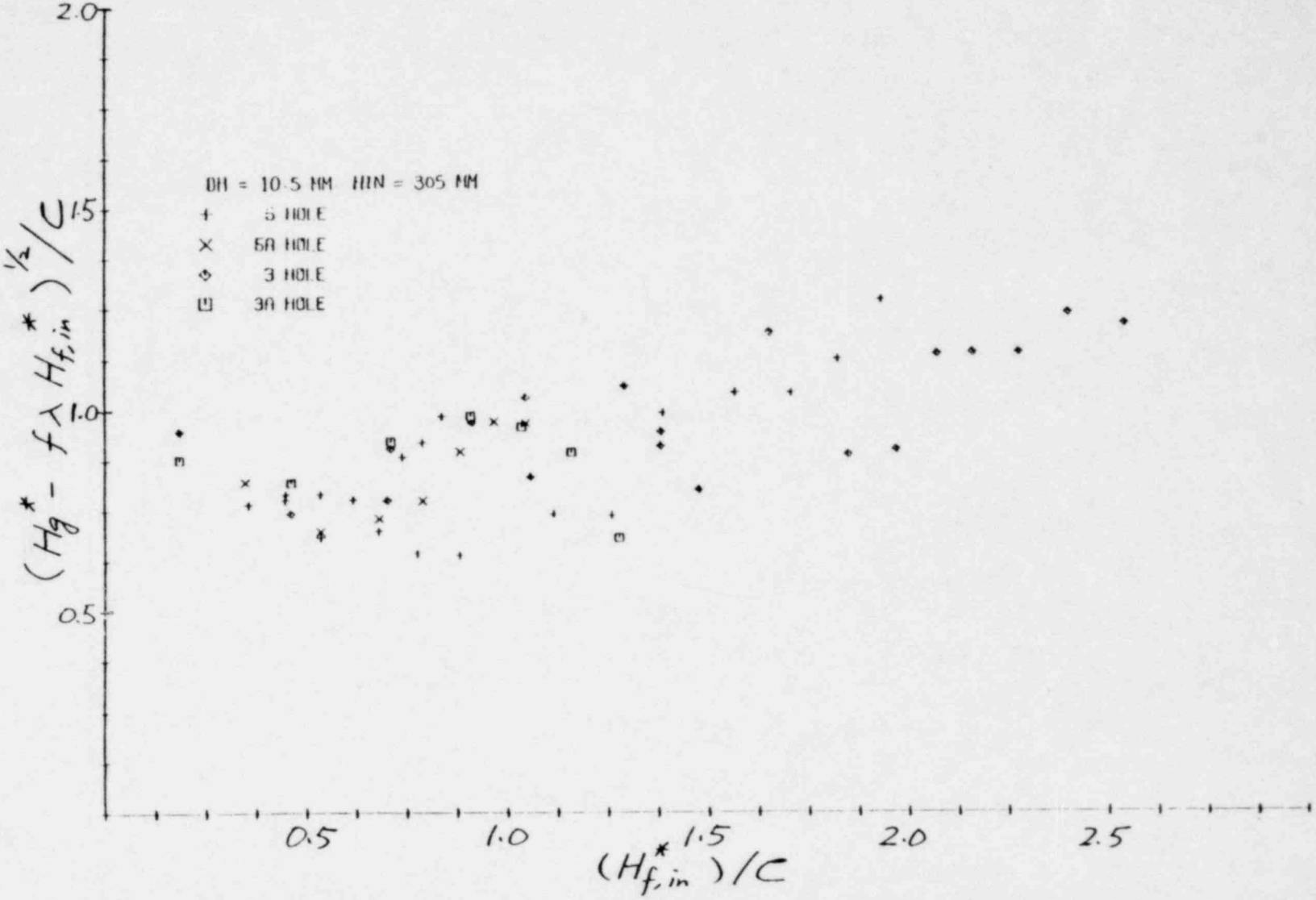

Figure 13. Comparison of 5 Hole, 5A Hole, 3 Hole, and 3A Hole Data with EOCB Correlation, Eq. (9).

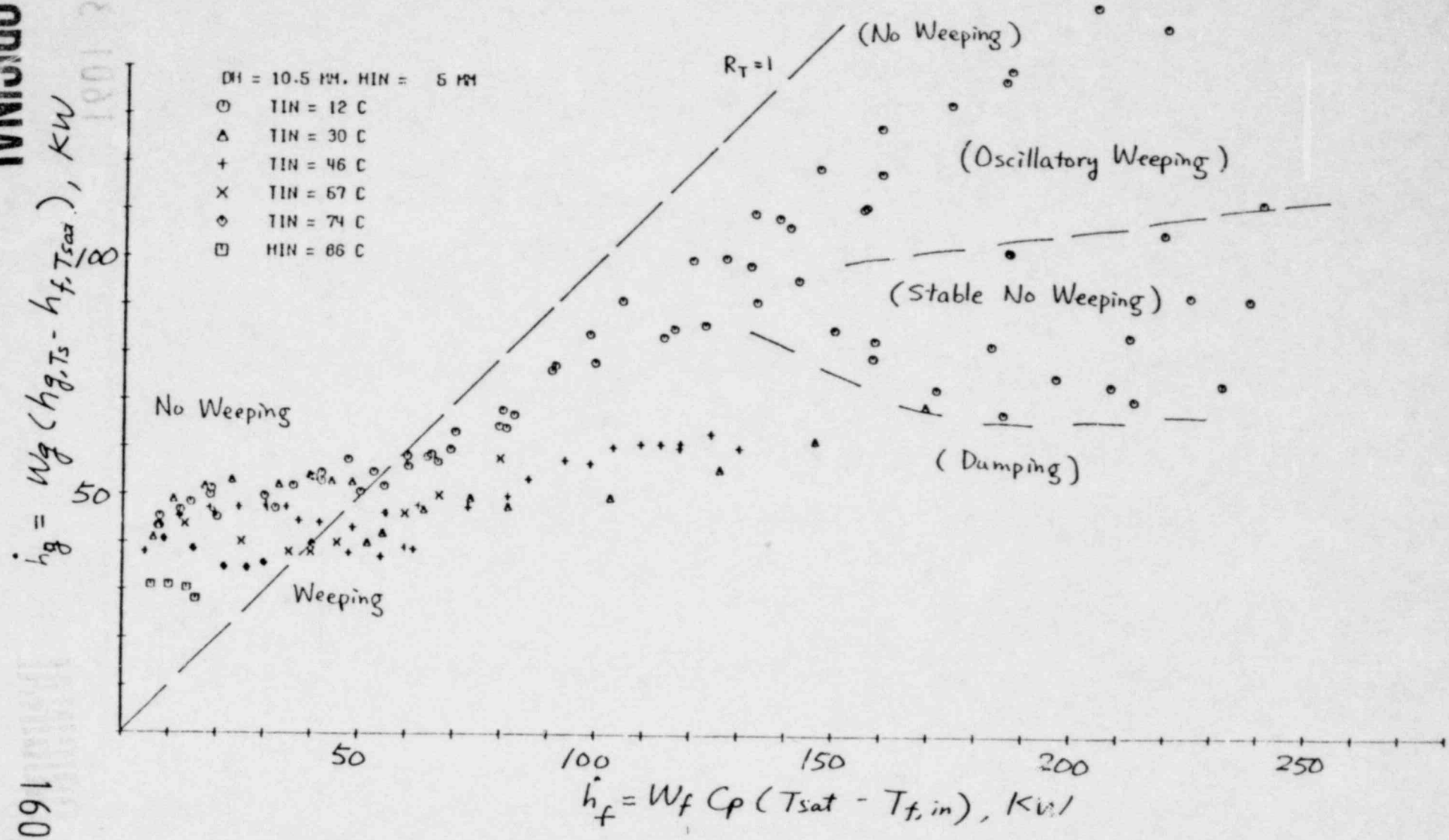

Figure 14. 15 Hole Liquid Penetration Data Obtained with Water Injected at Plate. (EOCB) End of Complete Bypass ≡ Onset of Weeping. End of Bypass (EOB) ≡ Dumping.

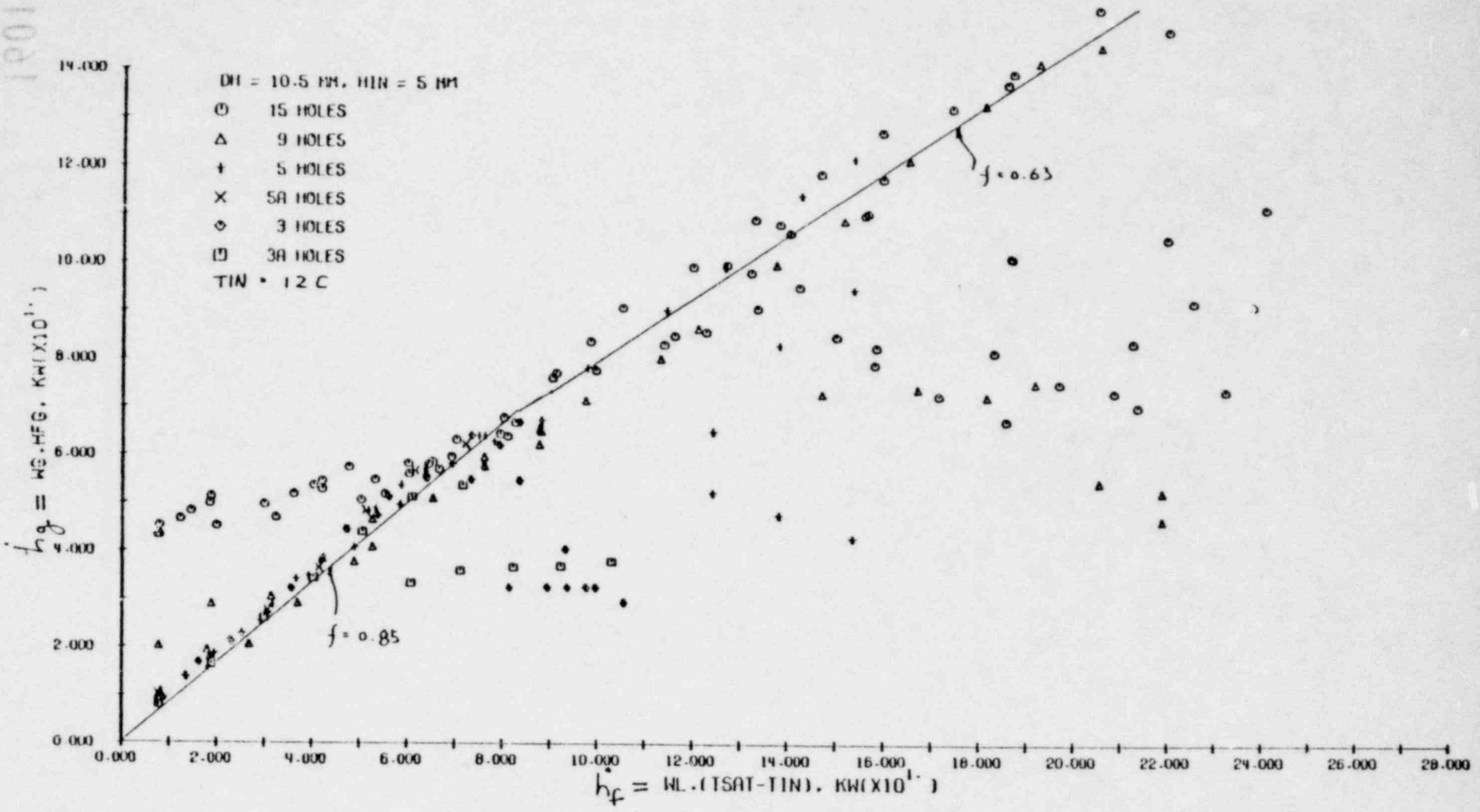

Figure 15. Liquid Penetration Data with 12°C Water Injected at the Plate for Various Perforation Ratios.

Figure 16. Effect of Liquid Inlet Spray Nozzle Position on Weep Point, 15 Hole Data.

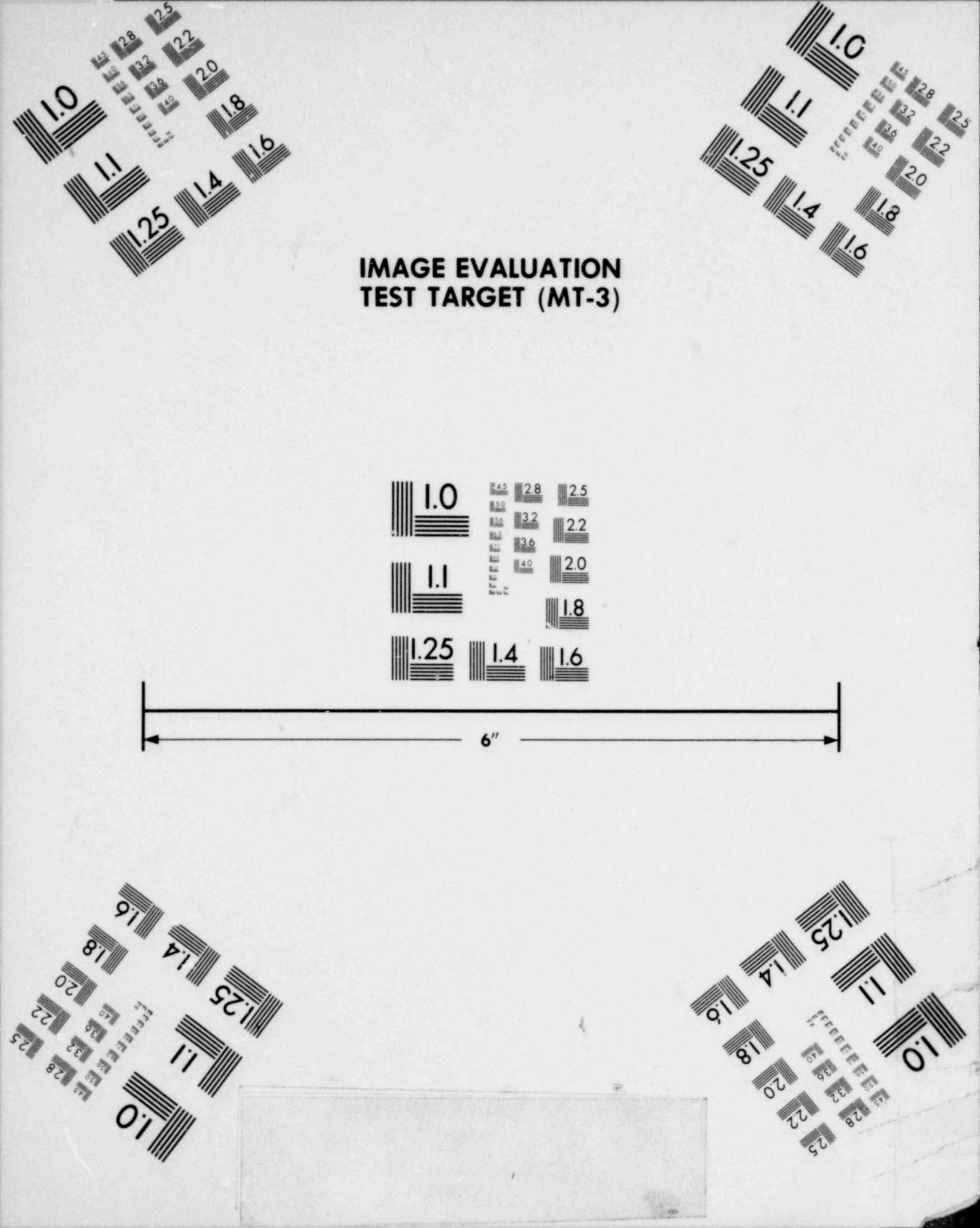
IMAGE EVALUATION
TEST TARGET (MT-3)
1.0
1.1
1.25
1.4
1.6
1.8
2.0
2.2
2.5
2.8
3.2
3.6
4.0
4.5
5.0
5.6
6.3
7.1
6"

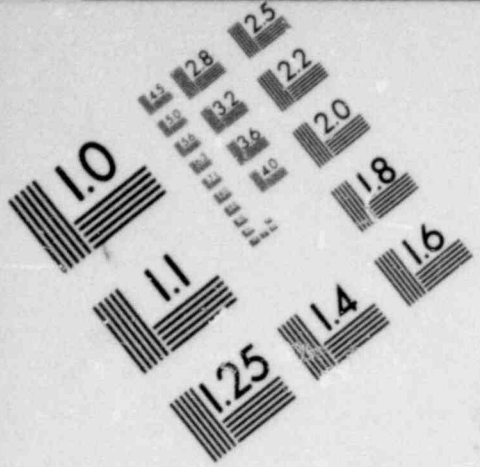

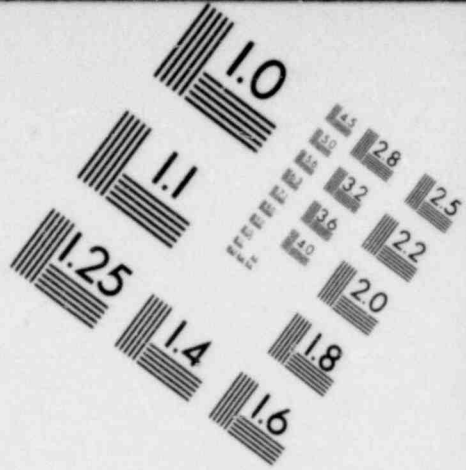

IMAGE EVALUATION TEST TARGET (MT-3)

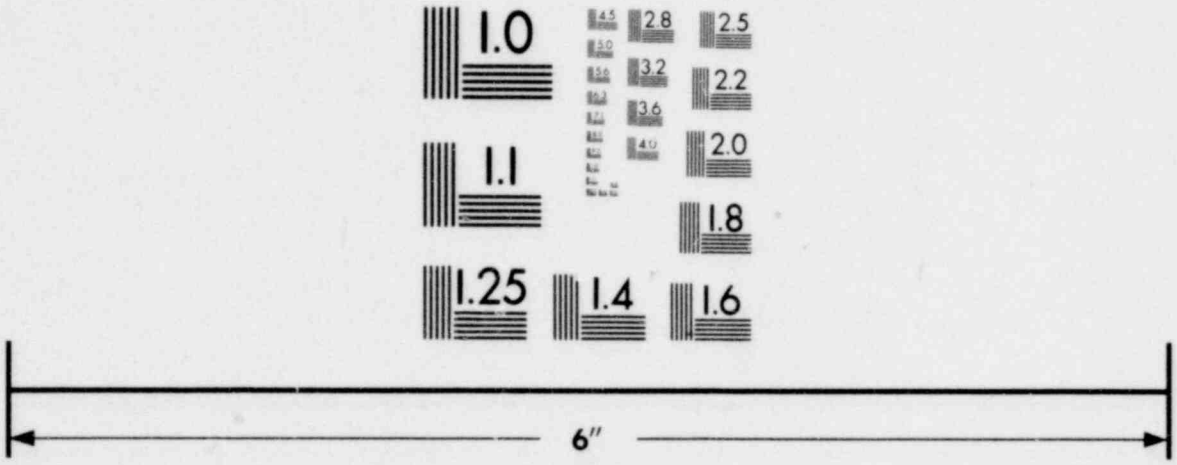

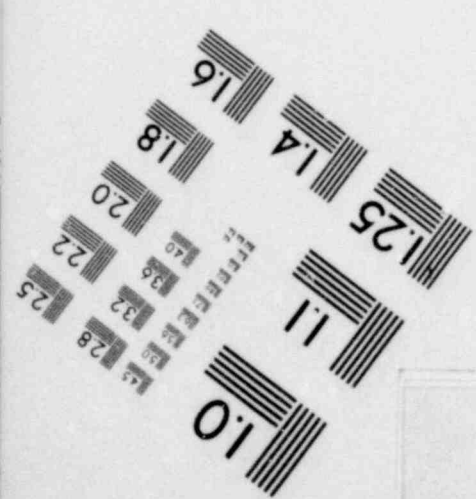

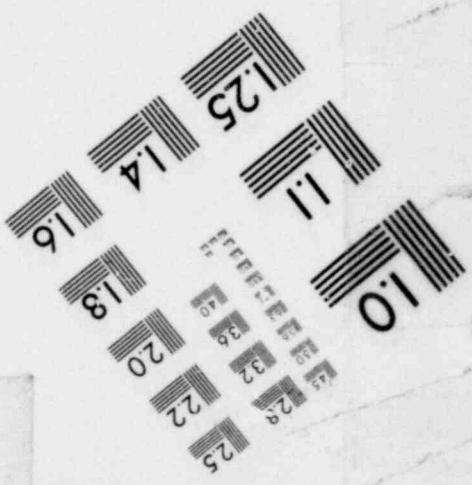

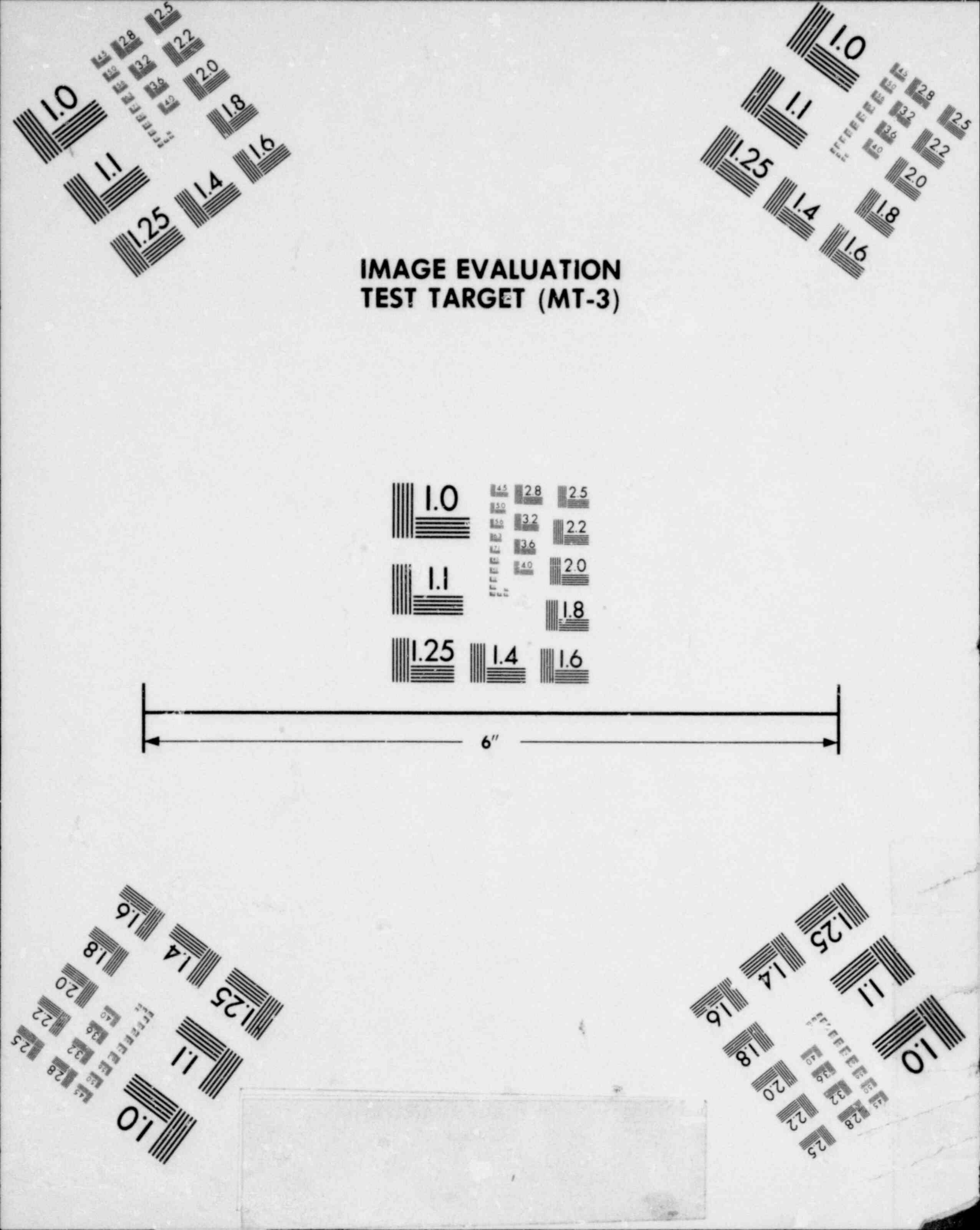
IMAGE EVALUATION
TEST TARGET (MT-3)
1.0
1.1
1.25
1.4
1.6
1.8
2.0
2.2
2.5
2.8
3.2
3.6
4.0
4.5
5.0
6.3
6"

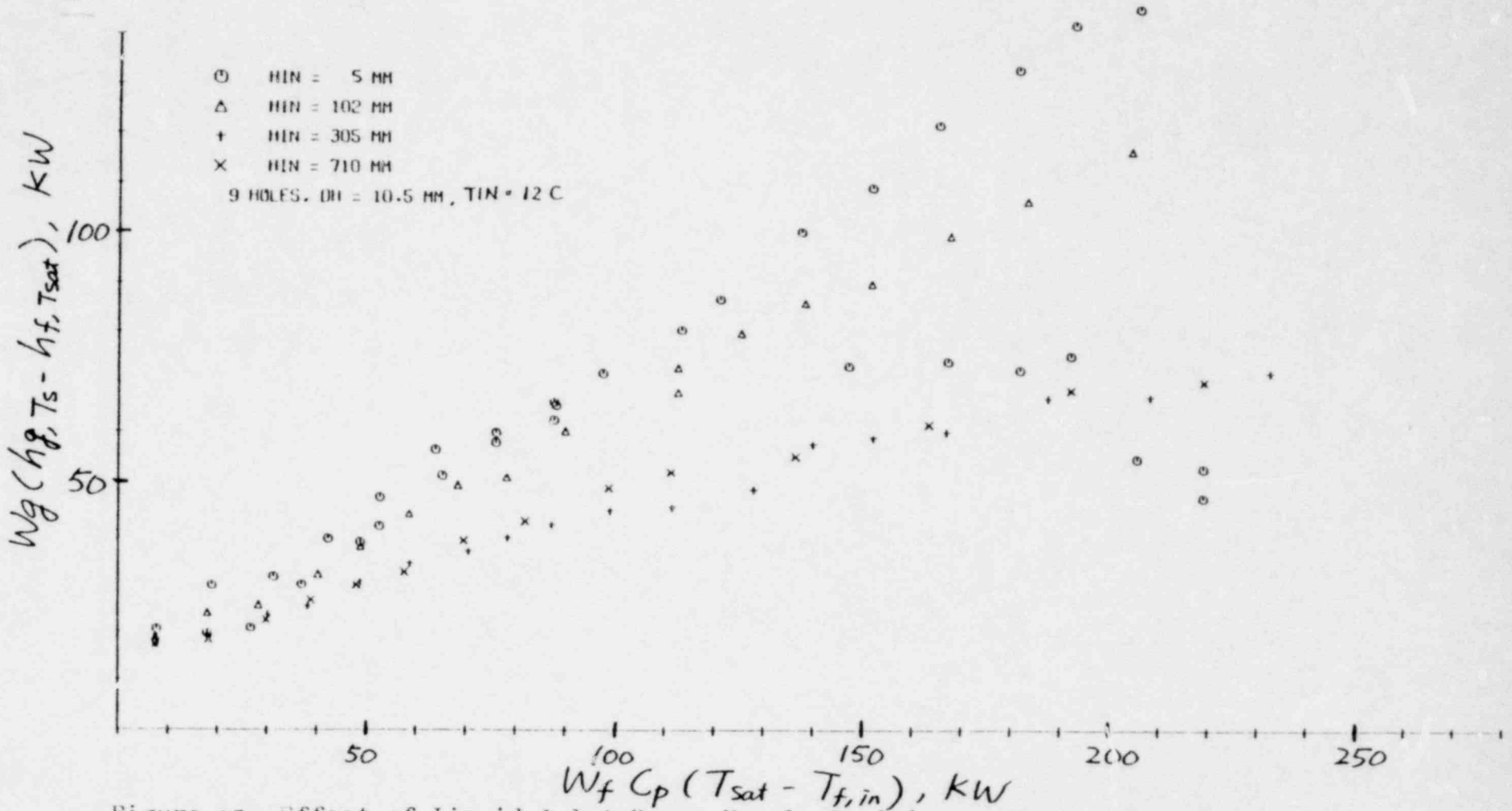

Figure 17. Effect of Liquid Inlet Spray Nozzle Position on Weep Point, 9 Hole Data.

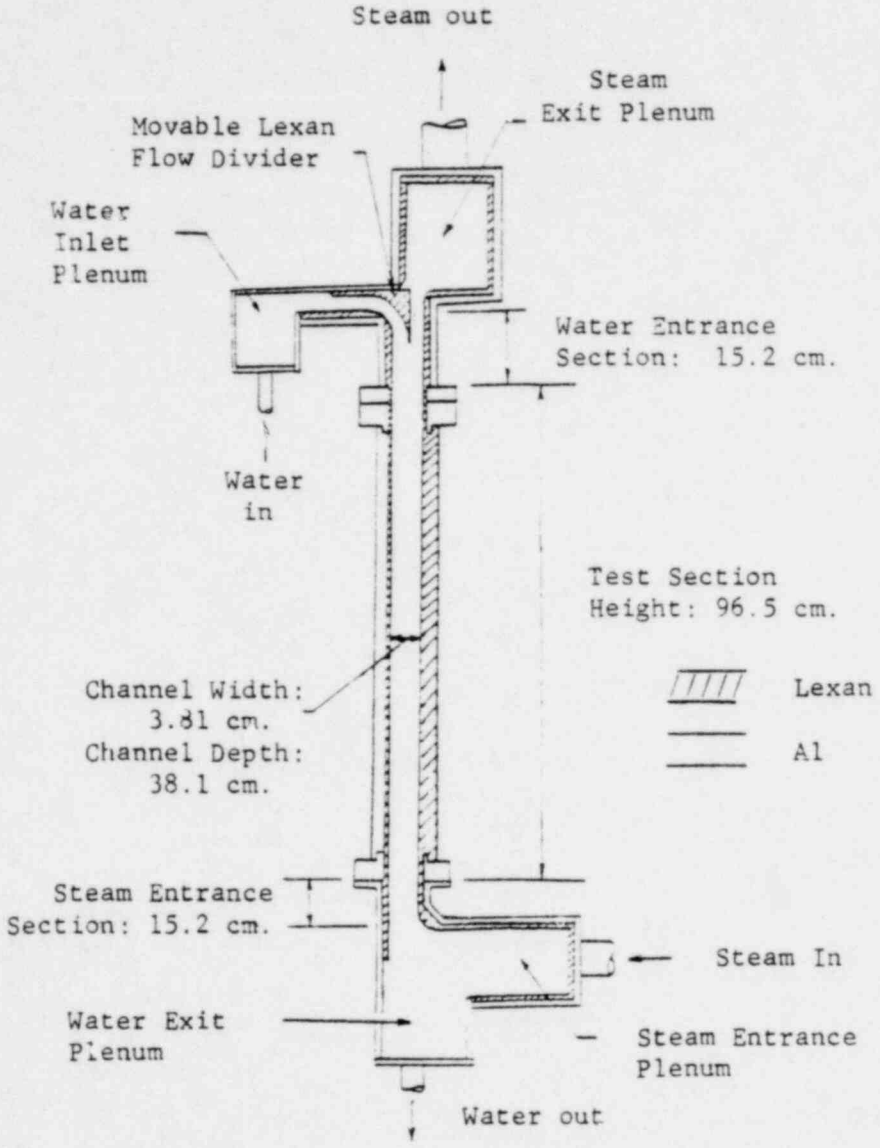

Figure 18: TEST SECTION AND END SECTIONS

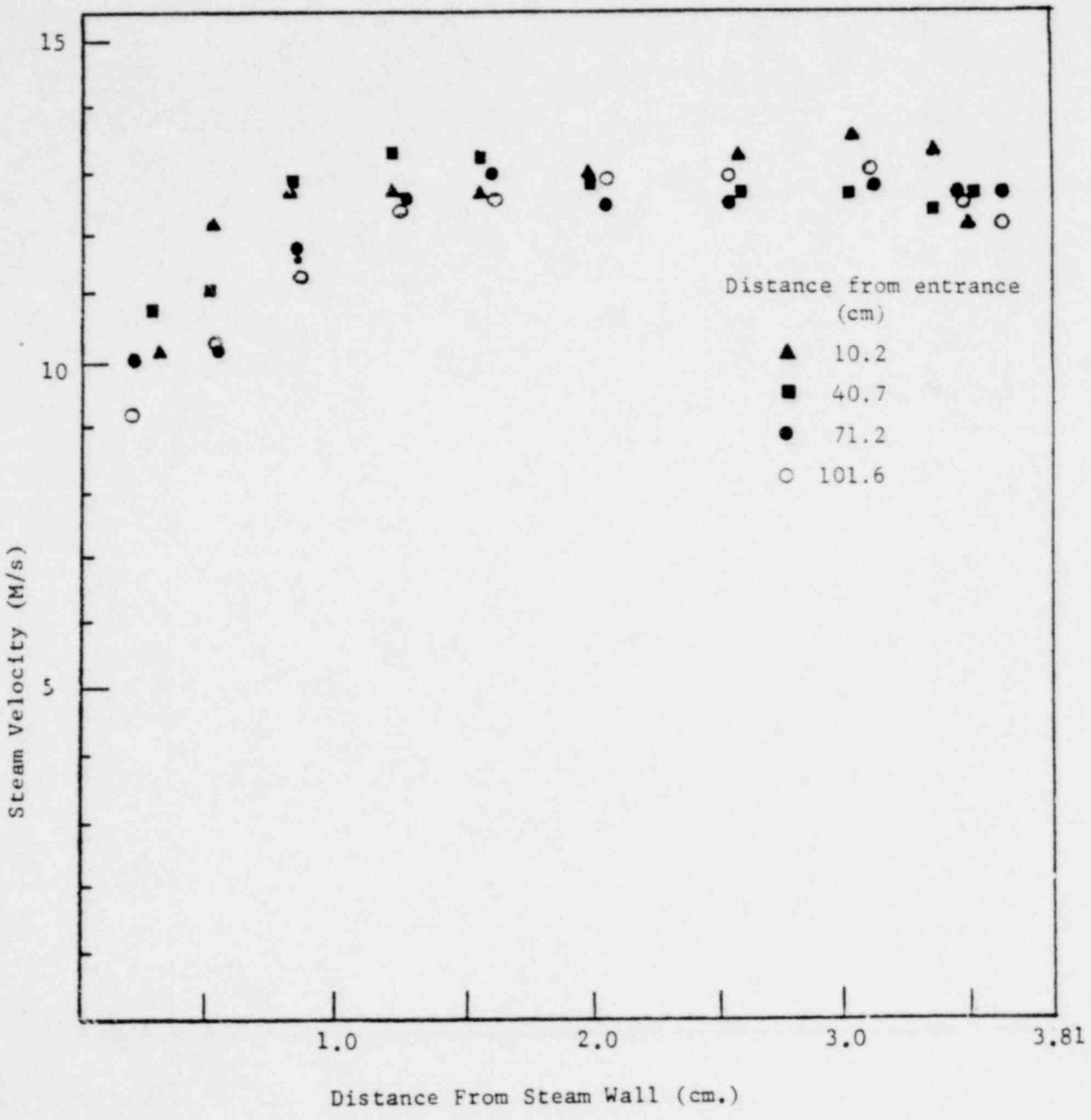

Figure 19: TYPICAL STEAM VELOCITY PROFILE

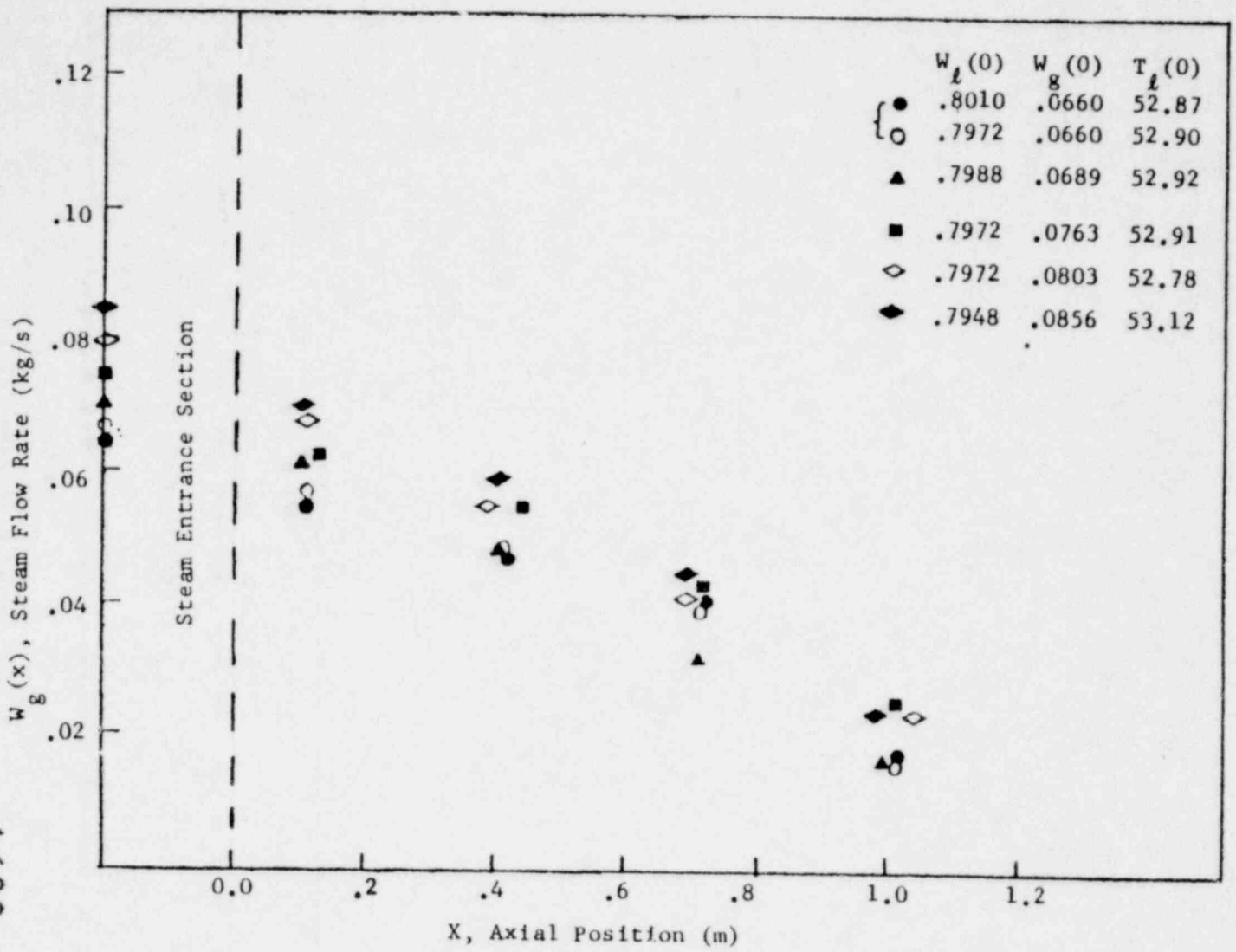

Figure 20 : AXIAL STEAM FLOW PROFILE

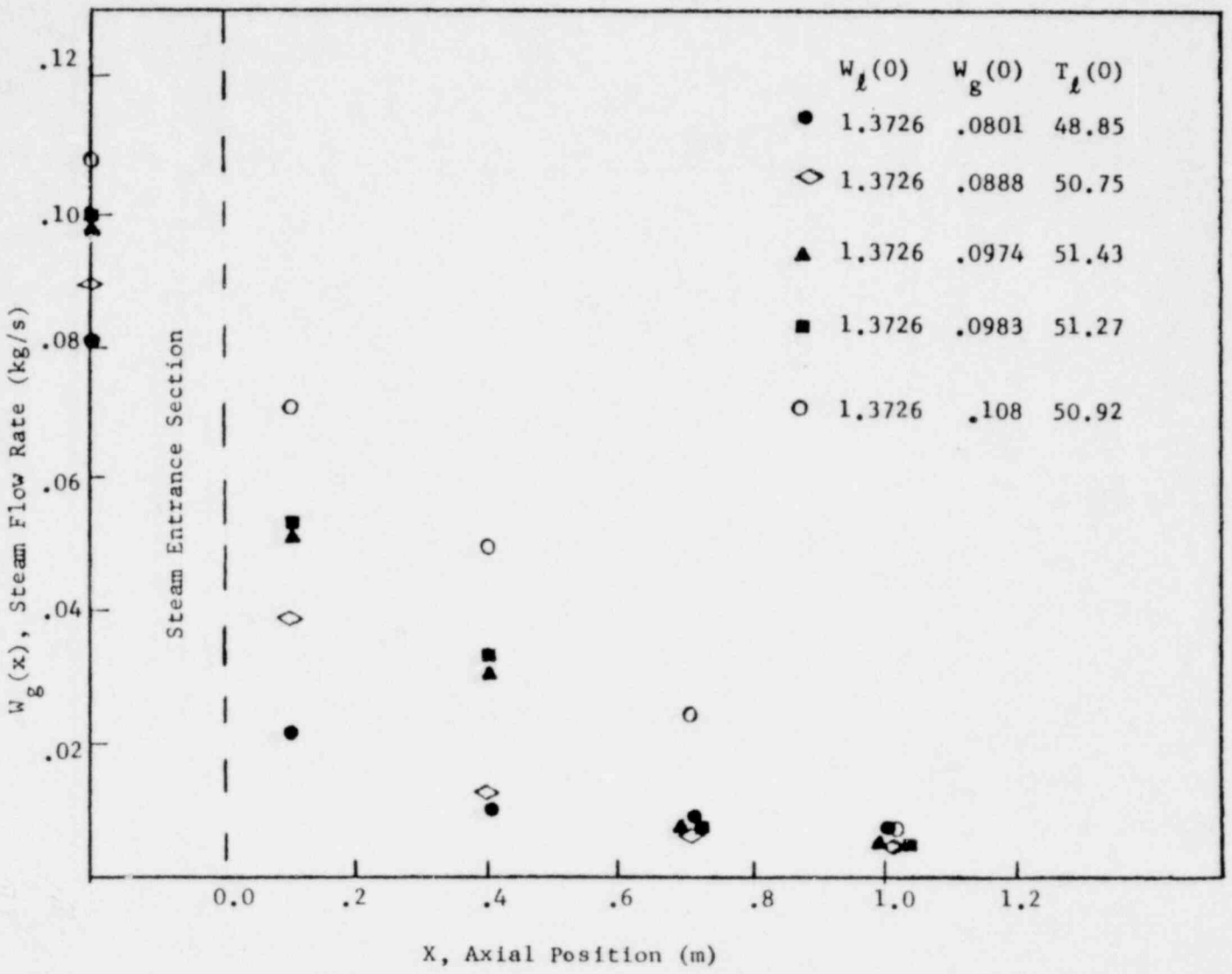

Figure 21 : AXIAL STEAM FLOW PROFILE

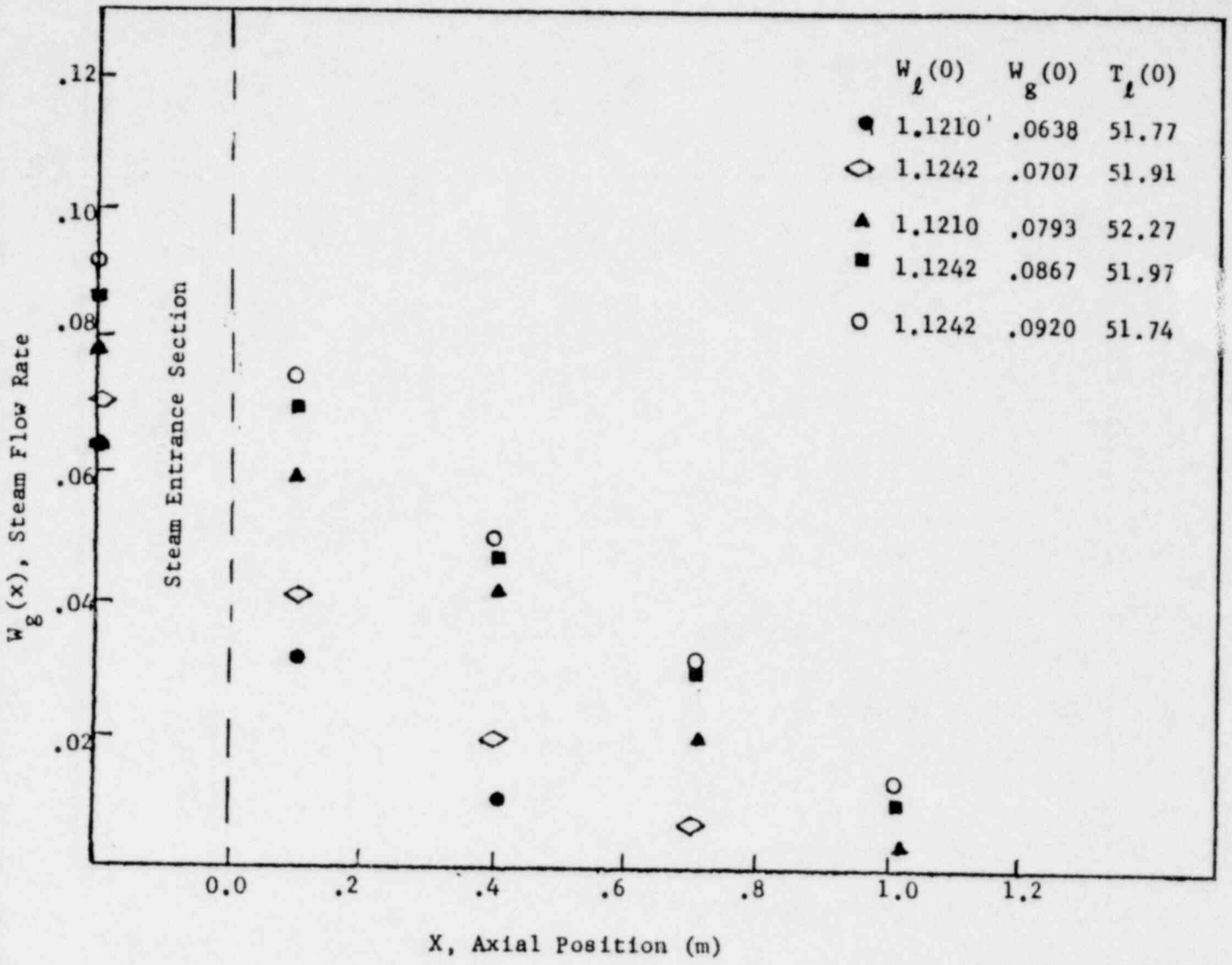

Figure 22 . AXIAL STEAM FLOW PROFILE

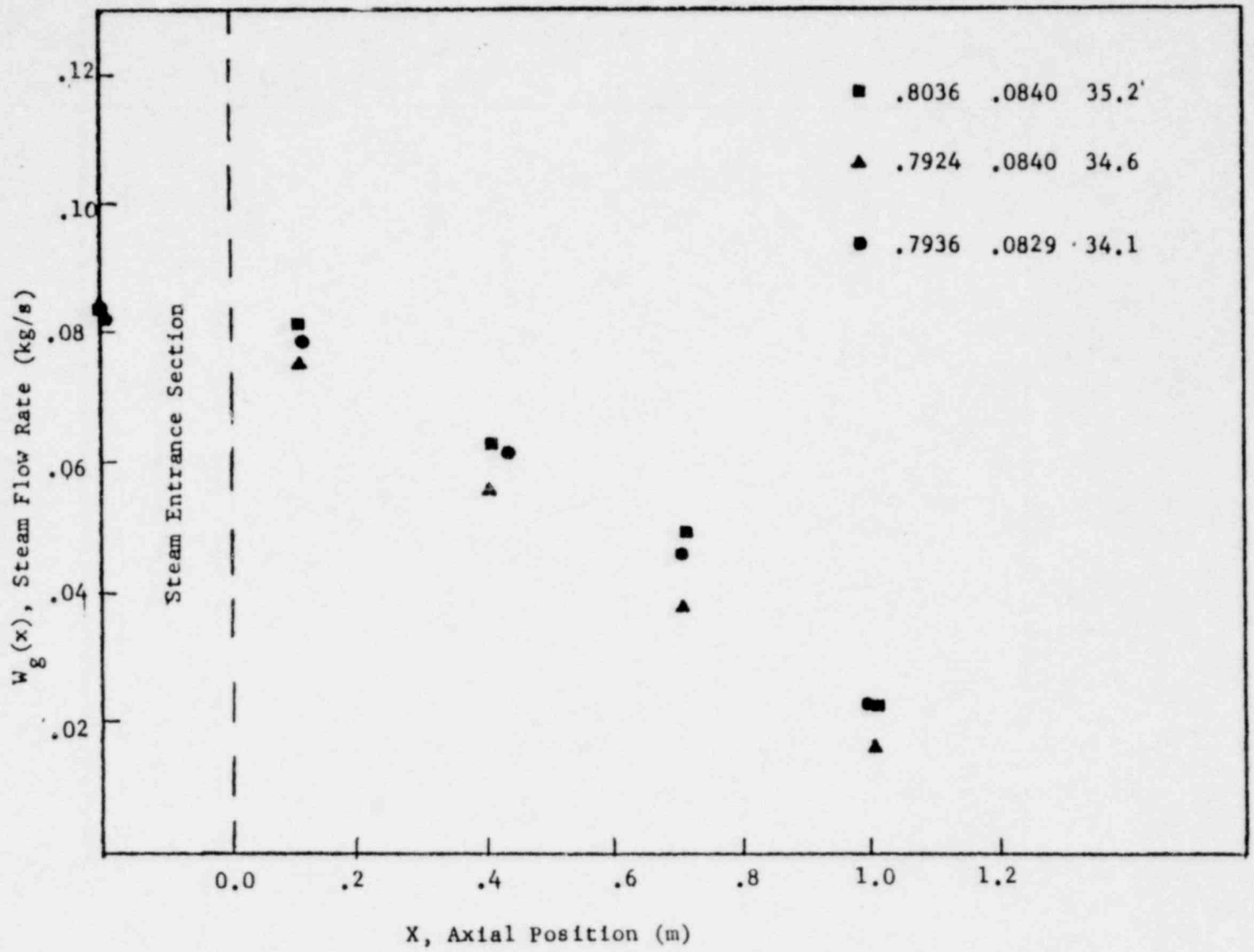

Figure 23: AXIAL STEAM FLOW PROFILE

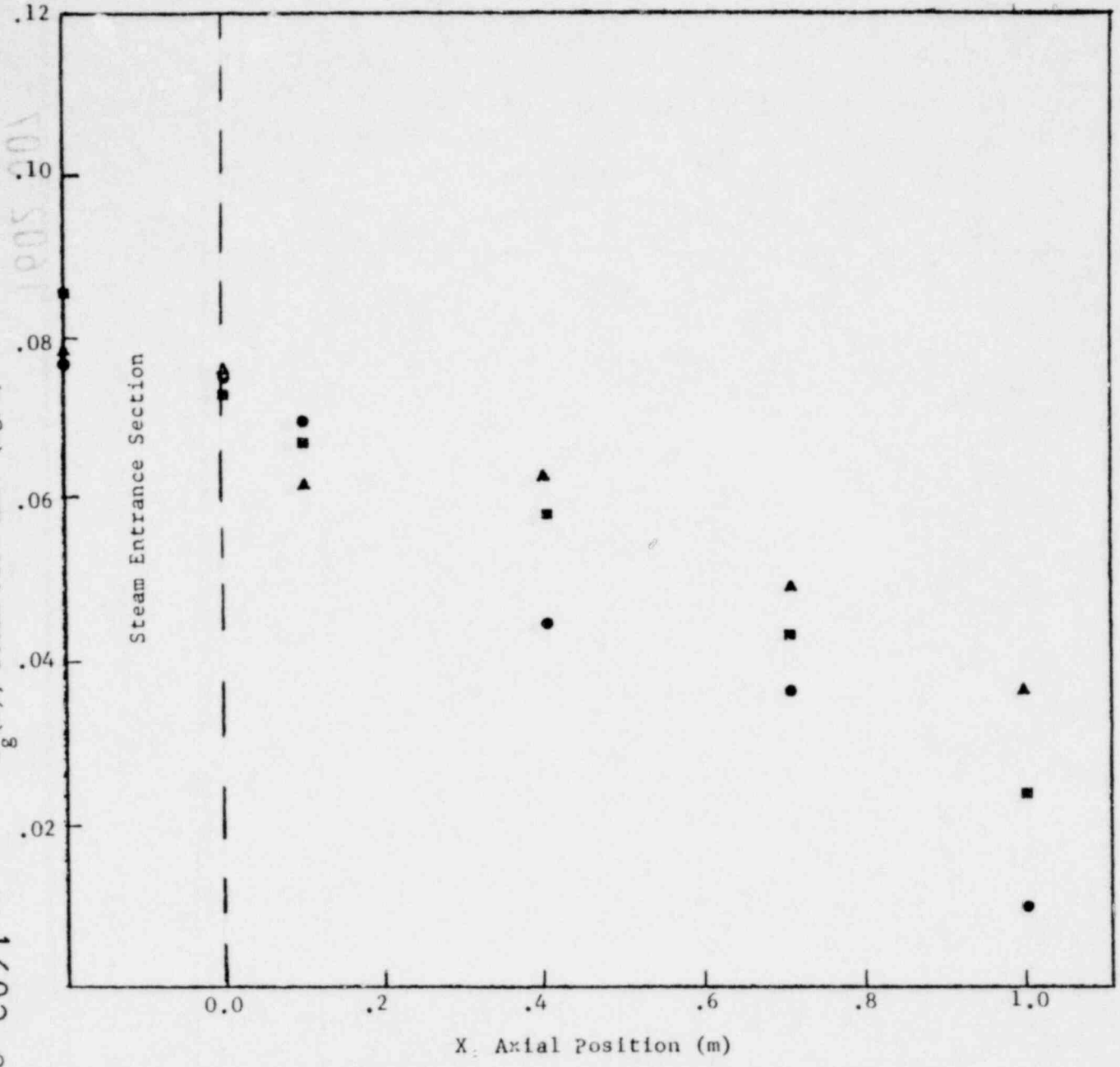

	$W_\ell(0)$	$W_g(x=0)$	$T_\ell(0)$
●	.7896	.075	34.02
■	.7948	.074	53.20
▲	.8163	.076	66.20

Figure 24 AXIAL STEAM FLOW PROFILE AS A FUNCTION OF INLET WATER TEMPERATURE

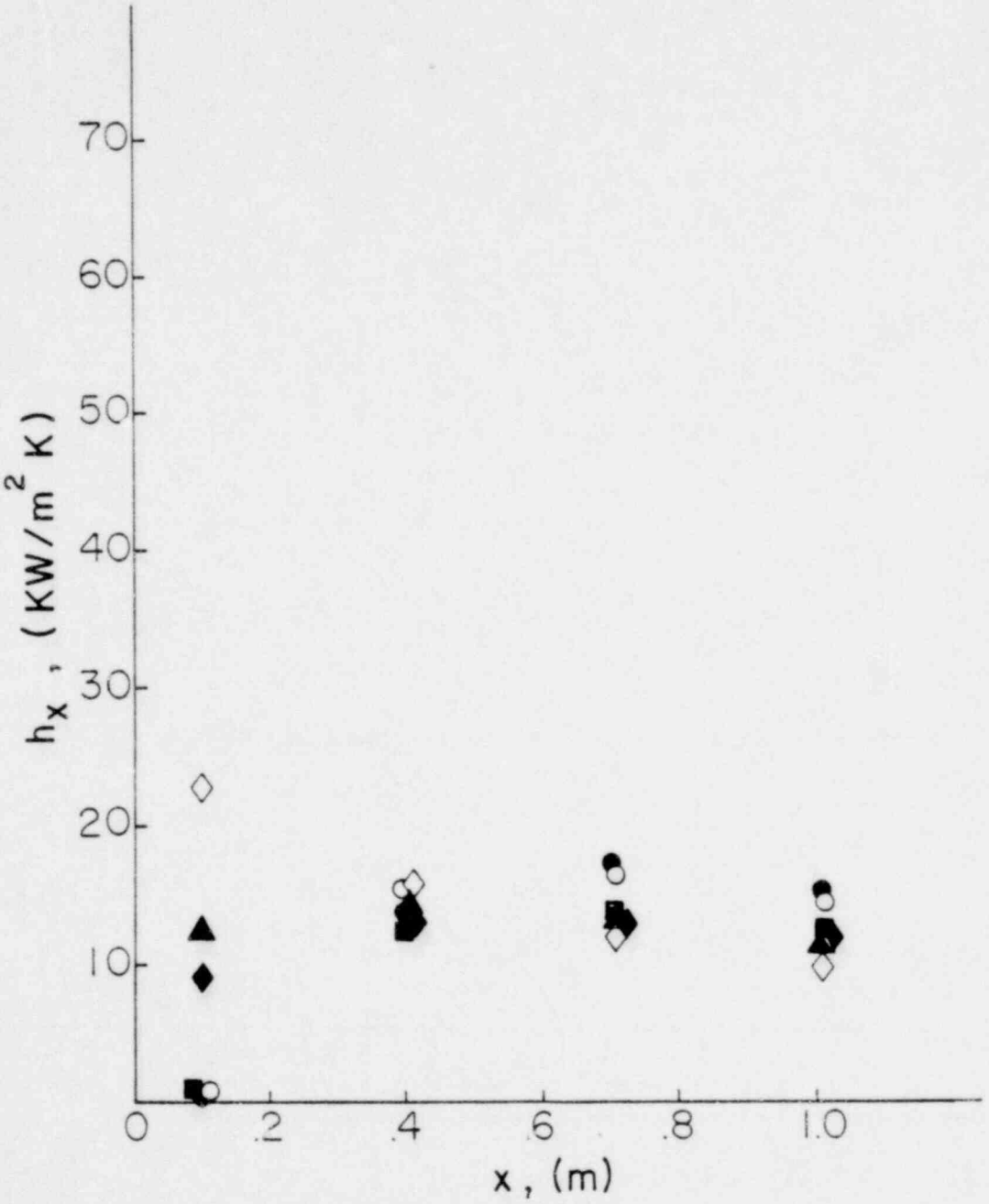

Fig. 25 Local Heat Transfer Coefficient vs. Distance from Bottom. Data as Fig. 20.

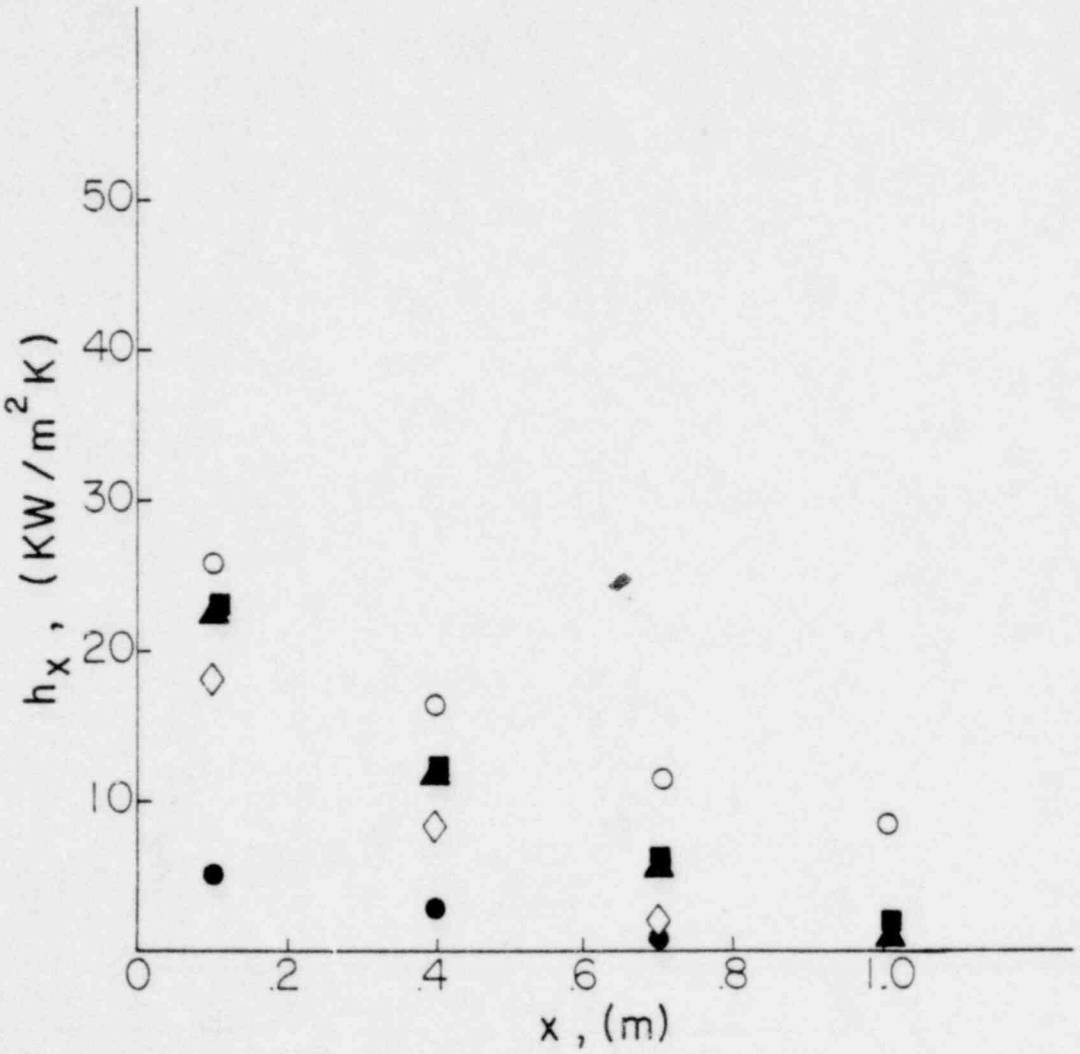

Fig. 26 Local Heat Transfer Coefficient vs. Distance from Bottom. Same Data as Fig. 21.

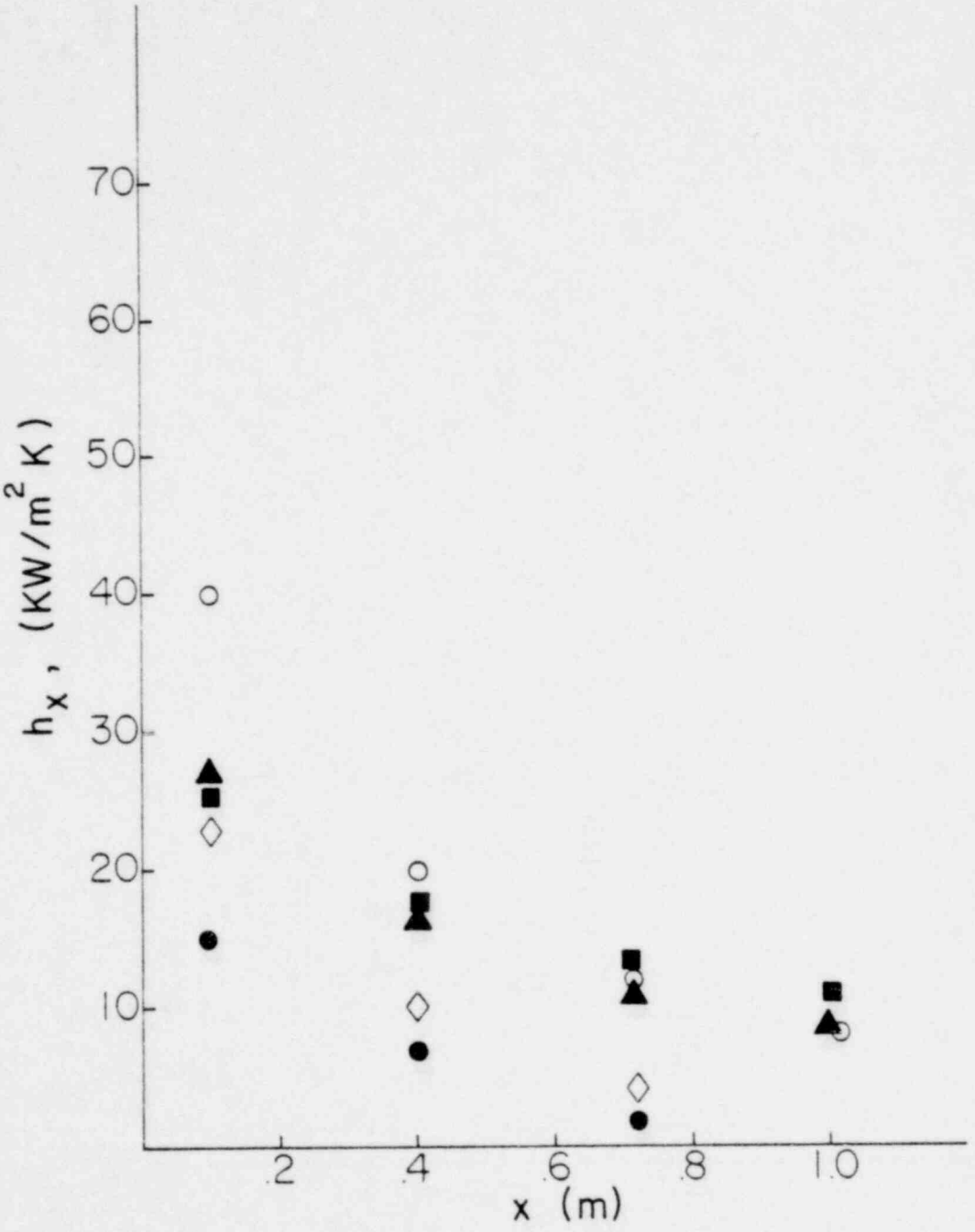

Fig. 27 Local Heat Transfer Coefficient vs. Distance from Bottom. Same Data as Fig. 22.

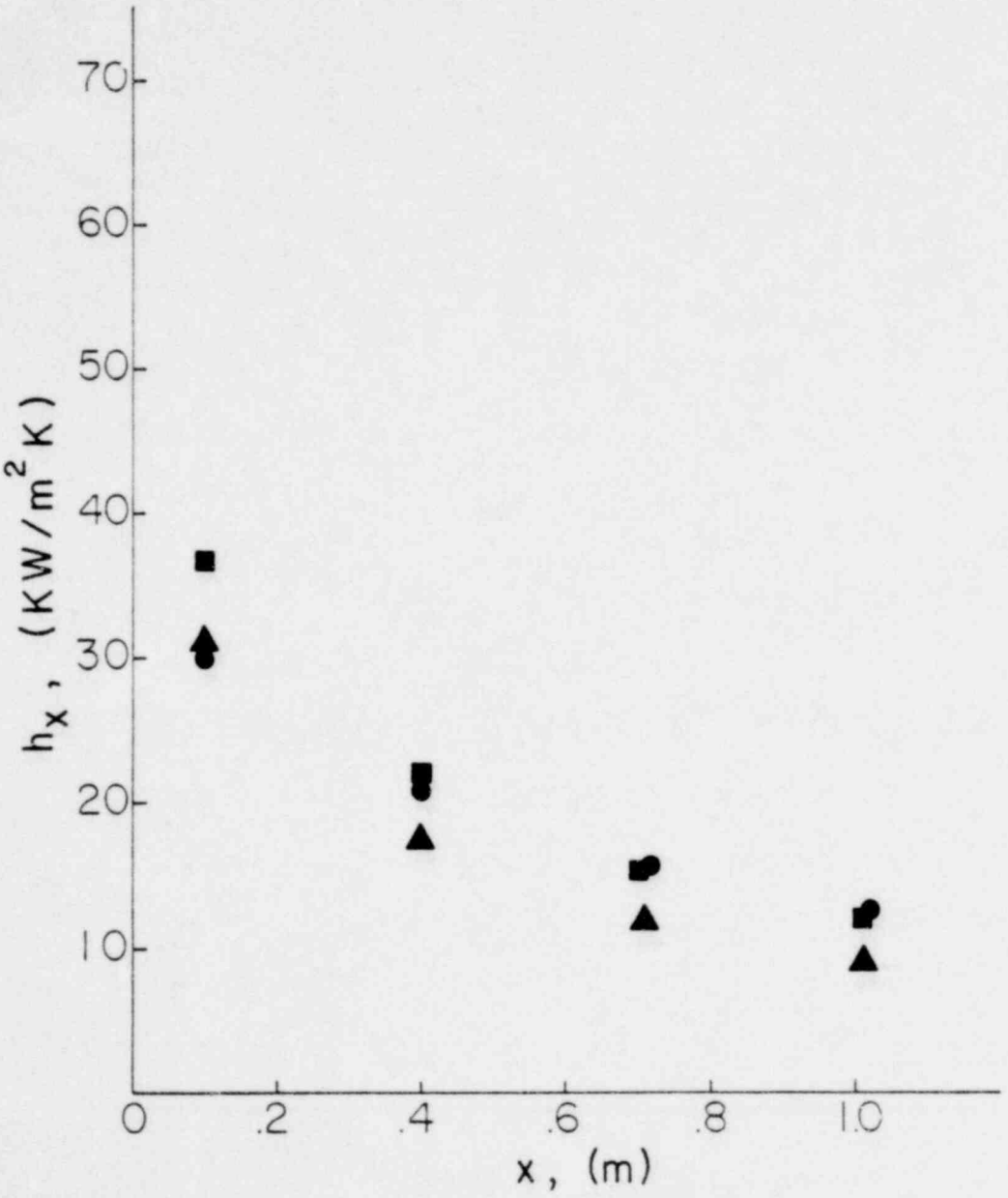

Fig. 28 Local Heat Transfer Coefficient vs. Distance from Bottom. Same Data as Fig. 23.

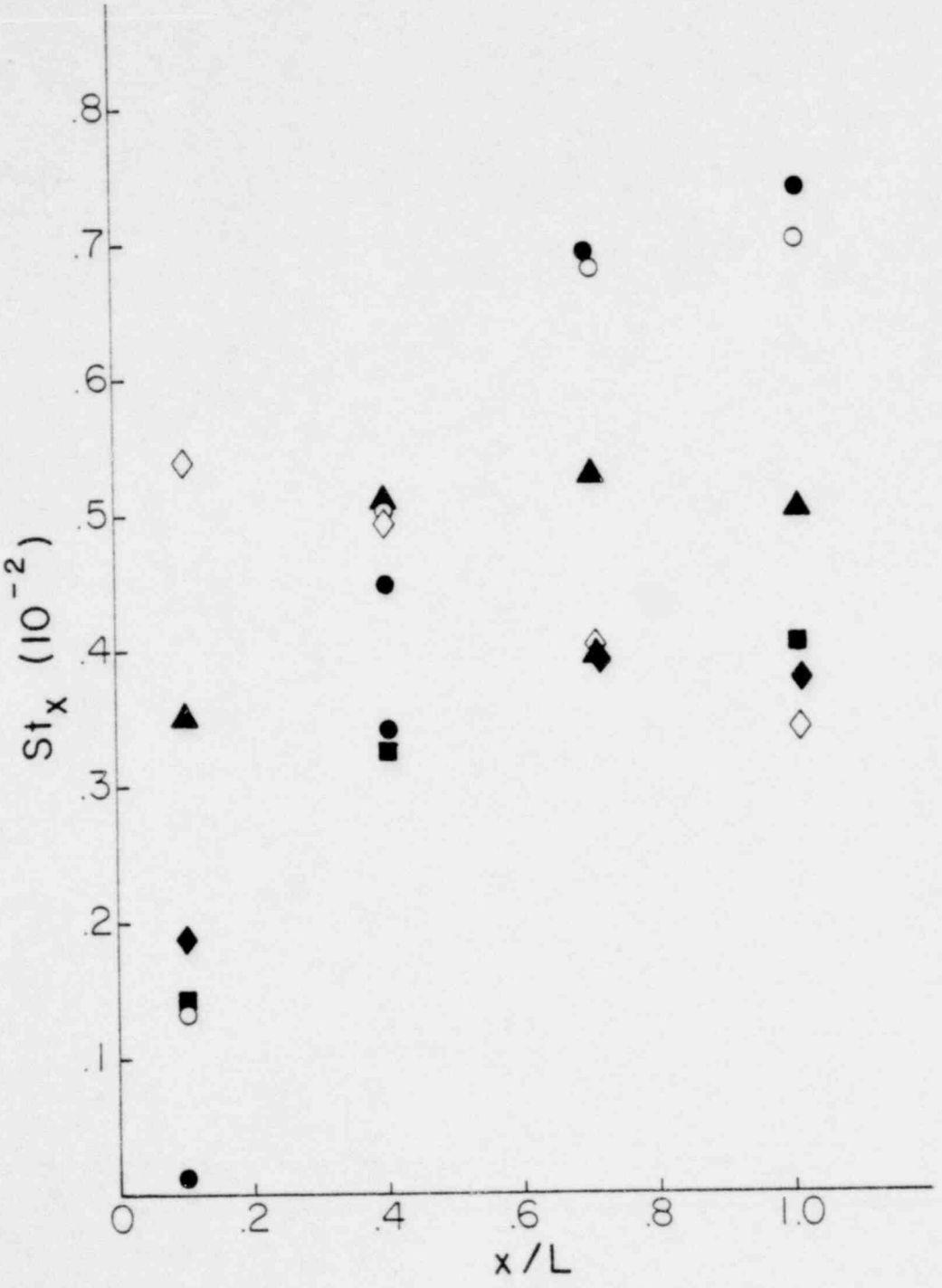

Fig. 29 Local Stanton Number as Function of Dimensionless Axial Distance. Same Data as Fig. 20.

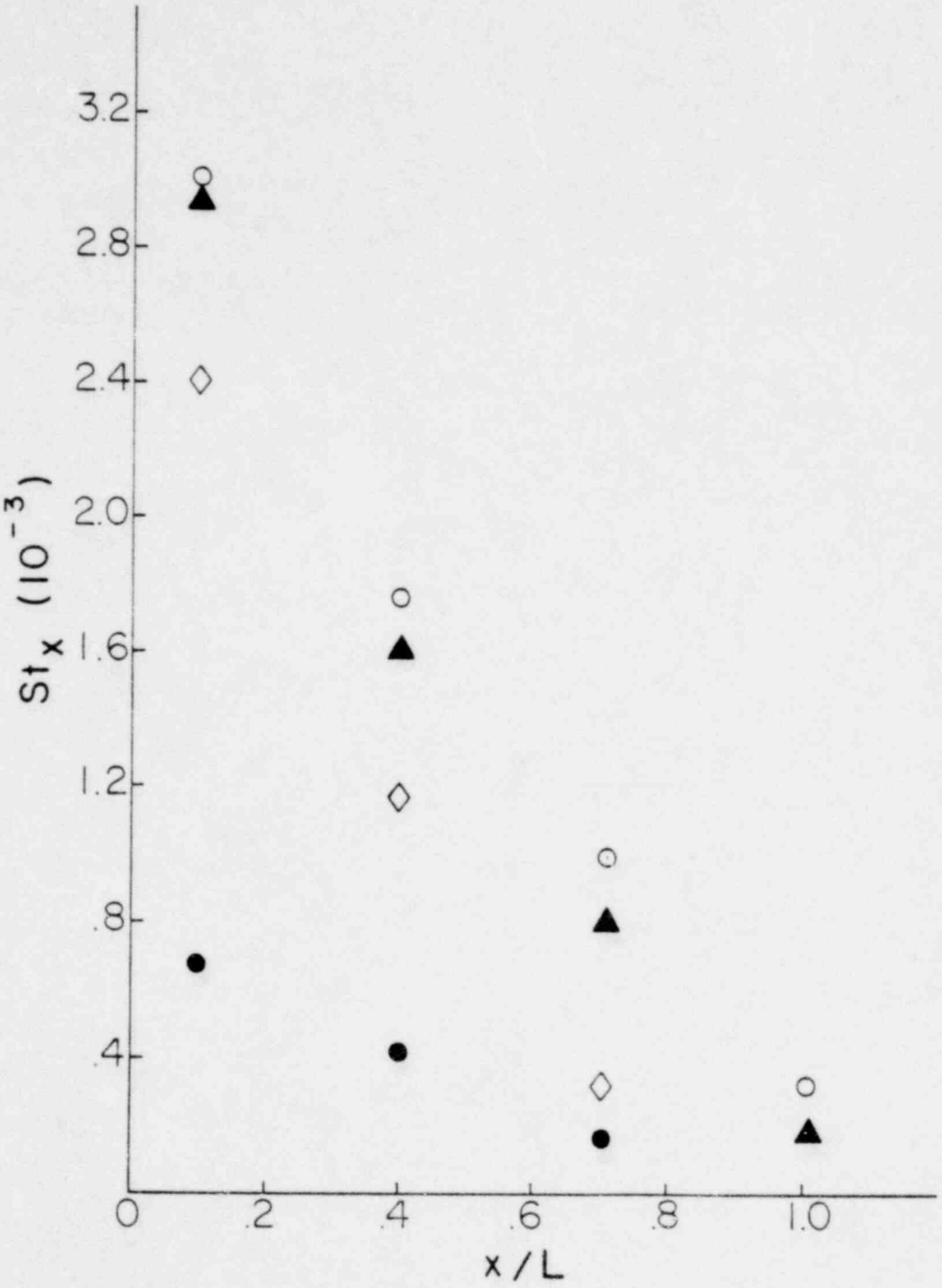

Fig. 30 Local Stanton Number as Function of Dimensionless Axial Distance. Same Data as Fig. 21.

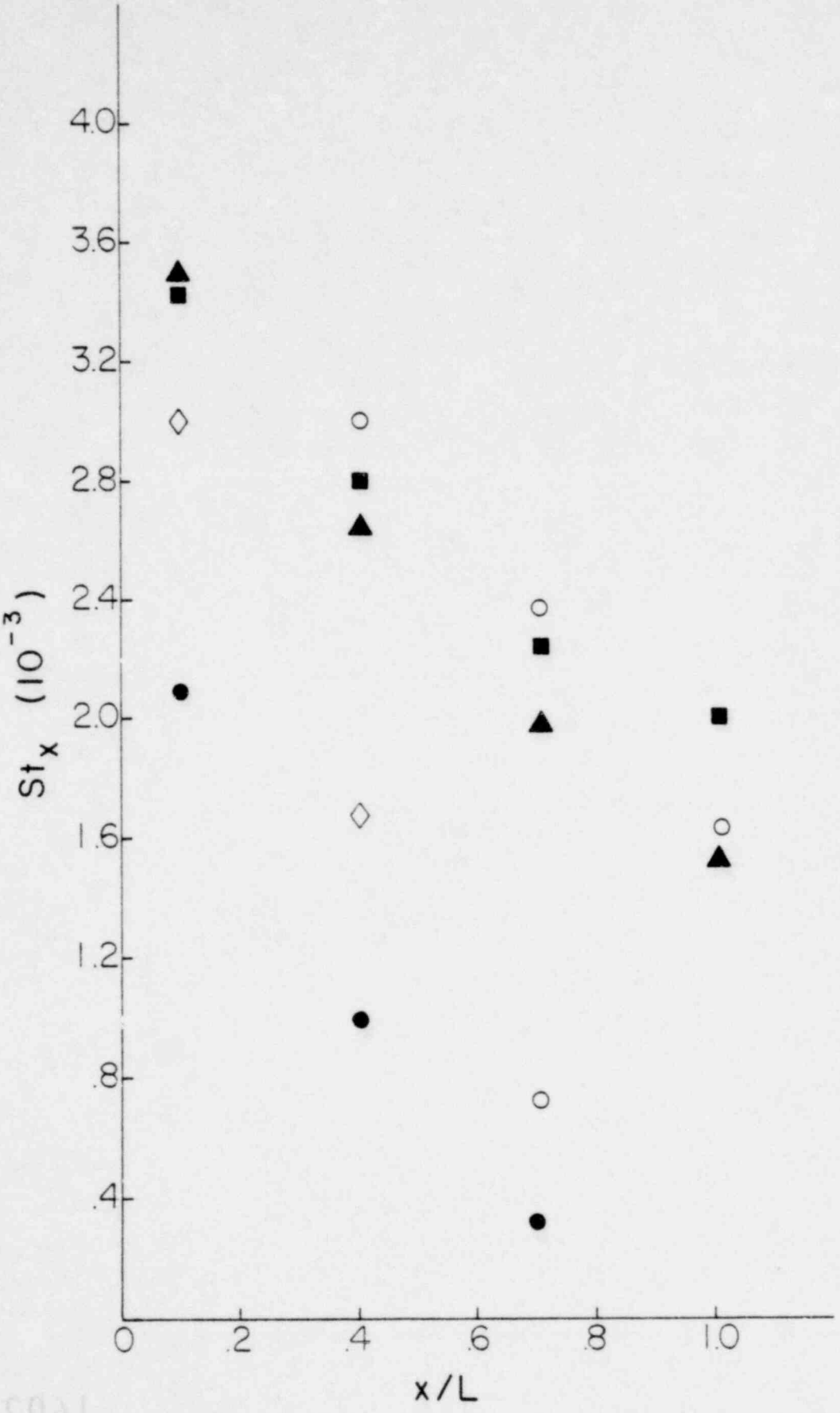

Fig. 31 Local Stanton Number as Function of Dimensionless Axial Distance. Same Data as Fig. 22.

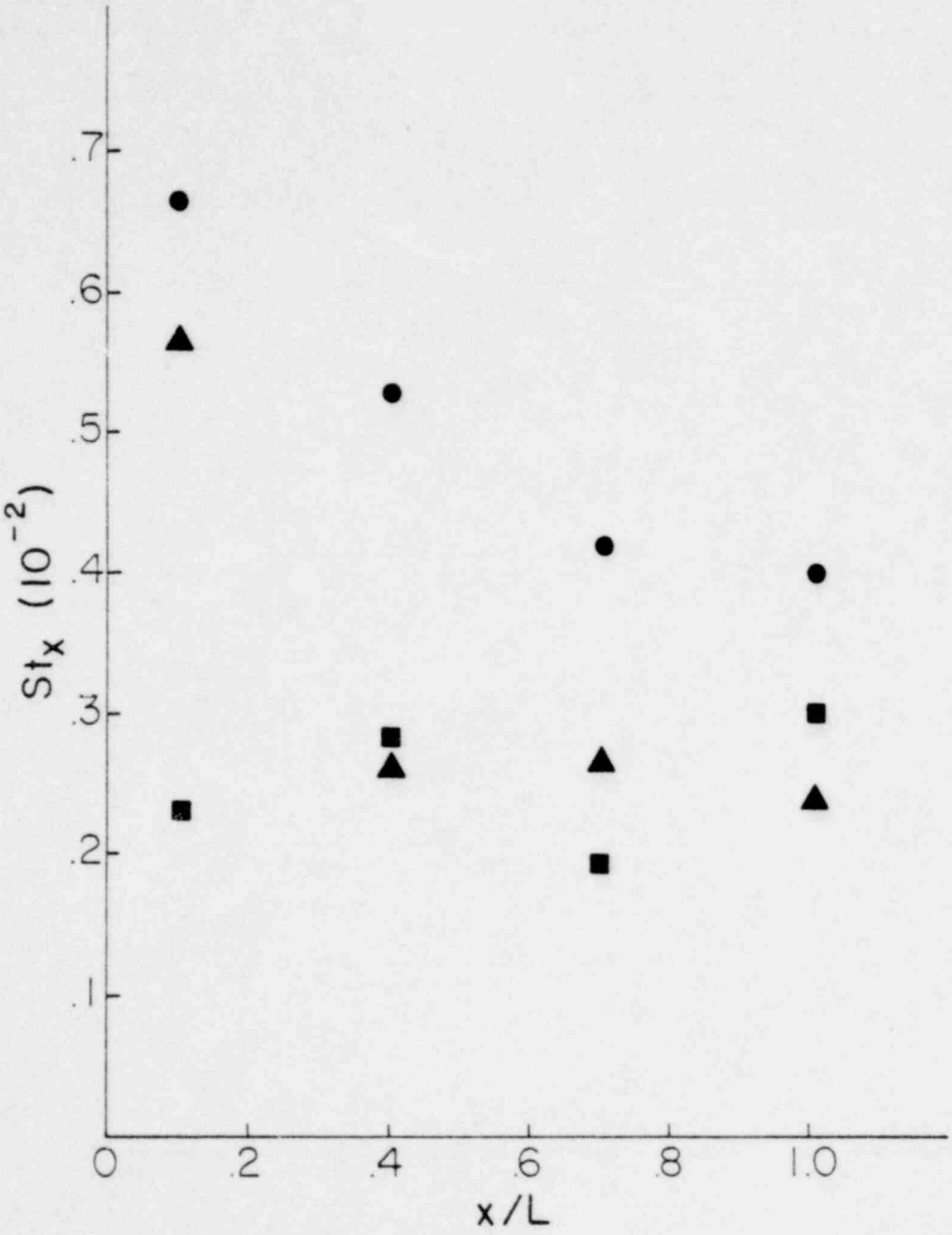

Fig 32 Local Stanton Number as Function of Dimensionless Axial Distance. Same as Fig. 22.

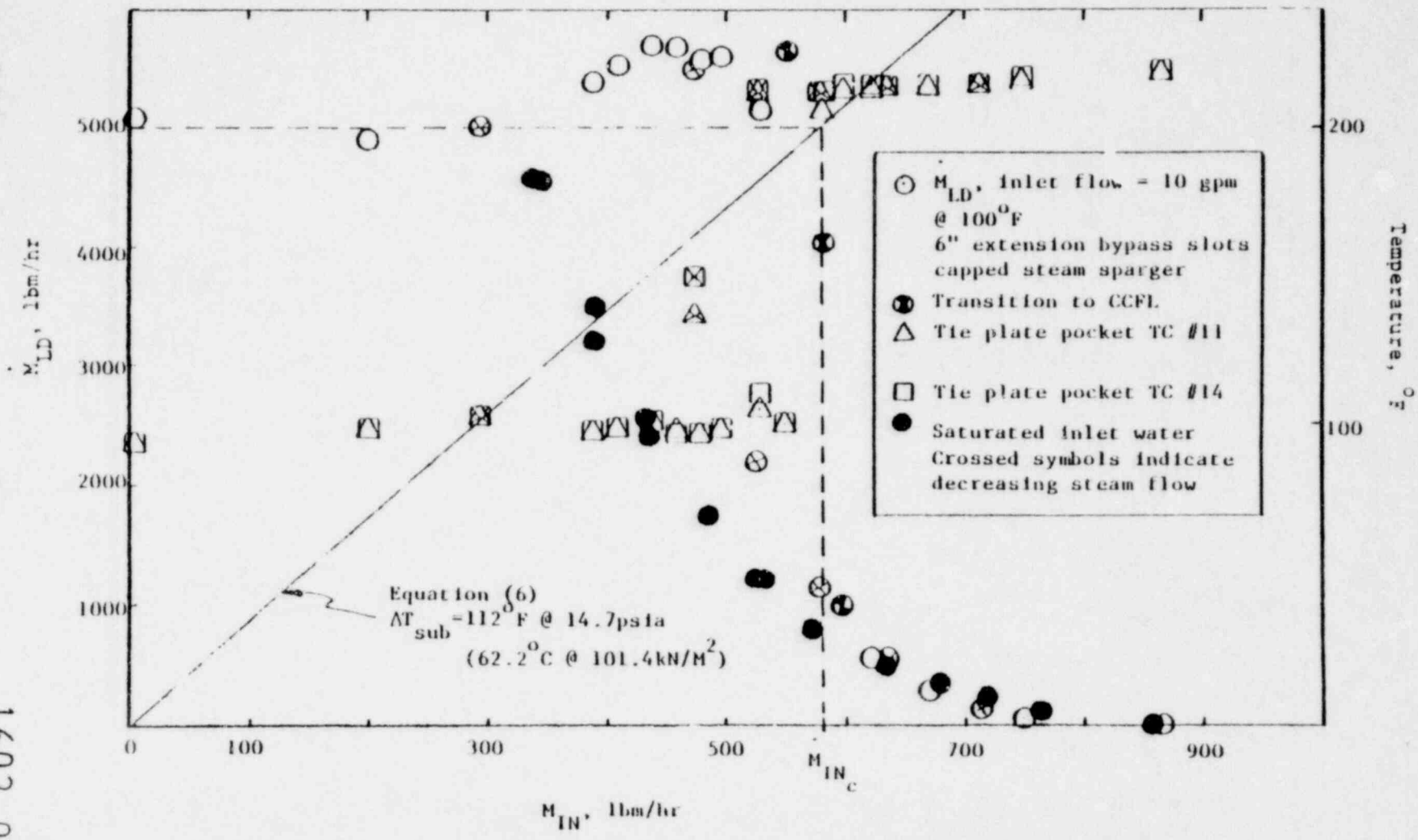

Fig. 33 Subcooled CCFL Characteristics in a Simulated BWR Tube Bundle (Jones)[6]. $M_{in} \equiv W_g$; $M_{LD} \equiv W_{fd}$; Eq. (6) is $R_T = 1$.

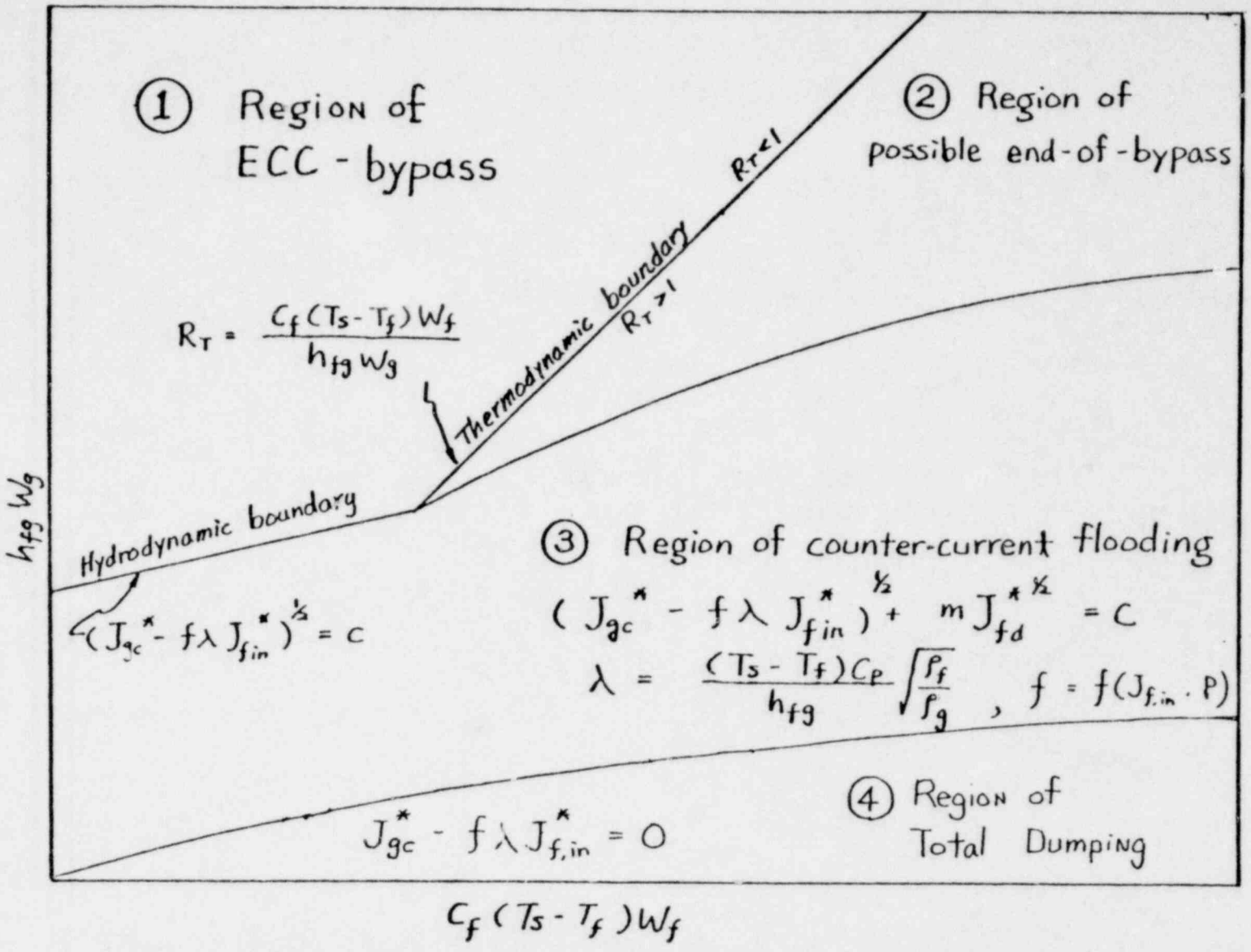

Figure 34 Suggested Flow Regime Map for KKU Geometry Perforated Plate with Elevated Water Inlet.

DROPLET ENTRAINMENT STUDIES OF DISPERSED FLOW THROUGH TIE PLATE IN LOCA BY LDA METHOD

* * *

BY
RICHARD S. L. LEE
J. SRINIVASAN
S. K. CHO

* * *

DEPARTMENT OF MECHANICAL ENGINEERING
STATE UNIVERSITY OF NEW YORK AT STONY BROOK
STONY BROOK, N.Y. 11794

PRESENTED AT SEVENTH WATER REACTOR SAFETY RESEARCH
INFORMATION MEETING, NATIONAL BUREAU OF STANDARDS
GAITHERSBURG, MARYLAND
NOVEMBER 5-9, 1973

SUMMARY

The deentrainment and reentrainment of water droplets in flow of a mixture of vapor and droplets through the upper plenum during the reflooding of a Pressurized Water Reactor following a loss of coolant accident are phenomena of great importance to the safety of the reactor. It has been generally assumed that this mixture emerges from the rod-bundle passage of the reactor core essentially unaffected by the presence of the tie plate which separates the core and the upper plenum. A typical model used for this type of investigation is the cross flow of a mixture around an array of vertical rods. Droplets are usually released from a sprayer arrangement placed in the middle of a horizontal air stream. Two serious questions arise concerning the size range of these droplets and the orientation of the flow as a result of the interaction between the mixture coming up from the core and the flow passages in the tie plate.

The range of size of droplets in a vapor-droplet mixture has a variety of implications in heat and mass transfers in the dispersed flow. In the flow passage in the reactor core, where heat transfer is of primary concern, the small droplets (<100μ) are expected to play a dominant role due to their large surface to volume ratios and their pronounced transverse migratory interaction with the boundary walls. On the other hand, in the upper plenum above the tie plate where mass transfer is of primary concern, the large droplets (>1mm) are expected to play a dominant role due to their overwhelming share of total mass in the dispersion. Consequently, the flow of a gas-droplet mixture through the tie plate deserves a great deal of attention.

The flow of an air-water droplet dispersion in a simulated 3-D test section in the reflood portion of LOCA is studied. For this purpose, a new scheme of Laser-Doppler Anemometry for the simultaneous measurement of size and velocity of large-size (1mm-6mm) droplets has been developed and utilized. In terms of droplet reentrainment from the tie plate, three flow regimes have been identified, depending on the velocity level of the flow: the dome formation stage, the oscillating dome stage and the wall film breaking up stage. It has been observed that the size

distribution of the reentrained droplets depends mainly on the flow regimes and is essentially independent of that of the incoming dispersion below the tie plate. These reentrained droplets are found to be mostly below 1mm in size and their trajectories on leaving the tie plate essentially oriented close to the vertical direction.

REFERENCES

1. Lee, S. L. and Srinivasan, J., "Measurement of Local Size and Velocity Probability Density Distributions in Two-Phase Suspension Flows by Laser-Doppler Technique", Int. J. Multiphase Flows, Vol.4, 1978, pp. 141-155.

2. Lee, S. L. and Srinivasan, J., "An Experimental Investigation of Dilute Two-Phase Dispersed Flow Using L.D.A. Technique", Proceedings of the 1978 Heat Transfer and Fluid Mechanics Institute, Stanford University Press, 1978, pp. 88-102.

3. Srinivasan, J. and Lee, S. L., "Measurement of Turbulent Dilute Two-Phase Dispersed Flow in a Vertical Rectangular Channel by Laser-Doppler Anemometry", Measurements in Polyphase Flows, Edited by D. E. Stock, 1978. The American Society of Mechanical Engineers, pp. 91-98.

4. Srinivasan, J., "Development of a Laser-Doppler Anemometer Technique for the Measurement of Two-Phase Dispersed Flow, NUREG/CR-0457, U. S. Nuclear Regulatory Commission, 1978.

5. Lee, S. L. and Srinivasan, J., "Laser-Doppler Anemometry Technique Applied to Two-Phase Dispersed Flows in a Rectangular Channel", NUREG/CP-0006, Proceedings of U. S. Nuclear Regulatory Commission Review Group Meeting on Two-Phase Flow Instrumentation, March 13-14, 1978, Rensselaer Polytechnic Institute, Troy, N. Y., pp. I.7-1-I.7-20.

6. Srinivasan, J. and Lee, S. L., "Application of Laser-Doppler Anemometry Technique to Turbulent Flow of a Two-Phase Suspension", Proceedings of the International Symposium on Papermachine Headboxes, McGill University, Montreal, Canada, June 3-5, 1979, pp. 25-30.

7. Lee, S. L., Srinivasan, J., Cho, S. K. and Malhotra, A., "A Study of Droplet Hydrodynamics Important in Upper Plenum in LOCA", Proceedings of U. S. Nuclear Regulatory Commission Reactor Safety Instrumentation Review Group Meeting, Silver Spring, Maryland, July 24-26, 1979. (in print).

OVERVIEW

* * *

- TWO-PHASE DISPERSED FLOW PHENOMENA IN THE SIMULATED 3-D TEST SECTION IN THE REFLOOD PORTION OF LOCA
  - IN ROD BUNDLE FLOW PASSAGE:
    SMALL DROPLETS (< 100 μ) PLAY A DOMINANT ROLE IN HEAT TRANSFER DUE TO THEIR PRONOUNCED TRANSVERSE MIGRATORY INTERACTION WITH BOUNDARY WALLS
  - IN UPPER PLENUM ABOVE TIE PLATE:
    LARGE DROPLETS (> 1MM) PLAY A DOMINANT ROLE IN MASS TRANSFER DUE TO THEIR OVERWHELMING SHARE OF TOTAL MASS IN DISPERSION

- OBJECTIVE OF EFFORT:

  TO STUDY THE SIZE AND VELOCITY DISTRIBUTIONS OF LARGE DROPLETS BELOW AND ABOVE TIE PLATE OF A SIMULATED 3-D TEST SECTION

  - DEVELOP LASER DOPPLER ANEMOMETRY FOR MAKING MEASUREMENTS OF:
    - SIZE AND NUMBER DENSITY DISTRIBUTION OF LARGE (1MM-6MM) WATER DROPLETS
    - VELOCITY DISTRIBUTIONS OF DROPLETS AND SURROUNDING CONTINUOUS PHASE
  - DESIGN AND CONSTRUCTION OF A FLOW CHANNEL TO SIMULATE THE DISPERSED FLOW THROUGH REPRESENTATIVE SECTION OF TIE PLATE

FLOW THROUGH TIE PLATE

* * *

- FLOW ARRANGEMENT
  - REPRESENTATIVE SECTIONS OF TIE PLATE (FIGURES 1 AND 2)
  - FLOW LOOP (FIGURE 3)
- PRELIMINARY TESTS
  - WATER DOME FORMATION (FIGURE 4A)
  - WATER DOME OSCILLATION (FIGURE 4B)
  - WATER DROPLETS BREAKING OUT FROM OSCILLATING DOME (FIGURE 5)
  - WATER DROPLET ENTRAINMENT FROM WATER LAYER (FIGURE 4C)
- FLOW REGIME CLASSIFICATION FOR TIE PLATE DROPLET ENTRAINMENT (TABLE 1)

NEW LDA OPTICAL TECHNIQUE

* * *

- DEVELOPMENT OF A NEW OPTICAL TECHNIQUE USING LASER-DOPPLER ANEMOMETRY FOR LARGE DROPLET MEASUREMENT
  - NEEDS FOR USING LDA (VELOCITY, SIZE AND TRAJECTORY LOCATION OF EACH DROPLET AT LOCAL MEASURING STATION
  - LASER SIGNAL DUE TO PASSAGE OF A LARGE DROPLET (REFERENCE-BEAM MODE LDA) (FIGURE 6)
    - BLOCKING LENGTH (SIZE) (FIGURE 7A)
    - DOPPLER SIGNAL (VELOCITY, LOCATION) (FIGURE 7B)
- INSTRUMENTATION
  - PHOTO DIODE FOR OBTAINING BLOCKING LENGTH (FIGURE 8)
  - INSTRUMENTATION BLOCK DIAGRAM (FIGURE 9)
  - SAMPLE DATA SHEET (TABLE 2)

- CALIBRATION
  - DIFFICULTIES IN:
    - OBTAINING CONTROLLED LARGE SPHERICAL DROPLET
    - MAINTAINING PRECISE DROPLET TRAJECTORY RELATIVE TO OPTICAL MEASURING VOLUME
  - INDIRECT CALIBRATION USING SPHERICAL PARTICLES (SPHERICITY: 0.00005 IN) OF CONTROLLED SIZES
- ACHIEVEMENTS
  - ON-LINE DATA ACQUISITION SYSTEM FOR OBTAINING ALL NECESSARY PARAMETERS HAS BEEN DEVELOPED
  - BLOCKING LENGTH AGAINST MEASURED SIZE (FIGURE 10)
  - DOPPLER SIGNAL AMPLITUDE VS. SIZE
    - STEEL BALL (FIGURE 11)
    - WATER DROPLET (FIGURE 12)
  - SAMPLE SCATTERING DIAGRAM (FIGURE 13)
  - DROPLET SIZE DISTRIBUTION (FIGURE 14)
  - DROPLET VELOCITY DISTRIBUTION (FIGURE 15)

CONCLUSIONS

* * *

- FLOW REGIMES OF TWO-PHASE DISPERSED FLOW THROUGH 3-D SIMULATED TIE PLATE HAVE BEEN IDENTIFIED

- A NEW LASER-DOPPLER ANEMOMETRY TECHNIQUE AND ACCOMPANYING ELECTRONICS AND COMPUTER INTERFACES CAPABLE OF MEASURING SIZE AND VELOCITY OF LARGE DROPLETS HAVE BEEN DEVELOPED

TABLE 1. FLOW REGIME CLASSIFICATION FOR TIE PLATE DROPLET ENTRAINMENT

FLOW REGIME	(I) INITIAL STAGE OF WATER DOME FORMATION	(II) DROPLET ENTRAINMENT FROM OSCILLATING DOME	(III) DROPLET ENTRAINMENT FROM WALL LAYER
AIR VELOCITY IN CHANNEL	UP TO ~ 5 M/SEC	~ 5-18 M/SEC	ABOVE ~ 18 M/SEC
AIR VELOCITY IN TIE PLATE HOLES	UP TO ~9 M/SEC	~9-30 M/SEC	ABOVE ~30 M/SEC
SIZE OF DROPLETS SUPPLIED	~1-5MM	~1-5MM	1-5MM
HEIGHT OF WATER DOME FORMED ON TOP OF TIE PLATE	SLOW FORMATION UP TO 3MM	OPTIMUM HEIGHT OF OSCILLATING DOME ~5-6MM	NO DOME REMAINS
CRITICAL FREQUENCY OF WATER DOME OSCILLATION	NONE	ORDER OF 10 HERTZ	NONE
PREDOMINANT SIZE OF DROPLET ENTRAINMENT	NONE	~0.5-1.5MM BREAKING OUT FROM OSCILLATING DOME	RANDOM BUT SMALL, < 0.5MM

TABLE 2. SAMPLE DATA SHEET

BLOCK NUMBER:	0			
AXIAL VEL (M/S C)	BLOCK LNTH (MICRONS)	PATH LNTH (MICRONS)	PEAK VOLT (VOLTS)	TIME BTWN SAMP (MILLI SEC)
0.26691E+01	0.63563E+04	0.26318E+03	0.56812E+01	0.25500E+03
0.26711E+01	0.63685E+04	0.26551E+03	0.57495E+01	0.23900E+03
0.26638E+01	0.63509E+04	0.26265E+03	0.57446E+01	0.23800E+03
0.26658E+01	0.63525E+04	0.26284E+03	0.56714E+01	0.23900E+03
0.26772E+01	0.63841E+04	0.26505E+03	0.57349E+01	0.23900E+03
0.26644E+01	0.63472E+04	0.26271E+03	0.57153E+01	0.23900E+03
0.26806E+01	0.63847E+04	0.26645E+03	0.57495E+01	0.23800E+03
0.26644E+01	0.63472E+04	0.26271E+03	0.57104E+01	0.23900E+03
0.26685E+01	0.63536E+04	0.26418E+03	0.57495E+01	0.23800E+03
0.26705E+01	0.63552E+04	0.26224E+03	0.56616E+01	0.23900E+03
0.26664E+01	0.63531E+04	0.26184E+03	0.56226E+01	0.23800E+03
0.26658E+01	0.63461E+04	0.26284E+03	0.57007E+01	0.23800E+03
0.26766E+01	0.63697E+04	0.26391E+03	0.56714E+01	0.23900E+03
0.26820E+01	0.63858E+04	0.26552E+03	0.57104E+01	0.23800E+03
0.26631E+01	0.63397E+04	0.26258E+03	0.56616E+01	0.23900E+03
0.26806E+01	0.63793E+04	0.26431E+03	0.56812E+01	0.23800E+03
0.26745E+01	0.63670E+04	0.26478E+03	0.57056E+01	0.23800E+03
0.26685E+01	0.63525E+04	0.26418E+03	0.57837E+01	0.23900E+03
0.26759E+01	0.63755E+04	0.26491E+03	0.56860E+01	0.23800E+03
0.26671E+01	0.63557E+04	0.26404E+03	0.57642E+01	0.23900E+03
0.26577E+01	0.63461E+04	0.26099E+03	0.55981E+01	0.23900E+03
0.26631E+01	0.63525E+04	0.26258E+03	0.57251E+01	0.23900E+03
0.26597E+01	0.63456E+04	0.26225E+03	0.56812E+01	0.23900E+03
0.26604E+01	0.63546E+04	0.26125E+03	0.56665E+01	0.23900E+03
0.26711E+01	0.63846E+04	0.26444E+03	0.56860E+01	0.23900E+03
0.26604E+01	0.63610E+04	0.26019E+03	0.54712E+01	0.24000E+03
0.26551E+01	0.63483E+04	0.26285E+03	0.57739E+01	0.23900E+03

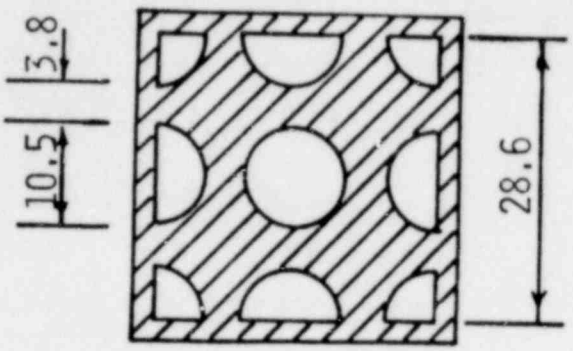

ALL UNITS: MM

FIGURE 1. REPRESENTATIVE SECTION OF 3-D TIE PLATE

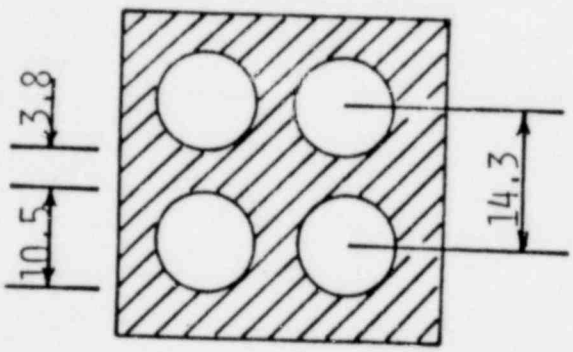

ALL UNITS: MM

FIGURE 2. ALTERNATIVE REPRESENTATIVE SECTION OF 3-D TIE PLATE

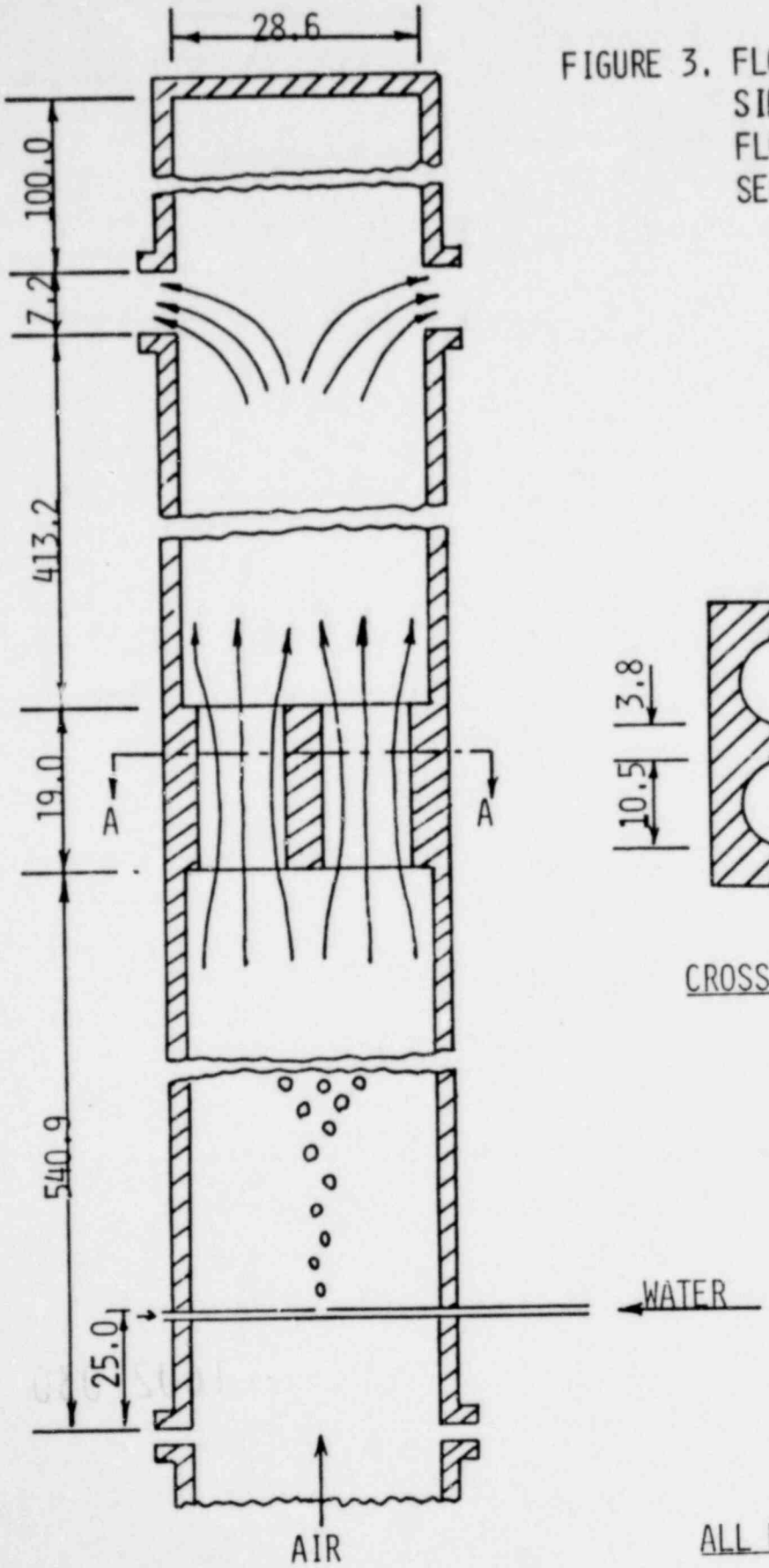

FIGURE 3. FLOW ARRANGEMENT FOR SIMULATED 3-D DISPERSED FLOW THRU REPRESENTATIVE SECTION OF TIE PLATE

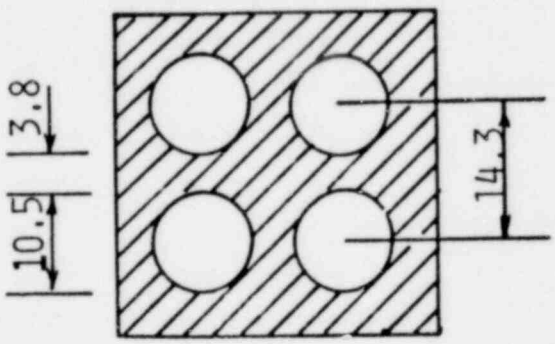

CROSS SECTION A-A

ALL UNITS: MM

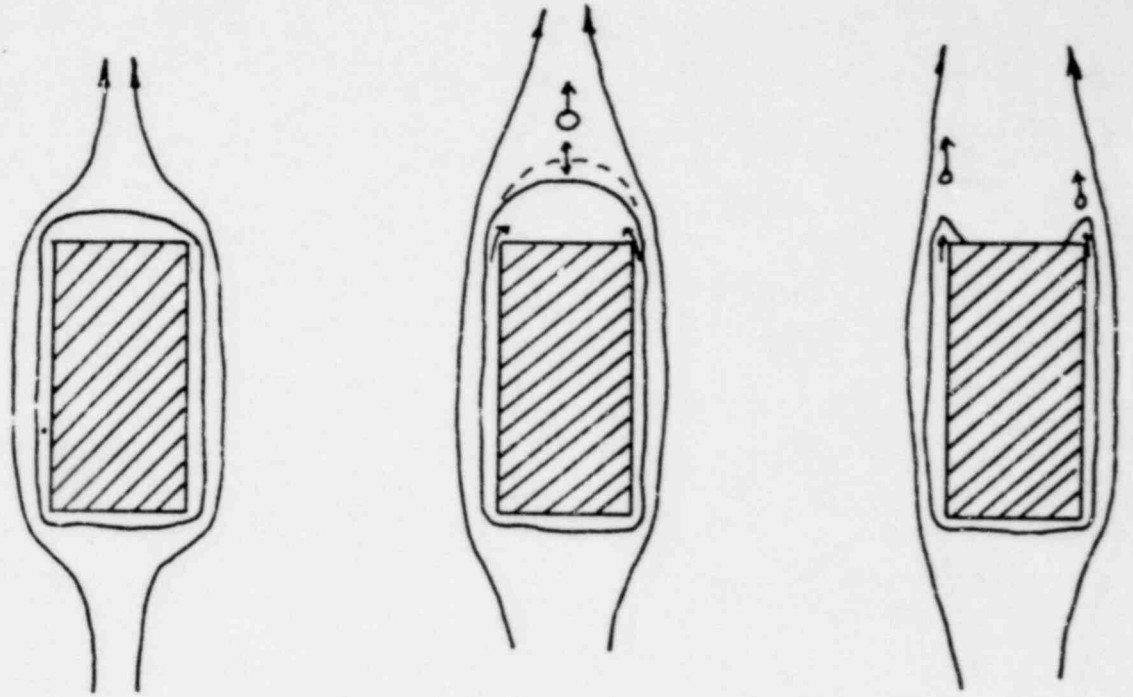

FIGURE 4. PATTERNS OF DISPERSED FLOW THROUGH TIE PLATE

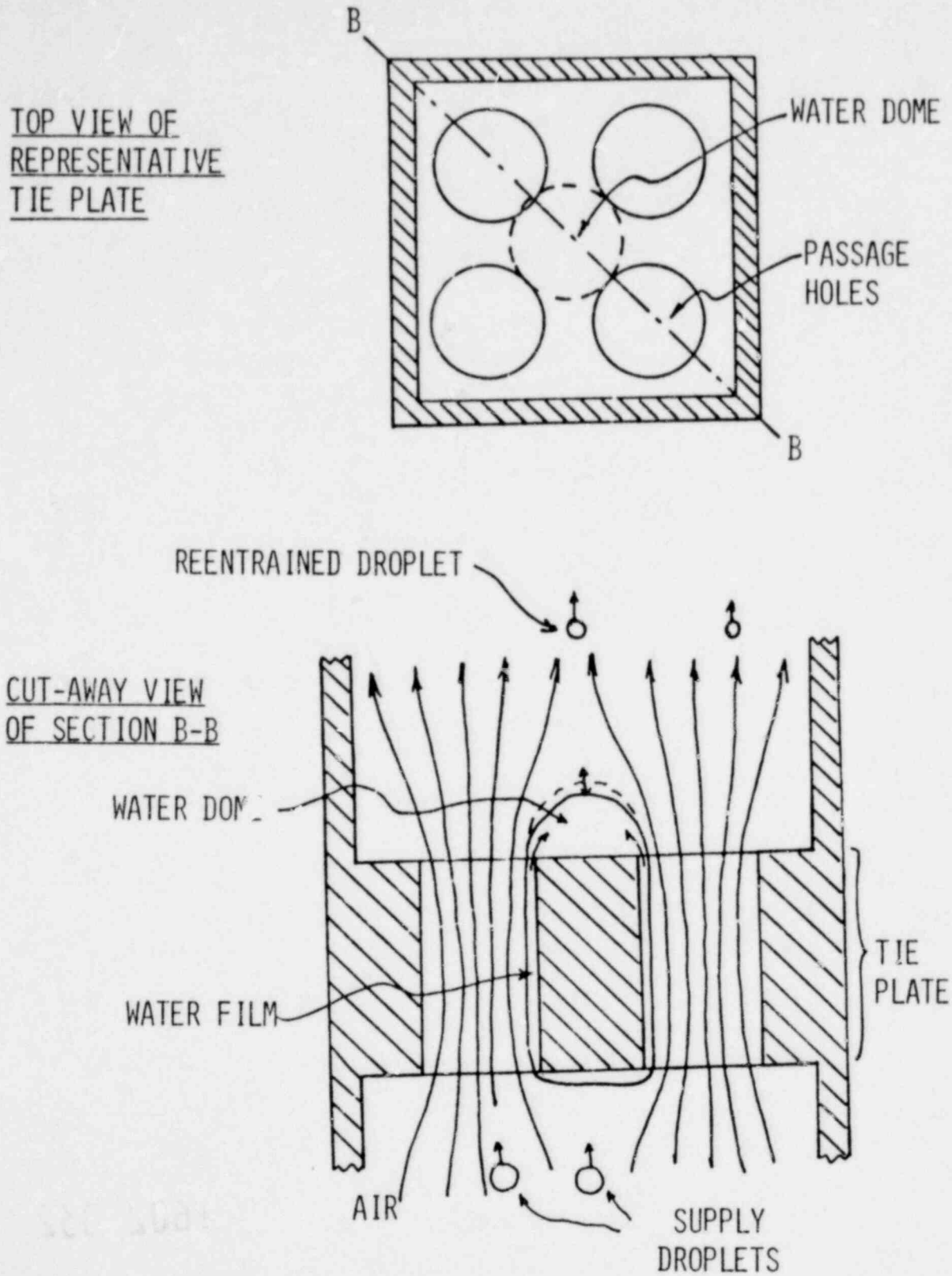

FIGURE 5. OSCILLATING WATER DOME

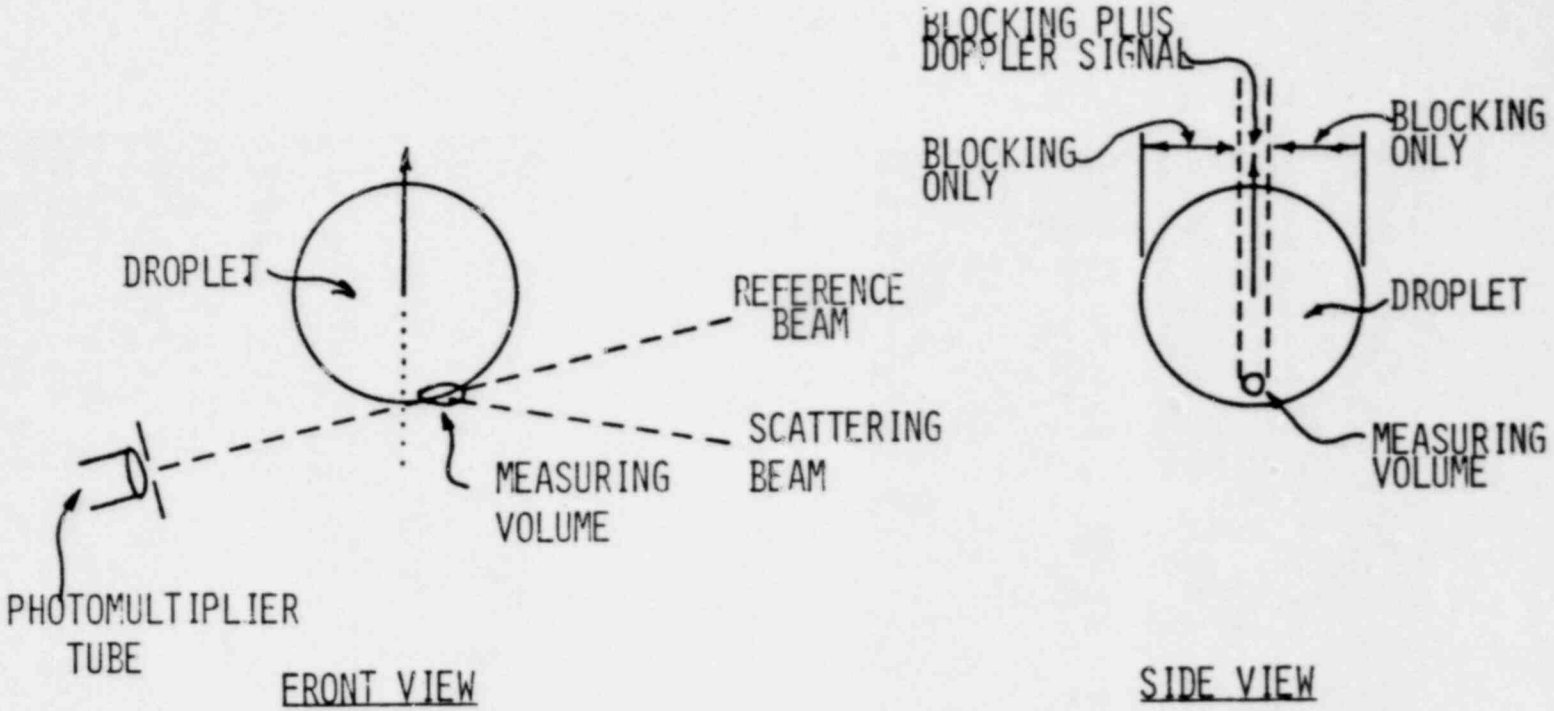

FIGURE 6. LASER-DOPPLER ANEMOMETRY SCHEME DEVELOPED FOR LARGE-SIZE DROPLET MEASUREMENT

LASER DOPPLER SIGNALS

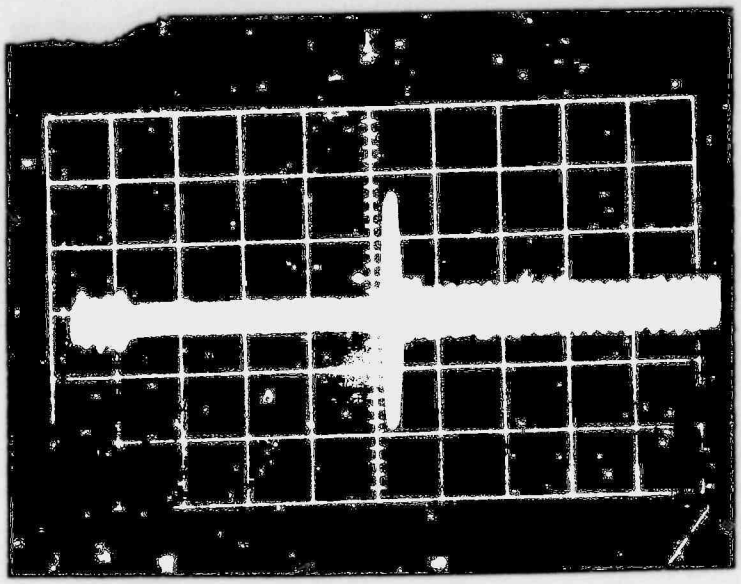

FIGURE 7A. BLOCKING LENGTH (SIZE)

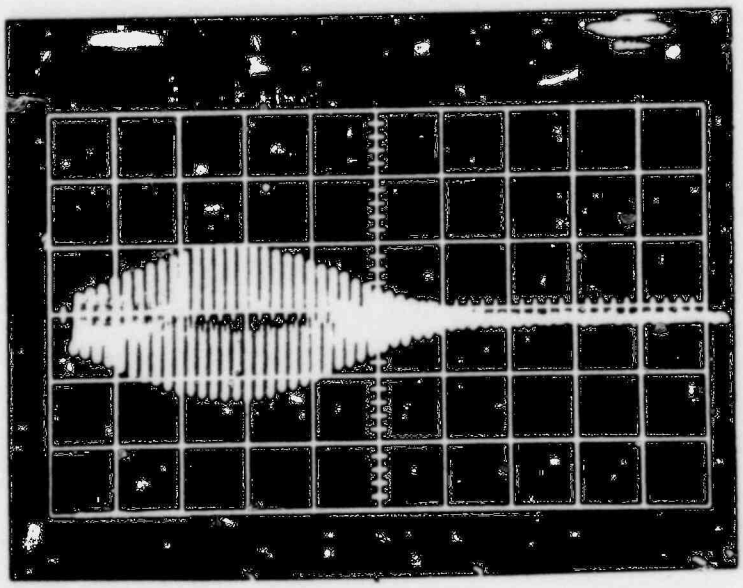

FIGURE 7B. DOPPLER SIGNAL (VELOCITY, LOCATION)

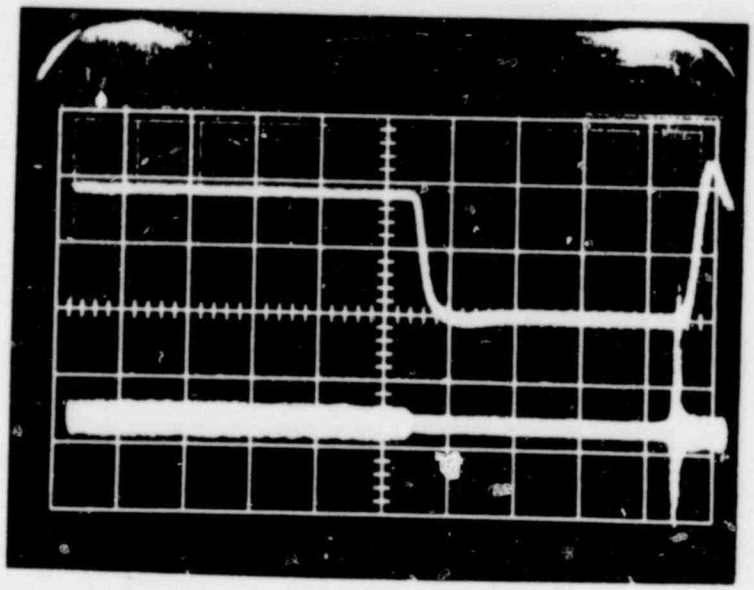

FIGURE 8. PHOTO DIODE OUTPUT AND DOPPLER SIGNAL

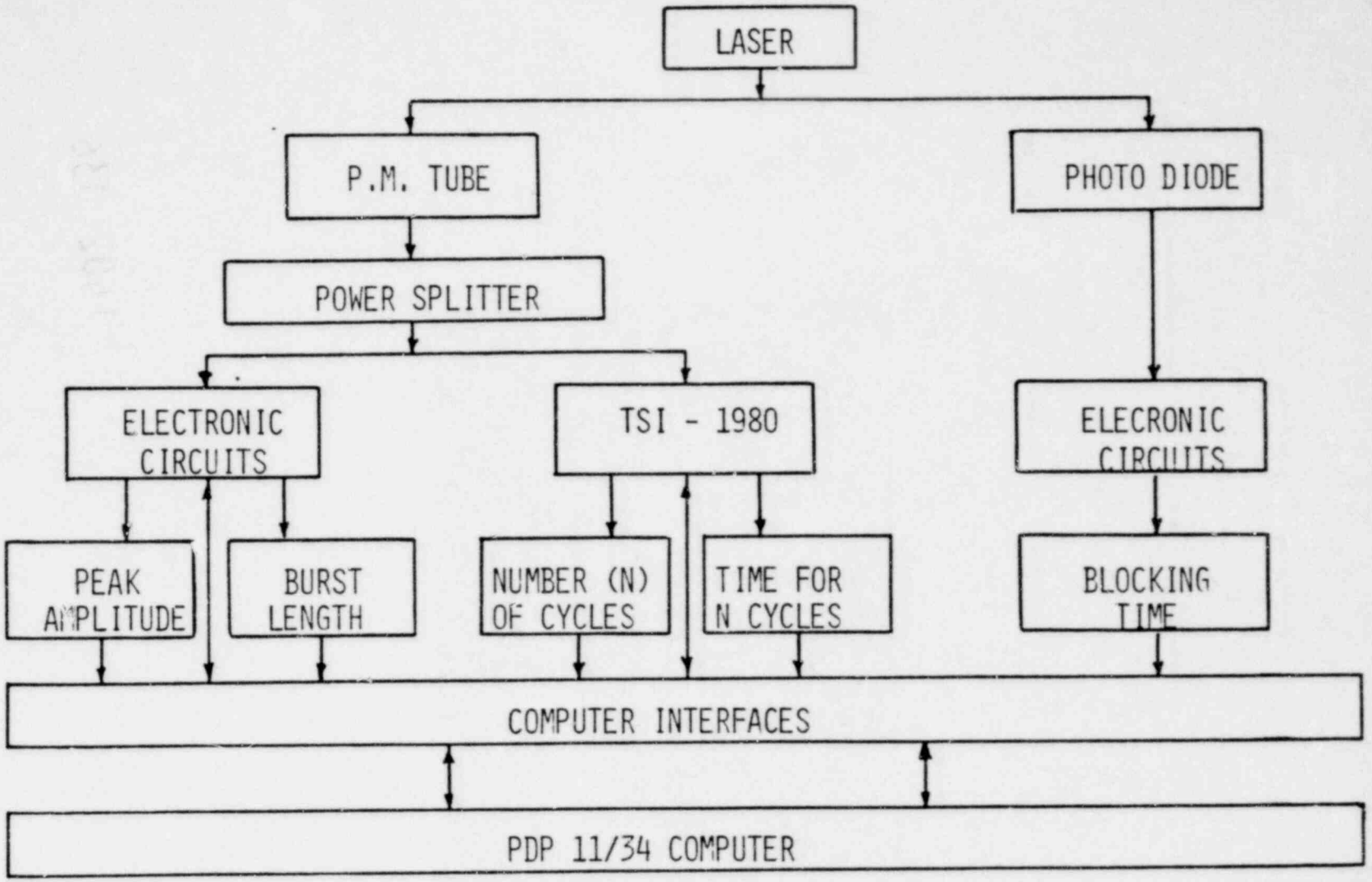

FIGURE 9. INSTRUMENTATION BLOCK DIAGRAM

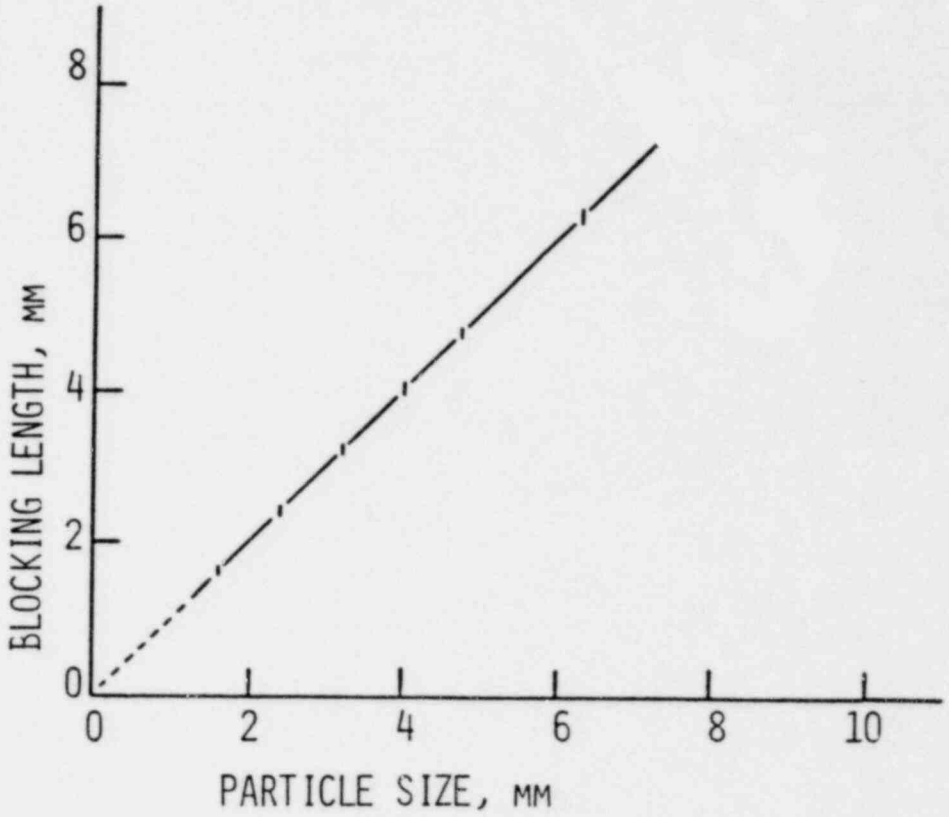

FIGURE 10. BLOCKING LENGTH AGAINST MEASURED SIZE (STEEL BALL)

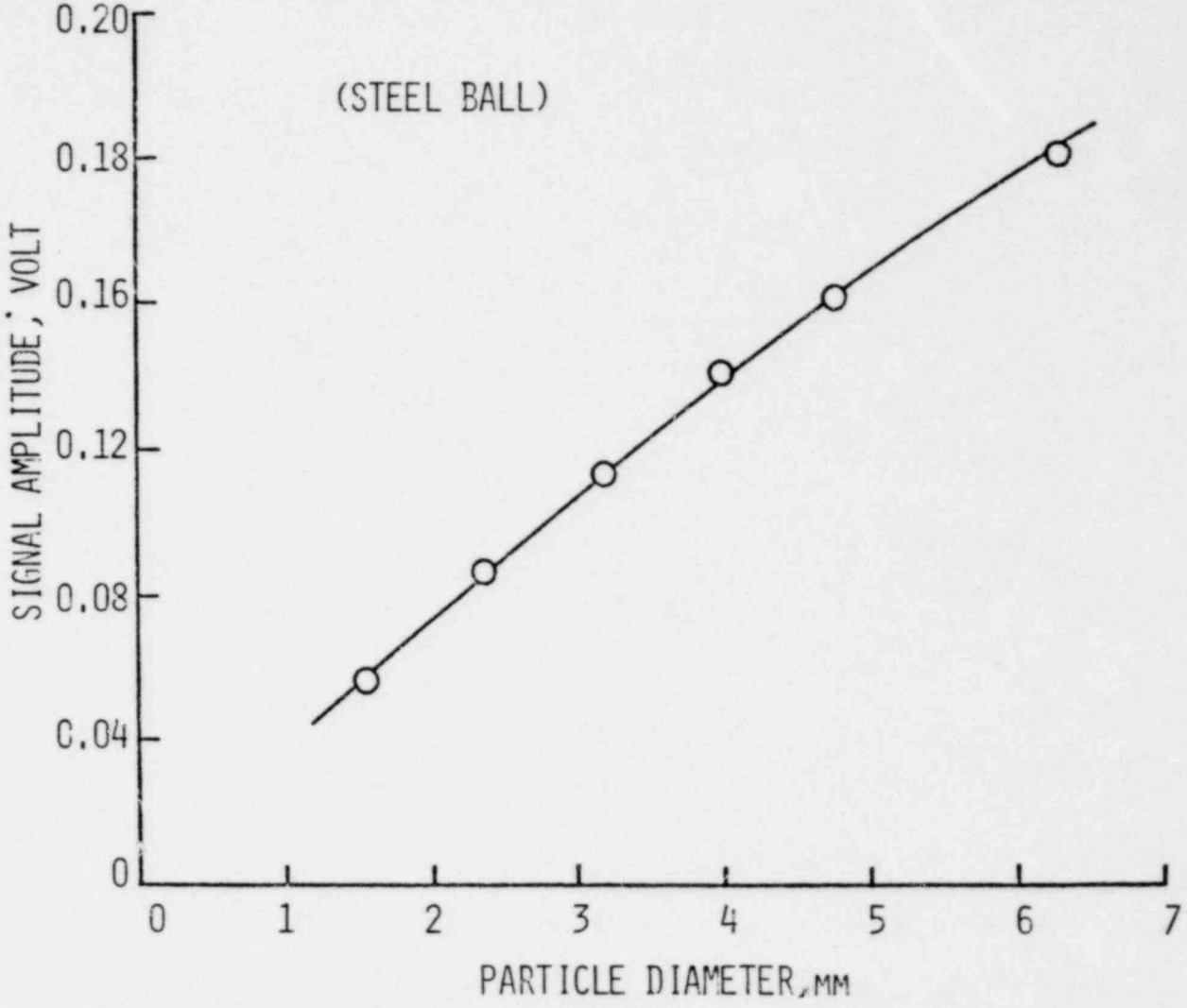

FIGURE 11. DOPPLER SIGNAL AMPLITUDE VS SIZE (STEEL BALL)

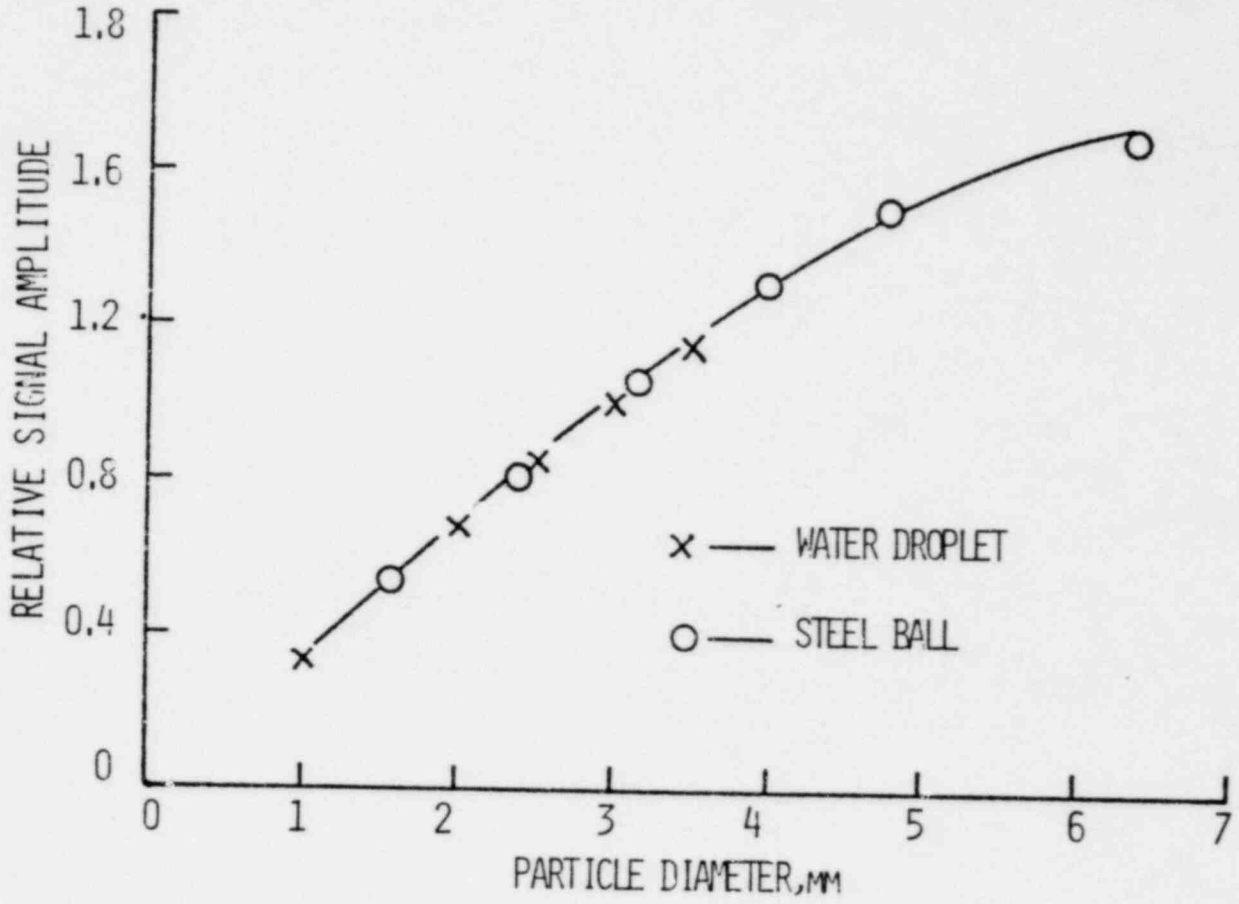

FIGURE 12. DOPPLER SIGNAL AMPLITUDE VS. SIZE (WATER DROPLET)

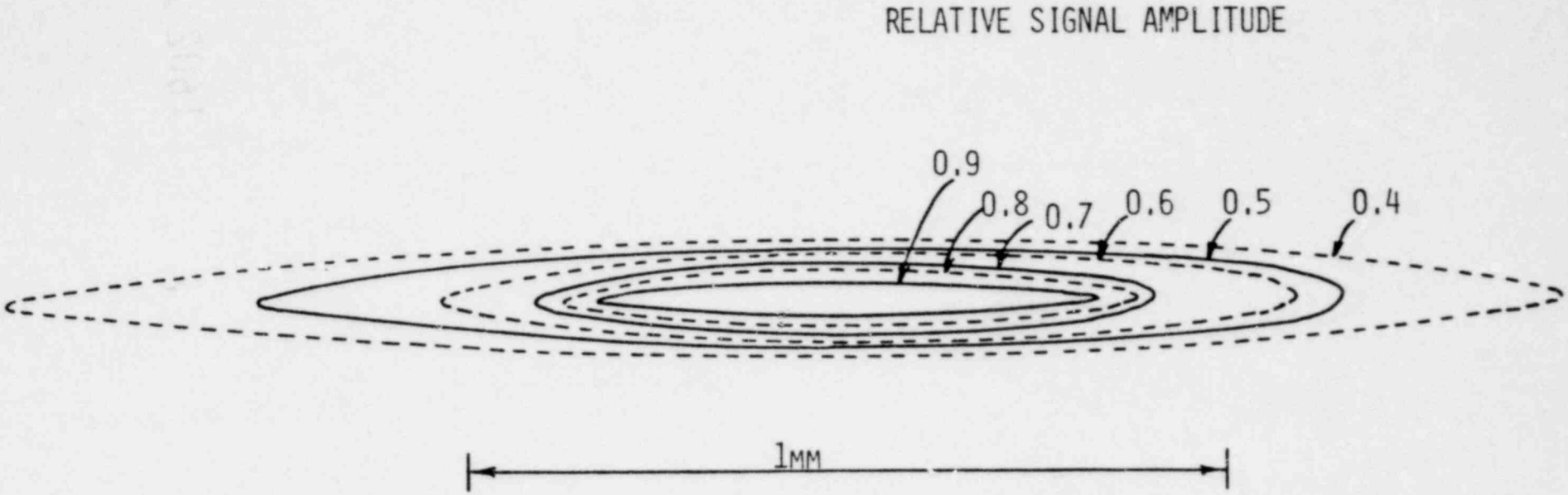

FIGURE 13. SAMPLE SCATTERING DIAGRAM

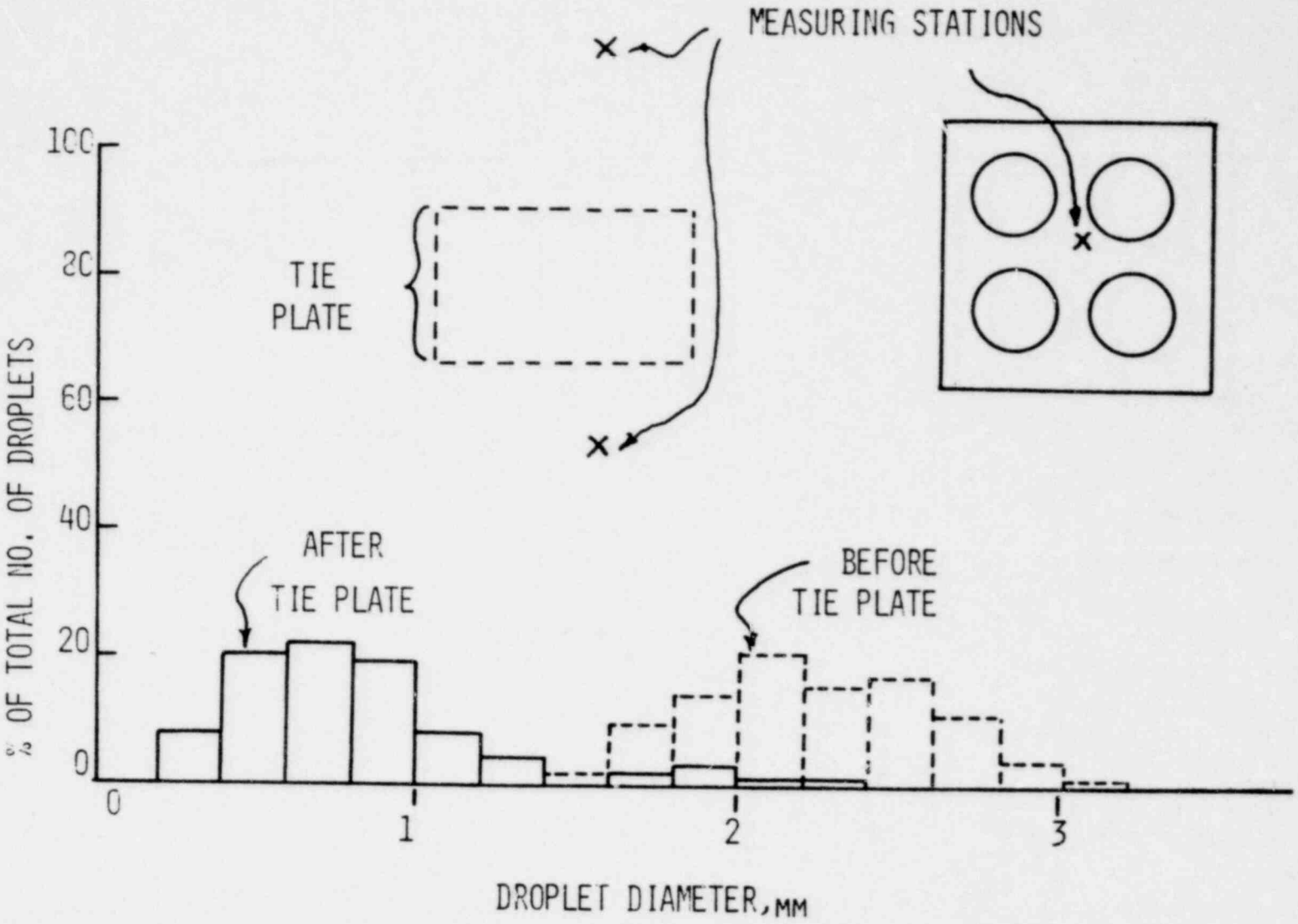

FIGURE 14. DROPLET SIZE DISTRIBUTION

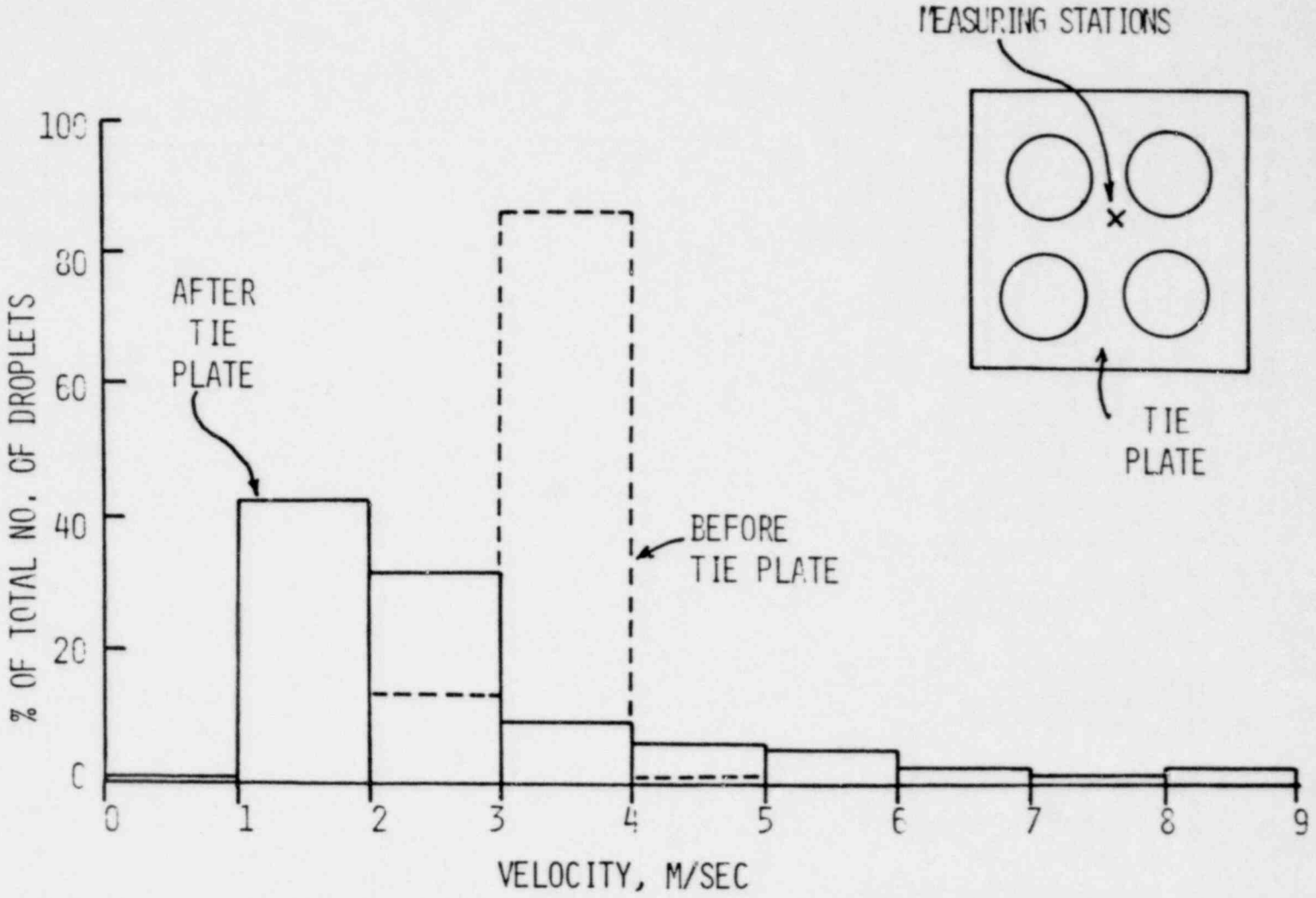

FIGURE 15. DROPLET VELOCITY DISTRIBUTION

LA-UR 79-1661

TITLE: DROPLET CROSS FLOW PHENOMENA IN AN LPWR UPPER PLENUM

AUTHOR(S): John C. Dallman and Walter L. Kirchner

Presented at: Seventh Water Reactor Safety Meeting
Gaithersburg, MD
November 6, 1979

los alamos
scientific laboratory
of the University of California
LOS ALAMOS, NEW MEXICO 87544

Form No. 836
St. No. 2629
1/75

UNITED STATES
ENERGY RESEARCH AND
DEVELOPMENT ADMINISTRATION
CONTRACT W-7405-ENG. 36

Droplet Cross Flow Phenomena in an LPWR Upper Plenum

John C. Dallman and Walter L. Kirchner
Energy Division
Los Alamos Scientific Laboratory
Los Alamos, New Mexico

Steam-droplet flows in the upper plenum of a Large Pressurized Water Reactor (LPWR) during a postulated LOCA can directly affect the peak fuel clad temperatures. The droplet flow, generated from the core region during the reflood stage of the accident, may either de-entrain on the upper plenum internals or be carried out a hot leg. Significant liquid de-entrainment in the upper plenum results in a potential reduction of the steam binding problem, and may enhance the reflood rate by draining back into the core region.

Earlier related work on the icing of aircraft wings and filtration of liquid/dust carryover from industrial plants has resulted in a number of de-entrainment efficiency measurements for cylinders in two-phase cross flows. The resultant theory of "inertial impaction" applied to flow conditions of interest in reactor applications would predict efficiencies of at least 90%. Recent studies by the authors using air-water flow across vertical cylindrical and square tubes have generated significantly different results.[1] Drop splattering and/or bouncing upon impact with the tubes appears to be the primary phenomenon diminishing the de-entrainment efficiency from that predicted by "inertial impaction" theory. This is in qualitative agreement with the work of Finlay and McMillan,[2] although their studies involved horizontal

cylinders. Re-entrainment from the draining liquid films on the tubes appears to cause only a small degradation in de-entrainment efficiency over the air velocities investigated in this study (velocities were chosen to be representative of expected LOCA conditions).

A convenient way to characterize liquid de-entrainment on structures is to measure the rate of liquid de-entrainment per unit area and the total mass flux at the structure surface. The ratio of these quantities is the de-entrainment (capture) efficiency. Measurement of single rod efficiencies using air-water drop flows has indicated a strong dependence on mass flux for flux rates less than 2 kg/m^2s (see Figure 1). At higher mass flux rates the capture efficiency, for the limited range of parameters of this study, tends toward a constant value. In addition, for velocities of 7 and 14 m/s no significant dependence on air velocity could be resolved (the data in Figure 1 are a representative sampling of results to date).

Figure 2 indicates that for air velocities of 7 and 14 m/s, volume mean drop diameters of about 1300 to 1600 μm, and mean droplet velocities from about 10 m/s to 18 m/s the single rod capture efficiency is only a weak function of particle Weber number. Also of interest is that no significant dependence on cylinder diameter is apparent for mass flux rates above 2 kg/m^2-s. However, the 76.2 mm square tube, facing perpendicular to the mean flow, did have a slightly better capture efficiency than the cylindrical tubes.

Extension of the single rod measurements to multiple rows in an infinite array can be accomplished using some strong assumptions: (1) the

flow is completely mixed between the rows, (2) the inter-row vortices are effective mixers but do not enhance re-entrainment, and (3) the changes in drop size and velocity spectra do not change the local de-entrainment efficiencies markedly from those of the first row. Using these assumptions an equation of the form

$$\eta_{mr} = 1 - A(1-\eta_{sr1})(1-\eta_{sr2})....(1-\eta_{srn})$$

can be used. Where A is a geometric factor dependent upon pitch-to-diameter ratios, staggered versus in-line arrays, etc., and η_{srn} is the capture efficiency of a single rod with a droplet mass flux typical of the n^{th} row. Application of this equation to the 76.2 mm square pin measurements is presented in Figure 3. From preliminary work on multiple row arrays it is felt that the results of Figure 3 are conservative, but further investigation is warranted.

In conclusion, the data presented indicate a de-entrainment efficiency for single structures substantially less than expected from theory. However, internal structure arrays typical of an upper plenum appear to exhibit a high net efficiency.

1. J. C. Dallman, W. L. Kirchner, and V. S. Starkovich, "De-entrainment Phenomena from Droplet Cross Flow in Vertical Rod Bundles," ANS Transactions, Vol. 30, pp. 381-384 (1978).

2. I. C. Finlay and T. McMillan, "Heat Transfer During Two-Component Mist Flow Across a Heated Cylinder," Proc. Instn. Mech. Engrs., Vol. 182, Pt. 3H, pp. 277-288 (1967).

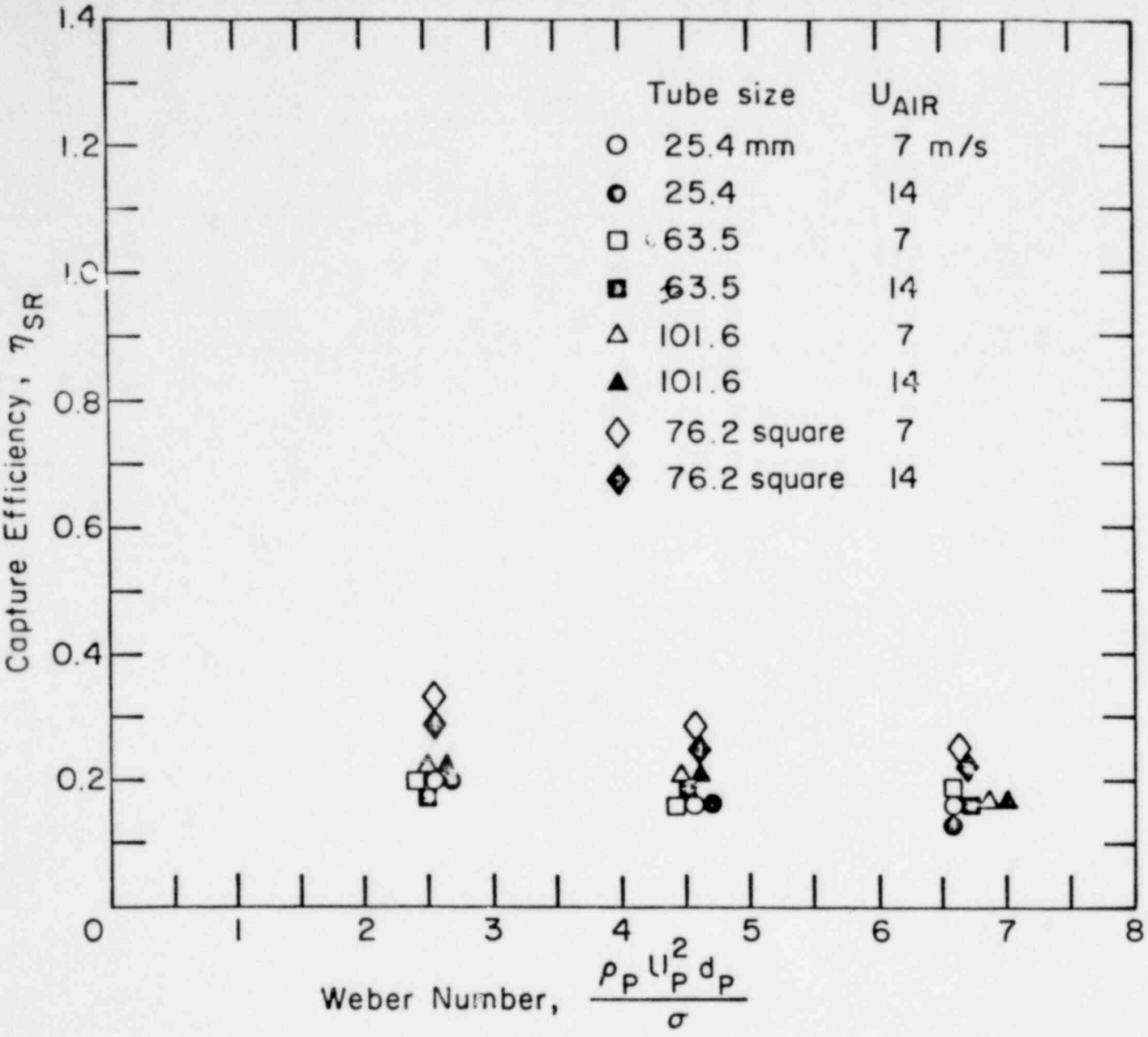

Figure 2 - Capture efficiency as a function of Weber Number.

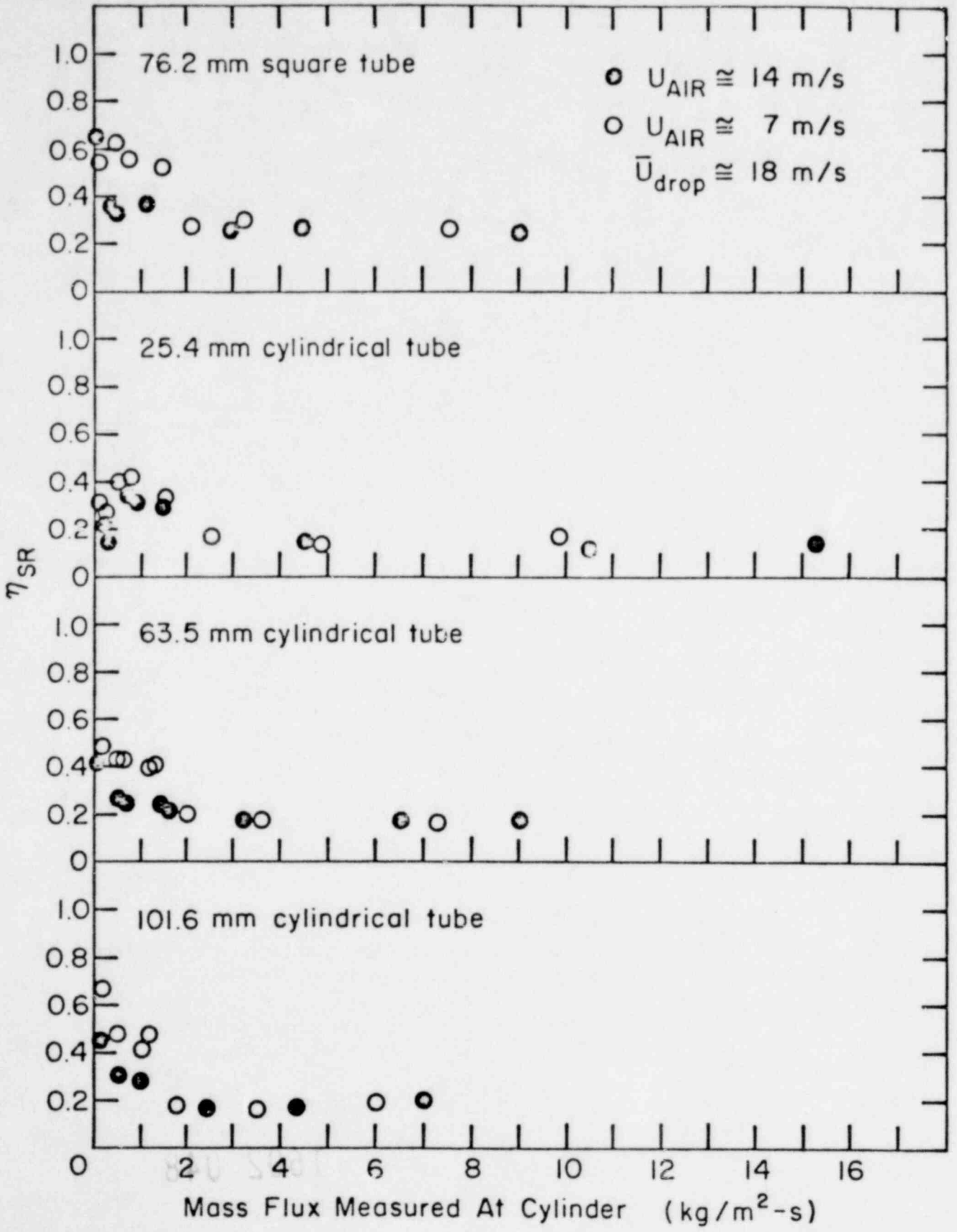

Figure 1 - Single tube de-entrainment efficiencies.

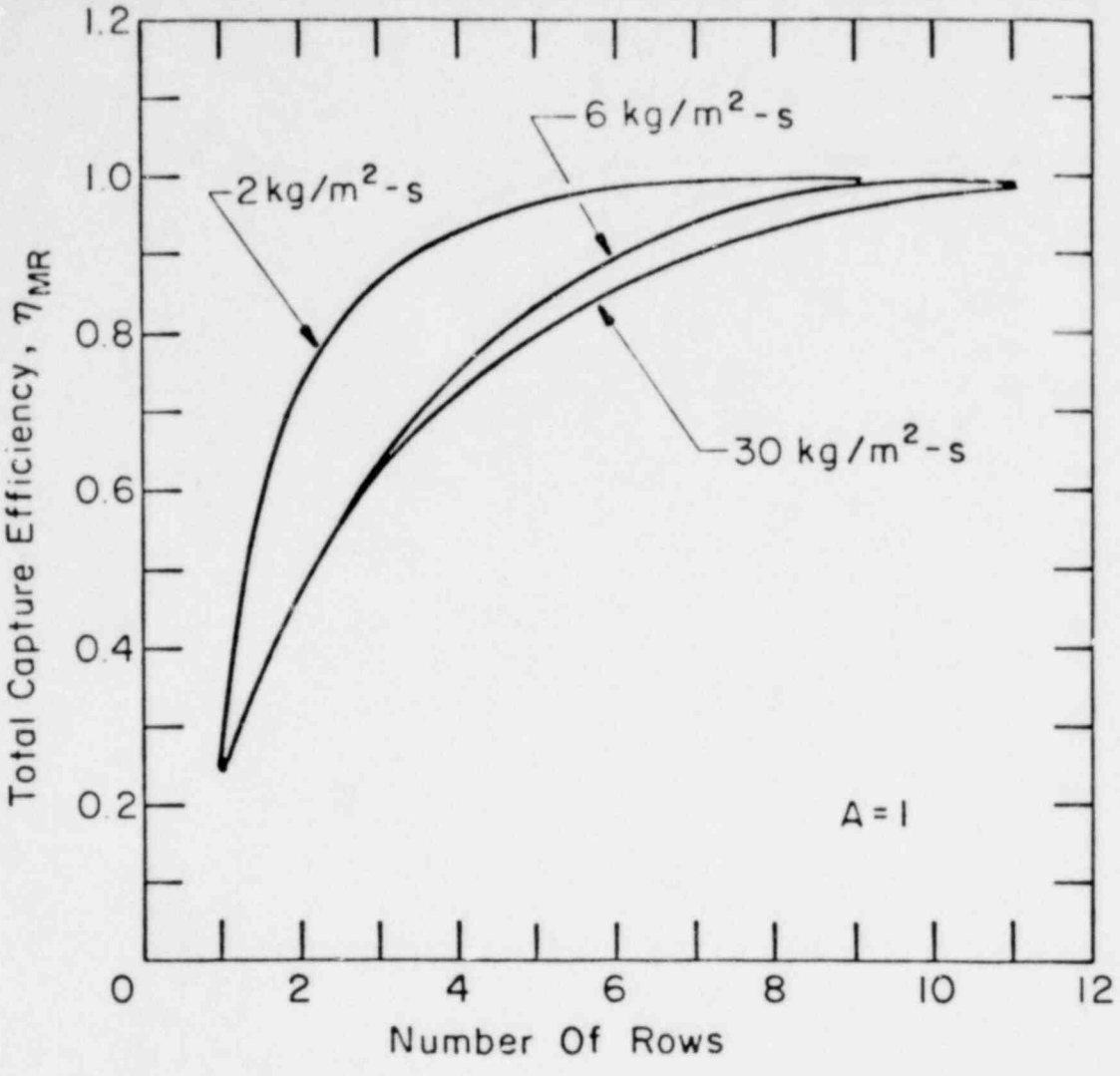

Figure 3 - Estimated multiple row capture efficiency.